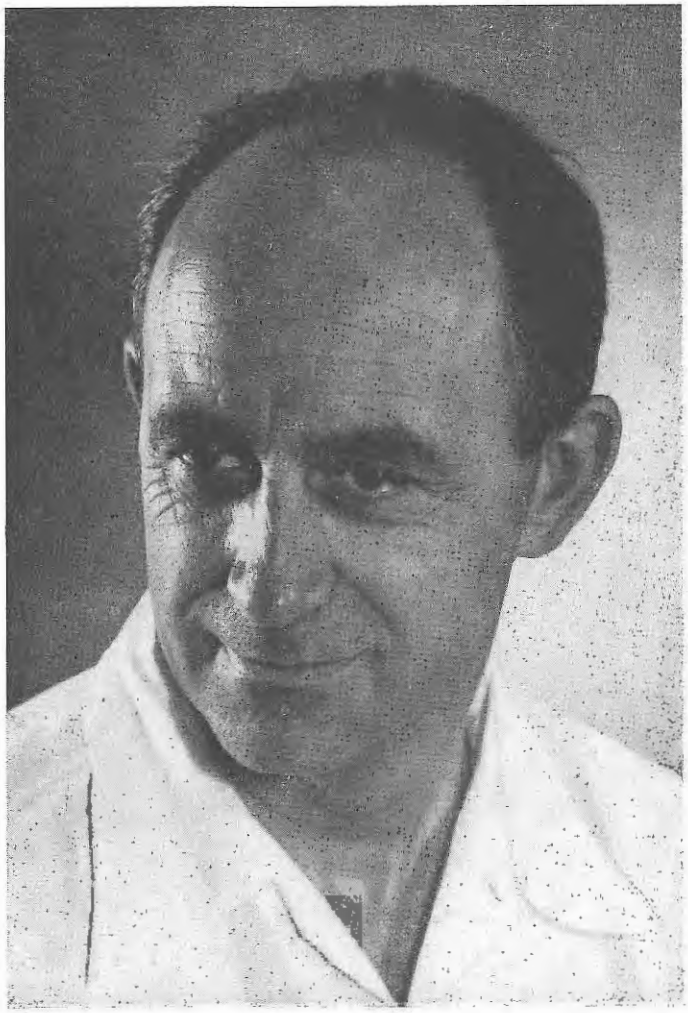

E. FERMI – *Los Alamos*, 1946.

ENRICO FERMI

NOTE E MEMORIE

(COLLECTED PAPERS)

VOLUME II

UNITED STATES 1939-1954

ACCADEMIA NAZIONALE DEI LINCEI - ROMA

THE UNIVERSITY OF CHICAGO PRESS

ACCADEMIA NAZIONALE DEI LINCEI, ROMA, ITALIA
THE UNIVERSITY OF CHICAGO PRESS, CHICAGO E LONDRA
THE UNIVERSITY OF TORONTO PRESS, TORONTO 5, CANADA

COMPOSTO E STAMPATO IN ITALIA

ROMA, 1965 — Dott. G. Bardi, Tipografo dell'Accademia Nazionale dei Lincei

COMITATO DI REDAZIONE

L'edizione di questo volume è stata curata dai proff. Edoardo Amaldi, Herbert L. Anderson, Enrico Persico, Emilio Segrè (Redattore Capo) e Albert Wattenberg, come è indicato nelle introduzioni delle singole note.

INDICE E BIBLIOGRAFIA

(I lavori preceduti da asterisco non sono ristampati in queste « Note e Memorie »).

LIBRI

* *Elementary Particles*, pp. XII+110, Yale University Press, New Haven, 1951. Tradotto come: *Particelle elementari*, Traduzione e complementi di P. CALDIROLA, pp. 192, Einaudi, Milano (1952).

* *Nuclear Physics.* A course given at the University of Chicago. Notes Compiled by J. OREAR, A. H. ROSENFELD, and R. H. SCHLUTER, pp. VII+246, The University of Chicago Press, Chicago, 1949.

Conferenze di Fisica Atomica (Fondazione Donegani), Accademia Nazionale dei Lincei, Roma 1950.

* *Notes on Quantum Mechanics*, pp. VII+171, The University of Chicago Press, Chicago 1961.

* *Lezioni di elettrodinamica*, pubblicata a cura dello studente Adelino Morelli. Roma, Stabilimento Tipolitografico del Genio Civile, [s. d.], 95 p., ill., 24 cm, litografato.

* *Lezioni di Fisica teorica*, dettate dal Prof. E. Fermi. Raccolte dai dott. Dei e Martinozzi. Roma, 1926–27, 60 p. ciclostilato.

* *Intervista con Enrico Fermi*, 11 novembre 1938, in « Ric. Scientifica », *9* (2), 638-639 (1938).

PREFAZIONE

Il primo volume di quest'opera contiene i lavori di Fermi scritti durante il periodo italiano della sua vita, dal 1921 alla fine del 1938, quando emigrò per gli Stati Uniti d'America. Il presente secondo volume comprende la fase americana della sua attività.

Per quanto cio che è stato detto nella Prefazione al Primo Volume si applichi, naturalmente, anche a questo Secondo Volume, è necessario tuttavia aggiungere alcune avvertenze.

I lavori del precedente volume, salvo eccezioni senza importanza, furono pubblicati da Fermi stesso. Il secondo volume contiene, invece, un numero rilevante di lavori che originariamente non erano destinati alla pubblicazione e che non furono riveduti dall'Autore. Tali sono per esempio i lavori che si riferiscono alla pila. Durante la seconda guerra mondiale essi furono fatti circolare come documenti segreti e rapporti di vari Enti del Governo Statunitense. Essi si riferiscono tutti, direttamente o meno, allo sviluppo dell'energia nucleare. Alcuni di questi scritti sono semplici rapporti sul lavoro compiuto durante un certo periodo, alcuni contengono il risultato di una sola misura importante, altri hanno scopo didattico o contengono presentazioni complete di teorie o di serie di esperimenti. Per quanto non li pubblichiamo tutti, i più importanti sono contenuti in questo volume – alcuni, sono ancora classificati e quindi inaccessibili. Altri lavori sono riproduzioni di corsi svolti in speciali circostanze durante la guerra. Essi sono stati scritti da uditori, senza revisione da parte di Fermi, e contengono imperfezioni che sarebbero certo state corrette dall'autore se egli li avesse preparati per la pubblicazione. Il Comitato di Redazione non può però sostituirsi all'autore in questo compito e le lezioni sono presentate nella redazione originale. Esse dànno un esempio interessante dello stile didattico di Fermi nei suoi anni maturi.

Tutti questi lavori, dopo la guerra, sono rimasti segreti, e quindi inaccessibili al pubblico, per un tempo più o meno lungo. Quando, infine, sono stati declassificati, Fermi stesso, per varie ragioni, decise di non pubblicarli. Il Comitato di Redazione ha peraltro deciso di includerli in questa opera a causa della loro importanza storica. Essi infatti sono una fonte indispensabile per ogni futura storia della tecnologia nucleare.

Poiché questi lavori non sono apparsi in regolari riviste scientifiche, è talora difficile rintracciarli tra le pubblicazioni ufficiali governative. Originariamente i lavori avevano una siglatura convenzionale. Spesso però lo stesso lavoro riappare con denominazioni diverse: così CP–413 è riapparso anche come AECD–3269.

Nelle introduzioni ai vari lavori abbiamo cercato di chiarire, per quanto possibile, le denominazioni ufficiali. Quando poi nel corso di lavori vengono citate altre pubblicazioni con una siglatura convenzionale, se esse sono contenute in questo volume, abbiamo dato il Numero sotto cui esse appaiono in questa rac-

colta. Per le altre il lettore interessato dovrà consultare un catalogo delle pubblicazioni dell'« Atomic Energy Commission » degli Stati Uniti d'America.

Abbiamo aggiunto in Appendice una lista di onori ricevuti da Fermi, una cronologia della sua vita e una breve descrizione dei manoscritti e di altri documenti storici a lui relativi, con l'indicazione della loro ubicazione.

Dobbiamo ringraziare il Dr. H. D. Young, bibliotecario dell'« Argonne National Laboratory », e il Dr. Robert Rosenthal della University of Chicago Library per il loro valido aiuto in diverse occasioni; nonché la Sig. O. Malaguti per l'aiuto prestato nella preparazione della bibliografia. Le Signore Laura Fermi ed Elfriede Segrè ci hanno validamente aiutato, sia in questo che nel precedente volume, in varie guise, e le ringraziamo cordialmente.

Il Comitato di Redazione

E. AMALDI, H. L. ANDERSON
E. PERSICO, F. RASETTI
C. S. SMITH, A. WATTENBERG
E. SEGRÈ (*Presidente*).

FOREWORD

The first volume of this book contains Fermi's scientific papers written during the Italian period of his life, from the beginning of 1921 to the end of 1938 when he emigrated to the United States of America. The present second volume covers the American phase of his activity.

The Foreword to Volume I applies also to this volume. There are, however, some additional remarks relevant especially to this volume.

The contents of the previous volume were prepared for publication by Fermi himself, with insignificant exceptions. Volume II contains a large number of papers which were not destined for publication, such as the reports of work connected with the pile. These papers have been issued as classified reports by different agencies of the U. S. Government concerned with nuclear energy during the Second World War. Some are only records of work performed during a certain period of time, some contain only the result of one important measurement, some are more elaborate presentations of theory or of a series of experiments. Although we do not publish them all, the most important are here. A few are still classified.

Some papers are reproductions of courses of lectures given in special circumstances during the war. They were written by members of the audience and were not revised by Fermi thus, they contain many imperfections which he would have removed if he had prepared them for publication. However, the Editorial Committee could not replace the Author in this work and the lectures are presented as written down. They are interesting samples of Fermi's didactic style in his later years.

After the war, all these papers remained classified for some time and became available for publication at different dates. Fermi himself decided, for various reasons, not to publish them after declassification. The Editorial Committee, however, has included them in this volume because they are historically interesting. In particular, they are indispensable source material for any future history of nuclear technology.

Because all these papers have not been published in standard journals, we have been faced with the problem of a suitable system of references. The papers were issued under code names such as CP–413, and often the same paper was reissued under different names:e. g., CP–413 is the same as AECD–3269. We have given this type of information in the introductions to the different papers. The papers contain also references to other reports issued under similar circumstances. We have left these references unaltered and the interested reader will have to consult the catalogs of publications issued by the U.S.A. Atomic Energy Commission.

We have added as Appendixes a list of honors received by Fermi, a chronology of his life and a catalog of the known manuscripts existing and of their location.

We thank Dr. H. D. Young of the Argonne National Laboratory and Dr. R. Rosenthal of the University of Chicago Library for their help on different occasions. Mis. O. Malaguti has helped in checking the bibliography. Mrs. Laura Fermi and Elfriede Segrè have contributed invaluable aid to the preparation of both volumes.

The Editorial Board

E. AMALDI, H. L. ANDERSON
E. PERSICO, F. RASETTI
C. S. SMITH, A. WATTENBERG
E. SEGRÈ, *Chairman*

NOTE E MEMORIE

(COLLECTED PAPERS)

Enrico Fermi had hardly arrived in the United States in January 1939 when the news of the discovery of the fission of uranium reached him. Hahn and Strassmann [1] in Berlin had just completed their important experiment showing the occurrence of barium from the bombardment of uranium by neutrons. They communicated this result and its implication that uranium could be split by neutrons to their erstwhile colleague, Lise Meitner, who had fled to Sweden because of the Nazi persecutions. The Christmas holidays found her at a favorite vacation place near Göteborg. Her nephew, Otto Frisch, had taken the occasion to join her and together they discussed the implications of these experiments, foreseeing as one of the consequences the large amount of energy release in the fission process.

These developments were communicated to Niels Bohr, who appreciated immediately the underlying reason for the fission process. He was about to depart for a visit to the United States and so couldn't wait to see the experimental tests which Meitner and Frisch had devised [2]. However on his arrival in New York, he hurried with his news to Columbia University. He wanted to discuss the new developments with Fermi.

Fermi saw directly, that in so violent a reaction neutrons might be released too. If the arrangement were such that the emitted neutrons could produce further fissions, the process might become multiplicative. If the circumstances were favorable enough, a chain reaction might be developed and large amounts of energy released.

At that time I was a graduate student working under the direction of Professor John R. Dunning. I had spent several years assisting E. T. Booth and G. N. Glasoe in the construction of the cyclotron. The cyclotron had begun to operate and I was readying an ionization chamber-linear amplifier combination for a thesis research in neutron scattering. Noting Fermi's evident interest in the new development as well as his lack of equipment, it seemed natural to offer to join forces with him. I proposed a rather simple modification of my ionization chamber which would allow us to observe the intense ionization caused by the fragments from the fission of uranium. We saw pulses from the fission of uranium on the screen of my cathode ray oscilloscope on January 25, 1939, only a few days after Frisch had carried out essentially the same experiment in Copenhagen.

The Fifth Washington Conference on Theoretical Physics took place the next day and Fermi was able to speak about the fission process with the conviction of personal experience. The discussion by Bohr and Fermi about the implications of the new development aroused the greatest interest in the scientific world. Many laboratories set about to verify the essential features of the process [3].

By the time he returned to Columbia the next day, Fermi knew what questions he wanted to answer. Were neutrons emitted in the fission of uranium? If so, in what numbers? How could these neutrons be brought to produce further fissions? What competitive processes were there? Could a chain reaction be developed?

In carrying further the experiments that could be done with the ionization chamber-linear amplifier combination, all the members of the group who, under Dunning, were working with the cyclotron, participated. E. T. Booth and G. N. Glasoe had worked several years constructing the cyclotron. While F. G. Slack had only recently arrived to spend a year in research at Columbia. The subsequent developments caused him to extend his stay several years beyond his original intention. Fermi's insistence that quantitative measurements be carried out prevailed, and in the first paper, written only one month after

(1) O. HAHN and F. STRASSMANN, « Naturwiss. », *27*, 11 (1939).

(2) L. MEITNER and O. R. FRISCH, « Nature », *143*, 239 (1939).
O. R. FRISCH, « Nature », *143*, 276 (1939).

(3) For an early review of the development of fission physics, see L. A. TURNER, « Rev. Mod. Phys. » *12*, 1 (1940).

Fermi had arrived at Columbia, the value of the fission cross-section for slow neutrons as well as for fast neutrons was reported. The measurements were quite crude, but they gave numerical values to essential quantities and served in this way to begin to bring realism to pure speculation. In addition, evidence was found which indicated that the fission cross-section had a 1/v dependence at low energies and the implication was drawn, based on an argument which we now know is not completely valid, that it was the rare isotope of uranium, U^{235}, which was involved. Fermi conceived the fission as taking place very rapidly, from which fact the 1/v dependence could be expected as a natural consequence. It was a surprise to him when, several years later, velocity selector measurements showed resonances in the low energy fission crosssection of U^{235}.

Curiously, these experiments with the ionization chamber were done mostly with a radon beryllium neutron source rather than the cyclotron. The cyclotron could serve as an intense but unsteady source of neutrons and in those days it was more frequently in need of repairs than operating reliably. For most of the work Fermi preferred the weaker but much more reliable radon-beryllium source which Dunning's good offices could also make available. On the other hand, the cyclotron served in the demonstration that fission products could be collected by recoil.

H. L. ANDERSON.

129.

THE FISSION OF URANIUM (*)

H. L. ANDERSON, E. T. BOOTH, J. R. DUNNING, E. FERMI, G. N. GLASOE, and F. G. SLACK.
« Phys. Rev. », *55*, 511–512 (1939) (Letter).

This letter is a preliminary report of some of the experiments which we have undertaken on the fission process of the uranium nucleus by neutron bombardment.

The phenomenon was discovered by Hahn and Strassmann (1) who were led by chemical evidence to suspect the possibility of the splitting of the uranium nucleus into two approximately equal parts. Through the kindness of Professor Bohr we were informed of these results some days before receiving them in published form, as well as of the suggestion of Meitner and Frisch that the process should be connected with the release of energy of the order of 200 Mev.

It seemed worth while to attempt the detection of the fragments by their high ionization. The interior of a parallel plate ionization chamber was coated with a thin layer of uranium oxide. When this chamber was connected to a linear amplifier a large number of small pulses from the alpha-particles of uranium were observed, but when exposed to the bombardment of neutrons from the cyclotron or from a Rn—Be source very large pulses occurred in addition. From the ratio of the maxima of these large pulses to the maxima of those due to the alpha-particles it was estimated

(*) Publication assisted by the ERNEST KEMPTON ADAMS FUND for Physical Research of Columbia University.

(1) O. HAHN and F. STRASSMANN, « Naturwiss. », *27*, 11 (1939).

that the energies of the fragments of uranium range up to about 90 Mev. This value of the energy seems to be somewhat smaller than the theoretical expectation. If we assume that the energy release in the fission is approximately 200 Mev, and that the two fragments may have somewhat different masses, then fragments with energies up to 120 or 130 Mev might be expected in some cases. However, these values probably do not lie outside our experimental error since lack of linearity in the amplifier and incomplete collection of the ions might explain the difference.

After this experiment had been performed, Professor Bohr received a cable from Dr. Frisch stating that he had obtained the same results some days before.

A number of measurements have been made of the cross section for the fission process for neutrons of different energies. For this the interior of an ionization chamber was coated, by electrolytic deposition, with a layer of uranium oxide of only 0.5 mm air equivalent, so that all the fission processes could be observed. In order to know the number of neutrons, a Rn—Be source of known intensity was utilized in a standard position inside a paraffin block [2]. In order to obtain the contributions of the thermal neutrons only, the difference in the number of fissions was measured with and without a cadmium absorber. These experiments gave a cross section of thermal neutrons for the fission process alone of about 2×10^{-24} cm^2. Fast neutrons from a Rn—Be source have instead an average cross section of about 0.1×10^{-24} cm^2.

By using a similar chamber with a thicker uranium oxide coating, the changes in the fission activity due to the interposition of cadmium and boron filters were determined and compared with those obtained when the same chamber was coated with boron instead of uranium. Within the limits of the experimental error the behavior for slow neutrons of the absorbers for the fission process and for the boron disintegration was the same. This suggests that the efficiency of slow neutrons for the fission process follows a $1/v$ law. As mentioned above, fast neutrons are relatively more efficient in producing the fission process than they are in the boron disintegration.

The validity of the $1/v$ law makes it probable that the levels of the compound nucleus are broadened by the short lifetime (probably not more than 10^{-17} sec.) of the fission process. There seems to be some contradiction between this result and the known fact that uranium has a sharp resonance for slow neutrons of about 25 ev that does not lead, however, to the fission but to the formation of U^{239}. As suggested by Professor Bohr a possible explanation is that the fission does not occur from U^{238} but from U^{235}, which is present in an amount of somewhat less than 1 percent.

The range of the fragments has been measured by allowing the fragments to enter a shallow ionization chamber 1.0 cm from the uranium through a grid. By varying the pressure the maximum range has been determined to be approximately 1.7 cm.

The recoil fragments from irradiated uranium have been collected upon a Cellophane foil placed next to it. After a ten-minute irradiation with slow

(2) E. AMALDI and E. FERMI, « Phys. Rev. », *50*, 899 (1936).

neutrons from the cyclotron, the Cellophane foil showed an activity of about 400 counts per minute when wrapped around a counter. The decay of this activity indicated the presence of several periods which have not yet been analyzed. Interposition of an 0.0012 Cellophane foil between the uranium and the collecting foil showed that a small fraction of the recoil fragments passes through, in fair agreement with the range measurement. While these experiments were in progress we were informed by Professor Bohr that a similar experiment had been suggested by Miss Meitner.

We are indebted to Dr. J. Steigman, H. B. Hanstein and E. Haggstrom for their assistance in carrying out these experiments.

Pupin Physics Laboratories, Columbia University, New York, New York, February 16, 1939.

N° 130.

Fermi preferred, for himself, to pursue the question of the neutron emission, leaving for others the study of those aspects of the fission process which seemed to bear less directly on the possibility of producing a chain reaction. I continued working with Fermi, giving up, at least for a time, the cyclotron and my ionization chamber-linear amplifier apparatus. I took over the production of the radon beryllium sources which were used in the next experiment. In this we were joined by H. B. Hanstein, also a graduate student, who contributed the electrometer with which we measured the radioactivity induced in the neutron detectors.

In the first experiment a radon-beryllium neutron source was used to irradiate a bulb containing uranium oxide, the whole being immersed in a large container of water. It was Leo Szilard who pressed upon us a radium-beryllium photoneutron source which he had managed to procure. The energy of the neutrons from this source being lower than that of those emitted from fission would allow the latter to reveal themselves in the experiment with the radon-beryllium source. It was possible to show that neutrons were emitted in about the same number as they were absorbed. These experiments were parallel to but carried out independently of those by von Halban, Joliot, and Kowarski [1].

H. L. ANDERSON.

130.

PRODUCTION OF NEUTRONS IN URANIUM BOMBARDED BY NEUTRONS (*)

H. L. ANDERSON, E. FERMI, and H. B. HANSTEIN

« Phys. Rev. », *55*, 797–798 (1939) (Letter).

It is conceivable that the splitting of the uranium nucleus may have associated with it the emission of neutrons. These could either evaporate from highly excited fragments (this process is made more probable by the large neutron excess of the fragments, which lowers the binding energy of the neutrons) or be emitted at the instant of fission. This letter is a preliminary report on experiments undertaken to ascertain whether, and in what number, neutrons are emitted by uranium subject to neutron bombardment, and also

(1) H. VON HALBAN, F. JOLIOT, and L. KOWARSKI, « Nature », *143*, 470 and 680 (1939).

(*) Publication assisted by the Ernest Kempton Adams Fund for Physical Research of Columbia University.

whether the number produced exceeds the total number absorbed by all processes whatever.

A source of neutrons was placed in the center of a spherical bulb, 13 cm in diameter, which was immersed in the center of a large tank of water, 90 cm in diameter and 90 cm high. The activity induced in a rhodium foil placed in the water at various distances from the source was measured with and without uranium oxide inside the bulb. If we denote by $a(r)$ the activity induced at the distance r, the integral $\int a(r)\, r^2\, dr$ is proportional to the total number of slow neutrons present in the water. A comparison of the integrals with and without uranium gives, in principle, the possibility of deciding whether or not, with uranium present, there is a net increase in the number of neutrons. This result will be independent of the initial energy of the neutrons since in the water they all become slow neutrons.

With radon + beryllium as a source of neutrons a 6 percent increase in tbe integral with uranium was found. If this increase were caused only by neutrons emitted by the processes discussed above, it would correspond to a yield of about two neutrons per each neutron captured. Since, however, a radon + beryllium source emits also neutrons with energies of several million electron volts one can also interpret the increase observed, or at least part of it, as due to $(n, 2n)$ processes in which a high energy neutron knocks out a nuclear neutron without being captured.

The experiment was therefore repeated with photoneutrons emitted from a block of beryllium irradiated with the gamma-rays from one gram of radium. Since these neutrons have energies considerably lower than 10^6 ev an $(n, 2n)$ process is highly improbable. Because of the large dimensions and the shape of the beryllium block and the radium source, it was not feasible, however, to secure, in this experiment, the requisite spherical symmetry. The resulting loss of precision makes a comparison of the two integrals inconclusive. Since, however, at large distances from the source the activity with uranium is about 30 percent larger than without uranium, it follows that neutrons of energy larger than that of the photoneutrons are produced in the process. This result is in agreement with the direct observations of Szilard and Zinn; we thank them for informing us of their results prior to publication. Close to the bulb the activity with uranium is, instead, about 60 percent of the activity without uranium. This decrease is due to the absorption of neutrons by uranium; the total absorption cross section of uranium, due to fission and other processes, can be deduced from this result to be of the order of 5×10^{-24} cm^2.

If the volume integral of the differences in the activities with and without uranium is calculated, the contribution from parts in the neighborhood of the bulb is negative and gives the order of magnitude of the number of neutrons absorbed. The contribution of the distant parts of the volume is positive and gives the order of magnitude of the number of neutrons produced. These two contributions are of the same order of magnitude and the present accuracy is inadequate to decide which one is larger. Improved experiments are in progress in order to increase the accuracy.

Roberts, Meyer, and Wang [1] have reported the emission of delayed neutrons subsequent to the bombardment of uranium by neutrons. Such delayed neutrons cannot contribute appreciably to the effects that have been described here. This was ascertained by observing that no activity was induced in the rhodium detector after the removal of the source.

We are indebted to the Association for Scientific Collaboration for the loan of the photoneutron source used in these experiments.

Pupin Physics Laboratories, Columbia University, New York, New York, March 16, 1939.

(1) ROBERTS, MEYER, and WANG, « Phys. Rev. », 55, 510 (1939).

N° 131.

Besides producing fission, slow neutrons can also, by simple capture, give rise to a radioactive isotope of uranium, U^{239}. This process competes with fission in taking up the neutrons which are needed to sustain a chain reaction. We wanted to know how much of the absorption was due to this process, and whether adding its contribution to that of the fission, all of the absorption ascribed to uranium could be accounted for. It is the simple capture of neutrons by U^{238} that leads through neptunium to the production of plutonium, which subsequently proved to be of great importance. The capture of thermal neutrons is due to a strong resonance absorption at somewhat higher energies. A major problem in making the chain reaction was to avoid losses due to this absorption. The following Letter reported the first of many measurements made to establish quantitatively the importance of this process. The value reported here turned out to be too small by a factor of two, but Fermi knew that a weakness of the experiment was in the source standardization and we subsequently devoted a considerable effort to improve the knowledge of the neutron output of the sources we used.

H. L. ANDERSON.

131.

SIMPLE CAPTURE OF NEUTRONS BY URANIUM (*)

H. L. ANDERSON and E. FERMI

« Phys. Rev. », *55*, 1106–1107 (1039) (Letter).

It is known (1) that slow neutrons, besides producing fission, can also by simple capture give rise to a radioactive isotope of uranium (U^{239}) which emits beta-rays with a period of 23 minutes. We have attempted to ascertain the contribution of this process to the capture of thermal neutrons, in order to determine whether this absorption could account for the difference (2-5) between the total capture cross section and the cross section for fission. According to Meitner, Hahn and Strassmann, the simple capture of neutrons is a typical resonance process with a sharp absorption band at about 25 volts.

(*) Publication assisted by the Ernest Kempton Adams Fund for Physical Research of Columbia University.

(1) MEITNER, HAHN, and STRASSMANN, « Zeits. f. Physik », *106*, 249 (1937).

(2) ANDERSON, BOOTH, DUNNING, FERMI, GLASOE, and SLACK, « Phys. Rev. », *55*, 511 (1939).

(3) WHITAKER, BARTON, BRIGHT, and MURPHY, « Phys. Rev. », *55*, 793 (1939).

(4) ANDERSON, FERMI, and HANSTEIN, « Phys. Rev. », *55*, 797 (1939).

(5) MICHIELS, PARRY, and THOMSON, « Nature », *143*, 760 (1939).

They give 1200×10^{-24} cm² as the cross section at resonance, but they give no information as to the width of the absorption band and the capture cross section for thermal neutrons.

Our measurement was based on a determination of the number of disintegrations per second of the 23-minute period of uranium produced by thermal neutrons and of the number of thermal neutrons effective under the conditions of irradiation.

The procedure was as follows: (1) Purification of uranium from uranium X by dissolving uranyl nitrate in ether and shaking with a small amount of water. UX and other impurities remain in the water, while a large fraction of uranium remains in ether solution and a purified uranyl nitrate may be obtained by evaporating the ether. (2) Irradiation inside paraffin by means of the cyclotron with an indium foil as monitor placed elsewhere in a fixed position. (3) Second ether purification in order to separate the 23-minute life from all other activities which are not due to isotopes of uranium. (4) Measurement, by means of an ionization chamber, of the decay of the 23-minute life and the growth of the UX activity.

If the beta-rays of U^{239} and of UX (practically, only those of UX_2 are effective since the beta-rays of UX_1 are too soft to enter our chamber) had the same energy distribution, the ratio of initial activity of U^{239} reduced to infinite time of irradiation, to the saturation activity of UX would give the ratio of the number of disintegrations of U^{239} to the known number of disintegrations of UX_2, namely, 5×10^{-18} per atom per second. However, the absorption coefficients of the two beta-radiations are different. According to our measurements, the mass absorption coefficients in aluminum are 10 cm²/g for U^{239}, and 5.5 cm²/g for UX_2. We have therefore corrected our results for the absorption of beta-rays in the substance itself, in the container and in the window of the ionization chamber, and for the sensitivity of the chamber. The total correction factor was 3.4. Under our conditions of irradiation, the two activities so corrected were of the same order of magnitude.

(5) The activation was performed with and without Cd absorbers in order to isolate the contributions of thermal neutrons. (6) The number of thermal neutrons for a given indication of the monitor was obtained by comparing the activity induced in an indium foil when irradiated either in the uranium position with the cyclotron or in a paraffin arrangement of standard geometry (center of the surface of a cylinder of paraffin containing the source 3 cm below the surface) with a known Rn-Be source. The number of thermal neutrons per millicurie per cm² per second effective in activating the indium foil was taken [6] to be $7\sqrt{3}$.

In this way we found, in a first experiment, a cross section for the production of U^{239} by thermal neutrons of 1.0×10^{-24} cm².

In a second experiment, using the same method on a mixture of uranium and manganese, we determined simultaneously the capture cross sections for uranium and for manganese, and found 1.2×10^{-24} cm² and 10×10^{-24}

(6) E. AMALDI and E. FERMI, « Phys. Rev. », *50*, 899 (1936). The factor $\sqrt{3}$ appears in order to take into account the obliquity of the emerging neutrons.

cm², respectively. The good agreement of this last value with that obtained as the difference between the scattering plus capture cross section [7] 14.3×10^{-24} cm² and the scattering cross section [8] 2.1×10^{-24} cm² may be interpreted as a check on the accuracy of the method.

The width, Γ, of the resonance level at 25 volts may be calculated from the intensity of activation, and turns out to be of the order of one volt. This width and our value for the thermal neutron cross section for simple capture are not consistent with an interpretation in terms of the single-level formula of Breit-Wigner.

Summing the fission cross section of 2×10^{-24} cm² with the above cross section for simple capture of 1.2×10^{-24} cm² we find as the total absorption cross section for thermal neutrons 3.2×10^{-24} cm². Because of the large errors which can affect such measurements, this may not be inconsistent with the value 5×10^{-24} cm² previously reported [4] from absorption measurements, or with the value of 5.9×10^{-24} cm² reported by Michiels, Parry and Thomson [5]. If, instead, the total absorption is considerably larger, as reported by Whitaker *et al.* [3], there must be some other process of absorption to account for the difference.

Pupin Physics Laboratories, Columbia University, New York, New York, May 17, 1939.

(7) DUNNING, PEGRAM, FINK and MITCHELL, « Phys. Rev. », *48*, 265 (1935).
(8) M. GOLDHABER and G. H. BRIGGS, « Proc. Roy. Soc. », *162*, 127 (1937).

N° 132.

While the work described in paper N° 131 was going on, Szilard was busy obtaining a large amount of uranium oxide for a more ambitious experiment with the object of observing directly an increase in the number of neutrons due to the presence of uranium. The uranium oxide, which was on loan, was packed in tin cans. In this way, some 20 kilograms could be placed around Szilard's photo-neutron source, and the whole assembly immersed in a bath of manganese solution. The neutron intensity was measured by measuring the radioactivity induced in the manganese. With the uranium in place, a ten percent increase was observed. Thus, it became certain that more neutrons were emitted by the uranium than it absorbed. When an attempt was made to deduce what the ratio was of fast neutrons emitted per thermal neutron absorbed by uranium, it became apparent that there was a large correction due to the resonance absorption by the uranium. Our discussion as to what to do about this proceeded aimlessly for a while. Then Fermi asked to be left alone for 20 minutes. This was long enough for him to make a rough estimate of this effect, and this was duly recorded in the paper. He never revealed, neither to Szilard nor to me, the details of how he arrived at this estimate, presumably because his basis was largely intuitive. Fermi was never far wrong in such things, and he was taken at his word. The episode did pinpoint the importance of the resonance absorption and provided the clue of how, by lumping the uranium, the losses due to the resonance absorption could be reduced. It also became clear that thermal neutron absorption by hydrogen was too large for water to be a usable medium for slowing down neutrons in a chain reaction.

This was the first, and also the last, experiment in which Szilard and Fermi collaborated together. Szilard's way of working on an experiment did not appeal to Fermi. Szilard was not willing to do his share of the experimental work, neither in the preparation nor in the conduct of the measurements. He hired an assistant to do what we would have required of him. The assistant, S. E. Krewer, was quite competent, so we could not complain on this score, but the scheme did not conform with Fermi's idea of how a joint experiment should be carried out, with all work distributed more or less equally and each willing and able to do whatever fell to his lot. Fermi's vigor and energy always made it possible for him to contribute somewhat more than his share, so that any dragging of feet on the part of the others stood out the more sharply in contrast.

H. L. ANDERSON.

132.

NEUTRON PRODUCTION AND ABSORPTION IN URANIUM (*)

H. L. ANDERSON, E. FERMI, and LEO SZILARD
Columbia University, New York, New York
« Phys. Rev. », *56*, 284–286 (1939)
(received July 3, 1939).

It has been found[1–3] that there is an abundant emission of neutrons from uranium under the action of slow neutrons, and it is of interest to ascertain

(*) Publication assisted by the Ernest Kempton Adams Fund for Physical Research of Columbia University.

(1) v. HALBAN, JOLIOT and KOWARSKI, « Nature », *143*, 470 (1939).

(2) L. SZILARD and W. H. ZINN, « Phys. Rev. », *55*, 799 (1939).

(3) ANDERSON, FERMI and HANSTEIN, « Phys. Rev. », *55*, 797 (1939).

whether and to what extent the number of neutrons emitted exceeds the number absorbed.

This question can be investigated by placing a photo-neutron source in the center of a large water tank and comparing, with and without uranium in the water, the number of thermal neutrons present in the water. In the previous experiments of this type [1-3] it was attempted to have as closely as possible a spherically symmetrical distribution of neutrons. The number of thermal neutrons present in the water was determined by measuring along one radius the neutron density ρ as a function of the distance r from the center, and then calculating $\int r^2 \rho dr$. A difference in favor of uranium of about five percent was reported by von Halban, Joliot and Kovarski [4].

Since one has to measure a small difference, slight deviations from a spherically symmetrical distribution might give misleading results. The present experiments which are based on the same general principle do not require such symmetry. In order to measure the number of thermal neutrons in the water we filled the tank with a ten-percent solution of $MnSO_4$. The activity induced in manganese is proportional to the number of thermal neutrons present. A physical averaging was performed by stirring the solution before measuring the activity of a sample with an ionization chamber. To obtain an effect of sufficient magnitude, about 200 kg of U_3O_8 was used.

The experimental arrangement is shown in fig. 1. A photo-neutron source, consisting of about 2 g of radium and 250 g of beryllium was placed in the center of the tank. The geometry was such that practically all neutrons emitted by the source and by the uranium oxide were slowed down and absorbed within the tank. Each irradiation extended over several half-life periods of radiomanganese and the observed activity of the solution was about four times the background of the ionization chamber. Alternating measurements were taken with the cans filled with uranium oxide, and with empty cans of the same dimensions. The activity proved to be about ten percent higher with uranium oxide than without it. This result shows that in our arrangement more neutrons are emitted by uranium than are absorbed by uranium.

In order to find the average number of fast neutrons emitted by uranium for each thermal neutron absorbed by uranium, we have to determine what fraction of the total number of neutrons emitted by the photo-neutron source is, in our experiment, absorbed in the thermal region by uranium. The number of photo-neutrons emitted by the source is indicated by the activity of the solution in the tank when the irradiation is carried out with empty cans surrounding the source. We obtained a measure of this number by taking into account that in our solution about 20 percent of the neutrons are captured by manganese and the rest by hydrogen. In order to obtain, in the same units, a measure of the number of neutrons absorbed by uranium we proceeded in the following way: A mixture of sand and manganese powder, having the same thermal neutron absorption as uranium oxide replaced

(4) v. HALBAN, JOLIOT and KOWARSKI, «Nature», *143*, 680 (1939).

the uranium oxide in 1/4 of the cans which were distributed uniformly among the other uranium oxide-filled cans. After irradiation, all this powder was mixed together, a ten-percent $MnSO_4$ solution was prepared from a sample, and its activity was measured with our ionization chamber.

In this way we found that about 50 percent of the neutrons emitted by the source are absorbed as thermal neutrons by uranium in our arrangement. It follows that, if uranium absorbed only thermal neutrons, the observed ten-percent increase in activity obtained with uranium present would correspond to an average emission of about 1.2 neutrons per thermal neutron

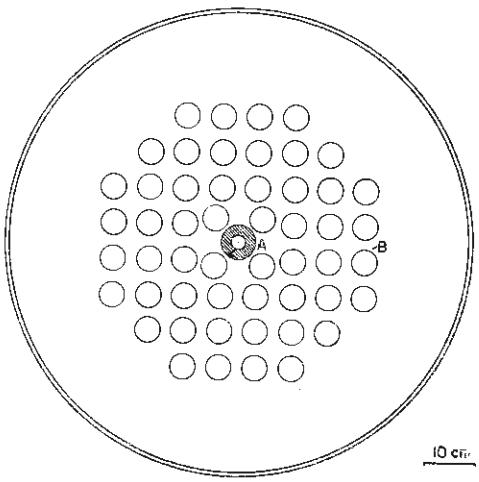

Fig. 1. – Horizontal section through center of cylindrical tank which is filled with 540 liters of 10-percent $MnSO_4$ solution. A, photo-neutron source composed of 2.3 grams of radium and 250 grams of beryllium. B, One of 52 cylindrical cans 5 cm in diameter and 60 cm in height, which are either empty or filled with uranium oxide.

absorbed by uranium. This number should be increased, to perhaps 1.5, by taking into account the neutrons which, in our particular arrangement, are absorbed at resonance in the nonthermal region by uranium, without causing neutron emission.

From this result we may conclude that a nuclear chain reaction could be maintained in a system in which neutrons are slowed down without much absorption until they reach thermal energies and are then mostly absorbed by uranium rather than by another element. It remains an open question, however, whether this holds for a system in which hydrogen is used for slowing down the neutrons.

In such a system the absorption of neutrons takes place in three different ways: The neutrons are absorbed at thermal energies, both by hydrogen and uranium, and they are also absorbed by uranium at resonance before they are slowed down to thermal energies. Our result is independent of the ratio of the concentrations of hydrogen and uranium, insofar as it shows that, for thermal neutrons, the ratio of the cross section for neutron production

and neutron absorption in uranium is greater than one, and probably about 1.5. What fraction of the neutrons will reach thermal energies without being absorbed will, however, depend on the ratio of the average concentrations of hydrogen and uranium. Since there is an appreciable absorption even far from the center of the resonance band, it follows that the fraction of neutrons absorbed by uranium at resonance will increase with decreasing hydrogen concentration. This has to be taken into account in discussing the possibility of a nuclear chain reaction in a system composed essentially of uranium and hydrogen. A chain reaction would require that more neutrons be produced by uranium than absorbed by uranium and hydrogen together. In our experiment the ratio of the average concentration of hydrogen to uranium atoms was 17 to 1, and in the experiment of von Halban, Joliot and Kowarski this ratio was 70 to 1. At such concentrations the absorption of hydrogen in the thermal region will prevent a chain reaction. By reducing the concentration of hydrogen one would obtain the following effect: On the one hand a larger fraction of those neutrons which reach thermal energies will be absorbed by uranium; on the other hand fewer neutrons reach the thermal region due to an increased absorption by uranium at resonance. Of these two counteracting factors the first is more important for high hydrogen concentrations and the second is more important for low hydrogen concentrations. Starting with high hydrogen concentrations, the ratio of neutron production to total neutron absorption will thus first rise, then pass through a maximum, and, as the hydrogen concentration is decreased, thereafter decrease. We attempted to estimate the quantities involved from the information available about resonance absorption in uranium [5-7] and from the observed net gain of 0.2 in the number of neutrons in our experiment. The effect of the absorption at resonance turns out to be so large that even at the optimum concentration of hydrogen it is at present quite uncertain whether neutron production will exceed the total neutron absorption. More information concerning the resonance absorption of uranium as well as more accurate measurement of some of the values which enter into our calculation are required before we can conclude whether a chain reaction is possible in mixtures of uranium and water.

We wish to thank Dr. D. W. Stewart, of the Department of Chemistry, and Mr. S. E. Krewer, for advice and assistance in carrying out some of these experiments. We are much indebted to the Eldorado Radium Corporation for enabling us to work with large quantities of uranium oxide in our experiments, and to the Association for Scientific Collaboration for the use of the photoneutron source and other facilities.

(5) MEITNER, HAHN and STRASSMANN, « Zeits. f. Physik », *106*, 249 (1937).
(6) v. HALBAN, KOWARSKI and SAVITCH, « Comptes rendus », *208*, 1396 (1939).
(7) H. L. ANDERSON and E. FERMI, « Phys. Rev. », *55*, 1106 (1939).

N° 133.

By now summer had arrived. Fermi left for Ann Arbor, where the University of Michigan conducted a Summer School of Theoretical Physics, in which Fermi had participated before (see paper N° 67), and of which he was very fond. I took up a careful study of the uranium resonance absorption process, which was to be my doctoral dissertation. Meanwhile, Szilard convinced himself that with graphite to slow down the neutrons the chain reaction was practically a certainty. With this certainty in mind he and E. P. Wigner prevailed upon Einstein to write his famous letter to President Roosevelt. The letter outlined the possibilities for nuclear energy and the need for supporting the work. It led to the establishment of the "Advisory Committee on Uranium" which was to look into the problem and report to the President. It also led, early in 1940, to a first government grant of $ 6,000 and to the delivery of enough graphite to determine its neutron absorption. (Fermi and Dean G. B. Pegram of Columbia had also made an attempt to alert the government to the implications of atomic energy—the previous March. Introduced by a letter from Pegram, Fermi had talked to Admiral S. C. Hooper and a group of Navy men in Washington. Perhaps because of his, and Pegram's, cautious language no action followed. (*)

During his stay at Ann Arbor some correspondence was exchanged between Fermi and Szilard on the subject of the use of graphite for making a chain reaction, but Fermi's attention was diverted by an interesting problem in cosmic rays. Mesotrons (now called μ-mesons) were newly discovered particles found among the cosmic rays. It had been shown that they have a considerably greater absorption in air than in equal masses of condensed material. This was interpreted as evidence that the mesotron was an unstable particle decaying with a lifetime of about two microseconds. Fermi thought that some of the difference in behavior might be due to the higher dielectric constant which is characteristic of condensed matter. In material having a high dielectric constant the electric field intensity of a rapidly moving charged particle is reduced in such a way that its loss of energy by ionization is diminished. When he returned to Columbia at the end of the summer, Fermi made a simple classical calculation which showed that the effect could be quize sizable. This was reported in the following letter. (Note the recurrence of the ideas first developed in papers N° 23 *a*, *b* and 95).

H. L. ANDERSON.

133.

THE ABSORPTION OF MESOTRONS IN AIR AND IN CONDENSED MATERIALS (**)

« Phys. Rev. », *56*, 1242 (1939) (Letter).

It has been pointed out by several authors that the absorption of mesotrons in air is considerably larger than the absorption by equal masses of condensed materials. This fact has been interpreted as evidence for a spon-

(*) L. L. STRAUSS, *Men and Decisions*, Doubleday & Co., 1962.

(**) Publication assisted by the Ernest Kempton Adams Fund for Physical Research of Columbia University.

taneous decay of the mesotron. A lifetime of about 2×10^{-6} sec. is required in order to account for the difference.

The great theoretical importance of this conclusion justifies a careful investigation of possible alternative explanations of the observed difference in absorption. I have therefore considered the following effect which seems to explain the observations, at least to some extent, without assuming a decay of the mesotron.

The ionization loss of energy by a fast particle passing through matter is partly due, as is well known, to close impacts between the particle and the material electrons; a large fraction of the loss, however, is due to impacts at distances greater than the atomic radius. For a mesotron with energy of the order of some billions of ev the ionizing effects of the particle can reach to distances of over 10^4 times the interatomic distances.

In a rarefied gas the action of the field of the passing particle on every molecule is independent of the perturbation due to the surrounding molecules. This is no longer true for a condensed material in which the electric field of the passing particle is largely affected by the reaction of the electric polarization of the substance. A calculation of this effect based on the classical theory of the ionization loss shows that it is by no means negligible.

Simple formulas can be obtained if the dielectric properties of the medium are schematized by assuming all the electrons (n per unit volume) to be elastically bound with the same frequency ν_0. The dielectric constant for low frequencies would then be $\varepsilon = 1 + ne^2/\pi m \nu_0^2$. With these assumptions it can be proved that the energy loss per unit path for a particle moving with velocity v is less than the loss calculated with the ordinary theory by the following amount:

$$\frac{2\pi ne^4}{mv^2} \log \varepsilon \quad \text{for} \quad v < c/\sqrt{\varepsilon},$$

$$\frac{2\pi ne^4}{mv^2} \left| \log \frac{\varepsilon - 1}{1 - v^2/c^2} + \frac{1 - \varepsilon v^2/c^2}{\varepsilon - 1} \right| \quad \text{for} \quad v > c/\sqrt{\varepsilon}.$$

The result is not essentially dependent on the special assumption as to the dielectric properties of the substance.

While these formulas give a relatively unimportant change in the stopping power of gases and solids for slow particles like protons or α–particles, the difference in behavior becomes rather large when the velocity approaches that of light. Let us consider for example the energy loss of a mesotron of 3×10^9 ev in two different media: A condensed material for which we take $\varepsilon = 2$; and air for which we take $\varepsilon = 1.00054$. Neglecting the present effect one would expect the energy loss to be approximately 2.3 Mev·cm²/g for both media. The reduction of loss due to the interaction is negligible in the case of air; it is instead about 0.5 Mev·cm²/g for the condensed substance. This reduces the loss in the latter case to only 1.8 Mev·cm²/g.

The effect of this difference on the absorption of cosmic rays can be estimated if we assume the number of mesotrons with energy $> W$ to vary as $W^{-1.9}$. The ratio of the mesotron intensity observed under equal amounts of air and of condensed materials should then be $(2.3/1.8)^{1.9} = 1.6$. According to Ehmert the experimental value of the ratio is about 2.

It seems therefore that the theory accounts for the order of magnitude of the effect even without any contribution from the decay of the mesotron.

Whether all the effects, and especially the somewhat greater differences of absorption reported as results of observations with relatively thin absorbers, can be interpreted on the outlined basis is doubtful. Indeed the theoretical result seems to be near one-half of the experimental difference. But in any case the interactions between atoms represent an important factor to be taken into account in the interpretation of experiments of this type.

I hope to be able to give soon the details of the theory and of its applications in a more extensive publication.

Pupin Physics Laboratories, Columbia University, NewYork, New York, October 1, 1939.

N° 134.

Fermi worked most of the fall calculating in some detail the magnitude and consequences of the effect discussed in paper N° 133. It turned out to be important only at very high meson energies. The experiment of Rossi, Hilberry and Hoag (« Phys. Rev. », *56*, 837, 1939) measured the absorption for mesons of energy sufficiently low for Fermi's effect to be rather unimportant. Thus, the decay of the mesotron was definitely established, and soon thereafter F. Rasetti observed the decay directly (« Phys. Rev. », *59*, 706, 1941). Subsequently, O. Halpern and H. Hall (« Phys. Rev. », *73*, 477, 1948) refined the calculations and showed that the effect was even smaller than Fermi had supposed.

H. L. ANDERSON.

134.

THE IONIZATION LOSS OF ENERGY IN GASES AND IN CONDENSED MATERIALS (*)

« Phys. Rev. », *57*, 485–493 (1940).
Pupin Physics Laboratories, Columbia University, New York, New York.
Received January 22, 1940.

It is shown that the loss of energy of a fast charged particle due to the ionization of the material through which it is passing is considerably affected by the density of the material. The effect is due to the alteration of the electric field of the passing particle by the electric polarization of the medium. A theory based on classical electrodynamics shows, that by equal mass of material traversed, the loss is larger in a rarefied substance than in a condensed one. The application of these results to cosmic radiation problems is discussed especially in view of the possible explanation on this basis of part of the difference in the absorption of mesotrons in air and in condensed materials that is usually interpreted as evidence for a spontaneous decay of the mesotron.

The determination of the energy lost by a fast charged particle by ionization and excitation of the atoms through or near which it is passing has been the object of several theoretical investigations. The essential features of the phenomenon are explained as well known in terms of a classical theory due to Bohr; the electrons near which the particle passes are treated as classical oscillators that are set in motion by the electric field of the passing particle. The energy thus absorbed by the electrons is equal to the energy lost by the

(*) Publication assisted by the Ernest Kempton Adams Fund for Physical Research of Columbia University.

particle. This theory gives a satisfactory description of the influence of the impacts for which the minimum distance b between the electron and the passing particle is larger than the atomic dimensions. Quantum mechanical corrections have to be introduced for the very close impacts, when the particle passes through the atom.

Both in the classical and in the quantum mechanical theories the action on every atom has been discussed so far by neglecting the perturbation of the field of the passing particle arising from the electric polarization of the surrounding atoms. A detailed analysis shows however that in some cases these polarization effects are very important [1].

The influence of the polarization has been calculated in the present paper on the basis of the classical theory. This may be expected to give correct results for at least that part of the energy loss which is due to collisions at distances b greater than the atomic radius.

THEORY.

The field of a charged particle moving through a medium having dielectric properties is affected by the polarization of the medium. We shall first calculate the field by applying classical electrodynamics. The amount of energy lost by the particle at distances greater than a certain minimum distance b from the path of the particle will then be calculated as flux of the Poynting vector across a cylindrical surface of radius b having the path of the particles as axis. We may reasonably hope to get in this way a correct estimate of the losses due to the atoms for which b is somewhat larger than the interatomic distances. Indeed we might then expect the quantum mechanical correction not to be very important: moreover a description of the dielectric properties of the medium with a continuum theory is permissible.

We write the Maxwell equations in the usual form:

$$\operatorname{div}(\mathbf{E} + 4\pi\mathbf{P}) = 4\pi\rho, \tag{1}$$

$$\operatorname{div}\mathbf{H} = 0, \tag{2}$$

$$c\operatorname{rot}\mathbf{E} = -\dot{\mathbf{H}}, \tag{3}$$

$$c\operatorname{rot}\mathbf{H} = \dot{\mathbf{E}} + 4\pi\dot{\mathbf{P}} + 4\pi\rho\mathbf{V}, \tag{4}$$

where $\mathbf{E}$, $\mathbf{H}$, $\mathbf{P}$, ρ, $\mathbf{V}$ are, respectively, the eletric and magnetic field strength, the electric polarization vector, the density and velocity of the electric charges. The magnetic polarization of the medium has been neglected.

The relationship between $\mathbf{E}$ and $\mathbf{P}$ can be simply expressed on the assumption that the electrons are elastically bound to equilibrium positions and are furthermore subjected to a friction force. It is then:

$$\mathbf{E} = \frac{m}{ne^2}(\ddot{\mathbf{P}} + 2p\dot{\mathbf{P}} + \nu_0^2\mathbf{P}). \tag{5}$$

(1) The possibility that a screening effect due to the polarization of the medium might reduce the ionization loss was suggested by W. F. G. SWANN, « Jour. Franklin Inst. », *226*, 598 (1938).

where m, e, n, are the mass, the charge and the number of electrons per unit volume; $\nu_0/2\pi$ is the frequency of the electronic oscillators when $E = 0$; $2p$ is the coefficient of the friction force.

Let $\mathbf{E}_\nu$ and $\mathbf{P}_\nu$ be the components of frequency $\nu/2\pi$ (with the time dependence: exp $(-i\nu t)$) in the harmonic analysis of $\mathbf{E}$ and $\mathbf{P}$: we have then:

$$\mathbf{E}_\nu = \frac{m}{ne^2}(\nu_0^2 - \nu^2 - 2ip\nu)\,\mathbf{P}_\nu . \tag{6}$$

In general we may assume between $\mathbf{E}_\nu$ and $\mathbf{P}_\nu$ a relationship of the type:

$$\mathbf{E}_\nu = 4\pi\gamma(\nu)\,\mathbf{P}_\nu \tag{7}$$

$\gamma(\nu)$ is in general a complex function of ν.

In the special case (5) that the dispersion law can be described in terms of one kind of dispersion oscillators only we have:

$$\gamma(\nu) = \frac{m}{4\pi ne^2}(\nu_0^2 - \nu^2 - 2ip\nu). \tag{8}$$

Our problem is to find the field produced by a concentrated charge e moving with the constant velocity v. We take the path of the particle as x axis and the position occupied by the particle at $t = 0$ as origin of the coordinates.

If we know the field at $t = 0$ we can obtain the field at any time by translating it with the uniform velocity v. This enables us to eliminate the time from the Maxwell equations by using the relationship:

$$\partial/\partial t = -v\partial/\partial x \tag{9}$$

Since at $t = 0$ the charge is at the origin we have further $\rho = e\delta(x)\,\delta(y)\,\delta(z)$; and the Maxwell equations become

$$\operatorname{div}(\mathbf{E} + 4\pi\mathbf{P}) = 4\pi e\delta(x)\,\delta(y)\,\delta(z), \tag{10}$$

$$\operatorname{div}\mathbf{H} = 0, \tag{11}$$

$$c\operatorname{rot}\mathbf{E} = v\mathbf{H}', \tag{12}$$

$$c(\operatorname{rot}\mathbf{H})_x = -vE_x' + 4\pi vP_x' + 4\pi ev\,\delta(x)\,\delta(y)\,\delta(z), \tag{13}$$

$$c(\operatorname{rot}\mathbf{H})_y = -vE_y - 4\pi vP_y' \quad ; \quad c(\operatorname{rot}\mathbf{H})_z = -vE_z' - 4\pi vP_z', \tag{14}$$

where a dash means the derivative with respect to x. Since the field moves with the uniform velocity v we may develop the field vectors in Fourier components with respect to x instead of t and interpret $\mathbf{E}_\nu$ and $\mathbf{P}_\nu$ in (7) as those components whose dependence on x is represented by factor exp $(i\nu x/v)$.

The integration of the equations (7) (10) (11) (12) (13) (14) with the boundary condition that the fields must vanish at infinite distance can be performed as follows. From (7) and (10) we first calculate div $\mathbf{P}$ and div $\mathbf{E}$ as:

$$\operatorname{div}\mathbf{P} = \frac{e}{2\pi v}\delta(y)\,\delta(z)\int_{-\infty}^{\infty}\frac{\exp(i\nu x/v)}{1+\gamma(\nu)}\,d\nu \quad ; \quad \operatorname{div}\mathbf{E} = \frac{2e}{v}\delta(y)\,\delta(x)\int_{-\infty}^{\infty}\frac{\gamma\exp(i\nu x/v)\,d\nu}{1+\gamma(\nu)} \tag{15}$$

we can then eliminate $\mathbf{H}$ from (13) and (14) in the usual way and eliminate also $\mathbf{E}$ with (7). Taking into account (15) we find an equation for each com-

ponent of **P**. Developing these components in Fourier integrals with respect to x one easily finds the solutions in terms of the Bessel functions K_0 and K_1

$$(16)\quad \begin{cases} P_x = -\dfrac{e}{4\pi^2 v^2}\displaystyle\int_{-\infty}^{\infty}\left(\frac{1}{1+\gamma}-\frac{v^2}{c^2\gamma}\right)K_0(kb)\exp(i\nu x/v)\,i\nu\,d\nu, \\ P_b = -\dfrac{e}{4\pi^2 v}\displaystyle\int_{-\infty}^{\infty}\frac{kK_1(kb)}{1+\gamma}\exp(i\nu x/v)\,d\nu, \end{cases}$$

where P_b is the component perpendicular to the x axis and

$$(17)\qquad k^2 = \frac{\nu^2}{v^2}\left(1-\frac{v^2}{c^2}\right)\frac{\nu^2}{c^2\gamma(\nu)}.$$

The sign of k is determined so as to have its real part ≥ 0. From (16) and (7) we obtain the components of the electric field

$$(18)\quad \begin{cases} E_x = -\dfrac{e}{\pi v^2}\displaystyle\int_{-\infty}^{\infty}\left(\frac{\gamma}{1+\gamma}-\frac{v^2}{c^2}\right)K_0(kb)\exp(i\nu x/v)\,i\nu\,d\nu, \\ E_y = -\dfrac{e}{\pi v}\displaystyle\int_{-\infty}^{\infty}\frac{\gamma k K_1(kb)}{1+\gamma}\exp(i\nu x/v)\,d\nu. \end{cases}$$

From these and (12) we finally obtain the magnetic field. This reduces to one component only, perpendicular to the x, b–plane. Its magnitude is given by

$$(19)\qquad H = \frac{e}{\pi c}\int_{-\infty}^{\infty} kK_1(kb)\exp(i\nu x/v)\,d\nu.$$

The amount of energy lost by the particle per unit time at distances larger than b is given by the flux of the Poynting vector out of a cylinder of radius b. Dividing this flux by v we obtain the corresponding loss of energy W_b per unit path. This is

$$(20)\qquad W_b = \frac{c}{4\pi v}\int_{\sigma}[\mathbf{E}\times\mathbf{H}]_n\,d\sigma = -\frac{cb}{2v}\int_{-\infty}^{\infty} HE_x\,dx.$$

We substitute in this expression (18) and (19) changing in the last the name of the integration variable to ν'. W_b is then expressed by a triple integral over x, ν, ν'. The integration over x gives a δ–function. This fact enables us to perform in the usual way also the integral over ν'. We find at last, taking into account $k(-\nu) = k^*(\nu)$

$$(21)\qquad W_b = \frac{e^2 b}{\pi v^2}\int_{-\infty}^{\infty}\left(\frac{\gamma}{1+\gamma}-\frac{v^2}{c^2}\right)i\nu k^* K_1(k^* b)K_0(kb)\,d\nu.$$

One easily recognizes that the integrand takes complex conjugate values for the values ν and $-\nu$ of the integration variable; we have therefore:

$$(22)\qquad W_b = \frac{2e^2 b}{\pi v^2}\,\mathrm{R}\int_{0}^{\infty}\left(\frac{\gamma}{1+\gamma}-\frac{v^2}{c^2}\right)i\nu k^* K_1(k^* b)K_0(kb)\,d\nu.$$

where we have indicated the real part of a by $\mathrm{R}a$

In order to calculate this integral we specialize our assumptions as to the dielectric properties of the medium by using (8). We find

$$W_b = \frac{8ne^4}{mv^2(\varepsilon-1)} \mathrm{R}\int_0^\infty \left(\frac{1-x^2-2i\eta x}{\varepsilon-x^2-2i\eta x} - \frac{v^2}{c^2}\right) ix\,dx\,k^*b\,\mathrm{K}_1(k^*b)\,\mathrm{K}_0(kb). \tag{23}$$

where

$$\varepsilon = 1 + \frac{4\pi ne^2}{m\nu_0^2} \tag{24}$$

is the dielectric constant for low frequencies [2]. We have further

$$\eta = p/\nu_0 \quad ; \quad x = \nu/\nu_0 \quad ; \quad k^2 = g^2x^2\frac{a-x^2-2i\eta x}{1-x^2-2i\eta x} \tag{25}$$

with

$$g^2 = \frac{4\pi ne^2}{mc^2(\varepsilon-1)}\left(\frac{c^2}{v^2}-1\right) \quad ; \quad a = \frac{c^2-v^2\varepsilon}{c^2-v^2}. \tag{26}$$

The integral (23) can be calculated when b is very small. In this case we may use for the Bessel functions the following expressions

$$\mathrm{K}_0(kb) = \frac{1}{2}\log\frac{4}{3.17\,k^2b^2} \quad ; \quad \mathrm{K}_1(k^*b) = \frac{1}{k^*b}, \tag{27}$$

in which $3.17 = \exp(2\times\text{Eulers constant})$.

(23) becomes now:

$$W_b = \frac{4ne^4}{mv^2(\varepsilon-1)} \mathrm{R}\int_0^\infty \left(\frac{1-x^2-2i\eta x}{\varepsilon-x^2-2i\eta x} - \frac{v^2}{c^2}\right) ix\,dx \log\frac{4(1-x^2-2i\eta x)}{3.17\,g^2b^2x^2(a-x^2-2i\eta x)}.$$

The integral can be reduced to the following integrals, that can easily be calculated by complex integration.

$$\mathrm{R}\int_0^\infty ix\,dx = 0 \quad ; \quad \mathrm{R}\int_0^\infty \frac{ix\,dx}{\varepsilon-x^2-2i\eta x} = -\frac{\pi}{2} \quad ; \quad \mathrm{R}\int_0^\infty ix\log x\,dx = 0;$$

$$\mathrm{R}\int_0^\infty \frac{ix\log x\,dx}{\varepsilon-x^2-2i\eta x} = -\frac{\pi}{4}\log\varepsilon - \frac{\pi}{2}\frac{\eta}{(\varepsilon-\eta^2)^{1/2}}\operatorname{artg}\frac{(\varepsilon-\eta^2)^{1/2}}{\eta};$$

$$\mathrm{R}\int_0^\infty \frac{ix\,dx}{\varepsilon-x^2-2i\eta x}\log\frac{a-x^2-2i\eta x}{1-x^2-2i\eta x}$$

$$= \begin{cases} 0 & \text{for } a > 0; \\ -\dfrac{\pi}{2}\log\dfrac{\varepsilon-a}{\varepsilon} + \dfrac{\pi\eta}{(\varepsilon-\eta^2)^{1/2}}\operatorname{artg}\dfrac{(\varepsilon-\eta^2)^{1/2}[(\eta^2-a)^{1/2}-\eta]}{\varepsilon-\eta^2+\eta(\eta^2-a)^{1/2}} & \text{for } a < 0; \end{cases}$$

$$\mathrm{R}\int_0^\infty ix\,dx\log\frac{a-x^2-2i\eta x}{1-x^2-2i\eta x} = \begin{cases} \frac{1}{2}\pi(1-a) & \text{for } a > 0; \\ \frac{1}{2}\pi(1-a) - \frac{1}{2}\pi[(\eta^2-a)^{1/2}-\eta]^2 & \text{for } a < 0. \end{cases}$$

(2) It should be noticed that ε is equal to the dielectric constant for small frequencies only when the description of the dielectric properties with dispersion oscillators of one frequency only is a sufficiently good approximation. When this is not the case ε might differ considerably from the actual value of the dielectric constant.

The integration path of these integrals is along the positive real axis. They can be calculated by deforming the integration path moving first from the origin in the positive imaginary direction to a very large distance from the origin and then coming back on the real axis along a quarter of a circle of very large radius with center in the origin and by taking proper account of the singularities. Notice further that only the real part of the above integrals is convergent. The divergence of the imaginary part has been introduced when we have used the approximate expressions (27) for the Bessel functions. This divergence is of course immaterial to us, since in our formulae only the real part of the integrals is used.

We obtain now:

$$(28)\qquad W_b = \frac{2\pi ne^4}{mv^2}\left\{\log\frac{mv^2}{3.17\,\pi ne^2 b^2} + \log\frac{\varepsilon-1}{\varepsilon(1-v^2/c^2)} - \frac{v^2}{c^2} - \frac{2\eta}{(\varepsilon-\eta^2)^{1/2}}\operatorname{artg}\frac{(\varepsilon-\eta^2)^{1/2}}{\eta}\right\} \qquad \text{for } v < \frac{c}{\sqrt{\varepsilon}}\,;$$

$$(29)\qquad W_b = \frac{2\pi ne^4}{mv^2}\left\{\log\frac{mv^2}{3.17\,\pi ne^2 b^2} - \frac{v^2}{c^2} + \frac{1-v^2/c^2}{\varepsilon-1}\left[\left(\eta^2+\frac{v^2\varepsilon-c^2}{c^2-v^2}\right)^{1/2}-\eta\right]^2 - \frac{2\eta}{(\varepsilon-\eta^2)^{1/2}}\operatorname{artg}\frac{(\varepsilon-\eta^2)^{1/2}}{\left(\eta^2+\frac{v^2\varepsilon-c^2}{c^2-v^2}\right)^{1/2}}\right\} \qquad \text{for } v > \frac{c}{\sqrt{\varepsilon}}\,.$$

When the damping is negligible ($\lim \eta = 0$) the above formulae become:

$$(30)\qquad W_b = \frac{2\pi ne^4}{mv^2}\left\{\log\frac{mv^2}{3.17\,\pi ne^2 b^2} + \log\frac{\varepsilon-1}{\varepsilon(1-v^2/c^2)} - \frac{v^2}{c^2}\right\} \qquad \text{for } v < \frac{c}{\sqrt{\varepsilon}}$$

$$(31)\qquad W_b = \frac{2\pi ne^4}{mv^2}\left\{\log\frac{mv^2}{3.17\,\pi ne^2 b^2} - \frac{1-v^2/c^2}{\varepsilon-1}\right\} \qquad \text{for } v > \frac{c}{\sqrt{\varepsilon}}\,.$$

These results should be compared with the corresponding energy loss calculated with the usual theory by neglecting the polarization effects:

$$(32)\qquad W_b \text{ (usual theory)} = \frac{2\pi ne^4}{mv^2}\left\{\log\frac{mv^2}{3.17\,\pi ne^2 b^2} + \log\frac{\varepsilon-1}{1-v^2/c^2} - \frac{v^2}{c^2}\right\}.$$

The comparison is shown in Fig. 1. The three curves represent the energy loss per unit path due to impacts at distances greater than 10^{-8} cm, measured taking $2\pi ne^4/mv^2$ as unit, according to the ordinary formula (32) and according to the present theory with formulae (30) and (31) for standard air and for water. In both cases the difference from the ordinary result is very small at low energies. For high energies, instead, the loss calculated with the ordinary theory keeps increasing logarithmically with increasing energy, whereas the effect of the polarization produces a flattening out of the curves for air and water in such a way that W_b remains finite even when the energy of the particle becomes infinite.

It can easily be seen from (28) and (29) that the limiting value of W_b for $v = c$ is independent on both the binding frequency ν_0 of the dispersion

oscillators and the damping constant n. It depends only on the number n of electrons per unit volume, and is given by:

$$W_b(v = c) = \frac{2\pi ne^4}{mc^2} \log \frac{mc^2}{3.17\,\pi ne^2 b^2} . \tag{33}$$

This shows that the energy loss of very high energy particles due to various materials in layers of such thicknesses as to contain always the same number of electrons per cm², is smaller for larger electronic densities n of the material (see on Fig. 1 the difference between air and water).

When the damping η of the dispersion oscillators is very small it is possible to calculate the integral (23) for arbitrary values of b by using the exact expressions for the Bessel functions instead of the approximate expressions (27). One finds:

$$W_b = \frac{2\pi ne^4}{mv^2}\left[-\frac{2\,b\nu_0\sqrt{\varepsilon}}{v} K_0\left(\frac{b\nu_0\sqrt{\varepsilon}}{v}\right) K_1\left(\frac{b\nu_0\sqrt{\varepsilon}}{v}\right) - \frac{v^2}{c^2} - \log\left(1 - \frac{v^2}{c^2}\right)\right] \tag{34}$$

for $v < c/\sqrt{\varepsilon}$;

$$W_b = \frac{2\pi ne^4}{mv^2}\left[\frac{2\,b\nu_0\sqrt{\varepsilon}}{v} K_0\left(\frac{b\nu_0\sqrt{\varepsilon}}{v}\right) K_1\left(\frac{b\nu_0\sqrt{\varepsilon}}{v}\right) - \frac{1 - v^2/c^2}{\varepsilon - 1} + \log\frac{\varepsilon}{\varepsilon - 1}\right] \tag{35}$$

for $v > c/\sqrt{\varepsilon}$.

For very small b these expressions go over into (30) and (31). It is interesting to note, however, that W_b in this case does not vanish, as one might expect, for very large b. Indeed it follows from (34) and (35) that for $b = \infty$ it is:

$$W_\infty = \frac{2\pi ne^4}{mv^2}\left[-\frac{v^2}{c^2} - \log\left(1 - \frac{v^2}{c^2}\right)\right] \qquad \text{for } v < c/\sqrt{\varepsilon}; \tag{36}$$

$$W_\infty = \frac{2\pi ne^4}{mv^2}\left[-\frac{1 - v^2/c^2}{\varepsilon - 1} + \log\frac{\varepsilon}{\varepsilon - 1}\right] \qquad \text{for } v > c/\sqrt{\varepsilon}. \tag{37}$$

W_∞ represents that part of the energy lost by the particle that is emitted in the form of radiation. Such an emission of radiation has actually been observed by Cerenkov [3], and can easily be seen to occur in those ranges of frequency for which the phase velocity of light in the given medium is smaller than the velocity of the particle. Its theory has been developed by Frank and Tamm [4] with methods very similar to those used here and with similar results. It is noteworthy that the Cerenkov radiation, as results from the preceding formulae, does not represent a loss of energy to be added to that calculated with the Bohr theory; but it forms instead part of the loss of the Bohr theory, as is seen from the fact that (30) (31), which include the Cerenkov radiation, give the same result (32) as the Bohr theory in the limit of very low densities ($\varepsilon = 1$) when the polarization effects become negligible.

We have considered so far only the phenomena occurring at distances greater than the interatomic distance, for which it is legitimate to apply the continuum electrodynamics. A description of the effects of impacts at

(3) P. CERENKOV, «Comptes rendus de l'Acad. Sci. U.R.S.S.», *14*, 101 (1937).
(4) I. FRANK and IG. TAMM, «Comptes rendus de l'Acad. Sci. U.R.S.S.», *14*, 109 (1937).

close distances requires a quantum mechanical description of the impact process as well as of the field of the passing particle and of its change due to the polarization of the other atoms. If we assume, however, that the effect of the polarization on the close distance impacts is not large we may use the ordinary theory, as developed by Bethe and Bloch for the calculation of the energy loss due to such impacts.

Under this assumption we may take the difference between the formulae (30) (31) of the present theory and formula (32) giving the result of the Bohr theory as the correction representing the polarization effects. We find thus that the energy loss per unit path is less than that given by the ordinary formulae by the following amount:

$$\frac{2\pi ne^4}{mv^2}\log\varepsilon \qquad \text{for } v < c/\sqrt{\varepsilon}\,; \tag{38}$$

$$\frac{2\pi ne^4}{mv^2}\left[\log\frac{\varepsilon-1}{1-v^2/c^2}+\frac{1-\varepsilon v^2/c^2}{\varepsilon-1}\right] \tag{39}$$

$$\text{for } v > c/\sqrt{\varepsilon}\,.$$

The correction is negligible for low velocities; for very large energies instead it reduces the energy loss to less than 50 percent of the loss calculated with the ordinary theory.

For very large energies we have from the ordinary theory the following energy loss:

$$\frac{2\pi ne^4}{mc^2}\log\frac{mc^2\,W}{(1-v^2/c^2)\,\hbar^2\nu_0^2}\,. \tag{40}$$

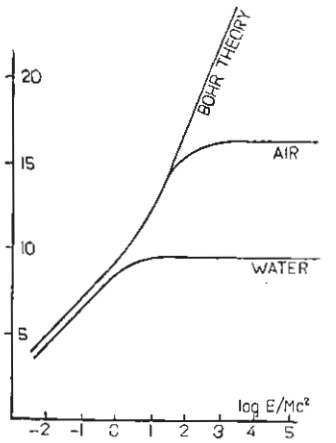

Fig. 1. – Energy loss per unit path due to impacts at distances greater than 10^{-8} cm. The curves marked air and water are calculated according to the present theory with formulae (30) and (31).

We obtain thus from (39) the following formula valid asymptotically for very large energies:

$$\frac{2\pi ne^4}{mc^2}\left[\log\frac{\pi m^2c^2\,W}{ne^2\hbar^2}-1\right]. \tag{41}$$

We note that this asymptotic formula does not contain the binding frequency of the electrons but only their number per unit volume.

Applications.

Only a very small polarization effect should be expected according to the present theory in the stopping power of different materials for α-particles, protons or deuterons having energies up to the order of magnitude of some Mev. In all these cases the velocity is rather small compared with c, so that we must use (38). This formula gives an entirely negligible correction in the case of air, since in this case E is very close to unity. Corrections of the order of several percent might be expected in the case of the stopping power in solid or liquids. It is doubtful whether such differences are large enough

to be observable. Moreover, when the velocity of the particle is small, as in the present case, the ionization produced by the particle does not reach far enough from the trajectory as to make the description of the field in terms of continuum electrodynamics a good approximation.

Greater effects are to be expected in the case of β–particles and especially for particles of several millions of ev. The correction for air is again negligible but an appreciable correction is found for condensed substances especially for high energy β–particles. The energy loss per cm of water calculated with the usual theories for β–particles of 10^6, 10^7, 10^8 ev is, respectively, 1.93, 2.15, 2.72 Mev. The correction (38) (39) reduces these losses to 1.83, 1.75, 1.94 Mev if we take $\varepsilon = 1.7$; since, however, the effective E may be as low as 1.1, the corrected energy losses may be 1.92, 1.91, 2.09 Mev. In spite of the fact that the differences are in some cases rather large, it is very difficult to compare these results with the available experimental material. Indeed the data for relatively low energies are largely affected by the scattering [5]; while those for large energies are perturbed by the radiation losses of energy.

The results for mesotrons are represented in fig. 2. The diagrams have been calculated for a rest energy of the mesotron of 80 Mev. The energy of the mesotron is plotted in a logarithmic scale on the abscissae; and the energy loss in units $2\pi ne^4/mv^2$ is plotted on the ordinates for standard air, water and lead. The curves A are calculated with Bloch's formula; the curves B are corrected for the polarization effects according to the present theory. It should be noticed that the incomplete knowledge of the dispersion law makes the shape of the curves B in the neighborhood of the point at which they begin to deviate appreciably from the corresponding curves A rather uncertain. For somewhat greater energies, instead, the curves B become practically independent of the dispersion law, being given by (41).

According to (41) the loss of energy in a layer containing N electrons per cm^2 depends on the electronic density n in the layer. For two layers having the same N and different electronic densities n_1 and n_2 the difference in energy loss is:

$$W_1 - W_2 = \frac{2\pi Ne^4}{mc^2} \log \frac{n_2}{n_1}, \tag{42}$$

the energy loss being smaller for the substance of greater density. (42) is valid only for rather large energies of the mesotron: for smaller energies the difference is considerably less, as can be seen on the curves of fig. 2, and it depends on the difference in atomic number between the different substances and not so much on the differences in density.

A difference in the absorption of mesotrons by air and by condensed substances in the sense that condensed substances have a smaller mass-absorption than air has been reported by several experimenters [6]. This difference is usually considered as evidence for a spontaneous decay of the mesotron. As the difference (42) is in the same sense as the experimentally

(5) M. M. SLAWSKY and H. R. CRANE, « Phys. Rev. », *56*, 1203 (1939).

(6) For a critical discussion of the literature on this subject see: B. ROSSI, « Rev. Mod. Phys. », *11*, 296 (1939).

observed differences, it is interesting to compare them quantitatively. Indeed if it were possible to prove that (42) accounts for all the difference observed experimentally, this would eliminate the strongest argument in favor of the decay of the mesotron.

The experiments on the difference in absorption have been performed using different techniques. In one type of experiment, as e.g. that of Ehmert [7], the absorption in thicknesses of air greater than the atmosphere is measured by inclining the counters by an angle θ with respect to the vertical, so that the thickness actually traversed by the rays is by a factor $1/\cos\theta$ greater than for the rays coming in a vertical direction. The absorption curve in air can be thus observed for thicknesses of air up to many atmospheres.

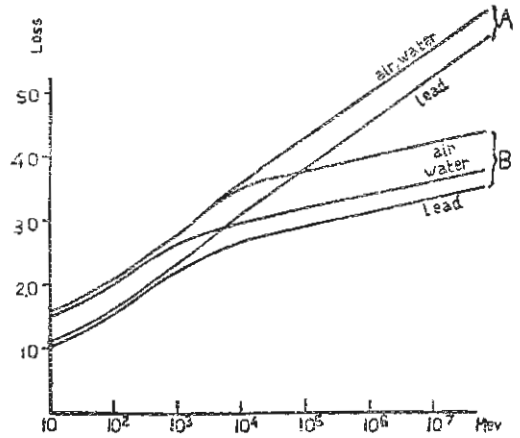

Fig. 2. – Energy loss in units of $2\pi ne^4/mv^2$ for mesotrons of various energies in air, water, and lead. Curves A are calculated with Bloch's formula and curves B are corrected for the polarization effects according to the present theory.

This absorption curve is compared with that obtained with the counters under water or under condensed materials. Experiments of this kind show that under large and equivalent thicknesses of air and of condensed materials the intensity of the mesotron component of the cosmic radiation is different. The intensity under condensed absorbers is about twice as large as under air.

In order to estimate what part of this difference can be accounted for by the present theory we take as average density of air along the path of the mesotron $1/e$ of the density at sea level, namely 0.00045, corresponding to an electronic density $n_{air} = 1.36 \times 10^{20}$. As a typical condensed substance we take water, for which the electronic density is $n_{water} = 3.35 \times 10^{23}$. According to (42) this corresponds to a difference of 0.60 Mev in the energy loss in one g/cm² of air and in a thickness of water containing the same number of electrons. For mesotrons of 10^4 Mev the energy loss is about 2.8 Mev × cm²/g. The loss in the equivalent amount of water is then only 2.2. The energies required for a mesotron to traverse a thick layer of air or an equivalent layer

(7) A. EHMERT, «Zeits. f. Physik», *106*, 751 (1937).

of water are therefore in the ratio $2.8/2.2 = 1.27$. Assuming the energy distribution of the mesotrons to be such that the number of mesotrons with energy greater than W is proportional to W^{-1} we conclude that the number of mesotrons observed under equivalent and very thick layers of condensed matter and of air should be in the ratio $1.27^{1.9} = 1.58$. The effect to be expected according to the present theory is therefore of the order of magnitude of the effect observed experimentally. The present theory, however does not appear sufficient to explain all the effect but only about one-half of it. If we interpret the residual effect as due to the decay of the mesotron the lifetime of this particle ought to be taken about twice as large as according to the usual estimates.

In a second type of experiment, like the one recently described by Rossi, Hilberry and Hoag [8], the vertical intensity of the mesotronic component of the cosmic radiation is measured at different heights with and without a graphite absorber; the absorptions in air and in graphite are thus directly compared. Graphite is used in order to eliminate as much as possible the effects due to the differences in atomic number. This arrangement has the advantage of being independent of the assumption that the primary radiation entering the atmosphere is isotropic. Furthermore the absorbers used are relatively thin (82 g/cm² graphite and 12.7 cm lead) and consequently the effect of a possible decay of the mesotron is measured for mesotrons of a relatively low energy, so that the apparent lengthening of the lifetime due to relativity effects is not very large. On the other hand, the observed absorptions are rather small (10 to 20 percent) and are therefore more sensitive to perturbations due to possible geometrical transition effects when the graphite is placed above the counters. Professor Rossi, however, informs me that he has very carefully excluded that his results might be considerably affected by such effects. Since this experiment involves mesotrons having energies of only a few hundreds of Mev the polarization effects discussed in this paper should affect its results only very little (see fig. 2). The effect observed in this experiment has therefore apparently to be attributed to a decay of the mesotron.

We notice finally that the estimates of the energy of the mesotrons penetrating to very great depths should be somewhat changed in order to take into account the polarization effects. For example the energy of mesotrons capable of traversing 1.5×10^5 g/cm² of matter should be reduced from 5.6×10^5 Mev to about 3.9×10^5 Mev.

(8) B. ROSSI, H. V. N. HILBERRY and J. B. HOAG, « Phys. Rev. », *56*, 837 (1939).

N° 135.

During the Spring of 1940 Fermi visited the University of California at Berkeley in order to give the Hitchcock Lectures there. At that time the phenomena of fission were paramount on his mind and I was also studying fission products. The new 60'' Crocker cyclotron had just started operation and had a beam of alpha particles. We decided to bombard uranium with alpha particles and observe the result. The following short paper describes what could be done at the time. The work was left essentially incomplete.

We did not discuss problems related to the chain reaction of uranium because of the secrecy involved.

During the same visit of Fermi to Berkeley we tried unsuccessfully to detect the density effect on the stopping power of a material for charged particles, discussed in paper N° 134.

E. SEGRÈ.

135.

FISSION OF URANIUM BY ALPHA-PARTICLES

E. FERMI and E. SEGRÈ
Department of Physics, Radiation Laboratory, University of California, Berkeley, California
« Phys. Rev. », *59*, 680–681, (1941) (Letter)
February 24, 1941.

Fission of uranium has been produced by neutrons, deuterons and gamma-rays. The 60'' cyclotron of the Crocker Radiation Laboratory with its 32-Mev alpha-particles afforded the possibility of trying to produce fission by alpha-bombardment of uranium.

A layer of ammonium uranate, a few millimeters thick was bombarded with a beam of several milliamperes intensity of 32-Mev alpha-particles for about one minute and was afterwards tested chemically for some of the characteristic fission products of uranium. The following were found: iodine (54 minutes), iodine (3.4 hours), I^{133} (22 hours), I^{131} (8 days). In some cases we found also tellurium members of the same chains.

In order to check that the activation was not due to secondary neutrons, both faces of the thick uranium target were tested. The face not directly exposed to the beam showed practically no activity. In order to rule out also the possibility of a deuteron contamination of the beam itself, it was checked that the ratio between the activity of 93^{239} and fission products was less, by order of magnitude, than the same ratio under deuteron bombardment. The 93 activity itself was possibily due to small residual deuteron contamination of the beam or to secondary neutrons.

We looked also for possible delayed fission by bringing the sample a few minutes after the end of the bombardment in front of an ionization chamber connected to a linear amplifier. No big kicks due to fission were observed.

The Gamow barrier for alpha-particles colliding with uranium is estimated to be almost 30 Mev. However, the transparency of the barrier for particles up to 4 or 5 Mev below the top of the barrier is still large enough to allow them to penetrate inside the nucleus with a large probability. If these estimates are correct, the formation of a compound nucleus by uranium and alpha-particles would have a large cross section even for energies somewhat below 25 Mev.

The excitation energy of the compound nucleus is less than the kinetic energy of the alpha-particle because at the top of the periodic system the process of emitting alpha-particles from the nucleus is exothermic. On account of this fact the excitation energy of the compound nucleus is probably from 5 to 10 Mev less than the kinetic energy of the alpha-particle. This leaves an excitation which may vary according to the energy of the primary particle from 15 to 27 Mev, and is therefore amply sufficient to produce the fission of the compound nucleus. Indeed it is so large that 2 or 3 neutrons may be evaporated, still leaving a sufficient energy available for the fission.

In conclusion, we wish to thank Professor E. O. Lawrence for his interest in this work, the Research Corporation for financial support and the Hitchcock Foundation for providing the opportunity for one of us to visit the Radiation Laboratory.

N° 136.

The results of the long calculations on the energy loss by ionization must have been somewhat disappointing to Fermi. They served to underline a remark he once made, that he could calculate almost anything to an accuracy of ten percent in less than a day, but to improve the accuracy by a factor of three might take him six months.

By the time this work was completed, Fermi decided that I had come far enough with my thesis research on the resonance capture of neutrons by uranium, so I wrote up my results and joined him again.

Szilard had been promoting the idea that the uranium research should be kept secret. The destructive possibilities of the chain reaction were very real to him. He was deeply concerned that the research would go forward more rapidly in Germany. If the Nazis had nuclear weapons in their hands before we did, world disaster seemed a certainty. It was very important that they should not know of our progress, or even of our interest. Szilard's earlier attempt to persuade Joliot and his group in France to withhold their results from publication failed, but now France was under the threat of the Nazi army. To set the pattern, of withholding papers from publication, at least in the Physical Review, Szilard needed a paper to withhold. For this, my thesis on the resonance absorption in uranium, already in the proof stage, would serve perfectly. A guarantee was given and a deposit of $ 75 made to the library of Columbia University by Dean G. B. Pegram. The ultimate publication of my thesis was thereby assured, and I was able to obtain my doctoral degree. Thereafter, those who submitted papers dealing with uranium research to the Physical Review could be asked to withhold them from publication by the editors. This was only necessary where the research had been conducted with private funds. The researches supported by government funds were written up in reports marked Secret and given limited circulation to a selected list of persons concerned.

At about this time Szilard's efforts to procure some graphite for a test of its neutron absorption properties began to bear fruit. Cartons of carefully wrapped graphite bricks began to arrive at the Pupin Physics Laboratory until one and one-half tons had come for the experiment. Fermi returned with enthusiasm to the quest for the way to make the chain reaction. This was the kind of physics he liked best. Together we stacked the graphite bricks into a neat pile. We cut narrow slots in some of the bricks for inserting the rhodium foil neutron detectors and were soon ready to take the measurements.

The rhodium foils were Fermi's favorite neutron detector. He had used them early in the Rome experiments. The radioactivity induced in rhodium by slow neutrons has a quite short half life: 44 seconds. This leaves very little time, after they have been irradiated, to get them under the Geiger counter for measurement. The Geiger counter was placed in Fermi's office, some distance down the hall from the laboratory in which the graphite pile had been built. This was done to keep the Geiger counter from being disturbed by the neutron source. A precise schedule was followed for each measurement. With the rhodium in place in the graphite, the source was inserted in its position and removed after one minute. To get the foil to the Geiger counter, set it in place under the Geiger tube, and close the lead shield in the allotted 20 seconds took some fast legwork. Stopwatch in hand he would always be ready to throw the switch of the counting device at the prescribed moment. Then, with obvious pleasure, he would follow the flashing lights of the scaling circuit, tapping his fingers on the bench in time with the clicking of the register. Such a display of the phenomenon of radioactivity never failed to delight him.

The results of the work had the greatest significance for the uranium project. Not only was it shown that the absorption of neutrons in graphite was small enough to make it the obvious choice of material for slowing down the neutrons, but also the basic theoretical techniques for describing the behavior of neutrons in such substances were set forth. The

slowing down process was described by means of a diffusion equation according to a theory which later became known as the "age theory" and enjoyed wide usage in the Uranium Project. The approach was one Fermi had already developed in his original work "Sul moto dei neutroni nelle sostanze idrogenate" (Paper N° 119). The case of graphite was actually simpler because the energy losses took place in smaller steps and because the scattering cross-section changed less rapidly than in the case of hydrogen. After the neutrons reached thermal energies, a second diffusion process began in which the neutrons continued to diffuse through the material until they either escaped, or were absorbed. The mathematical analysis following this point of view allowed the absorption cross section of graphite to be calculated from the exponential decrease in neutron intensity which was observed with increasing distance from the source. It was this method which was adopted to test all the subsequent batches of graphite which came in ever increasing numbers as the work proceeded.

This paper was reissued by the Metallurgical Laboratory as Report A–21 (CP), in August, 1943.

H. L. ANDERSON.

136.

PRODUCTION AND ABSORPTION OF SLOW NEUTRONS BY CARBON

H. L. ANDERSON and E. FERMI
Report A–21 (September 25, 1940).

The processes of slowing down of neutrons and of absorption of thermal neutrons in carbon have been investigated. The slowing down process is described as a diffusion of the neutrons and the corresponding diffusion constants are deduced from the experimental results. The diffusion of thermal neutrons that sets in after the slowing-down phase has also been studied in order to determine the capture cross section of carbon. This cross section for the graphite that we have used has been found to be 3×10^{-27} cm^2.

* * *

When fast neutrons are emitted by a source inside a slowing substance two essentially different diffusion processes take place. In the first, the fast neutrons collide many times with the nuclei of the substance, thereby losing energy until they reach thermal energy. After this the second diffusion process begins; the neutrons continue to diffuse through the material but without further loss of energy until they are finally absorbed. The length of the diffusion path in the slowing-down phase depends on the number of collisions required for reducing the initial energy of the neutron to thermal energy. The length of path during thermal diffussion depends on the absorption cross-section of the given material for thermal neutrons. We have investigated these two processes in graphite.

Before describing the experiments it will be convenient to write down a few relations which will be useful in the interpretation of the experiments.

Slowing down process.

On the assumption that the scattering of neutrons by carbon is elastic and spherically symmetrical in the center of gravity system it can easily be shown that if the energy before impact is E then the energy E′ after impact may take on with equal probability any of the values between the maximum E and a minimum $\frac{(A-1)^2}{(A+1)^2} E = 0.716\,E$, where $A = 12$ is the atomic weight of carbon. On the average the logarithmic decrement in the energy is given by the expression,

$$\mu = \overline{\log E/E'} = 1 - \frac{(1-\alpha)^2}{2\alpha} \log \frac{1+\alpha}{1-\alpha} = 0.158 \tag{1}$$

where $\alpha = 1/A$. It follows that a reduction in energy from 10^6 ev to 1 ev requires on the average about 87 collisions. The reduction to thermal energy would require instead some 110 collisions.

Consider a neutron having an initial energy E_0 inside an infinite mass of graphite. After a number N of impacts its energy is reduced to a value E_1. Let r be the distance between the initial and the final positions of this neutron. If we neglect the coherence in the directions of successive free paths and the dependence of the mean free path λ on the energy, we find for the average of r^2 the simple expression $\overline{r^2} = 2\lambda^2 N$. When those factors are taken into account it can be proved that:

$$\overline{r^2} = \frac{6}{(3-2\alpha)\mu} \int_{E_1}^{E_0} \lambda^2(E)\, dE/E = 13.4 \int_{E_1}^{E_0} \lambda^2(E)\, dE/E. \tag{2}$$

Owing to the uncertainties in the value of λ for fast neutrons this formula cannot be used for an exact calculation of $\overline{r^2}$.

If N is a large number the final position of the neutrons will have a Gaussian space distribution of the form

$$e^{-r^2/r_0^2}. \tag{3}$$

r_0 shall hereinafter be termed the *range* of the distribution. r_0^2 is related to $\overline{r^2}$ by the formula,

$$r_0^2 = \frac{2}{3}\overline{r^2}. \tag{4}$$

Actually, the distribution of the slow neutrons of a given resonance band around a point source of fast neutrons embedded in graphite will be only approximately Gaussian. Deviations may be expected because the neutrons emitted from the source are not initially homogeneous in energy and because the number N of collisions (about 87 for the rhodium band) is not sufficiently large.

We have studied the slowing down of neutrons emitted from a Rn + Be source to the energy of the resonance neutrons of rhodium (about 1 ev) and

of iodine (about 100 ev) by measuring at various positions the activity of rhodium and of iodine detectors, properly screened with cadmium so as to eliminate the thermal neutrons, in a mass of carbon. It would be desirable to use an amount of carbon large enough so that a fast neutron leaving the source cannot escape from the carbon before it has reached the resonance energy. Since the amount of carbon at our disposal (about 4 tons) was not sufficient for fulfilling this condition we arranged a number of graphite bricks in the form of a rectangular parallelepiped 91 × 91 × 245 cm³, as shown in fig. 1. The effect of the boundary may be neglected in the case of the largest dimension but not in the case of the smaller dimensions. The block of graphite was placed vertically in the center of a large room so as to minimize the effect

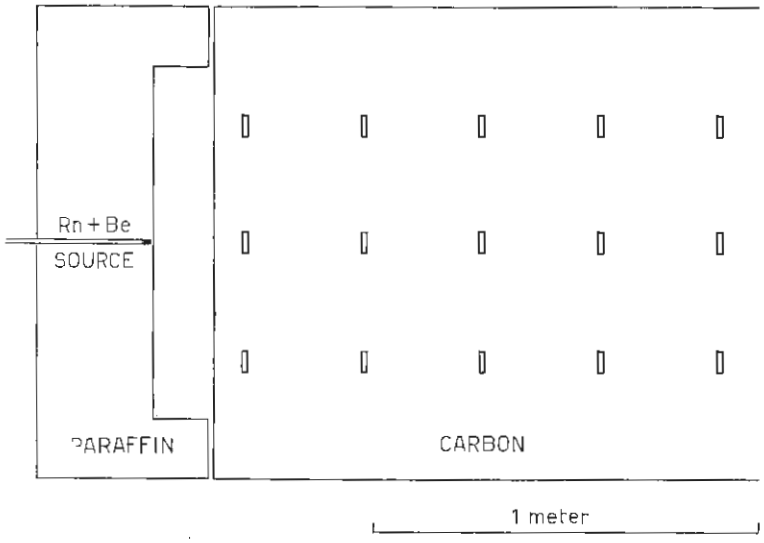

Fig. 1. – Arrangement for the measurement of the capture cross-section of carbon shown in section. The 15 slots for the detector are perpendicular to the plane of the figure.

of wall scattering. The source was placed in a fixed position inside the block while the detector was placed in various positions inside a vertical slot and its activity measured for each position. As detectors we used 5 × 5 cm² rhodium foils of thickness 0.126 gms/cm² and 6 cm diameter disks of PbI_2 of thickness 0.35 gms/cm². Taking a Cartesian set of axes with the z axis vertical, the x, y-plane passing through the source and the origin at one of the corners of a square cross-section of the parallelepiped, the source was at the position $x = 50.8$ cm, $y = 30.4$ cm and $z = 0$. The base of the parallelepiped was at $z = -91$ cm while the coordinates of the slot in which the detector was placed were $x = 40.6$ cm and $y = 45.7$ cm. The activity of the detector as a function of its z coordinate is given for Rh in Table I and for I in Table II. These results have also been plotted in fig. 2. The curves are only approximately Gaussian; the experimental points for large values of z lie considerably higher than the Gauss distribution adjusted to fit the initial points.

TABLE I.

Rhodium.

z (cm.)	Intensity
— 29.0	0.477
— 18.8	0.705
— 8.7	0.914
1.5	0.992
11.7	0.869
21.8	0.629
32.0	0.408
42,1	0.230
52.3	0.1162
62.5	0.0564
72.6	0.0273
82.8	0.0169
92.9	0.00778
103.1	0.00289

TABLE II.

Iodine.

z (cm.)	Intensity
— 20	0.602
0	1.000
20	0.584
40	0.189
60	0.0422
80	0.0081

Although the experimental results have been obtained with a very particular geometrical arrangement some general conclusions may be deduced from them. Let us assume that the slowing down process can be described as a diffusion process in which the neutron in slowing down to some definite value of energy undergoes a constant and large number N of impacts. The

process of slowing down may now be described by means of a diffusion equation

$$\Delta q = \frac{\partial q}{\partial t} \tag{5}$$

where q is the density of neutrons slowed down to a certain energy. t is a parameter dependent on the neutron energy having the dimensions of a length squared. t increases with decreasing energy and would be proportional to

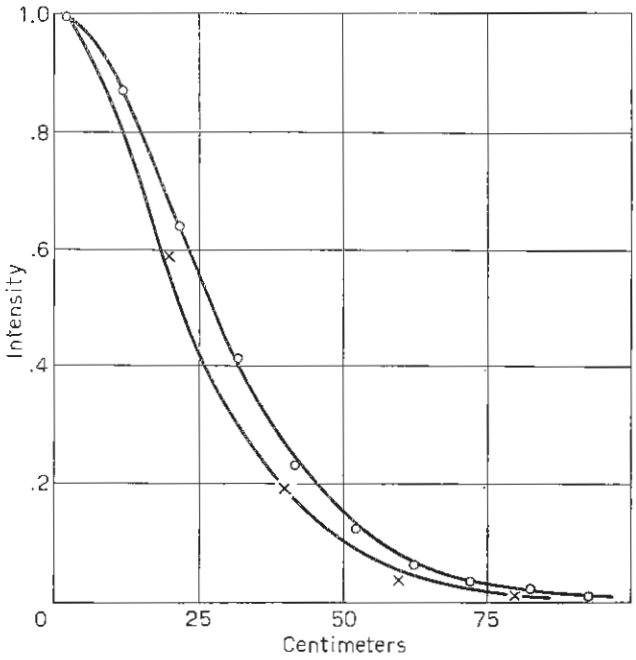

Fig. 2. – Intensity of rhodium resonance neutrons (o) and iodine resonance neutrons (x). The abscissae are the distances z of the detector from a horizontal plane through the source. The ordinates are the measured activations of a Rh and an I detector screened by cadmium. The curves are calculated with the formulae (11) and (12).

the number N of impacts required for slowing down the neutron to a given energy if λ were constant. The precise expression for t is,

$$t = \frac{13.4}{6} \int_{E}^{E_0} \lambda^2(E)\, dE/E. \tag{6}$$

This relationship may be found, for instance, by considering the case of a point source of neutrons inside an infinite mass of carbon. The solution of (5) for this case is,

$$\frac{1}{8\pi^{3/2} t^{3/2}} e^{-r^2/4t}.$$

The $\overline{r^2}$ corresponding to this distribution is $6t$ from which t may explicitly be related to the mean free path and the energy by means of (2). In terms of the range we have from (4),

$$r_0^2 = 4t. \tag{7}$$

With this definition of t the space distribution of neutrons of a given energy for our particular geometry may be derived by solving the diffusion equation (5) subject to the following boundary conditions: For $t = 0$, n is a δ–function at the position of the source. On the boundary of the carbon block $n = 0$. We may correct for the finite size of the mean free path by taking the boundary outside of the carbon block at a distance $\lambda/\sqrt{3}$ from its surface. For the case of a long rectangular parallelepiped the solution of (5) may be expressed in the form,

$$f(x, y, t)\, e^{-z^2/4t} \tag{8}$$

where $f(x, y, t)$ is a rapidly converging Fourier series of the arguments x and y which may readily be calculated given the dimensions of the base and the position of the source. It is seen that both the dependence of the distribution on z and the range of the distribution are independent of the size of the base and are the same as would be found for an infinite block.

We shall first interpret our results in terms of this simple theoretical description. The density of neutrons of a given resonance band is proportional to the activity of the corresponding detector suitably shielded with cadmium. We would expect the experimental points of Tables I and II to fit Gauss curves. Actually, only an approximate fit is obtainable. The rhodium curve may approximately be represented by a Gaussian function with a range r_0 (Rh) = 34 cm while for iodine r_0 (I) = 29 cm. The difference in the behavior between iodine and rhodium is due to the fact that the resonance energy of iodine lies above that of rhodium. The difference between the ranges for iodine and for rhodium makes possible a determination of the ratio of their resonance energies. From (2) and (4) taking λ as independent of the energy in this region, we have,

$$r_0^2(\mathrm{Rh}) - r_0^2(\mathrm{I}) = 20.6\, \lambda^2 \log_{10}(\mathrm{E_I}/\mathrm{E_{Rh}}). \tag{9}$$

Taking $\lambda = 2.55$ cm [1] for our graphite of density 1.63, this gives $\log_{10} \mathrm{E_I}/\mathrm{E_{Rh}} = 2.35$ and $\mathrm{E_I}/\mathrm{E_{Rh}} = 220$. This value is more than twice that obtained by the boron method (about 100). It should be pointed out that in our experiment the logarithm of the energy ratio is measured. A 20 % error in this logarithm, which would not be incompatible with our accuracy, would account for the difference.

From the distribution of neutrons in the rhodium band we may easily derive the distribution of those neutrons which have just reached thermal energies. Assuming a ratio of 40 between the rhodium resonance energy and thermal energy we obtain as in (9), r_0^2 (thermal) $- r_0^2$ (Rh) $= 20.6\, \lambda^2 \log_{10} 40$; r (thermal) = 37 cm. In this we have neglected the small chemical binding effect.

A more accurate phenomenological description of the slowing down process may be obtained on essentially similar lines by assuming two groups of neutrons diffusing with different ranges. Some justification for this assumption may be had by considering that some neutrons are slowed down to a

(1) H. B. HANSTEIN and J. R. DUNNING, « Phys. Rev. », *57*, 565 (1940).

given energy with fewer impacts, others with more impacts. An empirical description which represents quite accurately the experimental results is the following: For the distribution law for neutrons which have just become thermal in an infinite mass of carbon we superimpose two Gaussian groups:

$$q_{\text{th}} = 0.16\, e^{-r^2/29.9^2} + 0.84\, e^{-r^2/46.4^2} \tag{10}$$

The ranges for the rhodium and for the iodine neutrons are correspondingly smaller and can be calculated from the thermal ranges by proceeding as in (9). For rhodium the two ranges are 26 cm and 44 cm and for iodine 19.3 cm and 40.4 cm. Using these results and applying the differential equation (5) subject to the boundary conditions imposed by our geometry we obtain the distribution curves for rhodium:

$$0.5\, e^{-r^2/26^2} + 0.5\, e^{-r^2/44^2} \tag{11}$$

and for iodine

$$0.51\, e^{-r^2/19.3^2} + 0.49\, e^{-r^2/40.4^2}. \tag{12}$$

These have been plotted in Figure 1 and are seen to be in good agreement with the experimental points.

Absorption of thermal neutrons in carbon.

Once the neutrons have been reduced to thermal energy they keep on diffusing in the carbon without, on the average, any further change in energy. Provided the number of impacts is large this diffusion process may be described by means of the following differential equation,

$$n = \frac{\lambda^2 N}{3} \Delta n + \frac{\lambda N}{v} q \tag{13}$$

here n is the density of thermal neutrons, λ is the mean free path for scattering of thermal neutrons by carbon, N is the number of impacts by thermal neutrons before being captured $= \sigma_{\text{scatt}}/\sigma_{\text{cap}}$, v is the neutron velocity, and q is the number of thermal neutrons produced per cm^3 per second. By studying the distribution of thermal neutrons in a mass of carbon it is possible to obtain the coefficient $\lambda^2 N/3$ and since λ is known the capture cross-section is readily obtainable.

In our experiment we proceeded as follows. We arranged our graphite bricks in the form of a rectangular parallelepiped $122 \times 122 \times 152.5$ cm^3. The block was covered on all sides with cadmium sheet of 0.45 gms/cm^2 thickness. The cadmium could be removed from one of the square faces. Next to this face an arrangement of paraffin was constructed as shown in Figure 2 in the center of which was placed a Rn + Be source. Some 15 slots were cut in the carbon block to facilitate the introduction of a rhodium detector and the activity of this detector was measured for 45 positions both with and without the removable cadmium sheet.

The activity of the detector in the two cases is due in part to the resonance neutrons—and this part is obviously not affected by the cadmium—and the

remainder to the thermal neutrons. Taking the difference of the activity with and without the removable cadmium we get a result which is proportional to the difference $n_1 - n_2$ between the density of thermal neutrons in the two cases. n_1 and n_2 both obey the differential equation (13) and q is the same in both cases. Thus, the differential equation for $n_1 - n_2$ which is obtained by subtraction does not contain q. It is,

$$n_1 - n_2 = \frac{\lambda^2 N}{3} \Delta (n_1 - n_2). \tag{14}$$

The boundaries at which $n_1 - n_2 = 0$ are removed a distance $\lambda/\sqrt{3}$ from the actual surfaces of the carbon block. The integral of (14) subject to these boundary conditions is,

$$n = \sum_{j,k=1}^{\infty} A_{jk} \sin \frac{\pi j x}{a} \sin \frac{\pi k y}{a} \left[e^{-\alpha_{jk} z} - e^{-2\alpha_{jk} b} e^{\alpha_{jk} z} \right] \tag{15}$$

with

$$\alpha_{jk}^2 = \frac{3}{\lambda^2 N} + \frac{\pi^2}{a^2} (j^2 + k^2). \tag{16}$$

The origin of the coordinates is at one corner of the face nearest the source. This face is a square whose side a is greater than the actual side of the carbon block by $2\lambda/\sqrt{3}$. b is the length of the carbon block in the z direction increased by $\lambda/\sqrt{3}$. In our case we had $a = 123.4$ cm; $b = 153.9$ cm.

We need only evaluate one of the coefficients (e.g. the first, $j = k = l$) of a two-fold Fourier expansion of the intensity in a cross-section of the block. According to (15) this must vary as

$$e^{-\alpha_{11} z} - e^{-2\alpha_{11} b} e^{\alpha_{11} z}. \tag{17}$$

Since the second term represents a small correction which can easily be taken into account, we expect for this coefficient an exponential variation. The coefficient of this exponential is directly related to $\lambda^2 N/3$ by (16).

The first Fourier coefficient was determined by measuring with the rhodium detector the neutron density at 9 points over a cross-section and taking a suitable linear combination of these in order to minimize the influence of the other Fourier coefficients. Our geometry was such that the first harmonic was by far the most important. The effect of the other harmonics could perturb the result by only a negligible amount.

In figure 3 the observed values of the first Fourier coefficients are plotted logarithmically against z. A small correction has been applied to take into account the second term in (17) so that we would expect the experimental points to lie on a straight line. The dotted curve is the curve expected if there were no absorption and its slope is determined essentially by the dimensions of the graphite block. The solid curve has been drawn to fit as well as possible the experimental points. It corresponds to a cross-section for capture of 3×10^{-27} cm^2. This result is consistent with the upper limit of 10^{-26} cm^2 given by Frisch, Halban, and Koch [2].

(2) O. R. FRISCH, H. v. HALBAN and J. KOCH, « K. Danske Vidensk. Selsk. », *15*, No. 10 (1937).

It is clear that this result refers to the graphite which was actually used. Since the cross-section turns out to be exceedingly small, very small amounts of neutron absorbing materials might be, to some extent at least, responsible

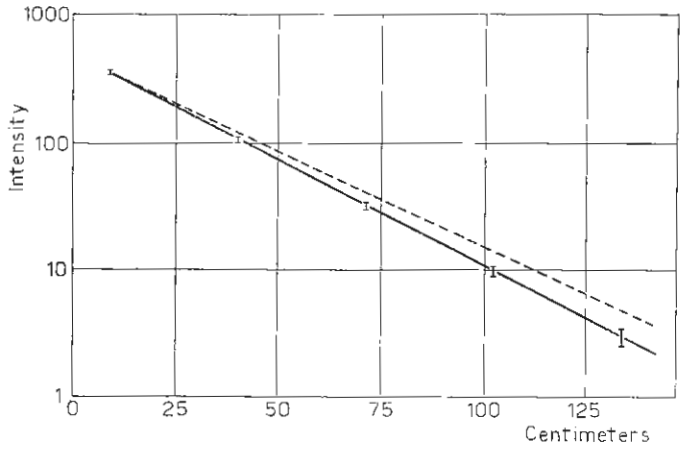

Fig. 3. – Logarithmic plot of $n_1 - n_2$ as a function of the distance from the face of the carbon block nearest to the source. The broken line would be expected in case of no absorption. The solid line corresponds to an absorption cross-section of 3×10^{-27} cm^2.

for this absorption. For instance, a content of water of less than one per cent could account for the observed absorption. We excluded the presence of an amount of water large enough to affect appreciably our result by comparing the weights of some of our graphite bricks before and after heating at 200°C for many hours. A small impurity which certainly accounts for part of the observed absorption is atmospheric nitrogen. Assuming that the gaps between the microcrystals in our graphite were filled with air, nitrogen would account for about one-tenth of the observed cross-section. If larger amounts of nitrogen were adsorbed the effect would be correspondingly larger.

N° 137.

After the success of the graphite measurements, there was an opportunity to study the fission process itself in some detail. Although a large number of radioactive series had been found among the fission products, most of the work had been confined to the identification and the genetic relationships of these radio-elements. Fermi always wanted to know the quantitative aspects of the relationships. In the present case he wanted to know what was the probability that when fission occurred in uranium, a given radioactive series would appear. This probability was called the branching ratio.

The work went forward along these lines, because an able radio-chemist, A. V. Grosse, had come to Columbia on a Guggenheim Fellowship in order to participate in the new work. It was Grosse's enthusiasm and buoyant personality, plus the fact that the cyclotron was working well, that made Fermi think that this research would be amusing as well as enlightening. Things worked out very well; Grosse devised the methods of radio-chemical separation, and these were carried out by Fermi and me. It amused Grosse to see the conversion of his physics colleagues into chemists. In watching us work it appeared as if I, who was supposed to be the assistant, was doing the supervising; Fermi himself was doing most of the hard work.

A great many ether separations were carried out. This involved boiling away fairly large quantities of ether. Fermi had none of the requisite patience of a good chemist and tried to speed this process beyond what was prudent. There would be an explosion, the ether would burst into flame, Fermi's eyebrows would be singed, but he wasn't deterred. Later, when the ether method became an important way to purify uranium, Fermi could give some cautionary advice.

The measurement of fission yields was later carried out in an extensive way by large groups of radio-chemists in the Metallurgical Laboratory, principally under the direction of N. Sugarman and C. D. Coryell. The following paper was the first quantitative work on this subject. There seemed no compelling reason to withhold this paper from publication.

H. L. ANDERSON.

Enrico Fermi was a rare combination of both an outstanding theoretical and an experimental physicist. In the universality of his genius he was also no mean chemist. It was fascinating to see Fermi *disappear* in dense fumes of sulfuric acid as he was carrying out some chemical separation in the corner room of the basement of the Pupin Laboratories in the very early days of the atomic energy project at Columbia University (1939). His voice could be clearly heard out of the " London fog " giving instructions as to what should be done next.

I had the privilege of working with Enrico Fermi and Herbert Anderson on a problem that interested all three of us, namely, what are the final chemical products of the fission of the uranium atom? The physicist refers to this problem as determining the probability that a given radioactive series is formed or what the branching ratio of a particular radioactive series is in the fission of U^{235}. The problem consisted usually of a quick chemical separation of a well-known fission product and the determination of its amount quantitatively, by making measurements in a Geiger counter in a well defined geometry.

Geiger counters were installed next to Fermi's desk in this office. The chemical separations were carried out a few rooms away at the end of a corridor. It was a common sight to see Herbert Anderson run " interference " for Enrico Fermi, opening the doors for Fermi who would be running close behind him, holding the radioactive preparation, usually a precipitate on a filter, in his hands. The filter was usually Scotch-taped into position in the warmed up Geiger counter within a few seconds after Fermi entered the room.

The amazing thing about Fermi's experimentation was his ability, by penetrating analysis, to always keep in mind the goal of his investigation, and to estimate, by intuition, approximate error possibilities so that his guess in many cases was better than other people's measurements. Because of these qualities his rate of progress in arriving at new results was the fastest I have ever seen.

A. V. GROSSE.

137.

BRANCHING RATIOS IN THE FISSION OF URANIUM (235) (*)

H. L. ANDERSON, E. FERMI, and A. V. GROSSE
Pupin Physics Laboratories, Columbia University, New York, New York
Received October 14, 1940
« Phys. Rev. », *59*, 52–56 (1941).

A survey has been made on the percentages of slow neutron-induced uranium fissions that give rise to the formation of various radioactive series. These percentages were obtained by measuring the numbers of β–disintegrations of a suitable member of the series after an irradiation under specified geometrical conditions and a quantitative chemical separation. The percentages found for the series thus far investigated vary from about 0.1 percent to 10 percent.

A large number of radioactive series found among the fission products of uranium have been reported. Thus far, however, the work has been confined mostly to the identification and the genetic relationships of the radio-elements which arise from uranium fission. The present work is part of a systematic attempt to determine in a quantitative way the probability that when uranium fission occurs a given radioactive series will appear. We shall call this probability the branching ratio of the radioactive series.

In Table I † are listed those radio-elements which have been found to date with indication, wherever possible, of their genetic relationships and atomic weights. In compiling this table we have relied mainly on the critical survey of Livingood and Seaborg (1), supplemented by data which have appeared subsequently. In Table I the fission fragments have been arranged in two groups; a light group having atomic weights in the range from 82 to 100 and a heavy group with weights ranging from 127 to 150. To date, 10 radioactive chains have been identified in the light group and 12 in the heavy group. Because of greater analytical ease we have concentrated our effort on the heavy group and have determined the branching ratios of 9 out of 12.

(*) Publication assisted by the Ernest Kempton Adams Fund for Physical Research of Columbia University.

† *Note added in proof.* — The 22–hour and the 6.6–hour iodines have now been assigned to atomic weights 133 and 135, respectively, by C. S. WU, « Phys. Rev. », *58*, 126 (1940).

(1) J. J. LIVINGOOD and G. T. SEABORG, « Rev. Mod. Phys. », *12*, 30 (1940).

TABLE I.

Radioactive series from uranium fission. S *indicates a stable isotope.*

HEAVY GROUP

	127	128	129	130	131	132	133	134	135	136	137	138	139	140	—	—	—	—	—	—	—
Sb 51	80 hr		4.2 hr												5 min	10 min	10 min				
Te 52	10 hr	S	70 min	S	25 min										77 hr	60 min	43 min	15 min			
I 53	S				8 day										24 hr	22 hr	54 min	6.6 hr			
Xe 54		S	S	S	S	S		S		S			30 sec.	short		5 day		9.4 hr	15 min		
Cs 55							S						6 min	40 sec.					32 min		
Ba 56				S		S		S	S	S	S	S	86 min	300 hr						14 min	1 min
La 57													S	40 hr						2.5 hr	18 min
% . . .	**0.18**		**0.34**		**1.6**								**6.4**	**8.4**	**5.2**	**7.6**	**12**	**9 (?)**			

LIGHT GROUP

	82	83	84	85	86	87	88	89	90	---	—	—	—	—	—	—
Br 35		2.3 hr								40 min	3.8 hr					
Kr 36	S	1.9 hr	S		S		3 hr	5 min								
		S														
Rb 37				S		S	18 min	15 min								
Sr 38			S		S	S	S	15 day				6 hr	7 min			
Y 39								S				3.3 hr				
Zr 40									S					17 hr	70 day	
Cb 41														75 min		
Mo 42																67 hr
— 43																6.6 hr
% . . .														**6.1**		

The sum of these heavy group fission series amounts to only about 50 percent, (see Table I) indicating that our present knowledge of fission fragments is still incomplete.

The presence of a variety of series may be interpreted by assuming that the original splitting may take place into different fragments. The emission of one or more neutrons further increases the number of possibilities. If no neutrons were emitted the sum of the weights of the two fragments ought to be equal to 236, in the case of fission produced by slow neutrons in U^{235}. If neutrons are emitted this sum is correspondingly less. Since, presumably, the same number of neutrons is not always emitted, we need not expect that when a given series in the heavy group occurs it will always be accompanied by the same series in the light group. Very little information is available as to the relative probability of the formation of the various fission products. We have, therefore, undertaken a study of these probabilities. Since we shall be unable to continue this research for some months because of the rebuilding of the Columbia cyclotron now in progress, it was thought worth while to report on the results obtained thus far.

Experimental method.

In each measurement we irradiated a solution containing 50 grams of uranium element inside a paraffin block placed in a fixed position near the cyclotron. Usually, uranyl nitrate was used, but the sulphate was employed for the antimony determination. Neutrons were produced in the cyclotron by the bombardment of Be with 6-Mev protons. These neutrons have an energy up to about 2 Mev and our geometrical arrangement was such that practically only slow neutrons were effective in producing fission. Our results, therefore, refer to the fission of U^{235}. The intensity of irradiation was monitored by means of a gold foil placed in a fixed position inside the paraffin block. The activity of the gold foil was compared to that of a standard uranium plaque by means of an ionization chamber. In a few cases a Rn + Be source was used for the irradiation instead of the cyclotron.

For the investigation of each element a known amount of the element in a suitable chemical form was added as a carrier to the uranium solution, together with smaller quantities of all other known fission products. The desired element was subsequently purified and separated. A weighed fraction of the added amount was painted on a thin aluminum strip, covered with Scotch cellulose tape and wrapped around a thin walled silvered-glass counter [2]. The strip was held by means of a suitable aluminum container so as to insure the reproducibility of its disposition relative to the counter. Taking into account the absorption of the β-rays, the geometrical efficiency of the counting arrangement, and the finite time of irradiation, as explained below, the number of β-disintegrations per second at saturation of the element in question

(2) Made by Eck and Krebs, New York City.

was obtained. The branching ratio, i.e., the fraction of fissions giving rise to a particular radioactive series, was calculated from the formula,

$$R = I\eta/gf\,MFN.$$

I is the observed initial activity of the preparation measured in counts per minute; f is the ratio of the weights of carrier element used for the activity measurement to that added to the irradiated solution; M is the intensity of irradiation as measured in arbitrary units with the gold monitor; F is the fraction of saturation of the activity in question accumulated during the time of irradiation; η is the correction factor for the absorption of the β–rays. For its determination an aluminum cylinder of thickness 0.043 g/cm², equivalent to the combined thickness of the counter wall and the Scotch tape, was inserted between the sample and the counter. If an exponential law of β–ray absorption is assumed, η is the ratio of the measured activity without the aluminum to that with it. Values of η are given in Table II. The thickness of the counter wall was found by comparing, with a second counter as detector, the absorption for β–rays of radium E of the counter used with an aluminum cylinder of known thickness under the same geometrical conditions. In this way the thickness of the counter wall was found to be equivalent to 0.029 g/cm² of aluminum. The Scotch tape had a thickness equivalent to 0.012 g/cm². A small increment was added to take into account the absorption in the average sample measured.

TABLE II.

Absorption factors η for 0.043 g/cm² of aluminum.

ELEMENT	HALF–LIFE	η	ELEMENT	HALF–LIFE	η
$_{51}Sb^{129}$	4.2 hr	1.67	$_{53}I$	22 hr	1.85
$_{52}Te^{129}$	70 min	1.81	$_{53}I^{131}$	8 days	4.9
$_{51}Sb^{127}$	80 hr	1.61	$_{56}Ba^{139}$	86 min	1.26
$_{52}Te^{127}$	10 hr	1.66	$_{56}Ba^{140}$	300 hr	1.52
$_{53}I$	54 min	1.60	$_{57}La^{140}$	36 hr	
$_{53}I$	2.4 hr	1.60	$_{40}Zr$	17.2 hr	1.39
$_{53}I$	6.6 hr	1.0	$_{41}Cb$	75 min	

The symbol g is the geometrical efficiency of the counting arrangement. It was determined by measuring in our standard way the β–activity of a weighed amount of U_3O_8 and was found to be 1/3. Differences in this efficiency caused by possible differences in the back-scattering of the various β–rays were neglected. The measurement of g was repeated several times with varying amounts of U_3O_8 and was found to give the same result to within a few percent.

N is the number of fissions per minute taking place in the uranium solution for unit intensity of irradiation. In order to determine N we proceeded in the following way: In place of the uranium solution we used 140 cc of a solution of $MnSO_4$. In order to alter the distribution of neutrons as little as possible the concentration of this solution was adjusted so that the number of neutron captures per second would be roughly the same as in the uranium case. The activity of a known fraction of these manganese atoms was then determined with the counter in our standard way. The number of fissions per uranium atom is equal to the number of disintegrations per manganese atom times the ratio of the fission cross section of uranium to the capture cross section of manganese for thermal neutrons. We found that for unit intensity of irradiation 960,000 fissions took place in our uranium solution per minute.

On the assumption that a series of radio-elements has no branchings we chose for each radioactive series one convenient radio-element for determining the percentage of fissions of the series. The chemical elements investigated were I, Sb, Ba and Zr. The series investigated are those of Table I for which the percentages are given.

Iodine.

Iodine was separated by the following method: A standard solution of 5 KI + 1 KIO_3 was added to the uranium solution and acidified with dilute H_2SO_4 to free all of the iodine. The free iodine was then steam distilled into a flask containing water and converted into iodide ion by titrating with $NaHSO_3$; the iodine was then precipitated as either PdI_2 or AgI.

Originally, our practice was to paint PdI_2 precipitated in the presence of Br ion on the aluminum strip. Since on several occasions the PdI_2 reacted with the aluminum with some loss of iodine, these measurements could be relied on for giving only relative branching ratios of the various iodine isotopes. For absolute determinations we used a precipitate of AgI. Bromine is not separated in this case, but since the bromine products are short-lived the determinations could be made on the longer-lived iodines. For these last measurements we used a Rn + Be source.

Separation of iodine has permitted us to investigate the following series [3],

(1) Te^{131} (30 min) or (30 hr) → I^{131} (8 day),

(2) Sb (10 min) → Te (60 min) → I (22 hr) → Xe (5 day),

(3) Te (~ 15 min) → I (6.6 hr) → Xe (9.4 hr),

(4) Sb (5 min) → Te (77 hr) → I (2.4 hr),

(5) Sb (< 10 min) → Te (43 min) → I (54 min).

In one experiment iodine was separated 24 hours after the end of a 7-hour irradiation. The decay curve was readily analyzed into an 8-day

(3) P. H. Abelson, « Phys. Rev. », *56*, 1 (1939).

and a 22–hour activity; no evidence for the presence of the 5–day Xe could be found and it was assumed that this gas escaped from the sample during measurement.

We were able to determine that the 8–day iodine arises principally from the 30–minute rather than the 30–hour isomer of tellurium. This was done by irradiating for 2 hours and separating the iodine after 22 hours and again after 89 hours. If the 8–day iodine arose from the 30–hour tellurium the ratio of its activity from the second separation to that from the first would be 1.1. If instead, it arose from the 30–minute tellurium this ratio would be zero. A ratio of 0.1 was found which indicates that the 8–day iodine arises principally from the 30–minute tellurium.

The branching ratio of the 2.4–hour activity was obtained as follows. The parent substance of this radio-element has a much longer life (77 hours) than the parent elements of all other radio-iodines produced in the fission. It follows that the 2.4–hour radio-iodine is the only radio-iodine which can be regenerated in an irradiated uranium solution from which iodine has been removed once one or two days after irradiation. We therefore irradiated a solution and after about one day performed a first iodine separation. The collected iodine has a decay curve in which all the following periods were represented: 8 days, 2.4 hours, 66 hours and 22 hours. The solution was then allowed to stand for about one more day; the 7–hour tellurium, which was still present in the solution, reproduced during this time the 2.4–hour iodine; a second iodine separation collected, therefore, the 2.4–hour iodine almost pure.

The activity of the 54–minute iodine could easily be distinguished from all other activities because of the large difference in period from the other activities and the fact that a separation of iodine soon after a short irradiation yields this activity with a much greater intensity than any other.

We were, however, not able to get a very convincing decay curve of the 6.6–hour iodine, perhaps because the daughter substance (9.4–hour Xe) was occluded only in part in our sample. The corresponding branching ratio given in the table is somewhat doubtful. The branching ratios in the case of the 22–hour and the 2.4–hour iodines were measured using AgI precipitation. The branching ratios of the other isotopes were obtained by analyzing decay curves of PdI_2 precipitations and comparing initial activities of the 22–hour and 2.4–hour activities with the others. Irradiations of various lengths of time gave reasonably consistent results.

Antimony.

Antimony and some tellurium were added to the uranium sulphate solution in the form of a solution of $SbCl_3$ in 50–percent H_2SO_4 and reduced with granulated zinc and sulphuric acid in a hydrogen generator to SbH_3, and absorbed in a $AgNO_3$ solution. The silver antimony precipitate was filtered, decomposed with concentrated HCl and antimony precipitated with H_2S from the solution in the usual way and weighted as Sb_2S_3 after drying in a stream of CO_2.

The activity of the Sb samples was analyzed in order to determine the branching ratios of the following series [3].

(1) $$Sb^{127}\ (80\ hr) \rightarrow Te^{127}\ (10\ hr) \rightarrow I^{127},$$

(2) $$Sb^{129}\ (4.2\ hr) \rightarrow Te^{129}\ (70\ min) \rightarrow I^{129}.$$

The decay curves show evidence of the growth of the two radio-telluriums (10 hours and 70 minutes) out of the chemically separated samples of antimony. The branching ratios of these two series are considerably smaller than any other found so far. This fact may perhaps be related to the circumstance that these series are at the low atomic weight end of the heavy group.

Barium.

This element was separated from the irradiated solution by first eliminating most of the $UO_2(NO_3)_2$ by ether extraction and precipitating Ba and Sr as sulphates in the aqueous extract. These sulphates were melted with $KNaCO_3$ in the presence of the oxides of Te, Mo and Cb, the washed carbonates dissolved in dilute HCl and precipitated, in the presence of Th (to eliminate UX), for a second time as sulphates. After converting these to carbonates Ba was separated from Sr as $BaCrO_4$ in acetic acid solution and reconverted into $BaSO_4$.

From the activity of the barium samples we determined the branching ratios of the two series [4]:

(1) $$Xe^{139}\ (< 30\ s) \rightarrow Cs^{139}\ (6\ min) \rightarrow Ba^{139}\ (86\ min) \rightarrow La^{139},$$

(2) $$Xe\ (short) \rightarrow Cs\ (40\ s\ ?) \rightarrow Ba\ (300\ hr) \rightarrow La\ (40\ hr).$$

A first barium sample was separated from a uranium solution irradiated for many hours. Special care was taken to purify the sample as thoroughly as possible from UX contamination. Since this purification process took several days only the 300-hour activity was found in the decay curve. Actually, the lifetime appeared from our measurements to be somewhat longer. The first part of the decay curve shows evidence of the growth of the 40–hour lanthanum. This growth was, however, not sufficiently intensive for a reliable separate determination of the absorption factors of Ba and La. In determining the branching ratio we used the average absorption factor of the complex radiation of Ba and La. This procedure may of course introduce some additional error into this determination.

The activity of the 86–minute barium was measured on a $BaCrO_4$ sample separated from a uranium solution irradiated about one hour. Because of the short time available for the purification an appreciable UX background was observed in this sample. The 86–minute activity was, however, much more intensive and could be analyzed without difficulty.

(4) O. Hahn and F. Strassmann, « Naturwiss. », *27*, 529 (1939); G. N. Glasoe and J. Steigman, « Phys. Rev. », *58*, 1 (1940).

Zirconium.

For the chemical separation of zirconium the U solution was acidified with concentrated HCl to about 25 percent, the Zr precipitated as a phosphate and the ZrP_2O_7 purified as previously described [5] and finally converted into ZrO_2.

The chain investigated was:

$$Zr\ (17.2\ hr.) \rightarrow Cb\ (75\ min).$$

A zirconium oxide sample separated from a solution irradiated about two hours was measured. The decay curve showed an initial rise caused by the growth of the 75–minute columbium and then a decay with the 17.2–hour period of zirconium. A rather small background, presumably caused by a long-living zirconium was also observed. We were unable to separate the two absorption factors of 17.2–hour zirconium and 75–minute columbium from these curves and we used, therefore, an average absorption coefficient. Two irradiations, one of 2 hours and another of 10 hours, gave, in good agreement, 5.9 and 6.3 for the branching percentages.

Assuming that one radioactive fragment in the light group and one radioactive fragment in the heavy group are produced in each fission, we would expect the sum of the branching percentages to be 100 for each of the two groups. The percentages for the nine series analyzed in the heavy group add to about 50. Apart from possible errors, especially in the determination of the number of fissions, this low result is partly caused by incomplete analysis (9 out of 12) of the known series and probably also by series not yet discovered.

In conclusion the authors wish to express their indebtedness to the Research Corporation for financial aid. One of us (AVG) is also indebted to the John Simon Guggenheim Memorial Foundation for the grant of a fellowship.

(5) A. V. Grosse and E. T. Booth, « Phys. Rev. », *57*, 664 (1940).

N° 138.

The advantages of graphite as a means to slow down neutrons became apparent after the experiment which used a pile of graphite to measure the absorption of carbon. In such a pile of graphite, the neutrons were slowed down more slowly than in water, but once they reached thermal energies the neutrons would diffuse longer and reach greater distances from the source. A physical separation of the thermal neutrons from higher energy neutrons could be obtained and Fermi saw many ways to use this to advantage.

The graphite column was rebuilt. It was provided with a gap in which a layer of uranium could be inserted. With a radon + beryllium source placed inside the column some 70 centimeters below the gap, the neutrons in the neighborhood of the gap were almost entirely at thermal energies. A large fraction of these were absorbed when uranium was inserted in the gap. The neutrons emitted by the uranium could now be distinguished easily from those originating from the source. A fourfold increase in the resonance activity of indium in the neighborhood of the uranium showed clearly the production of neutrons by the uranium.

Another advantage of using graphite came because the slowing down and diffusion of neutrons could be calculated in a much more reliable way than in the case of either water or paraffin. Thus it became possible to measure the most important property of uranium for the chain reaction, the average number of neutrons produced per thermal neutron absorbed. This quantity, which he called η, was found to have the value 1.73, as reported in the following paper. This augured well for the chain reaction, and further work was pushed forward, with increasing interest. A later repetition under improved conditions brought the number down to 1.29 (see paper N° 163).

This and the previous paper are interesting in that the nomenclature and notations used in them for the first time found wide acceptance in the further work on the slowing down of neutrons and in their reproduction by uranium.

This paper was reissued by the Metallurgical Laboratory as Report CP–6, in August, 1943.

H. L. ANDERSON.

138.

PRODUCTION OF NEUTRONS BY URANIUM

H. L. ANDERSON and E. FERMI
Columbia University, New York, New York
Report A–6 (January 17, 1941).

The average number η of neutrons produced by uranium upon the capture of a thermal neutron was determined by using a column of graphite for slowing down the neutrons. The column was provided with a gap in which a layer of uranium oxide could be inserted. A Rn + Be source was placed inside the column on its axis 70 cm below the gap. With this arrangement the production of neutrons by uranium was clearly demostrated by a fourfold increase of the resonance activity of indium in the neighborhood of the gap with the uranium in place. In *Section I* a study is made of the slowing down and of the thermal diffusion of neutrons in graphite. In *Section II* measurements of the distribution of indium resonance neutrons with and without uranium in the gap are analyzed to obtain the

number of neutrons produced per second by the uranium. In *Section III* measurements of the distribution of thermal neutrons with and without uranium are analyzed to give the number of thermal neutrons captured per second by uranium. From these numbers η is found to be 1.73.

This paper is a report of an experimental investigation to determine the average number of neutrons produced by uranium upon the capture of a thermal neutron. This number, which we shall denote by η, differs from the number of neutrons produced per fission because a fraction of the thermal neutrons captured by uranium gives rise to U^{239}. For a discussion of chain reactions produced with unseparated uranium isotopes it is the number η rather than the number per fission which is of immediate importance.

The previous attempts [1] to measure η have not been entirely satisfactory because the neutrons produced by uranium were measured as a small difference between the total number of neutrons present with and without uranium in the neighborhood of a primary source of neutrons. Furthermore, a considerable uncertainty was due to the difficulty of estimating the number of neutrons absorbed while being slowed down across the resonance band of uranium. In the present experiments these difficulties were minimized by using carbon instead of water for slowing down the neutrons. This has the advantage of making possible a much more complete separation of the thermal neutrons from those of higher energy. Indeed, in a tall column of graphite of square cross-section three feet on a side, the intensity of indium resonance neutrons (energy about 1 ev) at a distance of 70 centimeters from a Rn + Be source is already quite small while the intensity of thermal neutrons is still rather large. A layer of uranium placed at this position absorbs from the primary source practically only the thermal neutrons. An indium detector screened with cadmium, which is insensitive to the thermal neutrons, placed in the neighborhood of the uranium is very little affected by the primary neutrons produced by the Rn + Be source. The response to the secondary neutrons produced by the uranium, however, can be clearly distinguished and may be as large as four times that due to the primary neutrons.

The use of carbon has the further advantage that the diffusion of the neutrons may be calculated in a much more reliable way than in the case of either water or paraffin. This makes possible a complete analysis of the activity curves taken under various conditions and thereby permits a separate identification of those factors which enter into the experiment.

Section I: The slowing down and diffusion of neutrons in graphite.

In a previous report, " Production and Absorption of Slow Neutrons by Carbon ", (hereafter to be referred to as I) we described experiments on

(1) H. Halban, F. Joliot, and L. Kowarski, « Nature », *143*, 470, 680 and 939 (1939). H. L. Anderson, E. Fermi, and L. Szilard, « Phys. Rev. », *56*, 284 (1939). [Paper N° 132. (Editor note)].

the slowing down of neutrons in graphite. In the present experiments we required a more detailed analysis of this process as well as of the diffusion of thermal neutrons taking place after the energy of the neutrons had been reduced to thermal values. Accordingly, some technical improvements were introduced to allow for a more accurate placement of the detectors; indium instead of rhodium detectors were used to permit more precise measurements, especially of the weaker points; and a closer mathematical description along the same general lines as in I was used in analysing the slowing down process. In addition, the measurements were extended to include the distribution of thermal neutrons in the graphite column.

The neutrons from a Rn + Be source were slowed down inside a column of graphite bricks (density 1.63 gms/cm^3). The base of the column was 3 × 3 feet and the height was 8 feet. The Rn + Be source was placed inside the column on its axis about 3 feet above the base. The detectors (indium foils 4×6.4 cm^2 and of thickness 0.094 gms/cm^2) were inserted in slots at various heights above the source as shown in fig. 1. (The gap shown in the figure was introduced only in experiments to be described later in sections II and III). The activity of the 54-minute period of indium was measured with a counter. The counting was started 3 minutes after the end of the irradiation in order to allow the 13-second period to decay. No perturbation due to other activities of indium could be detected.

The results of measurements made without the gap are tabulated in Table I. *Column 1* gives a conventional notation for the position of the detector. The position 0 is the place where, in later experiments, the dural frame shown in fig. 1 was inserted. The spacing between two consecutive numbers in this notation corresponds to a distance between detector positions of 4 inches. The center of the source was placed on the axis of the column 1/4 inch below the plane at –7. *Column 2* gives the distance z in centimeters between the horizontal plane of the source and the various detector positions. A small correction of 0.6 cm must be applied in the case of measurements of the resonance neutrons to take into account the self-absorption of our indium detectors. In *Column 3* the effective values of z taking this correction into account are tabulated. Two series of measurements were taken; in one (Cd In Cd) the detector was covered on both sides with cadmium (thickness 0.9 gms/cm^2) to eliminate the thermal neutrons and in the second (Ni In Ni) the detector was covered with nickel foils having a negligible absorption for neutrons of all energies. The measured activities are given in *Columns 4 and 6*, respectively. The usual procedure for obtaining the activity due to thermal neutrons would be to subtract Column 4 from Column 6. This is not quite correct, however, because the absorption by cadmium of the indium resonance neutrons is neglected. For the cadmium thickness used this absorption was corrected for by multiplying Column 4 by 1.15 before subtracting it from Column 6. A further small correction has been applied in order to take into account the scattering of thermal neutrons by the walls of the room. This correction is appreciable only for points far from the source where it amounts to 0.063. The correction would be somewhat greater for points near the source. Since, however, the correction is unimportant near the source we have not taken

into account its variation and have subtracted 0.063 for all the points. In *Column 7* the experimental thermal neutron activity taking these corrections into account is tabulated. Finally, *Columns 5 and 9* give the values of the

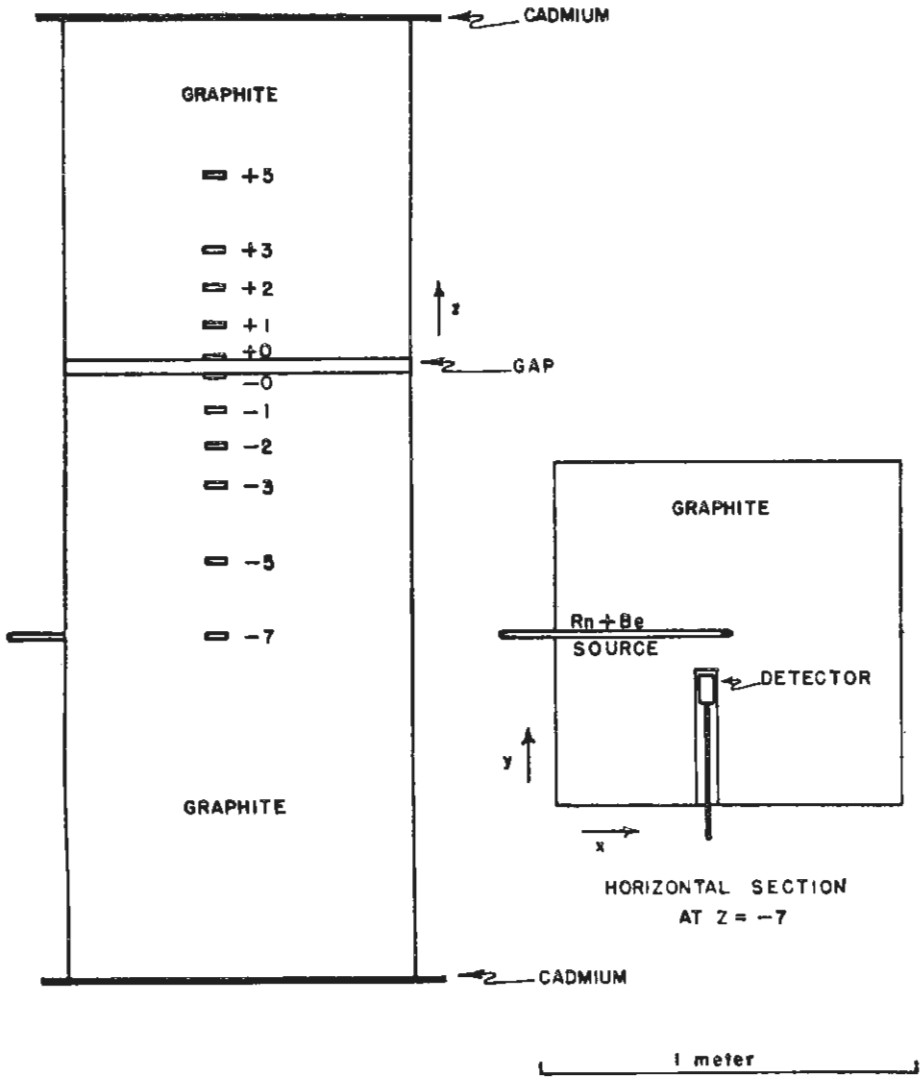

Fig. 1.

resonance and the thermal activities, respectively, calculated as will be discussed below.

The experimental and calculated data of Columns 4, 5, 7 and 8 normalized to give unity at $z = 0$ are shown in fig. 2. The property of a carbon column to separate the thermal from the resonance neutrons is clearly revealed by these curves.

TABLE I.

The resonance and thermal neutron activities of indium in the graphite column without gap.

			Cd In Cd		Ni In Ni	Thermal Neutrons	
pos	z	z_{res}	Expt	Calc	Expt	Expt	Calc
1	2	3	4	5	6	7	8
— 7	0.6	0	16.50	16.50	75.1	56.06	54.7
— 5	20.9	20.3	10.43	10.43	57.4	45.34	44.5
— 3	41.2	40.6	3.52	3.48	30.2	26.09	26.1
— 2	51.4	50.8	1.79	1.76	20.17	18.05	18.2
— 1	61.6	61.0	0.844	0.835	13.04	12.01	12.2
0	71.7	71.1	0.372	0.371	8.32	7.83	7.93
1	81.9	81.3	0.159	0.160	5.17	4.92	5.06
2	92.0	91.4	0.070	0.070	3.25	3.11	3.18
3	102.2	101.6	0.028	0.032	2.046	1.95	1.96
5	122.5	121.9	0.0075	0.0068	0.797	0.725	0.735

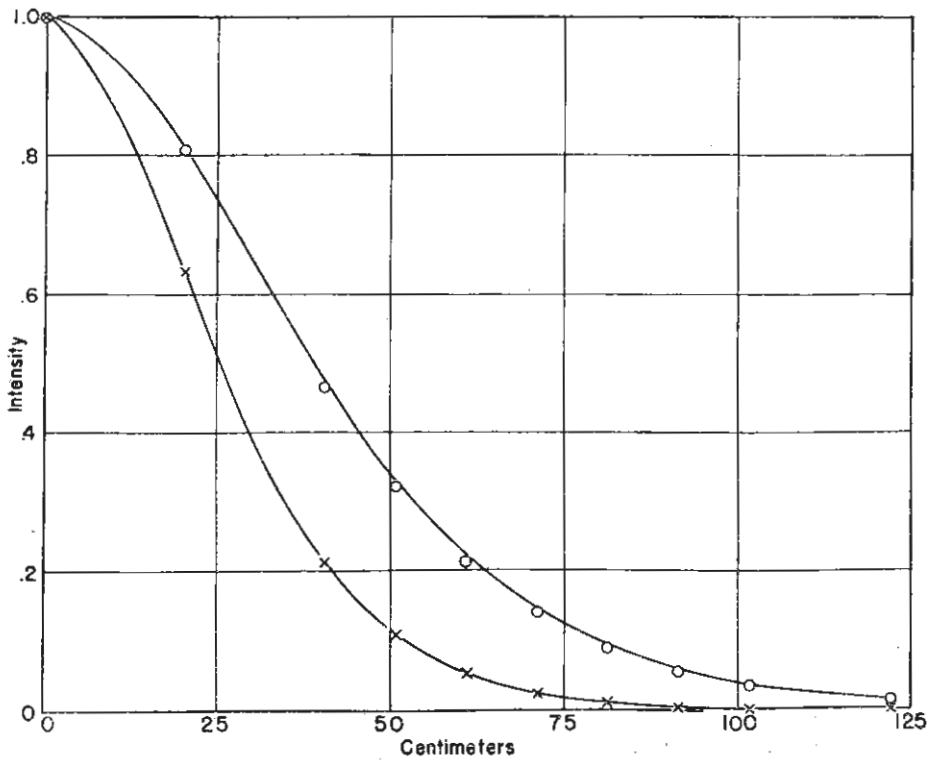

Fig. 2.

Discussion of the results of Table I.

In I we described measurements of the resonance activity of rhodium taken under conditions analogous to the indium measurements given in Column 4 of Table I. In that report we described a method for analyzing those results on the assumption that the slowing down of neutrons is essentially a diffusion process obeying the differential equation:

$$\Delta q = \frac{\partial q}{\partial t} \tag{1}$$

where the neutron age t (which is not a time) was given in I to be:

$$t = 2.233 \int_{E}^{E_0} \lambda^2 (E) \frac{dE}{E} \tag{2}$$

and q is the number of neutrons per unit volume which in unit time are slowed down from above to below the energy E, corresponding to the age t. λ is the mean free path taken to be 2.55 cm for slow neutrons in our graphite. The quantity q is related to $n(t)\,dt$ the density of neutrons having an age between t and $t + dt$ by the relation:

$$q(t)\,dt = \frac{\lambda v}{3} n(t)\,dt. \tag{3}$$

If our assumptions were strictly correct we would expect that the resonance activity of the indium detector given in Column 4 could be obtained as a solution of (1) corresponding to the boundary conditions imposed by our particular geometry. For a point source of neutrons of unit intensity this solution is:

$$q = \frac{4}{a^2} \frac{1}{2\sqrt{\pi t}} e^{-\frac{z_{res}^2}{4t}} \sum_{m=1}^{\infty} \sum_{n=1}^{\infty} e^{-\frac{\pi^2 t (n^2+m^2)}{a^2}} \sin\frac{n\pi x}{a} \sin\frac{m\pi y}{a} \sin\frac{n\pi u}{a} \sin\frac{m\pi v}{a} \tag{4}$$

where a is the side of the column increased by $2\lambda/\sqrt{3}$ and in our case is 94.4 cm. The positional coordinates in the horizontal plane x, y and u, v refer to the detector and source, respectively. In our case $u = v = a/2$. The distribution function (4) contains z in a Gaussian factor whose *range* is given by:

$$r_0^2 = 4t \tag{5}$$

as was already noticed in I.

The experimental data cannot be fitted with a single Gauss function. In I a phenomenological description was obtained by assuming two groups of neutrons diffusing with different ranges. To obtain a more accurate description in the present work we have analysed the experimental resonance activities of indium as follows:

$$A_{res} = 6.44\, e^{-\left(\frac{z_{res}}{22.8}\right)^2} + 9.42\, e^{-\left(\frac{z_{res}}{37.0}\right)^2} + 0.64\, e^{-\left(\frac{z_{res}}{57.0}\right)^2}. \tag{6}$$

Values calculated using this formula are listed in Column 5 of Table I; the agreement with the experimental points is as good as the experimental accuracy. This recipe may be obtained by taking a linear combination of three terms of the type (4) corresponding to the assumption that there are three groups of neutrons having different ranges and intensities as follows:

Range in cm for Indium Resonance	Intensity in percent f
22.8	14.0
37.0	65.8
57.0	20.2

To calculate the distribution of the thermal neutrons it is first necessary to take into account the additional diffusion from the resonance energy of indium (1 ev) to thermal energies (0.025 ev) by increasing the above ranges by an amount which may be obtained from a formula given in I:

$$(r_{th})^2 - (r_{In})^2 = 20.6\,\lambda^2 \log_{10} \frac{E_{In}}{E_{th}}. \tag{7}$$

The thermal neutron ranges are, thus, 27.1, 39.8, and 58.9 cm, respectively.

The diffusion of thermal neutrons may be described by means of the differential equation, (see I):

$$\Delta n - \frac{3}{\lambda^2 N} n + \frac{3}{\lambda v} q = 0 \tag{8}$$

where n is the density of thermal neutrons, λ is the mean free path for thermal neutrons in carbon, N is the number of impacts by thermal neutrons before being captured; its value was determined in I to be 1600, v is the neutron velocity, and q is the number of thermal neutrons produced per cm³ per second. The quantity q is given by a linear combination of terms of the type (4) using the thermal neutron ranges and the percentages f_i given above. For our geometry the solution of (8) which gives the distribution of thermal neutrons is:

$$n = \sum_{j,k=1}^{\infty} C_{jk} \frac{b_{jk}}{2} \sum_{i=1,2,3} f_i\, e^{\frac{3 r_i^2}{4 \lambda^2 N}} \left\{ \left[1 - \Theta\left(\frac{z}{r_i} + \frac{r_i}{2 b_{jk}} \right) \right] e^{\frac{z}{b_{jk}}} + \left[1 + \Theta\left(\frac{z}{r_i} - \frac{r_i}{2 b_{jk}} \right) \right] e^{-\frac{z}{b_{jk}}} \right\} \tag{9}$$

where

$$C_{jk} = \frac{6}{\lambda v a^2} \sin \frac{\pi j u}{a} \sin \frac{\pi k v}{a} \sin \frac{\pi j x}{a} \sin \frac{\pi k y}{a}$$

$$\frac{1}{b_{jk}^2} = \frac{3}{\lambda^2 N} + \frac{\pi^2}{a^2} (j^2 + k^2)$$

$$\Theta(x) = \frac{2}{\sqrt{\pi}} \int_0^x e^{-y^2} dy.$$

The values calculated with this formula are given in Column 8 of Table I. One constant only, proportional to the sensitivity of the detector, has been adjusted so as to fit in the best possible way the experimental data. The agreement is seen to be within a few percent.

In order to convert the quantities q and n used in the above formulas to indium resonance and thermal neutron activities measured in our experiments the following relations are useful:

$$A_{res} = 1253\, q\,(\mathrm{In})\,\frac{\sqrt{\pi}\,a^2}{4} \tag{10}$$

$$A_{th} = 17.5\, n\,\frac{\lambda v a^2}{6} \tag{11}$$

where q (In) is the value of q calculated using the indium resonance ranges.

Section II: Neutron production by uranium.

The neutrons produced when uranium captures thermal neutrons were observed as follows. A dural frame was inserted in the graphite column as shown in fig. 1. This frame left a gap of $1\,{}^1/_4$ inches in which a layer of uranium could be inserted. We used 74.2 kilograms of U_3O_8 placed in nine flat square iron boxes of one foot side and about 1 inch thick. These boxes could be easily placed in or removed from the gap and thereby permitted frequent comparisons of the neutron intensities with and without uranium in the gap. The results of measurements taken with and without uranium using the indium detectors shielded with cadmium are given in Columns 2 and 3 of Table II. The first column gives the detector position with the same notation as in Table I, except that the positions — 0 and + 0 refer to the positions immediately below and immediately above the gap. The marked increase in the indium resonance activity in the neighborhood of the uranium layer is mainly due to the production of neutrons by uranium.

Table II.

The resonance neutron activity of indium in the graphite column, with and without uranium in the gap.

Position	With uranium	Without uranium	Difference
1	2	3	4
— 0	0.522	0.338	0.18
+ 0	0.489	0.341	0.15
1	0.357	0.144	0.22
2	0.2554	0.0634	0.1920
3	0.1471	0.0280	0.1191
5	0.0412	0.0052	0.036

Corrections are due to the resonance absorption of neutrons by the uranium and to the escape of neutrons sidewise from the gap. In general, in analyzing these and other results, we have introduced sources of neutrons having appropriate energy and intensity, sometimes positive and sometimes negative, in order to account for the various ways by which neutrons could be produced or lost in our graphite column. Thus, the sources which are responsible for producing the difference listed in *Column 4* of Table II are the following:

1) A positive source of fast neutrons generated by the uranium. This source is not distributed uniformly throughout the uranium layer since the density of thermal neutrons, which after absorption by the uranium give rise to these fast neutrons, is greatest at the center and approaches zero near the edge. It is sufficiently accurate to take the intensity proportional to

$$\sin\frac{\pi x}{a}\sin\frac{\pi y}{a}$$

with the same notations as used in Section I. In what follows a source having such a distribution will be called a sine-sine source.

2) A negative sine-sine source of neutrons having an energy equal to that of the uranium resonance (10 ev) representing the absorption of neutrons by uranium at resonance.

3) A positive source representing the difference between the losses by sidewise escape from the gap, with and without uranium, of neutrons originating from the primary source.

4) A negative source representing the loss by sidewise escape from the gap with uranium of neutrons originating from the secondary source.

5) A positive source representing the effect of the gap on the 10 ev source mentioned above.

TABLE III.

Indium resonance activities due to the various sources: This table was constructed from Tables A and B of the Appendix by multiplying the numbers given there by the values of the source strengths I, the effective gap lengths L, and the activities A at the gap, indicated at the head of each column.

pos	fast source $I_U = 0.0218$	10 ev source $I_{res} = 0.0013$	gap sources			Calculated	Experimental
			primary $L = 3$ cm. $A_{In} = 0.34$	secondary $L = 5$ cm. $A'_{In} = 0.29$	resonance $L = 5$ cm. $A''_{In} = 0.1$		
1	2	3	4	5	6	7	8
0	+ 0.3196	— 0.1130	+ 0.0136	— 0.0465	+ 0.0057	0.1794	0.166 ± 0.023
1	+ 0.2888	— 0.0572	+ 0.0058	— 0.0305	+ 0.0014	0.2083	0.216 ± 0.017
2	+ 0.2123	— 0.0062	+ 0.0025	— 0.0171	+ 0.0001	0.1916	0.1920 ± 0.008
3	+ 0.1280	— 0.0013	+ 0.0011	— 0.0083		0.1195	0.1191 ± 0.004
5	+ 0.0383	— 0.0001	+ 0.0002	— 0.0014		0.0370	0.036 ± 0.004

The activities due to all the sources which need be considered are calculated in the Appendix. There in Table A we have tabulated, for various positions of the detector, the activities due to sources of unit intensity as defined in Appendix A. The activities due to the gap effects are calculated in Appendix B and tabulated in Table B. We have considered that the gap is equivalent to a layer of carbon of thickness L which differs from the geometrical thickness of the gap as discussed there. We have taken for the empty gap, L = 8 cm, and for the gap with uranium, L = 5 cm. These values have been determined in several different ways; by comparing the activities with and without the gap, by analysing the activities obtained with the source placed closer to the gap, and by comparing directly at the side of the column the neutrons emerging from the gap with those from an equal thickness of carbon.

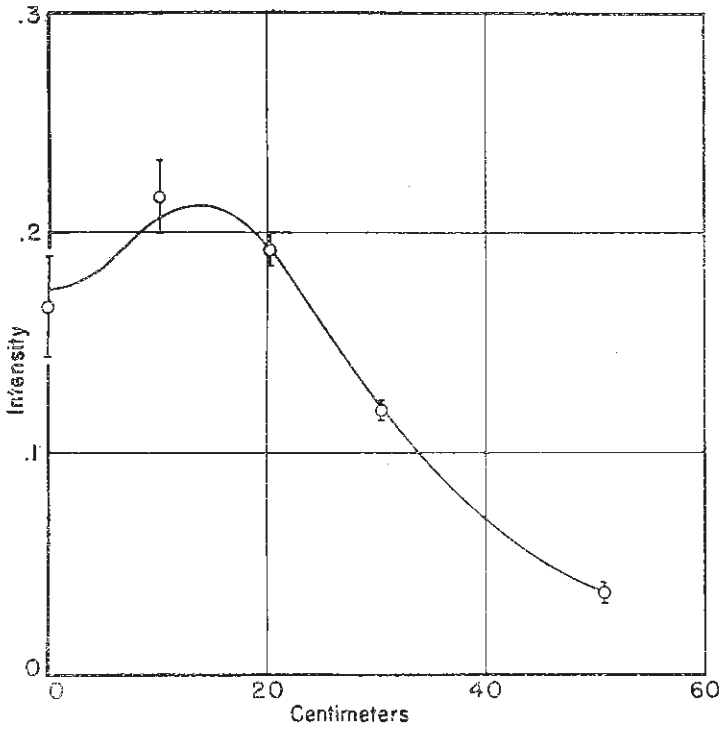

Fig. 3.

An analysis giving the indium resonance activities due to each of the above sources at various detector positions is given in Table III. This table was constructed by multiplying the numbers given in Tables A and B by the values of the source strengths I, the effective gap lengths L, and the activities A at the gap, indicated at the head of each column. In order to obtain a good fit with the experimental data we have taken as the intensity of the fast uranium source $I_U = 0.0218$ [2], and for the uranium resonance source $I_{res} =$

(2) We have tacitly assumed that the secondary neutrons have the same energy distribution as the primary neutrons. However, a measurement of the fast neutron source based on measurements at positions 2 and 3 would be altered by about 2 % if the initial energy differed by a factor of 10 from those of the primary source.

— 0.0013. The algebraic sum of the activities due to all the sources is given in Column 7 and is to be compared with the observed increase in the resonance activity due to uranium given in Column 8. The data of Column 7 was used to construct the solid curve of fig. 3 while the plotted points are those of Column 8. It is seen that the agreement is well within the experimental accuracy. It is to be pointed out that at positions 2 and 3, where measurements were made with the most care, the perturbation due to the resonance absorption and the gap amounts to only 10 % of the observed effect. The estimate of the strength of the secondary source based on these measurements should be, therefore, quite reliable [3].

The experiment was repeated using the resonance neutrons of iodine. The energy of these neutrons is presumably above the uranium resonance and the results should not be perturbed by the resonance absorption of the uranium. On the other hand, the activability of the iodine detectors is considerably less than that of the indium detectors and hence the accuracy obtainable is not as good. The strength of the secondary source as obtained from the iodine measurements was in quite good agreement with the value 0.0218 obtained from the indium measurements.

Section III: The thermal neutron absorption of uranium.

The negative source representing the absorption of thermal neutrons by uranium was obtained by taking measurements with and without uranium in the gap with the indium detectors covered only with nickel. The results of these measurements are given in Columns 2 and 3 of Table IV. The corresponding thermal neutron activities were obtained as for Table I and are listed in Columns 4 and 5. The difference between the thermal neutron activities with and without uranium is tabulated in Column 6.

The analysis of this difference was carried out in a manner similar to that used in Section II by making use of the thermal activities due to the various sources as given in Tables A and B of the Appendix. The details of the analysis are given in Table V. This table was constructed by multiplying the numbers given in Tables A and B by the appropriate values of the source strengths I, the effective gap lengths L, and the activities A at the gap, indicated at the head of the columns 2 to 6 of Table V. The sum of these contributions and the observed difference in the thermal neutron activities with and without uranium is given in *Column 8*. The activities given in this column are to be ascribed to a negative thermal neutron source. Its intensity was obtained by dividing the activities of Column 8 by the activities A_s of a thermal source of intensity given in Table A. The results are listed in *Column 9*, and the average 0.0107 has been taken as the intensity of the negative thermal neutron source. This source is made up in part by a positive source due to the fact that the absorption of aluminum is greater without than with uranium in the gap, by a negative source due to the absorption

(3) Much less accurate is the measured strength — 0.0013 of the resonance absorption source, since its effect is difficult to separate from that of the gap leakage.

of the iron in the uranium containers, and by a positive source due to the fact that fewer thermal neutrons escape sidewise out of the gap with uranium than without. The balance represents the absorption by uranium.

TABLE IV.

The thermal neutron activities in the graphite column with and without uranium in the gap.

pos	Ni In Ni		thermal neutrons		
	with U	without U	with U	without U	Difference
1	2	3	4	5	6
—0	4.533	6.363	3.870	5.911	2.041
0	3.853	6.050	3.227	5.595	2.368
1	2.800	3.860	2.326	3.631	1.305
2	2.230	2.488	1.873	2.352	0.479
3	1.606	1.550	1.374	1.455	0.081

The absorption of the dural and of the iron was determined by means of our graphite column. We removed the gap and inserted the dural plates at the position 0 and observed a decrease in the thermal neutron activity which varied exponentially with distance from the gap. At the gap the observed activity was 7.74 and the decrease due to the dural 0.54. In Column 6 of Table IV the difference at the position of the gap in the thermal neutron activity with and without uranium is seen to have an average value of 2.204. With this activity the decrease due to the dural would be 0.154. According to (23) the thermal neutron source which would give this activity is obtained by dividing this number by 302. Since in the experiment 1.1 times as much dural was actually used in the gap frame we have taken for the intensity of the thermal neutron source due to the dural 0.00056. In a similar way we obtained for the intensity of the thermal neutron source due to the absorption of the iron, 0.00079. The thermal source due to the loss of thermal neutrons from the gap was obtained with the help of A_5 of Table B and equation (23) to be 0.00206. The intensity of the thermal source which represents the absorption of the uranium obtained by subtracting these from the total thermal source is found to be 0.0126.

The decrease in the thermal neutron activity due to an absorbing layer in the graphite column is a measure of the absorption cross-section of the layer. For a layer containing ν absorbing atoms per cm^2 the absorption cross-section is given by the expression

$$\sigma = \frac{2\lambda}{3b\nu}\frac{\Delta A}{A}, \tag{12}$$

where $\Delta A/A$ is the relative decrease in the activity due to the absorbing layer at its position.

TABLE V.

Thermal neutron activities due to the various sources. This table was constructed from Tables A and B of the Appendix by multiplying the numbers given there by the values of the source strength I, the effective gap length L, and the activity at the gap A, indicated at the head of the columns.

pos	fast source $I_U = 0.0218$	10 ev source $I_{res} = 0.0013$	gap sources: pri $L_O - L_U = 3$, $A_{In} = 0.34$	gap sources: sec $L_U = 5$, $I_U = 0.0218$	gap sources: res $L_U = 5$, $I_{res} = 0.0013$	obs. diff.	Total	I_{th}
1	2	3	4	5	6	7	8	9
0	1.168	— 0.205	0.041	— 0.211	0.014	2.205	3.012	0.0100
1	1.111	— 0.183	0.035	— 0.192	0.012	1.305	2.088	0.0115
2	0.964	— 0.134	0.026	— 0.151	0.008	0.479	1.192	0.0109
3	0.771	— 0.086	0.017	— 0.126	0.006	0.081	0.680	0.0103
								0.0107 = average I_{th}

We have calculated the absorption cross-section of uranium for thermal neutrons using in (12) the following values; $\lambda = 2.55$ cm, $b = 20.0$ cm, ν for 8.85 gms/cm^2 U_3O_8 is 1.90×10^{22}, A, corresponding to a source of 0.0126 using (23) is 3.81. A may be obtained as the average of the measurements at + o and —o of Column 4 of Table IV. A correction of about 10 % has to be applied to take into account the fact that due to the absorption the neutron density inside the layer is lower than that measured outside. We have taken $A = 3.22$. In this way we have obtained $\sigma = 5.3 \times 10^{-24}$ cm^2. This result is in good agreement with that reported in a previous communication, " Fission and Capture Cross-section of Uranium for Thermal Neutrons " (*). In that report we measured the ratio of the uranium to the manganese absorption cross-sections and found for this ratio 0.59. Taking 9.4×10^{-24} cm^2 for the cross-section of manganese as recently measured by Rasetti this would give for uranium a total absorption cross-section of 5.5×10^{-24} cm^2.

The average number of neutrons produced per thermal neutron captured by uranium may be obtained as the ratio of the fast neutron source $I_U = 0.0218$ to the source due to the thermal neutron absorption of uranium $I = 0.0126$. The ratio is:

$$\eta = 1.73, \tag{13}$$

The error in this result is partly due to accidental errors. From the consistency of the experimental data this may be estimated to be less than 10 %. However, due to the uncertainties in the corrections which were made the actual error might be appreciably larger.

APPENDIX A.

The activity due to source of unit intensity.

In all our measurements we have always divided the observed activities by the neutron intensity of the source in order to render the results independent of both the decay of the source and the changes of the source from week to week. It is convenient to take as unit intensity of a point source of neutrons the intensity 1 of our Rn + Be sources.

In the case of a source distributed on a horizontal plane with a sine-sine distribution it is expedient to call intensity 1 that of a source having the local intensity:

$$\frac{4}{a^2} \sin \frac{\pi u}{a} \sin \frac{\pi v}{a} \, du \, dv. \tag{14}$$

This definition is convenient because if a point source of unit intensity located on the axis of our column is analyzed in a twofold Fourier series in the horizontal section of the column passing through the source (14) represents the first harmonic component. In what follows we shall denote by the index zero the value at the axis of the column of any sine-sine magnitude.

(*) We were not able to locate this paper. (Editors' note).

1) *The resonance neutron activity due to a fast sine-sine source:*

If the distribution of the resonance neutrons could be represented by one range only, the activity due to such a source would be proportional to the term $n = 1$, $m = 1$, of the double sum (4), with $u = v = a/2$, i.e. for the source on the axis; thus:

$$q = \frac{4}{a^2\sqrt{\pi}} \frac{1}{r_0} e^{-\frac{z_{res}^2}{r_0^2}} e^{-\frac{\pi^2 r_0^2}{2a^2}} \sin\frac{\pi x}{a} \sin\frac{\pi y}{a}. \tag{15}$$

Actually, we superimpose three neutron groups as was done in Section I, using the indium resonance ranges and percentages given there. Making use of (10) the final formula for the activity is found to be:

$$A_1 = 5.00\, e^{-\left(\frac{z}{22.8}\right)^2} + 9.02\, e^{-\left(\frac{z}{37}\right)^2} + 0.636\, e^{-\left(\frac{z}{57}\right)}. \tag{16}$$

2) *The thermal neutron activity due to a fast sine-sine source:*

The density of thermal neutrons from such a source of unit intensity is given by the term $n = 1$, $m = 1$, of the equation (9). Using (11) the thermal neutron activity is given by the expression:

$$\begin{aligned} A_2 = 22.3 &\left\{\left[1 - \Theta\left(\frac{z}{27.1} + 0.678\right)\right] e^{\frac{z}{20.0}} + \left[1 + \Theta\left(\frac{z}{27.1} - 0.678\right)\right] e^{-\frac{z}{20.0}}\right\} \\ + 111.5 &\left\{\left[1 - \Theta\left(\frac{z}{39.8} + 0.995\right)\right] e^{\frac{z}{20.0}} + \left[1 + \Theta\left(\frac{z}{39.8} - 0.995\right)\right] e^{-\frac{z}{20.0}}\right\} \\ + 39.2 &\left\{\left[1 - \Theta\left(\frac{z}{58.9} + 1.472\right)\right] e^{\frac{z}{20.0}} + \left[1 + \Theta\left(\frac{z}{58.9} - 1.472\right)\right] e^{-\frac{z}{20.0}}\right\}. \end{aligned} \tag{17}$$

3) *The resonance neutron activity due to a sine-sine 10 ev source:*

This may be calculated using (15) assuming for the slowing down of neutrons from the uranium resonance (10 ev) to indium resonance (1 ev) a range, calculated as in (7):

$$\left(20.6\,\lambda^2 \log_{10}\frac{E_U}{E_{In}}\right)^{1/2} = 11.6 \text{ cm}. \tag{18}$$

Using (10) the expression for the indium resonance activity is:

$$A_3 = 86.6\, e^{-\left(\frac{z_{res}}{11.6}\right)^2}. \tag{19}$$

4) *The thermal neutron activity due to a sine-sine 10 ev source:*

Proceeding as for the fast sine-sine source but using only one range, namely:

$$r_0 = \left(20.6\,\lambda^2 \log_{10}\frac{E_U}{E_{th}}\right)^{1/2} = 18.7 \text{ cm} \tag{20}$$

we obtain for the thermal neutron activity the expression:

$$(21)\quad A_4 = 155.5\left\{\left[1-\Theta\left(\frac{z}{18.7}+0.468\right)\right]e^{\frac{z}{20.0}}+\left[1+\Theta\left(\frac{z}{18.7}-0.468\right)\right]e^{-\frac{z}{20.0}}\right\}.$$

5) *The thermal neutron activity due to a sine-sine thermal neutron source*:

The solution of (8) for our geometry is:

$$(22)\quad n = \frac{6\,b_{11}}{\lambda v a^2}\,e^{-\frac{z}{b_{11}}}\sin\frac{\pi x}{a}\sin\frac{\pi y}{a}\,.$$

Using (11) the thermal neutron activity at our detector positions is given by the expression:

$$(23)\quad A_5 = 302\,e^{-\frac{z}{20.0}}.$$

For convenience, we have collected in Table A the values for these activities calculated for our detector positions.

TABLE A.

The resonance and thermal neutron activities of indium due to various sine-sine sources of unit intensity at the position 0.

pos	fast source		10 ev source		thermal source
	res A_1	therm A_2	res A_3	therm A_4	therm A_5
0	14.66	53.56	86.6	158.0	302
1	13.25	50.97	44.0	140.7	182
2	9.74	44.22	4.8	103.1	109
3	5.87	35.36	0.1	66.2	66
5	1.76	18.48	—	24.4	24

APPENDIX B.

DECREASE IN ACTIVITY DUE TO LOSS OF NEUTRONS FROM THE GAP.

We consider first that the gap is filled with carbon. The number of neutrons which escape sidewise from the gap per unit time from an element of area du dv is:

$$(24)\quad Q = \frac{\lambda w}{3}L\left(\frac{\partial^2 n}{\partial x^2}+\frac{\partial^2 n}{\partial y^2}\right)du\,dv$$

where L is the length of the gap and n is the density of neutrons. In the region

of the gap $n = n_0 \sin \frac{\pi x}{a} \sin \frac{\pi y}{a}$. Thus, the effect of the gap may be represented by a negative sine-sine source having an intensity:

$$I = \frac{\pi^2}{6} \lambda v \, L n_0 \tag{25}$$

in units as defined in Appendix A.

For thermal neutrons the above formula applies directly; for fast neutrons we replace n_0 by $n_0(t)\,dt$, the density of neutrons in the age interval dt on the axis of our column. This is related to $q_0(t)$ by the relation (3) so that the negative sine-sine source which represents the sidewise loss of fast and epithermal neutrons from the gap is:

$$dI = \frac{\pi^2}{2} L q_0(t)\, dt. \tag{26}$$

When the gap is either empty or filled with some other substance we may apply similar formulas provided we take into account the different scattering properties by introducing an *effective* length L. L will be greater than the geometrical length of the gap if the mean free path of the substance in the gap is greater than that of carbon.

1) *Effect of the Loss of Thermal Neutrons from the Gap:*

We begin with a discussion of this case because it is the simplest. Introducing the sine-sine source whose intensity is given by (25) into the differential equation (8) we obtain for the density of thermal neutrons due to this source at a distance ζ from the gap.

$$n(\zeta) = \frac{\pi^2 b}{a^2} \cdot L n \; e^{-\frac{|\zeta|}{b}} \tag{27}$$

where b is equal to b_{II} as used in (9) and n_g is the actual density of thermal neutrons at the gap. The thermal neutron activity due to the gap is thus:

$$A_6 = 0.022 \, L A_{th} \, e^{-\frac{|\zeta|}{b}} \tag{28}$$

where A_{th} is the observed thermal activity at the gap.

2) *Effect of the Gap on the Fast Neutrons from the Primary Source:*

The escape of fast neutrons from the gap during the slowing down process perturbs both the indium resonance and the thermal neutron measurements in the neighborhood of the gap. In order to calculate in a simple way the effect on the indium resonance activity of the loss through the gap of neutrons originated in the primary source, we note that over a wide region about the gap the observed density of indium resonance neutrons varies (see Table 2) approximately as

$$e^{-\frac{z}{l}} \tag{29}$$

with $l = 12$ cm. This suggests that for a limited age interval we may take the solution of (1) to be:

$$q = e^{-\frac{s}{l}} f(t) \tag{30}$$

Thus, in the case of a sine-sine distribution we find from (1) at the position of the gap the expression:

$$q_g(t) = q_g(\mathrm{In})\, e^{-\left(\frac{2\pi^2}{a^2}-\frac{1}{l^2}\right)(t-t_{\mathrm{In}})} \tag{31}$$

From (26) the negative source which represents the effect of the gap has the intensity:

$$dI(t) = \frac{\pi^2 L}{2} q_{0g}(\mathrm{In})\, e^{-\left(\frac{2\pi^2}{a^2}-\frac{1}{l^2}\right)(t-t_{\mathrm{In}})}\, dt. \tag{32}$$

It follows that the neutron intensity due to this gap source will be given by the expression:

$$q(\mathrm{In}) = q_g(\mathrm{In}) \frac{2\pi^{3/2} L}{a^2} \int_0^\infty \frac{1}{2\sqrt{T}}\, e^{-\frac{T}{l^2}-\frac{\zeta^2}{4T}}\, dT = \frac{\pi^2 L l}{a^2}\, e^{-\frac{|\zeta|}{l}}\, q_g(\mathrm{In}) \tag{33}$$

where $T = t_{\mathrm{In}} - t$ and ζ is the distance from the gap. The indium resonance activity is thus:

$$A_7 = 0.0133\, L A_{\mathrm{In}}\, e^{-\frac{|\zeta|}{l}} \tag{34}$$

where A_{In} is the observed indium resonance activity at the gap.

In order to obtain the thermal neutron activity due to this source we need the distribution of the nascent thermal neutrons. Proceeding as for (33) we obtain:

$$q(th) = \frac{\pi^2 L l}{a^2}\, e^{-\frac{|\zeta|}{l}}\, q_g(th) \tag{35}$$

which becomes, by making use of (31):

$$q(th) = \frac{\pi^2 L l}{a^2} q_g(\mathrm{In})\, e^{-\left(\frac{2\pi^2}{a^2}-\frac{1}{l^2}\right)(t_{\mathrm{th}}-t_{\mathrm{In}})}\, e^{-\frac{|\zeta|}{l}}. \tag{36}$$

The solution of the differential equation (8) for this expression for q is:

$$n = \frac{3\pi^2 l L q_g(\mathrm{In})\, e^{-\left(\frac{2\pi^2}{a^2}-\frac{1}{l^2}\right)(t_{\mathrm{th}}-t_{\mathrm{In}})}}{\lambda v a^2 \left(\frac{1}{b^2}-\frac{1}{l^2}\right)} \left(e^{-\frac{\zeta}{l}} - \frac{b}{l}\, e^{-\frac{|\zeta|}{b}} \right). \tag{37}$$

From this equation the thermal neutron activity may be obtained by using (10) and (11) and is:

$$A_8 = 0.0602\, L A_{\mathrm{In}} \left(1.67\, e^{-\frac{|\zeta|}{20.0}} - e^{-\frac{|\zeta|}{12}} \right). \tag{38}$$

3) *Effect of the Gap on the Neutrons Produced by the Uranium*:

The simplification used above in 2) is not applicable in this case because the neutron intensity due to the uranium source does not have an exponential behavior in the neighborhood of the gap. The negative source which repre-

sents this effect of the gap has the intensity given by the expression,

$$dI(t) = \frac{\pi^2 L}{2}\sqrt{\frac{t_{In}}{t}}\, e^{-\frac{2\pi^2}{a^2}(t-t_{In})}\, q_{og}(In)\, dt. \tag{39}$$

The intensity of indium neutrons due to this gap source at a distance ζ from the gap is:

$$q(In) = q_g(In)\frac{\pi^{3/2} L r_{In}}{2a^2}\int_0^1 \frac{e^{-\left(\frac{\zeta}{r_{In}}\right)^2 \frac{1}{\xi}}}{\sqrt{\xi(1-\xi)}}\, d\xi. \tag{40}$$

The indium resonance activity is:

$$A_9 = 0.01\, L A'_{In}\int_0^1 \frac{e^{-\left(\frac{\zeta}{32}\right)^2 \frac{1}{\xi}}}{\sqrt{\xi(1-\xi)}}\, d\xi \tag{41}$$

where A'_{In} is that part of the observed resonance activity at the gap which is due to the uranium source. We have taken $r_{In} = 32$ cm as the best single range which fits the experimental data.

We proceed now to calculate the effect on the thermal neutron activity. At the position of the gap the intensity of neutrons of age t due to a uranium source having an intensity I_U from (5) and (15) is:

$$q_{og}(t) = \frac{e^{-\frac{2\pi^2 t}{a^2}}}{2\sqrt{\pi t}}\,\frac{4}{a^2} I_U\,. \tag{42}$$

These neutrons give rise to a negative sine-sine source because some of them are lost sidewise from the gap. The intensity of the nascent thermal neutrons due to this source, using equation (26), may be found to be:

$$q(th) = \frac{2\pi I_U L}{a^4}\sin\frac{\pi x}{a}\sin\frac{\pi y}{a}\, e^{-\frac{2\pi^2 t_{th}}{a^2}}\int_0^1 \frac{e^{-\frac{\zeta^2}{4 t_{th}\xi}}}{\sqrt{\xi(1-\xi)}}\, d\xi. \tag{43}$$

The density of thermal neutrons is the solution of (8) with this expression for q, namely:

$$n = \frac{3}{\lambda v}\,\frac{\pi b}{a^4}\, L I_U \sin\frac{\pi x}{a}\sin\frac{\pi y}{a}\, e^{-\frac{2\pi^2 t_{th}}{a^2}}\int_{-\infty}^{\infty} F\left(\frac{\zeta_o^2}{4 t_{th}}\right) e^{-\frac{|\zeta-\zeta_o|}{b}}\, d\zeta \tag{44}$$

with

$$F\left(\frac{\zeta_o^2}{4 t_{th}}\right) = \int_0^1 \frac{e^{-\frac{\zeta_o^2}{4 t\chi}}}{\sqrt{\chi(1-\chi)}}\, d\chi.$$

The corresponding thermal neutron activity may be written, taking as average $t_{th} = 309$ cm^2.

$$A_{10} = 0.0272\, L I_U \int_{-\infty}^{\infty} F\left(\frac{\zeta_o^2}{1236}\right) e^{-\frac{|\zeta-\zeta_o|}{20.0}}\, d\zeta_o. \tag{45}$$

4) *Effect of the Gap on the 10 ev Source:*

This calculation is identical to that in 3) except that we must replace t_{In} by the quantity $t_{In} - t_{res}$ where t_{res} is the age of the uranium resonance neutrons. Also, t_{th} must be replaced by $t_{th} - t_{res}$. The corresponding expressions for the indium resonance and the thermal neutron activities are, respectively:

$$A_{11} = 0.00363\, LA''_{In} \int_0^1 \frac{e^{-\left(\frac{\zeta}{11.6}\right)^2 \frac{1}{\xi}}}{\sqrt{\xi(1-\xi)}}\, d\xi \tag{46}$$

and

$$A_{12} = 0.0446\, LI_U \int_{-\infty}^{\infty} F\left(\frac{\zeta_0^2}{4\,[t_{th} - t_{res}]}\right) e^{-\frac{|\zeta - \zeta_0|}{b}}\, d\zeta_0 \tag{47}$$

where A''_{In} is that part of the indium resonance activity which is due to the 10 ev source.

TABLE B.

The effect of the gap on the indium resonance and the thermal neutron activities due to the neutrons originating from the various sources. To obtain the activities the numbers tabulated must be multiplied by the quantities indicated at the head of each column.

pos	Thermal source	Fast source, primary		Fast source, secondary		10 ev source	
	therm A_6	res A_7	therm A_8	res A_9	therm A_{10}	res A_{11}	therm A_{12}
	$L \times A_{th}$	$L \times A_{In}$	$L \times A_{In}$	$L \times A'_{In}$	$L \times I_U$	$L \times A''_{In}$	$L \times I_{res}$
0	0.0220	0.01330	0.0403	0.0314	1.94	0.0114	2.14
1	0.0131	0.00571	0.0344	0.0210	1.76	0.0028	1.78
2	0.0078	0.00244	0.0253	0.0118	1.39	0.0002	1.21
3	0.0047	0.00104	0.0171	0.0057	0.99		0.76
5	0.0017	0.00019	0.0041	0.0010	0.44		0.28

In Table B we have collected of the indium resonance and thermal neutron activities of the above gap sources. The activities given there are all for unit length of gap. A_6 is given per unit of observed thermal neutron activity at the gap, A_7 and A_8 per unit of observed indium resonance activity at the gap, A_9 per unit of indium resonance activity due to the uranium source, A_{10} per unit intensity of the uranium fast source, A_{11} per unit of indium resonance activity due to the resonance absorption of the uranium, and A_{12} per unit of intensity of the 10 ev source.

N° 139.

It became important to have some more detailed information about the resonance absorption of uranium. The results obtained in my thesis could be used to calculate this absorption for thin layers of uranium but couldn't be relied upon for massive amounts. The idea of using the uranium in lumps, in order to reduce the resonance absorption, had by now taken hold. Fermi wanted to know how much resonance absorption took place in spheres of uranium oxide (metal was not yet available) and in particular, when these spheres were embedded in graphite. He was already beginning to plan a large scale experiment which would test fairly directly the neutron reproduction capabilities of a lattice of uranium and graphite. He wanted to know how big to make the uranium oxide lumps and how to space them in the graphite.

The Uranium Committee had by this time come to be organized under the National Defense Research Committee. A group at Princeton University, under Professor H. D. Smyth, had been drawn into the widening program. Princeton physicists had been interested in fission since the time Niels Bohr had brought them news of its discovery. They had carried out experimental and theoretical work on the subject and would have liked to correlate their research with that of Columbia. Misunderstanding and security practices had a first prevented collaboration between the two universities. Then at a special conference in Washington, in January 1941, E. P. Wigner and J. A. Wheeler learned from Fermi the results of some of the Columbia experiments. This fact and Wigner's independent study of the theoretical aspects of the chain reaction made it possible for the Princeton physicists to plan further work relevant to the uranium project.

In March it was decided that the experiment on resonance absorption of uranium would be carried out at Princeton under the direction and the collaboration of Fermi and myself. There were at Princeton a working cyclotron and two capable young nuclear physicists, R. R. Wilson and E. C. Creutz, and the joint experiment would serve to introduce the Princeton group to the techniques in slow neutron physics which had been developed at Columbia.

I moved to Princeton during this period while Fermi came to participate in the work at frequent intervals. The occasion brought us into close contact with E. P. Wigner, who had taken an active interest in the work and gave our results his sharpest scrutiny.

The quantity measured in the experiment at Princeton was the ratio of the number of resonance neutrons captured per second by a uranium sphere, divided by the slowing down density, i.e., the number of neutrons per cm^3 which per second pass across the resonance levels of uranium. This was called the resonance absorption volume of the sphere. The following paper, which appeared as an appendix to a Princeton report to the National Defense Research Committee, describes the work and gives the result of the measurement.

H. L. ANDERSON.

139.

CAPTURE OF RESONANCE NEUTRONS BY A URANIUM SPHERE IMBEDDED IN GRAPHITE

E. FERMI, H. L. ANDERSON, R. R. WILSON, and E. C. CREUTZ

Appendix A of Report A–12, to the National Defense Research Committee
by H. D. SMYTH, Princeton University (June 1, 1941).

For slowing down neutrons to thermal energies, graphite is a substance which may be used effectively. When uranium is imbedded in the graphite some of the neutrons are captured by resonance absorption before they reach

thermal energies. The purpose of the present experiments was to obtain a measure of the number of neutrons captured in this way when the uranium is in the form of a sphere of U_3O_8.

It is convenient to express the property of a given uranium sphere of capturing resonance neutrons in its neighborhood as a volume. Physically speaking, this is the volume of graphite from which the uranium sucks resonance neutrons. If we denote by ν_U the number of resonance neutrons captured per second by the uranium sphere and by q (U) the slowing down density, i.e., the number of neutrons per cm^3 which per second pass from above to below the resonance level (there may be more than one) of uranium, then the ratio of these two quantities, which has the dimensions cm^3, is the volume referred to. We shall call it resonance absorption volume of the given sphere.

Number of captures by the uranium sphere.

In the measurement of the number of captures of resonance neutrons by the uranium sphere use was made of the fact [1] that the resonance capture process leads to the production of a radioactive isotope of uranium of 24 minutes half-life. If suitable cadmium protection is provided to eliminate the thermal neutrons, the number of resonance captures per second taking place in the sphere is equal to the number of β–disintegrations per second of the 24–minute life at equilibrium. This number was obtained from a measurement of the β–activity of a small representative sample of the U_3O_8 which had been purified from the fission products and from uranium X. For the measurement the sample was spread as uniformly as possible over an area of 4×6 cm^2 on an aluminum foil and covered with Scotch cellulose tape. It was then wrapped inside a thin bakelite tube and slipped in a definite position over a Geiger-Muller counter so as to cover most of the sensitive area. We used a thin-walled silvered glass counter having a diameter of 2 cm and a sensitive length of 5 cm filled with 9 cm of argon and 1 cm of alcohol. The counter was used with a stabilized voltage supply and a scale of 16 recorder. The activity which is observed is composed not only of the decaying 24–minute activity but also of the rising activity due to the build-up of uranium X. From an analysis of the activity measurements ν_U may be calculated from the formula:

$$\nu_U = \frac{A_U}{A_{UX}} \cdot \frac{\eta_U}{\eta_{UX}} N, \tag{1}$$

where A_U is the saturation activity of the 24–minute life of the sample in counts per minute; A_{UX} is the saturation activity of UX of the sample in counts per minute; $N = 9.42 \times 10^7$ is the number of β–disintegrations of UX taking place per second in the uranium sphere (containing 9170 gm U_3O_8). The factors η_U and η_{UX} take into account the absorption of the β–rays.

In order to take into account the absorption of the β–rays the thickness of the counter wall was measured. With a second counter to detect the β–rays,

(1) L. Meitner, O. Hahn, and F. Strassmann, «Zeit. f. Physik», *106*, 249 (1937). These authors give 23 minutes as the half–life.

the absorption of the counter for β–rays of radium E was compared with that of an aluminum cylinder of known thickness under the same geometrical conditions. It was found that our counter had a thickness equivalent to 0.029 gms/cm² of aluminum. The correction factor for the absorption of the β–rays, on the assumption that the absorption follows an exponential law, was found as follows: An aluminium tube of thickness 0.043 gms/cm², having an absorption equivalent to the counter wall, the Scotch tape, and the average sample combined, was inserted between the sample and the counter; η is equal to the ratio of the measured activity without aluminum to that with it.

THE SLOWING-DOWN DENSITY.

The slowing-down density q may be measured by means of thin detectors of resonance neutrons placed in the neighborhood of the uranium sphere and covered with cadmium. The saturation activity A of such a detector is proportional to the slowing-down density q in graphite, for the resonance energy of the detector:

$$A = \varkappa q . \tag{2}$$

The proportionality factor $\varkappa$ can be measured by the procedure indicated in another report [2] by a comparison of the activity of the detector in graphite with the activity of the same detector in a large water tank at a known distance from a Rn + Be source of neutrons.

The quantity q obtained in this way with a given detector may differ appreciably from the quantity q (U) which is required for the present experiment since the spatial distribution of the neutrons is a function of the neutron energy. In order to obtain q (U) from q the differential equation for slowing down [3] may be applied. This equation is:

$$\Delta q = \frac{\partial q}{\partial t} , \tag{3}$$

where for graphite

$$t = 2.233 \int_{E}^{E_0} \lambda^2 (E) \frac{dE}{E} .$$

SPATIAL DISTRIBUTION OF INDIUM AND IODINE RESONANCE NEUTRONS.

Experiments were performed with a graphite block of face 61 × 61 cm² and of 81 cm length, constructed of graphite bricks 4″ × 4″ × 12″. The face of the block was some 36.5 cm distant from the target of the Princeton cyclotron which was the source of the neutrons. The neutrons were those produced by the bombardment of Be with 8 Mev protons. For the detectors, weighed amounts of In_2O_3 (about 25 mg) were spread on paper over an area

(2) H. L. ANDERSON and E. FERMI, «Standards in Slow Neutron Measurements», [Paper N° 140. (Editors' note)].

(3) H. L. ANDERSON and E. FERMI, «Production and Absorption of Slow Neutrons in Carbon». [Paper N° 136. (Editors' note)].

of 1.9 × 3.8 cm² and covered with Scotch cellulose tape. Iodine detectors were made from about 60 mg of PbI_2 prepared in the same way. Using 10 such detectors, a complete distribution curve could be made with one irradiation In all the experiments the detectors were shielded with 0.45 gms/cm² of cadmium. In figure 1 the results of measurements made parallel to the face at a distance of 30.5 cm from it on the median plane are plotted. If the block were isolated in space, the activity would extrapolate to zero at a distance $\lambda/\sqrt{3}$ from the side. The effect of the surroundings was to increase the effective width to about 70 cm. The observed curve is quite closely a cosine distribution for a width of this amount.

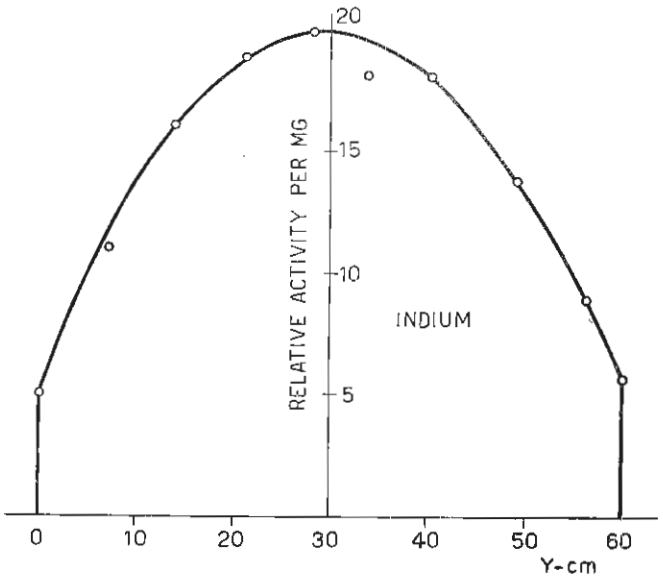

Fig. 1.

In figures 2 and 3 are shown the distribution along the axis for both iodine and indium neutrons. Making use of (3) and taking 70 cm for the effective width of the graphite parallelepiped, the indium curve can be obtained from the iodine curve if the ratio of the energies [4] is taken to be $E_I/E_{In} = 100$.

Experiments with the uranium sphere.

The uranium sphere contained 9,170 grams of U_3O_8 inside a thin copper shell of 8.5 cm radius. The sphere was provided with a conical cavity in which a cadmium cone containing ahout 4 grams of purified U_3O_8 could be placed. The graphite block was provided with a spherical cavity into which the uranium sphere could be inserted. The center of the sphere was placed on the axis at various distances from the front face of the block and oriented so that the axis of the cadmium cone was parallel to this face. Iodine and indium detectors shielded with cadmium were placed together near the surface of the

(4) H. L. Anderson, « Resonance Capture of Neutrons by Uranium ». « Phys. Rev. », *80*, 499, 1950.

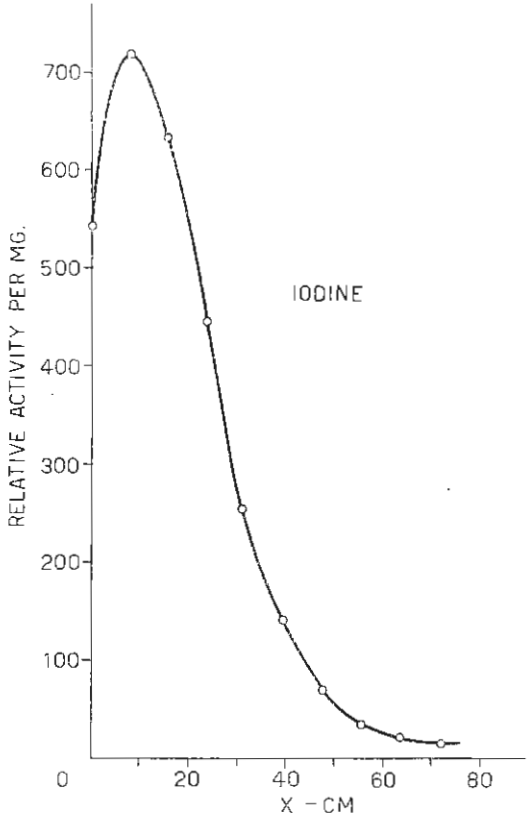

Fig. 2.

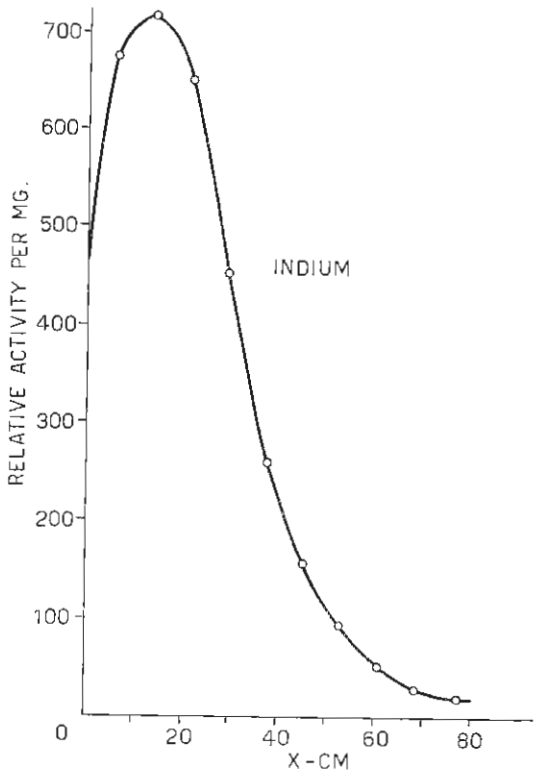

Fig. 3.

sphere at the position of the cone, and also at various positions along the axis. After the irradiation the U_3O_8 from the cadmium cone was dissolved in nitric acid and purified from uranium X and the fission products by means of an ether extraction. [4] The results of these measurements are tabulated in Table I; the saturation activities are given per milligram of detector.

In Table II we have collected the essential results of the experiments. Column 1 gives the distance of the center of the sphere from the front face of the graphite block. Columns 2 and 3 give the slowing-down densities for iodine and indium resonance neutrons respectively. Column 4 gives the total number of resonance captures per second by the U_3O_8 sphere. Columns 5 and 6 are the ratios of the data of column 4 to those of columns 2 and 3 respectively. If the resonance energy of iodine and indium were equal to the effective mean energy of the neutrons captured by the uranium sphere, we would expect the data of columns 5 or 6 to be constant and equal to the resonance absorption volume of the uranium sphere. It is seen that the data of column 5 are constant within the accuracy of these measurements whereas the data of column 6 show a definite decrease with distance. This behavior indicates that the effective energy of the neutrons absorbed is not very far from the iodine resonance energy and that it is larger than the resonance energy of indium. This seems quite reasonable in the light of the previous knowledge about the resonance bands.

TABLE I.

Detector	Weights in mg		Dist.	Sphere at 20.2 cm			Dist.	Sphere at 61 cm		
	In_2O_3	PbI_2		Sat. Act. of In_2O_3 per mg	Sat. Act. of PbI_2 per mg	Sat. Act. of U_3O_8 per mg		Sat. Act. of In_2O_8 per mg	Sat. Act. of PbI_2 per mg	Sat.Act. of U_3O_8 per mg
1	33.5	65.7	1.7	6550	947		6	7100	978	
2	28.0	66.8	6.0	7820	1082		15	7440	978	
3	21.2	66.6	11.9	6940	975		24	6060	671	
4	25.7	57.5	20.3	5250	718	46.4	33	3960	377	
5	27.6	74.5	31	3810	442		42	2203	224	
6	34.4	60.3	38	2800	298		51	1005	82.7	2.66
7	29.3	80.3	45	2165	182		61	542	38.5	
8	26.6	71.7	52	1365	105		71.3	325	24.7	
9	32.8	69.7	59	780	57		75.5	213	22	
10	25.8	69.2	66	522	39		79.5	172	15.1	

At 30.5 cm.

Detector	Weights	Sat. Act. per mg
U_3O_8	203.5	27
PbI_2	115.1	368
In	285	2310

Detector	Weights	Sat. Act. per mg
U_3O_8	147	23.8
PbI_2	112.3	292
In	196	2590

TABLE II.

Dist.	q (Iodine)	q (Indium)	Total Number of Resonance Capt. by U_3O_8 per Second	V_I	V_{In}
20.3 cm	7580	4910	33×10^6	4400 cm^3	6700 cm^3
30.5	3480	4300	18×10^6	5200	4200
61.0	406	507	1.9×10^6	4700	3700

As a result of the experiments we may take as the resonance absorption volume the average of the data of column 5, namely, 4800 cm^3. The experimental error is indicated by the discrepancies between the individual measurements.

N° 140.

Many of the measurements which were needed in the design of the chain reaction required knowledge of neutron source strengths and fluxes. Fermi felt quite strongly that it was worth a special effort to set up standard methods for calibrating sources and detectors so that these could always be compared to one another. Moreover, the response of the detectors could then be expressed in absolute units. The paper " Standards in Slow Neutron Measurements " was our best effort in this direction and can really be taken as a sequel to the earlier work with E. Amaldi, " On the Absorption and the Diffusion of Slow Neutrons " (Paper N° 118). Standard procedures were introduced by which indium and rhodium foils could be calibrated so that a measurement of their radioactivity could be used to give either the slow neutron density or the slowing down density in absolute units. The calibrations depended on the knowledge of the number of neutrons emitted from the source of neutrons used (here, radon plus beryllium) and this was in doubt by about 20 %. Moreover, the quantities themselves were somewhat conventionally defined since they depended on the nature of the slowing down material (here paraffin) as well as on the special response of the detector used. In spite of these uncertainties, Fermi was quite insistent that the calibrations be established as well as the state of the art allowed. A certain amount of error was frequently tolerable, but to think and measure in the same terms was essential. When, for example, it was the slow neutron density that one needed to know, Fermi wanted to measure it as he used it in his formulas, in neutrons per cm^2 per second.

There were important applications of these calibrations. In the study of the resonance absorption of uranium oxide spheres (see paper N° 139) the value of the slowing down density was needed. It became my job to make a continuing effort to improve the knowledge and the technique of measuring these fundamental neutron quantities.

H. L. ANDERSON.

140.

STANDARDS IN SLOW NEUTRON MEASUREMENTS

H. L. ANDERSON and E. FERMI
Columbia University, New York
Report A–2 (June 5, 1941).

In the course of experiments on the chain reaction with uranium and graphite the need for absolute neutron measurements became evident. Indeed, it became increasingly important to have some basis for planning in a quantitative way. To this end we have developed some methods which are described in this report for making such absolute neutron measurements. This has opened the possibility of evaluating certain experiments to obtain information essential in the design of a chain reaction experiment. In particular, these absolute determinations were necessary for evaluating the results of the experiment performed in collaboration with the Princeton group, " The

Capture of Resonance Neutrons by a Uranium Sphere Embedded in " Graphite " (*).

Measurements with slow neutrons are generally performed by observing the radioactivity induced in certain suitable chemical elements. It is the purpose of this paper to show that if such measurements are carried out in a standard way the results may be expressed in absolute units. The standardizations have been carried out for neutrons which have been slowed down by water, paraffin, or graphite, and include both the thermal and the resonance neutrons.

The measurements involved primarily are a determination of the absolute number of β–disintegrations from a thin detector (Section 1) and a determination of the mass absorption coefficient for thermal neutrons of the detector material (Section 2). In Section 3 we use these results for determining the density of thermal neutrons in water, paraffin and graphite. Once the densities of thermal neutrons have been determined in a given arrangement of material, thick detectors which are more conveniently handled may be calibrated. In Section 4 we use the calibrated detectors in order to determine the total number of neutrons emitted per second by a Rn + Be source. Measurements were performed using neutrons slowed down in water, also in graphite. In Section 5 we describe the measurements for the determination of the " slowing down density ". In Section 6 these results are applied to the determination of the Resonance Activability of a detector.

Section 1: Absolute number of β–disintegrations of a detector.

The measurement of the absolute number of β–disintegrations was performed by the use of a counter calibrated by means of known uranium X and radium–E sources. The sources were very thin deposits on an aluminum foil 2×2 cm^2. The amount of UX was determined both by weighing the U_3O_8 and by counting with a linear amplifier the alpha particles emitted by the source. The amount of radium–E was determined by counting the alpha particles of polonium growing out of the disintegration of radium–E. These sources were covered with cellulose " Scotch tape " and wrapped in contact with the counter in a definite position and the ratio of the observed counts to the known number of β–disintegrations was determined. The efficiency of the counter was found to be 0.390 for the UX_2 β–rays (mass absorption coefficient in Al 5.4 cm^2/gm (1)) The efficiency for the radium–E β–rays (mass absorption coefficient in aluminum 17.8 cm^2/gm) was found to be 0.215. From these data we have adopted the following practical formula for calculating the efficiency η of our counter for β–rays of mass absorption coefficient μ:

$$\eta = 0.5\, e^{-0.048\mu}.$$

(*) Paper N° 139 (Editors' Note).

(1) The mass absorption coefficients which are given in this paper are not corrected for the geometry used in their measurement. In our geometry source and absorber were cylindrical in shape and disposed concentrically with the counter.

It is to be pointed out that this formula holds only for our particular counter and our particular way of conditioning the samples. A considerable error may be incurred if the β–ray spectrum of a given radioactive emitter does not have the typical shape. For this reason we have tried to use several substances as detectors so as to have some sort of internal check among the results.

TABLE I.

Element	Period	Mass abs. coeff. of β-rays cm^2/gm			Observed number of thermal neutron disintegrations per gram per second (ν)	
		Al	Ag	Au	Paraffin	Graphite
Ag	22 sec	2.7	5.8		3119	999
Ag	2.3 min	7.4	12.0		1316	413
Au	2.7 days	18.5		28.4	4500	
In	13 sec	3.0	3.8		3100	(1020)
In	54 min	17.1	23.1		10400	3390
Rh	44 sec	4.8	7.4		10400	3573
Rh	4.2 min	4.8	7.4		1030	356

We have applied this formula for calculating the absolute number of β–disintegrations in various thin neutron detectors applying a small correction for the self-absorption of the β–rays in the detector material itself. The absorption coefficients used are listed in Table I. In calculating the small correction due to the self-absorption of the β–rays we have used for Ag, In, and Rh the mass absorption coefficients in silver since the atomic number of these elements is nearly the same.

SECTION 2: ABSORPTION COEFFICIENTS FOR THERMAL NEUTRONS.

The mass absorption coefficients for thermal neutrons have been measured for Ag, Au, In, Rh and B using the geometrical arrangement shown in figure 1. A Ra + Be source of about 500 mc was used as a source of neutrons and indium foils were used for detection of the thermal neutrons. The arrangement was chosen so as to have a rather small obliquity correction (the correction amounted to 2.3 %). Furthermore, the effect of scattering was very much reduced by placing the absorber quite close to the detector. In this arrangement only 1/2 of the scattered neutrons do not reach the detector; the remaining 1/2 strike the detector with oblique incidence so that the efficiency of detection is increased by a factor which is actually very close to 2, thereby cancelling

almost completely the effect of the scattering. That this was indeed the case was confirmed by a test of the apparent absorption of a graphite slab, which came out zero within the experimental error. The results of these measurements are summarized in Table II. The mass absorption coefficients and the

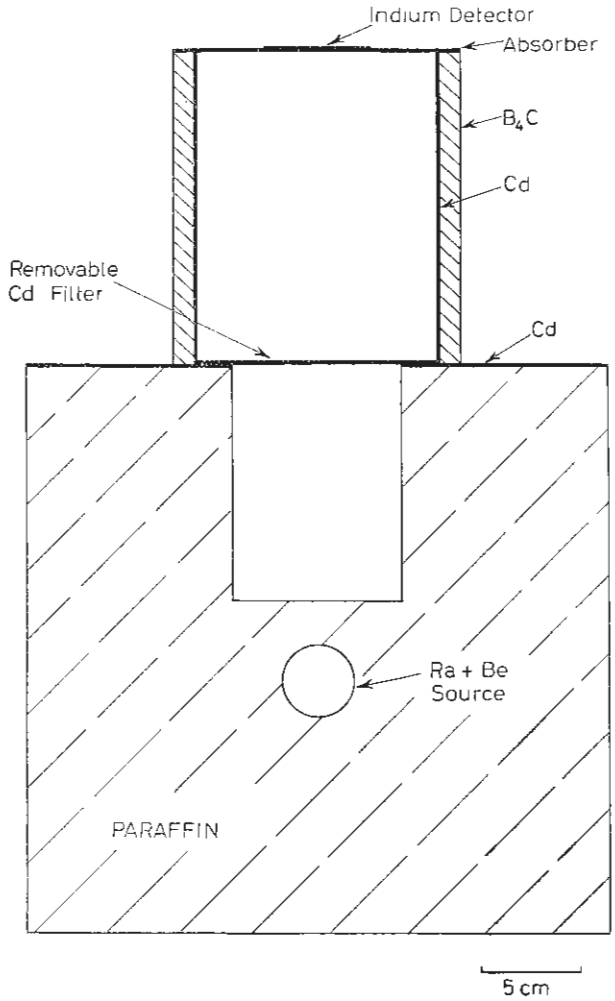

Fig. 1.

capture cross-sections as given in columns 2 and 3 refer to neutrons having a velocity

$$v_T = \sqrt{\frac{2kT}{m}} \tag{2}$$

where T = 293 degrees is the room temperature, k is Boltzmann's constant, and m is the neutron's mass. In the calculations which follow we have used these values for the absorption coefficients although they seem to be somewhat higher than the available published values.

TABLE II.

Element	$\varkappa$	σ	$\nu/\varkappa = nv_T$	
			$cm^{-2}\ sec^{-1}$	
	cm^2/gm	$cm^2 \times 10^{24}$	Paraffin	Graphite
Ag	0.334	60	13300	4230
Au	0.263	86	17100	
In	0.879	167	15400	5010
Rh	0.819	140	14000	4800
B	32.4	582	—	—
		Average. . .	14900	4680

SECTION 3: THE DENSITY OF THERMAL NEUTRONS.

We were interested in calibrating the thick indium detectors which we had employed in many of our measurements so as to be able to interpret the results of those measurements in absolute units. The indium detectors are of weight 2.42 grams and of dimensions 4×6.5 cm^2 and are measured by wrapping them inside a brass tube which was slipped over the counter. For the calibration of these detectors in paraffin we set up geometry in which the detector could be irradiated inside paraffin, with and without cadmium, using neutrons from the Ra + Be source. The average activity of the two faces of the foil was 9400 counts per minute at saturation with cadmium and 115,400 counts per minute at saturation without cadmium. The difference, 106,000 counts per minute, is the activity of the detector due to thermal neutrons. In the same position we irradiated also with and without cadmium various very thin detectors of Ag, Au, In, and Rh and measured by the technique described in Section 1 the number of disintegrations per gram of substance. These numbers are tabulated in column 6 of Table I.

The number ν of disintegrations per gram and per sec for a thin detector is given by the expression:

$$\nu = n\varkappa v_T \tag{3}$$

where n is the density of thermal neutrons, $\varkappa$ is the mass absorption coefficient for neutrons of velocity v_T, given by (2). The ratio $\nu/\varkappa$ should be a constant and equal to nv_T for all these irradiations. This ratio is given in column 4 of Table II. In compiling these ratios we have neglected to include the contributions of the 225-day activity of silver and the 48-day activity of indium. These contributions are presumably small and we plan to measure

them in the near future. We have taken nv_T to be equal to the average ratio, namely:

$$nv_T = 14{,}900 \text{ cm}^{-2} \text{ sec}^{-1}.$$

The thermal neutron activity of our standard indium detectors was 106,000 counts per minute. Since the activity is proportional to nv_T we obtain the relation:

$$nv_T = 0.14 \, A_{th} \text{ (for water and paraffin)}. \tag{4}$$

A_{th} being the saturation activity of the standard indium detectors due to thermal neutrons measured by our counter in counts per minute.

Since the albedo of paraffin and water is practically the same we may take this formula to be valid also in water. The albedo effect is, however, different in graphite. The coefficient of (4) cannot be used for measurements in graphite. By a procedure similar to that described we found for graphite:

$$nv_T = 4680 \text{ cm}^{-2} \text{ sec}^{-1}.$$

at a place where our standard indium detectors had an activity due to thermal neutrons $A_{th} = 46{,}300$ counts per minute at saturation. We have, therefore, for measurements in graphite:

$$nv_T = 0.101 \, A_{th} \text{ (for graphite)} \tag{5}$$

Section 4: Number of neutrons emitted by a Rn + Be source.

The measurement of the number of neutrons emitted by a Rn + Be source has been performed independently on neutrons slowed down in water and on neutrons slowed down in graphite. For the measurements in water we placed the source in the center of a large tank of water. The neutrons are slowed down by collisions with hydrogen until they reach thermal energies and are ultimately captured by hydrogen. The number of captures per cubic centimeter and per second is given by the relation:

$$\nu = nv_T \varkappa_w \rho \tag{6}$$

where $\rho = 1$ is the density of water, n the density of thermal neutrons and $\varkappa_w$ the mass absorption coefficient of water for neutrons of velocity v. The quantity $\varkappa_w$ has been obtained by combining the result of Frisch, Halban and Koch [2] who give 1940 as ratio of the capture cross-sections of boron and hydrogen with our measurement of the mass absorption coefficient of boron that has been reported in Table II. We find in this way $\varkappa_w = 0.00201$. With these values of the constants we obtain from (4) and (6):

$$\nu = 2.81 \times 10^{-4} A_{th}. \tag{7}$$

The total number of neutrons emitted by the source is the volume integral of ν. The integral could be readily calculated by measuring A_{th} at various distances from the source. We actually have measured A_{th} only at a few

(2) O. R. Frisch, H. Halban, and J. Koch, « K. Danske Vidensk. Selsk.», *15*, N° 10 (1938).

distances and assumed the dependence on the distance as given by Amaldi and Fermi and plotted in fig. 2.

For a 1 curie Rn + Be source the activity A_{th} at a distance r from the source is obtained by multiplying the ordinate of the curve of fig. 2 by 8.2×10^5. The total number of neutrons emitted by a 1 curie source per second is given by:

$$23.0 \times 4\pi \int f_{th}(r)\, r^2\, dr = 23.0 \times 4896 = 11.3 \times 10^6. \tag{8}$$

It is clear that the number of neutrons emitted by a Rn + Be source of given γ-ray strength depends somewhat on the packing and size of the Be grains. For this reason we have measured the neutron intensity of our sources in

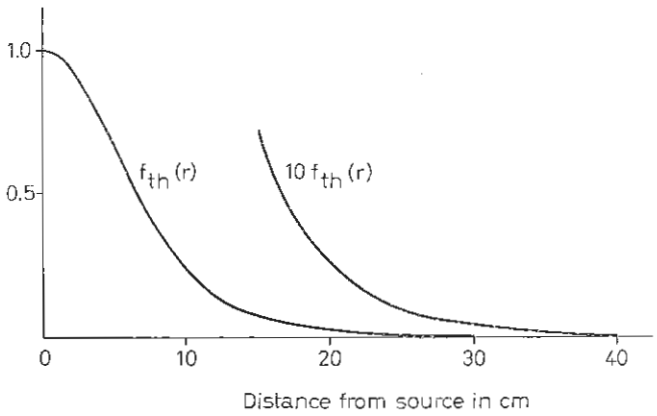

Fig. 2.

a conventional way. The neutron unit which we have adopted corresponds to about 228 millicuries and for this unit the value of Q is:

$$Q = 2.57 \times 10^6. \tag{9}$$

An independent evaluation of Q may be had from measurements in graphite. In Formula (11) [3] of our report " Production of Neutrons by Uranium " [*] hereafter to be referred to as II the density n of the thermal neutrons is expressed taking the number Q of neutrons which are emitted per second by a source of unit strength. At the place in graphite where the measurements described in Section 3 have been performed, we have measured the intensity A_{th} of the indium detectors by the same procedures as were specified in the above report, and found the intensity to be 127.6. From the value $nv_T = 4{,}680$ found above it follows that $Q = 2.75 \times 10^6\ \text{sec}^{-1}$. We take:

$$Q = 2.6 \times 10^6 \text{ neutrons per second} \tag{10}$$

with an estimated error of about 20 %.

(3) It is to be noticed that $\bar{v} = \frac{2}{\sqrt{\pi}} v_T$.

(*) Paper N° 138 (Editors' note).

SECTION 5: THE SLOWING DOWN DENSITY.

In measurements which involve the epi-thermal neutrons, e.g., those neutrons which activate the resonance levels, the quantity which is of importance is what we have called the slowing down density. The slowing down density q (E) is defined as the number of neutrons per unit volume which per unit time pass from above to below a given energy E. When a source of fast neutrons is placed inside a slowing down material of very large size, q is a function of E and the distance r from the source. Assuming that no captures of neutrons take place during the slowing down process, it follows

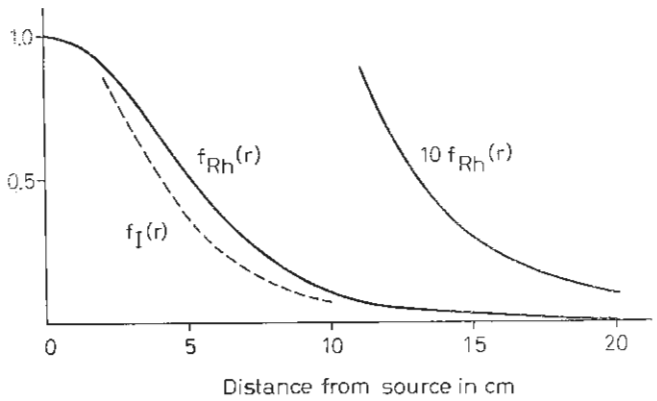

Fig. 3.

from the definition that in the steady state the volume integral of q is equal to the number Q of neutrons emitted by the source per unit time. Namely,

$$Q = 4\pi \int_0^\infty q\,(r\,,\,\mathrm{E})\, r^2\, dr. \tag{11}$$

When Q is known this formula enables us to determine q in absolute units. As an example let us consider the case of the neutron distribution due to a Rn + Be source of neutron intensity 1 placed inside a very large tank of water. Amaldi and Fermi [4] have determined for various detectors the intensity of activation due to resonance as a function of the distance from the source. In fig. 3 we have plotted the two curves $f_{Rh}(r)$ and $f_I(r)$ giving the resonance activity of a rhodium and an iodine detector. The two functions are normalized by taking their values at $r = 0$ equal to unity.

Since $f(r)$ is proportional to $q(r)$ we may write from (11),

$$q(r) = \frac{Q f(r)}{\int_0^\infty 4\pi f(r)\, r^2\, dr}. \tag{12}$$

(4) E. AMALDI and E. FERMI, « Phys. Rev. », *50*, 899 (1936) (Paper N° 118-*b*. Editors' note).

The volume integral has the value 2,600 cm³ for rhodium and 1730 cm³ for iodine. In order to determine q for neutrons of resonance energy E it is usually sufficiently accurate to use a logarithmic interpolation between the rhodium and the iodine resonance energies which are approximately 1 and 100 ev, respectively.

It is to be noted that at a distance of 7.5 cm q (I) = q (Rh) and it is to be expected that for the usual resonance detectors the value of q at this distance should be fairly independent of the resonance energy.

These considerations find useful application if the absolute value of q is desired at some place inside water or paraffin. The ratio of the resonance activity of a detector at this place having a resonance energy E to its resonance activity in a large tank of water at a distance of 7.5 cm from a Rn + Be source is measured. Then

$$q(r, \mathrm{E}) = 9.61 \times 10^{-5}\, \mathrm{Q}\, \frac{\mathrm{A}_{\mathrm{res}}(r)}{\mathrm{A}_{\mathrm{res}}(7.5\ \mathrm{cm})} \cdot \tag{13}$$

In order to measure the value of q in graphite it is necessary to take into account the different slowing down properties of this substance. The quantity to which the resonance activity of a detector is proportional, independent of the medium used for slowing down, is the density of neutrons in a given energy interval and not the slowing down density.

For a given value of q the ratio of the resonance activity in graphite to that in water is given by:

$$\frac{\mathrm{A}_{\mathrm{res}}(\mathrm{graphite})}{\mathrm{A}_{\mathrm{res}}(\mathrm{water})} = \frac{\lambda_g}{\lambda_w} \times \frac{1}{0.158} = 20.5 \tag{14}$$

where $\lambda_g = 2.55$ cm (graphite of density 1.55 gm/cm²) and $\lambda_w = 0.75$ cm are the mean free paths for resonance neutrons in graphite and water, respectively, and the factors 0.158 and 1 are the logarithmic averages of the energy loss per collision in the slowing down in graphite and water, respectively.

The absolute value of q can also be obtained from measurements in graphite alone by making use of formula (10) of II. We have determined the value of q by both methods and found reasonably good agreement.

If q in graphite is determined for a given energy by the methods described above, the value of q for some other energy may be calculated by the application of the differential equation of slowing down which was extensively applied in II.

$$\Delta q = \frac{\partial q}{\partial t} \cdot \tag{15}$$

Section 6: Application to the measurement of the resonance activability.

The number of resonance activations per second of a thin detector in water is given by the formula:

$$\nu = q\lambda_w \int_{\mathrm{res}} \sigma(\mathrm{E})\, \frac{d\mathrm{E}}{\mathrm{E}} \tag{16}$$

where $\sigma(E)$ is the cross-section of the detector for neutrons of energy E. The methods described above for the measurement of the number of β–disintegrations of a thin detector and for the determination of q enable us to obtain this integral which we shall call the *resonance activability*. We have measured the resonance activability for rhodium, indium, silver, gold, iodine, and uranium. The values obtained are given in column 2 of Table III. In obtaining these results corrections were made for the self-absorption of both the neutrons and the β–rays in the detectors; the detectors were thin enough so that these corrections were fairly small.

TABLE III.

	$\int_{res} \sigma(E)\frac{dE}{E}$	$\sigma(E_R)$	$\sigma(kT)$	E_R	BW
	10^{-24} cm²	10^{-24} cm²	10^{-24} cm²	*ev*	
Rh	940	4100	140	0.85	0.95
Ag 225 *d*	786	7200	42.4	2.7	1.46
Ag 2.3 *m*	61	—	17.6		
In	3260	23000	167	1.0	1.33
I	124	2100	5.1	100	3.0
Au	1280	26000	86	3.5	0.93
U	239	10000	2.7	10	2.06

These results may be combined with the known data on the resonance cross-sections, the resonance energy and the thermal neutron cross-sections for the resonance levels in question to determine what we have called the Breit-Wigner index for the level. This index is given by:

$$\text{B. W.} = \frac{1}{\pi}\left(\frac{E_R}{kT}\right)^{1/4} \frac{\int_{res} \sigma(E)\frac{dE}{E}}{\sqrt{\sigma(E_R)\,\sigma(kT)}}. \tag{17}$$

The BW index should have the value unity if the Breit-Wigner formula holds. Values for this index are tabulated in column 6 of Table III. It is seen that the Breit-Wigner formula holds quite well for the case of rhodium and gold while in the case of uranium and iodine a marked deviation is not outside of the experimental error. It should be mentioned that the measurements on the resonance activability were made in the early days of this work and since that time the procedures have been somewhat improved. We have not had time to repeat the experiments with the present technique and for this reason it is to be expected that the results might be subject to some revision.

N° 141.

Until the summer of 1941 greater emphasis was placed on the possible use of a chain reaction for production of power than for explosion in a bomb. Accordingly, Fermi prepared a report on the problems that would arise during the release of atomic energy, and presented it to the Uranium Committee on June 30, 1941.

It is of interest to note that Fermi limited his discussion to a chain reaction occurring in natural uranium, which was then the only form of uranium available. Fermi thus remained within the boundaries of the practical problem as it was at the moment, although both the separation of U^{235} and the production of plutonium were by then under study and achieved on a very small scale.

H. L. ANDERSON.

141.

SOME REMARKS ON THE PRODUCTION OF ENERGY BY A CHAIN REACTION IN URANIUM

Report A–14 (June 30, 1941)
Columbia University, New York, New York
(Presented at a meeting of the Committee on Uranium).

This report contains primarily a discussion of some general points of view as to the methods that could be employed for the use of a chain reaction in uranium as a source of energy. Even in the case that the chain reaction were not used as a source of energy but, for example, either as a source of radiations (neutrons and gamma rays) or as a source of large quantities of radioactive elements or a method for producing elements 93 and 94, the problem of dissipating the large amounts of energy released in the reaction would be of paramount importance. Indeed the rate of the reaction most probably would be limited by the amount of energy that could be dissipated.

Several methods have been proposed so far for producing a chain reaction, and this report shall discuss mainly those in which uranium is used without separation of the isotopes. In these methods the uranium may be assembled in the form of lumps of metal or of oxide distributed in a lattice array throughout a mass of light element (carbon, beryllium, heavy water) that is used for slowing down the neutrons produced in the fission process and enabling them thereby to react again with uranium reproducing new fission processes. In order to make this discussion as definite as possible we shall consider the case that carbon, in the form of graphite is used as slowing down material.

The energy produced in the reaction is due to:

a) The kinetic energy of the fission fragments.

b) The β–rays and γ–rays of the various radio-elements formed in the process.

c) The kinetic energy of the neutrons produced in the fission.

d) The nuclear affinity of the neutrons produced in the fission, which emit gamma-rays when they are captured.

All these various forms of energy are ultimately transformed into heat and it is important for our discussion to know at what places inside or outside of the reacting mass this transformation occurs.

We do not have at present a detailed knowledge of this distribution of the thermal energy. We have attempted nevertheless to give in Table I a plausible guess as to the distribution of the production of thermal energy. It should be stressed that the data of the table are purely indicative. They are furthermore affected to a considerable extent by the geometrical details of the reacting mass.

TABLE I.

Energy source	Amount in billion joules per gram of U-235	Place where thermal energy is released
Kinetic energy fission fragments	70	Uranium lumps
β–rays of radioactive elements	5	Uranium lumps
Gamma-rays of radioactive elements	2	70 % Uranium lumps 25 % Graphite 5 % Outside
Kinetic energy of neutrons .	3	90 % Graphite 10 % Outside
Nuclear affinity of neutrons. (gamma-rays)	8	60 % Uranium lumps 25 % Graphite 15 % Outside

It follows from this table that for every gram of U^{235} that is transformed 81.2 billion joules thermal energy are produced in the uranium lumps; 5.2 billion joules are produced in the graphite and 1.6 outside. Although these figures may be affected by very large uncertainties it appears that the bulk of the energy (90 % or more) is released in the uranium lumps, while only about 2 % is released outside of the reacting mass.

If the reaction is conditioned so as to produce the energy at a relatively slow rate the thermal conductivity of the mass may be sufficient for transporting outside the heat produced inside without having the temperature in the central portion of the mass become dangerously high. It can be estimated easily that even on fairly optimistic assumptions the maximum amount

of heat that could be taken out of the mass in this way would be of a few hundred large calories per second or about 1000 Kw of thermal energy.

At this rate of the reaction about one gram of U^{235} per day would undergo fission. The rate of production of element 94 would also be of about one gram per day so that it would take several years to accumulate a sufficient amount of this element for a " little " chain reaction unit on the assumption that the fission properties of element 94 are similar to those of U^{235}.

A larger power and a faster rate of reaction could be obtained only by increasing artificially the transport of heat from inside to outside the reacting mass.

In discussing the devices that could be used for this purpose we must bear in mind the fundamental fact that most chemical elements have such a high absorption for neutrons that only very small amounts of them introduced in any form inside the reacting mass would absorb so many neutrons as to stop the reaction. It is difficult with our present knowledge to put this statement in a much more precise form. Indeed the tolerance of the various elements depends on how critical are the conditions of the reaction. It is conceivable that some moderate amounts of substances like steel might be used without preventing the reaction and it is possible that the conditions might be much more critical so that only elements with very low neutron absorption may be used. In the following discussion we shall assume this latter case.

All the methods that have been considered for increasing the transport of heat out of the reacting mass involve the use of a fluid that is passed across the mass through suitable channels and takes away the heat. Such a fluid could be a gas or a liquid; or the heat could be used for vaporizing a suitable liquid, in which case the chain reacting mass could be at the same time the boiler of a thermal engine. We shall discuss separately the three methods indicated.

Gases. Convenient gases having a very low neutron absorption are helium, carbon dioxide and oxygen. This last must be probably ruled out on account of its chemical properties.

The amount of heat removed from the reacting mass is given by

$$c_p \mathrm{M} (\mathrm{T}_2 - \mathrm{T}_1)$$

where c_p is the specific heat at constant pressure, M is the mass of gas passed across the reacting unit and T_1 and T_2 are the temperatures of the gas before and after the passage. If we assume $T_2 = 400^\circ C$ we find that 20 Kgs of helium or carbon dioxide per second should be passed through a unit for the production of 10,000 large calories per second or 42,000 Kw.

The quantities of gas indicated are very large (of the order of 100 cubic meters at n.p.t.). The corresponding high velocities of flow could be appreciably reduced by increasing the pressure. Even if it is not possible to lead the cooling gases through pipes it would be probably feasible to enclose all the reacting unit in a steel container and pass the gases through narrow channels in the graphite having possibly ramifications in the uranium lumps where most of the heat is primarily produced.

The heated gases could be used either for heating a secondary boiler of a thermal engine or they could operate directly a gas engine or turbine. In the former case there would be the obvious advantage to be able to use directly well-known devices. The second method would presumably give a better yield; it would, on the other hand, require some development of the gas engine to adapt it to the new problem.

Liquids. There are not many liquids that are stable at high temperatures, do not have a too high vapor pressure, and have a low neutron absorption. Among them some organic compounds in which hydrogen is substituted with deuterium may be considered. Dr. Szilard has particularly stressed the advantage of using liquid bismuth.

Due to the much larger thermal capacity per unit volume, liquids would have over gases the advantage to require a considerably smaller velocity of flow; the greater viscosity would, on the other hand, introduce additional difficulties.

Liquids could be used only for transferring the heat from the chain reaction unit to the boiler of a thermal engine for the transformation into mechanical power.

Vapors. The use of vaporizing liquids appears of some promise for the production of mechanical energy. Here again the choice of suitable liquids is rather limited. Heavy water, some organic deutero-compounds or, according to the suggestion of Dr. Urey, some carbon fluorides could be conveniently used. The chain reacting unit would be used as the boiler; the liquid would be injected at one side and most of the heat would be absorbed as heat of vaporization. The advantage would be to avoid the necessity of a secondary boiler and to utilize the vaporization heat, which would enable to work in good conditions at not too high temperatures.

In conclusion it should be borne in mind that what we have presented here are only some general points of view. It is possible that the conditions of the chain reaction may be such as to allow a considerably greater freedom in the choice of the materials that can be used. Only after actual experimental realization of the chain reaction it will be possible to discuss in a precise way the best methods for its use.

Control of the reaction. Any use of the chain reaction for the production of power presupposes the possibility to control the rate of energy production.

The chain reaction may reach a steady state only when the multiplication factor of the neutrons (including neutron losses due to diffusion outside of the reacting mass) is equal to 1. Any change of the conditions that makes the multiplication factor greater than one will be followed by an exponential increase of the rate of the reaction, whereas a change of the conditions in the opposite sense will be followed by an exponential decrease of the rate of reaction.

If all the neutrons emitted after a fission were instantaneously emitted the relaxation time for the reproduction of the neutrons would be of the order of one thousandth of a second. Consequently, even very small differences of the multiplication factor from 1 would produce very violent increases or

decreases of the rate of reaction, so that the control of the reaction would be very difficult.

As a matter of fact, the actual state of affairs is much more favorable due to the existence of the delayed neutrons. It can be easily seen that when the multiplication factor is very close to unity, the relaxation time is determined essentially by the period of the delayed neutrons which is of the order of 10 seconds. This circumstance makes the adjustment of the rate of reaction to a desired value easily obtainable.

It appears also possible that the reaction may automatically reach a stable rate. Indeed a rise in temperature reduces the absorption of neutrons by both uranium and carbon and increases thereby the loss of neutrons due to diffusion outside the mass. If this effect of self regulation actually takes place a rise of the temperature to any desired level could he obtained by adjusting the size of the reacting unit or the reflection properties for neutrons of the materials surrounding the unit.

Protection from the radiations. A chain reaction unit that were operated at the rate of 10,000 large calories per second would emit several hundreds of kilowatts in the form of radiations (neutrons and gamma rays) that would be exceedingly dangerous unless properly screened. Neutrons can be conveniently screened by large tanks of water which may also be used for protection from the gamma radiations. The problem is similar to that of protection from the radiations emitted by large cyclotrons. Probably a thick ness of water for a few feet would offer a very substantial protection.

Some very reduced production of energy would continue for some time after the chain reaction has been shut off. This energy, due to the various radioactive products accumulated during the reaction would represent a few percent of the original energy and would be emitted for several hours and to a much lesser extent also for some weeks after the reaction has been interrupted.

142.

THE ABSORPTION OF THERMAL NEUTRONS BY A URANIUM SPHERE IMBEDDED IN GRAPHITE

E. FERMI and G. L. WEIL
Columbia University
Report A–1 (July 3, 1941).

The planning of a chain reaction experiment in a uranium-graphite system in which spheres of uranium (metal or oxide) are imbedded in a graphite mass requires the knowledge of the number of thermal neutrons that are absorbed by the uranium spheres. This number can be calculated by a mathematical analysis of the absorption and scattering of the neutrons inside the uranium sphere and in the surrounding graphite. Since, however, there is considerable uncertainty as to the absorption and scattering properties of U and U_3O_8 it appeared worth-while to determine the absorption of thermal neutrons also by a more direct method.

We consider a sphere of radius R imbedded in a graphite mass. We shall assume for simplicity that neutrons are produced with spherical symmetry so that the thermal neutron density will be a function of the distance r from the center of the sphere. In the graphite near the sphere the absorption of thermal neutrons by the sphere will manifest itself as a decrease of the neutron density close to the sphere. Inside the graphite the neutron density obeys the differential equation [eq. (8) of the report " Production of neutrons by uranium ",(*) henceforth referred to as I.]

$$\Delta n - \frac{3}{\lambda^2 N} n + \frac{3}{\lambda v} q = 0. \tag{1}$$

At the surface of the sphere n obeys a boundary condition of the form

$$\frac{n(R)}{\left(\frac{dn}{dr}\right)_{r=R}} = L \tag{2}$$

L is a constant that depends on the scattering and absorbing properties of the material as well as on the radius R of the sphere.

All the absorption properties of the sphere for thermal neutrons may be expressed in terms of L. We shall therefore call L the " absorption length " of the sphere for thermal neutrons. For instance the number of thermal neutrons absorbed by the sphere per unit time is given by

$$\mathfrak{A} = 4\pi R^2 \frac{\lambda v}{3} \left(\frac{dn}{dr}\right)_{r=R} = \frac{\lambda v}{3} \frac{4\pi R^2}{L} n(R) \tag{3}$$

(*) Paper N° 138. (Editors' note).

provided a and L are large compared to λ. We may combine this result with [(11) of I] and we obtain

$$\mathfrak{N} = \frac{4\pi R^2}{L} \times 1.283 \times 10^{-5} A_{th}(R) \tag{4}$$

where $\mathfrak{N}$ is expressed in units of the number of neutrons emitted by the primary source and $A_{th}(a)$ is the activity near the surface of the sphere of a standard indium detector measured according to the prescriptions of Report I.

If we want to have $\mathfrak{N}$ expressed in absolute units we may use instead formula (5) of the Report "Standards in slow neutron measurements" (*) and we have in absolute units

$$\mathfrak{N} = \frac{2}{\sqrt{\pi}} \frac{\lambda}{3} \frac{4\pi R^2}{L} v_T n(a) = \frac{4\pi R^2}{L} \times 0.096 A_{th}(R) \tag{5}$$

where $A_{th}(R)$ represents now the activity of our standard indium detectors measured according to the prescriptions of that report. (Counts per minute at saturation on our counter No. 2)

Before describing the methods for the experimental determination of L we report here some formulae for its approximate theoretical calculation. Since these formulae have already been the object of correspondence with the theoretical members of the Uranium Committee they are given here without proof.

We call γ the albedo of the uranium sphere defined as the probability that a thermal neutron entering the sphere re-emerges out of it without being absorbed. If γ is known, L can be approximately calculated with the formula

$$L = \frac{\lambda}{\sqrt{3}} \frac{1+\gamma}{1-\gamma}. \tag{6}$$

If the scattering and absorption properties of the material in the sphere are known, γ can be calculated. By applying the diffusion theory to the interior of the sphere one finds γ from the following approximate formula

$$\frac{1-\gamma}{1+\gamma} = \frac{1}{\sqrt{N_i}} \frac{e^{R/l_i} + e^{-R/l_i}}{e^{R/l_i} - e^{-R/l_i}} - \frac{\lambda_i}{\sqrt{3}\,R} \tag{7}$$

λ_i is the mean free path of thermal neutrons inside the sphere. N_i is the ratio of the total to the capture cross-section for thermal neutrons inside the sphere. l_i is the diffusion length inside the sphere:

$$l_i = \lambda_i \sqrt{\frac{N_i}{3}}. \tag{8}$$

It follows from (6) and (7) that L is a function of $R\rho$ for spheres made of the same material in states of different density ρ. In fig. 1 the values of L calculated with (6) and (7) are plotted as functions of $R\rho$ for spheres of U_3O_8 (upper curve) and of uranium metal (lower curve).

(*) Paper N° 140. (Editors' note).

In these calculations we have assumed

$$\lambda = \text{mean free path in graphite} = 2.55 \text{ cm}$$

$$\lambda_i = \frac{22.0}{\rho} \text{ for U–metal} \quad ; \quad \lambda_i = \frac{15.9}{\rho} \text{ for } U_3O_8$$

$$N_i = 3.3 \text{ for U–metal} \quad ; \quad N_i = 5.3 \text{ for } U_3O_8$$

$$l_i = \frac{23.1}{\rho} \text{ for U–metal} \quad ; \quad l_i = \frac{21.2}{\rho} \text{ for } U_3O_8 .$$

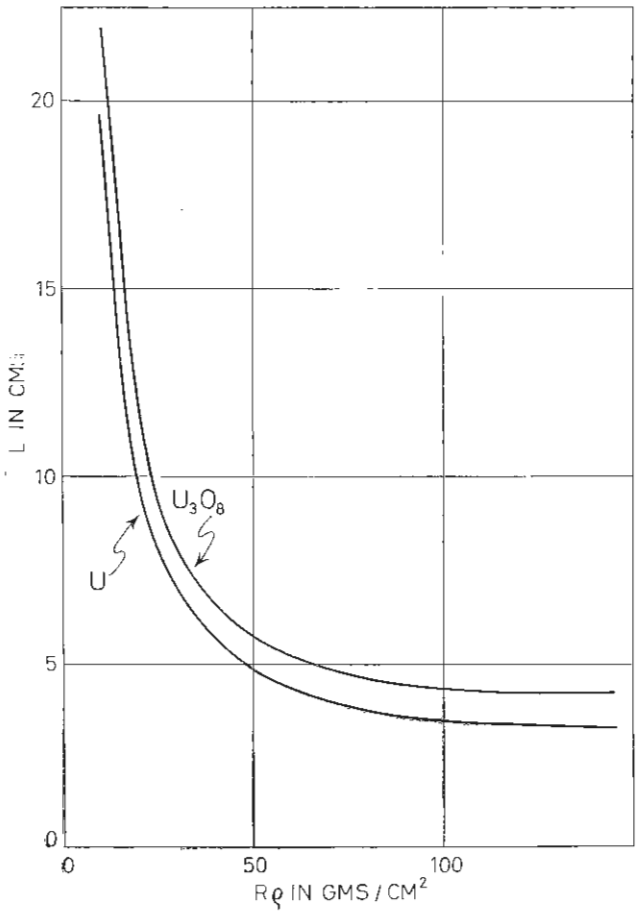

Fig. 1.

These theoretical results are affected by a considerable uncertainty because the diffusion theory can be expected to give only a rather bad approximation for our problem. Furthermore also the scattering and absorption cross-sections used in the calculation may be appreciably in error.

It appeared worth-nile therefore to attempt an experimental determination of L. The measurements have been performed on two spheres, one filled with U_3O_8 and one with powdered uranium metal. We illustrate the methods employed by describing in detail the measurements on the U_3O_8–sphere.

A thin spherical shell of spun copper sheet with a radius R = 8.5 cm was filled with 9300 gr U_3O_8 and placed in the center of a spherical cavity inside a graphite block of $4\times4\times5$ feet. A tuhe reaching to the center of the U_3O_8 sphere permitted the insertion of a Rn + Be source in the center of the sphere.

Measurements of the activity of various indium detectors were taken at several distances from the sphere. Since only data for points rather close to the sphere were used, the activities observed depend practically only on the distance r from the source at the center of the U_3O_8–sphere.

Activity measurements were taken using three types of indium detectors

a) 2.42 gr/4×6.5 cm²

b) 0.376 gr/4×6 cm²

c) 0.12 gr/6×0.2 cm².

The detectors *a*) were used also in the experiments of Report I. They have been used in the present experiments because our results of Report I [formulae (10) (11)] permit to express the " slowing down density " q and the density n of thermal neutrons in terms of their activities A_{Res} (detectors screened by Cd) and A_{th} (activity due to thermal neutrons). Throughout this report the units used shall be the same as in Report I.

The detectors (*a*) are rather wide and thick so that they introduce an appreciable perturbation in the neutron distribution around them. To avoid such perturbation at the positions where it would have affected our results we have used the thinner detectors (*b*). The narrow detectors (*c*) have been used for a direct measurement of the albedo to be described later.

If it were possible to measure the density of thermal neutrons with infinite accuracy we could calculate I. directly with (2). Actually it is not feasible to have the accuracy of the measurements better than 1 %. Consequently the error in the derivative $(dn/dr)_{r=R}$ would be very large.

We tried therefore to fit the observed $n(r)$ to a solution of the differential equation [(8) Rep. I]

$$\Delta n - \frac{3}{\lambda^2 N} n + \frac{3}{\lambda v} q = 0. \tag{9}$$

For this we must first determine $q(r)$, namely the number of nascent thermal neutrons per cm³ and second at a given distance from the source.

$q(r)$ was obtained by measuring the activity A_{Res} of our detectors (*a*) screened by cadmium. Equation [(10) Rep. I] gives then the " slowing down density " q_{In} for neutrons of energy of 1 ev (resonance energy of indium). From this we can determine easily q by integrating the differential equation [(1) Rep. I], and assuming an age difference $t = 50$ cm² [(2) Rep. I] between indium-resonance and thermal neutrons.

In fig. 2, the upper curve represents the observed values of the function $rq_{In}(r)$ plotted against r; the lower curve represents the result of the numerical integration and gives $rq_{th}(r)$ for the nascent thermal neutrons. It is seen that $rq(r)$ may be represented in the interval from $r = 8.5$ to $r = 35$ within the limits of the experimental accuracy by the expression

$$rq(r) = 4.73\times10^{-5} \sin(3°\cdot8\, r). \tag{10}$$

We substitute this expression of q in (9) and introduce instead of n the thermal activity A_{th}, related to n by [(11) Rep. I]. Since A_{th} is a function of r only, we obtain finally the following differential equation:

$$\frac{d^2}{dr^2}\left(rA_{th}(r)\right) - \frac{1}{l^2}\, rA_{th}(r) + 3.687 \sin(3^{\circ}\cdot 8\, r) = 0 . \tag{11}$$

We take, according to the latest measurements on the carbon cross-section

$$l = \lambda\sqrt{\frac{N}{3}} = 46.7 \text{ cm}. \tag{12}$$

The general integral of the differential equation is

$$rA_{th}(r) = 759 \sin(3^{\circ}.8\, r) + pe^{r/46.7} + qe^{-r/46.7}. \tag{13}$$

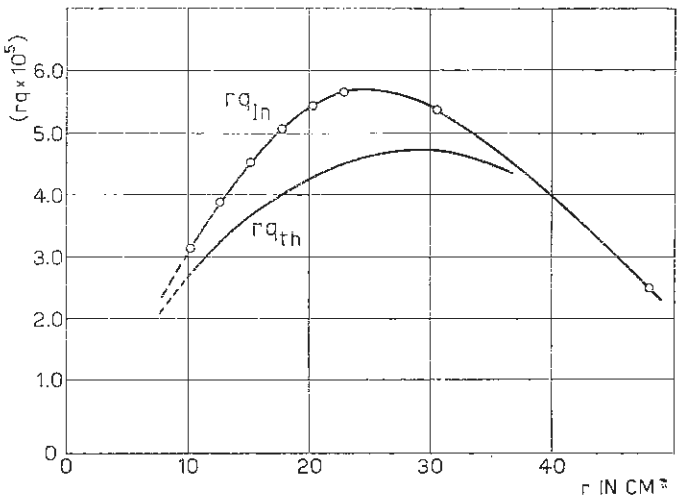

Fig. 2.

We determine the two integration costants p and q so as to fit in the best possible way the observed values of $A_{th}(r)$. For the reasons already explained, however, we have used for this measurement the thinner detectors (b) instead of the normal detectors (a) and multiplied the results by a transformation factor 4.193 that we found experimentally to be the ratio between the intensities of the two types of detectors at positions in graphite where the thermal neutron density is rather uniform.

The best fit is obtained by taking $p = 721$; $q = -1121$. The comparison between calculated and observed activities is shown in Table I. The agreement is seen to be very good.

We now can calculate A_{th} and dA_{th}/dr at $r = 8.5$ with a considerably greater accuracy than would be possible by a direct measurement. We find

$$A_{th}(8.5) = 333\left(\frac{dA_{th}}{dr}\right)_{r=8.5} = 41.8.$$

Since A_{th} is proportional to n we obtain from (2)

$$L = \frac{A_{th}(8.5)}{\left(\frac{dA_{th}}{dr}\right)_{r=8.5}} = 8.0 \text{ cm}. \tag{14}$$

An independent method for measuring L consists in determining first the albedo γ of the sphere. For this we observe that an indium detector that is backed by cadmium on one side is sensitive only to the thermal neutrons that arrive from the side not covered. The thermal neutron activity A_1 of such a detector when placed on the surface of the U_3O_8–sphere with its sensitive side facing outwards is proportional to the number N_1 of neutrons entering the sphere from outside. If the detector is placed with its sensitive side facing the sphere, its activity A_2 due to thermal neutrons is instead proportional to the number N_2 of thermal neutrons coming out of the sphere. The albedo γ is therefore given by the ratio A_2/A_1.

TABLE I.

rA_{th}

r	expt	calculated
10.2	475	469
12.7	648	659
15.2	837	833
17.8	984	990
20.3	1131	1128

In performing this measurement one should use detectors small enough so that the perturbation of the thermal neutron distribution due to the detector and to its cadmium protection should be negligible. We used therefore the narrow detectors (c) whose width is less than 1/10 of the mean free path of the neutrons. The observed intensities in arbitrary units were as follows:

	Activity
Uncovered face outside	3189
Uncovered face inside	2672
Both faces covered	1472

This gives $A_1 = 1717$; $A_2 = 1200$

$$\gamma = \frac{A_2}{A_1} = 0.70. \tag{15}$$

The correction due to the production of thermal neutrons inside the sphere can be estimated to be about 0.5 % and is therefore negligible.

With this value of γ we calculate from (6), taking $\lambda = 2.55$ cm.

$$L = 8.35 \text{ cm} \tag{16}$$

in good agreement with the previous value (14).

Similar measurements were performed also on a sphere of 5.65 cm radius filled with 5.5 Kg of powdered uranium metal. The two methods already described for the U_3O_8–sphere were applied and they gave for L the following results:

First method $L = 4.3$ cm

Second method $L = 3.7$ cm.

In Table II we summarize the results of the measurements and we compare them with the theoretical results:

TABLE II.

Substance	Radius cm	Density gm/cm³	L		
			First Method	Second Method	Theory
U_3O_8	8.5	3.6	8.0	8.35	8.0
U	5.65	7.3	4.3	3.7	5.4

The agreement is quite good for the U_3O_8–sphere; much worse for the metal sphere. The discrepancy is partly due to the fact that the metal powder used contained a very appreciable contamination by boron, as was shown by a chemical analysis. The amount of boron actually found can account, however, for only about one half of the observed discrepancy. The residual difference, which is however not much larger than the experimental error, seems to indicate a failure of the simple theory to represent quantitatively the observed absorption.

This is not surprising in view of the fact that the radius of the sphere is only twice the mean free path of the neutrons.

N° 143.

In the spring of 1941, at the request of the National Defense Committee,[1] the National Academy of Sciences appointed a special committee to review the military importance of the uranium work. Up to then, although some scientists like Szilard were convinced that atomic bombs were feasible, several members of the Uranium Committee had mainly taken in consideration a controlled chain reaction and doubted that atomic energy would come in time to affect the current war.[1]

The opinion of the National Academy committee evolved rapidly, as information from the scientists in the field became available to them: in May the committee submitted a first cautious report which placed the emphasis on power and discussed the difficulties of separating a sufficient amount of U^{235} for a bomb. The second report, in July, revealed the results of work on plutonium and mentioned the possibility of a plutonium bomb. Shortly afterwards the outlook for a U^{235} bomb brightened, owing both to progress in isotope separation and to information received from the British.

The following September, Arthur H. Compton, the chairman of the National Academy committee, sought first-hand information on the feasibility of a U^{235} bomb and went to see Fermi at Columbia University.[2] Compton writes that he had so far been very " cautious " in his conversations with Fermi for security reasons—clearly he could not bring himself to trust " a recently arrived émigré ". But then Samuel K. Allison had succeeded in allaying Compton's apprehension, at least to a certain extent. At Columbia Fermi stepped to the blackboard and worked out for Compton, according to Compton's own account, " simply and directly, the equation from which could be calculated the critical size of a chain reaction ". (Similar calculations had been made and discussed informally by others, according to Gregory Breit, member of the Uranium Committee). Compton learned that " the amount of fissionable metal needed to effect a nuclear explosion could hardly be greater than a hundred pounds ". On the train to Chicago he recalculated the critical size of a U^{235} bomb, and found his results in agreement with those of Fermi. (When a year later members of the Du Pont Company inquired on the trustworthiness of certain émigrés, Compton did not say directly that Fermi was all right, but stated that he had gone through Fermi's calculations himself and found the same results. Fermi, however, had the full confidence of the Uranium Committee and was appointed Chairman of the Subcommittee on Theory).

Gregory Breit asked Fermi to put his calculations in writing, but Fermi's notes on fast neutron reactions were brief, and in them he did not derive the formulas he used. Breit prepared the " Explanatory Remarks " that are here reproduced after Fermi's paper for his own as well as the Uranium Committee's edification.

On November 6, 1941, the National Academy committee submitted its third and most encouraging report. It discussed, among other questions, the feasibility and critical size of a U^{235} bomb. My guess is that the content of Paper N° 143 was the link between Compton's visit at Columbia and the third report of the Academy committee.

H. L. ANDERSON.

(1) H. D. SMYTH, *Atomic Energy for Military Purposes*, Princeton University Press, 1945.

(2) A. H. COMPTON, *Atomic Quest*, Oxford University Press, 1956.

143.

REMARKS ON FAST NEUTRON REACTIONS

Report A-46 (October 6, 1941).

Critical volume

$$V_c = 8.9 \frac{[\overline{(r^2)}]^{3/2}}{(\log k)^{3/2}}.$$

Assuming for U^{235}

$$\text{density} = 18\ \text{gm/cm}^3 \qquad \log k = 1\ (*).$$

Follows the critical mass:

$$M_c = \frac{4 \times 10^6}{(\sigma_t \sigma_f)^{3/2}} \text{grams}$$

σ_t and σ_f are the total and fission cross section in units of 10^{-24} cm^2.

Protecting with a scatterer of neutrons may reduce somewhat the critical amount.

σ_t and σ_f are not known for the energies of the secondary fission neutrons.

A possible guess may be $\sigma_t = 10$ $\sigma_f = 1$. This would give

$$M_c = 130{,}000 \text{ gr.}$$

However the cross sections may be very different and consequently M_c may be quite different. One cannot, in my opinion, exclude the possibility that M_c may be as low as 20,000 grams or as high as one or more tons.

Experiments on partially separated uranium isotopes seem to bear out the assumption that the fissions observed with neutrons of energy below 1 MeV are due to U^{235}. Such data might give only upper estimates if (*a*) a small percentage of higher energy neutrons is present in the source, or (*b*) the threshold for U^{238} fission is 0.35 ± 0.1 MeV as according to Haxby, Shoupp, Stephens, and Wells [1].

If a mass about twice the critical mass is assembled, the rate of multiplication of the neutrons will be about

$$1.4$$

each generation. Multiplication of the number of neutrons by e will then take place in a time of the order

$$t = \frac{1}{\log 1.4} \frac{\lambda}{v} \frac{\sigma_t}{\sigma_f}.$$

λ = mean free path

v = neutron velocity $\cong 10^9$ cm/sec.

(*) For definitions of symbols compare the «Explanatory remarks» by G. Breit, following this paper. (Note of Editors).

(1) O. R. HAXBY, W. E. SHOUPP, W. E. STEPHENS and W. H. WELLS, «Phys. Rev.», *58*, p. 199 (1940).

For $\sigma_f = 1$ it is

$$t = 6 \times 10^{-8} \text{ sec.}$$

If it were instead $\sigma_f = 3$ we would have

$$t = 2 \times 10^{-8} \text{ sec.}$$

The rate of the reaction increases by 10^4 in a time of the order of $10\,t$ and the velocity of the flying fragments shall be of the order

$$\frac{R}{10t}\ ^{(*)}$$

or about 10^7 cm/sec.

The estimate of this velocity and of the energy released in the reaction is again made very uncertain by our lack of detailed knowledge of the cross-sections of U^{235}.

The amount of energy released could be somewhat increased by surrounding the reacting unit with a very dense and thick layer of materials. This would increase the time before the reacting mass scatters and would also reflect in part the neutrons thereby reducing the amount of U^{235} needed.

EXPLANATORY REMARKS

G. Breit

The above notes of Professor Fermi's give a general picture of the process. On account of their brevity a few explanatory remarks may be in order. The formula for the mass can be understood as follows. Consider first an infinite medium in which the neutrons diffuse without slowing down. The diffusion is then described approximately by:

$$\Delta n - \frac{3}{\lambda_t \lambda'} n + \frac{3q}{v\lambda_t} = 0 \tag{1}$$

where

n = neutron density

λ_t = *m.f.p.* for any kind of collision

λ' = *m.f.p.* for a collision leading to absorption

v = neutron velocity

q = number of neutrons produced per cm^3 per sec. Assume that the only absorption is due to collisions leading to fission. Then:

$$\lambda' = \lambda_f$$

λ_f = *m.f.p.* for fission collisions.

One has:

$$q = \frac{v}{\lambda_f} n \cdot \eta$$

η = number of neutrons emitted per fission.

Hence

$$\Delta n + \frac{3(\eta - 1)}{\lambda_t \lambda_f} n = 0.$$

(*) R is the separation distance between the fragments at which the reactivity falls appreciably.

At the boundary of the sphere containing the uranium one sets $n = 0$. This boundary condition would be exact if the radius of the sphere were large compared with the mean free path and the distance within which a neutron reproduces itself. On these assumptions the differential equation for n gives the radius of the critical sphere R_c as:

$$R_c = \pi \left[\frac{\lambda_t \lambda_f}{3(\eta - 1)} \right]^{1/2} \tag{2}$$

and the mass:

$$M_c = \frac{4\pi}{3} \rho R_c^3 = \frac{4\pi^4}{3^{5/2}} \rho \frac{(\lambda_t \lambda_f)^{3/2}}{(\eta - 1)^{3/2}} \tag{3}$$

where ρ is the density.

In the notation:

$$10^{-24} \sigma = \text{cross section in cm}^2$$

one has for $\rho = 18$:

$$\lambda\sigma = 21.4$$

and:

$$M_c = \frac{4.4 \times 10^6}{(\eta - 1)^{3/2} (\sigma_t \sigma_f)^{3/2}} \text{ grams} \tag{4}$$

This formula is essentially the same as Fermi's. His $\log k$ is replaced here by $\eta - 1$. If $\eta - 1 \ll 1$ the two agree. For larger η the above discussion is not applicable because the diffusion equation (1) with an approximate q is then a poor approximation.

The replacement of $\eta - 1$ by $\log k$ is familiar in the theory of chain reactions with slowing down. Inside the medium one has [Report A – 9, Equus (1) to (4)]

$$\frac{\lambda}{3} \Delta n_t - \frac{n_t}{\lambda'} + \frac{\eta}{\lambda'_U} \int n_t(\vec{r}') \frac{e^{-\frac{(\vec{r} - \vec{r}')^2}{4\tau}}}{8(\pi\tau)^{3/2}} d\vec{r}' = 0 \tag{5}$$

where

n_t = density of thermal neutrons

λ = *m.f.p.* for a collision of thermal neutrons either of the scattering or absorption type

λ' = *m.f.p.* for a collision leading to absorption

λ'_U = *m.f.p.* for a collision leading to absorption in uranium which leads to fission

τ = neutron age $= \overline{r^2}/6$.

From (5) one finds:

$$-\frac{\lambda}{3} k^2 - \frac{1}{\lambda'} + \frac{\eta}{\lambda'_U} e^{-k^2\tau} = 0 \tag{6}$$

$$n = \sin kr/r.$$

For $\lambda\lambda' k^2 \ll 3$ i.e. for negligible diffusion after the neutrons have been slowed down one has:

$$k^2 \tau = \log \frac{\eta \lambda'}{\lambda'_U}$$

so that:

$$k^2 = \frac{6}{r_2} \log k \tag{7}$$

where

$$k = \frac{\eta \lambda'}{\lambda'_U} . \tag{8}$$

The quantity k is the number of fission neutrons per absorbed neutron times the chance that there is fission if the slowed down neutron is absorbed. It is the number of neutrons produced in one generation of the process of slowing down with consequent absorption leading to disappearance or to fission. The approximate boundary condition leads then to:

$$k R_c = \pi$$

so that:

$$R_c = \frac{\pi}{6^{1/2}} \frac{(\overline{r^2})^{1/2}}{(\log k)^{1/2}}$$

and:

$$V_c = \frac{4\pi^4}{3 \times 6^{3/2}} \frac{(\overline{r^2})^{3/2}}{(\log k)^{3/2}} = 8.8 \frac{(\overline{r^2})^{3/2}}{(\log k)^{3/2}} . \tag{9}$$

For small k one has $\log k = k - 1$. If all the absorption takes place by the uranium one has then $\log k = \eta - 1$ and Eq. (4) is obtained. If the replacement of $\log k$ by $\eta - 1$ is not made then one has:

$$M_c = \frac{4.4 \times 10^6}{(\sigma_t \sigma_f)^{3/2} (\log k)^{3/2}} . \tag{10}$$

Here $\overline{r^2} = 2 \lambda_t \lambda_f$ has been used in accordance with $\Delta n - (3/\lambda_t \lambda_f) n = 0$.

The use of $\log \eta$ instead of $\eta - 1$ in the last formula increases the estimated M_c. For the slow neutron chain reaction the use of $\log k$ is qualitatively correct. The difference between $\log k$ and $k - 1$ takes into account in this case the difference between a sinusoidal neutron density and its osculating parabola. On account of the presence of $e^{-k^2 \tau}$ in (6) a large η cannot lead to a very small R_c because a small R_c gives a large k which decreases the total number of fission neutrons represented by $\eta e^{-k^2 \tau}/\lambda'_U$. The effect of a large η is thus not as pronounced as it might be for a slow neutron chain.

This type of estimate may be too pessimistic because in the fast neutron case it may not be necessary for the neutrons to be slowed down by any appreciable amount and also because formula (5) is not quantitatively applicable in this case. One arrives in fact at a different result by considering the neutrons as diffusing without slowing down. A calculation carried out along the lines of Wigner's absorption considerations [Report A-20] gives:

$$\frac{\tan^{-1} (\pi \lambda_t / R_c)}{(\pi \lambda_t / R_c)} = \frac{1}{1 + (\eta - 1) \lambda_t / \lambda_f} . \tag{11}$$

This calculation should be an improvement on considerations starting with the approximate formula (1). It is not accurate in the treatment of the bound-

ary. For $\lambda_t/\lambda_f = 0.1$ and $\eta = 2.718$ the right side of (11) is 1/1.172. This is sufficiently close to unity to use:

$$\left(\frac{\pi\lambda_t}{R_c}\right)^2 \cong 3\,(\eta - 1)\,\frac{\lambda_t}{\lambda_f}$$

as an approximate solution. This agrees with (2). The error in using this approximation is not large. The approximation gives $\pi\lambda_t/R_c \cong \sqrt{3 \times 0.172} = 0.718$. The solution of $\tan^{-1}(\pi\lambda_t/R_c)/(\pi\lambda_t/R_c) = 1/1.172$ is $\lambda\pi_t/R_c = 0.76$. If one uses (4) instead of (10) the value of M_c comes out smaller by a factor of about 2.2. It is of course, premature to try to fix the mass to within a factor 2 on account of the lack of knowledge regarding cross sections.

N° 144.

The need to understand more thoroughly the slowing down of neutrons in graphite prompted Fermi to apply his earlier theory of the effect of chemical binding (paper N° 119 *a*, *b*) to this case. The following paper records his elementary calculations. This paper was probably written in October 1941.

H. L. ANDERSON.

144.

THE EFFECT OF CHEMICAL BINDING IN THE SCATTERING AND MODERATION OF NEUTRONS BY GRAPHITE

Report C–87.

The slowing down of neutrons by elastic collisions with atoms is determined by the simple laws of conservation of energy and momentum if the energy of the colliding neutron is so large that the atoms may be considered as free. Such an assumption is, however, not permissible when the energy of the neutrons is somewhat smaller than 1 ev. In this case the energy of the neutron becomes comparable to the quanta of elastic vibration of the atoms. This fact produces several effects:

a) The slowing down power of the substance per collision decreases below the normal value that would be observed in the case of free atoms.

b) The scattering cross-section for elastic collisions increases.

c) The angular distribution of the scattered neutrons is also affected.

An estimate of these effects can be obtained rather simply if we assume that each atom is bound by elastic forces to a fixed equilibrium position. In this case the theory can be carried through when graphite or any other substance with atomic weight larger than 1 is used as a moderator by the same method used in the case of slowing down by hydrogen [1]. Indeed, the discussion in the two cases is so similar that it is not worth while to repeat it for moderation by atoms heavier than hydrogen. Only the results shall be collected and discussed here for the case of moderation by carbon.

NOTATIONS AND FORMULAE.

We assume that each atom of the moderator is bound by elastic and isotropic chemical forces to an equilibrium position. Let ν be the frequency of the vibration.

(1) E. FERMI, « Ricerca Scientifica », 7, 2 (1936). [Paper N° 119-*a* and *b*. (Editors' note)].

Let p_0 and p be the momenta of the neutron before and after the collision. We introduce in place of them two proportional dimensionless quantities

$$P_0 = \frac{p_0}{\sqrt{2\,M h\nu}} \quad ; \quad P = \frac{p}{\sqrt{2\,M h\nu}} \tag{1}$$

where M is the mass of the neutron. P^2 is the ratio between the kinetic energy of a neutron of momentum p and the vibrational quantum.

When a neutron collides against an atom that is initially in the vibrational quantum state 0, the quantum state of the atom after the collision may be 0 or 1 or 2 or 3, $\cdots$ In the first case no energy is lost by the neutron in the collision; in the second case the neutron loses the energy $h\nu$; in the third case it loses the energy $2\,h\nu$, and so forth. We shall indicate by σ_0, σ_1, σ_2, $\cdots$ the cross-sections for these various processes. They are given by the following expressions:

$$\left.\begin{aligned} \sigma_n &= \frac{4\,a^2}{P_0^2}\cdot\frac{\pi A}{n\,!}\int_{\frac{2P_0^2 - n - 2P_0\sqrt{P_0^2-n}}{A}}^{\frac{2P_0^2 - n + 2P_0\sqrt{P_0^2-n}}{A}} \xi^n e^{-\xi}\,d\xi \qquad \text{for } n < P_0^2 \\ \sigma_n &= 0 \qquad\qquad \text{for } n > P_0^2 \end{aligned}\right\} \tag{2}$$

where A is the atomic weight of the moderator (more exactly the ratio between the atomic mass of the moderator and that of the neutron). a is a constant with the dimensions of a length that represents the strength of the interaction between the neutron and the atom. a is related to the limiting value of the scattering cross-section when the effect of the chemical binding becomes negligible by the following equation:

$$\sigma = 16\,\pi a^2\left(\frac{A}{A+1}\right)^2 \qquad \text{for } \frac{P_0^2}{2M} \gg h\nu. \tag{3}$$

The angular distribution of the scattered neutrons may be expressed in terms of a differential cross-section $\sigma_{n,d\omega}$ for processes in which the neutron excites the moderator atom to the vibrational quantum state n and is scattered inside the element of solid angle $d\omega$. This differential cross-section is given by the formula:

$$\sigma_{n,d\omega} = 4\,a^2\,\frac{P}{P_0}\,d\omega\,\frac{(\mathbf{P}-\mathbf{P}_0)^{2n}}{n\,!\,A^n}\,e^{-\frac{(\mathbf{P}-\mathbf{P}_0)^2}{A}} \tag{4}$$

where the bold type means that the corresponding momenta have to be taken as vectors. The value of the dimensionless momentum P after the collision is given by the conservation of energy. With our notations this gives: $P^2 = P_0^2 - n$.

Numerical results for carbon.

The numerical results calculated with the above formulae for the case of carbon, A = 12, are collected in Table I.

The top row of Table I represents the ratio $W/h\nu$ between the energy of the neutron before the collision and the vibrational quantum. The next six rows give for each value of $W/h\nu$ the percentage of collisions in which the neutron loses an amount of energy equal to 0,1,2,3,4, or 5 vibrational quanta. The next row gives the average change s of the logarithm of the energy. (This is the so-called slowing down power per collision; its limiting value for collisions with carbon when the chemical binding becomes negligible is 0.158). The last row gives the ratio between the scattering cross-section for neutrons of the given energy and the cross-section for neutrons of energy very large compared with the vibrational quantum.

TABLE I.

$\frac{W}{h\nu}$		0	0.5	1	1.5	2	2.5	3	3.5	4	4.5	5	5.5	6
Vibrational quanta lost by neutron	0	100	100	100	91.2	85	79.2	73.8	68.9	64.7	60.4	56.4	53.5	50.7
	1				8.8	15	19.8	23.3	26.1	28.4	29.8	31.3	31.5	31.9
	2						1.0	2.9	4.8	6.4	8.6	10.4	12.0	13.5
	3								0.2	0.5	1.1	1.8	2.7	3.5
	4										0.05	0.1	0.3	0.4
	5												0.006	0.03
s		0	0	0	0.097	0.104	0.117	0.127	0.133	0.133	0.139	0.141	0.143	0.142
σ/σ_∞		1.174	1.084	1.000	1.015	1.009	1.003	1.006	1.006	1.001	1.006	1.012	1.003	1.001

One can see from the preceding table that the chemical binding effect on the scattering cross-section is rather small. Its maximum value, $(A+1)^2/A^2$, corresponds to only 17 % (instead of 300 % in the case of hydrogen) and the difference is practically negligible for neutron energies in excess of one vibrational quantum. The effect on the slowing down power s is somewhat greater and the difference still amounts to about 10 % for neutron energies six times the vibrational quantum.

N° 145 and 146.

The interest in the fission of uranium by fast neutrons, partly because of the possibility of a fast neutron reaction (see paper N° 143), but also because of its contribution to the slow neutron chain reaction, led to the need for numbers, in this case for the cross sections involved. The available neutron sources were radon-beryllium, and radium-beryllium. Neutrons from these do not have the same energy spectrum as the fission neutrons, but one could at least come to know the order of magnitude, and there was reason to believe that the cross section would not be greatly energy-dependent (paper N° 145).

A sequel to this was a series of measurements of absorption cross sections for a number of elements, also with the radon-beryllium neutron source. This was a rough experiment made to have an idea of the magnitude of the cross sections. In particular, the cross section for the production of U^{239} was measured with somewhat more care.

H. L. ANDERSON.

145.

FISSION CROSS SECTION OF UNSEPARATED URANIUM FOR FAST Rn + Be NEUTRONS

H. L. ANDERSON and E. FERMI
Report C–83.

Report on experiments performed at Columbia University in November 1941 for the determination of the fission cross section of unseparated uranium by fast Rn + Be and Ra + Be neutrons.

The fissions were produced in a sample of 2.652 mg. of U_3O_8 spread on an area of about 10 sq. cm. This was placed inside an ionization chamber connected to a linear amplifier. The Rn + Be source was placed a few centimeters away from the ionization chamber. Care was taken to avoid the presence of substances that might have slowed down the neutrons. The data on the measurements are collected in Table I.

As an average result of the preceding measurements we find the fission cross section for fast radon plus beryllium and radium plus beryllium neutrons of about 0.45×10^{-24} cm^2. This result is dependent, of course, on the assumed

number of neutrons emitted per second by the source. Later measurements seem to indicate that this number might have been somewhat overestimated. If this is the case, the cross section should be correspondingly increased.

TABLE I.

Source	Q_0	r	Fiss/min	$\sigma_{fiss} \times 10^{24}$
Rn + Be	7.55×10^6	7.13	1.87	0.46
Rn + Be	7.81×10^6	10.1	0.83	0.43
Ra + Be	14.4×10^6	10.1	1.78	0.46

Column 1 – indicates the source of neutrons used.
Column 2 – gives the number of neutrons emitted by the source per second that was assumed in calculating the cross section.
Column 3 – gives the average distance between the source and the uranium samples.
Column 4 – gives the average number of fissions per minute.
Column 5 – gives the calculated cross section.

N° 146.

For the introduction to this paper see N° 145.

146.

ABSORPTION CROSS SECTIONS FOR Rn + Be FAST NEUTRONS

H. L. ANDERSON, E. FERMI, and G. L. WEIL
Report C–72.

The experiments described below on some capture cross sections measured for Rn + Be fast neutrons were carried out at Columbia University during November, 1941. The cross sections were measured by observing with a standardized Geiger-Müller counter the β activity induced in several substances by irradiation with the fast neutrons of a Rn + Be source from which the number of neutrons emitted per second was known.

In order to obtain adequate intensities, the substance to be irradiated was compressed in the form of a cylindrical ring 1.0 cm high, with outside diameter 1.16 cm and inside diameter 0.65 cm. The glass bulb containing the radon-beryllium mixture was approximately cylindrical in shape. It was about 0.65 cm diameter and 1 cm long. The compressed powder was supported by means of a light metal holder in the center of a room, so as to minimize the number of neutrons which might be slowed down and scattered into it.

The irradiation was started hy inserting the Rn + Be bulb in the center of the cylindrical ring. After irradiation, the powder was thoroughly mixed, spread in a thin layer of known weight on a piece of paper, covered with Scotch tape, and wrapped snugly around our Geiger-Muller counter in the manner described in report A–2, (N° 140) "Standards in Slow Neutron Measurements."

The results for Br, Au, In, I, Mn, and La are summarized in Table I. In the first line is given the substance irradiated and the half-life of the β–radioactivity investigated. In the second line is given the weight W in milligrams of the sample whose activity was measured. The third line gives the initial activity A_i observed in counts per minute. On the fourth line, the fraction of saturation activation achieved in the irradiation is given. In the fifth line is given the efficiency of the counter as calculated from the formula: Efficiency $= 0.48\, e^{-0.046\,\mu}$, where μ is the absorption co-efficient of the β–rays in gms per square cm. This formula is discussed in report A–2. In the sixth line is given the factor a by which the activity observed should be increased in order to take into account the absorption of the β–rays in the sample itself·

TABLE I.

	$PbBr_2$ (18 m.)	$PbBr_2$ (4.4 hr.)	Au (2.7 d.)	In (54 m.)	PbI_2 (25 m.)	MnO_2 (155 m.)	La_2O_3 (31 hr.)
Weight	360 mg.	360 mg.	96.4 mg.	141 mg.	645 mg.	239 mg.	365 mg.
Init. Act.	333	64	21	172	748	41	82
Irr. fraction	0.993	0.321	0.143	0.654	0.540	0.63	0.365
Efficiency	0.370	0.370	0.205	0.219	0.365	0.38	0.225
Abs. in sample	1.09	1.09	1.12	1.11	1.26	1.06	1.22
Q	3.38×10^6	3.38×10^6	3.12×10^6	2.86×10^6	3.46×10^6	3.8×10^6	2.55×10^6
Geom. factor	0.253	0.253	0.137	0.105	0.253	0.253	0.253
Atomic weight	184	184	197	115	231	87	163
σ	1.62×10^{-26}	0.96×10^{-26}	10.5×10^{-26}	9.9×10^{-26}	5.36×10^{-26}	0.19×10^{-26}	23×10^{-26}

The seventh line gives Q, the number of neutrons emitted per second by the source at the time of irradiation. In the eighth line is given the geometrical factor G for the irradiation. This is the ratio of the average path of neutrons through the substance in cm, to the volume of the substance in cm^3. In the case of Au and In, we used thin foils instead of compressed powder and for these substances, the geometrical factor was somewhat different. In the ninth line is given the atomic weight M of the element in question. The tenth line gives σ, the atomic cross section in cm^2 for neutron capture yielding the activity observed, as calculated by means of the formula given below.

$$\frac{A_i\, aM}{W f E\, 6.03 \cdot 10^{20} \cdot 60} = QG\sigma .$$

The above measurements were made only once, for it was our intention to obtain only a semi-quantitative indication of the order of magnitude of the cross section for these elements and an extensive investigation would have required more time than it appeared worth while to use. A somewhat more careful study was made in the case of uranium.

We were interested in determining the cross section for the formation of the 24–minute activity of U^{239}. This determination is made difficult by the presence of activities arising from fission. Since for neutrons of high energy the fission cross section is about 10 times larger than the capture cross section, it is necessary to eliminate the fission activities very completely in order to make the perturbation due to them reasonably small. In samples in which no separation was performed, the fission activities were about 20 times as intensive as the activity under investigation. We carried out several determinations and in all of them we made use of an ether separation to remove the fission activities. In two cases, we carried out in addition a phosphate precipitation of uranium and in two other cases we carried out an acetate precipitation in addition to the ether separation in order to remove more completely the activities arising from the fissions. In all cases we determined the number of atoms on the sample by observing the growth of uranium X. In the case of the ether separation only, we obtained for the cross section 13.0×10^{-26} cm^2. When the phosphate precipitation was carried out in addition, we obtained instead 6.6×10^{-26} cm^2 and 5.6×10^{-26} cm^2. With the acetate precipitation we obtained 4.8×10^{-26} cm^2 and 5.5×10^{-26} cm^2. This indicates that the ether separation alone was insufficient for a complete purification and the successive phosphate or acetate precipitation further removed some of the contaminating activities. Assuming that in these last cases all the impurities had been removed we find thus a cross section of about

$$6 \times 10^{-26}$$

for absorption of fast Rn + Be neutrons by uranium. This result is of the same order of magnitude observed for the other elements for which a fairly high level density is to be expected. From this point of view, the result obtained for uranium seems quite reasonable. However, in view of the fact that our separation from the first activities may not have been complete, we give this result as an upper limit.

N° 147 and 150.

Recently, in a biography of Galileo, I read an account of his activities immediately following the completion of his first telescope. As he trained it on the heavenly bodies, he recognized, immediately, that he had uncovered a new world of possible scientific exploration, and he could not resist setting out at once to chart this world. Systematically, night after night, he explored; he mapped the moon, discovered and labeled planetary satellites and analyzed their motion and the implications of his discoveries – until, when he was finished with his first fury of exploration, a map of the new world had been drawn. There were details to be filled in, the accuracy would be improved upon, better instruments would be made and they would explore further; but the main and important outlines were charted and the paths for further exploration marked.

What struck me most forcibly in this account is that, had the name Fermi been substituted for that of Galileo, it would have been completely in character. Here was Fermi immediately following the extraction of the first thermal neutron beams from the Argonne " pile ", or on any one of the other occasions when he was confronted with a new instrument.

Not that Galileo ever submerged himself so completely in the detail that he lost sight of the larger problem; he had always in mind, and periodically returned to, those systematic investigations which eventually destroyed the earth-centered universe; but with frequent excursions into new fields uncovered by reasoned extrapolation (i. e., theory) or improved instrumentation. And so it was with Fermi. Neither he nor Galileo could any more resist uncovering and following a promising scientific lead than they could resist breathing. (Before, I had thought of Fermi as a unique genius; or, if he had any precedents, possibly following in the tradition of Rayleigh. But it is clear that the genetic line runs straight from Galileo to Fermi).

My collaboration with Fermi in research was confined to work at Columbia University in 1941–42, during the formative stages of the " Plutonium Project ". The two papers on which our names appear together (N° 147 and 150), neither of them especially significant, illustrate (in a rather minor key) the points made above concerning Fermi's style of research. The more important one (N° 150) " concerns some experiments performed to ascertain whether a given lattice of uranium oxide lumps embedded in graphite could give a divergent chain reaction if its dimensions were made sufficiently large ". It is a report on the first of that long series of tests, of different lattice dimensions, materials of various fabrications and forms, which eventually led to the first successful chain reaction under the West Stands at the University of Chicago.

The results of this first test were inconclusive. Neither the uranium nor the graphite had the hoped-for purity; the density of the oxide was too low. All this was eventually to be improved, as a result of many efforts, but there remains the vivid memory of the unique excitement which accompanied those first attempts to see if the chain reaction was possible with the material then rapidly becoming available; the working out of the details of construction for the " exponential pile ", and of making measurements on it; with everyone joining in on all the details, from Fermi (face black from the dust of graphite-machining, now piling bricks but more often manipulating that sliderule, that link between his hands and his brain, from which he was inseparable), to the young graduate student borrowed from another group to provide another pair of hands.

The other paper (N° 147) represents one of those excursions into a short byway. The origin was an idea, advanced by Szilard, that it should be possible to find, in an appropriate photoneutron source, an energy spectrum resembling more closely that of the fission neutrons than was the case for the spectrum from the conventional mixture of radium and beryllium. (Experiments on the cross sections, etc., of various materials for fission neutrons had then to be performed, perforce, with artificial sources). The most rapid way of obtaining a comparison of fast neutron energies from different sources was to compare their " slowing-down

lengths " in some moderating material, say graphite, and Fermi suggested the of the use " exponential pile " of pure graphite for this purpose. The theory had already been worked out in connection with the exponential experiment for measuring neutron reproduction (probably it had already been worked out in the Rome days) and the application was straightforward and uncomplicated. But, with the data in hand, only a small amount more of computation would yield a new and basic piece of information: the absolute neutron yield from beryllium when bombarded in a standard geometry by the photons from radium. Why not take the small extra trouble to extract this number too; who could know when it might turn out to be useful?

As a student, one learned from Fermi mainly by observation and emulation. In an experiment, you did your assigned job, and more if you were able; but the pace was set by Fermi, and it was always fast. You had to get up early in the morning to be able to bring, to an enterprise in which Fermi was involved, some contribution which he had not already worked out. I mean this statement literally. I learned Fermi's secret quite by accident one morning, in the dormitory of the old Argonne Laboratory (transportation was difficult in those days, and we frequently stayed the night when we had an experiment going), when I happened to awake at around 5 A.M.; there he was, sitting cross-legged on his bunk, an Italian Buddha, slide rule on his lap, busily working out in his notebook the day's program. No wonder, when you rushed in bright and early with a new idea, it was already all worked out; you were never quite bright or quite early enough! In the classroom the pace was slower —it was Fermi's one concession—but, otherwise, it was not much different.

Paper N° 147 was reissued by the Atomic Energy Commission, Technical Information Branch, Oak Ridge, Tenn., as Report MDDC—1438, November 5, 1948.

B. T. FELD.

147.

NEUTRONS EMITTED BY A Ra+Be PHOTOSOURCE

B. T. FELD and E. FERMI

Report CP-89.

In this report an account is given of experiments performed at Columbia University in November 1941 on certain properties of the photoneutrons emitted by beryllium irradiated with gamma rays from radium.

The slowing down of the photoneutrons in graphite was investigated by taking activity measurements of indium detectors inside a graphite pile in which the source was included and the slowing down properties were expressed in terms of a two-range formula. Also the number of neutrons emitted by the photosource was measured by comparison with a Ra + Be source of known intensity.

DESCRIPTION OF PHOTONEUTRON SOURCE.

The photosource used consisted of a beryllium cylinder of 8 cm diameter and 8 cm height and a total weight of 608 grams. An axial cylindrical hole of 3.2 cm diameter was bored through this cylinder and the radium two-gram

source was inserted in this hole near the center of the beryllium block. Due to a somewhat indefined construction of the radium source this centering could be achieved only approximately.

Measurements in graphite column.

The photosource was inserted in a column of graphite bricks with a cross section of 4 by 4 feet and a height of 7 feet. The source was placed on the axis, 2 feet from the bottom face of the column. Indium detectors of the standard Columbia type were inserted and measured at various positions inside the pile. The result of these measurements is given in Table I; for comparison also the results of a similar measurement with the source No. 1 (1.16 gr Ra + Be) is given.

Table I.

Position	Photosource				Ra + Be Source		
	No Cd	Cd	Thermal	Calc. (Cd)	No Cd	Cd	Thermal
4,2,0	66417	17856	45884	17730	169200	34710	129200
8,2,0	50833	10595	38649	10690	140800	25040	112000
12,2,0	33874	4846	28303	4810	109200	14970	91970
16,2,0	21489	1773	19448	1710	78600	7920	69530
20,2,0	13887	524	13283	507	54080	3954	49530
28,2,0	5412	30	5377	27	24360	770	23470
36,2,0	2340	2	2337	1	10730	149	10560
44,2,0	1026		1026		4683	28	4652
52,2,0	419				1788	7	1780

In Table I the first column gives the coordinates of the position of the detector in a system of coordinates having the source as origin and the x axis vertical along the axis of the column. The coordinates are expressed in inches. The next three columns give the intensities of indium detectors in counts per minute reduced to the normal counter " Heffalump " without cadmium (column 2), with cadmium (column 3), and due to thermal neutrons (column 4). This last is calculated by subtracting from column 2 the data of column 3 multiplied by 1.15 in order to take into account the absorption of the cadmium on the resonance neutrons. Column 5 gives the activity with cadmium (as in column 3) calculated with a formula to be discussed later. The last three columns give the activities without cadmium, with cadmium, and due to thermal neutrons obtained when the photosource was substituted with Ra + Be source No. 1.

Discussion of results.

A comparison of columns 3 and 7 of Table I shows immediately that the resonance activity of the indium detectors decreases as a function of the distance from the source much more rapidly in the case of the photoneutron source than it does with the Ra + Be source. This different behavior is due to the fact that the photoneutrons have a mean energy much lower than the neutrons emitted by the Ra + Be source.

The resonance activity of the indium detectors given in column 3 may be represented rather accurately in terms of the following two-range formula:

$$(1) \qquad A_{res} = 9000\, e^{-(x/29)^2} + 13000\, e^{-(x/22)^2}.$$

The data of column 5 in Table I are calculated with this formula and it can be seen that they agree very well with the experimental data given in column 3. From equation 1 we can calculate in the usual way the percentages of neutrons belonging to the two ranges. The result is:

$$\text{Photoneutrons} \begin{cases} 61.3\ \% \text{ have indium range } 29 \text{ cm} \\ 38.7\ \% \text{ have indium range } 22 \text{ cm}. \end{cases}$$

As a mean indium range (calculated as square root of the mean square) we find for the photoneutrons 26.5 cm.

This last value should be compared with the mean range calculated in a similar way for the neutrons of a Ra + Be source which is 39.2 cm. The large difference between these two mean ranges is due to the difference in the energy of the neutrons emitted by the two sources.

Quantitatively the difference in the mean square ranges is related to the energies W_1 and W_2 of the neutrons emitted by the two sources by the following expression:

$$(2) \qquad r_2^2 - r_1^2 = 8.93\, \lambda^2 \log \frac{W_2}{W_1}$$

where λ is a suitable mean value of the mean free path in the energy interval between W_1 and W_2. We find:

$$\lambda^2 \log \frac{W_2}{W_1} = 93.4.$$

If we assume the mean free path in the energy interval in question to be about 6 cm, this formula gives a reasonable estimate of the ratio between the energy of the neutrons emitted by the two sources.

The data of Table I give also the ratio between the number of neutrons emitted by the two sources. We find by a simple calculation: Intensity of photosource = 0.231 × Intensity of Ra + Be source. Taking the intensity of the Ra + Be source No. 1 to be 14×10^6 neutrons per second, we find that the intensity of the photosource is 3.2×10^6 neutrons per second.

This result enables us to find that the number of photoneutrons emitted by one gram of beryllium at a distance of 1 cm from one gram of radium is 30,000 per second.

N° 148.

An interesting application of the graphite column which we had erected at Columbia was to use it as a source of thermal neutrons in a measurement of the cross section of boron. Boron had importance in absolute neutron measurements because its neutron absorption cross section was high and had a $1/v$ dependence. Previous measurements had given too low values for this cross section because the neutrons used, generally from paraffin, were not in thermal equilibrium. Neutrons from graphite were more likely to be thermal, and the measurement described in the following paper gave indeed a much higher cross section. A little too high, as it turned out because of an interesting property of crystalline graphite, which we were to study later (see paper N° 191), to produce neutrons somewhat colder than the room temperature.

H. L. ANDERSON.

148.

THE ABSORPTION CROSS SECTION OF BORON FOR THERMAL NEUTRONS

H. L. ANDERSON and E. FERMI
Report C–74.

In previous experiments, the absorption cross section of boron had been measured, using neutrons which had been slowed down in paraffin. It was generally assumed that neutrons emerging from a paraffin block which were captured by cadmium were practically identical to thermal neutrons. Since, however, the cut-off of cadmium extends beyond the thermal energy region, the energy distribution of neutrons absorbed by cadmium will be different from the Maxwell-Boltzmann distribution. The fact that the several determinations of the boron cross section reported in the literature vary widely between 500 and 650 is probably to be ascribed to this fact. Presumably, different amounts of paraffin were used around the source so that the average energy of the neutrons absorbed by cadmium might be expected to differ appreciably.

The importance of this fact has been demonstrated and stressed recently by the experiments performed by Manley (Report C–19) and by Bacher and Baker (Report C–25).

When neutrons are slowed down by carbon, it is possible to separate completely neutrons which are in thermal equilibrium from those of higher energy. This is due to the long diffusion path of thermal neutrons in carbon. We have carried out a measurement [1] of the boron absorption cross section

(1) The measurements were performed at Columbia University in January, 1942.

with neutrons emerging from the top surface of a large graphite column (cross section 4 feet hy 4 feet). The top surface of the column was 4 feet from the source, so that virtually only thermal neutrons could emerge.

The experimental arrangement is shown in fig. 1. As an absorber we used boron trifluoride gas in a fairly thin-walled (1 mm thick) dural cylindrical container. As detector, two large boron trifluoride counters were used and were placed somewhat above the top center of the cylindrical chamber. The

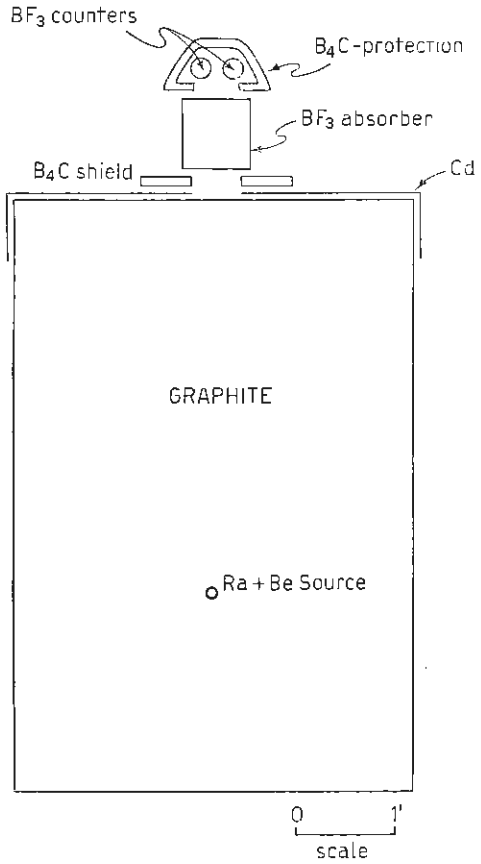

Fig. 1.

top surface of the graphite column was completely covered with cadmium, except for a circular opening 13 cm in diameter in its center. The absorption chamber and the boron trifluoride counters were placed directly above this opening. A circular disk of cadmium could be placed so as to cover the 13 cm opening and measurements were taken with and without this cadmium cover. Additional B_4C shields were used to protect the counters from stray neutrons.

The results are tabulated in Table I. In the first column is given the pressure of boron trifluoride in the chamber reduced to 0° C; in the second column is given the number of counts per minute ohserved without cadmium; the third column gives the number of counts per minute observed with cadmium, due to a large extent to radioactive contamination of the counters;

the fourth column gives the difference between columns 2 and 3 and represents the number of disintegrations observed due to thermal neutrons which were transmitted by the absorber. In the fifth column the transmission of the absorber is tabulated. In the sixth column is given the effective energy of the neutrons traversing the absorber as taken from the curves given in Bethe.[2]

TABLE I.

Boron absorption.

Pressure at 0° C	Observed Counts per Minute		Difference	Transmission	Effective Neutron Energy
	No Cd	Cd			
0	195.4 ± 1.0	46.1 ± 0.5	149.3	100	—
70.5	143.0 ± 1.0	45.8 ± 0.8	97.2	65.1	0 935 kT
145.1	109.2 ± 0.4	44.0 ± 0.7	65.2	43.7	1.034 kT

The length of the absorber was 20.4 cm. However, the actual length of path has to be increased slightly on account of two corrections, obliquity of the path, which amounts to 3.2 per cent, and the effect of the scattering of the walls of the container, which amounts to about 1 per cent. Thus we have taken as effective length 21.3 cm.

From these data we calculate a cross section of boron trifluoride for neutron energy equal to kT ($T = 300°$ K) of 469 cm² per mole, corresponding to a cross section of 778×10^{-24} cm² per molecule. The scattering cross section of the molecule may be estimated to be about 12×10^{-24} cm². Due to our particular geometry some of the scattered neutrons strike the detector, and we may consider that the absorption cross section per atom of boron is 770×10^{-24} cm², corresponding to a cross section of 464 cm² per gram atom.

This result is the cross section for the boron trifluoride which we used. It is probable that the impurities in this gas may have been of a few per cent, although air components were eliminated by freezing the BF_3 with liquid air and pumping away the non-condensable impurities. A determination of the molecular weight of the gas used was made and it was found to correspond quite closely to the theoretical value. This fact precludes the possibility that more than one boron atom per molecule could have been present in our gas.

A quantity of this gas was stored in a copper container so that it could be used to fill boron trifluoride counters, the cross section of which it was desired to know.

(2) H. BETHE, « Rev. Mod. Phys. », **9**, 136 (1937).

N° 149 and 150 (*).

It became clear from the measurements on uranium and graphite that the chain reaction in a natural uranium-graphite system might be possible, but only by exercising the greatest care in guarding against undesirable losses of neutrons. In particular, the loss by leakage of the neutrons from the confines of the structure could only be reduced sufficiently by making a very large structure indeed. To test with a smaller structure whether a larger one would work, Fermi invented the exponential experiment. The scheme was the same as that used to measure the absorption in graphite. In a rectangular column, this time made up with the uranium-graphite lattice, a neutron source is placed near the base. The exponential decrease in the neutron density along the length of the column will be greater or less than that expected due to leakage according to whether the reproduction factor is less than or greater than one.

The accuracy of the experiment increases with the size of the column, so that it was necessary to wait until a fairly large amount of graphite and uranium oxide could be obtained. A new grant of $ 40,000 was obtained from the Uranium Committee and by the end of September 1941, enough material had arrived to permit a definitive test with a particular choice of lattice, using a column of base 8 feet by 8 feet, and 11 feet high. The result of the measurement gave for the reproduction factor $k = 0.87$. This was appreciably under 1, but it was possible to think of enough improvements in purity, geometry, and density of uranium so that the prospects for a k greater than 1 looked fairly promising.

It had now become quite clear how to proceed. All the essential ideas were collected and written in paper N° 149, which is the basic paper on the chain reaction, and makes clear how the results of the exponential experiment were to be interpreted. The second, companion paper, describes and gives the result of the first exponential experiment.

H. L. ANDERSON.

149.

NEUTRON PRODUCTION IN A LATTICE OF URANIUM AND GRAPHITE

Theoretical Part.
Report C–12 (March 17, 1942).

This report contains some general theoretical points of view for the discussion of chain reaction experiments in which uranium (metal or oxide) is used in the form of lumps imbedded in a mass of graphite and disposed in a lattice structure.

Such an experiment has been discussed already several times from the theoretical point of view. It seemed advisable, however, to collect the various results in a systematic form. In particular, the theoretical questions that

(*) See also the introduction to N° 147 and 150 by B. T. Feld.

have arisen in connection with the interpretation of the first "intermediate experiment" with U_3O_8 and graphite shall he presented and discussed in this report.

Summary.

1. Reproduction factor in an infinite lattice.

We consider an array of uranium lumps disposed in a lattice of cell side o in a mass of graphite. Fast neutrons after being produced in the uranium lumps are slowed down to thermal energies by collisions, primarily against the carbon atoms and after reaching thermal energy keep on diffusing through the mass until they are absorbed by either the uranium or the carbon atoms. Some of the neutrons absorbed by the uranium atoms produce fission processes in which new fast neutrons are emitted, and a new cycle of slowing down and absorption begins. A cycle as described above shall be called a "generation." Thus we may talk of primary neutrons, of neutrons produced in the first generation, in the second generation, and so forth.

For the discussion of the chain reaction the fundamental magnitude to be considered is the reproduction factor k. This is by definition the average number of new fast neutrons produced in an infinite lattice by one original fast neutron in the first generation. For one primary neutron produced in the lattice there will be in the average 1 neutron in the 0 generation; k in the first generation; k^2 in the second; etc. . . or altogether

$$1 + k + k^2 + \cdots \tag{1}$$

neutrons. This series diverges for $k > 1$, in which case the production of neutrons is infinite. If $k < 1$ the sum (1) converges to the limit $1/1 - k$.

If the lattice is not infinite the reproduction factor will be reduced on account of the loss of neutrons due to leakage outside. Besides k we shall, therefore, have to consider also an effective reproduction factor $k_{eff} < k$ for lattices of finite dimensions.

We shall first consider the properties of an infinite lattice.

We consider a fast neutron emitted in one of the lumps. This neutron diffuses through the mass and after about one hundred collisions against the carbon atoms its energy is reduced to thermal energy. During this slowing down process some of the neutrons will, however, be absorbed by uranium in the resonance process. Let p be the fraction of the neutrons that is not absorbed at resonance.

Once a neutron is reduced to thermal energy it may be absorbed finally either by the uranium or by the carbon. Let f be the probability that a thermal

neutron is absorbed by uranium. We indicate by η the average number of fast neutrons produced when a thermal neutron is absorbed. We have then the equation,

$$k = \eta p f. \tag{2}$$

The density of neutrons of the various energies throughout the lattice is a function of the position. If each uranium lump in an infinite cubic lattice produces the same number of fast neutrons that are subsequently slowed down and ultimately absorbed, the symmetry is such that the normal derivative of the density at the boundary of each lattice cell having a uranium lump in its center is zero. This boundary condition is clearly equivalent to surrounding the cell with a perfect reflector for neutrons of all energies so that we may treat a cell as a separate unit.

2. The thermal neutron absorption in a cell.

We may simplify the mathematical problem without introducing a large error by discussing the behavior of a spherical instead of a cubical unit. We shall later discuss in some detail the differences between the spherical and the cubical cell.

We shall discuss first the case of a spherical uranium lump of radius R_1 imbedded in the center of a graphite sphere of radius R_2. The radii are chosen so that the volumes of the two spheres are equal to the volume of the uranium lump and to that of the cubical cell.

The density n of the thermal neutrons in graphite obeys the differential equation (eq. (13) of report A–21) (*)

$$\Delta n - \frac{3}{\lambda N} n + \frac{3}{\lambda v} q = 0 \tag{3}$$

where q is the rate of production of nascent thermal neutrons in the graphite. In integrating (3) we shall assume q to be constant in the graphite between the two spheres R_1 and R_2. This assumption is quite good for cells that are not too large and sufficiently correct for cells of the sizes that have been actually used.

The differential equation (3) must be integrated in the space between the two spheres R_1 and R_2 with the following boundary conditions

$$\frac{dn}{dr} = 0 \qquad \text{for } r = R_2 \tag{4}$$

$$\frac{n(r)}{\frac{dn}{dr}} = \frac{\lambda}{\sqrt{3}} \frac{1+\gamma}{1-\gamma} \qquad \text{for } r = R_1. \tag{5}$$

The second of these boundary conditions is obtained from equations (2) and (6) of report A–1.(**) γ is the albedo of the uranium sphere given by formula (7) of the same report. See also Report A–40 by Creutz, Wilson and Wigner.

(*) Paper N° 136. (Editors' note).

(**) Paper N° 142. (Editors' note).

The integral of (3) satisfying the boundary conditions (4) and (5) is

$$n = \frac{q\lambda N}{v} + \frac{1}{r}\left[Ae^{r/l} + Be^{-(r/l)}\right]. \tag{6}$$

where we have used the following notations

$$l = \lambda\sqrt{\frac{N}{3}} \qquad \alpha = \frac{R_1}{l} \qquad \beta = \frac{R_2}{l} \qquad s = \frac{1}{\sqrt{N}}\,\frac{1+\gamma}{1-\gamma} \tag{7}$$

$$\left.\begin{aligned} A &= -\frac{3l^3 q}{\lambda v}\,\frac{\alpha^2(1+\beta)e^{-\beta}}{(\alpha+s-\alpha s)(1+\beta)e^{-(\beta-\alpha)} - (\alpha+s+\alpha s)(1-\beta)e^{\beta-\alpha}} \\ B &= \frac{3l^3 q}{\lambda v}\,\frac{\alpha^2(1-\beta)e^{\beta}}{(\alpha+s-\alpha s)(1+\beta)e^{-(\beta-\alpha)} - (\alpha+s+\alpha s)(1-\beta)e^{\beta-\alpha}} \end{aligned}\right\} \tag{8}$$

The fraction f of the thermal neutrons absorbed by uranium is determined as follows. Thermal neutrons are produced in the volume

$$\frac{4\pi}{3}(R_2^3 - R_1^3) = \frac{4\pi}{3}l^3(\beta^3 - \alpha^3)$$

between the two spheres at the rate of q per cm^3 and per second. The rate of production is thus $\frac{4\pi l^3 q}{3}(\beta^3 - \alpha^3)$ per second. On the other hand the number of neutrons absorbed per second by the carbon between the two spheres is the integral $\int \frac{vn}{\lambda N}\,dt$ taken on the volume t between the spheres. The thermal neutrons absorbed by uranium are given by the difference between the number of thermal neutrons produced and the number of thermal neutrons absorbed by carbon, i.e.:

$$\frac{4\pi}{3}l^3 q(\beta^3 - \alpha^3) - \int \frac{vn}{\lambda N}\,dt.$$

The fraction f of the thermal neutrons absorbed by uranium is by definition the ratio of this number to the total number of nascent thermal neutrons. This expression can be calculated easily by substituting for n expression (6) and performing the integral. We find:

$$f = \frac{3\alpha^2}{\beta^3 - \alpha^3}\,\frac{(1-\alpha)(1+\beta)e^{-\beta+\alpha} - (1+\alpha)(1-\beta)e^{\beta-\alpha}}{(\alpha+s-\alpha s)(1+\beta)e^{-\beta+\alpha} - (\alpha+s+\alpha s)(1-\beta)e^{\beta-\alpha}}. \tag{9}$$

We shall also need the expression of the density of the thermal neutrons at the edge of the carbon sphere. This is calculated by putting $r = R_2$ in (6). Its explicit expression is:

$$n(R_2) = \frac{3ql^2}{\lambda v}\left[1 - \frac{2\alpha^2}{(\alpha+s-\alpha s)(1+\beta)e^{-\beta+\alpha} - (\alpha+s+s\alpha)(1-\beta)e^{\beta-\alpha}}\right]. \tag{10}$$

In the experiment described in the experimental part of this report cubical boxes of 8″ side filled with 60 pounds of U_3O_8 powder were imbedded in a graphite mass and disposed in a cubic lattice of 16″ cell side.

For the graphite used (density 1.63) we take

$$\lambda = 2.55 \text{ cm} \qquad l = \lambda\sqrt{\frac{N}{3}} = 45 \text{ cm}.$$

We have, furthermore,

$$R_1 = 12.6 \text{ cm} \qquad R_2 = 25.2 \text{ cm}$$

$$\alpha = 0.28 \qquad \beta = 0.54 \qquad \frac{1+\gamma}{1-\gamma} = 4.32 \qquad p = 0.141.$$

With these values we calculate from (9)

$$f = 0.873 \tag{11}$$

and from (10)

$$\frac{vn(R_2)}{q} = 327 \text{ cm}. \tag{12}$$

Experimental verification of this result is discussed in the experimental part. The number of nascent thermal neutrons produced per unit time in the cell is

$$\frac{4\pi}{3}(R_2^3 - R_1^3)\, q .$$

Of these

$$\nu_u = \frac{4\pi}{3}(R_2^3 - R_1^3)\, q f$$

are absorbed by uranium and

$$\nu_c = \frac{4\pi}{3}(R_2^3 - R_1^3)(1 - f)$$

are absorbed by carbon. From (11) and (12) we obtain for our special case

$$\begin{cases} \nu_u = 156\, vn(R_2) \\ \nu_c = 23\, vn(R_2) . \end{cases} \tag{13}$$

3. Comparison of the spherical with the cubical cell.

We have also calculated for the cell used in the experiment the differences introduced by substituting the actual cubical cell by a spherical cell.

In a cubical cell the density of the thermal neutrons is different at various points on the surface. It is a minimum at the center of the faces and a maximum at the corners. If we substitute a spherical cell in place of the cubical cell the intensity $n(R_2)$ on the surface must be taken with a value intermediate between the minimum and the maximum values on the surface of the cube. A numerical calculation for the cell used in the experiment gives the following ratios for the densities n at various points on the surface of the cubical cell to the density $n(R_2)$ on the surface of the equivalent spherical cell

$$n \text{ (center of face)} = 0.81\, n(R_2)$$

$$n \text{ (center of side)} = 0.98\, n(R_2)$$

$$n \text{ (corner)} = 1.10\, n(R_2) .$$

4. Resonance absorption.

The problem of determining p, the fraction of neutrons which escape resonance capture by uranium, has been studied quite extensively by the Princeton group. From their results one can calculate the " resonance volume " for a uranium lump. A simple formula for estimating the resonance volume is the following

$$V_R = 0.42\,M + 1.2\,S$$

where M is the mass of the lump in grams and S its surface in cm^2. The coefficients in the preceeding formula have been calculated making use of data obtained at Princeton and communicated by Wigner at the Chicago colloquium. It was indicated that such data were still based on preliminary results and could be still subject to revision.

For the lumps used in the Columbia experiment of 1941 the formula gives

$$V_R = 14400 \text{ cm}^3$$

from which it can be estimated

$$p = 0.79.$$

5. Behavior of a uranium-graphite system of finite size.

In the so-called " intermediate experiments " on uranium-graphite systems, measurements are performed on lattices containing a fairly large number of cells; the dimensions, however, are considerably smaller than the expected critical dimensions. Indeed the main purpose of such " intermediate experiments " is to determine whether for the given lattice k is larger or smaller than 1, and to estimate the critical dimensions if k proves to be > 1, without using the large amounts of materials required to reach actually the critical dimensions.

The behavior of a lattice containing a large number of cells can be described in first approximation by neglecting the small scale periodic structure and substituting for the actual inhomogeneous system an equivalent homogeneous system. The densities of neutrons of various energies inside the lattice are functions of the position. Such densities, besides a more or less regular variation from cell to cell, have local variations inside the cell reproducing the periodicity of the lattice structure. The approximation introduced in this section consists in averaging n over such local variations so as to represent the various densities as smooth functions such as one would expect in a homogeneous uranium-carbon mixture.

We may describe the diffusion of thermal neutrons in terms of an equation similar to (3); we notice, however, that in a uranium-carbon system the absorption of thermal neutrons is much greater than in pure graphite on account of the absorption of uranium. In actual cases uranium may absorb up to

ten times more than graphite. The average number N of collisions of a thermal neutron before being captured is, therefore, much less than it would be in graphite. We call Λ the mean free path for absorption (corresponding to λN in (3)) and we write

$$\Delta n - \frac{3}{\lambda\Lambda} n + \frac{3}{\lambda v} q_{th} = 0. \tag{14}$$

It should be noticed that λ in (3) and in (14) is not exactly the same, since also the mean free path is affected, although to a much smaller extent, by the presence of the uranium. If there were no resonance absorption, the density q of the production of nascent thermal neutrons could be calculated with the following equation (eq. (1) of the report A–21)

$$\Delta q = \frac{\partial q}{\partial t} \tag{15}$$

where

$$t = \frac{r_0^2}{4} \tag{16}$$

is the slowing down age for the nascent thermal neutrons and r_0 the corresponding range. Due to the resonance absorption a fraction $(1 - p)$ of the neutrons is absorbed during the slowing down process. We can take into account this factor by taking at $t = 0$ in equation (15) q equal to the density of production of fast neutrons multiplied by p. Assuming that we have a primary source of fast neutrons of density Q besides the production of fast neutrons by uranium $\left(\text{density: } \eta f \frac{v}{\Lambda} n\right)$ we obtain taking into account (2):

$$q\,(t = 0) = pQ + k \frac{v}{\Lambda} n. \tag{17}$$

A solution of (14), (15) (17), may be obtained easily for the case that depends on the space coordinates as a simple harmonic wave, $e^{i\boldsymbol{\omega}\cdot\boldsymbol{r}}$. In this case it is easily verified that the following solution fulfills our equations:

$$\left\{\begin{aligned} q &= \frac{\left(1 + \frac{\lambda\Lambda}{3}\omega^2\right) pQ}{\left(1 + \frac{\lambda\Lambda}{3}\omega^2\right) e^{\frac{r_0^2}{4}\omega^2} - k} \\ n &= \frac{\Lambda p Q / v}{\left(1 + \frac{\lambda\Lambda}{3}\omega^2\right) e^{\frac{r_0^2}{4}\omega^2} - k}. \end{aligned}\right. \tag{18}$$

By superposing such harmonic wave solutions it is possible to obtain solutions corresponding to more general problems.

Consider for instance the case of a cube of side a having a point source of intensity Q_0 at the center. If the cube is isolated and a is very large compared to the mean free paths we may take as boundary conditions on its surface that all neutron densities must vanish. The point source at the center may be developed as follows:

$$Q = \frac{8 Q_0}{a^3} \sum_{i,j,l} \cos\frac{\pi i x}{a} \cos\frac{\pi j y}{a} \cos\frac{\pi l y}{a} \tag{19}$$

the sum being extended to odd values of the indices i, j, l. From (18) we now find:

$$(20)\qquad \left\{\begin{aligned} q &= \frac{8\,\phi Q_0}{a^3}\sum_{i,j,l}\frac{\left(1+\frac{\lambda\Lambda}{3}\omega_{i,j,l}^2\right)\cos\frac{\pi ix}{a}\cos\frac{\pi jy}{a}\cos\frac{\pi lz}{a}}{\left(1+\frac{\lambda\Lambda}{3}\omega_{i,j,l}^2\right)e^{\frac{r_0^2}{4}\omega_{i,j,l}^2}-k}\\ n &= \frac{8\,\Lambda\phi Q_0}{a^3 v}\sum_{i,j,l}\frac{\cos\frac{\pi ix}{a}\cos\frac{\pi jy}{a}\cos\frac{\pi lz}{a}}{\left(1+\frac{\lambda\Lambda}{3}\omega_{i,j,l}^2\right)e^{\frac{r_0^2}{4}\omega_{i,j,l}^2}-k}\end{aligned}\right.$$

where we have put

$$(21)\qquad \omega_{i,j,l}^2=\frac{\pi^2}{a^2}(i^2+j^2+l^2).$$

6. Theory of the exponential experiment.

Besides this solution we shall use also in the interpretation of the experiments one corresponding to the case when no primary source Q is present in the domain in which measurements are performed. We write such a solution for the case of a column having a square cross-section of side a with the boundary condition that all neutron densities vanish at the boundary. The solution may be expanded in a double Fourier series in the cross-section:

$$(22)\qquad \sum_{j,l} c_{jl}\cos\frac{\pi jx}{a}\cos\frac{\pi ly}{a}\,e^{-z/b_{jl}}$$

where again the indices j and l are odd numbers. b_{jl} is a constant that fulfills the following equation

$$(23)\qquad k=\left\{1-\frac{\lambda\Lambda}{3}\left[\frac{1}{b_{jl}^2}-\frac{\pi^2}{a^2}(j^2+l^2)\right]\right\}e^{-\frac{r_0^2}{4}\left[\frac{1}{b_{jl}^2}-\frac{\pi^2}{a^2}(j^2+l^2)\right]}.$$

The largest of all the b_{jl} is b_{11}, corresponding to the main Fourier component. Consequently the solution for large values of z reduces to this component only. We have for it

$$(24)\qquad k=\left\{1-\frac{\lambda\Lambda}{3}\left(\frac{1}{b_{11}^2}-\frac{2\pi^2}{a^2}\right)\right\}e^{-\frac{r_0^2}{4}\left(\frac{1}{b_{11}^2}-\frac{2\pi^2}{a^2}\right)}.$$

It follows in particular from this equation that:

$$(25)\qquad b_{11}\gtrless\frac{a}{\sqrt{2}\,\pi}$$

according to whether $k\gtrless 1$. Consequently, a measurement of b_{11} offers directly a criterion for deciding whether a chain reaction in a given lattice may or may not be obtained by simply increasing its dimensions.

The practical importance of the last result makes it desirable to discuss how the result (25) is dependent upon the assumptions adopted in the theory of the preceding section, and in particular on the substitution of the lattice by a continuous medium. It can be shown that (25) is almost independent of such assumptions.

We consider a lattice structure having $k = 1$. In an infinite lattice of that structure a permanent solution shall exist in which neutrons are produced in equal number by all uranium lumps and each cell absorbs as many neutrons as it produces. In a cubic lattice each lump is surrounded by " shells " of lumps. Each shell is the ensemble of lumps having the same distance from the lump in question. The absorption of neutrons by a lump depends on the emission of neutrons by the surrounding cells and is clearly not affected by changing the intensity of the emission of neutrons in a surrounding cell, provided this is done in such a way as not to change the average intensity of the lumps of the shell.

Consequently our infinite lattice shall be still in equilibrium provided all lumps are surrounded by shells in which the average intensity of emission is equal for each shell to the emission of the lump at the center. Such condition is obviously verified if all the lumps emit neutrons with equal intensity.

A simple numerical calculation proves that such a condition is fulfilled with a very good accuracy, also for a distribution of the intensity of emission of the various lumps given by the expression

$$I_0 e^{-z/b} \cos \frac{\pi x}{a} \cos \frac{\pi y}{a} \tag{26}$$

where x, y, z are the coordinates of the lump, $b = \frac{a}{\pi\sqrt{2}}$ and a is large compared with the cell side.

This calculation has been carried out for the case in which a is 6 times the cell side corresponding to the experiment and found to hoid quite accurately. A more elaborate discussion of the approximations involved in this exponential method has been carried out by E. Teller.

N° 150.

For the introduction to this paper see N° 147 and 149.

150.

NEUTRON PRODUCTION IN A LATTICE OF URANIUM OXIDE AND GRAPHITE (EXPONENTIAL EXPERIMENT)

H. L. ANDERSON, B. T. FELD, E. FERMI, G. L. WEIL, and W. H. ZINN
Report C–20 (March 26, 1942).

This report concerns some experiments performed to ascertain whether a given lattice of uranium oxide lumps embedded in graphite could give a divergent chain reaction if its dimensions were made sufficiently large. From this point of view the fundamental properties of a given lattice structure may be described in terms of a reproduction coefficient k which is defined as the average number of neutrons produced in the first generation by a primary neutron in a lattice of the given structure having infinite extension.

In the experiments to be described in this report we have investigated the properties of a lattice of U_3O_8 lumps embedded in graphite. We used a cubic lattice with a cell side of 16 inches. In the center of each cell there was a cubical box of $8'' \times 8'' \times 8''$, containing about 60 pounds of uranium oxide. The box was made of thin tinned iron sheet and weighed about 500 gms. This structure was chosen especially because of its constructional simplicity since it could be assembled without cutting our graphite bricks of $4'' \times 4'' \times 12''$. Although we did not expect that this structure would approach too closely the optimum proportions, we thought it desirable to obtain some preliminary information as soon as possible. It turned out that for this particular structure k is about 0.87.

Two series of experiments were performed:

a) An "exponential experiment" having primarily the purpose to determine k.

b) With a view to investigate the detailed mechanism of the reproduction process measurements were also taken with the source in the center of a large cubical block and the intensities of resonance and thermal neutrons measured at various points and compared with the theoretical expectation (This experiment will be described in the third part of this report) (*).

(*) Paper N° 151. (Editors' note).

Exponential experiment.

The measurements to be described in this section were performed at Columbia University beginning in August 1941. At the end of September, 1941, a new and taller exponential pile was set up and the accuracy was further increased by using a 2 gram Ra + Be source instead of the original source of about 600 mg. We describe here this second series of experiments.

1. *Measurements.*

The final structure on which the measurement was performed was a column with square base $8' \times 8'$ (6×6 lattice periods). The column was 11' high (8 complete lattice periods) plus one 4' layer of graphite bricks at the hase.

The column rested on a paraffin base $10' \times 10'$, and about 1' thick. The source (2 grams Ra mixed with Be) was placed directly under the center of the lower base in a channel in the paraffin . For convenience we shall denote the points in our system using Cartesian axes x , y , z, having the origin in the centre of the lower base with the x–axis vertical and the y–axis pointing to the north.

A system of eleven horizontal slots (about $2'' \times 3/8''$ and 5' long) was provided for taking intensity measurements throughout the structure. Seven of these slots (numbered 1, 2, 3, 4, 5, 6, 7 in fig. 1) enabled us to introduce the detector on points close to the axis of the column. For practical reasons these slots passed 2'' west of the axis so that the measurements could not be taken exactly on the axis.

On the plane of slot 4 the additional slots 4 W, 4 WW, 4 E, 4 EE, were introduced in such a way as to make it possible to map completely the intensity in this plane for the determination of the correction due to higher harmonics.

Since the neutrons spontaneously produced by the uranium contribute appreciably to the activation, measurements were taken with and without source. We used as detectors indium foils with or without cadmium.

The result of the measurements is summarized in Tables I and II.

The measurements listed in Table I are all taken at the point of the slot nearest to the center of the column. The first column indicates the slot as in fig. 1. An eighth row has been added to indicate the position on top of the column. Columns 2 and 3 give the intensity measured with the source without and with cadmium around the detector. Column 4 is the ratio of the two preceding columns. It is seen that this ratio is fairly constant with the exception of point 7 where the intensity with cadmium is too low to allow any accuracy, and of point 1 where the perturbation due to the source close by is still appreciable. This " cadmium ratio " offers a simple criterion for deciding up to what distance the perturbation due to the source is considerable. It appears that in our case all the points except the first are only very little perturbed by the source.

Column 5 gives the intensity measured without source (and without cadmium) due to the spontaneous neutron emission.

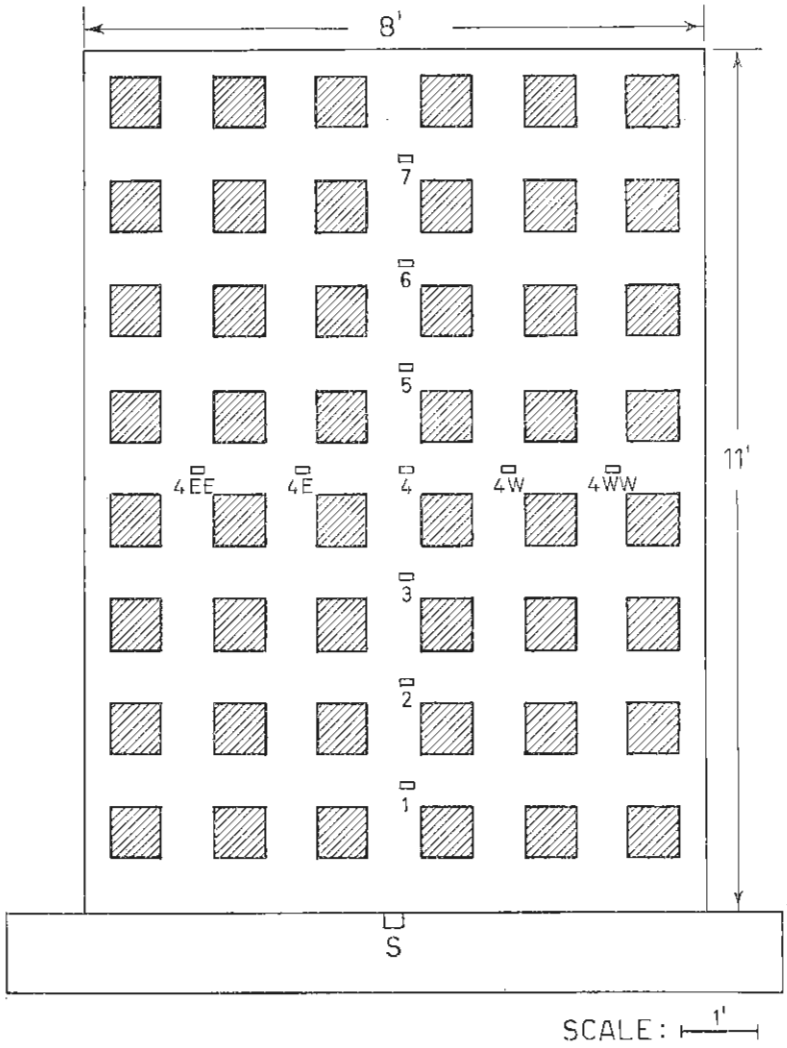

Fig. 1.

TABLE I.

Measurements near axis.

Position	Int. with source		Cd ratio	Int. without source no Cd	Net effect of source no Cd
	no Cd	Cd			
1	234.8	44.4	5.29	0.252	234.5
2	69.37	12.00	5.78	0.320	69.05
3	23.64	4.143	5.71	0.365	23.28
4	8.93	1.610	5.54	0.365	8.57
5	3.594	0.638	5.63	0.394	3.200
6	1.572	0.286	5.50	0.324	1.248
7	0.684	0.112	6.11	0.235	0.449
8 (top)	0.070				

TABLE II.

Measurements in plane 4.

Slot Distance from center	Intensity with source and without source (data in bracket)				
	4 EE	4 E	4	4 W	4 WW
0	4.79	7.71	8.93 (0.365	7.50	4.055
16″	4.115 (0.248)	6.645	7.73	6.24 (0.277)	3.50
32″	2.41 (0.1849)	3.765	4.36 (0.2495)	3.52	2.00 (0.2268)
46.5″	0.361	0.526	0.660	0.550	0.347

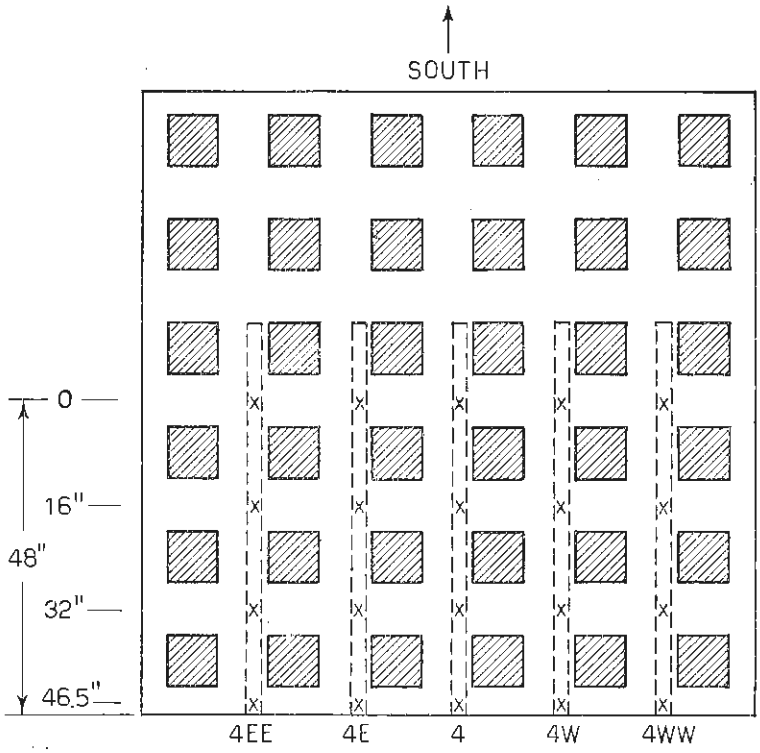

Fig. 2.

Column 6 is the difference of columns 2 and 5, and gives the net effect of the source.

In Table II we have collected the results of the measurements taken in the plane of slot 4. The slots are given in the top row of this table. For each slot measurements have been taken in four points at distances from the point of the slot nearest to the axis of the pile 0″, 16″, 32″, 46.5″ (see fig. 2).

The figures in Table II give the results of the measurements with the source. At some representative points also measurements without source have been taken. The result is given in bracket below the other figure.

2. *The harmonic correction.*

The correction due to higher harmonics was obtained as follows: The points on plane 4, at which measurements have been taken, are close to points having x and y equal to integral multiples $a/6$, where a is the effective side of the column. A simple and rather safe interpolation from the data of Table II, taking into account also the symmetry of the arrangement, enables us to calculate the intensity due to the net effect of the source at points on plane 4 having as coordinates integral multiples of $a/6$ ($a = 246.9$ cm = side of column increased by $2\lambda/\sqrt{3}$). The result is given im Table III.

TABLE III.

x/y	0	$a/6$	$2a/6$	$3a/6$
0	8.57 (0.36)	7.30 (0.32)	4.01 (0.24)	0
$a/6$		6.09 (0.28)	3.37 (0.21)	0
$2a/6$			1.89 (0.16)	0
$3a/6$				0

The numbers in bracket represent the correction that has been applied to take into account the effect of the spontaneous neutrons.

By taking the symmetry into account we can calculate from these data the coefficients of the development of the intensity in a twofold Fourier series

$$c_{11}\cos\frac{\pi x}{a}\cos\frac{\pi y}{a}+c_{13}\cos\frac{\pi x}{a}\cos\frac{3\pi}{a}y+c_{31}\cos\frac{3\pi x}{a}\cos\frac{\pi y}{a}+$$

$$+c_{33}\cos\frac{3\pi x}{a}\cos\frac{3\pi y}{a}+c_{15}\cos\frac{\pi x}{a}\cos\frac{5\pi}{a}y+c_{51}\cos\frac{5\pi x}{a}\cos\frac{\pi x}{a}+\cdots.$$

The result is:

$$c_{11}=8.19$$

$$c_{13}=c_{31}=0.19 \qquad c_{33}=0.01$$

$$c_{15}=c_{51}=0.02.$$

It can be seen that the-harmonic correction is rather small. Its most important term is the 1,3 and 3,1 harmonic component. Indeed c_{33} and $c_{15}=c_{51}$ are

so small that the experimental accuracy is not large enough to determine their sign, although, theoretically, all the harmonic coefficients must in our case (point source) be positive.

From the observed values of the harmonic coefficients on the 4 plane, it is possible to calculate the harmonic correction on the other planes by making use of the relationship between the exponential " relaxation length " for the various harmonic components:

$$\frac{1}{b_{jk}^2} = \frac{1}{b_{11}^2} + \frac{(j^2 + k^2 - 2)\,\pi^2}{a^2}. \tag{1}$$

Taking the experimental value $b_{11} = 45.5$ (see later), it follows $b_{13} = 23.7$, $b_{33} = 18.04$, $b_{15} = 15.03$.

TABLE IV.

Position	Harmonic Correction
1	—
2	(21.2)
3	2.79
4	0.43
5	0.073
6	0.012
7	0.002

Since the " step " in our measurement is equal to the cell side of $16'' = 40.64$ cm, we have the following Table IV, for the harmonic correction in which we have taken into account only the 1,3 and 3,1 harmonics.

This estimate of the harmonic correction is probably reliable for the positions 3, 4, 5, 6, 7, where the harmonic correction is small. For the positions closer to the source, the contribution of the harmonics is higher than 1,3 becomes appreciable and the measurements on the 4 plane allow only an exceedingly rough estimate of their contribution. For this reason it would not be advisable to use in the evaluation of the final result data taken from measurements performed on the planes 1 and 2.

3. *Room scattering corrections.*

If the scattering of the walls of the room were negligible, the neutron intensity curve extrapolated to the outside of the structure should vanish at a distance $\lambda/\sqrt{3}$ from the surface.

The room scattering has the effect of increasing the neutron density near the surface of the structure, thereby increasing the " effective side " of the column.

In order to estimate this effect, measurements have been taken of the intensity on the outer surface of the column at various heights above the center of the sides of the lower base. The heights were intermediate between those of the measuring slots. The result of these measurements is summarized in Table V.

TABLE V.

Position	Intensity	Intensity on axis	effective side
$4\,^1/_2$	0.218	5.66	249.6
$5\,^1/_2$	0.170	2.36	254.5
$6\,^1/_2$	0.129	1.03	262.5

Column 1 indicates the position intermediate between that of the slots. Column 2 gives the observed intensity. For comparison the intensity at the center of the slot obtained by interpolation from the data of Table I is given in column 3.

The " effective side " given in column 4 is calculated with the formula:

$$\frac{\text{Intensity at surface}}{\text{Intensity on axis}} = \cos\frac{\pi}{2}\,\frac{a_0}{a_{\text{eff.}}} \tag{2}$$

where $a_0 = 96'' = 243.84$ cm is the geometrical side of the column.

The room scattering has also been measured on the top surface where the intensity at the center is 0.07 (see Table I).

From this, and from the other data of Table I, one can calculate the " effective top " of the column, namely, the height at which the intensity extrapolated from the inside would vanish. One finds that the " effective top " is about 10 cm above the true top.

This result is used in calculating the correction factor on the intensity data due to the fact that the column has a finite height. This correction factor is given by the formula:

$$\frac{1}{1 - e^{-(z_0 - z)/b}} \tag{3}$$

where $z_0 - z$ is the distance from the " effective top " and b, the exponential relaxation distance. This correction factor is given in Table VI.

TABLE VI.

Position	Correction Factor
5	1.003
6	1.02
7	1.13

4. *Evalutation of the characteristic length c.*

$$\frac{1}{c^2} = \frac{1}{b^2} - \frac{2\pi^2}{a^2} . \tag{4}$$

We have shown in section 6 of the theoretical part (*) that a simple relationship (24) exists between the magnitude (4) and the reproduction factor k. We shall try therefore to evaluate (4) from the preceding measurements.

In Table VII, the first column represents, as usual, the position. Both integral and half integral positions have been included. Column 2 gives the intensity corrected for the higher harmonics (column 5 of Table I minus harmonic correction of Table IV). Column 3 gives the intensity of the harmonic 1,1 corrected for the effect of the top (from Table VI).

TABLE VII.

Position	Intensity of 1,1 harmonic	Intensity corrected for top effect	Ratio r	$b = \frac{40.64}{\log r}$	a	$\frac{1}{c^2} = \frac{1}{b^2} - \frac{2\pi^2}{a^2}$	c
2	(47.85)	(47.85)					
2 1/2			(2.335)	(48.0)	(246.9)	(1.10×10^{-4})	
3	20.49	20.49					
3 1/2			2.518	44.0	246.9	1.93×10^{-4}	72
4	8.14	8.14					
4 1/2			2.596	42.7	249.6	2.31×10^{-4}	64
5	3.127	3.136					
5 1/2			2.486	44.7	254.5	1.96×10^{-4}	71
6	1.236	1.261					
6 1/2			2.497	44.5	262.5	2.18×10^{-4}	68
7	0.447	0.505					

Column 4 is the ratio between adjacent pairs of values of the intensities given in column 3. At position 2 1/2 we have 2.335, e.g., the ratio 47.85/20.49 of the two intensity values at positions 2 and 3 and so forth. Column 5 gives the exponential relaxation length calculated from each of the preceding ratios with the formula:

$$b = \text{length of step/log ratio}$$

(length of step 16" = 40.64 cm).

Column 6 gives the "effective side" a. This is partly taken from Table V; for the lower positions, where the room scattering becomes unim-

(*) Paper N° 149. (Editors' note).

portant, it is assumed:

$$a = a_0 + 2\lambda/\sqrt{3} = 246.9.$$

Column 7 gives the values of (4) calculated from the data of columns 5 and 6.

We take the average of the data from this last column, excluding however, the first term, which is unreliable on account of the large harmonic correction, and we obtain:

$$\frac{1}{c^2} = \frac{1}{b^2} - \frac{2\pi^2}{a^2} = (2.09 \pm 0.09) \times 10^{-4} \tag{5}$$

$$c = 69 \text{ cm}.$$

We calculate now the reproduction factor with formula (24) of theoretical part:

$$k = \left(1 - \frac{\lambda\Lambda}{3}\frac{1}{c^2}\right) e^{-\frac{r_0^2}{4}\frac{1}{c^2}} \tag{6}$$

where we have assumed

$$\frac{\lambda\Lambda}{3} = 315 \qquad \frac{r_0^2}{4} = 340. \tag{7}$$

We obtain finally:

$$k = 0.87.$$

The error of this result is due:

a) To error in the measurements which from the internal consistency of the data may be estimated about $\pm$ 0.01.

b) To the uncertainty of the assumptions (7). In this respect it should be noted, however, that any error in these assumed values would affect proportionately the small difference of k from 1. For example, a 20 % error on (7) would result in an error of only 0.026.

c) To the errors in the theory of the exponential experiment. According to the discussion in the theoretical part, and to the more complete calculation of E. Teller, this error appears to be quite small.

It should be pointed out that this result refers to the particular lattice used.

It was found by auxiliary measurements that a 4 % loss in the reproduction factor k was due to the absorption in the iron cans containing the oxide. Furthermore, the oxide used was rather impure and a gain in k of a few percent can be expected by using purer oxide. Further improvements can be expected by the use of a better geometry, of compressed oxide, or of uranium metal.

We thank Dr. H. B. Hanstein and Dr. H. C. Paxton, who contributed to the early part of this experiment.

N° 151 and 152.

The exponential experiments reported in these two papers were the last ones performed at Columbia University. The results were encouraging and demonstrated an understanding of the effects being studied. More precise measurements were not made because of the deadline for shipping the material to Chicago.

The decision to move this work to Chicago was made early in January 1942, about a week after Fermi had offered me the opportunity of joining his group. At that time the physicists in his group were Anderson, Feld, Marshall, Weil, and Zinn. Fermi sent some of the group to Chicago almost immediately and made several trips there himself. The rest of us remained in New York until April, with Zinn in charge of the experiments and getting things ready for shipping.

During these three months, despite increasing pressure for decisions and advice, Fermi was intimately involved in the work and the measurements. When he came in, he wanted to see not only the results, but also the original measurements of the counts taken on each foil. In the tables of the reports one sees his desire to provide the data from which others could also calculate the results for themselves.

A. WATTENBERG.

151.

PRELIMINARY REPORT ON THE EXPONENTIAL EXPERIMENT AT COLUMBIA UNIVERSITY

Report CP–26 (March, April 1942).

Constants of the lattice cell, dimensions $8'' \times 8'' \times 8''$.
Cylindrical lumps of pressed U_3O_8:

Diameter	7.52 cm
Height	7.51 cm
Average weight	1795 gr.

Particular care was taken to eliminate as much as possible the moisture. The pressed uranium oxide bricks were preheated to about 250° C. Afterwards the structure was put together and covered with an iron sheet about 1/16" thick and evaporated to a pressure of a few millimeters of mercury while the temperature was raised to about 100° C. Subsequent tests proved that the moisture content had been thereby reduced to 0.03 percent, whereas the moisture contained before the treatment was about ten times as much.

The lattice contained 15 layers of 12×12 cells each. This structure rested on a base of graphite 16" thick. The source was inserted at the center of the lower base of the structure.

Measurements of neutron intensities.

A series of measurements was taken with indium detectors introduced in a series of slots throughout the structure. The positions of such detectors are indicated by a system of coordinates, as follows:

1. Origin of coordinates in the series:

x axis vertical

y and z axes horizontal and parallel to two bases of the structure. For convenience, a unit of 8″ is used for indicating the positions so as to have them represented by integral numbers.

2. Two series of measurements were taken, one without source and one with a source of about two grams of radium and beryllium. Measurements with the source, also measurements with the detector screened by cadmium, were taken. The measured intensities are given in Table I.

Table I.

Position	Source No Cd.	Source Cd.	No Source No Cd.
100	189227	46405	27.8
105	9490		
300	61120	8897	36.2
305	7204		
500	20876	3003	
502	16772		
504	8029		
505	3785		
700	7933	1154	41.3
702	6790		41.3
704	3533		27.9
705	1744		16.3
720	6613		41.6
722	5636		35.8
724	2951		23.1
725	1429		12.7
740	3508		26.6
742	2953		26.5
744	1593		17.2
745	779		7.9
750	1702		12.2
752	1411		13.7
754	782		9.5
755	397		5.4
900	3218	453	41.3
902	2719		
904	1484		
1100	1311	193.4	39.4
1102	1111		
1105	318		
1200	823	117.1	32.3
1300	485	75.2	28.8
1302	417		
1304	245		
1305	127		
1400	239.7	38.1	16.8
1500 (top)	22.4		3.5

HARMONIC CORRECTION.

The correction due to higher harmonics in the Fourier development of the intensity in a horizontal plane was calculated theoretically and compared with experimental intensities observed on the planes $x = 5$ and $x = 7$.

The theoretical calculation of the amounts was made on the assumption that far enough from the source the intensity of each harmonic is proportional to

$$b_{jl}\, e^{-x/b_{jl}}$$

where b_{jl} is the exponential relaxation distance for the harmonic component in question. This is given by the formula:

$$\frac{1}{b_{jl}^2} = \frac{1}{b_{11}^2} - \frac{j^2 + l^2 - 1}{a^2}\pi^2$$

"a" was taken 93.8" (geometrical side 92") and b_{11} was taken 46 cm. Subsequent measurements indicate that b_{11} is more closely 46.13. The small difference, however, is not significant for the present purpose of calculating the harmonic correction. The relative intensity of the various harmonic components calculated with this formula is given in Table II.

TABLE II.

x	1,1	1,3 3,1	3,3	1,5 5,1	3,5 5,3	5,5 1,7 7,1	Fraction due to 1,1 harmonic
1	29.55	19.21	5.48	7.32	5.24	4.72	0.625
3	12.21	3.355	0.539	0.435	0.222	0.104	0.723
5	5.05	0.586	0.053	0.029	0.009	0.002	0.8318
7	2.085	0.1023	0.0052	0.0017	0.0004	0.0001	0.950
9	0.863	0.0179	0.0005	0.0001	–	–	0.979
11	0.357	0.0031	0.0001	–	–	–	0.931
12	0.229	0.0013	–	–	–	–	0.994
13	0.1474	0.00054	–	–	–	–	0.996
14	0.0949	0.00022	–	–	–	–	0.998

The above theoretical representation of the harmonics would be correct only on the assumption that the base of the lattice has a constant reflection coefficient. Since it is questionable whether this assumption is correct, the theoretical intensity of the harmonics has been compared with experiment. The comparison gives for the points at $x = 5$ and the points at $x = 7$, harmonic correction factors of 0.8812 and 0.9570, whereas the theory gives at the same

positions 0.8818 and 0.950. Since the difference is not outside of experimental error, it appears legitimate to use throughout the calculated harmonic correction factor.

TABLE III.

x	Harmonic Correction	Top Correction	Cd–ratio Correction	Total Correction	Corrected intensity of main harmonic due to source
1	0.625	1	0.863	0.539	101978
3	0.723	1	1	0.723	44164
5	0.882	1	1	0.882	18376
7	0.950	1.001	1	0.951	7504
9	0.979	1.005	1	0.984	3125
11	0.981	1.028	1	1.008	1283
12	0.994	1.070	1	1.064	841
13	0.996	1.188	1	1.184	540
14	0.998	1.617	1	1.613	359

In Table III the various correction factors are collected. The first column gives the position. The second column gives the harmonic correction factor from the preceding table. The third column gives the correction factor due to the effect of the top of the column. This is calculated with the formula

$$\frac{e^{(x_0-x)/b}}{e^{(x_0-x)/b}-1}$$

x_0 is the abscissa of the effective top, which was taken 1.88 cm above the actual top of the column. The fourth column gives a Cd–ratio correction due to the fact that the Cd–ratio is anomalous for the point at $x = 1$ due to the fact that the source is very close to this point. Consequently, the ratio between the thermal neutron intensity and the indium activity at this point is different from the similar ratio at the other points.

The fifth column gives the total correction factor (product of the three preceding columns).

The sixth column gives the corrected intensity of the main harmonic. (This is obtained by multiplying the difference between the intensities at the points $(x, 0, 0)$ with source and without source from Table I by the correction factor given in column 5 of Table III).

If the intensities from column 6 of Table III are plotted in a logarithmic scale against the abscissae, the points lie very approximately on a straight line.

Determination of the exponential relaxation lengths.

The exponential relaxation length was determined by the method of least squares from the intensity data at positions 5, 7, 9, 11, 12, 13. The first two and the last positions were discarded because the corrections at these points are rather large and uncertain. However, these points also lie quite close to the straight line determined by the others.

The intensity of the main harmonic can be represented by the following formula:

$$164900\, e^{-x/46.13}$$

where x is now measured in centimeters. This gives a relaxation distance:

$$b = 46.13 \text{ cm}.$$

Calculation of the reproduction factor.

The reproduction factor is calculated with the formula

$$k = e^{-\frac{r_0^2}{4}\left(\frac{1}{b^2}-\frac{2\pi^2}{a^2}\right)}\left[1 - \frac{\lambda\Lambda}{3}\left(\frac{1}{b^2} - \frac{2\pi^2}{a^2}\right)\right].$$

We can assume $a = 237.74$ cm constant throughout the length of the column. This is perhaps not quite correct as there is some indication of a slight increase of the effective side of the column with increasing height. Since the measurements of the side of the column taken so far are not sufficiently accurate, no attempt was made at present to correct for this effect. From this value of a, and the previous value of b, follows:

$$\frac{1}{c^2} = \frac{1}{b^2} - \frac{2\pi^2}{a^2} = 1.207 \times 10^{-4}.$$

In order to calculate the reproduction factor, we have further assumed:

$$\frac{r_0^2}{4} = 324 \text{ cm}^2$$

and:

$$\frac{\lambda\Lambda}{3} = 372 \text{ cm}^2$$

This gives:

$$k = 0.918.$$

Interpretation of Cd-ratio.

In Table IV we have collected the ratios between the intensities at points on the axis without and with Cd around the detector.

We have excluded the first point, which is strongly perturbed by the source, and the last point, where the intensity is too low for a reliable meas-

urement. This Cd–ratio appears to be constant within the experimental accuracy, and its mean value is

$$\text{Cd–ratio} = 6.86.$$

TABLE IV.

x	Cd–ratio
1	4.06
3	6.87
6	6.93
7	6.87
9	7.10
11	6.78
12	7.03
13	6.45
14	6.29

The sensitivity of our detectors for thermal and resonance neutrons has been standardized in a separate series of measurements, with the following result

$$q = 6.33 \times 10^{-11}\, Q A_{Cd}$$

$$\lambda n v = 1.216 \times 10^{-8}\, Q\, (A - 1.15\, A_{Cd})$$

where A and A_{Cd} are the observed intensities without and with Cd; Q is the number of neutrons emitted per second by the source. From the previous value of the Cd–ratio follows:

$$\frac{\lambda n v}{q} = 1097.$$

From this value we can calculate the fraction f_T of thermal neutrons that is absorbed by uranium. This is given by the formula:

$$f_T = 1.005 \left(1 - \frac{n \lambda v}{3 l^2 q}\right)$$

where l is the diffusion length of thermal neutrons in graphite ($l = 45$ cm). The factor 1.005 is a correction due to the fact that the thermal neutron density is not constant throughout the cell. Inserting the numerical values in the preceding formula, we find:

$$f_T = 0.824.$$

Absolute value of intensity.

If a source is placed on the axis of a square column of side a the intensity of thermal neutrons at points far from the source is given by the formula

$$nv\lambda = Q\frac{6p}{a^2}\,\frac{\lambda\Lambda}{3}\,\frac{4}{r_0^2}\,b\,\frac{e^{-x/b}}{k+\frac{4}{r_0^2}\,\frac{\lambda\Lambda}{3}\,e^{-\frac{r_0^2}{4}\left(\frac{1}{b^2}-\frac{2\pi^2}{a^2}\right)}}\,.$$

Since the conditions under which this formula is valid do not correspond exactly to our experimental conditions, we cannot expect to find a too close agreement between these results and the observed intensities.

Since our column is extended only in one direction from the source, we expect the formula to give a too high estimate for the intensity. A comparison with the intensity observed and calculated gives actually the intensity observed equal to about 68 per cent of that calculated with the formula.

Natural neutrons.

The intensity observed without source can be used for calculating the number of neutrons emitted spontaneously by uranium, or rather the ratio of this number to the number of neutrons emitted by our source. The result of the calculation is

$$\text{Number of neutrons per kilogram uranium} = 5.77\times 10^{-7}$$

$$\times \text{ number of neutrons emitted by the source}$$

Taking this last number to be 24.6×106 neutrons per second, the number of natural neutrons per kilogram of uranium per second results 14.2, in good agreement with a similar result obtained from the intermediate experiment performed in August, September, 1941, at Columbia University.

N° 152.

For the introduction to this paper see N° 151.

152.

EFFECT OF ATMOSPHERIC NITROGEN AND OF CHANGES OF TEMPERATURE ON THE REPRODUCTION FACTOR

Report C–85 (May 19, 1942).

A. Effect of nitrogen.

In the exponential experiments performed at Columbia University in March and April of 1942, the exponential pile was conditioned in such a way that it was possible to use different gases inside the pile. In the experiment described in report C–26 (*), carbon-dioxide was used in order to eliminate the absorption due to atmospheric nitrogen. It appeared interesting however, to test by a direct experiment the effect of atmospheric nitrogen. For this the carbon-dioxide was pumped away and air was admitted inside the structure. The fraction of the total volume occupied by air was about 0.23 of the total volume.

Table I.

Position	CO_2	Air	Ratio
5,0,0	20944	20530	1.020
9,0,0	3218	3085	1.043
13,0,0	487	459	1.061

The intensity of activation of indium foils was measured at the positions 5, 9 and 13 along the axis of the structure. The results of the measurements are summarized in Table I, together with the result of the measurement with carbon-dioxide that are given for comparison.

(*) Paper N° 151. (Editors' note).

Column 1 indicates the position of the indium foil represented with the same notations as in report C-26. Column 2 gives the intensity observed when carbon-dioxide was admitted inside the structure. Column 3 represents the intensities at the same positions with air inside the structure. Column 4 gives the ratio between the data with carbon-dioxide and with air.

It is apparent that the intensity decreases with increasing distance from the source more rapidly when air is inside the structure than it does with carbon-dioxide.

From the data of Table I, it is possible to calculate the change in relaxation distance b, with much greater accuracy than it is possible to calculate the length b, itself. The reason is that all corrections due to higher harmonics to the effect of the end and to the uncertainty in the effective size of the pile disappear in the comparison. The result is

$$b_{CO_2} - b_{air} = 0.52 \text{ cm}. \tag{1}$$

The relaxation distance b, is related to the reproduction factor k, by the approximate relationship.

$$k = 1 - 700\left(\frac{1}{b^2} - \frac{2\pi^2}{a^2}\right). \tag{2}$$

The observed change of b, corresponds to the following change of k in passing from carbon-dioxide to air.

$$k_{CO_2} - k_{air} = 0.0073. \tag{3}$$

This change amounts to about 0.8 %.

B. Effect of changes of temperature.

The same exponential pile was also used in order to obtain a preliminary estimate of the effect of a temperature change on the reproduction factor. Due to the extremely short time at our disposal for such an experiment, the test could not be conducted with all the care that would have been desirable. In particular, the effect was investigated over a rather small change of temperature from 310° K to 372° K. Furthermore, in the experiment with the hot pile we had no time to achieve a uniform temperature inside the pile. The temperature decreased from the bottom to the top by about 20°.

In order to keep the temperature reasonably constant during the experiment, it was found necessary to keep the pile covered with a sheet of thermal insulator during the hot measurement. This made it necessary to compare the hot experiment with a cold experiment in which a similar sheet of thermal insulation was around the pile. The result of the measurement may be summarized by saying that no appreciable difference in the exponential relaxation distance could be detected between the hot and the cold pile.

From this result follows that the reproduction factor at high temperature is smaller than at low temperature. Indeed, the diffusion distance in the hot pile is larger than in the cold pile due to the fact that all absorption cross-sections for thermal neutrons are inversely proportional to the velocity

of the thermal neutrons and therefore, inversely proportional to the square root of the absolute temperature. The diffusion term decreases, therefore, as the square root of the absolute temperature. From this, one can easily estimate that the reproduction factor in our hot pile was about 0.4 percent smaller than in the cold pile. The difference is further increased if one takes into account the fact that in our hot experiment the temperature was decreasing from bottom to top of the pile. A somewhat complicated estimate of the correction due to this indicates that the decrease in the reproduction factor due to the increasing temperature is even larger possibly by about a factor 2 than indicated. It must be emphasized finally, that for the reasons already indicated, such a result must be considered as only very preliminary and that the experimental error is of the same order of magnitude as the effect itself.

N° 153.

The last two reports of the National Academy committee, as already mentioned, had been encouraging. The committee saw in the chain reaction not only its possibility for producing power but also, more important for the immediate emergency, its application as a producer of plutonium, a likely competitor to U^{235} as a material from which atomic bombs might be made (*). It was time to push the uranium work vigorously. On december 6, 1941, the National Defense Research Committee announced an " all-out " effort. The next day came the attack on Pearl Harbor and immediately afterwards the United States entered the war against Japan, Germany and Italy. It was deemed essential that if atomic weapons were feasible the United States should have them before the Nazis. Since Italy and the United States were at war, Fermi, still an Italian national, became an enemy alien.

It was under these circumstances that the Metallurgical Laboratory was organized. It first operated under the Office of Scientific Research and Development and six months later was placed under the United States Army's Corps of Engineers, Manhattan District, together with the uranium 235 separation projects. The purpose of the Metallurgical Laboratory was first to develop the chain reaction with natural uranium, using this to produce plutonium. The choice of a place and leader for the Metallurgical Laboratory was subjected to practical considerations. Fermi would have liked to pursue his uranium work at Columbia University. But Columbia, already engaged in two different uranium separation projects headed one by H. C. Urey, the other by J. R. Dunning, was hesitant to underwrite a third project in the same general area.

As a leader, Fermi was not considered eligible to hold major responsibilities, being an enemy alien. Instead, A. H. Compton, of the University of Chicago, was chosen as the director, and decided to make Chicago the center of the work. Fermi, more than a little unwillingly, could hardly do otherwise than take his little group to Chicago to continue what he had started at Columbia.

The move to Chicago began in the early spring of 1942. The United States was now heavily engaged in the war, the outcome of which appeared very uncertain. The work of the Metallurgical Laboratory acquired a great sense of urgency, and was given a high priority rating; it grew rapidly in size and number of personnel, and its work was classified *secret*. Fermi's little group of physicists was quickly outnumbered by the influx of many other groups: chemists to work out the chemistry of the fission products and plutonium, engineers to try to design the plants, metallurgists to fabricate uranium metal, even doctors and biologists to study the effects of massive amounts of radiation and recommend safeguards against their possible damage. These groups were set within an organizational framework which tried to administer the work and enforce the rules of military security.

In this complex, Fermi's role was greatly changed. He was much sought after for advice. There were a great many meetings organized to exchange information, to hear criticism, and to decide policy. The engineers had to produce a design without a handbook and with little knowledge in a field completely new to them. A large part of the burden of giving them the unobtrusive guidance they needed fell upon Fermi. It was for them that he invented the word " danger coefficient " which first appeared in the following table, prepared to emphasize the importance of impurities for the chain reaction. Note the use of the term *alloy*, the word adopted as code for uranium.

The following notation developed for the reports. The Columbia reports, written before the organization of the Metallurgical Laboratory were prefixed with the letter A. Chicago reports were prefixed with the letter C, to which a P was added for physics, F for work involving fast neutrons, and E for engineering. The Columbia work which was written up for the project at Chicago was nevertheless given the notation C.

H. L. ANDERSON.

(*) See introduction to paper N° 207.

153.

A TABLE FOR CALCULATING THE PERCENTAGE OF LOSS DUE TO THE PRESENCE OF IMPURITIES IN ALLOY

Report C–5 (February 10, 1942).

The first column of the table is the name of the element present as impurity.

In the second column the " danger coefficient " of the element in question is given. When alloy is used in a slow neutron experiment, the percentage of neutrons absorbed by the impurity is obtained by multiplying the weight percentage of the impurity present by the danger coefficient. If several impurities are present, their contribution should be added.

A dash indicates very small danger coefficient. No danger coefficient is given in cases where it is not known.

H	13+	Cr	2	Ag	24	Yb	~20
D	—	Mn	8	Cd	1300	Cp	100
He	—	Fe	1.6	In	62	Hf	
Li	280	Co	24	Sn	0.2	Ta	4
Be	—	Ni	4.3	Sb	1.7	W	3.5
B	2400	Cu	2.4	Te	2	Re	20
C	—	Zn	0.6	I	2.3	Os	4
N	4	Ga		Xe		Ir	63
O	—	Ge	44	Cs		Pt	4
F	—	As	3.7	Ba	0.4	Au	19
Ne	<6	Se	6	La	25	Hg	81
Na	1	Br	4	Co	6	Tl	<0.5
Mg	0.5	Kr	14	Pr	6	Pb	0.1
Al	0.3	Rb		Nd	66	Bi	—
Si	<1	Sr	0.6			Po	
P	1.4	Y	250	Sm	1350		
S	0.5	Zr	4	Eu	300	Em	
Cl	34	Nb	4	Gd	8000		
A	<2	Mo	1	Tb	~250	Ra	
K	3.5			Dy	200	Ac	
Ca	0.4	Ru	2	Ho	~100	Th	
Sc		Rh	58	Er	35	Pa	
Ti	5	Pd	2	Tu	~100	U	
V	5						

No 154.

One worry that arose as the prospect of making a chain reaction became more likely was the question, would the chain reaction be stable? That is, if enough heat were developed to produce an increase in temperature, would the pile become more or less reactive? It was quite important for safety reasons that the temperature coefficient should be negative. Fermi looked into the problem at a fairly early date and in the following paper outlined the principal ways by which the reactivity might have a temperature coefficient. The temperature coefficient was always watched with care in the subsequent development. More detailed calculations were carried out by others later. When the first pile was built one of the first things that Fermi wanted to measure was the temperature coefficient.

H. L. ANDERSON.

154.

THE TEMPERATURE EFFECT ON A CHAIN REACTING UNIT

EFFECT OF THE CHANGE OF LEAKAGE

Report C–8 (February 25, 1942).

INTRODUCTION.

When the temperature of a chain reacting unit is increased the effective reproduction factor of the system is changed mostly for three reasons:

a. The resonance absorption increases on account of the doppler broadening of the resonance levels.

b. The fraction of the thermal-neutrons lost by carbon absorption decreases on account of the general decrease in the thermal cross-section of both alloy and carbon. This has the effect that the thermal neutron density shows less pronounced minima on the alloy lumps.

c. The decrease of the thermal cross-sections due to the rising temperature has also the effect of increasing the diffusion length of thermal neutrons, thereby producing an increase of the loss of neutrons due to leakage outside of the mass.

While *a* and *b* would act to change the reproduction factor even in a structure of infinitely large dimensions, *c* operates only on a structure of finite size.

In this report a discussion of the effect of *c* shall be given.

Change in leakage.

We assume a chain reacting unit of spherical shape of radius R, and we introduce the following notations:

r_0 = slowing down range;

λ = mean free path of thermal neutrons;

N_0 = average number of collisions before capture of a thermal neutron at the temperature T_0;

N_1 = average number of collisions before capture of a thermal neutron at the temperature T_1.

At the temperature T_0 the system will be chain reacting providing the reproduction factor k_0 is related to R by the following relationship:

$$k_0 = \left(1 + \frac{\pi^2}{3}\frac{\lambda^2 N_0}{R^2}\right)\exp\left(\frac{\pi^2}{4}\frac{r_0^2}{R^2}\right). \tag{1}$$

When the temperature changes to T_1 the only element in the left hand side in the preceding formula that is affected appreciably is N_0, which changes to the new value N_1. If the $1/v$ law is valid, and N_0 and N_1 are proportional to the square roots of the temperatures T_0 and T_1, we have:

$$N_1 = N_0\sqrt{\frac{T_1}{T_0}}. \tag{2}$$

At the higher temperature T_1 a larger value k_1 of the reproduction factor shall be needed in order to maintain the chain reaction. k_1 is given by a formula entirely analogous to (1)

$$k_1 = \left(1 + \frac{\pi^2}{3}\frac{\lambda^2 N_1}{R^2}\right)\exp\left(\frac{\pi^2}{4}\frac{r_0^2}{R^2}\right). \tag{3}$$

From (1), (2), and (3) it follows that:

$$\frac{k_1}{k_0} = \frac{1 + \frac{\lambda^2 N_0 \pi^2}{3 R^2}\sqrt{\frac{T_1}{T_0}}}{1 + \frac{\lambda^2 N_0 \pi^2}{3 R^2}} \cong 1 + \frac{\lambda^2}{3}\frac{N_0}{R^2}\pi^2\left(\sqrt{\frac{T_1}{T_0}} - 1\right). \tag{4}$$

In order to estimate the importance of the effect, we may assume that in a practical case the term

$$\frac{\lambda^2 N_0}{3}\frac{\pi^2}{R^2} \tag{5}$$

may be of the order of magnitude

$$\frac{k_0 - 1}{2}. \tag{6}$$

If this is the case, the percentage loss in effective multiplication factor due to the increase of the leakage is about

$$\frac{k_0 - 1}{2}\left(\sqrt{\frac{T_1}{T_0}} - 1\right). \tag{7}$$

If we assume, for example, $k_0 = 1.1$, a change from $T_0 = 300°\,K$ to $T_0 = 1000°\,K$, produces a change in the effect of the multiplication factor of about 4 %.

It follows from the preceding discussion that the importance of this temperature effect shall be particularly felt for structures having a large reproduction factor. Since the effect under discussion has a tendency to stabilize the system with respect to temperature changes, one might perhaps expect that systems of very small reproduction factor, and consequently of very large dimensions, may be unstable, whereas systems of somewhat larger reproduction factor, and consequently smaller dimensions, may be thermally stable.

It should be further noted, as pointed out especially by Wigner, that a change in the leakage is due also to the thermal dilatation of the system. This produces a decrease of the effective reproduction factor by the amount

$$6\gamma\,(T_1 - T_0)\,(k_0 - 1) \tag{8}$$

where γ is the coefficient of linear thermal dilatation of the system. If we assume, as in the previous example, $T_1 - T_0 = 700$, and we assume further $\gamma = 8 \times 10^{-6}$, we find that a change due to this reason amounts to about 0.3 %. This effect should be added to the one calculated previously.

N° 155.

This report was the outcome of a discussion between the authors (Fermi and Breit) during the first month or two of the Metallurgical Laboratory at Chicago. Fermi had been thinking intensely about " piles " and had made estimates regarding the possible usefulness of reflectors. He showed these to the writer. They were in pencil and all the essentials were contained in a few lines on one sheet of paper. The other author had made related estimates suggested by the possibilities of a reactor system which was to contain a central uranium core enriched with U^{235}. Water around this " seed " was to serve as a moderator. The " water boiler " calculations were contained in a report of the A-series. The details of preparation of Report C-11 (paper N° 155), which was based on the combined views of the authors, were attended by the undersigned. Before the report was issued it was critically inspected by Fermi. The order of names was alphabetical and no other implication was involved. Fermi's feel for essentials of reactor design was, of course, superior by far to that of the present writer.

G. BREIT.

155.

THE USE OF REFLECTORS AND SEEDS IN A POWER PLANT

G. BREIT and E. FERMI
Report C-11 (March 9, 1942).

I. INTRODUCTION.

According to present data natural uranium graphite systems are not likely to give a multiplication factor k very much greater than unity. If these data are right, it will probably be necessary to use uranium metal and graphite of high purity in order to achieve the desired result. In view of this situation, it will be desirable to look for means of conserving the materials of high purity and of increasing their effectiveness in producing a chain reaction by using them together with materials of somewhat lower quality. This purpose may be accomplished by concentrating the highest grade materials in the core or seed of the arrangement. The core is to be surrounded by a lattice or some other neutron regenerative structure made of less valuable materials and having possibly a multiplication factor slightly less than unity.

Without any attempt at considering the practicability of using separated isotopes, it is nevertheless possible to discuss the pros and cons of having uranium enriched in the 235 isotope in the core. It turns out that the use of reflectors cuts down greatly the amount of enriched uranium needed for establishing a chain reaction.

The utilization of U^{238} for the production of Pu^{239} will also be briefly considered. It is found that it is possible to have greater numbers of neutrons in the reflector than in the seed so that the main production of Pu^{239} would take place in the reflector. This circumstance is likely to be of value in a power plant intended for the production of Pu^{239} because extraction of disintegration products can take place mainly in the reflector. The inner seed need not be disturbed as much as the outer envelope.

II. Calculation of critical size and of relative numbers of neutrons.

The critical size for an arrangement of a seed surrounded by a reflector is treated here somewhat schematically by means of the diffusion equation:

$$\frac{\lambda}{3}\Delta n + \frac{(k-1)}{\Lambda} n = 0 . \tag{1}$$

Here λ, Λ are respectively the mean free paths for collisions of any type and for collisions leading to capture. A fission neutron has some chance of being absorbed before it reaches thermal energies and it also has some chance of being absorbed at thermal energies without producing fission. Some of the fission neutrons survive premature death by absorption and succeed in landing into a U^{235}, which then undergoes fission and produces new neutrons. The average number of fission neutrons produced by one fission neutron during this life cycle is denoted by k and is referred to as the reproduction factor. It can be described as the average number of children produced during the life of one neutron.

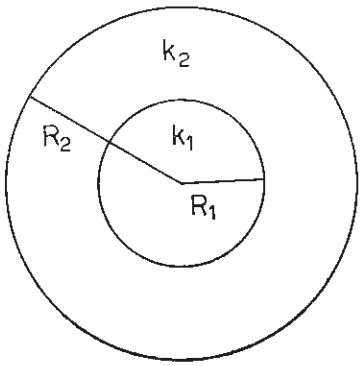

Fig. 1.

The seed and reflector are supposed to be spherical and to have respectively radii R_1, R_2 and reproduction factors k_1, k_2. It will be supposed that $k_2 < 1$ and that $k_1 > 1$. The diffusion lengths characteristic of the problem are

$$l_1 = \sqrt{\frac{\Lambda_1 \lambda_1}{3(k_1 - 1)}} \quad , \quad l_2 = \sqrt{\frac{\Lambda_2 \lambda_2}{3(1 - k_2)}} .$$

The solutions for n inside the seed and the reflector are respectively

$$n_1 = \frac{1}{r} \sin \frac{r}{l_1} , \tag{1.1}$$

$$n_2 = \frac{1}{r} \cdot \sin \frac{R_1}{l_1} \frac{e^{-\frac{r}{l_2}} - e^{\frac{r-2R_2}{l_2}}}{e^{-\frac{R_1}{l_2}} - e^{\frac{R_1-2R_2}{l_2}}} \tag{1.2}$$

The solution n_2 is adjusted so as to be zero at $r = R_2$ and so as to be equal to n_1 at $r = R_1$. The constant arbitrary factor by which both n_1 and n_2 may

be multiplied is omitted for simplicity. In addition to having $n_1(R_1) = n_2(R_1)$ it is also necessary to require that $\lambda_1 \partial n_1(R_1)/\partial R_1 = \lambda_2 \partial n_2(R_1)/\partial R_1$ so as to have continuity of neutron flow. This condition gives:

$$1 - \frac{R_1}{l_1}\cot\frac{R_1}{l_1} = \frac{\lambda_2}{\lambda_1}\left(1 + \frac{R_1}{l_2}\coth\frac{R_2 - R_1}{l_2}\right) \tag{1.3}$$

as the equation which determines R_1 in terms of R_2. The following special cases of this formula are worth noting:

$$\cot\frac{R_1}{l_1} + \frac{l_1}{l_2}\coth\frac{R_2 - R_1}{l_2} = 0 \qquad (\lambda_1 = \lambda_2) \tag{1.4}$$

$$\left(1 - \frac{\lambda_2}{\lambda_1}\right)\frac{l_1}{R_1} - \cot\frac{R_1}{l_1} = \frac{l_1\lambda_2}{l_2\lambda_1} \qquad (R_2 = \infty) \tag{1.5}$$

$$\cot\frac{R_1}{l_1} = -\frac{l_1}{l_2} \qquad (\lambda_1 = \lambda_2\ ,\ R_2 = \infty). \tag{1.6}$$

All of these equations can be readily solved by trial. This is especially easy for the last equation, which gives for example $R_1 = (3\pi/4)\,l_1$ if $l_1 = l_2$. In this case the radius is 3/4 of what it would be if the screen were not used. Correspondingly, the mass of the seed is $27/64 = 0.42$ of what it would have to be without the reflector. If in Eq. (1.5) one makes $\lambda_2 = 0$, keeping l_2 at a fixed value, this equation approaches $l_1/R_1 - \cot R_1/l_1 = 0$ with the solution $R_1 = 0$. This condition corresponds to perfect reflection at the boundary and is, of course, unattainable practically because it corresponds to $\lambda_2 = 0$ as well as to an infinite number of collisions before capture. A somewhat easier limit to come close to is that obtained by keeping l_2/λ_2 at a fixed value and making $\lambda_2 \to 0$. In this limit

$$\frac{l_1}{R_1} - \cot\frac{R_1}{l_1} = \frac{l_1}{\lambda_1}\lim\left(\frac{\lambda_2}{l_2}\right); \qquad (\lambda_2 \to 0\ ,\ R_2 = \infty). \tag{1.7}$$

For $k_2 = 1$ one obtains, by setting $l_2 = \infty$:

$$1 - \frac{R_1}{l_1}\cot\frac{R_1}{l_1} = \frac{\lambda_2 R_2}{\lambda_1 (R_2 - R_1)}; \qquad (k_2 = 1)\,. \tag{1.8}$$

The latter limit corresponds to using a reflector for which the condition of having a self-sustaining chain reaction in an infinite mass is barely fulfilled. By putting a seed with $k_1 > 1$, inside a finite mass of such a reflector, the chain reaction can be produced with relatively small amounts of materials. Finally, if $\lambda_2 = \lambda_1$ in the latter formula then:

$$\cot\frac{R_1}{l_1} = -\frac{l_1}{R_2 - R_1}; \qquad (k_2 = 1\ ,\ \lambda_1 = \lambda_2)\,. \tag{1.9}$$

The number of neutrons inside according to (1.1) is proportional to:

$$N_i = \int_0^{R_1} n(r)\, r^2\, dr = l_1^2\left[\sin\frac{R_1}{l_1} - \frac{R_1}{l_1}\cos\frac{R_1}{l_1}\right] \tag{2}$$

and on the same scale the number of neutrons outside is

$$N_{ou} = \int_{R_1}^{R_2} n(r)\, r^2\, dr = l_2^2 \sin\frac{R_1}{l_1}\left[1 + \frac{-\frac{R_2}{l_2} + \frac{R_1}{l_2}\cosh\frac{R_2 - R_1}{l_2}}{\sinh\frac{R_2 - R_1}{l_2}}\right]. \tag{2.1}$$

The ratio of the number of neutrons inside to that outside is

$$\frac{N_i}{N_{ou}} = \frac{l_1^2 \lambda_2}{l_2^2 \lambda_1} \frac{1 + \frac{R_1}{l_2} \coth \frac{R_2 - R_1}{l_2}}{1 + \frac{R_1}{l_2} \coth \frac{R_2 - R_1}{l_2} - \frac{R_2}{l_2 \sinh \frac{R_2 - R_1}{l_2}}} . \tag{2.2}$$

For large R_2 this formula simplifies to

$$\frac{N_i}{N_{ou}} = \frac{l_1^2 \lambda_2}{l_2^2 \lambda_1} = \frac{\Lambda_1}{\Lambda_2} \frac{(1 - k_2)}{(k_1 - 1)} \qquad (R_2 = \infty). \tag{2.3}$$

The ratio of the number of absorptions of all sorts inside and out is, according to the model used,

$$(N_i/\Lambda_1)/(N_{ou}/\Lambda_2) = (1 - k_2)/(k_1 - 1) \qquad (R_2 = \infty). \tag{2.4}$$

This simple formula shows that a large $k_1 - 1$ and a small $1 - k_2$ are both helpful in keeping the absorption of neutrons principally in the reflector rather than in the seed. In particular, if $k_2 = 1$ then the absorption of neutrons in the seed is negligible in comparison with that of the reflector. For the purpose of producing Pu^{239} this is a rather ideal condition because the seed need not be disturbed if Pu^{239} is to be extracted out of the reflector. This high efficiency of an arrangement with $k_2 - 1$ is due to the slow decrease of neutron density within the reflector and can be made use of only if large amounts of material are used in the reflector. It is, therefore, possibly premature to claim too much for it because it involves chemical extraction out of very large masses of material. The numerical results obtained by means of the more elaborate formula (2.2) show, however, that a reasonable compromise between size and concentration of Pu^{239} in the seed can be obtained.

For $k_2 = 1$ it is found that (2.2) becomes

$$\frac{N_i}{N_{ou}} = \frac{6 R_2 l_1^2 \lambda_2}{(R_2 + 2 R_1)(R_2 - R_1)^2 \lambda_1} . \tag{2.5}$$

III. Numerical results.

The first example to be considered here is $k_1 = 1.05$, $k_2 = 0.95$, $\lambda_1 = \lambda_2$, $l_1 = l_2$. In this case the equation connecting R_1 and R_2 is

$$\cot \frac{R_1}{l} + \coth \frac{R_2 - R_1}{l} = 0.$$

The values in Table I are obtained by means of this equation. They are tabulated so as to apply for any case in which $k_1 - 1 = 1 - k_2$ and $\lambda_1 = \lambda_2$.

In Table II these values are put into a more practical but less certain form by assuming that the effective number of collisions before capture is 200 so that:

$$l_1 = 2.6 \sqrt{\frac{200}{3(k_1 - 1)}} \quad , \quad l_2 = 2.6 \sqrt{\frac{200}{3(1 - k_2)}} .$$

TABLE I.

Factors representing saving for $k_1 - 1 = 1 - k_2$; $\lambda_1 = \lambda_2$.

R_1/l	$(R_2 - R_1)/l$	R_2/l	$(R_1/\pi)^3$ = Ratio of volume of seed to critical volume of seed in absence of reflector	$(R_2/\pi)^3 - (R_2/\pi)^3$ = Ratio of volume of screen to critical volume of seed in absence of reflector
$3\pi/4$	∞	∞	0.42	∞
$(\pi/2) + 0.80$	2.11	4.48	0.43	2.46
$(\pi/2) + 0.85$	1.37	3.79	0.46	1.29
$(\pi/2) + 0.90$	1.08	3.55	0.48	0.96
$(\pi/2) + 0.95$	0.90	3.42	0.52	0.76
$(\pi/2) + 1.00$	0.76	3.33	0.55	0.64
$(\pi/2) + 1.05$	0.65	3.27	0.58	0.55

TABLE II.

Masses for $k_1 = 1.05$, $k_2 = 0.95$, $l_1 = l_2 = 95$ cm.

$(R_2 - R_1)/l_1$	Oxide in Seed	Oxide in Screen	Total Oxide	Content of 235 in seed (Normal Isotopic Mixture)
∞	13.8 tons	∞	∞	217 lbs
2.11	14.0	81 tons	95 tons	220
1.37	15.0	42	57	236
1.08	15.8	31	47	250
0.90	16.9	25	42	265
0.76	17.9	21	39	280
0.65	19.0	18	37	300
0	33.0	0	33	0

For $k_1 = 1.05$, $k_2 = 0.95$ this gives $l_1 = l_2 = 95$ cm. The density of the graphite is taken to be 1.6. The volume needed in order to have a chain reaction in the material composing the seed without a reflector is $(4\pi/3)\ \pi^3 l_1^3 = 1.12 \times \times 10^8$ cm^3 and the mass is 1.79×10^8 gm $\cong$ 180 tons. [For simplicity of conversion we take here 1 ton = 1000 kgs = 2200 lbs]. In lattices used at

present the 3'' cubes of oxide with a density of 5.5 and a spacing of 8'' between cubes the volume of the oxide divided by the volume of the graphite is 1/19 corresponding to a mass ratio 1/5.5. In order not to be too optimistic, the saving in the amount of graphite due to the space occupied by the oxide will be neglected and the mass of oxide will be assumed to be 180 tons/5.5 = 32.7 tons, which will be rounded off to 33 tons. One finds with these conventions by means of Table I the masses listed in Tahle II. It is apparent that the masses of valuable material needed for the seed are decreased considerably through the use of the reflector.

TABLE III.

Factors representing saving for $k_2 = 1$, $\lambda_2 = \lambda_1$.

$R_1/l_1 - \frac{\pi}{2}$	$\frac{R_2 - R_1}{l_1}$	$\left(\frac{R_1}{\pi l_1}\right)^3$ = volume of seed divided by critical volume of seed	$\left(\frac{R_2}{\pi l_1}\right)^3$ = volume of reflector and seed divided by critical volume of seed	$\frac{\text{Neutrons inside}}{\text{Neutrons outside}}$ « Eq. (2.5) »
0		0.125	∞	0
0.1	9.967	0.151	50.9	0.047
0.2	4.933	0.179	9.70	0.161
0.3	3.233	0.212	4.29	0.333
0.4	2.365	0.246	2.62	0.56
0.5	1.830	0.286	1.91	0.87
0.6	1.462	0.330	1.54	1.28

The advantage of using the seed is more pronounced if k_2 is increased. For $k_2 = 1$ the saving in the material used for the core and the ratio of the number of neutrons inside and out depends only on R_1/l_1 and R_2/l_1. Some numerical values are given in Table III. The saving in the volume of the seed is seen to be quite appreciable in this. In the table, from 1/8 to 1/3 of the amount needed without a reflector is seen to suffice if a reflector is used. The table shows also that for a seed mass of 1/6 of the critical only about 5 percent of the neutrons are inside the seed, the remaining neutrons being in the reflector.

In Table IV the values listed in Table III are used for estimating the masses involved on the supposition that $k_1 = 1.10$, $\lambda_1 = \lambda_2$ and that the effective number of collisions is about 200. The diffusion length is then $l_1 = 2.6\ (200/0.3)^{1/2} = 67.1$ cm. The critical radius is $67.1\ \pi = 211.2$ cm, the critical volume is 4.0×10^7 cm^3, the critical mass of graphite with density 1.6 is 6.4×10^7 gm = 64 tons. The mass of oxide in the seed of critical size is

then of the order 64 tons/5.5 = 11.6 tons, wich will be taken to be 12 tons in round numbers. The amounts of oxide needed for the screened arrangement of Table III are then as in Table IV.

TABLE IV.

Masses for $k_1 = 1.10$, $k_2 = 1$, $l_1 = 67$ cms.

$(R_1/l_1) - \frac{\pi}{2}$	Oxide in Seed	Oxide in Screen	Total oxide
0	1.5 tons	∞	∞
0.1	1.8	610 tons	612 tons
0.2	2.1	114	116
0.3	2.5	49	51
0.4	2.9	28.6	32
0.5	3.4	19.4	23
0.6	4.0	14.5	18

The amounts of high grade oxide needed are here of the order of a few tons, which is encouraging.

N° 156, 157, and 160.

For the greatly increased staff of physicists that had gathered at Chicago, Fermi instituted a series of lectures on the physics of neutrons and the chain reaction. These were wonderful examples of his teaching abilities. He made the subject seem clear and simple so that everyone could follow. Because of them the work on the project went forward with an insight and an understanding on the part of a widened group of scientists, that would have been hard to come by otherwise. The notes on the lectures are incomplete and were written not by Fermi, but by one or another of the physicists who attended them. The first series is not complete.

H. L. ANDERSON.

156.

SLOWING DOWN AND DIFFUSION OF NEUTRONS

Report C–29 (Notes on Lecture of March 10, 1942).

I. INDIVIDUAL COLLISION IN HYDROGEN.

The slowing down, or damping, of fast neutrons as they diffuse through a damping medium is the result of the neutrons' loss of energy as they collide with atoms of the damping medium. This energy loss per collision depends on two factors: (a) the relative masses of the neutron and the scattering atom; and (b) the change in direction suffered by the neutron because of the collision. It can be shown from the laws of conservation of momentum and energy that the energy loss decreases as the damping atom becomes heavier; for this reason hydrogen is the most effective damping medium.

The collision between a neutron moving with velocity v and a proton at rest (at "rest" because its thermal velocity can be neglected compared with the velocity of all but thermal neutrons) can be described most conveniently in a coordinate system moving with uniform velocity $v/2$ with respect to the stationary laboratory reference system so that its origin always coincides with the center of mass of the two colliding particles. In this center of mass (c.m.) system the relative velocities of the neutron and proton are equal and oppositely directed vectors, $\boldsymbol{v}/2$ and $-\boldsymbol{v}/2$ while the total momentum is zero (fig. 1). Since the momentum after collision is also zero the only effect relative to the c. m. system of the collision is a rotation of the velocity vectors through some angle θ.

We can translate these results from the c. m. to the laboratory system by adding to each velocity a vector, $\mathbf{V}_{c.m.}$ representing the absolute velocity of the c. m. (fig. 2).

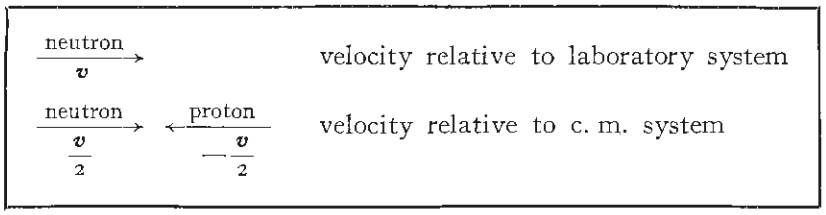

Fig. 1.

The main results of this calculation may be summarized:

(1) The angle between $\mathbf{U}_n$ and $\mathbf{U}_p$, the final velocities of neutron and proton, is 90°. This implies that the new path of a neutron after each collision makes an acute angle with its old path. Thus, for collisions in hydrogen, the neutron path after many collisions has a *forward* trend (fig. 3).

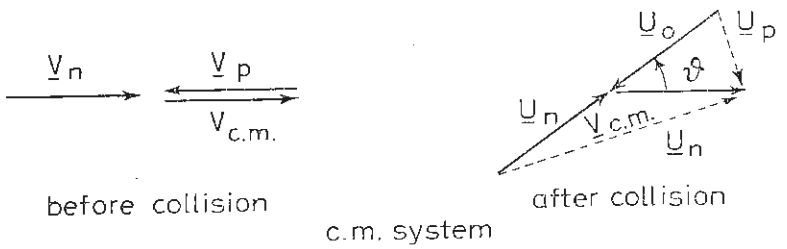

Fig. 2.

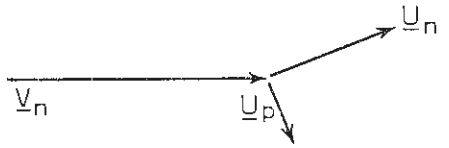

Fig. 3.

(2) Any final neutron energy between 0 (for head on collision) and E_o (for grazing collision) when E is the initial neutron kinetic energy, is possible.

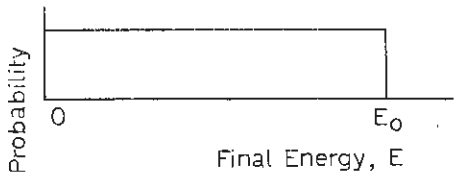

Fig. 4.

(3) If the scattering angles θ are all equally probable (as is predicted, at least for small velocities by quantum mechanics) all values of the final neutron energy between 0 and E_o are equally probable. This is represented in fig. 4.

II. Individual collisions in heavy media.

The situation is slightly different if the scattering atoms are heavier than neutrons. In this case:

(1′) The angle between $\mathbf{U}_n$ and $\mathbf{U}_p$ may be larger than 90° and so the forward trend of the neutrons tends to disappear as the scattering atom becomes heavier. In the limit, for very heavy atoms, the neutron scattering becomes isotropic in direction.

(2′) The smallest possible final neutron energy is αE_0, where:

$$\alpha = \left(\frac{A-1}{A+1}\right)^2,$$

A being the atomic weight of the scattering atom. This expression for α can readily be calculated by considering a head on collision. The maximum percentage loss in energy, $1-\alpha$, may be taken as a measure of the slowing down power of the medium. It is zero for a very heavy atom, 1 for Hydrogen.

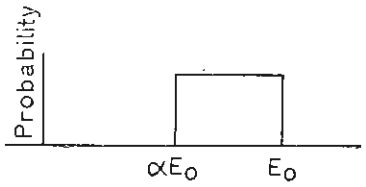

Fig. 5.

(3′) Under the same assumption as before, all values of the final energy between αE_0 and E_0 are equally probable (fig. 5).

III. Introduction of a logarithmic energy scale.

Let us assume, for the moment, that all neutron-atom collisions result in the maximum neutron energy loss, $(1-\alpha)E$. Then after each such collision the final energy represents a constant proportion of the initial energy, the

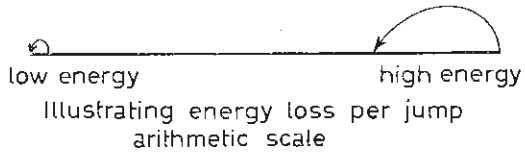

Fig. 6.

constant of proportionality being α. If we should represent the "jump" in energy for each collision on an arithmetic scale, a collision at high energy would represent a very long jump, a collision at low energy a very short one (fig. 6). For this reason it is convenient to introduce a logarithmic energy

scale—on this scale, the maximum loss per collision is $\log E_o - \log \alpha E_o = \log 1/\alpha$, which is independent of energy. Actually, since all final energies between o and E are equally probable, it is necessary to consider the average logarithmic energy loss per collision, $l \equiv \overline{\log (E_o/E)}$. This can be shown by integration to be unity for hydrogen, 0.158 for carbon, and $2/A$ for an element of large atomic weight. From the energy loss per collision it is very easy to calculate the number of collisions required for a neutron to lose any amount of energy.

Exercise. – Calculate the number of collisions required for a neutron to go from 10^6 ev to 1 ev when the damping medium is (a) carbon; (b) hydrogen.

IV. Limitations of simple damping theory.

It is clear that the above theory, since it is based on a picture of scattering atoms at rest, must break down at thermal energies (1/30 ev) where the velocities of the neutrons and the scattering atoms are comparable. Two further factors make the theory inaccurate at energies as high as 1 volt:

(1) Since the energy of, say, H atoms is quantized, the minimum energy which may be imparted by a neutron to a damping H atom is $h\nu$, where, since ν is of the order of the spectral frequencies of the H atom, $h\nu$ is of the order of 1/3 ev. Consequently, the probability of neutron energy loss by collision changes as the energy of the neutron becomes comparable with $h\nu$, and when this energy falls to about 1 ev, the simple theory is inapplicable. Actually, because the hydrogen atom is not a simple oscillator, the situation is rather more complicated.

(2) A hydrogen atom in chemical combination with another atom does not behave like a free proton in a collision process, but, because of the chemical binding energy, acts like a more or less stationary, massive particle. This effect tends to increase the effective reduced mass of the proton-neutron colliding system; it manifests itself in an apparent increase of the collision cross-section as the neutron energy decreases.

V. Mean square diffusion distance.

In slowing down from an initial energy E_o to a final energy E_1 any given neutron traverses a range or distance r from the source. The mean square distance from the source can be roughly estimated as follows:

The neutron path is an open polygon of $\frac{1}{l} \log \frac{E_o}{E_1}$ sides (i.e., the number of collisions to go from E_o to E_1), and each side has length λ, where λ is the mean free path. Then if we assume:

(1) That the collisions are incoherent so that the ranges for all the neutrons constitute a probability aggregate.

(2) That the probability of an individual path of length x is given by the usual kinetic theory expression:

$$e^{-x/\lambda} \frac{dx}{\lambda},$$

then the mean square range $\overline{r^2}$ for energy loss E_0 to E_1 is given by:

$$\overline{r^2} = \frac{2\lambda^2}{l} \log (E_0/E_1) .$$

This formula must be modified if, as in the case of scattering hy H, there is a forward tendency in the paths after collisions (thus increasing $\overline{r^2}$):

$$\overline{r^2} = \frac{2\lambda^2}{\left(1 - \frac{2}{3A}\right) l} \log (E_0/E_1)$$

(note that this correction is small for heavy atoms in which this scattering is isotropic).

Finally, if λ is a function of E:

$$\overline{r^2} = \frac{2}{\left(1 - \frac{2}{3A}\right) l} \int_{E_1}^{E_0} \lambda^2(E) \frac{dE}{E} .$$

The effect of the dependence of λ on energy is not very great in graphite, where there is perhaps a two-fold increase of λ when the energy falls from 10^6 to 10^4 ev. In water, however, λ changes by a factor of 5 in this

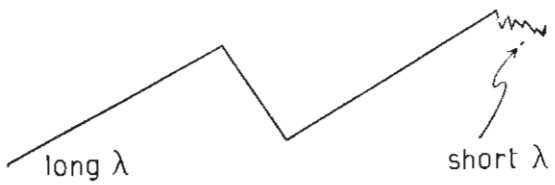

Fig. 7.

same energy range. This means that practically all of the neutron's range is covered at high energy when the mean free path is long—very little is traversed at low energy (fig. 7). The effect is particularly noticeable in experiments on the spatial distribution of neutrons—in carbon this distribution is practically Gaussian, in water it falls off much less rapidly than a Gaussian curve.

VI. Neutron energy distribution.

Suppose a steady source of neutrons is emitting a total of Q neutrons per second at a certain high energy E_0 (or $\varepsilon_0 = \log E_0$). These neutrons will pass through a continuum of energies until they reach thermal energy; how many neutrons will be found in a logarithmic energy interval ε and $\varepsilon + d\varepsilon$ at any time?

To solve this problem we find it convenient to represent the flow of neutrons through energy by dots " drifting " on a logarithmic energy scale (fig. 8). Each collision is represented in the diagram by a small arc; if, as

we assume, the damping medium is hydrogen, the logarithmic energy lost per collision is unity. The average "energy velocity" of drift = energy lost per jump × number of jumps per second $= l \frac{v}{\lambda}$ where v is the ordinary

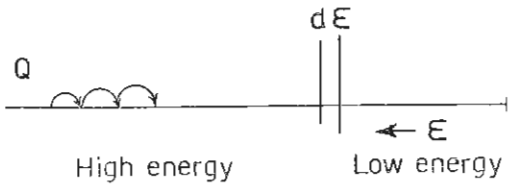

Fig. 8.

average neutron velocity, and if $\rho(\varepsilon)\, d\varepsilon$, is the density of neutrons in the range ε and $\varepsilon + d\varepsilon$, the total number of neutrons passing through this energy range is:

$$\rho(\varepsilon) \frac{v}{\lambda}.$$

This must be the same as the number of neutrons emitted at high energy (conservation of matter), and so:

$$\rho(\varepsilon) \frac{v}{\lambda} d\varepsilon = Q d\varepsilon$$

$$\rho(\varepsilon)\, d\varepsilon = \frac{\lambda}{v} Q d\varepsilon = \frac{\lambda}{v} Q \frac{dE}{E}.$$

Since $v \sim E^{1/2}$,

$$\rho(E)\, dE \sim \frac{\lambda\, dE}{E^{3/2}}.$$

Exercise. – What is the physical significance of the ratio v/λ.

N° 157.

For the introduction to this paper see N° 156.

157.

DETERMINATION OF THE ALBEDO AND THE MEASUREMENT OF SLOW NEUTRON DENSITY

Report C–31 (Notes on Lecture of March 17, 1942).

Determination of the albedo.

Let us consider a thermal neutron which enters a large block of paraffin or water and proceeds to diffuse inside the medium. The number of collisions without absorption which the neutron will undergo is relatively high in paraffin, and so there will be an appreciable probability that the neutron will re-emerge. This probability is a measure of the reflecting power or " albedo " of the absorbing medium; it is about 0.83 for thermal neutrons in H_2O.

Fig. 1.

Experimentally, the albedo of H_2O can be determined in the following manner. The activity of a thermal neutron detector (Dy, or CdInCd–NiInNi) is measured in a large tank of H_2O—first with no other materials near it, and second, with a Cd foil (which absorbs *almost* all the thermals) covering one face of the detector (fig. 1). If the measured activity in the first case is A, in the second case B, one should expect the ratio A/B = 2, for, since the Cd foil absorbs all neutrons striking from one side, its presence halves the number of neutrons crossing the thermal detector. Actually, the ratio is about 12.

To explain this large ratio, let us consider the no Cd experiment. Ideally, each neutron which crosses the detector and is absorbed ultimately is recorded by the G. M. counter. If there is no Cd to absorb the neutrons, a neutron which crosses the detector from right to left has a finite probability β (=albedo) of recrossing the foil from left to right. Consequently, for every neutron crossing once, β neutrons cross twice, β^2 neutrons cross three times, etc., or, the total number of crossings per neutron is the geometric series:

$$1 + \beta + \beta^2 - \cdots = \frac{1}{1-\beta} \cdot \tag{1}$$

Since no reflection can take place in the Cd experiment, a neutron can cross the detector no more than once, and so the ratio of the activities in the two cases must be:

$$\frac{A}{B} = \frac{2}{1-\beta}, \tag{2}$$

where the factor 2 is introduced because in one experiment the foil is bombarded from both sides, in the other experiment only from one side. For the experimentally observed ratio $A/B = 12$, the albedo for water is 0.83.

Relation between albedo and number of collisions before capture of thermal neutrons.

Since the albedo is a measure of the probability that a neutron will re-emerge once it enters a medium, and since this probability depends upon N, the number of collisions which the neutron can make before it is captured, there must be some relation between β and N. To arrive at this relation we shall consider the previous experiment with the detector now consisting of a single atom of cross section σ. The activity in the no Cd case, A, is proportional to $nv\sigma$, the number of collisions with the detector per second (n = neutron density per cm^3, v = velocity).

In the Cd experiment we must calculate the total number of thermal neutrons reaching the Cd per sec. from a knowledge of:

(a) The number q of neutrons becoming thermal per cm^3 per second (density of nascent thermals).

(b) The probability $P(x)$, of a nascent thermal neutron at distance x from Cd reaching the Cd without a capture.

This latter probability may be shown to be very nearly:

$$P(x) = e^{-x/L} \tag{3}$$

where L, the diffusion length, is given by:

$$L = \lambda \sqrt{N/3}, \tag{4}$$

λ being the mean free path. The total number of nascent thermals from a region between x and $x + dx$ which reach each cm^2 of Cd is:

$$P(x) \times [\text{number born in } dx] = q\,dx\,e^{-x/L}, \tag{5}$$

and so the total number which strike the detector atom from all directions and all distances in front of the atom is (for *uniform q*):

$$\sqrt{3}\int_0^\infty q\, e^{-x/L}\,\sigma\, dx = \sqrt{3}\, q\,\sigma L = B. \tag{6}$$

The factor $\sqrt{3}$ arises from the fact that each direction (fig. 2) must be weighted by a factor cos 0, and the average value of this weighting is $\sqrt{3}$.

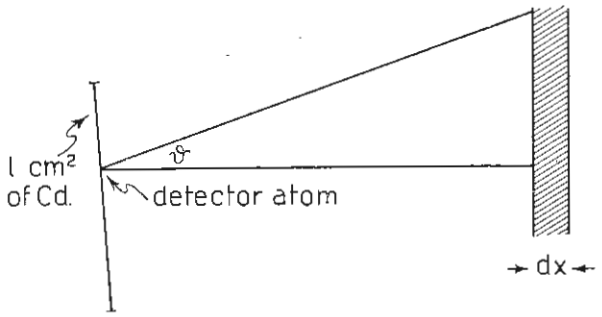

Fig 2.

Since $A = nv\,\sigma$, we have:

$$\frac{A}{B} = \frac{nv}{\sqrt{3}\, qL}. \tag{7}$$

To express this result in terms of N, we note that in the stationary state,
number of thermals born/sec/cm³

= number captured/sec/cm³

= Probability of capture/sec times number of thermal neutrons/cm³

$$= \frac{v}{N\lambda}\, n = q \tag{8}$$

$$\frac{A}{B} = \sqrt{N}. \tag{9}$$

Comparing (9) and (2), we have:

$$\beta = 1 - \frac{2}{\sqrt{N}} \tag{10}$$

a result which is correct for large N and which gives N = 144 for $\beta = 0.83$ (water), and $N = \infty$ for $\beta = 1$ (perfect reflector). When N is small this formula must be modified to:

$$\beta = \frac{\sqrt{N} - 1}{\sqrt{N} + 1}. \tag{11}$$

The albedo for graphite calculated by (10) is 0.94 if we take $N \sim 1000$. This means that a A/B in a graphite experiment should be > 12, whereas

actually A/B in graphite is less than 12; in other words, in graphite the activity with Cd backed foils is greater than it should be according to the simple theory. This extra activity in the Cd case is attributed to neutrons which actually curve around the Cd shield and strike the detector " from behind " (fig. 3); this effect is appreciable in graphite because λ is so large (3 cm compared with 0.3 cm in water). To prevent this " corner turning " a Cd backing, large compared with the diffusion length in carbon (45 cm), and a very small detector, should be used.

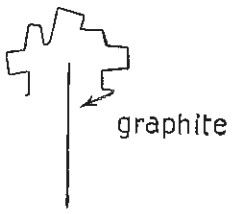

Fig. 3.

Certain other complications which enter in the interpretation of the experiments may also be mentioned:

(1) The theory outlined here assumes that the thermal neutron production is uniform throughout a region which is large compared with L. This can be realized with a point source in water (L = 2 cm) but is impractical in graphites (L = 45 cm).

(2) The neutron loss by leakage through the sides has been neglected; this effect is diminished by increasing the size of the diffusing medium.

(3) The self absorption of the detector reduces the observed activity, especially if the detector is thick. For this reason, the thinnest detector compatible with the available sensitivity should be used in measuring neutron density. A very narrow detector behaves like a thin detector in this respect because the probability of a neutron hitting such a detector more than once (and thus being absorbed) is very small.

Measurement of neutron density.

We shall now consider the problem of determining neutron density and source intensity from measurements of neutron activity. Again consider a single atom detector at a distance r from a source in an infinite medium. Then:

$$\text{number of collisions/sec} = \text{activity} = v\sigma n(r) = A(r),$$

or

$$n(r) = \frac{A(r)}{v\sigma}. \tag{12}$$

This gives us the density from the measured activity. We can get the source strength thus:

If Q = total neutrons produced by source/sec = total disappearing/sec, and number disappearing/sec in volume element $4\pi r^2 dr = \frac{n(r)v}{\lambda N} \times 4\pi r^2 dr$,

$$Q = \frac{v}{\lambda N} 4\pi \int_0^\infty n(r) r^2 dr = \frac{4\pi}{\lambda N \sigma} \int_0^\infty A(r) r^2 dr \tag{13}$$

and, if $A(r)$ is determined, Q is found by integration.

FERMI'S THEORY OF SLOW NEUTRON CAPTURE BY HYDROGEN.

Capture of a neutron by H atoms is generally supposed to result in the combination of a neutron (n) and proton (p) to form a deuteron. To account for the observed probability of capture the rate of energy dissipation must be calculated; this can be done by considering the spins and magnetic moments of two elementary particles. The proton has a spin and a magnetic moment of about 3 (in nuclear magnetons); the neutron has a spin 1/2 and magnetic

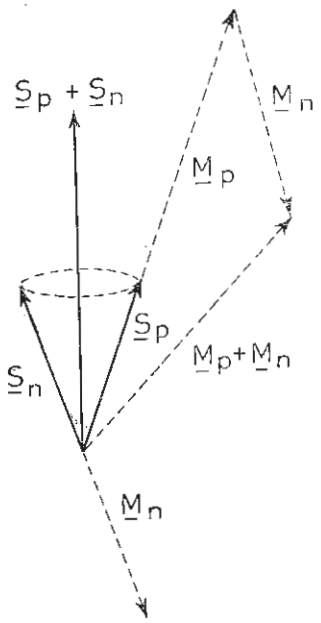

Fig. 4.

moment of about —2 (negative because it corresponds to a +charge spinning). When the n and p are sufficiently close together, the two spins are coupled (as in atomic spectra) and each spin processes around its vector sum which is invariant in space (fig. 4). The resultant magnetic moment vector, $\mathbf{M}_p - \mathbf{M}_n$, being *off* the resultant spin axis, also precesses; this precession gives rise to electromagnetic radiation whose power dissipation determines the probability of the formation of an $n - p$ combination.

N° 158.

One of the first experiments to be done at Chicago was a measurement of the number of neutrons from one of the Ra–Be neutron sources, making use of the graphite column and the newly measured boron cross section. For Fermi this was a necessary part of getting organized in a new laboratory. We had to have neutron sources and detectors calibrated. I went about this automatically; M. H. Whitaker and J. H. Roberts were brought in to be indoctrinated into the Fermi way of doing things.

This paper was issued also as Report C–21. It was reissued by the Atomic Energy Commission, Technical Information Branch, Oak Ridge Tennessee as Document MDDC–880, in January, 1947.

H. L. ANDERSON.

158.

THE NUMBER OF NEUTRONS EMITTED BY A RA+BE SOURCE (SOURCE I)

H. L. ANDERSON, E. FERMI, J. H. ROBERTS, and M. D. WHITAKER
Report CP-21 (March 21, 1942).

In order to simplify the design of experiments directed toward the production of a chain reaction involving uranium, it is desirable to know the actual number of neutrons emitted by the primary sources used. A series of experiments have been planned whose aim is to determine this number. The measurements described are a part of this series. Here, the number of neutrons per cm^2 emerging from the top of a carbon parallelepiped is measured and calculated, and from a knowledge of the neutron distribution in the carbon, with a given placement of source, this measurement is reduced to the neutron emission from the source.

A radium–beryllium neutron source containing about 1.16 grams of radium was placed 28 inches from the bottom of a carbon parallelepiped five feet on a side and of variable height (fig. 1). The source was placed on the vertical axis of the pile, and the number of neutrons emerging from the top surface at the center was determined for two different heights. These neutrons were detected by a BF_3 proportional counter of 3.62 cm inside diameter, which was filled with BF_3 gas to a pressure of 12.1 cm of mercury at 0°C. A 10 cm section of the counter was exposed to the neutron flux, the rest being shielded by a close fitting cadmium wrapper, in which a semicylindrical window 10 cm long had been cut. The glass walls of the counter tube and the metal cathode (a nickel cylinder 0.010 inches thick) were found, experimentally, to have an absorption factor of 1.13. This absorption factor was measured before

the assembly of the counter by observing the decrease in the counting rate of a smaller BF_3 counter placed near a graphite surface, when the glass tube and nickel cylinder were slipped over it.

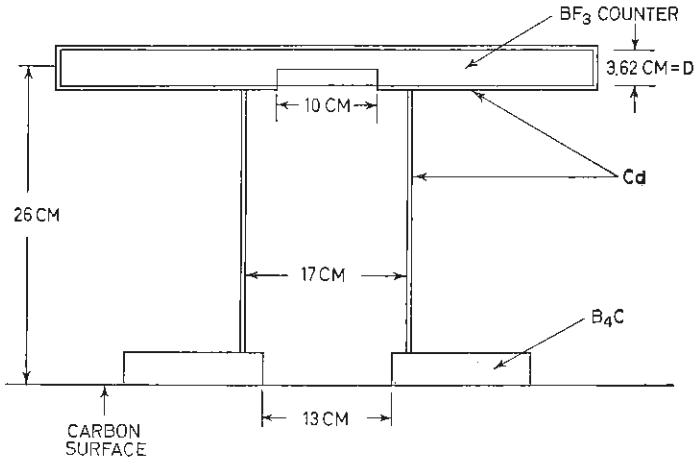

Fig. 1.

A boron carbide shield, containing a circular hole 13 cm in diameter, was used to define the part of the upper carbon surface from which the counter could receive C neutrons. The counter tube was mounted horizontally on a vertical cadmium sheet cylinder, in such a manner, that the semicylindrical opening in the cadmium wrapper around the counter was symmetrically placed, with respect to the circular opening in the boron-carbide shield. The axis of the counter was 26 cm above the carbon surface. Additional cadmium shields were arranged so that it was impossible for the counter tube to receive C neutrons, other than those originating in the carbon surface defined by the boron carbide shield. The number of disintegrations produced in the tube was counted with and without a cadmium shield over the 13 cm opening. The difference between the number of counts per minute observed with and without cadmium was taken with the carbon surface 40 inches above the source, and again with the surface 44 inches above the source as a check. These numbers were found to be 90/min and 63/min. These numbers must be reduced to the number of neutrons per second, J_0, emerging from unit area of the carbon surface at its center by suitable geometrical considerations, and by making use of the known angular distribution of the neutrons coming from the carbon surface. After J_0 is known, the number of neutrons emitted by the source can be calculated from a knowledge of the neutron distribution in the carbon pile.

An approximate calculation of the number of neutrons producing disintegrations in the counter tube in terms of J_0 will be done, and the accuracy will be improved by determining correction factors to take care of the approximations made.

The angular distribution of the neutrons coming from the surface varies with the angle θ, which any neutron makes with the normal to the surface

as $\cos\theta + \sqrt{3}\cos^2\theta$. The fraction of the neutrons which come off at any angle θ is then:

$$\frac{\cos\theta + \sqrt{3}\cos^2\theta}{\pi\left(1+\frac{2}{\sqrt{3}}\right)}$$

where the denominator is the definite integral of the numerator between the limits 0° and 90°. For angles close to 90° this becomes:

$$\frac{1+\sqrt{3}}{\pi\left(1+\frac{2}{\sqrt{3}}\right)}$$

and the number of disintegrations taking place per second in the counter is approximately:

$$\frac{\pi R^2 J_0 \sigma_{(kT)}}{D^2} \cdot \frac{1+\sqrt{3}}{\pi\left(1+\frac{2}{\sqrt{3}}\right)} = 1.2679 \cdot \frac{R^2 J_0 \sigma_{(kT)}}{D^2}$$

where πR^2 is the area of the emitting carbon surface, D is the distance between the surface and the counter, and $\sigma_{(kT)}$ is the cross section of the counter for absorption of a neutron of energy kT. $\sigma_{(kT)}$ will be calculated later.

H. W. Ibser has calculated this numerical factor accurately for the actual geometry used and finds it equal to 0.9265 of the value.

We have assumed in the approximation that the neutron current is the same for all parts of the carbon surface from which neutrons were counted in the above experiment. Since the neutron flux falls off as $\cos(\pi x/a) \times$ $\times \cos(\pi y/a,)$ it follows that the average neutron current would not be J_0, which is the value at the center, but 0.9948 J_0 for the surface of 13 cm diameter.

The approximation used does not take into account the fact that the window, through which neutrons pass through the cadmium shield around the counter tube, is in the form of a semicylinder. This means that the cadmium boundaries which define the length of the counter tube are at a lower level than the level at which the width is defined, by an amount that has a maximum value equal to the radius of the tube. This results in the tube having an effective length that is 1.07 times as great as the length of the semicylindrical opening in the cadmium surrounding the tube.

Even before we calculate the cross section of the counter, which has been designated as $\sigma_{(kT)'}$ we will calculate the amount by which we must correct this cross section, in order to have it apply to the Maxwellian neutron distribution which we actually have, instead of applying only to the neutrons of energy kT. Since the cross section of the boron used varies as $1/V$, in order to get a factor relating the cross section for neutrons of energy kT to the average cross section for the neutrons having a Maxwellian distribution about the energy kT, we must get the ratio of the velocity of a neutron of energy kT to the average velocity of the neutron having the Maxwellian

distribution. Or, if $C=\sqrt{2\,kT/m}$, then the cross section will vary as the average of C/V.

$$\overline{\left(\frac{C}{V}\right)}=\frac{\int_0^\infty \frac{C}{V}V^3 e^{-V^2/C^2}\,dV}{\int_0^\infty V^3 e^{-V^2/C^2}\,dV}=\frac{\sqrt{\pi}}{2}=0.8862\,.$$

Now, if we apply all these correction factors to the first numerical constant 1.2679, we find that this becomes 1.1218 and the number of neutron captures per second in the counter becomes:

$$1.108\cdot\frac{R^2\,J_0\,\sigma}{D^2}=0.06925\;J_0\sigma$$

where $\sigma_{(kT)}$ has been changed to σ by the inclusion of the last correction factor.

If we neglect the attenuation of the neutron current by absorption in the BF_3 of the counter, which we can do in this case with an error of less than 1 %, then we can say that the total cross section of the counter is the number of boron atoms in the tube times the cross section of each, or, the number of moles of the gas times the cross section per mole, which is 473 cm² for boron and neutrons of energy kT. Then

$$\sigma\ \text{counter}\ (kT)=\frac{\text{number of moles}\times 473}{1.13}$$

where 1.13 is the absorption factor of the wall material of the counter tube.

$$\text{Volume of counter tube}=\frac{\pi D^2}{4}\times 10=\frac{\pi}{4}(3.62)^2\times 10=102.92\ \text{cm}^3;$$

$$\text{Pressure}=\frac{12.1}{76}\ \text{atmospheres at } 0^\circ\text{C};$$

$$\text{Number of moles}=\frac{102.92}{22412}\times\frac{12.1}{76}=7.311\times 10^{-4}\ \text{moles}$$

$$\sigma\ \text{counter}\ (kT)=\frac{7.311\times 10^{-4}\times 473}{1.13}=0.306\ \text{cm}^2.$$

With the top of the carbon 40 inches above the source, the number of disintegrations per second due to C neutrons was observed to be 1.5. Therefore

$$1.5=0.06925\;J_0\times 0.306$$

and

$$J_0=1.5\cdot\frac{1}{0.06925\times 0.306}=70.78\,\frac{\text{neutrons}}{\text{cm}^2\,\text{sec}}$$

and for the case where the top of the carbon pile is 44 inches above the source

$$J_0=\frac{63}{60}\,\frac{1}{0.06925\times 0.306}=49.54\,\frac{\text{neutrons}}{\text{cm}^2\,\text{sec}}\,.$$

In the report A–21, Formula 15 gives the density n of thermal neutrons as a function of z. For a (Ra+Be) source, the neutrons may be represented

as a superposition of three groups having ranges for slowing down to thermal energy and percentages as follows:

Per cent	Range in graphite
15.0	27.1 cm
69.3	39.8
15.7	58.9

For large z and a 5 ft column the formula reduces to:

$$\frac{\lambda NV}{Q} = 0.008565\, e^{-z/27.61}.$$

Near the top of the column an additional term must be added to represent the effect of the nearby boundary. We have then:

$$\frac{\lambda NV}{Q} = 0.008565\, [e^{-z/27.61} - e^{+z/27.61}\, e^{-(z/27.61)(Z_0+\lambda/\sqrt{3})}$$

where Z_0 is the ordinate of the top. Since the diffusion coefficient is $\lambda V/3$ we have

$$\frac{J_0}{Q} = -\frac{\lambda V}{3Q}\left(\frac{\partial N}{\partial z}\right)_{z=Z_0} = \frac{0.008565}{3\times 27.61}\,[1 + e^{-(z/27.61)(2.55/\sqrt{3})}]\, e^{-Z_0/27.61}$$

$$= 1.9636\times 10^{-4}\, e^{-\frac{Z_0}{27.61}}$$

$$\frac{J_0}{Q} = 4.95\times 10^{-6} \quad \text{at} \quad Z_0 = 40 \text{ inches}$$

$$\frac{J_0}{Q} = 3.432\times 10^{-6} \quad \text{at} \quad Z_0 = 44 \text{ inches}$$

$$\therefore Q = \frac{70.78}{4.954\times 10^{-6}} = 14.29\times 10^6 \frac{\text{neutrons}}{\text{sec}}$$

from the data taken at $Z_0 = 40$ inches and

$$Q = \frac{49.54}{3.432\times 10^{-6}} = 14.43\times 10^6 \frac{\text{neutrons}}{\text{sec}}$$

from the data taken at $Z_0 = 44$ inches

$$\therefore \text{avg } Q = 14.36\times 10^6 \quad \text{for source No. I.}$$

For the three sources I, II, and III, we have the results given in the following tabulation in which we combine the value of Q and the comparisons given in the report C–10.

Source No.	Q	Grams radium	Q/gram
I	1.44×10^7	1.16	1.24×10^7
II. . . .	1.28×10^7	1.0308	1.24×10^7
III . . .	1.05×10^7	0.84	1.25×10^7

N° 159.

Waiting for the arrival of sufficient material for the first chain reactor, Fermi continued to improve his knowledge of the pertinent constants. He liked to analyze the data himself, because he preferred his knowledge to be first-hand. Looking over the data on the exponential experiments, he wrote this paper.

H. L. ANDERSON.

159.

THE DETERMINATION OF THE RATIO BETWEEN THE ABSORPTION CROSS SECTIONS OF URANIUM AND CARBON FOR THERMAL NEUTRONS

Report C–84 (May 15, 1942).

The so called " cadmium ratio " observed in the exponential experiment offers a simple and probably rather reliable method for the determination of the ratio between the absorption cross sections of uranium and carbon for thermal neutrons. We shall illustrate this method and its results on the data obtained in the exponential experiment No. 5, in which uranium-oxide D 1 (*) of fairly high purity was used.

From the observed value 6.68 of the cadmium ratio in this experiment, it is possible to determine the magnitude $\lambda\, nv/q$ by the same method described in the sub-title " Interpretation of cadmium ratio " of report C–26 (**). The result is:

$$(1) \qquad \frac{\lambda\, nv}{q} = \frac{1.216\times 10^{-8}}{6.33\times 10^{-11}}\,\frac{6.68-1.15}{1} = 1062\,.$$

The fraction of thermal neutrons absorbed by uranium can be calculated in terms of this magnitude, as in C–26 (**). The result is:

$$(2) \qquad f_{\mathrm{T}} = 0.829.$$

This indicates that the number of neutrons absorbed by uranium and by carbon in the cells are in the ratio 0.829 to 0.171. If the density of neutrons within the cell of our lattice were constant the ratio between these two num-

(*) D 1 was the label of a particular grade of material. (Editors' note).
(**) Paper N° 150 (Editors' note).

bers should be equal to the ratio between the product of the thermal absorption cross section × the number of atoms in the cell for uranium and for carbon respectively. A correction, however, must be applied to take into account the fact that the density of thermal neutrons is, in average, larger in carbon than in uranium, because absorption takes place inside the uranium lump. This correction is not very large and can be estimated by applying the diffusion theory to the diffusion of thermal neutrons within the cell. The result is that the density of thermal neutrons in carbon is in the average 1.273 times larger than in uranium. The number of gram atoms of uranium in the cell is 6.70 and the number of gram atoms of carbon is 1090. On account of the preceding correction, this latter number must be increased by the factor 1.273. Consequently, the ratio between the effective number of atoms of carbon and uranium is:

$$\frac{\text{Atoms of C}}{\text{Atoms of U}} = \frac{1090 \times 1.273}{6.70} = 207. \tag{3}$$

We have finally:

$$\frac{207\,\sigma_C}{\sigma_U} = \frac{0.171}{0.829}. \tag{4}$$

From this we obtain the final result

$$\frac{\sigma_U}{\sigma_C} = 1003. \tag{5}$$

It should be noted that this result is relative to the uranium and the graphite used in the experiment.

N° 160.

For the introduction to this paper see N° 156.

160.

THE ABSORPTION OF GRAPHITE FOR THERMAL NEUTRONS

Report C–154 (Notes on Lecture of June 30, 1942).

The recent measurements of the diffusion length of thermal neutrons in graphites of various origins together with the results on the " diffusion mean path " enable us now to calculate the absorption cross section of graphite with a somewhat greater accuracy than it had been possible so far.

In what follows all the data on diffusion length, mean free paths and similar magnitudes are reduced to graphite of density 1.6.

The following data and definitions have been used:

Mean free path λ calculated on the assumption of an atomic scattering cross section of $4.8\ 10^{-24}$. $\lambda = 2.60$ cm. Diffusion mean free path:

$$\lambda_0 = \frac{\lambda}{1 - \cos\theta}$$

where $\cos\theta$ is the scattering angle of a single collision. We have taken from the latest measurements of Anderson: $\lambda_0 = 2.73$ cm.

The absorption mean free path A and the diffusion length L are related by the equation:

$$L^2 = \frac{\lambda_0 A}{3} = \frac{\lambda_0 \lambda}{3} \frac{\sigma_x}{\sigma_a(\bar{v})}$$

where σ_x is the scattering cross section and $\sigma_a(\bar{v})$ is the absorption cross section of graphite for neutrons having the mean velocity:

$$\bar{v} = \frac{2}{\sqrt{\pi}} \sqrt{\frac{2\,kT}{m}} = \frac{2}{\sqrt{\pi}} v_{kT}.$$

If the $1/v$ law holds, the absorption cross-section for neutrons of energy kT is $2/\sqrt{\pi}$ times larger than $\sigma_a(\bar{v})$.

We find ultimately:

$$\sigma_a(v_{kT}) = \frac{2}{\sqrt{\pi}} \frac{\lambda_0 \lambda \sigma_x}{3 L^2} = \frac{12.8 \times 10^{-27}}{L^2}.$$

The numerical results for our brands of graphite are as follows

Graphite	Effective Cross-section $\sigma_a(v_{kT})$ (Carbon + Impurities)
Speer (*)	5.49×10^{-27}
AGX (*)	6.68×10^{-27}
US (*)	6.38×10^{-27}

The differences are presumably due to the different content of impurities.

(*) Name of a particular brand of graphite. (Editors' note.)

N° 161.

Eugene Wigner had asked me to look into the question of how much the diffusion coefficient for neutrons would be increased if the moderator were pierced by parallel, empty cooling channels. After I had carried out the computation, Fermi happened to mention to me that he too had calculated the increase in diffusion coefficient. I met with Fermi that afternoon, and we compared our results. Fermi suggested that we write a joint report on the calculation.

Fermi's calculation consisted essentially of computing the mean square distance of travel in directions parallel and perpendicular to the channels. His result could be expressed as

$$D_{\parallel} = \frac{\lambda}{3}\left[1 + \Phi + \Phi \cdot \frac{3}{2}\frac{a}{\lambda} Q\right]$$

$$D_{\perp} = \frac{\lambda}{3}\left[1 + \Phi + \Phi \cdot \frac{3}{4}\frac{a}{\lambda} Q\right]$$

where Q is the ratio of mean square chord length in the channel to square of mean chord length (= 4/3 for a circular cylinder). My calculation was done as indicated in the paper. However, I could not evaluate the triple integral of equation (13) directly; hence I evaluated it by comparing the final result with Fermi's calculation of $D_{\parallel}$. This gave the value $N' c\pi a^2 \lambda/3$ for the triple integral of equation (13).

I wrote the paper, and I never was certain whether Fermi read it through carefully. I think he was content that the final result agreed with his result. The whole matter of diffusion through channels has since been worked out in detail by D. F. Behrens, (« Proc. Phys. Soc. », *52*, 607 (1949)).

A. M. WEINBERG.

161.

LONGITUDINAL DIFFUSION IN CYLINDRICAL CHANNELS

E. FERMI and A. M. WEINBERG
Report C–170 (July 7, 1942).

ABSTRACT.

The increase in leakage of the neutrons because of the presence of empty cylindrical channels in a pile has been calculated. The overall diffusion coefficient parallel to the duct is $D = \frac{1}{3} c\lambda\left(1 + \Phi + \Phi\frac{2a}{\lambda}\right)$ where c = average velocity of neutrons, λ = mean free path in pile, a = diameter of channel, and Φ = fractional volume of total pile occupied by the channels. The longitudinal flow in a single channel is shown to be greatest at the center of the channel, and the average flow per square centimeter per unit gradient inside a channel is $D_c = \frac{1}{3} c\lambda\left(1 + \frac{2a}{\lambda}\right)$.

1. Introduction.

The increased neutron leakage along cylindrical ducts inside the pile is of considerable importance in estimating the overall dimensions required for the pile to operate. Clearly, the diffusion of neutrons along empty channels proceeds much more readily than diffusion through the lattice; consequently the leakage through such a duct will be much greater than the leakage from a similar solid channel, and so an operating pile containing cooling ducts must be larger than one which is completely solid. In the present note we shall compute the average longitudinal diffusion flow in a single isolated channel and in a pile containing several such channels. The treatment will follow rather closely the ordinary kinetic theory computation of diffusion; however the results will be somewhat more reliable than in the kinetic theory case because neutron-neutron collisions can be neglected.

Suppose a cylindrical channel is bored through an infinite pile in which there was an originally constant neutron density gradient running parallel to the axis of the channel. The density will have a (different) *constant* gradient even after the channel has been bored through the medium; for if we assume the density gradient is constant, the increase in diffusion flow to a point P in the channel due to contributions from any point at higher density is just equal to the decrease in diffusion flow due to the symmetrical point at lower density. Consequently a linear density distribution in the channel is self consistent with the same linear distribution outside the channel. It should be pointed out that although the density gradient inside and outside the channel is the same, the diffusion *flow* is not constant but is highest on the axis of the cylinder and tapers off to its usual value inside the pile within a mean free path or so of the edge of the cylinder.

2. Diffusion into an empty space, general.

In this section we shall write down an expression for the number of neutrons per sec per cm² thrown across a surface element ds in empty space from a volume element dv inside a medium in which there is a linear distribution of neutrons. Consider an element ds lying in the xy plane at the point (x, o) (fig. 1). Let the overall distance from dS to the element dv be denoted by r; the distance from dS to the point w where r intersects the wall of the medium by ρ. Then since the constant gradient is assumed to lie along the z axis, the number of particles, $N dv$, in dv is:

$$N\,dv = \left(N_o + \rho \frac{dN}{dz}\right) dv = (N + rN' \cos\theta)\, dv\,. \tag{1}$$

where prime denotes derivative with respect to z, and N_o is the density in the xy plane. Since each neutron makes c/λ collisions per second, where c is the average velocity and λ the mean free path in the medium, the number of particles in dv starting new mean free paths per second is:

$$\frac{c}{\lambda}(N_o + rN' \cos\theta)\, dv\,. \tag{2}$$

Of these, only the fraction $\frac{\cos\theta}{4\pi r^2}\,ds$ are directed towards dS, (assuming spherically symmetric scattering), while only $e^{-\frac{r-\varrho}{\lambda}}$ of those properly directed will survive the journey from dv to dS without suffering a collision. Consequently the number reaching dS per second from dv is:

$$(3)\qquad \frac{c}{4\pi\lambda}(N_0 + rN'\cos\theta)\,e^{-\frac{r-\varrho}{\lambda}}\cos\theta\sin\theta\,dr\,d\theta\,d\varphi\,dS.$$

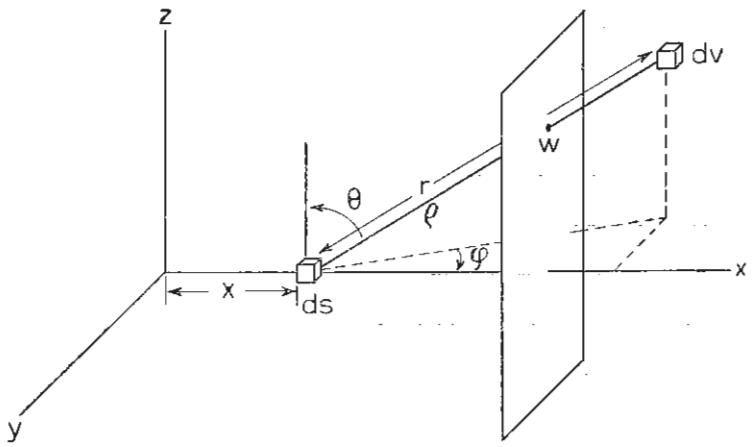

Fig. 1.

The total contribution from above and below the xy plane can be found by integrating (3) over all space in which the neutrons make collisions.

3. Cylindrical channel, interior point, uniform transverse distribution.

We shall now apply the formula of the preceding section to calculate the longitudinal flow in the interior of a long cylindrical channel of radius a, whose axis coincides with the Z–axis. From geometry we have that ρ, the distance cut off on the radius vector by the cylindrical wall, is:

$$(4)\qquad \rho(x,\theta,\varphi) = \left(-x\cos\varphi + \sqrt{a^2 - x^2\sin^2\varphi}\right)^{\csc\theta}.$$

The number per second striking dS in all directions from above is, from (3),

$$(5)\qquad F_{\perp}\,dS = \frac{c\,dS}{4\pi\lambda}\int_0^{2\pi}\int_0^{\pi/2}\int_{\varrho}^{\infty}(N_0 + rN'\cos\theta)\,e^{-\frac{r-\varrho}{\lambda}}\cos\theta\sin\theta\,dr\,d\theta\,d\varphi =$$

$$= \frac{N_0 c}{4}\,dS + \frac{N'c\lambda}{6}\,dS + \frac{N'c\,dS}{4}\,a\,E\left(\frac{x}{a}\right)$$

where $E(x/a)$ is the complete elliptic integral of the second kind. The number striking from below is the same as (5) except that the last two terms are negative. Hence the total flow from all sides is:

$$(6)\qquad F(x) = \frac{N'c}{3}\left[\lambda + \frac{3a}{2}\,E\left(\frac{x}{a}\right)\right].$$

and the interior diffusion coefficient is:

$$D(x) = \frac{F(x)}{N'} = \frac{c}{3}\left[\lambda + \frac{3a}{2} E\left(\frac{x}{a}\right)\right]. \tag{7}$$

In fig. 2 the diffusion flow given by (6) has been plotted as a function of x/a, the relative distance from the cylinder axis; the ratio a/λ was taken to be 5.

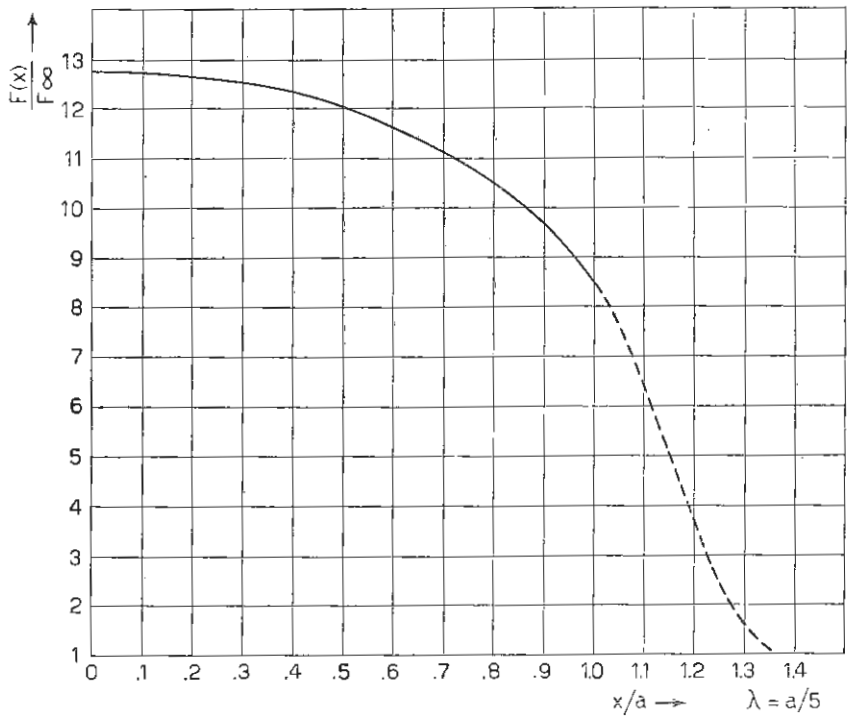

Fig. 2.

The flow outside the cylinder was sketched in roughly by assuming that the flow reduces to its ordinary value:

$$F_\infty = \frac{N' c \lambda}{3} \tag{8}$$

exponentially with a relaxation length of about λ.

The average flow over the cylinder $\bar{F}$, is found by integrating (6) with respect to x and interchanging the order of integration in the elliptic integral. The result is

$$\bar{F} = \frac{2\pi \int_0^a x F(x)\, dx}{\pi a^2} = \frac{N' c}{3}(\lambda + 2a), \tag{9}$$

and the average longitudinal interior diffusion coefficient is

$$\bar{D} = \frac{c}{3}[\lambda + 2a]. \tag{10}$$

The forms of the expressions for $\overline{F}$ (or $\overline{D}$) are not altogether unexpected; for the mean free path of a particle inside the channel is of the order of the diameter of the channel, and so $L + 2a$ is of the order of the overall mean free path of a particle which passes through the channel. From this point of view we may write:

$$\overline{D} = 1/3 \times \text{average velocity} \times \text{overall mean free path}$$

which is identical with the ordinary kinetic theory formula for the diffusion coefficient.

The flows at the center and at the cylinder surface can be computed from (6). The results for these two points compared with the average flow are:

$$F(a) = \frac{N'c}{3}\left(\lambda + \frac{3}{2}a\right)$$

$$\overline{F} = \frac{N'c}{3}(\lambda + 2a)$$

$$F(0) = \frac{N'c}{3}\left(\lambda + \frac{3\pi}{4}a\right).$$

For $a = 5\lambda$, the flows are in the ratio:

$$F(a) : \overline{F} : F(0) = 1 : 1.3 : 1.5 .$$

4. Cylindrical channel, interior point, cosine transverse distribution.

The transverse distribution in the actual pile is given by:

$$N_{trans} = N_0 \cos \alpha x \cos \alpha y \approx N_0\left[1 - \frac{\alpha^2}{2}(x^2 + y^2)\right]$$

where $\alpha \approx \frac{\pi}{w}$, w being the width of the pile. The diffusion flow through a channel oriented perpendicularly to such a distribution can be calculated exactly as before, except that the distribution to be inserted in (3) is:

$$N = (N_0 + rN' \cos\theta)\left(1 - \frac{\alpha^2}{2} r^2 \sin^2\theta\right).$$

The result of the integration in this case is

$$(11) \qquad \overline{F} = \frac{N'c}{3}\left[\lambda + 2a\left(1 - d'^2\left\{\frac{8}{5}a^2 + \frac{3}{4}\lambda a + \frac{3}{4}\lambda^2 + \frac{9}{20}\frac{\lambda^3}{a}\right\}\right)\right].$$

For a pile 6 meters in width, and a channel of 10 cm radius, the term in the brackets is less than 0.003; hence a transverse cosine distribution of such large wave length can be neglected in considering the diffusion flow through the channels.

5. Cylindrical channel, exterior flow, uniform transverse distribution.

In order to compute the overall increase in diffusion flow caused by a large number of parallel channels, it is first necessary to compute the increased flow *outside* each channel considered in isolation. In this case the net flow per square centimeter at a point x centimeters from the center of the cylinder is given by

$$(12) \qquad F(x) = \frac{N'c\lambda}{3} + \frac{N'c}{\pi}\int_0^{\arcsin\frac{a}{x}}\int_0^{\pi/2}\sqrt{a^2 - x^2\sin^2\varphi}\; e^{-\frac{x\cos\varphi - \sqrt{a^2 - x^2\sin^2\varphi}}{\lambda\csc\theta}}\cos^2\theta\, d\theta\, d\varphi .$$

The first term is the ordinary unperturbed diffusion flow which would exist in the absence of a channel, while the second term represents the added flow due to the presence of the channel. The contribution of this term is indicated very roughly by the dotted part of fig. 2.

The total excess external flow due to a single channel is found by integrating the excess flow density over a plane outside the cylinder:

$$(13) \qquad F_{excess} = 2\pi\cdot\frac{N'c}{\pi}\int_a^{\infty}\int_0^{\arcsin\frac{a}{x}}\int_0^{\pi/2} x\sqrt{a^2 - x^2\sin^2\varphi}\; e^{-\frac{x\cos\varphi - \sqrt{a^2 - x^2\sin^2\varphi}}{\lambda\csc\theta}}\cos^2\theta\, d\theta\, d\varphi\, dx$$

$$= N'c\,\frac{\pi a^2\lambda}{3}.$$

6. Many parallel cylindrical channels.

We can now compute the total diffusion flow parallel to a set of identical parallel cylinders embedded in the pile. If Φ is the fractional volume occupied by the cylinders and S the total area of the face of the pile normal to thecylinders, we have:

Total cross-sectional area of cylinders $= \Phi S$

Total number of cylinders $= \frac{\Phi S}{\pi a^2}$

Total area not occupied by cylinders $= (1 - \Phi)\, S$.

The total flow is the sum the flow through the cylinders + the total excess external flow due to each of the cylinders + the total unperturbed flow through the surface between the cylinders:

$$(14) \qquad F_{total} = \frac{N'c\lambda}{3}\left(1 + \frac{2a}{\lambda}\right)\Phi S + N'c\,\frac{\pi a^2\lambda}{3}\cdot\frac{\Phi S}{\pi a^2} + \frac{N'c\lambda}{3}(1 - \Phi)\, S =$$

$$= \frac{N'c\lambda}{3}\, S\left(1 + \Phi + \Phi\,\frac{2a}{\lambda}\right).$$

The average flow per square centimeter is

$$\overline{F} = \frac{F_{total}}{S} = \frac{N' c\lambda}{3}\left(1 + \Phi + \Phi\frac{2a}{\lambda}\right) \tag{15}$$

and the average longitudinal diffusion coefficient is

$$D_{II} = \frac{\overline{F}}{N'} = \frac{c\lambda}{3}\left(1 + \Phi + \Phi\frac{2a}{\lambda}\right). \tag{16}$$

These expressions for $\overline{F}$ and D_{II} are required for estimating the net leakage due to the presence of channels in the pile.

N° 162.

The following paper is interesting in that it reflects the change in the way of working which was enforced on Fermi in the large and powerful organization, which in just a few months the Metallurgical Laboratory had become. He no longer had the time to participate directly in the experimental work. Instead, he could order an experiment done and a skilled group would carry it through forthwith and deliver all the data to him for analysis. He could even have the analysis done for him by a member of the theoretical physics group. It is doubtful how much he enjoyed it. He commented to Segrè in a visit that he was making physics by the telephone.

As an exercise of his powers, Fermi decided to repeat an earlier work (see paper N° 138) with a larger graphite column and better accuracy. Assigned to Group III under the leadership of M. D. Whitaker and W. H. Zinn, it was promptly executed. The analysis of the data, however, Fermi refused to delegate. It is given in some detail in his report. The new value of $\eta = 1.29$ was appreciably smaller than that found before and underscored the wisdom of repeating the experiment.

H. L. ANDERSON.

162.

THE NUMBER OF NEUTRONS EMITTED BY URANIUM PER THERMAL NEUTRON ABSORBED

Report C–190 (July 16, 1942).

SUMMARY. — The experiments on the emission and absorption of neutrons described in the report for the week ending July 3rd, 1942, C–164, (*) are interpreted with the result that the absorption cross-section of uranium for neutrons of energy kT is 6.77×10^{-24} and the ratio is 1.29.

In report A–6 by Anderson and Fermi (**), a method was applied for the determination of the number of neutrons emitted when a thermal neutron is absorbed by uranium. Since the amount of carbon that was available at the time was rather limited, it appeared worthwhile to repeat now the same experiment under improved conditions. The main improvements are:

a. Use of a graphite column of a larger side (about 150 cm. instead of 90.),

b. Use of compressed uranium oxide, which makes it possible to keep the gap into which the uranium layer can be introduced considerably narrower, so as to make the gap correction much smaller.

c. Use of uranium of considerably higher purity.

The details of the experiment and the results of the various intensity measurements are given in report C–164. The present report is concerned with the interpretation of the data given there.

In discussing this interpretation we shall use essentially the same notation as in report A–6. In particular we shall express the slowing down density and the density of neutrons

(*) C–164 is not one of the reports prepared by Fermi. (Editors' note).

(**) See paper N° 138. (Editors' note).

by taking as unity the number of neutrons emitted by the Ra + Be source used in the experiment.

The experiment as described in the weekly report C–164 consisted essentially of a series of measurements of neutron intensities in a graphite column having a Ra+Be source on the axis. A gap situated at about 100 cm from the source was empty in some of the measurements and, in a second series of measurements, it was filled with a layer of pressed uranium oxide of a thickness of 3.82 gm/cm^2. More details as to the experimental arrangement are given in the weekly report. The measurements with the empty gap are used for the standardization of the indium detectors employed for the measurements, whereas the difference between the measurements with uranium and without uranium in the gap which is due primarily to the opposing effects of the neutrons produced by uranium and of the neutrons absorbed by uranium, is used for a calculation of these effects.

We shall divide the analysis into the following sections:

1. Standardization of detectors.
2. Determination of the number of neutrons produced by uranium.
3. Determination of the number of thermal neutrons absorbed by uranium.
4. Conclusions.

1. Standardization of the Detector.

The measurements without uranium in the gap have been taken with and without Cd around the indium foils. The measurements with Cd give an intensity proportional to the slowing down density q for the indium resonance neutrons. From a comparison between the observed intensity and the slowing down densities calculated in the usual way, we can find the coefficient by which the observed activity has to be multiplied in order to obtain the slowing down densities. Such a comparison is carried out in Table I.

Table I.

Position	A_{Cd}	$10^6\, q$	$10^{11}\, q/A_{Cd}$	
3	30143	1.789	5.94	
5	8256	0.4893	5.93	
7	1716	0.1022	5.96	
9	327	0.01916	5.86	
10 —	143	0.008637	6.04	5.93
gap →				
10 +	147	0.008613	5.86	
11	64	0.004013	6.27	
12	—	0.001881	—	
13	16	0.000836	5.23	
14	10	0.000365	3.65	

The first column gives the position of the Cd covered indium detector from the source. The number indicating the position is very closely equal to the distance of the detector from the source in units of 10 cm. Column

two, taken from the weekly report C–164, gives the activity A_{Cd} observed without uranium in the gap; column three is calculated on the assumption that the neutrons emitted by the source are divided into three groups, having indium ranges 22.8, 37 and 57 cm, and having a relative number of neutrons 0.150, 0.693, and 0.157. The formula used is:

$$(1) \qquad 10^6 q_{In} = 2.274\, e^{-(r/22.8)^2} + 2.455\, e^{-(r/37)^2} + 0.152\, e^{-(r/57)^2}.$$

Column four gives the ratio between q and the observed resonance activity. It is seen that the ratio is reasonably constant except for the last points where the large fluctuations are probably due to experimental inaccuracy in the reading of very low intensities. As a mean value of the ratio we have taken 5.93×10^{-11}. We have thus the standardization of the resonance neutrons expressed by the following formula:

$$(2) \qquad q = 5.93 \times 10^{-11} A_{Cd}.$$

As we have already stated, this is not an absolute standardization, since the number of neutrons emitted by the source has been taken to equal 1. For the source actually used, the number of neutrons emitted is probably about 25×10^6 per second.

The data on which the standardization of thermal neutrons has been carried out are collected in Table II.

TABLE II.

Pos.	A_{Ni}	A_{Cd}	A_{th}	Top Correction Factor	Product	Gap Effect	Activity Corrected	$10^6\, nv\lambda$	$\frac{10^8\, nv\lambda}{A_{th}}$ corrected
7	59480	1714	57509	1.0001	57515	140	57655	656	1.138
9	27673	327	27297	1.0003	27305	294	27599	316	1.145
10 —	19020	143	18856	1.0005	18865	426	19291	219	1.135
10 +	19008	147	18839	1.0005	18848	426	19274	219	1.136
11	13062	64	12988	1.0011	13002	294	13296	151	1.136
12	9173	(32)	9136	1.0024	9158	203	9361	104	1.111
13	6207	16	6189	1.0050	6220	140	6360	71.6	1.126
14	(4226)	10	(4214)	1.0105	(4258)	97	(4355)	49.3	1.132

The values in parentheses are calculated for the purpose of interpolation.

The first column gives again the position of the detector as in Table I, the second and third columns give the activities without Cd(A_{Ni}) and with Cd(A_{Cd}) around the detector. These data are taken from the weekly report C–164. The fourth column gives the activity A_{th} due to thermal neutrons.

This has been calculated by the formula:

$$A_{th} = A_{Ni} - 1.15\, A_{Cd}. \tag{3}$$

The fifth column represents the correction due to the effect of the top. The sixth column represents the thermal intensity corrected for the effect of the top. The seventh column is a small correction to take into account the leakage of neutrons through the gap. In the present experiment this correction is much less important than it was in the experiment described in A–6, because the side of the column is greater and the gap is shallower. The correction has been calculated by using the formula 27 of report A–6:

$$n(\zeta) = \frac{\pi^2 b}{a^2} \mathrm{L}\, n_g\, e^{-\frac{|\xi|}{6}}. \tag{4}$$

In calculating this formula we have taken $a = 153.45$ cm ; $b = 26.99$, corresponding to a diffusing length of 43.25 cm as was found recently for the AGX graphite. L is the effective thickness of the gap. L has to be taken somewhat larger than the geometrical thickess (1.1 cm) because the transversal diffusion across the gap is greater than it would be if the gap were filled with graphite. For the empty gap we have actually taken $\mathrm{L} = 2$. The eighth column gives the activity corrected for everything. The ninth column gives λnv calculated by the same formula as in the weekly report C–92, using, however, the value for the diffusion length and for the size of the column corresponding to the brand of graphite and to the size used in the present experiment. The tenth column gives the ratio of the two last columns. This ratio is constant within the experimental error and we have taken as mean value for it, 1.132×10^{-8}. We obtain finally the standardization of our detectors for the determination of thermal neutron densities given by the following formula:

$$\lambda nv = 1.132 \times 10^{-8} \times [A_{Ni} - 1.15\, A_{Cd}]. \tag{5}$$

As before the standardization corresponds to taking as unit the number of neutrons emitted by the source.

2. Determination of the Number of Neutrons Produced by U.

A comparison between columns 6 and 4 of Table I, of report C–164, shows that the resonance activity of indium near the gap is much greater with uranium in the gap than without uranium in the gap. This difference is due to the fact that fast neutrons are emitted by uranium and are slowed down to indium resonance energy in the vicinity of the gap, adding thereby to the intensity of indium resonance neutrons emitted directly by the source. Although the source emits a number of neutrons much greater than the uranium layer, only a few of them reach the environment of the gap before being slowed down to thermal energies, so that the resonance activity at and beyond the gap is very low without uranium.

In Table III, we give in the first column the position of the detector; in the second and third columns the resonance activity with and without uranium in the gap; in the fourth column the difference; in the fifth column the same difference multiplied by the factor 5.93×10^{-11} to give q_{exc}, namely the excess of the slowing down density due to the effect of the U_3O_8 layer. From these values of q_{exc} we can calculate the number of neutrons emitted by the uranium in the gap.

TABLE III.

Pos.	Cd		Diff.	$q_{exc} \times 10^{10}$
	U	no U		
9	950	327	623	369
10 —	804	143	661	388
10 +	793	147	646	
11	728	64	664	394
12	559.5	(32)	527.5	313
13	363.9	16	347.9	206
14	201.5	10	190.5	113

We call I_F the source of fast neutrons at the gap. This is defined as in Appendix A of Report A–6.(*) The slowing down density of neutrons due to this source on the axis of the column is given by formula 15 in A–6:

$$q_F = I_F \frac{4}{a^2\sqrt{\pi}} \frac{1}{r_0} e^{-\frac{\pi^2 r_0^2}{2a^2} - \left(\frac{x}{r_0}\right)^2} \tag{6}$$

where r_0 is the range of the neutrons emitted by U.

From the data of Table III we take $r_0 = 35$ cm. From (6) follows by integration

$$I_F = \frac{a^2}{4} e^{\frac{\pi^2 r_0^2}{2a^2}} \int q_F \, dx = 7612 \, q_F \, dx \, . \tag{7}$$

The integral in this last formula can be obtained by numerical integration of the last column of Table III. Some corrections must be applied, however, to the result in order to take into account the effect of the resonance neutrons absorbed by uranium, of the neutrons lost through the gap and of the natural neutrons emitted by uranium. The numerical integration of the last column of Table III gives

$$\int_{-\infty}^{\infty} q_{exc} \, dx = 2.618 \times 10^{-6} . \tag{8}$$

(*) N° 138 (Editors' note).

The experimental data of the table have been extrapolated beyond the range of measurement by assuming $r_0 = 35$ cm. It has been further assumed that q_{exc} is symmetrical with respect to the gap. The resonance correction has been calculated by using the data on the resonance absorption as measured in Princeton. It has been found in this way that the correction of 0.118×10^{-6} must be added to the previous integral for this reason. The gap correction has been calculated by integrating the formula (40) of No. 138. The correction to the integral assuming as effective length of the gap 1.3 cm is 0.026×10^{-6}. The correction due to the natural neutrons is even smaller and amounts to only 0.003×10^{-6}. In conclusion, we find:

$$(9) \qquad \int_{-\infty}^{\infty} q_F \, dx = (2.618 + 0.118 + 0.026 - 0.003) \times 10^{-6} = 2.789 \times 10^{-6}.$$

It follows from formula (9):

$$(10) \qquad I_F = 7612 \times 2.759 \times 10^{-6} = 0.0210$$

3. Determination of the Number of Thermal Neutrons Absorbed By Uranium.

In Table IV we have collected the data needed for the calculation of the number of thermal neutrons absorbed by the uranium layer in the gap.

Table IV.

Pos.	with U			$\lambda vn \times 10^5$ (U)	$\lambda vn \times 10^5$ (Air)	$\lambda vn \times 10^5$ (Excess)	$\lambda vn \times 10^5$ (Abs)	$\lambda vn \times 10^5$ (Abs) gap
	A_{Ni}	A_{Cd}	A_{th}					
7	60022	(2066)	57646	65.255	65.100	3.923	3.768	11.45
9	27045	950	25952	29.378	30.900	5.170	6.692	9.69
10—	14809	804	13884	15.717	21.345	5.364	10.992	10.99
10—	14108	793	13196	14.938	21.326	5.364	11.752	11.75
11	11651	728	10814	12.241	14.702	5.170	7.631	11.05
12	9137	559.5	8494	9.615	10.342	4.664	5.391	11.31
13	6947	363.9	6528	7.390	7.006	3.923	3.539	11.75
14	5031	201.5	4800	5.434	4.770	3.105	2.441	10.74

The first column gives the position; the second and third columns give the intensities observed without and with Cd around the detector when uranium is inside the gap; the fourth column is the fraction of the activity due to thermal neutrons calculated with formula (3); the fifth column is obtained by multiplying the fourth column by the factor 1.132×10^{-8} in

order to obtain the expression $\lambda\, nv$ when uranium is in the gap. The sixth column, which is obtained by multiplying by the same factor the data of column four of Table II, gives λnv when air instead of uranium is in the gap. The difference between the sixth and fifth column is partly due to the absorption of thermal neutrons by the uranium layer; since, however, uranium produces also fast neutrons which are subsequently slowed down and ultimately reduced to thermal energies, we must calculate their contribution in order to obtain the effect due to the uranium absorption of thermal neutrons only. The number of thermal neutrons due to the q_{excess} is given in column seven and has been calculated by the method described below (1). Column eight is obtained by subtracting column five from the sum of columns six and seven. This column represents the decrease of λnv due to the fact that the uranium layer absorbs some thermal neutrons. It follows from formula (22) of report A–6 (*)

$$\lambda vn = \frac{6\,b}{a^2}\, e^{-\frac{z}{b}} \tag{11}$$

(1) Column seven of Table IV is calculated as follows: (In this note we systematically omit the subscript " excess " which is always meant to be there). $\lambda\, nv$ for a sin-sin distribution of neutrons obeys the differential equation:

$$\frac{d^2}{dz^2}(\lambda\, nv) - \frac{1}{b^2}\,\lambda vn + 3\,q = 0\,.$$

From this follows:

$$\lambda\, nv = \frac{3\,b}{2}\int_{-\infty}^{\infty} q\,(\zeta)\, e^{-\frac{|z-\zeta|}{b}}\, d\zeta\,.$$

In calculating column seven, we have put in the integral the value for the density of nascent thermal neutrons that can be obtained from the measured value of q_{excess} for indium resonance by integrating the slowing down differential equation:

$$\Delta q = \frac{\partial q}{\partial t}$$

for an age difference between indium resonance and nascent thermal neutrons of 60 cm^2. The values of the density of nascent thermal neutrons obtained in this way as a function of the distance from the gap are as follows:

Distance from the gap	$q_{\text{th (excess)}} \times 10^{10}$
0	375
10	333
20	285
30	203
40	125
50	65
60	30
70	12
80	4
90	2
100	0

The numerical integration of formula (*a*) gives the $\lambda\, vn$ (excess) of Table IV.

(*) See paper N° 138. (Editors' note).

that the intensity due to a negative sin-sin thermal source as the one representing the absorption of our oxide decreases exponentially with the distance from the absorbing layer and with a relaxation distance b, which in our case is equal to 26.99 cm. The data of column eight multiplied by the exponential factor:

$$e^{\left|\frac{z-z_0}{b}\right|}$$

where $|z - z_0|$ is the distance of the place on the axis where the measurement is taken from the gap, should give a constant. The products of the data of column eight by the exponential are given in column nine. Besides fluctuations presumably due to experimental error, there is an indication that the mean value of the data of column nine corresponding to points below the gap is slightly lower than the same mean value for points above the gap. This is due to the fact that the uranium layer, besides absorbing the neutrons, also scatters them. The difference between the mean values above and below the gap can be well interpreted both in sign and order of magnitude in terms of this explanation. Taking the mean value of the mean values of the data of column nine above and below the gap, we find at the gap $\lambda\, nv \times 10^5$ (absorption) = 10.91. This decrease of the intensity at the gap is essentially due the absorption of thermal neutrons by the material in the gap. A small correction must, however, be applied to take into account the fact that the number of thermal neutrons leaking outside of the gap without and with uranium is different. This, like all other gap corrections, is in the present experiment quite small and can be calculated by the methods explained in report A–6. This value of $\lambda\, nv$ corrected for this reason is:

(12) $$\lambda\, nv\,(\mathrm{Abs}) = 11.17 \times 10^{-5}.$$

Formula (11) gives the intensity due to a unit source absorption. Dividing (12) by $6\,b/a^2 = 0.006877$, we find the intensity of the negative thermal absorption source. A very small correction should be applied to this to take into account the absorption due to the 0.002'' aluminum layer on which the uranium was resting and of some small pieces of scotch tape used for keeping the pressed uranium oxide blocks in place. The two corrections together amount to less than 0.1 %. We obtain finally the thermal source due to the absorption by U_3O_8.

(13) $$I_{th} = 0.01623.$$

4. Conclusions.

The number η of neutrons produced per thermal neutron absorbed is given by the ratio between the intensity I_F of the fast neutron source given by (10) and the intensity I_{th} representing the thermal absorption source.

We have thus:

(14) $$\eta = \frac{0.0210}{0.01633} = 1.29.$$

From (13) we may also find the cross section for the absorption of thermal neutrons by uranium. Taking into account the definition of unit source as given in Appendix A of Report A–6, we find that the absorption cross section for neutrons of energy kT is given by the following formula:

$$\sigma_U(kT) = \frac{4}{a^2}\,\frac{2}{\sqrt{\pi}}\,\frac{\lambda}{\lambda nv}\,\frac{I_{th}}{N} \tag{15}$$

where N is the number of uranium atoms per cm² in the gap, and for λnv we must take the value at the gap when uranium is inside the gap, which is given by the mean of the two values at positions 10+ and 10— in column five of Table IV, namely $\lambda nv = 15.327 \times 10^{-5}$. In calculating this cross section we have further assumed $\lambda = 2.6$ cm. N is calculated from the density 3.82 grams/cm² of uranium oxide in the gap as $N = 8.18 \times 10^{21}$. We find in this way:

$$\sigma_U(kT) = 6.77 \times 10^{-24}. \tag{16}$$

It should be noted that this value of the absorption cross-section of uranium corresponds to neutrons of thermal energy and not to the so-called C neutrons emerging from paraffin which have a considerably higher mean energy.

The experimental error on the data (14) and (16) may be of the order of 5 or 10 %.

N° 163.

This paper was written by Christy; I performed some of the computations. Fermi had analyzed the Columbia measurements on temperature effects in exponential experiments. At that time we used to hold a theoretical seminar under Wigner's general guidance. Fermi spoke to the seminar on his analysis of the temperature effect, and the present paper was written shortly after the seminar. I remember that at this seminar Fermi raised his dissatisfaction at the state of our understanding of the behavior of thermal neutrons in a moderator. I might add that even now, sixteen years later, our understanding is still imperfect.

A.M. WEINBERG.

163.

EFFECT OF TEMPERATURE CHANGES ON THE REPRODUCTION FACTOR

R. F. CHRISTY, E. FERMI, and A.M. WEINBERG
Report CP–254 (September 14, 1942).

ABSTRACT.

The experimental data on the heated Columbia and Chicago piles give the following results:

Expt.	ΔT	Δk
Columbia	62° C	$0.8\,\% \pm 1.0\,\%$
Chicago	109° C	$0.39\,\% \pm 0.4\,\%$

The experimental error in each case is larger than the observed effect and the interpretation is further complicated by the presence of thermal gradients in the graphite. The smallness of the observed effects suggests that the "thermal" neutrons in a lattice may have a temperature considerably higher than the temperature of the pile.

* * *

The effect of temperature change on k has been measured in two exponential piles (Columbia Pile No. 2a and Chicago Pile No. 2), and a preliminary report on the Columbia pile has already appeared (CP–85) (*). Roughly, the

(*) See paper N° 151 (Editors' note).

rise in temperature causes a Doppler widening of the resonance lines, and a decrease in thermal absorption cross sections. The first effect would decrease k, because of the increased resonance absorption, by an amount which cannot, as yet, be estimated with certainty. Because of the decreased self absorption and increased neutron density in the uranium, the second effect would increase k by about $3\left(1 - \sqrt{\frac{T_0}{T}}\right)$ percent: where T_0 is the initial and T the final "thermal" neutron temperature. The preliminary results on the Columbia pile indicated a net decrease of k with temperature, but the size of the effect was less than the experimental error.

The interpretation of both the Chicago and Columbia experiments is somewhat complicated by the fact that in both cases the temperature was not uniform through the pile. In the experiment at Columbia there was an appreciable longitudinal gradient of temperature giving rise to a rather large correction. In the Chicago experiment, the longitudinal gradient was practically absent; the temperature on the axis was, however, a few degrees higher than on the sides. This transversal thermal gradient introduces a very small correction.

(1) Columbia experiment – Longitudinal gradient.

In the Columbia experiment there was a longitudinal temperature gradient of 20° C in the height of the pile (142 cm), the top of the pile being at 360° K, the bottom at 380° K. Because of this gradient, the mean free path for capture Λ, the neutron velocity v, and k will all vary from the top to the bottom of the pile. For simplicity we shall assume that the temperature T varies exponentially:

$$T \sim e^{-\varepsilon z} \tag{1}$$

where ε is very small compared with $\beta = \frac{1}{b}$, and b = relaxation length. Although it is true that such an assumption does not make T harmonic, the error involved is quite small because the temperature gradient is so gradual.

With this assumption it follows that:

$$\Lambda \sim T^{1/2} \sim e^{-\frac{1}{2}\varepsilon z} \qquad v \sim T^{1/2} \sim e^{-\frac{1}{2}\varepsilon z} \tag{2}$$

and we may assume, without loss of generality:

$$k \sim T^{-\mu} \sim e^{\mu\varepsilon z}, \tag{3}$$

where μ is a small positive number. The procedure now is to solve the slowing down equation (t = age of neutrons):

$$\Delta q = \frac{\partial q}{\partial t} \tag{4}$$

subject to the initial condition:

$$q(0) = \frac{kv}{\Lambda} n \tag{5}$$

where n, the density of thermal neutrons is given by:

$$\frac{\lambda\Lambda}{3}\Delta(nv) - nv + \Lambda q(t) = 0, \tag{6}$$

and $\lambda\Lambda/3$ is the square of the diffusion length.

The expressions for q obtained from (6) and (4), when equated, yield a characteristic equation which is the expression for k.

The first harmonic solution of (6) is:

$$n \sim \cos \alpha x \cos \alpha y \, e^{-\beta z}; \tag{7}$$

hence, from (6):

$$q(t) = \frac{nv}{\Lambda}\left[1 - \frac{\lambda\Lambda}{3}\left\{\left(\beta + \frac{\varepsilon}{2}\right)^2 - \alpha^2\right\}\right] \tag{8}$$

and, by (5):

$$q(0) \sim \cos \alpha x \cos \alpha y \, e^{-(\beta - \mu\varepsilon)z}. \tag{9}$$

For this spatial variation of q, we can write the solution of (5) as

$$q(t) = q(0)\, e^{t[(\beta-\mu\varepsilon)^2 - \alpha^2]} = \frac{kv}{\Lambda} n e^{t[(\beta-\mu\varepsilon)^2-\alpha^2]}. \tag{10}$$

Equating the two expressions (8) and (10), we have:

$$k = e^{-t[(\beta-\mu\varepsilon)^2-\alpha^2]}\left\{1 - \frac{\lambda\Lambda}{3}\left[\left(\beta + \frac{\varepsilon}{2}\right)^2 - \alpha^2\right]\right\} \tag{11}$$

or

$$k \approx 1 - \frac{1}{c^2}\left[t + \frac{\lambda\Lambda}{3}\right] + \left(2\mu t - \frac{\lambda\Lambda}{3}\right)\beta\varepsilon. \tag{12}$$

The correction term $\left(2\mu t - \frac{\lambda\Lambda}{3}\right)$ arises because of the non-uniformity of the temperature field.

Equation (12) together with

$$k = \left(\frac{T_0}{T}\right)^{\mu}$$

enables us to compute k at any temperature T, and μ, from two measurements at T and T_0. The Columbia data is summarized in the following table:

T	t	$\frac{\lambda\Lambda}{3}$	β	$\frac{1}{c^2} = \beta^2 - \alpha^2$	ε	μ	k	% change in k
310° K	350	360	1/46	1.2×10^{-4}	0	0.044	0.915	0
372° K	350	394	1/46	1.2×10^{-4}	3.9×10^{-4}	0.044	0.9077	0.8 % ± 1 %

The value of k from the first two terms alone (uniform temperature) is 0.9107, while its value from all three terms is 0.9077; hence the temperature gradient accounts for almost half of the calculated change in k.

(2) Chicago experiment – Transverse gradient.

In the Chicago experiment the heating was from the sides, and the temperature on the axis of the pile was 395° K while the temperature at the edge was 388° K. The longitudinal gradient was only 1° in the height of the pile and may therefore be neglected. In this case, we assume for the temperature:

$$T = T_0 [1 + \varepsilon (\cos 2\,\alpha x + \cos 2\,\alpha y)]. \tag{13}$$

This distribution has the proper symmetry and is not too far wrong if ε is small.

The transverse variation of T introduces higher harmonics in the thermal neutron distribution. For this reason, we assume:

$$vn = [\cos \alpha x \cos \alpha y + \gamma (\cos 3\,\alpha x \cos \alpha y + \cos \alpha x \cos 3\,\alpha y)\, e^{-\beta z}$$

where γ is a small parameter; also, as before:

$$\Lambda = \Lambda_0 [1 + \varepsilon (\cos 2\,\alpha x + \cos 2\,\alpha y)],$$

$$k = k_0 [1 - 2\,\varepsilon\mu (\cos 2\,\alpha x + \cos 2\,\alpha y)],$$

$$\frac{k}{\Lambda} vn \approx \frac{k_0}{\Lambda_0} [(1 - \varepsilon (2\,\mu + 1)] [\cos \alpha x \cos \alpha y\, e^{-\beta z} + \text{higher harmonics}],$$

$$\frac{\lambda\Lambda}{3} \Delta\, vn \approx \frac{\lambda}{3} (\beta^2 - \alpha^2)\, \Lambda_0 (1 + \varepsilon) (\cos \alpha x \cos \alpha y\, e^{-\beta z} + \text{higher harmonics}),$$

$$\Lambda q\,(t) \approx k_0 [1 - \varepsilon (2\,\mu + 1)] [1 + \varepsilon] (\cos \alpha x \cos \alpha y\, e^{-\beta z} + \text{higher harmonics}).$$

Substituting these expressions into (7), and neglecting higher harmonics (which are important only for determining γ), we find

$$k_0 = [1 + \varepsilon (2\,\mu + 1)]\, e^{-\frac{t}{c^2}} \left[1 - \varepsilon - \frac{\lambda\Lambda_0}{3\,c^2}\right] \approx 1 - \frac{1}{c^2}\left(t + \frac{\lambda\Lambda_0}{3}\right) + 2\,\mu\varepsilon; \tag{14}$$

from (3) and (14) k and μ may be computed as in the previous case.

In the Chicago experiment the porous graphite was filled with atmospheric N_2 whose density decreased with rise in temperature. At ordinary temperatures there is sufficient N_2 in the pile to decrease k by 0.8 %; this figure is proportional to the density of the N_2 in the graphite pores. The density would be proportional either to the temperature if the diameter of the pores is large compared with the mean free path of N_2, or to the square root of the temperature if the diameter of the pores is small compared with the mean free path. In the first case, the effect of the N_2 would be a 0.22 % increase in k, in the second case, a 0.11 % increase in k. The effect of temperature alone on k must, therefore, be increased by this amount; that is, to 0.39 % or 0.28 %. In both cases the effect is still less than the experimental error.

The Chicago data is summarized in the following table:

T_o	t	$\frac{\lambda\Lambda}{3}$	$\frac{1}{c^2}$	ϵ	μ	k	$\Delta k_{(\text{with } N_2)}$	Δk_{N_2}	Δk_{vacuum}	
297° K	350	350	0	0	0.0065	1.0000	0	0		
388° K	350	403	2.4×10^{-6}	0.0045	0.0065	0.9982	0.17 %±0.4 %	0.22 % or 0.11 %	0.39 % or 0.28 %	±0.45

In this case the value of k without the non-uniformity correction term is 0.99819, while its value including the correction is 0.99822. The non-uniformity correction is therefore negligible.

(3) Conclusion.

The magnitude of the temperature effect is less than the experimental error in both the Chicago and the Columbia experiments, although in both cases the direction of the effect was toward smaller k. The actually observed experimental effects were null in the Columbia experiment

$$\left(\frac{1}{c^2}\right)_{310^\circ} = \left(\frac{1}{c^2}\right)_{372^\circ}$$

and almost null in the Chicago experiment

$$\left(\frac{1}{c^2}\right)_{297^\circ} - \left(\frac{1}{c^2}\right)_{372^\circ} = 2.4\times10^{-6}.$$

The following question may, therefore, be legitimately raised: Does a temperature change at low temperatures have much effect on the velocity or thermal absorption of the neutrons? The answer to this question would be negative if the " thermal " neutrons in a lattice are not really in thermal equilibrium with the carbon, but are at considerably higher temperatures. Indeed, there is other evidence to suggest that this is actually the case.

If the change in the diffusion length is smaller than would be expected for truly thermal neutrons, the discrepancy between the Chicago and the Columbia experiments would be decreased. For in the Columbia experiment the entire decrease in k was attributed to a theoretically calculated increase in diffusion length; if this increase were less than the calculated amount because the neutrons are not truly thermal, the calculated change in k would be less, thus tending to iron out the difference between the Chicago and Columbia results.

N° 164 and 165.

In the beginning, reports of progress in the Metallurgical Project were written weekly. An early example of one of these reports is paper N° 164. Fermi, as the head of the Experimental Nuclear Physics Division, wrote a summary of the work completed, current, and under consideration. There followed more detailed reports by the leaders of the groups working under Fermi's general direction. The Chicago cyclotron had been pressed into service for some of the experiments under the leadership of A. C. G. Mitchell. J. H. Manley was in charge of the experiments done with the D–D source. M. D. Whitaker and W. H. Zinn jointly carried out the exponential experiments; I did the experiments with Ra–Be sources. V. C. Wilson was in charge of the group assigned to manufacture electronic circuits and controls.

Theoretical Physics was under E. P. Wigner. His report noted that the exponential pile experiments were being systematically analyzed by R. F. Christy and J. Williamson, while a detailed theoretical study of this type of experiment had been prepared by E. Teller. Wigner's interest in water cooling for the large scale producing piles was apparent in this report and marked the heginning of a long struggle with competitive schemes, notable among which was the helium cooled proposal favored by the engineering group headed by T. V. Moore. Finally, N. Hilberry reported the progress in the procurement of materials. Paper N° 164 is Fermi's part of the report.

Paper N° 165 is another example of these reports, which provide an interesting record of the progress of the work leading to the first chain reaction.

H. L. ANDERSON.

164.

STATUS OF RESEARCH PROBLEMS IN EXPERIMENTAL NUCLEAR PHYSICS

Excerpt from Report C–133 for Week Ending June 20, 1942.

PROBLEMS COMPLETED.

Since the last report(*) on the status of research problems in experimental nuclear physics the results on pile no. 6 have been worked out with the result that the optimum size of the U_3O_8 lumps appears to be intermediate between the size originally used (2,200 grams) and that used in experiment no. 6 (18,000 grams). The optimum would be to use lumps of about 5,000 grams. The advantage to be expected by such a change of size, however, is only a small fraction of a percent.

Work has also been completed on the comparison between various brands of graphite: AGX, used in the early work at Chicago, US, used in the early work at Columbia, and the new Speer graphite. The result indicates that

(*) By M. D. Whitaker and W. H. Zinn. (Editors' note).

the Speer graphite has an absorption considerably lower than the two other brands. A gain in the reproduction factor of the order of 2.5 to 3 percent may be expected by substituting in our present piles this better graphite in place of the other brands. Consequently, the problem of securing large amounts of very pure graphite seems to be of paramount importance.

Measurements on the absorption of U_3O_8 have been performed by observing the intensity of thermal neutrons inside a U_3O_8 sphere embedded in a graphite mass placed near the cyclotron. The result seems to indicate that the absorption is somewhat greater than according to the previous estimates.

The considerable discrepancy in the measurements of the number of neutrons emitted by the radium beryllium sources have been eliminated to a large extent by the use of MnO_2 detectors. Apparently the indium detectors used in the previous measurements had the resonance band so close to the thermal region as to produce a sizeable deviation from the $1/v$ law.

Problems current.

Measurements on the absorption of beryllium are being performed and it is hoped that a reliable value for the diffusion length may be available next week. The study of the anisotropic diffusion of neutrons in carbon is still being carried on in the attempt to get a reliable value for the " diffusion mean free path " for graphite. There are some indications that an even greater difference between the " diffusion mean free path " and ordinary mean free path would be found in beryllium.

Exponential pile No. 7 has just been set up. Its structure is similar to that of pile No. 3 (3 inch oxide cubes in a cell of 8 inches side) except that about 120 grams of paraffin have been placed on the side of the uranium lumps. It is hoped to get from the measurements some information as to the effect of hydrogenated systems inside a carbon uranium pile.

A $5' \times 5'$ carbon column with a gap for introducing a layer of pressed U_3O_8 has been set up for the measurement of the absorption cross section of uranium for thermal neutrons and of the number of neutrons emitted when a thermal neutron is absorbed.

Problems under serious consideration.

After completion of the exponential experiment No. 7, a similar experiment will be carried out using about the same geometry of carbon and uranium as in no. 7 and placing beryllium blocks near the U_3O_8 cubes instead of paraffin. It is hoped to get in this way some information on the effect of beryllium on the reproduction factor. The first batches of ether purified U_3O_8 from Mallinckrodt are expected to arrive at the end of the week or early next week and work will be started immediately to test the effect of the further purification on the reproduction factor. After this experiment, a comparison test between U_3O_8 and UO_2 will be carried out.

Plans for the development of a portable detector of radiations suited for large scale production are under consideration.

Determination of the possible existence of resonance absorption in carbon.

Measurement of the number of neutrons produced in the fission of uranium by fast Rn+Be neutrons.

Investigation of the resonance absorption in cells of various dimensions and various materials in view of obtaining information on the various possibilities of cooling.

N° 165.

For the introduction to this paper see N° 164.

165.

STATUS OF RESEARCH PROBLEMS IN EXPERIMENTAL NUCLEAR PHYSICS

Excerpt from Report C–207 for Week Ending July 25, 1942.

Since the last report on the status of research problems in experimental nuclear physics the following work has been completed.

The exponential piles Nos. 7, 8 and 9 have been set up and measured.

No. 7 is a pile made of oxide cubes of 3″ side imbedded in a cubic lattice of AGX (*) graphite of 8″ cell side. Two slabs of paraffin of the total weight of 127 gms were added near each uranium lump in order to test the loss in reproduction factor due to the presence of hydrogenated materials. Otherwise, materials and geometry were identical with those used in pile No. 3 *a* and *b*. The result indicated an appreciable decrease in the reproduction factor due to the presence of paraffin. This decrease corresponds to a " danger coefficient " for paraffin, slightly larger than 1.

Exponential experiment No. 8 is similar to experiment No. 7, except that beryllium instead of paraffin was placed near the uranium lumps. The result indicates an exceedingly small difference between the experiment with beryllium, and the control experiment without beryllium. Indeed the difference in reproduction factor between the two is a small fraction of the experimental error. This result indicates that no appreciable advantage from the neutron point of view can be expected with the use of beryllium. This material might, however, be of considerable interest as a possible technological material to be used inside the reacting piles.

Exponential experiment No. 9 is a test of the reproduction factor that can be obtained at present with the use of very pure U_3O_8 from Mallinckrodt. It is believed that no significant amounts of impurities are left in this product so that no further advantage on the result of this experiment can be expected due to a further purification of the oxide. This experiment was carried out with the same geometry as used in experiment No. 5. (Cylindrical lumps of pressed oxide in an 8″ cell side cubic lattice). The graphite used was the same U.S. (*) graphite used in experiment No. 5, so that the only difference

(*) This is the name of a particular brand of material. (Editors' note).

between the two tests was the change from D-1(*) to Mallinckrodt(*) oxide. The new experiment indicated an increase in the reproduction factor of about 1.2 percent. The result of the measurement gave a reproduction factor slightly in excess of 1 ($k = 1.007$ or $k = 1.004$, according to the method of calculation). Some further increase in the reproduction factor in graphite uranium oxide systems may be expected by:

a) Use of pure graphite. A change from the US graphite to Speer(*) graphite may be expected to yield an increase in k from 2 to 2.5 percent.

b) Removal of nitrogen may give an increase in k by somewhat less than 1 percent.

c) Change from U_3O_8 to UO_2.

The following experiments in pure nuclear physics have been completed:

A) A measurement of the "diffusion mean free path" in graphite of density 1.6, gave $\lambda_D = 2.73$ cm. This result is slightly higher than the mean free path calculated from the scattering cross section 4.8×10^{-24} of carbon. The difference is presumably due to some small amount of angular coherence in the scattering of thermal neutrons by graphite. This new value of the mean free path should be used in the diffusion equation for thermal neutrons in graphite.

B) A new measurement of the number η of neutrons emitted when a thermal neutron is absorbed by uranium and of the total absorption cross-section of uranium for thermal neutrons was performed. The results are $\eta = 1.29$ and $\sigma_U(kt) = 6.77 \times 10^{-24}$, both data with a probable error of 5 to 10 percent.

C) The diffusion of thermal neutrons in beryllium of average density 1.735 was investigated using a considerable larger amount of this metal than had been available in previous experiments. The diffusion length and the "diffusion mean free path" were found to be 26 and 2.56 cm. This corresponds to an absorption cross section of about 0.011×10^{-24}.

D) Experiments were performed by the cyclotron group on the nuclear distribution inside and in the neighborhood of uranium lumps imbedded in a graphite for various geometries. In particular, the difference between a sphere with or without a gap surrounding it was investigated and cylindrical units with a paraffin core were studied in order to obtain some information to be used in the discussion of the water cooled plant.

Routine tests on various batches of Mallinckrodt oxide have been conducted by the neutron absorption method. The results have indicated so far a loss of absorption of the order of less than 0.1 percent. Two new Ra to Be sources of 200 mg each have been procured. These sources have been designed so as to keep their size as small as possible. For this a very small Ra+Be proportion has been used and the Ra+Be mixture has been pressed in a suitable die. These sources are very convenient when very definite geometrical conditions are desirable, although, their yield is somewhat smaller than for the usual sources. Some technological work has been completed in view of collecting data needed for the design and construction of the experimental plant.

(*) This is the name of a particular brand of material. (Editors' note).

In particular, an investigation has been conducted in order to determine the behavior of lumps of pressed uranium oxide imbedded in graphite when energy is produced inside the lump at the rate of about 100 watts per lump. (Also the cooling of graphite by means of a water circulation in copper pipes in good thermal contact with the graphite has been investigated).

Work has also been conducted in order to test various methods for the removal of the uranium out of the experimental pile after operation.

The tedious but exceedingly useful work of developing and producing measuring instruments has been carried on as usual.

The most important problems that are in consideration by the physics division in the near future are concerned with an investigation of the properties of UO_2 to be substituted for U_3O_8 in the exponential piles. It is also planned to set up, as soon as possible, an exponential pile with a volume about twice as large as the exponential piles investigated so far, in order to ascertain whether the reproduction factor as measured in a larger unit turns out to be the same as that obtained from a smaller unit. This experiment is intended to be a check on the exponential method for measuring reproduction factors, which is very desirable in view of the important decisions that are based on the results of such measurements.

General nuclear physics experiments and measurements will go on; however, it is planned to shift a considerable fraction of the activity of the physics division from experiments on pure nuclear physics to research in connection with the technology of the experimental pile.

N° 166 and 167.

Worth noting in paper N° 165 is the result, with the very pure uranium oxide delivered by the Mallinckrodt Chemical Company, of a reproduction factor greater than *1* for the first time. The earlier deliveries of uranium oxide, guaranteed to be " chemically pure " by the previous supplier, had been, in Fermi's own privately expressed words, " filthy with dirt." He had been " swindled by a slick sales talk " and it had taken one year and a move to Chicago to prove it.

In the following monthly review (paper N° 166) Fermi could show that the reproduction factor which could be obtained in a graphite-uranium oxide system was as much as 1.04. With a 4 % excess available, the chain reacting structure could have a reasonable size and there was still some margin left over for a limited amount of impurity.

Exponential Pile N° 11 (paper N° 167) was considerably larger than its predecessor and served to check the reliability of the theoretical interpretation. The experiment was carried out by Zinn, but the results were given by Fermi.

H. L. ANDERSON.

166.

STATUS OF RESEARCH PROBLEMS OF THE PHYSICS DIVISION

Excerpt from Report CP–235 for Month Ending August 15, 1942.

This is a review of the main problems on which work had been performed by the physics division in the past month. The details of the methods and of the results are to be found in the reports of the various group leaders under whose supervision the work has been conducted.

EXPONENTIAL EXPERIMENTS.

Two exponential piles No. 9 and 10 have been set up and measured. They are both geometrically similar to pile No. 5 (cylinders of 3″ diameter and 3″ height of pressed oxide in a cubic graphite lattice of 8″ side).

In No. 9, U_3O_8 from Mallinckrodt was used. The analysis indicates that this oxide is free from appreciable amounts of impurities. The reproduction factor found in pile No. 9 was $k = 1.007$ or $k = 1.004$ according to the method of calculation. The second value is probably more nearly correct. This experiment indicates an increase in reproduction factor somewhat more than 1 % due to the change from the D1(*) oxide to the purified Mallinckrodt(*) oxide.

(*) This is the name of a particular brand of material. (Editors' note).

In experiment No. 10, when UO_2 was used instead of U_3O_8, a further increase of about 1 % was found in the reproduction factor. This increase bears out the theoretical expectation that an appreciable loss of reproduction factor is due to the presence of oxygen in the oxide lumps.

Some further increase in the reproduction factor of graphite uranium oxide systems may be expected by:

a) Use of pure graphite. A change from the US (*) graphite to Speer (*) graphite may be expected to yield an increase in k from 2 to 2.5 %.

b) Removal of nitrogen may give an increase by somewhat less than 1 %.

It appears probable therefore that the best reproduction factor for graphite-oxide systems will be close to 1.04.

Since important decisions are based on the results of the measurements of reproduction factors by the experimental method, it appeared worthwhile to check on the reliability of the method by setting up a larger pile of the same internal structure as pile No. 10 in order to verify whether the reproduction factor obtained in the larger structure is the same as that of the smaller pile. For this purpose, a new experimental pile No. 11 having about twice the volume of pile No. 10 has been set up and is going to be measured in the next few days.

Nuclear properties of various materials.

A number of tests of neutron absorption of various materials have been performed.

(*a*) The routine tests on the absorption of the Mallinckrodt oxide have been carried out regularly on the various batches. The absorption found so far are below the experimental accuracy of about 0.05 %. It is planned in the near future to carry out control measurements in order to check on the reliability of this test by adding known amounts of various neutron absorbers to batches of oxide in order to determine whether the neutron absorption method carried out according to the present routine gives a correct indication of their amount.

(*b*) A measurement of the absorption cross section of beryllium by the method of the diffusion length has been carried out using a considerably larger amount of this metal than had been available in previous experiments. The diffusion length and the diffusion mean-free path were found to be 26 and 2.56 cm for beryllium of average density to 1.735. This corresponds to an absorption cross section of about 0.011×10^{-24}.

(*c*) A measurement of the diffusion length in the carbon brick " Kenproof " has been carried out in order to explore the possibility of using this material as a reflecting shield for neutrons. The diffusion length of this material is about 22 cm.

(*d*) A graphite pile of about 5×5 feet cross section has been set up for measurements of fairly small absorption cross sections of various materials.

(*) This is the name of a particular brand of material. (Editors' note).

A layer of the material is introduced in a suitable gap and the absorption cross section is calculated from the decrease in neutron density near by. This method has been applied so far to the determination of a brand of pure commercial lead. A cross-section of 0.15×10^{-24} was found for this material.

Provisions are made to measure the absorption of the new batches of Speer graphite as soon as they shall be available.

Miscellaneous experiments in nuclear physics.

(*a*) Determination of the number of neutrons produced in the fission by fast Ra+Be neutrons has been carried out by determining the total number of resonance neutrons produced by a source imbedded or not in a uranium metal sphere covered with cadmium. The experiment indicated an increase of about 16 % in the number of neutrons observed with the metal sphere. This increase is of the same order of magnitude as expected according to the calculations of Szilard and Feld. It is hoped to increase the accuracy of this result by using a stronger source of small geometrical dimensions.

(*b*) Experiments were performed with neutrons emitted by the cyclotron on the neutron distribution inside and near uranium lumps imbedded in graphite with various geometrical dispositions. Cylindrical units with a paraffin core were investigated in order to obtain some information to be used in the discussion of the water cooled plant. Also the neutron distribution inside a large metal sphere has been studied. The result seems to indicate a hardening of the neutrons that penetrate near the center of the sphere so as to give an effective absorption lower than the absorption for thermal neutrons. Further work is being done on this problem.

(*c*) The admission of photo-neutrons by beryllium irradiated with hard gamma rays from long living fission products has been observed. The yield is of the same order of magnitude as that found for the gamma rays of radium C.

(*d*) A test designed to determine whether there is any appreciable absorption of neutrons during the slowing down process in carbon has been in progress for some time and it is hoped that the results will be available soon.

(*e*) A counter has been constructed specially designed for an absolute determination of the beta ray activity.

Preparatory work for the experimental pile.

Considerable activity has been devoted by the Physics Division to preliminary design and testing of various devices to be used in the experimental plant.

Work has been done in particular on the controlling devices. A material that presents interesting features for the controlling rods is iron containing

a small percentage of boron. Various possible mechanisms and electric devices for the operation of the controlling rods have been investigated.

Ways of connecting graphite bricks to form a stringer that could be pulled out of the pile after operation have been designed and tested for strength.

The heating transmission between pressed oxide lumps and graphite, between adjoining graphite bricks, and between the graphite and water cooled copper pipes has been determined. An interesting result is the strong dependence of such heat transmission coefficients upon the gas in which the system is imbedded. The heat transmission in a helium atmosphere is about three times higher than in air. Since the air shall have to be substituted by helium in the operating pile, it is expected to get thereby a considerable improvement in the heat transmission.

Some preparatory work has been done for testing the properties of vacuum tight coverings of metal sheet and of balloon cloth.

Instruments.

Somewhat more than 50 counting sets are at present operating in the various divisions of the laboratory. An organization has been set up for keeping such sets in shape and it is hoped that this may help to improve the quality of the measurements. The Instruments Section has also been working on the production of a reliable fast neutron detector and of electric devices for the operation of the controls.

N° 167.

For the introduction to this paper see N° 166.

167.

EXPONENTIAL PILE No. 11

Excerpt from Report CA–247 for Week Ending August 29, 1942.

The measurements of the reproduction factor in graphite oxide systems have been performed so far by measurements of intensity in the exponential piles. Up to now the sizes of the exponential piles on which experiments have been performed have not been varied between wide limits. Indeed, the sides of the columns have ranged from 90 to 96''. As a check on the reliability of the theoretical interpretation of the exponential experiment, it appeared worthwhile to perform a measurement at least once using the same internal lattice geometry on two columns of rather widely different side. This provides a check on whether the reproduction factor measured with the two arrangements is the same.

The two exponential piles compared in this way are No. 10 and No. 11. The lattice is the same in both piles, namely a cubic lattice of 8'' cell side with cylindrical lumps of pressed UO_2 having a diameter and height of about 3''and a total mass of about 2070 grams. The side of the pile used in experiment No. 10 was 92''. Pile No. 11 has the same internal structure but its side is 132''. A complete description of experiment No. 10 has been given by Whitaker and Zinn in the weekly report C–223. The most probable value for the reproduction factor in experiment No. 10 was $k = 1.014$.

The value for the reproduction factor obtained for experiment No. 11 is slightly lower, namely, between 1.012 and 1.013. The difference between the results of the two experiments appears, therefore, to be within the limits of accuracy of measurement, although there is some indication that experiments on small size piles might give a somewhat high value for the reproduction factor, probably due to an underestimate of the effects of room scattering.

Table I gives a comparison of the essential features of the two experiments. The geometric side and the effective side a are given in the first and second row. The third row gives the relaxation distance $a/\pi\sqrt{2}$ that would be expected in the two cases for the reproduction factor $k = 1$. The fourth row gives the relaxation distance b actually observed. In both cases b is larger than $a/\pi\sqrt{2}$, indicating that the reproduction factor is > 1. The fifth

row gives the magnitude $\frac{1}{c^2} = \frac{2\pi^2}{a} - \frac{1}{b^2}$. This magnitude should be equal in the two experiments if there were no errors either in the experiment or in the theoretical interpretation. The sixth row gives the reproduction factor. The seventh row gives the number of counts obtained in the two cases from the natural neutrons at the center of the pile. The difference between the two values is quite consistent with the difference expected theoretically due to the change of dimensions.

TABLE I.

	No. 10	No. 11
Side	92'' = 233.7 cm	132'' = 335.3 cm
a	240	340.6
$\frac{a}{\pi\sqrt{2}}$	54.1	76.7
b	55.82	81.32
$\frac{1}{c^2} = \frac{2\pi^2}{a^2} - \frac{1}{b^2}$	22×10^{-6}	19×10^{-6}
k	1.014	1.012_5
Natural neutrons	67	116

A few features of the exponential pile No. 11, which is the largest so far constructed, may be of interest. The effective reproduction factor defined as the reproduction factor obtained when the losses due to leakage outside of the pile of finite dimensions are included, was about

$$k_{\text{eff}} = 0.83.$$

From this follows that a neutron originally produced by an external source in the geometrical distribution corresponding to the main harmonic would be reproduced in the average about six times, if all the generations are included.

The critical dimensions for a cubical pile of the same internal structure as No. 11 would be about 13 m side. For a pile of the same structure of spherical shape the critical radius would be somewhat more than 7 m, corresponding to a critical mass of graphite of about 2500 tons.

N° 168.

In the summer of 1942 the United States Army was assigned an active part in the uranium project, and in August it organized a special district of the Corps of Engineers, the Manhattan District. In September, Brigadier General L. R. Groves was placed in charge of all Army activities concerning the uranium project, a post that he held throughout the war years and until the civilian Atomic Energy Commission was established. Although for several months the project remained under the joint control of Army and Office of Scientific Research and Development, from the summer of 1942 its whole effort was increasingly directed toward military objectives [1].

Even before the Army took over, it had become evident that the physical facilities of the project needed to be greatly expanded and a search for a suitable tract of land had begun. A site at Argonne Forest, near Palos Park, was purchased in June, and plans were made to move the project there. But the demand for buildings and special facilities was so great that a larger site was located at Oak Ridge, Tennessee (the Manhattan District purchased it later in the summer), leaving the first one freed from all purposes other than the construction of the first chain reacting pile. The plans for building the first reactor could now go forward unimpeded by the myriad needs of the chemists, metallurgists, biologists, and engineers who had many urgent problems to solve before the large scale production of plutonium could become a reality. Eventually, however, the plans had to be changed, and the pile was built on the campus of the University of Chicago (see paper N° 178).

Meanwhile, at the Metallurgical Laboratory in Chicago the exponential experiments were continued under the direction of Zinn. Fermi's report for September, 1942 showed considerable improvement in the purity of the latest deliveries of Speer Graphite. It also revealed the plan to encase the pile in a rubberized balloon cloth housing, so as to make possible a gain of about 1 % in the reproduction factor through the removal of air.

Report CP-257, of which this paper is an excerpt, was issued also as A-287.

H. L. ANDERSON.

168.

STATUS OF RESEARCH PROBLEMS OF THE PHYSICS DIVISION

Excerpt from Report CP-257 for Month Ending September 15, 1942.

This is a review of the main problems on which work has been performed by the physics division in the past month. The details of the methods and of the results are to be found in the reports of the various group leaders under whose supervision the work has been conducted.

(1) H. D. SMYTH, *Atomic Energy for Military Purposes*, Princeton University Press (1945).

EXPONENTIAL EXPERIMENTS.

During the past month a test on the validity of the methods used for calculating the reproduction factor from the measurements in the exponential experiments has been performed by setting up an exponential pile having the same internal structure but appreciably larger size than any of the piles previously constructed. The two experiments that are so compared are No. 10 and No. 11. In both cases UO_2 lumps of about 2070 grams are embedded in a cubic graphite lattice of 8" cell side. The side of the exponential column in the two cases was, however, different (92" for Pile No. 10 and 132" for Pile No. 11). The volumes of the two piles were approximately in the ratio of 1 to 2. The value of the reproduction factor for experiment No. 10—$k = 1.014$—has already been reported. The value found in experiment No. 11 was $k = 1.012$. The difference between the two results is of the order of magnitude of the experimental error. It was also checked that the density of the natural neutrons in the piles 10 and 11 was in the ratio expected from the theory. (For details, see the report of Group III – Zinn).

A new attempt was made to determine the dependence of the reproduction factor on the temperature. For this an exponential pile was set up and provided with a set of heaters and with thermal insulation and was measured first at room temperature and then at a temperature of about 120° C. Only a very small decrease of the order of the experimental error was observed in the relaxation distance. The interpretation of this experiment is discussed in Report CP–254 (*) by Fermi, Christy, and Weinberg, and the result indicates a decrease in the reproduction factor of 0.4 % per 100° with an experimental error of the order of magnitude of the effect itself. The conclusion is obviously somewhat doubtful and more work shall have to be done on the sensitivity to temperature changes.

A considerable amount of uranium metal in the form of sintered blocks has been received from the Alexander factory and this material is at present being used in an exponential pile in order to test its properties. The amount of material available so far is not sufficient to make up a complete pile but only three or four layers. It is hoped, nevertheless, to be able to get in this way some useful indication as to the properties of metal. It should be noticed that the metal in question contains a considerable amount of impurities and has pyroforic properties which make its handling even in the sintered form unpleasant and dangerous.

The following exponential experiments are also being considered:

1. An exponential pile with Speer graphite and UO_2 in order to check whether a better brand of graphite will give the expected advantage.

2. An exponential experiment in which a large amount of bismuth will be placed near the uranium lumps in order to test the effect of a pure commercial brand of bismuth on the reproduction factor.

(*) See paper N° 163 (Editors' note).

3. An exponential experiment in which a rod of paraffin will be inserted in a hole drilled through each uranium lump in order to obtain a geometry as close as possible to that which it is proposed to use in the water cooled plant.

Nuclear properties of various materials.

The tests of the Mallinckrodt production of UO_2 have been conducted regularly. Except for one single case in which the absorption found was 0.3 %, all the rest of the samples gave indication of a quite negligible absorption. (See report of Group IV–Anderson).

Measurements of the diffusion length of a batch of 50 tons of Speer graphite have been performed. Two samples have been tested, one of bricks taken from the ends of the furnace and one of bricks taken primarily from the central portion. The diffusion length reduced in both cases to the normal density 1.6 was 47.93 cm for the first sample and 48.63 cm for the second sample. From the value of the diffusion length one can calculate the absorption cross sections for neutrons of energy kT for the various brands of graphite. Such cross sections are recorded in Table I.

Table I.

Brand of Graphite	$\sigma_{(kT)\times 10^{27}}$	ppm–B equivalent
U.S.	6.4	1.8
AGX	6.7	2.1
Speer (7 tons)	5.5	0.7
Speer (1st 50 ton lot end of furnace)	5.6	0.9
Speer (1st 50 ton lot center of furnace)	5.4	0.6

The last column of this table represents the ppm of boron required to give the observed cross section on the assumption that boron is the only impurity present and that the cross section of pure carbon is 4.9×10^{-27}. (See report of Group III–Zinn).

There are still some elements that may be present as impurities in our materials for which the neutron absorption is not yet known. Experiments are in progress in order to determine the absorption cross section of some of these elements, particularly in the group of the rare earth.

Miscellaneous experiments in nuclear physics.

The tests on the neutron distribution inside small samples of a lattice structure placed near the cyclotron have been continued during the past month. The results seem to indicate that the absorption coefficient of

cadmium absorbable neutrons in the lattice is less than that of thermal neutrons. The simplest interpretation seems to be that due to the strong absorption of neutrons in a lattice, the number of collisions is not sufficient to reduce the neutrons to thermal energy. (See report of Group I–Snell).

The previous results, as well as the rather obscure results obtained in the thermal experiment on the exponential pile, make it appear worthwhile to investigate in a somewhat more systematic way the conditions under which neutrons are or are not slowed down to thermal energies by collisions in graphite. A graphite column has been set up by Mr. Anderson's group with facilities for heating in order to perform such experiments. (See report of Group IV–Anderson).

New measurements of the absorption cross section of uranium for thermal neutrons have been taken. (See reports of Anderson and Snell). Although the method used in the two measurements is quite different, both experiments seem to indicate that the value of the total thermal cross section is somewhat higher than indicated by previous measurements. The reason for such a discrepancy is not yet cleared up. Preliminary results obtained by Mr. Anderson's group give the values 4.6×10^{-24} and 3.2×10^{-24} for the cross sections of uranium for thermal neutrons leading to fission and to formation of U^{239}. Assuming these values and assuming that the number of neutrons emitted when a thermal neutron is absorbed is for natural uranium $\eta = 1.3$, it would follow that the number of neutrons emitted is 2.2 per fission.

Some more work has been performed by Mr. Anderson's group on the standardization of absolute measurement of β–ray intensities giving particular attention to the error introduced in such measurements by the use of different foils backing the samples.

Preparatory work for the experimental pile.

A number of tests have been made to investigate the possibility of using a sheet of rubberized balloon cloth for evacuating the first chain reacting pile that is at present being planned. This material appears to have several very convenient features. In a test a number of graphite blocks were wrapped in balloon cloth, cemented with ordinary rubber cement, and evacuated to about 1 mm of mercury. (See report of Group IV–Anderson).

A test has been performed on the conduction and dissipation of heat in a graphite pile cooled with a water current in a system of copper pipes embedded in the outer portions of the graphite. The system was embedded in balloon cloth and first evacuated and then filled with helium. The energy dissipated per unit area was of the same order of magnitude as expected in the experimental pile in order to provide a test under conditions as close as possible to those expected in the operating pile. (See report of Group IV–Anderson).

Work is in progress on the construction of four control rods with mechanisms for operation to be used in the first chain reacting pile. (See report of Group V–Wilson).

N° 169 and 174.

Fermi organized a second series of lectures in September. He had quite clear ideas about how he was going to carry out the chain reaction experiment. The lectures to the young people of the Metallurgical Laboratory gave him an opportunity to review these ideas and check, in his own mind, the soundness of his plans.

All the bases, both theoretical and experimental, of the chain reaction, he collected together and recast in the simplest possible form which could yet give adequately accurate quantitative results. Anyone with a reasonably good training in physics could follow the argument and learn how the lattice constants and the size of the pile were arrived at, what the behavior would be during the approach to criticality, how the controls worked, including an estimate of their effectiveness, and what the time response of the reactivity of the pile would be. Doubts could be settled, questions answered, and the physicists who were engaged in various phases of the work could have an understanding, in some detail, of the whole. The lectures were fresh, clear, and convincing; they showed Fermi's wisdom, his knowledge, his complete suitability for the job at hand. It was a privilege and a thrilling experience to be associated with him in those days.

The notes, taken by one or another of his listeners, have not been revised: they are still mostly in concise mathematical language, but here and there they have recorded Fermi's use of slang, which he was picking up from his younger associates and of which he was very fond.

Several subsequent books on the chain reaction by various authors were based on these lectures, though often without reference to them.

H. L. ANDERSON.

169.

PURPOSE OF THE EXPERIMENT AT THE ARGONNE FOREST. MEANING OF THE REPRODUCTION FACTOR "k"

Report CP–283 (Notes on Lecture of September 23, 1942).

PURPOSE OF EXPERIMENT AT ARGONNE FOREST.

1. To determine if a self sustaining chain reaction is possible.
2. To demonstrate whether or not power may be obtained from such a reaction.

MEANING OF REPRODUCTION FACTOR "k".

"k" is the number by which one multiplies the number of neutrons of one generation to find the number of neutrons in the next generation. For instance, if there are N_r neutrons in a given generation, there will be

$k N_1$ daughter neutrons and there will be $k^2 N_1$ in the second generation, or $k^n N_1$ in the nth generation. Thus, if $k < 1$, $k^n N_1 \to 0$, and the reaction is not self-sustaining. If $k = 1$, the reaction is self sustaining, while if $k \gg 1$, "run quick-like behind a big hill many miles away."

In a self sustaining chain reaction, the initial neutrons are provided by spontaneous fissions in the pile. These are reduced to an energy suitable for producing fissions before they come in contact with special materials in which neutrons are born very readily. A fraction of this new generation then repeats the life history of their parents.

The structure which will be built at the Experimental Plant will consist of carbon blocks and uranium units. The pile will be a cube whose edge

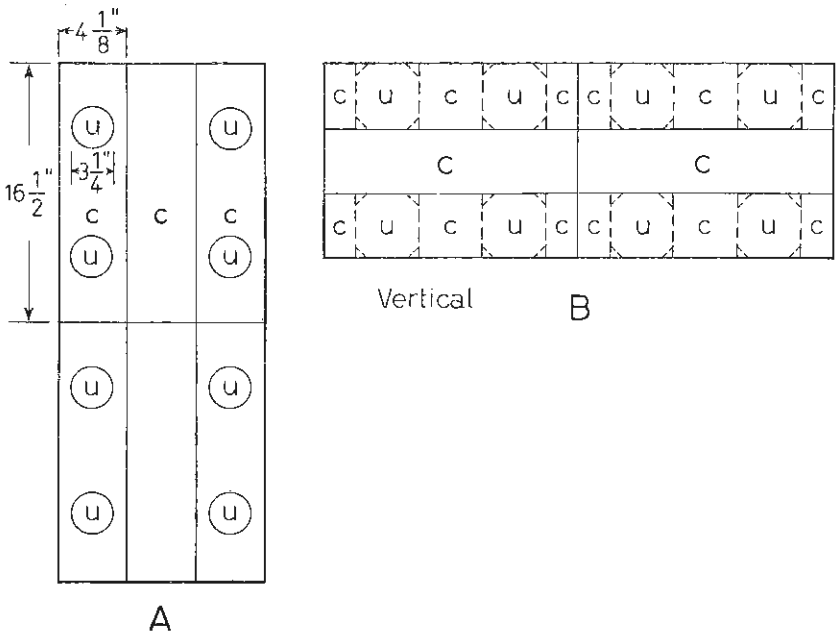

Fig. 1.

will be 6.4 meters. The structure is indicated in fig. 1. The unit which is repeated throughout alternate horizontal layers in the pile is shown in A of fig. 1. The unit which is repeated through the vertical is shown in B, fig. 1. In each case, U denotes the region in which neutrons are produced most copiously and C the region in which they are moderated.

A neutron may terminate its existence in the pile by:

1. Escaping from the pile.
2. A sterile encounter with an atom (parasitic capture). In this, the neutron is captured, when its energy is not such that a fission results or the neutron is captured in a material in which fissions do not result.
3. Producing a fission which in turn releases daughter neutrons.

The materials and geometry are selected so as to reduce No. 2 and increase No. 3. No. 1 is decreased by making the pile larger.

The number of neutrons in the pile at any time is

$$N_1 + N_1 k + N_1 k^2 + \cdots + N_1 k^n$$

or

$$N_1 (1 + k + k^2 + \cdots + k^n),$$

a geometric series hence

$$S = \frac{\text{Lim}}{n+\infty} N_1 \frac{(1-k^n)}{(1-k)} = \frac{N_1}{1-k} \qquad (\text{if } k < 1).$$

Hence, the total number of neutrons in a pile is a means of measuring k.

This will enable us to define the effective production factor k_e. If the production factor is k and the fraction of neutrons escaping from the pile is f,

$$k_e = (1-f)\, k.$$

Thus if the production factor is 1.05 and 5 per cent of these escape

$$k_e = (0.95)\ (1.05).$$

A boron counter measures neutron density because the probability of a neutron producing an ion in such a counter is proportional to $1/v$ and the number of ions passing through a region is proportional to nv, where n is the neutron density, hence the total number of pulses is proportional to:

$$\frac{1}{v}\, nv = n.$$

This indicates a method of building the pile. Counters will be placed in the pile and S determined as the size of the pile increases. When $k \to 1$, S will rise very rapidly, and before the pile can be made larger the parasitic capture of neutrons must be increased. This can be done by inserting some material, which readily absorbs thermal neutrons, into the pile. The plan is to have four rods which may be moved in or out of horizontal slots near the center of the pile. These rods will be inserted and if "k" is lowered according to predictions the construction work will continue.

When the pile is completed it will be sealed in an air tight tent made of rubberized halloon cloth and the whole will be evacuated. The removal of the air will reduce parasitic capture and enhance the value of k.

The control rods, each of which will kill about 1/2 of one per cent of the neutrons, will then be pulled out until "k" approaches 1. Then it will be determined whether "k" can be sufficiently regulated by the movement of the rods both manually and automatically. When it has been shown that a self-sustaining reaction can be established and controlled, the laboratory and territory will be evacuated and the pile will be operated for a short while from the "dug out" in no man's land to determine if power may be obtained from such a plant.

N° 170.

For the introduction to this paper see N° 169.

170.

THE CRITICAL SIZE—MEASUREMENT OF "k" IN THE EXPONENTIAL PILE

Report CP–289 (Notes on Lecture of September 30, 1942).

In the actual carbon piles in which k has been measured there are two neutron sources placed near the bottom of the pile as indicated in fig. 1 and the piles are in a room in which walls may scatter neutrons.

In order to treat of the problem of production of neutrons in this pile the following simplifying assumptions are made:

1. The entire medium is homogeneous:

A. Actually the medium is a lattice work made up of carbon throughout which are placed uranium metal or uranium oxide units. (See Fermi's first lecture)(*);

B. This assumption also means the source is distributed uniformly throughout the region.

2. The neutrons are monoenergetic.

3. There is no back scattering by the walls.

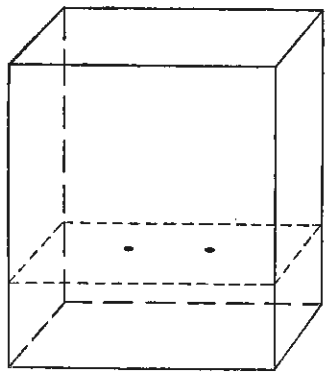

Fig. 1.

This means that the neutron density $n(x, y, z)$ is a function of position only.

The neutron density at any point may vary with time by

1. Diffusion,
2. Absorption,
3. Production.

EQUATION OF NEUTRON DENSITY FOR STEADY STATE.

$$D\Delta n + (k - 1)\frac{vn}{\Lambda} + q = 0$$

is the equation for steady state under preceding assumptions. D is the diffusion coefficient, that number by which the neutron density gradient is multiplied

(*) See paper N° 169.

to give the number of neutrons crossing unit area in unit time. n is the number of neutrons per cm^3. v is the velocity of neutrons, assumed uniform. Λ is the mean free path of neutrons, the mean distance a thermal neutron travels before capture. k is the reproduction factor for neutrons. q is the number of neutrons per unit time per unit volume which the source sends into pile.

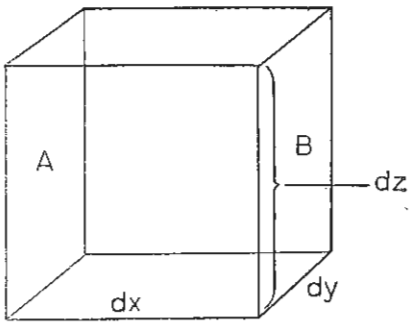

Fig. 2.

Let the neutron density at the center of the elemental cube $d\tau = dx\,dy\,dz$ be n and the respective rates of change of neutron density in the x, y and z directions at this point be $\partial n/\partial x$, $\partial n/\partial y$, and $\partial n/\partial z$ (fig. 2). The rate of change of neutron density at face A is $\frac{\partial n}{\partial x} - \frac{\partial^2 n}{\partial x^2}\frac{dx}{2}$ and that at face B is $\frac{\partial n}{\partial x} + \frac{\partial^2 n}{\partial x^2}\frac{dx}{2}$. Thus the respective rates of influx through faces A and B are $D\left(\frac{\partial n}{\partial x} - \frac{\partial^2 n}{\partial x^2}\frac{dx}{2}\right)dy\,dz$ and $D\left(\frac{\partial n}{\partial x} + \frac{\partial^2 n}{\partial x^2}\frac{dx}{2}\right)dy\,dz$. Hence, the contribution to the number of neutrons within the cube due to diffusion along the x axis is $D\frac{\partial^2 n}{\partial x^2}dx\,dy\,dz$. Likewise, the contributions to the number of neutrons within this element due to diffusion along the z and y axis are respectively $D\frac{\partial^2 n}{\partial y^2}dx\,dy\,dz$ and $D\frac{\partial^2 n}{\partial z^2}dx\,dy\,dz$.

Hence the total contribution of diffusion to the neutron density with the element $d\tau$ is:

$$D\left(\frac{\partial^2 n}{\partial x^2} + \frac{\partial^2 n}{\partial y^2} + \frac{\partial^2 n}{\partial z^2}\right)\frac{dx\,dy\,dz}{d\tau} \equiv D\Delta\, n.$$

THE CHANGE IN NEUTRON DENSITY DUE TO ABSORPTION AND REPRODUCTION.

If Λ is the mean distance a thermal neutron travels before absorption, the probability of absorption in a distance ds traveled in a time dt is ds/Λ and the number absorbed per unit volume is:

$$n\frac{ds}{dt}\frac{1}{\Lambda} = \frac{nv}{\Lambda}.$$

The change in density due to reproduction is:

$$k\frac{nv}{\Lambda},$$

since by definition for each neutron absorbed k neutrons are produced.

Now, q neutrons per unit volume per second are supplied by the source, and the total contribution to the density by diffusion, reproduction and the source is:

$$D\Delta n + \frac{knv}{\Lambda} + q$$

and the loss by absorption is nv/Λ. In the steady state, the net contribution of all factors is zero and:

$$D\Delta n + (k-1)\frac{nv}{\Lambda} + q = 0.$$

It is shown in kinetic theory that $D = \frac{v\lambda}{3}$ where λ is the mean distance a thermal neutron travels between successive collisions. Substituting this value and multiplying through by $3/v\lambda$ we have:

$$\Delta n + (k-1)\frac{3n}{\lambda\Lambda} + \frac{3q}{\lambda v} = 0. \tag{1}$$

Solution of equation (1).

We consider a cube of side a and assume the source diffused throughout the cube.

Since n is a function of x, y and z and a Fourier series may represent the solution for any distribution of sources, the leading term of this Fourier series is assumed as a solution. Thus let

$$n = n_0 \cos\frac{\pi x}{a}\cos\frac{\pi y}{a}\cos\frac{\pi z}{a}$$

where the origin is taken at the center of the pile.

$$\Delta n = \frac{\partial^2 n}{\partial x^2} + \frac{\partial^2 n}{\partial y^2} + \frac{\partial^2 n}{\partial z^2} = -\frac{3\pi^2}{a^2} n_0\left(\cos\frac{\pi x}{a}\cos\frac{\pi y}{a}\cos\frac{\pi z}{a}\right) = -\frac{3\pi^2}{a^2} n.$$

Substituting these values in equation (1) we have:

$$-\frac{3\pi^2}{a^2} n + \frac{3(k-1)n}{\lambda\Lambda} + \frac{3q}{\lambda v} = 0,$$

which gives:

$$n = \frac{3q}{\lambda v}\Big/ 3\left(\frac{\pi^2}{a^2} - \frac{(k-1)}{\lambda\Lambda}\right);$$

n increases as a increases provided $\frac{\pi^2}{a^2} > \frac{k-1}{\lambda\Lambda}$. The variation of n with a is indicated in fig. 3;

a_0 is given by

$$\frac{\pi^2}{a_0{}^2} = \frac{k-1}{\lambda\Lambda} \quad \text{or} \quad a_0 = \pi\sqrt{\frac{\lambda\Lambda}{k-1}}.$$

At $a = a_0$ the pile is unstable and the theory does not hold beyond this point as equilibrium was assumed. Also for a_0 to be real $k > 1$. It should also be noted that as k increases a_0 decreases.

If one does not assume monoenergetic neutrons, the formula becomes:

$$a_0 = \sqrt{\frac{3\pi^2}{k-1}}\sqrt{\frac{\lambda\Lambda}{3} + \frac{r_0^2}{4}}$$

r_0 is the mean distance a high energy neutron diffuses before becoming a thermal neutron. For example:

$$\frac{\lambda\Lambda}{3} + \frac{r_0^2}{4} = 700 \text{ cm}^2.$$

Let $k = 1.05$. Then:

$$a = \sqrt{\frac{700 \times 3\pi^2}{0.05}} = 700 \text{ cm.}$$

This is the size of side of the pile required for k to be equal to 1.05. The experimental pile will be a cube of approximately this size.

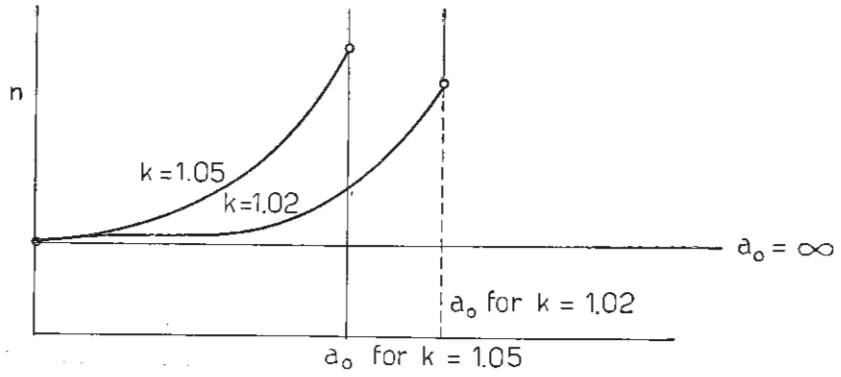

Fig. 3.

MEASUREMENT OF k IN THE EXPONENTIAL PILE.

In measuring k in the exponential pile, neutron density measurements with counters are taken starting at a distance from the localized source, such that q may be assumed to be zero. The differential equation then becomes

$$\Delta n + \frac{3(k-1)n}{\lambda\Lambda} = 0.$$

If one measures the neutron density along a vertical line the solution is of the form

$$n = f(z) \cos\frac{\pi x}{a} \cos\frac{\pi y}{a}$$

$$\Delta n = f''(z) \cos\frac{\pi x}{a} \cos\frac{\pi y}{a} - \frac{2\pi^2}{a^2} f(z) \cos\frac{\pi x}{a} \cos\frac{\pi y}{a}.$$

Substituting these values in the equation we get the following differential equation for $f(z)$

$$f''(z) - \left[\frac{2\pi^2}{a^2} - 3\frac{(k-1)}{\lambda\Lambda}\right] f(z) = 0$$

whose general solution is of the form:

$$f(z) = Ae^{-z\sqrt{\frac{2\pi^2}{a^2} - \frac{3(k-1)}{\lambda\Lambda}}} + Be^{+z\sqrt{\frac{2\pi^2}{a^2} - \frac{3(k-1)}{\lambda\Lambda}}}.$$

For an infinite pile, the term $e^{+z\sqrt{\ }}$ cannot be a solution, since it becomes infinite as $z \to \infty$. Therefore B = 0.

The relaxation distance is the distance required to reduce the neutron intensity by a factor of $1/e$. In a pile the neutron density follows the law

$e^{-\frac{z}{b}}$ and thus

$$\frac{1}{b^2} = \frac{2\pi^2}{a^2} - \frac{3(k-1)}{\lambda\Lambda}.$$

If we do not assume monoenergetic neutrons the formula becomes

$$\frac{1}{b^2} = \frac{2\pi^2}{a^2} - \frac{k-1}{\frac{\lambda\Lambda}{3} + \frac{r_0^2}{4}} \quad \text{or,}$$

$$k - 1 = \left(\frac{\lambda\Lambda}{3} + \frac{r_0^2}{4}\right)\left(\frac{2\pi^2}{a^2} - \frac{1}{b^2}\right) \quad \text{or,}$$

$$k - 1 = 700\left(\frac{2\pi^2}{a^2} - \frac{1}{b^2}\right).$$

Therefore:

k	> 1	< 1	1
b	$> \frac{a}{\pi\sqrt{2}}$	$< \frac{a}{\pi\sqrt{2}}$	$= \frac{a}{\pi\sqrt{2}}$

Numerical example:

$a = 233$ cm. If the length of the side is corrected for the mean free path a becomes about 238 cm.

Thus:

$$\frac{a}{\pi\sqrt{2}} = 53.8 = b.$$

The relaxation distance in the present pile is about 55 cm.

Comments after lecture.

$\frac{\Lambda\lambda}{3} = \frac{2500 \times 2.5}{3} = 2000$, for carbon. The reason $\Lambda\lambda/3$ is small is due to uranium absorption. Of the total absorption of neutrons about one part is due to carbon and seven to uranium. This reduced Λ by a factor of about eight, hence,

$$\text{Effective } \frac{\Lambda\lambda}{3} = 350.$$

To determine k, neutron densities are measured as a function of z and are found to fit the curve $n = n_0 e^{-\frac{z}{b}}$. Thus:

$$\log n = \log n_0 - \frac{z}{b}$$

and if n is plotted against z on semi-log paper, the slope $= -\frac{1}{b}$. Knowing a and b, k can be found.

To compute r_0, a source is placed in a column of graphite. The density of 1 volt electrons is measured as a function of the distance from a source.

This intensity is found to follow the Gaussian law and

$$n = n_0 e^{-\frac{x^2}{r_0^2}}$$

where r_0 is the mean value of x. The graph is shown below (fig. 4)

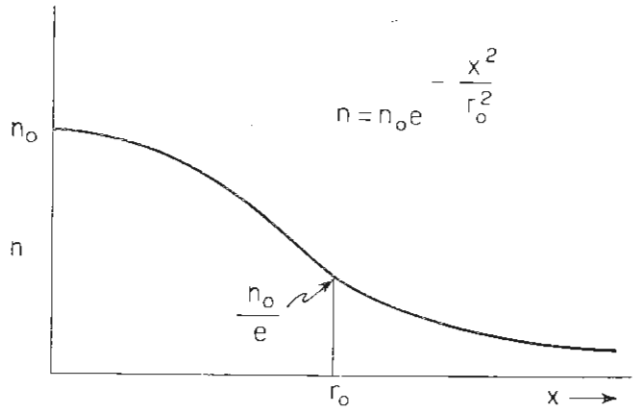

Fig. 4.

r_0 is the mean distance from the source at which a high energy neutron is reduced to thermal, which is the distance for the intensity of these neutrons to be reduced by a factor of $1/e$. Since the above is for one volt neutrons corrections are made for neutrons of thermal energy.

Distinction between Λ and $\sqrt{\frac{\Lambda\lambda}{3}}$.

$\sqrt{\frac{\Lambda\lambda}{3}}$ is roughly equal to the air line distance between the birthplace S and the site of capture P of a thermal neutron. This is represented by the

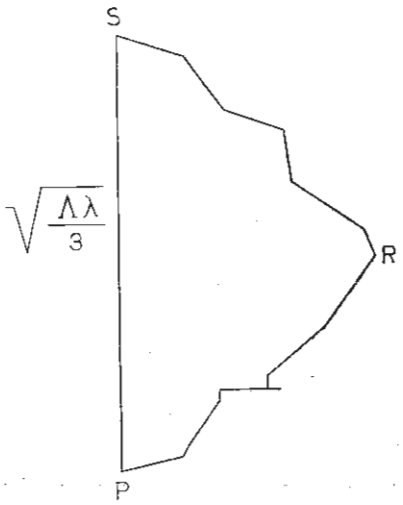

Fig. 5.

straight line SP in fig. 5. Λ is the total distance a thermal neutron travels during its life time. This is represented by the broken line SRP.

LIFE HISTORY OF 100 NEUTRONS.

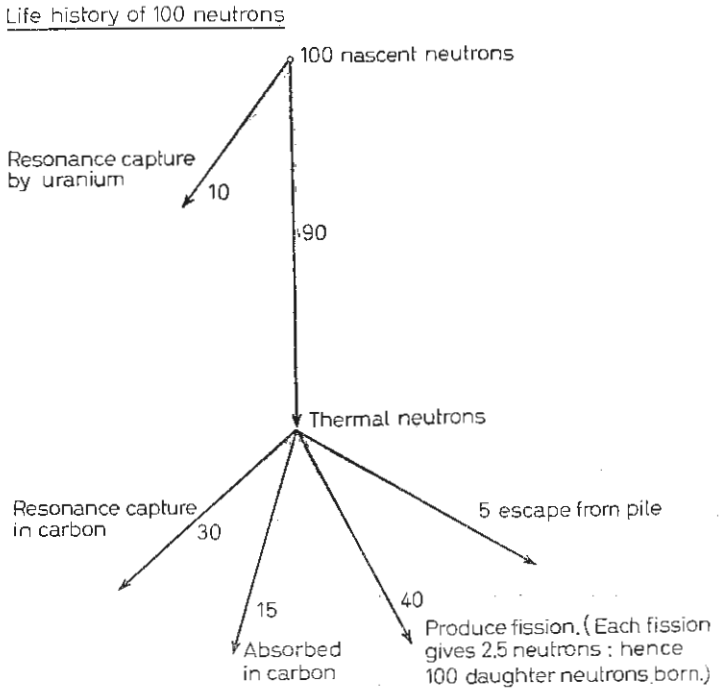

N° 171.

In paper number 171 Fermi gives a simplified derivation of the time dependence of a reactor. The procedure that Fermi followed in starting up the fist pile was based on the formulae in this lecture combined with the method (see paper number 169) for estimating criticality from a series of subcritical measurements. The same procedure was followed in starting up subsequent reactors.

This lecture is of historical interest. It clearly illustrates that there was a good understanding of pile kinetics despite implications to the contrary in some melodramatic accounts of the events of December 2nd, 1942 given in the press. See also the introduction to N° 169.

A. WATTENBERG.

171.

PROBLEM OF TIME DEPENDENCE OF THE REACTION RATE: EFFECT OF DELAYED NEUTRONS EMISSION

Report CP–291 (Notes on Lecture of October 7, 1942)

A. SIMPLE THEORY NEGLECTING DELAYED EMISSION OF NEUTRONS.

Assume $k = 1 + \varepsilon$, where ε is a small positive number, k is the reproduction factor for a pile of finite size. A fast neutron becomes thermal in about 100 collisions, then after about 1000 more collisions it is absorbed. It moves much more slowly in its thermal stage, therefore the thermal life is long compared with the early " fast " life.

Because $\frac{\text{absorption by uranium}}{\text{absorption by carbon}} = \frac{10}{1}$, the lifetime of a neutron in a lattice of uranium and carbon is about 1/10 of the lifetime in pure graphite. If the lifetime in graphite is 1/100 sec, then the lifetime of a neutron or time of one generation in the lattice is 1/1000 sec.

If $k = 1.001$, the nth generation of descendents from one neutron is $(1.001)^n$. To multiply the initial number of neutrons by e there must be $1/\varepsilon$ generations as shown below

$$\log (1 + \varepsilon) = \varepsilon \quad \text{approximately}$$

$$e^{\varepsilon} = 1 + \varepsilon$$

$$e = (1 + \varepsilon)^{1/\varepsilon}.$$

The time for $1/\varepsilon$ generations, if $\varepsilon = 0.001$ and the time of one generation is 1/1000 seconds, is equal to $\frac{1}{\varepsilon} \times \frac{1}{1000} = 1$ second.

After 10 minutes there have been 6×10^5 generations since:

$$n\times\frac{1}{1000}\text{ sec} = 600\text{ seconds}, \qquad n = 6\times10^5$$

and the number of neutrons produced from one neutron is $(1+\varepsilon)^n = e^{n\varepsilon} = e^{6\times10^5\times10^{-3}}$.

The control rods will probably change k by about 1 % if moved from all out to all in the pile.

If the rods are 6 meters long, and $k = 1.001$ for the rods completely out, then $k = 0.991$ for the rods completely in. Since 600 cm of rod change k by 1 %, 6 cm of rod charge k by 0.01 % or by 0.0001 units of k.

If the control rod is moved out 6 cm, k changes from 1.0009 to 1.0010. The relaxation time, or time to change the number of neutrons by the factor e, is given by:

$$\frac{1}{\varepsilon}\times\frac{1}{1000} = \frac{1}{0.001}\times\frac{1}{1000} = 1\text{ second}.$$

This theory however is not correct because there is a time delay in the emission of some of the neutrons.

B. Simple theory including delayed emission of neutrons.

Upon fission, 99 % of neutrons are emitted right away. 1 % is emitted after an appreciable time lag described by a complicated law which depends on about 3 lifetimes. The mean lifetime is about 10 seconds.

(a) If $k = 1.20$, without delayed neutrons $k = 1.19$. The reaction rate is not changed appreciably by removal of delayed neutrons. (b) If $k = 1.005$, their elimination reduces k to 0.995 and the delayed neutrons are needed to sustain the chain reaction. The reaction can not explode in less than 10 seconds—not until the needed neutrons are supplied. The lifetime of the delayed neutrons controls the relaxation time in case (b) but not in (a).

Let $\tau = 1\frac{1}{1000}$ sec = normal time of one generation

$T = 10$ sec = time of one generation of delayed neutrons

n = number of neutrons present in the reacting mass

c = number of existing radioactive atoms which will decay to give delayed neutrons (c stands for " credits ").

$\frac{dn}{dt}$ = rate of change of number of neutrons

$p = 1$ % = fraction of neutrons which produce delayed neutrons.

c atoms decay with lifetime T to give c/T new neutrons per second.

All neutrons are absorbed after an average lifetime τ (tau) at the rate n/τ neutrons per second.

Each absorbed neutron forms k new neutrons. k includes emission of both credit neutrons and instantaneous neutrons. These statements may be expressed by the equations (1) and (2)

$$(1)\qquad \frac{dn}{dt} = \frac{c}{T} - \frac{n}{\tau} + k(1-p)\frac{n}{\tau}$$

where $k(1-p)$ neutrons produce instantaneous neutrons.

(2) $$\frac{dc}{dt} = kp\frac{n}{\tau} - \frac{c}{T}$$

where $kp\frac{n}{\tau}$ = new credits formed per second

$\frac{c}{p}$ = credits lost per second from radioactive decay.

These equations have exact solutions of the form:

(3) $$c = c_0 e^{\alpha t}$$

(4) $$n = n_0 e^{\alpha t}.$$

They may be differentiated to obtain

$$\frac{dc}{dt} = c_0 \alpha e^{\alpha t}$$

$$\frac{dn}{dt} = n_0 \alpha e^{\alpha t}$$

and these substituted with (3) and (4) in equations (1) and (2). After dividing the equations by $e^{\alpha t}$, there is obtained:

$$n_0\left(\alpha + \frac{1}{\tau} - \frac{k(1-p)}{\tau}\right) - \frac{c_0}{T} = 0.$$

$$n_0\frac{kp}{\tau} - c_0\left(\alpha + \frac{1}{T}\right) = 0.$$

The condition that these equations for n_0 and c_0 have solutions is that the determinant of their coefficients be zero.

These equations may be solved approximately however by neglecting appropriate terms containing τ, because τ is very small compared with T.

Let $N = \frac{n}{\tau} = \frac{\text{number of neutrons}}{\text{lifetime for absorption}}$ = neutrons absorbed per second.

The equations may be rewritten

$$\begin{cases} \frac{dc}{dt} = kpN - \frac{c}{T} \\ \tau\frac{dN}{dt} = \frac{c}{T} - N\{1 - k(1-p)\} \end{cases}$$

τ is very small. Terms which contain it may be neglected, and one thus obtains

$$\frac{dc}{dt} = kpN - \frac{c}{T}$$

$$\frac{c}{T} = N\{1 - k(1-p)\}.$$

This approximation is good below $k = 1.01$ where T is the determining factor of the relaxation time, is no good if τ is the determining factor

$$c = TN\{1 - k(1-p)\}$$

$$\frac{dc}{dt} = T\frac{dN}{dt}\{1 - k(1-p)\} = kpN - N\{1 - k(1-p)\}.$$

After simple algebra, the equation becomes:

$$\frac{dN}{dt} = \frac{N}{T}\left\{\frac{k-1}{1-k(1-p)}\right\}.$$

The solution is

$$N = e^{Q\times\frac{1}{T}\times t} \quad \text{where } Q = \frac{k-1}{1-k(1-p)}$$

t, the relaxation time, or time for the number of neutrons to change by a factor e, is given by:

$$t = \frac{T}{Q} = T\left\{\frac{1-k(1-p)}{k-1}\right\}$$

$(1-p)$ = fraction of neutrons producing instantaneous neutrons,
p = fraction of neutrons producing delayed neutrons,
$k(1-p)$ = reproduction factor if there were only instantaneous neutrons.

The relaxation time is thus clearly the product of the lifetime for delayed neutrons and the ratio of the amounts by which the two reproduction factors differ from one.

If $p = 1\,\%$, $k = 1.003$, and $T = 10$, then the relaxation time t is given by

$$t = 10 \text{ sec } \frac{[1-1.003(1-0.01)]}{1.003-1} = 23 \text{ seconds}$$

k	relaxation time
1.0000	
1.0001	910 seconds
1.001	90
1.002	40
1.003	23
1.004	15
1.005	10
1.009	1
1.0101...	0

Note that although the relaxation time becomes zero for $k = 1.0101$, this has no significance because the approximation used is no longer valid. The relaxation time for $k = 1.001$ from this theory is 90 seconds, while if the delayed neutrons are neglected, simple theory gives the quite different value of 1 second.

N° 172, 173 and 174.

The lectures in papers 172, 173 and 174 were the application of pile theory to the reactor we were building. In these lectures instead of dealing with general theoretical cases (see later lectures at Los Alamos), Fermi simplified the situation by taking the appropriate geometrical case and he put in the numerical values for the lattice that would be used.

These lectures were for the groups that were building the reactor, and they demonstrated Fermis strong desire that those working with him comprehend the measurements they were making and the plans for the future. See also the introduction to N° 169.

A. WATTENBERG.

172.

A SIMPLIFIED CONTROL. OPTIMUM DISTRIBUTION OF MATERIALS IN THE PILE

Report CP-314 (Notes on Lecture of October 20, 1942).

The k of metal is lower than that expected. Since critical size $a \sim \frac{1}{\sqrt{k-1}}$ it follows that volume $\sim \frac{1}{(k-1)^{3/2}}$ because volume is proportional to a^3. To better utilize the material available, the new pile is to be spherical. For the same critical size,

$$\frac{\text{vol sphere}}{\text{vol cube}} = 1.24.$$

The sphere has a volume of 24 % more than does the cube.

A SIMPLIFIED CONTROL.

Consider a small control sphere at the center of the spherical pile. How is k affected by this control? The equation which describes the density of neutrons in the pile is

$$L^2 \Delta n + (k-1)\, n = 0 \quad \text{where} \quad L^2 = \frac{\lambda \Lambda}{3}.$$

If $n = n(r)$ as it does in a spherical pile and $\Delta = \frac{1}{r^2} \frac{\partial}{\partial r} \left(r^2 \frac{\partial}{\partial r} \right)$ then the equation reduces to

$$n''(r) + \frac{2}{r} n'(r) + \frac{k-1}{L^2} n = 0.$$

Let $n = \frac{1}{r}\varphi(r)$. This is valid for a spherical pile. The equation then becomes:

$$\varphi''(r) + \frac{k-1}{L^2}\varphi(r) = 0$$

and if $k > 1$, which is true in this case,

$$\varphi(r) = A \sin \frac{\sqrt{k-1}}{L} + B \cos \frac{\sqrt{k-1}}{L} r.$$

Now n becomes:

$$n = \frac{1}{r}\left\{ A \sin \frac{\sqrt{k-1}}{L} r + B \cos \frac{\sqrt{k-1}}{L} r \right\}.$$

Consider two cases:

(1) spherical pile no control,

(2) spherical pile, small concentric spherical control pile.

Case (1).

To determine the constants A and B, the boundary conditions must be considered.

(a) $$n = 1 \quad \text{at} \quad r = 0.$$

Therefore

$$B = 0 \quad \text{and} \quad A = 1.$$

Actually n has some value different from 1. However, we shall neglect this factor of proportionality for simplicity.

(b) $$n = 0 \quad \text{at} \quad r = R$$

where R is the critical dimension.

$$\frac{1}{R} \sin \frac{\sqrt{k-1}}{L} R = 0.$$

This condition requires $\frac{\sqrt{k-1}}{L} R$ to be either zero or π. Since R is not zero, it follows that:

$$\frac{\sqrt{k-1}}{L} R = \pi$$

$$R = \frac{\pi L}{\sqrt{k-1}}$$

$$k - 1 = \frac{\pi^2 L^2}{R^2}.$$

Case (2).

The boundary conditions now differ: $n = 0$ at R_1 and at R_2

$$n = \frac{1}{r}\left\{ A \sin \frac{\sqrt{k-1}}{L} r + B \cos \frac{\sqrt{k-1}}{L} r \right\}$$

$$\frac{1}{R_1}\left\{ A \sin \frac{\sqrt{k-1}}{L} R_1 + B \cos \frac{\sqrt{k-1}}{L} R_1 \right\} = 0$$

$$\frac{1}{R_2}\left\{ A \sin \frac{\sqrt{k-1}}{L} R_2 + B \cos \frac{\sqrt{k-1}}{L} R_2 \right\} = 0.$$

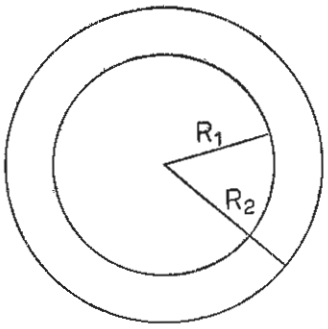

For these equations to have a solution, the determinant of their coefficients must vanish:

$$\begin{vmatrix} \sin a R_1 & \cos a R_1 \\ \sin a R_2 & \cos a R_2 \end{vmatrix} = 0 \quad \text{where} \quad a = \frac{\sqrt{k-1}}{L}$$

$\sin a R_1 \cos a R_2 - \cos a R_1 \sin a R_2 = 0 = \sin a (R_2 - R_1)$. The condition is $\frac{\sqrt{k-1}}{L}(R_2 - R_1) = \pi$.

Such a shell of thickness $R_2 - R_1$ acts as a sphere of radius $= (R_2 - R_1)$

$$k - 1 = \frac{\pi^2 L^2}{(R_2 - R_1)^2}$$

$$k = 1 + \frac{\pi^2 L^2}{(R_2 - R_1)^2}.$$

A control of cylindrical shape or even a slab is roughly similar in effect.

To improve the chances of achievement of a chain reaction, a core of metal lattice will be at the center of the sphere. k of the metal lattice is a few percent higher than k of the oxide lattice. To use a core is more effective than to scatter the metal throughout the pile, because the neutron density is higher at the center. The pile will consist of

(1) a core of good graphite + metal,
(2) a shell of good graphite + oxide,
(3) a shell of inferior graphite + oxide,
(4) a shell of poor graphite (no lattice),
(5) a shell of wood.

The poorer grades of graphite must be used because unhappily there is not enough of the best grade.

Amount of metal in each lattice hole, plotted vs, k

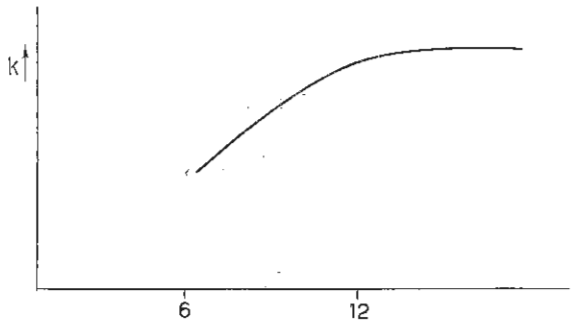

k may go down past a concentration of 12 unts per lattice hole.

There must be some compromise in this first pile between optimum core size and amount of metal in each lattice hole, because the supply of metal is limited.

Let $k_o = k$ oxide , $k = k$ metal , V_{core} = volume of core .

$(k - k_o) V_{core}$ must be made a maximum for the material available.

N° 173.

For the introductions to this paper see N° 169 and N° 172.

173.

DESIGN OF THE GRAPHITE-URANIUM LATTICE: EXPERIMENTAL DETERMINATION OF f_t FROM THE Cd RATIO

Report CP–337 (Notes on Lectures of October 27 and November 3, 1942).

PROPER DIMENSIONS OF A GRAPHITE-URANIUM LATTICE.

A lattice is defined by the size of the lattice cell and by the size of the uranium lump within the cell.

Let the effect of too little or too much metal within the cell be considered:

Case of Too Much Metal	Case of Optimum Amounts of Metal	Case of Too Little Metal
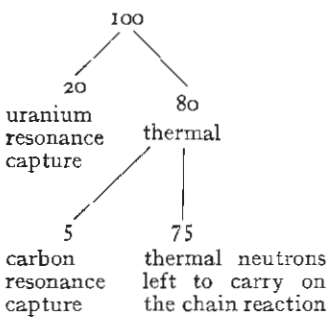	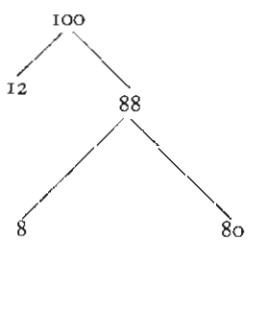	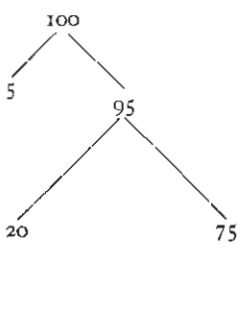

In these simple pictures, all neutrons (both thermal and fast) lost by resonance absorption of uranium are lumped in the single figures 20, 12, 5.

Most thermal neutrons will die in the uranium, but some will die in the carbon and be lost to the chain reaction. If there is too little metal, more neutrons will die by carbon resonance absorption; if too much metal, more neutrons will die by uranium resonance absorption. If the number of neutrons lost by carbon and uranium resonance absorption is minimized by proper

choice of relative amounts of metal and carbon, more neutrons are left for the chain reaction.

Let σ_c = cross section of 1 gram of carbon for neutrons.

Let σ_m = cross section of 1 gram of metal for neutrons.

If for every gram of carbon there are x grams of metal, the probability that a neutron will be absorbed by metal and not by carbon is proportional to

$$\frac{x\sigma_m}{\sigma_c + x\sigma_m}.$$

However, this statement is not strictly true. The metal acts as a sink for neutrons, and the neutron density in and near the metal is lower than elsewhere. Therefore probability of absorption by the metal is somewhat less than this quantity, but by an amount which will be neglected in this treatment.

The expression may be rewritten

$$\frac{1}{1 + \frac{\sigma_c}{\sigma_m x}} = e^{-\frac{\sigma_c}{\sigma_m}\frac{1}{x}} = e^{-\frac{\beta}{x}} \qquad \text{where} \quad \beta = \frac{\sigma_c}{\sigma_m}$$

$e^{-\frac{\beta}{x}}$ is the fraction of neutrons reaching thermal energies which are used in the chain reaction.

Let $e^{-\alpha x}$ = fraction of neutrons which become thermal.

$e^{-\alpha x} e^{-\frac{\beta}{x}}$ = fraction of thermal neutrons (necessarily therefore below the uranium resonance energies) which are absorbed by uranium and which cause

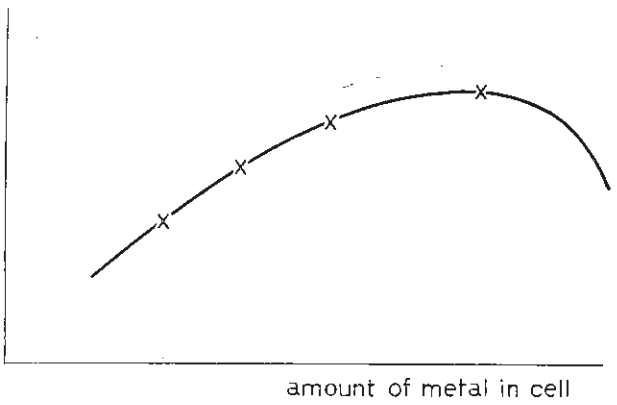

Fig. 1. – x = experimental points. There is as yet no experimental verification for *decrease* in the curve after the maximum.

fission. Then fraction of total neutrons utilized $= e^{-\left(\alpha x + \frac{\beta}{x}\right)}$. α and β are approximately constants. The coefficient $\alpha x + \frac{\beta}{x}$ must be minimized to make this fraction a maximum. This can be done by setting its derivative

equal to zero:

$$\alpha - \frac{\beta}{x^2} = 0 \qquad x^2 = \frac{\beta}{\alpha} \qquad x = \sqrt{\frac{\beta}{\alpha}} \qquad \text{max. fraction} = e^{-2\sqrt{\alpha\beta}}.$$

The maximum fraction for the chain reaction is obtained when the fractions absorbed by uranium and the fraction reaching thermal energies are approximately equal. See fig. 1.

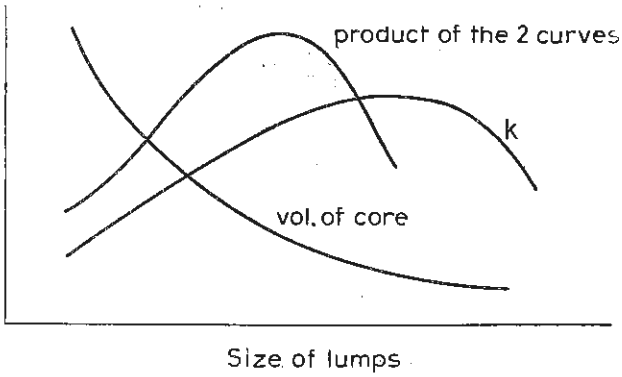

Fig. 2.

At the last lecture Fermi indicated that lack of sufficient metal for the entire lattice made it desirable that the size of the metal core of the lattice and the size of the metal lumps be such that $[k_{\text{oxide}} - k_{\text{metal}}]\, V_{\text{vol. of metal core}}$ is a maximum. See fig. 2.

Design of a lattice cell.

Consider an infinite lattice. At the boundary between 2 cells of the lattice, the normal derivative of the neutron density is zero, because the density is symmetrical with respect to the boundary.

Let q = number of thermal neutrons produced per cm³/sec,

$\bar{q}$ = average value of q,

T = lifetime of thermal neutrons,

V = volume of carbon,

n = neutron density.

The equation for diffusion of thermal neutrons is

$$\frac{\lambda v}{3} \Delta n - \frac{n}{T} + q = 0$$

Let f = thermal utilization of the metal

$$= \frac{\text{net number of thermal neutrons which diffuse into the metal}}{\text{total number of thermal neutrons produced in the cell}}.$$

Then

$$f = \frac{\frac{\lambda v}{3}\left(\frac{\partial n}{\partial r}\right)_{r=a} 4\pi a^2}{\bar{q} V_{\text{carbon}}}.$$

a is the radius of the metal lump. $\frac{\lambda v}{3}\left(\frac{\partial n}{\partial r}\right)_{r=a} 4\pi a^2$ gives the net number of neutrons which flow into the metal lump per unit surface area of the lump.

The cells are of such a size in this case that q is approximately constant over the cell. Here it will be considered so for simplicity. This approximation is good if the cell dimensions are small compared with the slowing down range of the neutron.

Boundary conditions.

(1) At boundary of cell, $\frac{\partial n}{\partial r} = 0$. If the metal surface absorbed all neutrons which strike it, the boundary condition at $r = a$ would be $n = 0$. However, about 40 % of the neutrons are reflected into the carbon. The mean free path is not small compared with the dimensions of the sphere, consequently the boundary condition is more complicated.

It is

$$\frac{n}{\left(\frac{dn}{dr}\right)_{r=a}} = \frac{\lambda}{\sqrt{3}} \frac{1+\gamma}{1-\gamma}$$

where γ is the reflection coefficient known as the albedo of the sphere.

For $\gamma = 0.4$ and $\lambda = 2.7$, $\frac{n}{\left(\frac{dn}{dr}\right)_{r=a}} = 3.6$ cm.

To simplify the problem, the boundary of the cell shall be assumed spherical, fig. 3 an error not greater than other errors introduced by the inaccurate value of the albedo, and errors in theory caused by the lack of thermal equilibrium among the neutrons and by the large mean free path.

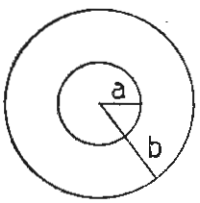

Fig. 3

$$\frac{\lambda v}{3}\Delta n - \frac{n}{T} + q = 0$$

$$\Delta n - \frac{n}{l^2} + \frac{3}{\lambda v} q = 0 \qquad l^2 = \frac{\lambda v T}{3} = 50 \text{ cm}^2.$$

$$\Delta = \frac{1}{r^2}\frac{\partial}{\partial r}\left(r^2 \frac{\partial}{\partial r}\right)$$

$$\frac{d^2 n}{dr^2} - \frac{2}{r}\frac{dn}{dr} - \frac{n}{l^2}\frac{3}{\lambda v} q = 0$$

Boundary conditions: (1) $n = \left(\frac{dn}{dr}\right)_{r=a} \frac{\lambda}{\sqrt{3}} \frac{1+\gamma}{1-\gamma}$;

(2) $\left(\frac{dn}{dr}\right)_{r=b} = 0.$

Let $n = \frac{1}{r}\varphi(r)$

$$\frac{d^2\varphi}{dr^2} - \frac{\varphi}{l^2} + \frac{3}{\lambda v} q = 0 \qquad \frac{3}{\lambda v} q = \text{constant}.$$

The solution is $\varphi = \frac{3 l^2}{\lambda v} q + Ae^{r/l} + Be^{-r/l}$ where A and B are determined by the boundary conditions. The thermal utilization becomes

$$f_t = \frac{\frac{\lambda v}{3}\left(\frac{\partial n}{\partial r}\right)_{r=a} 4\pi a^2}{q\bar{V}} = \frac{3\alpha^2}{(\beta^2-\alpha^2)} \left\{ \frac{(1-\alpha)(1+\beta)e^{-(\beta-\alpha)} - (1+\alpha)(1-\beta)e^{+(\beta-\alpha)}}{(\alpha+s-s\alpha)(1+\beta)e^{-(\beta-\alpha} - (\alpha+\beta+s\alpha)(1-\beta)e^{+(\beta-\alpha)}} \right\}$$

where $\alpha = a/l$, $\beta = b/l$, $s = \frac{\lambda}{\sqrt{3}\,l}\frac{(1+\gamma)}{(1-\gamma)}$. γ is given by theory but may be inaccurate by 1 percent.

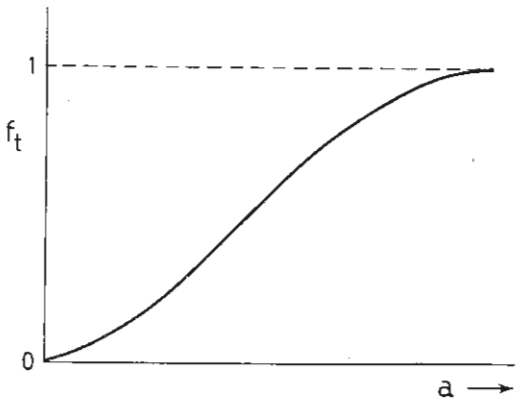

Fig. 4.

When a is small the absorption of the metal is proportional to its own volume, a^3. When $a = b$, all neutrons are absorbed by the metal of course. The optimum value for f_t is about 0.87. See fig. 4.

Experimental determination of f_t from the Cd ratio.

The activity of an indium detector with and without Cd is measured in the lattice. Activity when shielded with Cd is activity not caused by thermal neutrons. The unshielded activity is caused by both thermal and resonance neutrons.

$$A_{Cd} = A_{res}\frac{1}{1.15}$$

$$A = A_{th} + A_{res}$$

$$\frac{A}{A_{Cd}} = 6 \quad \text{or} \quad 7 = 1.15\frac{(A_{th}+A_{res})}{A_{res}} = \left(\frac{A_{th}}{A_{res}} + 1\right)1.15$$

$$A = A_{Cd} = A_{th} + 0.13\ A_{res}$$

$A_t = K_t n$ The activity caused by thermal neutrons $\simeq$ density of thermal neutrons.

$A_r = K_r \bar{q}$ The activity caused by resonance energy neutrons $\simeq$ production of thermal neutrons.

The K's are constants of proportionality.

$\bar{q} V_{Carbon} f_t$ = number of thermal neutrons absorbed in metal. Therefore $(1 - f_t)\,\bar{q} V_{carbon}$ is the number of thermal neutrons absorbed by graphite $= \frac{n}{T} V_{carbon}$, where $\frac{n}{T}$ = average rate which neutrons die per cm³.

$$\frac{A}{A_{Cd}} = \left(1 + \frac{A_{th}}{A_{res}}\right) 1.15 = 1.15 \left\{ K \frac{n}{\bar{q}} + 1 \right\}$$

$$(1 - f_t)\,\bar{q} V_{carbon} = \frac{n}{T} V_{carbon} (1 - f_t) = \frac{n}{\bar{q} T}$$

but

$$l^2 = \frac{\lambda v T}{3} \simeq 50 \text{ cm}^2. \qquad T = \frac{3 l^2}{\lambda v}.$$

Therefore

$$f_t = 1 - \frac{n \lambda v}{\bar{q}\, 3 l^2} = 1 - \frac{\lambda v}{3 l^2} \left\{ \frac{1}{1.15} \frac{A}{A_{Cd}} - 1 \right\} \frac{1}{K}.$$

λ, v, l^2 are known. $\frac{A}{A_{Cd}}$ is measured, K is determined and then f_t can be calculated.

N° 174.

For the introductions to this paper see N° 169 and N° 172.

174.

CALCULATION OF THE REPRODUCTION FACTOR

Report CP–358 (Notes on Lecture of November 10, 1942).

CALCULATION OF THE REPRODUCTION FACTOR.

A neutron is born in the lump with KE = 2 MeV. During its travels, before it escapes the lump, the fast neutron may:

(a) Collide elastically with a metal nucleus, transferring a small part of its KE to the translational motion of the nucleus but leaving the state of the nucleus unchanged. The neutron of course travels on with smaller KE.

(b) It may collide inelastically with a metal nucleus, itself escaping but giving a large part of its KE to excite the nucleus to another state. The excited nucleus may then for instance emit a γ–ray. Szilard and Zinn found the cross section for this process in the metal to be 2.8×10^{-24} cm^2 per atom in the metal.

(c) It may collide with the nucleus and cause fission. The neutron in this case is captured. Szilard found the cross section for this process $= 0.5 \times 10^{-24}$ cm^2 per atom in the natural metal.

Fission in 235 is caused by both very fast and very slow neutrons. To produce fission in 238 the neutron must have energy $>$ 1 MeV. For neutrons of energy above 2 MeV the probability that a neutron born deep within the metal lump will produce a fast fission $= \frac{0.5}{2.8 + 0.5} = \frac{5}{33}$.

If fission occurs the neutron disappears and somewhat less than 2.6 neutrons appear. The net gain of neutrons is $(2.6 - 1) = 1.6$ = average multiplication factor per neutron for the process of fast fission in natural metal. The average multiplication factor for a neutron produced deep within the metal lump $= \frac{5}{33} \times 1.6 = 0.24$ contribution to k from fast fission if all neutrons were born at center of lump.

Actually conditions are much less favorable for increase of k by the process of fast fission:

(1) Most neutrons escape the metal lump because they are born near the surface; more neutrons are born near the surface because they are created

by fission induced by thermal neutrons which come in from the graphite and die near the surface. Thermal neutrons have high probability to be absorbed in the surface of the lump.

(2) The lumps of the Argonne pile are small. The probability of fast fission is proportional to the radius of the lump if the lump is small.

For metal of density 18.0 the increase in reproduction factor due to fast fission is given in the following table and diagram:

Radius of lump	k
1 cm	4.0 %
2	7.6
3	10.6
4	13.0

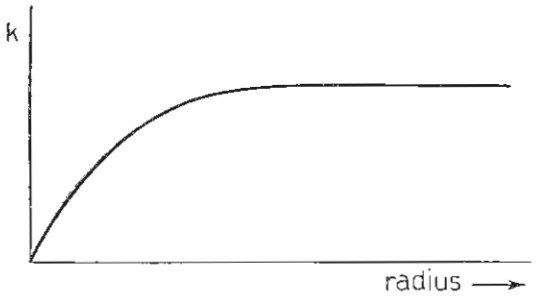

Fig. 1.

k reaches saturation as the radius of the lump increases because most neutrons are produced near the surface. The experimental errors in determination of constants are probably in such a direction as to increase the apparent size of k. If $r = 3$ cm, 0.11 % of neutrons cause fast fission.

Quantitatively the neutron resonance absorption spectrum of U^{238} is not accurately known. Qualitatively it is like the scheme in fig. 2.

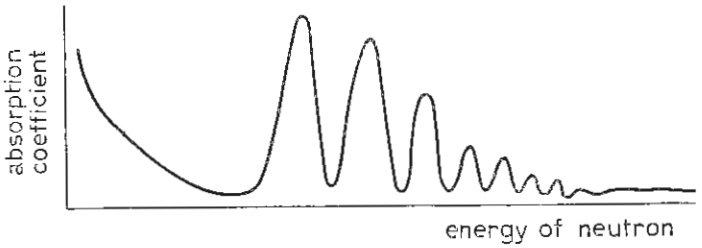

Fig. 2.

As a neutron slows it may be caught in one of the resonance bonds of the metal. The fraction of neutrons lost by resonance absorption may be calculated. If q neutrons per second are produced in a metal lump, the lump absorbs in the resonance process an amount of neutrons $V_r q$. V_r is a constant dependent on the size of the lump. It is the volume from which neutrons are drained by the lump and it is called the resonance volume.

$V_r = A$ (mass of lump in grams) $+ B$ (surface in cm^2). A and B are empirical constants. If a neutron has the energy of a resonance absorption peak it is absorbed almost as soon as it hits the metal lump. Hence the number of neutrons absorbed by the lump is proportional to the surface of the lump. A neutron of energy corresponding to a low absorption coefficient may travel some distance into the lump before being absorbed. Consequently the number

of neutrons absorbed by the lump is also proportional to the mass of the metal lump.

For the metal which is now used, $V_r = 0.358$ (mass in grams) $+ 1.06$ (surface in cm^2). The metal lump for the Argonne pile $= 2720$ grams, its surface, 153 cm^2. $V_r = 1136$ cm^3.

Neutrons come from a volume of more than 1 liter to be caught in the metal by the resonance absorption, but the actual volume of the metal is: $\frac{2720\text{ gm}}{18.0\text{ gm/cm}^3} = 150$ cm^3.

The fraction of neutrons absorbed by the resonance process $= \frac{V_r q}{Vq} = \frac{V_r}{V}$, where V is the volume of the metal graphite cell. The fraction of neutrons escaping resonance absorption by the metal $= 1 - \frac{V_r}{V}$. $1 - \frac{V_r}{V} = e^{-\frac{V_r}{V}}$ is a valid approximation if $V_r \ll V$.

V for the Argonne pile $= 9200$ cm^3 $e^{-\frac{V_r}{V}} = 0.887$ fraction of neutrons escaping resonance absorption in the Argonne pile = fraction of neutrons which reach thermal energies.

The thermal utilization coefficient is 0.868. For every thermal neutron produced, only 0.868 thermal neutrons are reabsorbed by the metal. It is thought that for every thermal neutron absorbed, 1.29 neutrons are produced.

0.868×0.887 = fraction neutrons which reach thermal energies and are reabsorbed by metal for every original fast neutron.

$0.868 \times 0.887 \times 1.29$ = fraction of new neutrons from slow fission per original fast neutron.

This result must be corrected for the increase in k by fast fission. If $r = 3$ cm, increase in $k = 106\,\%$.

$(1 + 0.106) \times 0.868 \times 0.887 \times 1.29 = k$ = average number of neutrons produced by one neutron. $k = 1.086$.

1.29 = number of neutrons produced when a thermal neutron is absorbed by metal.

2.6 = average no. of neutrons produced when a thermal neutron *causes* fission.

Probability of fission $\times 2.6 = 1.29$.

Probability of fission = ratio of abundances $\times \frac{\sigma_{238}}{\sigma_{235}}$.

N° 175.

During October the tempo of the preparations for the chain reaction experiment increased. Anderson's group was joined to Zinn's so that nine exponential experiments were carried out. The first tests of the uranium metal arriving from Metal Hydrides and Westinghouse were carried out and some changes in the plan of the structure were made in the light of these results.

Report CP–297, of which this paper is an excerpt, was issued also as A–318.

H. L. ANDERSON.

175.

THE PROJECTED EXPERIMENT AT ARGONNE FOREST AND THE REPRODUCTION FACTOR IN METAL PILES

Excerpt from Report CP–297 for Month Ending October 15, 1942.

The main problem facing the physics division during the past month has been the organization of the experiment at Argonne Forest. In connection with this experiment, it has been necessary to organize in the West Stands the work of pressing about 50 tons of uranium oxide and of machining about 500 tons of graphite. The organization of this work, which is now about halfway completed, is discussed in the report of Zinn and Anderson. Besides this work, nine exponential experiments have been performed in the past month in order to try to get information as to the behavior of metal lumps.

The construction of the building at Argonne Forest has been progressing during the month of October, and it is expected that the pile room will be ready for occupation early in November. Mr. Stearns has taken charge of keeping the contacts with the Army and with Stone and Webster to arrange for the details of the work carried out there. Mr. Wilson and his group, together with Mr. Froman, are in charge of developing the controls and the various instruments that will be used in connection with the Argonne pile.

This exceptional amount of work has required a considerable expansion of the personnel, both laborers and physicists. In order to make available a sufficient number of physicists, the two groups III and IV have been temporarily fused into one unit and the work on standardization has been practically discontinued.

EXPONENTIAL EXPERIMENTS.

Of the nine exponential experiments numbered 13 to 21 performed in the last month, one, namely No. 18, was designed in view of determining the reproduction factor for a lattice of pressed UO_2 and Speer graphite as closely as possible similar to the lattice that will be used in part of the structure to be erected at Argonne Forest. The details of this experiment are given in the report of Zinn and Anderson. The reproduction factor was found to be 1.032 and is, therefore, about 0.5 % below the expectation. This reproduction factor can be increased to some extent by evacuating the structure. A further small increase may be expected by substituting in at least part of the mass AGOT graphite in place of Speer, since the measurements seem to indicate that the AGOT graphite absorbs slightly less than Speer.

Eight exponential experiments, Nos. 13–17 and 19–21, have been performed in order to get some preliminary information as to the behavior of metal lumps. Two brands of metal, sintered blocks from Metal Hydrides (experiments No. 13–17) and fused blocks from Westinghouse (experiments No. 19–21) have been used. In both cases, the amount of metal available was not sufficient to set up a complete exponential pile and therefore the sandwich method was used by interposing a few metal bearing layers in an exponential pile of U_3O_8. The geometry of these experiments and the results of the measurements are described in detail in the report of Zinn and Anderson.

Experiments of this type are not as reliable as the conventional type of exponential experiment. This is particularly the case when the metal lattice has a cell different from that of the oxide lattice. In this case it is very difficult to avoid transition effects which may vitiate the result to a considerable extent. A tentative interpretation of this set of experiments is given in what follows. In Table I is given a summary of the results of the eight experiments. Column 1 gives the number of the experiment. Column 2 indicates the type of uranium used. Pile 13 with U_3O_8 is used for comparison; MH stands for Metal Hydrides metal and West for Westinghouse metal. The third column gives the volume of the cell in liters. The experiments in which the cell volume is 8.4 liters have the usual cubic cell structure of 8″ side. The experiments in which the cell volume is 28.3 liters have a cubic cell of 12″ side. Experiment No. 17, in which the cell volume is 4.2 liters, corresponds to a body centered lattice. The graphite used in all these experiments has been U. S. graphite.

Column 4 gives the number of lattice layers bearing metal in the various experiments. Column 5 gives the mass of metal lump in grams. The lumps were assembled out of small blocks $1'' \times 1'' \times \frac{1''}{2}$ on the side in the case of Metal Hydrides metal and 1″ on the side in the case of Westinghouse metal in a disposition as compact as possible. Such blocks were placed in a cylindrical hole 3″ in diameter and 3″ deep, drilled in the carbon block. The hole was appreciably wider than the metal lump and left, therefore, a

considerable clearance around the lump. Colums 6 and 7 give the intensity observed on the axis of the pile at position 4 below the metal bearing layer and at position 10 above the layer. Inspection of the data of column 4 indicates that the intensity helow the layer is fairly constant in all experiments. Somewhat greater variations from the mean are found for experiments 15, 16 and 17 and are probably due to transition effects rather complicated to interpret and due primarily to the fact that the metal lattice used is for these cases widely different from the oxide lattice in which it is embedded.

TABLE I.

Pile	Uranium	Cell volume (liters)	No. of layers	Mass of lump (grams)	Pos 4	Pos 10	b	* $10^6 \nabla^2$ (cm^{-2})	L^2	k	Cd ratio
13	U_3O_8	8.4	—	1800	31132	3335	54.25	3	700	1.002	6.88
14	M.H.	8.4	4	2022	30943	3444	55.45	18	682	1.012	6.60
15	M.H.	28.3	2	6826	30573	3237	52.87	— 14?	855	0.988 ?	8.15
16	M.H.	28.3	2	8848	30752	3271	53.34	— 8?	744	0.994 ?	7.57
17	M.H.	4.2	6	885	29764	3445	55.87	23?	654	1.015 ?	6.17
19	West	8.4	4	2121	31219	3644	57.68	42	677	1.028	6.53
20	West	8.4	4	1818	31020	3520	56.26	27	707	1.019	7.00
21	West	8.4	4	2424	31436	3737	58.72	53	660	1.035	6.26

* In the Project the symbol ∇^2 (nabla^2) became identified with the numerical value obtained from applying this operator tn neutron distributions for pilessof specific sizes and shapes. In other reports we have used Δ to indicate the differential operator. (Editors' note).

The intensities observed at position 10 above the layer show relatively much larger variations. These are due primarily to the fact that the reproduction factor inside the layer and consequently of the exponential relaxation distance inside the layer are different from the same magnitudes in the surrounding oxide lattice: as the relaxation distance in the layer is longer than in the oxide, the intensity above the layer will be higher in the experiment with metal than it is in the control experiment No. 13 with oxide. If we indicate by b_0 the exponential relaxation distance for the control experiment No. 13, and with A the thickness of the metal bearing layer, with b_M the relaxation distance in the layer, and with I_0 and I_M the intensities in the oxide pile and in the metal bearing pile at some point above the layer, we have the following relation:

$$\log \frac{I_M}{I_0} = \frac{A}{b_0} - \frac{A}{b_1}.$$

The values of b given in column 8 are calculated with this formula. From the usual type of analysis of the data of Pile No. 13, we have used for b_0 the value

$$b_0 = 54.25 .$$

It should be noticed that these results are not quite free from ambiguity since the intensities measured at position 10 may be appreciably perturbed by transition effects especially in experiments 15, 16 and 17. For this reason the results for these three experiments are given as tentative. In column 9 we have calculated the values of the magnitude

$$\nabla^2 = \frac{2\pi^2}{a^2} - \frac{1}{b^2} .$$

It should be noticed that it is this magnitude (nabla^2) and not the reproduction factor that determines essentially the critical dimensions of a pile of the proposed structure. Indeed, the critical radius for a spherical shape is

$$R = \frac{\pi}{\nabla^2}$$

and in case of a cube, the critical side is

$$a = \frac{3\pi}{\nabla^2} .$$

We have also calculated the reproduction factor "k" for the various experiments. $k-1$ is given by the product of nabla^2 times the square of the migration length L^2 for which the values given in column 10 have been assumed. The values of the reproduction factor are given in column 11. For the discussion of this result we have also listed in column 12 the Cd ratio observed inside the metal layer in the various experiments.

The four experiments Nos. 14–17 in which Metal Hydrides metal has been used had as primary purpose the determination of the optimum cell side. Due to the rather limited amount of metal available, it proved impossible to carry out such a determination in a really conclusive way. Indeed, by examining the reproduction factor as listed in column 11 of the table, we would be led to the conclusion that the cell used in Experiments 15 and 16 was too large and that the optimum lies somewhere between the cell sides used in Experiments 14 and 17. It should be noticed, however, that the Cd ratio in Experiments 15 and 16 is far too high due to lack of metal so that it would appear that the reproduction factor for the large cell side ought to be taken appreciably larger than indicated by the measurement. On the other hand, in Experiment 17, where a small cell was used, the reproduction factor was somewhat closer to the optimum value than in Experiment 14 so that the increase in reproduction factor observed in this last case is probably unreal. It would appear that a cell side of 8″ as used in Experiment 14 is not far from the optimum. This conclusion, however, is given only tentatively and more work shall have to be done on this problem as soon as larger amounts of metal become available.

It is known that the Metal Hydrides metal contains a fairly large amount of dangerous impurities so that all the values of the reproduction factor are appreciably lower than with pure metal.

Experiments Nos. 19, 20 and 21 have been performed with Westinghouse metal and their primary purpose is to determine the reproduction factor to be expected by using a purer brand of uranium and also to determine the best amount of metal to be used with a cell of 8'' side. The values of the reproduction factor observed in these three experiments indicate an increase of the reproduction factor with the mass of the metal lump. Such an increase is in agreement with the estimates made by Wigner. Further experimentation with larger masses of the lump will be carried out as soon as more Westinghouse metal becomes available so that a slight increase of the best value of the reproduction factor observed in Experiment No. 21 may be expected. The value of the reproduction factor 1.035 found in this case could be increased probably by about 2.5 % by using pure graphite and by removing the air from the structure. Some small amount of impurity is still present in the Westinghouse metal accounting probably for a loss of about 0.5 % in the reproduction factor.

General features of the pile planned at Argonne Forest.

In view of the expectation that the final values of the reproduction factor obtainable with metal will fall somewhat lower than the previous estimates, the plans for the structure to be set up at Argonne Forest have been somewhat revised and it is planned at present to use all the materials that will be available and processed by about the end of November in the form of a spherical structure having a diameter of about 26 feet. All the metal that will be available to that date will be put in the central portion of the lattice in lumps of about 6 lbs. each. The outer portions of this sphere will consist of dead layers of graphite for a thickness of about 1 ft. The present estimates indicate that the size of this structure will probably be somewhat below the critical dimensions although it cannot be excluded that the critical dimensions may be reached already at this stage. If this should not be the case, more material shall have to be added before the critical dimensions are reached.

N° 176 and 177.

In the Metallurgical Project a considerable amount of effort went into the design of a suitable plant for the production of plutonium even before the chain reaction had been demonstrated experimentally. The principal problem was the choice of an adequate cooling system with sufficiently low neutron absorption. The most obvious choices were to cool hy gas, preferably helium, or by water. An ingenious proposal by Szilard was to use liquid hismuth, but this found few supporters because of the lack of engineering experience with this material. Other possibilities included circulating the uranium itself, either as liquid UF_6 or as oxide in a slurry. Once the coolant was chosen, it had to be demonstrated that the plant was practical and that it could be built in the short time allowed. To provide useful amounts of plutonium the plant (or plants) needed to dissipate some hundreds of megawatts of heat, carefully controlled, with a minimum of corrosion, with means for extracting and replacing the uranium, and with adequate safeguards against the dangerous effects of the radiations, including the effects on the chemical and mechanical properties of the materials used. These were mighty engineering problems, but somewhat outside the purview of even the best of engineers, who could hardly have heard of the neutron before they had been persuaded to join the Project. Nevertheless, an Engineering Group had been set up and given the directive to design a production plant. An able theoretical physicist, John Wheeler took up the task of guiding them. In due course the engineers T. V. Moore and M. Leverett submitted their design for a helium cooled plant. Fermi was asked to serve as chairman of the review committee which included the three physicists, Allison, Wigner and Szilard and an able engineer from the Du Pont Company, C. M. Cooper.

This was not a role of Fermi's liking. He did not like to sit in judgment of others and he did not like committees. He served on them mainly out of a sense of duty.

Fermi took these responsibilities seriously, however, and put his best efforts into them. He was an ideal man in an organization. He always did somewhat more than what could be considered his part and rarely made any demands on the others. His way of preparing for his role as reviewer was to try to work out his own solution to the problem. He considered several ways to cool the pile. Two of these are given in paper N° 176.

For Szilard, whose interest was in the liquid bismuth cooled plant, Fermi had a measurement on the neutron absorption of this substance carried out. The results were favorable, as he reported in a memorandum to Szilard (paper N° 177).

H. L. ANDERSON.

176.

METHODS OF COOLING CHAIN REACTING PILES

(CP) Memo 10 (October 5, 1942).

Memorandum to: S. K. ALLISON (October 5, 1942)
From: E. FERMI

I am collecting here some estimates concerning the heat transfer properties and the neutron properties of some possible types of chain reacting piles. Similar estimates for a different type of pile are being prepared at the same time by Mr. Wigner. Mr. Moore has undertaken a preliminary study

of the external equipment that should be provided in connection with the types of reacting units discussed here.

In the present memorandum two types of construction are discussed primarily. The first involves essentially a cooling of the graphite by means of a system of water pipes passing through it. The cooling of the uranium lumps is by conduction into the graphite. The second proposal discussed in this report follows a suggestion by Mr. Cooper to use the uranium metal in the form of shot. In this scheme, the uranium is disposed in cylindrical units located inside suitable channels through the graphite and cooled by a water pipe placed on the axis of each channel.

The properties of these two types of plant are discussed in Sections 1 and 2. A comparison of the relative advantages of the two methods and also of a plant with external cooling only is given in Section 3.

Section 1.

10^4 *kw Plant with Graphite Cooled by Water Pipes.*—The internal structure proposed for this plant is represented in fig. 1. The graphite is

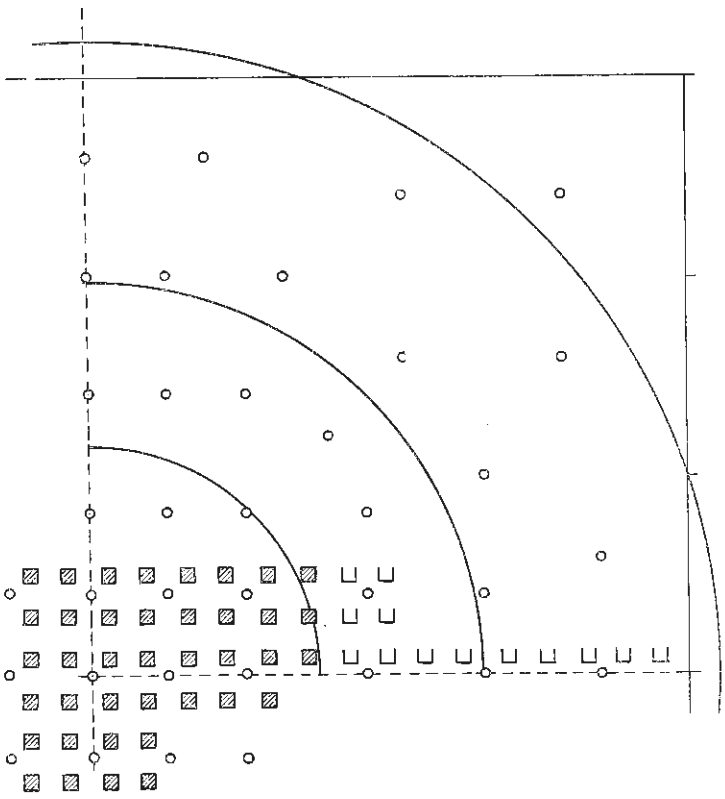

Fig. 1.

disposed in the form of a cube of about 6 meters side and the uranium metal is in the form of lumps of spherical or cylindrical shape disposed in a cubical lattice of 20 cm side. Such a geometry can be easily obtained starting with

graphite in the form of 4''1/4×4''1/4 bars as ordered. The graphite is cooled by a set of 97 pipes which could be disposed as indicated in fig. 1 with a greater concentration near the center of the pile where the heat development is larger. In the central portion, the pipes are disposed in a square pattern of 40 cm side. The density with which the pipes are distributed in the outlying portions of the pile decreases in such a way as to have approximately the same amount of energy dissipated in each pipe. Indeed, for a total energy production of 10,000 kw, the heat dissipated by each pipe is about 25,000 cal/sec. The heat dissipated per unit length of the pipe is, of course, greater near the center of the pile than at the ends. Near the center of the pile it amounts to about 65 cal/sec cm. Since the central portion of the pile is the one where the temperature rises are the greatest, all the following estimates refer to this position.

If we allow for a temperature rise of 25°C of the cooling water, the water flow in each pipe must be 1,000 cc/sec. The pressure of the water required to drive the water at this rate through the pipe is given by:

$$\text{Pressure} = \frac{8.5}{D^{24/5}} \text{ atmospheres}$$

where D is the internal diameter of the pipe. The pressure drop of the pipe calculated with the formula is 8.5 atmospheres for one cm internal diameter; 1.2 atmospheres for 1.5 cm diameter; and 0.3 atmospheres for 2 cm diameter. To this pressure drop, of course, the pressure drop in the water system outside of the pile should be added.

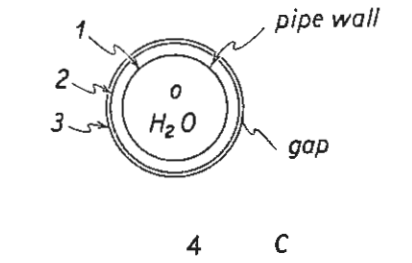

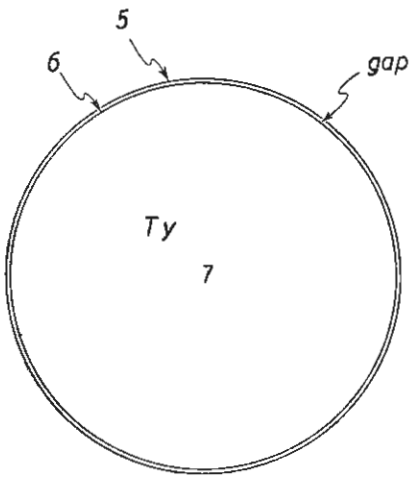

Fig. 2.

In fig. 2 a schematical presentation of the main thermal resistances inside the pile is given. The numbers from 0 to 7 indicate positions at which we have to know the temperature in the operating pile. The main heat resistances are:

0–1 Heat resistance inside the water pipe from the water to the internal surface of the pile. The temperature drop due to this heat resistance is 30°C for 1 cm internal diameter; 22°C for 1.5 cm; and 17°C for 2 cm.

1–2 The temperature drop across the thickness of the pipe wall is negligible in case of copper or aluminum pipes. For a lead pipe it amounts to about 20°C.

2–3 The heat resistance in the contact between the pipe and the graphite is very hard to estimate in a reliable way as it depends very closely on the clearance between the pipe and the graphite. For a 1.5 cm pipe in a helium atmosphere, the temperature drop is about 115°C × the clearance in thousandth's inch. It is seen that this temperature

drop may constitute a very serious objection to this method and requires an exceedingly accurate mechanical fitting of pipes, which could perhaps be achieved by using a pipe of elliptical section pressed against the graphite by an internal pressure as discussed by Newson.

3–4 The temperature drop from the surface of the graphite near the pipe to the bulk of the graphite may be calculated with the practical formula:

$$T_4 - T_3 = 5 \times \text{cal/cm}$$

and it amounts, therefore, to about 325°C.

4–5 The temperature drop from the bulk of the graphite to the surface of the graphite near the metal lump is 88°C by assuming a practical graphite conductivity of 0.1.

5–6 The heat resistance between the surfaces of the graphite and the lump depends again on the clearance and is given by about 25° × the clearance in thousandth's inch. The conduction byr adiation is a small fraction of the gas conduction at the temperature under consideration.

6–7 The temperature drop from the center of the metal lump to its surface is 86°C for lumps located near the center of the pile.

These data are summarized in Table I where the temperatures at the various places have been estimated for a production of 10,000 and of 5,000 kw. In estimating these temperatures, clearances of 0.002 inches have been assumed.

TABLE I.

	10^4 kw	5×10^3 kw
T_0 Water	40°C	40°C
T_1 Internal surface of pipe	62	51
T_2 External surface of pipe	82	61
T_3 Graphite near pipe	312	176
T_4 Bulk of graphite	637	339
T_5 Graphite near lump	725	383
T_6 Surface of lump	775	408
T_7 Center of lump	861	451

It appears from these figures that a pile of this construction could perhaps operate at 10,000 kw only if the clearances could be safely kept at a limit of 0.002 inches as indicated. It would probably be difficult to get out of the pile more than 5,000 kw without increasing the number of pipes.

The loss of reproduction factor in the proposed system is estimated for a pipe of 1.5 cm diameter, as follows:

Loss due to water	0.6 %
Loss due to material of pipe	0.1 % for lead pipes
	0.2 % for aluminum pipes
	3.9 % for copper pipes

It would seem that copper pipes, which certainly would be the best from the structural point of view, have to be excluded on account of the large loss of reproduction factor, whereas aluminum or lead pipes probably would be satisfactory.

Section 2.

Use of Metal in the Form of Shot.—Mr. Cooper has pointed out the advantage of using metal in the form of shot. The main advantage is the ease with which the metal could be removed if this plan should be adopted. The main drawback of the use of shot, besides its relatively low density compared with that of the metal, is the fact that internal conduction of the shot is considerably lower than that of the compact metal. For this reason, it would appear difficult to use shot in a pile for very high energy production. It is not impossible, however, that shot may be used in piles with power outputs of a few thousand kw.

In the absence of experimental evidence on the subject, I have tried to estimate what would be the heat conduction of shot embedded in helium. My estimate gives a conduction coefficient of 0.003 (cal, cm, °C). Mr. Cooper has also made an estimate of the same magnitude and found about twice as much. The following calculations are on the assumption of a conductivity of 0.003.

I have calculated a pile of the following internal structure—an equilateral triangular pattern of uranium rods with a side of 20 cm as suggested in the plans for the water cooled pile designed by Wigner's group. Each rod is located in a cylindrical hole in the graphite with a diameter of 3.5 cm. On the axis of this hole, there is an aluminum pipe of an external diameter of 1.05 cm, through which the cooling water is circulated. The uranium shot is dumped between the outer surface of the aluminum pipe and the internal cylindrical surface of the hole in the graphite. In fig. 3, a sketch of the cross section of one of such rods is given. The live part of the pile is a cylinder of 6 meters diameter, 5 meters long. The amount of metal used for these dimensions would be about 38,000 kg of metal disposed in 820 rods. The figures given in what follows are for a power of 10,000 kw. It will be found, however, that a pile of this construction may be able to operate only at a considerably lower power.

It is easily seen that by far the greatest heat resistance in a pile of this construction is across the uranium shot. On the assumption, that is only slightly pessimistic, that most of the energy is produced near the outer portions

of the uranium rod, one can calculate the temperature drop (δT) by the formula:

$$w = \frac{2\pi k \delta T}{\log \frac{r_2}{r_1}}$$

where w is the energy dissipated per cm of pipe length, k is the thermal conductivity of the uranium shot and r_2 and r_1 are the radii of the rod and of the cooling pipe. With this formula, assuming $k = 0.003$, one can calculate this temperature drop for an energy output of 10,000 kw and for the central portion of the pile. This temperature drop is 1500°C. Such a high temperature drop would evidently be too high. The pile would probably

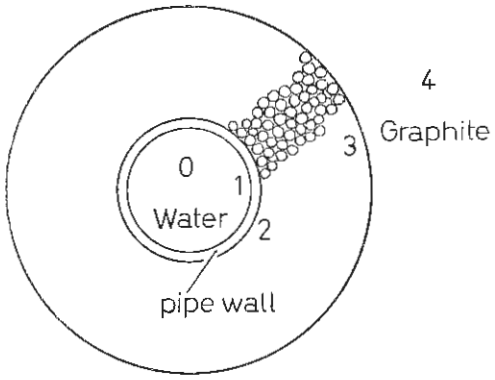

Fig. 3.

be run at about 3,000 kw, in which case the maximum temperature of the uranium would be between 500 and 600°C.

The reproduction factor loss in this pile is somewhat greater than in the one previously discussed on account of the greater number of pipes that is necessary. The loss due to the water and aluminum of the pipes may be estimated as about 1.3 %. Some additional loss would be due to the fact of using rods instead of lumps and to the lower density of the shot compared with the compact metal. It would seem probable that the total loss would be between 1 and 2 1/2 %.

Section 3.

Conclusions.

I. *Cooling of Graphite by Water Pipes.*

Advantages:

1. Neutron properties very similar to those adopted so far.

2. Small number of cooling pipes and consequently small loss in reproduction factor.

3. Mechanism for taking apart the structure not too dissimilar to what has been already planned for a pile with external cooling only.

Disadvantages:

1. Necessity of exceedingly small clearances between the graphite and the pipes and the lumps. To keep such low clearances would be particularly difficult in view of the thermal distortions in the operating pile.

2. Difficulty of taking apart the structure after end of the operation. In addition to the difficulties already considered for taking apart a pile with external cooling only, additional facilities should be provided for cutting the pipes.

II. *Shot Method.*

Advantages:

1. Very convenient method for removing the uranium after end of the operation in a form that makes it directly suitable for further chemical handling.

2. Simple mechanical construction. No necessity of great accuracy in the machining of the mechanical parts and only minor risks involved in possible breakage due to thermal distortions.

Disadvantages:

1. A fairly large loss in the reproduction factor. It is hard to estimate how serious such a loss may be before we know what loss of reproduction factor is allowable.

2. Necessity of developing a technique for the production of uranium shot.

In view of the difficulties connected with both schemes, it appears worthwhile to consider also the possibility of going back to the scheme for the cooling of the external surface only. Such a method would, of course, allow an energy output of about one tenth of that expected with the previous methods, but would on the other hand involve less uncertainty as to the neutron operation.

N° 177.

For the introduction to this paper see N° 176.

177.

THE EFFECT OF BISMUTH ON THE REPRODUCTION FACTOR

Excerpt from Report CA–320, Bulletin for Week Ending October 31, 1942.

(Letter)

To: L. SZILARD October 31, 1942.
From: E. FERMI

Two exponential experiments, No. 25 and No. 26, have been performed recently in order to determine what reduction in the reproduction factor is found when large amounts of bismuth are introduced in a carbon-uranium pile. In the exponential experiment No. 25 the amount of bismuth introduced was about equal to the amount of uranium present. Experiment No. 26 was in all respects similar to experiment No. 25 except that the bismuth had been removed. The comparison of these two experiments indicated that the reproduction factor with bismuth was slightly lower than the one without bismuth. The difference of reproduction factor calculated from the experimental data was about 0.009.

It should be noticed that a certain amount of asymmetry had to be introduced in the cell to accomodate the bismuth. The diffusion coefficient of the neutrons in the vertical direction is consequently slightly different from the diffusion coefficient in a horizontal direction. This produces a slight error in the exponential method of calculating the reproduction factor, which would be rather hard to calculate but may be estimated to be probably a relatively small fraction of the observed difference.

Assuming for bismuth a cross section of 0.016×10^{-24} as measured by Wilkinson and Levinger, one would calculate for bismuth a danger coefficient of about 0.0035 and, consequently, a loss of reproduction factor of 0.0035. Taking into account the effect of asymmetry previously mentioned, it appears that the actual danger coefficient is about twice as large as the calculated value.

The amount of bismuth that would be needed in a bismuth cooled plant is appreciably less than the amount of bismuth used in the present experiment. It appears likely that 1/3 of the amount that has been used could be adequate for cooling purposes. Consequently, the loss of reproduction factor would be only 0.2 or 0.3 %.

cc to: A. H. COMPTON
W. H. ZINN
S. K. ALLISON
E. P. WIGNER
C. COOPER
T. W. MOORE

N° 178.

By November the rate of arrival of materials had mounted sufficiently so that it became apparent that there would be enough for the chain reaction by the end of the month. A strike of labor unions, however, had held up the preparation of the building at the Argonne Forest site, originally scheduled for completion on October 20. Fermi went to Compton with the proposal that the chain reactor be built in the West Stands of the stadium on the University campus instead. The inherent danger associated with the possible release of a large amount of radioactivity in the middle of a large city in case something went wrong, made this a difficult suggestion to accept. In war, brave men, even those who feel their responsibility keenly, take risks. Compton told Fermi to go ahead, nor was his order rescinded by General Groves when he was told. The final decision to build the pile in the West Stands was made on November 14. Report CP–341, of which this paper is an excerpt, was issued also as A–368.

H. L. ANDERSON.

178.

THE EXPERIMENTAL CHAIN REACTING PILE AND REPRODUCTION FACTOR IN SOME EXPONENTIAL PILES

Excerpt from Report CP–341 for Month Ending November 15, 1942.

ORGANIZATION OF THE EXPERIMENT FOR THE PRODUCTION OF A CHAIN REACTION.

In the past month, as in the previous month, most of the attention of the Physics division has been devoted to the organization of the experimental production of a chain reaction. It had been planned originally to perform the experiment at the new laboratory at the Argonne Forest. A considerable delay in the date of delivery of the building has made it necessary to change this plan and to organize the experiment in the large handball court in the West Stands. It will be impossible to operate the pile in the West Stands at more than a nominal power. It is hoped, however, to be able to achieve most of the results expected from this experiment in the West Stands. In case that it should be desirable to operate the pile at a somewhat higher energy, the structure should have to be transported to the Argonne laboratory that will be completed in the meanwhile.

The details of the present state of the work on this experiment are given in the report of Zinn and Anderson and in that of Wilson.

Exponential experiments in the past month.

In the past month, seven exponential experiments have been completed, (Nos. 22–28). The structural details of these exponential piles are given in the report of Zinn and Anderson. The interpretation of the experiments shall be given here.

Exponential Experiments with Metal.—Experiments 22 and 23 are a continuation of the series of Experiments 19, 20 and 21, already discussed in the last monthly report. Their purpose is to determine the reproduction factor, using a variable amount of Westinghouse metal imbedded in a U. S. graphite lattice of 8'' cell side. In Experiment 22, a sandwich geometry, as described in Experiments 19, 20 and 21 discussed in the last monthly report, was used. Each lump consisted of an aggregate of nine Westinghouse metal cubes of a total weight of 2727 gm. The metal-bearing sandwich consisted of four lattice layers. In Experiment 23, the geometry was similar, except for the fact that each lump consisted of 12 cubes of a total weight of 3636 gm and the sandwich had three instead of four lattice layers.

Table I is similar to Table I of the monthly report CP-297 (of which No. 175 is a part) and summarizes the essential data derived from these two experiments. For convenience, the corresponding data of Experiments 19, 20 and 21 are collected in the same table.

Table I.

Experiments 22 and 23.

Exp. No.	No. of Layers	Mass of Lump (gm)	Pos. 4	Pos. 10	b	$10^6 \nabla^2$ (*) (cm^{-2})	L^2	k	Cd-ratio
20	4	1818	31026	3520	56.26	27	707	1.019	7.00
19	4	2121	31219	3644	57.68	42	677	1.028	6.53
21	4	2424	31436	3737	58.72	53	660	1.035	6.26
22	4	2727	31622	3863	59.47	60	647	1.039	6.06
23	3	3636	31546	3765	60.02	65	597	1.039	5.27

From an inspection of the data of Column 9, giving the reproduction factor k for the various lattices, it appears that the mass of metal lump for which the reproduction factor has the highest value is intermediate between 2727 gm and 3636 gm, the best reproduction factor being probably close to 1.04. An improvement of 3 % in the reproduction factor may be expected

(*) See Editors' note. Paper N° 175.

by using AGOT(*) graphite instead of U. S.(*) graphite and removing the atmospheric nitrogen. It appears, therefore, that a metal graphite lattice will give a reproduction factor of about 1.07.

Exponential Experiments with AGOT Graphite.—The tests on the diffusion lengths on the various brands of graphite have indicated that the absorption of the AGOT graphite is considerably lower than that of all other brands of graphite received so far. The mean of the values for the absorption cross sections in the AGOT samples examined so far, is 5.0×10^{-27}; whereas for the Speer graphite, a mean value of 5.45×10^{-27} has been found. The AGOT graphite has also a higher density than the Speer graphite, 1.62 instead of 1.54.

TABLE II.

Experiment 27.

Pos.	Average Intensity	Naturals	Net Intensity	Correction Factor	Corrected Intensities	Log I	Least Square Value $5.10980-0.14135\,n$
4	34261	84	34177	1.0283	35144	4.5458	4.5444
6	18158	91	18067	1.0064	18183	4.2596	4.2617
10	4881	80	4801	1.0368	4977.7	3.6970	3.6963

TABLE III.

Experiment 24.

							$5.14665-0.16522\,n$
5	20853	62	20791	1.0082	20961	4.5214	4.3206
7	9746	61	9685	1.0054	9718	3.9876	3.9901
9	4554	—	4497	1.0095	4540	3.6571	3.6597
11	2104	55	2049	1.0441	2139.4	3.3301	3.3292

It was expected, therefore, that the reproduction factor in a lattice with uranium oxide and AGOT graphite would be higher than in a lattice of similar composition with Speer graphite. Exponential Experiment 27 was performed in order to test this conclusion. The exponential Pile 27 is identical to exponential Pile 18 (already described in Report CP–297), the only difference being that AGOT graphite was used in 27 instead of Speer graphite as used in 18. The fundamental data on Exponential Experiment 27

(*) This is the name of a particular brand of graphite. (Editors' note).

are summarized in Table II. From these data, we calculate, as in the case of Pile 18, an exponential relaxation distance

$$b = 64.522$$

and

$$\frac{1}{c^2} = \frac{2\pi^2}{a^2} - \frac{1}{b^2} = 58.9 \times 10^{-6} \text{ cm}^{-2}$$

corresponding to a value of

$$c = 130 \text{ cm.}$$

The density of the graphite used in Pile 27 was about 1.62. From this density and from the Cd–ratio 6.66 observed in this pile, we calculate

$$L^2 = 666 \text{ cm}^2$$

and the reproduction factor

$$k = 1.039.$$

The increase in reproduction factor, with respect to Pile 18, is 0.7 %. A further advantage in using AGOT graphite instead of Speer is due to the fact that, owing to the high density, the migration length is smaller, and consequently, also the critical dimensions are somewhat smaller.

Pile 28 is entirely similar to Pile 27, except that it was set up in one of the small handball courts in the West Stands, since the large handball court had to be completely cleared when the construction of the chain reacting pile was started. Pile 28 gave results entirely similar to Pile 27 and shall be used for sandwich experiments with metal.

Tests on the Effect of Paraffin Cores.—At the request of Mr. Wigner, exponential Pile 24 was set up in order to test the effect on the reproduction factor of introducing a paraffin core on the axis of a cylindrical lump in a uranium graphite lattice.

The purpose of the experiment was to obtain some information to be used in estimating the loss of reproduction factor in a water cooled plant, in which water runs through a uranium pipe. Pile 24 had the usual U. S. graphite lattice with a 8″ side cubic cell. The lumps were UO_2 lumps of pressed Mallinckrodt oxide. A cylindrical hole of about 2 cm diameter was bored through the lump and was filled with a paraffin cylinder having the weight of 21.2 gm. The weight of the uranium oxide in the lump was 1930 gm. Except for the presence of the paraffin cores, Pile 24 had the same structure as Pile 10, already described.

In Table III, the data on the observed density and on the correction factor used are given. From these data, we calculate in the usual way the relaxation distance

$$b = 53.41 \text{ cm}$$

$$\frac{1}{c^2} = \frac{2\pi^2}{a^2} - \frac{1}{b^2} = -10 \times 10^{-6} \text{ cm}^{-2}.$$

From this value, one can obtain the reproduction factor of about 0.994.

The decrease in reproduction factor with respect to Experiment 10, is 1.9 %.

Part of this loss of reproduction factor is due, however, to the fact that the amount of uranium used in Experiment 24 is rather low. This is partly due to the fact that in boring the oxide lumps, the amount of uranium is actually decreased, and also to the fact that the presence of paraffin increases the slowing down power of the cell. A discussion of the influence of these factors has been given by Christy in Report CA–329 in which he finds that, in the present experiment, the danger coefficient of paraffin is 1.0.

The Influence of Bismuth on the Reproduction Factor.—At the request of Mr. Szilard, two exponential experiments, 25 and 26, were performed, with the purpose of determining the loss of reproduction factor to be expected in a Bi cooled plant. The two exponential Piles, 25 and 26, described in detail in the report of Zinn and Anderson, are identical in all respects, except that a Bi cylinder of the weight of 1527 gm was used near each U_3O_8 lump in the case of Experiment 25 and was removed in Experiment 26.

TABLE IV.

Experiment 25.

Pos.	Net Intensity	Correction Factor	Corrected Intensity	Log I	Least Square Value 5.13154-0.16487 n
4	29035	1.0187	29578	4.4710	4.4721
6	13867	1.0043	13927	4.1439	4.1423
10	2972	1.0215	3036	3.4823	3.4828

TABLE V.

Experiment 26.

					5.12333-0.16179 n
4	29378		29927	4.4761	4.4762
6	14153		14214	4.1527	4.1526
10	3134.6		3202	3.5054	3.5054

Tables IV and V summarize the results for the two Experiments, 25 and 26.

For Experiment 25, we calculate from these data,

$$b = 53.526 \text{ cm}$$

and

$$\frac{1}{c^2} = \frac{2\pi^2}{a^2} - \frac{1}{b^2} = -8.4 \times 10^{-6} \text{ cm}^{-2}$$

corresponding to a reproduction factor of about

$$k = 0.994$$

and for Experiment 26, we calculate

$$b = 54.545$$

and

$$\frac{1}{c^2} = \frac{2\pi^2}{a^2} - \frac{1}{b^2} = 4.5 \times 10^{-6}\ \mathrm{cm}^{-2}$$

corresponding to a reproduction factor

$$k = 1.003\,.$$

The reduction of reproduction factor due to the Bi is 0.009.

In the two Experiments, 25 and 26, the structure of the lattice had no complete symmetry due to the necessity of leaving space in which to put the Bi cylinders. One can estimate that this asymmetry may account for a difference of about 0.002 in the observed reproduction factor. The difference actually due to Bi is, therefore, only 0.007.

Since the amount of Bi was equal to the amount of uranium in the lump, 0.007 is the danger coefficient of Bi. This value is somewhat higher than the one that one would calculate out of the cross section of Bi as measured by Wilkinson and Levinger. This difference may be due, in part to experimental error, in part to some added absorption due to resonance in Bi, and in part to small amounts of impurities in the Bi.

N° 179.

In the fall of 1942 the Manhattan District selected a site for the construction of large piles for the production of plutonium at Hanford, Washington. On November 18, E. I. du Pont de Nemours and Company expressed their willingness to construct and operate the production plant at Hanford. The Metallurgical Laboratory was asked to prepare a series of reports which summarized the status of the project in terms which would be understandable to the du Pont management. Fermi wrote the section on Feasibility of a Chain Reaction, and Wigner, with a little help from me, wrote General Considerations Concerning the Lattice Structure. The whole report was completed within a few days. It consisted of three reports, of which only CP–383 (paper N° 179) was written by Fermi and is reproduced here. It is a model of clarity and economy, and shows Fermi's skill at simplifying complicated situations.

A. M. WEINBERG.

179.

FEASIBILITY OF A CHAIN REACTION

Report CP–383 (November 26, 1942).

Will the reaction be self-sustaining?

Since the early discussions on the possibilities to produce a chain reaction by making use of the neutrons emitted in the fission of uranium, it appeared that two essential factors determine whether the reaction will or will not be self-sustaining.

(a) One of them is the so-called reproduction factor k. This is defined as the average number of neutrons that are produced in one generation per neutron absorbed in a system of infinite large dimensions. It is clear that a system of sufficiently large size will be chain-reacting provided its reproduction factor is greater than 1. If the reproduction factor is less than 1, it is not possible to produce a chain-reaction by an increase of the dimensions.

(b) If the neutrons are generated in a system of finite size, some of the neutrons are lost by diffusion outside of the reacting mass. We express this factor in terms of a coefficient of retention l defined as the probability that a neutron produced inside the mass will not leak out.

It is clear that the leakage factor will increase with increasing dimensions of the system and will approach 1 when the dimensions become infinitely large. For a system of spherical shape the leakage factor is given approximately by the formula $l = \frac{1}{1 + \frac{A}{R^2}}$ where R is the radius and A is a constant.

For a uranium-graphite system A is of the order of 7000 cm^2.

The condition for the production of a self-sustaining chain reaction is that the total number of neutrons does not change. This is the case when the product of a reproduction factor and diffusion factor is equal to 1, i.e.:

$$kl = 1.$$

If kl is less than 1, the number of neutrons present in the system will gradually decrease. If kl is greater than 1, the number of neutrons present in the system will increase exponentially.

If the reproduction factor is larger than 1 by only a very small amount, the size of a chain-reacting system shall have to be very large so as to keep the loss of neutrons due to leakage very small.

If the reacting system has a spherical shape, one can find immediately from the two preceding formulas that the critical radius is given approximately by the expression $R = \sqrt{\frac{A}{k-1}}$.

* * *

It follows from the preceding discussion that one of the primary tasks for the experimental production of a chain-reaction is to develop methods for measuring the reproduction factor k for various arrangements.

In the early stages of the investigation attempts were made to obtain the value of k out of a detailed analysis of the processes by which neutrons are absorbed and reproduced. It was recognized, however, that this method could not reach the required accuracy due to the practical impossibility to measure with a high degree of precision the numerous constants involved in the process. Indeed the individual errors involved in each measurement sum up to a very large uncertainty in the final result. Even now after several years of work on the problem it would be difficult to obtain the reproduction factor by this method with an error less than ten or twenty percent. These early investigations indicated that for systems of graphite and uranium, the reproduction factor would be close to 1. However, it was not possible to decide in this way whether it would be above or below 1.

As soon as large amounts of graphite and uranium became available, new and better methods could be applied for the determination of the reproduction factor. This constant is now determined directly as result of a single measurement which can be performed with a very great precision. A column with a square cross-section and with the proper mixture of uranium and graphite is built. A radium-beryllium source of neutrons is placed at the bottom of this column. The density of neutrons is then measured at various heights along the axis of the column. It is found that except for some perturbations near the end of the column the intensity decreases exponentially as we move away from the source. The slope of the exponential function is directly related to the reproduction factor.

The limits of accuracy of the method may be estimated from the fact that values for the reproduction factor obtained in the same system in

different measurements usually differ by only a small fraction of 1 percent. This was found to be the case also in an experiment specially designed in order to test the reliability of the methods used for determining k. The reproduction factor was measured for two lattices of oxide and graphite identical both as to materials and as to lattice constants. The total amount of material used, however, was in one case twice that used in the other case. A difference of only 0.2 percent, well within the limits of the experimental error was found in the two experiments.

Since the summer of 1941 a large number of measurements of reproduction factors have been performed for systems of graphite and uranium oxide in order to determine experimentally the optimum arrangement. These investigations have stressed the importance of using materials of an exceedingly high purity since losses of several percent in the reproduction factor may be due to the absorption of neutrons in exceedingly small amounts of certain elements, particularly boron and several rare earth elements that may be present as impurities.

The best value of the reproduction factor that has been obtained using uranium oxide and graphite is about 1.04. If uranium is used in the metallic form the reproduction factor may be as high as 1.07.

It appears, therefore, that the question whether or not it is possible to produce a self-sustaining chain-reaction must be answered in the affirmative. It has been indicated that the measurements of the reproduction factor are affected with errors of a small fraction of 1 percent; consequently, even if we assume the actual error to be 1 or 2 percent, the measured values of the reproduction factor are so much above 1 as to make it appear exceedingly unlikely that the true value should be less than 1.

While the conclusion that suitable systems of uranium and graphite become chain-reacting provided their dimensions are sufficiently large, seems to be very well established experimentally, there is still some uncertainty as to the precise amount of materials required for a chain-reacting system. Indeed, in the case of uranium oxide and graphite, an error of 1 percent in the value of the reproduction factor would involve an error of about 40 percent in the estimate of the amount of materials required. For a metal-graphite system, the error involved would be about 15 percent.

Will the reaction be thermally stable?

From the practical point of view of planning and constructing chain reacting units in which large amounts of energy can be released, it is important to know the effect of changes of temperature on the reactivity of the system. If the reactivity increases with increasing temperature, the system would be thermally unstable because an accidental rise of the temperature would increase the development of energy and consequently determine a further rise of temperature. If, instead, the reactivity decreases with increasing temperature, the system is thermally stable.

A theoretical discussion of the problems of thermal stability seems to indicate that probably most chain-reacting systems will be thermally stable.

Since some of the assumptions made in these theoretical estimates may possibly be insufficiently accurate, it was thought desirable to obtain in addition some more direct experimental evidence, and several attempts have been made to determine the reproduction factor for systems heated artificially. The result of these experiments gave actually some indication that the reactivity of the systems under investigation probably decreases with increasing temperature. The effects observed were, however, so small as to be of the same order of magnitude as the experimental error.

We conclude, therefore, that the question whether chain-reacting systems with uranium and graphite are or are not thermally stable is still undecided although it appears probable that the systems will be thermally stable. If this shall prove to be the case, there will be a natural limitation to the operation temperature for a pile of a given size independent of any controlling device and determined essentially by the size. Controlling mechanisms would be needed in this case only for starting and for interrupting the reaction.

Will the reaction be controllable?

Since it is by no means certain that chain-reacting systems will be thermally stable, it is very important to develop methods for the control of the reaction capable of keeping the system operating at any required level of energy production. Most of the controlling devices that have been considered so far involve the use of substances having a strong neutron absorption that should be introduced inside the pile so as to reduce the number of neutrons available for the reaction. Such substances may be in the form of solid rods that can be pushed mechanically in suitable slots in the pile. Or they may be liquids that can fill up to a controlled level one or more pipes passing inside the pile. Or they may be gases which could be introduced at a variable pressure and would fill the empty spaces in the graphite conglomerate. Of these various possibilities, the only one that has been developed to a considerable extent is the use of solid rods.

The essential requirements of a controlling mechanism are:

(a) that it should be prompt enough in its response to a change of conditions so as to keep the reaction at a steady level in case that external perturbations should operate in the sense to offset its balance;

(b) that the range of control should be sufficiently wide so as to make it possible to keep the reaction within bounds even in case of as large a perturbation of the equilibrium as can be conceivably expected;

(c) that its operation should be as independent as possible of mechanical failures.

The present evidence indicates that there should be no special difficulty in fulfilling the first requirement. Our experiments indicate that the time needed to produce a sizable change in the rate of energy production

in case of a change of the reproduction factor due to some external perturbation will be very long and probably in most cases of the order of several minutes or even of a few hours. This long relaxation time gives ample time for the controlling devices to operate so as to bring back the system to the original level of operation if it should deviate from it in either direction. The controlling mechanism probably will be operated automatically by an ionization chamber filled with BF_3 which measures the density of neutrons.

The indications are that also the second requirement will be achieved easily. One can estimate that a controlling rod having a diameter of about 4 inches will reduce the reproduction factor by an amount of the order of 1 percent if introduced in the pile near its center. It is at present planned to use several controlling rods in order to increase further their range of operation.

Some more development work appears indicated in order to improve the mechanical reliability of the controlling devices. This applies particularly to the control of chain-reacting piles designed for the production of large amonnts of energy. In such systems, both the pile and the controlling rods will have a fairly high temperature that may produce a warping of the rod or of the channel in which the rod is moving.

The controlling rods in a pile designed for high energy production should be artificially cooled. This is not expected, however, to involve serious difficulties since the amount of energy developed in the rod is relatively very small.

Besides the controlling rods, that have the primary function of keeping the reaction at the desired level, it appears desirable to have also a number of safety rods which should operate in case that the intensity should rise above specified limits due to a failure of a controlling mechanism. Such safety devices should be designed in such a way as to operate even in case of a serious warping of the structure. For piles designed for operation at high energy, it might be desirable not to rely for the safety mechanism on the rods only, but to have the possibility of flooding the system with a neutron absorbing liquid or gas which would be operated only in case that all other mechanisms should fail.

N° 180 and 181.

Actual assembly of the pile was undertaken only after the decision, on November 14, to build it under the West Stands. (See introduction to paper N° 178). But work for its construction had begun in October, under Zinn's andmy direction, and Fermi's general supervision. Graphite was then being delivered at a steady pace and it was our responsibility to see that the graphite bars were machined to size and holes were drilled in them where needed to accommodate the uranium lumps. Zinn organized two special crews, one of which machined the graphite. The other pressed the uranium oxide powder into pseudo spheres, in a large hydraulic press. Both crews managed to keep their work up at a rate equal to that of the deliveries. Thus, in our report for the month ending October 15, Zinn and I could state that 210 tons of graphite had been machined. A separate group under Volney C. Wilson was in charge of control and measuring devices.

On November 16 (a Monday), we opened the rubberized balloon cloth envelope and started erection of the pile inside it. We organized into two shifts. Zinn, who was in charge of the day shift, now drove the press crews hard and managed to have them produce enough material not only for the layers that the day shift added to the pile, but also for those that would be assembled by the night shift under me.

The frame supporting the pile was of wooden blocks, and additional machines were installed to cut them. As blocks were put in place, the shape and size of the next were figured and specifications sent to the carpenter's shop: there were no detailed plans or blue prints for the frame or pile. Each day we would report on the progress of the construction to Fermi, usually in his office in Eckhart Hall. There we would present our sketch of the layers that we had assembled and reach some agreement on what would be added during the following shifts. Since some of the graphite was of better quality than the rest, it was important to arrange its disposition carefully. Fermi spent a good deal of time calculating what would be the most effective location for the various grades of graphite in hand.

A particularly difficult point was where to put the uranium oxide and where the uranium metal. We knew that because of its higher reproduction factor the metal should be in the central part of the pile, but we had to decide at what layer to begin to install it. When the construction began, only a small amount of metal was available, and so the original plan was to install it at a point fairly near the actual center. By good fortune, a substantial delivery of uranium metal of high quality arrived from Spedding's group in Ames after the construction was well underway. The plan was changed immediately to capture the advantage that this could give.

Thus, while before starting to assemble the pile we had a well thought-out but rather general plan for it, the details were determined day by day, as the construction proceeded out of those meetings in Fermi's office. One important detail was the location of the cadmium control strips. These were needed to keep the pile from becoming too reactive, once it began to approach the critical size.

We wanted a number of control rods distributed widely in the structure. This meant that some had to be installed at a rather early stage. A quite simple design of control rod was developed, which could be made on the spot: cadmium sheet was nailed to a flat wood strip made to be inserted in a slot machined in the graphite layer for this purpose. The strips had to be inserted and removed by hand. Except when the reactivity of the pile was being measured, they were kept inside the pile and locked using a simple hasp and padlock, the only keys of which were kept by Zinn and myself. One special control rod was built by Zinn: it operated by gravity and was called " Zip ". It was to be pulled out before the pile went into operation and fastened with a rope. In case of an emergency the rope could be cut and Zip would fall in place inside the pile.

Once the fifteenth layer had been reached, we introduced the practice of measuring the neutron activity at a fixed position in the structure. We did this with a boron trifluoride

in case of a change of the reproduction factor due to some external perturbation will be very long and probably in most cases of the order of several minutes or even of a few hours. This long relaxation time gives ample time for the controlling devices to operate so as to bring back the system to the original level of operation if it should deviate from it in either direction. The controlling mechanism probably will be operated automatically by an ionization chamber filled with BF_3 which measures the density of neutrons.

The indications are that also the second requirement will be achieved easily. One can estimate that a controlling rod having a diameter of about 4 inches will reduce the reproduction factor by an amount of the order of 1 percent if introduced in the pile near its center. It is at present planned to use several controlling rods in order to increase further their range of operation.

Some more development work appears indicated in order to improve the mechanical reliability of the controlling devices. This applies particularly to the control of chain-reacting piles designed for the production of large amounts of energy. In such systems, both the pile and the controlling rods will have a fairly high temperature that may produce a warping of the rod or of the channel in which the rod is moving.

The controlling rods in a pile designed for high energy production should be artificially cooled. This is not expected, however, to involve serious difficulties since the amount of energy developed in the rod is relatively very small.

Besides the controlling rods, that have the primary function of keeping the reaction at the desired level, it appears desirable to have also a number of safety rods which should operate in case that the intensity should rise above specified limits due to a failure of a controlling mechanism. Such safety devices should be designed in such a way as to operate even in case of a serious warping of the structure. For piles designed for operation at high energy, it might be desirable not to rely for the safety mechanism on the rods only, but to have the possibility of flooding the system with a neutron absorbing liquid or gas which would be operated only in case that all other mechanisms should fail.

counter, at the end of each shift, when the construction quota had been filled. Each day the measurements were reported to Fermi, who was ready with his latest calculation of R^2 eff, the effective square radius of the structure. From a plot of R^2 eff/A, the approach to criticality could be followed. The actual curve is reproduced in fig. 2 of paper N° 181.

From this plot we could tell that the pile would be critical when the 57th layer was completed, on the night between December 1st and 2nd, during my shift. That night the construction proceeded as usual, with all cadmium covered wood in place. When the 57th layer was completed, I called a halt to the work, in accordance with the agreement we had reached in the meeting with Fermi that afternoon. All the cadmium rods but one were then removed and the neutron count taken following the standard procedure which had been followed on the previous days. It was clear from the count that once the only remaining cadmium rod was removed, the pile would go critical. I resisted great temptation to pull the final cadmium strip and be the first to make a pile chain react. However, Fermi had foreseen this temptation and extracted a promise from me to make the measurement, record the result, insert all cadmium rods, and lock them all in place. The next morning, December 2, I was on hand, bright and early, to tell Fermi that all was ready. He took charge then.

Fermi had prepared a routine for the approach to criticality. The last cadmium rod was pulled out step by step. At each step a measurement was made of the increase in the neutron activity, and Fermi checked the result with his prediction, based on the previous step. That day his little six-inch pocket slide rule was busy for this purpose. At each step he was able to improve his prediction for the following. The process converged rapidly, and he could make predictions with increased confidence of being accurate. So it was that when he arrived at the last step, Fermi was quite sure that criticality would be attained then. In fact, once the cadmium rod was pulled out entirely, the pile went critical, and the first self-sustaining chain reaction took place.

Only some forty persons * were present at the experiment, mostly the scientists who had done the work. But there was also C. H. Greenewalt of the du Pont Company, for his people had to be fully convinced that the predictions about the pile could be made in a reliable way, that piles would work and produce plutonium. This was necessary, because at that very time the du Pont Company was considering whether to agree with the request of the project and undertake the construction of piles for the production of plutonium.

* Editor's Note: Those present were:

H. M. AGNEW
S. K. ALLISON
H. L. ANDERSON
H. M. BARTON
T. BRILL
R. F. CHRISTY
A. H. COMPTON
E, FERMI
R. J. FOX
S. A. FOX
D. K. FROMAN
A. C. GRAVES
C. H, GREENEWALT
N. HILBERRY
D. L. HILL
W. H. HINCH
W. R. KANNE
P. G. KOONTZ
H. E KUBITSCHEK
H. V, LICHTENBERGER
L. W. MARSHALL
G. MILLER
G. MONK JR.
H. W. NEWSON
R. G. NOBLES
W. E. NYER
W. P. OVERBECK
H. J. PARSONS
G. S. PAWLICKI
L. SAYVETZ
L. SEREN
L. A. SLOTIN
F. H. SPEDDING
W. J. STURM
L. SZILARD
A. WATTENBERGER
R. J. WATTS
G. L. WEIL
E. P. WIGNER
M. H. WILKENING
V. C. WILSON
W. H. ZINN

The test was run for 28 minutes, at a maximum intensity corresponding to an energy production of one half watt (the intensity was kept low in order to minimize the production of radioactivity by the pile). Today this experiment is regarded as the beginning of the atomic age, but in his December monthly report Fermi wrote simply: "The chain reacting structure has been completed on December 2 and has been in operation since then in a satisfactory way."

For Fermi's own description of the work on the pile, both at Columbia University and at the Metallurgical Laboratory, see papers Nos. 223, and 269.

For his discussion of the theory of a pile see paper N° 225.

H. L. ANDERSON.

N° 181, Appendix II.

The appendix to this paper is credited to a group of authors that represents a roster of the Instrument Division of the Metallurgical Laboratory. In this way, it is representative of the new era in which major research projects may be carried out by organized groups of scientists. In this case, we have one group of scientists carrying out the basic nuclear chain reaction experiment and a second working on instrumentation and controls.

Fermi exhibited unique ability in coordinating this type of organized effort. His gift for clear explanation of basic principles and requirements made it possible for others to understand the needs and to direct their talents toward such contributions as they were best qualified to produce.

The nuclear reactor turned out to be an extraordinarily tractable device from the viewpoint of instrumentation and control. Its response to control is practically instantaneous but is in terms of a rate of change rather than an abrupt change in operating level. This is a situation that is inherently stable and safe. Fermi confidently anticipated this mild behavior and, when asked what he would do if he was proved to be wrong, he said, "I will walk away—leisurely."

W. P. OVERBECK.

180.

WORK CARRIED OUT BY THE PHYSICS DIVISION

Excerpt from Report CP–387 for Month Ending December 15, 1942.

EXPERIMENTAL PRODUCTION OF A CHAIN REACTION.

The activity of the Physics Division in the past month has been devoted primarily to the experimental production of a divergent chain reaction. The chain reacting structure has been completed on December 2 and has been in operation since then in a satisfactory way. A program of tests on the operating conditions of the chain reacting unit and of experiments for the investigation of the various radiations inside and outside the pile is in progress. The results will be reported as soon as possible.

Exponential experiments with metal.

An exponential experiment, No. 29, has been performed in order to determine the reproduction factor that can be obtained using six-pound lumps of metal from Metal Hydrides. The experiment described and discussed in detail in the report of Zinn and Anderson is of the sandwich type and gives a comparison between the reproduction factors obtained with metal and with dioxide. The difference in reproduction factor resulted 3 %. Since the reproduction factor previously obtained with the dioxide (Report CP–341) is about 1.04 the reproduction factor in a lattice of Metal and AGOT (*) graphite results 1.07.

Effective temperature of the thermal neutrons.

Some experiments have been carried out in order to investigate to what extent neutrons reach thermal equilibrium with graphite under various conditions. These experiments described in the report of Zinn and Anderson indicate that the " effective temperature " of the thermal neutrons in most cases and in particular in a chain reacting pile is only slightly higher than the actual temperature of the graphite.

(*) This is the name of a particular brand of graphite. (Editors' note).

N° 181.

For the introduction to this paper see N° 180.

181.

EXPERIMENTAL PRODUCTION OF A DIVERGENT CHAIN REACTION (*) (**)

Institute for Nuclear Studies, University of Chicago, Chicago 37, Illinois
(Received June 27, 1952).
«Am. J. of Phys.», *20*, 536–558 (1952).

Except for minor editorial revisions this paper is the reproduction of a report written for the Metallurgical Laboratory of the University of Chicago almost ten years ago, after the experimental production of a divergent chain reaction. This report has now been declassified and can be published.

The present first part of the report contains a general description of the first pile and of its operation. The details of the construction, preparation, and testing of the materials and of the instrumentation are given by the members of the groups responsible for the work in Appendices I and II.

The pile had approximately the shape of a flattened ellipsoid of graphite having 388–cm equatorial radius and 309–cm polar radius. The uranium was distributed through the graphite mass in lumps partly of metal and partly of oxide arranged in a cubic lattice array with about 21–cm cell side. The experimental procedure followed in approaching the critical dimensions and in the actual operation of the pile is described. The observed critical dimensions are compared with the expectation from the tests on the various components of the structure.

This report gives a description of the construction and operation of a chain reacting pile. The pile was constructed in the West Stands Laboratory during the months of October and November 1942 and was operated for the first time on December 2, 1942.

It will appear from its description that an experiment of this kind requires the collaboration of a large number of physicists.

The two groups of Zinn and Anderson took charge of the preparation of the materials and of the actual construction of the pile; the group of Wilson

(*) The «American Journal of Physics» is pleased to have the opportunity of publishing this paper on the tenth anniversary of the achievement of a nuclear chain reaction, December 2, 1942.

(**) This report is based on work carried out under the auspices of the Manhattan District, U.S. Corps of Engineers, at the Metallurgical Laboratory, The University of Chicago.

prepared the measuring equipment and the automatic controls. The details of this work are given by the members of the two groups in the appendices.

A large share of the credit for the experiment goes also to all the services of the Metallurgical Laboratory and in particular to the groups responsible for the development of the production and the testing of the materials. The exceptionally high purity requirements of graphite and uranium which were needed in very large amounts probably made the procurement of suitable materials the greatest single difficulty in all the development.

General description of the pile.

The pile consists essentially of a lattice of lumps, party of uranium metal and partly of uranium oxide imbedded in graphite. Except for a small fraction near the surface of the pile the lattice cell is a cube of 8.25 inches side.

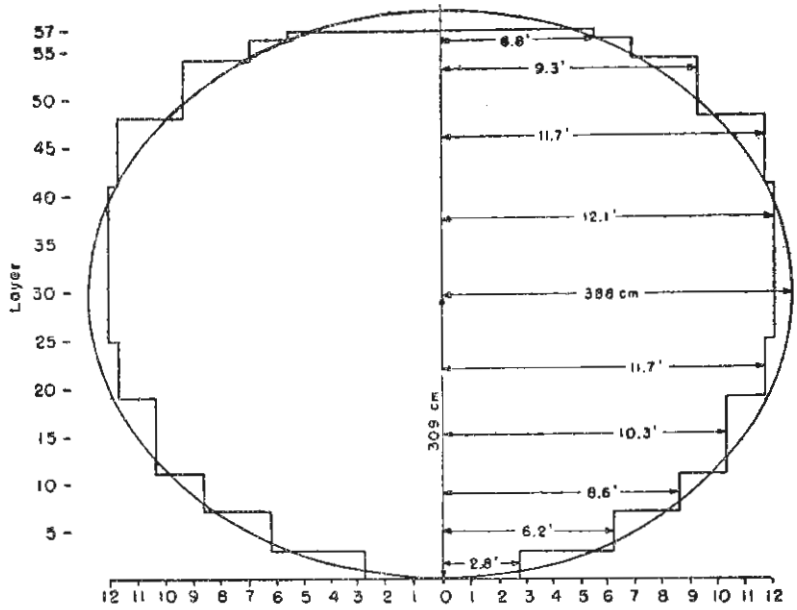

Fig. 1. – Vertical cross section of the pile, showing the equivalent ellipsoid.

Since only a relatively small amount of metal (about six tons) was available and since our graphite was of various brands of different purity it had been planned originally to construct the pile in an approximately spherical shape, putting the best materials as near as possihle to the center. It happened actually that the critical conditions were reached before the sphere was completed and construction was interrupted about one layer above the critical dimensions. For the same reason the top layers of the pile were made appreciably smaller than would correspond to the spherical shape originally planned. The present structure may be roughly described as a flattened rotational ellipsoid having the polar radius 309 cm and the equatorial radius 388 cm. (See fig. 1).

The graphite is supported on a wooden structure and rests on the floor on its lowest point.

The original plan foresaw the possibility that it might have been necessary to evacuate the structure in order to reach the critical conditions.. For this reason the pile was constructed inside a tent of rubberized balloon fabric that in case of need could have been sealed and evacuated.

Since the amount of metal available was only about 6 tons, the metal-bearing part of the lattice was designed for best utilization of the metal rather than for best reproduction factor. The metal lumps used weighed 6 pounds and consisted of metals of various origins (Westinghouse, Metal Hydrides, and Ames). An exponential experiment performed on the metal lattice had given for it a reproduction factor of 1.067 and $\nabla^2 = 101.7 \times 10^{-6}\ \mathrm{cm}^{-2}$. [1] The use of heavier metal lumps of seven or eight pounds would have given a better reproduction factor. Since, however, heavier metal lumps would have reduced the volume of the metal-bearing part of the lattice, it was deemed advisable to use lumps somewhat undersize.

The greatest part of the volume was occupied by a lattice having the same cell side of $8\frac{1}{4}$-inches with lumps of pressed UO_2 weighing about 2140 g. The reproduction factor for this lattice had been measured in a previous exponential experiment and had been found to be 1.039 with a $\nabla^2 = 59 \times 10^{-6}\ \mathrm{cm}^{-2}$.

Measurements performed during the construction.

A series of measurements was performed while the pile was being assembled in order to make sure that the critical dimensions could not be reached inadvertently without taking the proper precautions. These measurements had also the purpose of checking the neutron multiplication properties of the structure while it was being assembled so as to permit the determination of the critical point before actually reaching it.

The measurements were performed using two types of detectors. A BF_3 counter was inserted in a slot about 43 inches from the ground and its readings were taken at frequent intervals of time. In addition an indium foil was irradiated every night in a position as close as possible to the effective center of the structure and its induced activity was measured the following morning and compared with the readings of the BF_3 counter. For these measurements the natural neutrons spontaneously emitted by uranium are a perfectly adequate source and no other source of neutrons was added.

Typical results of these measurements are collected in Table I. The first column indicates the height of the structure expressed in number of

(1) The neutron density n varies approximately according to the equation $\nabla^2 n = an$, where a is a constant depending on the physical and geometrical structure of the lattice. The value of a is called the Laplacian of the lattice and is denoted by ∇^2. Larger values of ∇^2 correspond to a better structure.

layers (each layer approximately $4\frac{1}{8}$-in.). The second column gives the intensity A expressed in counts per minute of a standard indium foil, induced by the natural neutrons when the foil is placed at a central place inside the structure where the neutron intensity is a maximum. Actually, the foils were placed as close as possible to the best position and a small correction was applied in order to account for the fact that the foil was not exactly at the optimal position.

TABLE I.

Measurements on the pile during construction.

Layer	A	R_{eff} (cm)	R^2_{eff}/A
15	42	128	390
19	78	158	320
23	119	187	294
25	148	200	270
29	221	225	229
33	345	248	178
36	470	265	149
41	350	288	98
45	1360	308	70
47	1940	317	52
51	4400	332	25
54	12400	344	9.5
57	divergent	356	—

In a spherical structure having the reproduction factor 1 for infinite dimensions the activation of a detector placed at the center due to the natural neutrons is proportional to the square of the radius. For an ellipsoid a similar property holds, the intensity at the center being proportional to the square of an effective radius R_{eff} given by the formula

$$\frac{3}{R^2_{eff}} = \frac{1}{a^2} + \frac{1}{b^2} + \frac{1}{c^2}\,, \tag{1}$$

where a, b, and c are the semi-axes of the ellipsoid. For the case of spherical sectors such as were the shapes of our structure at various stages of its construction, it clearly would be a major mathematical task to determine exactly R_{eff}. It proves, however, rather easy and not too arbitrary to determine graphically for any height of the spherical sector an equivalent flattened ellipsoid. (See fig. 1.) The effective radius can then be calculated with formula (1). The values listed in the third column of Table I are calculated in this way.

If the reproduction factor were 1 for our lattice the expression given in the fourth column of the table should be a constant. It is seen instead that the values listed in column four decrease steadily and converge to zero at about the 56th layer. This is the point where the critical conditions are attained and where the intensity due to the natural neutrons would become infinitely large. The values of R^2_{eff}/A are plotted in fig. 2. The critical layer is at the intersection of the curve with the x axis.

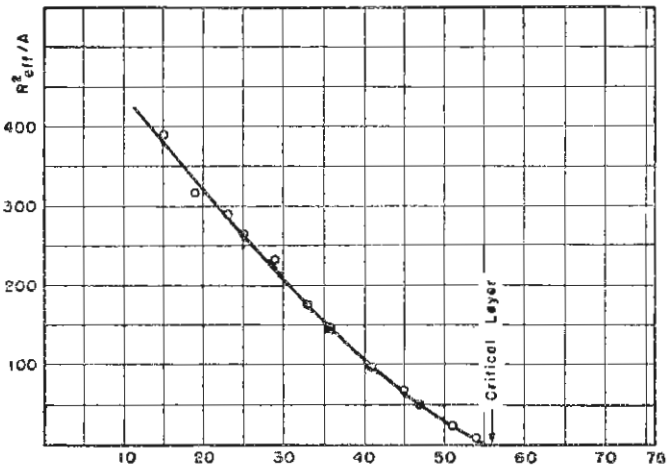

Fig. 2. – Plot showing the approach to the critical size during construction.

During the construction as a matter of precaution, appreciably before reaching this critical layer, some cadmium strips were inserted in suitable slots. They were removed once every day with the proper precautions in order to check the approach to the critical conditions. The actual construction was carried in this way to the 57th layer, about one layer beyond the critical dimensions. When all the cadmium is removed the effective reproduction factor of the structure is about 1.0006.

Measuring equipment and controls.

Any detector of neutrons or of γ–radiation can be used for measuring the intensity of the reaction. Neutron detectors are somewhat preferable since they give a more immediate response to the intensity of the reaction and are not affected by the radiations emitted by the fission products after shut-down of the reaction.

Actually used for determining the intensity of the reaction were several such neutron detectors, namely, two BF_3 proportional counters placed on the outside of the pile and several ionization chambers filled with BF_3 and placed near one of the walls of the pile. These chambers were connected to suitable amplifying systems, and the amplified current was used to operate recording instruments and the automatic controls and safety devices.

The controlling of the reaction was obtained by inserting in the pile some strips of neutron absorbing materials (cadmium and, in one case, boron steel).

When the pile is not in operation, several such cadmium strips are inserted in a number of slots so as to bring the effective reproduction factor considerably below 1. It was actually found that any one of the cadmium strips is alone sufficient to bring the pile below the critical conditions. Besides a number of cadmium strips that can be used for manual operation of the pile, the pile is provided also with two safety rods and one automatic control rod. The safety rods are normally out of the pile during operation. They are kept outside of the pile by a catch operated by a magnet and they are connected to a suitable system of weights so that they are drawn inside the pile by the weights if the catch is released. The magnets are energized by an amplifying system in such a way that they are automatically released if the intensity of the neutrons emitted by the pile rises above a specified limit.

The automatic control rod may be pushed inside and outside the pile by two electric motors and may be operated either by hand or by an amplifying system in such a way that the rod is pushed inside if the intensity of the reaction increases above the desired level, and is pulled outside if the intensity is below the desired level. The detailed description of the control and measuring devices is given in Appendix II.

Operation of the pile.

In order to operate the pile, all the cadmium strips except one are first taken out of the pile. The last rod is then slowly pulled out of the pile. As the critical conditions are approached, the intensity of the neutrons emitted by the pile begins to increase rapidly. It should be noticed, however, that when this last strip of cadmium is so far inside the pile that the effective reproduction factor is just below 1, it takes a rather long time for the intensity to reach the saturation value. In a similar way, if the cadmium strip is so far outside of the pile that the reproduction factor is greater than 1, the intensity rises at a rather slow rate. Indeed, for our pile, when all the cadmium is completely outside of the pile, the intensity rises approximately at the rate of a factor of 2 every minute. When the cadmium strip is close to the critical position, these relaxation times become exceedingly long. It has been found, for example, that for one of our controlling strips, the relaxation time is given by: 230 minutes/x, where x is the distance of the rod from the critical position expressed in cm. This means that if the rod is only 1 cm off the critical position, the relaxation time is about 4 hours. For the automatic control rod the corresponding constant is 180 minutes. These long relaxation times which are due to the existence of a small percentage of delayed neutrons emitted in the fission process make it rather easy to keep the pile operating at a constant level of intensity even without the use of automatic regulation. Indeed, to operate the pile at the desired level of intensity, one can usually proceed as follows.

First, the last strip of cadmium is pulled completely outside of the pile and the intensity as indicated by the various measuring devices begins to rise slowly. Since in these conditions, the relaxation time is about two minutes, the desired level of intensity is usually reached in a few minutes. As soon as the meters indicate that the desired level has been attained, the rod is pushed inside the pile to about the critical position. The measuring instruments indicate immediately a steadying of the intensity at about the desired level. In order to keep the level constant, it is sufficient to push the rod one or two cm in or out every once in a while so as to compensate for the small variations in the reproduction factor due primarily to changes of atmospheric pressure.

The diagram in fig. 3 was taken by the automatic intensity recorder during the first operation of the pile. The exponential rise of the intensity is clearly noticeable on the diagram. The intensity was permitted to increase up to a value corresponding to an energy production of about 1/2 watt. At this point, the automatic safety device operated, and the safety rods were pulled inside the pile and interrupted the reaction as evidenced on the diagram by the sudden drop in intensity.

A higher intensity test was made on December 12 when the pile was operated to an energy production of approximately 200 watts. The test was not run to a higher intensity on account of the limitations imposed by the necessity of keeping the radiation outside of the building well below the physiological tolerance dose. During the operation at high intensity which lasted about 45 minutes, some records of the intensity in various rooms inside the building and on the street outside were taken with standard R–meters and with BF_3 counters and indium foils to detect the neutron intensity. Typical values obtained in this survey are shown in Table II.

TABLE II.

Radiation survey in the vicinity of the pile.

	Milliroentgen per minute	Counts per minute of a standard indium foil at saturation
Near pile	50	8×10^6
Inside pile room far from pile	6	10^6
Corridors on side of pile room	2	2×10^5
Tower room	0.0005	negligible
Sidewalk of Ellis Street nearest to pile	0.05	6000
Sidewalk of Ellis Street farthest from pile	0.01	2700
Control	0.001	—

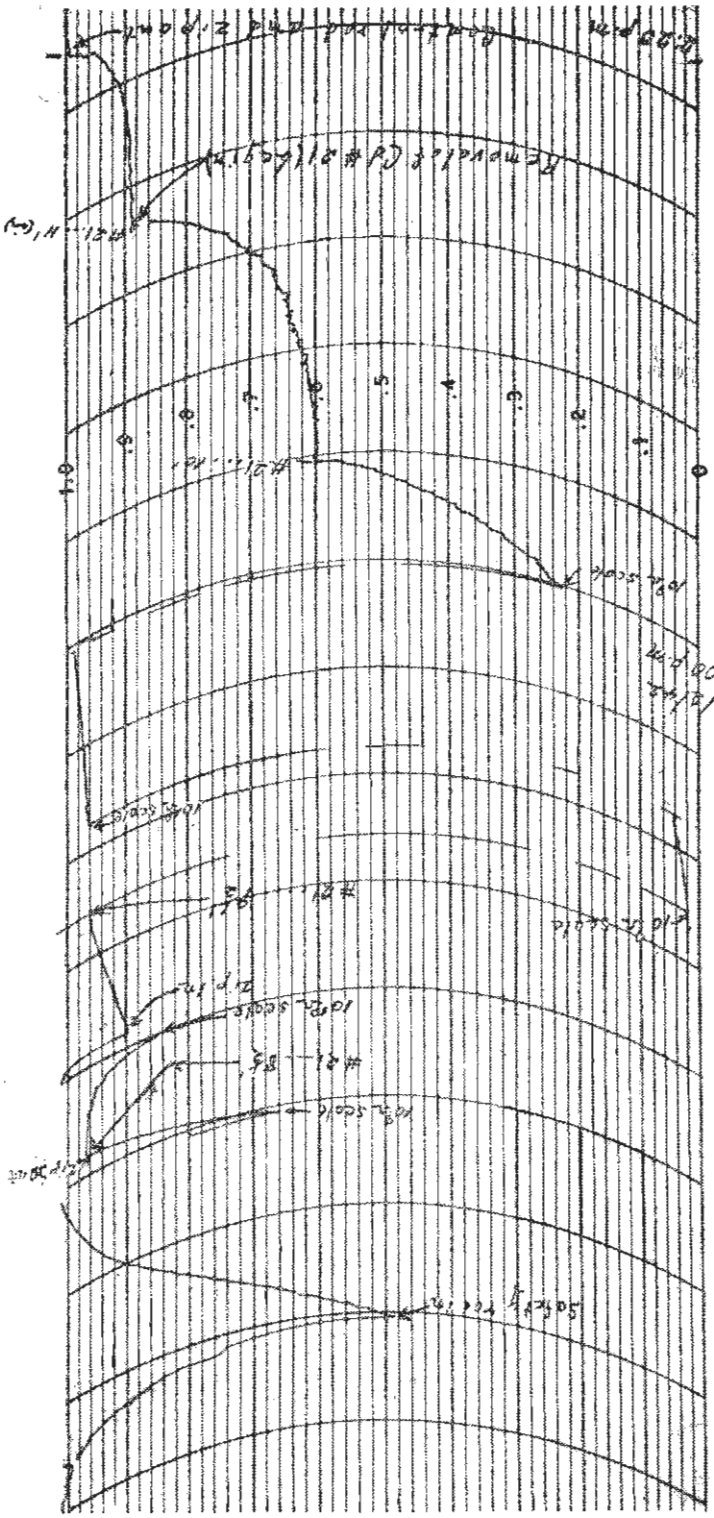

Fig. 3. – First operation of the pile. Automatic record of the reaction intensity.

COMPARISON OF EXPECTED AND OBSERVED CRITICAL DIMENSIONS.

In spite of the fact that the shape of the pile and its internal structure are far from regular, some conclusions may be obtained as to the actual reproduction factors of the various lattices used in the pile and their comparison with the reproduction factors expected from the results of exponential experiments.

We have already indicated (see fig. 1) that the outline of the structure is not far from that of a flattened rotation ellipsoid with a polar semi-axis of 309 cm and an equatorial semi-axis of 388 cm. Formula (1) gives then as effective radius of the structure,

$$R = 355 \text{ cm}.$$

This value of the radius corresponds to a ∇^2 of 78.3×10^{-6} cm^{-2} and to an average reproduction factor of about 1.054.

Since various lattices have been used at various places inside the structure, such values are only mean values for the various lattices used, and they can be compared with the individual values only if the statistical weight pertaining to each kind of lattice is known.

One can prove easily that the statistical weight of each component lattice is in first approximation proportional to its volume multiplied by the mean square density of neutrons over the volume occupied by the given lattice type. An attempt has been made to calculate in this way the statistical weight of the various lattices represented in our structure. The results of this calculation are given in Table III.

TABLE III.

Statistical weight of various lattices in the pile.

Type of lattice	Statistical weight	$\nabla^2 \times 10^6$ from exponential experiments
Metal	39.2 %	+ 102
AGOT Brown AGOT	53.5	+ 59
Speer	6.6	+ 45
U. S. Live	0.5	— 10
Dead	0.2	— 520
	Weighted average . .	73.4

The first column of the table gives the type of lattice. For the sake of simplicity, lattice types having presumably a rather similar reproduction factor have been grouped together under the denomination of Speer. The

second column gives the statistical weight of each kind of lattice expressed in percent. The third column gives the values of ∇^2 as obtained from exponential experiments. The weighted average of ∇^2 is 73.4 instead of the value of 78.3 as estimated from the critical dimensions.

This is an indication that the values of ∇^2 and of the reproduction factors as calculated from exponential experiments have been slightly underestimated, the correct values being probably about 0.003 or 0.004 higher than the published values.

Energy emitted by the pile.

The number of neutrons emitted by the pile, the number of fissions and the energy produced can be estimated in terms of the activity of standard indium foils placed inside the pile. The standardization of these indium foils has indicated that the following relationship exists between the resonance activity, A_{Res} expressed in counts/minute at saturation with the foil screened by cadmium, and the slowing down density of neutrons in graphite

$$q = 0.00156 \times A_{Res}. \tag{2}$$

The cadmium ratio in the greatest fraction of the volume of our structure is about 6.6; this means that if an activity of A counts/minute at saturation is recorded when the indium foil is not screened by cadmium, the activity with cadmium would be

$$A_{Res} = A/6.6$$

and consequently,

$$q = 0.00156 \times A/6.6 = 0.000236 \times A.$$

The total number of neutrons that are slowed down inside the pile from above to below indium resonance energy is given, therefore, by:

$$0.000236 \times \bar{A}V,$$

where $\bar{A}$ is the mean value of activity and V is the volume of the pile. We have assumed

$$V = 1.95 \times 10^8 \text{ cc.}$$

On the other hand, one can estimate that $\bar{A}$ is equal to about $0.3 \times$ the activity A_0 at the center of the pile. It follows that the total number of neutrons slowed down in the pile from above to below indium resonance is

$$1.4 \times 10^4 \times A_0.$$

The total number of neutrons produced in the pile is about 13 percent higher, since some of the fast neutrons produced are absorbed at resonance before reaching indium resonance energy and a small fraction escapes from the pile. The total number of neutrons produced is given, therefore, by

$$1.6 \times 10^4 \times A_0. \tag{3}$$

If we assume that 2.2 neutrons per fission are emitted, we obtain from this the number of fissions per second expressed by the formula

$$F = 7200\, A_0.$$

Assuming that the energy produced per fission is 200 Mev, equivalent to

3.2×10^{-4} erg, the power output of the pile is given by

$$2.3\ A_0\ \text{erg/sec} = 2.3 \times 10^{-7} \times A_0\ \text{watts}.$$

This formula has been used in the estimates of the power output already given.

APPENDIX I

CONSTRUCTION OF THE CHAIN REACTING PILE

H. L. ANDERSON, A. C. GRAVES, P. G. KOONTZ, L. SEREN, A. WATTENBERG, G. L. WEIL, and W. H. ZINN (*).

In the previous sections of this report some discussion of the general structural features of the chain-reacting pile is given. In this section the detailed plan of the graphite-uranium system is set forth, together with a brief description of the preparation and testing of the special materials. This work, which occupied a period of three months, required that very careful physical measurements be made on rather large quantities of material. Our indebtedness to the Research Assistants, H. Agnew, D. L. Hill, H. Lichtenberger, G. Miller, R. Nobles, W. Nyer, H. Kubitschek, L. Sayvetz, and W. Strum, upon whom the main burden for carrying out these measurements fell, is here acknowledged.

Two types of measurements on the materials with which it is proposed to build a chain reaction must be made. First, the reproduction factor for the particular graphite-uranium system being used must be determined and, secondly, reasonably large samples of the actual materials of construction must be checked in order to insure that the reproduction factor will not be lowered by the introduction of inferior batches of uranium or graphite. In this instance the problem was somewhat complicated by the fact that in the first chain reacting pile three different types of graphite-uranium systems had to be used.

(*) Present addresses: *

H. L. ANDERSON,
Institute for Nuclear Studies,
University of Chicago,
Chicago, Illinois.

A. C. GRAVES,
Los Alamos Scientific Laboratory,
P. O. Box 1663,
Los Alamos, New Mexico.

P. G. KOONTZ,
College of Wooster,
Wooster, Ohio.

LEO SEREN,
Betatron Section, Code 3116,
Nucleonics Division,
Naval Research Laboratory,
Washington, D. C.

ALBERT WATTENBERG,
Laboratory for Nuclear Science and Engineering,
Massachussets Institute of Technology,
Cambridge, Massachusetts.

G. L. WEIL, Consultant,
Suite 603,
1025 Connecticut Avenue, N. W.,
Washington 6, D. C.

W. H. ZINN,
Argonne National Laboratory,
P. O. Box 299,
Lemont, Illinois.

* On June 27th 1952 (Ed. Note).

Determination of the reproduction factor.

The exponential pile experiment is designed to determine the reproduction factor k of an infinite lattice of uranium lumps in graphite without the necessity of constructing piles of very large dimensions. From such pile experiments the optimum cell constants have been determined for pressed UO_2 (density = 6.1 g/cm^3) and cast uranium metal (density = 18 g/cm^3), together with the values of k associated with these optimum lattices in graphite of poorer quality than that available for the chain-reacting pile. For the purpose of designing the chain-reacting pile it was necessary to determine the value of k for the three components (cast uranium metal in AGOT graphite–pressed UO_2 in AGOT graphite-pressed UO_2 in Speer graphite) of its structure. The measurements and results of the exponential piles which were constructed to test these components will be given in this section.

Briefly, the theory of exponential pile measurements is as follows:

If one considers a uranium-graphite lattice structure of square cross section with side equal to a, and semi-infinite height, with a source of fast neutrons at the center of the base, then, at points sufficiently far removed from the source, the neutron intensity will be given by an equation of the form

$$n = \Sigma_{ij}\, B_{ij}\, e^{-x/b_{ij}} \cos\frac{i\pi y}{a} \cos\frac{j\pi z}{a}\,, \tag{1 a}$$

where the x axis is taken along the vertical axis of the pile, and the $x = 0$ plane coinciding with the base of the pile. Thus, for points on the axis, each harmonic of the neutron intensity decreases exponentially,

$$n = B_{ij} \exp(-x/b_{ij}), \tag{2 a}$$

with a relaxation distance equal to b_{ij}. At a sufficiently large distance from the source the first harmonic only is important. The relaxation length b (b_{11}) is related to the reproduction factor k through the following equation:

$$k = \left[1 - \frac{\lambda\Lambda}{3}\left(\frac{1}{b^2} - \frac{2\pi^2}{a^2}\right) \times \exp\left\{\frac{r_0^2}{4}\left(\frac{1}{b^2} - \frac{2\pi^2}{a^2}\right)\right\}\right], \tag{3 a}$$

where λ = mean free path of thermal neutrons in graphite, Λ = mean free path for absorption collision, and $r_0^2/4$ = the age of nascent thermal neutrons. The quantity

$$\left(\frac{1}{b^2} - \frac{2\pi^2}{a^2}\right) = \frac{1}{c^2}\,,$$

where c is the diffusion length. For the case that k is close to unity, c is very large and $1/c^2$ small so that one can write

$$k = \left[1 - \left(\frac{\lambda\Lambda}{3} + \frac{r_0^2}{4}\right)\left(\frac{1}{b^2} - \frac{2\pi^2}{a^2}\right)\right] \tag{4 a}$$

or

$$k = \left(1 - \frac{L^2}{c^2}\right), \quad \text{where } L^2 = \left(\frac{\lambda\Lambda}{3} + \frac{r_0^2}{4}\right). \tag{5 a}$$

Thus, if L, the migration length, is known, a measurement of the relaxation distance b, associated with the first harmonic of the neutron intensity, will

determine the reproduction factor corresponding to a lattice of infinite dimensions similar to the one being tested.

Because of the finite height (124 in.) of an actual exponential pile, two corrections must be applied to the neutron intensity measurements. First, a " harmonic correction " due to the presence of higher harmonics at points near the source; and second, an " end-correction " due to the proximity of the top of a pile to the measuring positions.

To determine the relaxation distance b, indium foils (0.0924 g/cm^2) are placed at positions along the axis of the pile, and the induced 54-minute activity measured on G–M counters. For these measurements the foil is held in a nickel holder; thus, the activation (A_{Ni}) is due to both thermal and indium resonance neutrons. (All measurements are corrected to give the activities that would be observed for infinite times of irradiation). The emission of neutrons by spontaneous fission of the uranium in the pile produces a " background " which must be subtracted from the intensity measurements. Finally, after making the harmonic and end corrections, one calculates b from the relation

$$b = \frac{D}{\log\left[(A_{Ni})_2/(A_{Ni})_1\right]}, \tag{6 a}$$

where D is the distance between the two positions at which (A_{Ni}) is measured.

The length of a side a to be used in calculating k from Eq. (4 a) must be that value for which the neutron intenisty actually becomes equal to zero. (Because of the finite length of the mean free path λ compared to the dimensions of the pile, the effective side is larger than the physical side.) From neutron intensity measurements near the edge of the pile one can estimate the effective value of a.

The migration length L (Eq. (5 a)) can be calculated from the graphite density and the cadmium ratio. The cadmium ratio $(A_{Ni})/(A_{Cd})$ is the ratio of the activity of a foil with nickel holder (A_{Ni}) and the activity (A_{Cd}) at the same position when the foil is covered with cadmium. Activation in the latter case is due only to indium resonance neutrons.

The three piles with which we are concerned had the following general features in common. A pile was constructed on a base (AGX graphite), 16 in. high, in the top layer of which a source channel was placed. Four (Ra+Be) fast neutron sources, each of approximately 0.5 g, were used, and these were divided into two closely equivalent 1 g sources. Each was placed in the channel at positions approximately halfway from the center to the edges of the pile. This arrangement, through cancellation of odd harmonics of the neutron intensity at points along the pile axis, considerably reduced the harmonic correction to be applied to the measurements. The lattice structure measured 99 in. $\times$ 99 in. $\times$ 123 $\frac{3}{4}$–in., and consisted of 15 layers $\left(\text{each } 4\ \frac{1}{8}\text{–in. high}\right)$ of graphite bearing uranium, alternating with 15 layers of solid graphite. Measuring slots extending to the center of the pile were inserted in horizontal sections corresponding to the even-numbered graphite layers.

In order to eliminate errors caused by slow neutrons being scattered back into the pile from the surroundings, the top and sides of the piles were covered with cadmium sheet.

In specifying the positions at which measurements were made, the following coordinate system and unit of length are used. The origin is taken at the center of the base of the lattice; the x coordinate along the pile axis, the y coordinate in the direction of the line joining the sources, and the z coordinate in the direction of the measuring slots. The fundamental lattice constant (also equal to the distance between two layers of the pile) is taken as the unit of length, and in the piles to be described, is equal to 8.25 in.

Pile No. 18.

The structure of this pile consisted of a cubic lattice of pressed UO_2 (Mallinckrodt ether purified) pseudo-spheres (average weight 2143 g) in Speer graphite. The lattice spacing was 8.25 inches, and the ratio of the weight of graphite to that of uranium per cell was 6.4.

A summary of the measurements is given in Table I.

Table I.

Measurements on Pile No. 18.

Position	Average intensities (*)			Net intensity
	With source		Without source	
x , y , z	A_{Ni}	A_{Cd}	A_{Ni}	A_{Ni}
4 , 0 , 0	33569		75	33494
6 , 0 , 0	17373	2747	82	17291
10 , 0 , 0	4513		70	4443

(*) Counts per minute.

In Table II are given the correction factors and corrected intensities together with a least square analysis of the results.

With the distance between positions 4 and 10 equal to 125.8 cm, we obtain for the exponential relaxation distance (Eq. (6a)) $b = 62.74$ cm. The effective side of the pile was estimated to be $a = 256.9$ cm. With this value, and that for b, we calculate

$$\frac{1}{c^2} = \frac{2\pi^2}{a^2} - \frac{1}{b^2} = 45 \times 10^{-6}\ \mathrm{cm}^{-2}$$

and $c = 149$ cm.

TABLE II.

Analysis of results of measurements upon Pile No. 18.

Position x , y , z	Net intensity from Table I	Harmonic correction	End correction	Corrected intensities	Log I	Least square value 5.11350– 0.14525 x
4 , 0 , 0	33494	1.0193	1.0006	34161	4.5445	4.5325
6 , 0 , 0	17291	1.0039	1.0022	17396	4.2403	4.2420
10 , 0 , 0	4443	1.0002	1.0323	4587	3.6615	3.6610

From Table I we obtain a cadmium ratio equal to 6.32. The value of the migration length, L (Eq. (5 a)), can be estimated knowing the graphite density (1.54) and the cadmium ratio. For this pile $L^2 = 7.2$ cm^2.

From Eq. (5 a) we obtain for the reproduction factor

$$k = 1.032.$$

PILE NO. 27.

This pile was identical with No. 18 with the exception that AGOT graphite was used throughout in place of Speer. Tables III and IV give summaries of the measurements and corrected intensities.

From these results we calculate $b = 64.52$ cm, $1/c^2 = 58.9 \times 10^{-6}$ cm^{-2}, and $c = 130$ cm.

TABLE III.

Measurements on Pile No. 27.

Position	Average intensities			Net intensity
	With source		Without source	
x , y , z	A_{Ni}	A_{Cd}	A_{Ni}	A_{Ni}
4 , 0 , 0	34261		84	34177
6 , 0 , 0	18158	2726	91	18067
10 , 0 , 0	4881		80	4801

TABLE IV.

Analysis of results of measurements upon Pile No. 27.

Position x , y , z	Net intensity from Table III	Harmonic correction	End correction	Corrected intensities	Log I	Least square value 5.10980–0.14135 x
4 , 0 , 0	34177	1.0193	1.0006	35144	4.5458	4.5444
6 , 0 , 0	18067	1.0039	1.0022	18183	4.2596	4.2617
10 , 0 , 0	4801	1.0002	1.0323	4977.7	3.6970	3.6963

For AGOT graphite, density 1.62 g/cc, and a cadmium ratio from Table I equal to 6.67, L^2 is estimated to be $L^2 = 666$ cm^2. From these values we obtain for the reproduction factor $k = 1.039$. Thus, the use of AGOT in place of Speer graphite gives an increase in the reproduction factor of 0.7 percent.

PILE NO. 29.

Since the amount of cast uranium metal available for testing was insufficient to fill a complete lattice of the usual size, the pile was constructed in the form of a sandwich in which four oxide bearing layers (at the planes $x = 6, 7, 8, 9$) of Pile No. 27 were replaced with four metal-bearing layers in the same lattice. In addition, the AGOT graphite in this same region was replaced with AGOT (Lots Nos. 10, 11), which lots showed the lowest absorption cross section. The uranium metal (from Metal Hydrides) was in the form of cast cylinders, $2\frac{1}{4}$–in. diameter, weighing approximately 2.7 kg each. The graphite-to-uranium ratio was 5.1.

The determination of the exponential relaxation distance for the metal lattice of the sandwich pile is based essentially upon a comparison of the ratio of the neutron intensity below and above the metal lattice with the ratio of the intensities at the same positions in Pile No. 27. Since, however, Pile No. 29 was built at a different location than that of Pile No. 27, it was necessary to repeat Pile No. 27 at the new location. The results of this Pile (No. 28) agreed with those obtained for the identical Pile No. 27. Pile No. 28 was, therefore, used as the control for Pile No. 29.

If R_o and R_m are, respectively, the ratios of the intensities at positions below and above the position of the metal lattice in the oxide and oxide-metal-oxide piles, b_o and b_m the exponential relaxation distance associated with the oxide and metal lattices, and A the height of the metal lattice in the sandwich pile, then:

(7 a) $$\log \frac{R_o}{R_m} = \frac{A}{b_o} - \frac{A}{b_m} .$$

TABLE V.

Measurements on Piles Nos. 28 and 29.

Position	Pile No. 28 Observed intensities		Pile No. 29 Observed intensities	
x , y , z	A_{Ni}	A_{Cd}	A_{Ni}	A_{Cd}
4 , 0 , 0	36680		37320	
6 , 0 , 0	19530	2865	20980	3200
10 , 0 , 0	5212		6001	

The measurements on Piles Nos. 28 and 29 are given in Table V.

For Pile No. 28: $R_0 = I_4/I_{10} = 7.021$;

For Pile No. 29: $R_m = I_4/I_{10} = 6.219$.

Since A = 83.82 cm, and b_0 for Pile No. 28, 64.472 cm, we obtain from Eq. (7 a)

(8 a) $$\log \frac{7.021}{6.219} = \frac{83.82}{64.472} - \frac{83.82}{b_m}$$

or

$$b_m = 71.10 \text{ cm}.$$

This gives an improvement of 42.8×10^{-6} cm^{-2} in the value of ∇^2 compared to Pile No. 28, or an increase in the reproduction factor for metal over dioxide (L^2 estimated to be 700 cm^2) of

$$700 \times 42.8 \times 10^{-6} = 0.03.$$

Therefore, k for the uranium metal lattice in AGOT graphite is

$$k = 1.04 + 0.03 = 1.07.$$

A summary of the results for the three piles discussed is given in Table VI.

TABLE VI.

Results of measurements upon test piles.

Pile No.	Form of U	Graphite	$\frac{\text{Graphite}}{\text{Uranium}}$	Cd-ratio	Thermal utilization factor	b (cm)	$\frac{10^6}{c^2}$ (cm^{-2})	L^2(cm^2)	k
18	UO_2	Speer . . .	6.4	6.32	0.866	62.74	45	712	1.032
27	UO_2	AGOT . . .	6.4	6.67	0.869	64.52	58.9	666	1.039
29	Metal	AGOT (Lot Nos. 10, 11)	5.1	6.56	0.871	71.10	101.2	700	1.07

Graphite cross-section measurements.

Accurate determination of the neutron capture cross section of the graphite to be used in a reacting pile is necessary for two reasons. First, if there is too much absorption in the graphite a chain reaction may be impossible or may require dimensions too large to be practical, and secondly, since the effect of the absorption is proportional to the square of neutron density the use of low cross-section material near the center will reduce the size of the structure. For these reasons cross-section measurements were made on each brand of graphite used in the structure. These were AGX (National Carbon Company), US (U. S. Graphite Company), Speer (Speer Graphite Company), and nine different lots of AGOT (National Carbon Company) graphite. For these measurements a series of σ cross-section piles, described in the following section, were constructed.

Description of σ–Piles.

Most of these piles were built on a base of Speer graphite approximately 5×5 ft and about 3 ft high. A source slot through the center of the center layer of this base parallel to one edge measured about 10×10 cm. $\frac{1}{4} \times \frac{1}{4}$–in. graphite strips were fastened to the top of this base in parallel rows 12 in. apart. On these strips a layer of Speer or AGX graphite was laid leaving a 1/4–in. gap into which cadmium could be inserted. In general, this layer was different from the graphite being measured and was used only because long pieces were available to bridge the 1/4–in. gap. Above this layer 15 layers of the material to be tested were laid with detector slots at the top of layers 3, 6, and 9. These slots, numbered 1, 2, and 3, respectively, passed through the vertical axis of the pile perpendicular to the source slot in order that small inaccuracies in placing the foils would have a minimum effect on the measurement and in order to reduce as much as possible the radiation absorbed by operators handling the foils. The entire pile above the gap was covered with cadmium in order to reduce to a minimum the number of thermal neutrons entering the pile from the room.

In those piles built to measure σ for AGX, US, and Speer 1 graphite the dimensions of this top portion were very nearly $5 \times 5 \times 5$ ft. The remaining Speer piles and the AGOT piles were about 168×157 cm and 157 cm high.

Theory.

The thermal neutron density n in a graphite structure containing a source is described by the following differential equation:

$$D\Delta n - (1/t)\, n + q = 0, \tag{1 b}$$

where D is the diffusion coefficient $= \lambda v/3$, λ is the mean free path for scatter-

ing, v is the neutron velocity, t is the mean life of a thermal neutron, and q is the nascent thermal density. If measurements are made with cadmium in the gap and without cadmium in the gap we will have two such equations for the two neutron densities n_1 and n_2. Subtracting these two equations and writing $n = n_2 - n_1$, we have

$$\mathrm{D}\Delta n - (1/t)\, n = 0, \tag{2 b}$$

or

$$\mathrm{L}^2 \Delta n - n = 0,$$

where L is the diffusion length $(= \sqrt{\mathrm{D}t})$.

We will give the solution of this equation for a rectangular pile whose sides are $[a - (2\lambda/\sqrt{3})]$, $[b - (2\lambda/\sqrt{3})]$, and $[\mathrm{Z} - (\lambda/\sqrt{3})]$ parallel to the x, y, and z axis, respectively. For boundary conditions we will assume that $n = 0$ when $x = \pm a/2$, $y = \pm b/2$ and $z = \mathrm{Z}$. The solution is

$$n = \sum_{lm} \mathrm{B}_{lm} \cos \frac{l\pi x}{a} \cos \frac{m\pi y}{b} \left(e^{-z/b_{lm}} - e^{-(2\mathrm{Z}-z)/b_{lm}}\right). \tag{3 b}$$

Here b_{lm}, the distance for the intensity of the lm harmonic to decrease by a factor of $1/e$ in a pile of infinite length is related to L by the following equation:

$$\frac{1}{\mathrm{L}^2} = \frac{1}{b_{lm}^2} - \pi^2 \left(\frac{l^2}{a^2} + \frac{m^2}{b^2}\right). \tag{4 b}$$

Along the vertical axis of the pile the first harmonic of neutron density is proportional to

$$e^{-z/b_{11}} - e^{-(2\mathrm{Z}-z)/b_{11}},$$

The second term of this expression is a reflection from the top of the pile and would not be present in an infinitely tall pile. Hence to correct for the finite height of a pile all intensities along the axis are multiplied by

$$\frac{1}{1 - e^{-2(\mathrm{Z}-z)/b_{11}}}, \tag{5 b}$$

the so-called end correction.

Equation (4 b) gives a means of determining L. One either measures b_{11} far from the source where the higher harmonics are small or corrects the measured intensities for these harmonics and obtains b_{11} closer to the source where the intensity is easier to measure.

This is done as follows: Assuming a value of L, Eq. (4 b) permits a calculation of the relaxation length of each harmonic. Writing Eq. (3 b) for the z axis we have

$$n = \sum_{lm} \mathrm{B}_{lm} \left(e^{-z/b_{lm}} - e^{-(2\mathrm{Z}-z)/b_{lm}}\right).$$

If two equal sources are used at $x = \pm a/4$, two such solutions must be added and a factor of $\cos l\pi/4$ appears. This causes the 1,3 harmonic to cancel the 3,1 harmonic and the 1,5 to cancel the 5,1 along the Z axis. The 3,3 harmonic is the first to appear and is negative.

To a good approximation we can write

$$n = B_{11}\,(e^{-z/b_{11}} - e^{-(2Z-z)/b_{11}}) - B_{33}\,(e^{-z/b_{33}} - e^{-(2Z-z)/b_{33}}) + \cdots .$$

The harmonic correction factor is therefore

$$\frac{B_{11}}{n}\,(e^{-z/b_{11}} - e^{-(2Z-z)/b_{11}}).$$

For σ–piles used in determining cross sections of AGOT graphite, the total harmonic and end correction factors were 1.0056 for slot 1 and 1.0131 for slot 3.

Measurements.

Measurements were made with indium foils of 26 cm² area weighing 92.4 mg/cm^{-2}. Two counters were used and each determined the activity of three foils from each of the three slots when there was cadmium in the slot and again when the slot was empty. Irradiation times were adjusted to keep the initial counting rates below 1500 counts per minute. The count was started three minutes after the foils were removed from the pile and continued for most measurements until more than 20,000 counts had been recorded. Assuming a half-life of 54 minutes for indium the initial activity after infinite irradiation was calculated. Since the sensitivities of the two counters were not the same, the activities measured on one counter were multiplied by the ratio of sensitivities as determined from measurements on a number of piles. The mean activities at slots 1 and 3 were corrected for harmonics and end effects as explained in the preceding section. Then if these corrected activities are called I_1 and I_3, respectively, b_{11} was obtained from the formula

$$b_{11} = Z_{13}/\log\,(I_1/I_3),$$

where Z_{13} is the distance between slots 1 and 3. Equation (4 b) of the preceding section was used to calculate the diffusion length. These values are given in Table VII, Column 2, for each of the graphites measured. Column 1 gives the name of the graphite as stamped on each piece. GX 2 refers to the shipment of AGX cut to 4×4×30 in. SP 1 refers to the shipment of Speer graphite cut to 10×10 cm cross section. SP 2 and SP 2′ refer to Speer graphite cut to $4\frac{1}{8}\times 4\frac{1}{8}\times 16\frac{1}{2}$ in. The prime denotes graphite taken from the ends of the furnace. This graphite was not stamped. TO 1 refers to the 1st lot of AGOT graphite; TO 2 refers to the second lot, and similarly for other lots up to lot 15. Column 3 gives the diffusion length corrected to a density of 1.600 grams/cc, and Column 4 gives the cross section calculated from the formula

$$\sigma_a = \frac{12.8\times 10^{-24}}{L^2_{1.6}}.$$

It will be noted that the best graphites measured were T 10 and T 11. These lots and some T 14 were used for the core of the pile. The rest of the

AGOT formed a rough sphere around this. SP 2 and SP 2′ graphite was placed outside this. At the very outside of the pile US and GX 2 graphite was used interchangeably.

TABLE VII.

Diffusion lengths and cross sections for various graphites.

Graphite	L	$L_{1.6}$	$\sigma_a \times 10^{24}$
SP 1	49.53	48.35	0.00549
SP 2	49.77	47.93	0.00563
SP 2′	50.53	48.63	0.00541
TO 1	50.32	50.64	0.00499
TO 0, 2, 3, 4, 5, 6 .	48.95	49.71	0.00518
TO 8, 9, 13	49.74	50.49	0.00502
T 10	50.83	51.40	0.00484
T 11	51.16	51.70	0.00479
T 12	49.86	50.42	0.00504
T 14	50.14	50.67	0.00499
T 15	49.71	50.96	0.00493
AGX	43.25	43.79	0.00668
U.S.	44.57	44.79	0.00638

PRESSING OF URANIUM OXIDE.

The greater part of the pile contains uranium dioxide lumps which were fabricated by compressing loose dry UO_2 powder in a die with a hydraulic press. The chief problem here was the design of the die. Figure 4 gives the details of the dies which were used to press the $3\frac{1}{4}$–in. pseudospheres. It is essential that the die be made of a good quality tool steel, hardened and ground and polished since the powder has a considerable abrasive action. The force used in making the briquettes was in the range of 150 to 175 tons. Lubrication of the die proved to be important and it was found that a dilute solution (0.5 percent by weight) of stearic acid in acetone was quite satisfactory. A small amount of a wetting agent (ethylene glycol) was added to the lubricant so that when it was brushed on the polished surface of the die it would spread evenly. After some experience in handling the dies had been obtained it was possible to fabricate with one press 400 to 500 briquettes in an 8–hour working day.

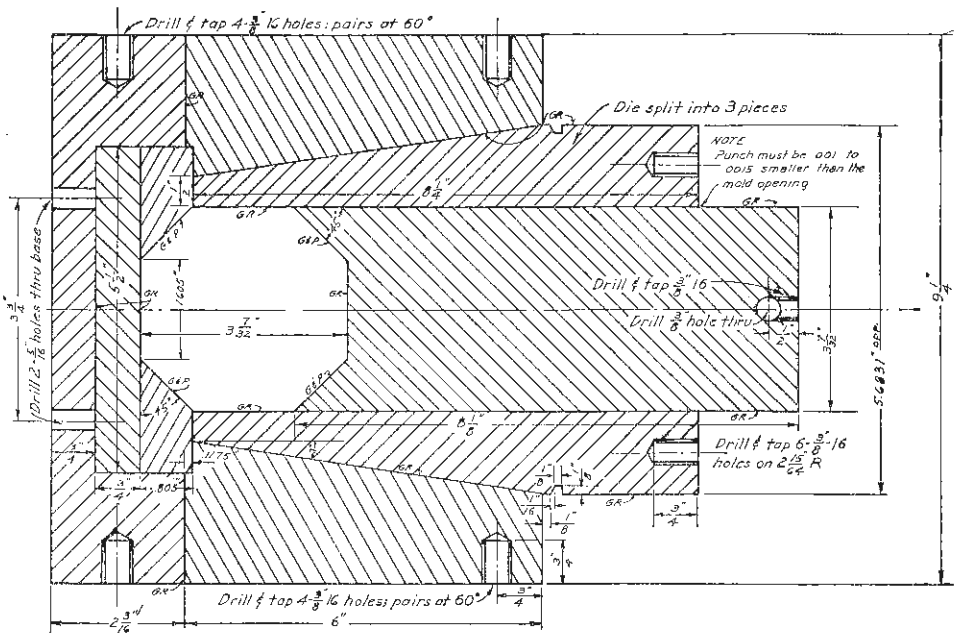

Fig. 4. – Die for pressing uranium oxide "pseudospheres."

Machining of Graphite.

The graphite is received from the manufacturer in bars of $4\frac{1}{4} \times 4\frac{1}{4}$ in. cross section and in lengths from 17 in. to 50 in. The surfaces are quite rough and therefore it is necessary that they be made smooth and that bricks of a standard length be cut.

For this work ordinary wood-working machines were used. Two surfaces are first made plane and accurately perpendicular to each other in a jointer and the remaining two surfaces are finished by a planer. A swing-saw was used for cutting to length. The surfaces were held to ± 0.005 inch and the length to ± 0.020 inch. The only departure from this was a slight rippling which appeared occasionally as the result of dull blades or improper manipulation of the work on the machines. Molybdenum steel cutting blades were used in these machines and resharpening, although a constant chore, was not so frequent as to cause any real difficulty. About 14 tons of material could be prepared in this way per 8-hour working day. In all 40,000 bricks were required.

A further graphite machining operation was the drilling of the $3\frac{1}{4}$-in. diameter holes with shaped bottoms, which were required to permit the insertion of the UO_2 briquettes into the graphite. These holes were drilled in a single operation by mounting a spade bit in the head stock of a heavy lathe and forcing the brick up to the tool with the lathe carriage. Due care had to be given to the design of the cutting tool, and to the alignment and centering of the bit.

These tools required frequent resharpening and, in fact, this proved to be the only difficulty in this operation. Carballoy bits showed the longest life but were rejected because of the greater effort required in preparing them. Bits ground from old files proved to be most satisfactory; about 60 holes could be drilled without resharpening. Actual drilling of the hole required about 20 seconds and from 60 to 100 holes per hour was the usual rate for the whole operation. A total of 22,000 holes were drilled.

CONSTRUCTION OF THE PILE.

The unit cell of the graphite-uranium lattice has a side of $8\frac{1}{4}$ in. and a volume of 0.324 cu ft. In order to achieve this lattice the graphite bricks were machined to a cross section of $4\frac{1}{8} \times 4\frac{1}{8}$ in. and were cut to a length of $16\frac{1}{2}$ in. The structure was planned as a sphere of maximum radius of 13 ft; the choice of a sphere being necessary because of the fact that probably not sufficient material would be available for any other shape which would be chain reacting. The decision to build a sphere necessitated two important additions to the structure. The first of these was a wooden framework in which the sphere was inscribed, and secondly, a graphite pier which supports the side of the sphere through which the control rods pass. It was believed to be entirely possible that after the structure was erected that the wood might warp or shrink and cause some displacement of the graphite above it. Since this would be undesirable from the point of view of passing control rods into the pile, that part of the pile through which the rods pass is entirely supported by this graphite pier. Originally it had been intended to evacuate the pile and, therefore, considerable pains were taken to see that the wooden framework fitted the graphite securely and that it presented a smooth continuous surface to the surrounding balloon cloth envelope. It turned out, however, that evacuation was not necessary and, therefore, these details are unimportant.

The cube in which the sphere is inscribed has a side of 24 ft 2 in. From this it follows that a part of the 26–ft diameter sphere is cut off on the sides; these parts represent a rather small percentage of the total volume of the sphere. As planned the sphere was to have a shell 1 in. thick on the outside made up of graphite without uranium or so-called dead graphite. The graphite-uranium lattice was expected to occupy a sphere of 12–ft radius and have a total volume of 7200 cu ft and hence about 22,300 cells were expected to be included in the structure.

As has been indicated earlier not all of the material available was of uniform quality and in order to use this material most efficiently that of highest quality was placed at the center with the less reactive types arranged in concentric shells; the quality decreasing outward from the center. The 26–ft diameter sphere would have required that about 75 layers of the $4\frac{1}{8}$–in. thick bricks would be piled up; however, the chain-reacting condition was

reached at the 57th layer. The actual amount of graphite in the pile is indicated in Table VIII in which also the amounts of each brand are given.

The US and AGX brands had dimensions somewhat different than the majority of the graphite and since they are of lower quality they were mostly used in the outer shell of dead graphite.

TABLE VIII.

Graphite in pile.

Source	Brand	Lbs
National Carbon Co.	AGOT	510,000
Speer Graphite Co.		145,000
U. S. Graphite Co.	U. S.	32,000
National Carbon Co.	AGX	60,000
AGX + Speer (Pier only) . .		24,000
		771,000 = 385.5 tons

In Table IX the details of the uranium lumps are given. Column 1 gives the geometrical forn of the lump.

TABLE IX.

Uranium in pile.

Geometrical shape	Compound	Weight	Density	Number	Total weight in pile
$2\frac{1}{4}$-in. cylinder . . .	Metal	6.0 lb	18 g/cm³	2,060	12,400 lb
$3\frac{1}{4}$-in. pseudosphere.	UO_2	4.72	6.10	14,840	70,000
$3\frac{1}{4}$-in. pseudosphere.	U_3O_8	3.99	5.17	1,200	4,790
3-in. cylinder	UO_2	4.56	6.14	540	2,460
3-in. cylinder	U_3O_8	3.97	5.20	840	3,340
				19,480	92,990 = 46.5 tons

The designation $3\frac{1}{4}$-in. pseudosphere indicates pressings which were cylinders of $3\frac{1}{4}$-in. diameter and $3\frac{1}{4}$-in. height, but which had the edges cut off at 45° so that they were roughly spherical. The designation 3-in. cylinder means a cylinder of height and diameter of 3 in. Since five varieties

of uranium lumps and four brands of graphite were used a considerable variation in the combination making up the cell was possible.

Metal—AGOT. Uranium metal cylinders combined with the highest quality AGOT graphite.

AGOT Br + AGOT. $3\frac{1}{4}$-in. pseudosphere of UO_2 inserted in an AGOT graphite brick and combined with undrilled AGOT bricks to make up the lattice.

Sp Br + Sp. $3\frac{1}{4}$-in. pseudosphere of UO_2 inserted in a Speer graphite brick and combined with undrilled Speer bricks to make up the lattice.

AGOT Bl + Sp. $3\frac{1}{4}$-in. pseudosphere of U_3O_8 inserted in a drilled brick of AGOT graphite and combined with undrilled Speer bricks to make up the lattice [1].

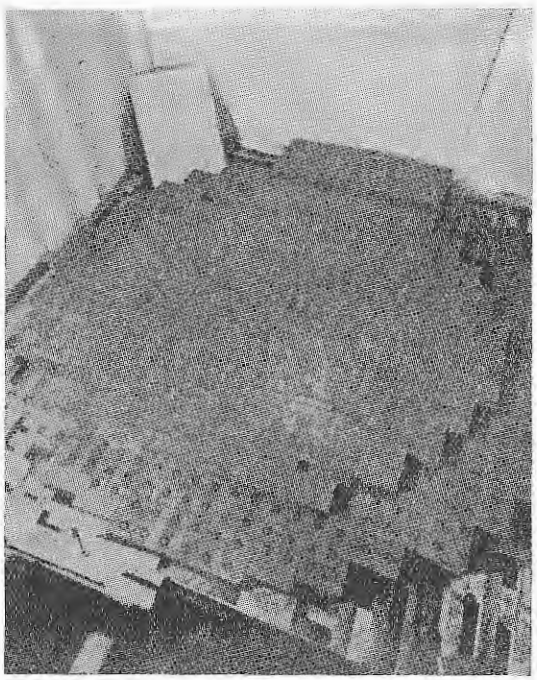

Fig. 5. – A layer of the pile.

Figure 5 is a photograph of the 19th and 18th layers. The roughly spherical form of the structure is shown and also some of the supporting wood frame work. The lattice is maintained in the vertical direction by inserting between two oxide bearing layers a layer of dead graphite. Layer 19 as shown in the photograph is only partially completed.

A total of 10 slots passing completely through the pile were provided. Three of these near the center are used for the control and safety rods, the

(1) A brief section at this point, omitted from the original report, involves discussion of diagrams not included in the report.—EDITOR.

remainder being available for experimental purposes. In addition one row of bricks carrying uranium lumps and passing very close to the center of the pile is arranged so that it can be pushed completely out of the pile. This construction permits the removal of samples from the pile and is useful for experimental purposes.

APPENDIX II.

MONITORING AND CONTROLLING THE FIRST PILE

H. BARTON, T. BRILL, S. FOX, R. FOX, D. FROMAN, W. HINCH, W. R. KANNE, W. OVERBECK, H. PARSONS, G. PAWLICKI, L. SLOTIN, R. WATTS, M. WILKENING, and V. C. WILSON (*).

The construction and operation of equipment for monitoring and controlling the first pile was undertaken by the circuit group. This job was subdivided as follows:

1. Monitoring the pile during construction.
2. Monitoring the pile while operating.
3. The control rods.
4. Electrical controls.

(*) Present addresses: *

H. M. BARTON, Jr.,
Phillips Petroleum Company,
Bartlesville, Oklahoma.

THOMAS BRILL,
Argonne National Laboratory,
P. O. Box 299,
Lemont, Illinois.

R. J. FOX,
508 Michigan Avenue,
Oak Ridge, Tennessee.

STEWART FOX,
Nuclear Instrument & Chemical Corporation,
223 W. Erie Street,
Chicago, Illinois.

DAROL FROMAN,
Los Alamos Scientific Laboratory,
P. O. Box 1663,
Los Alamos, New Mexico.

W. H. HINCH,
U. S. Bureau of Reclamation,
Denver Federal Center,
Denver, Colorado.

W. R. KANNE,
Knolls Atomic Power Laboratory,
Schenectady, New York.

W. P. OVERBECK,
E. I. du Pont de Nemours & Company,
Savannah River Plant,
P. O. Box 117,
Augusta, Georgia.

J. HOWARD PARSONS,
Los Alamos Scientific Laboratory,
P. O. Box 1663,
Los Alamos, New Mexico.

G. S. PAWLICKI,
Oak Ridge National Laboratory,
P. O. Box P,
Oak Ridge, Tennessee.

LOUIS SLOTIN,
(deceased).

R. J. WATTS,
Los Alamos Scientific Laboratory,
P. O. Box 1663,
Los Alamos, New Mexico.

M. H. WILKENING,
New Mexico Institute of Mining & Technology,
Campus Station,
Socorro, New Mexico.

V. C. WILSON,
General Electric Company,
P. O. Box 1088,
Schenectady, New York.

* On June 27th, 1952 (Editors Note).

1. Monitoring the pile during construction.

A slot of $2\frac{1}{2} \times 2\frac{1}{2}$-in. cross section running from the north face of the pile to slightly beyond the center of the pile was built into the 11th layer. A BF_3 proportional counter in a $2 \times 2 \times 12$-in. graphite block was pushed

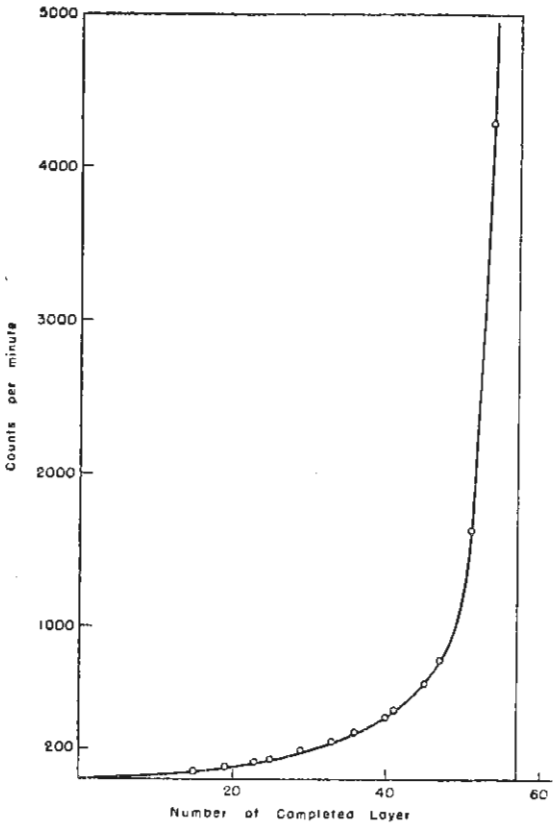

Fig. 6. – Intensity of reaction during construction.

along this slot to the center of the 11th layer. The counting rate was recorded both by a scale of 128 scaler and a pulse integrator operating a recording milliammeter. In this way a continuos history of the construction was obtained. The integrator also operated an alarm relay.

Figure 6 shows the counting rate as a function of the number of layers completed.

2. Monitoring the pile while operating.

When the pile was nearly large enough to become chain reacting, a second BF_3 proportional counter and four BF_3 ionization chambers were set up to monitor the pile. The automatic control rod and the safety rods

are actuated by signals originating in these BF_3 ionization chambers. The amplified ionization current is also used to operate recording power-level indicators. One chamber is battery operated. The other three chambers are powered by ordinary power packs with VR-tube stabilization. The power for these packs is derived from voltage regulating transformers. A diagram of the ionization chamber with the first two stages of amplification and the power supply is shown in fig. 7. The level indicator output terminals are

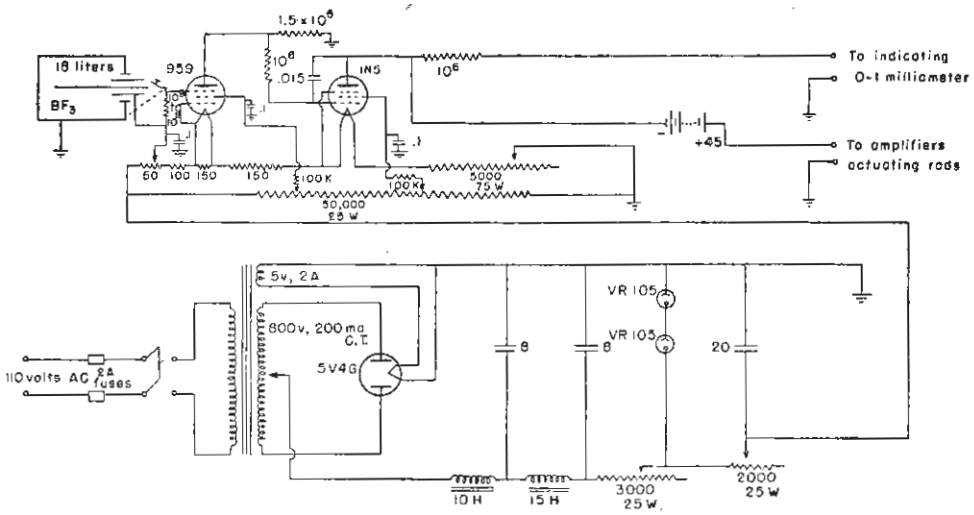

Fig. 7. – Ion chamber circuit.

shown as well as the output terminals to feed the amplifiers for the control and safety rods. Actually, different sets are used for the three different purposes.

The suppressor grid of the 959 tube is used for detection of the ionization current in order to secure a high leakage resistance of the tube. At the plate, screen, and filament voltages used, the over-all leakage resistance is greater than 10^{13} ohms at all voltages impressed on the suppressor grid in practice. This introduces no appreciable error when resistors less than 10^{11} ohms are used in the grid circuit. The voltage gain in the tube is about 1.5. If the control grid had been used the voltage gain would have been about 15, but except very near its floating potential, this grid shows an appreciable leakage. Moreover, this leakage is far from constant as the grid is swung over the values encountered in practice. In the circuit the connections are made to the suppressor grid terminal by soldering directly to it, thus eliminating leakage in a socket. The insulators in the ionization chamber were made of clean, dry plate glass. The outer surfaces of the insulators were heated and coated with ceresin wax. The 959 tube also was heated to about 100° C and dipped in molten ceresin. The wax keeps surface leakage to a minimum even under conditions of high humidity.

Operating experience with a divergent pile has brought to light several defects in these instruments. These defects are enumerated below with brief

suggestions for correction or improvement. An instrument with the improved design is to be tested on this pile before similar apparatus is constructed for future piles:

1. The chambers are too large to handle easily and are unnecessarily large for the required sensitivity. A volume of 2 liters instead of 18 seems adequate.

2. The variation of output of the instruments with line voltage is too great. A triode-pentode voltage regulator should be used, dispensing with the regulating transformers and VR tubes.

3. A more powerful tuhe such as 6J7 should be used in place of the 1N5 tube in thc second stage. This will allow using a 1 milliampere-movement recording meter as a voltmeter on the plate of this tube in place of using the meter in the plate circuit. This has the distinct advantage that the meter reading can be made accurately proportional to the current collected in the chamber. In the present instruments the meter reading decreases with increased intensity, and it becomes highly nonlinear as the tube goes to cut off.

4. The electric field for the collection of ions in the chamber is very far from the saturation value. This condition can be improved both by increasing the applied voltage and by a better shape of the electrodes.

5. The amplifiers being built right on the chambers are rather inaccessible and, in order to change sensitivity, a resistor must be replaced by soldering in the amplifier. The leads from the chamber to the amplifier should be long enough to pass through a protecting barrier and range change should be made with a multiposition switch.

6. For high power piles the chambers should bc made of, or lined with, a material from which no long-lived radioactive product is formed.

3. THE CONTROL RODS.

Since the power produced by a chain reacting pile is proportional to the neutron density, a pile may be controlled by controlling the neutron density. In the first pile this was done by means of rods of cadmium and boron steel. These rods could be moved in and out to regulate the fraction of neutrons absorbed in the rods.

During the construction several rods of cadmium were inserted in the pile. When tests indicated the pile was large enough to be chain reacting, these rods were removed one by one. This process is described in the main body of the report. Three of the rods were built specially as shown diagrammatically in figs. 8–10.

Figure 8 is a diagram of a safety rod. In normal operation, this rod is pulled entirely out and is held by a solenoid and catch which in turn are controleed by an automatic safety circuit adjusted to release if the neutron intensity becomes too great. This rod was made more complicated than necessary for several reasons. First, it was thought that the pile would need to be evacuated and so the rod was built in a vacuum-tight steel case with remote control. Secondly, it was thought that we should try to have the

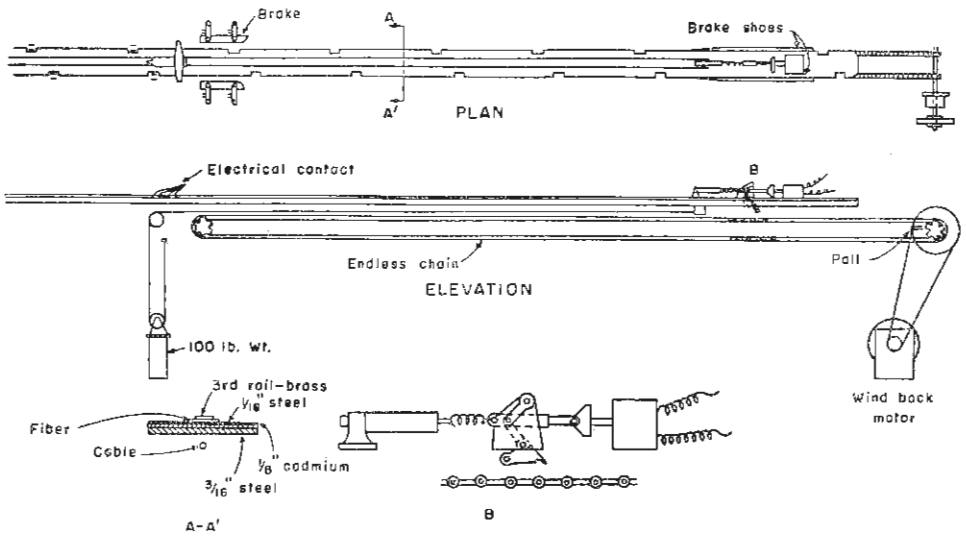

Fig. 8. – Details of safety rod.

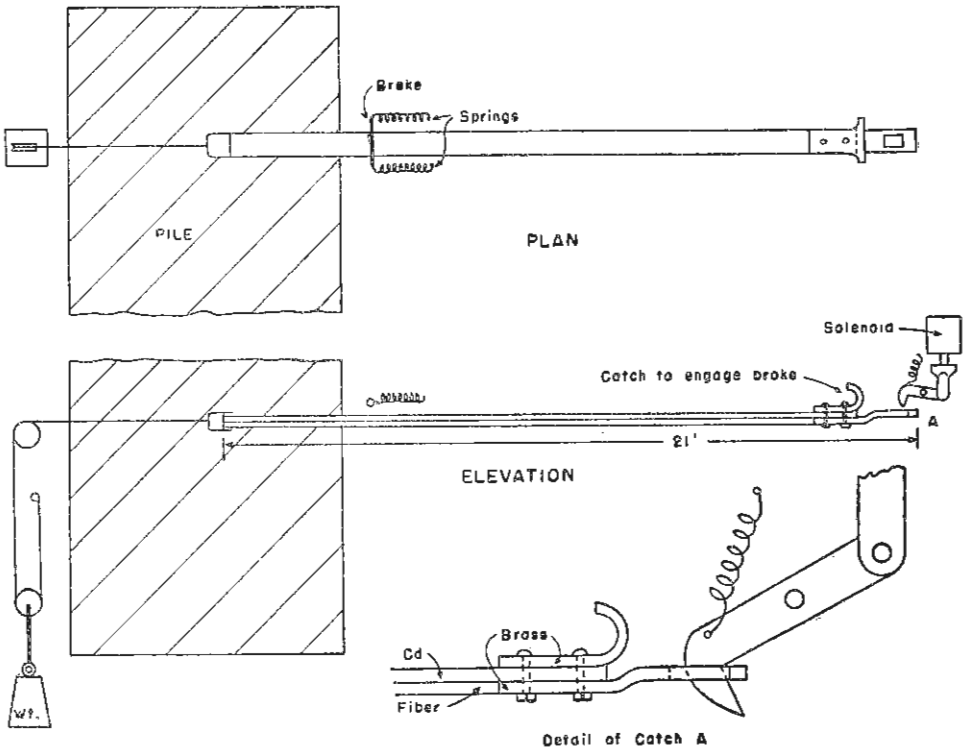

Fig. 9. – Details of " Zip " rod.

rod go in in less than a second. Third, it was thought that the pile would be run hot and so no rope could be placed in the pile and a steel cable would absorb too many neutrons. These restrictions prevented pulling the rod through. Fourth, it was planned to have the rod so that it could be pulled out to any desired position.

To meet the second and fourth requirements the catch was placed on the rod, and made to engage into an endless chain. When the solenoid is activated this engages. The circuits are arranged so that this cannot operate unless the neutron intensity is low. Therefore one cannot remove the rod from the pile unless the circuits agree that it is safe to do so. When the current in the solenoid is interrupted, the catch releases and the weight falls pulling only the rod without the extra drag of any pull out mechanism. This helps speed up the motion. The details of the catch are shown. When the knee action is adjusted so that it is not quite on the zero position when holding, the pull of both the spring and the weight tend to release the catch. To stop the rod a friction brake was designed which binds in the forward direction but automatically releases when the rod is pulled back.

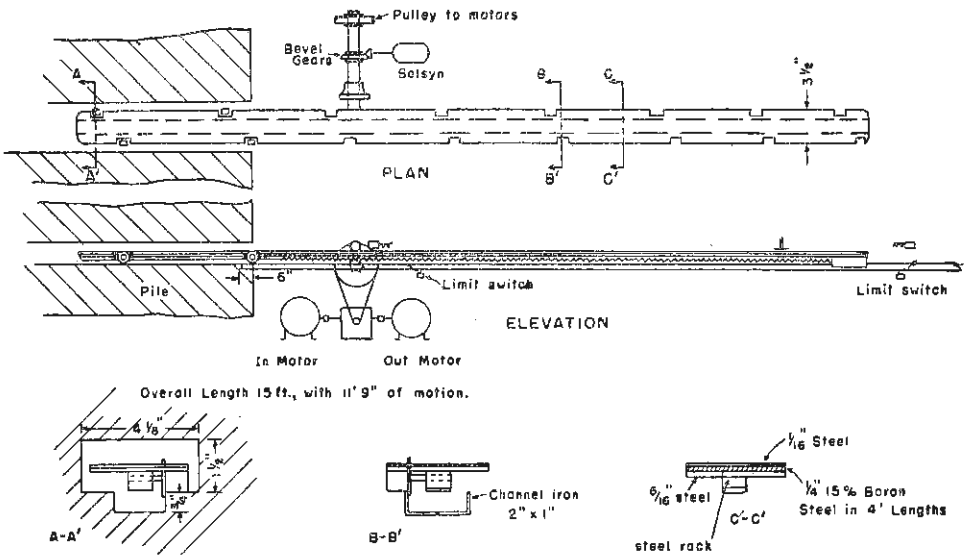

Fig. 10. – Control rod details.

Figure 9 is a diagram of a simpler safety rod which was built when it became apparent that it would not be necessary to evacuate the pile. This is pulled out and set by hand but may be released from the control table or by the safety circuits.

Figure 10 is a diagram of the regulating rod used. The rod was built as a sandwich. The center piece contained 1.5 percent of boron by weight.

Experience with these rods has shown that the regulating rods and the safety rods should be mounted on sufficiently rigid supports that the shock of the safety rods cannot destroy the settings of the regulating rods. A pneumatic safety rod has been designed and one will be tried in the second pile. The regulating rod seems adequate and only changes in the motor drives and gearing are contemplated for the second pile. Complete diagrams are available for the mechanical details of these rods.

4. Electrical controls.

In this section, a discussion will be given of the attempt to utilize the signals from the monitoring devices to move the control rods.

The initial lack of knowledge regarding behavior of the first pile led us to prepare a rather elaborate system of controls. While it has been found that these controls may be simplified and improved, our preparations have made it possible to test a variety of measurement and control devices.

a. *Measurement.*

The primary requirement of control is accurate measurement. We were equipped with ionization chambers and proportional counters, both filled with boron trifluoride. A simple method of checking these instruments was

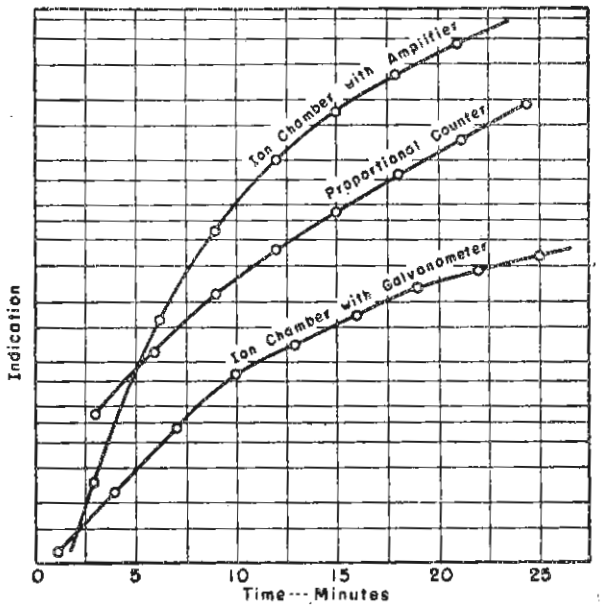

Fig. 11. – Recording of various monitoring devices.

found to be that of allowing the intensity to rise and fall at a natural rate obtained by placing a control rod outiside the critical position and then inside. This procedure results in exponential growth and decay of intensity and should therefore produce an indication which, plotted on semilog paper against time, is linear. Figure 11 shows such plots for the counter, the ion chamber current, and the output of the ion chamber amplifier. Obviously, the proportional counter is best as an indicating instrument since its response is most linear. The ion chamber, particularly with added amplification, is far from linear but is satisfactory as part of an automatic control system since its readings are reproducible.

The curve shown for the ion chamber with galvanometer was obtained with the circuit shown in fig. 12. This circuit is the simplest indicating system which we have used and has a great advantage in that only the ion chamber is located near the pile. Everything else is readily accessible.

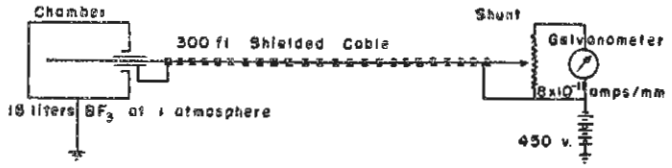

Fig. 12. – Connections of BF_3 chamber.

b. *Indication.*

One of our most important duties was to provide remote indication of the various actions of the pile. Since it will be impossible, at high intensities, to remain close to the pile, we must have remote indications of both intensity and of control rod positions. With regard to neutron intensity, our present

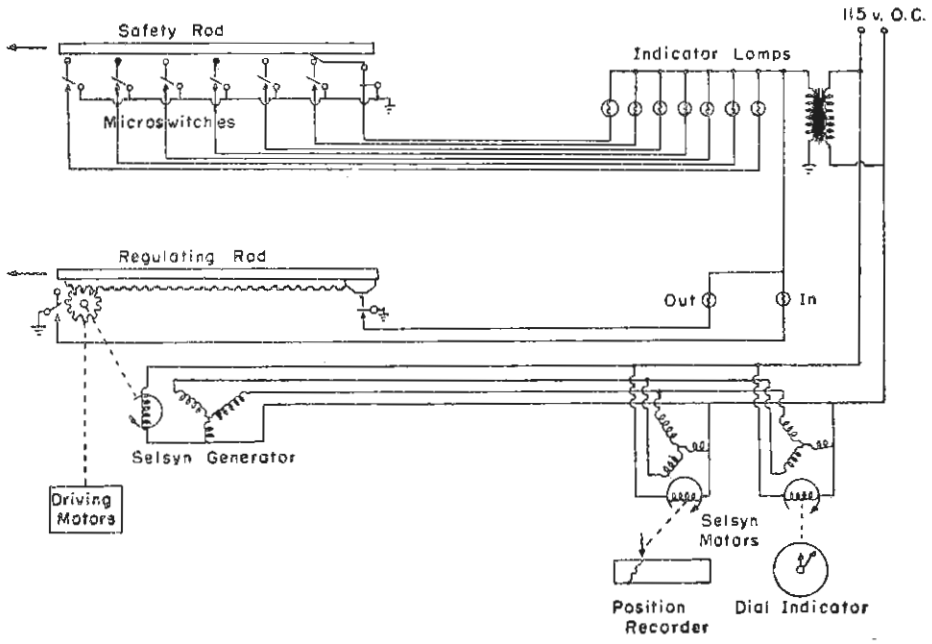

Fig. 13. – Rod position indicator system.

setup includes remote indication from four ion chambers and two proportional counters. Details of the circuits for these instruments are given elsewhere in this report.

Figure 13 shows the system employed to indicate control rod positions. The " safety " rod position is indicated only at intervals by means of microswitches lying along its track. " Regulating " rod position is more accurately indicated by selsyn units. As shown in the diagram, we have one selsyn generator coupled to the regulating rod mechanism and two selsyn motors;

one operating a dial indicator, the other a recording pen. In the present setup, it has been found possible to set the rod position within 0.05 inch of any desired value. A higher degree of accuracy would be possible if the gear ratio between selsyn and rod mechanism were increased.

c. *Controls.*

As mentioned above, the two types of control rod used in the pile are the safety rod and the regulating rod. The electrical circuit employed with these rods is shown in fig. 14. The safety rod (fig. 8) may be set to any desired position, usually all the way out, and is then held in place by a solenoid

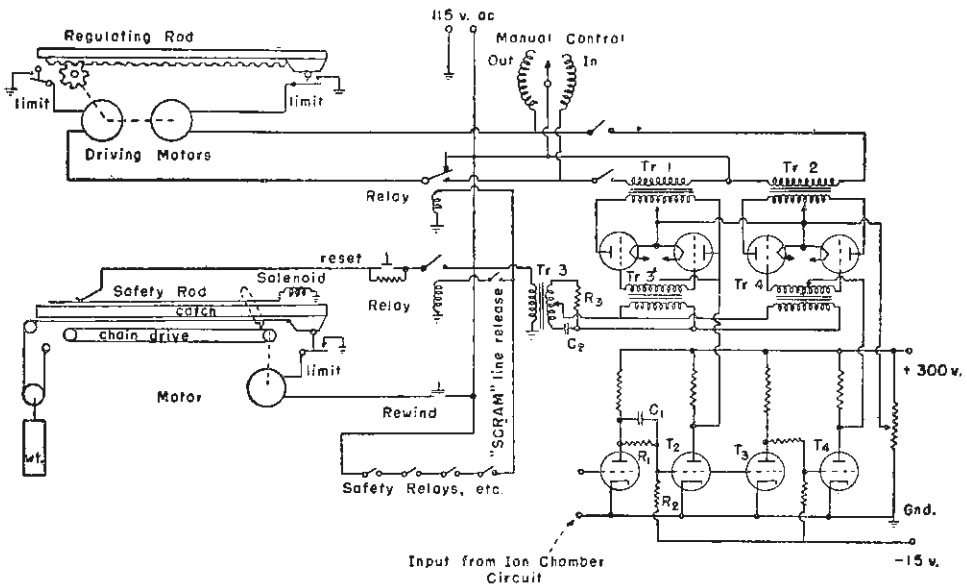

Fig. 14. – Simplified diagram of control system.

catch mechanism. Whenever current to the solenoid is interrupted, the rod is released and is pulled into the pile by a 100-lb weight.

The regulating rod is operated by two motors, one of which drives inward, the other outward. The use of two motors rather than a single reversible motor is for adaptation to an automatic regulating circuit to be described later.

The first section of the control system is an automatic safety control. It consists of two relays, one with normally open contacts in series with the solenoid on the safety rod, the other with normally closed contacts in series with the " IN " motor on the regulating rod. These relays are actuated through a common " SCRAM " line. If this line is opened at any point, all rods go in. The safety rods go in in about 2 seconds while the regulating rod requires 20 seconds. It was our intention to design any safety devices in such a manner as to open contacts in series with this " SCRAM " line. At the present time there are three automatic safety circuits operating from

three separate BF_3 chambers and holding separate relays. If any one relay is opened, the " SCRAM " line is broken and all the rods are sent in.

A second section of the control system is designed for manual regulation of the pile. It includes individual release switches for the safety rods, control of the rewind motors on the safety rods, a resetting switch for the solenoid catch, and a two directional variable speed control for setting the regulating rod. The latter consists simply of a variac whose winding is split so that it forms a variable inductance in series with each motor. Thus, direction of motion depends on direction of rotation of the variac knob and speed depends on the amount of rotation.

The final section of the control system includes an automatic circuit designed to operate the regulating rod in a manner such as to maintain constant intensity. The task of regulating intensity manually has been found so easy that this circuit has seen little service. However, with improved performance, it may be found very useful in experimental work and, in future plants, some modification of it may be essential. From present measurements, it seems that such a future control system may operate on temperature rather than neutron intensity since the pile appears to have a stable relationship between temperature and reproduction factor. The principles of precise control, however, remain similar. Controlling from neutron intensity, it seems possible to make the following assumption:

$$dn/dt = K_1 x,$$

where dn/dt is the rate of change of neutron intensity, and x is the distance of the rod from a neutral position at which intensity remains constant.

Suppose, then, that the control system is designed to move the rod at a speed partly proportional to the neutron intensity and partly proportional to rate of change of intensity, i.e.:

$$dx/dt = - K_2 n - K_3 dn/dt.$$

The minus signs indicate that the control system opposes any change of neutron intensity. Differentiating this last equation, we obtain

$$\frac{d^2 x}{dt^2} + K_3 \frac{d^2 n}{dt^2} + K_2 \frac{dn}{dt} = 0.$$

Substituting from the first equation, we obtain

$$\frac{d^2 x}{dt^2} + K_1 K_3 \frac{dx}{dt} + K_1 K_2 x = 0.$$

This is now an equation of motion for the rod alone and it is possible to insert any initial condition in terms of an initial error in rod position and solve for the motion followed by the rod in correcting for this disturbance. It is found that this motion is stable if K_3 is greater than $\sqrt{(K_2/K_1)}$ and, if this requirement is not fulfilled, the control will be unstable and oscillatory. In the event that a temperature control is found more suitable for high intensity operation, the rod may be replaced by a cooling system and x becomes a cooling rate. To increase intensity, it will be necessary only to increase the flow of the cooling medium. It seems most likely that a combination of

temperature and intensity controls will be needed since control from temperature alone may produce vicious transient conditions.

In the present system, the neutron intensity is measured by an ion chamber whose output, over a limited range may be considered proportional to neutron intensity. This signal is amplified by a vacuum tube (T_1 in fig. 14) and then passes through a network consisting of resistors R_1, R_2, and condenser C_1. The characteristic of this network is such that, over the range of possible frequency components of any reasonable disturbance, it applies to the grid of the next tube T_2 a voltage

$$e_g = K_4 n + K_5 dn/dt.$$

The constants in this equation are determined by the values of R_1, R_2, and C_1 and the latter may thus be used to adjust the entire control system for stable performance.

Tubes T_3 and T_4 produce an inversion of the control signal without amplification. Thus, changes in anode potential of T_2 are accompanied by equal and opposite changes at the anode of T_4.

In series with each of the regulating-rod motors, is the primary winding of a transformer, Tr_1 and Tr_2. Each transformer has a secondary winding across which two thyratron tubes are so connected that, when conducting, they short circuit the secondaries. The thyratron grid circuits are, however, arranged so that the amount of conduction may be smoothly varied. This is accomplished by adding to the control potentials, supplied by tubes T_2 and T_4, an ac voltage obtained from transformer Tr_3, phase shift network R_3 and C_3, and grid transformers Tr_4 and Tr_5.

The transformers Tr_1 and Tr_2 with their thyratrons now act as automatically variable impedances in series with the two motors and, due to the inverse relationship between the control potentials supplied by tubes T_2 and T_4, an increase of intensity drives the " IN " motor and a decrease drives the " OUT " motor.

Tests on this original circuit indicate that it will hold intensity constant to the order of ± 3 percent in the presence of rather violent disturbances such as insertion or removal of other rods.

5. Conclusions.

While our initial experiments indicate that fairly precise control may be obtained with simple manual regulation, it also indicates that stable automatic control is possible, and that it may be made much more precise than the present system. Our future program, already under way, therefore consists of further development and improvement of such controls so that they will be available when needed.

N° 182 and 183.

What thrilled Fermi most about the chain reacting pile was not so much its obvious promise for atomic energy and atomic bombs, which many others were now prepared to pursue, but an entirely new and unsuspected feature. It was a marvelous experimental tool. This wonder, three weeks old by the time Fermi wrote his next report, had a sensitivity for neutrons beyond the wildest dreams of those who had struggled so hard to make measurements before. It was, in fact, a neutron multiplier of almost unlimited power. Change the number of neutrons a little, and soon the effect would be multiplied by a million times or more. The sensitivity was, in fact, limited by even rather slight changes in the pressure and temperature of the air inside. The temperature coefficient of the reproduction factor, long an unanswered and difficult problem, was now measured precisely with the greatest of ease by the simple expedient of opening a window to allow some of the cold outside air to enter the pile.

The pile became a fine device for checking the purity of the uranium, an extensive standardization was carried out, and many features of the uranium graphite lattice, inaccessible before, were studied.

This was physicists' work: a new device to calibrate, measurements to make, methods to develop, limits to explore, new effects to notice, results to understand. Fermi would be too busy for committees for quite a while. Most of the work was done with the groups of Anderson and Zinn, with Fermi an active participant again. The progress was very rapid and was recorded in his monthly reports.

Paper N° 183 was issued also as Report A–475.

H. L. ANDERSON.

182.

SUMMARY OF EXPERIMENTAL RESEARCH ACTIVITIES

Excerpt from Report CP–416 for Month Ending January 15, 1943.

Most of the work of the nuclear physics division in the past month has been centered around the chain reacting pile.

One of the main problems that must be solved in order to use the pile as a tool for physical experimentation is that of determining the critical position of a control rod with very high accuracy. Two methods have been applied for this purpose. One is based on a determination of the periods of rise or of decay of activity, and one on the determination of the position of the control rod for which the intensity of the pile becomes steady at a high level of neutron emission. The sensitivity of both methods is about equal and corresponds to displacements of the order of 0.1'' of the control

rod. Such displacements correspond to changes in the effective reproduction factor of the order of 2×10^{-6}.

The changes of effective reproduction factor do not depend in a linear way on the position of the control rod. Equal displacements of the control rod produce a much greater variation of the effective reproduction factor when the end point of the rod is deep inside the pile than when the rod is far out. Over a fairly wide interval of positions, the changes of reproduction factor per inch of displacement of the rod are proportional to the square of the length of rod inside the pile. Since the critical position is normally not far from 7′ inside the pile, it is convenient to correct all displacements in such a way as to have a uniform sensitivity which is conventionally chosen equal to the sensitivity of the rod at 7′.

For the interpretation of many experiments, one must know the change of reproduction factor due to a displacement of one inch of the control rod. An approximate determination of this change indicates that it is about 18×10^{-6} per inch. Such figure is, however, only quite preliminary and work is in progress in order to improve its accuracy.

The effective reproduction factor is influenced very markedly by the changes in the nitrogen content in the pile due to variations of the atmospheric pressure. This effect is quite large and corresponds to a shift of the control rod of 3.9″ corresponding to about 7×10^{-5} for a change of atmospheric pressure of 1 cm of mercury at room temperature. Incidentally, such a pressure sensitivity of the critical position corresponds in a satisfactory way to the value to be expected from the knowledge of the capture cross section of nitrogen and of the amount of nitrogen present inside the pile.

When a neutron absorbing substance is introduced near the center of the pile, the critical position of the control rod changes in order to compensate for the neutron absorption in the substance introduced. The present evidence indicates that a determination of the shifts of the control rod obtained in this way may be developed in a very sensitive and convenient way to determine the absorption cross sections and danger coefficients of various materials. The order of magnitude of the sensitivity of the method is such that cross sections somewhat less than 1 square centimeter can be measured easily. Since very large samples can be used, the method promises to be very convenient to use in many cases.

Some investigation has been made of periods of rise or fall of the neutron intensity. When the control rod is close to the critical position, the period expressed in minutes is given by $7^4/x$, where x is the distance from the critical position in inches.

From the accepted values for the periods and the percentages of delayed neutrons, one would expect somewhat longer periods; the discrepancy is by about a factor of 2 and indicates that the percentage of delayed neutrons emitted in the fission is probably more nearly 0.5 than 1 %.

The temperature coefficient of the effective reproduction factor of the pile has been measured by cooling artifically the pile about 9° C and heating it back to room temperature afterwards. During the decrease and rise of temperature, which extended over a period of about three weeks, the critical

positions were determined. Correcting the results for the effect due to the changes in nitrogen content of the pile due to the variations of pressure and of temperature, a shift of critical position by 2.1''/°C was found.

Such a shift corresponds to a decrease of the effective reproduction factor by 3.8×10^{-5}/°C. It should be noticed that small changes in this figure may be expected as a consequence of changes in the standardization of the pile.

It is interesting to compare this result with the theoretical expectations.

Three main reasons for a variation of the effective reproduction factor with temperature are known, namely:

(a) Due to the higher temperature of the thermal neutrons, the leakage of neutrons outside of the pile increases with increasing temperature. This determines a decrease of the effective reproduction factor. On the assumption that the thermal neutrons are in perfect thermal equilibrium, this effect would amount to a decrease in "k" by 4.7×10^{-5}/°C. Since, however, the effective temperature of the neutrons is probably somewhat higher than room temperature, this effect is presumably somewhat smaller, probably about 0.4×10^{-5}/°C.

(b) The variation of the temperature of the neutrons produces also a leveling of the thermal neutron intensity within the lattice cell, which determines a decrease of the thermal "disadvantage factor" and consequently an increase of the reproduction factor. This effect can be calculated for our lattice and amounts to 8.6×10^{-5}/°C for the metal lattice and 5.2×10^{-5}/°C for the oxide lattice. Taking into account the distribution and amounts of various types of lattices in our pile, the average effect should be 6.5×10^{-5}/°C. Also, this value should be somewhat reduced since the neutrons are not in perfect thermal equilibrium and a more probable value is 5.6×10^{-5}/°C.

(c) The Doppler broadening of the resonance levels of uranium determines an increase in the resonance absorption which produces a decrease of the reproduction factor. No sufficient data are available so far for an independent estimate of this factor.

The observed effect is quite close to the effect expected from (a). It would appear, therefore, that the two effects (b) and (c) acting in opposite directions approximately cancel. This conclusion is, of course, limited to the lattice used in the present pile and to a narrow temperature interval near room temperature.

N° 183.

For the introduction to this paper see N° 182.

183.

SUMMARY OF EXPERIMENTAL RESEARCH ACTIVITIES

Excerpt from Report CP–455 for period ending February 6, 1943.

In the course of the past month most of the work of the nuclear physics division has consisted of experiments performed by using the chain reacting pile.

In the last monthly report it was indicated that the accuracy of setting of the control rod for the determination of the critical point of the pile is about 0.1 inches, corresponding to a determination of the reproduction factor with an error of 2×10^{-6}. Further work has indicated that it is possible to improve somewhat this accuracy for experiments performed in a short interval of time.

The high accuracy of this determination enables one to use the pile as a very sensitive tool for the test of the purity of uranium. This is done by substituting the lumps of a batch to be tested for the lumps in a few cells located in the central portion of the pile. The critical position is determined before and after the substitution and its difference is proportional to the loss due to the impurities present. Tests conducted so far by substituting the lumps in 14 cells have indicated that the sensitivity of the method amounts to about 1/20 of a percent. This test is therefore much more convenient than the test by an exponential pile, the main advantages being (a) the greater accuracy, (b) the fact that the tests can be performed on a sample of about 100 lbs instead of at least 2 tons, and (c) that the test can be performed in about one hour instead of several days.

Attempts have been made to use the pile in a similar way to perform the equivalent of an exponential experiment on a new type of lattice. For this, the lattice structure is modified in a few central cells and a corresponding change of the critical position of the rod is determined. The method is very sensitive. There are, however, some uncertainties as to the interpretation of the results whenever the cadmium ratio in the new lattice differs considerably from the cadmium ratio of the environment. A number of experiments of this type have been performed and are reported elsewhere.

Considerable attention has been given to the problem of standardizing the pile in such a way as to be able to express actual changes of reproduction factor in terms of the displacement of the rod. In some experiments, a change of the critical position of the rod is due to a change of the physical conditions of all the cells of the pile. This is the case, for example, when the nitrogen content of the pile changes due to change of atmospheric pressure. A second example of the same type is the shift of the critical position due to a change in temperature of all the pile. For the interpretation of experiments of this type, it is necessary to know the variation of reproduction factor per unit displacement of the rod. In what follows, we shall indicate by x the variation of reproduction factor for a displacement of the critical position of one conventional inch. In other experiments a change of physical conditions or of structure is introduced only in a few cells located in the central portion of the pile. In such cases the change of overall reproduction factor of the pile is given by $\delta k = (k_1 - k_0)\frac{N_1}{N}$, where $k_1 - k_0$ is the change of reproduction factor introduced in the modified cells, N_1 is the number of modified cells and N is the effective number of cells. In calculating N one must take into account the fact that the statistical weight of each cell depends on its position in the pile being approximately proportional to the square of the neutron density at the place of the cell.

The two constants, x and N are known so far with a considerable error. Some idea of the accuracy with which they are known may be obtained in the following way. 6 different experiments that give information on either x or N or their product, have been performed so far.

A. *Effect of pressure on the critical position of the control rod.*—It has been observed that the critical position shifts by 3.96 conventional inches for a pressure change of 1 cm of mercury. The corresponding variation of reproduction factor may be calculated as follows. The free volume occupied by air within a cell (including free space inside the graphite and actual macroscopic holes) is, on the average, 2236 cm^3. From this follows that the variation in the amount of nitrogen per cm of pressure and per cell is 1.89×10^{-3}. Assuming a nitrogen cross section of 1.7×10^{-24} for thermal neutrons, one can calculate a loss of reproduction factor of 6.9×10^{-5} per cm variation of pressure. Since the corresponding shift of the critical position is of 3.96 conventional inches, it follows that 1 conventional inch is equivalent to a variation of reproduction factor $x = 1.7 \times 10^{-5}$.

B. *The neutron intensity at various places within the pile has been determined experimentally.*—The effective number of cells, N, can then be calculated upon the assumption that the statistical weight of each cell is proportional to the square of the neutron intensity, with the formula $N = \Sigma (n_i/n_0)^2$ where n_i and n_0 are the neutron intensities in the i^{th} and in the central cell; the sum is to be extended to all the cells in the pile. Such a sum can be calculated by a process of numerical integration if the intensity at all places inside the pile were known. The result is $N = 2240$. This value can be appreciable in error due to the fact that the intensity is actually measured only at the few places inside the pile where there are slots

in which detectors can be placed. The values at other places must be obtained by an interpolation process which is made rather uncertain by the irregular structure of the pile.

C. *Standardization with a source.*—This experiment was performed by placing a radium-beryllium source at the center of the pile and by measuring the intensity of neutrons with a standardized detector when the control rod was displaced by a known amount from the critical position. The details and the interpretation of this experiment are given in another part of this report. The result is $Nx = 0.044$.

D. When a small amount of boron is placed at the center of the pile, the critical position shifts, due to the absorption of neutrons in the boron, at the rate of about 320 inches per gm atom. Assuming for boron an absorption cross section of 460 cm^2/gm atom and assuming an effective cross section of the cell of 27 cm^2 for neutrons of energy kT, one finds from this measurement: $Nx = 0.051$.

E. A similar experiment has been performed by distributing in the central portion of the pile some small cadmium pieces, either little squares of about 5 mm side or wires of 1.3 mm diameter. Such cadmium pieces absorb completely all the thermal neutrons that strike them, so that their cross section is equal to their actual geometric cross section. From the shift of the critical position of the rod due to the presence of the cadmium pieces, one can calculate $Nx = 0.053$.

F. The original Metal Hydrides (*) lumps in 14 cells in the central portion of the removable stringer were substituted by pressed pseudospheres of UO_2. A change in the critical position of 6.65 conventional inches was observed. Previous exponential experiments have indicated a difference of 3 % between the reproduction factors of 2 lattices with Metal Hydrides 6–lb. lumps and UO_2 pseudospheres. Taking into account the fact that the 14 cells in which the change was introduced are somewhat off the center of the pile, one can calculate from this experiment, $Nx = 0.051$.

A comparison of all these values shows a considerable lack of agreement between them. More work will be needed to improve our present knowledge of the standardization, primarily in view of the fact that the quantitative interpretation of most of the results obtained with the pile requires a knowledge of the 2 standardization constants, N and x. As best values for N and x, we can take at present $x = 2 \times 10^{-5}$ and $N = 2500$. The error in these values may however be as large as 20 percent.

Some metal lumps in the central portion of the pile have been thermally insulated from the surrounding graphite and provided with heaters by which their temperature can be raised about 500°C. From the changes of the critical position observed during the heating and cooling of these lumps, one can calculate the effect on the reproduction factor due to a change of temperature of the uranium lumps while the graphite temperature is not changed. A decrease of reproduction factor of 1×10^{-5} per °C was observed. This decrease

(*) Name of a brand of graphite, so called because produced by the Metal Hydrides Company. (Editor's note).

is presumably due to an increase of the resonance absorption with increasing temperature. In the discussion of the thermal effects given in the last monthly report, we had been led to the expectation that the resonance effect would be several times larger than actually observed. Since this is not the case, we are therefore led to conclude that there is some other mechanism of the variation of the reproduction factor with temperature besides those listed before, namely increased leakage, levelling of the neutron intensity within the cell, and change of resonance absorption.

A possible new mechanism that has not been considered so far could be a variation with temperature of the number η of neutrons produced per thermal neutron absorbed. Such a change could be expected if the fission cross section follows the $1/v$ law in the thermal region, whereas the capture process decreases with increasing energy of the neutrons less rapidly than according to the $1/v$ law. A quantitative estimate shows that an effect of the order of magnitude required to explain the observations is not out of the possibilities. Further work will be required in order to check on this possible explanation.

184.

THE UTILIZATION OF HEAVY HYDROGEN IN NUCLEAR CHAIN REACTIONS

Columbia University Report A–554
(Memorandum of Conference between Prof. E. FERMI and Prof. H. C. UREY on March 6, 7, and 8, 1943).

After a preliminary discussion of the general situation, we proceeded to a detailed consideration of available reports. The following were examined:

B–119 FENNING, F. W., KOWARSKI, L., and SELIGMAN, H. *Production and Absorption of Neutrons in Media Containing* U *and* H.

B–8 HALBAN, H., and KOWARSKI, L. *Study of Density Distribution of Thermal Neutrons in Widely Extended Media in View of Determination of Capture Cross-Sections.*

A–134 HALBAN, H., and WIGNER, E. P. *Possibility of a Resonance Absorption in Carbon.*

HALBAN, H., KOWARSKI, L., FENNING, F. W., and FREUNDLICH, H. F. *Evidence for the Disintegration of Deuterium by Fast Neutrons.*

B–29 HALBAN, H., and KOWARSKI, L. *Evidence for a Potentially Divergent Nuclear Reaction Chain in a System, below the Critical Size, Containing U and D.*

B–28 HALBAN, H., and KOWARSKI, L. *Technological Aspects of Nuclear Chain Reactions Used as a Source of Power.*

B–118 FENNING, F. W., and SELIGMAN, H. *Capture Cross-Sections of* N, Mg, S, *Ca and* Pb.

UREY, H. C., MURPHREE, E. V., and HALBAN, H. *Discussion on the Use of Uranium with Slightly Increased Content of Isotope 235.*

Most relevant for our discussion is Report B–29, in which Halban and Kowarski bring forth evidence that is interpreted by them as proof that a system containing a homogeneous mixture of U_3O_8 and D_2O may give rise to a divergent chain reaction.

Report B–8 by the same authors describes measurements on the absorption cross sections of oxygen, carbon and deuterium.

Report B–119 is a study of the chain reacting properties of systems containing uranium and natural hydrogen performed by a technique similar to that used for report B–29. Although this work is not in itself relevant to our discussion, we considered it important from the methodological point of view.

The report *Evidence for the Disintegration of Deuterium by Fast Neutrons*, discusses some evidence for the existence of $(n, 2n)$ processes, that may possibly increase the reactivity of deuterium containing systems.

CRITICAL REVIEW OF IMPORTANT PAPERS.

B–29. *Evidence for a Potentially Divergent Nuclear Reaction Chain in a System, below the Critical Size, Containing* U *and* D, by HALBAN and KOWARSKI, Dec. 1940. This paper describes work performed at the end of 1940, using about 112 liters of heavy water mixed with variable amounts of U_3O_8 powder inside an aluminum sphere of 60 cm diameter, which was surrounded by a liquid hydrocarbon. A source of neutrons was placed at the center of the system and measurements of neutron intensity were taken at various distances from the center, using Dysprosium detectors. The volume integral of the activity of these detectors is measured in the hydrocarbons surrounding the sphere, with and without the uranium heavy water mixture inside. The authors find an increase in this integral of the activity when the heavy water and uranium mixture is present. The observed increase is 6 ± 2 percent for a mixture of 380 atoms of deuterium to one of uranium, and 5 ± 1.5 percent for a mixture of 160 atoms of deuterium to one of uranium.

The authors develop a theory of their experiment and arrive at the equation

$$\nu_\infty - 1 = (q_{ext} - 1)\frac{1-p}{q_{int}}$$

where ν_∞ is the reproduction factor for an infinite amount of mixture (k in American notation), q_{ext} is the ratio between the integrals of the activity outside with and without heavy water uranium mixture inside the sphere, q_{int} is the ratio between the number of thermal neutrons absorbed inside the sphere, and the number of neutrons emitted by the primary source, and p is the fraction of neutrons absorbed at resonance by uranium during the slowing down process in an infinitely extended medium. [$(1-p)$ in the current American notation].

Some objection can be raised as to the validity of this formula, since it does not take into account neutrons which are slowed down outside the sphere, and subsequently absorbed within it. In a note at the end of the paper an attempt is made to take this effect into account. No justification is given, however, for neglecting, in the computation of the flow of neutrons across the boundary, the contribution of subresonance neutrons which have not yet reached thermal energies, and would not therefore be detected by the dysprosium detectors. Possible errors may also have been introduced in the results by the use of relatively thick dysprosium detectors, both on account of the fact that such detectors appreciably lower the neutron intensity in their neighborhood, and to the fact that dysprosium probably does not absorb according to the $1/v$ law. We were unable to make a judgment of the reliability of the conclusions obtained in this paper. Only the final results of a complex computation is given without any indication of the actual experimental data on which this is based.

In the report B–119, published by Fenning, Kowarski and Seligman, about two years later, the authors have become keenly aware of the possible errors of the technique used previously, and make some attempt to introduce corrections. Unfortunately, these new measures refer to properties of systems containing natural hydrogen and the old measurements on heavy water have not been repeated with similar improvements. Furthermore, the results are made somewhat indefinite by the lack of information on the purity of the uranium oxide used, and on the amount of light water present in the D_2O. Use of purer materials should improve the results.

Report B–8 deals with a method for the determination of absorption cross-sections of carbon, oxygen and heavy water. These measurements were performed at various times during 1940. We do not believe that more than the order of magnitude of these quantities can be inferred from this paper. The authors give a value for the cross-section of carbon which they believe is in error by only a few percent because of the limited size of the absorbing material which they used. Calculations which can now be made on the basis of experiments carried out in this country show that the error made was not so small as they state, but amounted to a factor of about two-thirds. Correcting, accordingly, their value for the cross-section of carbon turns out to be about half the accepted value today. Similar criticisms apply to the work on the cross-section of oxygen where the system used was even considerably smaller. Since the technique used was in both cases the same, we do not feel that the given values for the cross-sections of oxygen and of deuterium can really be trusted.

An interesting suggestion is offered in the paper *Evidence for the Disintegration of Deuterium by Fast Neutrons.* Some evidence is given in this paper, for the existence of an $(n, n\,2)$ reaction produced by fast Ra+Be neutrons colliding with D. Similar experiments are at present being repeated in Chicago. It is doubtful whether this $(n, 2\,n)$ process can actually be a very important factor in the chain reactions with heavy water. Indeed, only a small percentage of the neutrons emitted in the fission process has energy above the threshold (3.3 MeV) at which this reaction becomes energetically possible. Since a large fraction of the Ra+Be neutrons has energy much greater than the fission neutrons, it is doubtful whether any conclusion on their behavior can be applied in a reliable way to the case of fission neutrons.

Evidence for the reactivity of uranium-heavy hydrogen systems from other sources.

The same methods that are applied for the calculation of carbon-uranium systems, may be used for a general discussion of the behavior of uranium-heavy water systems. Calculations have actually been performed both on homogeneous and heterogeneous mixtures. The data entering into these calculations are:

(a) The number of neutrons emitted per thermal neutron absorbed by uranium. The value $\eta = 1.32$ has been taken for this number. From the well-established results on the reactivity of carbon-uranium systems, it

appears very improbable that η should be appreciably larger than this value.

(b) The absorption cross-section per molecule of heavy water has been taken as 8×10^{-27}. This is the value given in the Halban and Kowarski paper previously reported. We have already expressed some doubts as to the accuracy of this number, which has been used nevertheless for lack of better information. It is possible that the actual cross-section may be with about equal probability smaller or larger, in which case the reactivity of the system would be, respectively, larger or smaller than calculated. If the cross-section of heavy water or of oxygen were appreciably larger than the value used here, one could still use the theoretical results given for a system in which the slowing down medium is a deutero carbon of an approximate composition CD_2 and the cross-sections assumed in this calculation would apply very closely to such a system.

(c) The experimental information available to us does not permit a very reliable estimate of the fraction of neutrons absorbed at resonance in the case of a homogeneous system. The calculation has been performed using results published in H. L. Anderson's thesis.

A summary of the results of the calculations follows. For a homogeneous system, the best value of the reproduction factor occurs for a system containing 16 % in weight of uranium, and is $k = 1.02$.

In a heterogeneous system of uranium metal and heavy water, the best value of the reproduction factor is $k = 1.20$ for uranium metal lumps having a radius of about 2 cm, with a weight ratio of heavy water to uranium metal between 2 and 3. The estimated critical volume corresponding to these conditions is about 7 cubic meters, which could possibly be reduced further by suitable reflectors, e.g. ordinary water placed around the system.

In a system of aluminum pipes containing UF_6 embedded in heavy water the reproduction factor calculated with suitable allowance for the loss due to the aluminum pipes, is $k = 1.11$. This value is obtained for pipes of about 10 cm diameter and 2 mm wall thickness disposed in a square lattice of about 25 cm spacing. The critical volume corresponding to this case is about 20 cubic meters, which again could be somewhat reduced by suitable reflectors.

In spite of the fact that the theory applied here is entirely analogous to that of the carbon-uranium systems for which we have now a rather reliable experimental evidence, we do not feel that the preceding results are equally trustworthy. We have already mentioned the considerable uncertainty as to the absorption properties of oxygen. Additional uncertainties are due to the possibility that $(n, 2n)$ reactions or production of photo-neutrons in deuterium, may contribute appreciably to the reaction. The best estimates that we can make of such contribution indicate that they are not likely to be very important. There is, however, very little experimental evidence in support or against such a conclusion. It should be noticed further that the results given for the homogenous mixture are less reliable than the others, since we have no experimental evidence as to the behavior of homogeneous systems for carbon-uranium mixtures.

Summary of the evidence.

The comparison between the experiments of Halban and the theoretical expectation for the case of a homogeneous mixture indicates a very serious disagreement. Halban and Kowarski conclude that ν_∞ (or our k) for homogeneous system is $1.18 + 0.07$, whereas the theory would lead to a value of only 1.02. Unfortunately neither theory nor experiments are free from serious objections, so that we are not in a position to reach a conclusion that may be trusted. If the experimental results of Halban are right, a homogenous system containing a few tons of heavy water would be reactive. If this is the case the engineering advantages involved in the use of such a simple system would be so great as to warrant a much more serious effort on the heavy water production. If, on the otber hand, the theoretical estimates are correct, a homogeneous system if possible at all, would be almost prohibitively large. Even assuming a sizeable error in the pessimistic sense in the estimated valuc of the reproduction factor for this case, the critical amount would be of the order of 100 tons of heavy water. On the other hand, it appears to us that no matter what the conclusions are concerning the properties of homogencous systems, the possibilities of heterogeneous systems are very promising. Attractive features of these systems are their small size, the obvious advantage of the hexafluoride system, and some simplifications in the engineering features.

Recommended experimental program for the immediate future.

The present state of uncertainty as to the possibilities of heavy water could be somewhat improved by further experimental work, using amounts of this material available at present. If new experiments should confirm Halban and his co-workers, a considerable shift in the emphasis on the heavy water program might result.

It would be very desirable that the original experiments of Halban and Kowarski performed more than two years ago, be repeated, with improvements in technique that are now possible, both as to purity of materials and detecting devices. After this, consideration should be given to incorporating a uranium-heavy water mixture in the pile at Chicago. A test of the change of the reactivity of the pile would give a valuable indication of the behavior of the system.

A final test of the usefulness of heavy water must wait for the production of some tons of heavy water. Plans for the experiments should be laid well in advance and preparations made so as to have the results shortly after the arrival of the materials.

185.

THE SLOWING DOWN OF NEUTRONS IN HEAVY WATER

Report CP–530 (March 19, 1943).

ABSTRACT.

Numerical calculations of the sloving down range of neutrons in heavy water based on the results of cross-section measurements.

* * *

The recent measurements of J. H. Williams (Report CF–597) on the cross-sections of various elements for neutrons of energy up to 6 Mev enables one to make a somewhat better estimate than had been possible so far of the slowing down properties of heavy water for neutrons. The knowledge of the slowing down properties is important since they are one of the elements that enter in the calculation of the critical size of a heavy water plant.

In this report, the mean square distance, $\overline{r^2}$, for the slowing down of neutrons has been calculated numerically. $\overline{r^2}$ is related to the slowing down range r_0 by the relationship:

$$r_0^2 = \frac{2}{3}\overline{r^2} \tag{1}$$

$\overline{r^2}$ is given approximately by the following expression:

$$\overline{r^2} = \int_{E_1}^{E_0} \frac{2\lambda^2(E)}{1 - \overline{\cos\vartheta}} \frac{dE}{El} \tag{2}$$

where λ is the mean free path for neutrons of energy E; $\overline{\cos\vartheta}$ is the mean value of the cosine of the angle between the direction of motion of the neutron before and after a collision; l is the average change of the logarithm of the energy due to a collision.

The mean free path in heavy water is given by:

$$\lambda = \frac{29.85}{2\sigma_D + \sigma_0} \tag{3}$$

where σ_D and σ_0 are the cross sections of the deuterium and oxygen expressed in units of 10^{-24} cm^2.

For a collision of a neutron with an atom of atomic weight A, one finds:

$$\overline{\cos\vartheta} = \frac{2}{3A}. \tag{4}$$

This formula is valid on the assumption that the scattering is isotropic in the system of the center of gravity. We shall assume in the present report that this is the case.

Since the probabilities of collision against deuterium and oxygen are proportional to $2\,\sigma_D$ and σ_o, one finds:

$$\overline{\cos\vartheta} = \frac{\frac{2}{3}\sigma_D + \frac{1}{24}\sigma_o}{2\,\sigma_D + \sigma_o} \tag{5}$$

and

$$\frac{1}{1-\overline{\cos\vartheta}} = \frac{48\,\sigma_D + 24\,\sigma_o}{32\,\sigma_D + 23\,\sigma_o}. \tag{6}$$

In a collision against an atom, the average change in the logarithm of the energy is:

$$1 - \frac{(1-\alpha)^2}{2\,\alpha}\log\frac{1+\alpha}{1-\alpha} = \begin{cases} 0.725 & \text{for D} \\ 0.120 & \text{for o} \end{cases} \tag{7}$$

where $\alpha = 1/A$.

We find, therefore, for heavy water:

$$l = \frac{1.45\,\sigma_D + 0.12\,\sigma_o}{2\,\sigma_D + \sigma_o}. \tag{8}$$

Substituting these values in (2), we find:

$$\overline{r^2} = \int_{E_1}^{E_0} F(E)\,\frac{dE}{E} \tag{9}$$

where

$$F(E) = \frac{1}{(32\,\sigma_D - 23\,\sigma_o)(1.45\,\sigma_D + 0.12\,\sigma_o)}. \tag{10}$$

Table I gives the values used for the cross sections and for the function F in various energy intervals.

TABLE I.

E (in eV)		$\sigma_D \times 10^{24}$	$\sigma_o \times 10^{24}$	F (cm^2)
1	63000	3.3	3.8	42.3
63000	126000	3.3	4.1	40.5
126000	251000	3.3	4.4	38.9
251000	501000	3.3	5.2	35.1
501000	10^6	3.2	2.5	54.1
10^6	2×10^6	2.8	2.5	66.7
2×10^6	4×10^6	2.2	2.5	95.7
4×10^6	8×10^6	1.3	1.3	291

The values of the integral (9) taken for the energy interval from 1 to E electron volts are given in Table II.

The values from Table II are plotted in the diagram of fig. 1. The abscissa gives the energy in a logarithmic scale. The curve is split for convenience into three sections and the values of the energy are indicated on each section.

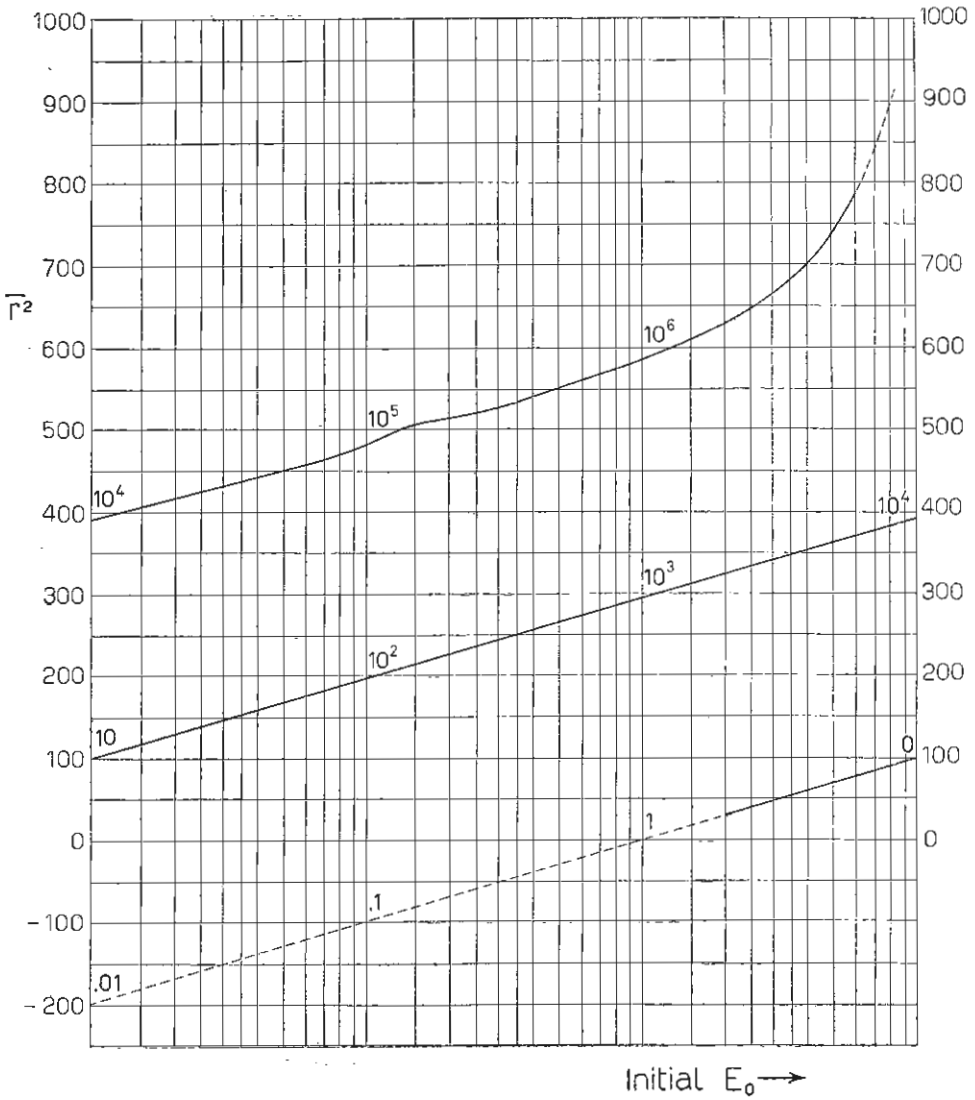

Fig. 1. – Curve gives $\overline{r^2}$ (E, 1 ev) in cm² for slowing down in D_2O.

With the help of this diagram, we can immediately calculate $\overline{r^2}$ for the slowing down of neutrons from an initial energy, E_o, to a final energy, E_1. $\overline{r^2}$ is given by the difference of the ordinates of the curve corresponding to the two values E_o and E_1 of the energy.

TABLE II.

E	$\overline{r^2}(1, E)$
1	0
63000	468
126000	495
251000	522
5×10^5	547
10^6	584
2×10^6	630
4×10^6	696
8×10^6	897

If we take, for instance, 2×10^6 ev as initial energy and 0.1 ev as final energy we find:

$$\overline{r^2}(0.1, 2\times10^6) = 630 - (-100) = 730 \tag{11}$$

corresponding to a slowing down range:

$$r_0 = \sqrt{\frac{2}{3}\overline{r^2}} = 22.0 \text{ cm.} \tag{12}$$

It should be noticed that the validity of these results is limited by the fact that the scattering has been taken as isotropic in the system of the center of gravity of the two colliding particles.

N° 186–188.

The original West Stands Pile, named CP–1 (chain reacting pile number 1) had a short life. After three months its uses had been explored sufficiently to know how to rebuild it with many improvements. The building at the Argonne site was now complete and a whole group of young and eager engineers from du Pont had been sent to Chicago for indoctrination in the new art. These were immediately put to work stacking graphite bricks so that by the middle of March the rebuilt pile CP–2 had reached criticality at Argonne.

There was an important assignment connected with the Argonne pile: this was to design and test a suitable radiation shield for the production piles that were to be built at the so-called " Site W, " Hanford, Washington, as mentioned in paper N° 187. For this work it would not have been essential to standardize the pile, but Fermi nevertheless insisted on doing a rather complete job of this. He wasn't happy unless he had control of and could account for, in a quantitative way, the behavior of all the elements that entered into his experiments. Fermi's role in the standardization of the pile is recordeded in the report of Anderson's group, paper N° 188.

In this group was Miss Leona Woods, who became one of Fermi's frequent collaborators. In the summer of 1943 she married John Marshall, a member of the same group.

Report CP–641, of which papers N° 187 and 188 are excerpts, was issued also as A–627.

H. L. ANDERSON.

186.

SUMMARY OF EXPERIMENTAL RESEARCH ACTIVITIES

Excerpt from Report CP–570 for Month Ending April 17, 1943.

ARGONNE PILE.

The construction of the chain reacting pile at the Argonne Laboratory is almost completed. Work is still going on to finish the shielding of the top and the north side of the pile and to complete the regulating and the safety mechanisms. When all the rods are out, the new pile has a reproduction factor of the order of 1.004, corresponding to a reactivity about eight times greater than the pile at the West Stands. Consequently, the period of rise of intensity is much shorter, being now about 8 seconds instead of about 100.

A series of measurements has been performed during the construction of the top layers of the pile in order to establish as accurately as possible the relationship between the period and the excess reproduction factor. These experiments are described in the report by Zinn and Anderson. It is hoped that the pile will be ready for operation at the end of the week.

CYCLOTRON GROUP.

The Cyclotron Group has been primarily concerned with the completion of a series of experiments which will be described in the CF reports. Besides this activity, a number of irradiations have been given for various chemistry groups.

EXPONENTIAL AND SIGMA PILES (*).

The activity of this group has been devoted to a standardization of the detectors used in the exponential experiments performed at Argonne. Attention has been given in particular to the possibility of improving the resonance neutron standardization of a cadmium covered indium detector by taking differences with and without a boron absorber. This has the purpose to eliminate as much as possible the perturbing influence of high resonance levels of indium. The results actually indicate a sizable perturbation due to these levels for the points close to the source.

This group is now ready to undertake a series of exponential experiments with a lattice cell of 8'' side and varying amounts of metal. As soon as the metal rods will be available, the group will undertake a measurement on the lattice to be used in the water-cooled plant.

(*) " Sigma piles " were graphite piles used to measure the absorption cross section of the graphite. (Editors' note).

N° 187.

For the introduction to this paper see N° 186.

187.

SUMMARY OF EXPERIMENTAL RESEARCH ACTIVITIES

Excerpt from Report CP-641 for Month Ending May 10, 1943.

ARGONNE PILE.

The construction of the chain reacting pile at the Argonne Laboratory is now completed and the pile has been operated for short times up to powers of about 140 KW. At this power output the heating of the lumps is at the rate of several degrees per minute and can be measured very easily.

The shielding of the pile, 5 feet of concrete on all sides except the top which is shielded with about 40 inches of wood and 4 inches of lead, proves to be quite adequate for physiological protection even when the pile is operated at the highest possible output. From the point of view of protection, considerable care must be exercised when materials are extracted from the pile after an intensive irradiation.

The main limitations to the operation of the pile at high energy are due to the necessity of avoiding too intensive heating of the lumps and accumulation of inconvenient amounts of fission activities.

The program of metal testing with the pile is already underway and metal testing will be carried out one day every week, on Wednesday.

Some preliminary standardization work has been carried out and experiments have been performed in order to test the effectiveness of the pile shield. (Work has been started on the test of an iron shield for the pile at site W (*) and it is expected to be completed in about one week).

EXPONENTIAL PILES.

Mr. Morrison has succeeded Mr. Froman in the leadership of this group.

Work has been completed on the standardization of the detectors. The group has been engaged on a series of exponential experiments with a lattice

(*) War time name for Hanford, Washington (Editors' note).

cell of 8 inches side and with increasing amounts of metal. The first of these experiments using four 1–inch cubes of metal per lump has been completed. This program has subsequently been interrupted in order to perform the exponential tests on the lattice of the water cooled pile. This experiment is now in progress.

Miscellaneous experiments in nuclear physics.

Mr. Feld's group has been concerned with the investigation of the properties of a radium-boron neutron source. Data have heen collected on the slowing down of the neutrons emitted by this source in a graphite pile in order to obtain the ranges and to compare the number of neutrons emitted by this source with the number of neutrons emitted by a radium-beryllium source. The measurements on the number of neutrons emitted by the fast fission when the source is placed at the center of a metal sphere, already performed with the radium-beryllium source, have been repeated with the radium-boron source. The result indicates that the number of neutrons due to fast fission is in this case considerably less than for radium-beryllium neutrons. The difference is presumably due to the lower average energy of the neutrons emitted by the radium-boron source.

Cyclotron group.

Most of the activity of the Cyclotron Group has been devoted to irradiations for various chemistry groups. Work has been started on fast neutron counters on the construction of a better spectrometer. An investigation of the emission of delayed neutrons and of the γ rays emitted subsequent to the thorium fission is in progress.

N° 188.

(See also introductions to papers 186–188).

In the spring and summer months of 1942 a number of newly graduated students, mainly from Columbia and Chicago, went to enlarge the ranks of the Metallurgical Laboratory. As one of them, I worked with Fermi on the graphite pile, saw its completion and early operation, and took part in the first experiments with it. The pile was then moved to the Argonne site, and our group began working there. Our first task was to calibrate the pile, as related in this paper.

The relationship in our group was informal from the start. While we worked in Chicago, it became a pleasant rule to go everyday for a swim in the late afternoon off the breakwater at the edge of Lake Michigan. On Sunday afternoons we would go on a bike ride or walk in the forest preserve where later on the Argonne laboratory was built. If there were laboratory visitors they came along.

On these occasions, Enrico liked to show superendurance, to swim farther, to walk farther, to climb farther with less fatigue, and he usually could. In the same way he liked to win at throwing the jacknife, pitching pennies, or playing tennis, and usually he did. These qualities of gaiety and informality of his character made it easy for the young members of the laboratory to become acquainted with him. He was an amazingly comfortable companion, rarely impatient, usually calm and mildly amused.

On hikes and swims we talked about wind and waves, geophysics, origins of the solar system, novas and supernovas, and the physical world. Rather markedly Enrico did not spontaneously like to talk politics and economics, nor about philosophy and the humanities, and rarely could be invited to join in such discussions. Also the visual fine arts had no particular attractions for him. For example, once when he had unenthusiastically gone along to an exhibit of portrait painting, he spent the time making a statistics of relative length of legs to total body height for people of the eighteenth century.

In the hours of relaxation away from the laboratory, his conversation was seldom pedagogical; instead he told of things that amused him as relaxed free association brought them to his mind. He sketched his ideas qualitatively and briefly so that one caught the image and felt a desire for deeper understanding. The same quality of brevity extended as well to his serious teaching, in that he strongly and colorfully described the main principles, but rarely filled in the details. In this way the student felt both excited by Fermi's broad view-point but also tantalised by a desire to understand a great many newly glimpsed problems.

While collaborating in experiments Enrico was flexible and openminded to suggestions. He said he had less technical experience than experimentalists and on this account he flatteringly assisted them rather than they him in preparing the equipment. But in the later stages of an experiment he led the way in crystallizing the concepts of what quantities were measurable and meaningful.

In data analysis he was especially impressive. For example, he insisted that integrals could be evaluated numerically in less time than it takes to look them up in a table, and he drove his colleagues to lightning slide rule manipulations to feed numbers to his speedy integration on a desk computer. He was learning to use the big computers at Los Alamos in the last year before he died and had already made them as useful to his purposes as his desk computer.

L. MARSHALL.

188.

STANDARDIZATION OF THE ARGONNE PILE

H. L. ANDERSON, E. FERMI, J. MARSHALL, and L. WOODS

Excerpt from Report CP–641 for Month Ending May 10, 1943.

(1) THE LINEAR INTENSITY.

The intensity at which the Argonne pile operates is measured by means of a galvanometer connected to a BF_3 ionization chamber. Due to the effects of saturation in the ionization chamber the deflection of the galvanometer is not proportional to the intensity throughout the range over which it is desired to make measurements. At low intensities the response is linear but at high intensities the galvanometer reading becomes proportional to the square root of the intensity. A linear scale for the galvanometer was determined by permitting the intensity of the pile to rise exponentially at a fixed period. The period was determined from observations taken in the region of linear response, from which the intensity corresponding to the higher galvanometer readings could be found by extrapolation. The following relation serves to convert galvanometer readings to linear intensity:

$$\mathrm{LI} = \mathrm{GR}\,(1 + 3.56 \times 10^{-4}\,\mathrm{GR}).$$

The relation holds reasonably well up to galvanometer readings of 50,000 cm.

(2) THE GOLD MONITORS (W. STURM).

The integral of the intensity of the pile is followed by means of gold monitors. Gold foils are placed in a fixed position conveniently located inside the cement shield during all irradiations. These foils are measured by means of a Lauritsen electroscope and from their activity the integrated intensity can be obtained. These foils were calibrated against the galvanometer scale by operating the pile at a given linear intensity for a known length of time, and then observing the activity induced in the gold. The activity of the gold in divisions per hour reduced to the end of the irradiation is related to the linear intensity as follows:

$$\mathrm{LI} \times \mathrm{seconds} = 6000 \times \mathrm{Au\ div/hr}.$$

(3) THE NEUTRON DENSITY.

Our standard indium foils were irradiated in the center of the pile and also in a certain standard position just inside of the shield so as to obtain the relation between the indium activity and the linear intensity. Thus, it appeared that

$$\text{Standard Indium counts/min} = 2400\ \mathrm{LI}$$

$$\text{Center Indium counts/min} = 1.13 \times 10^5\ \mathrm{LI}.$$

These are indium activities taken without cadmium. From the indium foil calibrations it follows that for the number of neutrons passing across one square centimeter per second in the center of the pile

$$nv = 1.13 \times 10^4 \, \mathrm{LI}$$

and for the slowing down density

$$q = 24.6 \ \mathrm{LI}.$$

(4) The power output.

The power output of the pile may be calculated by considering that the number of neutrons which are captured per second in the cell is q times the volume of the cell (8850 cm^3). Of these the fraction f_T (thermal utilization = 0.87) are captured by the lump and of these the fraction 0.59 produce fissions and release 2×10^8 ev of energy. Thus, for the central cell the power is 3.57×10^{-6} LI in watts. The effective number of cells is 6,127. The power output is given by:

$$\text{watts} = 0.022 \ \mathrm{LI}, \qquad \text{therefore: } nv = 6.14 \times 10^5/\text{watt}.$$

The power output has also been observed more directly by observing the rise in temperature of a lump by means of a thermo-couple during an irradiation. Such measurements gave somewhat larger power yields than that calculated above. As a rough rule for calculating the power output we use:

$$\text{watts} = \frac{\mathrm{LI}}{40}, \qquad \text{therefore: } nv = 4.52 \times 10^5/\text{watt}.$$

(5) Control rod calibration.

The period is the most direct measure of the reactivity of the pile. Due to the effect of the delayed neutrons, however, the relation between the reciprocal of the period and the excess effective reproduction factor $\delta k = (k_{\mathrm{eff}} - 1)$ is now a linear one. Since the relation between the reciprocal of the period and δk is not too well known, it is more accurate to introduce a new unit which is proportional to δk and equal to the reciprocal of the period for small values of this quantity. This unit is the inhour and it is the amount of reactivity which gives the pile a period of one hour. The relation between the inhours and the period has been obtained from the measurements of period during the construction of the Argonne pile and from the use of Snell's data on the delayed neutron periods. This relation is:

$$ih_{\mathrm{crit}} - ih = \frac{64}{\tau} + \frac{245}{\tau + 3.57} + \frac{688}{\tau + 10.1} + \frac{1938}{\tau + 34.5} + \frac{665}{\tau + 83}.$$

In order to calibrate the control rod in inhours, the critical condition was determined and the period was measured at various positions of the control rod. These data may be reduced to inhours by using the formula given above and making appropriate corrections for the changes in pressure. In addition,

the neutron intensity in the control rod slot was measured by means of copper foils. The square of the copper foil activity is proportional, in first approximation, to the sensitivity of the control rod in inhours per centimeter. The proportionality constant is determined by integrating this differential curve from the zero position to the position at which the period determinations were made. The ratio:

$$\frac{ih\,(x)}{\int_0^x \mathrm{A}^2\,dx}$$

is found to be substantially constant as indicated in the Table below:

TABLE I.

Control Rod	τ	Press	ih (740 mm)	$\int_0^x \mathrm{A}^2\,dx$	$ih\,(x) \Big/ \int_0^x \mathrm{A}^2\,dx$
439.33	—	741.1	0	0	—
360	62	—	39.47	89	0.443
330	37.1	—	54.92	123	0.447
300	24.5	740.9	70.20	158	0.444
250	14.3	740.6	92.75	214	0.433
200	9.8	740.6	110.19	255	0.432

TABLE II.

Control Rod	$\frac{d\,(ih)}{dx}$	ih
0	0.000	0.0
50	0.023	0.7
100	0.067	2.7
150	0.158	8.2
200	0.299	19.5
250	0.418	37.8
300	0.492	60.7
350	0.520	86.0
400	0.490	111.5
450	0.402	133.7
500	0.281	151.2
550	0.142	161.3

In Table II the sensitivity of the control rod and also the inhours is given for various control rod positions given in centimeters as indicated on the control rod dial. The relation between δk and the inhours was obtained from the data on the periods during the construction of the pile as reported in the previous monthly report is taken to be:

$$\delta k = 3.04 \times 10^{-5}\, \delta ih.$$

The pressure effect from the data taken on CP–1 is:

$$0.323 \text{ ih/mm Mg}$$

and the temperature effect from CP–1 data is:

$$0.814 \; ih/^{\circ}\text{C}.$$

In terms of the older unit used with CP–1

$$1 \text{ cinch} = 0.8135\, \delta ih.$$

From those data it would appear that the period of the Argonne pile with all rods removed will be about six seconds and the effective reproduction factor corresponding to this condition will be about 1.004.

The standardizations which are reported above are still considered to be tentative and in the course of the following month they will be checked by various methods. This will represent the principal effort of Group IV in May. In addition, it is planned to carry on experiments on the fast neutron effect by using separated 238 isotope.

N° 189 and 190.

First priority for the Argonne pile was to solve problems which came up in connection with the design of the Hanford plant (Site W). The June report mentions the completion of the design and testing of a suitable shield. A regular program of uranium metal testing was set up and tests were made of control rods and the neutron characteristics of the lattice. But the pile had a pet feature in which Fermi had a particular interest: the thermal neutron purification unit, that is, a graphite column set up on the top of the pile in which thermal neutrons could be found, now in quite substantial intensity and essentially free from those of higher energy. This was the " thermal column " which almost all subsequent experimental piles were to incorporate.

Report CP–718, of which paper 190 is an excerpt, was issued also as A–893.

H. L. ANDERSON.

189.

TESTS ON A SHIELD FOR THE PILE AT SITE W

E. FERMI, W. H. ZINN
Report CP–684 (May 25, 1943).

We have just completed a preliminary analysis of the data obtained in the shield experiment. From this data it is possible to set forth a reasonably satisfactory prescription for the pile at site W.

In the table attached, the number of neutrons and γ's coming from various parts of the particular iron and paraffin sandwich type shield which we used are given. These materials were placed above 70 cm of dead graphite.

The thickness of materials given in the right hand column indicates the total thickness of Fe or of paraffin for the measurement in question. For the experimental shield a reduction in γ radiation of 5.4×10^7 was observed. We have reason to believe that in increasing the thickness of Fe from 10.2 cm to 30.6 cm, an additional reduction of neutron intensity of only a factor of 2 may be expected. This would mean a total reduction in neutron intensity of 3×10^8. These figures refer to a sandwich shield having the composition given in the last line of the table.

If we assume that the W pile will operate at 250,000 kw and if we wish to know the radiation hazard for an 8–hour day, the figures would have to be multiplied by 7×10^9.

Assuming that 10^9 γ–rays are equivalent to an R of radiation, this sandwich gives for the W pile 0.14 R per 8–hour day. The number of neutrons is 3.5×10^7 per cm^2 per 8–hour day.

These results for the γ and neutron radiation escaping from the W pile should be reduced somewhat due to the fact that the W pile is considerably larger than the Argonne and hence the radiation will be spread over a larger area. This reduction factor could amount to as much as 2. In view of the radiation figures, it seems advisable to recommend that an additional hydrogen layer be introduced into the last 30 cm of Fe. The effect of this layer will be similar to that of the two previous ones and should make this shield quite adequate.

The particular way in which the hydrogenous material is distributed throughout the Fe is not believed to be critical. It might, for instance, be more practical to use more and thinner layers of hydrogenous material. It is necessary, however, to use a fairly substantial thickness of Fe in the first part in order that thermal and dissociation troubles be avoided in the first hydrogen layer. In this conviction, it is fortunate that Fe is an effective absorber of thermal neutrons.

If instead of hydrogen a material such as pressed wood or masonite is used, the hydrogen layer would be somewhat increased in thickness. If we assume that masonite contains 6 percent hydrogen and has a density of 1.3 gm/cm² the thicknesses given would have to be multiplied by about 1.5.

Shield Thickness & Composition (Thickness in cm)	Neutrons/cm²/sec/kw	γ-rays/cm²/sec/kw
0	1.7×10^6 (mostly thermal neutrons)	1.08×10^6
7.6 Fe	1.1×10^4	3.8×10^5
26.7 Fe	1100 (mostly fast neutrons)	3400
26.7 Fe + 19 CH_2	30 (mostly thermal neutrons)	2700
26.7 Fe + 19 CH_2 + 7.6 Fe		470
26.7 Fe + 19 CH_2 + 18.1 Fe	0.3 (mostly fast neutrons)	47
26.7 Fe + 19 CH_2 + 18.1 Fe + 15.2 CH_2		40
26.7 Fe + 19 CH_2 + 18.1 Fe + 15.2 CH_2 + 10.2 Fe	0.01	4
26.7 Fe + 19 CH_2 + 18.1 Fe + 15.2 CH_2 + 20.4 Fe		0.3
26.7 Fe + 19 CH_2 + 18.1 Fe + 15.2 CH_2 + 30.6 Fe		0.02

190.

SUMMARY OF EXPERIMENTAL RESEARCH ACTIVITIES

Excerpt from Report CP–718 for Month Ending June 12, 1943.

Argonne pile.

Work has been completed on the test of a composite shield of iron and paraffin. The results of this investigation have formed the basis for the design of the shield to be used in the pile at site W.

Measurements have been performed in order to determine the absorption cross section of oxygen and deuterium. Oxygen was introduced into the pile in the form of CO_2, and deuterium in the form of D_2O. Both experiments indicate a considerably smaller cross section for oxygen than had been so far assumed. An attempt to check on the cross section of oxygen by using beryllium oxide has not given constructive results so far due to some impurity introduced into the oxide.

The cross section of O^{18} has been newly measured by determining the activity of O^{19} formed by neutron capture. The result is in substantial agreement with the one obtained in the West Stands.

A test has been made for determining the relative effectiveness of control rods of different cross section: cylinder, cross, and plate.

Some investigation has been conducted on the radioactive gases that emanate from the pile. Most of the activity is due to gas emanating from pressed oxide lumps. Appreciable activity is also directly induced in air, primarily due to the activation of the atmospheric argon.

The usual program of testing of metal lumps has been regularly carried out during the month. The possibility of the use of the pile for testing of graphite has also been investigated with the result that it appears easily possible to determine absorption cross sections of graphite with a sensitivity of the order of magnitude of 1 percent using samples of the order of 50 or 100 kilograms.

The thermal neutron density across a lattice cell has been determined in order to obtain an experimental measurement of the disadvantage factor.

A series of measurements have been performed using the thermal neutron purification unit on top of the pile. The test has indicated that all epithermal neutrons are removed to a very great extent, so that cadmium ratios of the order of 20,000 have been observed with indium foils. The thermal neutrons escaping from the column have been used to produce a beam for

the measurement of cross sections. Certain irregularities in the results obtained in this investigation have led to the observation that neutrons of energy apparently much lower than thermal neutrons can be filtered out of such a beam using a graphite scatterer. These very slow neutrons have in most cases cross sections very substantially different from the cross sections for normal thermal neutrons; in particular, the increases by a factor between 3 and 4. It is expected that such large variations of the cross sections for neutrons of very low energy will have a considerable bearing on the discussion of the dependence of the reproduction factor on the temperature of the pile. The details of these investigations are given in the reports of Zinn, Weil, Anderson and Marshall.

Exponential piles.

Mr. Morrison's group has completed the exponential piles for the test of the reproduction factor in the "W" lattice with and without water in the pile. A test has also been conducted to determine the effect of adding some small amount of boron in the water in order to obtain a direct measurement of the migration length of the neutrons in this lattice.

Cyclotron group.

The time of the Cyclotron Group has been primarily taken by irradiations for the Chemistry and Health groups. Besides this work an investigation has been conducted of the absorption cross section of argon and the comparison of the global decay curves of thorium and uranium fission products has been extended to a longer interval of time.

N° 191.

Studies with the thermal column led directly to a new discovery. The neutrons emerging from this new facility did not have the correct energy distribution at all. There was a preponderance of very low energy neutrons. The effect was rather quickly traced to an interference effect of the Bragg type with neutrons. Such behavior had been anticipated in a theoretical paper by G. C. Wick (« Phys. Zeits. », *38*, 403 (1937)). Neutrons of sufficiently long de Broglie wave lengths could pass through the graphite lattice virtually unimpeded by scattering. Neutrons would have an important application in the study of crystal lattices.

This work is described in paper N° 191, which was first circulated as part of reports CP–718 (for month ending June 12, 1943) and CP–781 (for month ending July 10, 1943). It was also issued as document MDDC–54 by the Atomic Energy Commission, Technical Information Branch, Oak Ridge, Tennessee. This paper was also reported by me to the 1946 International Conference on Low Temperatures and Elementary Particles held at Cambridge, England. It was included in the report of this conference published in 1947 by the Physical Society of London.

H. L. ANDERSON.

191.

PRODUCTION OF LOW ENERGY NEUTRONS BY FILTERING THROUGH GRAPHITE (*)

H. L. ANDERSON, E. FERMI, and L. MARSHALL
Metallurgical Laboratory, University of Chicago, Chicago, Illinois

(Received September 19, 1946)
« Phys. Rev. » *70*, 815–817.

Neutrons of energy much lower than thermal were prouced by filtering a beam of thermal neutrons through a block of graphite 23 cm long. In such a block, Bragg scattering removes the neutrons whose wave-length is less than the largest Bragg wave-length in graphite, 6.69 angstroms. Measurement of the boron absorption of the filtered neutrons showed that they had an effective wave-length of 7.15 angstroms which corresponds to neutron temperatures around 18° Kelvin. The cross section of graphite for the filtered neutrons is 0.70×10^{-24} cm^2. That a part of this is caused by the incoherence due to thermal agitation of the atoms of the crystal was demonstrated by heating the crystal and observing the increase in this cross section. The filtered neutrons were used to show interference effects in other substances such as Be, Bi, and S. In water a fourfold increase in the scattering cross section of hydrogen due to chemical binding was observed.

A simple method to produce a beam of neutrons having average energy much lower than that corresponding to room temperature is described in this paper. The method consists in filtering ordinary thermal neutrons through a

(*) This paper is a result of work performed under contract W–7401–eng–37 with the Manhattan Project at the Metallurgical Laboratory, University of Chicago.

long and narrow block of graphite which, as will be shown, scatters out of the beam all the neutrons except those of very low energy.

On top of the graphite chain reacting pile which was constructed at the Argonne Laboratories, a graphite column was constructed with base 5′ × 5′ and 7′ high. The column rose above the pile through a hole in the shield which covers the whole of the chain reacting pile. In such a column the fast neutrons emitted by the pile are slowed down in the lower part of the column so that predominantly only thermal neutrons diffuse upward in the column. Thermal neutrons purified to a high degree from higher energy neutrons are obtained in this way.

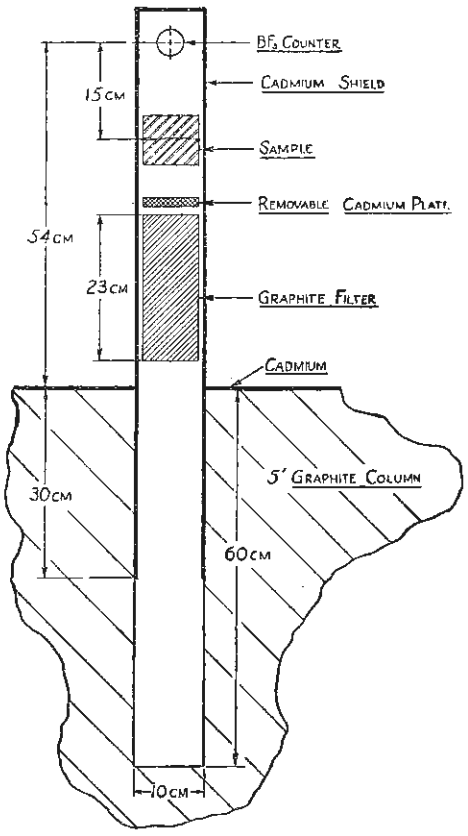

Fig. 1. – Arrangement of apparatus.

Attempts were made to measure the cross section of boron for neutrons emerging from the top of this column. We obtained 867×10^{-24} cm²/atom, a result considerably greater than the value 770×10^{-24} cm²/atom when a somewhat shorter column was used. These results indicated that lower energy neutrons penetrate more readily through large thicknesses of graphite than do the neutrons in the upper energy part of the Maxwell distribution.

In order to investigate this effect in a more systematic way a good beam geometry was set up as shown in fig. 1. To increase the intensity and yet maintain good collimation, the neutrons used were those emitted from the lower part of a hole extending two feet down in the graphite filter (which was removable) and then through the sample whose transmission it was desired to measure and finally to a BF_3 proportional counter used as a detector. The whole assembly was isolated from stray thermal neutrons by the cadmium shield. A cadmium plate could be inserted above the graphite filter in order to measure the background. In all measurements the small background observed with this cadmium plate in place was always subtracted.

Measurements by the transmission method were made of the total cross sections of a number of substances with and without the 23-cm long graphite filter. The results are given in Table I.

The first column gives the sample, the second its thickness in grams/cm², the third and fourth columns give the logarithm of the transmission and the total cross section σ in units of 10^{-24} cm²/atom obtained without the filter, while the fifth and sixth columns give the same quantities for neutrons which were filtered through 23 cm of graphite.

The marked decrease in the scattering cross section of graphite from 4.05×10^{-24} cm^2/atom to the value 0.70×10^{-24} cm^2/atom is quite striking. With the filter the log of the transmission of the Pyrex plates (boron) increase by a factor of 3.5. This corresponds to a reduction of energy by a factor of more than 12 for the neutrons which emerge from the graphite filter.

TABLE I.

Transmission of filtered neutrons.

Substance	g/cm^2	No filter		23-cm graphite filter	
		Log transmission	σ in 10^{-24} cm^2/atom	Log transmission	σ in 10^{-24} cm^2/atom
C (graphite)	12.96	2.639	4.05	0.453	0.70
Pyrex	0.241	0.437		1.537	
Be	4.52	0.977	3.25	0.219	0.73
Be	9.04	1.693	2.82	0.424	0.71
$^1/_2$ D_2O	4.352	2.008	7.65	2.475	9.44
$^1/_2$ H_2O	0.455			2.61	85.8
$^1/_2$ H_2O	0.265			1.461	82.5
Bi	76.39	1.469	6.68	0.226	1.03
S crystalline	19.91	0.617	1.66	1.08	2.89
S amorphous	8.02	0.530	3.52	1.063	7.06
S amorphous (next day)	8.02			0.497	3.31

Since graphite is a polycrystalline material, Bragg reflection scatters all neutrons whose wave-length is smaller than the two times the largest lattice spacing. (1) The low energy neutrons are transmitted through the filter because their wave-length is larger than the largest lattice spacing in graphite crystals. Interference takes place in all directions except the straight through direction for such neutrons.

A calibration of the Pyrex plates used in these experiments was carried out by E. Bragdon, E. Fermi, J. Marshall, and L. Marshall who determined their transmission as a function of neutron velocity, using a mechanical velocity selector. In order to obtain the average velocity of neutrons by a measurement of transmission in boron, some assumption has to be made about the velocity distribution of the neutrons, in order to take into account the hardening of the beam in its transmission through the Pyrex plate. For the neutrons emerging from the hole in the graphite column a Maxwell distri-

(1) W. M. ELSASSER, «Comptes rendus», *202*, 1029 (1936). G. C. WICK, «Physik. Zeits.», *38*, 403 (1937).

bution may be assumed and the correction for hardening can be made using the Bethe [2] correction. In this way we found that the kT energy of the neutrons from the hole was 0.023 ev, about 10 percent less than what corresponds to room temperature. The difference being presumably caused by a partial filtering of the neutron coming from the hole.

For the neutrons which filtered through 23 cm of graphite the transmission data with the Pyrex plate gave an effective neutron velocity of 533 meters per second. This corresponds to an effective neutron wave-length of 7.15 A. By effective wave-length we mean the wave-length we would measure if all the neutrons had the same velocity. For graphite the largest Bragg wavelength is 6.69 A. Our result for the effective wave-length is higher than this because of the contribution of the low energy tail of the Maxwell distribution. With a longer filter we obtained an even larger effective wave-length which showed that for our 23 cm filter the filtering was not yet complete.

TABLE II.

Temperature effect on the scattering of filtered neutrons by graphite.

Temp. of scatterer °C	Total cross section in 10^{-24} cm²/atom
20	0.71
69	0.84
117	0.97
254	1.33
370	1.92

Similar crystal effects were observed in Be and also in Bi in spite of the fact that both atoms have a nuclear spin different from zero.

In the case of water a fourfold increase in the cross section over the value [3] 21×10^{-24} cm² measured at 1.44 ev (indium resonance) was observed as was to be expected from the effects of chemical binding. [4] The effect of chemical binding is presumably also responsible for the increase in the cross section of D_2O.

Sulphur proved interesting. Sulphur prepared in the amorphous state gave a cross section of 7.06×10^{-24} cm² for the filtered neutrons, a value twice as high as the value obtained for the same sample with the unfiltered thermal neutrons. This increase is believed caused by the cooperative scatter-

(2) H. A. BETHE, « Rev. Mod. Phys. », 9, 136 (1937).

(3) H. B. HANSTEIN, « Phys. Rev. », 59, 489 (1941).

(4) E. FERMI, « Ricerca Scient. », 7, 13 (1936). H. A. BETHE, « Rev. Mod. Phys. », 9, 127 (1937).

ing in aggregates of sulphur atoms with dimensions small compared to the neutron wave-length. In such aggregates of n atoms the scattering is proportional to n^2 rather than to n. The next day the same specimen, having partially crystallized, showed a smaller cross section.

To show the effects of the thermal motion of the atoms in a crystal on the interference conditions, the scattering cross section for 15.4 g/cm^2 of graphite was studied with filtered neutrons as a function of temperature of the scatterer. The scatterer was heated with an oxyacetylene torch and the temperature measured using a thermocouple. Temperature equilibrium was not perfectly established in these experiments but the effect is evident. The results are given in Table II. These experiments show clearly that the thermal motion of the crystal atoms tends to destroy the interference conditions.

N° 192.

By summer 1943 the work at the Argonne site was in full swing. The concerted effort in which all those of us working with Fermi had joined in order to make the chain reaction idea a reality was now behind us. Fermi's " gang " had begun to separate, each taking up smaller tasks according to his inclination and competence. Formally, in the organization chart of the Metallurgical Laboratory, there were always groups. Thus, Walter Zinn, George Weil and I were, formally, Group Leaders. We each had our assistants who helped us in what we had to do. Now our tasks had become more distinct, and the separation became evident also in the way Fermi began to think of us. In his monthly reports we were referred to as Zinn's group, Weil's group, Anderson's group, etc. These and Marshall's Group did their work at the Argonne site, while Arthur Snell, Philip Morrison and Bernard Feld remained at the University.

As Director of the Physics Division, Fermi did not include in his report the activities of the Theoretical Section, which was under E. P. Wigner, but let Wigner write the summary for the groups working more directly with him.

As long as he collaborated closely with his group, Fermi put some enthusiasm in writing his monthly summaries of their work. As his connection with them became less direct, he resisted more and more taking credit for what they were doing. Those who wanted to know what was going on would have to look elsewhere than in Fermi's summary.

Report CP–781, of which this paper is an excerpt, was issued also as A–973.

HERBERT L. ANDERSON.

192.

SUMMARY OF EXPERIMENTAL RESEARCH ACTIVITIES

Excerpt from Report CP–781 for Month Ending July 10, 1943.

ZINN'S GROUP.

Absorption cross-sections of various gases, nitrogen, argon, boron, helium and hydrogen, have been determined by a measurement of the danger coefficient. A research has been conducted also to determine the activity induced in the various gases and to correlate the values of the activity to the values of their absorption cross-sections. Of particular interest in this respect is the activity induced in air, which apparently is due essentially to the argon content in the air. Commercial helium also shows a trace of activity, which is probably due to a small argon impurity. When air is extracted from the pile, an appreciable gaseous activity due to recoil and diffusion of fission products is also observed.

WEIL'S GROUP.

During the past month 110 lots of metal were tested.

The studies on the use of the pile for graphite testing have been completed hy experimental calibration of the effect of the graphite density.

The loss of reproduction factor due to the aluminum coatings of the "Hot Dogs" (*) has been determined.

The density distribution of the thermal neutrons across a cell has been measured and particular attention has been given to the determination of the drop in intensity across the gap surrounding the metal lumps.

The effect of beryllium has been investigated by placing some amount of Be in some experiments near a lump and in some other experiments far from the lump. The results indicate that beryllium is about equivalent to graphite when placed far from the lump, whereas there is an appreciable increase in the reproduction factor when the beryllium is near a lump. This seems to indicate a positive contribution of the n, $2n$ reaction in beryllium.

ANDERSON'S GROUP.

An attempt has been made to determine experimentally the contribution of the fast neutron fission to the reproduction factor in the pile. This has been made by comparing the fission activities in a sample of normal uranium and in a sample of uranium from which most of the 235 isotope has been removed. The result indicates a surprisingly high fast neutron effect which is actually somewhat larger than the upper limit for the effect that had been considered theoretically.

The investigation on the properties of the very slow neutrons filtered through graphite has been extended to a few more elements and it has been found that the low scattering cross-section found for graphite at room temperature increases appreciably when the graphite is heated.

A program of research is in progress to determine activation cross-sections of various elements by thermal neutrons.

MARSHALL'S GROUP.

Preliminary results on the comparison between the numbers of fission and capture processes in uranium as a function of the temperature of the neutrons in order to determine the so called η–effect, seem to indicate that the effect has a sign opposite to the one that would be needed in order to explain the dependency of the reproduction factor of the pile on the temperature.

The scattering cross-sections of various elements for indium and iodine resonance neutrons have been determined. The results may be used for a calculation of the slowing down power of these elements.

(*) The short uranium metal cylinders encased in aluminum that were being fabricated for the Hanford piles were at first colloquially called "hot dogs." (Editors' note).

SNELL'S GROUP.

The studies of the fission products responsible for the emission of delayed neutrons have been conducted with the result that the carriers of the 24 sec and 57 sec delayed neutrons are probably halogens. Determination has been made of the neutron capture cross-section for argon from a measurement of induced activity. The result is by about a factor of 2 larger than the similar result found by Zinn's group.

An investigation has also been made of the activities induced in lead.

MORRISON'S GROUP.

The migration length for the water cooled lattice has been determined by measuring the Laplacian when boron contaminated water was flowed through the lattice.

The Laplacian has been determined for a lattice of uncoated rods of 1.62 cm radius. The result applies directly to the calculation of the metal testing pile as is planned at site W.

The diffusion length in graphite containing channels has been investigated.

Further work is in progress to extend the information as to the values of the Laplacian as a function of the weight of the metal lumps and to determine the slowing down properties of beryllium.

FELD'S GROUP.

The spectra of the neutrons emitted in the fission process and by a Ra–Be and a Ra–B source have been compared by determining the ratio of activities induced in various fast neutron detectors. It was found that the Ra–B source has a spectrum appreciably closer to that of the fission neutrons than the Ra–Be source.

The investigation on the inelastic scattering cross-sections of bismuth, lead and iron have been extended.

193.

RANGE OF INDIUM RESONANCE NEUTRONS FROM A SOURCE OF FISSION NEUTRONS

E. FERMI and G. L. WEIL

Excerpt from Report CP-871 for Month Ending August 14, 1943.(*)

A rough estimate of the slowing down range of fission neutrons was obtained in the following manner. CdInCd activities were measured at three positions in the thermal purification column on the top of the pile when the pile was operated similarly for the two cases: (a) "Hot dog" at base of thermal column; (b) "Hot dog" removed. The results are given in Table I, where column 1 gives the distance in cm of the foil from the center of the "Hot dog"; column 2 the CdInCd activity (corrected to the end of the irradiation) with the "Hot dog" in position; column 3 the "background" with the "Hot dog" removed, and column 4 the net CdInCd activity due to fission neutrons from the "Hot dog."

TABLE I.

r cm	CdInCd "Hot Dog" in position	CdInCd Background	Net CdInCd
10.2	10,759	64	10,695
30.5	5,103	36	5,067
50.8	1,182	8	1,174

These data can be fitted with a Gaussian curve having a range $r_0 = 33$ cm. The actual value may be slightly larger since the value of the intensity observed at $r = 50.8$ cm is perturbed by the fact that this point is fairly close to the end of the column. The experiment shall be repeated with a taller column as soon as possible.

In the case of lamp black, however, the cross section for the unfiltered neutrons is found to be not only considerably higher than that of graphite, but also its value rose from 11 to 14.8 when filtered neutrons were used. This increase may be explained by supposing that the lamp black atoms are arranged in clusters whose dimensions are small compared to the wave

(*) Report CP-871 was issued also as A-1156 (Editors' note).

length of the neutrons. Since the atoms are not arranged in a regular way, destructive interference will not take place. Instead, the neutron waves of the scattered radiation will be in phase and the intensity of the scattering will then become proportional to the square of the number of atoms in a cluster rather than to the first power of this number as would be the case for smaller neutron wave lengths. The increase in the scattering cross section observed for paraffin and for D_2O is believed due to the effects of chemical binding. For uranium the increase is due to the increase in the absorption for lower energy neutrons. This increase is smaller than for boron because of the more important role played in uranium by the scattering.

TABLE II.

Substance	gm/cm²	No Filter		23 cm Graphite Filter	
		Log T	σ	Log T	σ
Paraffin	0.1244	0.626	58.4	1.117	104
Paraffin	0.2992	1.425	55.3	2.390	92.7
Be	4.52	0.977	3.25	0.219	0.73
Be	9.04	1.693	2.82	0.424	0.71
Graphite	12.96	2.637	4.05	0.453	0.70
Lampblack	1.69	0.936	11.0	1.260	14.8
Pyrex	0.241	0.437	—	1.537	
U	17.5	0.697	15.7	1.390	31.4
D_2O	4.352	2.008	7.65	2.475	9.44

The measurement of the boron cross section was also made using a paraffin filter of 3.8 cm thickness. The result was 368 cm²/mole, indicating that neutrons which penetrate through paraffin emerge with a higher average energy. From paraffin filtered neutrons to graphite filtered neutrons the energy is decreased by a factor of 25. This should be useful in studying the variation in nuclear cross sections for slow neutrons of different energies. These effects reopen the question of what is the value of the boron cross section for the neutrons of a given energy. It is planned to resolve this difference by measuring boron cross section for indium resonance neutrons, the energy of which has been measured to be 1.44 ev. In addition an attempt will be made to use the monochromatic radiation which may be obtained by Bragg reflection from a crystal.

N° 194.

In April, 1942, H. C. Urey had argued in favor of heavy water as neutron moderator instead of graphite. This had some obvious advantages but it did not appear that enough of it could be made in time to merit changing the original plan to use graphite. However, enough production was set up at Trail in British Columbia to make possible the construction of an experimental reactor. It was this P–9 pile, later called CP–3 that Zinn and his group began to design at Argonne with Fermi's encouragement. It would have much more power than CP–2 and very much extend the experimental possibilities.

In this paper and in those following " P–9 " is the code word for heavy water.

Report CP–1016, of which this paper is an excerpt, was issued also as A–1411.

H. L. ANDERSON.

194.

SUMMARY OF EXPERIMENTAL RESEARCH ACTIVITIES

Excerpt from Report CP–1016 for Month Ending October 23, 1943.

The plans for the construction of the P–9 pile at the Argonne Laboratory are being pushed ahead by Zinn's group with the collaboration of Vernon's group. The procurement of several items needed for the pile is already underway and part of the concrete shield has already been poured by the contractor of the new Argonne building. Besides this activity Zinn's group has devoted some attention to the problem of developing and testing measuring and safety equipment for the operating piles. Experiments have been conducted on safety devices containing a bimetallic strip in which one of the metals is uranium. Under the effect of irradiation the uranium heats up and the bimetallic strip bends, opening the contact.

The behavior of ionization chambers and thermocouples has been followed over a rather long period of time. The general conclusions are that a boron coated ionization chamber has kept its sensitivity unchanged for a period of about two months, during which it has never been exposed to very intensive irradiation. The boron coated thermocouple has proved so far satisfactory and has not given any indication of a change in sensitivity.

An experiment has been initiated by Anderson's group for the direct determination of the amount of product produced per kw–hr. Messrs. Seren, Moyer, Sturm and Miller, in Anderson's group, have carried out a very extensive survey of a cross section for the activation of 32 β activities. These cross sections will be useful in calculating the radioactivity induced in materials placed at various places within an operating pile.

Further measurements of cross sections for indium and iodine resonance neutrons have been performed by Marshall's group. Most significant among these measurements are the results obtained on uranium. The total cross section of this element at indium resonance energy (1.44 ev) is only 9.5×10^{-24}. Since about 1×10^{-24} is accounted for by absorption, this leaves a scattering cross section of only 8.5×10^{-24}. A peculiar behavior of the absorption curve observed for iodine resonance neutrons with uranium absorbers definitely indicates a partial overlapping of some resonance levels of these two elements. This overlapping should be taken into account in the interpretation of the Princeton experiments on the effective resonance cross section of uranium.

A new exponential pile with a very large graphite to uranium ratio has been constructed and is now being measured by Morrison's group.

This group has also standardized some sources for the Clinton Laboratories and performed some measurements of diffusion length.

The main activity of the group has been devoted to an attempt to investigate the dependence of diffusion length on the temperature. Unexpected difficulties make the interpretation of this experiment still somewhat obscure. The indications are, however, that the diffusion length varies with temperature less rapidly than one would expect on the basis of full thermal equilibrium and validity of the 1/v law.

Feld's group has been investigating the properties and number of photoneutrons of Ra–Be and Ra–D_2O. The group has been carrying out a survey of nine (n, α) and (n, p) reactions activated by uranium fission neutrons. Also, some sources recently acquired by the laboratory have been calibrated.

The Indiana University Project, directed by A. C. G. Mitchell, has investigated the resonance activities induced in uranium mixed with a varying amount of carbon. The main purpose of this experiment is to obtain elements for the calculations of the resonance loss in a homogeneous P–9 pile. The investigation will be extended to uranium hydrogen mixtures.

The activity of the Theoretical Physics Section is summarized by Mr. Young later in this report.

195.

SUMMARY OF EXPERIMENTAL RESEARCH ACTIVITIES

Excerpt from Report CP–1088 for Month Ending November 23, 1943.

Most of the activity of Zinn's group has been devoted to the planning and procurement for the P–9 pile. The concrete shield for this pile has been poured in the new building in construction at Argonne. The blocks of lead-cadmium alloy for the thermal shield are being cast. The procurement of the most critical items is underway and the delivery dates have been scheduled.

A measurement was performed of the slowing down range of delayed neutrons in graphite. The indium range of these neutrons is 30.7. This indicates that the energy of these neutrons is appreciably lower than the average energy of fission neutrons. An estimate based on this value of the range gives an average energy of about 600 kev.

Besides the routine activity of metal testing, M. Weil's group has performed measurements on the diffusion length of samples of Kendall, (*) Gulf Cleves (*) and Whiting (*) graphite. The results are in essential agreement with previous indications that the absorption of Kendall graphite is about 9 percent less than that of Whiting and the absorption of Gulf Cleves is about 4 percent less than that of Whiting. The Kendall graphite has, of course, an added advantage due to the considerably higher density.

The methods for graphite testing in the pile have been improved by a new calibration of the correction due to varying densities of the graphite samples used.

A preliminary survey has been made of the short period activities induced in water by the pile radiations. Indications have been found of a rather strong activity with a mean life of about 10 seconds, probably to be identified with N^{16}. The practical cross-section for pile neutrons seems to be about 10 times greater than the practical cross-section of activation of the 31 sec period of O^{19}. It is expected to study these activities more carefully in view of their importance in estimating the activity at the discharge end of the W pile during operation.

The Electronics Group has been recently organized by T. Brill and has devoted much attention to getting the laboratory fitted and a stock of materials assembled. In addition, this group has been improving the safety circuits of the Argonne pile and supplying the laboratory with a number of amplifiers and circuits.

(*) Name of a special brand of graphite. (Editors' note).

The efficiency of control rods in which neutrons are absorbed by water or by ammonia solutions has been investigated by Anderson's group. The results indicate that such rods are only about one half as efficient as a strip of Cd of a width somewhat less than the diameter of the pipe in which the water solution was contained.

Experiments have been performed to determine the concentration of neutrons near the tip of a control rod. The result is in essential agreement with the theoretical estimates that the number of neutrons absorbed in the rod near the tip increases by about a factor of 2.

The activation cross sections of several new isotopes have been measured.

The range of fission neutrons in graphite has been determined by Marshall's group by using a very small amount of uranium metal, so as to minimize the correction factors. An indium range of 35.6 cm was found.

Measurements have been performed on an enriched sample of uranium in order to determine the fission cross section and the value of ν. The results are $\sigma_f = 4.6 \times 10^{-24}$ for natural alloy and $\nu = 2.15$.

An extensive investigation on the capture cross-section of boron for thermal neutrons gives now as the most probable value 700×10^{-24} cm^2 for neutrons of 2200 meters per sec. velocity. The scattering cross-section of fluorine was measured and found to be 3.7×10^{-24} for indium resonance neutrons. The group performed also some measurements on gallium detectors. The resonance energy as determined from the boron absorption is about 100 volts.

Mr. Morrison's group has been working on experiments in order to determine the change of the diffusion length in graphite with temperature. The present indications are that the variations of the diffusion length with temperature are about 20 percent less than one would expect according to the elementary theory. This result reduces to some extent the discrepancies found in the interpretation of the temperature effect on the reproduction factor of a pile. It is only sufficient, however, to eliminate part of the discrepancy.

An extensive comparison has been performed by Feld's group on the activations of (n, α) and (n, p) processes by Ra + B, Ra + Be and fission neutrons. It appears that in most cases the fission neutrons show a behavior somewhat intermediate between those of Ra + B and Ra + Be sources.

196.

THE RANGE OF DELAYED NEUTRONS

E. FERMI and G. THOMAS

Excerpt from Report CP–1088 for Month Ending November 23, 1943.

A measurement of the slowing down range of neutrons in graphite was performed for the delayed neutrons emitted by a lump after a short and intensive irradiation inside the pile.

A uranium cylinder 6'' long and 1.26'' diameter, having the total mass of 2390 grams, was first placed in the center of the Argonne pile and given an irradiation with a period of about 15 seconds and a total energy of 2.05 kw. Immediately after the irradiation, the lump was withdrawn from the pile and placed on the axis of the $5' \times 5'$ column used for the standardization of sources. Standard In foils protected by Cd had previously been inserted in the column at proper intervals and the lump was placed in the column about 15 seconds after the end of the irradiation. The delayed neutrons emitted by the lump were slowed down in the graphite and activated the various indium foils. After a wait of a few minutes when the delayed neutron emission had ended, the foils were placed on a counter and the following activities observed.

Distance from the source (inches)	CdInCd Activity Counts per minute
4	61,900
12	21,830
20	3,355
28	315
36	44
44	5

The mean square distance, $\overline{r^2}$, at which the delayed neutrons attain indium resonance energy (1.44 ev) can be calculated by the numerical integration of the preceeding data. The result is $\overline{r^2} = 1416$ corresponding to an age $= \frac{1416}{6} \times 236$ and to a range $r_0 = \sqrt{\frac{2}{3} 1416} = 30.7$. This range is appreciably shorter than the range of fission neutrons which was found to be 35.6.

This indicates that the average energy of the delayed neutrons is appreciably less than the average energy of the fission neutrons. Using the relationship between range and energy given in CP–1084(*), we find the average energy of the delayed neutrons = 640 kilovolts.

(*) Paper N° 197. (Editors' note).

N° 197 and 198.

The great speed with which the work went forward under these wartime conditions of free spending and high quality leadership is indicated in the previous reports. The P-9 pile, a matter of talk in the preceding summer, had its shield complete in November in a new building. By the following August it was operating at rated power.

In the meantime, at Argonne, Fermi had recaptured many of the conditions of work which he liked best. His laboratory still had commitments in connection with the Hanford piles, but the questions of nuclear physics related to the piles, which had kept him busy in the past, were no longer the urgent ones. Pile engineering problems were being studied in other places. By late fall 1943 the center of the scene had shifted to Oak Ridge, Tennessee, then known as " Site X, " or " Clinton Engineering Works. " There, a pilot plant was built, not large enough to produce plutonium for a bomb, but sufficient for tests of the chemical separation of plutonium from uranium. There also, isotope separation plants were built, which at this time were already producing small amounts of uranium enriched in U^{235}. In Hanford, Washington, " Site W, " the du Pont Company was pushing construction of the piles for the production of plutonium following plans that were being prepared in Wilmington, Delaware, the du Pont's central office. In the laboratories at Los Alamos, New Mexico, known as " Site Y, " research on problems more strictly connected to the bomb was underway.

Thus, at the Argonne, 20 miles outside Chicago, Fermi could go back for a while to basic research, the work he enjoyed the most. The conditions were pleasant: there was a pleasant wood in which to walk, enthusiastic young people with whom to work, devoted followers able to help him build or otherwise obtain the apparatus he might want. In November and December he was doing experiments with the Marshalls. With them, he returned to experiments on the slowing down of neutrons in graphite, but this time he could perform them with the neutrons actually emitted in slow neutron fission. The pile provided the source of slow neutrons and a layer of uranium absorbed them and produced a true fission spectrum, with intensity adequate to permit accurate measurements (Paper N° 197). In December he took advantage of the new opportunities which had arisen once the isotope separation plants at Oak Ridge went into production. He now obtained samples of uranium greatly enriched in U^{235}. Even though these samples were small, they were adequate for improved measurements of the crucial neutron constants because for a source, Fermi now had the pile with its powerful thermal neutron column. (Paper N° 198).

Paper N° 197 was issued also as A–1475.

Paper N° 198 was issued also as A–1666.

H. L. ANDERSON.

197.

SLOWING DOWN OF FISSION NEUTRONS IN GRAPHITE

E. FERMI, J. MARSHALL and L. MARSHALL
Report CP–1084 (November 25, 1943).

ABSTRACT.

The slowing down range of fission neutrons from natural uranium in graphite has been measured. Its value reduced to graphite density 1.6 is 35.6 cm. A calculation of the same range based on the Bloch Staub spectrum of fission neutrons and on a calculated relationship between energy and range gives instead $r_0 = 34.3$.

* * *

A 293 gram cube of Westinghouse metal was placed 121.1 cm below the top of the thermal purification column of the Argonne pile. This column consists of 17 layers of graphite of average density 1.62, each 10.47 cm thick and is built above the top of the pile which has three more layers of dead graphite. Indium foils encased in cadmium boxes 0.102 inches thick were placed at distances approximately 10, 30, 50, 70, 90 and 110 cm from the cube. Since the activity of the 6 foils bombarded simultaneously varied over a range too wide for measuring, 4 foils were activated at a single time with low pile intensity in positions 1, 2, 3, 4 or with high pile intensity in positions 3, 4, 5, 6. The last foil, position 6, was protected by laying three additional layers of graphite on top of the thermal column. For each activation the pile intensity was run up on a 13.9 second period and scrammed at a definite intensity. The kilowatt hours were measured by observing the rise in temperature of a thermocouple in a metal lump in the pile. This method allows successive irradiations to be duplicated quite accurately. If only thermal neutrons were originally present in the column, the CdInCd activities would be due exclusively to the fission neutrons produced in the uranium cube. There is actually a background activity which is due to indium resonance neutrons not made thermal by the column. Its value was obtained by duplicating the measurement without the metal cube. The foils were read on two counters, Eeyore and Daleth, whose relative sensitivity is given by $\frac{\text{Eeyore}}{\text{Daleth}} = 1.248$. The activities were reduced to the same units and the background count was subtracted. The net activity was plotted against r^2 and interpolated values obtained. Using these, a numerical integration was made to obtain the mean square distance $\overline{r^2}$ for fission neutrons to become indium resonance neutrons.

Data On Counter Daleth Foil position cm (distance from cube)	CdInCd c/m			Background c/m
	I	II	III	
10.2	38,241	38,520	37,652	6,030
29.85	14,750	14,766	14,669	1,150
50.00	3,319	3,301	3,286	283
69.8	590	580	580	88
Temperature rise of lump in pile	0.46°	0.46°	0.45°	0.45° Average=0.455°

On Counter Eeyore Foil position cm (distance from cube)	CdInCd c/m			Background c/m
	I	II	III	
50.0		34,008	34,065	2,705
69.8	5,950	6,006	5,862	807
90.1	981	956	957	270
109.8	191	232	218	114
Temperature rise of lump in pile	3.85°	3.83°	3.85°	3.87° Average=3.85°

Interpolated Values cm	Activity net of background A CdInCd (Daleth)	$r^2 A \times 10^{-4}$	$r^4 A \times 10^{-7}$
0	35,100	0	0
10	31,700	317	32
20	22,100	884	354
30	13,100	1179	1061
40	6,620	1059	1694
50	2,970	742	1855
60	1,210	436	1570
70	480	235	1151
80	176	113	723
90	65.3	33	428
100	24.0	24	240
110	9.4	11	138
120	(3.6)	(5)	75
130	(1.35)	(2)	38
	(0.50)	(1)	19
	(0.18)		9
	(0.07)		4
	(0.025)		2
			1

Calculation of the range.

The column is sufficiently large so that the CdInCd activities measured on the axis are not perturbed appreciably by the effect of the sides. We calculate, therefore, the mean square distance from the cube with the formula:

$$\overline{r^2} = \frac{\int_0^\infty A r^4\, dr}{\int_0^\infty A r^2\, dr} = \frac{94{,}053 \times 10^7}{50{,}667 \times 10^4} = 1858 \text{ cm}^2.$$

We have further:

$$r_0^2 = \frac{2}{3} r^2 = 1237 \text{ cm}^2.$$

$$r_0 = 35.2 \text{ cm}.$$

The average stacking density of the graphite used is 1.62. The preceding value of the range can be reduced, therefore, to the normal value of the density 1.6 by multiplying by the factor 1.62/1.6. This gives the final result:

$$r_0 = 35.6$$

This value of the range corresponds to an age of 317 cm^2.

Number of neutrons emitted.

The total number of neutrons emitted by the lump during the irradiation can be calculated from the volume integral of the activation measured in the foil at various positions. A calibration of the standard indium foils measured on counter Daleth gives the following relationship between the slowing down density in graphite and the activity A_{Cd} of the foil protected by Cd, expressed in counts per minute at saturation:

$$q = 0.00143 \times A_{Cd}\,.$$

For a steady irradiation we could, therefore, obtain the number of neutrons emitted per second by the uranium cube by multiplying the volume integral of A_{Cd} by the factor 0.00143. Since our irradiation extends over a period of time very short compared to the life of indium, we obtain the total number of neutrons emitted during the burst by multiplying the volume integral of the initial activity of the foil at various positions by the factor 0.00143 and by the life time of indium expressed in seconds, namely, 4,674.

The number of neutrons emitted is, therefore:

$$4\pi A_{Cd} r^2\, dr \times 0.00143 \times 4674 = 4\pi \times 5.067 \times 10^8 \times 0.00143 \times 4674 = 4.26 \times 10^{10}.$$

The burst irradiation produced a temperature rise of 0.455°. Since a 1 kw-hr irradiation produces a temperature rise of 1.6°, the total energy of irradiation

amounted to 0.28 kw-hr. We conclude that the number of neutrons emitted by the lump in an irradiation burst of 1 kw-hr would have been 1.5×10^{11} or $\frac{1,5\times10^{11}}{3600} = 4.2\times10^{7}$ neutrons$\cdot$sec$^{-1}\cdot$kw^{-1}. If we assume the fission cross-section of uranium 4.6×10^{-24}, and we assume further that two neutrons per fission are emitted, we find that the cross-section for neutron emission of our lump weighing 293 grams is:

$$\frac{293\times0.602\times4.6\times2}{238} = 6.8 \text{ cm}^2.$$

If we neglect self-absorption, we find, then, the average flux of neutrons at the place of the lump by dividing the number of neutrons emitted per second by the cross-section of the lump, namely:

$$nv = \frac{4.2\times10^{7}}{6.8} = 6.2\times10^{6} \quad \text{per kw.}$$

This value of the flux is in agreement with values obtained by more direct estimates.

Comparison with theory.

The range of the fission neutrons in graphite could be calculated if the energy distribution of fission neutrons and the relationship between the slowing down range and energy of the neutrons were known. We denote by $\overline{r^2}(E)$ the mean square of the distance at which neutrons emitted with energy E attain indium resonance energy by slowing down in graphite. Let, further, $\Pi(E)\,dE$ give the number of fission neutrons emitted in the energy interval dE. We have, then:

$$\overline{r^2} = \frac{\int \overline{r^2}(E)\,\Pi(E)\,dE}{\int \Pi(E)\,dE}.$$

This expression has been calculated numerically by using for $\Pi(E)$ the energy spectrum measured by Bloch and Staub in (LA–17). The function $\overline{r^2}(E)$ has been recalculated using the carbon scattering cross-section measured by Williams. The following formula was used:

$$r^2(E) = 2\lambda^2(E) + 2\lambda^2(1.44_{ev}) + \frac{2}{0.158\times\frac{17}{18}}\int_{1.44ev}^{E}\lambda^2(E)\frac{dE}{E}.$$

The values for these two functions are given in the table, where the first column gives the energy expressed in Mev. The second column gives function $\overline{r^2}(E)$, and the third column gives $\Pi(E)$. This last column is taken from the data of Bloch and Staub up to the energy 3.2 Mev. The values beyond 3.2 Mev were extrapolated.

TABLE I.

E	r^2 (E)	(E)
0.1	1061	0.45
0.2	1157	0.60
0.3	1230	0.73
0.4	1290	0.84
0.5	1346	0.92
0.6	1398	0.97
0.7	1447	1.01
0.8	1491	1.03
0.9	1539	1.02
1.0	1580	1.00
1.2	1665	0.93
1.4	1748	0.84
1.6	1827	0.75
1.8	1917	0.65
2.0	2008	0.56
2.2	2090	0.47
2.4	2166	0.40
2.6	2236	0.33
2.8	2297	0.28
3.0	2350	0.23
3.2	2379	0.19
3.4	2387	(0.16)
3.6	2390	(0.13)
3.8	2415	(0.11)
4.0	2469	(0.09)
4.2	2480	(0.08)
4.4	2503	(0.06)
4.6	2564	(0.05)
4.8	2644	(0.04)
5.0	2743	(0.04)
5.2	2834	(0.03)
5.4	2917	(0.03)
5.6	3005	(0.02)
5.8	3085	(0.02)
6.0	3162	(0.01)

By a numerical integration we find:

$$\overline{r^2} = \frac{\int \overline{r^2}\,(\mathrm{E})\,\Pi\,(\mathrm{E})\,d\mathrm{E}}{\int \Pi\,(\mathrm{E})\,d\mathrm{E}} = \frac{3912}{2.213} = 1768$$

corresponding to a range

$$r_0 = \sqrt{\frac{2}{3}\,1768} = 34.3.$$

This value is somewhat smaller than the experimental value $r_0 = 35.6$.

N° 198.

For the introduction to this paper see N° 197.

198.

FISSION CROSS-SECTION AND ν-VALUE FOR 25(*)

E. FERMI, J. MARSHALL and L. MARSHALL
Report CP–1186 (December 31, 1943).

ABSTRACT.

The fission cross-section of U^{235} for thermal neutrons has been measured by transmission experiments. Its value for neutrons of velocity 2200 meters per second is 645×10^{-24} cm²/atom for pure U^{235} or 4.63×10^{-24} cm²/atom for natural uranium. The nunmber of neutrons produced per thermal capture of U^{235} has been found to be 2.14.

* * *

The fission cross-section of U^{235} for thermal (2200 meters/second) neutrons has been measured. The transmission of a sample A of U_3O_8 oxide in which the isotope 235 was enriched about 15 times was measured and compared with the transmission of a sample B of natural oxide containing an equal amount of U^{238}.. Neutrons coming from a hole in the thermal column of the Argonne pile were used. The average temperature of these neutrons was determined from the transmission of a Pyrex glass plate which had been calibrated with neutrons of known velocity from the velocity selector.

The same enriched sample was also used for the determination of the number, ν, of neutrons emitted per thermal fission of U^{235}. The changes in the critical position of the control rod were measured for (1) enriched oxide, sample A, (2) for the natural oxide, sample B, and (3) for a known weight of powdered Pyrex glass. ν can be calculated from these measurements, together with the previously measured transmissions.

DETERMINATION OF FISSION CROSS-SECTION.

The measurements were performed with three samples of U_3O_8 enriched by different amounts of U^{235}. Any such sample may be considered to contain B grams of natural oxide + C grams of pure $U_3^{235}O_8$. Then $B + C = A$,

(*) Code name for U^{235}. Similarly, 26 and 28 are code names for U^{236} and U^{238}. (Editors' note).

where A = weight of the enriched sample. Since the samples were not to be mixed, each one was enclosed in a separate aluminum can to protect it from absorption of atmospheric water vapor, and a duplicate can was prepared containing B grams of natural oxide, the weight contained by the enriched sample in the first can. The transmission, T_I, of the combined enriched samples, $A = (A_1 + A_2 + A_3)$, was compared with the transmission, T_{II}, of the combined amounts of natural oxide, $B = (B_1 + B_2 + B_3)$. The ratio T_I/T_{II} gives the transmission of the weight, $C = (C_1 + C_2 + C_3)$ of pure $U_3^{235}O_8$ and from this ratio the fission cross-section of U^{235} was determined. The weight B of natural oxide, equivalent to that contained in an enriched sample of A grams was calculated from the weight ratio R of U^{238} to U^{235} according to the formula:

$$M = \frac{140}{139} A \left\{ \frac{R}{R + 1.002} \right\}.$$

After the experiment was made, a new isotopic analysis of the 3 samples was communicated to us, indicating that the enriched samples had been compared with slightly more natural oxide than they actually contained. A correction on the log of the transmission has been applied for this error. The weights A of the enriched sample are given in the first column of the following table. The second column gives the original analysis,

$$R = \frac{wt\, U^{238}}{wt\, U^{235}};$$

the third column contains the calculated weights M of natural oxide contained in the enriched samples according to the first analysis. These amounts were actually used in the experiment. The 4th column gives the new analysis. The 5th column gives the weight, B′, of natural oxide which should have been used. The last column contains the amounts, C = A — B′, of separated $U_3^{235}O_8$.

A grams	$R = \frac{U^{238}}{U^{235}}$	B grams	R′	B′ grams	C: grams pure $U_3^{235}O_8$
I 5.7321	5.74	4.9326	5.56	4.8918	0.8403
II 10.8239	10.5	9.9860	9.70	9.8814	0.9425
III 10.2962	8.10	9.1875	7.72	9.1788	1.1174
Total-26.8522 . . .		24.1061		23.9520	2.9002

The transmissions were measured in a beam of neutrons from a hole 125 cm deep in the thermal column on top of the Argonne pile. The column is 17 layers of dead graphite, each layer about 10 cm thick, the lowest layer separated from the live pile lattice by 3 layers of dead graphite. Four counters containing BF_3 at 12.5 cm pressure were placed one above another at an average distance 146 cm above the hole. The cans containing the oxide were

supported midway between counters and the mouth of the hole. The beam of neutrons from the hole was collimated with Cd lined shields filled with B_4C. The counting rate, I_A, of the BF_3 counters was measured when the neutron beam was intercepted by sample A. The counting rate I_B was again measured, when the sample B, natural oxide, was in the beam. The small correction I_{Cd} due to epicadmium neutrons was measured and subtracted. The transmission of the 2.9002 grams of pure U^{235} is given by:

$$\frac{I_B - I_{Cd}}{I_A - I_{Cd}} = \frac{8717 - 165}{4758 - 165} = 1.862 .$$

The logarithm of the ratio of transmissions is

$$\log 1.862 = 0.621 .$$

The following corrections on the logarithm of the transmission should be made. The weight of natural oxide used contained an excess of 24.1061 — 23.9520 = 0.1541 grams, equivalent to 0.7819×10^{-24} moles/cm² of $UO_{8/3}$ (natural oxide). That is, the sample of natural oxide contained more natural U_3O_8 than was containcd in the total of enriched samples. The transmission of the samples of natural oxide then is too low, due to the extra oxide in the beam. On the other hand, the transmission of the enriched oxide includes the effect of scattering by U^{235} and by O. Assuming

$$\sigma \text{ scattering of } U^{235} = 8.5 \times 10^{-24}$$

$$\sigma \text{ total of natural uranium} = 16.3 \times 10^{-24}$$

$$\sigma \text{ scattering of O} = 4.1 \times 10^{-24}$$

one obtains for the correction terms respectively 0.001 and 0.017. The corrected logarithm of the transmission is

$$\log T = 0.621 + 0.001 - 0.017 = 0.605$$

for 0.001487 moles/cm² of $UO_{8/3}$ (U^{235} oxide). This figure was obtained from the area of the container, 7.022 cm², and the molecular weight of $U^{235}O_{8/3}$, 277.67 grams:

$$\frac{2.9002 \text{ grams}}{277.67 \times 7.022 \text{ cm}^2} = 0.001487 \text{ moles/cm}^2 \, UO_{8/3} .$$

Since the neutrons from the hole are not monoenergic, and assuming that the fission cross-section is inversely proportional to the neutron velocity, a Bethe correction must be applied.

$$\text{The Bethe correction} = \sqrt{0.980} = 0.990$$

$$(\log T) \text{ correction} = 0.990 \ (0.605) = 0.599 .$$

The calculated fission cross-section of U^{235} for neutrons from the hole in the thermal column then is found to be:

$$\sigma \text{ capture } U^{235} = \frac{0.599}{0.001487 \times 0.6023 \times 10^{24}} = 668 \times 10^{-24} \text{ cm}^{2/\text{mole}} .$$

Average temperature of neutrons from hole.

The effective temperature of the neutrons emerging from the hole is not equal to room temperature due to the long mean free path of very slow neutrons in graphite. It was necessary, therefore, to determine experimentally their effective energy in order to reduce the previous result to a definite velocity of the neutrons. This was done by comparing the transmission of two Pyrex plates of total thickness 0.483 grams/cm² for neutrons used in the previous experiment (neutrons from the hole, passed through the natural oxide sample B) with their transmission in the beam of the velocity selector.

For neutrons from the hole filtered through the sample of 24.1061 grams of natural oxide, the logarithm of the transmission of the two plates was ln T = 0.822. The transmission of the same plates was measured for neutron velocities, V, from 1800 to 4500 meters/second over the thermal neutron velocity selector, and the following equation was obtained:

$$\log T_{Pyrex} = \frac{(1.683) \times 10^3}{V} + 0.041$$

0.041 is a correction presumably due to scattering of thermal neutrons by Na, Si, O, et cetera, contained in the Pyrex glass.

After the log of the transmission of Pyrex over the hole is corrected for scattering, the Bethe correction may be applied:

$$0.822 - 0.041 = 0.781$$

$$\text{Bethe correction} = \sqrt{1.028}$$

$$(\log T) \text{ correction} = 0.781 \times \sqrt{1.028} = 0.792.$$

The average velocity of neutrons from the hole is directly obtained from the velocity selector equation and from the corrected log of the transmission over the hole:

$$V = \frac{1.683 \times 10^3}{0.792} = 2125 \pm 24 \text{ meters/second}.$$

It is convenient to correct the fission cross-section to 2200 meters/second corresponding to kT energy at 20.4° C:

$$\sigma_f U^{235} = 668 \times 10^{-24} \text{ cm}^2/\text{atom} \times \frac{2125}{2200} = 645 \times 10^{-24} \text{ cm}^2/\text{atom}.$$

For natural uranium the fission cross-section becomes:

$$\sigma_f (\text{natural U}) = \frac{645 \times 10^{-24}}{140} = (4.63 \pm 0.10) \times 10^{-24} \text{ cm}^2/\text{atom}.$$

Determination of the number ν of neutrons per thermal fission of U^{235}.

The samples of enriched oxide previously used in the transmission experiments were divided among 56 small aluminum dishes of about 3 cm diameter. A duplicate set of dishes was prepared containing an amount

of natural oxide equivalent to the total amount contained in the enriched samples. Either set of dishes was placed in receptacles in the blocks of a graphite stringer near the center of the pile. The distance between any two dishes was always greater than 6.5 cm. The critical position of the control rod was found successively for the enriched oxide and for the natural oxide. The measurements were repeated 5 times to improve the accuracy. The geometric position of the dishes was reproduced as nearly as possible for all measurements.

Critical positions were also determined for pure graphite dust and for pulverized Pyrex glass mixed with graphite dust. The materials were placed in the same aluminum lids in the same geometry. The glass was reduced to small particles with a steel mortar and pestle, pulverized in an agate mortar and sieved through 0.044 mm mesh (sieve 325). It was of such particle size and so distributed that the correction due to self absorption was no more than 1 percent. That the Pyrex powder contained no appreciable amount of adsorbed water was shown by the fact that its weight was unchanged after strong heating. The following table contains the observed data. The effect on the pile, of the various materials, is expressed in inhours.

2.9002 grams $U_3^{235} O_8$	$+ 1.321 \pm 0.018$ ih
2.9844 grams powdered Pyrex	$- 1.899 \pm 0.013$ ih.

Therefore, the weight of Pyrex whose influence on the critical position is equal in magnitude but opposite in sign to that of 2.9002 grams $U_3^{235} O_8$ is

$$2.9844 \times \frac{1.321}{1.899} = 2.0759 \text{ grams.}$$

From the transmission experiment the following values, corrected for scattering and corrected by the Bethe factor, were obtained:

Absorber	Corrected log Transmission
2.9002 grams $U_3^{235} O_8$ on 7.022 cm²	0.599
0.483 grams/cm² Pyrex plates	0.792

The weight of Pyrex having the same transmission as the $U_3^{235} O_8$ is given by:

$$0.4826 \text{ grams/cm}^2 \times 7.022 \text{ cm}^2 \times \frac{0.599}{0.792} = 2.5737 \text{ grams Pyrex.}$$

One may conclude from these data that when one thermal neutron is absorbed by the sample of U^{235} the reactivity of the pile changes as if

$$\frac{2.0759 + 2.5737}{2.5737} = 1.807 \text{ thermal neutrons were produced.}$$

If the neutrons produced in the fission process were thermal this number would be equal to ν. Since, however, the new neutrons produced in the fission process are fast, two correction factors must be applied to take into account:

(a) the fact that some of the new neutrons are captured at resonance while they are being slowed down to thermal energies. As usual we call p

the fraction of neutrons that is not absorbed at resonance. For the Argonne metal lattice $p = 0.87$. For this reason the value of ν must be corrected by a factor $\frac{1}{p} = \frac{1}{0.87}$;

(b) the fact that neutrons diffuse during the slowing down process away from the place where they have been produced. The correction factor due to this effect is:

$$1 + \frac{\tau}{\tau + \frac{\lambda\Lambda}{3}}(k - 1) = 1.031$$

where τ is the slowing down age of the neutrons ($\tau = 350\,\mathrm{cm}^2$) $\frac{\lambda\Lambda}{3} = 325\ \mathrm{cm}^2$ is the square diffusion distance of the thermal neutrons in the pile and $k = 1.06$ is the reproduction factor in the metal lattice of the pile where the measurement was performed.

With these corrections we obtain as final result:

$$\nu = 1.807 \times \frac{1}{0.87} \times 1.031 = 2.14.$$

199.

SUMMARY OF EXPERIMENTAL RESEARCH ACTIVITIES

Excerpt from Report CP–1175 for Month Ending December 25, 1943.

The design of the P–9 plant at the Argonne Laboratory has been completed in all details by Zinn's group. Work for the installation of the tank that will be delivered shortly has been started.

The metal testing group under George Weil has tested 133 lots of metal that were all found within the normal limits, and two lots of Gulf Cleves graphite which show the usual lower absorption with respect to the old types of AGOT graphite. In addition to this testing work, some further study has been performed on the short period activity in water. The results confirm the existence of a γ–radiation connected to the short period and indicate that the differences between distilled water and treated Columbia River water are negligible as far as the short lived activities are concerned. Some more work has also been performed on the study of the fine structure of the neutron density inside a cell.

The electronics group under Brill has been working on an improvement of the safety circuits of the Argonne pile, on the design of the control circuits for the P–9 pile, and on the construction of several amplifiers.

A direct determination of the yield of product for a given amount of energy developed in a pile has been completed in collaboration by Anderson's and Sugarman's groups. The results are given in Report CN–1190.

As a by-product of the same work, the energy release per fission was determined to be 210 Mev. It is planned to repeat experiments of this type in order to improve the accuracy of the results. Work has been continued by Anderson's group on the neutron yield for (α, n) reactions with polonium α–particles. A new and more complete list of these results is given in his report. Also, the studies of the cross sections for activation of radioactive isotopes by slow neutrons have been extended and a table including these results up to date is given in the report.

The purified helium to be used in the Hanford pile has been investigated in order to determine the danger of radioactive impurities. Some small activity due to presence of argon was detected, in addition to a small activity of about 20 min half life, whose origin has not yet been determined.

Marshall's group has been working on an attempt to determine the so-called η effect. It was recognized that the geometry used so far actually failed to give the desired difference in temperature between the neutrons

used in the comparison and a new geometry has been found that has the required properties. Also, some work has been performed on the absorption of uranium for gallium resonance neutrons.

Morrison's group has been getting ready for the exponential test on the latest edition of the W lattice. In addition to this, work has been performed on the technique of the σ pile measurements with special attention to the perturbation arising from the effect of the wall. Morrison's results give a cross section for Kendall graphite about 6 percent less than the one found for the standard AGOT graphite used in the first exponential experiment on the W lattice.

Feld's group is developing a technique for measuring the isotopic ratio of enriched alloy samples and has been collaborating with the physics section at Site X (*) in the work on the "Snell experiment."

(*) War time name for Oak Ridge (and Clinton), Tennessee. (Editors' note).

N° 200.

Another device made possible by the higher intensities available from the pile was a mechanical neutron velocity selector. Velocity selectors based on the Fizeau principle had been familiar to physicists for a very long time. In 1926 Stern [1] had proposed one of these selectors to measure molecular velocities. The apparatus was built by Lammert [2] in 1929. Later, when it was realized that neutrons had thermal velocities, confirmation was sought by mechanical experiments (see paper N° 92 *a* and *b*, Vol. I). A true velocity selector based on the Fizeau principle was first built by Dunning, Pegram, Mitchell, Fink, and myself [3] at Columbia University; it used cadmium shutters.

The increased neutron intensity due to the pile improved by orders of magnitude the attainable resolution with velocity selectors. The emphasis shifted from the desire of crudely demonstrating the velocity spectrum of neutrons to obtaining truly monochromatic beams for further experiments.

Fermi designed the velocity selector described in the following paper at Los Alamos, during a visit from Chicago, with some help from me. It was another example of Fermi's way of working: a discussion on the feasibility of the instrument led to a concrete plan developed on the spot: Fermi left Los Alamos with a detailed sketch of the apparatus, which was then built at Argonne. It had a rotating cadmium shutter and gave Fermi his chance to measure the boron cross section at a well defined neutron velocity.

Paper N° 200 was first circulated as *Measurements of the Cross Section of Boron for Thermal Neutrons* by E. Bragdon, E. Fermi, J. Marshall, and L. Marshall, Report CP–1098 (January 11, 1944). Under the same title as that of paper 200, it was also issued as MDDC–711. Although a note in the paper stated, hopefully, that the document would be reprinted in the Metallurgical Laboratory Physics Technical Series, it never was.

E. SEGRÈ.

200.

A THERMAL NEUTRON VELOCITY SELECTOR AND ITS APPLICATION TO THE MEASUREMENT OF THE CROSS-SECTION OF BORON

E. FERMI, J. MARSHALL, and L. MARSHALL
Argonne National Laboratory (*), *University of Chicago, Chicago* (**), *Illinois*
(Received April 25, 1947)
« Phys. Rev. », *72*, 193–196 (1947).

A mechanical velocity selector for the study of monochromatic neutrons in the range of energies below 0.3 ev is described.

The instrument has been applied to the measurement of the cross section of boron, which is found to be 703×10^{-24} cm^2 for neutrons of 2200 meters per second velocity.

(1) O. STERN, « ZS f. Phys. », *39*, 751 (1926).

(2) B. LAMMERT, « ZS f. Phys. », *56*, 244 (1929).

(3) DUNNING, PEGRAM, MITCHELL, FINK, and SEGRÈ, « Phys. Rev. », *48*, 704 (1935).

(*) The information contained in this document will appear in Division IV of the MPTS as part of the contribution of the Argonne National Laboratory.

(**) All three authors now at Institute for Nuclear Studies, University of Chicago.

INTRODUCTION.

Slow neutrons emerging from various moderators with different geometries usually have average velocities comparable, but by no means equal, to the thermal agitation velocity. Large differences, both positive and negative, are observed depending on the nature and the geometry of the moderating substance. This phenomenon has been observed by various experiments [4-7].

In this paper we have collected some typical examples of the variations of average velocity of slow neutrons using different moderators as indicated by changes in the apparent cross section of boron. Since boron is often used as a standard substance in slow neutron measurements, its cross section has been determined also by use of monochromatic neutrons obtained with a velocity selector of new design operated in connection with the thermal column of the Argonne graphite pile.

The observed temperatures of the neutrons emitted from the various moderators and arrangements of moderators appear to be in accordance with the individual arrangements employed. Within the experimental errors of the method, the cross section of boron varies as the $1/v$ law, and the measured cross section is 703×10^{-24} cm^2 per atom per neutrons of velocity 2200 meters per second.

TEMPERATURES OF NEUTRONS FROM VARIOUS SOURCES.

With the thermal purification column of the graphite pile at the Argonne Laboratory as a primary neutron source, a number of measurements were made of the cross section of boron. In all cases the detector was a proportional counter filled with BF_3 gas. By the use of cadmium diaphragms a neutron beam was obtained with small angular dispersion.

The absorber and detector in these experiments were both boron and consequently both obeyed the $1/v$ law of neutron absorption. It was possible, therefore, to use the correction method given by Bethe [8] to calculate the cross section of boron for mono-energic neutrons of energy kT where T is the absolute temperature of the Maxwellian distribution emitted from the source. Since the cross section of 2200 meters per second neutrons (kT at 293° K) is known, one can then determine the effective temperature of the neutron beam. It must be understood that these effective temperatures are based on the assumption that the neutron beam is Maxwellian in velocity distribution. This is certainly not strictly true for most sources employed.

The results of these experiments are given in Table I. It is quite clear from an inspection of the table that the effective temperature of the neutron

(4) J. RAINWATER and W. W. HAVENS, Jr., « Phys. Rev. », *70*, 136 (1946).
(5) W. W. HAVENS, Jr. and J. RAINWATER, « Phys. Rev. », *70*, 154 (1946).
(6) J. H. MANLEY, L. J. HAWORTH, and E. A. LUEBKE, « Phys. Rev. », *69*, 405 (1946).
(7) R. F. BACHER, C. P. BAKER, and B. D. MCDANIEL, « Phys. Rev. », *69*, 443 (1946).
(8) H. A. BETHE, « Rev. Mod. Phys. », *9*, 134 (1937).

beam depends strongly on the source of neutrons. During these experiments the temperature of the thermal column was in the neighborhood of 30° C or 303° K.

TABLE I.

Source of neutrons	Absorber	Cross section for kT neutrons (cm^2)	Effective temp.(°K)
1. Beam from surface of thermal column	Gaseous BF_3	$\sigma_B = 855 \times 10^{-24}$	198
2. Beam passed through a 3.7–cm slab of paraffin	Gaseous BF_3	598×10^{-24}	408
3. Beam passed through 7.6 cm. of heavy water at 33.7° C in a container 18-in. diam	Gaseous BF_3	Corrected to 20.4° C $\sigma_B = 710 \times 10^{-24}$	288
4. Beam passed through a 22 cm column of graphite 10 cm square	Pyrex plate calibrated in velocity selector	2800×10^{-24}	18.4
5. Beam from hole in thermal column 125 cm deep, 10 cm square . . .	Gaseous BF_3	701×10^{-24}	293
6. Beam from a "black hole" in thermal column, a hole 10 cm × 10 cm × 22 cm high connected to surface of thermal column by a 42–cm tube of cadmium of internal diam 2.5 cm	Gaseous BF_3	755×10^{-24}	255

The source arrangement given under case 1 produces low temperature neutrons because of the filtering action of the graphite in the pile and thermal column. [9] Very slow neutrons whose de Broglie wave-lengths are longer than periodicities encountered in the graphite crystals are scattered very little and can penetrate to the surface of the column more easily than the faster neutrons. In case 2 the slower neutrons are removed preferentially because both the absorption and scattering cross sections of hydrogen are larger and also because scattering in the forward direction is preferred at higher energy. Heavy water (case 3) acts somewhat in the same way because also for deuterium compounds the scattering cross section and the coherence of successive free paths vary with the energy in the same direction as for hydrogen compounds. Therefore, the effective temperature of the neutrons is raised from the initial 198° K to 288° K. The fact that this last temperature is quite close to the actual temperature of the heavy water probably is coincidental. In case 4 the filtering effect of the graphite is shown very strongly. Most neutrons that are scattered are removed from the beam and the graphite column is so long that almost none of the warm neutrons can travel the whole distance without being scattered. Case 5 gives a rather good approximation of the temperature of the source. The neutrons in the beam from the deep hole should be a fair sample of the neutrons present at the bottom of the hole.

(9) H. L. ANDERSON, E. FERMI, and L. MARSHALL, «Phys. Rev.», 70, 815 (1946).

Essentially it is a case of blackbody radiation from a hole in the wall of a furnace. Case 6 was expected to give a good temperature value, but failed to do so, probably because the hole was not deep enough.

VELOCITY SELECTOR.

The velocity selector makes use of a rotating shutter to interrupt the beam of neutrons from the thermal column of the pile. The shutter was constructed by inserting a multiple sandwich of 0.004–in. to 0.008–inch cadmium foils and $\frac{1}{32}$–in. aluminum sheet tightly into a steel cylinder about

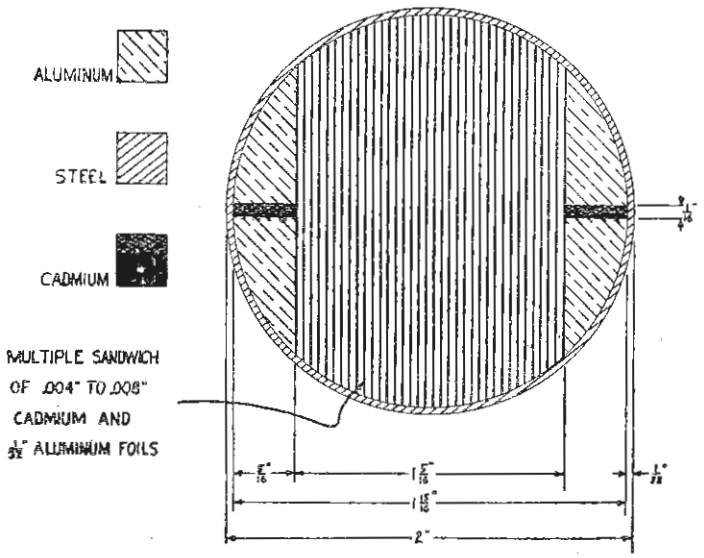

Fig. 1. – Cross section of the shutter of the velocity selector.

$1\frac{1}{2}$ in. in diameter with walls $\frac{1}{32}$ in. thick. The shutter was mounted in ball bearings on a heavy steel base plate and was belt and pulley driven by a Dumore grinder motor. Maximum rotational speeds of 15,000 revolutions per minute were possible. It was constructed in the shops of the Metallurgical Laboratory under the direction of Mr. T. J. O'Donnell who is responsible for its mechanical design.

A cross section of the shutter is shown in fig. 1. From the thickness of the aluminum spacers between the cadmium foils, and from the dimensions of the shutter, one would estimate that no neutrons from a parallel beam would be able to get through when the shutter was more than 1.2° from its full open position. In the experimental arrangement used, it was impossible to use a strictly parallel beam of neutrons. The collimators actually used allowed a maximum divergence of neutron direction in the beam of approximately 3°. Consequently, one would expect the shutter to be completely closed during each 180° of rotation except for an interval of $3° + 2 \times 1.2° = 5.4°$. Actually it was found that the counters indicated background intensity except when the shutter was in a 6° interval.

Through one end of the shutter was inserted a steel rod with its axis perpendicular to the axis of the shutter and with a minor surface ground and polished perpendicular to its axis at each end. Light from a projection lamp and lens system was reflected from these surfaces onto two photo-cells so placed that each photo-cell was illuminated twice during each revolution. One of the photo-cells was used with an amplifier and scaling circuit as a revolution counter. The other, adjustable and calibrated as to angular position, was connected to an electronic switch circuit which allowed pulses from the proportional counter to be recorded only when the photo-cell was illuminated.

BF_3 filled proportional counters were used as the neutron detector. A nest of four was connected in parallel and mounted at a distance of 146 cm from the shutter. A thick shield of wood, iron, and paraffin was placed between the counters and the pile to compensate somewhat for the fact that the top shield of the graphite pile was not so thick as might be desired. A hole in this shield allowed neutrons from the shutter to reach the counters.

The neutron beam between the shutter and the counters was collimated to make sure that no slow neutrons from sources other than the shutter could enter the counters. Slow neutrons reflected from the walls and roof of the building were eliminated by protecting the sides and back of the counters with a $\frac{1}{2}$–in. thick layer of boron carbide.

The shutter and an improved velocity selector arrangement are to be more fully described in a paper by Brill and Lichtenberger.

Determination of boron cross section for neutrons of known velocity.

The cross section of pure BF_3 at several different pressures was measured for neutrons from the thermal velocity selector for velocities ranging from 1700 to 5000 meters per second. Within the experimental accuracy of the method the cross section of boron varied according to the $1/v$ law. After corrections for scattering were made, the average cross section of boron for neutrons of 2200 meters per second velocity was 699×10^{-24} cm^2/atom. 2200 m/sec is the velocity of a neutron of energy kT where T is 293° K.

In order to verify this value a similar measurement was made with a different boron compound as absorber. $Na_2B_4O_7$ was ignited at about 400° and dissolved in heavy water. The solution was enclosed in a thin-walled aluminum cell, and a second cell of identical wall thickness, which contained an amount of heavy water equal to that in the solution, was prepared. The transmissions of these two absorbers for neutrons from the velocity selector were measured, and the value of the boron cross section for 2200 m/sec neutrons was found to be 700×10^{-24} cm^2 corrected for scattering.

In good agreement with these values was the cross section as calculated from measurements at the indium resonance energy[10]. Transmission measurements were made using a collimated beam of neutrons from the interior

(10) J. Marshall, «Phys. Rev.», *70*, 107 (1946).

of the graphite pile of the Argonne Laboratory. The indium foil detectors were protected from thermal neutron activation by thick cadmium covers. Background measurements were made by use of an indium filter. Thus the measurements were limited in more than one way to neutrons absorbed strongly by indium.

BF_3 gas in a steel cylinder was interposed in the collimated beam. The BF_3 was highly purified (the same gas as used in the thermal neutron transmission experiments described above). The transmission of the steel container filled with BF_4 at 44 and 68 lb/in^2 was compared with the transmission of the empty container. The density of gas used was determined by weighing the cylinder. The pressures used and the length of the cylinder (30 cm) were such that the transmissions were in an accurately determinable range (approximately a 2/3 transmission for the 68–lb sample).

TABLE II.

	Measurement	σ_{kT} (B) at 293° K
$Na_2B_4O_7$—D_2O . . .	Velocity selector	700×10^{-24} cm^2
BF_3	Velocity selector	699×10^{-24}
BF_3	In resonance	710×10^{-24}
	Average	703×10^{-24} cm^2

The total cross section of BF_3 for indium resonance neutrons was measured as 107.1×10^{-24} cm^2/atom. Assuming

$$\sigma_{\text{scattering}}(\text{F}) = 3.7\times10^{-24}\ \text{cm}^2,$$
$$\sigma_{\text{scattering}}(\text{B}) = 2\times10^{-24}\ \text{cm}^2,$$
$$\text{indium resonance energy} = 1.44\ \text{ev},$$

the boron absorption cross section for neutrons at velocity 2200 m/sec is 710×10^{-24} cm^2/atom.

The results of the three measurements are given in Table II.

This report is based on work done at the Argonne National Laboratory, the University of Chicago, under the auspices of the Manhattan District, U.S. Corps of Engineers, War Department.

201.

SUMMARY OF EXPERIMENTAL RESEARCH ACTIVITIES

Excerpt from Report CP–1255 for Month Ending January 24, 1944 (*).

The main activity of the experimental groups in the Nuclear Physics Division has been centering around the following experiments:

1. P–9 EXPERIMENTS.

The construction of the P–9 experimental pile has been absorbing for several months most of the activities of Zinn's group and it is expected that this will be the case for the next two or three months. Both the reactor and the storage tank have been received and some preliminary work for the jacketing of the metal rods has been started. Also, preparations have been completed for the exponential experiment with metal rods and P–9. This experiment will be performed as soon as about one ton of P–9 is delivered.

2. CROSS SECTIONS OF URANIUM.

The progress made in the past few months on the investigation of the various absorption cross sections of uranium begins now to yield a fairly clear picture of those properties. The relevant pieces of information in this respect are: A measurement of the cross section of 25 (**) already reported in CP–1186 (***) giving as fission cross section of unseparated alloy 4.6×10^{-24} for neutrons of 2200 meters per second velocity. In the past month a series of measurements have been performed to determine the ratio of capture to fission cross section. The result of these measurements, given in detail in Anderson's report, is:

$$\frac{\sigma_c}{\sigma_f} = 0.65 .$$

Together with the preceding result, this gives $\sigma_c = 3.0$. Interesting results have been communicated by the group working with the velocity selector of the Columbia cyclotron. They find strong resonance absorptions at 6.9,

(*) Report CP–1255 was issued also as A–1831. (Editors' note).
(**) Code Name for U^{235}. (Editors' note).
(***) Paper N° 198. (Editors' note).

24 and 45 ev. There is some indication of a small resonance absorption at 0.28 ev, apparently identical with one of the fission resonances recently discovered at site Y (*). At a velocity of 2200 meters per second, they find a total absorption cross section of 15.7×10^{-24}. This value is in essential agreement with values for the total cross section of uranium for thermal neutrons obtained at the Argonne Laboratory, 15.4×10^{-24}. If we take the average of these two values, namely 15.6×10^{-24}, to be the total cross section at 2200 meters per second, the scattering cross section turns out to be 8.0×10^{-24}. This value for the scattering cross section is much lower than any previously given. The high values reported by previous experimenters are probably due to a large extent to hydrogen impurities in the samples used. The discovery of resonances in the fission processes recently reported by the laboratory at site Y has also very materially broadened our understanding of the fission processes.

3. Possible absorption processes in 25.

The discovery of resonances in the fission already referred to has brought new emphasis on the possibility that a sizable fraction of the neutrons absorbed by 25 may produce an isotope 26 instead of giving rise to fission. Work is going on in the division along two lines in order to check on this possibility. Attempts are being made to determine whether the absorption cross section of 25 measured by counting the number of fissions in a standardized beam and measured by transmission experiments are equal. If it should turn out that they are not, the difference could be attributed to 26 formation. Also, preparations are made to test the alpha emission of a separated sample sent for irradiation to Clinton. It is expected that if 26 is an alpha emitter with a lifetime shorter than 10^4 or 10^5 years, it should be possible to detect its formation if the branching ratio is of the order of 10 percent. No results have been obtained to date in either of these experiments. It should be pointed out that any information of this type on the behavior of 25 could offer very valuable clues as to the behavior of our product, and it appears desirable to start similar experimentation on the product as soon as the production of this element reaches the stage when 50 mg of it can conveniently be spared for the purpose.

4. Thermal coefficient of the reproduction factor.

Considerable effort has been devoted by the division in the past to the attempt of understanding the complex phenomena that determine the dependency of the reproduction factor upon the temperature of the pile. It seems, at present, likely that the main factor that is still incompletely understood is the so-called η effect, namely the variation of the capture to fission ratio

(*) War time name for Los Alamos, New Mexico. See also introductions to papers N° 220 and 222. (Editors' note).

in uranium with the temperature of the neutrons. A new attempt is in progress to determine such ratio but so far no direct results are available. For the solution of the problem we had very valuable collaboration from the group at Y who undertook at our request a careful investigation of the deviations of the fission cross section from the 1/v law in the thermal region. Incomplete results received to date make it appear probable that the fission cross section decreases in the thermal region somewhat faster than according to the 1/v law, a fact that is in the direction needed to explain the discrepancies still remaining in the interpretation of the thermal effect.

5. Value of ν.

The average number ν of neutrons emitted per fission can be obtained from three completely different experiments performed recently. One of them is the measurement of the ratio σ_c/σ_f for thermal neutrons already referred to. Assuming that $\eta = 1.32$, it follows that

$$\nu = \eta \times \left(1 + \frac{\sigma_c}{\sigma_f}\right) \times 2.18.$$

This value corresponds to the assumption that all the absorption of 25 is due to fission. If we consider the possibility of an appreciable branching into 26 formation and call α the ratio of the number of processes leading to 26 formation to the number of processes leading to fission, the result for ν is

$$\nu = 2.18 + 1.32\,\alpha.$$

This value of ν should be compared with the other two values deduced from experiments already reported. The measurement reported in CP–1186 in which ν was measured by comparing the absorption of 25 as measured in a transmission experiment with the increase of activity of the Argonne pile when some 25 is inserted in it. The result given in that report is $\nu = 2.14$. If the possibility of a branching α of the 26 formation is considered, the result becomes

$$\nu = 2.14 + 2.14\,\alpha.$$

A third independent determination of ν may be obtained from the measurement of the yield of the product per kw–hr reported by Anderson in the monthly report for December. From these data, taken in conjunction with the packing fraction data of Dempster, follows that the ratio between the number of captures leading to product formation and the number of fissions is 0.92. Taking properly into account the contribution of fast fission resonance absorptions and leakage, one finds, ultimately:

$$\nu = 2.28 + 1.1\,\alpha.$$

If we assume $\alpha = 0$, the three values of ν are in excellent agreement and agreement would be about equally good if α were of the order of 10 or 20 percent.

6. Exponential experiments.

Mr. Morrison has now received the graphite for the exponential test on the Hanford lattice and the exponential pile is under construction. He has also performed some experiments on the diffusion in a structure containing channels.

7. Other activities.

Besides working on these experiments, the usual testing of metals and graphite has been going on, with increased emphasis on the graphite tests. Measurements of cross sections of various elements and technical materials have been performed. Brill's group has developed and constructed several amplifiers and other electronics equipment. Feld's group has completed and is ready to put into writing in a systematic form results on fast fission, inelastic scattering, and yields of various fast neutron reactions with Ra–α–Be and Ra–α–B sources. Anderson has constructed a model of a control rod driven by an Amplidyne system.

202.

SUMMARY OF EXPERIMENTAL RESEARCH ACTIVITIES

Excerpt from Report CP–1389 for Month Ending February 24, 1944 (*).

P–9 EXPERIMENTS.

An amount of P–9 adequate for carrying out the exponential experiment with metal rods embedded in P–9 has been received a few days ago. It is expected that the first exponential experiment of this type will be completed in about a week. The construction of the P–9 reacting pile is progressing satisfactorily and it is expected that the machine will be ready by the time a sufficient amount of P–9 will be available for filling it. The test samples for the determination of cross-section of P–9 of various origins in the pile have been assembled and some preliminary tests have been carried out.

THERMAL COEFFICIENT OF THE REPRODUCTION FACTOR.

The experimental determination of the so-called η effect has been concluded during the past month, with the result that the value of η actually depends on the temperature of the neutrons and shows a fractional decrease of $(5.2 \pm 1.1) \times 10^{-5}/^{\circ}C$. The sign and magnitude of this effect are such as to considerably reduce the discrepancies previously noted in the attempts to interpret theorctically the temperature coefficient of the reactivity of a pile. Taking as an example the case of the Clinton pile, which is somewhat simpler than that of the Argonne pile since it is constituted by a simpler type of lattice, one may analyze the various components of the thermal effect about as follows.

p is the fraction of neutrons escaping resonance absorption, f is the thermal utilization and M is the migration length. The effective change of reproduction factor is given by the following expression:

$$\delta k_{\text{eff}} = k\frac{\delta\eta}{\eta} - k\frac{\delta p}{p} + k\frac{\delta f}{f} - (k-1)\frac{\delta M^2}{M^2}$$

where the first term represents the η effect, the second term represents the change of the resonance absorption due to the heating of the metal, the third term represents the change of thermal utilization f, due to the so-called leveling effect and the fourth term represents the effect of the change of leakage.

(*) Report CP–1389 was issued also as A–2030. (Editors' note).

In estimating these various effects for the Clinton pile, we have assumed that the neutrons are in thermal equilibrium and we have taken the following values:

For graphite,

Diffusion length:

$$l = 50\,(1 + 0.000853\,t)$$

where t is the variation of the temperature in °C.

Absorption mean free path:

$$\Lambda = 2757\,(1 + 0.001706\,t).$$

For the metal

Diffusion length:

$$l_0 = 1.55\,(1 + 0.000991\,t).$$

Absorption mean free path:

$$\Lambda_0 = 3.24\,(1 + 0.001706\,t).$$

From these values one calculates with the formula developed by Christy and Monk in C–104:

$$f = 0.891\,(1 + 6.91 \times 10^{-5}\,t).$$

The migration length is calculated with the formula:

$$M^2 = \frac{r_0^2}{4} + l^2\,(1 - f) = 350 + l^2\,(1 - f) = 622\,(1 + 50 \times 10^{-5}\,t).$$

Assuming a reproduction factor for the Clinton pile, $k = 1.062$, one finds for the leveling term in the Clinton pile the following terms for the various contributions to the change of reproduction factor per °C.

Leveling effect:

$$k\,\frac{\delta f}{f} = + 7.3 \times 10^{-5}.$$

Leakage effect:

$$-(k - 1)\,\frac{\delta M^2}{M^2} = - 3.1 \times 10^{-5}.$$

Change of resonance absorption: This effect seems to have been somewhat underestimated in the previous computations and experimental indications obtained by flashing the pile both at Clinton and at Argonne seem to indicate that it amounts to about:

$$k\,\frac{\delta p}{p} = - 2 \times 10^{-5}.$$

The η effect: Assuming, according to the measurement, a fractional change of about $- 5.2 \times 10^{-5}$/°C, we find for this effect:

$$k\,\frac{\delta \eta}{\eta} = - 5.5 \times 10^{-5}.$$

From all these contributions we ultimately find as overall temperature effect:

$$\delta k_{\text{eff}} = - 3.3 \times 10^{-5}/°\text{C}.$$

This value coincides in sign with the observed effect. However, it is somewhat smaller in magnitude by one or two units. The discrepancy cannot be considered very serious if one takes into account the fact that the result is a small difference of fairly large terms which may all be appreciably in error. It seems to be legitimate to conclude that the main features determining the thermal coefficient of the reproduction factor are now understood, although the accuracy with which the effect can be calculated needs still to be improved considerably. It should also be remarked that the calculations have been performed so far on the assumption that fission is the only absorption process in 25. If a sizable fraction of the absorption of 25 is due to formation of the isotope 26, one might consider the possibility of a thermal effect due to a change with the temperature of the ratio between number of neutrons producing fission and the number of neutrons determining formation of 26 (*).

Cross-sections.

A considerable part of the activity of the division has been dedicated to the problem of improving our knowledge of the neutron cross-sections. The ratios of the boron and manganese absorption cross-sections to the absorption cross-sections of hydrogen have been determined. These values are important because the elements in question are often used as standards for cross-section measurements. Also, the list of activation cross-sections has been further extended and some more cross-sections have been determined in a beam geometry, both with neutrons of approximately thermal energy and with cold neutrons obtained by filtering through beryllium.

Experiments on enriched 25 Samples.

A number of experiments has been performed on a sample of enriched alloy recently received from site Y. The value of R (ratio between number of atoms of 28 and of 25 in the sample) has been determined by two entirely independent methods and has been found by both methods to be 0.05. The value of the absorption cross-section of 25 has been measured in a beam geometry and found to be 640×10^{-24} for neutrons of 2200 meters per second velocity. Also the value of ν has been measured again by observing the increase of reactivity of the pile when the sample is introduced near the center. The new value is almost identical to the one found previously, namely 2.15 instead of the previous value of 2.14. Both values are calculated on the assumption that fission is the only absorption mechanism for neutrons in 25. Further work has been devoted to the problem of finding out whether or not a process of absorption of neutrons in 25 with formation of isotope 26 exists.

A sample of enriched alloy was irradiated at Clinton and returned to us after an irradiation for which nvt was estimated to be about 4×10^{17}.

(*) U^{236} (Editors' note).

It was anticipated that if the isotope 26 was formed in this sample during the bombardment, the specific alpha activity of the irradiated sample might be larger than the specific alpha activity of the non-irradiated material. A careful comparison failed to show any difference and one can conclude that if an effect is there, it is less than 1 percent. The result indicates that either the probability of capture into 26 is quite small or the lifetime of 26 for alpha emission is very long. One might actually conclude from the experiment that $\tau > 10^6\ \alpha$ years, where τ is the lifetime of 26 for alpha emission and α is the probability that capture of a neutron by 25 leads to 26 formation. It is not believed that this negative result means that the probability of 26 formation has to be excluded. Indeed, the position of 26 among the known heavy alpha emitters, makes it appear probable that 26 is a fairly long-lived element with a lifetime perhaps as large as 10^7 years. If this is true, the failure of observing an increase in the alpha activity is by no means incompatible with a large value of the branching factor.

Exponential experiments.

A new exponential experiment with metal rods embedded in Gulf Cleves graphite has been performed during the month. The value of the Laplacian found is 120×10^{-6}, which is the largest found so far in an exponential experiment. In order to obtain a direct measurement of the effect of a control rod, a Cd cylinder was inserted in the exponential pile and the change of the relaxation distance produced by it was observed. The result yields a measurement of the efficiency of the control rod that can be compared with the theoretical estimates in order to check the assumptions that are used at present in estimating the effect of control rods.

Other activities.

Development and construction of amplifiers.

Construction of a cloud chamber for the investigation of the radiation coming out of the pile.

Testing of graphite and metal.

Investigation of the slowing down of neutrons produced by αn and γn reactions of radium radiations on boron and beryllium.

203.

REPORT OF FERMI'S ACTIVITIES WITH THE MARSHALL GROUP

Excerpt from Report CP–1389 for Month Ending February 24, 1944.

Fission chamber measurement of R

(E. FERMI, L. MARSHALL)

There is in the laboratory a sample of U_3O_8 which is enriched in 25. It was received from site Y and is labelled E 10 A. They gave the ratio of 28/25 as R = 8.5. The value of R was remeasured here using the thermal column of the Argonne pile.

For this measurement 4 foils were prepared by Cunningham. Two of them were prepared to contain 87.6 micrograms of natural U_3O_8. The other two contain 87.7 micrograms of enriched U_3O_8. With the pile run at a steady power the enriched foil gave 8984 — 7 (background) = 8977 counts/min while the normal foil gave 585.6 — 7 = 578.6 counts/minute. From these data R was calculated to be 8.05, assuming R for normal uranium to be 139. In other words, the sample contains 8.05 times as many atoms of 28 as it does atoms of 25.

Neutron Emission Measurement of R

(E. FERMI, JOHN MARSHALL)

The value of R for sample E 10 A was also measured by an independent method. A BF_3 counter was cast into a cylinder of paraffin which was then covered with 1/10″ of cadmium having no cracks for neutrons to leak through. This counter then became a detector of neutrons above the cadmium cut-off while its sensitivity to thermal neutrons was extremely low.

The counter was then placed in the thermal column of the pile so that samples of uranium could be slid under it. One sample contained about 30 grams of the enriched oxide spread out evenly in a shallow aluminum box 2″ in diameter. The other sample was in an identical box and contained ordinary uranium oxide to an amount equal to the amount of ordinary oxide contained in the enriched sample (as computed from the isotopic ratio given by the fission chamber experiment). This sample also contained finely powdered Pyrex glass. Just enough was added to bring up the absorption to that of the enriched sample. The enriched sample had been tested previously in a beam of thermal neutrons for its thermal absorption.

The pile was held at a constant intensity and the number of counts per minute was observed when no sample was under the counter, when the enriched sample was there, and when the natural sample was there. The following results were obtained:

enriched sample	3205	c/min.
natural sample	253.8	c/min.
no sample	72.2	c/min.

The enriched sample then contained $\frac{3205-72.2}{253.8-72.2} = 17.26$ times as much 25 as did the natural sample. From this ratio R is computed to be 8.05. This value of R should be good within about 1 percent.

Cross-section of Lithium Fluoride

(E. FERMI, L. MARSHALL)

The total cross-section of lithium flouride has been measured to be 69.5×10^{-24} cm^2 for neutrons with a velocity of 2200 meters/sec.

Measurement of ν *for 25*

(E. FERMI, J. MARSHALL, L. MARSHALL)

Using the enriched sample from site Y a value for ν has been measured under better conditions than were possible in the measurement reported in CP–1186. The result is $\nu = 2.15$. The same method was used that was used before.

Absorption cross-section for 25

(E. FERMI, L. MARSHALL)

The absorption cross-section for 25 has been measured to be 640×10^{-24} cm^2 for neutrons of velocity 2200 meters/sec. This also was done with sample E10A.

Cold neutrons from Be

(E. FERMI, L. MARSHALL)

Neutrons filtered through 9'' of beryllium metal emerge with an average temperature of 30.6°A. Cross-section measurements have been made with these neutrons as indicated in the following Table I.

TABLE I.

Material	Atoms/cm²	log T observed	log T corrected	Total cross-section
U	1.488×10^{22}	0.400	0.383	25.7×10^{-24} cm²
Au	2.306×10^{21}	0.629	0.622	270×10^{-24} cm²
Cd	2.574×10^{20}	1.340	—	5200×10^{-24} cm²
25	2.58×10^{21}	0.732	0.735	2850×10^{-24} cm²

The log of the transmission was corrected using the Bethe correction and assuming that the neutrons have a Maxwellian energy distribution (which they almost certainly don't) and assuming that the scattering cross-sections are constant (which they probably aren't).

204.

SUMMARY OF EXPERIMENTAL RESEARCH ACTIVITIES

Excerpt from Report CP–1531 for Month Ending March 25, 1944.(*)

P–9 EXPERIMENTS.

During the past month the first series of experiments using about one ton of heavy water were completed. Three measurements were performed, namely, (a) an attempt to determine the absorption cross section of heavy water by the sigma pile method. The result was that the cross section is too small to be detected with a sigma pile of the dimensions used and that the cross section is, if anything, smaller than had been estimated previously; (b) The range of fission neutrons in heavy water was measured and found to be somewhat smaller than had been expected theoretically. The age for the reduction of fission neutrons to indium resonance energy was found to be 96 cm^2; (c) An exponential experiment was performed in order to determine the Laplacian of the lattice to be used in the P–9 pile now in construction at Argonne. The Laplacian was found to be 880×10^{-6} cm^2, in good agreement with the theoretical expectation. There are certain indications that the agreement is to some extent accidental since a satisfactory explanation of the observed Cd ratio is still missing. Work is going on in order to clarify this point. The practical conclusion is that the design of the Argonne pile need not be changed.

EXPERIMENTS ON 25.

The experiments in order to determine what fraction of the neutrons captured by 25 gives rise to 26 formation instead of fission have been continued during the month. The present evidence is that the fission cross section is between 80 and 85 percent of the total absorption cross section of 25.

EXPONENTIAL EXPERIMENTS.

An exponential test of the lattice to be used at Hanford has been carried out and the results lead to the expectation of a considerable excess reproduction factor in the Hanford pile. The excess is estimated to be 1.2 ± 0.4 percent.

(*) Report CP–1531 was issued also as A–2209. (Editors' note).

Fission neutrons.

The slowing down of fission neutrons in water was investigated and the value of $\overline{r^2}$ for indium resonance neutrons was found to be 194 cm², a considerably larger value than had been expected.

Properties of graphite.

Some interesting preliminary results have been reported by the cyclotron group at Columbia working with a velocity selector on a study of the scattering cross section of graphite as a function of the energy of the neutrons. The cross section shows very remarkable features for thermal neutrons. Sudden drops in the cross section are observed for decreasing energy. The positions of these drops are at the energies to be expected from the crystal structure of graphite. A detailed report on this work will be given as soon as the results are completed.

Other activities.

Development and construction of amplifiers.

Construction of an amplidyne operated control rod which allows regulation of the pile intensity with much greater accuracy than had been possible with the present rods.

Determination of the range of recoils from the (n, p) reaction in Al which was found to be 3×10^{-5} cm.

A recalculation of the fast effect, taking into account the difference in the data curve of the fission products from 25 and from 28. The result is that the data on the fast effect from CP–644 are too high by about 20 percent.

Testing of metal, graphite, and heavy water.

205.

RANGE OF FISSION NEUTRONS IN WATER

H. L. ANDERSON, E. FERMI, and D. NAGLE
Excerpt from Report CP–1531 for Month Ending March 25, 1944.

The distribution of indium resonance neutrons from the fission of 235 was measured in water up to 30 cm distance. At 30 cm the relaxation distance was found to be about 9 cm. Using this relaxation distance for extrapolation of the curve beyond 30 cm the $\overline{r^2}$ was calculated to be 194 cm². This result is higher than any previously reported. Due to the low intensity and the necessity to use several large sources, this result may have a considerable error.

Measurements were carried out in a cylindrical water tank 18 inches in diameter on top of the thermal purification column of the Argonne pile. Several uranium sources were used and these were placed in the water 10 cm above the bottom of the tank in order to avoid the perturbations due to the boundaries. For measurements at near points a capsule (4.7 cm in diameter, 0.7 cm high) containing 32.4 grams of enriched U_3O_8 (R = 8.05) was used. For reasons of intensity at more distant points we used uranium metal disks 15.2 cm in diameter. The water level in the tank was maintained at 56 cm so that even at 30 cm there were 16 cm of water above the detector.

The detectors were standard indium foils (4 × 6.5 cm² × 0.1 gms/cm²) which were protected on all sides with 1.30 gms/cm² of cadmium.

The experimental data are listed in Table I. The distance given is the distance from the center of the source to the center of the detector. The intensity given is the initial activity of indium in counts per minute reduced to the end of irradiation. Since the weight of the source and the thermal neutron flux with which it was irradiated was different in the various experiments, the data has to be fitted together at the places where the measurements overlapped. The background is due to fast neutrons from the pile which penetrate the water tank and activate the detector.

If our source and detector were small enough, $\overline{r^2}$ could be obtained by integrating under the observed curve. However, due to the size of the source the detector receives contributions of intensity from a range of distances. Thus, for a small detector at a perpendicular distance x from a flat disk of radius R the intensity

$$I = \int_x^{\sqrt{x^2+R^2}} f(r)\, r\, dr$$

where $f(r)$ is the desired distribution function and I is the measured intensity. The function $f(r)$ was found by constructing a curve which satisfied the above

relation at all of the points measured. Table II gives the smooth curve obtained in this way.

TABLE I.

Source	Distance Center to Center cm	Initial Activity c/m	Background c/m
3433 gm U metal 15.2 cm diam. 1 cm thick.	14.9	—	20
	20.6	456	10
	25.1	173	10
	30.2	76	10
1690 gm U metal 15.2 cm diam. 0.5 cm. thick.	3	2462	5
	6	1350	2
	9	650.6	1
	14.9	113.6	0.5
	20.9	28.9	0.2
30 gm U_3O_8 enriched in 235. (R = 8,05)	2.9	1000	—
	5.5	619	—
	8.0	338	—

TABLE II.

r	$r^2 f(r)$	r	$r^2 f(r)$
0	0	16	960
2	730	18	688
4	2024	20	504
6	2928	22	376
8	2920	24	288
10	2380	26	218
12	1800	28	176
14	1365	30	144

In obtaining the value of $\overline{r^2}$ from the ratio

$$\overline{r^2} = \frac{\int_0^\infty r^4 f(r)\, dr}{\int_0^\infty r^2 f(r)\, dr}$$

the curve has been extrapolated beyond $r = 30$ cm by an exponential function with a 9 cm relaxation distance. The result found was $\overline{r^2} = 194$ cm^2. The usual difficulty of insufficient accuracy at the far points makes the final result somewhat uncertain. The extrapolation beyond 30 cm amounts to 30 percent of the integral in the numerator and neglects the tendency of the relaxation distance to increase with increasing distance from the source.

The older measurements in paraffin of Snell (report C–121) reduced to water gave $\overline{r^2} = 130$ cm^2 but this result is certainly low due to proximity of a graphite boundary 1 inch from the source, and also since the measurements we carried out to 25 cm, to an underestimate of the relaxation distance.

A calculation of $\overline{r^2}$ (report CP–1251) averaged over the fission neutron spectrum obtained by the photographic method (report LA–60) gave 180 cm^2.

206.

EVIDENCE FOR FORMATION OF 26

E. FERMI and L. MARSHALL

Excerpt from Report CP–1531 for Month Ending March 25, 1944.

A comparison was carried out between the ratio of the total absorption cross sections of 25 and lithium as measured in a beam geometry and the ratio of the fission cross section of 25 to the disintegration cross section of lithium measured by observing the number of pulses in an ionization chamber due to 25 or lithium when thin deposits of these two elements are placed in a thermal neutron beam of constant intensity.

The total absorption cross section for 25, reported in last month's monthly report is 640×10^{-24}. Since in the experiments to be described the same sample of enriched alloy was used, the results to be reported are not affected by any error in the estimate of the enrichment factor. The numbers given were calculated assuming for R the value 8.05 reported last month.

The absorption cross section of lithium was obtained in two different ways: (a) The total cross section of LiF was measured in a beam geometry and found to be 70.0×10^{-24} for neutrons of 2200 meters per second velocity. The cross section of LiF was also measured for indium resonance neutrons of 1.44 ev (see later in this report) and found to be 13.75×10^{-24}. From these two values, assuming that the absorption follows the 1/v law and the scattering is constant, one finds $\sigma_{abs} = 64.9 \times 10^{-24}$ and σ_{scatt} (LiF) $= 5.1$. (b) The cross section of LiF was also measured by the danger coefficient method, comparing it directly with the known absorption of Pyrex plates calibrated with the velocity selector. The result of this measurement is that one gram of LiF absorbs like 0.951 grams of Pyrex. One gram of Pyrex has an absorption cross section of 1.584 cm^2 for neutrons of 2200 meters per second velocity. From these data one finds that the absorption cross section of LiF is 64.9, in complete agreement with the previous result. In conclusion, we have assumed the absorption cross section of Li to be 64.9 ± 1.

The ratio of the total absorption cross section of 25 and Li is then 9.86, with an error of perhaps 2 or 3 percent.

In order to determine the ratio of the fission cross section of 25 to the disintegration cross section of Li, thin deposits of enriched uranium and of Li were prepared. The thickness of the deposits was of the order of 100 micrograms per square centimeter, so that the error due to self absorption in the sample was rather small. Actually, samples of various thicknesses were used and no trend in the rate of disintegrations per unit mass was observed. In both cases the deposits were obtained by spreading on platinum

foil a known aliquot of titrated solution. In the case of the uranium deposits, the thickness was checked by preparing first a number of samples of natural uranium checking that the number of alpha particles emitted corresponded very closely to the number expected theoretically. The deposit of enriched material was prepared subsequently following closely the same technique and the number of alpha particles was counted, in order to ascertain the consistency of the count obtained from various foils.

In the case of Li, both LiF and $LiCO_3$ deposits were prepared and a comparison showed that the number of disintegrations observed when the various deposits were placed in the beam of neutrons was proportional to the amount of Li in the deposits.

The counting of the various deposits was carried out in a thermal neutron beam on top of the thermal column of the Argonne pile. The deposits were successively placed inside an ionization chamber connected to a linear amplifier. There is no special difficulty in counting the fission pulses. For counting the Li recoils, the chamber was filled with two atmospheres of argon in order to reduce the number of spurious pulses due to nitrogen. Since the argon was only about 99.5 percent pure, a number of pulses was observed due to nitrogen impurities. These pulses formed a background to be subtracted. Actually, the background was observed by counting the number of pulses when a dummy foil was inserted in the chamber. These dummy foils had been prepared by following exactly the same procedure as for obtaining the Li deposit except that no Li was present. Table I gives a summary of the results.

TABLE I.

Measurements with 25.

Micromoles of 25	Fissions per minute	Fissions per minute per micromole	
0.07947	45.3	570	
0.2519	143	568	avg. 573
0.4732	275	581	

Lithium disintegration.

Micromoles of Li	Disintegrations Observed	Background	Li Disintegrations per minute	
4.949	433	88	69.9	
9.898	784	88	70.2	avg. 70.5
9.898 (different bias)	827	118	71.7	

The ratio of fission cross section of 25 to disintegration cross section of Li turns out to be $\frac{573}{70.5} = 8.13$. This value is appreciably lower than the ratio

9.86 found for the total absorption cross section of the two elements. Assuming that the neutron capture in Li gives rise in all cases to a detected Li ionization and assuming also that all the fissions in 25 are counted, one finds from the two numbers that of the neutrons absorbed by 25, only $\frac{8.13}{9.86} = 82.5\,\%$ gives rise to fission. The remaining $17.5\,\%$ are absorbed by some different process, probably formation of 26 by radiation absorption of one neutron.

The main reasons for error in the measurement are the following: (a) Some fission may be missed in the counting due for example to self absorption within the sample itself. This error, which would lead to an overestimate of the branching ratio into 26 formation is probably rather small, since the agreement in the fission count with deposits of various thicknesses is quite good. (b) If some counts have been lost in observing the Li disintegrations underestimate of the probability of 26 formation results. This is also the case if the assumption made that all the neutron absorption in Li leads to a heavy particle disintegration is incorrect. (c) The branching ratio of the 26 formation may be overestimated if the number of Li disintegrations is lower than the observed value, as may be due, for instance, to a small boron contamination of the thin deposits. It was primarily to reduce the probability that this may be the case that several deposits were used and a comparison was made between LiF and $LiCO_3$ deposits.

If we assume that the percentage 82.5 is correct, we find the following values for the fission cross section of 25 and for the cross section leading to 26 formation, for neutrons of 2200 meters per second velocity

$$\sigma_{\text{fiss}}\,(25) = 578 \times 10^{-24}\ \text{cm}^2$$

$$\sigma_{\text{rad. capt}}\,(25) = 112 \times 10^{-24}\ \text{cm}^2.$$

N° 207–209.

The overriding demands of the Project began to make themselves felt. The du Pont Company needed experienced physicists to help them with the Hanford piles. Of Fermi's closer collaborators, the first to go was George Weil. He was followed soon after by the Marshalls. I began to spend a major part of my time in Wilmington, and Fermi himself was becoming more and more involved in the work at other sites of the Manhattan District, especially in the work on the bomb at Los Alamos.

At Argonne, meanwhile, some samples of plutonium became available in the spring. The reports for April (N° 207–209) show that Fermi measured the neutron absorption of plutonium himself. A second experiment on the range of fission neutrons from plutonium was carried out with the help of two young assistants, Harry Heskett and Darragh Nagle.

In the table of paper N° 209 there is a slight mathematical mistake that does not affect the experimental results.

Report CP–1592, of which these papers are excerpts, was circulated also as A–2257.

H. L. ANDERSON.

Fermi's interest in plutonium dated back to 1939, when its existence had been postulated but it had not yet been separated. In December of that year Fermi and I had privately discussed plans for making Pu^{239}, and on the 16th of that month there was a conference between Fermi, Lawrence, Pegram, and myself at Columbia University on preparing enough plutonium to test its fissionability. On January 1, 1940 I started work on this problem in Berkeley and was soon joined by J. W. Kennedy, G. T. Seaborg, and A. C. Wahl. These men had been independently investigating the chemistry of plutonium, using tracer Pu^{238}, in Berkeley, during December 1939. The first samples of Pu^{239} in micrograms amounts were prepared with the 60'' cyclotron in Berkeley by Kennedy, Seaborg, Wahl and myself during the early months of 1940.

Larger amounts of plutonium became available early in 1944, from the Clinton pilot plant. The Clinton pile had begun operating in November 1943. By February 1944 the separation plant at Clinton had produced plutonium in milligrams amounts, and by March 1944, it had delivered several grams of this substance [1]. Fermi, at Argonne, received some samples for his experiments.

E. SEGRÈ.

207.

SUMMARY OF EXPERIMENTAL RESEARCH ACTIVITIES

Excerpt from Report CP–1592 for Month Ending April 24, 1944.

P–9 EXPERIMENTS.

The construction of the P–9 reactor pile is progressing satisfactorily. All the main items of equipment are now on hand. The metal rods have been jacketed and welded and are now being given the final test.

(1) H. D. SMYTH, *Atomic Energy for Military Purposes*, Princeton University Press, 1945.

Experiments on 25 and 49.(*)

The cross-section for absorption of thermal neutrons by 49 has been found to be 950×10^{-24} cm² for neutrons of 2200 meters per second velocity. Assuming the ratio between the fission cross-sections of 49 and 25 to be 1.4, as recently measured at Y, and assuming further that the capture branching ratio is equal for the two isotopes, one would find a cross-section of about 900. There is, therefore, some indication that α may be slightly larger for 49 than it is for 25, although the difference is not outside of experimental error.

The number of neutrons emitted by 49 and 25 has been compared. The ranges of the two types of neutrons for slowing down in graphite are equal within the experimental error. The number of neutrons emitted by 49 per neutron absorbed seems to be slightly less than the corresponding number for 25. A direct comparison of the ν values for the two isotopes is in progress.

A second attempt has been made in order to determine whether the activity of a 25 sample irradiated at Clinton increases due to the formation of an alpha active isotope. No evidence was found, and the result indicates that if 26 is formed, its lifetime must be greater than 6×10^5 years.

Exponential experiments.

An exponential experiment on the so-called Hanford B lattice has been performed by Morrison's group. The essential difference between the Hanford B and the Hanford A lattices is that in A, Gulf Cleves graphite was used; and in B, Kendall.

The difference in Laplacian was found to be 2.5×10^{-6} in favor of Hanford B. This result would seem to indicate a somewhat smaller advantage due to the different brand of graphite, than had been expected.

Diffusion length in uranium.

A measurement of this magnitude gave a diffusion length of 1.55 cm. This value is appreciably higher than the value 1.33 used in most of the lattice calculations. Some work to check on the dependence of the result upon the nature of the neutrons used is in progress.

Alpha particles emitted in fission.

Mr. Hughes has carried out a rather extensive investigation of emission of alpha particles by 25 under neutron radiation. He finds the existence of some long-range alpha particles whose maximum range seems, however, to be somewhat shorter than according to the Alvarez result. He finds also

(*) 49 was the code name for plutonium. (Editors' note).

a number of lower-range alpha particles. An estimate of the yield seems to indicate that the total number of alpha particles emitted by fission is of the order of a fraction of a percent, unless it should happen that a large number of very low energy alpha particles are emitted which seems to be theoretically a rather improbable occurrence.

Cross-section measurements.

A supplementary list of activation cross-sections for 16 isotopes is given in Mr. Anderson's report. Also, some work was done on determining the cadmium ratio for a few elements, in particular, Dy, for which the cadium ratio inside the Argonne pile is very high, indicating the probable existence of a resonance quite close to thermal energy, and Th, for which $\int \sigma \frac{dE}{E}$ was found to be 88×10^{-24}.

Recoils of aluminum.

The range of recoils of products of Al was found to be 3×10^{-5} cm for the 10–minute lifetime product of the (n, p) reaction. For the recoil of the (n, γ) reaction produced by thermal neutrons only an upper limit of 8×10^{-8} cm can be given at present.

Cross-section of graphite.

An extensive collection of data found with the Columbia velocity selector by Havens and Rainwater is found in Anderson's report. These results indicate an important influence of the crystalline structure of graphite on the neutron scattering properties.

Capture of O^{17}.

Hinks and May from Montreal have been guests of the Argonne laboratory during the month and have carried out a determination of the absorption cross-section of O^{17}. Their preliminary results indicate that the contribution of O^{17} to the total absorption of oxygen is of the order of 10^{-28} cm^2. This confirms the fact that probably no very serious trouble is to be expected in the P–9 piles in case that this isotope should be somewhat enriched in the P–9 used.

Testing of materials.

The routine tests on metal and P–9 samples have been kept on regularly during the month and have proved completely uneventful. (*)

(*) See paper N° 208. (Editors' note).

N° 208.

For the introduction to this paper see N° 207.

208.

ABSORPTION OF 49

Excerpt from Report CP–1592 for Month Ending April 24, 1944.

The total absorption cross-section of 49 for thermal neutrons has been measured.

The sample was in the form of powdered PuO_2 and was contained in a cylindrical aluminum box, having a diameter of 2.207 cm. Since it would be difficult to spread evenly the powder inside the box, the oxide was mixed with 2 gr of graphite powder and an even layer of the mixture was obtained. The help of Mr. Cunningham in preparing the graphite-plutonium oxide mixture was greatly appreciated.

Considerable attention must be given to keep the size of the oxide grains as small as possible since, if the grains are too coarse, the self-absorption inside the grains leads to an underestimate of the cross-section. In spite of the attention given to this point, it is felt that the present measurement may be still appreciably in error due to the grain size.

The measurement was performed on top of the thermal column of the Argonne pile, using a beam of thermal neutrons collimated through a cadmium geometry with a radius of 1.8 cm. The absorption of the sample was compared with the absorption of standardized Pyrex plates, and the data were corrected to a neutron velocity of 2200 m/sec. A small scattering correction of 17×10^{-24} sq. cm for the PuO_2 molecule was subtracted. The average of two series of measurements gives a total absorption cross-section of 930×10^{-24} sq. cm. It is estimated that this value should be increased by about 2 percent in order to take into account the correction due to the size of the grains, as the most probable value cross-section of plutonium we find, therefore:

$$\sigma_{abs} = 930 \times 10^{-24} \text{ for neutrons of 2200 m/sec velocity.}$$

Due to the somewhat unsatisfactory conditioning of the sample, the error in this measurement is somewhat larger than for similar measurements and may well be be 3 or 4 percent.

N° 209.

For the introduction to this paper see N° 207.

209.

COMPARISON OF THE RANGES IN GRAPHITE OF FISSION NEUTRONS FROM 49 AND 25

E. FERMI, A. HESKETT and D. E. NAGLE

Excerpt from Report CP–1592 for Month Ending April 24, 1944.

The ranges in graphite to indium resonance were compared for fission neutrons from 49 and from 25 and found to be very nearly the same.

Standard indium foils in sealed cadmium holders were used as detectors. These were placed in a graphite block on the vertical axis of the thermal column of the Argonne Pile. A comparison of ranges of the neutrons was made using three irradiations of equal duration and intensity, one with no sample, one with 1.119 grams of PuO_2 and one with about 13.754 grams of U_3O_8 with R = 8.05.

After each irradiation the indium activities were followed for about five hours on beta counters. Below are tabulated the observed indium activities. The more active foils were allowed to decay several hours, but for the several foils corresponding to each distance from the source, the time of decay was roughly the same.

Table I lists the saturated initial activities, before and after subtracting the blank irradiations. At each distance from the source is shown the ratio of indium activity from 49 neutrons to indium activity from 25 neutrons. Clearly the two distant points show large experimental error, only part of which can be explained by poor statistics. The variation of the ratio 49 to 25 with distance from the source is less than the experimental error.

The ratio averaged over the two near points is 1.045. The total absorption cross-section of the 49 is estimated to be 1.07 times that of the 25 sample. The ratio of neutrons emitted per absorption is:

$$\frac{n(25)}{n(49)} = \frac{1.07}{1.045} = 1.02.$$

This experiment, therefore, detects no difference between 49 and 25 in range of fission neutrons or in neutrons emitted per absorption.

It is planned to repeat the measurement with reconditioned samples and with other detectors.

TABLE I.

Comparison	I				II				III			
Sample	None	$\frac{(49-0)}{49}$	$\frac{(29-0)}{25}$	$\frac{49}{25}$	None	$\frac{(49-0)}{49}$	$\frac{(25-0)}{25}$	$\frac{49}{25}$	None	(49–0)	(25–0)	$\frac{49}{25}$
Distance from Source												
4″	136,970	1,122,400	1,108,300	1.014	56,478	420,800	412,990	1.023	56,478	426,430	414,940	1.043
		985,400	971,300			364,300	356,500			370,000	358,500	
12″	14,422	184,000	174,488	1.060	5,586	68,880	65,550	1.056	5,586	69,630	65,284	1.073
		169,670	160,000			63,290	59,960			64,040	59,700	
20″	2,404	14,540	14,094	1.038	1,067	5,715	4,881	1.219	1 ,067	5,325	5,237	1.021
		12,136	11,690			4,648	3,814			4,258	4,170	
24″	937	4,347	5,020	0.835	508	1,355	1,436	0.913	508	1,491	1,321	1.209
		3,410	4,083			847	928			983	813	

Average of $\left(\frac{49}{25}\right)$ for distances 4″ and 12″ = 1.045.

N° 210.

This is one of the few conventional scientific articles that contains work performed at the first pile in 1943–44. During the initial period of operation we were studying the characteristics of the pile and how to operate it. The method of measuring drifts or inverse periods, which is described in this article, developed as a convenient way to operate and use the pile for quantitative measurements.

Even in the first days, Fermi and Zinn put H. Lichtenberger and myself to work on using the pile as a tool to measure neutron absorption cross sections. Samples were put in the first pile, and the compensating changes in control rod position were determined. After the pile was rebuilt at the Argonne, Anderson and Weil devoted a great deal of effort into making this a high precision technique which they applied to many problems such as the determination of the number of neutrons emitted in fission. We measured thermal neutron absorption cross section in this way for about fifty elements.

The method also became a routine tool for checking for neutron absorbing impurities in the materials which were to be used in other reactors. Weil or I used the pile one day a week for this routine testing; later a special reactor was built at Hanford to handle this type of work.

Fermi almost always had estimated in advance the effect on the pile to be expected from the size of a sample and his knowledge of neutron cross sections. A few of the younger physicists were discouraged about bothering to make measurements which " the omniscient one " was able to predict in advance. However, I believe some of us did learn the lesson that he was trying to teach us of always calculating in advance what result to expect.

A. WATTENBERG.

210.

METHOD FOR MEASURING NEUTRON-ABSORPTION CROSS SECTIONS BY THE EFFECT ON THE REACTIVITY OF A CHAIN-REACTING PILE

H. L. ANDERSON, E. FERMI, A. WATTENBERG, G. L. WEIL, and W. H. ZINN
Argonne Laboratory, University of Chicago, Chicago, Illinois
(Received March 14, 1947)
« Phys. Rev. », *72*, 16-23 (1947).

This paper described a method for measuring neutron-absorption cross sections based on the following principle: Introduction of a neutron-absorbing substance into a pile decreases the reactivity and in order to keep the power level constant the control rods must be displaced. By proper calibration this displacement may be used as a precision measure of the absorption cross section.

1. Introduction.

The reactivity of a chain-reacting pile depends critically on the balance of neutron production, absorption, and leakage. A small change in the absorption of neutrons taking place in the pile produces a drift in the intensity at which the pile is operating. This effect has been utilized for measuring neutron-absorption cross sections.

This method was particularly useful in the development of piles since it gives directly the effect of the neutron absorption of various materials in the operation of a pile. The method measures the absorption directly while effects of scattering usually enter in a minor way. This has an advantage over methods which obtain the absorption as the difference between the total and the scattering cross section, especially where the difference is small.

2. Neutron reproduction.

In the first two chain-reacting piles which were constructed at the Metallurgical Project, neutrons were reproduced in a structure consisting of a lattice of uranium lumps embedded in a pile of graphite bricks. In this structure neutrons are reproduced in a cycle in which fast neutrons are slowed down to thermal energies by elastic collisions with carbon. Upon reaching thermal energies, the neutrons continue to diffuse without further loss in energy, on the average, until they are either absorbed in the pile or escape the pile by leakage. A fraction of the neutrons which are absorbed produce fission in uranium with the liberation of new fast neutrons. The average number of neutrons produced from one original neutron in such a cycle is called the reproduction factor, k. The value of k depends on the balance of neutron production, absorption, and leakage.

When the pile is operated at sufficiently high intensity, the neutron production is predominantly that from neutron-induced fission and the contribution from spontaneous fission (α, n) reactions, (γ, n) reactions, and cosmic rays becomes vanishingly small. The pile is said to be in the critical condition when the neutron intensity remains constant. The value of k is then just slightly less than unity, the deviation from unity measuring just the amount of neutron production which is contributed by other neutron sources than the neutron-induced fission. In the piles used in our work, the critical condition could be obtained by the adjustment of a cadmium control rod. Insertion of more or less cadmium in the pile served to increase or decrease the amount of neutron absorption with consequent decrease or increase in the value of k. In what follows, the neutron intensity at which the pile is operated will be taken to be high enough so that the value of k at the critical condition may be considered to be unity with sufficient accuracy.

When the value of k is slightly larger than unity, the neutron intensity will drift upwards, while with k slightly less than unity, the neutron intensity will drift downward. The reactivity is a measure of the excess of k over

unity. For $k - 1 = 2.5 \times 10^{-5}$, the neutron intensity will increase with a period of about 1 hour. For pile periods very long compared to the longest delayed neutron period (78 sec), $(k - 1)$ is inversely proportional to the period.

3. Control rod calibration.

In this work, we have measured the effect of the insertion of an absorber in the pile by observing the displacement of the control rod which was required to return the pile to the critical condition. It was found, however, that for a given change in reactivity, the displacement required, if measured in centimeters, was not always the same but depended on the position of the control rod in the pile. It was convenient to introduce a new unit of rod position such that displacements measured in the new units would always be proportional to $(k - 1)$. In order to provide a precise definition of such a unit, use was made of the property of the pile that its period is proportional to $1/(k - 1)$ in the limit of long periods. Accordingly, the unit of rod position was given the name *inhour* (from "inverse hour," symbol: ih), with the significance that when the control rod is displaced from the critical position by 1 inhour, the pile will have a period of (very nearly) 1 hour. (See Appendix I).

4. Neutron absorption.

The introduction of a neutron-absorbing substance into a pile reduces the value of k. To compensate for this loss of k, it is necessary to move the control rod out of the pile. The change in the critical position of the rod measured in inhours is a measure of the absorption of the substance.

The absorption of two substances may be compared by comparing the change in critical position which they produce. However, the number of neutrons absorbed by the substance depends on the way in which its cross section varies with energy, and on the energy distribution of the neutrons in the pile. It is clear that our measurement is a measure of the average value of the cross section for the particular energy distribution which obtains in the pile used. In the graphite piles which were used for this work, the contribution of the thermal neutrons predominates except in a few instances for those substances which have strong, low lying resonance levels. For most substances, the effect of scattering on the value of the reproduction factor enters in a relatively minor way. In most cases, then, a comparison of the effect on k of two substances is a comparison mainly of their thermal-neutron-absorption cross section.

5. Intensity measurement.

The intensity of operation of the pile was measured by observing the ionization current produced in a large BF_3 ionization chamber connected to a high sensitivity galvanometer. Small drifts were observed with a differ-

ential galvanometer, which was connected so as to measure the difference between the ionization current and that provided by a battery and potentiometer. By adjusting the neutron intensity to give an ionization current of 10^{-5} ampere, it was easy to observe drifts of 1/1000 in intensity, using a differential galvanometer with a sensitivity of 10^{-9} ampere for 1-mm deflection at 1 meter. Thus a displacement of 0.01 inhour from criticality would produce a drift of 5 mm in 3 minutes. This was ample sensitivity for most measurements, as will be discussed later.

6. Boron standard.

A standard absorber was prepared using known amounts of boron, the cross section of which is accurately known. The value of the absorption cross section for boron has been measured [1] by the transmission method for slow neutrons using a mechanical velocity selector. Such a measurement gives an absolute and accurate measure of the absorption cross section, because in boron the scattering cross section is very small compared to the absorption cross section, and it is easy to analyze the results obtained at different neutron velocities in terms of a part proportional to 1/v which is caused by the absorption, and a constant part which is caused by the scattering. At 2200 meters per second, these authors give 703×10^{-24} cm^2 for the absorption cross section of boron.

In carrying out an absorption comparison, it is important that every atom of the sample have the same chance to capture a neutron; or failing this exactly, it is sufficient if the unknown and the standard samples are conditioned in such a way that the situation is the same for both. In order to minimize the effects of self-absorption and yet obtain an easily measured effect, an arrangement was used which distributed the absorber over a fairly wide area. In the case of the boron standard, in some measurements we used BF_3 gas, in others we used borax for which we provided a graphite holder, $10 \times 10 \times 120$ cm^3 which could contain 92 aluminum dishes for the borax about 1 inch in diameter each, and distributed inside the graphite. This holder could be reproducibly inserted near the center of the pile, in a position symmetrically disposed with respect to the neighboring uranium lumps. (See Appendix II).

The boron standard was made by preparing a solution of borax and depositing one milliliter of this solution on a disk of filter paper in each of a set of 92 aluminum dishes. This solution, when evaporated, had the appearance of having distributed itself quite uniformly over the filter-paper disk. In making a comparison with an unknown absorber, equal filter-paper disks and equal aluminum dishes were always used to make the standard and the unknown identical in every respect except for the borax in the one and the material of the unknown in the other. The total absorption cross section of

(1) E. Bragdon, E. Fermi, J. Marshall, and L. Marshall, «Phys. Rev.» (to be published) (It was published without Bragdon's name. See paper N° 200 [Editors' note]).

the borax for the average pile neutrons was about 9 cm^2; and since this was distributed over a total area of 460 cm^2, the effect of self-absorption was of the order of 2 percent. If the size of the unknown is adjusted to give the same absorption cross section over the same area, no error resulting from self-absorption occurs in the comparison. The error in the relative absorption cross section occurs as the difference in the self-absorption effects.

The borax solution was analyzed for boron by first standardizing a solution of sodium hydroxide with potassium hydrogen tartrate. The borax was converted to boric acid with HCl, using a methyl orange indicator, and a titration was then carried out with the NaOH in the presence of mannitol. The method is that given in Treadway and Hall, «Analytical Chemistry» *2*, 502. Two sets of three measurements each were carried out in our borax solution, one by Mr. W. Sturm of the Argonne Laboratory, and the other, independently, by Mr. D. Revinson of the Analytical Chemistry Group of the Metallurgical Laboratory. The average of the first series gave 2.816×10^{-4} mole of boron per ml, and for the second set, 2.793×10^{-4} mole of boron per ml. The agreement was considered satisfactory and the average of these results, 2.804×10^{-4} mole per ml was used in determining the cross sections. To the cross section per atom of boron, which at 2200 meters per second is 703×10^{-24} cm^2, we added 1×10^{-24} cm^2 to take into account the contribution of the sodium and hydrogen, and used 704×10^{-24} cm^2 at 2200 meters/second for the atomic-absorption cross section of borax. The total cross section of 92 borax disks was thus 10.94 cm^2 at 2200 meters/second.

7. Critical position measurements.

The effect of this boron standard on the reactivity of the pile was studied by comparing the critical position obtained with a blank set of aluminum dishes, and filter-paper disks with that obtained with the 92 borax absorbers. Since the absorption was distributed among 22 neighboring cells, only a minor perturbation in the neutron intensity distribution was produced. Measurements of the critical position were made by setting the control rod to produce first a slow drift in one direction and then in the other, and interpolating between the two settings in inverse proportion to the period of drift observed.

The critical position may be altered during the course of the measurement because of changes in temperature and barometric pressure which may take place. It is always necessary to make corrections for these effects during the course of a measurement. In the Argonne graphite pile, the temperature effect amounted to —0.814 ih/°C while the pressure effect, which was caused by the change in the amount of air nitrogen in the pile, amounted to —3.23 ih/cm Hg. There was also a humidity effect caused by the change in water content of the air on the pile which amounted to —2.85 ih/cm H_2O vapor. Of these, the most serious was the pressure effect, and it was always necessary to read the barometric pressure to 0.01 mm of Hg using a special mercury or aneroid barometer. Barometric pressure changes rapidly and in a spurious way, and over the short interval of time of such a change the pressure may not have had a chance to equilibrate over all the pile structure. The limiting

sensitivity of the method is imposed by the pressure effect and amounts to ~0.01 ih.

The temperature effect is less troublesome because the temperature of the pile changed slowly and in a regular way, so that by arranging a series of measurements in a cyclic time sequence of the form ABBA the slow drift in critical position caused by temperature change would be automatically eliminated in the averages.

In Table I is listed a series of measurements of critical position expressed in inhours with, and without the borax standard. The effect of pressure has already been corrected for in these values.

From these data, the sensitivity of the method is seen to be 2.052 cm^2 (at 2200 m/s) per inhour of rod displacement, with a precision measure of about $\pm$ 0.03 cm^2.

TABLE I.

Standardization of absorption measurements.

Blank	Critical position in inhours Borax	Cadmium
105.127	99.806	98.926
105.144	99.806	98.902
105.163	99.821	
105.145	99.862	
105.190		
105.153	99.823	98.914

As an example of the method, the measurement of the absorption cross section of columbium is of interest. Columbium has only one isotope, and it was to be expected that the absorption of a neutron would give rise to a radioactive isotope so that the absorption cross section could be measured by observing the B emissions. Early activation cross section measurements by L. Seren, H. Friedlander, and S. Turkel at the Argonne Laboratory gave an apparent result of about 0.02×10^{-24} cm^2.

A high purity sample of Cb_2O_5 was obtained from the Fansteel Company. A preliminary measurement showed an absorption cross section of 1.4×10^{-24} cm^2, almost 100 times larger than that found by the activation method. A new sample was then obtained from the Fansteel Company which was reported to have even higher purity than the first. Spectroscopic analyses made on the two samples are given in Table II.

The Cb_2O_5 was pressed into pellets which were placed in the aluminum sample dishes covered with a disk of filter paper. In order to obtain approximately the same control-rod displacement, 46 of the standard boron dishes

were used. These were uniformly distributed in the graphite holder. The no-absorber critical position was obtained with empty aluminum dishes and blank filter-paper disks. The first sample contained 931.45 grams of Cb_2O_5, the second sample 934.31 grams, while there was 0.1395 gram of boron in the standard. Measurements of critical position of the rod in inhours are given in Table III. Corrections for changes in pressure during the measurement are already included in the numbers given.

TABLE II.

Analysis of columbium pentoxide.

Spectrochemical analysis Sample No. 1 (oldsample)		Mfg. spectrochemical analysis Sample No. 2 (new sample)	
	99 → Cb		
Ce	50 ppm	Ta_2O_5	None
Gd	10 ppm	TiO_2	Less than 0.001 %
Hf	50 ppm	Fe_xS	None
Mo	20 ppm	ZnCuMg	Very weak
Sc	5 ppm	SiO_2	0.03 %
Pr	5 ppm		
S	20 ppm		
Zr	100 ppm		

TABLE III.

Absorption of columbium.

	Critical position in inhours			
	Blank	Cb No. 1	Boron (std.)	Cb No. 2
Run A	117.66	115.14	115.39	115.14
Run B	117.67	115.17	115.39	115.15
			115.40	
	117.66	115.15	115.39	115.14

Change in critical position

Due to Cb No. 1	ih = 2.51
Cb No. 2	ih = 2.52
Boron std.	ih = 2.27

Absorption cross section of Cb

(referred to 2200 m/s) = 1.44×10^{-24} cm^2

With very good agreement for both samples, the experiment yielded for the ratio of the average absorption cross section, for pile neutrons, of columbium to that of boron the value 0.00204. On the assumption that the absorption cross section obeys the same law of variation with neutron velocity as does the boron (the 1/v law) the columbium-absorption cross section may be given the value of 1.4×10^{-24} cm² at 2200 m/s.

8. Cadmium standard absorber.

In a large part of the work it was found convenient to use cadmium as a standard absorber rather than boron. A wire of cadmium has the property that practically all neutrons with energy less than about 0.3 ev which strike it will be absorbed. Since most of the neutrons in the pile are below 0.3 ev, cadmium serves as a convenient standard absorber, whose neutron cross section may be obtained from its geometrical dimensions.

Cylindrical cadmium wires of diameter D and length l have a geometrical cross section for isotropically distributed neutrons

$$A = \frac{1}{4}\pi D l$$

neglecting end effects.

In comparing the effect of cadmium to that of the standard borax absorbers, we used wires which had an average diameter of 0.1006 cm and a total length of 128.25 cm, giving a neutron cross section of 10.14 cm². These wires were distributed uniformly over the graphite holder together with blank aluminum dishes and blank filter-paper disks. Control-rod displacements resulting from the cadmium and compared to the borax are given in inhours in Table I. The effect of the cadmium is seen to be 6.239 ih or 1.625 cm²/ih.

The neutron cross section of cadmium may be converted to that of a 1/v absorber at 2200 meters per second by multiplying by the factor 2.052/1.625 = 1.26.

9. Temperature of pile neutrons.

Since the boron absorption of neutrons varies according to the 1/v law, the number of neutrons which are absorbed by thin absorbers is proportional to the neutron density, and is independent of the neutron velocity distribution. Thick cadmium, however, captures every thermal neutron which strikes it, hence the absorption by cadmium depends also on the average velocity of neutrons.

A comparison of the effect of the absorption of these two substances gives information about the average velocity of pile neutrons. In making the comparison it is necessary to subtract that part of the effect of boron which is caused by absorption of neutrons above the cadmium limit. This was done by means of a BF_3 counter placed above a hole extending into the center of the pile. Using boron carbide collimation, the counter could not see neutrons which might be reflected by the pile shield, but only those emerg-

ing directly from near the bottom of the hole. Such neutrons have a distribution quite close to that which is present inside the pile. With no cadmium in the beam we observed 5200 counts per minute; with cadmium, 112 counts per minute; and with 3 inches of B_4C powder in the beam, 4 counts per minute. The contribution of the neutrons above the cadmium limit is thus 2.08 percent. Thus, an absorber whose cross section is 2.095 cm^2 at 2200 m/s, and which absorbs according to the 1/v law up to the cadmium limit and not at all above, changes the critical position hy 1 inhour. For an absorber which absorbs all neutrons up to the cadmium limit with equal probability the same change in critical position is produced by 1.625 cm^2 of cross section. It follows that the average velocity of the neutrons which are in the center of the pile and below the cadmium limit is 2836 meters per second. This corresponds to a neutron temperature of 383° Kelvin.

10. Effect of scattering.

A neutron scatterer may affect the reactivity of a pile either by altering the spatial, or the energy distribution of neutrons in the pile. A scatterer placed near a uranium lump may reduce the number of neutrons which can diffuse into the lump and thereby diminish the reactivity. An increase in the reactivity may be obtained if the scatterer is placed near the edge of the pile so that the neutron leakage is reduced. A pure scatterer can, however, produce no change in the spatial distribution if it is placed in a region where the gradient of the neutron density is zero. For this reason, absorption measurements are always made with the sample symmetrically disposed with respect to the uranium lump, and near the center of the pile.

With a scatterer in this position, its effect on the energy distribution does alter the reactivity of the pile in a non-negligible way. By increasing the slowing-down power of the moderator, the resonance absorption in uranium is decreased and the result is an increase in the reactivity.

11. Absorption cross section of beryllium.

For certain light elements with very small neutron absorption, the increase in the reactivity due to slowing down (see Appendix III) may be comparable to the decrease due to absorption and must be taken into account. We describe, as an example, a determination of the absorption cross section of beryllium. Beryllium metal blocks were placed in the Argonne pile distributed in 16 cells, 456 grams per cell. The results of the inhour measurements are given in Table IV.

The measurement with cadmium wires standardizes the geometry used for absorption. As discussed above, the cadmium standardization may be reduced to that of a 1/v absorber at 2200 meters per second by multiplying its cross section by the factor 1.26. Thus the cadmium standardization gives: $3.80/8 \times 1.26 = 0.377$ ih/cm^2.

TABLE IV.

Measurement of the beryllium cross section.

Sample	Change in inhours
7296 grams Be	— 0.11
12960 grams C	0.00
8 cm^2 Cd	— 3.80

The measurement with graphite shows that the effect of slowing down on the reactivity of the graphite we used is equal to the effect of its absorption. The absorption cross section of our graphite as measured by a diffusion method was known to be 0.0049×10^{-24} cm^2 at 2200 m/s. The effect of the slowing down is proportional to $\sigma_s \xi$, where σ_s is the cross section for scattering for resonance neutrons, and ξ is the average logarithmic loss of energy per collision (see Appendix III). For graphite $\sigma_s = 4.8 \times 10^{-24}$ cm^2 per atom and $\xi = 0.158$ while for beryllium $\sigma_s = 6.1 \times 10^{-24}$ cm^2 per atom and $\xi = 0.202$ so the effect of slowing down in beryllium is:

$$\frac{6.1 \times 0.202}{4.8 \times 0.158} \times 0.377 \times 4.9 \times 10^{-27} \times \frac{7296}{9} \times 6.02\, \xi \times 10^{23} = 1.46 \text{ ih}.$$

Subtracting this from the total effect — 0.11 ih we have for the effect of absorption —1.57 ih. Thus, the absorption cross section of beryllium at 2200 m/s is:

$$\frac{1.57}{0.377} \frac{9}{7296 \times 6.02 \times 10^{23}} = 8.5 \times 10^{-27} cm^2/\text{atom}.$$

Since an accurate chemical analysis for the beryllium blocks we used was not available this result represents an upper limit of the capture cross section of beryllium. We have reason to believe, however, that the material was of high purity.

APPENDIX I

THE INHOUR

The inhour is proportional to $k - 1$, thus,

$$\text{ih} = C\,(k - 1)$$

where the value of C is given by

$$C = \lim_{k \to 1} \frac{1}{T\,(k - 1)},$$

and T is the period of the pile in hours.

The relation between the displacement from criticality in inhours and the period of the pile may be obtained from the intensities and periods of the delayed neutron emission. For the uranium-graphite pile, the following formula has been used in our work:

$$\text{ih (crit)} - \text{ih} = \frac{64}{T} + \frac{245}{T + 3.57} + \frac{688}{T + 10.1} + \frac{1938}{T + 34.5} + \frac{665}{T + 83},$$

where T is the period of the pile in seconds. The numbers in the denominators are the periods of the various delayed neutron emissions in seconds. The contribution of some shorter periods has been disregarded. It is to be noted that because of the way in which the inhour has been defined, the accuracy with which this formula gives the period becomes greater and greater for larger and larger values of the period. According to the above formula, the pile has a period of 1 hour when

$$\text{ih (crit)} - \text{ih} = 0.990.$$

Calibrations of the control rod may always be effected with the use of this formula by observing the period of the pile for a given displacement of the control rod from the critical position. The value of the inhour is measured from its zero value corresponding to control rod out of the pile. Table V gives the sensitivity of the control rod $d\,\text{ih}/dx$ as a function of the position of the rod in the pile in centimeters. The integral of this curve is also given.

TABLE V.

Calibration of control rod of Argonne pile.

x cm	$d\,\text{ih}/dx$	ih
0	0.000	0
50	0.023	0.7
100	0.067	2.7
150	0.158	8.2
200	0.299	19.5
250	0.418	37.8
300	0.492	60.7
350	0.520	86.0
400	0.490	111.5
450	0.402	133.7
500	0.281	151.2
550	0.142	161.3

The inhour is useful as a measure of rod displacement because it is a measure of pile reactivity which is independent of the position of the control rod, so that linear interpolations are accurate in comparing the effects of different absorbers. Moreover, its value has an almost unambiguous significance for all graphite-uranium piles.

The value of the constant C is known for uranium-graphite piles to be

$$C = 2.5 \times 10^{-5} \text{ hours}^{-1}$$

with an accuracy of about 20 percent.

APPENDIX II

EFFECT OF POSITION

The effect of a given absorber on the reproduction factor depends on its position in the pile. Because of the inhomogeneous character of the structure the general variation of neutron density has superimposed on it a strong local variation. Thus the density n of neutrons at the position x, y, z may be represented by

$$n(x, y, z) = \alpha(x, y, z)\,\beta(x, y, z),$$

where α is a smooth function, and β has the same periodicity as the cells and describes the local variations of intensity. For small absorbers which do not perturb the neutron distribution appreciably, the effect on the reactivity is proportional to the square of α and depends also in a complicated way on the position of the absorber within the cell.

In order to minimize the variations caused by this last factor it is preferable to place the absorbers not too close to the uranium lumps. For the graphite-uranium piles, the variation of α may be obtained with sufficient accuracy from the solutions of the diffusion equation

$$\Delta\alpha + B^2\alpha = 0$$

subject to appropriate boundary conditions. In a uniform cubic structure of side a, α may be expected to vanish near the boundary so that the solution is

$$\alpha(x, y, z) = \alpha(0, 0, 0)\cos(\pi x/a)\cos(\pi y/a)\cos(\pi z/a),$$

in which the origin of the coordinates is taken at the center of the pile. Thus, the effect on k of an absorber added to the central cell is 8 times greater than if it were added to the average cell. The number of neutrons which it absorbs is only $\pi^3/8$ times greater.

In the Argonne pile used in this work, the design of the cell was such that an absorber having a cross section for pile neutrons of 1 cm^2 placed midway between two lumps would absorb about 1/28 of the neutrons absorbed by the cell itself. Thus, inappreciable perturbations of the neutron distribution would be caused in general if the amount of absorber added per cell had less than 1 cm^2 of absorption.

APPENDIX III

ENERGY DISTRIBUTION OF PILE NEUTRONS

It is convenient to distinguish two groups of neutrons in the pile, in consideration of the property of cadmium, in quite thin sheets, which absorbs completely one of these with only a minor effect on the other. Cadmium has a fairly sharp absorption limit between 0.3 and 0.5 ev depending on its thickness. Neutrons whose energy is below this limit are cadmium-absorbable and sometimes are termed C-neutrons. The neutrons of higher energy are not appreciably absorbed by cadmium and are sometimes termed epicadmium neutrons.

Because of the nature of the slowing-down process, the number of neutrons in a logarithmic energy interval is proportional to dE/E. Since the distance for slowing down is large compared with the spacing of the uranium lumps, but small compared with the dimensions of the pile, the distribution of sources may be taken to be uniform and the loss by leakage and absorption (which amounts to about 10 percent down to 1 ev) may be neglected in general. It is thus appropriate to speak of the slowing-down density $q(E)$ which is the number of neutrons per cm^3 which is slowed from above to below the energy E within one second. This

quantity is conserved in the pile except for losses caused by leakage and absorption, as mentioned. The relation to the density of neutrons $n(E)$ per unit energy interval is generally

$$n(E) = Q(E)\frac{1}{v\bar{E}}\frac{1}{\xi_s \sigma_s}.$$

Here v is the neutron velocity, and σ_s is the reciprocal mean free path for collision with the moderator (carbon), and ξ_s is the average logarithmic loss of energy per collision.

The value of ξ for elastic collisions and isotropic scattering for a moderator of mass M of atomic weight A is:

$$\xi = 1 - \frac{(A-1)^2}{2A}\log\frac{A+1}{A-1},$$

which for not too small A reduces to $\xi \approx 2/A$. For carbon ξ has the value 0.158, for oxygen it is 0.121, while for hydrogen its value is unity. The product $\xi_s \sigma_s$ is the slowing-down power per cm^3 of the moderator.

Once the neutrons fall below the cadmium limit, the mechanism of the slowing down is greatly altered. The neutron energy becomes comparable to the energy of crystal binding of the atoms with which they collide, and to the energy of thermal agitation. The slowing down proceeds more slowly, and indeed, because of the preferential absorption of neutrons having lower energies, thermal equilibrium is never established exactly. For most purposes, it is sufficiently accurate to consider the C–neutrons in the pile as a group of neutrons having a Maxwellian energy distribution with a temperature somewhat higher than the true temperature of the pile, as discussed in the text.

Neglecting the variation of $q(E)$ and σ_s with neutron energy, the number of epicadmium neutrons which are absorbed per second by a substance with absorption cross section $\sigma_a(E)$ is

$$A_{res} = \int_{E_{Cd}}^{\infty} \sigma_a(E)\, n(E)\, v\, dE = \frac{q}{\xi\sigma_s}\int_{E_{Cd}}^{\infty} \sigma_a(E)\frac{dE}{E},$$

where the upper limit has been extended to infinity because the contribution to the absorption at high energies is usually quite small. The integral has been called the resonance-absorption integral, and in general its principal contributions come from the low energy neutrons.

Below the cadmium threshold, the neutrons have approximately the Maxwellian distribution as was pointed out above. This is a rather narrow energy range and the chance that a resonance occurs in it is fairly rare. Except for those cases where a resonance below 0.3 ev is known to occur, it is reasonable to suppose that the absorption has a $1/v$ dependence so that the thermal activation is given by:

$$A_{th} = n\bar{v}\sigma(\bar{v}).$$

Here $\bar{v}$ is the average velocity of the C–neutrons, and n is their density. The ratio of the activations is given by:

$$\frac{A_{res}}{A_{th}} = \frac{q}{n\bar{v}}\int_{E_{Cd}}^{\infty} \sigma_a(E)\frac{dE}{E}\Big/\xi\sigma_s\,\sigma(\bar{v}).$$

The quantity $(q/n\bar{v})\cdot(1/\xi\sigma_s)$ can be determined from the measurements described above in which a BF_3 counter was exposed to the neutrons from a hole in the pile. These data gave

$$\left(\frac{A_{th}}{A_{res}}\right)(\text{boron}) = 47.1.$$

Since the boron absorption follows the $1/v$ law, we have

$$\sigma(\bar{v})\Big/\int_{E_{Cd}}^{\infty} \sigma(\bar{v})\left(\frac{E(v)}{E}\right)^{1/2}\frac{dE}{E}\left(\frac{E_{Cd}}{2E(\bar{v})}\right)^{1/2}$$

for 0.90 gm/cm² of Cd we may take $E_{Cd} = 0.4$ ev, while for $E(\bar{v})$ we take 0.042 ev and obtain, thereby, the general expression

$$\frac{A_{res}}{A_{th}} = \frac{0.045}{\sigma(\bar{v})} \int_{E_{Cd}}^{\infty} \sigma(E) \frac{dE}{E}$$

with an uncertainty of about 10 percent resulting from the uncertainty in E_{Cd}. The coefficient 0.045 is in good agreement with the value obtained from an independent method of obtaining this number based on the use of a calibration of indium foils in a "standard graphite pile" which is described elsewhere. This relation is useful in determining the value of $\int \sigma_a(E)\, dE/E$ from a comparison of the activations induced in a substance with and without cadmium protection.

The work reported here was done in 1943–44. It was carried out under contract between the University of Chicago and the Manhattan District Corps of Engineers, War Department.

N° 211 and 221.

Already at this early stage of reactor development, Fermi and other men at the Metallurgical Laboratory were considering the possibility of achieving *breeding*, namely of producing in a reactor more fissionable material than was consumed. In a pile using natural uranium, breeding would be achieved if more plutonium were produced than U^{235} is burned up. Whether this is possible depends on neutron economy. Since it was known that between two and three neutrons were produced per fission, breeding appeared theoretically possible.

A number of discussions on breeding were held at the Metallurgical Laboratory in which Fermi played an active role. He was so impressed in the practical importance of developing breeder reactors that after the war he encouraged Zinn, by then director of the Argonne laboratory, to design and build such a reactor. In recognition of this interest, the first commercial breeder plant in the United States was called " The Enrico Fermi Atomic Power Plant ".

Included here are the notes on Fermi's part in two of the discussions at the Metallurgical Laboratory: the first took place in April 1944 (paper N° 211), the second in June 1945 (paper N° 221).

Paper N° 211 was circulated also as Document LAO–17.

H. L. ANDERSON.

211.

DISCUSSION ON BREEDING

Excerpt from Report N–1729. (Notes on meeting of April 26, 1944).

Present: FERMI, ALLISON, SZILARD, WIGNER, WEINBERG, SEITZ, MORRISON, COOPER, VERNON, TOLMAN, WATSON, OHLINGER.

The first speaker in today's meeting was Mr. Fermi. His remarks follow.

It was assumed for today's discussion that the aim of the chain reaction would be the production of power.

The first type of pile assumed for this purpose was a permanent large pile of about the Hanford size (but not the Hanford type necessarily) for production of energy in the neighborhood of 10^6 kilowatts. The arrangement suggested was one in which one large mother plant would produce 49 for consumption in a series of smaller plants. In the mother plant, the energy produced would be used to reduce the cost of the 49 produced. (Mr. Fermi mentioned that he viewed the use of this power for the heating of cities with sympathy). There may be non-technical objections to this arrangement, for example, the shipment of 49 to the smaller consuming plants offers the serious hazard of its falling into the wrong hands, but these objections were to be omitted from this discussion.

The fundamental aim in the mother plant would be to get the maximum possible yield, with full utilization of the metal as the goal. If a solution to such a proposal can be found, then the schemes for isotope separation are not of great interest. If such a solution is not possible, then the schemes for isotope separation should undoubtedly be investigated further.

In the following discussion of full metal utilization, the isotopes 28 and 49 will be referred to as 8 and 9, respectively. In the reaction cycle suppose that one fission of 9 and ψ fissions of 8 take place in a single cycle or generation. Then the production of neutrons will be $\nu_9 + \psi\nu_8$. Some neutrons are lost in the moderator, coolant, etc. Let L = the number lost and α = the number used in producting 40–10. Then the excess of neutrons available for absorption by 8 to produce 9 will be:

$$(1 - L)(\nu_9 + \psi\nu_8)$$

and the production of 9 per cycle will be:

$$(1 - L)(\nu_9 + \psi\nu_8) - 1 - \alpha - \psi.$$

The term $1 + \alpha$ represents the destruction of 9. Therefore, the ratio of production of 9 to its destruction, which we will call γ, will be:

$$\gamma = \frac{P}{1+\alpha} = (1 - L)\left(\frac{\nu_9}{1+\alpha} + \psi\,\frac{\nu_8}{1+\alpha}\right) - 1 - \frac{\psi}{1+\alpha}.$$

To utilize all the metal, γ obviously must be greater than 1. If γ is only very little greater than 1, the chain reaction would keep going with maximum economy of fissionable materials and would continue to go on until all the metal were used, but the value of such a pile would not be great and it would only be good for, say, hardening materials (the Wigner effect) or possibly (though less desirable) heating cities. The effective ν_9 is around 2.1 to 2.2.

Assume first a Hanford type pile with an equivalent amount of 49 substituted for the 25, i.e., in the early stages, 25 would be burned to produce 49 which would gradually improve its condition. The earlier estimate of 1.9 for the ratio of the fission cross section of 49 to that of 25 has been more recently estimated by site Y as 1.4. The ratio of absorption cross section for 49 to that of 25 is around 1.5. Under these conditions, ν_9 is about 10 percent higher than it was previously thought to be. (The actual values of ν and ν effective are not really known so the discussion can only show ranges). The situation then in a pile of Hanford design and lattice would be for a ν effective (which will be referred to hereafter as μ) of 2 to 2.2, γ will be from 0.8 to 0.98. In the latter case, the pile is close to a balanced situation but not quite there. To adjust such a pile without drastic changes of design, large diameter slugs or more metal could be used to improve the thermal utilization and increase ψ. However, over-sized lumps increase the difficulty of cooling since the annular type cooling is badly limited in power production by the metal temperature.

The second type pile considered for the production of power was the P–9 moderated pile. For a μ of 2 to 2.2, γ would be 0.93 to 1.13. These values do not necessarily represent the optimum but are merely indicative of what

can be done with P–9 piles, and one with such a γ of 10 to 15 percent may or may not be an operable plant. The practical difference between continuous and discontinuous P–9 plants is not large in this respect since the loss by absorption for the coolant and its tubes practically compensates for the less efficient reproduction in slurry piles. One might hope to improve the situation by capturing the escaping neutrons in a reflector but the absorption in the pile container is an important problem.

Another type of pile to consider is one with very little or no moderator (fast chain reacting type). From the nuclear point of view this is very desirable and is simple in principle but, practically, it involves serious problems in removing the heat. Ignoring the cooling, and considering only the nuclear point of view, this type pile may be of either one of two forms:

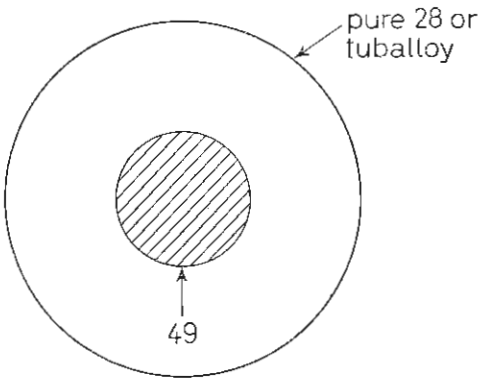

Fig. A.

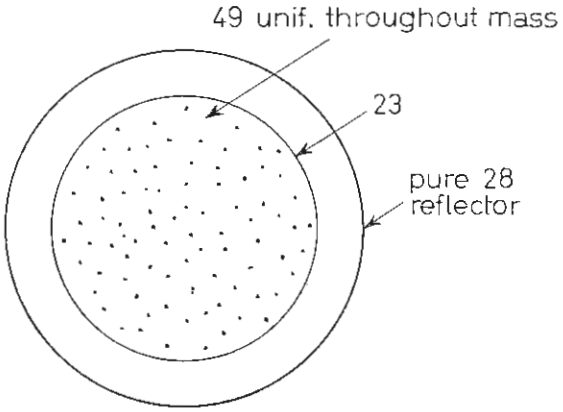

Fig. B.

In fig. A, a small spherical core of 49, say, 10 cm in diameter, would be surrounded by a sphere of 28 or normal tuballoy (*) about 40 to 60 cm in diameter. This arrangement is good from a γ standpoint and one might expect a γ of 1.3 to 1.4, because L can be made small since the fast neutrons from the 49 get into the 28 readily. (Mr. Allison pointed out that if 25 is not considered for the surroundings here, thorium might be used). The pile shown in fig. A only requires a few kilograms of 49. To utilize more 49 it would be possible to construct units like A with multiple 49 cores spherical or cylindrical in shape.

Fig. B represents a homogeneous sphere of 28 with 49 uniformly distributed throughout the mass, the whole surrounded by a reflector of pure 28 to catch the leakage neutrons. In this arrangement about 70 percent of the neutrons get into 28 immediately to produce fast fission. Assuming a mixture of 49 and 28 in which X represents the percentage of 49, critical conditions (i.e., where the chain reaction continues if the pile is of infinite size) would be reached with about 5 percent of 49 in the mixture (X=0.049). For values of μ of 2 to 2.2, γ would be 1.37 to 1.57. As the pile size is decreased, the results in Table I would be obtained. They are calculated without reflector.

(*) Code name for natural uranium. (Editors' note).

Adding a reflector would decrease the critical radius of the active sphere by about 10 cm and improve very considerably the value of γ since the reflector would utilize the neutrons escaping from the active core. Taking the case of the 70 cm sphere above, this represents about $1\frac{1}{2}\,\bar{m}^3$ or say 30 tons of the mixture. Therefore, 6 percent or about 2 tons of 49 would be required to keep this machine running. Thus a plant of this type requires a large quantity of 49 for operation although this is not sufficient reason for discarding this type of pile as a possibility.

TABLE I.

Critical Radius of Sphere	X (fraction of 49)	γ	
		$\mu = 2$	$\mu = 2.2$
100 cm	0.054	1.23	1.43
70 cm	0.060	1.10	1.30
50 cm	0.067	0.98	1.18

The serious objection to these fast chain piles is the removal of the heat. Since practically all the heat is produced in the 49 (about 70 to 80 percent), piles like those in fig. A are harder to cool since it is mainly the tiny core which must be cooled while in fig. B the whole mass is to be cooled.

As another possibility, a compromise enriched pile might be designed which would have enough moderator to reduce the percentage of enrichment required to keep the chain reaction going. But not as large an amount would be required for the conventional optimum conditions.

Mr. Fermi suggested that at a later meeting he would consider the question of how to use the 49.

N° 212.

As a result of his own experiments and his contact with the work at Site Y (Los Alamos), Fermi was the expert on the neutron properties of 49 (Pu^{239}). This was to be the product of the Hanford plant and its properties were of interest not only to the designers of the bomb, but also to the designers of the pile.

It was very important to measure, among other nuclear properties of Pu^{239}, $\alpha = \frac{\sigma_c}{\sigma_f}$, the ratio between capture and fission cross section, and the spontaneous fission constant. These measurements were assigned to the Los Alamos Laboratory, which received the first Pu available from the pilot plant at Oak Ridge. Fermi took a lively interest in them and arranged with Segrè, who was in charge of this work at Los Alamos, for the use of the pile for the measurement of α. In this work there was active collaboration between Chicago and Los Alamos, with Segrè coming to Chicago and working with D. Nagle, a member of Fermi's group.

The results of Fermi's measurements and some of the interesting and somewhat unexpected properties of plutonium were reported to the Chicago group by H. H. Goldsmith. The notes, not always grammatical, that were taken from Goldsmith's report constitute this paper. It was circulated also as Report A–2617.

H. L. ANDERSON.

212.

REPORT ON RECENT VALUES OF CONSTANTS OF 25 AND 49

Report CK–1788 (May 19, 1944).

Present: FERMI, ALLISON, W. W. WATSON, COOPER, WIGNER, SZILARD, SEABORG, MULLIKEN, WEINBERG, MORRISON, ANDERSON, SUGARMAN, SEITZ, DANCOFF, MISS CASTLE, YOUNG, TURKEVICH, BURTON, HUGHES, SNELL, GOLDSMITH.

1. CROSS SECTION OF 49 AS A FUNCTION OF ENERGY.

We have recently measured the absorption cross section of 49 by the transmission method. Because of the large cross section, a very thin layer of absorber must be used. (A few tenths of a mm of oxide will absorb about 50 percent of neutrons.) To approximate a uniform layer we mixed 1 gm of 49 with 2 gm of graphite powder. Despite the apparent uniformity of surface, the neutrons traverse only 4–5 grains of 49 on average. This leads to large fluctuations in transmitted intensity across the sample with resultant inaccuracy in cross section measurement. Our value for kT neutrons was $\sigma = 950$ b.

At site Y somewhat better samples were obtained by pressing the 49 between Al surfaces. The samples were only $\sim$ 1 inch in diameter due to

the scarcity of 49. This limited the modulated neutron beam to such small apertures that measurements were confined to the region below 1 ev.

A study of the transmission of 49 in the region between 0.01–0.5 ev revealed a very strong and narrow resonance with a maximum at ~ 0.3 ev. A curve showing the cross section as a function of neutron energy in this region was exhibited. The cross section at 0.01 ev is 1600 b, then falls off as $1/v$, flattens out and reaches a minimum of ~ 600 b at 0.1 ev, then rises to an observed value of ~ 3800 b at 0.3 ev. The height of the resonance line is reduced and its width is broadened by the poor resolution of the velocity selector.

The results were also shown in the form of a graph relating σv as a function of the neutron energy. The value at 0.01 ev is 2.27×10^6 (in units of 10^{-24} $cm^2 \times m/sec$). The curve is practically horizontal up to 0.05 ev and rises to a maximum value of 26×10^6 at 0.3 ev. Making a rough correction for the resolving power of the instrument, would estimate the maximum value to be $\sim 40 \times 10^6$ (the absorber had an appropriate thickness for the measurement of σ at the kT; however, in the resonance region the transmission is only ~ 5 percent, resulting in large background difficulties).

Can fit data approximately by a modified Breit-Wigner formula:

$$\sigma v = 1.36 + \left[\frac{40}{1 + \left(\frac{E - 0.3}{0.042} \right)^2} \right] \times 10^6.$$

The first term within the bracket represents the $1/v$ absorption (and perhaps the residual effect of minor resonances, both negative and positive); the second is the Breit-Wigner contribution. The narrow width of the resonance — 0.042 ev — is noteworthy (estimate the width as > 0.02 ev and < 0.05 ev). Such a narrow resonance indicates a relatively long lifetime for the intermediate nucleus. Theoretical physicists at Y had guessed that the 49 resonance would be broader than those of 25. Actually it is about 1/3 of the 25 widths. It should be noted that the Y value of the kT cross section of 49 is ~ 1020 b. This is probably more accurate than our own value of 950 b. Provisionally we may take the value 1000 b as correct.

The remarkable height and sharpness of the 49 resonance as compared to the 25 resonances was emphasized by plotting the velocity selector data for both substances on the same $\sigma v - E_n$ graph. The difference in the two sets of experiments should be recalled. In the case of 49 the sample was used as an absorber; the neutrons were detected by a boron counter. The measured transmission gives σ_{total} *vs* E_n. For 25, the ratio of the activation cross sections of B and 25 was measured by detecting the modulated neutron beam with a B counter and a 25 fission chamber respectively. Assuming the $1/v$ law for B, one gets directly σv for the fission of 25.

In answer to a question by Weinberg, Fermi calculated $\int \frac{\sigma \, dE}{E}$ for 49 to be ~ 2000 b. This is of the same order of magnitude as observed for the resonances of In, Au, etc. In answer to a suggestion by Morrison, Fermi indicated that there was as yet no evidence to justify the assumption that the level systems for fission and capture are of a different order of magnitude.

This led to a discussion of the intuitive reasons behind the insistence that such levels are identical. It was agreed that a measurement of the 25 resonances by a transmission method would be worth-while. It was also agreed that an accurate study of the 49 resonance by the activation method would not be feasible, due to the large α background. (This would limit the amount of 49 in a fission chamber to $\sim 10\,\mu$gm; whereas 25 fission chamber in the Y experiments contained ~ 1 gm of 25).

2. Present status of the branching ratio of 25 and 49.

The first Argonne measurement of the branching in 25 yielded the values $\frac{\sigma_f}{\sigma_{(f+c)}} = 0.825$, giving a branching ratio $\alpha = 0.175/0.825 = 0.21$. More recent measurement gives $\alpha = 0.15/0.85 = 0.18$.

At site Y, using essentially the same methods, first results gave $\alpha \sim 0.1$. Most recent experiments give ~ 0.15. It seems that the best estimate of the branching ratio at present is 16–17 percent.

(a) There is now some evidence pointing to a greater branching ratio in 49 than in 25

$$\frac{\sigma_a(49)}{\sigma_a(25)} = 1.57.$$

However,

$$\frac{\sigma_f(49)}{\sigma_f(25)} = 1.4 \text{ (Y value is 1.38; Anderson's is 1.41).}$$

If α in 25 is taken to be 0.16 then the branching in 49 is 0.3.

This larger value for the branching in 49 as compared to 25 is consistent with the narrower resonance level in 49.

(b) At Argonne we have measured:

$$\frac{\eta_{49}}{\eta_{25}} = 0.97 \quad (\eta = \text{no. of neutrons emitted/neutron absorbed}).$$

At site Y, ν_{49}/ν_{25} was found to be 1.18 (ν = no. of neutrons emitted/fission). This gives a 49 branching ratio $\sim 1.18/0.97$ or $\alpha \sim 0.4$. Knowing the two branching ratios, we find $\nu_{25} = 2.15 \times 1.16 = 2.4$; $\nu_{49} = 2.15 \times 1.3 \sim 2.8$.

The existence of the 49 resonance will effect our work to some extent. One possible application may be given. The resonance occurs at the relatively low energy of 0.3 ev. This corresponds to kT with T = 3000° C. This means that at neutron temperatures of $\sim 200°$ C the tail of the Maxwellian distribution will overlap the 49 resonance. Consequently, temperature changes will affect the number of fissions of 49. After a few months of W (*) operation 49 will contribute a few percent of k. This contribution will be highly temperature sensitive and should be calculated.

(*) Site W was the wartime name of Hanford, Washington. (Editors' note).

3. THE LONG RANGE α PARTICLES.

Segrè has constructed a chamber for studying the coincidence between long range α particles and fission fragments. Finds that most of the long range α particles are coincident with fission. Yield is ~ 1 α/200 fissions. He finds the α particles have range extending to 21 cm in air. This agrees with Alvarez's ionization chamber measurements. Hughes, employing a cloud chamber has found the α's to have the same yield but smaller range (up to ~ 15 cm). Segrè also reports that perhaps 1/3 of the α's he observes show no coincidence with fission. The results of Segrè and Hughes indicate that the α's coincidente with fission are not monoenergetic.

Two possible mechanisms for the emission of α's during the fission process are: (a) fission fragment is so highly excited that emission from fragment becomes energetically possible; (b) a three particle fission, the α particle left behind as the fission fragments separate. Though neither mechanism is plausible, (a) is preferred.

Fermi, Wigner, and Dancoff discussed the relative probability of α and p emission during the fission process.

H. H. GOLDSMITH.

213.

SUMMARY OF EXPERIMENTAL RESEARCH ACTIVITIES

Excerpt from Report CP–1729 for Month Ending May 25, 1944 (*).

During the month of May the P–9 pile at the Argonne Laboratory has been partly filled with liquid to the point of actually reaching the critical condition. It turned out that the amount of water needed for this was about 20 % less than had been estimated from the results of the exponential experiment. It is not yet quite clear what the reason is for the discrepancy. The construction of the pile is now practically complete, and the machine will be put in operation to power as soon as the balance of the P–9 arrives.

A number of experiments have been carried out in Mr. Anderson's section on nuclear properties of product, reported in CK–1761.

The long range alpha particles emitted by 25 under neutron irradiation have been studied by Mr. Hughes in the Wilson chamber. He reports a cross-section of about 2×10^{-24} for the production of alpha particles of ranges between 5 and 10 cm, and a cross-section of 1.6×10^{-24} for ranges between 10 and 15 cm. The total cross-section of 3.6 for emission of these alpha particles corresponds to about 1/200 of the absorption cross-section of 25.

Mr. Hughes carried out some measurements on the diffusion of thermal neutrons in uranium metal through a thickness of 5.5 cm. He finds that the average value of the diffusion length is 1.55 cm with a slight indication of a gradual hardening of the neutrons with increasing depth.

Mr. Seren has carried out additional measurements on the activation cross-sections of various isotopes. His results are summarized in a table in the report.

A measurement was performed in order to determine the increase in neutron density at the end of a W–slug when aluminum spacers of 7/8'' thick are interposed between slugs. It was found that the density of neutrons increases by about 40 percent.

An experiment was performed in order to determine whether the decomposition products of water by fission fragments reach a saturation pressure. No indication of a saturation was observed up to 14 atmospheres pressure of the detonation mixture.

(*) Report CP–1729 was issued also as A–2443. (Editors' note).

Mr. Anderson constructed a BF_3 chamber for the detection of very weak neutron sources. It is possible with this chamber to detect sources emitting about 1 neutron per second.

In Mr. Morrison's group work has been going on in order to determine the reproduction factor of various types of Hanford lattices. Some points on the technique of the measurement have to be cleared up before final results can be quoted.

N° 214.

An interesting item in the May report had to do with the study of the dissociation of water by fission. Already in the '30s Fermi had discussed at length this process with Trabacchi, but at that time alpha particles and not fission fragments were the dissociating agents. The emanation for the Rome experiments was extracted from a radium chloride solution. There was always some decomposition of the water, and for safety's sake, the mixture of hydrogen and oxygen had to be ignited before the emanation was extracted. Even earlier, Madame Curie had worked on this problem, which was of considerable practical interest. The dissociation of water by fission is a way of producing chemical energy directly from fission.

H. L. ANDERSON.

214.

DISSOCIATION PRESSURE OF WATER DUE TO FISSION

H. L. ANDERSON and E. FERMI

Excerpt from Report CP–1729 for Month Ending May 25, 1944.

The gas pressure developed in a closed vessel containing a water solution of uranyl nitrate under neutron bombardment was observed up to 14 atmospheres. The pressure increased linearly with uniform irradiation. There

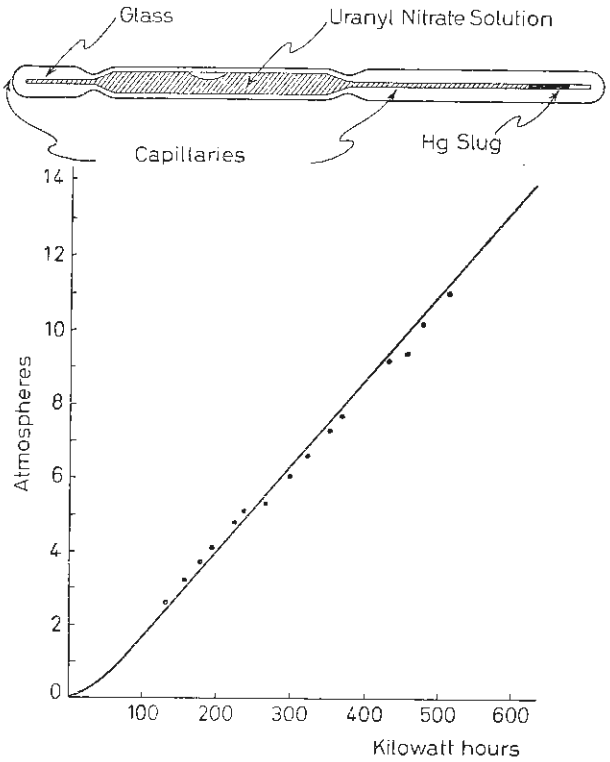

Fig. 1.

was no indication of a saturation pressure at which the rate of combination equals the rate of dissociation. The low rate of recombination may be due to removal of oxygen by some alternative process, or to some inhibiting action of the walls — we have not been able to check these points as yet.

A sketch of the arrangement is given which shows a solution of 2.4×10^{-4} moles of 25 in about 1.2 cc of solution as urangl nitiate. The solution is enclosed in a Pyrex glass tube provided with capillary tubing at each end. The pressure was observed by observing the displacement of a mercury pellet toward the closed end of one of the capillary tubes.

The amount of gas produced was approximately what might be expected from the number of fissions after 622 kw–hr (3×10^{13}) and a yield of 1 molecule of water dissociated per 100 ev of fission energy.

215.

SUMMARY OF EXPERIMENTAL RESEARCH ACTIVITIES

Excerpt from Report CK–1761 for Month Ending May 25, 1944 (*).

A number of experiments have been carried out in Mr. Anderson's section on nuclear properties of the product (**). The ratio of the fission cross-sections for 49 and 25 was observed for neutrons of different energies, and the following results are reported: Ratio for thermal neutrons, 1.41; ratio for the fraction of the pile neutrons absorbed by cadmium, 1.64; same ratio when the neutrons are filtered through a pyrex plate in order to reduce the percentage of thermal neutrons in the spectrum, 1.89. These results are clearly due to the influence of the resonance level reported from Y. In the same series of measurements also the values of $\int \sigma \frac{dE}{E}$, above the cadmium cut-off, were obtained for 25 and 49; the value for 25 is 340×10^{-24}, and for 49, 450×10^{-24} cm^2.

Some measurements were performed on the comparison of the delayed neutrons emitted by 25 and 49. So far only the data on the component of the longest period are available. The half period of this component was measured to be 55 sec, and the number of delayed neutrons emitted per fission in 49 is one-half of the corresponding number in 25.

Mr. Anderson constructed a BF_3 chamber for the detection of very weak neutron sources. It is possible with this chamber to detect sources emitting about 1 neutron per second. This will enable to check whether the purity is adequate using a few grams of product. This chamber has been used for the determination of the yield for neutron emission by sulphur when bombarded with alpha particles from polonium. A yield of 0.0035×10^{-6} neutrons per alpha particle was observed.

The high-sensitivity neutron detector described on pages 13–14 of CP–1729 (q.v.) can measure the emission of 1 neutron per second in 6 hours of observation with a statistical accuracy of $\pm$ 0.25 neutrons per second.

This high sensitivity should make it useful in studying low yield α, n reactions and in measuring the impurity in the product.

(*) Report CK–1761 was issued also as A–2468. (Editors' note).

(**) By " the product " is meant 49. (Editors' note).

216.

SUMMARY OF EXPERIMENTAL RESEARCH ACTIVITIES

Excerpt from Report CP–1827 for Month Ending June 25, 1944.

During the month the P–9 pile has been operated to a power of about 150 kw. From the records of the temperature of the various parts of the pile there is no indication of difficulties to step up the power to the rated value of 250 kw. This will be done as soon as the standardization measurements, now in progress, shall be completed. Preparations are being made for the use of the new pile in the experimental program of the laboratory. Samples of lithium and nitrogen have been put in one of the experimental holes for the production of H^3 and C^{14}.

A program for the systematic measurement of the scattering cross sections of the elements for thermal neutrons has been started by Mr. Hughes' group. Several scattering cross sections obtained by this method are reported.

In the same group work has been going on with the Wilson chamber in order to determine the possible contribution of B^{11} to the total absorption of boron, and to study further the long range alpha particles emitted by 25 on capture of neutrons.

The same problem is being studied by a different method by Mr. Hill, who is developing a coincidence chamber in which absorbers can be introduced without opening the chamber. Mr. Hill reports further data on the beta activity following a fission, both for 28 and for 25.

Mr. Seren's group has further extended the table on the activation cross sections of the elements.

Mr. Roberts is developing standards of β–ray activity made out of thin deposits of RaE.

In Nagle's group Mr. Seidl has completed a run, apparently successful, on the measurement of the number of neutrons emitted by a source, determined by measuring the amount of helium formed in the boron reaction. The experiment shall have to be repeated several times in order to evaluate and to improve the accuracy of the method.

Also, Nagle's group has developed a fission counter that will be used for monitoring the operation of the pile. Nagle reports also some results of a study on the delayed neutrons emitted by 25 and 49.

N° 217 and 220.

The construction of the heavy water pile (CP–3) was completed in June (see paper N° 216), and almost at once this new, more powerful reactor was used for experimental purposes. The collimation of a neutron beam from the thermal column gave Fermi the possibility of beginning to investigate the optical properties of the neutrons. Some preliminary work with the thermal column of the graphite pile had already shown that the wave properties of neutrons would have interesting consequences (see paper N° 191). There was a certain fascination associated with experiments which depended so clearly on the wave rather than the corpuscular properties of these particles. Their wave lengths and scattering cross-sections were comparable with those of x–rays, and it seemed possible that various materials would have an index of refraction for neutrons.

In July 1944 Fermi and Zinn undertook to investigate the possibility of determining the index of refraction by the total reflection method (paper N° 217). This was the beginning of a series of experiments on neutron optics that were performed first by Fermi and Zinn, then by Zinn alone, and after the end of the war by Fermi with Leona Marshall and with other collaborators.

In their work on the reflection of neutrons with mirrors, Fermi and Zinn recognized one difference between neutrons and x–rays: unlike x–rays, the phase of the scattered neutron wave might have the same or opposite sign as that of the incident (paper N° 220).

In paper N° 220 Fermi and Zinn refer to " experiments performed during the summer of 1945 ". This is probably a mistake, as paper N° 217 indicates that the experiments were made in the summer of 1944. Paper N° 220 was also issued as document MDDC–56 by the office of the District Engineer, Manhattan District, Oak Ridge, Tennessee, 1946. I presented this paper together with two others dealing with neutron diffraction effects at the 1946 International Conference on Low Temperatures and Elementary Particles held at Cambridge, England.

H. L. ANDERSON.

217.

COLLIMATION OF NEUTRON BEAM FROM THERMAL COLUMN OF CP–3 AND THE INDEX OF REFRACTION FOR THERMAL NEUTRONS

E. FERMI and W. H. ZINN

Excerpt from Report CP–1965 for Month Ending July 29, 1944.

Some exploratory measurements have been made of the collimation which can be obtained for the neutrons which issue from a thermal column. A $4'' \times 4''$ channel, 8′ deep was opened in the thermal column. The bottom of this channel was 71 cm from the tank wall and separated from it by graphite. The intensity of the beam issuing from this channel and its collimation

were investigated by means of indium foils at a distance of 3352 cm from the face of the column. The central portion of the beam showed a saturated activity for a standard indium foil of 79500 C/min for 250 KW. At a distance of 8382 cm the corresponding value was 1600 C/min. The beam was further collimated by some cadmium slits, and it was found that the width of the beam at these distances from the machine was what one would expect from the geometry of the arrangement. A cadmium slit 1 mm wide was placed at the face of the thermal column and a second slit 1 mm wide, 5 meters beyond the first slit. A BF_3 counter with a slit 2 mm wide and 4.7 meters from the second slit was used to examine the beam. The width agreed closely with what one expects from the collimation imposed on the beam, and at the maximum intensity the counting rate was 10,000 C/min for 250 KW.

The highly collimated thermal neutron beam discussed above suggests that it might be possible to determine the index of refraction for a beam of neutrons by the total reflection method. The theory indicates that

$$n - 1 = \frac{\pm h^2 N \sqrt{\sigma}}{8 \pi^{3/2} mE}$$

where N is the number of nuclei per cm^3, m the neutron mass, and E the neutron energy. Since it cannot be predicted whether a particular substance will have an index greater or smaller than 1, it was decided to look for the totally reflected beam from a number of substances, namely, aluminum, beryllium, graphite, glass, and iron. A graphite mirror 33 cm long and 8 cm wide was prepared by rather crude polishing methods and set up on a spectrometer table. Angles of 1 min of arc could be measured. The mirror was first adjusted so that its plane surface was parallel to the beam and then it was displaced through a small angle. The counter was moved perpendicularly to the beam to find the reflected maximum. A typical result, such as was first obtained, is given in figure 1. Reflected beams have been observed for a graphite mirror for grazing angles as high as 24 min. However, as these large angles are reached, the intensity of the reflected maximum is reduced considerably. This is to be expected since the angle of total reflection will depend upon the energy of the neutrons, and the more energetic parts of the velocity distribution will be refracted into the mirror at angles less than those of the less energetic parts. To determine definitely that the phenomena of total reflection is here being observed, the transmission of the reflected maximum was measured in pyrex plates. It was found that the transmission decreased steadily as the grazing angle was increased; for instance, for a glancing angle of 4 min the transmission through one pyrex plate was found to be 68 percent. For a glancing angle of 12 min the transmission through this same plate was found to be 54 percent. The fact that total reflection is found from graphite indicates that the index of refraction for thermal neutrons in graphite is less than 1. The magnitude of the index cannot be given at present, but the impression exists that the displacements predicted by the formula above are somewhat larger than those actually observed. Refinements in the apparatus are being made, and it is hoped that it will be possible to establish the value of an index quite well by using the boron

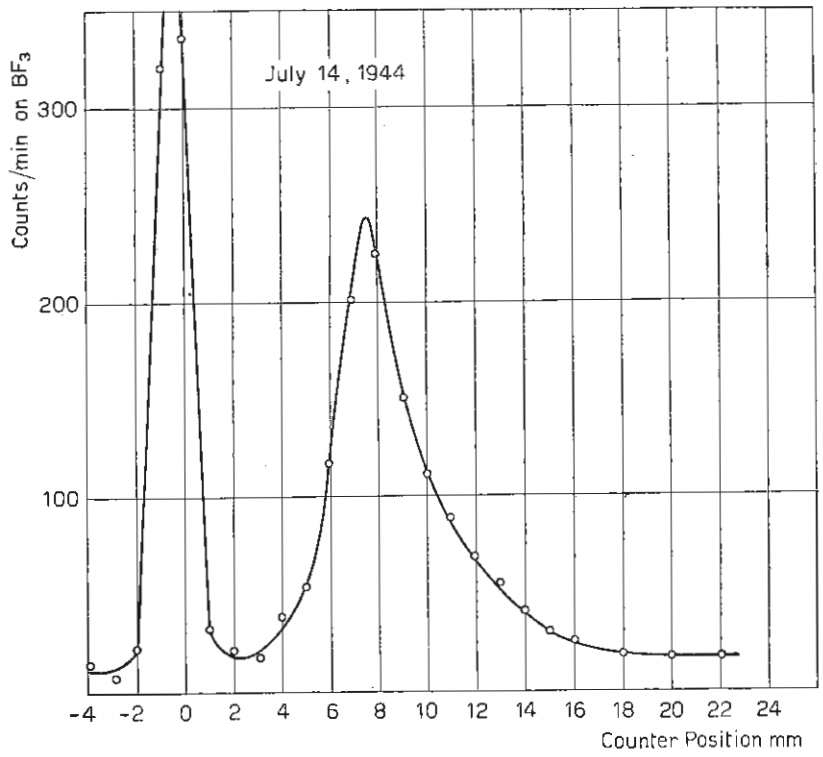

Fig. 1. – Graphite mirror. Glancing angle 3 minutes. Refected beam displaced 0.8 cm.

absorption technique. A search was made for the reflected beam in the case of a glass mirror and for grazing angles from 1 to 5 min no reflected maximum was observed. This indicates that for this substance the index of refraction is more than 1.

N° 218.

From the summer of 1943 much of Fermi's work at Argonne had to do with problems of the Hanford piles. He also went often to Hanford where he helped solve more problems, related to design and construction of the plant. As C. H. Greenewalt, later President of the du Pont Company, recalled, Fermi " buckled down to do everything he could to make the project a success. " One result of this collaboration is paper N° 218, written in August 1944, when the first production pile at Hanford was nearing completion. This report, in which he suggests a method for measuring the amount of nitrogen in the pile, is in the form of a letter to C. H. Greenewalt from " E. Farmer. " At that time Fermi, like a few other top men in the project, used an assumed name when away from Chicago.

One of Fermi's contributions at Hanford, perhaps his most important, is not recorded in any reports or papers, but lives in the memory of those who witnessed the start-up of the pile in early September 1944. Fermi had been called to be present because, as Compton wrote, (1) " Enrico Fermi was our anchor man in such occasions. " The pile started up with no difficulties, but before the power developed reached the operating level, the reactivity began to decline. Soon the chain reaction stopped altogether. Complete failure was feared, but within the next few hours Fermi and J. A. Wheeler independently realized that the trouble was due to xenon poisoning, and Fermi predicted under which conditions the pile would operate again.

A few men who were then at Hanford have sent me their recollections, from which I have excerpted the parts that help to piece the story together.

D. F. Babcock, of the du Pont Company, writes: " John Wheeler, very early in the project, became interested in the possibility that there might be a fission product of moderate half life, with a high cross section for thermal neutrons. His prediction was one chance in a hundred that the multiplication factor would be reduced by 0.01 as a result of this phenomenon. " Wheeler tried to get experimental data on this possible poisoning effect using the Oak Ridge pile, but could not go far, because calibration of the control rod was not sufficiently accurate.

Babcock goes on: " The story now jumps to the eventful day at Hanford when B-Reactor started up so smoothly, then died. " Greenewalt's faith in Fermi was so deep that for a while he was inclined to attribute the failure to causes not related to the pile's physics. P. F. Gast recalls that "on the day in question he caught a ride with Greenewalt, who talked at great length on his view that the difficulties could not possibly arise from any nuclear physics source since this had clearly been well worked through by Fermi, and the troubles must be due either to ' something in the river water, ' which was plating on the process tubes due to the then not well-understood effects of pile radiations, or to just a plain leak in one of these tubes. "

John Wheeler, as Babcock recalls, " was able to evolve the theory that a radioactive poison was the culprit. " Independently Fermi and Greenewalt reached the same conclusion. Greenewalt writes: " I was there, in the control room, until a very early hour in the morning and with my limited knowledge could conclude only that the poison was due to some fission product in view of the characteristics of the decay. I left the data for Fermi and Wheeler and went to bed. "

Babcock goes on with his story: " John Wheeler predicted from the reactor data that the poison was the daughter (or granddaughter) of a fission fragment and the combined half lives of the chain was about 15 hours. He selected three fission chains that had about this half life. " Each chain was assigned for study to a team of two people. Although Fermi, with Leona Marshall, had his assignment, he volunteered to help Babcock's team. From the analysis of the three chains, " it was soon apparent that the culprit chain was tellurium, iodine and xenon and that the cross section of xenon-135 must be about 3.5 million barns. "

(1) A. H. COMPTON, *Atomic Quest*, Oxford University Press, 1956.

Fermi evaluated all data. " In no case did Fermi choose the arithmetic mean between conflicting data, " Babcock writes, " He would weigh the data... This skill in evaluating experiments (and experimenters) was most amazing to me. About two hours after the Xe^{135} had been discovered Enrico predicted that completing the reactor charge to the maximum possible would give almost enough reactivity for successful operation, and burnout of graphite poisons and Pu growth could give the remainder. The success of Fermi's prediction is now known to all. " (This was in fact a victory for the conservative engineering practices of the du Pont Company. They had designed the active zone of the pile big enough to take care of this unanticipated inhibitor of reactivity).

In reminiscing about those days Greenewalt writes: " The thing that impressed me the most about Fermi in the very earliest days of our acquaintance, when the du Pont Company first entered the picture, was the extraordinary clarity of his exposition. To me as a chemical engineer what was done at Chicago was almost in the " black magic " category, but Fermi I remember, made it all very clear, very simple and very possible. "

H. L. ANDERSON.

218.

METHODS FOR ANALYSIS OF HELIUM CIRCULATING IN THE 105 UNIT

Document HW 3-492 (August 7, 1944).

Letter

To: C. H. GREENEWALT
From: E. FARMER

It is desirable to provide sensitive methods for the analysis of the helium circulating in the 105 Unit. In particular, it is desirable to keep a close check on the amount of nitrogen since changes in the nitrogen content will affect the critical position and make it impossible to draw any conclusions as to the poisoning and other changes due to operation of the pile.

A simple method for the nitrogen analysis consists in detecting the nitrogen disintegrations due to capture of thermo neutrons. The method proposed is, in brief, as follows:

One should construct a thermal graphite column on top of the 305 pile. This column should have suitable holes for insertion of an ionization chamber connected to a linear amplifier. Successively a chamber containing the gas to be analyzed and the chamber containing a standard gas to which a known amount of nitrogen is added should be produced in the same position insider the slot and the nitrogen disintegration counted. The ratio of the number of counts is equal to the ratio of the amounts of nitrogen.

It is my expectation that this will not be the only use for the thermal column in the 305 unit and I would strongly recommend that such a column be installed.

(*s*) *E. Farmer*

EF: al

219.

BORON ABSORPTION OF FISSION ACTIVATION

H. L. ANDERSON and E. FERMI

Excerpt from Report CF–2161 for Month Ending September 23, 1944.

In order to study the average behavior of the fission activation in the region up to about 1000 electron volts, experiments were made in which the fission activity was observed due to the neutrons from the thimble of CP–3 with various thicknesses of boron absorbers inserted in the beam. We have obtained fairly reliable data with boron absorbers up to 4.3 gr/cm², corresponding to a cut-off energy of 720 ev. We have also made measurements up to 17 gr/cm² of boron, but the effects of multiple scattering have confounded the results. Steps are being taken to overcome these difficulties. The beam was defined by a boron carbide shield 4.7 cm thick. The fission chamber was 25 cm above this opening and boron absorbers could be inserted in the intervening space. The whole arrangement was protected on all sides by 4.7 cm of B_4C. The boron absorbers were those kindly preparaed for us at Los Alamos. They were made of a mixture of boron and lead borate. The approximate chemical analysis was:

B	70.3 %
Pb	16.0 %
C	0.5 %
Fe	3.0 %
O	10.2 %

The absorbers were covered with a cellophane protection weighing 9.5 mg/cm². The boron absorption of boron, 28, 25, 49, 23 and nitrogen were observed with this arrangement. The boron data was observed using a small BF_3 counter. The effects of 28 and 25 were separated by using depleted and enriched material. The nitrogen data was obtained by using the fission chamber without any foil inside. The data has been collected in the table below. Except for boron and nitrogen the values given are in counts per minute for 10^{18} atoms at 300 kw. In the case of boron and nitrogen, the number of atoms effective was not known very accurately but could be inferred from the known cross-sections of these elements in the thermal region.

Filter	Approx. Cut-off ev	BF_3	10^{18} atoms 28	25	49	23	N_2
No Cd		1,000,000	36	1,144,000	1,820,000	983,000	13,900
Cd —	0.5	26,316	35.1	39,200	57,400	88,400	1,190
Cd 0.269 gm/cm² B .	3	8,893	36.2	20,380	22,630	36,468	921
Cd 0.543	11	4,494	33.3	13,570	14,040	20,196	873
Cd 1.169	53	1,971	32.6	7,490	6,811	9,420	758
Cd 2.161	180	840	27.4	3,778	3,390	4,478	636
Cd 4.311	720	289	21.3	1,381	1,153	1,582	471

The behavior of 28 is easily interpreted. Since 28 is fissionable only by fast neutrons, the diminution in the intensity is due only to the scattering by the boron absorbers. The scattering cross-section which follows from the 28 data is 2.2 B/boron atom in good agreement with the scattering data of Zinn, Cohen and Seeley (« Phys. Rev. », *56*, page 260 (1939)) measured at 2.88 Mev. For the substances which exhibit thermal neutron fission the behavior is most conveniently studied by comparison with a 1/v detector. Since the energy distribution of a neutron flux is approximately $\varphi_0 \frac{dE}{E}$ above the cadmium limit, the activation of a 1/v detector with a boron absorber of N atoms/cm² is given by

$$A = \int_{0.5}^{\infty} \frac{\sigma_d}{E^{1/2}} \varphi_0 \frac{dE}{E} e^{-\left(N \frac{\sigma_a}{E^{1/2}} + N\sigma_s\right)}.$$

In which A is the number of disintegrations · sec^{-1} · $atom^{-1}$ of the detector;

σ_d is the disintegration cross-ection of the detector at 1 ev;

σ_a is the absorption cross-section of the absorbers at 1 ev; and

σ_s is the scattering cross-section of the absorber. The lower limit of integration is the cadmium cut-off energy 0.5 ev. Thus:

$$\frac{AN}{\left(1 - e^{-\frac{N\sigma_a}{(0.5)^{1/2}}}\right)} = 2 \frac{\sigma_d}{\sigma_a} \varphi_0 e^{-N\sigma_s}.$$

The product of the activation and the thickness of the absorber with a small correction due to the cadmium cut-off varies only due to the scattering of the absorber.

With the BF_3 counter the product of activation × absorber thickness has an exponential variation corresponding to a scattering cross-section of 3.7 B/boron atom. This value is in good agreement with that observed by Lichtenberger with these same absorbers but using thermal neutrons. The value of the constant φ_0, which is the neutron flux per unit logarithmic energy interval, may be obtained from the no cadmium minus cadmium

data of 25 and boron by using the value 1.28 for the ratio of the boron to the 25 cross-sections in the region. In this way we found

$$\varphi_0 = 1.0 \times 10^6 \text{ at } 300 \text{ kw.}$$

The nitrogen curve can be analyzed into a combination of the boron curve and the 28 curve. This shows that the behavior of nitrogen is due to a 1/v behavior on which is superimposed a relatively large fast neutron effect. The thermal fissionable elements 25, 49 and 23 all show a departure from the 1/v law. The 25 cross-section, as is already well-known, rises above that of boron. The present data shows that it is 3.5 times greater than boron for the neutrons around 700 volts. In the high energy region the behavior of all three substances is fairly similar.

The principal deviations in their properties occur below 10 volts since the behavior here is largely determined by the chance position of the resonances. Thus the high thermal cross-section of 49 is known to be due to the resonance at 0.3 ev. The behavior of 23 is striking in that its thermal activation is smaller than either 25 or 49, while the activation above the cadmium limit is considerably greater than either. This implies an interesting interaction of the low energy resonances.

N° 220.

For the introduction to this paper see N° 217.

220.

REFLECTION OF NEUTRONS ON MIRRORS

E. FERMI and W. H. ZINN
Physical Society Cambridge Conference Report, 92, 1947, Chicago.

When a beam of neutrons crosses a boundary between two different media, refraction and reflection phenomena are expected that are qualitatively similar to those observed in the case of light but are quantitatively different from it because the refraction index of neutrons differs from 1 by amounts of the order of 10^{-6}. In this respect the properties of neutrons are rather similar to those of x–rays.

The existence of an index of refraction of the de Broglie waves representing the neutrons is related to the fact that neutrons are scattered by atoms. One can prove in an elementary way that the following relationship exists between the index of refraction n and scattering cross-section σ:

$$n - 1 = \pm \frac{N\lambda^2 \sigma^{1/2}}{4\pi^{3/2}}, \tag{1}$$

where N is the number of atoms per unit volume and λ is the de Broglie wavelength. The sign is plus or minus, dependent on whether the phase of scattering by a single atom is equal or opposite to that of the primary wave. In the case of x–rays the phase is normally such that the index of refraction is less than unity; in the case of neutrons, however, both cases are theoretically possible.

When the index of refraction is less than 1 (scattering phase negative), we shall expect total reflection of neutrons striking a surface under a sufficiently small glancing angle. From the previous expression of index of refraction one finds that the limiting angle of reflection is approximately

$$\theta_0 = \sqrt{2(1-n)} = \sqrt{\frac{N\lambda^2 \sigma^{1/2}}{2\pi^{3/2}}}. \tag{2}$$

Putting the numerical values to the formula one finds that the limiting angles will be on the order of 10 minutes.

The total reflection of neutrons has actually been observed in experiments performed during the summer of 1945 at the Argonne Laboratory. Since

the glancing angle for total reflection must be very small, the beam of neutrons used in the experiment must be very well collimated. This was obtained by passing a beam of thermal neutrons emerging from the thermal column of the heavy water pile through two slits 1 mm wide and placed 5 m apart. The beam was allowed to fall on polished surfaces of various materials with a very small and adjustable angle. The reflected beam was detected with BF_3–filled proportional counters provided with an entrance slit 2 mm wide. The counters were placed at a distance of 4.7 m from the second collimating slit.

Very intensive reflected beams were observed for a number of surfaces and for glancing angles up to about 10 minutes. The mirrors used were graphite, glass, aluminium, beryllium, copper, zinc, nickel and iron. They had dimensions in most cases of 5 × 10 in. and were given a very high polish on the reflecting surface. In this respect the various substances were differently suited to give a good polished surface and this may be the reason why differences in intensity were observed from the various mirrors. Even at small angles, where most of the thermal neutrons would be totally reflected, the intensity of the reflection seemed, however, to be too large to be explained as a reflection phenomenon which is to be expected, with small intensity, even when the index of refraction of the surface is greater than 1. Since the limiting angle is proportional to the wavelength, one cannot expect a sharp determination of the limiting angle using non-monochromatic thermal neutrons.

It is planned to perform in the future similar experiments using monochromatic neutrons.

E. FERMI – *Los Alamos*, 1945.

N° 221.

For the introduction to this paper see N° 211.

221.

RELATION OF BREEDING TO NUCLEAR PROPERTIES

Excerpt from Report CF–3199 (Discussion on Breeding)
Chicago, June 19–20, 1945.

Present: ALLISON, BARTKY, BROWN, BURTON, CAPT. CHAPMAN, CHIPMAN, COHN, COLE, COMPTON, DANCOFF, DANIELS, DEMPSTER, DOAN ESTERMANN, FERMI, FOOTE, FRANCK, FRIEDMAN, GOLDSMITH, GRENINGER, HAMILTON, HILBERRY, HOGNESS, HOWE, HUGHES, JESSE, JOHNSON, LANGSDORF, LATIMER, LEVERETT, LICHTENBERGER, MANNING, MAURER, MONK, MULLIKEN, MURPHY, NICKSON, NORDHEIM, OHLINGER, PERLMAN, RABINOWITCH, RUSSELL, SEABORG, SHANKA, SIMPSON, SMYTH, SOODAK, SPEDDING, STEARNS, SZILARD, WAKEFIELD, WARNER, WATSON, WAY, WEINBERG, WHEELER, WHITAKER, WIGNER, WILHELM, G. YOUNG, ZINN.

Minutes by E. RABINOWITCH.

A certain value of η means that for each neutron entering the fissionable nucleus, η new neutrons are produced. One of these neutrons must be reserved for the next link in the nuclear reaction chain, while the remaining $\eta - 1$ can

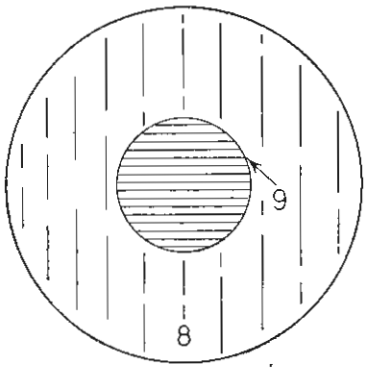

Fig. 1.

be fed to Th (or U^{238}) to produce breeding. The maximum net breeding gain is thus $\eta - 1 - 1 = \eta - 2$. This relationship makes $\eta = 2$ a " critical value " for successful breeding (in absence of all neutron losses). Let's talk specifically about the conversion of U^{238} into Pu^{239}, or $8 \rightarrow 9$ for short. Each fission of 9 produces η_9 neutrons. Let us designate by β the number of fissions

of 8 per fission of 9. We then have, for the number of atoms of 9 produced per fission of 9:

$$\nu_9 + \beta\nu_8 - 1 - \alpha - \beta - (\text{“ engineering ” losses}).$$

This leads to the equation

(1) $$\text{Breeding ratio (without losses)} = \frac{\nu_9 + \beta\nu_8 - 1 - \alpha - \beta}{1 + \alpha}.$$

What value of this ratio can we hope to obtain in a “ fast ” pile (with a core of 9 surrounded by 8) ?

The most important term in (1) is $\nu_9 - \alpha - 1$. It can be evaluated essentially by a single experiment:

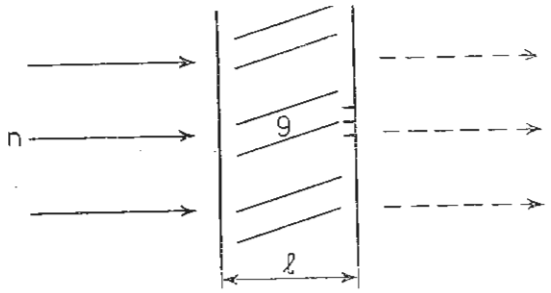

Fig. 2.

The neutron beam traversing a layer l cm thick of 9, is decreased by absorption and swelled by fission neutrons. The intensity of the transmitted beam is changed by a factor of

$$1 + \sigma_f l (\nu_9 - 1) - \sigma_f \alpha l$$

or

$$1 + l [\sigma_f (\nu_9 - \alpha - 1)].$$

A simple transmission experiment thus permits to evaluate the expression in square brackets. The result of such an experiment, performed at Y is

$$\nu_9 - \alpha - 1 = 1.85$$

ν_8 is unknown; let's assume that it, too, is not far from 2.5, so that $\nu_8 - 1 \simeq 1.5$.

The factor β depends on geometrical conditions.

The best estimate at present is $\beta = 0.28$.

The factor α is small ($= 0.05$). We thus obtain:

Breeding ratio $(8 \rightarrow 9) = 2.16$ (This is the “ theoretical ” value, which neglects all losses).

Breeding gain 1.16.

A small “ bonus ” could be obtained by dispersing 9 in 8 instead of lumping all 9 together.

For a large mass of a 49/28 alloy, one calculates

Breeding ratio	2.29
Breeding gain	1.29

For a thermal 23 breeder, the values are

Breeding ratio	1.35
Breeding gain	0.35.

N° 222.

Fermi started to visit Los Alamos from the very beginning of that project. He was there for a preliminary conference in the spring of 1943 when programs for the organization of the future laboratory were being discussed. I met him there together with several of our old friends who had been connected with other phases of the war effort and were preparing to move to Los Alamos.

Fermi visited Los Alamos accompanied by his bodyguard, J. Baudino. Those of us who were there permanently took advantage of every occasion to go on hikes with him in the New Mexico mountains. The walks were usually in part working sessions during which we discussed important subjects, in the freedom and peace of the woods and alpine meadows. During these visits Fermi was also initiated to trout fishing, but his original ideas on the subject were not as practical and successful as his ideas on physics.

His primary responsibility was to Chicago, and he moved from Chicago to Los Alamos only in September 1944, when the pile program was sufficiently advanced not to need his continuous attention. By that time Los Alamos was reaching a critical stage, and Fermi had been asked to go there. He did not want a fixed administrative post, although he was on the Governing Board of the Laboratory, the highest managerial council, and nominally was also an Associate Director. He took special interest in the water boiler, a small homogeneous reactor containing a solution of enriched uranium in water, and was closest to the group contructing and operating it. As usual, he exerted a very strong influence on the scientific personnel of this group, although he had met most of them for the first time in Los Alamos.

Los Alamos, as any such closed community, developed strange quirks in the mind of people who under normal circumstances would not have paid attention to details of prestige and etiquette. Consequently, it was of major concern to some families to have their homes on the proper streets. Apartments were all practically identical, but distinction was conferred by certain addresses. The best address was " Bathtub Row, " where a few houses had the only bathtubs in town and where the authorities lived. When the Fermis arrived, the housing shortage was very acute and they were temporarily housed in a " popular " section of town, among younger physicists and machinists. They chose to remain there after a house on Bathtub Row became available, because they preferred the beautiful view from their windows to an aristocratic status. This did not pass unremarked, and may have contributed to the morale of the place.

Shortly after his arrival, Fermi began giving isolated lectures on many subjects and in the fall of 1945 he taught a regular course in neutron physics (paper N° 222). He also consulted with anybody who came to him for help. I can remember only a few instances in which I was personally involved, but I am sure that there are many more. One day J. R. Oppenheimer, the Director of the Laboratory, asked B. Rossi and me to prepare a report on the effects to be expected from a nuclear explosion of a certain magnitude. At that time the subject was quite new, and we were laboriously trying to estimate and guess the effects. Fermi happened to go by, and we asked him some questions. In no time he clarified the whole subject, and we were able to make a report, which hindsight shows was remarkably accurate. At another time we discussed with him complicated instrumental problems of some apparatus which baffled even the experts, and again he found a simple and original solution.

During his stay in Los Alamos he struck up a friendship with J. von Neumann. I am sure that the friendship was cemented by mutual admiration and a common interest in computers. Fermi had always been adept at numerical calculations and saw immediately the new possibilities opened by fast electronic computers. He spent many hours learning about, and experimenting with them (see papers N° 256 and 260).

Fermi took a direct and active part in the preparations for " Trinity, " the test of the first atomic bomb at Alamogordo, in July, 1945 and was present at the explosion.

After this test and the end of the war his attention turned to teaching, including an interesting series of lectures on thermonuclear reactions, and finally to plans for the new Institute at Chicago. When he moved back to Chicago, several of the younger physicists working in Los Alamos followed him, to finish their studies at the University of Chicago. An incomplete list includes: Agnew, Argo, Chamberlain, Chew, Farwell, Goldberger. Some of these had been originally my students and some Teller's.

After the end of the war Fermi returned several times to Los Alamos in summertime, to work with computers and help solve difficulties of various kinds. These summer visits may have helped him also to discarge his duties as member of the General Advisory Committee of the Atomic Energy Commission. According to Fermi's way of working, these duties required an uncommon amount of firsthand knowledge.

Fermi's reports on his work at Los Alamos in wartime are still classified, and only his course on neutron physics (paper N° 222) can be included here. (Chronologically papers N° 221 and 223 also belong to this period, but they are unrelated to Los Alamos).

Paper N° 222 contains the course on neutron physics mentioned above, given to the young physicists of Los Alamos. The students attending it had very different preparation ranging from beginners to graduate students. I estimate their number, by memory, to be about 30. The lectures were written down by a number of students and a rough draft was prepared without help or revision from Fermi, for the benefit of the audience.

The lectures of Part I containing neutron physics without reference to chain reactions were promptly declassified and the notes assembled by I. Halpern were circulated in mimeographed form. They have been issued as LADC 225, MDDC 320, and LAMS 347. Tbey were later rewritten and to an extent polished by D. J. Beckerly as AECD 2664. The lectures of Part II have been declassified only in 1962. They were preserved only as raw notes taken by unknown students.

The original versions of both parts are included here. The notes were obviously not destined for publication and it is apparent that they contain an almost verbatim account of Fermi's presentation, occasionally marred by defects of style or even by lack of understanding on the part of the writer. It has been decided not to attempt to give a more finished version because it would be impossible to do it in the form that Fermi would have given to the lectures if he had published them. The lectures are interesting as a sample of his didactic style and contain a large amount of material which appeared later in standard textbooks.

E. SEGRÈ.

N° 222.

In the summer of 1944 J. Robert Oppenheimer, the scientific director of " Project Y " at Los Alamos, came several times to Chicago and persuaded Fermi to move to Los Alamos. Fermi had been there for the first time in April 1943, when the project was beginning to function, and had participated as a consultant in conferences at which a concrete program of research was prepared. (1) He returned there on other occasions and as a result some of his work at Chicago was done for, or in collaboration with the Los Alamos project. Now he was wanted full time, not for any specific assignment, but because of his general wisdom. Oppenheimer felt that Fermi should have an official position, and so he was named Associate Director of the project. He planned to move to Los Alamos in August, but at the last moment he was called to Hanford for the starting of the pile. Only in September, after the difficulties due to the poisoning of the pile were solved, could he take up his new duties at site Y, where he remained through December 1945.

Upon his arrival Fermi became the leader of the especially organized F Division (in which F stands for Fermi) whose general responsibility was to investigate problems that

(1) For this and other details in this introduction see: Los Alamos Scientific Laboratory of the University of California, Los Alamos, New Mexico – Document LAMS–2532 (December, 1961): *Manhattan District History, Project Y, The Los Alamos Project*; Vol. I, *Inception Until August 1945*, by DAVID HAWKINS.

did not fit in the work of other divisions. Four groups were placed in the F Division. One, under Edward Teller, pursued the theoretical study of a super bomb (hydrogen bomb) in which Teller had been engaged for some time. Egon Bretscher headed another group on the super bomb, which was the experimental counterpart of Teller's. Fermi's greatest personal participation was in the other two groups: the Water Boiler group, under L. D. P. King, which included several young people, among them Joan Hinton, a student in physics, who a few years later left the United States to join her fiancé in Communist China; and the F–4 group which was organized under me, after I joined the project in November.

A water boiler unit of low power (about 0.05 watt) had been built in the spring of 1944, as soon as enough uranium enriched in U^{235} had arrived from the separation plants at Oak Ridge and it had been used for experiments of significance in the construction of the bomb. After the first series of experiments was completed, it was decided to rebuild the water boiler for operation at a higher power (5 kilowatts). The Water Boiler group was making plans for this unit at the time Fermi arrived at Los Alamos.

He took a great interest in this reactor, the first to use enriched fuel and the first homogeneous one: the system fuel-moderator was a solution of enriched uranium salt in ordinary water. Fermi was especially intrigued by the idea that here was a reactor which, though extremely simple and of very small size, was a strong source of neutrons. (The solution for this reactor was contained in a sphere of one foot diameter). Although the construction of the water boiler was under King's leadership, Fermi made a habit of spending as much time as he could at the special " Omega site " in the Los Alamos Canyon. It became his routine, whenever he could, to go to the site every day, especially in the initial phase of planning, and to carry out many of the design calculations himself. In December the reactor was completed, and Fermi participated in its first test and in its calibration.

My group, meanwhile, had been assigned to help construct the water boiler, but was considered uncommitted and available to study problems that might come up. I was invited to attend the meeting of the advisory board, of which Fermi was a member. Non-members like myself were invited on occasions when the problems that needed solution were discussed. It was hoped that in this way more ideas would be generated and that those present would volunteer for some of the tasks. Thus, when the problem arose of how to determine the critical size of the U^{235} bomb, I proposed that my F–4 group undertake experiments to measure the fission produced in a U^{235} sphere by using the neutrons from the water boiler. Fermi and I agreed on the general method but disagreed on the details. I wanted to use a fission chamber for detector, Fermi wanted to catch the fission fragments on cellophane foils. We both went ahead to test our ideas, Fermi with Joan Hinton's help, I with my group. We obtained very similar results.

The experiments on criticality took up January and February 1945. In March it was recognized that no amount of experimental work would yield as much information as an actual explosion, and plans were made for an atomic test, under the code name of " Project Trinity ".

In preparation for Trinity, the advisory board posed the problem of measuring the efficiency of the plutonium bomb (plutonium was to be used in the Trinity test). It seemed to me that a good measurement of the efficiency could be made by comparing the radioactivity of the fission products with the amount of the plutonium residue. My proposal was accepted and placed under the F Division. For this purpose the number of radiochemist was greatly increased. The final test was to be made right after the explosion: then we would get into the area right under the exploded device and collect dirt samples from which the radioactivity of the various fission products and of the plutonium residues could be compared.

The Trinity test was made at Alamogordo, in the desert land of southern New Mexico, on July 16, after long preparations. Fermi was there in a general advisory capacity and to participate in many of the activities. At the moment of the explosion he stood with the others at an observation point some 10 000 meters away from the steel tower supporting the atomic device. He later related that he did not hear the noise of the explosion, so great was his concentration on a simple experiment that he was performing: he dropped small pieces of paper and watched them fall. When the blast of the explosion hit them, it dragged them along, and they fell to the ground at some distance. He measured this distance from which

he calculated the power of the explosion. His results turned out to agree well with those obtained with much more elaborate operations.

The successful Trinity test was the climax of the Los Alamos wartime period. Within one month after it two atomic bombs were dropped on Japan, and the war ended. Many of the men in Los Alamos began to make plans for peace time activities, for a return to the universities and teaching.

The life at Los Alamos had suited Fermi very well: it had the regularity that he liked best, and that, nnder those unusual wartime circumstances, was set by army rule. His work day starded early and continued, except for the hour break at lunch, until the dinner hour. Evenings were reserved for relaxation, which in Los Alamos frequently took the form of dinner parties. These occurred more than at usual frequency to make up for the isolation of the town; besides, there were many old as well as new-found friends to see. Work was six days a week, and Fermi spent most of his Sundays in open-air activities. He enjoyed the close proximity to the outdoors, the wild, beautiful landscape of New Mexico, the many mountain trails to follow, on foot in summer, on ski in winter, and the young people who became his steady companions on his Sunday excursions. The company of many of the best men in their fields and the frequent occasions for informal conversations with them provided excellent intellectual stimulation.

If Los Alamos could have had a university, Fermi might have stayed there. Instead, on December 31, 1945 he left, and went back to Chicago, where he had been many times, on visits, during this period. He was now a member of the Institute for Nuclear Studies, one of three newly established Institutes for Basic Research at the University of Chicago. These institutes reflected the changed conditions of science after the end of the war. The war experience had made clear the importance of science in general, of physics in particular. The nation had been taught a lesson it would not easily forget. It would support its physicists, help them in their work. But the war had taught the physicists too. It had taught them how to work with larger means, with more assistants, with more facilities and money. They could be more effective this way, and this was the way they wanted to continue to work. Besides, in the war projects they had learned and enjoyed the advantages of collaborating with scientists outside the field of physics, especially with chemists, metallurgists, biologists. It would be a drawback if this collaboration could not go on because of the highly departmentalized universities.

The University of Chicago recognized the new era: forewarned by A. H. Compton it established the new institutes in which men could work together in related fields, with expanded means. When the idea of the Institute for Nuclear Studies began to materialize, Fermi was asked to become its director, but, not feeling suited for administrative tasks, he declined and joined the Institute as a simple member. S. K. Allison became the first director.

H. L. ANDERSON.

222.

A COURSE IN NEUTRON PHYSICS

PART I

Document LADC-225 (February 5, 1946)
(Notes by I. HALPERN).

A Course in Neutron Physics was given by E. Fermi in the Fall of 1945 as part of the program of the Los Alamos University. The course consisted of some thirty lectures, almost all of which were given by Fermi. In his absence, R. F. Christy and E. Segrè gave several lectures.

These notes are, except for a few rearrangements, omissions and insertions, those taken down in class. The omissions were necessary because some of the material of the course is still classified information. The division into chapters and sections was made only when the notes were put together for printing,(*) but the chronological order of presentation was everywhere preserved. The homework assignments are given in their proper place.

Mr. B. T. Feld kindly read these notes before they were printed and made some corrections and valuable suggestions. Miss Arva Frazier typed up the notes.

I. HALPERN.

(*) These notes were not printed but only mimeographed (Editors' note).

TABLE OF CONTENTS

PART I (LADC 225)

CHAPTER I

NEUTRON SOURCES.

(1) (α, η) *Reactions.*

(A) Li^7 (α, n) B^{10} will mean $Li^7 + He^4 \rightarrow B^{10} + n^1 + Q$ (fig. 1), where Q is the energy balance. As an example let us calculate:

The masses of the atoms involved in the reaction are available from mass-spectrographic data:

	atomic mass		
Li^7 :	7.01804	B^{10}:	10.01605
He^4:	4.00388	n^1 :	1.00893
left side	11.02192	right side	11.02498

Note that the mass on the right exceeds that on the left by 0.00306 mass units (the reaction is endothermic, i.e., Q is negative). Now one mass unit is 931 Mev so that $Q = -2.85$ Mev.

The threshold for the reaction is, however, somewhat larger than 2.85 Mev. For 2.85 Mev would suffice only if neither end-product particle moved. In order to satisfy the conservation of momentum this cannot be so, for the α particle is moving at a stationary Li^7 to begin with, and so the center of gravity has a momentum which it will still have after the reaction.

Homework assignment: As an assignment (and in the future, all assignments will be in small type) explain why you can use atomic masses for such calculations, when it is true that nuclear masses alone are involved in the reaction.

Homework: Prove that one mass unit equals 931 Mev using $E = mc^2$. Convert from mass units to gms, to ergs, to Mev.

Under this assumption of stationary Li^7, let us calculate the threshold energy for the reaction. V_c, the velocity of the center of gravity is $\frac{4V}{7+4} = \frac{4}{11}V$. The minimum kinetic energy of the reaction products is

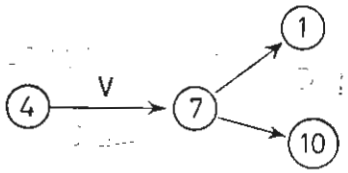

Fig. 1. – The numbers represent masses.

then $1/2 \times 11 \times \left(\frac{4}{11}V\right)^2$. Therefore, for the reaction to go, the minimum velocity V of the α particle must be given by:

$$\frac{1}{2} \times 4 \times V^2 = 2.85 \text{ Mev} + \frac{1}{2} \times 11 \times \left(\frac{4}{11}V\right)^2$$

or $\frac{7}{11}\left(\frac{1}{2}\times 4\times V^2\right) = 2.85$ Mev (i.e. only 7/11 of the kinetic energy of the α particle is available for conversion to mass). Hence the threshold is $2.85 \times \frac{11}{7} = 4.5$ Mev.

(B) Be^9 (α, n) C^{12} is the most probable reaction with Be^9, although Be^9 (α, n) 3 He^4 also occurs. This is exothermic, $(Q = 5.5$ Mev) and is the basic reaction in one the most common neutron sources (radium+beryllium). There is no sharp threshold in this reaction, the yield curve rising slowly with E_α (because of the Gamow formula for penetration of a Coulomb barrier by charged particles) (fig. 2). Three natural neutron sources in common use are based on this reaction.

Ra + Be (~ 5 gms Be to 1 gm Ra)
Rn + Be (Rn gas in a Be capsule; very light, ~ 4 day half life)
} These sources emit too many gammas for some uses.

Po + Be (relatively low intensity)

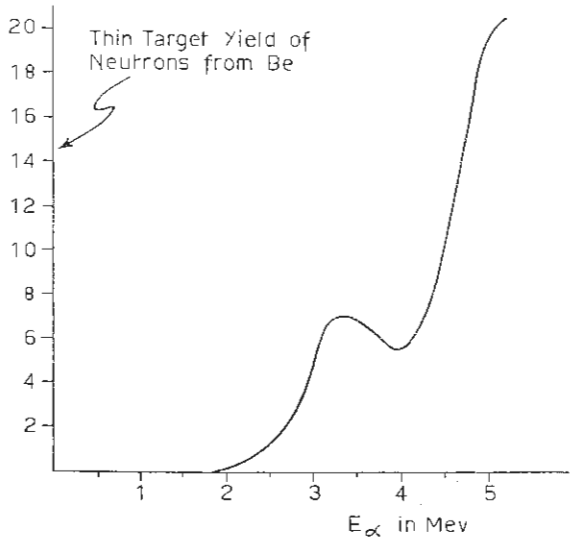

Fig. 2. – Neutron yield in Be (α, n) reaction as a function of energy.

To see what α's are emitted in each case, one must turn to the decay series of the uranium family.

The part from Ra to RaF is shown in fig. 3.

Normal radium is a mixture of Ra and the products emitting the 4 α's to RaD. Rn emits 3 α's. Po emits but 1 α and is quite a bit weaker.

The strengths of these natural (α, n) sources are:

$$\left.\begin{matrix}\text{Ra} + \text{Be}\\ \text{Rn} + \text{Be}\end{matrix}\right\} \quad 10 \text{ to } 15 \times 10^6 \ \frac{\text{neutrons}}{\text{sec curie}};$$

$$\text{Po} + \text{Be} \quad 2{,}8 \times 10^6 \ \frac{\text{neutrons}}{\text{sec curie}};$$

where a curie of a substance disintegrates at the same rate as 1 gm of radium.

In a Ra + Be source the neuts will have all sorts of energies up to $7.68 + 5.5 \cong 13$ Mev. The spectrum will be fairly continuous for in addition to the various α's involved, there's the matter of penetrating Be crystals, and the fact that C^{12} needn't necessarily be left in the ground state.

$B(\alpha, n)N$, gives $\sim 2 \times$

$\times 10^6 \frac{\text{neutrons}}{\text{sec curie}}$ with Ra α's.

$F(\alpha, n)Na^{22}$.

Sometimes you can use Ra α's in BF_3. You'd get about $10^5 \frac{\text{neutrons}}{\text{sec curie}}$.

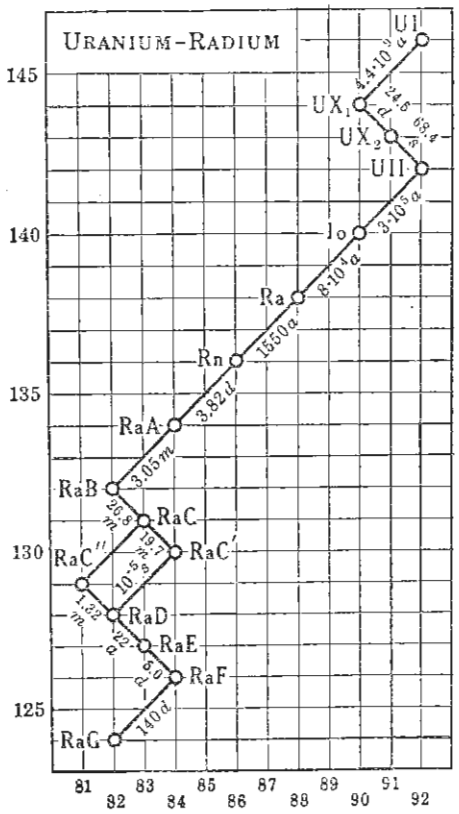

Fig. 3. – Half-lives and energies in U^{238} radioactive family.

(2) *Photo Sources* (γ, n).

Be and D alone among the isotopes have low enough (γ, n) thresholds (1.61 Mev & 2.17 Mev respectively) to be useful with natural γ's.

We can get with such sources low energy monochromatic neutrons. Ra γ's on Be, however, give neuts in 2 groups (0.12 Mev, 0.51 Mev) since 2 Ra γ's lie above the threshold.

Homework: Neglecting absorption of γ's, what's the strength of the source shown in fig. 4?

A practical rule for the calculation of the total number of neuts per second from a γ + Be source is 1 gm Ra at 1 cm from 1 gm Be gives $3 \times 10^4 \frac{\text{neutrons}}{\text{sec}}$.

Other photo sources.

Ms Th γ D_2O 0.220 Mev neutrons

Ms Th γ Be 2 groups 0.88, 0.16 Mev neutrons.

Using artificially radioactive γ emitters.

Reaction	Sb γ Be	Ga γ D_2O	Na γ D_2O	La γ Be	Na γ Be
Neutron Energies	0.030	0.12	0.24	0.62	0.80 Mev

(3) *Artificial Neutron Sources.*

(A) The D—D reaction.—Bombard heavy ice or heavy paraffin with deuts.) Based on:

$$D + D \begin{cases} \nearrow He^3 + n & \text{exothermic} \\ \searrow H^3 + H^1 & \sim 3.2 \text{ Mev} \end{cases}$$

about half and half

Yield for a thick target of heavy ice.

Energy (kev)	Yield $\frac{\text{neutrons}}{\text{deut}}$
0	0
50	0.2×10^{-7}
100	0.68
200	3.0
300	6.9
500	19
1000	81
2000	400

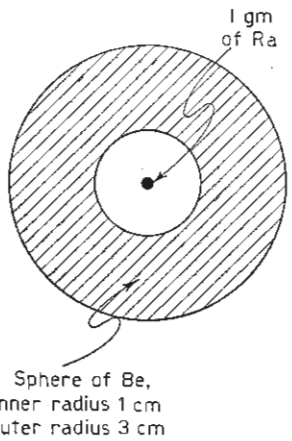

Fig. 4. – Photoneutron source.

Homework: How many n/sec could one get from a beam of 500 kev deuts if the current were 1 ma.?

Advantagesof this reaction: reasonable yields at low energies; monochromatic yields.

Disadvantage: troublesome target.

(B) Protons on Lithium.—This reaction

$$Li^7 + H^1 \rightarrow Be^7 + n - 1.62 \text{ Mev}$$

can give monochromatic neuts down to rather low energies. The threshold is $8/7 \times 1.62 = 1.85$ Mev.

If the target is bombarded with threshold protons, the neuts come off with a finite energy ($\sim$30 kev) for then they move with the speed of the center of gravity. If we raise the proton energy, there is enough energy to give the neuts a velocity *with respect* to the c. of g. For the net velocity, one adds vectorially the velocity of the center of gravity to the neutron velocity with respect to the center of gravity. For high enough energies, neuts can show resultants of zero velocity, or even backward velocities.

(4) *Deuterons on Beryllium.*

The Cyclotron source yield rises rapidly with energy. For a thick target, 1 Mev deuterons give 10^8 neutrons per second per microamp. 8 Mev deuterons give 10^{10} neutrons per sec per microampere.

CHAPTER II

Collisions of Neutrons with Nuclei.

Examples of such processes are (n, n) which are called scattering processes, (elastic when K. E. of neut before collision=sum of K. E.'s of neutron and recoil nucleus after collision; inelastic when the kinetic energy is not conserved—some energy may go into nuclear excitation). Reaction where a neutron comes in and other "particles" come out are (n, γ), (n, p), (n, α). A third distinct type is the $(n, 2n)$ reaction. A fourth type would be $(n,$ fission.)

(1) *Neutron Cross-Sections as a Function of Energy.*

Description of intensities of reactions is usually given in terms of cross-sections. In unit time $nv\,\sigma$ neutrons will hit a nucleus (fig. 5). Actually the representation is rather fictitious inasmuch as σ is not a well-defined geometrical quantity. We might make more general our notion of σ using semi-classical ideas. We would consider σ as describing the projected area of the nucleus and of a zone including the range of nuclear forces. But even this area would be of the order 3×10^{-24} cm^2. We would conclude that all σ's must be $\sim 3 \times 10^{-24}$ cm^2. But there are observed σ's of the order $10^4 \times$ $\times\ 10^{-24}$ cm^2. We must adopt a wave mechanical point of view to account for this. A neutron becomes a large body at slow velocity. It can't be considered a point compared to the nucleus but may be much larger. Its linear dimension would be given by $\lambda = \frac{h}{mv}$. At low velocities σ would be restricted (in orders of magnitude) only by $\sigma < \lambda$. Let us see therefore how λ depends on E (neutron energy in electron volts).

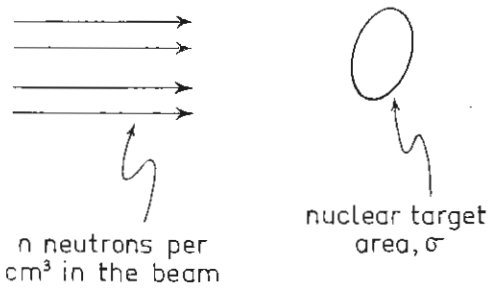

Fig. 5. – Definition of Cross-Section.

$$\frac{1}{2} mv^2 = \mathrm{E} \times 1.6 \times 10^{-12} \text{ ergs}$$

$$\therefore\ mv = \sqrt{3.2 \times 10^{-12}\, m\mathrm{E}} \text{ and } m = 1.6 \times 10^{-24} \text{ gm}$$

whence $\lambda = \frac{h}{mv} = \frac{2.8 \times 10^{-9}}{\sqrt{\mathrm{E}}}$. λ is called the de Broglie wave length.

In practical limits E goes from about 0.001 volts to several million volts. Thermal neuts, for example, are about 1/40 ev which makes $\lambda = 2 \times 10^{-8}$ cm (of the order of interatomic distances). For 1 volt neuts, $\lambda = 3 \times 10^{-9}$; for 10^6 volts, $\lambda = 2 \times 10^{-12}$ (of the order of nuclear dimensions). At a high enough energy λ becomes small compared to 10^{-12}. Then we can use the classical corpuscular notion, and for higher energies than this we must use $\sigma < 10^{-24}$ rather than $\sigma < \lambda^2$ to set an upper limit on σ. In keeping with these ideas one could define:

$$\sigma \equiv \frac{\text{processes per nucleus per unit time}}{nv}$$

and we've seen σ will be less than the largest of the two quantities 3×10^{-24} or λ^2.

(2) *The Measurement of Total Cross-Section.*

Without the absorber, the detector measures intensity I_0. We then put in the absorber (fig. 6). The measured intensity is I. We assume that the solid angle of absorber at source and de tector is infinitesimally small (one must make sure that neuts scattered even a little bit can't get to the detector.) Our geometry is thus such that any neutron "affected" will not be detected. Take a closer look at the absorber: $dI = -\sigma_t N dx \cdot I$ whence $I = \text{constant} \times e^{-\sigma_t N x}$ and the constant must be I_0 (fig. 7). If the length of the slab is "a". $I = I_0 e^{-\sigma_t N a}$ and σ_t can be calculated from the measurements of I and I_0

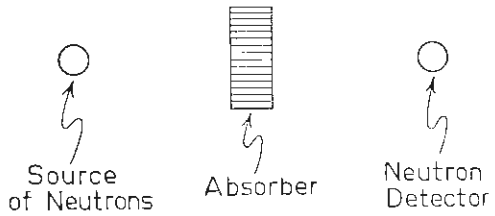

Fig. 6. – Attenuation measurement.

$$\sigma_t = \frac{1}{Na} \log \frac{I_0}{I}$$

σ_t may represent the sum, $\sigma_{\text{elastic}} + \sigma_{\text{inelastic}} + \sigma_{\text{absorption}}$ where $\sigma_{\text{absorption}}$ includes all processes in which a neutron disappears, i.e., (n, α) (n, p) (n, γ) etc.

Homework: A copper plate 1 cm thick reduces the intensity of thermal neuts by the factor 0.36. What is the σ_t for copper for thermal neuts? Express result in units of 10^{-24} cm^2 (Barns).

(3) *The General Features of Collisions.*

As an example, you may be thinking of an (n, α) reaction altho what follows is quite general. (figs. 8 and 9) Final state refers to either the α or the recoil, for if we are given the α momentum and direction, the laws of momentum conservation assign the momentum and direction to the recoil, and from the conservation of energy law, one can determine now the state of excitation of the recoil. Thus a specification of momentum and direction of the α specifies the final state completely.

What is the probability that a transition will occur for which the energy of the α is E? (i.e. between E and $E + dE$). From Quantum Mechanics, it can be shown that this is given by a product. It is $M' \times \rho$ where M' is $\frac{4\pi^2}{h} \times |H|^2$ and H is a matrix element depending on the energies of the initial and final states, and $\rho(E)$ is the density of possible final states in the neighborhood of E.

$$-\frac{dI}{I} = N\sigma\, dx$$

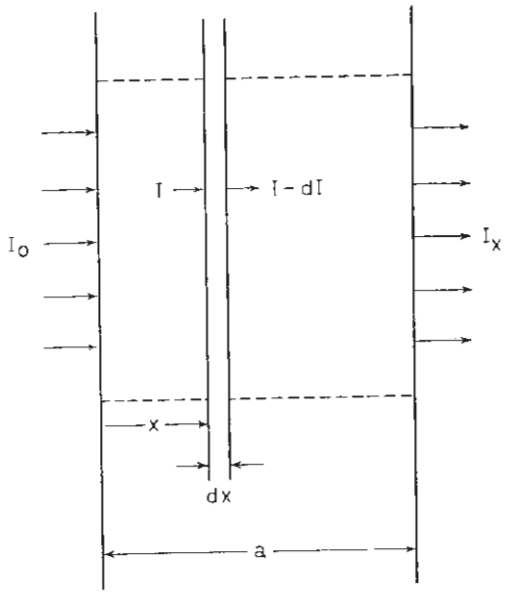

Fig. 7. – N the number of absorber atoms/cm³ The probability that a neutron will suffer a collision in a layer of thickness dx is $\sigma_t N dx$, where σ_t, is the cross-section for all neutron processes in which a neutron is removed from the beam $\sigma_t = \sigma_{el} + \sigma_{inel} + \sigma_{abs}$.

Fig. 8. – Nuclear collision.

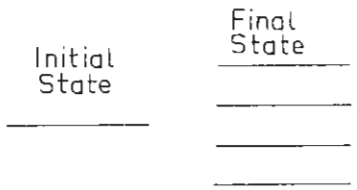

Fig. 9. – For a given energy of the initial state, there are a number of possible final states

The matrix element is too tough to calculate here, but we can get ρ. Actually the α can come off with any energy and so we'd get a continuum (i.e. $\rho = \infty$) everywhere. However we can put the system in a box of finite volume Ω and this will make the distribution of final energies discrete and ρ (the number of states per unit energy interval) will be finite.

The question "How many states per unit energy occur at E?" becomes "How many states of an α particle in a box of volume Ω have energy E?" For the answer to this we turn to statistical mechanics and say, it is proportional to the volume in phase space which corresponds to this energy. If h is the linear dimension of a cell in phase space (a cell can contain one state) then the number of states for which p_x is betwen p_x and $p_x + dp_x$ etc. is:

$$\frac{\Omega}{h^3}\, dp_x\, dp_y\, dp_z$$

(where the integration over configuration space i.e. over $dx\,, dy\,, dz$ has already been done). Hence the number of states for which the total momentum is between p and $p + dp$ is proportional to the volume of the spherical shell at $p = (p_x^2 + p_y^2 + p_z^2)^{1/2}$ in momentum space. This volume is: $4\pi\, p^2\, dp$

$$\delta N = 4\pi p^2\, dp\, \frac{\Omega}{h^3}$$

represents the number of states with momentum p to $p + dp$. For particles, (i.e.: $\alpha\,, p\,, n$) $E = \frac{1}{2}\, m v^2 = \frac{p^2}{2m}$ so that $dE = (p/m)\, dp$, for photons $E = h\nu$; $p = h\nu/c$ so that $dE = c\, dp$.

In general, therefore $dE = v\, dp$ where v is the velocity of the particle or photon. Thus the number of states per unit energy range, $\rho = \frac{\delta N}{\delta E}$ becomes:

$$\frac{4\pi\Omega}{h^3}\frac{p^2}{v} \text{ in general or } \frac{4\pi\Omega m p}{h^3} \text{ for particles, } \frac{4\pi\Omega}{hc^3}\nu^2 \text{ for photons.}$$

Although Ω occurs in ρ, Ω^{-1} will occur in M′ so that the transition probability is independent of Ω as it must be if our taking of an arbitrary Ω is to be justified. Thus the probability of a transition to a state where the particle or photon has momentum p_{out} is proportional to $M' \times \frac{p_{\text{out}}}{v_{\text{out}}}$. This probability will be proportional to $v_{\text{incident}} \times \sigma$ where σ is the cross-section for neuts of velocity v_{incident} to be "converted" into outgoing particles of velocity v_{out}.

$$\sigma = M \times \frac{p_{\text{out}}^2}{v_{\text{out}}} \times \frac{1}{v_{\text{in}}}\,.$$

It is convenient to define a new $M = M' \times$ (constants of proportionality).

(4) *Applying This Result to Several Situations.*

As an example note that for elastic scattering ($v_{\text{in}} = v_{\text{out}}$) we get simply: $\sigma = M \times m^2$ (for $p = mv$) so that for slow neuts (M wouldn't change much in so small an energy range) σ is independent of the velocity of the slow neutrons. The elastic scattering cross-section of slow neutrons does not depend appreciably on their energy. It should be pointed out that for elastic scattering from light nuclei $v_{\text{in}} = v_{\text{out}}$ only in the center of gravity system and it is in this system that the above is true.

As a second example, consider one of the so-called absorption processes (fig. 10). Let's say recoil is heavy so that the light particle gets all the energy. Then:

$$\frac{1}{2} m_1 v_{out}^2 = \frac{1}{2} m v_{in}^2 + Q$$

$$\text{or } p_{out}^2 = m_1^2 \left[\frac{m}{m_1} v_{in}^2 + \frac{2}{m_1} Q \right]$$

where m = neutron mass; m_1 = light particle mass.

Then:

$$\sigma = M \times \frac{m_1^2}{v_{in}} \left[\frac{m}{m_1} v_{in}^2 + \frac{2}{m_1} Q \right]^{1/2}.$$

Note that when Q is positive (exothermic) and v_{in} is small, then σ goes as $1/v_{in}$ [the $1/v$ law]. Obviously a negative Q and very small v_{in} doesn't make

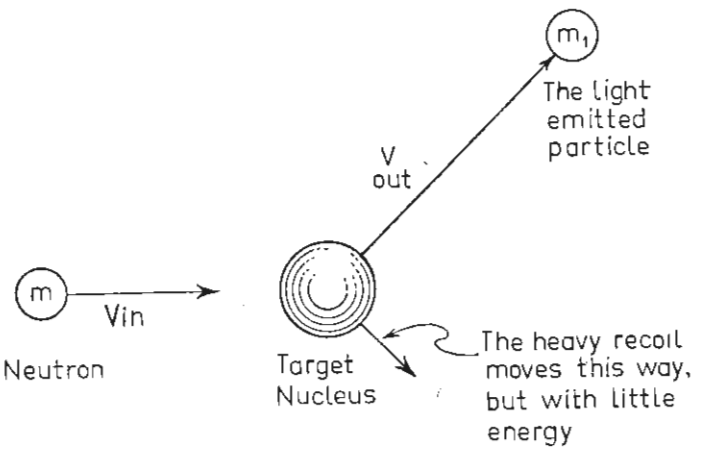

Fig. 10. – An " absorption " process. (A neutron is absorbed by the target and another type of particle is emitted).

physical sense. The result we get is imaginary. This shows mainly that the formula doesn't cover that case. σ should be zero in such a condition.

Homework: Find an example of each of the processes (n, n) [elastic and inelastic] (n, γ) $(n, \alpha) \cdots$ etc. and record the cross-section. (From the literature).

Consider next inelastic scattering (Assume that you're working in the center of gravity system. In this case neutron mass should be replaced by its reduced mass $\frac{m m_A}{m + m_A} = \mu$. If m_A is large, the reduced mass is practically the neutron mass and the following results will hold approximately in the lab system). If the first excitation level of the nucleus is W, and the neutron has $\frac{1}{2} \mu v_{in}^2 < W$ then no inelastic scattering can take place. But if $\frac{1}{2} \mu v_{in}^2 > W$ then, if the nucleus is excited to this level, W:

$$\frac{1}{2} \mu v_{in}^2 - W = \frac{1}{2} \mu v_{out}^2$$

substituting in the cross-section formula:

$$\sigma = M \times \frac{1}{v_{in}} \frac{(\mu v_{out})^2}{v_{out}} = M \mu^2 \frac{v_{out}}{v_{in}}.$$

Figure 11 is a plot of the factor $\frac{v_{out}}{v_{in}}$. Writing:

$$W = \frac{1}{2} \mu v_0^2 \quad , \quad v_{out} = (v_{in}^2 - v_0^2)^{1/2}$$

which is:

$$[(v_{in} + v_0)(v_{in} - v_0)]^{1/2}.$$

showing that v_{out} goes as the square root of the velocity above the threshold. There would be a small cross-section for the production of slow neuts by this metod since $\sigma \sim v_{out}$.

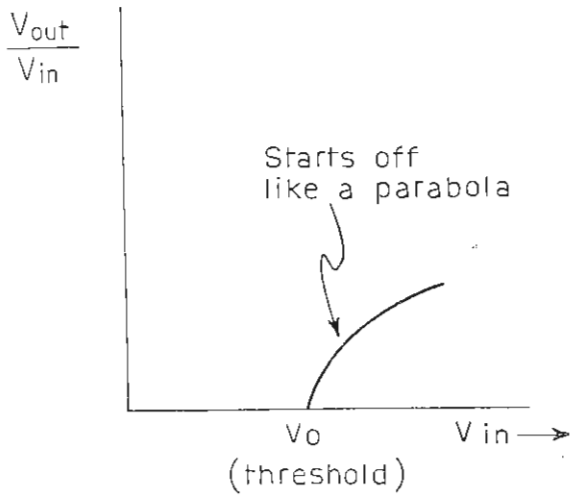

Fig. 11. – Cross section asa function of energy for a threshold reaction (no barrier).

Next, we take up (n, γ) Here $p = \frac{h\nu}{c}$, $v_{out} = c$ so that $\sigma = M \times \frac{1}{v_{in}} \frac{h^2 \nu^2}{c^3}$. Let's say a neutron hits a nucleus (Z , N) so that the compound nucleus is (Z , N + 1). Neutron capture is almost always (exception = helium) exothermic. The energy available for photon emission is $\frac{1}{2} + \mu v_{in}^2 + W$ where W is the neutron binding energy (the so called energy balance for this case). If the first photon corresponds to a drop to the level L (not necessarily ground) we may write $h\nu = \frac{1}{2} \mu v_{in}^2 + W_L$. As $v \to 0$, $\frac{h^2 \nu^2}{c^3}$ approaches a fixed number [depending on W_L]. But in the expression for σ the $1/v_{in}$ part increases rapidly. Slow neutron (n, γ) reactions go as $1/v_{in}$ (assuming again sufficient constancy of M).

Next consider the (n, α) processes. [The (n, p) processes are of the same type]. $n + A \to B + \alpha$. These reactions can be endothermic or exo-

thermic (Q negative or positive). The energy equation is:

$$\frac{1}{2}\mu v_{in}^2 = \frac{1}{2}\mu_\alpha v_\alpha^2 - Q \qquad \text{(in center of gravity system).}$$

First take $Q > 0$; here v_α is at least $\left(\frac{2Q}{\mu_\alpha}\right)^{1/2}$. Hence

$$\sigma = M \times \frac{1}{v_{in}} \frac{(\mu_\alpha v_\alpha)^2}{v_\alpha} = M \frac{\mu_\alpha^2 v_\alpha}{v_{in}}.$$

For low energies, with $Q < 0$ the (n, α) process obeys the $1/v$ law (reasoning similar to that in the (n, γ) situation above). But for $Q < 0$, things are different. There is a threshold. Write

$$Q \equiv -\frac{1}{2}\mu v_o^2 \qquad \text{so that} -\frac{1}{2}\mu v_o^2 + \frac{1}{2}\mu v^2 = \frac{1}{2}\mu_\alpha v_\alpha^2$$

i.e. $v_{in}^2 - v_o^2 = \frac{\mu_\alpha}{\mu} v_\alpha^2$ showing clearly that $v_{in} = v_o$ is the threshold velocity.

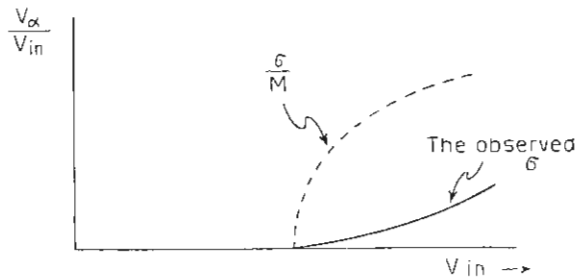

Fig. 12. – Cross section as a function of energy for a threshold reaction (with barrier).

Again we'd expect a parabolic rise in the value v_α/v_{in}. But the observed σ is quite different as can be seen in fig. 12. The reason is the sharp variation of M in this case. Slow charged particles have very much trouble getting out of Gamow barriers.

(5) *Some Examples of the Foregoing Reaction Types.*

$B^{10} + n \rightarrow Li^7 + He^4 + 2.99$ Mev (Normally Li^7 s left excited so that only about 2.5 Mev are available for kinetic energy). In view of the discussion in section (4) this reaction should go as $1/v$ for slow neuts. It does. In unseparated boron (B^{10} & B^{11} mixed) σ is 705 barns for room temperature neutrons. Since the velocity of such neuts is 2.2×10^5 cm/sec the cross-section goes as $\frac{705 \times 2.2 \times 10^5}{v}$. It might be noted that for pure B^{10} the room temperature cross-section is 3800 barns. This reaction is rather important inasmuch as several neutron detectors are based on it. For example, see fig. 13.

Homework: We have a boron layer of 0.05 gm/cm² penetrated by a one ev neutron beam. What is the reduction in intensity of such a beam?

There are many variations of this scheme. You might build the electrodes for more multiplication, i.e. cylindrically symmetrical. One might use argon in the chamber and put boron (in some compound) on one of the electrodes. If the layer is thin, the escaping Li^7 or He^4 might get through to the argon to cause the necessary ionization.

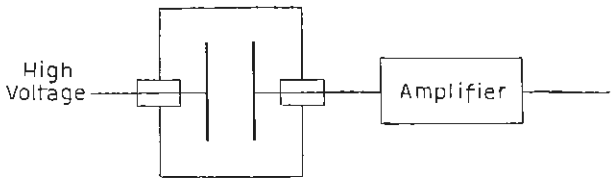

Fig. 13. – BF_3 Ionization chamber. Especially sensitive to slow neutrons.

$Li^6 + n \rightarrow H^3 + He^4 + 4.5$ Mev. (The most convenient way to make H^3). For ordinary lithium (Li^6 & Li^7 mixed) the cross-section is 65 barns for room temperature neuts, and the $1/v$ law is followed for slow neuts, (up to about 0.1. Mev) (fig. 14). The $1/v$ law holds to higher energies for light nuclei (where the energy levels are spaced far apart) than for heavy nuclei with their close packed levels (which would cause sharp variations in M). It is well to keep in mind that the $1/v$ law holds for *relative* velocities. That is, when v becomes small for the neuts, the thermal agitation of the target nuclei must be considered in the application of the $1/v$ law. Let us calculate the number of slow neutrons captured in some material per unit time as a function af the velocity of the neutrons if σ obeys the $1/v$ law. Consider those atoms with velocity v. What is the number of captures per unit time due to atoms of velocity v? Since σ goes as A/v_{relative} and the number of "meeting" per/sec goes as $N_v \times v_{\text{relative}}$, the capture probability which is proportional to the product goes as $N_v A$ where A may be considered constant (N_v is the concentration of atoms of velocity v). The total capture probability becomes $\sum_v AN_v = AN$, a constant. That is, the number of captures per unit time is constant and indipendent of v_{relative} whenever σ goes as $1/v$.

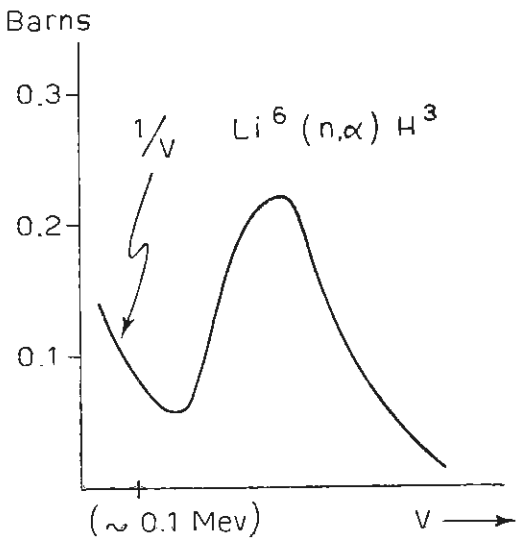

Fig. 14. – Cross section as a function of energy for the $Li^6(n, \alpha) H^3$ reaction.

Homework: What is the average life of a neut in a chunk of lithium (or in BF_3) at standard conditions?

$n + N^{14} \rightarrow C^{14} + H^1 + 0.6$ Mev. Although Q is positive, it is small and the Gamow factor plays a part, so that the cross-section is only 1.7 barns for room temperature neutrons.

Homework: What is the mean life of a neutron in air?

CHAPTER III

The Chart of Stable Isotopes and What it Implies about Nuclear Reactions Involving Neutrons.

(1) *The Segrè Isotope Chart.*

In this chart a nucleus is identified by the number of protons and the number of neutrons it contains. The plot looks somewhat as shown in fig. 15.

For convenience the strip of stable isotopes is usually broken up and plotted as in fig. 16.

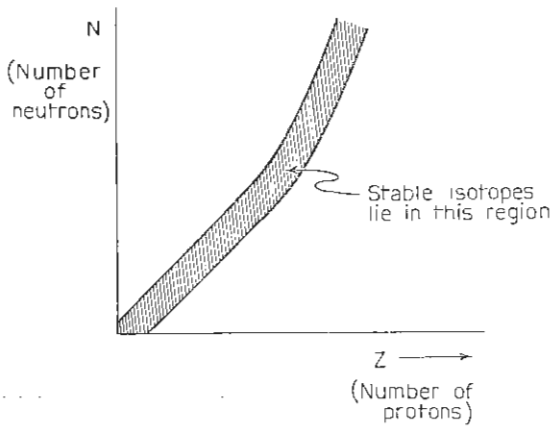

Fig. 15. – N–Z diagram of nuclei (Segrè Chart).

Along with the stable nuclei are plotted unstable nuclei (formed by some sort of bombardment). As an example, let us plot the part of the diagram around aluminum (fig. 17).

It so happens that in the case of aluminum 3 neutron reactions (and these are the 3 most common ones) all yield unstable end products. These are usually β emitters. Thus in the (n, p) reaction discussed, we end up where we started except for the fact that the neutron has become a proton + electron:

$$Al^{27} + n \rightarrow Mg^{27} + H^1 \qquad \text{followed by} \quad Mg^{27} \rightarrow Al^{27} + e^-.$$

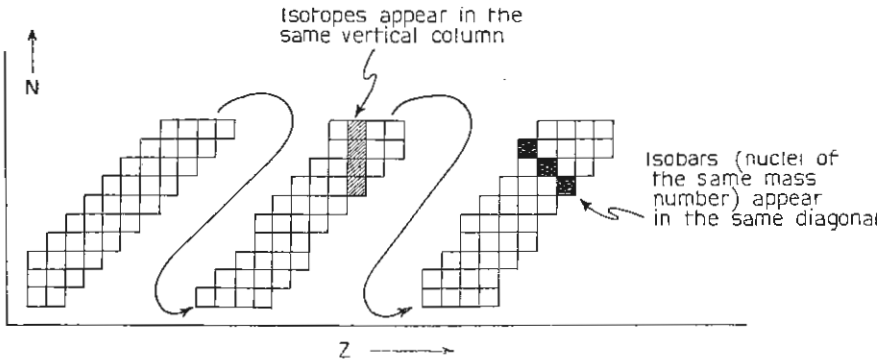

Fig. 16. – Detail of a Segrè Chart.

The net effect can be written $n \rightarrow p + e^-$. There exists also (p, n) reactions for which the net result is $p \rightarrow n + e^+$. Consider Al^{27} again and note that by "substituting" neuts for protons and vice versa we obtain a set of nuclei for which $Z + N = 27$. These will lie on a line of slope — 1 on the chart, (fig. 18). Most nuclei in this set are of course, unstable.

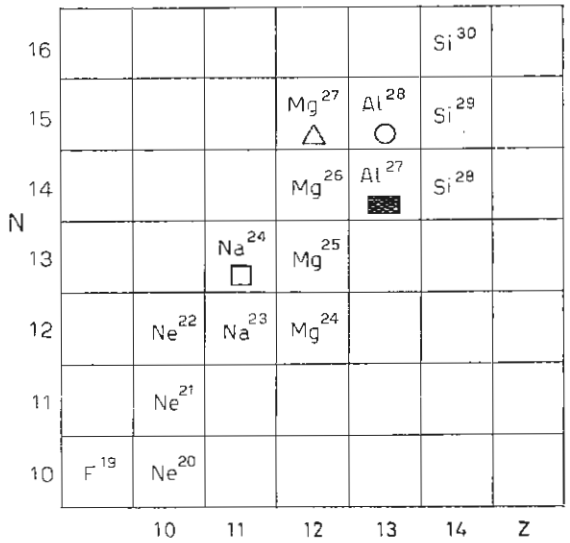

Fig. 17. – Al^{27} is marked with a ■
The end products of the following 3 neutron reactions on Al^{27} are also marked.

○ Represents the product in $Al^{27}(n, \gamma)Al^{28}$
△ Represents the product in $Al^{27}(n, p)Mg^{27}$
□ Represents the product in $Al^{27}(n, \alpha)Na^{24}$.

Actually the unstable nuclei below the stable region need not emit positrons. They may move in the right direction by K–electron capture. This has been observed.

The 3 unstable nuclei considered in connection with Al^{27} are all β emitters as would be expected since they are all above the stable curve. They

all possess characteristic half lives. These are:

Al^{28} 2.3 min Mg^{27} 10 min Na^{24} 15 hours

If Al^{27} is bombarded by neuts of assorted energies, all 3 products may appear and some sort of chemical separation could be used to separate the activities.

Homework problem: Find 5 examples each of (n, α), (n, p), (n, γ) processes. Record the half lives of the radioactive product nuclei.

Were we to isolate one of the activities by chemical means or by using neutrons of proper energy, we could examine the energy spectrum of the emitted β particles; we would find a continuous spectrum (fig. 19). This was (and still is) a somewhat unexpected result. In order to explain this spectrum one usually assumes that the total equation is (take radioactive Mg^{27} as an example) $Mg^{27} \rightarrow$ $\rightarrow Al^{27} + e^- + \nu$ (where ν stands for Pauli's neutrino). The neutrino takes the extra energy, i.e., $E_\nu + E_{e^-} = E_0$ where E_0 is a constant which gives the energy of the β decay. E_0 is the maximum energy on the graph above. For Mg^{27}, this E_0 is 1.8 Mev. Thus the neutrino is here invoked to help conserve energy. Before such a scheme is acceptable, one should show that the maximum β energy (and not, say the average β energy) is the energy lost per nucleus in β decay. Let us assume this in the case of Mg^{27} and see that it leads to observed results $Mg^{27} \rightarrow Al^{27} + e^- + 1.8$ Mev. But

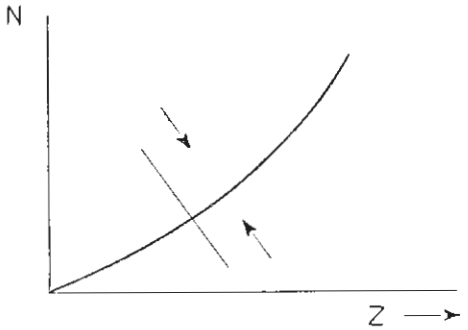

Fig. 18. – Unstable nuclei will move to the curve of stable isotopes as shown; those lying above the curve by the emission of electrons, those below by positron emission.

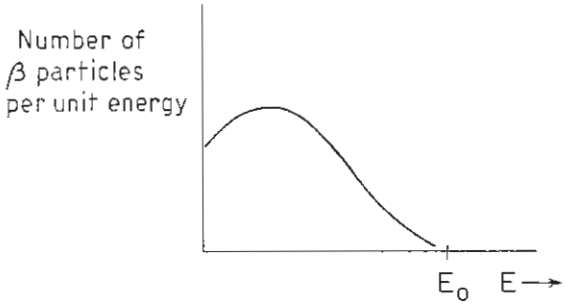

Fig. 19. – Beta ray spectrum.

now, we know the reaction $Al^{27} + n \rightarrow Mg^{27} + H^1 + Q$, and adding these we find, 0.75 Mev $= Q + E_0$ (0.75 is the difference in mass of the neutron and hydrogen atom). Thus $Q = -1.05$ Mev. Thus the observed β-spectrum of Mg^{27} implies (if our assumptions are correct, i.e., if the maximum energy in the β-spectrum corresponds to the total energy of the reaction

of β emission) that the (n, p) reaction on Al^{27} is endothermic with $Q = -1.05$ Mev. And this is observed, for the process has a threshold corresponding to this Q. If the observed Q were, say,—1.2 Mev, this would imply that the energy given out upon β–decay exceeds the max imum of the β–spectrum. To satisfy energy conservation one would assign a non-negligible rest mass to the neutrino.

(2) *Isotope Weights and* (n, γ) *Reactions.*

One might crudely reason that all such reactions are exothermic by about 8 Mev, because we could write

$$A + n \rightarrow (A + 1) + Q$$

as the energy equation. Assuming (and this is quite crude) that the mass of a nucleus containing protons and neutrons of total number A is equal to A, we find

$$Q = 0.009 \text{ mass units or about } 8 \text{ Mev.}$$

Actually the true atomic weight differs appreciably from A in many cases. It has, in fact, been found convenient to define the packing fraction

$$\frac{\text{Atomic Weight} - A}{A}$$

This packing fraction appears in the expression for the energy of formation of a nucleus. Per particle the energy of formation = 0.0085 — (packing fraction). This can be seen from the following considerations.
Total energy of formation is Z (1.0081) + N (1.0089) – atomic weight. Assuming that $Z \sim N$ this can be written approximately

$$(Z + N)\ (1.0085) - \text{Atomic Weight.}$$

Dividing by A gives the above result. For our present purposes the implication of all this is that (n, γ) reactions are not always exothermic with Q = 8 Mev, but that in order to get Q one must know the packing fractions of the nuclei involved.

Homework: Look up 10 nuclear masses in the low end of the chart and calculate the binding energy of the neutron to each. Take H^1 H^2 Li^6 Li^7 Be^9 B^{10} B^{11} C^{12} C^{13}...

We have seen that neutron binding energies are of the order 8 Mev through the periodic table. There are irregular variations of the binding energy with A but in addition there is a regular variation that should be mentioned. This variation involves the packing fraction which is not wholly irregular with respect to the position of the isotope in the periodic table (fig. 20).

Let us then use this observed packing fraction curve to determine any regular variation of binding energy with A. Write

$$\text{P. f.} = \frac{M - A}{A} = f(A)$$

then $M(A) = A\,[1 + f(A)]$; similary $M(A + 1) = (A + 1)\,[1 + f(A + 1)]$.

The binding energy of a neutron (or proton) is roughly $-(A+1)[1+f(A+1)]+A[1+f(A)]+1.0085$ (where 1.0085 is the average mass of neutron & proton). This is $0.0085-[(A+1)f(A+1)-Af(A)]$ which can be written $0.0085-\frac{d}{dA}[Af(A)]$. The function $Af(A)$ looks as shown, in (fig. 21). From the curve, note that at very low A the binding energy is erratic (it doesn't mean much to consult the curve here). It soon becomes $>$ 8 Mev (the slope of the curve is negative). At fairly high A, the binding energy become less than 8 Mev.

Homework: Look up the actual mass defect curve. Find the average binding energy for nuclei in the following neighborhoods: Fe, Ag, Pb, U.

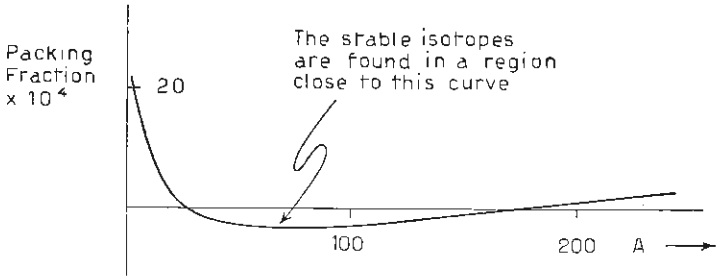

Fig. 20. – Packing fraction curve.

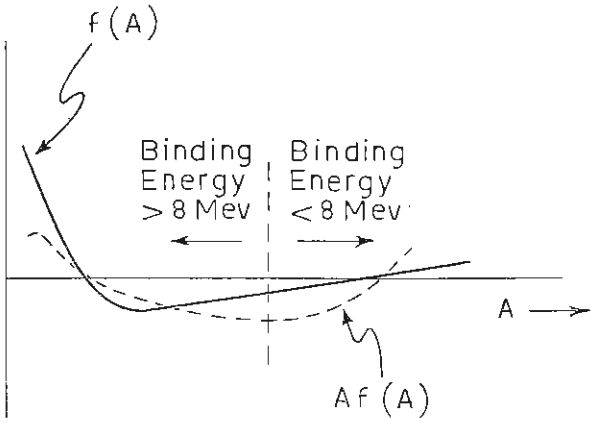

Fig. 21. – Packing fraction curve.

At any rate, the (n,γ) reaction will involve energies of the order 8 Mev. (The only "stable" isotopes that we know do not bind neutrons at all are He^4 and the neutron itself. Tritium also would probably not bind a third neutron, and this would be true of all the unstable nuclei with enough excess neutrons). In the curve of fig. 22 we refer the nuclear binding of neutrons to the stable isotope curve. The closer an isotope is to the top dashed curve the more likely it will emit neutrons (as does a fission fragment). Isotopes only slightly above the stable curve will emit β particles in order to become stable.

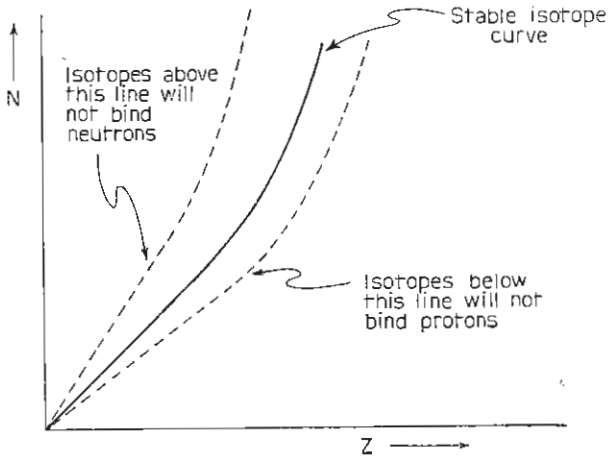

Fig. 22. – Regions of nuclear stabilty.

It should be pointed out that this 8 Mev rule for (n, γ) reactions is just a rough guide and would often be misleading. For example, the opposite processes, or (γ, n) reactions, on deuterium and Be^9 show thresholds of 2.2 Mev and 1.7 Mev respectively showing that the neutron binding energies can be rather lower than 8 Mev.

CHAPTER IV

Models of Nuclei and of Nuclear Reactions.

(1) *The Compound Nucleus.*

We have seen (Chapter II, section (4)) that for an (n, γ) process the cross-section near the origin (i.e. low energy) goes as $\frac{1}{v}\left(\frac{h\nu}{c}\right)^2 \frac{1}{c}$. About 100 (n, γ) reactions are known and the $1/v$ law holds for most only very close to $v = 0$. This is because σ is complicated by the M values. These M values show very sharp variations or resonance levels. An explanation of resonance etc. has to be made in terms of some model. Our picture of a nuclear reaction is somewhat as follows. (fig. 23) A neutron when hitting a nucleus will not knock out the first particle it hits. It will distribute its energy among the various members of the nucleus. The combination of neutron + old nucleus is called a compound nucleus. Whether a particle comes out, depends on the probability of concentrating the necessary escape energy on one particle in the course of the interactions within the nucleus. According to this picture an (n, γ) process can be represented

$$A + n \longrightarrow (A + n)^*, \qquad \text{where } * \text{ means excited}$$

$$(A + n)^* \longrightarrow (A + n) + h\nu \qquad \text{(takes a relatively long time)}.$$

One usually says that the compound nucleus is "relatively stable". This means that it takes many times the time it would take a nuclear particle to cross the nucleus for a compound nucleus to concentrate the necessary energy on a constituent so that the latter escapes. The crossing time

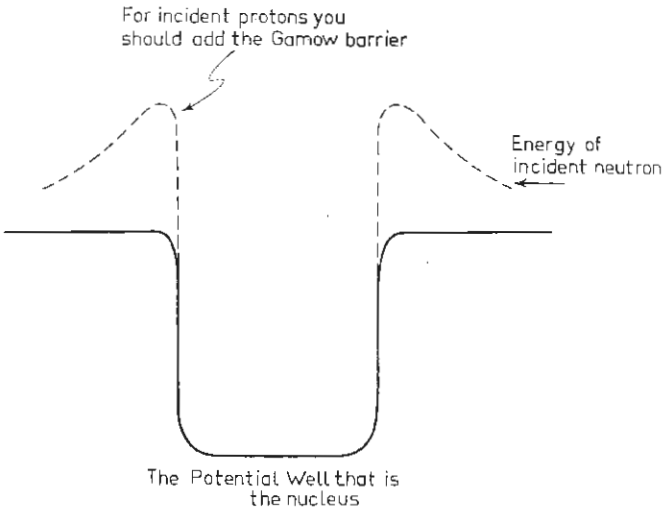

Fig. 23. – The nucleus as a potentiall well.

is of the order $\frac{10^{-12}}{10^{9}} = 10^{-21}$ seconds. The time of existence of a compound nucleus can be inferred from $\hbar \sim \Delta E\, \Delta t$ and a knowledge of widths of resonance levels. Sometimes Δt is of the order 10^{-14} seconds.
This is 10^{7} times the crossing time.

Homework: Find all the information in the literature you can about indium and gold resonances for neutrons.

(2) *Neutron Resonances and Spacing of Nuclear Levels.*

Having seen that the mechanism of a nuclear collision involves the formation of a relatively stable "compound nucleus", let us again consider the (n, γ) process in order to get some more information about nuclei. The cross-section for such a process, we have shown, will follow the $1/v$ law for v small, and will show resonances at higher v, (Section (1) of this chapter). These resonances can be related to the energy levels of the compound nucleus, as is indicated in fig. 24. Neutrons will be absorbed according to the $1/v$ law from very low velocities until they have enough energy, such that the sum of their energy + the binding energy of a neutron to A becomes equal to the energy of some excited state of $(A + n)$, the compound nucleus. At this neutron energy, the absorption cross-section will show a peak.

If the first such resonance peak occurs on the average, for, say, nuclei of medium weight, when neutrons have energy of the order of magnitude E, we would conclude that the energy level spacing of medium weight nuclei

is of order E (in the region of excitation corresponding to the binding energy of a neutron). For medium weight nuclei such "first capture resonances" occur at the order of 10 volts. Thus the energy level spacing at ~ 8 Mev

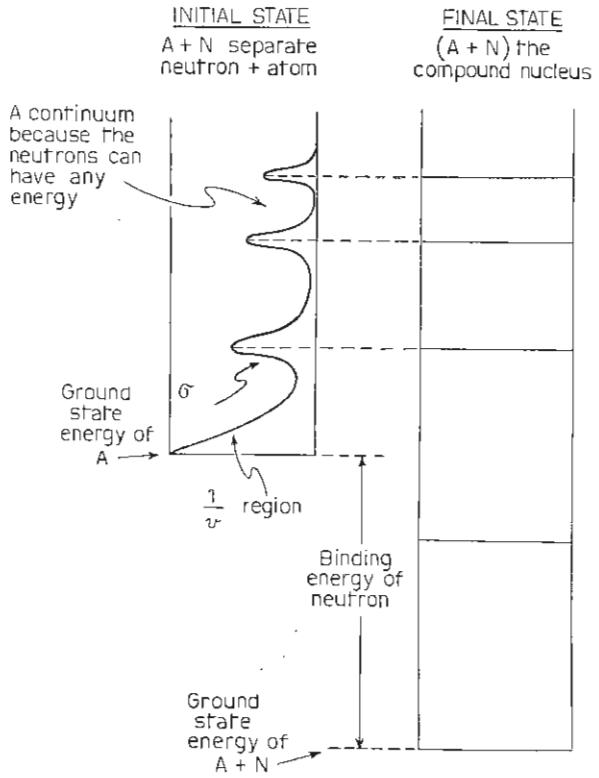

Fig. **24.** – Nuclear energy levels.

excitation is of the order 10 volts. Experiments dealing with such nuclei near their *ground* states indicate, however, that the spacing between energy levels is of the order 10^5 & 10^6 volts at low energies.

Homework: Find from the literature the first resonances for nuclei A = 100 to A = 150. Make an estimate of the level spacing here. A is the mass number.

(3) *Two Models of the Nucleus.*

In constructing a nuclear model we thus have at least two observations to account for (1) Why are relatively stable compound nuclei formed in nuclear collisions? (2) Why does energy level spacing decrease so rapidly with excitation energy in medium or large sized nuclei? (The above discussion does not apply too well to very light nuclei). The first problem is dealt with essentially as follows, no matter what the model. A nucleus is considered to be a mass of close packed particles bound by short range forces. The interactions with neighbors are strong. Whereas in the case of the electrons around the atom, these interactions between neighbors are weak and the collision

of a fast moving particle with such an electron can be considered approximately as a two body problem, in the case of nuclear collision this is no so. The strong interactions act as shock absorbers, and if a particle succeeds in colliding with a nuclear particle, the energy of the collision is quickly shared by the nuclear constituents. This energy is distributed and redistributed as the nuclear particles move about and it is only when, by chance, enough energy is concentrated on a single particle that we have a " disintegration " and this particle leaves the nucleus. It is for this reason that a compound nucleus can exist for so long a time without disintegrating.

In answer to the second question, we shall consider two models. First let us think of the nucleus as a mechanical system with A members, each having 3 degrees of freedom. This system will sustain vibrations and there will be 3 A characteristic frequencies for there are 3 A degrees of freedom in the system. With a frequency of vibration ν_1 there is associated energy $h\nu_1$. If the system is vibrating with frequencies ν_1 and ν_5 at once, it has energy $h\nu_1 + h\nu_5$. In general it will have energy

$$a_1 h\nu_1 + a_2 h\nu_2 + a_3 h\nu_3 + \cdots + a_{3A} h\nu_{3A}$$

where the a's are integers. If $\nu_1 \neq \nu_2 \neq \nu_3$ etc. it is easy to see that at high energies there would be more levels per unit energy. This argument is qualitative and quite inexact, but the basic idea is reasonable. A system of many degrees of freedom will pack its energy levels at high energy.

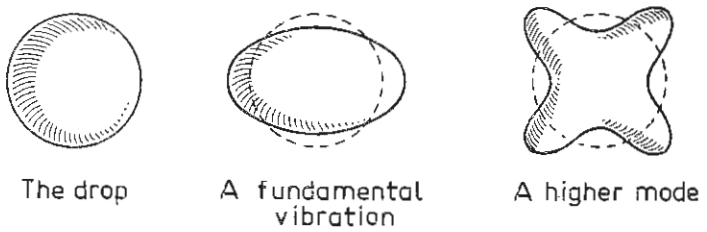

Fig. 25. – Drop model of nucleus.

This type of consideration can be refined somewhat. Bohr suggested that a nucleus be thought of as a drop. Both nuclei and drops are held together by short range forces (shorter than the dimension of the drop or nucleus) and the volumes of each are proportional to the mass. So that nuclei are not very dissimilar to drops.

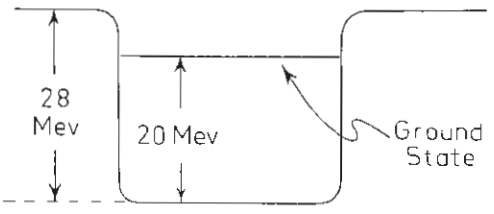

Fig. 26. – Gas model of nucleus.

One can ask about the possible modes of vibration of a drop (fig. 25). This can be calculated under various assumptions in a not obviously incorrect manner. All theories lead to an expression for energy level density of the form $e^{-f(E)}$ but to say too much about $f(E)$ would not really be justified. It can be said, however, that results based on the drop model are in the right direction.

The second model of the nucleus is one quite different. We consider a nucleus as a gas of protons and neutrons in a well (fig. 26). We speak of a temperature T of this gas. At T = 0 the nucleus is in the ground state (but some particles are moving rather fast nonetheless, because of the Pauli exclusion principle). If energy is fed in to the gas, some particles get faster and T goes up. It can be shown that for a degenerate gas of the type here considered the energy is proportional to T^2 rather than T. In fact

$$U = \frac{1}{4}\pi^2\left(\frac{A}{\zeta}\right)\tau^2$$

where U is the energy, A the number of particles in the nucleus, ζ the energy in the ground state ($\sim$ 19 Mev) and $\tau = kT$. If U is written $\alpha\tau^2$ then the entropy

$$S = \frac{\partial U}{\partial \tau} = 2\,a\tau = 2\sqrt{aU} = \pi\sqrt{\frac{A}{\zeta}U}.$$

It is customary to write $S = \log P + \text{const}$ where P is the probability of the state in question. Statistically P is the number of states per unit energy interval. We can thus write: number of states per unit energy $= Ce^{\pi\sqrt{\frac{A}{\zeta}U}}$.

(Thus $-\pi\sqrt{\frac{A}{\zeta}U}$ corresponds to the $f(E)$ of the drop model).

Applying this to a medium nucleus with 8 Mev excitation ($A \sim 100$, $\zeta \sim 19$) we find as the number of states per unit energy Ce^{20} or $C \cdot 10^8$. That is, the density of states at 8 Mev is 10^8 times what it is at the ground state. This is somewhat too high.

In conclusion it should be warned that these points of view shouldn't be taken for more than they are worth. They serve to indicate the trends. Essentially the idea is that a nucleus is a system with many degrees of freedom. Almost any attack would show the logarithmic variation we have found. For more details see *Nuclear Physics Part B* – Bethe, § 53, «Reviews of Mod. Phys.», 9, April 1937.

Homework: Make a table of level density for the following nuclei at the given excitations (in Mev) using the gas model:

Be Fe Ag Au E = 4, 6, 8, 10.

CHAPTER V

THE SCATTERING OF NEUTRONS.

(1) *The Breit-Wigner Formula.*

We have already spoken of a general formula for the cross-section of a nuclear process (page 448). In the case that resonance levels of a compound nucleus are far apart and we are interested in the cross-section in the neighborhood of one of the resonance levels, the expression for the cross-sec-

tion of an (a, b) process can be shown to take the form

$$\sigma(a, b) = \pi\lambda\!\!\!^{-2}_a \frac{\Gamma_a \Gamma_b}{(E_a - E_r)^2 + \Gamma^2/4}.$$

This is the Breit-Wigner formula. $\lambda\!\!\!^{-}_a$ and E_a are the wavelength $\left(\frac{\hbar}{mv_a}\right)$ and energy the incident particle. E_r is the resonance level energy and Γ is the width of the resonance peak at half its maximum value. Actually the above expression for σ should be multiplied by factors depending on the spins of the initial particles and the compound nucleus. But, for simplicity let us consider these factors incorporated in the Γ_a and Γ_b. Γ_a & Γ_b are the partial widths of the resonance peak and are associated with the probability of emitting "a" and "b" particles, respectively. Their exact form is rather complicated but since the probability of emission of a particle b of momentum p (page 450) is proportionalt o $\rho \frac{p^2_{\text{out}}}{v_{\text{out}}}$, so is Γ_b.

The relative probability that the outgoing particle will be an "a" particle is Γ_a/Γ etc. In order that these be true relative probabilities $\sum_{i=a,b\cdots} \Gamma_i = \Gamma$.

It should also be remarked that $\Gamma_i \times \tau_i \cong \hbar$ where τ_i is average time of emission of a particle i after the formation of the compound nucleus. Thus the probability that no particle i has been emitted from the nucleus up to the time t is $\prod_i e^{-t/\tau_i} = e^{-t\sum_i (1/\tau_i)}$ and $\tau = \left[\sum_i (1/\tau_i)\right]^{-1}$ is the average life of the compound nucleus. It will be seen that τ, as well as the individual τ_i's, will satisfy the Heisenberg relation $\Gamma \times \tau \cong \hbar$.

The Breit-Wigner formula can be applied as it was given, to any nuclear collision involving the formation of a compound nucleus provided that the resonance levels are not so close together that they appreciably distort this one-level formula. It can be applied, for example, to (n, γ) processes. Let us do a typical problem. For resonance capture in indium, $E_r = 1.44$ ev and $\sigma(n, \gamma)_{\text{res}} = 26{,}000$ barns. Γ is 0.05 ev. Find the number of neutrons emitted for each γ emitted, given the information that experimentally only γ's and neutrons are observed to be emitted (i.e., $\Gamma = \Gamma_n + \Gamma_\gamma$) and that more γ's are emitted than neutrons ($\Gamma_\gamma > \Gamma_n$). From $\sigma_{\text{res}} = \pi\lambda\!\!\!^{-2}_{n\,\text{res}} \frac{\Gamma_n \Gamma_\gamma}{\Gamma^2}$ $\Gamma_n \Gamma_\gamma$ can be evaluated. The result is that $\Gamma_n = 0.0008$ ev and $\Gamma_\gamma = 0.05$ ev whence $\frac{\Gamma_n}{\Gamma_\gamma} = 0.015$. For gold, $E_r = 4.8$ ev and σ_{res} is also $\sim 26{,}000$ barns and $\Gamma = 0.07$ ev. From this data, $\Gamma_n = 0.0035$ and $\Gamma_\gamma \sim 0.07$. For silver, $E_r = 5.5$ ev. $\sigma_{\text{res}} = 7200$ barns, $\Gamma = 0.19$ ev. These capture reactions are very useful as methods of slow neutron detection.

(2) *Some General Considerations on the Scattering of Neutrons.*

From the Breit-Wigner formula, the elastic scattering cross section for low energy neutrons becomes $\sim \pi\lambda\!\!\!^{-2}_n \frac{\Gamma_n^2}{E_n^2}$. Now $\lambda\!\!\!^{-}_n$ goes as $1/v_n$ and Γ_n goes as $\rho^2_{\text{out}}/v_{\text{out}}$ or as v_n. Hence the cross section is independent of energy. Thus one

would expect that σ should be fairly constant for scattering of neutrons with energies less than the first resonance energy.

The curve for the total cross section in hydrogen (paraffin) is given in fig. 27. This differs very little from the scattering cross section. At low energies the cross section does level out, as predicted, at about 19 barns. But then for very low velocities there is a sudden increase in σ. This is ex-

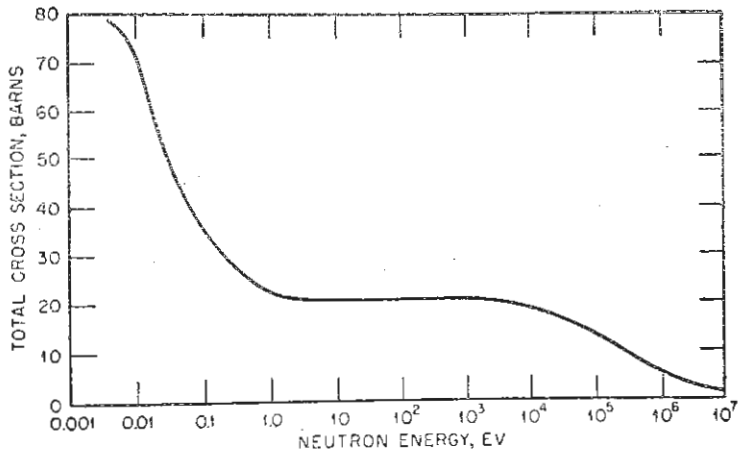

Fig. 27. – Cross section for n–p collision as a function of energy.

plained as follows. Since Γ_n is proportional to m^2, σ must go as m^2. In the application of the B. W. formula this m is the reduced mass of the problem and the velocities are the relative velocities involved. For neutrons scattered from hydrogen, m is therefore half the neutron mass, except where the hydrogen is bound in a molecule and the relative neutron-proton velocity provides too little energy to free the hydrogen or excite the molecule. Then the hydrogen effectively has infinite mass and the reduced mass is the neutron mass itself. Since σ goes as m^2, the cross section for bound hydrogen is ~ 4 times that of free hydrogen. For slow neutrons on chilled paraffin, the relative velocities are low and σ approaches $\sim$ 80 barns.

(3) *Scattering by a Potential.*

The use of the B. W. formula for scattering involves the calculation of Γ's and it is often simpler to use the following approach to the problem of scattering. We consider what happens to the wave function of a particle scattered by a potential representing a nucleus. One advantage of this approach stems from the fact that quite exact information on σ is available even if the potential is but crudely known. A moving particle will satisfy the Schrödinger equation

$$\Delta\psi + \frac{2m}{\hbar^2}(E - U)\psi = 0$$

where U represents the potential of the problem. Let us consider a U that looks as in fig. 28.

If we consider only *s*–scattering (zero angular momentum), then the Schrödinger equation in spherical coordinates is simply

$$r\psi'' + 2\psi' + \frac{2m}{\hbar^2}(E - U)\, r\psi = 0 \qquad \text{or} \qquad \frac{d^2}{dr^2}(r\psi) + \frac{2m}{\hbar^2}(E - U)(r\psi) = 0 .$$

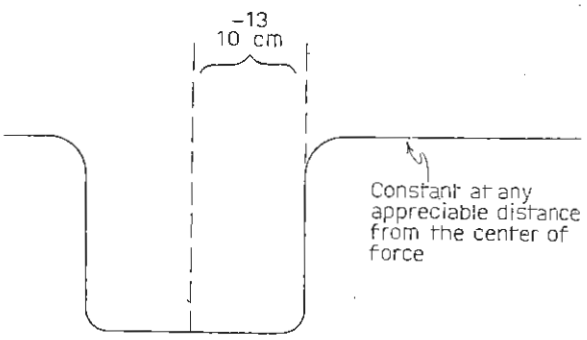

Fig. 28. – Potential well.

Thus for *s*–scattering $r\psi$ (let us call it u) obeys a rather simple one-dimensional differential equation

$$u'' + \frac{2m}{\hbar^2}(E - U)\, u = 0$$

which one would solve (given a U) under boundary conditions $\psi = 0$ at infinity and finite throughout.

Given an arbitrary potential what can be said about u at sight (fig. 29)?

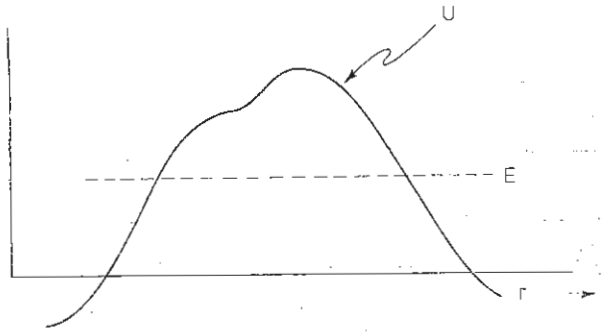

Fig. 29. – Behaviour of u function.

Aside from the $2m/\hbar^2$, the equation reads:

$$u'' = -(E - U)\, u .$$

Whenever $(E - U) > 0$, u'' and u have opposite sign. This means that the function u curves toward the r axis. The concavity is toward the r axis. On the other hand $(E - U) < 0$ implies that the concavity is away from the r axis. In case $E - U = 0$ there is no curvature of the function u. In a qualitative way one can thus draw u for a U of any shape. [Of course when an analytical expression for U is available, one can integrate the equation,

but in any case our rough consideration can quickly furnish information about the general shape].

Consider the three situations: $E = 0$, $E > 0$, $E < 0$. Take $E = 0$ to begin with (fig. 30).

The number of bumps in the region of the nucleus is determined by the depth of the well. The deeper the well the sharper the curvature and the more changes of direction u exhibits within the nucleus.

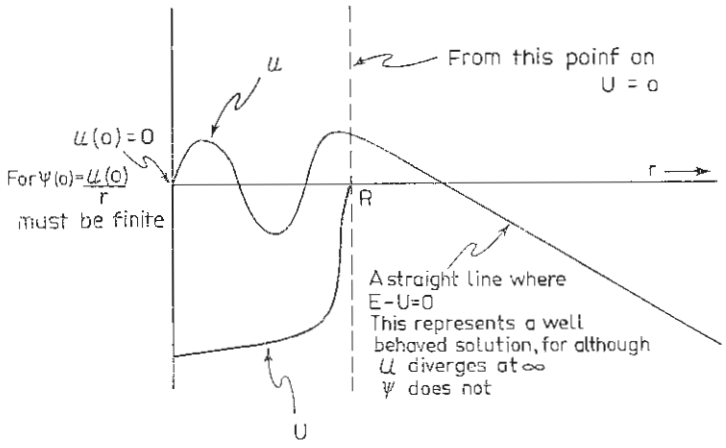

Fig. 30. – Behaviour of u function.

For $E > 0$, the equation to be satisfied past R is $u'' + \frac{2m}{\hbar^2} E u = 0$. The solutions are $\cos \sqrt{\frac{2mE}{\hbar^2}} r$ and the similar sine. This must be matched to the curve within the nucleus (u and its first derivative must be continuous at the junction). The wave length of these cosine and sine functions, it should be remarked, is the de Broglie wave length of the particle being described.

For $E < 0$, the equation at distances outside the range of action R becomes $u'' = \frac{2m}{\hbar^2} (-E) u$. The solution is well known:

$$u = e^{\pm \sqrt{\frac{2m}{\hbar^2}(-E)}\, r} \qquad (-E) \text{ is a positive quantity.}$$

A linear combination of these two exponentials would give a catenary that grows rapidly with r. Such solutions would have to be discarded because they are not well behaved at infinity. Say the energy is E_1, and the curvature is such that the matching exponential solution is as in u_1 (fig. 31). For a lower energy E_2, the curvature will be such that u_2 is the solution. Now between E_1 & E_2 there will be a solution that does not diverge. That is B is neither negative nor positive in $u = Ae^{-\sqrt{\frac{2m}{\hbar^2}(-E)}\, r} + Be^{+\sqrt{\frac{2m}{\hbar^2}(-E)}\, r}$, but is exactly zero. From this we see that there are a discrete group of energies giving allowable (non–diverging) ψ functions in the case that $E < 0$.

Consider again the case where $E > o$, for this corresponds to the case of an incident particle. We shall take up the scattering of such a particle by the nucleus. (See Mott & Massey for details). The sine function that represents the wave outside the nucleus will not necessarily seem to come (when extrapolated) from the origin (fig. 32). It will have a phase shift.

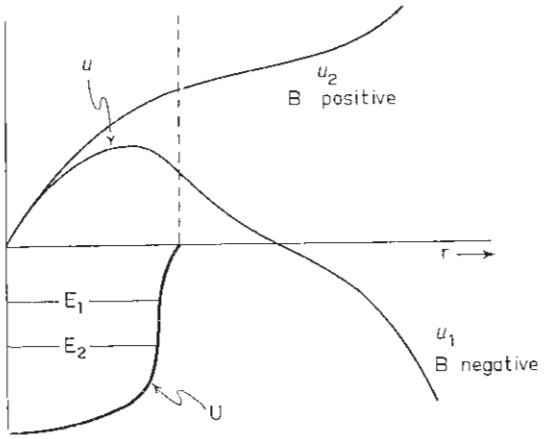

Fig. 31. – Behaviour of u function.

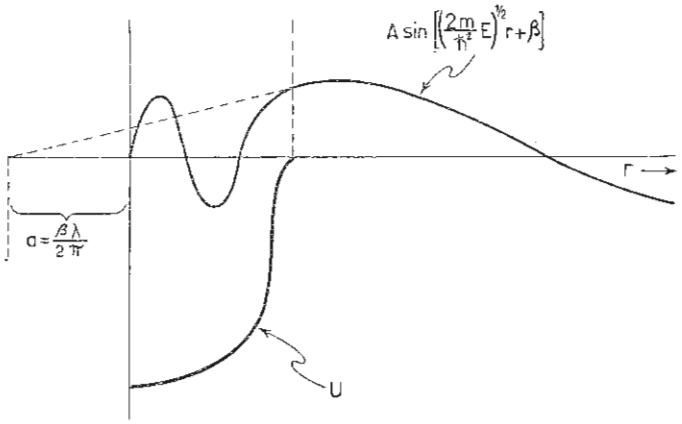

Fig. 32. – Scattering length definition.

This phase shift will depend on the wave function (within the nucleus) to which we must join the sine.

It can be shown (See Mott) that for s–scattering the cross-section depends on the phase shift as follows

$$\sigma_{scat} = 4\pi \frac{\hbar^2}{m^2 v^2} \sin^2 \beta .$$

When does one have only s–scattering (i.e. the incident particle comes in without angular momentum) ? If a particle would pass a nucleus at a distance b (if it were unaffected by the nuclear force) and has velocity v at a great distance from the nucleus, then its angular momentum would be mvb.

But in quantum mechanics the angular momentum is quantized. $mvb = \hbar l$. Then $b = \frac{\hbar}{mv} l$ where l takes on integer values. The region $b = 0$ to $b = \frac{\hbar}{mv} \cdot 1$ gives the region in which we have s–scattering. We would have p–scattering for b between $\frac{\hbar}{mv}$ and $2\frac{\hbar}{mv}$. If, however, $R < \frac{\hbar}{mv}$ there would obviously be no p–scattering (particles passing at "p–distances" from the nucleus would not be aware of its existence). In this case there would be only s–scattering. This condition can be stated, " there is s–scattering only if the neutrons are slow. "

For very low velocities, the above scattering formula is therefore seen to hold and takes on a very simple form. If λ is very big and if a is the distance of the shift of the sine at the origin, the phase shift is $\beta = 2\pi \cdot \frac{a}{\lambda}$. " a " is pretty much the same for all low velocity particles. For very low velocity, λ is big enough so that β may be substituted for sin β. In this case

$$\sigma_{scat} = \frac{4\pi\hbar^2}{m^2 v^2} \times \frac{4\pi^2 a^2}{\lambda^2} = 4\pi a^2.$$

Homework: Given $R = 0.228 \times 10^{-12}$ (the classical electron radius) and a depth of a rectangular potential well of 10.8 Mev (the singlet state of the deuteron) and of 19.7 Mev (triplet state), answer the following questions concerning the scattering of neutrons by protons.

(1) Are there any bound states in each of these cases?
(2) What is the value of " a "?
(3) What is the average cross-section for low velocity neutrons in hydrogen?

It can be shown that the formula

$$\sigma_{scat} = \frac{4\pi\hbar^2}{m^2 v^2} \sin^2 \beta$$

reduces in the case of the existence of bound states, to

$$\sigma_{scat} = \frac{4\pi\hbar^2}{m\left(\varepsilon + \frac{E}{2}\right)}$$

where ε is the binding energy of the bound neutron and E the incident kinetic energy. Even when a virtual state exists, this formula is valid, but here ε is negative and $|\varepsilon|$ is used in place of ε in the formula. In the case of the deuteron, the triplet state has a bigger ε than the singlet. In fact the ε for the singlet (spin of neutron opposite to that of the proton) is so small that it is difficult to decide whether it is positive or negative. In any case the observed scattering cross section of neutrons in hydrogen would be

$$\sigma = \frac{4\pi\hbar^2}{m}\left(\frac{3}{4}\,\frac{1}{\varepsilon_1 + E/2} + \frac{1}{4}\,\frac{1}{|\varepsilon_2| + E/2}\right).$$

The 3 : 1 weighting of states follows from the fact that there are $2S + 1$ states of spin S, and in our case $S = 0$ (singlet) and $S = 1$ (triplet) are the two possible values of S. One can determine whether the " singlet " deuteron state is real or vitual by scattering neutrons from para and ortho hydrogen. It can be shown that the scattering for real states is about 180°

out of phase with that for virtual states. In parahydrogen the spins of the 2 atoms in the molecule are antiparallel and if one were to scatter slow neutrons from parahydrogen, and if the singlet state were virtual, the 2 atoms would scatter out of phase and the scattering cross section would be low. For orthohydrogen (the atoms have spins parallel) the scattering amplitudes for the 2 atoms would always be in phase and the scattering cross section would be greater. This has been observed and the singlet deuteron state is believed to be virtual.

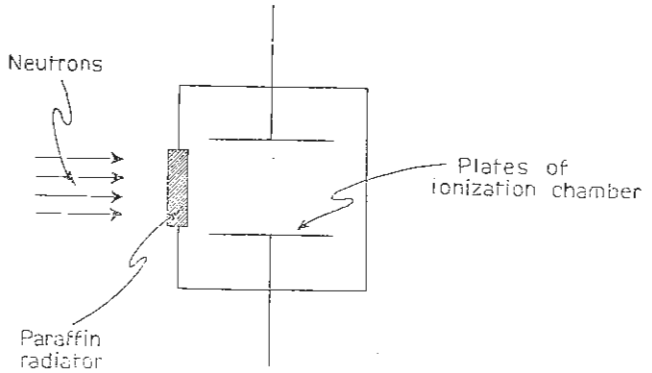

Fig. 33. – Ionization chamber for neutron detection.

Before leaving the subject of the scattering of neutrons in hydrogen, it should be mentioned that this scattering is the basis of an important method of neutron detection. One exposes a thin paraffin layer to the neutron flux. The neuts get scattered in the paraffin and in each scattering a proton recoils with energy of the same order as the neutron energy. One can detect fast protons with ionization chambers. Hence a fast neutron detector can be built as in fig. 33.

In order to measure neutron energies, a collimating device can be used to allow only forward scattered (maximum energy) protons into the chamber (fig. 34).

The pulse in the chamber can be calibrated in terms of proton energy and in this way the original neutron energy can be ascertained (fig. 35).

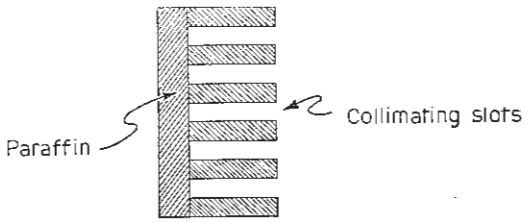

Fig. 34. – Proton collimator.

It should be remarked that in general neutron scattering cross sections show complicated variations with energy, as these examples show. These irregularities are related to involved resonance phenomena, which would not be covered by the simple theory of this section. Incidentally, one usually measures total cross sections. When the absorption cross section is very small compared to the scattering cross section, such measurements give, in effect, the scattering cross section.

(4) *The Scattering of Neutrons by Crystals.*

If neutrons have energy of about 1 ev or less, they have de Broglie wavelengths of the order of Ångstroms or greater. Interatomic distances are measured in Ångstroms and it might be expected, therefore that atoms will interfere in the scattering of slow neutrons. This is actually the case, as we have seen in the discussion of scattering in ortho and para-hydrogen of the last section. One might do an experiment of scattering slow neutrons from

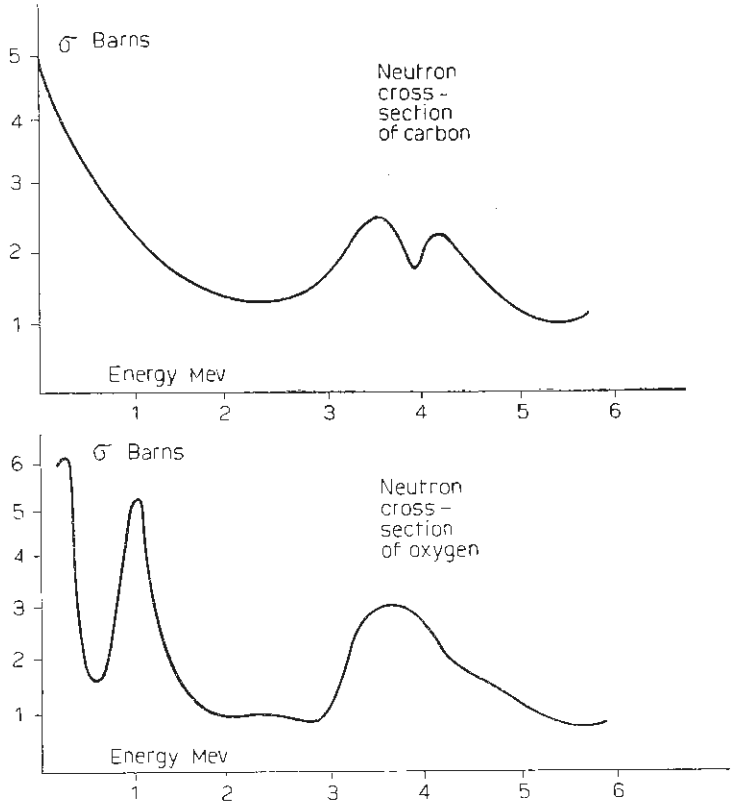

Fig. 35. – Neutron cross section of carbon and oxigen.

a crystal, in order to observe these effects, for the regular arrangement of atoms in a crystal would tend to emphasize any interference phenomena. If one uses an apparatus of the type illustrated in fig. 36, to measure the angular distribution of scattered intensity as a function of angle of incidence, it is found that neutrons obey a Bragg-like formula.

$$n\lambda = 2a \sin\theta$$

where n is the order, λ the neutron wavelength and a the interatomic spacing. For the first order this can be written:

$$v = \frac{h}{2ma\sin\theta}.$$

If a beam of neutrons with a continuous spectrum impinged on a crystal, those neutrons of the proper v for the angle θ would be reflected in a sharp beam at an angle equal to the angle of incidence. Neutrons with other velocities woul simply be scattered in the material in a normal way. One can easily check that the reflected beam really contains those neutrons whose velocity

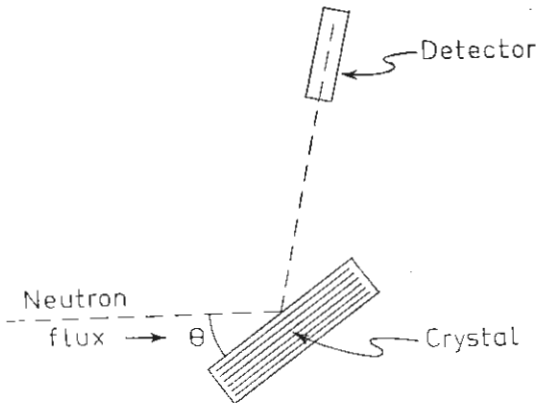

Fig. 36. – Bragg reflection.

is given by the Bragg formula, by taking readings with and without a boron absorber in front of the detector for various angles. The boron cross section as a function of v is well known and from the observed curve for σ *vs* θ one could easily get one for v *vs* θ, and this would be found to give the Bragg relation (aside from complications due to higher order reflections, etc.). It can be seen, therefore, that the combination of a crystal and neutron detector can be used to analyze a beam of neutrons for the velocity distribution. In such a way, for example, slowed down neutrons from a tank of water are found to show a Maxwell distribution. It is found that microcrystalline substances scatter much better than regular crystalline substances. The explanation is along the following lines. The neutron arrives at the first microcrystal. (Fig. 37). If the Bragg condition is not fulfilled the neutron can get through. Otherwise it will be reflected. When the neutron arrives at the next microcrystal it once again must pass the test of not fulfilling the Bragg condition if it is not to be scattered. Were there but one crystal, it would have but one test to pass. The more microcrystals, the greater the chance to be scattered. For a single large crystal only those neutrons are removed whose velocity satisfies the Bragg relation. For the microcrystalline structure, sooner or later all velocity neuts of the original beam will be removed as the beam moves from crystal to crystal in the microcrystalline structure.

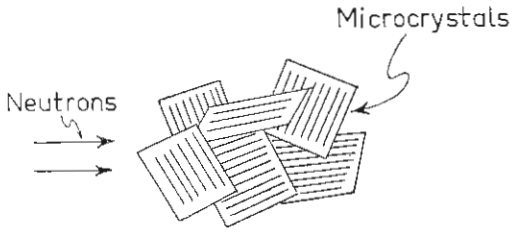

Fig. 37. – Microcrystals in neutron beam.

There is one very important difference between x–ray and neutron scattering. If the crystal is composed of 2 isotopes the x–ray scattering is not particularly disturbed, for x–ray scattering depends on extra–nuclear properties of an atom (and these are pretty much the same for 2 isotopes). For neutrons it is the nucleus itself that enters into the scattering process. And nuclei are such that in addition to determining scattering cross-sections, they determine the phase of scattering. Consider a neutron being scattered by 2 isotopes. For species one the scattering intensity is proportional to σ_1. The scattering amplitude for species one is $\sqrt{\sigma_1}$ and for species 2, $\sqrt{\sigma_2}$. Write

$$\sqrt{\sigma_1} = \frac{\sqrt{\sigma_1} + \sqrt{\sigma_2}}{2} + \frac{\sqrt{\sigma_1} - \sqrt{\sigma_2}}{2} \qquad \sqrt{\sigma_2} = \frac{\sqrt{\sigma_1} + \sqrt{\sigma_2}}{2} - \frac{\sqrt{\sigma_1} - \sqrt{\sigma_2}}{2}.$$

Thus $\sqrt{\sigma_1}$ & $\sqrt{\sigma_2}$ have a part in common (they scatter the same for this part, the so–called coherent part). In addition there is an incoherent (opposite phase) part. The coherent part does give rise to interference. The incoherent part gives rise to scattering as if from an unordered assembly of atoms.

Homework: For NaCl (using the (001) planes only) make a table of the λ reflected (1st & 2nd order) at various angles θ

$$1, 2, 3, 4, 5, 10, 20, 30, 40^\circ.$$

Calculate the ev for each λ. What is the relative intensity of first and second order beams, assuming a Maxwell distribution ($T = 300^\circ$ K) for the neutrons?

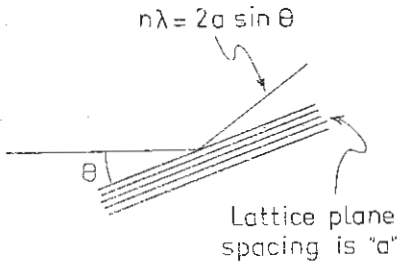

Fig. 38. – Bragg reflection.

How deep will a beam of neutrons penetrate inside a crystal if the Bragg reflection is satisfied ? Let us take a finite piece of crystal, say a crystal of M planes with $N \times N$ atoms in each plane (fig. 38). There are then $N \times N \times M$ atoms in the crystal. If there were but one atom and its cross section were σ the scattered intensity of a beam of intensity I is $I\sigma$. This would be isotropic and at distances r the intensity would be $\frac{I\sigma}{4\pi r^2}$. This implies that the amplitude of the scattered beam at this point is $\sqrt{\frac{I\sigma}{4\pi r^2}}$. Since this is but an order of magnitude calculation we are doing, let us call the amplitude simply $\frac{\sqrt{I}\sqrt{\sigma}}{r}$. Now let us estimate the amplitude in the reenforced direction. In this direction the amplitudes add. Hence the amplitude is $\frac{\sqrt{I}\sqrt{\sigma}}{r} N^2 M$. This makes the intensity $\frac{I\sigma}{r^2} N^4 M^2$; now we ask, " What is the width of the angular spread of the reflected beam ? " From physical optics this angle $\theta = \frac{\lambda}{d}$, where d is the dimension of the " mirror ". In our case $d = N \times a$. This gives a patch of " light " of size $\frac{\lambda r^2}{Na}$ at the distance r in the right direction. Thus the total energy reflected is

$$I\sigma N^2 M^2$$

under the assumptions: *a*) that the crystal is so small that there is practically no attenuation in the crystal, *b*) that λ is of the order of magnitude *a*. Were the crystal a perfect mirror it would remove energy $I(Na)^2$. It could certainly not remove more.

Hence certainly

$$I\sigma N^2 M^2 < I(Na)^2$$

or $\sigma M^2 < a^2$; what does this inequality imply ? It means that if $M > \frac{a}{\sqrt{\sigma}}$, then the layers beyond $M_0 = \frac{a}{\sqrt{\sigma}}$ do not count. We say the beam doesn't penetrate past M_0 layers. The depth of penetration then is $M_0 a$ or $\frac{a^2}{\sqrt{\sigma}}$. The distance *a* will be of order 3×10^{-8}; $\sqrt{\sigma}$ will be about 2×10^{-12}. This means about 10^{+4} planes play a vital part in Bragg reflection. This is of the order of microns.

If a heterogeneous beam of neutrons is made to hit a large perfect crystal, those neutrons of the " right " velocity will be weeded out right off (within a micron or so). But the rest of the neutrons won't be transmitted 100 percent. There are several reasons for the attenuation of even the " wrong " velocity neutrons.

(1) The presence of isotopes presents a random irregularity and this would give incoherent scattering for all velocities;

(2) Another element of irregularity is the random variation of spin direction of the nuclei;

(3) The crystal may not be too regular, but even if it were, the thermal motions of the atoms would complicate matters,

(4) The crystal atoms might absorb as well as scatter neutrons.

How to obtain very slow neutrons using interference phenomena: The Bragg formula can be written $\lambda = 2a\frac{\sin\theta}{n}$. This implies that $\lambda < 2a$. Thus neutrons whose wavelength is larger than twice the maximum crystal spacing do not in any case get Bragg-reflected. All scattering of such neutrons would be due to the above 4 phenomena. Graphite has almost one isotope (99 percent) and the spin is zero (atoms of even atomic weight have spin zero usually). For graphite $2a = 6.69 \times 10^{-8}$ cm. This makes the energy of neutrons of this λ equal to 0.0018 volts [1 volt neutrons have $\lambda = 0.286 \times 10^{-8}$ cm]. For thermal distributions, the peak is at about 0.025 volts. This implies that a piece of graphite will (in an appreciable distance) weed out almost the entire spectrum of thermal neutrons. Only the very slow neutrons (shaded in diagram of fig. 39) will not be weeded out (they have too large a λ and can be scattered only by the 4 processes mentioned above and these are small for graphite). Thus we can get a very " cold " beam using thermal neutrons and a polycrystalline graphite " filter. "

Reflection of neutrons from polished surfaces: If one sends a beam of *x*-rays on a polished surface at a glaxcing angle, one observes a total reflection. (Most substances have indices of refraction for *x*-rays very slightly less than one). The index of refraction of a substance is intimately connected with the scattering properties of the substance. The interference of scattered

x–rays and original x–rays produces a change in phase of the original ray. This change of phase can be described most conveniently by assigning an index of refraction that describes the change of wave velocity within the substance. At any rate the same phenomena of total reflection from polished surface occurs for neutrons too. But the index of refraction for neutrons is very close to one. This means that a converging lens for neutrons would have to bulge very much along the axis to do any good if it were made of

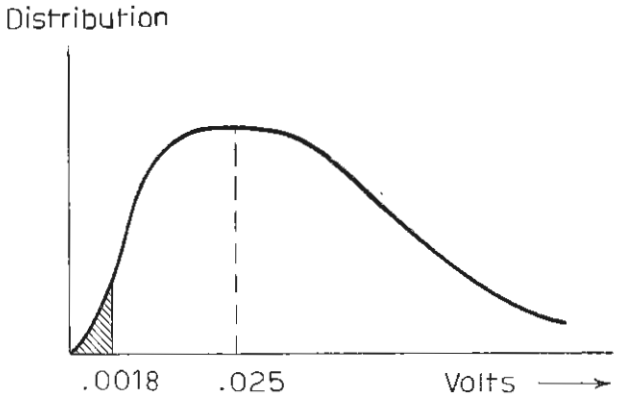

Fig. 39. – Neutron filtering action.

substances where n is slightly greater than one. For substances in which $n < 1$ a converging lens would look like the diverging lenses of optics. These lenses are possible in principle, but because $|n - 1|$ is so small, they are not at all practical.

Homework: Show that if a continuous distribution of neutrons impinges on a microcrystalline substance when $M < M_0$, the scattered intensity is of the order of that expected from a non-crystalline substance of the same number of atoms for all energy neutrons. Use the fact that the resolution of a microcrystal reflecting neutrons of wavelength λ according to the Bragg formula is given by $\frac{\delta\lambda}{\lambda} \sim \frac{1}{M}$.

CHAPTER VI

The Slowing Down of Neutrons

(1) *The Change of Direction and Energy upon Collision.*

Suppose a beam of neutrons is made to hit some hydrogen. A neutron loses on the order of half its energy per collision. At this rate a million volt neutron becomes thermal in about 24 collisions. (Hydrogen is particularly good for slowing down neutrons, because in addition to its being light, it has a high scattering cross-section for neutrons; ~ 20 barns compared to 3 or 4 barns for other light nuclei).

Assuming isotropic scattering in the center of gravity system, let us investigate the results of a collision of a neutron of velocity v against an atom of weight A at rest. The velocity of the center of gravity is $\frac{v}{1+A}$. The velocities of A and n relative to the center of gravity are $\frac{v}{1+A}$ and $\frac{vA}{1+A}$ respectively (fig. 40). In a scattering process, the magnitudes of velocities

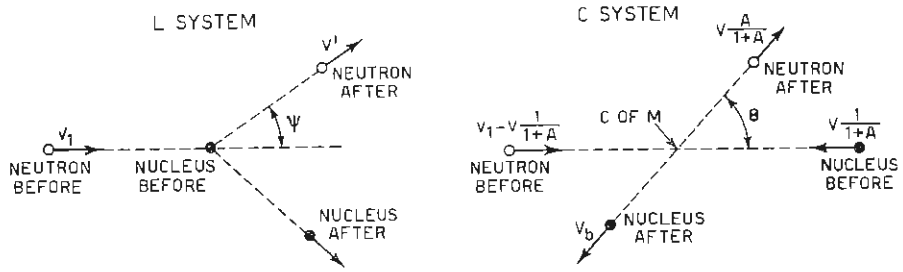

Fig. 40. – Neutron scattering in laboratory (L) and center of mass (C) systems.

in the center of gravity system don't change. Only the directions change. Going back to the lab system, we can get v', the resultant velocity of the neutron in the lab system, by adding (vectorially) its velocity in the center of gravity system to the velocity of the center of mass in the lab system (fig. 41).

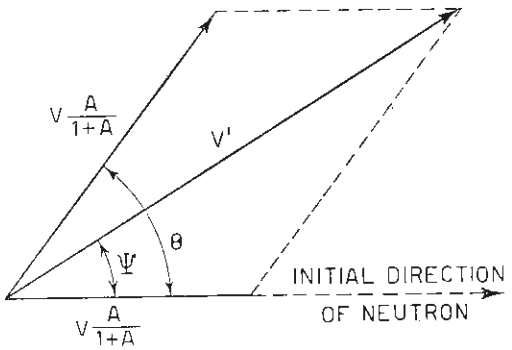

Fig. 41. – Transformation from C system to L system.

From the diagram

$$\frac{1}{2}mv'^2 = \frac{1}{2}m\frac{v^2}{(1+A)^2}[A^2 + 1 + 2A\cos\theta] .$$

Thus the ratio of neutron energies before and after collision is

$$\frac{E'}{E} = \frac{A^2 + 1 + 2A\cos\theta}{(A+1)^2} .$$

It should be noted that θ is an angle in the c. of g. system. If β is the angle in the lab system between initial and final neutron directions, it is easy to show that:

$$\cos\beta = \frac{A\cos\theta + 1}{(A^2 + 1 + 2A\cos\theta)^{1/2}}$$

$\overline{\cos\beta}$ is (unlike $\overline{\cos\theta}$) not equal to zero, but is some positive number showing that colliding particles show a tendency to preserve their direction of motion. In fact,

$$\overline{\cos\beta} = \int_0^{\pi} \frac{A\cos\theta + 1}{\sqrt{A^2 + 1 + 2A\cos\theta}} \cdot \frac{2\pi\sin\theta\, d\theta}{4\pi} = \frac{2}{3A}$$

showing that this tendency to keep going in the original direction, is greatest for collisions with light particles, as expected.

Let us look more closely at the formula for E'/E. The maximum and minimum values are:

$$\left.\begin{aligned} &= 1 \text{ for } \theta = 0 \text{ (practically no collision)} \\ &= \left(\frac{A-1}{A+1}\right)^2 \text{ for } \theta = \pi \text{ (head–on collision)} \end{aligned}\right\} \quad \frac{A^2 + 1 \pm 2A}{(A+1)^2}$$

For collisions with hydrogen ($A = 1$) the limits are thus 1 and zero. For heavier atoms, it is, of course, impossible to bring the neutron to rest. In fact where A is big, $\left(\frac{A-1}{A+1}\right)^2 \cong 1 - \frac{4}{A}$ neglecting higher terms in 1/A. Thus for $A = 100$, the biggest possible loss in energy is 4 percent. For $A = 200$ it is 2 percent and so on.

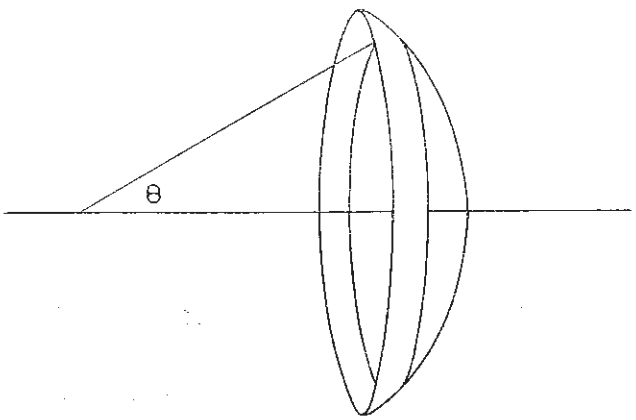

Fig. 42. – Solid angle between θ and $\theta + d\theta$.

We would like to know what is the relative probability of a neutron coming off with any energy E' between the limits just described. Let us assume that the scattering is isotropic in the c. of g. system. What is the solid angle between θ and $\theta + d\theta$ (fig. 42)? It is

$$\frac{2\pi\sin\theta\, d\theta}{4\pi} = \frac{\sin\theta}{2} d\theta .$$

From the formula for E',

$$dE' = -E\frac{2A}{(1+A)^2}\sin\theta\, d\theta = -E\frac{4A}{(1+A)^2} dp$$

where dp is the probability $\left(\frac{1}{2}\sin\theta\, d\theta\right)$ that the angle is between θ and $\theta + d\theta$ or that the energy E′ lies between E′ and E′ + dE′. Thus:

$$dp = \frac{(A+1)^2}{4A}\,\frac{dE'}{E}\,.$$

Thus the probability of coming off with energy E′ is independent of E′. The curve for the probability of coming off with energy E′ as a function of E′/E is shown in fig. 43. For hydrogen the figure would be a square with a corner at the origin.

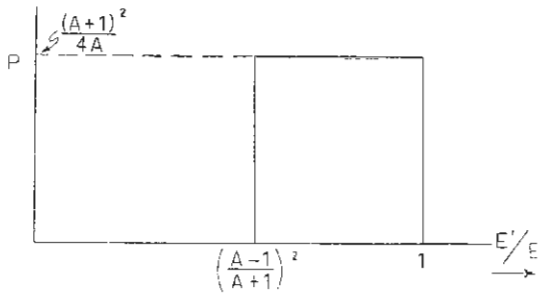

Fig. 43. – Neutron energy after one collision.

What would be the influence on neutron energy of a large number of collisions ? It is more convenient in this discussion to consider $\varepsilon = \log E$. This comes from the result that E′/E is independent of E. In fact since the percent loss in energy is on the average the same, the neutron's energy looks like fig. 44 after collisions 1 , 2 , 3 · · · .

Fig. 44. – Energy decrease in successive neutron collisions.

and in each collision it is log E rather than E that changes by a more or less fixed amount. Let us call $\xi \equiv \overline{\log \frac{E}{E'}}$ and evaluate it.

$$\text{It is } \int_{E'_{min}}^{E'_{max}} \log\frac{E}{E'}\cdot P(E')\,dE' \quad \text{which is } \int_{\left(\frac{A-1}{A+1}\right)^2 E}^{E} \log\frac{E}{E'}\,\frac{(A+1)^2}{4A}\,\frac{dE'}{E}\,.$$

This is a fairly simple integral and

$$\xi = 1 - \frac{A\left(1-\frac{1}{A}\right)^2}{2}\log\frac{A+1}{A-1}\,.$$

For carbon, for example, A = 12 and ξ is equal to 0.158. For hydrogen $\xi = 1$. This means that for hydrogen E′/E is on the average $1/e$. To reduce a 1 Mev neutron to thermal energies $\left(\frac{1}{40}\text{ ev}\right)$ by means of hydrogen one would

require $\log(4\times10^7) = 17.5$ collisions. About 110 collisions $\left(\frac{17.5}{0.158} = 110\right)$ would be required in carbon.

Homework: Calculate ξ for H^2, He^4, Be^4, O^{16}, U^{238}. How many collisions will be needed to reduce a neutron's energy from 10^6 to 1 volt?

(2) *Distribution of Neutrons from a Point Source—Experimental Methods.*

It is because neutrons are slowed down by collisions, that the treatment of most problems in which neutron fluxes are introduced into media requires

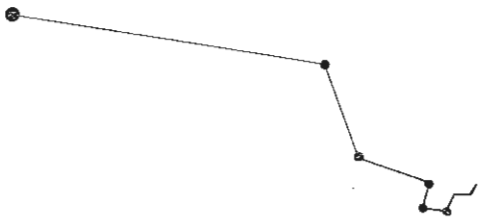

Fig. 45. – In water the mean free path decreases as the energy does.

some knowledge of the nature of the slowing down process. The simplest question to ask is "Given a point source of monoenergetic neutrons, what is the steady-state spatial distribution as a function of energy?" The solution will be basic; for any source distribution can be considered a superposi-

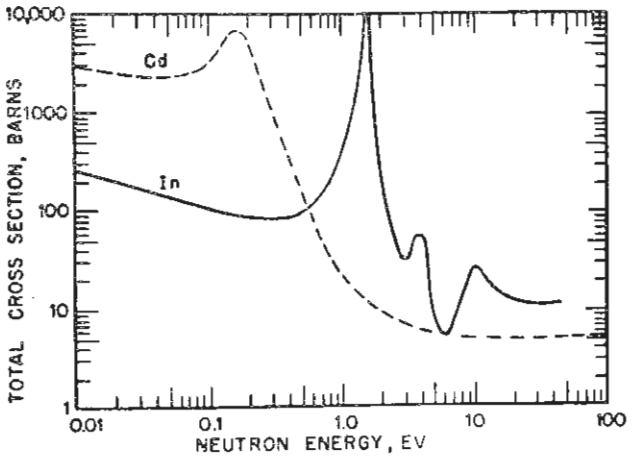

Fig. 46. – Cross section of cadmium and indium as functions of neutron energy.

tion of point sources. Consider a Ra + Be source in a large tank of water (fig. 45). For hydrogen, the scattering cross section is particularly large at low energies and so a neutron does most of its traveling on the first one or two of its paths if it starts with 10^6 volts. One could investigate the distribution of neutrons from the source in water by using detectors sensitive to different energy neutrons. For example one might use an indium foil and get a plot such as in fig. 46. The cross section for indium is also shown. To

make the indium more useful, we prevent its responding to thermal neuts by surrounding it with cadmium foils. We could use Rh foils ($\sim$ 1 ev resonance energy) too (fig. 47). We could use a Cd–In–Cd sandwich and subtract it from the simple In (unshielded) activation in order to get the distribution of thermal neutrons in space. To detect the spatial distribution of neutrons of about 37 volts one would use iodine. One would get for the detectors mentioned a set of curves like that shown. The curves here are all normalized to unit activation at $r = 0$.

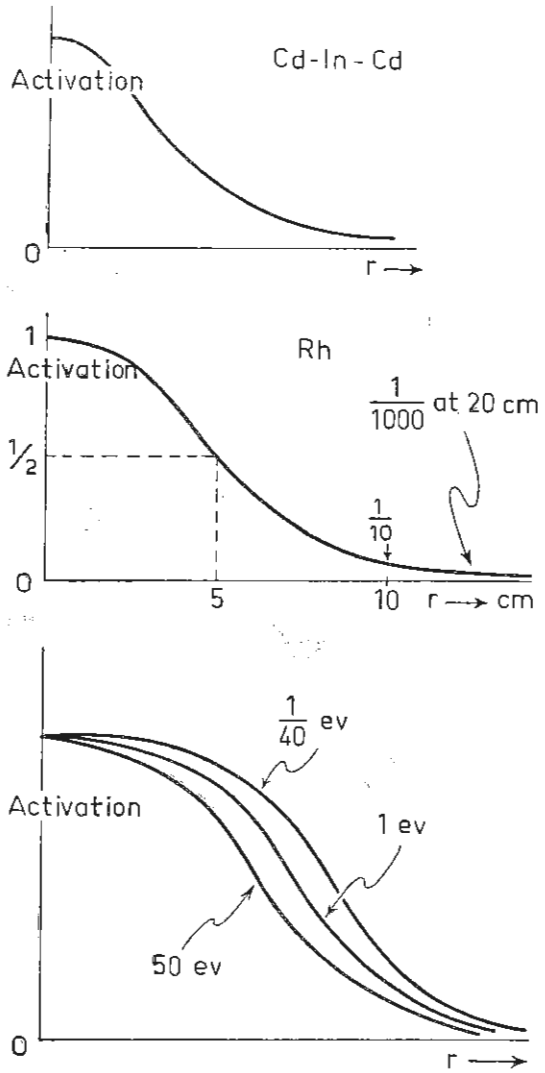

Fig. 47. – Neutron density as a function of energy and distance.

(3) *Distribution of Neutrons from a Point Source—The Calculation of* $\overline{r^2}$.

We would now like to solve the following problem. A point source of neutrons of energy E_0 is located in some medium. The neutrons get slowed down by collisions upon leaving the source. Consider all the neutrons of

energy E. How far away from the origin or source are they on the average? What is their $\overline{r^2}$?

Consider a typical path (fig. 48). The resultant displacement

$$\boldsymbol{r} = \boldsymbol{l}_1 + \boldsymbol{l}_2 \cdots + \boldsymbol{l}_n$$

and

$$r^2 = l_1^2 + l_2^2 + \cdots + l_n^2 + 2\,(\boldsymbol{l}_1 \cdot \boldsymbol{l}_2 + \boldsymbol{l}_1 \cdot \boldsymbol{l}_3 + \cdots + \boldsymbol{l}_2 \cdot \boldsymbol{l}_3 + \cdots).$$

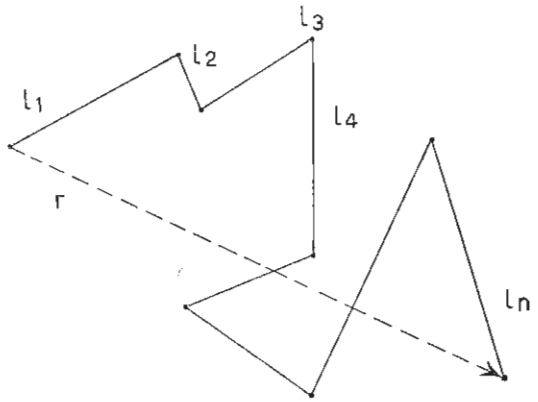

Fig. 48. – Vector sum of $\boldsymbol{l}_i$.

We would like to average this expression, and shall do one parameter at a time. First consider all the lengths l fixed and all the angles β fixed, but not fixed as to φ (see diagram fig. 49). Later we shall average over various lengths l and angles β, but for the moment let us do this part of the averaging.

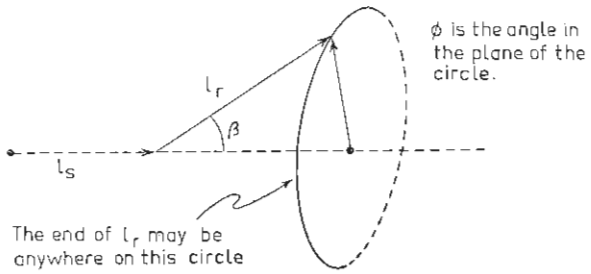

Fig. 49. – Definitions of β and φ.

Under these assumptions we should like to prove that

$$\overline{\cos \widehat{14}} = \cos \widehat{12} \cos \widehat{23} \cos \widehat{34}$$

where $\cos \widehat{rs}$ is the cosine of the angle between $\boldsymbol{l}_r$ and $\boldsymbol{l}_s$. From the diagram (fig. 50)

$$\cos \widehat{14} = \cos \widehat{13} \cos \widehat{34} + \sin \widehat{13} \sin \widehat{14} \cos \widehat{134}.$$

On the average

$\cos \widehat{134} = 0$ (As 4 rotates about 3). Hence $\overline{\cos \widehat{14}} = \overline{\cos \widehat{13}} \cos \widehat{34}$

and now we repeat the same scheme and again an average of a dihedral angle vanishes

$$\overline{\cos \widehat{13}} = \overline{\cos \widehat{12} \cos \widehat{23}} \qquad \text{But } \cos \widehat{12} \text{ is } \beta_{12},$$

a constant. Hence in general,

$$\overline{\cos \widehat{rs}} = \cos \widehat{rl} \cos \widehat{lm} \cdots \cos \widehat{ts}$$

where $\boldsymbol{l}_r, \boldsymbol{l}_l, \boldsymbol{l}_m \cdots$ are successive vectors.

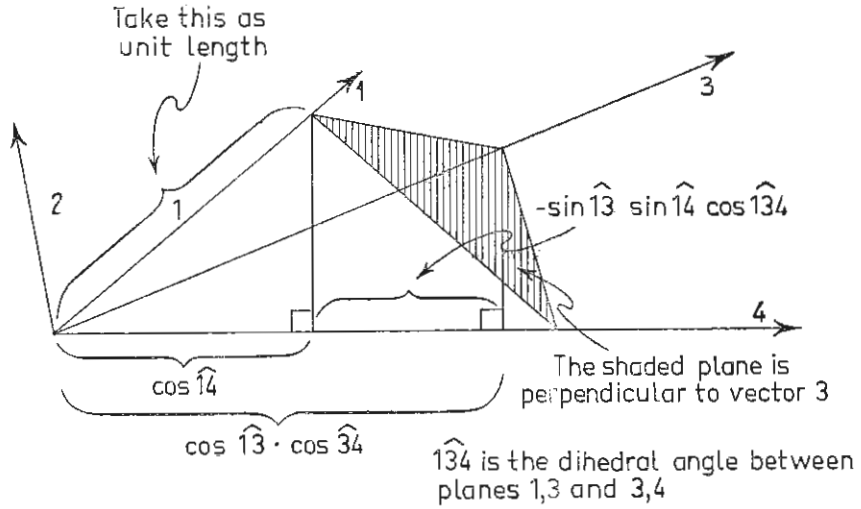

Fig. 50. – Diagram for the calculation of $\cos \widehat{14}$.

Now consider the mean free paths. The probability that l_r lies between l_r and $l_r + dl_r$ is $e^{-\frac{l_r}{\lambda_r}}$. From this we can get $\overline{l_r} = \int_0^\infty l_r e^{-\frac{l_r}{\lambda_r}} \frac{dl_r}{\lambda_r}$ and $\overline{l_r^2} = \int_0^\infty l_r^2 e^{-\frac{l_r}{\lambda_r}} \frac{dl_r}{\lambda_r}$. These integrals are of the form $\int_0^\infty x^n e^{-\alpha x} dx = \frac{n!}{\alpha^{n-1}}$ and we find $\overline{l_r} = \lambda_r$ the mean free path (this is why λ_r can be called the mean free path) and $\overline{l_r^2} = 2\lambda_r^2$.

Recalling the results of our average over angles and using these last results for the average l's, $\overline{r^2}$ for the set of angles $\beta_{12} = \widehat{12}$, $\beta_{23} = \widehat{23} \cdots$ is

$$\overline{r^2} = 2\lambda_1^2 + 2\lambda_2^2 \cdots + 2\lambda_n^2 + 2[\lambda_1\lambda_2 \cos \widehat{12} + \lambda_1\lambda_3 \cos \widehat{12} \cos \widehat{23} + \cdots + \lambda_2\lambda_3 \cos \widehat{23} + \cdots].$$

In the case of hydrogen this calculation can be completed in an exact way. In general, however, it is now convenient to make some approximation. Let us assume it takes a large number of collisions to produce a small change in energy. This is the more true the heavier the atom collided with.

The angles $\widehat{12}$, $\widehat{23}$ etc., may take on all values from zero to π. To determine $\overline{r^2}$ we must average over the various possible angles. Notice that the coefficient of λ_1 in $\overline{r^2}$ is

$$2\,[\lambda_2 \cos \widehat{12} + \lambda_3 \cos \widehat{12} \cos \widehat{23} + \cdots].$$

But since $\overline{\cos \beta} = \frac{2}{3\,A}$ and since later terms consist of products of an increasing number of such cosines, for A large these terms rapidly become small. One would need but the first few terms in the series to approximate the coefficient of λ_1. Furthermore, the first few λ's will not differ appreciably from λ_1 and $\cos \widehat{12}$ is on the average $\frac{2}{3\,A}$. Call this c. The quantity $\cos \widehat{12}$ $\cos \widehat{23}$ is c^2 on the average. The coefficient of λ_1 is therefore $2\,\lambda_1\,(c + c^2 + c^3 + \cdots)$. There will not be much error if we consider this an infinite series. The true $\overline{r^2}$ is then

$$2\,\lambda_1^2 + 2\,\lambda_2^2 + \cdots + 2\,\lambda_1^2 \frac{c}{1-c} + 2\,\lambda_2^2 \frac{c}{1-c} + \cdots = \frac{2}{1-c} \sum_{i=1}^{n} \lambda_i^2.$$

This can be written as an integral over the λ's rather than a sum.

$$\overline{r^2} = \frac{2}{1 - \frac{2}{3\,A}} \int_{\log E_1}^{\log E_0} \frac{\lambda^2(\varepsilon)\,d\varepsilon}{\xi} = -\frac{2}{\xi\left(1 - \frac{2}{3\,A}\right)} \int_{E_1}^{E_0} \frac{\lambda^2(E)\,dE}{E} \qquad [\text{Valid for } A \gg 1]$$

were $\varepsilon = \log E$, $\xi = \overline{\log (E_n/E_{n+1})}$.

It was mentioned that for hydrogen the formula for $\overline{r^2}$ could be worked out exactly.

The result is

$$\overline{r^2}_{E_1} = 2\,\lambda^2(0) + 2\,\lambda^2(a) + 2\int_0^a \lambda^2(x)\,dx + 2\,\lambda(0) \int_0^a \lambda(x)\, e^{-\frac{x}{2}}\,dx + 2\,\lambda(0)\,\lambda(a)\, e^{-\frac{a}{2}}$$

$$+ 2\,\lambda(a) \int_0^a \lambda(x)\, e^{-\frac{a-x}{2}}\,dx + 2 \int_0^a \lambda(u)\,du \int_0^{a-u} \lambda(u+x)\, e^{-\frac{x}{2}}\,dx$$

where

$$x \equiv \log \frac{E_0}{E} \qquad a = \log \frac{E_0}{E_1}.$$

From about 1 volt (chemical binding forces no longer play a part) to $\sim$ 10 kv, σ for neutron in hydrogen is fairly constant. For slowing down in this region, it can be shown that (because λ is fairly constant).

$$\overline{r^2}_{E_1} = f(E_0) - 6\lambda^2 \log E_1.$$

This is derived from the complete formula for slowing down in hydrogen.

Using Ra + Be as a neutron source in a tank of water, we find the following data experimentally.

Slowing to Rh resonance ($\sim$ 1 volt) $\quad \overline{r^2} = 276.6$ cm^2

Slowing to I resonance ($\sim$ 50 volt) $\quad \overline{r^2} = 262.2$ cm^2.

Using the formula for $\overline{r^2}_{E_1}$ that holds from 1 ev to $\sim$ 10 kv and subtracting r^2 of I from that of the Rh resonance neutrons

$$\overline{r^2}\,(\mathrm{Rh}) - \overline{r^2}\,(\mathrm{I}) = 6\lambda^2 \log \frac{50}{1} = 14.4\ \mathrm{cm}^2.$$

Since log 50 is $\sim$ 3.9, this implies that $\lambda = 0.61$. In this way, one can get the mean free path in water at energies from 1 to about 10 KV. This is an average mean free path and compares well with actual appropriate averages of differential data.

Homework:

r	0	1	2	3	4	5	6	7	8	9	10
A (Rh)	1000	960	890	710	630	500	390	290	210	150	110
r	11	12	13	14	15	16	17	18	19	20	
A (Rh)	88	67	57	39	29	23	19	16	12	10	

r = Distance from point source in cm.

A = Activity Induced in detector.

From this data calculate $\overline{r^2}$. You might have to extrapolate grater distances. This is best done by using the last 5 or 6 points on a semilog plot.

(4) *Distribution of Neutrons from a Point Source—The Age Equation.*

In the last section we have discussed one description of the space distribution of neutrons in a tank. Namely $\overline{r^2}$. We shall here discuss another. Call $\varepsilon = \log E$ once again and assume that neutrons are fed into a system at energy E_0 within a certain region. We shall be interested in the space distribution of neutrons of various energies. Accordingly define a neutron density $n(x, y, z, \varepsilon)\,d\varepsilon$ which is the number of neuts per unit volume at x, y, z in energy range ε to $\varepsilon + d\varepsilon$. Consider a volume element (fig. 51) and the neutrons in it in the given energy range. Per unit time this volume will receive neuts in this range from two sources. First from diffusion of neuts of this energy from other volumes. Second, from the degradation of neutrons of higher energy. Consider first the diffusion. From kinetic theory the diffusion ceofficient is:

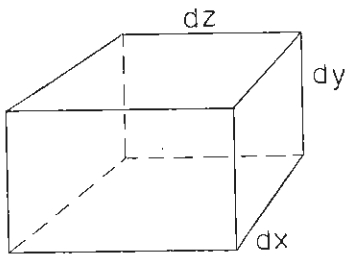

Fig. 51. – Figure for the diffusion equation.

$$D = \frac{\lambda v}{3\,(1 - \overline{\cos\beta})}\ (*) \qquad \left(\text{where we recall that } \overline{\cos\beta} = \frac{2}{3A}\right)$$

and is used as follows. Consider the face $dz\,dy$ of our volume element. The net number of neutrons in the energy range $d\varepsilon$ diffusing out across this face is

$$d\varepsilon \cdot D \left(\frac{\partial n}{\partial x}\right) dy\,dz \qquad \text{per unit time.}$$

(*) $\dfrac{\lambda}{1 - \overline{\cos\beta}}$ is called the transport mean free path.

The number of neutrons diffusing in across the opposite face is:

$$d\varepsilon \cdot \mathrm{D}\left(\frac{\partial n}{\partial x} + \frac{\partial^2 n}{\partial x^2} dx\right) dy\, dz .$$

The net number entering the volume across this opposite pair of faces is:

$$d\varepsilon \cdot \mathrm{D} \frac{\partial^2 n}{\partial x^2} dx\, dy\, dz$$

and the total number of neuts in the energy range $d\varepsilon$ diffusing into the volume per unit time is:

$$\mathrm{D}\Delta n\, d\varepsilon \qquad \text{per unit volume.}$$

Next consider the other source of neutrons in the energy range $d\varepsilon$ at ε. Since v/λ would be the number of collisions of a neutron in unit time, $\xi \frac{v}{\lambda}$ gives the degradation of ε in unit time. Consider the interval ε to $\varepsilon + d\varepsilon$ on an

Fig. 52. – $\xi \frac{v}{\lambda}$ is the velocity with which a neutron proceeds down the axis.

ε axis (fig. 52). At ε the number of neutrons per unit volume moving out of the range in question in unit time is:

$$\xi \frac{v(\varepsilon)}{\lambda(\varepsilon)} n(\varepsilon) .$$

Similarly per unit volume per unit time

$$\left[\frac{v(\varepsilon)}{\lambda(\varepsilon)} n(\varepsilon)\, \xi + d\varepsilon \frac{\partial}{\partial \varepsilon}\left(\frac{vn}{\lambda}\xi\right)\right]$$

neutrons enter the energy range in question at $\varepsilon + d\varepsilon$.

In the stationary state there is no net change in n at any point. Hence considering both "sources" of neutrons:

$$\mathrm{D}\Delta n + \frac{\partial}{\partial \varepsilon}\left(\xi \frac{vn}{\lambda}\right) = 0 \qquad \text{where} \quad \mathrm{D} = \frac{\lambda v}{3\left(1 - \frac{2}{3A}\right)} .$$

This is then the slowing down differential equation for the steady state. It is often more convenient to deal with

$$\xi \frac{vn}{\lambda} \equiv q$$

the so-called slowing down density rather than with n itself. The reason for this name for q follows from the fact that, as was noticed, $\xi \frac{v}{\lambda}$ is the velocity of a neutron along the ε axis. $n\xi \frac{v}{\lambda}$ is then the number of neuts per unit volume per unit time crossing any value ε on the ε axis. In the steady

state and in the absence of capture, if q is integrated over all space, the number of neuts crossing any energy value ε per unit time is certainly the number of neutrons fed into the system in unit time, a constant; i.e., $\int q(\varepsilon)\, dx\, dy\, dz =$ constant for all ε. Thus q is in some sense a simpler quantity than n. This is indicated somewhat by the differential equation we get if we write our differential equation in terms of q rather than n

$$\frac{\lambda^2(\varepsilon)}{3\xi\left(1-\frac{2}{3A}\right)}\Delta q + \frac{\partial q}{\partial \varepsilon} = 0.$$

Here the differential operators operate on q only—no longer on $\lambda(\varepsilon)$, v, etc. In addition to trasforming the dependent variable, let us transform the independent variable ε according to

$$\tau \equiv \frac{1}{3\xi\left(1-\frac{2}{3A}\right)} \int_{\varepsilon}^{\varepsilon_0} \lambda^2(\eta)\, d\eta \qquad \text{where}$$

τ is called the "age". It has dimensions (length)^2

Then $\frac{\partial q}{\partial \varepsilon} = \frac{\partial q}{\partial \tau}\frac{\partial \tau}{\partial \varepsilon} = -\frac{\partial q}{\partial \tau}\frac{1}{3\xi\left(1-\frac{2}{3A}\right)}\lambda^2(\varepsilon)$ whence

$\Delta q = \frac{\partial q}{\partial \tau}$, a simple and well known classical equation (recall heat conduction).

Why τ is called "Age"? The heat conduction equation is $\Delta T = \frac{c\rho}{K}\frac{\partial T}{\partial t}$ and τ is seen to correspond to t, the time in this equation. Perhaps a better reason for the name is that "at birth" the neutron has energy ε_0. As time goes on ε goes down and the integral τ increases as the "time since birth" or the "age" of the neutron increases.

Homework: Consider a substance where λ = constant. What is, in this case, the relation between τ and the actual "time from birth"?

To use our age differential equation we must specify boundary conditions. Let us do the point source problem to begin with. Given a point source of neutrons of energy E_0 in an infinite medium (this corresponds somewhat to a large graphite block with a Ra + Be source in the middle), what is n as a function of ε and position? We first solve the equation for q. (Let us borrow the corresponding solution of the heat equation, which is rather well-known)

$$q = \frac{Q}{(4\pi)^{3/2}\tau^{3/2}} e^{-\frac{r^2}{4\tau}}.$$

The solution is a Gaussian function of r. Q is the number of neutrons of energy E_0 introduced into the system in unit time, i.e. the source strength. The solution clearly shows that as E decreases from E_0 (i.e. as τ increases) the space distribution for the energy E gets broader and broader (fig. 53). This is as it should be. Fast neutrons are distributed close to the source. Slow neutrons are considerably spread out.

It was mentioned before that q has the property that $\int q\,dx\,dy\,dz = \text{const.}$ Let us check this with our particular solution:

$$4\pi\int_0^\infty q r^2\,dr = \frac{4\pi Q}{(4\pi\tau)^{3/2}}\int_0^\infty e^{-\frac{r^2}{4\tau}} r^2\,dr = Q, \text{ a constant since } \int_0^\infty e^{-\alpha x^2} x^2\,dx = \frac{\sqrt{\pi}}{4\alpha^{3/2}}.$$

This establishes that Q is truly the source strength as we have asserted.

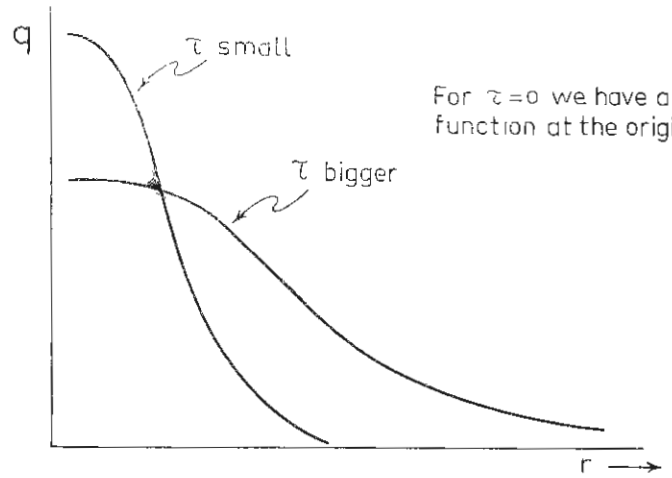

Fig. 53. – Gaussian curve.

It migth be remarked that this Gaussian distribution for q of a particular τ could have been arrived at without the detailed calculation. Let us consider n instead of q (the space distribution of q and n for the same τ is the same except for a multiplying function of τ). The spatial distribution of n can be arrived at somewhat as follows. Consider the x axis with the source at the origin. We are interested in the distribution n as a function of x for a particular τ. A particular τ means a particular number of collisions since birth, or a particular number of path lengths travelled. If the number of paths is a large number and all mean free paths are small compared to the total distance travelled (and such is the case) then we can use a theorem in the study of large numbers which says that "If one sums a large number of numbers which are equally likely positive and negative, and whose magnitudes are all less, by far, than the sum of their magnitudes, one finds that the values of these sums (always taken for the same number of small numbers) distribute on a Gaussian curve provided no additional information is known about the numbers summed". (This theorem, incidentally can be used to show why repeated measurements of some physical quantity like a length fall on a Gaussian curve, provided that the errors are what we call random). In our case the theorem implies that $n_x \sim e^{-\frac{x^2}{k}}$ where k is some measure of the width of the distribution. Similarly for the y and z directions. Hence $n = n(x, y, z)$ goes as $e^{-\frac{r^2}{k}}$.

CHAPTER VII

THE DISTRIBUTION OF SLOW NEUTRONS IN A MEDIUM.

(1) *The Differential Equation for Slow Neutrons.*

To find the distribution of neutrons of various energies in a medium, one usually deals with two separate problems. First there is the slowing down problem, and this was dealt with in the last chapter. But the neutrons do not continue to get slowed down indefinitely, for the nuclei they collide with are not at rest, but have vibrational energies corresponding to their temperature. The neutrons eventually come into thermal equilibrium with these nuclei, and show a Maxwellian distribution corresponding to the temperature of the medium. Clearly the problem of the distribution of these slowed down or thermal neutrons is quite distinct from that of the distributions of the neutrons being slowed down and must be handled by separate methods.

In approaching this second problem we ask: "Given a source of thermal neuts, what can be said about their distribution in a medium in a stationary state?" We seek a differential equation as our description. Let $n\,(x\,,y\,,z)$ be the density of thermal neuts at $x\,,y,\,z$. Consider a unit volume. There are 3 mechanisms by which the number of neutrons in this volume changes with time. First the diffusion. This gives a net contribution to $\partial n/\partial t$ which is $\mathrm{D}\Delta n$. Second some neutrons are captured or absorbed [2]. This number will be proportional to n. We write $-\frac{n}{\theta}$. Lastly we have those neutrons generated in the volume by the slowing down to thermal of fast neutrons. This term is q_{T}, the value of q at this place for τ corresponding to thermal energies. Thus the desired differential equation is

$$\mathrm{D}\,\Delta n - \frac{n}{\theta} + q_{\mathrm{T}} = \frac{\partial n}{\partial t}\,.$$

In the steady state $\frac{\partial n}{\partial t} = 0$. Here we must put in the proper space dependence of q_{T} as determined from the age equation before we attempt to solve this equation under the proper boundary condition. Recalling that $\mathrm{D} = \frac{\lambda v}{3}$ the equation can be written

$$\Delta n - \frac{3\,n}{\lambda v \theta} + \frac{3\,q_{\mathrm{T}}}{\lambda v} = 0 \quad \text{or} \quad \Delta n - \frac{n}{l^2} + \frac{3\,q_{\mathrm{T}}}{\lambda v} = 0$$

for the steady state. Here $l = \sqrt{\frac{\lambda v \theta}{3}}$ and is called "the diffusion length." $v\theta$ is often written A and is the capture mean free path.

(2) This term should perhaps also have been considered in the slowing down process. But whereas orders of magnitude are such that in the slowing down, the consideration of absorption is usually a refinement, here it is a necessity.

For a point source of slow neutrons, the solution is $n = A\frac{e^{-r/l}}{r}$ where A is a normalization coefficient. For a point source, the last term in the equation is zero everywhere in space (except that we have a delta–function source at the origin). In order to evaluate A, consider a small sphere drawn about the source, which we assume emits one slow neutron each second. Then for $r \ll l$, $n \cong \frac{A}{r}$ and the flux through the sphere is $D \times 4\pi r^2 \times \text{grad}\,(A/r)$ which must be equal to one. Since $D = \frac{\lambda v}{3}$ this gives $A = \frac{3}{4\pi\lambda v}$. One can check the now complete solution of the homogeneous equation

$$n = \frac{3}{4\pi\lambda v}\frac{e^{-r/l}}{r}.$$

(The name " diffusion length " for l stems from its role in this expression) by substituting into

$$\left(\frac{\partial^2}{\partial r^2} + \frac{2}{r}\frac{\partial}{\partial r}\right)n - \frac{3n}{\lambda v\theta} \quad \left(\text{recalling } l^2 = \frac{\lambda v\theta}{3}\right).$$

This should, of course, be zero, and it is. The point source solution is particularly important because any source can be represented by a proper assembly of point sources and the corresponding solution would be a superposition of these point source solutions.

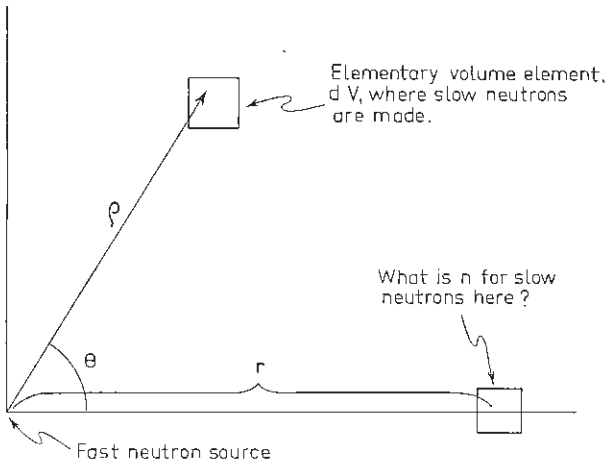

Fig. 54.

To solve this equation for a point source of fast neutrons, one can set up an integral over a distribution of slow neutron point sources all over space that arises from the slowing down of the fast neutrons. We ask " What is the density of slow neuts at a distance r from the point source of fast neutrons? " (fig. 54). At any point there arc q_T point sources of slow neutrons per unit volume where $q_T = \frac{Q}{(4\pi\tau)^{3/2}}e^{-\varrho^2/4\tau}$ where τ corresponds to thermal neuts. But for a point source of slow neutrons at (ρ, θ) the slow neutron density at r is

$$n = \frac{3}{4\pi\lambda v}\frac{e^{-\frac{|\varrho - r|}{l}}}{|\varrho - r|}, \quad \text{where} \quad |\varrho - r| = \sqrt{\rho^2 + r^2 - 2\rho r\cos\theta}\,.$$

Thus the density of slow neutrons at r is given by the integral

$$\int_{\varphi=0}^{2\pi}\int_{\varrho=0}^{\infty}\int_{\theta=0}^{\pi}\frac{Q}{(4\pi\tau)^{3/2}}\,e^{-\varrho^2/4\tau}\,\frac{3}{4\pi\lambda v}\,\frac{e^{-|\varrho-r|/l}}{|\varrho-r|}\,d\varrho\,\varrho^2\sin\theta\,d\theta\,d\varphi\,.$$

(2) *The Boundary Conditions for the Differential Equation.*

In order to solve the slow neutron differential equation, one must know how n or some function of n behaves at the spatial boundaries. Consider a finite convex medium with a neutron source in it and free space everywhere around it. What can be said of q or n at the bounding surface? To a first approximation one can take q or n equal to zero. This is made somewhat plausible by the argument that free space acts as a perfect sink. It absorbs all neutrons and returns none. It therefore acts as so heavy a drain on the neutron density at the boundary that no density can be maintained there.

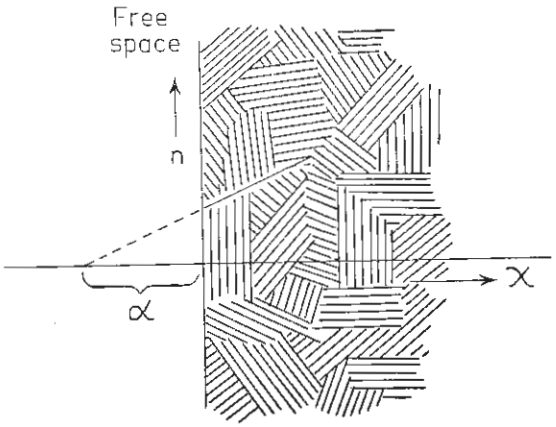

Fig. 55. – Boundary condition. Extrapolated length.

Actually a more refined calculation will show that a more proper boundary condition is the vanishing of n or q at a surface 0.66 λ away from the bounding surface (where λ is the neutron mean free path in the medium). An even more refined argument leads to 0.70 λ as the distance of this outside surface from the true boundary. We shall consider at least the first refinement.

Consider a plane bounding surface (fig. 55). We shall assume that in the neighborhood of the houndary the neutron density n is a linear function of distance, i.e.:

$$n = p\,(\alpha + x)$$

Let us now calculate the neutron flux Φ at the bounding surface. Certainly it is gradient $n \times$ (the diffusion coefficient), i.e.:

$$\Phi = p\cdot\frac{\lambda v}{3} \quad \text{for } p = \frac{dn}{dx} \quad \text{in this problem.}$$

The flux can, however, also be calculated as follows. Consider a unit volume at a distance x from the boundary (fig. 56). There are n (x) neutrons here. The probability that a neutron going off at the angle θ will escape is $e^{-\frac{x}{\cos\theta}\cdot\frac{1}{\lambda}}$. Assuming that neutrons leave this volume in an isotropic fashion, the number of neutrons crossing the boundary per unit time coming from this volume is

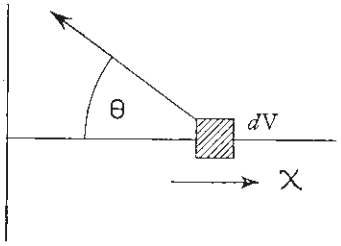

Fig. 56.

$$\frac{1}{2}\int_0^{\pi/2} p\,(\alpha + x)\,\frac{v}{\lambda}\,e^{-\frac{x}{\lambda\cos\theta}}\sin\theta\,d\theta\,dV.$$

Consider that the volume has unit area perpendicular to the x axis and depth dx. Then to integrate the above expression over x, would be to find the total amount of neutrons coming each second to the surface from an infinite column of unit cross sectional area perpendicular to the surface. But this is readly seen to be the flux, or the number of neutrons crossing unit area of the surface per second, provided, of course, that everything can be assumed uniform perpendicular to the x direction. Hence

$$\Phi = 1/2\int_0^{\pi/2}\int_0^{\infty} p\,(\alpha + x)\,\frac{v}{\lambda}\,e^{-\frac{x}{\lambda\cos\theta}}\sin\theta\,d\theta\,dx$$

and writing $\mu = \cos\theta$ this integral is seen to be a rather simple one. The solution gives

$$\Phi = \frac{vp}{2\lambda}\left(\frac{\alpha\lambda}{2} + \frac{\lambda^2}{3}\right).$$

Equating this to our previsious result for Φ we get $\alpha = \frac{2}{3}\lambda$. But α is the x intercept. Therefore we have shown that n vanishes at a distance $\frac{2}{3}\lambda$ outside the bounding surface. This is the boundary condition we sought to derive. It is to be noted that this boundary condition really describes n at the *boundary*. The x intercept is used only to describe this. In particular, the boundary condition does not mean that n vanishes at $x = -\frac{2}{3}\lambda$ and is negative beyond that distance. Our conclusion is simply "The density at a bounding surface behaves as though n is a linear function of x vanishing at $x = -\frac{2}{3}\lambda$".

(3) *The Diffusion Length l.*

In order to be able to use the slow neutron differential equation one must know the value of l. To measure l in the case of water for example, one can use a pile and a tank of water (fig. 57). Neclecting end effects this is essentially a one dimensional problem

$$\frac{\partial^2 n}{\partial x^2} - \frac{1}{l^2}n = 0$$

and the non-diverging solution is $n = Ae^{-x/l}$. One makes measurements with and without cadmium separating the pile and water tank to ascertain (by a subtraction) n for thermals as a function of x in the water. From the data obtained for n we can evaluate l for water. It is ~ 2.8 cm. For paraffin we get a result that shows that the absorbing mechanism in the case of water and paraffin is the same, hydrogen capture (i.e., one need assume no carbon or oxygen absorption to account for the observed l's).

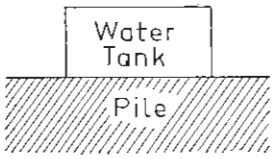

Fig. 57. – Measurement of the diffusion length.

There are other schemes to determine l and related constants for H_2O. Some are described in a paper by Fermi and Amaldi («Phys. Rev.», *50*, 899 (1936)) (*). l shows a temperature dependence and it is sometimes of interest to know this temperature dependence. For water it has been measured and $l = 2.64 + 0.0061$ T (T in degrees centigrade). Since $l^2 = \frac{\lambda\Lambda}{3}$ where Λ is the capture or absorption mean free path and λ is the transport mean free path $\frac{\lambda}{1-\overline{\cos\theta}}$ we can use our information about l and λ to calculate Λ or vice versa.

Homework: Calculate λ from information about l and Λ for water $l = 2.8$ cm and $\Lambda = \frac{1}{\sigma_c n_c}$ where σ_c at 2200 m/sec $= 0.31$b. 2200 m/sec corresponds to v in $(1/2)\,mv^2 = kT$ for room temperature. But if there is a Maxwell distribution $\bar{v} = \frac{2}{\sqrt{\pi}}\,v$, i.e. $\bar{v} = \left(\frac{8\,kT}{\pi m}\right)^{1/2}$ one can simply show that for water at room temperature, we would want σ_c corresponding to $\bar{v}$, not v. Calculate n, Λ and finally λ, the transport mean free path.

For a substance such as graphite, the procedure of last page does not sufficiently represent a one-dimensional problem for us to obtain l by measurement as simply as for water. (l becomes a length of the order of the dimensions of the medium). One must solve the 3 dimensional problem. Consider a block of graphite as that shown in fig. 58, with a fast neutron source placed at $(v, u, 0)$. It can be shown that the solution of the slowing down equation

$$\Delta q - \frac{\partial q}{\partial \tau} = 0$$

is, in this case

$$q = (4/a^2)\,(Q/\sqrt{4\pi\tau})\,e^{-z^2/4\tau} \sum_{r,s=1}^{\infty} e^{-\pi^2\tau(r^2+s^2)/a^2} \sin(\pi s x/a) \sin(\pi r y/a)$$

where Q is the source strength. This solution is obtained by fairly straightforward Fourier methods.

Experimentally it is found that a Ra + Be neutron source has 3 well defined neutron energies. Such a source gives 3 superposed distributions.

(*) Paper N° 118 *b* (Editors note).

	percent	τ Indium Resonance	τ Iodine Resonance
1)	15.0	130 cm²	54 cm²
2)	69.3	340	268
3)	15.7	815	736

This table gives the value of τ for the 3 components in graphite at different energies, and the percent of each component present. Sometimes such data are given in terms of the range r_0 which is equal to $2\sqrt{\tau}$.

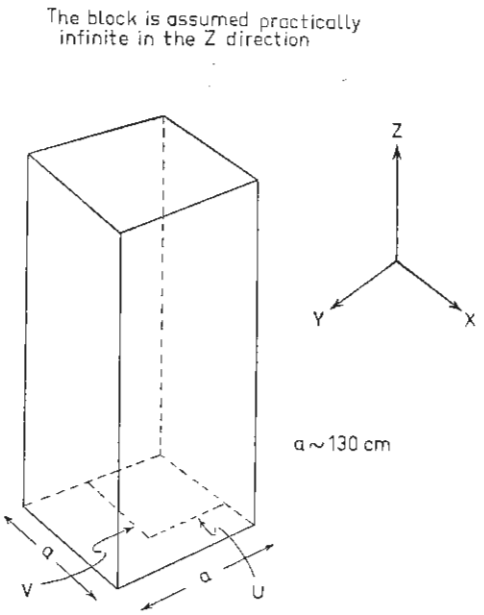

Fig. 58. – Block in which q is calculated.

From the numbers in this table, it is seen that at 30 or so centimeters from the source q becomes very small. Then it will be true that the " source " term in the slow neutron diffusion differential equation will be small. The slow neutron density n, will obey quite closely

$$\Delta n - \frac{1}{l^2} n = 0.$$

At such distances from the source, because of the boundary conditions, one assumes a solution of the form:

$$n = \sum_{r,s=1}^{\infty} n_{rs}(z) \sin\frac{\pi r y}{a} \sin\frac{\pi s x}{a}$$

substituting into the differential equation, we get an equation for $n_{rs}(z)$

$$\frac{d^2 n_{rs}}{dz^2} - \left[\frac{\pi^2}{a^2}(r^2 + s^2) + \frac{1}{l^2}\right] n_{rs} = 0.$$

This is of the form:

$$\frac{d^2 n_{rs}}{dz^2} - \frac{1}{b_{rs}^2} n_{rs} = 0$$

and the solution is well known, $e^{\pm z/b_{rs}}$.

We omit the diverging solutions $e^{+z/b_{rs}}$, so that

$$n = \sum_{r,s=1}^{\infty} e^{-\frac{z}{b_{rs}}} \sin\frac{\pi ry}{a} \sin\frac{\pi sx}{a}$$

where

$$\frac{1}{b_{rs}^2} = \left[\frac{\pi^2}{a^2}(r^2 + s^2) + \frac{1}{l^2}\right].$$

Because for $r, s > 1$ the solution for n is one quickly damped, experimentally it will suffice to compare activation measurements by slow neuts in such a column with the $r = s = 1$ component,

$$n = e^{-z\sqrt{\frac{2\pi^2}{a^2} + \frac{1}{l^2}}} \sin\frac{\pi y}{a} \sin\frac{\pi x}{a}.$$

For a typical graphite sample, we have constants:

$$\rho = 1.551\,\frac{\text{gm}}{\text{cc}} \qquad b_{11} = 28.38 \qquad a = 150.49 \text{ cm}$$

(we must add $2 \times \frac{2}{3}\lambda$ to "a" [end of section (2) this chapter] so that the effective dimension, $a = 150.49 + \frac{4}{3}\lambda$; which happens to be 153.29 cm ($\lambda = 2.1$ cm)). This information and some good measurements will allow us to find l. Since l depends on density, by convention, l for all samples of graphite (graphite is tested by measuring its l in this way) is reduced to the value it would have at $\rho = 1.60$ in order that one may compare different samples of graphite and make statements as to their purity.

Here we briefly record some of the results obtained in this way for 4 common substances.

	ρ	n Atoms/cc	l	l^2/Λ
H_2O	1.0 gm/cc	0.0334×10^{24}	2.85 cm	0.142 cm
D_2O	1.1	0.0331	> 100	0.80
Be	1.8	0.1235	31	0.87
C	1.62	0.0871	50.2	0.903

Actually the 2 microscopic constants in such problems are σ_{scat} and σ_{abs}. For convenience let us list some of the relations between these and the more easily measured constants:

$$\lambda = \frac{1}{\sigma_{scat} \cdot n} \quad ; \quad v\theta = \Lambda = \frac{1}{\sigma_{abs} \cdot n} \quad ; \quad l^2 = \frac{\lambda\Lambda}{3} \quad ; \quad N = \frac{\sigma_{scat}}{\sigma_{abs}} \frac{3l^2}{\lambda^2} = \frac{\Lambda}{\lambda}$$

where n is the number of atoms/cm^3 and where N is the average number of scattering collisions made per capture.

(4) *The Albedo, or the Reflection Properties of Bounding Surfaces for Neutrons.*

We have so far in this chapter outlined the methods of obtaining neutron distributions in media due to sources within them. However, neutrons are often introduced into a medium from the outside. It is convenient to define a reflectivity, or as it is called, albedo (whiteness in Latin) for a surface. It is simply the fraction of the incident neutrons eventually returned or " reflected " from the surface. An albedo of one means perfect reflection; an albedo of zero means perfect (black body) absorption. See Fermi's paper on the motions of neutrons in hydrogeneous substances: *Sul moto dei neutroni nelle sostanze idrogenate* in « Ric. Sci. » 7, 13 (1936) (*).

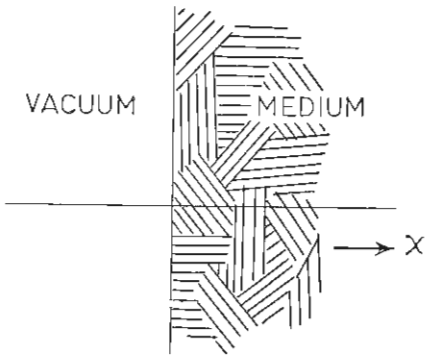

Fig. 59. – Albedo.

Let us solve a typical problem. We shall calculate the albedo of an infinite plane surface for slow neutrons. But first it shall be necessary to solve the following problem. " Given a medium bounded at $x = 0$ (fig. 59) and occupying all of space to the right of this plane, what is the probability that a slow neutron starting at a point d units distant from $x = 0$ will escape from the medium, i.e. will reach $x = 0$? "

We shall do this problem twice, using two very different approaches. First we shall use the slow neutron diffusion equation and assume that the problem is one dimensional, i.e., that the neutrons move only in the x–direction.

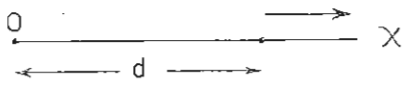

Fig. 60.

Assume a point source of neutrons at d on the x axis (fig. 60). We must calculate the flux at the origin for unit source strength (for this is precisely the escape probability). The slow neutron diffusion equation is in this case:

$$\Delta n - \frac{n}{l^2} = 0$$

(everywhere but at $x = d$) and since this is a one dimensional problem the solution is:

$$n = Ae^{-\frac{x}{l}} - Ae^{\frac{x}{l}}$$

for $0 < x < d$, assuming the boundary condition $n(0) = 0$. For $x > d$, $n = Be^{-x/l}$. These two solutions must join at d (fig. 61) so that n is continuous and the gradient dn/dx has a finite discontinuity. To find the amount of this discontinuity, integrate the complete diffusion equation throughout a small

(*) [See paper N° 119. (Editors' note)].

" volume " surrounding the source:

$$\int_{d-\varepsilon}^{d+\varepsilon} \frac{d^2 n}{dx^2} dx - \int_{d-\varepsilon}^{d+\varepsilon} \frac{n}{l^2} dx = -\int_{d-\varepsilon}^{d+\varepsilon} \frac{q}{D} dx \qquad \text{(Section (1) this chapter).}$$

The first term is $\frac{dn}{dx}\Big|_{d-\varepsilon}^{d+\varepsilon}$, the discontinuity in dn/dx. The second term vanishes as $\varepsilon \to 0$ for n must for physical reasons be a continuous function of x. The last term is simply $-Q/D$ where Q is the source strength. Thus the conditions on n and dn/dx at d are:

$$Ae^{-\frac{d}{l}} - Ae^{+\frac{d}{l}} = Be^{-\frac{d}{l}}$$

$$-\frac{A}{l} e^{-\frac{d}{l}} - \frac{A}{l} e^{\frac{d}{l}} = -\frac{B}{l} e^{-\frac{d}{l}} + \frac{Q}{D}$$

$$\text{whence} \quad A = -\frac{lQ}{2D} e^{-\frac{d}{l}} \quad , \quad B = \frac{lQ}{2D}\left(e^{\frac{d}{l}} - e^{-\frac{d}{l}}\right).$$

The flux at $x = 0$ is then $D \cdot \left(\frac{dn}{dx}\right)_{x=0} = Qe^{-\frac{d}{l}}$, and for unit source strength it is simply $e^{-\frac{d}{l}}$. This gives the probability, $p(d)$ that a slow neutron at d will eventually escape from the medium.

Before we use this result to find the albedo of such a one-dimensional medium for neutrons incident on the boundary from the outside, let us redo the problem in another way. In addition to the methods of diffusion, there is a more exact, more rigorous way to attack problems of the type being discussed. To find the neutron density in a particular volume V at a time t, one could investigate the density of neutrons that are moving toward V and are in other volumes at various earlier times t' so that (considering their velocities and distances from V) they would be in V at the time t. The neutron density at V at the time t, could be expressed as some sort of sum or integral of these other neutron densities. We would be led to an integral equation in the neutron density n.

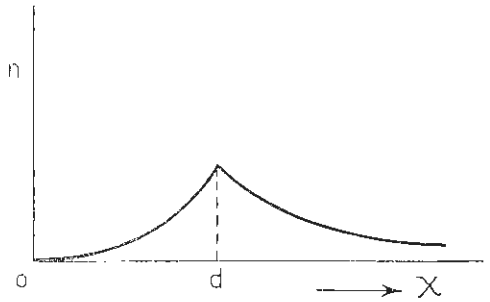

Fig. 61. – Joining of the solutions.

Thus in addition to the differential equation method of solving diffusion problems, there is an integral equation method too. It would be well to stop a moment and compare the relative merits of the two approaches. In setting up the diffusion differential equation it had to be assumed that the quantities like n, $\frac{dn}{dx}$ etc. vary slowly with respect to the mean free path of the diffusing particles. Further it was assumed that densities of particles were large enough so that speaking of quantities like dn/dx made sense. In particular

one would not expect that the solution of a problem like the following by diffusion methods would give physically true results : " Find $n(r, \theta, \varphi)$, the density of slow neutrons in a sphere of radius $\lambda/2$, if there is a point slow neutron source at the center of the sphere. (λ is the mean free path of slow neutrons in the medium of the sphere)." There are, however, no such restrictions on the use of integral equation methods. No assumptions about the variation of dn/dx with distance, etc., need be made. Integral equation methods are more general. However, they are usually more difficult. It often becomes expedient to do the diffusion problems by means of the differential equation and proper boundary conditions first in order to get a rough idea about the function in question. Then one gets the more exact solution by means of an integral equation. This is the procedure we shall follow here. We have obtained $p(d)$ the probability that a neutron d units from the boundary of a one dimensional medium will escape from it, by means of the diffusion differential equation. Let us now apply integral methods.

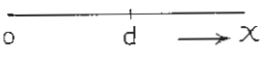

Fig. 62.

Consider a neutron at d (fig. 62). As it leaves d, one of two things may occur. It may go to the left or it may go to the right, each with a 50 percent chance. If it goes to the left, it may escape before it suffers a collision or it may collide. The probability that a neutron at d will escape without a collision is therefore the product

$$\frac{1}{2} \times e^{-\frac{d}{\lambda}}$$

where λ is the total mean free path. However a neutron may escape even if it suffers a collision Say the neutron suffers its first collision at x, and that $\Pi(x)$ is the probability that a neutron from d suffers its first collision at x (either to the right or left of d). $p(x)$ is the probability that a neutron at x will eventually escape. Clearly then, $p(d)$ can be written as some sort of sum or integral

$$p(d) = \frac{1}{2} \cdot e^{-\frac{d}{\lambda}} + \sum_{\text{all } x} \Pi(x)\, p(x)$$

where it is assumed that there is isotropic scattering in the lab system, i.e., that $p(x)$ depends only on x and not on the side from which the neutron arrives at x. In detail the sum should be written:

$$\left.\begin{aligned} &\frac{1}{2}\int_0^d e^{-\frac{d-x}{\lambda}} \frac{dx}{\lambda}\, p(x) \frac{N-1}{N} \\ &+ \frac{1}{2}\int_d^\infty e^{-\frac{x-d}{\lambda}} \frac{dx}{\lambda}\, p(x) \frac{N-1}{N} \end{aligned}\right\}$$

where the first integral gives the probability that a neutron starting from d will go left, suffer a collision at x, but will eventually escape.

The second integral gives the probability for the same thing with initial motion to the right.

The factor $\frac{N-1}{N}$ appearing in these integrals gives the probability that the collision at x is a scattering collision. There are N scattering collisions

per absorbing collision. Thus the integral equation is:

$$p(d) = \frac{1}{2} e^{-\frac{d}{\lambda}} + \frac{1}{2} \int_0^\infty e^{-\frac{|x-d|}{\lambda}} \frac{dx}{\lambda} p(x) \frac{N-1}{N} .$$

The solution of the differential equation gave $p(d) = e^{-d/l}$. Let us therefore try $p(d) = Ae^{-ad}$ as the solution of this integral equation. So doing, we find:

$$p(d) = \frac{\sqrt{N}}{\sqrt{N}+1} e^{-\frac{d}{\lambda\sqrt{N}}}$$

($\lambda\sqrt{N}$ is $\sqrt{3}\,l$; see end of Section (3), this chapter). Thus this solution goes as $e^{-\frac{d}{\sqrt{3}\,l}}$ rather than as the differential equation solution $e^{-d/l}$.

We are now in a position to do what we originally set out to do—to find the albedo. Say a beam of slow neutrons moving along the x axis from the left hits the plane $x = 0$. The probability that a neutron of the beam will make its first collision in dx at x is $e^{-\frac{x}{\lambda}} \frac{dx}{\lambda}$. The probability of not being absorbed and escaping from here is $p(x)\frac{N-1}{N}$. Hence the albedo is:

$$\beta = \int_0^\infty e^{-\frac{x}{\lambda}} \frac{dx}{\lambda} p(x) \frac{N-1}{N} = \frac{\sqrt{N}-1}{\sqrt{N}+1} .$$

A non-absorbing medium would eventually return all neutrons and have an albedo of 1.

If we wish to know β for an angle of incidence θ, we are forced to drop the one-dimensional attack and the problem becomes more difficult. The result is that

$$\beta(\theta) = \frac{\sqrt{N}-1}{\sqrt{N}+\sqrt{3}\cos\theta} .$$

This is inconsistent with first result ($\theta = 0$) only because this solution allows for the fact that although $\theta = 0$ for the incident neutrons, they are not restricted to move along the x axis in the medium. The effect of allowing motion at angles to the x axis is to allow longer paths and hence more change for absorption. This makes β slightly smaller.

Suppose we wish to measure the albedo for slow neutrons on paraffin. A direct measurement would be difficult, for even if a collimated slow neutron beam can be made to impinge on some paraffin, neutrons would be coming off at all angles from all over the surface of the paraffin and their detection would be no easy matter. A much neater way of finding the albedo is the following. Place a thin foil slow neutron detector somewhere in the middle of a mass of paraffin whose boundaries are far enough away from the foil that the paraffin can be considered infinite in extent (fig. 63). (By a thin foil is meant one where there is little modification of the neutron distribution due to the presence of the foil, i.e., one for which $\sigma n \delta \ll 1$), where σ is the atomic cross-section, n the number of atoms/cc and δ the thickness of the foil). By means of some neutron source we induce an activity in the foil.

Call this activity A. Next back the foil on one side with some cadmium (enough so that it can be assumed that the cadmium absorbs practically all the slow neutrons hitting it, but not enough to distort the neutron flux

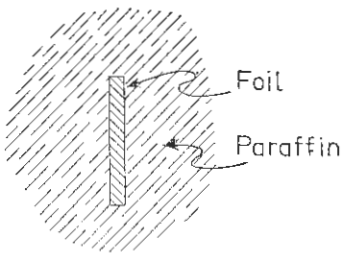

Fig. 63. – Measurement of the Albedo.

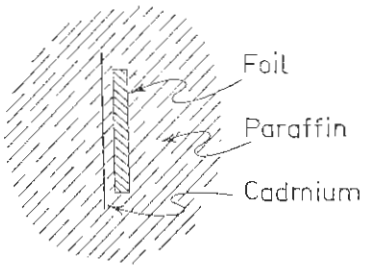

Fig. 64 – Measurement of the Albedo.

field appreciably) (fig. 64). Remeasure the activity in the detector foil. Call this activity B. Now the ratio A/B bears a simple relation to the albedo. To see how this comes about, consider the number of neutrons N hitting the foil each second in situation B. It is clear that for a uniform distribution of slow neutrons, the foil in case A would have N neutrons per second hitting from each side, and would have at least 2 N slow neutrons hitting it per second. But that is not all, for some of the neutrons passing through the foil can return and pass through it again (for there is no cadmium about to prevent this) (fig. 65). In fact we can calculate the average number of times a neutron about to impinge on the foil will pass through it before it is eventually absorbed in the paraffin. Certainly the probability that this neutron will return through the foil is β, the albedo of the paraffin for slow neutrons. The probability that it will make at least two trips is $\beta \times \beta$ or β^2 and so on. Thus the total number of passages through the foil for a neutron is on the average:

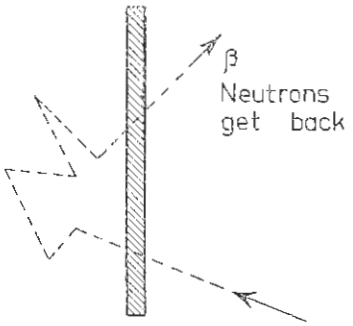

Fig. 65.

$$1 + \beta + \beta^2 + \beta^3 + \cdots = \frac{1}{1-\beta}.$$

Hence there would be $\frac{2N}{1-\beta}$ slow neutrons hitting the foil each second, rather than simply 2N neutrons. From this it follow that $\frac{A}{B} = \frac{2N}{(1-\beta)\overline{N}}$. Hence a measurement of the two activites A and B suffices to let us calculate the albedo. For paraffin A/B is 11. This makes $\beta = 0.82$. This type of measurement would not be feasible with poor absorbers of neutrons for it has to be assumed that the diffusion length in the medium is small compared to the foil size, i.e., that most of the "reflection" takes place close to the foil. Further, if the detector is not thin it acts as its own cadmium, so to speak, and a correction must be made for the absorption in the foil.

Homework: If ζ is the average fraction (averaged over angles of incidence) of incident neutrons absorbed in the foil, find the relation between A/B and the albedo.

CHAPTER VIII

NUCLEAR FISSION.

(1) *The Binding Energies of Nuclei.*

Before we proceed to take up the subject of fission, it is necessary to get some understanding of what it is that holds nuclei together. For this purpose we should like to find an expression for the nuclear binding energy [or the nuclear mass—since mass and binding energy are related through

nuclear mass = (number of neutrons × neutron mass) + (number of protons × proton mass) — binding energy]

in terms of the general nuclear parameters, A and Z. A is the number of particles in the nucleus and Z the number of protons; (A — Z) is therefore the number of neutrons.

In the absence of exact knowledge concerning the nuclear force, the problem of finding the dependence on binding energy on Z and A is a difficult one. We must examine our empirical knowledge about nuclei for implications concerning the nuclear forces or the binding energy.

(A) The sizes of nuclei and the binding energy: From scattering and other experiments with heavy nuclei it is found that nuclear radii go as $A^{1/3}$. In fact:

$$R = 1.48 \times 10^{-13} A^{1/3} \text{ cm}$$

fairly well fits the known data. (It should be remarked that this formula does not mean very much if applied to the very lightest nuclei). For our purposes the formula implies that the average density of constituent particles is about the same in all nuclei. It is quite likely that the density within a single nucleus does not vary much from one region within the nucleus to another. If a certain binding energy due to nuclear forces is to be associated with two nuclear particles within the nucleus a given distance apart, it is clear from the foregoing that this binding energy per unit volume of nucleus is constant inasmuch as the average distances between constituent particles is everywhere the same. We conclude, therefore, that the binding energy of nuclei is essentially proportional to their volume or to A. In terms of the energy of a nucleus (the negative of the binding energy) we have then $E \sim -a_1 A$ where a_1 is some positive coefficient which these considerations have not sufficed to determine.

(B) The surface of the nucleus and the binding energy: We know that the above discussion is not the whole story. For example, even if it is assumed that nuclear constituents are everywhere spaced the same distance apart and are subject to equal forces everywhere, it is clear that an exception must be made of the particles at the surface. They are not surrounded by as many particles and are therefore not bound as strongly as particles

inside a nucleus. The number of such particles is proportional to the surface, and we must subtract a number proportional to them from our previously discussed binding energy, for we see now that we have somewhat overestimated the binding energy. Since surface area goes as R^2 we must add to E a factor $a_2 A^{2/3}$. Thus $E = -a_1 A + a_2 A^{2/3}$.

(C) The fact that Z tends to be A/2 and its relation to the binding energy: In addition to the foregoing, we have other bits of information about nuclei that have certain implications about how E must depend on Z and A. Let us investigate these relations and incorporate them into our expression for E as correction terms. For example, it is found that the number of protons and that of neutrons in any nucleus are very nearly the same. (It is true that for heavy nuclei there are less protons than neutrons, but we shall assume that this is due to the electrostatic repulsion between protons which we shall consider next. That is, we assume that if it were not for the Coulomb forces between protons, there would be equal numbers of protons and neutrons in nuclei). There are at least 3 types of nuclear forces within a nucleus; neutron-proton proton-proton, neutron-neutron. In view of the equality of the number of protons and neutrons in nuclei, the last two types of forces must be of the same order of magnitude. For were the proton-proton forces stronger, nuclei with more protons than neutrons would tend to be more strongly bound and hence more stable than those with equal numbers of each. If the energy E of isobars (same A, different Z) were plotted against Z (fig. 66), we should get a curve symmetric about $Z = A/2$, for nuclei with Z protons and $(A - Z)$ neutrons would have the same E as those with Z neutrons and $(A - Z)$ protons since neutron-neutron and proton-proton forces are assumed equal. The curve as drawn shows a minimum at $Z = A/2$ since nuclei for which $Z = A/2$ are the most stable. Thus E_3, the energy associated with the departure from equality in the number of protons and neutrons, must go as some even power of $[Z - (A/2)]$. For simplicity consider that in the neighborhood of A/2, E_3 goes as $[Z - (A/2)]^2$. To see what the dimension of the coefficient should be, consider two nuclei with the same value for Z/A, one having an A twice the other. (Thus both nuclei have the same fractional excess of neutrons over protons, but one has twice as many particles). The larger nucleus will have twice the E_3 if we associate with each extra or unpaired particle a certain fixed energy. It appears, therefore, that E_3 should be proportional to A. We write:

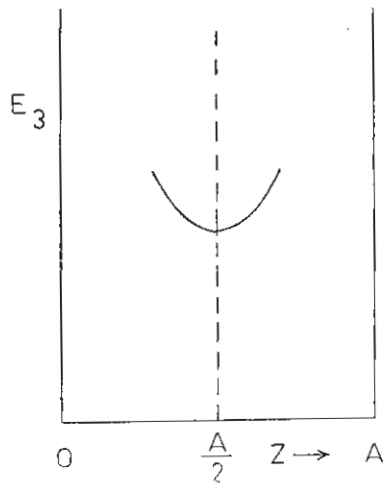

Fig. 66. – Nuclei tend to have $Z = A/2$.

$$E_3 = + a_3 A\left(\frac{Z}{A} - \frac{1}{2}\right)^2 \quad \text{or} \quad a_3 \frac{\left(\frac{A}{2} - Z\right)^2}{A}.$$

(D) The Coulomb forces between protons and the binding energy: The problem of finding the energy, E_4, due to the electrostatic forces between the protons can be approximated by the solution of the following straightforward electrostatic problem, " What is the energy of a charge Z uniformly distributed throughout a sphere of radius R? " The result is

$$\frac{3}{5}\frac{Z^2}{R}$$

written with a proper coefficient so that the energy is m mass units

$$E_4 = + 0.000627\frac{Z^2}{A^{1/3}}.$$

(E) Even or odd numbers of protons and neutrons and the binding energy: It is found empirically that there are very few stable nuclei with even atomic weight A and odd atomic number Z. In fact it can be said that the most stable tend to have both Z and (A — Z) even. Slightly less stability occurs in the cases Z–odd, (A — Z) even and Z even, (A — Z) odd. And, as we have said Z–odd, (A — Z) odd is the least stable arrangement for a nucleus. Clearly, forces between nuclear constituents must therefore show a dependence on whether an even or odd number of neutrons and protons are about, and so must the binding energy. Some sort of explanation has been advanced based on the idea that constituents tend to fill the nucleus' lowest energy levels and that strong forces exist between the pairs of neutrons or protons that can fill the same level. It has been empirically determined that $E_5 = \delta$ can be assigned as a correction term to our expression for E on the following basis:

$$\delta = \begin{cases} \text{A odd} & 0 \\ \text{A even} \begin{cases} \text{Z even} & -\left(\dfrac{0.036}{A^{3/4}}\right) \\ \text{Z odd} & +\left(\dfrac{0.036}{A^{3/4}}\right) \end{cases} \end{cases}.$$

We must now evaluate the coefficient a_1, a_2, a_3 in our complete expression:

$$M(A, Z) = 1.00893\,A - 0.00081\,Z - a_1 A + a_2 A^{2/3} + a_3\frac{\left(\frac{A}{2} - Z\right)^2}{A} + 0.000627\frac{Z^2}{A^{1/3}} + \delta.$$

To find a_3 get dM/dZ and set this equal to zero. The resulting equation between Z and A is

$$Z_A = \frac{0.00081 + a_3}{2a_3 + 0.001254\,A^{2/3}}\cdot A$$

is one for which M is a minimum and therefore gives the stablest values of Z for any A. Fitting this equation to the known stable isotopes gives one a best value for a_3. It is 0.083. One determines a_1 and a_2 by fitting the equation for M (A, Z) to the known data for nuclear masses. The result is that $a_2 = 0.014$ and $a_1 = 0.00504$. Hence

$$M(A, Z) = 0.99389\,A - 0.00081\,Z + 0.014\,A^{2/3} + 0.083\frac{\left(\frac{A}{2} - Z\right)^2}{A} + 0.000627\frac{Z^2}{A^{1/3}} + \delta.$$

Homework: This makes $Z_A = \frac{A}{1.981 + 0.015\,A^{2/3}}$. Compare this with the known stable isotopes; try picking ~ 10 of them and plotting a graph. Dempster in the « Physical Review », *53*, 870 (1938) gives a curve of packing fraction, $\frac{M(A,Z) - A}{A}$, vs. A. Using the above equation, plot the packing fraction expected " theoretically " along with Dempster's experimental curve and note the degree of agreement.

Using the formula for M one can calculate the binding energies of neutrons to isotopes of uranium. This information will be very closely connected with the ability of slow neutrons to fission these various isotopes as we shall see. Let us calculate the binding energy of a neutron to U^{235}.

$$\begin{aligned} M(U^{235}) &= 235.11240 \text{ (given by our formula)} \\ +M(n) &= 1.00893 \\ \text{Sum} &= 236.12133 \\ -M(U^{236}) &= 236.11401 \\ \text{Binding Energy} &= 0.0073 \text{ mass units} = 6.81 \text{ Mev.} \end{aligned}$$

In such a way one finds that the binding energies of neutrons to U^{236}, U^{237}, U^{238}, would be 5.51, 6.56, 5.31 Mev, respectively. This alternation of the magnitude of the binding energies comes from the factor δ. This alternation is superposed on the regular variation of M (A , Z) with A and Z given by the other 5 terms.

(2) *The Fission Process.*

In what follows, we shall try to account in a rough way for the existence of fission in the heavy isotopes.

Homework: Calculate the binding energies of neutrons to

$$Th^{232} \quad Au^{197} \quad Sm^{149} \quad In^{115} \quad Mn^{55}$$

Use the formula for M (A , Z) as we have done to obtain the masses. Sufficiently accurate *experimental* data for nuclear masses (for such an application as we have here) exists only for the lightest nuclei.

An examination of the packing fraction curve shows that in the region of uranium the packing fraction is of the order + 0.0006 whereas for middle weight nuclei the packing fraction run of the order — 0.0007. This implies that the heavy nuclei are not energetically stable against breaking into 2 middle sized nuclei. Let us look into this more closely. Clearly the energy that would be released in such a splitting is of the order $M(A,Z) - 2M(A/2, Z/2)$ and if this is positive, the splitting is energetically possible. This difference can be written:

$$A\left[\frac{M(A,Z) - A}{A} - \frac{M(A/2, Z/2) - A/2}{A/2}\right]$$

or A times the difference in the packing fractions. So that when the difference of the packing fractions is positive fission is energically possible. It is to be noted, however, that A [p.f. (A) — p.f. (A/2)] does not give the energy released in a fission process. It gives the energy for the transition from P to Q (see fig. 67). Actually the end state R is of lower energy than Q. Hence the total energy released in a fission is $>$ A [p.f. (A) — p.f. (A/2)]. If A were 240, A/2 is 120 and Z_A comes out 93.74 for the nucleus A (p. 503). $Z_A/2$ is then 46.87, but using A/2 and the formula for $Z_{A/2}$ the stable Z_{120} is 51.15

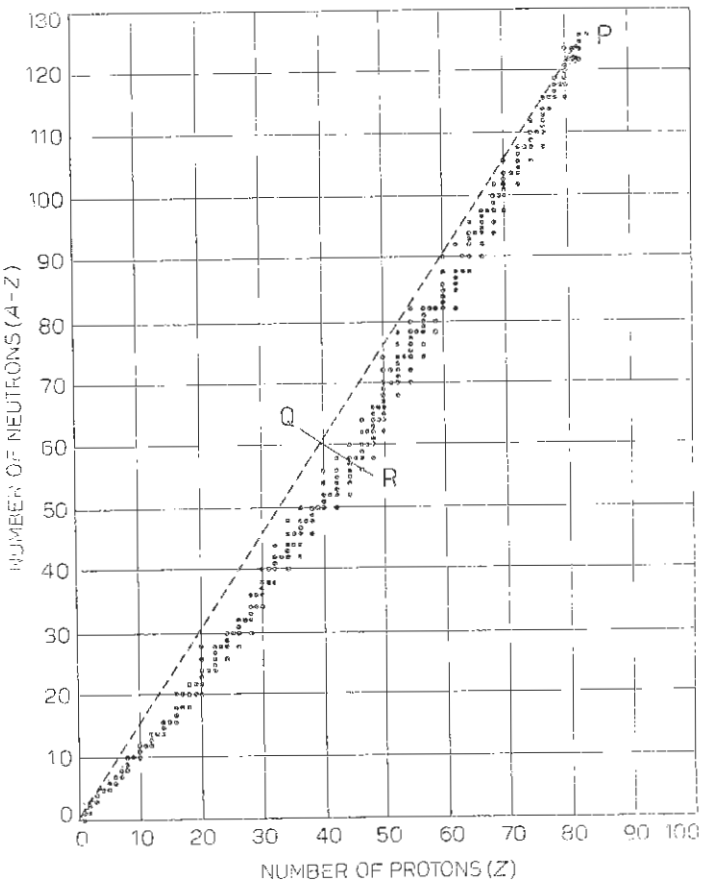

Fig. 67. – Numbers of neutrons and protons in stable nuclei (Segrè Chart).

or about 4 units from $Z_A/2$. This means that about four beta particles will be emitted per fragment. From the packing fraction curves it appears that fission is exoenergetic for all nuclei with A greater than about 100. Why then is fission such a rare process? Consider a nucleus that breaks into 2 fission fragments. Plot the energy of the nucleus (i.e., the fragments) as a function of the distance between the 2 parts (fig. 68). At infinite separation we take the energy at zero. When the fragments are combined ($r = 0$) we know from measurements that E is about 180 or 200 Mev greater. This lets us plot a point for $r = 0$. What about points between $r = 0$ and infinity? Up to distances of the order of the diameter of the fragments, it is the Coulomb

energy between the particles that alone contributes to the energy between particles since that is the only force acting between them. This energy is $\frac{\left(\frac{Z}{2}e\right)^2}{r}$. The value of this term at distances the order of the nuclear diameter is either smaller, equal to, or greater than the 180 or 200 Mev at $r = 0$.

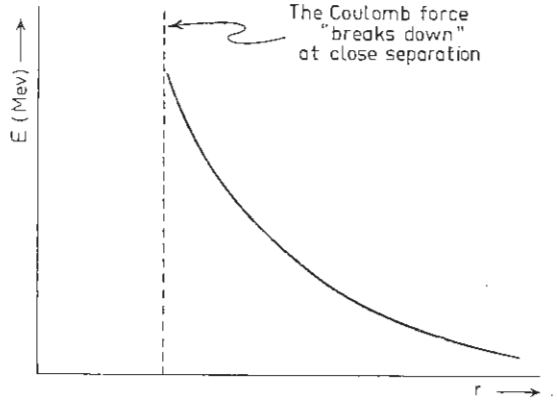

Fig. 68. – Potential energy between a fission fragment and a nucleus.

We would be able to draw three different transition curves from $r = 0$ to such distances (see diagram, fig. 69). Presumably stable nuclei with $A > 100$ are represented by curves of the type I, with barrier heights of the order

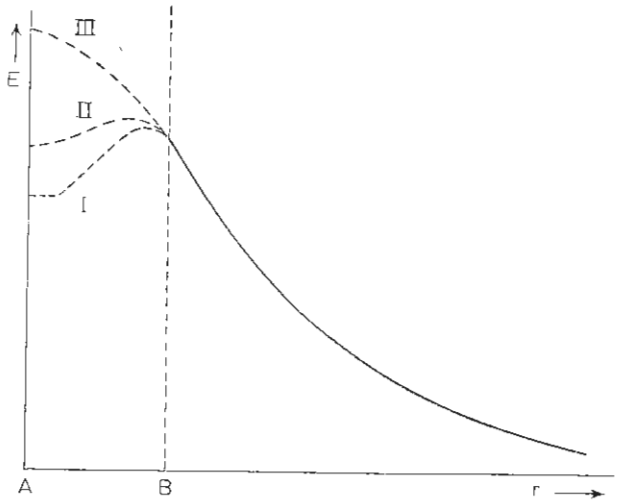

Fig. 69. – Nuclear energy as a function of deformation.

of 50 Mev. Presumably, too, uranium would be represented by a curve like II where the barrier is about 6 Mev. Substances whose curve would be given by III would naturally not exist for long in nature. This curve presumably represents non-existing transuranics. For a somewhat more detailed discussion of the transition distances ($r = 0$ to $r = B$), see the Bohr-Wheeler pa-

per in the «Physical Review» of Sept. 1939. Let us think of $r = B$ as being of the order of diameter of a fission fragment. Then $B = 2 \times 1.48 \times 10^{-13} \left(\frac{A}{2}\right)^{1/3}$. We can draw a curve for E_B as a function of atomic weight (fig. 70). The curve for E_A gives the excess of mass or energy of a mother nucleus of weight A over that of its two fragments. This curve becomes negative below $A = 85$. It crosses the curve for E_B in the neighborhood of $A = 250$. From such a graph one can get $(E_B - E_A)$ for any A. $(E_B - E_A)$ is a measure of the height of the energy barrier against fission.

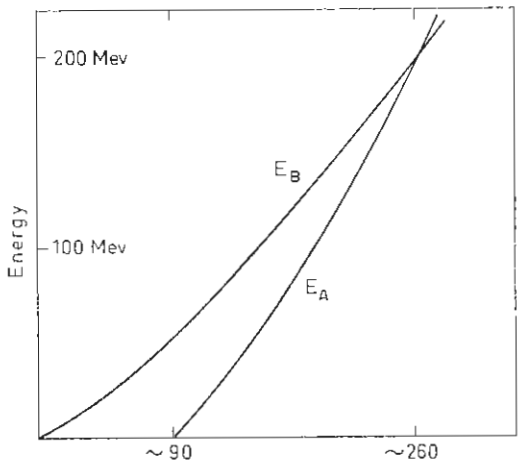

Fig. 70. – Dependence of critical fission energy on mass number.

One can of course investigate more precisely the shape of the energy vs. separation curve in the neighborhood of $r = 0$, if some specific model is assumed. Consider the Bohr liquid drop model. Here we assume that the original nucleus is a sphere and we calculate the change in energy for a small deformation. We assume that the first deformation of a sphere that is beginning to split is a very simple one, namely that the sphere stretches a bit in one direction and flattens out perpendicular to this direction. The sphere becomes an ellipsoid.

If we assume that the sphere does not change its volume on becoming an ellipsoid (and this is reasonable in view of the fact that all nuclei tend to maintain the same density of nuclear particles, as we have seen), the change in the energy of the nucleus upon deformation will be due to only two of the five factors discussed in the last section. First there will be the surface energy which will tend to increase with deformation because more surface will be exposed, and second we have the electrostatic energy which will decrease upon deformation because the repelling charges are effectively separated a little.

Thus we have at least two energies changing in opposite ways with deformation of a spherical nucleus. Since the surface or capillary energy goes as the surface area or $A^{2/3}$ and the electrostatic energy $\sim \frac{Z^2}{A^{1/3}}$ or $\sim A^{5/3}$ the latter energy becomes more important for heavy nuclei. Thus, for

heavy nuclei it is likely that the energy of a nucleus tends to decrease with deformation and a spherical nucleus is unstable. The opposite is true for light nuclei. From this picture it is in heavy nuclei that we would expect fission. Let us investigate the change of energy of a spherical nucleus upon distortion, in some detail. The electrostatic energy of a charge Z distributed throughout the volume of an ellipsoid (fig. 71) can be shown to be:

$$\frac{3}{10}\,\frac{Z^2 e^2}{\sqrt{a^2 - b^2}}\,\log\frac{a+\sqrt{a^2-b^2}}{a-\sqrt{a^2-b^2}}$$

and the surface energy is proportional to the surface area which can be shown to be:

$$2\pi b^2 + 2\pi\,\frac{a^2 b}{\sqrt{a^2-b^2}}\,\arccos\frac{b}{a}\,.$$

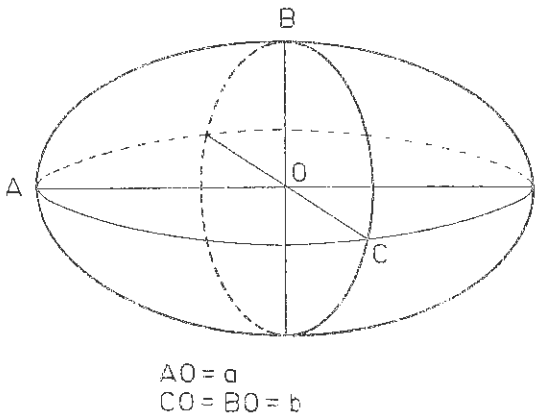

Fig. 71. – An Ellipsoid of revolution.

Now consider a sphere of original radius R. We stretch it in one direction $a = R\,(1+\varepsilon)$. What should b be in order that the volume of the ellipsoid is that of the original sphere? $\frac{4\pi}{3}\,a b^2 = \frac{4\pi}{3}\,R^3$ whence $b = \frac{R}{1+\varepsilon}$. Substituting for a and b in the two energy expressions above and developing the results in powers of ε we find, the electrostatic energy is

$$\frac{3}{5}\,\frac{Z^2 e^2}{R}\left(1 - \frac{1}{5}\varepsilon^2 + \cdots\right)$$

(where it is to be noted that the first term is simply the electrostatic energy of the sphere and the second, a correction term that gives a decrease of energy with deformation as predicted). The surface energy is proportional to:

$$4\pi R^2\left(1 + \frac{2}{5}\varepsilon^2 + \cdots\right).$$

Using the proper coefficients for these energies from the formula for M (A , Z) (p. 503), the excess in energy of the ellipsoid over the sphere is

$$\varepsilon^2\left[\frac{2}{5} \times 0.014\, A^{2/3} - \frac{1}{5} \times 0.000627\,\frac{Z^2}{A^{1/3}}\right].$$

The condition for stability against deformation is that the bracket be positive. That is, that

$$\frac{Z^2}{A} < 44.7 .$$

Homework: At what atomic number is instability reached according to this inequality? Use the expression for Z_A, the proper value of Z for a nucleus of weight A that has been developed (p. 503).

For uranium $\frac{Z^2}{A} = 36$ and for lower elements its value is even smaller.

Actually instability will come quite a bit before the point given by the solution of the preceding problem. For curves of the shape shown in fig. 72, the barrier is already rather transparent and one could expect appreciable spontaneous fission. Even for U^{233} there are $\sim$ 20 fissions per gm per hour spontaneously, so that for heavier atoms this may soon become a prominent phenomenon.

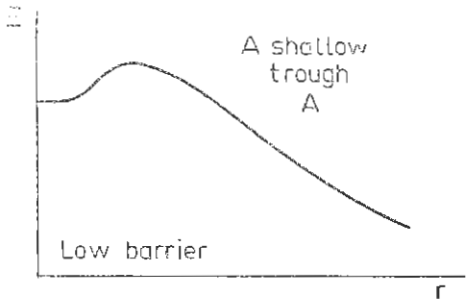

Fig. 72. – Barrier against fission.

We shall be more interested, in what follows, in fissions brought about by neutrons than in spontaneous fissions. Neutrons can cause fission by contributing their kinetic energy and their binding energy to the nucleus. This energy is at least $\sim$ 5 or 6 Mev (the binding energy of the neutron) and may raise the energy of the nucleus high enough within the barrier for a fission to take place before the excess energy is lost by a γ radiation. Because of the fact that the binding energy of neutrons to nuclei with an odd number of neutrons is larger than it is to those with an even number of neutrons (p. 503), it is reasonable to expect fission for thermal neuts to be more prevalent for those nuclei with an odd number of neutrons. This is so. (238 won't fission with thermals, but 235 will).

From facts like these and photofission thresholds, one can estimate that for uranium the height of the fission barrier is of the order 5 Mev.

It is to be kept in mind that in the consideration of the competition of fission with other processes, it is not sufficient to consider energies alone as we have done. For fission, one must have the energy rise to the top of the barrier, but in addition it is necessary that this energy be concentrated in the proper modes of motion for fission. This may take some time and competing processes may therefore occur at the expense of fission. Since the number of modes (and hence of useless non-fission modes) increases with excitation energy, it may therefore be very likely that the reason photofission with $\sim$ 100 Mev γ's on lower nuclei has not been observed is because the energy doesn't get concentrated in a proper mode before it is lost by some other way than fission.

(3) *The Particles of Fission.*

In addition to the appearance of the fission fragments, one can observe neutrons, β particles, γ rays and fast α particles following or accompanying fission.

As to the fission fragments themselves, their atomic weight present an interesting problem. The distribution of fission fragments as a function of atomic weight appears in fig. 73. At the half point (if U^{235} is fissioned by

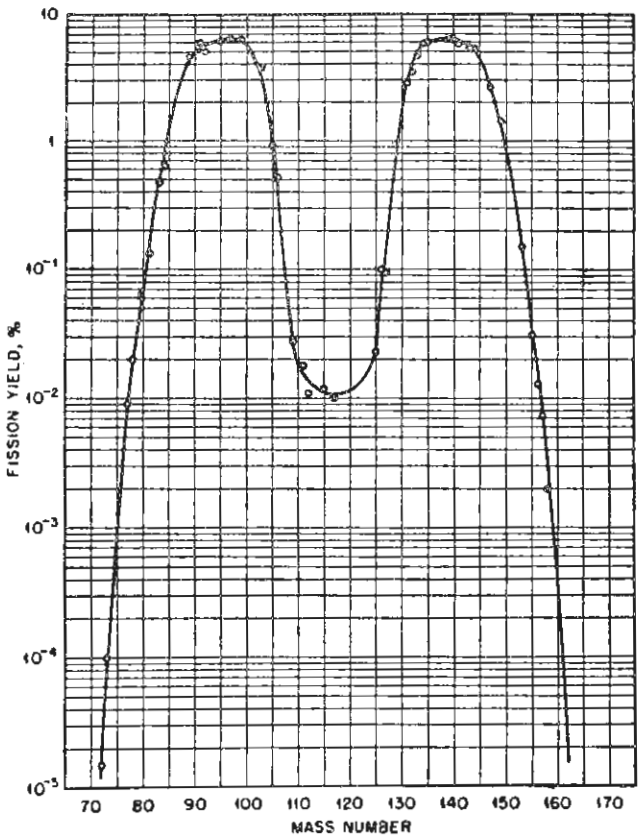

Fig. 73. – Fission yields of products of various mass numbers.

a neutron and 2 are emitted in the course of fission, one would get A = 117 if it is assumed that a nucleus splits into 2 equal fragments), the observed yield is very low. Instead of even splitting, the splitting is very uneven as this experimental curve shows. This phenomenon has not yet been explained theoretically.

As for the neutrons of fission, they are classed as either prompt or delayed, "prompt" meaning that they leave the fission fragment after its formation in times shorter than we can measure. One can estimate that they leave within 10^{-15} seconds under circumstances such as the following. Consider the fission process once again as the splitting of a drop (fig. 74). The

final fragments are not of spherical shape. Hence there will be a considerable vibrational energy associated with oscillations about the equilibrium (spherical) shape of the fragment. This excitation energy may be sufficient to evaporate a neutron, especially since neutron binding energies in fisssion

Fig. 74. – Liquid-drop model of fission.

fragments are small because of the excess of neutrons. For example, assume that U^{235} is made to fission by a neutron and 2 fragments with $A = 118$ and $Z = 46$ appear. Using the formula for $M(A, Z)$ (p. 503) one can calculate binding energies for various nuclei of weight $A = 118$.

Z	44	45	46	47	48	49	50
Binding Energy	2.5	6.8	3.6	7.8	4.7	9.0	5.8

(where $Z = 50$ is the stable value for Z if $A = 118$). Thus neutrons may be lightly bound to fission fragments. Whenever neutron emission is energetically possible, neutron emission is likely, because of the absence of a barrier for neutrons. As a matter of fact, one could conclude from observations that considerable excitation energy must be present in the fragments because from one to three neutrons are emitted per fission in the case of U^{235}, for example.

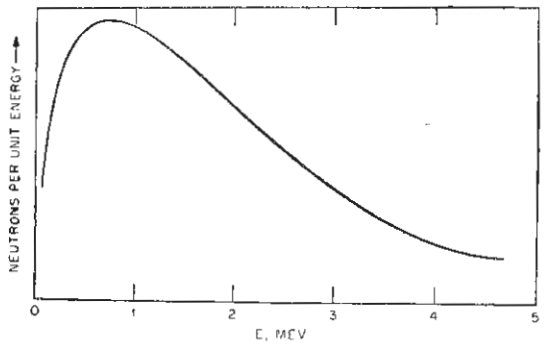

Fig. 75. – Fission neutron energy spectrum.

The energies of the neutrons that come off at fission are given in the distribution curve in fig. 75. In the center of gravity system of neutron and fission fragment the neutron energy distribution would be sort of Maxwellian with a "temperature" corresponding to the excitation of the fragment. To get the theoretical curve for the distribution in the lab system one would have to take account of the motion of the fission fragment and the dependence of emisssion probability on neutron energy.

Homework: Derive an energy distribution curve for fission neutrons assuming a velocity V for the fission fragment and a Maxwell distribution of energies in the c. of g. system. Also assume that the probability of neutron escape is proportional to their velocity.

In addition to these prompt neutrons some ($\sim$ 1 %) come off delayed. To explain the emission of delayed neutrons, consider a fragment A which undergoes a β-disintegration to a nucleus B* (fig. 76). Usually this disin-

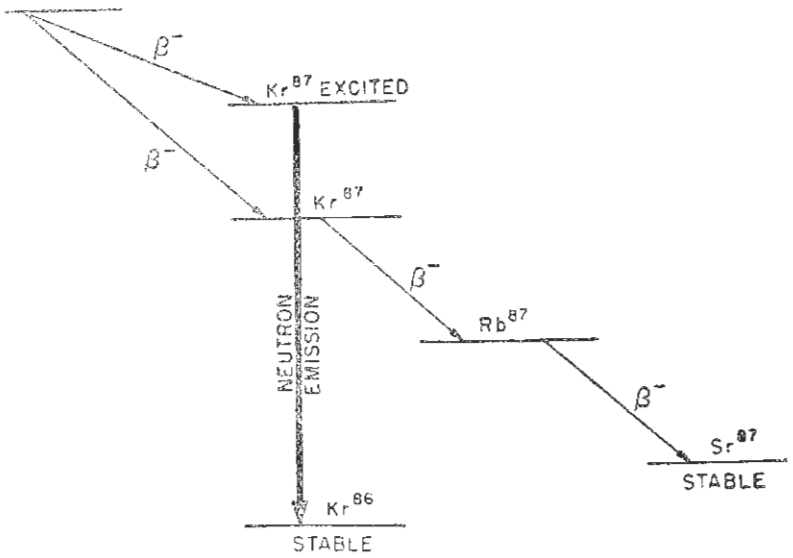

Fig. 76. – Interpretation of delayed neutron emission.

tegration will go to the ground state of B*, but occasionally the nucleus B* may end up excited with excitation energy greater than the binding energy of a neutron. In such a case neutron emission becomes quite likely. Such neutrons would come off very quickly after the β decay and would therefore show decay periods that correspond to the periods of the disintegration of A to the excited state of B*.

The delayed neutron periods that have been observed and their yields are at the right. The first 2 periods are rather well verified. The short time ones are as yet not definitely confirmed.

1/2 life	Delayed neut per prompt
55.6 sec	0.00021
22.0	0.00139
4.51	0.00178
1.53	0.00201
0.42	0.00071
Total . . .	0.006

(4) *Cross-Sections for Fission and Competing Processes in the Heavy Isotopes.*

The cross-section for capture and fission for the isotopes of uranium and plutonium that have so far been investigated show a rather complicated dependence on energy. For some isotopes the (n, f) cross-section decreases with neutron energy whereas for others it increases. Some isotopes show an (n, f) threshold whereas some have an (n, f) cross-section that follow the $1/v$ law at low energies. Pronounced resonances for capture are apparent at low neutron energies is isotopes like U^{238}. The resonances becomes less striking at higher energies where they tend to get smeared out.

TABLE OF CONTENTS

PART II

(Declassified in 1962)

(Notes)

CHAPTER VIII

NUCLEAR FISSION (*cont.*).

(5) *Cross Section for Absorptive Processes in Fissionable Materials.*

For Pu^{239} the thermal (0.025 ev) cross sections are $\sigma_f = 705$ barns, $\sigma(n, \gamma) = 345$ barns, and the total cross section is, therefore, $\sigma_t = 1050$ barns. The variation of the fission cross-section with energy is indicated in the table below. The capture cross-section becomes relatively less important. This is fortunate for the multiplication rate.

ev	σ_f
0.025 (thermal) . .	705
0.1 to 0.2	$1/v$
0.3	6000 (resonance)
10^4	3
$3 \cdot 10^5$	2
$3 \cdot 10^5$	1.96

CHAPTER IX

NUCLEAR PILES.

(1) *Construction of a Chain Reacting Pile.*

Returning to uranium, let us now plot on one graph the capture and fission cross sections of U^{235} and of U^{238} (fig. 77). Since in natural uranium only 1/140 is U^{235} we shall plot $\sigma/140$ for U^{235} and $(139/140)\,\sigma$ for U^{238}.

The cross section observed with ordinary uranium would be the sums of the cross sections plotted above, or roughly as in fig. 78. It is seen that below about 1 ev and above 1.4 Mev $\sigma_f > \sigma_c$ and in between the capture cross section is greater. One would conclude that if it were possible to get a chain reaction going in natural uranium, it would be sustained by neutrons whose energy is greater than 1.4 Mev or by neutrons near thermal.

Consider first the high energy region. It will be shown that the existence of a large inelastic scattering cross-section prevents the realization of a chain

reaction. Given a big mass of natural uranium and a fission occurring somewhere in the middle, let us see what is likely to happen. About 2.5 neutrons will be produced per fission so that we start with 2.5 neutrons. The fission neutron energy spectrum is such that we can assume that one neu-

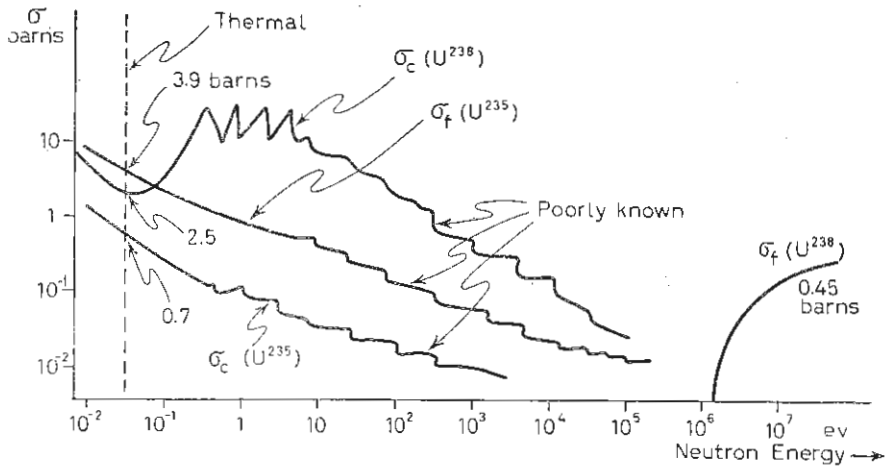

Fig. 77. – Uranium cross sections (separated isotopes).

tron is produced with energy below the effective fission threshold of U^{238} (1.5 Mev) and that there are 1.5 neutrons left with energy greater than 1.5 Mev. The low energy neutron will probably be absorbed because of the high capture cross section at its energy. In fact, the probability that it causes a

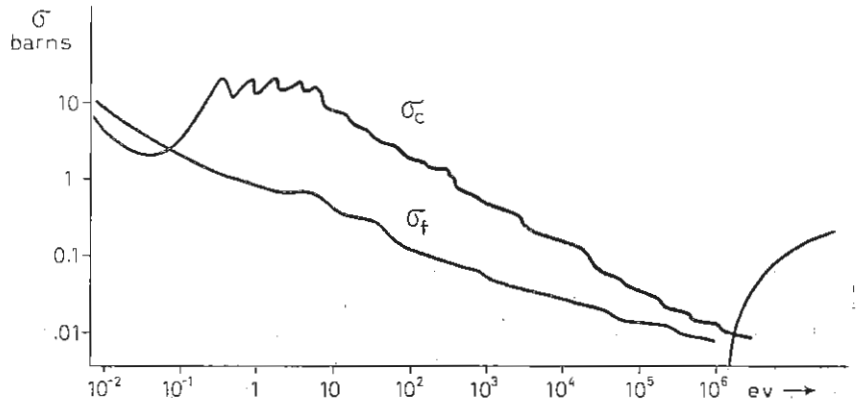

Fig. 78. – Ordinary uranium neutron cross sections.

fission is only 0.05. Were there no inelastic scattering, the remaining 1.5 neutrons could cause a chain reaction, because they have about four times the probability of causing a fission than of being captured. (i.e. 1.2 of the 1.5 fast neutrons would lead to new fissions, and the necessary condition for a chain, that the number of neutrons per fission that lead to new fissions

be greater than one is satisfied). But there is inelastic scattering of these fast neutrons and the cross section for scattering from above to below the 28 threshold is of the order 2.3 barns. Since σ_f is only 0.4 (and $\sigma_e = 0.1$) only 4/23 of the 1.5 fast neutrons will produce fissions. This is about 0.2 and therefore there can be no self-sustaining chain due to the high energy neutrons.

Now let us consider the thermal region. For 0.025 volt neutrons $\sigma_f = 3.9$ and $\sigma_e = 3.2$ barns, so that the total cross section is 7.1 barns. All of these behave as $1/v$ and so their relative values are appreciably the same throughout the region. If the 2.5 neutrons produced in a fission manage to get slowed down to thermal values, without absorption, one would expect them to make $(3.9/7.1) \times 2.5 = 1.37$ (1.32 is actually believed to be more accurate) new fissions. One would have a going chain. The problem, then, is to reduce the fission neutron energies to thermal before the neutrons are absorbed. One would be led to a scheme such as the following in order to solve the problem. Mix the uranium with a substance that does not absorb neutrons. Spread the uranium thin enough so that there is sufficient probability for the required amount of fission neutrons to be slowed down to thermal energies (without capture in the U) to keep the chain going.

One might consider using He^4 as the slowing down substance or moderator for it is believed that He^5 does not exist. However, such a moderator would not be practical, the mean free paths would be long and a structure of about one cubic mile might be required. One might think of using liquid helium in such a pile. This is also not very practical. One can say the following: If one can succeed in increasing the density of a pile by a factor f, as in the case of liquefying helium, then the linear dimensions of the pile can be reduced by the factor f, and the operation of the pile will be exactly as it was before changes were made, for the ratio of mean free path to a distance in the pile stays fixed. The overall result is to multiply the volume by f^{-3} and the mass by f^{-2}.

Actually, one is forced to use substances that do absorb neutrons, but they do not absorb them very much. Chain reactions have been obtained with graphite and heavy water. Possibly Be or even H_2O may be successful moderators.

Consider a graphite pile. It is so large that leakage from the surface can be neglected. Assume U is uniformly spread through the pile. For graphite at thermal energies, $\sigma_{sc} = 4.8$ barns, $\sigma_e = 0.0048$ barns. What is the maximum ratio R of the number of carbon to uranium atoms required to keep the pile going? This maximum is set by the absorption of the carbon at thermal energies. Assume $\nu = 2.4$. Assume further (in order to get an upper limit on R) that no absorption takes place during the slowing down to thermal. From the diagram (fig. 79), it is seen that for the pile to go, $(3.9/\sigma_t) \times 2.4$ must be greater than 1. (Where σ_t is the total cross section for absorbing processes at thermal energies $\sigma_t = 3.9 + 3.2 + 0.0048$ R). This gives 0.0048 R less than 0.226 or R must be less than 470. Or in terms of weight, the ratio of weight of carbon to U must be less than 25. Actually a consideration of losses during slowing down, and the consideration that U is not spread uniformly

through actual piles (resulting in higher neutron densities in the carbon, away from the U neutron sinks) both tend to lower this upper limit.

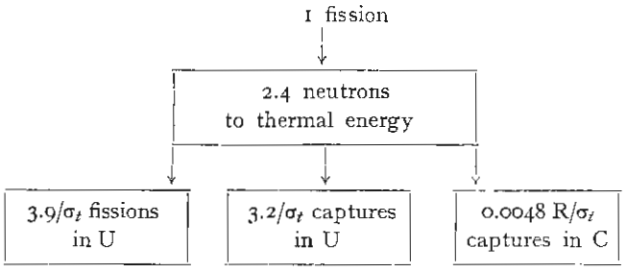

Fig. 79.

There is a lower limit for R, for, as we have seen, a pile will not go without a moderator and this lower limit must be less than our upper limit if the whole scheme is to be feasible.

(2) *Capture During Slowing Down.*

We have heretofore neglected this effect. Assume that q, the slowing down density, is constant. That is that $q(x, y, z, E)$ the number of neutrons per cc that change from energy above E to below E in unit time (1) does not depend on position and (2) does not depend on E. The physical conditions that would give such a q would be a uniform medium with a uniformly spread steady source. We have seen that the velocity with which a neutron drifts down the $\varepsilon = \log E$ axis is $\xi v(\varepsilon)/\lambda$ where $\xi = \overline{\log (E_i/E_f)}$. Hence, $q = n(\varepsilon)\,\xi v(\varepsilon)/\lambda(\varepsilon)$. We can write the number of neutrons per cc in the logarithmic energy interval:

$$n(\varepsilon)\,d\varepsilon = q\,\frac{\lambda}{\xi}\,\frac{1}{v}\,\frac{dE}{E}.$$

Now consider an atom of U in the pile. How many neutrons in this energy interval will it absorb in unit time? This will be: $n(\varepsilon)\,d\varepsilon\,v\sigma(\varepsilon)$ and in terms of E, the total number of neutrons absorbed per atom per unit time is then:

$$\frac{q\lambda}{\xi}\int \sigma(E)\,\frac{dE}{E}.$$

The upper limit of the integral need not be picked too carefully for the integrand decreases rapidly as E increases. The lower limit is usually taken as the Cd absorbtion edge which is approximately 0.3 ev. Under these circumstances the integral (omitting $q\lambda/\xi$) is, for U, 240 barns. This is determined empirically.

Since q neutrons are produced per unit time per unit volume, and each atom absorbs $\frac{q\lambda}{\xi}\int_{0,3} \sigma\,\frac{dE}{E}$ neutrons in unit time, one can associate with each atom an "absorption volume" $\frac{\lambda}{\xi}\int \sigma\,\frac{dE}{E}$ (note that this has the dimensions of a volume) where we can say that each atom will absorb all the neu-

trons made in the absorption volume surrounding it. For U, this volume is 4×10^{-21} cc which is much greater than the size of a U nucleus (10^{-35} cc) as is to be expected.

The total number of neutrons absorbed per cc in a pile would be in unit time: $q \times 4 \times 10^{-21} \times$ number of atoms of U/cc. Assume the number of atoms of U/cc to be 1.6×10^{20} (and the number of atoms of C to be 8×10^{22} per cc). We take here the number of C atoms/number of U atoms = 500. Then 0.64 q neutrons are absorbed per cc per sec, or 64 % of the neutrons are absorbed.

However this is a considerable overestimate. This stems from the fact that the absorption cross section has sharp resonances. The absorption of n atoms is not the same as n times the absorption of one atom. The atoms absorb each other's neutrons, so to speak, and " shield " each other. This can be clarified somewhat as follows. The spectrum of neutrons in the pile is not what it would be if the cross sections were smooth. There are depressions in the spectrum at resonance energies because neutrons with such energies are quickly removed. Nuclei of U are therefore presented with relatively few absorbable neutrons.

To cut down the slowing down absorption, one would lump the U in the pile rather than spread it, for then within a lump there would be no moderator which would tend to even out the neutron spectrum by continually feeding neutrons into resonance regions. These nuclei on the surface of a lump would quickly remove all incident resonance neutrons and interior nuclei would see very few. But how would lumping affect the absorption of thermal neutrons by the uranium and the carbon? The carbon absorption per cc per second would be:

$$n_C \times \sigma_C \times N_C \times v$$

where n_C is the density of neutrons of thermal energies at the carbon, and σ_C and N_C are the carbon neutron cross section and the number of atoms of carbon per cc respectively. For uranium, the absorption per cc per second is:

$$n_U \times \sigma_U \times N_U \times v$$

Since the uranium acts as a neutron sink if it is lumped, n_C is greater than n_U. Hence, from the point of view of absorption of thermals to get fission, lumping is undesirable.

This result and the previous one can be considered quantitatively to give a value for the optimum size of the lumps because from the point of view of slowing down absorption, the bigger the lumps the better, but from the point of view of fission absorption of thermals, the smaller the lumps the better.

It is found empirically that for a *uniform* mixture of uranium and carbon

$$\left(\int \sigma \frac{dE}{E} \right)_{eff} = 2.95 \times (\sigma_{scat})^{0,47}$$

holds for (σ_{scat}) " scattering cross section," less than 1600. Here (σ_{scat}) is the scattering cross section of one atom of uranium plus that of the number

of moderator atoms per uranium atom. We have seen that if we were simply to add atomic absorptions, $\int \sigma \frac{dE}{E}$ is 250 barns. Substituting the known scattering cross section for uranium and carbon in the empirical formula we get approximately 124; or even for a uniform distribution the "self-absorption" effect is of the order of a factor of two.

If one lumps the uranium the discrepancy should be even greater. It is found empirically that the "absorption volume" of a lump of uranium in some carbon is:

$$0.385 \text{ (mass in grams of U)} + 1.03 \text{ (surface area in cm}^2 \text{ of U)}$$

Can one construct a pile by uniformly disbursing uramium in carbon? To see this let us do the problem of the calculation of the reproduction factor. Take C/U = 200 $\nu = 2.4$. Empirically

$$\int \sigma \frac{dE}{E} = 75$$

using the fact that σ_{scat} for carbon is about 4.8 barns and for uranium about 10 barns. This gives as the total absorption per cc during slowing down: (It is assumed that the density of C is about 1.6 gms/cc)

$$q \times \frac{2.6}{0.158} \times 75 \times 10^{-24} \times 4 \times 10^{20} = \text{approx. } 0.5\, q.$$

This means that about 50 percent of the neutrons are absorbed during slowing down. Thus 1.2 neutrons per fission reach thermal energies. Now the capture cross section for carbon is 0.0048 barns and that of uranium is 7.1 barns. Since there are 200 carbon atoms per uranium atom, the number of neutrons absorbed by the uranium is

$$\frac{7.1}{(200 \times 0.0048) + 7.1} \times 1.2 = 1.06.$$

Since 3.9/7.1 absorptions in uranium lead to fission, we get

$$1.06 \times \frac{3.9}{7.1} = 0.58.$$

Thus the pile will not go. It is possible to show that no uniform distribution (no value of C/U) will make a chain reaction.

One could design an inhomogeneous pile by using one of many structures such as a cubical lattice of spherical lumps or a cylindrical geometry.

(3) *Calculation of k for Spherical Lumps in a Cubical lattice.*

Start with one neutron in a sphere. $1 + \varepsilon$ neutrons will escape the sphere as there is a small probability that the original fission neutron will, while still fast, give rise to a fast fission. Let f_r be the probability that a neutron is absorbed in a resonance during slowing down. Then $(1+\varepsilon)(1-f_r)$ neutrons will reach thermal energy. Let f_t be the probability that a thermal neutron is absorbed by uranium. Then $f_t(1+\varepsilon)(1-f_r)$ neutrons will

be absorbed by the uranium. In order to find out how many neutrons on the average are made by such an absorption, multiply the above by η which is:

$$\begin{pmatrix}\text{probability that absorption of thermal}\\ \text{neutrons will give a fission } \left[\text{for uranium } \frac{3.9}{7.1}\right]\end{pmatrix} \times \begin{pmatrix}\nu\text{, the number of neutrons}\\ \text{per fission [2.4 for uranium]}\end{pmatrix}$$

Thus $\eta = 1.32$ and the reproduction factor is:

$$k = \eta f_t (1 - f_r)(1 + \varepsilon).$$

Let us see how the three factors f_t, $1 - f_r$, and $1 + \varepsilon$, can be calculated. Let us first get an order of magnitude calculation for $1 + \varepsilon$. The order of magnitude of a path of a neutron escaping from a spherical lump is the radius of the lump. Assume that there is only a 60 percent chance of the original fission neutron to be at the high end of the fission spectrum, in particular that it has energy greater than 1.4 Mev, that being taken as the 28 fission threshold. Now $\sigma_f = 0.45$ barns and $\lambda_f = 50$ cm. Then our original neutron would make this many new ones, due to fast fission:

$$0.6 \times (R/\lambda) \times (\nu - 1).$$

The last factor is the net number of neutrons per fission, which is 1.4. Thus in order of magnitude,

$$1 + \varepsilon = \frac{R}{\lambda}(\nu - 1).$$

Actually $(1 + \varepsilon)$ can be calculated by somewhat more refined methods, giving more accurate results.

Next we calculate $(1 - f_r)$. We have seen that empirically the absorption volume of a lump of uranium is:

$$V_r = 0.385\ \text{Mass}_{\text{gm}} + 1.03\ S_{\text{cm}^2}$$

qV_r neutrons are absorbed per second by a lump and qV_c neutrons are produced per second by a lump. Here V_c is the volume of a cell of the lattice. Thus $f_r = V_r/V_c$. Actually a somewhat better calculation gives $f_r = 1 - e^{-V_r/V_c}$ but the results of this and the simpler formula are not too different.

Now it remains to see how f_t is calculated. If the lattice is infinite, then at any symmetry plane the gradient of neutron density for thermal neutrons, for example, must vanish. Now the boundaries of a cell are all symmetry planes and we have a boundary value problem. Actually for purposes of calculation the cubic cell is replaced by a spherical one and one finds n, the thermal neutron density, as a function of position in the cell. One can then calculate the rate of absorption of thermal neutrons by the uranium. In this way one obtains:

$$f_t = \frac{3\alpha^2\left[(1-\alpha)(1+\beta)e^{-(\beta-\alpha)} - (1+\alpha)(1-\beta)e^{\beta-\alpha}\right]}{(\alpha^3-\beta^3)\left[(\alpha+s-s\alpha)(1+\beta)e^{-(\beta-\alpha)} - (\alpha+s+\alpha s)(1-\beta)e^{\beta-\alpha}\right]}$$

where $\alpha =$ (radius of lump)/(diffusion length in carbon)

$\beta =$ (radius of cell)/(diffusion length in carbon)

$s = \frac{1+\gamma}{1-\gamma}\frac{1}{\sqrt{N}}$ where $N = \sigma_{tot}/\sigma_{abs}$ (approx. 1100 for graphite)

$\gamma =$ albedo (from outside)

$$\frac{1-\gamma}{1+\gamma} = \frac{\sqrt{3}\, l_i}{\lambda_i N_i}\left\{\frac{e^{2R/l_i}+1}{e^{2R/l_i}-1} - \frac{l_i}{R}\right\} \qquad \begin{matrix} l_i = \text{diffusion length} \\ N_i = \sigma_{tot}/\sigma_{abs} \end{matrix}$$

$$\text{for U}\ , l_i = \frac{24.0}{\rho\ (\text{density})} \qquad \lambda_i = \frac{21.1}{\rho} \qquad N_i = 2.71\ \text{(for U)}.$$

And so one calculates the four factors in k. For a typical lattice, these numbers may be of order $\eta = 1.32$, $f_t = 0.88$, $f_r = 0.12$, $1+\varepsilon = 1.05$. For such a lattice $k = 1.07$. (The best k's for a uranium-carbon system are about 1.10).

In industrial piles, or even in lab piles to give strong neutron fluxes, one runs the pile at high power. The Argonne pile which is 20 feet on a side can't be run higher than 2 kw because no special provision was made for cooling. For higher power piles one must introduce a cooling system. In Clinton, for example, there is a rod lattice with air cooling through channels in which the rod lie. The power of this pile is 5000 kw. (The air coming out is about 100°). Other piles are water cooled and aluminum jackets must be used. The point of all this is that for high power piles k cannot be maintained at 1.1 because of the introduction of absorbing material, i.e. air, water, aluminum.

(4) *The Relation between the Reproduction Factor and the Critical Size of the Pile.*

Assume we have calculated k, the reproduction factor, for a particular lattice and it turns out to be slightly greater than one, say 1.05. Were we to have an infinite lattice we would have a super critical pile. How big should we make the pile so that in can still be under control? If n is the thermal neutron density in the pile, it will look roughly as follows: it will show a maximum at the middle of the pile; superposed on this will be the fluctuations due to the uranium in each lattice cell. Let us assume that there are many lattice cells and that we can, in what follows, consider only the general shape of n, neglecting the lumps. We have derived once before the differential equation for n, the density of thermal neutrons

$$\frac{\lambda v}{3}\Delta n - \frac{v}{\Lambda} n + q = 0.$$

It is to be noted that Λ, the absorption mean free path, is some sort of average of Λ for graphite and for uranium. For pure graphite it is 25 m, and in the proportions of uranium and graphite usually used the average Λ is about one tenth of this.

k is the reproduction factor of the lattice (infinite). We have seen that k is the product of four factors. This product can be written ηf_t times the number of thermal neutrons eventually absorbed for each fast fission neutron created per cc per sec. The number of neutrons absorbed per cc per second is $\frac{v}{\Lambda} n$. Thus the number of fast neutrons produced is $\eta f_t \frac{vn}{\Lambda}$. The effective number of fast neutrons is the number that eventually becomes thermal. This is:

$$\eta f_t \frac{v}{\Lambda} n (1 + \varepsilon) (1 - f_r) = k \frac{vn}{\Lambda} .$$

Call this q_0, the number of effective fast neutrons produced per cc per unit time. We now must solve the age equation $\Delta q = \frac{\partial q}{\partial \tau}$ with the boundary condition that $q = q_0$ at $\tau = 0$. For simplicity assume that the pile is shaped as a cube, Because n vanishes at the boundary (actually, as we have seen, the true boundary condition is $n = 0$ at 0.7λ outside the surface, but in this case this is only a few centimeters which is small compared to a for piles) we expand $n(x, y, z)$ as

$$n(x, y, z) = \sum_{ijk} n_{ijk} \sin\left(\frac{i \pi x}{a}\right) \sin\left(\frac{j \pi y}{a}\right) \sin\left(\frac{k \pi z}{a}\right) .$$

Take only the n_{111} term for our solution. That is, we assume $n = n'$

$$n = n' \sin\left(\frac{\pi x}{a}\right) \sin\left(\frac{\pi y}{a}\right) \sin\left(\frac{\pi z}{a}\right)$$

and

$$q_0 = q_0' \sin\left(\frac{\pi x}{a}\right) \sin\left(\frac{\pi y}{a}\right) \sin\left(\frac{\pi z}{a}\right) .$$

These must satisfy the pair of equations:

$$\frac{\lambda v}{3} \Delta n - \frac{v}{\Lambda} n + q = 0 \qquad \text{(for slow neutrons)}$$

$$\Delta q = \frac{\partial q}{\partial \tau} \qquad \text{(slowing down for the effective number of fast neutrons).}$$

Also

$$\frac{kv}{\Lambda} n' = q_0' .$$

Substituting the above assumed sinusoidal solution one gets:

$$-\frac{\lambda v}{3} \frac{3 \pi^2}{a^2} n' - \frac{v}{\Lambda} n' + q = 0$$

$$-\frac{3 \pi^2}{a^2} q' = \frac{\partial q'}{\partial \tau}$$

$$\frac{kv n'}{\Lambda} = q_0' .$$

The second of these readily lets us evaluate the constant q':

$$q' = q_0' e^{-\frac{3 \pi^2}{a^2} \tau}$$

or

$$q' = \frac{kv}{\Lambda} n' e^{-\frac{3 \pi^2}{a^2} \tau}$$

If this is substituted into the first equation we get a condition on the constants of the pile which must be satisfied for a solution:

$$n'\left(-\frac{\lambda v}{3}\frac{3\pi^2}{a^2}-\frac{v}{\Lambda}+\frac{kv}{\Lambda}e^{-\frac{3\pi^2}{a^2}\tau}\right)=0.$$

This can be written:

$$k=e^{\frac{3\pi^2}{a^2}\tau}\left(1+\frac{3\pi^2}{a^2}\frac{\lambda\Lambda}{3}\right)$$

where k is the k for the infinite lattice. Since our equation have been solved for an equilibrium pile, this equation gives the size of a pile that would be in equilibrium if k were the reproduction factor for the infinite lattice. This can be written more simply if the exponential is expanded

$$k=1+\frac{3\pi^2}{a^2}\left(\tau+\frac{\lambda\Lambda}{3}\right).$$

Let us put in some numbers. $\tau = 300$ cm^2 and $\frac{\lambda\Lambda}{3} = 350$ cm^2. Thus $k = 1 + 20000/a^2$ or $k = 1 + 2/a_m^2$ where a is in meters. Since the best k for a graphite pile is about 1.1, then a_m is about 4.5 as a minimum. For $k = 1.03$ we would need an 8 meter pile. In general $a_m = \frac{\sqrt{2}}{\sqrt{k-1}}$ or the volume is $a^3 = [2/(k-1)]^{3/2}$.

If the pile were a rectangular parallelepiped, it can be shown that the condition on the dimensions would be:

$$k=1+\pi^2\left(\frac{i^2}{a^2}+\frac{j^2}{b^2}+\frac{k^2}{c^2}\right)\left(\tau+\frac{\lambda\Lambda}{3}\right)$$

where a, b, c, are the sides of the pile. It can be shown that our neglect of the higher harmonics is justified for an actual pile. Had we assumed ijk th harmonic and had constructed the pile so that the 1 1 1 harmonic was just critical, then in general this higher harmonic would have a k less than one and would thus die out with time. For any shape of pile it can be shown that the main harmonic present after a long time is the fundamental.

(5) *The Time Dependent Equations of the Pile, Prompt Neutrons only.*

Last time we derived three equations to describe a pile at equilibrium. Today we shall discuss the time dependence of the pile. We shall assume for simplicity that all neutrons are prompt. We also assume, and this is not a bad assumption, that the slowing down takes a time that is negligible compared to the time spent by a neutron as a thermal neutron. Actually this ratio is about 1 to 100.

The first equation of the last lecture becomes, in the time-dependent case,

$$\frac{\lambda v}{3}\Delta n-\frac{v}{\Lambda}n+q=\frac{\partial n}{\partial t}$$

and the other equations

$$\Delta q = \frac{\partial q}{\partial \tau} \qquad \text{and} \qquad q_0 = \frac{kv}{\Lambda} n$$

remain unchanged because of the above assumptions, i.e. it is assumed that q_0 is still proportional to n at all times.

In general for a general shape of pile the problem is to solve a differential equation

$$\Delta\varphi(x, y, z) + \omega\varphi = 0$$

where the ω are eigenvalues and the boundary condition is that $\varphi = 0$ at (really near) the boundary.

To find a solution we assume that the time-dependent solutions are expressihle as products:

$$(1) \qquad \begin{cases} n = f(t)\,\varphi(x, y, z), \\ q = g(t, \tau)\,\varphi(x, y, z), \\ q_0 = g_0(t)\,\varphi(x, y, z). \end{cases}$$

Considering the age equation, it becomes:

$$\Delta q = g(t, \tau)\,\Delta\varphi = -\omega g(t, \tau)\,\varphi = \frac{\partial q}{\partial \tau} = \varphi \frac{\partial g}{\partial \tau} \qquad \text{or} \qquad \frac{\partial g}{\partial \tau} = -\omega g.$$

Whence $g = g_0 e^{-\omega\tau}$. From the above relationships for q_0 and n:

$$g_0 = \frac{kv}{\Lambda} f(t)$$

and

$$g = \frac{kv}{\Lambda} f(t)\, e^{-\omega\tau}$$

we can therefore write for q

$$q = \frac{kv}{\Lambda} f(t)\,\varphi(x, y, z)\, e^{-\omega\tau}.$$

Now let us find the form of solution for n. From the first equation (1) we get

$$-\frac{\lambda v}{3}\omega n - \frac{v}{\Lambda} n + \frac{kv}{\Lambda} e^{-\omega\tau} n = \frac{\partial n}{\partial t}$$

The solution is

$$n = n(0)\, e^{t\left[\frac{kv}{\Lambda} e^{-\omega\tau} - \frac{v}{\Lambda} - \frac{\lambda v}{3}\omega\right]}.$$

The exponent is a decreasing function of ω. Recall that ω is a constant denoting the harmonic of the stationary solution corresponding to it. Because the set of equations is linear, the time dependence of the various harmonics is:

$$e^{tF(\omega_1)} \qquad , \qquad e^{tF(\omega_2)}$$

and since $F(\omega)$ decreases as ω increases it means that after a time the fundamental harmonic will outgrow the others even if we started at $t = 0$ with

a complicated distribution of neutrons in which some higher harmonics were important.

When the exponent is zero, we have a time independent or equilibrium solution:

$$\frac{kv}{\Lambda} e^{-\omega_1 \tau} - \frac{v}{\Lambda} - \frac{\lambda v}{3} \omega_1 = 0$$

(for the cube $\omega_1 = 3\pi^2/a^2$ and for a sphere $\omega_1 = \pi^2/R^2$ etc.). This is precisely the k equation of the last lecture giving pile sizes for equilibrium

$$k = \left(1 + \frac{\lambda\Lambda}{3} \omega_1\right) e^{\omega_1 \tau}$$

where the proper ω is substituted as determined by the shape of the pile.

Taking ω to mean ω_1, the ω for the fundamental, let us rewrite the exponent:

$$k \frac{v}{\Lambda} e^{-\omega\tau} \left[1 - \left(1 + \frac{\lambda\Lambda}{3} \omega\right) \frac{e^{\omega\tau}}{k}\right].$$

If the reproduction factor were $k_0 = \left(1 + \frac{\lambda\Lambda}{3} \omega\right) e^{\omega\tau}$ then the pile would be just going. The exponent can be written:

$$k \frac{v}{\Lambda} e^{-\omega\tau} \left(1 - \frac{k_0}{k}\right)$$

or the time dependence is:

$$\exp\left[\frac{v}{\Lambda} (k - k_0)\, t\, e^{-\omega\tau}\right]$$

which shows that k_0 is what we said it was, i.e. the reproduction factor corresponding to equilibrium. Write:

$$\frac{n(t)}{n(0)} = e^{\frac{v}{\Lambda}(k-k_0)t} = e^{t/T}$$

where T is the period of the pile $= \frac{\Lambda/v}{k - k_0}$ (we have neglected $e^{-\omega\tau}$ because it is of the order of unity). This can be written:

$$T = \frac{\text{lifetime of a neutron}}{k - k_0}.$$

(6) *Effect of Delayed Neutrons.*

Let us reconsider the first three equations of the previous section, taking into account the delayed neutrons. The two equations:

$$\frac{\lambda v}{3} \Delta n - \frac{v}{\Lambda} n + q = \frac{\partial n}{\partial t}$$

$$\Delta q = \frac{\partial q}{\partial t}$$

remain unchanged. The third equation must be changed. If a neutron is absorbed at $t = 0$, 99 percent of the fission neutrons are delivered imme-

diately and 1 percent are delivered later. At any instant about 99 percent of the neutrons delivered are prompts and about 1 percent are delayed neutrons from previous fissions. If p is the fraction of neutrons that are delayed, the number of neutrons made per unit time in an *equilibrium* pile is:

$$q_0 = \underset{\uparrow}{\frac{k\upsilon}{\Lambda}(1-p)\,n} + \underset{\uparrow}{p\frac{k\upsilon}{\Lambda}n} = \text{same number as if all were prompt}$$

prompt neutrons delayed neutrons from previous fissions.

If the n's in the two terms are different, we are not dealing with an equilibrium pile and it is necessary to know the time distribution of delays. The fraction of delayed neutrons emitted in time dt at the time t is:

$$\sum_i \frac{p_i}{\theta_i} e^{-t/\theta_i}$$

where the θ_i are the various delayed neutron periods.

If we are at a time t and we look back an interval of time dt' at a time $t-t'$, we see that there were $k(v/\Lambda)\,n(t-t')\,dt'$ absorptions then. The number of neutrons appearing at t as delays from these absorptions in the interval dt' is:

$$\frac{k\upsilon}{\Lambda} n(t-t')\,dt' \sum_i \frac{p_i}{\theta_i} e^{-t'/\theta_i}.$$

Thus,

$$q_0 = \underset{\uparrow}{\frac{k\upsilon}{\Lambda} n(t)(1-p)} + \underset{\uparrow}{\frac{k\upsilon}{\Lambda}\int_0^\infty n(t-t')\,dt' \sum_i \frac{p_i}{\theta_i} e^{-t'/\theta_i}}.$$

prompt delayed

This then is the equation we must use instead of the third equation of the previous section when we wish to take the delayed neutrons into account.

We seek a solution of the same form as before:

$$n = c\,\varphi(x,y,z)\,e^{t/T}$$

substituting this into the q_0 equation:

$$q_0 = \frac{k\upsilon}{\Lambda}(1-p)\,n + \frac{k\upsilon}{\Lambda} c\varphi\, e^{t/T} \int_0^\infty e^{-t'/T}\,dt' \sum_i \frac{p_i}{\theta_i} e^{-t'/\theta_i}$$

which is:

$$\frac{k\upsilon}{\Lambda} n(t)\left[(1-p) + \sum_i \frac{p_i}{\frac{\theta_i}{T}+1}\right] \equiv An.$$

Just as before we find:

$$q = q_0 e^{-\omega\tau} = An\, e^{-\omega\tau}$$

for the q equation, but for the n equation,

$$-\frac{\lambda\upsilon}{3}\omega n - \frac{\upsilon}{\Lambda} n + An\, e^{-\omega\tau} = n/T$$

so that the life time is:

$$T = \left[-\frac{\lambda v}{3}\omega - \frac{v}{\Lambda} + \frac{kv}{\Lambda}\left(1 - p + \sum_i \frac{p_i}{(\theta_i/T)+1}\right) e^{-\omega\tau}\right]^{-1}.$$

Homework: Calculate the dimension for a cylindrical pile of arbitrary relative dimensions given k and the fact that the pile is in equilibrium.

The expression for T can be rewritten:

$$T = \left[-\frac{\lambda v}{3}\omega - \frac{v}{\Lambda} + e^{-\omega\tau}\left(1 - \sum_i \frac{p_i \theta_i}{\theta_i + T}\right)\frac{kv}{\Lambda}\right]^{-1}$$

and one can solve for k as a function of the period T.

$$k = \frac{e^{\omega\tau}\left(\frac{\Lambda}{v}\frac{1}{T} + 1 + \frac{\lambda\Lambda}{3}\omega\right)}{1 - \sum_i \frac{p_i \theta_i}{T + \theta_i}}$$

where $\left(1 + \frac{\lambda v \omega}{3}\right) e^{\omega\tau}$ is k_o, the k needed to keep the pile in equilibrium, i.e.,

$$k = \frac{k_o + \frac{\Lambda}{vT} e^{\omega\tau}}{1 - \sum_i \frac{p_i \theta_i}{\theta_i + T}}.$$

Note that as T approaches infinity (pile at equilibrium) k approaches k_o.

Since the second term of the denominator is small, we can write without appreciable error

$$k = \left(k_o + \frac{\Lambda e^{\omega\tau}}{vT}\right)\left(1 + \sum_i \frac{p_i \theta_i}{\theta_i + T}\right).$$

Since Λ = about 300 cm, v = about 2×10^5, T = about 1 sec, the second term in the first factor is small compared to k_o, which is about = 1. Therefore, multiplying out,

$$k = k_o\left(1 + \frac{\Lambda e^{\omega\tau}}{v k_o T} + \sum_i \frac{p_i \theta_i}{\theta_i + T}\right).$$

The relative excess of reactivity $(k - k_o)/k_o$ can be written:

$$\frac{k - k_o}{k_o} = \frac{\theta_o}{T} + \Sigma \frac{p_i \theta_i}{\theta_i + T} \qquad \text{where } \theta_o = \frac{\Lambda e^{\omega\tau}}{v k_o}$$

θ_o is approximately Λ/v (since $e^{\omega\tau}$ and k_o are of order 1), which is the life-time of a neutron. For T large:

$$\frac{k - k_o}{k_o} = \frac{\theta_o + \Sigma p_i \theta_i}{T}.$$

What is the physical meaning of the numerator in this expression? The average length of time of a generation is:

$$\theta_o (1 - p) + \sum_i p_i (\theta_i + \theta_o)$$

where θ_o is the generation time for prompts and $\theta_i + \theta_o$ is the generation time for a neutron delayed θ_i seconds. This expression is exactly equal to the numerator in $(k - k_o)/k$ for T large.

Some of the known neutron delays for U^{235} are given below. Using these data, let us get an idea of the magnitude of the average length of time of a generation. θ_o is about 0.0015 sec and $\Sigma p_i \theta_i$ is about 0.083 sec. Thus, the contribution to the generation time of the delays is about 60 times that of the prompt.

$p_i \times 100$	θ_i
0.077	0.6 sec
0.220	2.2
0.194	6.51
0.152	31.7
0.023	80.2
0.666	

Were there no delays, it is seen that T would be very short even for small excess k.

Writing the formula for $(k - k_o)/k_o$ for short periods, i.e., for T much less than θ_i, we have

$$\frac{k - k_o}{k_o} = \frac{\theta_o}{T} + p$$

and the excess k depends mainly on the prompts, for p is small. In practice one operates a pile with T much greater than θ_i, and there, we have seen that the delayed neutrons do play a considerable role.

Homework: Given $\theta_o = 0.0015$, plot $(k - k_o)/k$ vs. $1/T$ using the complete formula:

$$\frac{k - k_o}{k_o} = \frac{\theta_o}{T} + \frac{\Sigma p_i \theta_i}{\theta_i + T}.$$

Since the critical dimensions of a pile depend on $k - 1$ where k is close to one, small errors in k give rise to large uncertainties in necessary pile dimension. To ckeck these dimension and k one can do the following experiment. Construct a small (say 1/10 the size of the pile) lattice work of the type to be used and place a neutron source at the middle of one end. If the neutron intensity is measured up along the axis of this column away from the source, one finds an exponential decay, and it can be shown that the period of this decay is very simply related to the critical dimensions of the pile.

Consider the three equations:

$$\frac{\lambda v}{3}\Delta n - \frac{v}{\Lambda}n + q = 0 \quad , \quad \Delta q = \frac{\partial q}{\partial \tau} \quad , \quad q_0 = \frac{kv}{\Lambda}n$$

once again. Assume again that the space dependence in the steady state solution for our piece of lattice is: $\varphi(x, y, z)$ where $\Delta\varphi + \omega\varphi = 0$. We take the form $\varphi = \sin\frac{\pi x}{a}\sin\frac{\pi y}{a}e^{-\frac{z}{b}}$ (a is the side of the column, b is the decay factor in the exponential). For this φ, ω is simply $\frac{2\pi^2}{a^2} - \frac{1}{b^2}$. With this ω, we can find the reproduction factor from the three equations of the pile. As before $k = \left(1 + \frac{\lambda\Lambda\omega}{3}\right)e^{\omega\tau}$ and we can, therefore, measure a and b and find k. To find the critical size of a cubical pile of side A, we merely write $\omega = \frac{2\pi^2}{a^2} - \frac{1}{b^2} = \frac{3\pi^2}{A^2}$, for the equation $k = \left[1 + \frac{\lambda\Lambda}{3}\left(\frac{2\pi^2}{a^2} - \frac{1}{b^2}\right)\right]e^{\left(\frac{2\pi^2}{a^2} - \frac{1}{b^2}\right)\tau}$ gives the k of the infinite lattice for the substance discussed in terms of the measured quantities, and we have already seen that $k = \left(1 + \frac{\lambda\Lambda}{3}\frac{3\pi^2}{A^2}\right)e^{\frac{3\pi^2}{A^2}\tau}$ gives the dimension A of an equilibrium cubical lattice, for any k. Thus, A is determined as a function of a and b.

(7) *Control of a Pile.*

A pile is always constructed somewhat over critical size, because for a pile to be workable T must be reasonably small. Furthermore, k is temperature dependent and one must be able to compensate for this. One must also be able to compensate for the absorption due to the foreign materials, if one wants to use the pile for, say, making radioactive substances. Thus, a pile is planned with excess activity and control rods are relied upon to vary k from below to above 1. One might use a cadmium rod which is inserted to various depths in a channel of the pile.

(8) *Absorbers in the Pile.*

If $n \sim \sin\frac{\pi x}{a}\sin\frac{\pi y}{b}\sin\frac{\pi z}{c}$ it is not true that the absorptivity at any point in the pile is proportional to n. Consider an atom at the center of a pile and one near the periphery. The effect of these atoms is proportional approximately to the square of n at the two positions as far as absorption is concerned. The reason for this is along the following lines. Neutrons absorbed by a centrally located atom are more likely to be of service in the pile than peripheral neutrons. The effective absorption is really neutron density $\times$ effectiveness of neutrons. It can be shown that the second factor is proportional to n and so the product goes as n^2. Thus, if a control rod is inserted into a pile to depth d, (fig. 80) the dependence of the absorption of the rod on d is proportional to

$$\int_0^d \left(\sin\frac{\pi x}{a}\right)^2 dx.$$

One can use control rods to test samples of graphite or absorbing materials. One builds the pile with a channel for the insertion of samples (fig. 81).

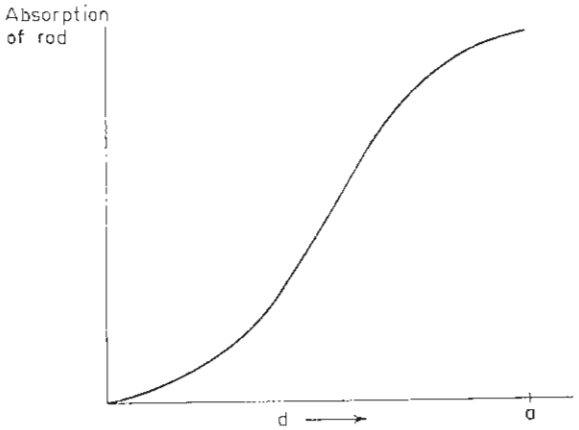

Fig. 80. – Absorption of rod as a fuction of length inserted.

The critical (equilibrium) position for the control rod with no sample is determined. Then new critical positions are determined and the differences in critical position are a measure of absorptivity of the sample. One can use such a scheme to determine reactivities correct to five significant figures for pieces of uranium.

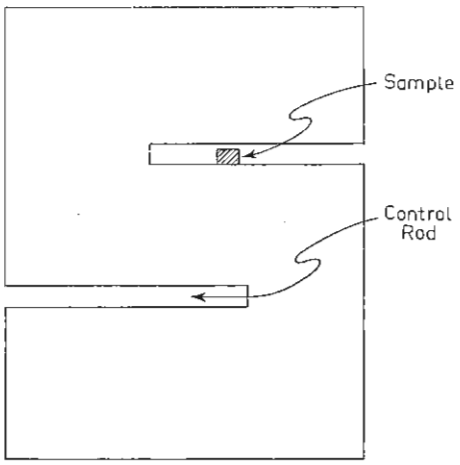

Fig. 81. – Method for measuring absorption of a sample.

(9) *Energy Production of a Pile.*

The number of fission produced per cc per second in a pile is $(f_t \, nv/\Lambda) \frac{3.9}{7.2}$ where the factors are: the fraction of thermals absorbed by the uranium, the neutron density, the reciprocal lifetime of a thermal neutron, and the fraction of neutrons absorbed by uranium that lead to fissions. Assum-

ing 200 Mev per fission, we must multiply the number of fissions/sec cc by 200 Mev/fission = 0.00032 ergs/fission in order to get ergs/sec cc. In the resulting expression the product nv, the flux appears. We should use $\overline{nv}$ the average flux, and it can be shown that for a cube this is related to $n_0 v$, the flux at the middle by equation: $\overline{nv} = n_0 v \frac{8}{\pi^3}$. Finally, kilowatts $= n_0 v \left(\frac{8}{\pi^3} V \frac{f_i}{\Lambda} \frac{3.9 \times 3.2}{7.2} \times 10^{-14}\right)$. Putting in proper numbers, this is approximately $4 \times 10^{-9}\ n_0 v$. One can obtain powers of the order 2.5×10^3 kw (at Clinton) which means that the flux at the center is approximately 10^{+12}. At Hanford neutron fluxes at the center of the piles are approximately 10^{13} n/sec cm^2.

(10) *Pile Shielding.*

In a 1 kilowatt pile there are 3×10^{13} fissions/sec. Asssuming 20 Mev of gamma radiation per fission and that 50 percent of this is not absorbed then the total radiation from the pile of kw is 3 kw $\times 10^{13}$ gammas of approximately 1 Mev or the equivalent. For a pile of area $4\pi (500)^2$ someone near the pile would get in one day (10^5 sec)

$$\frac{\text{kw} \times 3 \times 10^{13}}{4\pi (500)^2} \times 10^5 \sim 10^{12} \times \text{kw} \frac{\text{1 Mev photons}}{\text{cm}^2 \text{ day}}.$$

Now a daily dose is approximately 10^8 photons/cm^2 day. This corresponds to about 1 R unit. Thus, a pile gives of the order

10^4 kw daily doses/day.

This gives an idea of the difficulty of the shielding problem. For large piles we must shield by a factor of a billion or so. In addition to the problem of shielding from the gammas, one must shield from the neutrons. One can use cadmium to shield from thermal neutrons, but one must be careful to put the cadmium inside the lead shield used to cut out the gammas since the (n, γ) reaction in the cadmium makes many gammas. However, neither the Cd nor the Pb are very effective against the very fast neutrons. Concrete can be used to help cut down the fast neutrons. It helps slow them down and capture them. However, concrete is bulky. Layers of Fe alternated with layers of paraffin form a less bulky and somewhat more effective shield. Around 4 feet will absorb the gammas by a factor 10^9 and a reasonable amount of the neutrons.

Since gammas will attenuate approximately 1/e in 25 gr/cm^2, we would need at least 500 gr/cm^2 to attenuate only the gammas by 10^8. Since we need neutron protection too, a compromise shield will be at least 1000 gr/cm^2. This makes the lightest portable nuclear energy source about 50 tons.

In Clinton the cooling system is an air system, which blows through the channels for the uranium. None of the fission product gases give trouble (the uranium slugs are in Al cans) but some of the argon in the air becomes radioactive. The air is disposed of through a 100 foot stack. The cooling

system at Hanford is a water system. There the problem of disposing of radioactive water arises. It is diluted to harmlessness (the salmon of the Columbia River are still healthy).

(11) *Other Types of Piles.*

Heavy Water:

At Argonne there is a D_2O pile that can run at 300 kw (fig. 82). For this pile $n_0 v = 10^{12}$ or the same as for the 5000 kw Clinton pile. The reason the latter has so much more power is due to the fact that there is more uranium in the

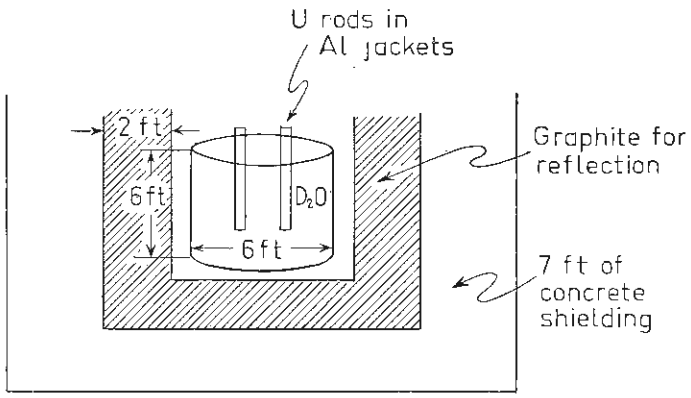

Fig. 82. – Heavy water pile.

Clinton pile. Heavy water has the advantage over carbon that it makes a low power pile easier to cool. It also can be made smaller in size. An important disadvantage is the decomposition of water by the radiation of the pile. Only 100 ev will decompose a molecule. In a homogenous pile, (for example a solution), this would be especially serious for most of the 200 Mev per fission would be picked up by the water and approximately 2 mg per kw per sec would be decomposed. This would necessitate schemes for recovery of the D_2.

Enriched Uranium Water Boiler:

One can use different materials as moderators if enriched rather than natural uranium is used. Since for every 3.9 neutrons absorbed in 235 giving fission, 0.7 and 2.5 give gammas in 235 and 238 respectively, it is seen that the number of neutrons per thermal absorbed by uranium would be $3 \cdot 9/4.6 \times 2.4 = 2.05$ rather than $3.9/7.1 \times 2.4 = 1.32$ if we used pure 235. Actually even a 14 percent enrichment of 235 makes a considerable difference, and this is the material used with the water boiler at Omega (*) (fig. 83). Water

(*) This is the name of a canyon at Los Alamos, where the water boiler was built. (Editors' note.)

makes a good enough moderator. This particular pile can run approximately 5 kw. One problem connected with this pile is the disposal of radioactive fission products. Such piles are small and it is feasible to build them for use as sources of neutrons for experimental purposes.

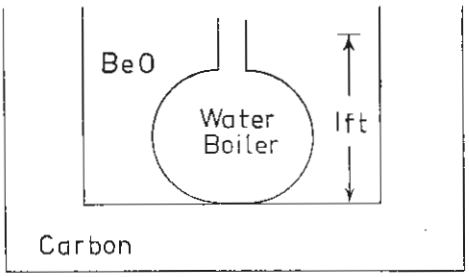

Fig. 83. – Los Alamos water boiler.

CHAPTER X

Fast Neutron Chain Reactions.

In a thermal pile a neutron lives approwimately 10^{-3} sec. With $k = 1.1$ a generation will last of the order $10^{-3}/0.1 = 10^{-2}$ sec. This is the e–folding time for we have seen that T, the e–folding time, is the lifetime of a neutron divided by $(k - k_0)$. In a water boiler $\Lambda = 50$ cm, $v = 10^5$ cm/sec and $k = 2$ so that the e–folding time is $\Lambda k/v = 10^{-4}$ sec. In a fast reactor (say U^{235} or Pu) $\Lambda = 10$ cm, $v = 10^9$, $k = 2$ so that for a fast reactor $T = 10^{-8}$ sec. All the times given are minima, i.e., we have assumed the most favorable conditions in each type of reactor. For the industrial problem the advantage is in longer e–folding times, for it is such reactors which are most controllable. Foe explosives it is short e–folding time that is important.

In a kg of fissionable material there are about 2×10^{24} atoms. If a is the reciprocal of the e–folding time, then a reaction could continue less than t seconds where $e^{at} = 10^{24}$. This would give times $t = 0.5$, 0.005 seconds and 0.5 micro seconds for the graphite pile, water boiler, and fast reactor respectively. Actually mechanical effects begin to take place at 5 or 6 e–folding times before the end (using up all the material). What happens here is that after many generations the energy release is great enough so that pressures expand the reactor, its surface increases, leakage increases and eventually the reactor falls below critical and from there on the reaction dies out (fig. 84).

Let us consider this more quantitatively. Say the pressure goes up as $p = p_0 e^{at}$, and we are dealing with a spherical reactor. The surface will feel an acceleration that is of order $\ddot{R} = pR^2/M$. Since the exponential varies much more rapidly with time than R, in orders of magnitude the displacement of the surface as a function of time is:

$$\delta R = \frac{p_0 R^2}{M} \frac{e^{at}}{a^2} = \frac{pR^2}{Ma^2}$$

where p is the pressure at time t. Let us use this to find the maximum pressure. δR at this time will be of order of the difference of R_0 and the radius of the just critical sphere. The energy released up to the point that the

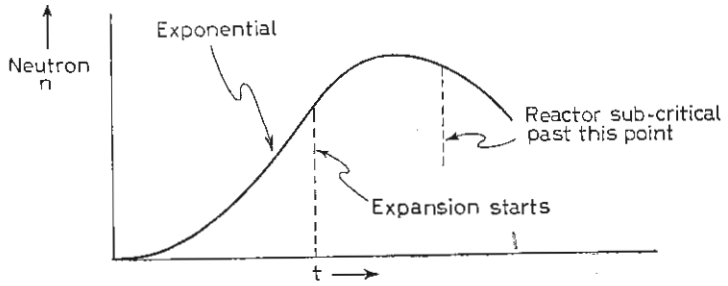

Fig. 84. – Neutron density as a function or time.

criticalty goes below 1 is of order $p_{max}\, 4\pi R^3/3 = (p$ times the volume). Thus, the energy, W = approximately M a^2 R δR, and it is seen that a enters as the square. Clearly, to produce an explosion, we must use a reactor with the shortest possible e–folding time.

Let us calculate the critical properties of a fast reactor of the type shown. in fig. 85. In such a reactor the size of active material is about 10 cm and the mean free path is about 10 cm. Consequently, we cannot use the approach we used in pile theory, that is we cannot use diffusion theory for it is not true that mean free paths are much less than the dimensions of the system. In the approach to be considered we shall have to introduce the transport cross section, (i.e., the cross section modified to take account of the non-isotropic elastic scattering). Let us call σ the total transport cross section of all the atoms per cc. Then (since $\sigma N\lambda \equiv 1$) this cross section is simply the reciprocal of the transport mean free path. In addition to elastic scattering there are other processes.

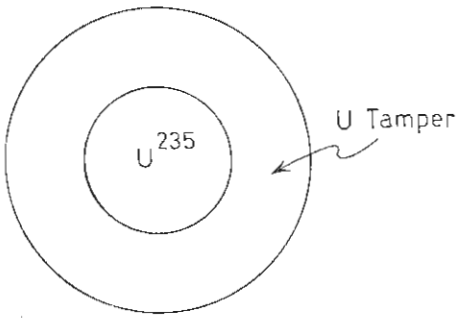

Fig. 85. – Fast reactor.

	Number of Neutrons Hitting Nucleus	Number of Neutrons Leaving
Capture	1	0
Inelastic Scattering . .	1	1
Fission	1	ν

On the average, for every neutron hitting a nucleus, $1 + f$ come out, where f is either positive or negative depending on the type of material

used. $1+f$ can be written in general:

$$1+f=\frac{0\times\sigma_a+1\cdot\sigma_{sc}+\nu\sigma_f}{\sigma_{tot}} \qquad \text{or} \qquad f=\frac{-\sigma_a+(\nu-1)\sigma_f}{\sigma_{tot}}.$$

In a non-fissionable material $f=-\frac{\sigma_a}{\sigma_{sc}+\sigma_a}$ and f is negative and the absolute value of f is less than 1. For a chain reaction $f>1$. In order to describe a reactor, we will specify σ and f where σ is the transport cross section defined above. In a proper calculation one would consider what happens to neutrons in various energy ranges, but for our purposes we shall assume that all the neutrons have some average energy.

We must establish an integral equation for the neutron density. If at a certain point, one neutron is produced each second, what is the neutron density at a distance r from this point if the emission is isotropic? The time spent in a shell of volume $4\pi r^2 dr$ by a neutron is dr/v. The average number of neutrons found in the shell is also dr/v since 1 neutron is emitted per second. The neutron density at the distance r is then dr/v divided by the volume element or $1/4\pi r^2 v$. It is to be remarked that this result is based on the assumption that there is no absorption in the medium. We wish to find $n(\mathrm{A})$, the neutron density at a point A in the medium. To find this, find the contributions to this density of a volume element at B, i.e., we find how many collisions at B result in scatterings in the direction of A. We then integrate the volume element $d\mathrm{B}$ over all space. In the volume element $d\mathrm{B}$ there are $n(\mathrm{B})\,v\,\sigma(\mathrm{B})\,d\mathrm{B}$ collisions per second. $n(\mathrm{B})\,v\,\sigma(\mathrm{B})\,[1+f(\mathrm{B})]\,d\mathrm{B}$ neutrons come out of the volume element $d\mathrm{B}$ each second. Thus, $d\mathrm{B}$ can be thought of as a neutron source of this strength. But we have seen that such a source will give a density:

$$n(\mathrm{B})\,d\mathrm{B}\,v\,\sigma(\mathrm{B})\,[1+f(\mathrm{B})]/4\pi r^2 v$$

at a point r away if there is no absorption and the emission is isotropic. We can account for the absorption by multiplying by a factor $e^{-\int_{\mathrm{A}}^{\mathrm{B}}\sigma\,dr}$. Thus,

$$n(\mathrm{A})=\int\frac{n(\mathrm{B})\,\sigma(\mathrm{B})\,[1+f(\mathrm{B})]\,e^{-\int_{\mathrm{A}}^{\mathrm{B}}\sigma\,dr}}{4\pi r_{\mathrm{AB}}^2}d\mathrm{B}$$

and this is the integral equation we sought. A system in chain reacting equilibrium will obey:

$$\int_{\text{all space}} n(\mathrm{A})\,d\mathrm{A}\,\sigma(\mathrm{A})\,f(\mathrm{A})=0$$

for there will be no net production of all space neutrons in the system.

Before we solve these equations for a particular problem, let us return to differential theory. We had $l=\lambda\sqrt{\mathrm{N}/3}$ where $\mathrm{N}=\sigma_{tot}/\sigma_{abs}$. We assumed that the flux of neutrons is proportional to the gradient (neglecting higher

derivatives). This is the same as assuming that $n(x)$ is a function that is fairly linear for distances of order λ. In a one dimensional problem $n(x)$ goes as $e^{x/l}$. For this function to show little curvature in a distance λ, it is necessary that λ/l be a small number, or that N be large. Thus, our original diffusion equation implicitly assumed that N be large. In addition, we assumed isotropic scattering and a one velocity problem. We shall retain these assumptions, but try to modify differential diffusion theory to be valid for N small. Say we have a gradient of neutrons travelling in the direction of the x axis. Because of this gradient the density of neutrons travelling at any angle θ to the x axis is not the same for all θ at a given point, but is a maximum for neutrons moving in the direction of the gradient. The neutron density moving at the angle θ at the point x is: $n(x, \theta)\, 2\pi \sin\theta\, d\theta$, or writing $\xi = \cos\theta$, is $n(x, \xi)\, 2\pi d\xi$ where $2\pi d\xi$ is the element of solid angle. We wish to establish an equation for $n(x, \xi)$. We follow the procedure of examining all the factors for the variation of n with time.

Since we are assuming that all neutrons have the same velocity, neutrons everywhere moving in a direction ξ will have an x component of velocity $v\xi_0$. If n varies with x, then the change in $n(x, \xi_0)$ in time dt will be:

$$n(x - v\xi_0\, dt) - n(x) \qquad \text{which is simply}$$

$$-v\xi_0\, dt\, (dn/dx)$$

where we have considered neutrons moving in the specific direction ξ_0.

Another source of loss of neutrons out of the element $dx\, d\xi$ being considered is the fact that in each unit time, a number of neutrons, vn/λ will suffer collisions. If the neutrons in dx were initially moving in direction ξ, once they have collided they will be moving in some other direction and will no longer belong to the same $dx\, d\xi$.

We must now find how many neutrons are scattered into the solid angle $d\omega$ where $d\omega$ is the element $2\pi d\xi$ of solid angle considered. For the various direction ξ' at x there will be $n(x, \xi')\, d\omega' v/\lambda$ collisions out of $d\omega'$ in unit time. $(N - 1)/N$ of these neutrons will be moving in other directions after collision. $1/N$ will be absorbed. Therefore, the number of neutrons initially moving in direction ξ' that are scattered into the direction ξ in unit time is:

$$n(x, \xi')\, d\omega' \frac{v}{\lambda} \frac{N-1}{N} \frac{d\omega}{4\pi}.$$

We must integrate this over $d\omega'$ to get the total number of neutrons at x scattered into the direction ξ. Per unit solid angle the term to be added to our equation is:

$$\frac{N-1}{2N} \frac{v}{\lambda} \int_{-1}^{+1} n(x, \xi')\, d\xi'.$$

At equilibrium:

$$-\xi \frac{\partial n}{\partial x} - \frac{n}{\lambda} + \frac{N-1}{2N\lambda} \int_{-1}^{1} n(x, \xi')\, d\xi' = 0.$$

To solve this we assume that the solution is separable, i.e., $n(x, \xi) = n(x) f(\xi)$. Further we assume, because of our past experience, that $n(x)$ will be of the form $e^{x/l}$ where l must be determined from the costants of the problem. Substituting into the equation, we find that $f(\xi)$ must obey the following equation:

$$\frac{1}{\lambda} f(\xi) + \frac{1}{l} \xi f(\xi) = \frac{N-1}{2N\lambda} \int_{-1}^{+1} f(\xi')\, d\xi'$$

or:

$$\left(\frac{\lambda}{l} \xi + 1\right) f(\xi) = \frac{N-1}{2N} \int_{-1}^{+1} f(\xi')\, d\xi'.$$

But the right side of the equation is some constant, so that f must be of the form $f(\xi) = \dfrac{c}{1 + \frac{\lambda}{l}\xi}$. We must now make sure, however, that this f has at least some values of l that do give solutions. That is: we have established that if there are solutions, they are of the form above, but we have yet to see if this is true for all l, for some l, or for no l. Substituting into the equation, we find:

$$1 = \frac{N-1}{2N} \int_{-1}^{+1} \frac{d\xi}{1 + \frac{\lambda}{l}\xi}$$

whence:

$$1 = \frac{N-1}{2N} \frac{l}{\lambda} \log\left(\frac{l+\lambda}{l-\lambda}\right).$$

This is an equation that tells us what values of l will solve our problem. To see what the solution is when N is still a fairly large number, develop both sides. First $2N/(N-1) = 2(1 + 1/N + 1/N^2 + \cdots)$. Writing $\lambda/l = \varepsilon$ and assuming that ε is small:

$$\frac{1}{\varepsilon} \log \frac{1+\varepsilon}{1-\varepsilon} = \frac{1}{\varepsilon}\left[\left(\varepsilon - \frac{\varepsilon^2}{2} + \frac{\varepsilon^3}{3} - \cdots\right) + \left(\varepsilon + \frac{\varepsilon^2}{2} + \frac{\varepsilon^3}{3} + \cdots\right)\right] =$$

$$= 2\left(1 + \frac{\varepsilon^2}{3} + \frac{\varepsilon^4}{5} + \cdots\right).$$

Hence $(1/N) + (1/N^2) = \dfrac{\varepsilon^2}{3} + \dfrac{\varepsilon^4}{5}$.

The first approximation gives $\varepsilon^2 = 3/N$, which gives precisely $l = \pm\lambda\sqrt{N/3}$, the result from our rougher differential diffusion theory. In the next approximation we can substitute for the correction term $\varepsilon^4/5$, the first approximation result. Then $(1/N) + (1/N^2) = \dfrac{\varepsilon^2}{3} + \dfrac{9}{5}\dfrac{1}{N^2}$ which gives:

$$\frac{\lambda}{l} = \pm\sqrt{\frac{3}{N}\left(1 - \frac{4}{5N}\right)}.$$

We shall now return to our integral equation making use of what we have developed. In the integral equation $1 + f$ stood for the number of neutrons coming out, on the average, after a collision. For a medium where

there is only capture (no fission) $f = -1/N$ and $\sigma \equiv 1/\lambda$. One can therefore write

$$\frac{1}{l} = \sigma\sqrt{-3f\left(1+\frac{4}{5}f\right)}.$$

It can be shown that this formula applies even with f positive (say for U^{235}) in which case the density goes as $e^{ix/l}$ and $e^{-ix/l}$ and we have sines and cosines. The method of proof that this applies when f is positive would be essentially a repetition of the calculation, where allowance be made for fission.

The equation for $1/l$ was developed under the assumption that n goes as $e^{x/l}$ and is a function of x only. We shall, however, apply this in our more general equation, (for a more exact and laborious calculation can be shown to give quite similar results). This method was developed by Serber and we shall apply it to a simple geometry, i.e., f greater than zero in a spherical core and f less than zero outside. We begin by writing $\Delta n - \frac{1}{l^2} n = 0$ where l is tbe corrected l. That is, we begin with a somewhat improved diffusion theory. On the inside l^2 is less than zero and the solutions are like sines and cosines. Outside l^2 is greater than zero and the solutions are exponentials. We may summarize our results up to this point:

Inside the Sphere (r less than a)	Outside the Sphere (r greater than a)
$\Delta n - \frac{n}{l^2} = 0$	$\Delta n - \frac{n}{l'^2} = 0$
$\frac{1}{l} \equiv \sigma h \qquad \mathrm{H}i = h$	$\frac{\lambda'}{l'} \equiv h' \quad \text{and} \quad \frac{N}{N-1} = \frac{1}{2h'} \log \frac{1+h'}{1-h'}$
$\frac{1}{1+f} = \frac{1}{2i\mathrm{H}} \log \frac{1+i\mathrm{H}}{1-i\mathrm{H}}$	$\text{or} \quad \frac{1}{1+f'} = \frac{1}{2h'} \log \frac{1+h'}{1-h'}$
$= \frac{1}{\mathrm{H}} \arctan \mathrm{H}$	$\text{since} \quad f' = -\frac{1}{N} \quad , \quad \sigma' = \frac{1}{\lambda'}.$

In either case $\Delta n(r) = d^2n/dr^2 + (2/r)(dn/dr)$ so that:

$$r\frac{d^2n}{dr^2} + 2\frac{dn}{dr} = \frac{1}{l^2} nr$$

but the left side is $\frac{d^2}{dr^2}(nr)$, whence we have an equation of the one-dimensional form in nr. The solutions are $nr = Ae^{-r/l'} + Be^{r/l'}$ on the outside. On the inside $l = -i/\sigma\mathrm{H}$ so that the solutions are $rn = C \sin(\sigma \mathrm{H}r)$ and $D \cos(\sigma \mathrm{H}r)$. In terms of σ' rather than l', the outside solutions are:

$$Ae^{\sigma' h' r} \quad , \quad Be^{-\sigma' h' r}.$$

The first solution is neglected because it represents a diverging case. Similarly the $D \cos(\sigma \mathrm{H}r)$ solution is rejected for the inside. Let us normalize our solutions so that $n(0) = 1$. Then $n = \sin(\sigma \mathrm{H}r)/\sigma \mathrm{H}r$. Outside the solution

is $Be^{-\sigma nr}/r$ where B is determined by fitting the solutions inside and outside at the boundary. Our solutions must fulfill 2 conditions:

$$n(\mathrm{A}) = \int \frac{n(\mathrm{B})\,\sigma(\mathrm{B})\,[1+f(\mathrm{B})]\,e^{-\int_{\mathrm{A}}^{\mathrm{B}}\sigma\,dr}}{4\pi r_{\mathrm{AB}}^2}\,d\mathrm{B}$$

$$\int_{\text{all space}} n(\mathrm{A})\,\sigma(\mathrm{A})\,f(\mathrm{A})\,d\mathrm{A} = 0.$$

We will be unable to do this exactly. We shall try to satisfy the 2nd equation, and the first one only at the center. The 2nd equation will suffice to determine B. Then we substitute into the first equation. If it checks, we are dealing with a critical (equilibrium) assembly. If, however, the first equation does not check, the sphere is either too large or too small for the particular f and f' and we must try a different radius.

Let us, therefore, substitute into the 2nd equation. The integral must be written in 2 parts

$$4\pi\int_0^a \sigma f\,\frac{\sin \sigma \mathrm{H} r}{\sigma \mathrm{H} r}\,r^2\,dr + 4\pi\int_a^\infty \sigma' f'\,\frac{\mathrm{B}e^{-\sigma' h' r}}{r}\,r^2\,dr = 0.$$

Since f' is negative, we may write:

$$\sigma f\int_0^a \frac{\sin \mathrm{H}\sigma r}{\mathrm{H}\sigma r}\,r^2\,dr = \sigma'\,|f'|\,\mathrm{B}\int_a^\infty \frac{e^{-\sigma' h' r}}{r}\,r^2\,dr.$$

This gives:

$$\mathrm{B} = \frac{h'^2\sigma' f}{\mathrm{H}^3\sigma^2(1-f')}\;\frac{\sin(\mathrm{H}\sigma a) - \mathrm{H}\sigma a\cos(\mathrm{H}\sigma a)}{1+h'\sigma' a}\,e^{h'\sigma' a}.$$

We now substitute into the first integral equation, letting A refer to the point $r = 0$. Since $n(0) = 1$, we may write (once again splitting the integral into two parts):

$$1 = \int_0^a \frac{\sin \sigma \mathrm{H} r}{\sigma \mathrm{H} r}\,\sigma(1+f)e^{-\sigma r}\,\frac{4\pi r^2}{4\pi r^2}\,dr + \int_0^\infty \mathrm{B}\,\frac{e^{-\sigma' h' r}}{r}\,\sigma'(1+f')\,e^{-\sigma a-\sigma'(r-a)}\,\frac{4\pi r^2}{4\pi r^2}\,dr.$$

The integrals here are slightly more difficult than the others, but they are in the tables. Putting in the value of B the result is:

$$\frac{1+f}{f}(\mathrm{H}\sigma a)^2\,\frac{e^{\sigma a \arctan \mathrm{H}} - \int_0^{\sigma a}\frac{\sin \mathrm{H}x}{x}e^{-x}\,dx}{\sin \mathrm{H}\sigma a - \mathrm{H}\sigma a\cos \mathrm{H}\sigma a} = \frac{1+f'}{f'}\,\frac{(h'\sigma' a)^2 e^{-\sigma' a(1+h')}}{1+h'\sigma' a}\left[\int_{(1+h')\sigma' a}^\infty \frac{e^{-x}}{x}\,dx\right].$$

On the left appear quantities related to the core. On the right are the quantities related to the reflector or tamper. We substitute in this equation the values for f and H for the particular materials being considered. We then can plot the left and right hand sides as a function of a. The curves will intersect at some point and this value of a is the critical or equilibrium radius.

Having found the critical radius, we may find B and we can plot n as a function of r. It will be found that the curves show a discontinuity. This discontinuity, will not actually exist, but will almost exist. That is, the gradient of n is fairly sharp at the boundary, as can be shown by a more exact calculation.

With not very involved modifications, the theory here discussed can give information about supercritical as well as equilibrium systems. We had written:

$$n\,(\mathrm{A}) = \int n\,(\mathrm{B})\,\sigma\,(\mathrm{B})\,\frac{(1+f_{\mathrm{B}})\,e^{-\int_{\mathrm{A}}^{\mathrm{B}}\sigma\,dr}}{4\pi r_{\mathrm{AB}}^2}\,d\mathrm{B}.$$

This equation says that all the neutrons in A at a time t come from points B where they suffered their last collision at some earlier time, t'. In a system at equilibrium the times are of no moment in the final results, but for a supercritical system we should know $t - t' = r/v$. If the intensity goes as $e^{\alpha t}$ all over the system, the intensity at B at the time t' was $e^{-\alpha r/v}$, what it is at t. Thus, we can substitute into the equation for $n\,(\mathrm{A})$,

$$n\,(\mathrm{A}) = \int n\,(\mathrm{B})\,\sigma\,(\mathrm{B})\,\frac{(1+f_{\mathrm{B}})\,e^{-\int_{\mathrm{A}}^{\mathrm{B}}\sigma\,dr-\frac{\alpha r}{v}}}{4\pi r_{\mathrm{AB}}^2}\,d\mathrm{B}.$$

The equation is now modified to say: "The neutrons at A at the time t are the neutrons suffering their last collisions at a distance r away (and coming off in the proper direction) at a time r/v earlier than t." We have simply substituted $n\,(\mathrm{B})\,e^{-\alpha r/v}$ for $n\,(\mathrm{B})$ to take account of the variation in $n\,(\mathrm{B})$ with time. It is to be noted, however that the term $e^{-\alpha r/v}$ appears in the same form as $e^{-\int_{\mathrm{A}}^{\mathrm{B}}\sigma\,dr}$, the absorption term. Regarding this new term in this light, we can solve for α, the reciprocal of the e-folding time, for a supercritical assembly as follows. Say that we have a core of material with $a = 20$ cm, but that a solution of the equilibrium type indicates that $a = 10$ cm is the critical radius. It is clear that if there were more absorption, the critical radius would be larger and that one could, in fact, find how much absorption would be necessary to make $a = 20$ cm the critical radius. We solve the problem by finding an α that will make $a = 20$ the critical radius. With this value of α both integral equations will hold for the value $a = 20$. In this way one can determine the e-folding time.

N° 223.

Shortly after the end of the war, while he was still living in Los Alamos, Fermi had his first opportunity to talk about the work on the chain reaction and the pile before an academic audience. The partial lifting of secrecy had created the desire, in those who had worked in the atomic field, to let the scientific community know what had been done. At the same time, the scientific community was very eager to learn how atomic power was achieved.

The American Philosophical Society of Philadelphia took the initiative and planned to devote its general autumn meeting to atomic energy. Because this topic would be of interest also to members of the National Academy of Sciences, this academy was approached and a joint meeting was arranged. The *Symposium on Atomic Energy and its Implications* took place in Philadelphia on November 16 and 17, 1945. Other speakers, beside Fermi who presented a paper on the development of the first chain reaction (N° 223), were: for the scientific aspects, J. D. Smyth, H. C. Urey, E. P. Wigner, J. A. Wheeler; for atomic weapons, J. R. Oppenheimer; for health protection, R. S. Stone; for the social, international and humanistic implications, J. H. Willits, J. Viner, and A. H. Compton; for the problems of controlling energy, J. T. Shotwell and I. Langmuir.

The importance of the subject, the joint sponsorship of the two outstanding societies, and the caliber of the speakers made the symposium very successful and drew an attendance of about six hundred members of the two societies and special guests.

H. L. ANDERSON.

223.

THE DEVELOPMENT OF THE FIRST CHAIN REACTING PILE

(*Read November 17, 1945, in the Symposium on Atomic Energy and its Implications*)
« Proc. Amer. Phil. Soc. », 90, 20–24 (1946).

It has been known for many years that vast amounts of energy are stored in the nuclei of many atomic species and that their release is not in contradiction with the principle of the conservation of energy nor with any other of the accepted basic laws of physics. In spite of this recognized fact, it was the general opinion among physicists until recently that a large scale release of the nuclear energy would not be possible without the discovery of some new phenomenon.

The reasons for this somewhat negative attitude were the following: Two types of processes in which nuclear energy could be released might be considered in principle. Various nuclear reactions take place spontaneously with production of energy when two nuclei are brought in contact. The simplest of many possible examples is perhaps that of ordinary hydrogen. Two hydrogen nuclei when brought in contact are spontaneously capable of

reacting forming a deuterium nucleus and emitting an electron. The energy liberated in this process is about 1.4 Mev per process, equivalent to 1.6×10^{10} calories per gram or about two million times the combustion energy of an equal amount of coal. The reason why hydrogen is not a nuclear explosive is that two hydrogen nuclei never come in contact under ordinary conditions, owing to the repulsion of the positive electric charges of the two nuclei. There is no theoretical reason that prevents the coming together of the two nuclei; indeed this could be achieved both by very high temperatures and by very high pressures. Temperatures or pressures that are, however, well beyond the limits that could be achieved by ordinary means. Actually, temperatures large enough to permit nuclear reactions to proceed at an appreciable rate are prevalent in the interior of many stars, in particular of the sun; these reactions are generally recognized as the main source of the energy irradiated by the stars.

A second possible pattern for the liberation of nuclear energy is the chain reaction. In most nuclear disintegrations particles are emitted (α-particles, protons, or neutrons) which in their turn are capable of producing new reactions. One can then conceive the possibility that when a first reaction takes place the particles produced by it may have a sufficient activity to determine in the average more than one similar reaction. When this is the case, in each "generation" the number of reacting nuclei increases until the process "burns" a sizable fraction of the original material. Whether the chain reaction develops or not depends on whether the number of new processes produced by the particles emitted by a first process is larger or smaller than one. This number is called "reproduction factor."

For all processes known until the discovery of fission early in 1939, however, the reproduction factor was in all cases enormously smaller than one. The fission process opened a new way. Almost immediately after the announcement of the discovery the possibility was discussed that when the two fragments separate they may be excited so highly that neutrons may "evaporate" out of them. This conjecture was soon confirmed by experimental observations on both sides of the Atlantic.

In the spring of 1939 it was generally known that a fission that can be produced by the collision of a single neutron with a uranium atom was capable of producing more than one new neutron, probably something of the order of two or three. It was felt at that time by many physicists that a chain reaction based on the uranium fission was a possibility well worth investigating.

At the same time this possibility was viewed with hope and with great concern. Everybody was conscious early in 1939 of the imminence of a war of annihilation. There was well founded fear that the tremendous military potentialities that were latent in the new scientific developments might be reduced to practice first by the Nazis. Nobody at that time had any basis for predicting the size of the effort that would be needed, and it well may be that civilization owes its survival to the fact that the development of atomic bombs requires an industrial effort of which no belligerent except the United States would have been capable in time of war. The polit-

ical situation of the moment had a strange effect on the behavior of scientists. Contrary to their traditions, they set up a voluntary censorship and treated the matter as confidential long before its importance was recognized by the governments and secrecy became mandatory.

To proceed with the steps that led to the development of the chain reaction, I would like to point out that, on the basis of the information available at the end of 1939, two lines of attack to the problem appeared worthwhile. One involved as a first step the separation out of ordinary uranium of the rare isotope 235 which is responsible for the slow neutron fission of uranium. Since this separation eliminates the parasitic absorption of neutrons by the abundant isotope 238, it was felt that once uranium containing a high percentage of 235 were available it would be easy to produce a chain reaction. The real difficulty was of course to obtain isotope separation on a large scale.

The second line of attack, the one that I propose to discuss in this paper, envisaged the use of natural uranium. The problem to assemble this material in a way proper to produce a chain reaction is of course considerably more tricky than the similar problem for U^{235}. Indeed the neutrons produced by a primary fission must be used very sparingly in order to keep a positive surplus in spite of the loss due to the large parasitic absorption of U^{238}. Great care must be exerted in order to make the balance between useful and parasitic absorption of the neutrons as favorable as possible. Since the ratio of the two absorptions depends on the energy of the neutrons and, aside from details, is greater for neutrons of low energies, one of the steps consists is slowing down the neutrons from their initial high energy, which is of the order of 1 Mev, to an energy as low as that of thermal agitation. A simple process to achieve this end has been known for some time. It is based on the obvious fact that when a fast neutron collides against an atom and bounces off some of its energy is lost as recoil energy of the atom. The effect is greater for light atoms which recoil more easily and is maximum for hydrogen but quite appreciable also for all light elements.

In order to slow down the neutrons we shall have, therefore, to spread the uranium throughout a mass of some convenient light element. The most obvious choice would be the lightest element, hydrogen, which has currently been used in its combination forms of water or paraffin for the slowing down of neutrons. Further study indicates, however, that hydrogen is not well suited to the purpose. This is due to the fact that the hydrogen nuclei have an appreciable tendency to absorb neutrons with which they combine to form the heavy hydrogen nucleus, deuterium. For this reason when hydrogen is used for slowing down the neutrons a new parasitic absorption is introduced which eats up dangerously into the small positive excess of neutrons needed to maintain the chain reaction.

Other light elements had, therefore, to be considered for slowing down the neutrons. None of them is as effective as hydrogen for this purpose but it was hoped that their lower absorption might overcompensate for this drawback. Very little was known in 1939 of the absorption properties of many light elements. Only in a few cases rather uncertain upper limits

were to be found in the literature. The most obvious choices appeared at the time to be deuterium in the form of heavy water, helium, beryllium, or carbon in the form of graphite.

In the discussions that we had in the group working on the problem at Columbia University in 1939 and 1940, and which included George Pegram, Leo Szilard, and Herbert Anderson, we reached the conclusion that graphite offered the most hopeful possibilities due primarily to the ready availability of this substance. In the spring of 1940 experimental work on the properties of graphite was initiated at Columbia University using a few tons of graphite supplied to us through the Chairman of the Uranium Committee, Dr. Briggs. Two problems were attacked and solved at that time. One consisted in the determination of the absorption properties of graphite for neutrons and one in the study of its effectiveness for slowing down neutrons. The technique used in these experiments consisted in setting up a square column of graphite a few feet thick. A small source of neutrons consisting of a few grams of beryllium mixed with radon, or radium, was placed on the axis of this column. The neutrons emitted by it diffuse through the column and are gradually slowed down to thermal agitation energy; they keep on diffusing after this until they are either absorbed or diffuse out of the column. The distribution, both in space and energy, of the neutrons throughout the column was mapped using detectors sensitive to neutrons of various energies and the results were fitted into a mathematical theory of the diffusion process. The results of these investigations permitted to develop a mathematical method for calculating with fair accuracy all the life history of a neutron from the moment of its emission as a fast neutron to the moment of its final absorption.

At the same time work was initiated in order to determine the excess number of neutrons emitted by natural uranium when a thermal neutron is absorbed by it. Since a considerable fraction of the thermal neutrons absorbed by uranium is captured by U^{238} and does not give rise to fission, this excess turns out to be fairly small and makes it therefore very essential to avoid as much as possible parasitic losses so as to end up with a positive margin that may make the chain reaction a possibility. A simple trick permits a very considerable reduction of the parasitic losses that take place while the neutron is being slowed down. Instead of spreading the uranium uniformly throughout the mass of graphite, it is more convenient to arrange it in lumps distributed in some suitable lattice configuration throughout the graphite. This device makes it less probable for a neutron to encounter a uranium atom during the slowing down process when its energy makes it particularly vulnerable to parasitic absorption.

In working out the effectiveness of this method, the group working at Columbia was very materially reinforced by the collaboration with a new research group that was set up at Princeton University. In the spring of 1941 sufficient data on the details of the process had been gathered to enable one to form a relatively clear picture of the importance of the various factors and of the best devices to be used in order to minimize the unfavorable items.

In principle it would be possible to measure with great accuracy the absorption and scattering properties of neutrons for all energies and for all

atoms involved and to use these results in a mathematical theory of the process so elaborate as to make it possible to predict the behavior of a given system accurately enough to answer the question whether a given system would or would not be chain reacting purely on a basis of calculation. The practical feasibility of this program did not appear too hopeful. We know now that the positive excess that makes possible a chain reaction in a graphite-uranium system is of only a few percent. Since many factors of absorption and production of neutrons enter in the final result, it is clear that they should be known individually with extreme accuracy to make a prediction possible. The measuring methods developed up to 1941 seldom permitted the measurement of nuclear properties with an accuracy hetter than 10 percent and were therefore inadequate to give a basis for calculations that would permit answering in a reliable way the question of whether the chain reaction with natural uranium and graphite was or was not possible.

In any system of finite dimensions some neutrons escape by diffusing out of its surface. This loss of neutrons by escape can in principle be eliminated by increasing the size of the system. It was clear in 1941 that the balance of neutrons capable of sustaining a chain reaction, even if at all positive, would be so small as to make it necessary to use a system of very large size in order to eliminate most of the loss of neutrons by escape. It was important to devise methods capable of answering the following questions: (1) whether a system containing lumps of uranium distributed through the graphite in a given lattice arrangement would become chain reacting provided its dimensions were infinitely large, and (2) assuming a positive answer to the previous question, what minimum dimensions would be needed actually to achieve the chain reaction? The minimum dimensions are usually called the critical size of the pile. Since the method of detailed calculation from the values measured for the constants was inadequate as explained before, one had to devise some way that would give more directly the required answers.

A brute-force method for this would be to set up a system of the given structure and keep on adding to it until a chain reaction actually is achieved or the system refused to react even when built up to enormous size. This method obviously would be exceedingly expensive both in materials and labor. Fortunately it is possible to obtain a fairly accurate answer to the two questions by using a relatively small sample of the structure under investigation. The first experiments of this type, the so-called intermediate or exponential experiments, were set up at Columbia University in the summer and fall of 1941. A lattice structure was set up containing cans filled with uranium oxide spread throughout a mass of some thirty tons of graphite. A primary source of neutrons was inserted at the bottom of this mass and the distribution of the neutrons throughout the mass was investigated in detail and compared with the theoretical expectation.

The results of this first experiment was somewhat discouraging in that it indicated that a system of that structure, even if built up to infinite size, would still have a negative balance of neutrons and more precisely a loss of 13 percent of the neutrons each generation. In spite of this negative result

hope was not abandoned. Indeed sizable improvements to this first structure could be expected as indicated below.

Early in 1942 all the groups working on the production of a chain reaction were united at the Metallurgical Laboratory of the University of Chicago under the general leadership of Arthur Compton. During 1942 some twenty or thirty exponential experiments were carried out at Chicago in the attempt to improve on the conditions of the first experiment. Two different types of improvements were pursued. One consisted in a better adjustment of the dimensions of the lattice and the other in the use of better materials. Impurities had to be eliminated to a surprisingly high extent from both uranium and graphite since the parasitic absorption due to elements appearing as common impurities in uranium and graphite was responsible for a loss of an appreciable fraction of the neutrons. The problem was tackled to organize large-scale production of many tons of graphite and uranium of an unprecedented purity. Also the production of uranium in metallic form was vigorously pursued. Up to 1941 uranium metal had been produced only in very small amounts, often of questionable purity. Uranium metal was mostly produced in the form of a highly pyrophoric powder which in several cases burst spontaneously into flames when coming in contact with air. These pyrophoric properties were only somewhat reduced by sintering the powder into compact blocks. Some of these sintered blocks were used in exponential experiments carried out in order to obtain information on the properties of a system containing metallic uranium; while the experiments were in progress the blocks were burning so fast that they felt hot to the touch and we were afraid that they might actually burst into flames before we could go through with the experiment.

Toward the fall of 1942 the situation as to the production of materials gradually improved. Through the joint efforts of the staff of the Metallurgical Laboratory and of several industrial firms, better and better graphite was obtained. Industrial production of practically pure uranium oxide was organized and some amount of cast uranium metal was produced. The results of the exponential experiments improved correspondingly to the point that the indications were that a chain reacting unit could be built using these better brands of materials.

The actual erection of the first chain reacting unit was initiated in October 1942. It was planned to build a lattice structure in the form of a huge sphere supported by a wooden structure. The structure was to be erected in a Squash Court on the campus of the University of Chicago. Since we were somewhat doubtful whether the dimensions as planned would be sufficiently large, the structure was actually built inside a huge tent of balloon cloth fabric that in case of need could have been sealed for the purpose of removing the air in order to avoid the parasitic absorption of the atmospheric nitrogen. This precaution actually proved unnecessary.

It took a little over one month to build the structure. A large number of physicists, among them W. H. Zinn, H. L. Anderson, and W. C. Wilson, collaborated in the construction. During this time the approach to the chain reacting conditions was followed day by day by measuring the neutron in-

tensity building up inside the pile. Some neutrons are produced spontaneously by uranium in very small numbers. When the system approaches the critical size, each of these neutrons multiplies for several generations before final absorption. Indeed, when the reproduction factor of the pile is, for instance, 99 percent, each neutron multiplies in the average one hundred generations. Consequently, the density of neutrons increases throughout the mass as the critical dimensions are approached and tends to diverge at the critical size. By watching the rise of the neutron density, one obtains, therefore, a positive method for extrapolating to the critical size.

Appreciably before the dimensions originally planned for the structure were reached, the measurements of the neutron density inside the structure indicated that the critical size would soon be attained. From this time on work was continued under careful supervision so as to make sure that criticality would not be inadvertently reached without proper precautions. Long cadmium strips were inserted in slots that had been left for this purpose in the structure. Cadmium is one of the most powerful absorbers of neutrons and the absorption of these strips was large enough to make sure that no chain reaction could take place while they were inside the pile. Each morning the cadmium strips were slowly removed, one by one, and a determination of the neutron intensity was carried out in order to estimate how far we were from the critical conditions.

On the morning of December 2, 1942, the indications were that the critical dimensions had been slightly exceeded and that the system did not chain react only because of the absorption of the cadmium strips. During the morning all the cadmium strips but one were carefully removed; then this last strip was gradually extracted, close watch being kept on the intensity. From the measurements it was expected that the system would become critical by removing a length of about eight feet of this last strip. Actually when about seven feet were removed the intensity rose to a very high value but still stabilized after a few minutes at a finite level. It was with some trepidation that the order was given to remove one more foot and a half of the strip. This operation would bring us over the top. When the foot and a half was pulled out, the intensity started rising slowly, but at an increasing rate, and kept on increasing until it was evident that it would actually diverge. Then the cadmium strips were again inserted into the structure and the intensity rapidly dropped to an insignificant level.

This prototype of a chain reacting unit proved to be exceedingly easy to control. Intensity of its operation could be adjusted with extreme accuracy to any desired level. All the operator has to do is to watch an instrument that indicates the intensity of the reaction and move the cadmium strips in if the intensity shows a tendency to rise, and out if the intensity shows a tendency to drop. To operate a pile is just as easy as to keep a car running on a straight road by adjusting the steering wheel when the car tends to shift right or left. After a few hours of practice an operator can keep easily the intensity of the reaction constant to a very small fraction of 1 percent.

The first pile had no device built in to remove the heat produced by the reaction and it was not provided with any shield to absorb the radiations

produced by the fission process. For these reasonsi t could be operated only at a nominal power which never exceeded two hundred watts. It proved, however, two points: that the chain reaction with graphite and natural uranium was possible, and that it was very easily controllable.

A huge scientific and engineering development was still needed to reduce to industrial practice the new art. Through the collaboration of all the men of the Metallurgical project and of the Du Pont Company, only about two years after the experimental operation of the first pile large plants based essentially on the same principle were put in operation by the Du Pont Company at Hanford, producing huge amounts of energy and relatively large amounts of the new element, plutonium.

N° 224.

Soon Fermi had another opportunity to speak publicly about atomic energy. He was invited to the George Westinghouse Centennial Forum held in Pittsburgh on May 16, 17, and 18, 1946, under the sponsorship of the Westinghouse Educational Foundation, to celebrate the hundredth anniversary of George Westinghouse's birth. The purpose of this forum, called *Science and Life in the World*, was to present a summary of the scientific knowledge gained during the war and to examine its implications.

Fermi spoke in the section on *The Future of Atomic Energy*, and chose as his topic the peaceful applications of atomic energy. At an early stage of his work, Fermi had become interested in the possibility of using reactors to produce useful power. (See, for instance, papers 211 and 221). He realized that there would be great technical, economical, and, especially, political difficulties, but that the application of neutrons and radioactive materials in scientific techniques would bring important advances in knowledge in many fields. It is of interest that both he and the previous speaker, J. R. Oppenheimer, should have mentioned a proposal of an international agency for the control of atomic energy. Since the end of the war, many of those who had worked on the atomic bomb had recognized the need for international control and had been pressing for it.

The papers presented at this forum were published in three volumes, by McGraw Hill Book Company. Fermi's paper was published in the first volume, which included the sections on *Science and Civilization* and *The Future of Atomic Energy*. His paper was also circulated as Document MDDC–1 by the U.S. Atomic Energy Commission, Technical Division, Oak Ridge, Tennessee (May 27, 1946).

H. L. ANDERSON.

224.

ATOMIC ENERGY FOR POWER

The George Westinghouse Centennial Forum
Science and Civilization – The Future of Atomic Energy (May 1946).

I am going to talk on peaceful applications of atomic energy. It is a subject more pleasant to talk about than the one that Dr. Oppenheimer has discussed (*). Still, the two subjects are so deeply interrelated that we, unfortunately, cannot expect very much good to come for humanity out of peaceful applications unless a satisfactory solution of the tremendous problems of preventing the destructive use of the military potentialities is found.

If we try to look into the future and we take the optimistic point of view that mankind may succeed in organizing itself so as to eliminate the fear and the danger of atomic weapons, we might speculate as to what may be the development of atomic energy as a constructive force.

(*) J. R. OPPENHEIMER had spoken on *A Future for Atomic Weapons*. (Editors' note).

Any such speculation, you will realize, can only be exceedingly sketchy. One can point to some probable developments, but one cannot make the list even approximately complete.

The first point that I propose to discuss is the use of nuclear reactions for the production of controlled and usable power. Chain-reacting piles, in which energy is produced at an easily controllable rate, have been operated for over 3 years. Starting with the first pile, which was run only up to 200 watts, the power has been stepped up in successive units by enormous factors. The piles operated at Hanford for the synthesis of plutonium produce energy in amounts comparable to that of the largest hydroelectric plants.

The energy that is produced in the piles built until now, however, is delivered at such a low temperature that it is of no practical use. In the Hanford plants it actually is wasted for the extremely unconstructive purpose of heating, by a small amount, the waters of the Columbia River.

Most of you know, I presume, that the physical basis of the chain reaction is the fission of uranium. This is a phenomenon that was discovered just before the beginning of the war by Otto Hahn and Strassmann working in Berlin. It consists in a very violent disintegration of the uranium atom, which takes place when a neutron strikes it. The atom splits into two fragments, which fly apart with a very high velocity and with a relatively enormous release of energy.

Still, what makes the chain reaction possible is not the large amount of energy released but is the fact that a few neutrons are emitted together with the fission products. If we assume, for the purpose of this discussion, that 2 neutrons are emitted in each fission and also that all neutrons originating in the system produce a fission, we have the conditions that would lead to an explosive chain reaction. Indeed, if in a system of this type we introduce 1 first neutron, this will give rise to fission and produce 2 neutrons. In turn they will produce 2 neutrons each, and so on.

The number of neutrons will then double at each step, or "generation," so that their number will rapidly multiply until the reaction reaches extreme violence and great amounts of heat are developed. This sudden release of energy produces the atomic explosion. The system as just discussed is said to have a reproduction factor of 2, because at each generation 1 neutron gives rise to 2 new neutrons.

In designing a bomb, one tries to achieve conditions in which the fission energy is released as fast as possible. This requires that the generation time be as short as possible and that at each generation the number of neutrons should increase by the largest possible factor. In order to make the generation time short, one will use fast neutrons. In order to make the reproduction factor as large as possible, one will try to adjust things in such a way that a large percentage of the neutrons ends up by producing new fissions and thereby the largest possible number of new neutrons.

If, instead, we want to produce a controllable chain reaction, the reproduction factor will have to be very close to 1 and there will be no need to have a short generation time. Indeed it would be, if anything, more desirable that the generation time be rather long, because this would make control

more easy. It is possible, therefore, to use slow neutrons in a controlled chain reaction.

There is one more fundamental difference between the bomb and a controlled chain reaction. The fast reaction on which the bomb is working is operated using " valuable " fissionable materials like U^{235}, which is separated from uranium at Oak Ridge, Tennessee, or plutonium, a new element actually fabricated at Hanford, Washington.

Controllable chain reactions instead can be obtained using natural uranium. This material was used in producing the first chain reaction, for the simple reason that at that time the " valuable " fissionable materials were not available. It also is used in all the industrial piles that have been constructed so far. Natural uranium consists primarily of a mixture of U^{238}, representing about 99.3 percent of the total, and U^{235}, representing about 0.7 percent. It is this small amount of U^{235} that makes the reaction possible, since U^{238} does not react, giving rise to fission, when bombarded by slow neutrons.

A chain reaction can be obtained quite easily using pure U^{235}, since thereby one avoids the parasitic absorption due to the U^{238}. When ordinary unseparated uranium is used, the problem is appreciably more difficult, since the positive excess in the neutron balance in each generation is in this case very small, and all unavoidable losses must be kept to a minimum so as to end up with a reproduction factor larger than unity.

From this point of view, therefore, the presence of U^{238} is very undesirable. On the other hand, U^{238} plays a very essential role in the plutonium production. Indeed U^{238} is transformed during the reaction into plutonium by the mechanism represented in the following nuclear process:

$$U^{238} + n \rightarrow U^{239}$$

$$U^{239} \rightarrow Np^{239} + e^{-}$$

$$Np^{239} \rightarrow Pu^{239} + e^{-}$$

The first of these reactions represents the absorption of a neutron by the nucleus 238, which is thereby transformed into the isotope U^{239}. U^{239} is an unstable isotope of uranium, which spontaneously disintegrates by emitting an electron and transforming into the new element, neptunium, of atomic charge 93 and weight 239, as indicated in the second reaction.

The transformation of uranium into neptunium takes place in a time of the order of one-half hour. Also Np^{239}, which is thereby formed, is unstable and spontaneously emits an electron changing in a few days into the final reaction product Pu^{239} as indicated by the last equation. If we examine the over-all balance of a chain reaction of this type, it is clear therefore that U^{235} will gradually be destroyed to keep the reaction going, whereas U^{238} will slowly be transformed into Pu^{239}.

In order to operate a chain-reacting pile at a steady level, the reproduction factor must be equal to 1. If it is larger than 1, the intensity increases; if it is smaller, the intensity drops. For this reason the operator must have

means to adjust the reproduction factor to any desired value in the vicinity of 1. This usually is achieved by means of organs called "control rods." They are rods—made of some material having a strong absorption for neutrons—which the operator can insert into the pile at a depth that can be accurately adjusted.

The number of neutrons absorbed by the rods and thereby removed from the reaction will depend on how deeply the rod reaches into the pile. Consequently, the reproduction factor will also depend upon the position of the rod and will have its largest value when the rod is outside and its smallest valued when the rod is completely inside.

Conditions are usually adjusted in such a way that the reproduction factor is equal to 1 when the rod is in some intermediate position called "critical position," and it takes values larger than 1 if the rod is pulled farther out than the critical position, smaller than 1 if the rod is pushed farther in.

If the operator wishes to increase the rate of reaction, the rod is pulled out so that the reproduction factor exceeds 1 by some small amount and the number of neutrons gradually increases. If the operator wants to reduce the rate of reaction, all he has to do is to insert the rods somewhat farther than the critical position. The reproduction factor will then be less than 1 and the rate of reaction will gradually decrease. If he wants to keep the power at a steady level, he will place the rods at the critical position.

It is clear from this that the problem of controlling the rate of reaction in the pile can be solved in a very simple way. Experiment actually has shown that the controlling problem can also be solved very easily in practice. To keep a pile—whether capable of producing a large or a small amount of power—running at a steady level is an art that can be completely mastered in a few hours. It is also easily possible to keep the intensity of the pile steady at any desired level by moving the rods with mechanical devices operated automatically. In this case all the operator has to do is watch the control panel.

The chief technical difficulty that stands at present in the way of production of atomic energy for practical uses is the following. In all the reacting units that have been constructed until now, the energy is produced at a very low temperature. This undoubtedly is due to a great extent to the fact that the primary purpose for which the piles have been constructed during the war was not the production of useful power, but the production of plutonium. For this reason no effort was made in the direction of constructing a pile with materials capable of standing a very high temperature, since such development undoubtedly would have retarded very considerably the achievement of the essential objectives.

The following points are important. There is no known practical limitation to the temperature at which energy can be produced by a fission chain reaction. Indeed there is reason to believe that, in the explosion of the atomic bombs, temperatures higher than 1,000,000 degrees (centigrade) may have been obtained. Only for machines designed to operate at a steady level a practical limitation is imposed by the refractory properties of the materials

used. In this respect, the choice of the materials is quite critical because not only their ability to stand high temperatures must be taken into account, but also one must consider the adverse effect that adding foreign materials in the reaction system has on the nuclear reaction itself. This adverse effect is due to the fact that most materials absorb neutrons sometimes more and sometimes less. Any material that has to be added as a coolant, for instance, to remove heat from the pile or as a lining for the pipes through which a cooling fluid is conducted determines a loss of neutrons. When this loss is so large that the reproduction factor drops below 1, the reaction stops.

And now comes the question: Could large amounts of energy be released?

The essential fuel in piles of the Hanford type is U^{235}, which represents only 0.7 percent of the total weight of natural uranium.

The content in fission energy of uranium is roughly 3,000,000 times that of an equal weight of coal. If only 0.7 percent of the uranium is utilized, the practical uranium to coal ratio will be about 20,000. These figures point to the great importance of devising methods for the complete utilization of the energy of uranium.

The demand for a technical solution of this prohlem may not be very urgent in the immediate future, since there still are fairly large uranium deposits that can be mined at relatively low cost. If we conceive, however, a development in which large amounts of atomic energy would be produced by U^{235}, the rich deposits of uranium would rapidly be exhausted and further production would have to use very poor ores with a consequent increase of several orders of magnitude in the cost of the primary material. In this case, the importance of a complete utilization of the energy stored in uranium would naturally become much greater. It is clear on the other hand that the energy value of 1 pound of uranium is so great that even an enormous increase of cost of this material may not interfere with its economical use as a source of power. Three million tons of coal, equivalent in energy content to 1 ton of uranium, cost about $ 8 million. Consequently, as far as cost of the raw materials, uranium and coal would become equivalent for a price of uranium of $ 4,000 a pound. Before the war the cost of uranium was about $ 2 a pound, so that an increase of the order of a thousand times the prewar price would not be necessarily uneconomical.

We might conceive that twenty or thirty years from now the general scheme of atomic energy production may be perhaps about as follows. There will be large central installations in which very great amounts of power will be produced and transformed into electrical energy or steam for local power consumption. Besides producing directly power, these large units may also produce some amount of plutonium, which will be extracted and distributed to small installations in which plutonium and not uranium will be used as the primary fuel. This plan would have the advantage of permitting wide use of relatively small power units, thereby reducing very greatly the difficulties of distribution.

A general scheme of this type has recently been discussed in a report by the State Department, on which Dr. Oppenheimer has made very inter-

esting comments. According to this report, the large central units in which plutonium is produced, as well as all sources of uranium and thorium, would be controlled and operated by an international agency, which would distribute or sell plutonium in a denatured form for use by individual consumers. The authors of this report express the view that it perhaps might be possible to denature plutonium so as to make its use for military uses exceedingly difficult and time-consuming, and express the hope therefore that it may be feasible to exert only a minimum of international control on the users of denatured plutonium without danger that it may be diverted secretly to construction of weapons.

The attractive feature of this report is, in my opinion, its denial of the chances of success of an international scheme predicated on a set of prohibitions, and prohibitions only. I am afraid, however, that the report may have been somewhat overinterpreted by the public, in an optimistic sense, in its estimate of the difficulties to divert denatured plutonium to military uses. There is no denying the fact that the possible use of plutonium for aggressive warfare constitutes a difficulty for the industrial uses of atomic energy that is much greater than any technical difficulty that we can foresee. The problem of preventing this use is essentially political and not technical, and I do not see much hope of solving it unless the very basis of the relationships among nations should be thoroughly changed in the future years.

Going back to the technical problems, I should like to mention one more feature of atomic energy units that will prove a serious limitation to their general use. During the process of fission, which is basic to the production of atomic energy, not only energy but also radiations of various kinds—particularly neutrons and gamma rays—are produced. Unless they are prevented from doing so by a shield, these radiations escape from the pile and their intensity is so terrific that they would kill in a very short time any living beings who were to approach an unshielded operating unit. It is therefore an essential necessity to shield the pile with such materials as to prevent the escape of lethal radiations. In principle the problem is not at all difficult to solve. It is sufficient, for example, to surround the pile with a concrete wall several feet in thickness in order to eliminate completely any danger. On the other hand, there is no way to eliminate the radiations without the use of a very heavy shield. Indeed in many designs of piles that have been discussed, the shield represents by far the greatest part of the weight of the installation. The necessity of surrounding the pile with a heavy shield will prevent several uses of atomic power. It does not appear possible, for instance, to design an atomic power unit light enough to be used in a car or in a plane of ordinary size. Perhaps a large locomotive may be the smallest mobile unit in which an atomic power plant conceivably could be installed.

We may summarize this discussion on atomic power by stating that there is definitely a technical possibility that atomic power may gradually develop into one of the principal sources of useful power. If this expectation will prove correct, great advantages can be expected to come from the fact that the weight of the fuel is almost negligible. This feature may be particularly valuable for making power available to regions of difficult access and far

from deposits of coal. It also may prove a great asset in mobile power units; for example, in a power plant for ship propulsion. On the disadvantage side we have some technical limitations to the applicability of atomic power, of which perhaps the most serious is the impossibility of constructing light power units; also there will be peculiar difficulties in operating atomic plants, as for example the necessity of handling highly radioactive substances which will necessitate, at least for some considerable period, the use of specially skilled personnel for the operation. But the chief obstacle in the way of developing atomic power will be the difficulty of organizing a large-scale industrial development in an internationally safe way. This presents actually problems much more difficult to solve than any of the technical developments that are necessary. It will require an unusual amount of statesmanship to balance properly the necessity of allaying the international suspicion that arises from withholding technical secrets, against the obvious danger of dumping the details of the procedures for an extremely dangerous new method of warfare on a world that may not yet be prepared to renounce war. Furthermore, the proper balance should be found in the relatively short time that will elapse before the "secrets" will naturally become open knowledge by rediscovery on the part of scientists and engineers of other countries.

One might be led to question whether the scientists acted wisely in presenting the statesmen of the world with this appalling problem. Actually there was no choice. Once basic knowledge is acquired, any attempt at preventing its fruition would be as futile as hoping to stop the earth from revolving around the sun.

Power production is not the only peaceful use of atomic chain reactions that is in sight. There are other possibilities, which may not compete with the power production in direct economic importance but perhaps may prove to be ultimately the most fruitful field of development. An operating pile is a source of radioactive materials many orders of magnitude stronger than any source previously obtained. Radioactive materials are produced partly as a direct consequence of the fission process, since the fragments into which the uranium atoms split are radioactive isotopes of elements located in the middle part of the periodic system. These radioactive elements can be purified chemically. Other radioactive substances can be produced as follows: In a going pile, neutrons are emitted continuously in very great numbers. Any substance that is inserted in the pile is exposed to an intensive bombardment by these neutrons. When a neutron strikes the nucleus of a substance, several reactions may take place, and many of them result in the formation of radioactive isotopes. Most elements can be obtained in this way in a radioactive form. Their lifetimes range from a fraction of a second to thousands of years. Among the more significant artificial radio elements, one should mention carbon 14, with a lifetime of about three thousand years. Radioactive substances can be used for a variety of purposes. The radiations emitted by them are equivalent to the radiations emitted by radium and could be used for medical purposes on a much greater scale than has been possible with radium. From the point of view of radiotherapy, the hope has been expressed that it might be possible to take advantage of

the fact that the artificial radioactive substances are available in a variety of chemical elements, and one might use the chemical properties in order to achieve a concentration of the active material in the tissue that is to be exposed to the radiations.

Still greater hopes have been raised by the possibility of using large amounts of radioactive materials as tracers. Particularly attractive in this respect appears the possibility of using carbon 14 as a tracer for carbon in organical chemical and biochemical work. The use of carbon 14 in biology is expected to offer means to follow easily the reaction of carbon in the complicated chemical processes of life, and it is hoped that the availability of carbon 14 will be adequate to allow research in this direction to proceed on a very large scale.

It would not be very surprising if the stimulus that these new techniques will give to science were to have an outcome more spectacular than an economic and convenient energy source or the fearful destructiveness of the atomic bomb.

225.

ELEMENTARY THEORY OF THE CHAIN-REACTING PILE (*) (**)

Institute for Nuclear Studies, University of Chicago
« Science », *105*, 27–32 (1947).

The results and the methods discussed in the following outline of the theory of a chain-reacting pile working with natural uranium and graphite have been obtained partly independently and partly in collaboration by many people who participated in the early development work on the chain reaction. Very important contributions to the theoretical ideas were given by Szilard and Wigner. Many physicists contributed experimental results that helped to lead the way, among them, H. L. Anderson and W. H. Zinn, first at Columbia University and later at the Metallurgical Laboratory of the University of Chicago; R. R. Wilson and E. Creutz, at Princeton; and Allison, Whitaker, and V. C. Wilson, at the University of Chicago. The production of the chain reaction was finally achieved in the Metallurgical Laboratory directed by A. H. Compton.

Absorption and Production of Neutrons in a Pile.

We consider a mass, " the pile," containing uranium spread in some suitable arrangement throughout a block of graphite. Whenever a fission takes place in this system, an average number (ν) of neutrons is emitted with a continuous distribution of energy of the order of magnitude of 1,000,000 ev. After a neutron is emitted, its energy decreases by elastic collisions with the atoms of carbon and to some extent also by inelastic collisions with the uranium atoms. In the majority of cases the neutrons will be slowed down to thermal energies. This process requires about 100 collissions with carbon atoms. After the energy of the neutron is reduced to thermal value, the neutron keeps on diffusing until it is finally absorbed. In several cases, however, it will happen that the neutron is absorbed before the slowing-down process is completed.

(*) This paper, presented at the Chicago meeting of the American Physical Society, June 21, 1946, is based on work performed under Contract No. W-7401-eng-37 with the Manhattan District at the Metallurgical Laboratory, University of Chicago.

(**) This paper was also circulated as document MDDC-74 by the Atomic Energy Commission, Oak Ridge, Tennessee (June 18, 1946) (Editors' Note).

The neutron may be absorbed by either the carbon or the uranium. The absorption cross-section of carbon for neutrons of thermal energy is quite small, its value being approximately 0.005×10^{-24} cm^2. For graphite of density 1.6, this corresponds to a mean free path for absorption of about 25 m. It is believed that the absorption cross-sections follows the $1/v$ law, and consequently the absorption cross-section, which is already quite small at thermal energies, becomes practically negligible for neutrons of higher energy. It is therefore a sufficiently good approximation to assume that absorption by carbon during the slowing-down process can be neglected.

The absorption of a neutron by uranium may lead either to fission or to absorption by a (n, γ) process. We shall refer to this last possibility as the process of resonance absorption. The relative importance of fission and resonance absorption in the different energy intervals is not the same. In this respect we can consider roughly three intervals:

(1) *Neutrons with energy above the fission threshold of* U^{238}.—We can call these conventionally "fast neutrons." For fast neutrons the most important absorption process is fission, which normally takes place in the abundant isotope U^{238}. Resonance absorption is smaller but not negligible.

(2) *Neutrons of energy below the fission threshold of* U^{238} *and above thermal energy.*—We shall refer to these neutrons as "epithermal neutrons." For epithermal neutrons the most important absorption process is the resonance capture. The cross-section for this process as a function of energy is quite irregular and presents a large number of resonance maxima that can be fairly well represented by the Breit-Wigner theory. In practical cases the resonance absorption becomes important for neutron energy below about 10,000 ev and increases as the energy of the neutrons decreases.

(3) *Neutrons having thermal agitation energy or "thermal neutrons."*—For thermal neutrons both the resonance and fission absorption process are important. In this energy range both cross-sections follow approximately the $1/v$ law, and therefore their relative importance becomes practically independent of the energy. Let σ_f and σ_r be the cross-sections for fission and resonance absorption for neutrons of energy kT, and η be the average number of neutrons emitted when a thermal neutron is absorbed by uranium. Then η differs from ν, since only the fraction $\frac{\sigma_f}{(\sigma_\nu + \sigma_f)}$ of all the thermal neutrons absorbed by uranium produces a fission. It is, therefore,

$$\eta = \frac{\nu\sigma_f}{(\sigma_f + \sigma_r)} . \tag{1}$$

The preceding discussion leads one to conclude that only a fraction of the original fast neutrons produced will end up by producing a fission process. For systems of finite size, further losses of neutrons will be expected by leakage outside the pile.

Limiting ourselves for the present to systems of practically infinite dimensions, we shall call P the probability that a fast neutron ultimately is absorbed by the fission process. The average number of neutrons produced in the

"second generation" by the first neutron will then be

$$k = P\nu. \tag{2}$$

Usually, k is called the "reproduction factor" of the system. A self-sustaining chain reaction evidently is possible only when $k > 1$. If this is the case, the reaction actually will take place provided the leakage loss of neutrons is sufficiently small. This, of course, can always be achieved if the size of the pile is large enough.

Life History of a Neutron.

When a fast neutron is first emitted in our pile, the following events may take place:

(1) There is a small probability that the neutron will be absorbed by uranium before its energy has been appreciably decreased. If this is the case, the absorption leads often to fission of U^{238}. The probability of such fast fissions, however, is usually only a few percent. Indeed, if the system contains little uranium and a large amount of carbon, the elastic collisions with carbon tend to reduce the energy very rapidly to a value below the fission threshold of U^{238}. If, on the other hand, the system is very rich in uranium, the inelastic collision processes become very probable and rapidly reduce the energy of the original fast neutron to a fairly low value before it has a chance to produce a fission in U^{238}.

(2) In the large majority of the cases, therefore, the neutron is not absorbed as a fast neutron and rapidly loses its energy, mostly due to collision against the carbon atoms. One can prove in an elementary way that it takes about 6.3 collisions against the carbon atoms to reduce the energy by an average factor of e. Consequently, it will take about 14.6 collisions in order to reduce the energy by a factor of 10, and about 110 collisions to reduce the energy from 1,000,000 ev to the thermal energy value of 1/40 ev. While this slowing-down process is in progress, the neutron may be absorbed by the resonance process in uranium. We shall call p the probability that a neutron is not absorbed before reaching thermal energy. One of the most important factors in designing a pile consists in trying to minimize the probability that neutrons are removed from the system by resonance absorption during the slowing down.

(3) If the neutron is not absorbed during the slowing-down process, it eventually reaches thermal energy and ultimately will be absorbed by either uranium or carbon. If uranium and carbon were mixed uniformly, the probability for these two events would be in the ratio of the absorption cross-sections of uranium and carbon for thermal neutrons multiplied by the atomic concentrations of the two elements. Since actually the mixture is not uniform, this is only approximately true. We shall call f the probability that a thermal neutron is absorbed by uranium. In designing a chain-reacting pile one will normally try to adjust things so as to have both f and p as large as possible. Unfortunately, the two requirements are contradictory,

because in order to make f large, one shall try to build a system very rich in uranium in order to reduce the probability of absorption of thermal neutrons by carbon. On the other hand, in a system containing a relatively small amount of carbon the slowing-down process will be relatively slow, and consequently the probability of resonance absorption during the slowing down will be large.

It is clear, therefore, that one shall have to conciliate two opposite requirements by finding an optimum value for the ratio of uranium to carbon.

In a homogeneous mixture of uranium and carbon the values of f and p depend only on the relative concentrations of the two elements. If we do not restrict ourselves, however, to homogeneous mixtures only, one can try to obtain a more favorable situation by proper arrangement of the geometrical distribution of the two components. This actually is possible to a considerable extent, because of the following circumstances. The resonance absorption which is responsible for the loss of neutrons during the slowing down has very sharp cross-section maxima of the Breit-Wigner type. Therefore, if the uranium, instead of being spread through the graphite mass, is concentrated in rather sizable lumps, we will expect that the uranium in the interior of a lump will be shielded by a thin surface layer from the action of neutrons with energy close to a resonance maximum. Therefore, the resonance absorption of a uranium atom inside the lump will be much less than it would be for an isolated atom. Of course, self-absorption in a lump reduces not only the resonance absorption but also the thermal absorption of uranium. One can expect theoretically, however, and experiment has confirmed, that at least up to a certain size of lumps the gain obtained by reducing the resonance loss of neutrons overbalances by a considerable amount the loss due to a lesser absorption of thermal neutrons.

The typical structure of a pile is a lattice of uranium lumps embedded in a matrix of graphite. The lattice may be, for example, a cubic lattice of lumps or a lattice of rods of uranium. This latter arrangement is slightly less efficient from the point of view of the neutron absorption balance but often presents some practical advantages, since it makes easier the removal of the heat produced by the pile. In the present discussion we shall consider only lattices of lumps.

It is useful to give some typical figures for the probabilities of the various absorption processes. These probabilities, of course, are not constant but depend on the details of the structure of the lattice. Average figures for a good lattice will be given as an example. When a neutron is first produced by a fission taking place in a lump of uranium, it may have a probability of the order of 3 percent of being absorbed, giving rise to fission before loosing any appreciable amount of energy. In 97 percent of the cases when this does not happen the neutron will initiate its slowing-down process, and it may either be absorbed by the resonance process during the slowing down or reach thermal energy. The probability of resonance absorption during the slowing down may be of the order of 10 percent, so that 87 percent of the original neutrons will be slowed down to thermal energies. Of these, perhaps 10 percent may be absorbed by carbon and the remaining 77 percent by uranium.

If we assume for the purpose of example that $\nu = 2$, we shall have in one generation the processes summarized in Table I. For the example given, the reproduction factor will be, therefore,

$$k = 0.06 + 0.77\,\eta. \tag{3}$$

Consequently, a lattice of the type described would have a reproduction factor larger than 1, provided η is larger than 1.22.

TABLE I.

Probability (%)	Type of process	Neutrons produced per neutron absorbed	Neutrons per generations by one neutron
3	Fast fission.	2	0.06
10	Resonance absorption	0	0.0
10	Absorption by carbon	0	0.0
77	Absorption by uranium at thermal energies	η	$0.77\,\eta$

In order to evaluate the reproduction factor one must be able to calculate the probabilities for the various processes mentioned. Some points of view which may be used in the practical calculation will be indicated briefly.

Probability of Fission Before Slowing Down.

The value of this quantity is very easily calculable for a very small lump of uranium. In this case it is obviously given by

$$P_F = \sigma_F\, nd, \tag{4}$$

where σ_F is the average value of the fission cross-section for fission neutrons; n is the concentration of uranium atoms in the lump; and d is the average value of the distance that the neutron produced in the lump must travel before reaching the surface of the lump. The case of a lump of larger size is more complicated, since then multiple collision processes become important and both elastic and inelastic scattering play a considerable role. In particular, the last process for a lump of large size effectively slows down the neutrons before the fission threshold of U^{238} and brings them down to an energy level in which they are readily absorbed by the resonance process.

Resonance Absorption.

If we had a single atom of uranium in a graphite medium where fast neutrons are produced and slowed down to thermal energy, the probability per unit time of a resonance absorption process of neutrons with energy

larger than thermal energy would be given by the following expression:

$$\frac{q\lambda}{0.158}\int \sigma(E)\,\frac{dE}{E}\,, \tag{5}$$

where q is the number of fast neutrons entering the system per unit time and unit volume, λ is the mean free path, and $\sigma(E)$ is the resonance absorption cross-section at energy E. The integral must be taken between a low limit just above thermal energy and an upper limit equal to the average energy of the fission neutrons. One will expect that the largest contribution to the integral will be due to the Breit-Wigner peaks of $\sigma(E)$.

The above formula would be very much in error in the case of a lattice of lumps. As already indicated, this is due to the fact that inside a lump there is an important self-screening effect that reduces very considerably the density of neutrons having energy close to a resonance maximum.

The best approach to a practical solution to the problem is therefore a direct measurement of the number of neutrons absorbed by resonance in lumps of uranium of various sizes.

Measurements of this type have been performed first at Princeton University, and the results have been summarized in practical formulas that are used in the calculations.

Probability of Absorption at Thermal Energies.

If uranium and carbon were uniformly mixed, a thermal neutron would have a probability

$$\frac{N_U\,\sigma_U}{N_C\,\sigma_C + N_U\,\sigma_U} \tag{6}$$

to be absorbed by uranium. In this formula N_C and N_U represent the numbers of atoms of carbon and of uranium per unit volume, and σ_C and σ_U represent the cross-sections of carbon and uranium for thermal neutrons.

More complicated is the case of a lattice distribution of lumps of uranium in graphite, since the density of thermal neutrons throughout the system is not uniform but is large at the places far from the uranium lumps and smaller near and inside the uranium lumps, due to the fact that the absorption of thermal neutrons is much greater in uranium than in graphite. Let $\bar{n}_C$ and $\bar{n}_U$ be the average densities of thermal neutrons in the graphite and in the uranium lumps. The number of thermal neutrons absorbed by uranium and by carbon will be proportional to $N_U\,\sigma_U\,\bar{n}_U$ and $N_C\,\sigma_C\,\bar{n}_C$, and we will have, therefore, instead of Equation (6), the corrected formula,

$$f = \frac{N_U\,\sigma_U\,\bar{n}_U}{N_U\,\sigma_U\,\bar{n}_U + N_C\,\sigma_C\,\bar{n}_C}\,. \tag{7}$$

For practical purposes it is usually sufficiently accurate to calculate $\bar{n}_C$ and $\bar{n}_U$, using the diffusion theory. The approximation is made to substitute the lattice cell by a spherical cell having volume equal to that of the actual cell,

with the boundary condition that the radial derivative of the density of neutrons vanishes at the surface of the sphere. It is also assumed that the number of neutrons that are slowed down to thermal energies per unit time and unit volume is constant throughout the graphite part of the cell. This approximation is fairly correct, provided the dimensions of the cell are not too large. With these assumptions one finds the following formula for the probability, f, that thermal neutrons be absorbed by uranium:

$$f = \frac{3\alpha^2}{\alpha^3 - \beta^3} \frac{(1-\alpha)(1+\beta)e^{-\beta+\alpha} - (1+\alpha)(1-\beta)e^{\beta-\alpha}}{(\alpha+s-s\alpha)(1+\beta)e^{-\beta+\alpha} - (\alpha+s+s\alpha)e^{\beta-\alpha}} \tag{8}$$

where α and β represent the radius of the lump and the radius of the cell expressed taking the diffusion length in graphite, $l = \sqrt{\lambda\Lambda/3}$, as unit of length. It is further

$$s = \frac{\lambda}{\sqrt{3}} \frac{1+\gamma}{1-\gamma}, \tag{9}$$

where γ is the reflection coefficient of the lump for thermal neutrons.

Lattice Containing a Large Number of Cells.

The density of neutrons of any given energy in a lattice containing a large number of cells is a function of the position in the lattice. One can arrive at a simple mathematical description of the behavior of such a system by neglecting in first approximation the local variation of such functions due to the periodic structure of the lattice and substituting for the actually inhomogeneous system and equivalent homogeneous system. In this section we shall accordingly simplify the problem by substituting for all densities of neutrons values obtained by averaging the actual values over the volume of the cell. The densities will then be represented by smooth functions such as one would expect in a homogeneous uranium-graphite mixture.

Let $Q(x, y, z)$ be the number of fast neutrons produced per unit time and unit volume at each position in the lattice. These neutrons diffuse through the mass and are slowed down. During this process some of the neutrons are absorbed at resonance. Let $q(x, y, z)$ be the number of neutrons per unit time and unit volume which become thermal at the position x, y, z; then q is called the "density of the nascent thermal neutrons."

We shall assume that if an original fast neutron is generated at a point, zero, the probability that it becomes thermal at a given place has a Gaussian distribution around zero. This assumption may be justified by considering that the diffusion process of slowing down consists of very many free paths. Experimentally one finds that the distribution curve of the nascent thermal neutrons aroud a point source of fast neutrons is represented only approximately by a Gaussian distribution, and formulas have been used in which the actual distribution is described as a superposition of two or three Gaussian curves with different ranges. For the purpose of the present discussion, however, we shall take only one. For each fast neutron produced only p

neutrons reach thermal energy. The distribution of nascent thermal neutrons produced by a source of strength 1, placed at the origin of the coordinate, shall then be represented by

$$q_1 = \frac{p}{\pi^{3/2} r_0^3} e^{-r^2/r_0^2}. \tag{10}$$

For graphite of density 1.6 the range, r_0, is of the order of 35 cm. The density of nascent thermal neutrons at point P can be expressed in terms of Q by adding up the contribution of all the infinitesimal sources, $Q(P')\,d\tau'$ ($d\tau'$ represents the volume element around the point, P'). We obtain in this way

$$q(P) = \frac{p}{\pi^{3/2} r_0^3} \int Q(P')\, e^{-\frac{(P'-P)^2}{r_0^2}}\, d\tau'. \tag{11}$$

The density, $n(x, y, z)$, of the thermal neutrons is connected to q by the differential equation,

$$\frac{\lambda v}{3} \Delta n - \frac{v}{\Lambda} n + q = 0, \tag{12}$$

where λ is the collision mean free path of thermal neutrons, v is their velocity, and Λ is the mean free path for absorption of a thermal neutron. Equation (12) is obtained by expressing a local balancing of all processes whereby the number of thermal neutrons at each place tends to increase or decrease. The first term represents the increase in number of neutrons due to diffusion ($\lambda v/3$ is the diffusion coefficient of thermal neutrons); the second, the loss of neutrons due to absorption; and the third, the effect of the nascent thermal neutrons.

It should be noted that the absorption mean free path Λ in Equation (12) is much shorter than the corresponding quantity, Λ_0, in pure graphite. Indeed, the absorption in a lattice is due mostly to the uranium. In first approximation Λ is given by

$$\Lambda = (1 - f)\,\Lambda_0. \tag{13}$$

In practical cases Λ may be of the order of magnitude of 300 cm, whereas Λ_0 in graphite without uranium is about 2,500 cm.

When a thermal neutron is absorbed by uranium, η new neutrons are produced by fission. This number should be increased by a few percent in order to take into account the effect of the small probability of fast fission. Let $\varepsilon\eta$ be the total number of fast neutrons so corrected.

The number of thermal neutrons absorbed per unit volume and unit time is vn/Λ. Of these, the fraction f is absorbed by uranium. We have, therefore,

$$Q = f\eta\,\varepsilon \frac{v}{\Lambda} n + Q_0, \tag{14}$$

where $f\eta\,\varepsilon \frac{v}{\Lambda}$ represents the number of fast neutrons produced in the chain reaction process, and Q_0 represents the number of fast neutrons produced by an outside source if one is present. In most cases, of course, Q_0 will be

equal to zero. From Equations (11), (12), and (14) we can eliminate all unknowns except n, and we find

$$(15)\quad \frac{3}{\lambda\Lambda}n - \Delta n = \frac{3\not{p}\varepsilon\eta f}{\pi^{3/2} r_0^3 \Lambda\lambda}\int n(\mathrm{P}')\, e^{-\frac{(\mathrm{P}'-\mathrm{P})^2}{r_0^2}}\, d\tau' + \frac{3\not{p}}{\pi^{3/2} r_0^3 \lambda v}\int Q_0(\mathrm{P}')\, e^{-\frac{(\mathrm{P}'-\mathrm{P})^2}{r_0^2}}\, d\tau'.$$

A solution of this equation is obtained readily by developing both Q_0 and n in a Fourier series. The general term of this development, corresponding to Q_0 of the form $Q_0 \sin \omega_1 x \sin \omega_2 y \sin \omega_3 z$, is:

$$(16)\quad n = \frac{(\Lambda\not{p}\, Q_0/v)\sin\omega_1 x \sin\omega_2 y \sin\omega_3 z}{\left(1 + \frac{\lambda\Lambda}{3}\omega^2\right) e^{\omega^2 r_0^2/4} - \varepsilon p f \eta},$$

where $\omega^2 = \omega_1^2 + \omega_2^2 + \omega_3^2$.

When the dimensions of the pile are finite but very large compared with the mean free path, the boundary condition is that all densities must vanish at the surface. If the pile, for example, is a cube of side a and the origin of the coordinates is taken in one of the corners, it is:

$$(17)\quad \omega_1 = \frac{\pi n_1}{a} \quad ; \quad \omega_2 = \frac{\pi n_2}{a} \quad ; \quad \omega_3 = \frac{\pi n_3}{a},$$

where n_1, n_2, n_3 are positive integral numbers that define the various Fourier components. The critical dimensions of the system are such that the denominator of Equation (16) vanishes for the 1, 1, 1 harmonic, since in this case the density of the neutrons becomes infinitely large. The critical condition can be expressed, therefore, by the equation:

$$(18)\quad \left(1 + \frac{3\pi^2}{a^2}\frac{\lambda\Lambda}{3}\right) e^{\frac{3\pi^2}{a^2}\frac{r_0^2}{4}} = \varepsilon p f \eta.$$

The right-hand side in this formula is the reproduction factor, k, for a system of infinite size. We can therefore write the critical condition as follows:

$$(19)\quad k = \left(1 + \frac{3\pi^2}{a^2}\frac{\lambda\Lambda}{3}\right) e^{\frac{3\pi^2}{a^2}\frac{r_0^2}{4}}.$$

In most cases both the exponent of e and the term added to 1 in the parentheses are small compared with 1, and so the previous expression can be simplified to:

$$(20)\quad k = 1 + \frac{3\pi^2}{a^2}\left(\frac{\lambda\Lambda}{3} + \frac{r_0^2}{4}\right).$$

This formula can be used in order to calculate the critical side of a pile of cubical shape. If, for example, we assume for a special lattice numerical valued of $\lambda = 2.6$ cm, $\Lambda = 350$ cm, $r_0^2 = 1{,}200$ cm^2, and $k = 1.06$, we find for the critical side of a cubical pile, $a = 584$ cm. Naturally, these constants are merely hypothetical, and though included within the possible range, are in practical cases strongly dependent on the details of the lattice structure.

It is useful to derive an approximate relationship between the power produced by a pile and the intensity of thermal neutrons inside it. Roughly 50 percent of the thermal neutrons absorbed in a pile give rise to fission, and the energy released per fission is of the order of 200 Mev. This corresponds to about 1.6×10^{-4} ergs per thermal neutron absorbed. Since the number

of thermal neutrons absorbed per unit volume is vn/Λ, the energy produced is approximately

$$\frac{vn}{\Lambda}\, 1.6\times 10^{-4} \cong 4.6\times 10^{-7}\, vn \text{ ergs/cm}^3 \text{ sec.} \tag{21}$$

Naturally, the power is not produced uniformly throughout the pile because n is a maximum at the center and decreases to zero at the edge of the pile. For a cubical pile n is represented approximately by

$$n = n_0 \sin\frac{\pi x}{a} \sin\frac{\pi y}{a} \sin\frac{\pi z}{a}\,, \tag{22}$$

where n_0 is the density of neutrons at the center of the pile. Integrating the previous expression (21) over all the volume of the pile, one obtains the following formula for the power:

$$W = \frac{8}{\pi^3}\, 4.6\times 10^{-7}\, nv\, a^3 = 1.2\times 10^{-7}\, n_0\, va^3\,. \tag{23}$$

If, again, we take as an example a pile with a side of 584 cm, we find $W = 24\, n_0\, v$ ergs/sec. When the pile is operating at a power of 1 kw, the flux of thermal neutrons at the center is therefore about $n_0 v = 4\times 10^8$ neutrons/cm² sec.

Description of a Graphite Pile at Argonne Laboratory.

The first pile was erected under the West Stands on the campus of the University of Chicago at the end of 1942. After having been operated there for a few months it was moved to the Argonne Laboratory, near Chicago, where it has been used until now for various research purposes.

The lattice of that pile is not the same throughout the structure. Since only a small amount of uranium metal was available at that time, metal has been used in the central portion of the pile and uranium oxide in the outer portion.

The intensity of operation of the pile is recorded by a number of BF_3 ionization chambers connected to amplifiers or to galvanometers.

Since this pile has no cooling devices built into it, the power produced is limited by the necessity of avoiding an excessive temperature rise. The pile could be operated indefinitely at a power of 2 kw and is often operated for periods of the order of one or two hours up to about 100 kw.

One feature that is often used for neutron research work is the thermal column, a column of graphite having sides of about 5×5 feet, which is built on the center of the top of the pile and goes through the top shield. The neutrons that diffuse from the pile into this column are rapidly reduced to thermal energy so that the neutrons inside the column a few feet above the top of the pile are practically pure thermal neutrons.

The pile is also equipped with a number of holes in the shield and removable stringers of graphite that make it possible to explore phenomena inside the pile or to introduce samples for neutron irradiation.

When the pile is operated at 100 kw, the flux of thermal neutrons at the center is about 4×10^{10} neutrons/cm² sec.

N° 226, 228–230, 234, and 235.

Upon returning to Chicago at the end of the war, Fermi renewed his interests of 1943 in making use of the intense neutron flux from the CP–3 reactor which was at the original Argonne National Laboratory. His presence in the Chicago area influenced the Atomic Energy Commission in choosing a place near Chicago as the permanent site for the Argonne National Laboratory. Fermi and L. Marshall were working there in 1946. During the spring of 1947, I joined them and we regularly drove out to the old Argonne site about three times a week.

One of Fermi's interests was to use neutron interference phenomena to study the structure of liquids and solids. This interest resulted the following year in Owen Chamberlain doing a thesis on the diffraction of neutrons by liquid metals (« Phys. Rev. », 77, 305 (1950)).

At this time Fermi was also interested in measuring the magnetic moments of the radioactive nuclei which could be produced abundantly in the reactor. He started the construction of a molecular beam apparatus. He had me work on this until it became obvious that it was going to take several months to get the apparatus built. His efforts eventually led to a molecular beam program at the Argonne National Laboratory. However, before this effort was fruitful he was attracted to meson physics.

A more productive area of research at the Argonne was the study of phase shifts for slow neutron scattering; these experiments grew out of the earlier experiments with Anderson and L. Marshall (see papers N° 148, 191, and 224). During 1946 and 1947 he did a series of experiments with L. Marshall and the one measurement with W. Sturm. Fermi also wanted to have a beam of polarized neutrons and he played around with Bragg diffraction from magnetite. However, he probably was discouraged from working with polarized neutron beams because D. J. Hughes and his associates were involved in a major effort along these lines at the Argonne.

His experiments at the Argonne are all characterized by employing comparatively simple apparatus and placing the importance upon the physical concepts involved. This period of time was a beautiful manifestation of Fermi's ability to choose areas of research where his efforts would be most effective.

A. WATTENBERG.

N° 226.

This paper is the outcome of Fermi's interest in experiments carried out by W. J. Sturm who made use of the " chopper " technique developed by Fermi and the neutron crystal spectrometer developed by Zinn to measure the detailed energy dependence of the slow neutron cross section for Be and for BeO, both in the form of crystalline powders. Discussions between Fermi, Sturm, and Sachs led to the interpretation of the data in terms of crystal structure effects. Although the detailed theory of slow neutron scattering from crystals had been presented much earlier by Halpern, Hammermesh, and Johnson (« Phys. Rev. », 59, 981 (1941)); and by Weinstock (« Phys. Rev. », 65, 1 (1944)), Fermi had his own very simple way of deriving the essential features of the energy dependence of the cross section of the powder sample. His argument is presented in the paper but the more detailed theory is used to complete the analysis of the data.

Just at this time, Fermi had been looking for methods to measure the neutron scattering lengths for various nuclei. The coherent scattering length was of interest in connection with a number of fundamental questions including such matters as the spin dependence of the neutron scattering and the location of the nearest neutron resonance. The determination of the sign of the scattering length was of particular interest for the latter question. In our discussion of the interpretation of the data on BeO, it quickly became apparent that the results were very sensitive to the relative sign of the scattering lengths of beryllium and

oxygen, and the method was exploited to determine this sign. In fact this paper serves as the original illustration of a rather powerful method for determining the relative sign and magnitude of the scattering lengths of two nuclei when they can be formed into a crystalline compound.

This paper was circulated also as Document MDDC–1184, Atomic Energy Commission, Technical Information Division, Oak Ridge, Tennessee, January 13, 1947.

Parts of this paper were included, in a somewhat different form, in quarterly Report CF–3574, Argonne Laboratory, July 26, 1946.

R. G. SACHS.

226.

THE TRANSMISSION OF SLOW NEUTRONS THROUGH MICROCRYSTALLINE MATERIALS(*)

E. FERMI(**) W. J. STURM, and R. G. SACHS
Argonne National Laboratory, Chicago, Illinois
(Received January 27, 1947)
« Phys. Rev. », 71, 589–594 (1947).

The transmission of monochromatic slow neutrons through microcrystalline Be and BeO has been determined. The source of neutrons was the Argonne heavy water pile. These neutrons were monocromatized by means of a mechanical velocity selector for low energies and a neutron crystal spectrometer for higher energies. The results are in excellent agreement with the theory of elastic scattering from crystals. It is found by comparison of the results on BeO with the theory that the scattering amplitudes of Be and O have the same sign. This method may be used to determine the relative scattering phases of other pairs of nuclei which can be combined to form a crystalline material. The sample must consist of crystals smaller than a micron in linear dimensions. Other possible sources of disagreement between theory and experiment are discussed in Section 5.

1. INTRODUCTION.

The measurement of the effective scattering cross section of crystalline materials for slow neutrons is of considerable interest in connection with problems of neutron diffusion. If the material consists of nuclei having a small absorption cross section, the scattering cross section can be determined by measuring the transmission coefficient for slow neutrons. It is known that the scattering cross section determined in this way is a very sensitive function of neutron energy which shows violent fluctuations for small changes in the energy. These fluctuations are associated with the appearance of Bragg reflections from the appropriate planes in those of the microcrystals which are properly oriented. The shape of the transmission curve has been

(*) This document is based on work performed under the auspices of the Manhattan Project at the Argonne National Laboratory. This paper was submitted for declassification on November 27, 1946.

(**) Also a member of the Institute for Nuclear Studies, University of Chicago.

determined theoretically by Halpern, Hammermesh, and Johnson [1] and by Weinstock [2] for materials containing one atomic species. The generalization to multi-atomic materials is simple and will be given in Section 4.

With the intense monochromatic neutron sources which are now available, it is possible to obtain a rather precise measurement of transmission curves as a function of energy. Measurements of this kind have been carried out for microcrystalline Be and BeO. It is the purpose of this paper to present the results of these measurements and to compare them with theory. In particular, it will be shown in Section 4 how the results can be used to determine the relative phases of the Be and O scattering.

In Section 2, the experimental methods for obtaining monochromatic neutron beams are discussed and in Section 3 the experimental results obtained with these beams are given. Section 4 contains a discussion of the theory with particular reference to its application to materials containing more than one atomic species. The limits of applicability of the theory are considered in Section 5.

2. Experimental Method.

The monoenergetic neutron beams required for the measurements were obtained by means of two velocity selectors in conjunction with the heavy water pile at the Argonne Laboratory. The first was the mechanical velocity selector first used by Fermi, Marshall, and Marshall [*] as modified by Brill and Lichtenberger, [3] which by use of a motor driven cadmium shutter and proper timing devices can be applied to the measurement of cross sections for the range of neutron energies between 0.004 and 0.20 electron volt. The second, which extended the measurements in one case to about 1.0 electron volt, made use of the monoenergetic beams of neutrons diffracted from LiF(100) in the neutron crystal spectrometer which has been previously described. [4]

The burst of neutrons periodically released by the rotating shutter of the mechanical velocity selector passed through a neutron detector after traversing a measured path between the shutter and detector. The output of the detector, recorded during short measured intervals after the release of the initial burst and during the time the burst was passing through the counter, made it possible to record only neutrons in a very small velocity range. By introducing a sample of a microcrystalline substance into the periodic beam released by the shutter, it was possible to measure the trans-

(1) O. Halpern, M. Hammermesh, and M. H. Johnson, « Phys. Rev. », *59*, 981 (1941).

(2) R. Weinstock, « Phys. Rev. », *65*, 1 (1944).

(*) See paper N° 200 (Editors' note).

(3) This velocity selector will be described in forthcoming papers by E. Fermi, L. W. Marshall, and J. Marshall and by T. Brill and H. D. Lichtenberger. This description of a use of the instrument before publication of their papers is presented with the permission of these authors.

(4) W. J. Sturm and S. H. Turkel, « Phys. Rev. », *70*, 103 (1946); W. H. Zinn, « Phys. Rev. », *70*, 102 (1946).

mission of the substance as a function of energy by measuring the fraction of neutrons scattered by the sample in each small energy interval. The value of the effective scattering cross section was calculated for this interval from the measured transmission data.

The neutron source was a beam from the graphite thermal column of the chain reactor collimated by a series of three absorbing slits to a $3/4'' \times 3''$ area. The spectrum of neutrons emitted from this source had an approximate Maxwellian distribution of velocities with its peak at about 0.04 electron volt. The intensities in the range between 0.004 to 0.20 electron volt were sufficient for these measurements; outside this range intensities were generally too low to be used. Passing through the shutter the interrupted beam fell upon the absorber and reached the detector, 150 cm from the rotating cylinder. The detector, mounted with its axis normal to the beam, was a BF_3 proportional counter, 3.8 cm in diameter and 11 cm long, having a central wire 0.002 inch in diameter. The filling gas was enriched in the isotope B^{10} to increase its counting efficiency. In order to minimize the effect of background neutron radiation, the whole counter except for a port to admit the beam was surrounded by a 2.5–cm shield layer of boron carbide.

Measurement of transmission was made by comparing the beam intensity at the various energies with the scattering sample interposed in the beam to the intensity of the unfiltered beam. A second series of similar measurements was taken at each energy to evaluate the intensity of neutrons leaking through the shield plus those fast neutrons which passed through the closed shutter. This measurement was made by stopping the shutter and setting it at the position which it assumed at the time the signal from the detector was sent to the recorders. In this position only fast neutrons could pass through the shutter to reach the detector. In all cases this background intensity was less than 5 percent of the total flux in each energy interval, reaching this fraction only in the extremes of the energy range. The transmission was then calculated from the relation

$$T = \frac{R(a)}{R(0)},$$

where $R(a)$ is the counting rate in the filtered beam corrected for background, and $R(0)$ is the counting rate of the open beam similarly corrected.

3. Results.

A) *Beryllium.*—The sample for the measurements was prepared from a block of very pure microcrystalline beryllium metal reduced to chips by turning on a lathe. These chips, subsequently further pulverized by trituration in a mortar and pestle made of beryllium metal, were reduced to their final size in a beryllium ball mill. A 3.25″ diameter cylindrical disk of the material having a surface density of 2.45 grams/square centimeter was prepared by pressing in a die. The cross section per atom shown plotted in fig. 1 was calculated from the relation

$$\sigma = -\log \frac{T}{N}$$

in which N is the number of atoms of Be per cm² and T is the transmission measured in the manner discussed above. Solid lines represent theoretically predicted values. Uncertainties in the cross section were evaluated by assigning a statistical uncertainty equal to the square root of the number of counts to each of the four measured components of the transmission value. Because the intensities were lowest at the extreme of the energy range, cross-section measurements at these energies show the greatest statistical uncertainty.

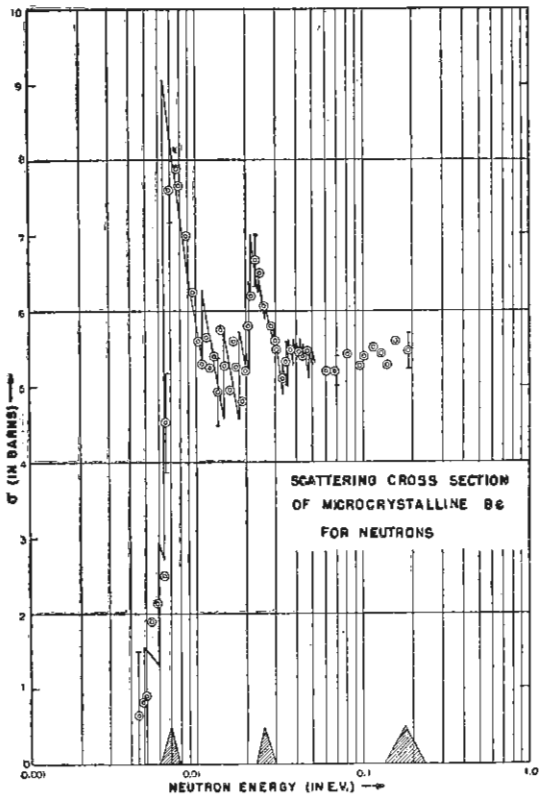

Fig. 1. – The microcrystalline beryllium cross section. The solid line represents the cross-section function as calculated in Section 4. Triangles at the base of the curve indicate the resolution of the instrument in the various ranges of measurement. The cross sections, σ, are given in units of 10^{-24} cm²/atom (barns).

B) *Beryllium Oxide.*—A sintered block of BeO, prepared from very fine powder crystals was used to measure the scattering cross section for this compound. Cross-section values were calculated from transmission measurements, and, as can be seen from fig. 2, agree very well with the theoretical treatment given below.

In the case of the beryllium oxide curve, mechanical velocity selector measurements were repeated on the neutron crystal spectrometer in the range between 0.04 and 0.20 electron volt and extended to 1.0 electron volts by this method.

4. Theory.

Although the theory of the coherent scattering of neutrons by microcrystalline materials has been given [1,2], it seems worth while to indicate the physical factors which go into the results. For this purpose, we consider a beam of neutrons moving in a given direction incident upon a single microcrystal. The wave-lengths of the neutrons in the beam are assumed to be

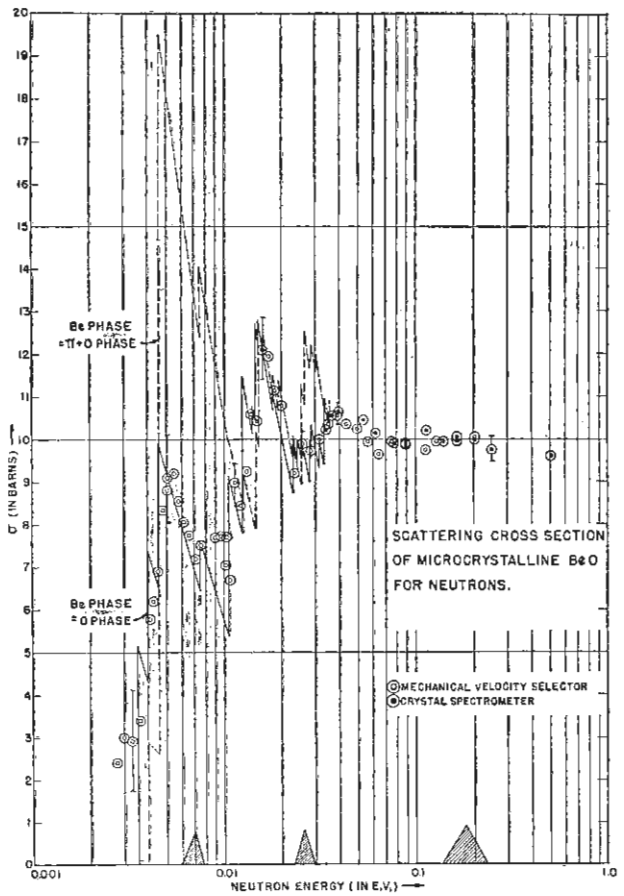

Fig. 2. – Scattering cross section of BeO. Alternate theoretical curves for same and opposite phase of neutron scattering are shown as solid and dotted lines, respectively. Results indicate that the Be phase is the same as the oxygen phase.

distributed uniformly between λ and $\lambda + \Delta\lambda$. The orientation of the microcrystal is such that one of the wave-lengths in the interval $\Delta\lambda$ undergoes Bragg reflection from some particular set of lattice planes. Then, since the scattered wave is undergoing constructive interference, the scattered intensity is proportional to the square of the number of scattering centers. Thus, if N_0 is the number of nuclei in the microcrystal and F the scattering cross section of a nucleus, the scattered intensity is proportional to $N_0^2 F$.

Since the crystal is finite in size, the scattered beam is spread by diffraction over a solid angle of the order of $\frac{(\lambda/l)^2}{\cos\theta}$ where l is the average linear dimension of a microcrystal and θ is the angle between the scattered beam and the normal to the crystal plane responsible for Bragg reflection. Since $\cos\theta = \frac{b\lambda}{2}$ where b is the product of the order of the reflection and the reciprocal of the spacing between lattice planes, the intensity of the scattered beam integrated over its spatial width is proportional to

$$\frac{\lambda N_o^2 F}{l^2 b}. \tag{1}$$

Only neutrons within a small range of wavelengths in the interval $\Delta\lambda$ contribute to this scattering. The fraction of the neutrons with the proper wavelength can be obtained from the resolving power of the crystal which is $\frac{d\lambda}{\lambda} = \frac{1}{bl}$ where bl is equal to the product of the order of the reflection and the number of crystal planes contributing to the reflection. The fraction of the incident neutrons which are scattered is therefore $\frac{d\lambda}{\Delta\lambda} = \frac{\lambda}{bl\Delta\lambda}$, so the ratio of the intensity scattered to the incident intensity is proportional to

$$\frac{N_o^2 F\lambda^2}{l^3 b^2 \Delta\lambda}. \tag{2}$$

This scattered intensity is now to be averaged over all orientations of the microcrystal. Since the crystal gives rise to a Bragg reflection only if its orientation is such that the Bragg condition is satisfied for some wave-length within $\Delta\lambda$, a contribution to the scattering is obtained only in the solid angle $2\pi\Delta(\cos\theta) = \frac{2\pi b\Delta\lambda}{2}$. The average over-all orientation, therefore, gives rise to the factor $\frac{\Delta(\cos\theta)}{2} = \frac{b\Delta\lambda}{4}$. The final result for the scattering cross section per nucleus corresponding to scattering of a particular order from a particular set of lattice planes is, apart from numerical factors,

$$\sigma_b = \frac{NF\lambda^2}{b}. \tag{3}$$

where N is the number of nuclei per unit volume. This cross section is to be summed over all sets of crystal planes and all orders of reflection which are consistent with the Bragg conditions; i.e., for which $b \leq 2/\lambda$.

From this result it can be seen that for very low neutron energies of wavelength large compared to twice the spacing between any adjacent lattice planes, no Bragg reflection can occur so there is no coherent scattering. When the energy is increased to the point at which the Bragg condition is just satisfied for the most widely spaced pair of lattice planes, there is a discontinuous jump in the scattering given by Eq. (3). Then the cross section decreases proportionally to the square of the neutron wave-length until the Bragg condition is satisfied for the next most widely spaced pair of lattice planes. At that point, another term of the type Eq. (3) is introduced so the cross section again increases discontinuously. This behavior repeats itself

as the energy is increased so a jagged curve of the form shown in fig. 1 is obtained.

The exact form of the elastic scattering cross section with the correct numerical factors including a factor which takes into account the zero point and thermal oscillations of the crystal is [2]

$$\sigma_e = \sum_{b \leq 2/\lambda} \frac{FN\lambda^2 \exp(-\omega b^2)}{8\pi b}, \tag{4}$$

where ω is a constant which depends on the Debye temperature and temperature of the lattice and is to be obtained from reference 2, Eq. (30). F is to be interpreted as the form factor of the unit cell in the crystal and N the number of unit cells per unit volume. Then σ_e is the cross section per unit cell.

Since the Be lattice is hexagonal close packed, the form factor is given by

$$F_{Be} = \frac{2\sigma_{Be}[1 + \cos\pi(2l + 4m + 3n)/3]}{\mu_{Be}^2}, \tag{5}$$

where σ_{Be} is the cross section of the free Be atom, μ_{Be} is the reduced mass, in units of the neutron mass, of the neutron and a free Be atom, and l, m, n are the products of the order of the reflection and the Miller indices of the plane leading to the particular Bragg reflection under consideration. The appearance of the factor $1/\mu_{Be}^2$ is owing to the very large effective mass of a Be atom which scatters neutrons with an energy small compared to the binding of the Be in the lattice [5]. The theoretical curve obtained from Eq. (4) for Be at room temperature ($T = 293°$ K) is given in fig. 2. The cross section σ_{Be} has been taken to be 6.1×10^{-24} cm^2. This value is obtained from the mean experimental cross section for a neutron energy of the order of several volts (an energy at which the Be atom may be treated as free). The Debye temperature of Be has been taken to be [6] $\Theta = 1000°$ K.

The generalization of these considerations to polyatomic crystals leads again to Eq. (4). In this case, however, the form factor depends on the positions of the different atomic species in the unit cell and on the relative signs of the amplitudes of the waves scattered from the different nuclei. If our considerations are limited to biatomic crystals, the form factor is given by

$$F = 4\pi \left| A_1 \sum_{abc} \exp[2\pi i(la + mb + nc)] + A_2 \sum_{\alpha\beta\gamma} \exp[(2\pi i(l\alpha + m\beta + n\gamma)] \right|^2, \tag{6}$$

where *abc* are the positions in terms of the primitive translations of the lattice of the nuclei which scatter with amplitude A_1, and $\alpha\beta\gamma$ are the corresponding positions of the nuclei which scatter with amplitude A_0. For the BeO crystal this reduces to

$$F_{BeO} = 4\pi \left| A_{Be} + A_O \exp(3\pi i n/4) \right|^2 F_{Be}$$

where F_{Be} is to be obtained from Eq. (3). In particular, for $n = \pm 1$, the

(5) E. FERMI, « Ricerca Scient. », *7*, No. 2, 13 (1936). See also R. G. SACHS and E. TELLER, « Phys. Rev. », *60*, 18 (1941).

(6) MOTT and JONES, *Properties of Metals and Alloys* (Oxford, 1936).

amplitude dependent factor is

$$A_{Be}^2 + A_O^2 - \sqrt{2}\, A_{Be} A_O .$$

Since A_{Be} and A_O are of the same order of magnitude, this quantity depends rather sensitively on the relative signs of the amplitudes A_{Be} and A_O. It is larger if the signs are opposite. Thus, for the reflections from the twelve sets of planes $(l, m) = (\pm 1, 0), (0, \pm 1), (1, 1), (-1, -1)$ with $n = \pm 1$, there will be a considerable difference in the strength of the Bragg peak between the two cases of like sign and opposite sign. This makes it possible to determine experimentally by a transmission measurement whether the signs A_{Be} and A_O are equal or opposite.

The theoretical curves for the cross section as a function of energy are given in fig. 2 for both possible choices of sign. In obtaining these curves, the magnitudes of the scattering amplitudes were obtained from

$$4\pi |A_{Be}|^2 = \frac{\sigma_{Be}}{\mu_{Be}^2} \quad , \quad 4\pi |A_O|^2 = \frac{\sigma_O}{\mu_O^2} , \tag{7}$$

where σ_O is the scattering cross section of a free O atom (found as before from the scattering of one volt neutrons to be 4.1×10^{-24} cm^2) and μ_O is the reduced mass of the neutron plus a free O atom. The Debye temperature of BeO was estimated from the velocity of sound and found to be $\Theta = 1200°$ K. Comparison of the experimental points and the theoretical curves shows clearly that the signs of the amplitudes of the Be and O scattering are the same.

5. Conclusion.

The good agreement between theory and experiment indicates that the application of Eq. (4) to other crystalline materials should give an adequate representation of the scattering cross section as a function of energy. There are, however, a number of conditions that may lead to deviations from this result.

Probably the most important of these would be the occurrence of such large microcrystals in the sample that the peaks in the scattering are wiped out by extinction in the crystals. An estimate of the maximum size of the microcrystals to be used can be obtained by determining what fraction of those neutrons of a given energy which hit a particular crystal at the Bragg angle are scattered. This fraction can be obtained by dividing the expression (1) by the projected cross-sectional area of the crystal which is given by $l^2 \cos\theta = \frac{l^2 \delta\lambda}{2}$. If we introduce the correct numerical factor which can be obtained by comparing Eqs. (1)–(4), the fraction of the neutrons scattered by a particular set of crystal planes turns out to be

$$\frac{N^2 l^2 F^2}{\pi b^2} . \tag{8}$$

Since it is desirable to have not more than 1 percent of the beam scattered

by one microcrystal, the upper limit on the crystal dimensions may be taken to be

$$l \leq \frac{(\pi)^{1/2}\, b}{10\, N\, (F)^{1/2}} . \tag{9}$$

If $b = 3 \times 10^{7}\ \mathrm{cm}^{-1}$, $F = 10^{-23}\ \mathrm{cm}^{2}$ and $N = 4 \times 10^{22}$, Eq. (9) becomes $l \leq 5 \times 10^{-5}$ cm. Thus, for crystals of linear dimensions smaller than a micron, one would not expect an appreciable reduction in the peaks because of extinction. These dimensions refer to the perfect microcrystals of which the material is composed. Considerably larger crystallites would be acceptable if the crystallites consist of many such microcrystals oriented at small angles with respect to each other. In order to be sure that this condition was satisfied for the Be crystals on which were made the measurements discussed in Section 3, it was necessary to break the material up mechanically; for BeO, there was no such difficulty.

Other sources of deviations from the theory may be the following:

(1) The microcrystals not randomly oriented. This may occur when the sample is prepared by extrusion.

(2) The temperature of the sample not small compared to its Debye temperature. Then an appreciable amount of inelastic scattering would be expected. This would render the peaks less sharp and would introduce appreciable scattering below the first Bragg limit.

(3) The crystal contains two or more isotopic constituents which have appreciably different scattering properties. The incoherent scattering background would then be appreciable. However, it is necessary that there be a very strong dependence of the scattering amplitude on the isotopic identity of the nucleus for this to be a large effect.

(4) The nuclei of the sample have a spin different from zero and the scattering is strongly spin dependent. This would again lead to an incoherent background which would be large only if the spin dependence of the scattering were very strong.

(5) If the sample used is made up of a very fine powder, the surface area will be so large that there is a chance that adsorbed surface films may contribute appreciably to the cross section. This may lead to an erroneous interpretation of the results, particularly if one is trying to distinguish between two possibilities corresponding to two different combinations of the signs of the scattering amplitudes. If a large amount of water, for example, is adsorbed on the crystals, there will be a smooth background cross section rising rapidly at low energies which could easily transform the lower curve in fig. 2 into a curve that could hardly be distinguished from the upper curve.

If care is taken to avoid the difficulties mentioned above, it is believed that the transmission method offers a good procedure for determining the relative phases of the scattering of pairs of nuclei which can be compounded to form a microcrystalline material. This would then make it possible to determine the absolute sign of the scattering phases of a series of nuclei if the phase were determined for one particular nucleus.

The numerical work required for determining the theoretical curves in figs. 1 and 2 was carried out by M. G. Goldberger.

N° 227–231, 234 and 235.

At the end of the war, the physicists who returned to the University of Chicago to form the Institute for Nuclear Studies found a physics department with bare shelves. Almost every usable meter, tool, and accessory of particle physics had long since been absorbed into wartime research. For example, even the small cyclotron had been shut down, and required many months of cleaning before it could resume operation.

It was reasonable, therefore, that we turned to the excellent heavy water reactor facility of the Argonne Laboratory with its high thermal neutron flux, to investigate aspects of neutron physics which had been bypassed in the drive to the wartime objectives.

The series of investigations of scattering processes of slow neutrons show the main features of Fermi's often expressed philosophy of experimentation. That is, one should begin to make any straightforward measurement in a situation where there is a promising ignorance. The attempt to understand the results should in turn suggest new measurements. In his collaboration, we felt his sweet reasonableness, steady competence with situations he could influence, and restrained amusement at frustrations beyond his control.

We already knew from wartime research (see paper N° 191) of the production of very cold neutrons by filtration through microcrystalline graphite, whose crystal planes removed from the transmitted beam those neutrons of wave length sufficiently short to be Bragg scattered. It was a natural step, therefore, to examine the neutron scattering properties of single crystals and in particular to use their Bragg scattering to produce monochromatic neutron beams.

In this way, we found strong differences of intensity of neutrons reflected from various planes of a given crystal, differences which could be interpreted in terms of scattering interferences between elements of the crystal. We quickly found that lithium scattered in opposite phase from that of most elements, a result which impelled us to test many crystals borrowed from several museums in the neighborhood of Chicago until we finally found a second example, namely manganese.

The experiment on the neutron-electron interaction developed from a desultory conversation on the subject of " How could one measure ? " during which many impractical experiments were mentioned. It was an exciting surprise when such a good idea evolved.

In a somewhat different form, papers 227–230 were included in quarterly reports CF–3574 and CP–3750, Argonne Laboratory, July 26, 1946, and January 17, 1947. Paper N° 227 was presented by Herbert Anderson, together with Paper N° 191 and 220, at the 1946 International Conference on Low Temperatures and Elementary Particles held at Cambridge, England.

LEONA MARSHALL.

227.

PHASE OF NEUTRON SCATTERING

E. FERMI and LEONA MARSHALL

Physical Society Cambridge Conference Report, 94–97 (1947).

Bragg scattering of neutrons is analogous to that of x–ray scattering except in one respect. x–rays are always scattered in the same phase, but neutrons may be scattered in the same phase or in opposite phase. The

purpose of this investigation was to examine the phase of neutron scattering of various nuclei.

A beam of thermal neutrons from the Argonne pile was made monoenergic by Bragg reflection from the 100 face of a fluorite crystal at an angle of about 15°. By rotating a second crystal in the monoenergic beam, Bragg reflections of various orders were obtained. A study of the relative intensities of the orders allows one to compare the phase of neutron scattering of the different nuclei which compose the second crystal.

The simplest case is that of a crystal in which the planes are equidistant and consist alternately of two kinds of atoms. Such is the case, for instance, for the 111 planes of NaCl, which are equidistant and contain alternately sodium and chlorine. In the first-order Bragg reflection, the optical path for reflection from sodium planes differs from that for reflection from chlorine planes by $\lambda/2$. Consequently, if sodium and chlorine scatter in the same phase their contributions will subtract and the order will have low intensity; if they scatter in opposite phase the order will have high intensity.

The situation is different for the second order, where the difference in optical path for reflection from the two kinds of plane is λ, and, consequently, if sodium and chlorine scatter in the same phase the order will have high intensity and, if in opposite phase, low intensity. By analogous reasoning it follows that if the two types of nuclei scatter in the same phase the odd orders will be weak and the even orders will be strong. Conversely, if they scatter in opposite phase the odd orders will be strong and the even orders weak.

Analogously to x-ray scattering, there is superimposed upon this effect a continuous decrease from order to order due to geometrical factors, to thermal agitation, and to imperfections of the crystal.

Aside from this regular decrease the intensity of the various orders is determined by the form factor

$$F = \left| \sum_j \pm \sqrt{\sigma_j} \exp\left(2\pi i n \delta_j / d\right) \right|,$$

where σ_j is the scattering cross-section, d is the spacing of the lattice planes, n is the order of the Bragg reflection, δ_j is the perpendicular distance from the jth atom to the plan of reflection. The + sign is used if the neutrons are scattered in phase, and the — sign if they are scattered in opposite phase. In the case where an element has more than one isotope, the weighted average of the square roots of the isotopic scattering cross-sections is used.

The observed intensities of Bragg reflections from various crystals are given in Table II. They have not been corrected for the continuous decrease of intensity with order because this correction is different for various crystals. The theoretical form factors calculated from the above expression, assuming that all elements scatter in the same phase, and therefore using always the + sign, are also given. The square root of the scattering cross-section of an atom taken with the proper sign is represented in the form factor by the chemical symbol for the atom itself.

TABLE I.

Crystal	Plane	Order	Max. intensity (c./s.)	Theoretical form factor
NaCl	111	1	2376	Na—Cl
		2	2750	Na+Cl
NaCl	100	1	8200	Na+Cl
		2	2960	Na+Cl
		3	650	Na+Cl
PbS	111	1	7250	Pb—S
		2	10700	Pb+S
		3	808	Pb—S
		4	750	Pb+S
PbS	100	1	6893	Pb+S
		2	1354	Pb+S
		3	726	Pb+S
CaF_2	100	1	16300	Ca—2 F
		2	20300	Ca+2 F
		3	1287	Ca—2 F
FeS_2 (Pyrite)	100	1	6893	Fe+0.6 S
		2	1354	Fe—1.6 S
		3	726	Fe—1.6 S
MnS_2	111	1	7930	Mn—1.06 S
		2	2560	Mn+0.06 S
		3	670	Mn+0.06 S
Fe_3O_4	111	1	12000	2.3 Fe+ 1.2 O_x
		2	12600	16.0 Fe—31.9 O_x
		3	12800	13.7 Fe— 3.5 O_x
		4	21000	8.0 Fe+31.5 O_x
		5	5100	23.7 Fe+ 5.9 O_x
$CaCO_3$ (Calcite)	111	1	2820	Ca—CO_3
		2	2000	Ca+CO_3
		3	1060	Ca—CO_3
$CaCO_3$ (Calcite)	211	1	10990	Ca+C+0.9 O_x
		2	3360	Ca+C—1.0 O_x
		3	2400	Ca+C+1.3 O_x
KBr	111	1	1545	K—Br
		2	2853	K+Br
		3	19	K—Br
		4	~ 0	K+Br
MgO	111	1	764	Mg—O
		2	14175	Mg+O
		3	132	Mg —O
MgO	100	1	10352	Mg+O
		2	6258	Mg+O

Continued: TABLE I.

Crystal	Plane	Order	Max. intensity (c./s.)	Theoretical form factor
LiF	100	1	740	Li+F
		2	236	Li+F
LiF	111	1	10080	Li–F
		2	~ 13	Li+F
		3	382	Li—F
$BaSO_4$	011	1	1015	—3.4 Ba+3.8 S+4.7 O_x
		2	1632	+1.9 Ba+3.1 S–9.6 O_x
		3	651	+0.4 Ba+2.0 S—7.9 O_x
		4	36	—2.5 Ba+0.8 S—2.2 O_x
		5	~ 0	+3.8 Ba—0.6 S+0.9 O_x
	010	1	3606	4 (Ba+S)+ 0.4 O_x
		2	4837	4 (Ba+S)+14.6 O_x
		3	756	4 (Ba+S)+ 3.1 O_x
	101	1	737	0.9 Ba—1.2 S— 1.5 O_x
		2	1946	1.1 Ba—2.0 S— 4.6 O_x
		3	1477	3.8 Ba+1.0 S+ 2.6 O_x
		4	~ 0	0.3 Ba—0.1 S+ 2.1 O_x
		5	587	1.0 Ba+2.1 S—10.4 O_x

It is at once evident that the components of the pairs, Na and Cl, Ca and F, Pb and S, Fe and S, K and Br, Mg and O, Fe and O, scatter with the same sign. Furthermore, Li and F scatter neutrons with opposite phases. The measurements of MnS_2 do not allow a unique interpretation, although they indicate that Mn and S probably scatter with opposite phases.

Assuming this last statement to be true, it follows from the measurements on calcite that Ca and O scatter with the same phase. The analysis of the measurements on $BaSO_4$ is facilitated by using the fact that S and O scatter which the same phase since the measurements on pyrite and magnetite proves that both are like Fe. With this assumption one finds that Ba also has the same phase as C.

From these data it follows that O, Fe, Mg, Ba, Ca, S, F, and Pb all scatter neutrons in the same phase. Li and probably Mn scatter in the opposite phase. Na and Cl scatter with like sign, as do K and Sr, but are as yet unrelated to the others.

The fact that a mirror of Fe shows total reflection for neutrons indicates that this element changes the phase of the scattered neutron wave by 180° (negative phase), and permits the assignment of negative phase to C, Fe, Mg, Ba, Ca, S, F, and Pb, and of positive phase to Li and probably to Mn. Theoretical results lead to the expectation that hydrogen also scatters with negative phase.

In Table II the attempt has been made to give a set of values of $\sqrt{\sigma}$ that is consistent with the observed intensities.

TABLE II.

Element	O	Fe	S	Pb	Ca	F	Li	Ba	Mg
$\sqrt{\sigma} \times 10^{12}$ (cm)	—2.15	—2.9	—1.0	—1.7	—2.8	—2.1	+2.1	—2.8	—2.0

From this table it appears that most elements of the group investigated scatter with positive phase. This is somewhat puzzling since it is contrary to the theoretical expectation. We propose to carry out in the future some check, especially on the points on which this conclusion mainly rests.

N° 228 and 229.

In a somewhat different form, paper N° 228 was included in quarterly Report CP–3750, Argonne National Laboratory, January 17, 1947. Paper N° 228 was also circulated as Document MDDC–713, Atomic Energy Commission, Oak Ridge, Tennessee.

Paper N° 229 was aso circulated as document MDDC–843.

See also the introductions to papers N° 226 and 227.

H. L. ANDERSON.

228.

INTERFERENCE PHENOMENA OF SLOW NEUTRONS

E. FERMI and L. MARSHALL
Argonne National Laboratory and University of Chicago, Chicago, Illinois

(Received February 7, 1947)
« Phys. Rev. », 71, 666–677 (1947).

Various experiments involving interference of slow neutrons have been performed in order to determine the phase of the scattered neutron wave with respect to the primary neutron wave. Theoretically this phase change is very close to either 0° or 180°. The experiments show that with few exceptions the latter is the case. The evidence is based on the following types of measurements: (*a*) measurement of the intensities of Bragg reflection of various orders of many crystals, and comparison with the theoretical values of the form factor; (*b*) total scattering cross section of gas molecules for wave-lengths long compared with the molecular dimensions; and (*c*) determination of the limiting angles for total reflection of neutrons on various mirrors. The elements Ba, Be, C, Ca, Cu, F, Fe, Mg, N, Ni, O, Pb, S, and Zn were found to scatter neutrons with 180° phase difference; Li and probably Mn scatter with zero phase difference. The five elements I, Br, Cl, K, and Na behave alike and the phase with which they scatter is tentatively identified as 180°. Coherent scattering cross sections have been determined for several elements.

INTRODUCTION.

The scattering processes of slow neutrons are greatly complicated by interference phenomena due to the fact that the de Broglie wave-length is comparable with interatomic distances. The general pattern of interference phenomena of slow neutrons is similar to that of x–rays, since both the wave-length and the scattering cross section of x–rays are comparable to those of neutrons. On the other hand there are considerable differences due to several factors. Among them is the fact that the scattering of x–rays varies regularly with atomic number while that of neutrons is a rather erratic

property. Furthermore, in the case of neutrons the phase difference between scattered and incident wave may be either 0° or 180° as will be discussed in Section 1. For x-rays instead, it is always 180° because x-ray energies are larger than most electronic resonance energies. Also, the absorption properties of neutrons differ markedly from those of x-rays.

The main purpose of this work was the investigation of various interference phenomena in order to determine the phase change of the scattered neutron wave for a large number of elements. Section 1 contains a summary of the theoretical background of this work. Section 2 describes the measurements of the intensities of Bragg reflections of various orders and their interpretation. Section 3 is a discussion of some experiments on filtered neutrons. In Section 4, experiments on scattering of neutrons by gas molecules are presented. Section 5 describes measurements of the limiting angle for total reflection of neutrons. The general conclusions are discussed in Section 6.

1. Theoretical Considerations.

When a slow neutron is scattered by a nucleus, its de Broglie wave at some distance from the scattering nucleus may be written as the sum of a term $\exp(ikx)$ representing the primary wave and a term $-a[\exp(ikx)]/r$ representing the scattered wave. This is true for the case of slow neutrons because with very good approximation the scattering is spherically symmetrical. The coefficient of the latter term has been written with the minus sign for reasons of convenience that will be apparent later. If the constant a is positive, there is a phase change of 180° between scattered and incident wave, and if a is negative, the phase change is 0°. One proves in an elementary way that the scattering cross section is related to the constant a by the equation

$$\sigma = 4\pi |a|^2 \tag{1}$$

and also that the constant a is with very good approximation for slow neutrons a real number. Its imaginary part is very small and can usually be neglected except in case of extremely high absorption. The quantity a which has the dimensions of a length and the order of magnitude of 10^{-12} cm shall be referred to as the "scattering length." The main purpose of this paper is the experimental determination of the scattering length and in particular of its sign.

For elements consisting of one isotope only and without nuclear spin, the magnitude of the scattering length can be immediately obtained from (1), so that only its sign needs to be determined. Even in this simple case a small correction must be applied depending on whether the atom is free or bound. Because of the change in the reduced mass, the cross section of a fre atom differs from that of the same atom bound in a crystal, by a factor $[(A + 1)/A]^2$, where A is the atomic weight [1].

(1) For example see H. A. Bethe, « Rev. Mod. Phys. », 9, 71 (1937).

Since the scattering length is proportional to the square root of the cross section, the correction factor will be (A + 1)/A. It follows that

$$a = \left[\frac{(A+1)}{A}\right] a_f \tag{2}$$

where a indicates the scattering length of the atom bound in a crystal and a_f the scattering length for the free atom. For elements that are mixtures of several isotopes with probabilities of occurrence $p_1, p_2, \cdots, p_n$, and scattering lengths $a_1, a_2, \cdots, a_n$ the scattering length is the average

$$a = p_1 a_1 + p_2 a_2 + \cdots + p_n a_n . \tag{3}$$

This is the magnitude that determines the interference properties of the element. The scattering cross section is no longer given by (1) but by

$$\sigma = 4\pi \{ p_1 a_1^2 + p_2 a_2^2 + \cdots + p_n a_n^2 \} . \tag{4}$$

Actually in this case the relationship between a and σ can be expressed by the inequality

$$| a | \leq \left(\frac{\sigma}{4\pi}\right)^{1/2} . \tag{5}$$

The knowledge of the scattering cross section is insufficient, therefore, to determine even the magnitude of the scattering length.

A similar situation obtains if the nucleus has a spin I different from zero. Here the spin vector of the scattering nucleus is oriented either parallel [total spin I + (1/2)], or antiparallel [total spin I — (1/2)] to the spin vector of the neutron. Consequently the scattering length may take either of two values, $a_{I+1/2}$ or $a_{I-1/2}$. The effective scattering length is the average of these two scattering lengths, each being weighted by the probability of occurrence of the corresponding spin orientation, namely

$$a = \frac{I}{2I+1} a_{I-1/2} + \frac{I+1}{2I+1} a_{I+1/2} . \tag{6}$$

The scattering length will obey (5), the equal sign corresponding to the case that $a_{I+1/2}$ is equal to $a_{I-1/2}$ both in magnitude and sign.

A simple geometrical interpretation of the scattering length can be obtained if the interaction between the neutron and the nucleus is represented by a potential well. Let the eigenfunction of the neutron for an s state of energy zero be $\psi(r)$. In fig. 1, $r\psi(r)$ is plotted *versus* r. The curve becomes a straight line for r greater than the radius r_0 of the potential well. This straight line can be extended to intersect the r axis at the point P. One can prove that the scattering length a is the abscissa of the point P. Figure 1 A corresponds to a case in which a is positive, and fig. 1 B to a case in which a is negative. By inspecting the two figures it is apparent that the probability is much higher for a positive than for a negative, especially for heavy elements. This remark on the relative probability for a to be positive or negative is due to E. Teller and V. Weisskopf.

A simple formula can be obtained in the case that the scattering is due to the effect of a single Breit-Wigner resonance level. It is, then

$$a = \frac{-\lambda_R \Gamma_n}{[W - R + i\Gamma]} \tag{7}$$

where W is the energy of the neutron, R is the resonance energy, Γ_n and Γ are the neutron and total half width at half maximum, and $\lambda\!\!\!^{-}_R$ is the de Broglie wave-length at enery R, divided by 2π. Since in most cases Γ is small

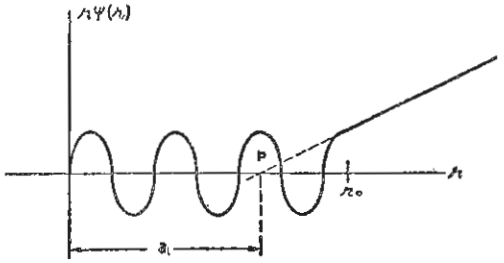

Fig. 1 A. – Positive scattering length.

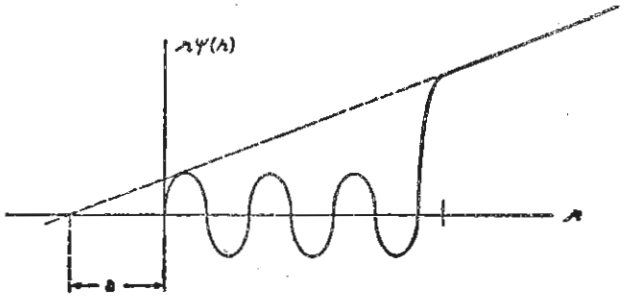

Fig. 1 B. – Negative scattering length.

compared with (W — R), it follows that a will be positive or negative depending on whether the energy of the neutron lies below or above the resonance energy. This picture is a great oversimplification since there are no cases in which the Breit-Wigner scattering of a single level is the dominant phenomenon, and complicated situations arise due to interference of Breit-Wigner and potential scattering.

2. Intensities of Various Orders of Bragg Reflection.

One can compare the changes in phase in the neutron scattering of different elements by measuring the intensity of the Bragg scattering for various orders and various crystalline planes of crystals containing at least two elements.

The simplest case is that of a crystal in which the planes are equidistant and consist alternately of two kinds of atoms, as for example, the 1 , 1 , 1 planes of NaCl. These planes are equidistant and consist alternately of sodium and of chlorine. In the first order Bragg reflection, the optical path for reflection from sodium planes differs from the path for reflection from chlorine planes by $\lambda/2$. Consequently if sodium and chlorine nuclei cause

the same change in phase of the scattered neutron wave, their contributions will subtract and the order will have low intensity. If they scatter with opposite phase change their contributions will add and the order will have high intensity.

The situation for the second order is reversed. Here the difference in optical path for reflection from the two kinds of planes is λ. Consequently if sodium and chlorine scatter with the same change in phase the order will have high intensity, and if with opposite change in phase, low intensity. Similarly it follows that if the two kinds of nuclei scatter with the same change in phase the odd orders will be weak and the even orders will be strong. Conversely, if they scatter with opposite change in phase, the odd orders will be strong and the even orders weak.

Analogously to x–ray scattering, there is super-imposed upon this effect a continuous decrease in intensity from order to order due to geometrical factors, to thermal agitation, and to imperfections of the crystal.

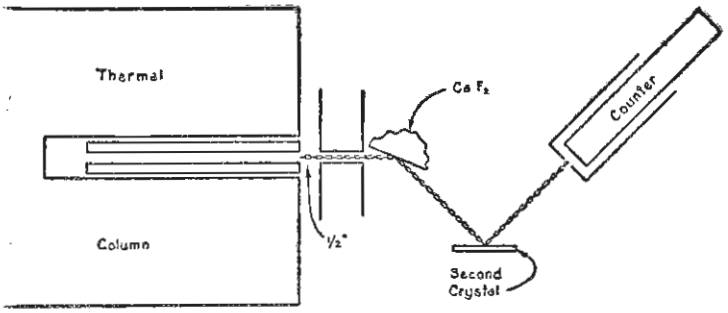

Fig. 2. – Apparatus for measuring intensity of Bragg orders.

For more complicated cases the intensity of the various orders is determined as for x–rays by the form factor

$$F = | \Sigma_j a_j \exp (2\pi i n \delta_j/d) | \tag{8}$$

where a_j is the scattering length, d is the spacing of the lattice planes, n is the order of the Bragg reflection, and δ_j is the perpendicular distance from the jth atom to the plane of reflection. Naturally the form factor is strongly dependent on the relative signs of the scattering lengths of the various atoms of the crystal. An analysis of the intensities for various orders and various planes of the crystal will often allow the determination of the relative signs of the scattering lengths of the elements involved. In several cases it is possible to determine also the ratios of the values of the scattering lengths.

A comparison of intensities for Bragg reflections of various orders of many crystals have been made using monochromatic neutrons. The experimental arrangement is schematically represented in fig. 2. A beam of non-monochromatic thermal neutrons emerges from a $4'' \times 4''$ hole containing a long collimator $1/2''$ wide by $1\ 1/4''$ high in the thermal column of the Argonne heavy water pile. This beam falls on the 1, 0, 0 plane of a large CaF_2 crystal at a glancing angle of about 16°. Neutrons of energies satisfying

the Bragg conditions ($\lambda \sim 1.50$ angstroms for the first order) are reflected to form a beam that is used for investigating various crystal specimens. The beam contains a main component of neutrons of wave-length 1.50 A plus a small fraction of neutrons of energy four times as large due to the second order reflection on the CaF_2 crystal. The second order component is fairly unimportant because there is only a small number of neutrons of this relatively high energy in the Maxwell distribution. We can, therefore, consider the beam reflected on the calcite to be approximately monochromatic. This monochromatic beam of neutrons falls on some plane of the second crystal, which is mounted on a rotating table. The neutrons undergo a second Bragg reflection, and are finally detected by an enriched BF_3 proportional counter. The counter is supported by an arm which rotates about the axis of the crystal table. Additional Cd slits not shown are used for more precise collimation of the neutron beam.

A typical measurement was carried out as follows. Both counter and second crystal were set approximately at angles corresponding to a reflection of a given order. By rocking each separately the setting of maximum intensity was found. Also the inclination of the crystal was adjusted for maximum intensity. From the intensity measured in these conditions was subtracted a background, measured by turning the crystal a small angle off the Bragg position. In the majority of cases the background was a small fraction of the total count.

The results of these measurements are summarized in Table I. Columns 1 and 2 indicate the crystal and the plane. Column 3 is the form factor. Here the chemical symbol of the element has been used to represent its scattering length. The fourth column gives the absolute value of the form factor, using the values of the scattering length given in Table VII. The fifth column gives the measured intensities of the various orders in counts per minute. In the sixth column is the ratio of column 5 to column 4. If the values chosen for the scattering lengths are approximately correct, one expects that the values in column 6, corresponding to any given plane, should show a regular decrease in intensity with increasing order, since dividing the intensity by the form factor should correct it for the irregular change of intensity from order to order. Therefore only the regular decrease should remain.

There may be some doubt whether it is more appropriate to divide the intensity by the form factor or by its square. Theoretically one would expect that, for ideally perfect crystals, the form factor should be used, and for ideally imperfect crystals, its square. Actually, we have found that one obtains a much better fit by using the form factor.

For the simplest crystals containing two elements one can see immediately by inspecting the intensity data of column 5 whether the scattering lengths of the two elements have equal or opposite sign. For instance CaF_2 (100), NaCl (111), and PbS (111) show clearly superimposed on the general decrease of intensity with increasing order, an alternation of intensity with strong even orders and weak odd orders. Since, in these crystals, the planes consist alternately of the two kinds of atoms, we conclude that the scattering

lengths of each pair have the same sign. The opposite is the case for LiF (1 1 1) where the even orders have intensity so low that we could not measure them, and the odd orders have a normal intensity. Therefore Li and F have scattering lengths of opposite sign. In some of the more complicated cases the analysis is also quite straight forward as can he seen by comparison of the observed intensities with the formulae for the form factors in column 3. In a few cases the interpretation is not unique.

The following conclusions as to the signs of the scattering lengths can be drawn. The components of the following pairs have scattering lengths of the same sign: Na , Cl ; Pb , S ; Ca , F ; Fe , S ; Fe , O ; K , Br ; Mg , O ; K , Cl; K , I. The components of the pair, Li, F have scattering lengths of opposite sign. The measurements of MnS_2 do not allow a unique interpretation although the probable conclusion is that Mn and S also have scattering lengths of opposite sign.

Using the evidence to be presented in Sections 4 and 5 that carbon and oxygen have scattering lengths with the same sign, one can conclude from the measurements on calcite that Ca and O also have scattering lengths of the same sign.

From the measurements on FeS_2 and Fe_3O_4, one can conclude that S and O have the same sign ; and from data on $BaSO_4$, one is led to assign also the same sign to Ba. The measurements on $NaNO_3$ indicate that N and O have the same sign. (See confirmatory evidence in Section 4). The measurements of the (1 1 1) plane of $NaNO_3$ indicate although not quite conclusively that Na has the same sign as the group NO_3, and therefore as N and O.

From these data it follows that C , O , Fe , Mg , Ba , Ca , S , F , Pb, and N all have the same sign. Na , K , Cl , Br , I all have like sign. The partial evidence just mentioned, according to which Na has the same sign as O, indicates that all this latter group should be included with the former. That this conclusion is correct is strongly supported by evidence to be presented in Section 6. Li and perhaps Mn have scattering lengths of the other sign. They represent together with hydrogen (see Section 6) the only exceptions found so far to the behavior of the majority of elements.

This type of data allows only a comparison of the signs of scattering lengths of different elements but not their absolute determination. The absolute determination of sign of scattering length will be discussed in Section 5. The over-all conclusions from Section 2 will be presented in Table VII. There, an attempt has been made to give the actual value of the scattering lengths for several elements. In calculating these values the attempt was made to obtain the best possible agreement of the observed intensities given in Table I, with the form factor after proper account was taken of the natural decrease of intensity with increasing order.

In x–ray analysis of crystals the Debye-Scherrer method of powder photography is extensively used. For neutrons, however, the intensity of the Debye-Scherrer maxima is rather small, and in most cases the method will be impractical. For example, in the case of microcrystalline graphite, we were able to detect only the maximum corresponding to the first reflection on the 0 0 1 plane.

TABLE I.

Intensity of Bragg orders.

Crystal	Plane	Order	Form factor		Intensity	Ratio
CaF_2	(100)	1	Ca — 2 F	0.41	16300	39800
		2	Ca + 2 F	1.99	20300	10200
		3	Ca — 2 F	0.41	1287	3140
NaCl	(111)	1	Na — Cl	0.57	2376	3990
		2	Na + Cl	1.69	2750	1630
PbS	(111)	1	Pb — S	0.20	7280	36400
		2	Pb + S	0.76	10700	14100
		3	Pb — S	0.20	808	4040
		4	Pb + S	0.76	750	986
PbS	(100)	1	Pb + S	0.76	19650	25800
		2	Pb + S	0.76	11420	15000
		3	Pb + S	0.76	2249	2960
FeS_2	(100)	1	Fe + 0.62 S	0.99	6893	6960
		2	Fe — 1.6 S	0.37	1354	3660
		3	Fe — 1.6 S	0.37	726	1960
MnS_2	(111)	1	Mn — 1.06 S	0.74	7930	10700
		2	Mn + 0.06 S	0.42	2560	6100
		3	Mn + 0.06 S	0.42	670	1600
Fe_3O_4 (magnetite)	(111)	1	2.34 Fe + 1.20 O	2.65	21300	8040
		2	16 Fe — 31.9 O	6.34	19970	3150
		3	13.7 Fe — 3.55 O	9.06	12570	1390
		4	8 Fe + 31.50 O	25.78	16700	647
		5	13.7 Fe + 5.94 O	14.85	5120	344
$CaCO_3$ (calcite)	(111)	1	2 C + 6 O — 2 Ca	3.42	9500	2780
		2	2 C + 6 O + 2 Ca	6.58	8520	1290
		3	2 C + 6 O — 2 Ca	3.42	1840	538
$CaCO_3$ cleavage	(211)	1	2 Ca + 2 C + 1.76 O	3.99	10900	2730
		2	2 Ca + 2 C — 2.0 O	1.70	3360	1980
		3	2 Ca + 2 C + 2.7 O	4.57	2400	528
$BaSO_4$	(100)	1	4 Ba + 4 S + 0.42 O	4.54	3606	794
		2	4 Ba + 4 S + 14.6 O	13.19	4837	366
		3	4 Ba + 4 S + 3.1 O	6.17	756	123
$BaSO_4$	(011)	1	— 3.4 Ba + 3.8 S + 4.7 O	1.24	1018	821
		2	1.75 Ba + 3.1 S — 9.6 O	3.61	1632	452
		3	0.42 Ba + 2.0 S — 7.9 O	3.93	651	166
		4	— 2.46 Ba + 0.75 S — 2.2 O	3.07	36	12
$BaSO_4$	(101)	1	0.87 Ba — 1.25 S — 1.47 O	0.56	737	1320
		2	1.13 Ba — 2.02 S — 4.56 O	2.46	1946	791
		3	3.77 Ba + 0.98 S + 2.56 O	4.81	1477	307
		4	0.27 Ba — 0.10 S — 2.12 O	1.47	—	—
		5	1.04 Ba + 2.12 S — 10.4 O	4.93	587	119
MgO	(100)	1	Mg + O	1.17	10352	8800
		2	Mg + O	1.17	6258	5350

Continued: TABLE I.

Crystal	Plane	Order	Form factor		Intensity	Ratio
MgO	(111)	1	Mg — O	0.05	764	15300
		2	Mg + O	1.17	14175	12100
		3	Mg — O	0.05	132	2640
LiF	(111)	1	Li — F	1.19	10080	8470
		2	Li + F	0.01	~ 0	—
		3	Li — F	1.19	300	252
KBr	(111)	1	Br — K	0.21	1545	7360
		2	Br + K	0.91	2853	3140
KCl	(111)	1	Cl — K	0.78	2346	3010
		2	Cl + K	1.48	5620	3800
		3	Cl — K	0.78	334	428
		4	Cl + K	1.48	160	108
$NaNO_3$	(211)	1	Na + N + 0.88 O	1.96	29000	14800
		2	Na + N — 0.98 O	0.83	4171	5000
		3	Na + N + 1.34 O	2.25	4148	1800
$NaNO_3$	(111)	1	NO_3 — Na	2.14	29400	13700
		2	NO_3 + Na	3.26	16790	5150
		3	NO_3 — Na	2.14	2243	1050
KI	(111)	1	K — I	0.01	85	—
		2	K + I	0.71	348	500
		3	K — I	0.01	24	—

A second possibility to study microcrystalline substances is to measure the total cross section of the substance for neutron of wave-length close to $2d$ where d is the longest lattice spacing. An analysis of this case for substances containing two elements has been made by Fermi and Sachs, and indicates that the total cross section in this region depends strongly on whether the scattering lengths of the two elements have equal or opposite sign. The practicability of this method is somewhat limited by the fact that the theory applies only when the microcrystalline grain of the substance is exceedingly fine.

3. SPECTRUM OF FILTERED NEUTRONS.

In the study of interference in gas molecules, somewhat simpler results are obtained with neutrons of energy far below thermal energies and which have a wave-length long compared with interatomic distances. Such neutrons are present in very small percentage in the Maxwell distribution at room temperature. Consequently, one cannot isolate such low energy neutrons by Bragg reflection because in the reflected beam there is a contamination by high orders which is many times more intensive than the first order. A simple way to avoid this difficulty, without use of extremely low temperature

moderators, is to remove the high energy part of the Maxwell distribution by passing the beam of neutrons through a filter of a microcrystalline material of low absorption, [2] such as graphite or BeO. This filtering action of microcrystalline substances is due to the fact that neutrons of wave-length longer than $2\,d$, where d is the longest lattice spacing of the crystal, cannot satisfy the Bragg reflection condition for any of the many crystallites that they meet while crossing the filter. Consequently, they are scattered out of the beam only to a minimal extent. The production of very low energy neutrons by the filtering process has bene previously reported [2] for the case of graphite, where the limiting wave-length is 6.7 A. In the present experiments BeO filters have been used, for which the limiting wave-length is 4.4 A. In order to get experimental proof of the correctness of the interpretation of the filtering process, we have investigated with the crystal spectrometer the spectrum of the neutrons filtered by a prism 40 cm long and containing 100 g/cm². The side dimensions of the prism were about 10 × × 10 cm. The analysis was carried out with a crystal of celestite in the 001 plane. The results are plotted in fig. 3, where the wave-lengths are plotted on the abscissae, and the observed intensities are the ordinates. The figure shows clearly that the spectrum of the filtered neutrons has negligible intensity for short wave-length, rises abruptly to a maximum value at wavelength of approximately 4.5 A, and after that, decreases gradually with increasing wave-length.

Fig. 3. – Spectrum of neutrons filtered through BeO. Abscissa in Angstrom.

The decrease of intensity on the long wave-length side is somewhat more rapid than corresponds to the Maxwell distribution. This probably is due to the fact that the neutrons emerging from the graphite column are not fully slowed down to the lowest energies of the Maxwell distribution by the collisions in graphite.

The fact that microcrystalline BeO and Be metal are good filters for neutrons is an indication that the scattering lengths of Be for the two spin orientations of the neutron do not differ very considerably. Indeed if this were the case one would expect a strong incoherent scattering that should not vanish even for wave-lengths longer than $2\,d$. For filtered neutrons we found a residual cross section for BeO of 0.7×10^{-24} cm². If all this residual cross section were due to the difference in the scattering lengths a_1 and a_2 for the two spin orientations, it could be calculated that a_1 and a_2 certainly have the same sign and that their ratio is about 2. Probably the actual

(2) ANDERSON, FERMI, and MARSHALL, « Phys. Rev. », *70*, 815 (1946).

values are appreciably closer, because part of the observed residual cross section is certainly due to crystal imperfections and to thermal agitation.

4. Scattering of Neutrons by Gas Molecules.

Some conclusions on the scattering of neutrons can he drawn from the study of the total cross section of gas molecules. For neutrons of wavelength short compared with interatomic distances the molecular scattering cross sections is the sum of the individual scattering cross sections of the atoms in the molecule. When neutrons of longer wavelength are used, a number of complications arise, partly due to interference effects, and partly to the fact that the scattering now is due to atoms that no longer can be considered free.

The theoretical calculation of the cross section has been carried out by Teller and Schwinger [3] for the case of the H_2 molecule for low rotational states. For heavier molecules, such as N_2 or O_2, even when low temperatures and slow neutrons are used, a fairly large number of rotational states is always excited so that a detailed calculation of the contributions of all rotational states becomes impractical. Simple results can be calculated by neglecting the neutron mass in comparison with the mass of the atoms in the molecule. In this approximation one obtains results identical with those of the classical theory of interference. The approximation is quite good in the case of x–rays, where the particle scattered is a photon of very small effective mass, and has been used currently by Debye and his co-workers. For scattering of neutrons from molecules such as N_2, O_2, etc., the approximation is not nearly as good. The corrections, however, have not been calculated, and the results will be compared with those of the approximate theory except in the case of H_2 where the theory of Teller and Schwinger has been used.

The scattering cross sections of several molecules have been determined using very low energy neutrons obtained by filtration through a BeO filter. The spectrum of these neutrons is given in fig. 3. Although these neutrons are not monochromatic they belong to a fairly narrow band of average wavelength 5.1 A. For the measurements at room temperature the gas under investigation was contained in a long aluminum tube of 2.5″ i.d. and 365 cm long. Pressures up to 2 atmospheres were used. On H_2 we performed some measurements at liquid air temperature and in this case a tube 24″ long was used. A copper coil was soldered around this tube and liquid air was circulated in it. The entire assembly was protected with rock wool insulation. The conditions were such that the orthopara ratio was practically the same as at room temperature.

Only in the cases of CF_4 and H_2 measurements were performed also for neutrons of shorter wave-lengths obtained by Bragg reflection on a fluorite crystal.

(3) Teller and Schwinger, « Phys. Rev. », *52*, 286 (1937).

In Table II the total cross sections of BeO–filtered neutrons observed for various gases at room temperature are collected. In the third column of the table is given the sum of the total cross sections of the constituent atoms. One notices considerable differences between this sum and the observed cross sections. Except for the case of hydrogen which will be discussed later these differences are explained only to a small extent by the fact that the gas molecules are not at rest (so-called Doppler effect), and are due mostly to the interference of the waves scattered by the constituent atoms. In column 4 the values of σ calculated from the classical interference theory (see above) are given. For diatomic molecules containing two different atoms one obtains two different results, depending on the assumption that is made for the sign of the scattering lengths of the two atoms. In the cases of CO_2 and CF_4 a reasonably good agreement between theory and observation is obtained only if the scattering lengths of the component atoms are assumed to have the same sign. The same seems to be true for N_2O, though the sensitivity to a change in relative sign of the scattering length is not so pronounced here.

TABLE II.

Cross sections for $\lambda = 5.1$ A (gas at room temperature).

Molecule	σ (observed)	Sum of the total cross sections of constituent atoms	σ calcultated from classical interference theory
CO_2	24.5	13.0	24.8 or 4.1 for opposite phase
N_2O	57.8	34	55 or 4.1 for opposite phase
O_2	16.2	8.2	13.2
N_2	47.4	30	44.4
CF_4	41.5	21	38 or 7.5 for opposite phase
H_2	170	42	

The very large cross section observed for H_2 is strongly perturbed by the Doppler effect because here the thermal agitation velocity of the molecules is larger than the velocity of the neutrons, so that the phenomenon can be better described by saying that the molecules hit the neutron rather than the opposite. This fact is brought out by the strong temperature dependence of the cross section which drops from 170×10^{-24} cm^2 to 81×10^{-24} cm^2 when the H_2 is cooled from room temperature to liquid air temperature. This point will be discussed later.

Table III gives the cross sections observed for CF_4 at room temperature for neutrons of various velocities. The table shows a rise by about a factor 2 when the wave-length increases from 1.5 to 5.1 A. Up to 1.5 A the cross

values are appreciably closer, because part of the observed residual cross section is certainly due to crystal imperfections and to thermal agitation.

4. Scattering of Neutrons by Gas Molecules.

Some conclusions on the scattering of neutrons can be drawn from the study of the total cross section of gas molecules. For neutrons of wavelength short compared with interatomic distances the molecular scattering cross sections is the sum of the individual scattering cross sections of the atoms in the molecule. When neutrons of longer wavelength are used, a number of complications arise, partly due to interference effects, and partly to the fact that the scattering now is due to atoms that no longer can be considered free.

The theoretical calculation of the cross section has been carried out by Teller and Schwinger [3] for the case of the H_2 molecule for low rotational states. For heavier molecules, such as N_2 or O_2, even when low temperatures and slow neutrons are used, a fairly large number of rotational states is always excited so that a detailed calculation of the contributions of all rotational states becomes impractical. Simple results can be calculated by neglecting the neutron mass in comparison with the mass of the atoms in the molecule. In this approximation one obtains results identical with those of the classical theory of interference. The approximation is quite good in the case of x–rays, where the particle scattered is a photon of very small effective mass, and has been used currently by Debye and his co-workers. For scattering of neutrons from molecules such as N_2, O_2, etc., the approximation is not nearly as good. The corrections, however, have not been calculated, and the results will be compared with those of the approximate theory except in the case of H_2 where the theory of Teller and Schwinger has been used.

The scattering cross sections of several molecules have been determined using very low energy neutrons obtained by filtration through a BeO filter. The spectrum of these neutrons is given in fig. 3. Although these neutrons are not monochromatic they belong to a fairly narrow band of average wavelength 5.1 A. For the measurements at room temperature the gas under investigation was contained in a long aluminum tube of 2.5″ i.d. and 365 cm long. Pressures up to 2 atmospheres were used. On H_2 we performed some measurements at liquid air temperature and in this case a tube 24″ long was used. A copper coil was soldered around this tube and liquid air was circulated in it. The entire assembly was protected with rock wool insulation. The conditions were such that the orthopara ratio was practically the same as at room temperature.

Only in the cases of CF_4 and H_2 measurements were performed also for neutrons of shorter wave-lengths obtained by Bragg reflection on a fluorite crystal.

(3) Teller and Schwinger, « Phys. Rev. », *52*, 286 (1937).

section is fairly close to 21×10^{-24} cm², namely to the sum of the cross sections of one atom of carbon and four of fluorine. The rise is due in large measure to interference.

TABLE III.

Cross section of CF_4 (room temperature).

$\lambda \times 10^8$	Velocity of neutrons (m/sec)	$\sigma \times 10^{24}$
0.881	4590	19.5
1.099	3600	19.0
1.316	3000	21.5
1.492	2650	20.8
5.1	775	41.5

Tables IV and V give the results obtained on H_2 at room temperature and at liquid air temperature respectively. At room temperature one notices a steady rise in cross section with decreasing velocity of the neutrons. As previously indicated, this is to a large extent due to the thermal agitation velocity of the gas molecules. A correction factor, calculated on the assumption that the cross section is constant, is given in the fourth column. The last column gives the cross section corrected by this factor.

TABLE IV.

Cross section of H_2 (room temperature).

$\lambda \times 10^8$	Velocity (m/sec)	$\sigma \times 10^{24}$	Factor for Maxwell distribution	σ/factor
0.76	5212	50.9	1.048	48.6
0.93	4256	53.2	1.071	49.7
1.11	3546	56.2	1.099	51.1
1.46	2714	61.2	1.172	52.2
1.68	2347	64.4	1.231	52.3
2.24	1765	68.0	1.407	48.3
5.1	775	169.7	2.514	67.5

The data of Table V taken at liquid air temperature can be most easily compared with the Teller-Schwinger theory because at this temperature practically only rotatioual states 0 and 1 are involved. Column 3 of this table gives the observed cross section and column 4 gives the cross section corrected for the thermal agitation velocity of the gas molecules. The fifth column gives the theoretical values calculated with the Teller-Schwinger theory, assuming $a_0 = -2.40 \times 10^{-12}$ and $a_1 = 0.54 \times 10^{-12}$ for the singlet and triplet state of the neutron proton system. The agreement is not too good especially for the lowest velocity, though the last value may be vitiated by the large Doppler correction.

TABLE V.

Cross section of H_2 *at* 83° K (ortho-para ratio unchanged from room temperature).

$\lambda \times 10^8$	Velocity (m/sec)	$\sigma_{total} \times 10^{24}$ observed	$\sigma_{scat} \times 10^{24}$ corrected for absorption and Doppler effect	Teller-Schwinger theory
0.836	4730	44	43	—
1.202	3290	51	49	—
1.638	2420	55	52	56
1.884	2100	56	51	57
5.1	775	81	52	80

By performing a similar set of measurements on deuterium one might be able to draw some conclusions of the spin dependence of the cross section, and we hope to make such measurements in the future.

5. TOTAL REFLECTION OF NEUTRONS OF MIRRORS.

The total reflection of neutrons on mirrors is theoretically expected to occur at very small glancing angles for substances with a positive scattering length. The index of refraction is given by

$$n = 1 - \frac{\lambda^2 N a}{2\pi} \tag{9}$$

where a is the scattering length taken with the proper sign, N is the density of atoms in the mirror, and λ is the wave-length. Consequently n is less than 1 (case of total reflection) if a is positive. The limiting glancing angle is then given with very good approximation by

$$\theta_0 = [2\,(1 - n)]^{1/2} = \lambda \left(\frac{Na}{\pi}\right)^{1/2}. \tag{10}$$

In most cases $(n - 1)$ is of the order of magnitude of 10^{-6} and the limiting angle of the order of 10′. The total reflection of neutrons on mirrors has been previously observed [4] using non-monochromatized thermal neutrons. In this case of course one cannot observe a limiting angle because θ_0 [see (10)] is proportional to λ so that neutrons of the various wave-lengths of the Maxwell distribution drop out of the reflected beam gradually as the glancing angle is increased. In spite of this, the fact that strong reflection is observed on a substance can be construed as good evidence that the index of refraction for that substance is less than one, and that therefore a is positive. This is so because, although a substance which is not totally reflecting has a finite reflection coefficient, it is so small that no very prominent reflection could he observed in such cases. From the quoted experiments it could therefore be concluded that the following elements, Be, Cu, Zn, Ni, Fe, C, for which strong reflection has been observed, have positive scattering length.

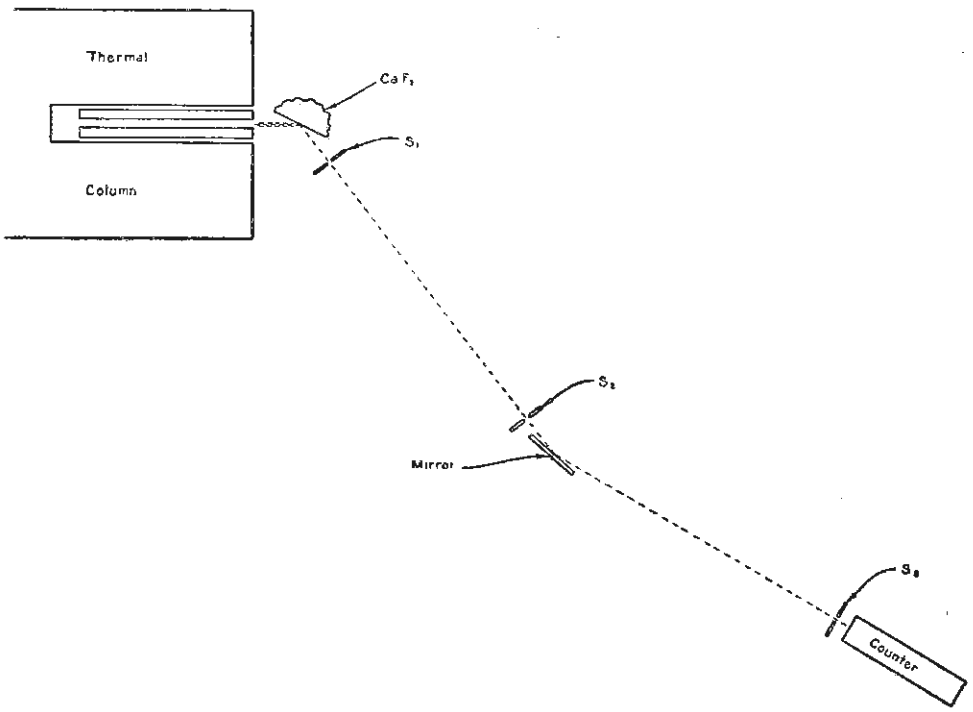

Fig. 4. – Monochromatic total reflection on mirrors.

In order to test conclusively the theory of total reflection, the reflection experiments were repeated using monochromatic neutrons. This made it possible to observe the sharp drop of the reflected intensity at the limiting angle and to measure this angle.

The experimental arrangement is shown schematically in fig. 4. A collimated beam of thermal neutrons emerging from the thermal column is made monochromatic by Bragg reflection on a fluorite crystal. It is further

(4) FERMI and ZINN, « Phys. Rev. », 70, 103 (1946).

collimated by passing through two very narrow cadmium slits, S_1 and S_2, 2 mm wide and about 3.5 meters apart. The narrow monochromatic beam emerging from the second slit falls on the mirror which can be rotated by small angles. The reflected beam is detected by a BF_3 proportional counter about 3.5 meters away and with a cadmium entrance slit 2 mm wide. By moving the counter across the beam, both direct and reflected beam are detected.

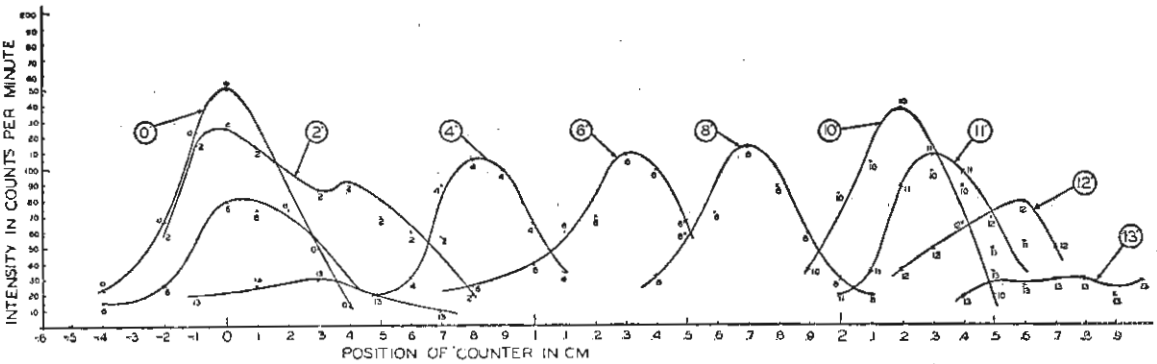

Fig. 5. – Typical results of measurements of a reflection on a Be mirror.

Typical results of these measurements are plotted in fig. 5 for the case of a reflection on a Be mirror. The abscissa is the position of the detector expressed in centimeters measured transversely to the direction of the beam. The ordinate is the neutron intensity in counts per minute. The curves whose experimental points are marked 0, 2, 4, etc., correspond to the intensity plots found when the mirror is set at an angle of 0, 2, 4, etc., minutes to the direction of the neutron beam. When the mirror is parallel to the beam, there is observed a single maximum corresponding to that of the main beam. When the mirror is rotated by 2′ the reflected beam is barely resolved from the direct beam. At 4′ the two maxima are well separated. For larger angles the direct beam has not been drawn in the plot except for the largest angle, 13′, at which the reflected beam has completely disappeared and also the direct beam has disappeared because the mirror has turned by such a large angle that it completely cuts off the main beam. These points therefore correspond to the background, which actually was about 20 counts per minute.

By inspecting the plot one sees that the intensity of the reflected beam drops sharply to background between the positions 10 and 13 minutes. This drop is not quite sudden because the angular resolution was about two minutes. A study of the intensity shows the limiting angle to be 12 minutes.

In Table VI the values of the limiting angles of several mirrors measured for neutrons of de Broglie wave-length $\lambda = 1.873$ A are given. The experimental values given in the second column of the table should be compared with the theoretical values calculated from formula (10) given in the third column. The agreement is excellent except in the case of carbon, for which a not too good graphite mirror was used.

TABLE VI.

Limiting angle for total reflection of neutrons of 1.873 A.

Mirror	Limiting angle (minutes)	
	Observed	Calculated
Be	12.0	11.1
C (graphite)	10.5	8.4
Fe	10.7	10.0
Ni	11.5	11.8
Zn	7.1	6.9
Cu	9.5	9.5

The absolute determination of the sign of the scattering length for the totally reflecting elements, taken together with the results of Sections 2 and 4, allows one to determine the actual sign for a large group of elements.

6. CONCLUSIONS.

In Table VII all the data available at present on scattering length have been summarized. The absolute sign given in the table has been obtained primarily from the data of Section 5 on total reflection, and indirectly, by combining these data with those of Section 2 on intensities of Bragg reflections, and Section 4, on molecular scattering. The absolute values have been obtained in various ways.

For the elements having only one isotope or one strongly dominant isotope, and no nuclear spin, the absolute value of the scattering length can be calculated from formulae (5) and (2) provided the total scattering cross section is known. For example, this method has been applied in assigning the value 0.61×10^{-12} cm for the scattering length of oxygen in a crystal. This differs by a factor 16/17 from the scattering length 0.57×10^{-12} cm for a free oxygen atom. In some cases this same method has been applied to elements having several important isotopes, or a spin, or both. In such cases the absolute value is naturally much less reliable. The method has been used when no better way was available. In the last column of Table VII the code letter A has been used to denote values obtained by this method.

The results of Section 2 allow the scattering lengths of several elements to be related directly or indirectly to that of oxygen whose scattering length 0.61×10^{-12} has been used as a standard for these cases.

TABLE VII.
Scattering lengths.

Element	$a \times 10^{12}$	$4\pi a_{at}^2 \times 10^{24}$	$\sigma_{scat} \times 10^{24}$	Remarks
Ba	0.79	7.7	8	C
Be	0.89	8.0	6.1	M
Br	0.56	3.9	< 7	C
C	0.67	4.8	4.8	A
Ca	0.79	7.5	9.5	C
Cl	1.13	15	15	A, no spin and isotope effect considered
Cu	0.81	8.0	7.2	M
F	0.60	4.1	4.1	A, no spin effect considered
Fe	0.82	8.1	9.2	M
H	−0.39	0.48	21	From theory
I	0.36	1.6	1.6	A, no spin effect considered
K	0.35	1.5	1.5	A, no spin and isotope effect considered
Li	−0.59	3.4	—	C
Mg	0.56	3.7	4	C
Mn	−0.44	2.4	2.4	A, no spin effect considered
N	0.87	8.3	8.3	A, no spin effect considered
Na	0.56	3.7	3.5	C
Ni	1.09	14	13	M
O	0.61	4.1	4.1	A
Pb	0.48	2.9	10	C
S	0.28	0.95	1.1	C
Zn	0.58	4.1	3.6	M

For the five elements, Na, K, Cl, Br and I, which are not conclusively related to the others (see Section 2), Cl has been taken as a standard with a scattering length of 1.13×10^{-12} cm. The sign has been taken positive partly on account of the evidence from Bragg reflection on $NaNO_3$, as discussed in Section 2. Furthermore, both theoretical and experimental evidence in-

dicate that cases of negative scattering length are very improbable. The probability that five elements all having the same sign should be negative is therefore exceedingly small.

In other cases the value of the scattering length has been calculated from the value of the limiting angle using formula (10). Code letter M indicates these instances.

In the third column of Table VII is given the expression $4\pi a^2\left(\frac{A}{A+1}\right)^2\times 10^{24}$. If there are no important isotopes and no spin this should coincide with the scattering cross section. Otherwise it should in general be smaller, the more so the greater the differences are in the scattering lengths for the various isotopes and spin orientations.

The values in column 3 therefore should be compared with the experimental values of the scattering cross section given in column 4. Naturally the comparison is trivial for the cases designated by A, where formulae (2) and (5) have been used to calculate a. Comparison in the remaining cases shows that usually the data of the third and fourth columns are rather close. The few exceptions for which the data in column 3 are less than those of column 4 can be explained as due to experimental inaccuracy. The fact that they are close seems to indicate that, in general, the spin and isotope dependence of the scattering length is not extremely pronounced.

There are two notable exceptions. One is hydrogen, a case well known from the Teller-Schwinger theories. The other one is lead where perhaps some of the many isotopes may have a negative scattering length.

The table shows that the scattering length is positive in the great majority of cases as discussed in Section 1.

This work was performed at the Argonne National Laboratory, and we greatly benefited by the help of the staff of the laboratory in providing and operating the neutron source, and in supplying many of the experimental facilities needed. Several of the crystals used were loaned to us by the Field Museum in Chicago through the courtesy of Mr. Changnon, by Dr. Howland of the Mineralogy Department of Northwestern University, and by Dr. Fisher of the Geology Department of the University of Chicago. Also some specimens were obtained from the Union Carbide and Carbon Research Laboratories, Inc., and the Eagle Picher Lead Company. Mr. Warren Nyer helped in some of the experiments.

This document is based on work performed under Contract No. W-31-109-eng-38 for the Manhattan Project, and the information covered therein will appear in Division IV of the Manhattan Project Technical Series as part of the contribution of the Argonne National Laboratory.

N° 229.

For the introduction to this paper see papers N° 226, 227 and 228.

229.

PHASE OF SCATTERING OF THERMAL NEUTRONS BY ALUMINUM AND STRONTIUM (*)

E. FERMI and L. MARSHALL
Argonne National Laboratory and University of Chicago, Chicago, Illinois

May 15, 1947
« Phys. Rev. », *71*, 915 (1947) (Letter).

In a previous paper (1) we have described a method for determining whether neutrons scattered by an atom have the same phase as the primary neutron wave or opposite phase. The method has now been applied to two more elements, Al and Sr. The crystals investigated were Al_2O_3 (corundum) and $SrSO_4$ (celestite). The measured intensities of various orders of Bragg reflections of monochromatic neutrons are given in the following table, which is arranged like Table I of reference 1.

TABLE I.

Intensities of reflection of thermal neutrons by Al_2O_3 *and* $SrSO_4$.

Crystal	Plane	Order	Form factor	Intensity
Al_2O_3	110	1	2 Al — 1.44 O	480
		2	2 Al — 1.34 O	700
		3	2 Al + 2.09 O	5940
$SrSO_4$	001	1	0.44 Sr + 0.77 S + 0.12 O	4351
		2	0.62 Sr — 0.19 S + 0.67 O	3576
		3	0.98 Sr + 0.48 S + 1.01 O	2182
		4	0.24 Sr + 0.93 S — 1.81 O	1682
	210	1	0.78 Sr + 0.66 S — 0.01 O	6021
		2	0.21 Sr — 0.14 S + 0.36 O	413
		3	0.44 Sr + 0.84 S + 1.09 O	1493
	101	1	0.46 Sr — 0.65 S — 0.54 O	702
		2	0.55 Sr — 1.16 S — 2.54 O	3182
		3	1.94 Sr + 0.83 S + 0.50 O	5759

(*) This document is based on work performed under Manhattan Project sponsorship at the Argonne National Laboratory.

(1) E. FERMI and L. MARSHALL, « Phys. Rev. », *71*, 666 (1947). [See paper N° 227. (Editors' note)].

Attempts to fit these data with actual values of the scattering length for aluminum and strontium have not been satisfactory. It seems unambiguous, however, that the sign of the scattering of aluminum is the same as that of oxygen, namely, positive according to our convention. This is proven by the low intensity of first and second order compared with that of the third order.

A similar behavior of the reflection from the (101) plane of celestite indicates that the scattering length of strontium is also positive. From the scattering cross sections of these two elements, 1.4×10^{-24} cm^2 for Al and 9.5×10^{-24} for Sr, one can calculate the scattering lengths 0.35×10^{-12} cm for Al and 0.88×10^{-12} cm for Sr.

N° 230.

Paper N° 230 was also included, in a somewhat different form, in quarterly Report CP–3750, Argonne National Laboratory, January 17, 1947. It was also circulated as Document MDDC–844, Atomic Energy Commission, Oak Ridge, Tennessee, April 30, 1947.

See also introductions to papers N° 226 and 227.

H. L. ANDERSON.

230.

SPIN DEPENDENCE OF SCATTERING OF SLOW NEUTRONS BY Be, Al, AND Bi

E. FERMI and L. MARSHALL
Argonne National Laboratory and University of Chicago, Chicago, Illinois
(Received May 16, 1947)
« Phys. Rev. », *72*, 408–410 (1947).

Some information has been obtained on the spin dependence of scattering of slow neutrons by Be, Al, and Bi by measuring the scattering cross section for filtered neutrons. The result is that in none of these three cases does the sign of the scattering length change when the spin orientation is changed. But in the case of Be and Bi the magnitude of the scattering length for one spin orientation may be up to twice as great as that for the other spin orientation, and in the case of Al the variation may be a factor of three.

Some information on the spin dependence of the scattering of slow neutrons can be obtained by measuring the cross sections of some microcrystalline substances for filtered neutrons.[1,2].

When a slow neutron is scattered by an atom having nuclear spin I, two values for the scattering length [2] can be expected according to whether the spin of the neutron is parallel or antiparallel to I ; these will be indicated by a_+ and a_-. If these two values are equal, there is no spin dependence of the scattering. In this case interference phenomena are not influenced by the spin, and the neutron waves scattered by the atoms behave as fully

(1) H. L. ANDERSON, E. FERMI, and L. MARSHALL, « Phys. Rev. », *70*, 815 (1946). [See paper N° 191. [Editors' note)].

(2) E. FERMI and L. MARSHALL, « Phys. Rev. », *71*, 666 (1947). [See paper N° 227. (Editors' note)].

coherent. When a_+ and a_- are different the coherent scattering of the atom is determined by an average scattering length: (see reference 2, formula (6))

$$a = \frac{I}{2I+1} a_- + \frac{I+1}{2I+1} a_+ .$$

The remaining scattering behaves as incoherent for interference phenomena.

In order to discuss the significance of coherent and incoherent scattering it is necessary to distinguish between collisions in which the spin orientation is not changed and those in which it changes. The first type of collision is responsible for coherent scattering, the second for incoherent. The reason is that interference takes place only when the scattering is due to the co-operative action of all atoms. This is the case when there is no spin change to indicate which atom has been responsible for the scattering. If there is a spin change, however, the scattering is attributed to the individual action of that atom whose spin has changed.

One can prove by elementary quantum mechanics that the coherent scattering cross section is

$$\sigma_{\text{coherent}} = 4\pi \left\{ \frac{I}{2I+1} a_- + \frac{I+1}{2I+1} a_+ \right\}^2, \tag{1}$$

and the incoherent scattering cross section is

$$\sigma_{\text{incoherent}} = 4\pi \frac{I(I+1)}{(2I+1)^2} (a_+ - a_-)^2. \tag{2}$$

This last vanishes when a_+ is equal to a_-.

The scattering cross section σ is the sum of (1) and (2)

$$\sigma = 4\pi \left(\frac{I+1}{2I+1} a_+^2 + \frac{I}{2I+1} a_-^2 \right). \tag{3}$$

The scattering of neutrons by micro-crystalline substance is largely due to the Bragg reflections on microcrystals which happen to be oriented in the proper way. Such Bragg reflections are possible only if the wave-length λ is less than $2d$, where d is the maximum lattice spacing of the crystal. Correspondingly, a large drop in the total scattering cross section of micro-crystalline materials is usually observed at this critical wave-length. The cross section usually does not drop to zero, however. The residual scattering is partly caused by the effect of irregularities of the crystal, both permanent and those due to thermal agitation, and partly by the incoherent scattering of Eq. (2), and to the effect of isotopes if they exist.

If the residual cross section could be measured for a substance containing only one isotope and made of perfect crystals at absolute zero, a measurement of the incoherent cross section of Eq. (2) could be obtained. From it one could calculate $|a_+ - a_-|$. Practically only an upper limit to this quantity can be obtained on account of the unavoidable irregularities of the sample.

Measurements have been performed on the residual cross section of micro-crystalline Be, Al, Bi, and Pb. A beam of neutrons from the thermal column of the Argonne heavy water pile was passed through a BeO filter (100 g/cm²) or a graphite filter (57 g/cm²). In this beam of filtered neutrons the transmis-

sions of the various elements were measured for samples of increasing thickness. In some cases the cross section decreased appreciably with increasing thickness of the sample. This is due to a further filtering of the neutron beam by the sample, as will be discussed later.

TABLE I.

Scattering cross sections for slow neutrons.

Element	Spin	$\sigma \times 10^{24}$ cm^2 for unfiltered neutrons $\lambda \sim 1.8$ A	$\sigma \times 10^{24}$ cm^2 for BeO filtered neutrons $\lambda > 4.4$ A	$\sigma \times 10^{24}$ cm^2 for graphite filtered neutrons $\lambda > 6.7$ A	Theoretical edge in A	Residual scattering cross section $\times 10^{24}$ cm^2	$\sigma_{scattering} \times 10^{24}$ cm^2	Limits for value of a_+/a_-
Be	3/2	6 0	0.49	0.64	3.95	0.47	7.5	0.6 to 1.8
Al	3/2	1.7	0.93	1.23	4.67	0.21	1.5	0.25 to 3.3
Bi	9/2	7.2	1.67 to 1.4	0.93	8.00	0.85	8.9	0.5 to 2.1
Pb	—	9.8	4.6 to 1.9	1.61	5.7	0.85	11	—

The results of the measurement are summarized in Table I. The cross sections observed for neutrons filtered through BeO and through graphite are given in columns 4 and 5, respectively. For comparison the cross section observed for unfiltered neutrons is given in column 3. These last values, in particular those of Bi and Pb, are appreciably decreased by the fact that the samples had a coarse crystalline structure. Consequently there is extinction of the Bragg reflection within the individual single crystals causing an apparent lowering of the cross section.

The cross sections of columns 4 and 5 are much lower than those of column 3 because the filters have removed a large fraction of the neutrons capable of being Bragg-scattered.

For Be, the theoretical edge ($2\,d$) is 3.95 A. Consequently both filters pass only wave-lengths longer than $2\,d$ and which cannot be Bragg-scattered. The increase in cross section from column 4 to column 5 is probably due to the Doppler effect resulting from thermal agitation of the Be nuclei. The residual cross section 0.47 given in column 7 has been chosen as the lower of these two values corrected for the small absorption of Be.

In the case of Al, the BeO filter does not completely eliminate all neutrons that may have Bragg reflections. Most of the rise in cross section from column 4 to column 5 is due to increase in the $1/v$ absorption. Actually the minimum scattering cross section is observed with the graphite filter. This value of 1.23 is decreased by 1.02 because of absorption of the Al. The residual scattering cross section is therefore taken as 0.21.

For Bi, the theoretical edge $2\,d$ is 8.0 A. Therefore neither filter is able to remove completely neutrons that can be Bragg reflected. For BeO filtered neutrons there is a decrease in cross section with increasing thickness

of Bi presumably due to a partial filtering of the neutrons by the sample itself. The graphite filter, because of its larger critical wave-length ($2d$), gives a lower cross section. This last has been decreased by 0.08 because of absorption, and therefore 0.85 has been taken as the upper limit to the residual scattering.

The theoretical edge for Pb is at 5.7 A. The BeO filter is therefore inadequate as is apparent from the fact that the cross section varies from 4.6 to 1.9 with increasing thickness of the absorber. As residual scattering cross section we have taken the one measured with the graphite filter corrected by 0.76 for absorption.

The values of the residual scattering cross section so obtained are collected in column 7 of the table. In column 8 are listed the scattering cross sections of the bound atoms obtained by correcting the cross sections of the free atoms by the factor $[(A + 1)/A]^2$ for the reduced mass.

For the elements Be, Al, and Bi, which have only one isotope, the residual scattering cross section is due only to spin dependence of the scattering length and to crystalline irregularities. The assumption that the residual cross section is due entirely to spin dependence leads to an overestimate of the difference between a_+ and a_-. The limits for the ratio a_+/a_- given in column 9 are calculated with this assumption and using the data of columns 7 and 8 together with formulae (2) and (3).

In the three cases investigated it is found that a_+ and a_- have the same sign. This is in accordance with the fact [2] that almost all elements have a positive scattering length. If one is allowed to generalize from these few cases, it would appear that the same is true for the scattering lengths for individual spin orientations. This is quite plausible also on theoretical grounds. On the other hand, differences of as much as a factor of 2 in the two scattering lengths produce a relatively small amount of incoherent scattering. The observation of the residual scattering becomes a sensitive method for investigation of spin dependence only when the difference between the two scattering lengths is quite large. It is quite possible that this difference is much less than the maximum values given, and that the observed residual scattering is due largely to crystal irregularities. An analysis of the data for Pb has not been given because this case is complicated by the presence of several isotopes.

This document is based on work performed under Manhattan Project sponsorship at the Argonne National Laboratory.

N° 231.

In the spring of 1946 a committee of scientists advising General Groves on postwar reorganization of research suggested the establishment of National Laboratories. Here, with government support, many universities would participate in programs of basic research too expensive for a single university. Groves accepted the suggestion eagerly, and Argonne was the first laboratory on which he acted. By the beginning of 1947 Argonne no longer issued its report as a division of the Metallurgical Laboratory, but as Argonne National Laboratory. By that time the Atomic Energy Commission had started functioning and the Manhattan Project was terminated.

Another sign of the return to normalcy is the fact that Fermi's post-war work at Argonne, although circulated at first in the laboratory's reports, was soon released for publication. Paper 231 presents non-published excerpts from quaterly reports CF–3574, CP–3750 and CP–3801 for July 26, 1946, January 17 and April 14, 1947. This work was done with L. Marshall, and section 1 with also W. Nyer.

See also the introduction to paper N° 227.

H. L. ANDERSON.

231.

FURTHER EXPERIMENTS WITH SLOW NEUTRONS

E. FERMI and L. MARSHALL

Excerpts from Quaterly Reports CF–3574, *Argonne Laboratory* (July 26, 1946), and CP–3750 and CP–3801, *Argonne National Laboratory* (January 17 and April 14, 1947).

1. SCATTERING OF MONOCHROMATIC NEUTRONS BY HYDROGEN MOLECULES.

It is planned to investigate the dependence of the scattering cross-section of gas molecules on the velocity of the neutrons. Preliminary measurements have been performed so far only in the case of hydrogen. The monochromatic neutrons were obtained by Bragg reflection at different angles on a fluorite crystal. A value of the cross-section for very low energy neutrons was obtained using filtered BeO neutrons. The results are summarized in Table I.

A striking feature of these results is the very large value for the cross-section observed at 760 m/sec. This appreciable rise of cross-section at low velocities, however, can be explained in great measure as due to the fact that the velocity of the neutron is less than the thermal agitation velocity of the molecule. (The temperature of the hydrogen was 29° C. At this tempera-

ture the root mean square velocity of a molecule is 1930 m/sec). The cross-sections given in the last column are corrected approximately for this effect and as one can see they show a much less pronounced change with the velocity. There is still apparently a rise in cross-section with decreasing velocity from about 2000 m/sec to 760 m/sec. This rise is probably due to the interaction of the neutron with the various rotational levels of the molecule. The theoretical analysis is not yet completed and will be presented at some future time.

TABLE I.

Cross-section of H_2*–Molecule.*

Velocity of Neutron m/sec		Cross-section Observed	Cross-section Corrected
760 (BeO–Filter)		170×10^{-24}	77×10^{-24}
1765	Bragg Reflection	68	48
2347		64.4	52
2714		61.2	52
3546		56.2	51
4256		53.2	50
5212		50.9	49

2. SPECTRUM OF NEUTRONS FILTERED THROUGH Be.

In fig. 1 is given the spectrum of neutrons filtered through a block of sintered Be metal of 36 gm/cm². The spectrum was obtained by monochromatising the neutrons with a crystal of $SrSO_4$. In the figure the intensity rises first at 3.6 Å, and the main rise is at 4.0 Å. The theoretical edge for Be is 3.95 Å in good agreement with the latter observation. The fact that neutrons of somewhat shorter wave length are also transmitted to some extent is due to the fact that there are only a few quite weak Bragg reflections for these neutrons. To eliminate them a longer filter should be used.

3. BREIT-WIGNER RESONANCES.

The Breit-Wigner theory predicts that at a resonance maximum not only the absorption cross section should be large but also the scattering cross section. The two cross sections are expected to have the ratio:

$$\rho = \Gamma_n/\Gamma_\gamma \tag{3}$$

of the neutron width to the gamma width. For σ_{abs} and σ_{scat} due to a single

resonance level we can write with the usual notations

$$\sigma_{abs} = \pi\lambda_R^2 \left[I \pm \frac{1}{2I+1} \right] \frac{\Gamma_n \cdot \Gamma_\gamma}{\Gamma^2 + (E-R)^2} \tag{4}$$

$$\sigma_{scat} = \pi\lambda_R^2 \left[I \pm \frac{1}{2I+1} \right] \frac{\Gamma_n^2}{\Gamma^2 + (E-R)^2} . \tag{5}$$

The existence of a remarkably high scattering at resonance has already been reported by Langsdorf for the case of In. We have tried to study in more detail the resonance scattering for the resonances of In and Ag in order to make a somewhat more quantitative test of the theory for these cases. A description of the experiment follows.

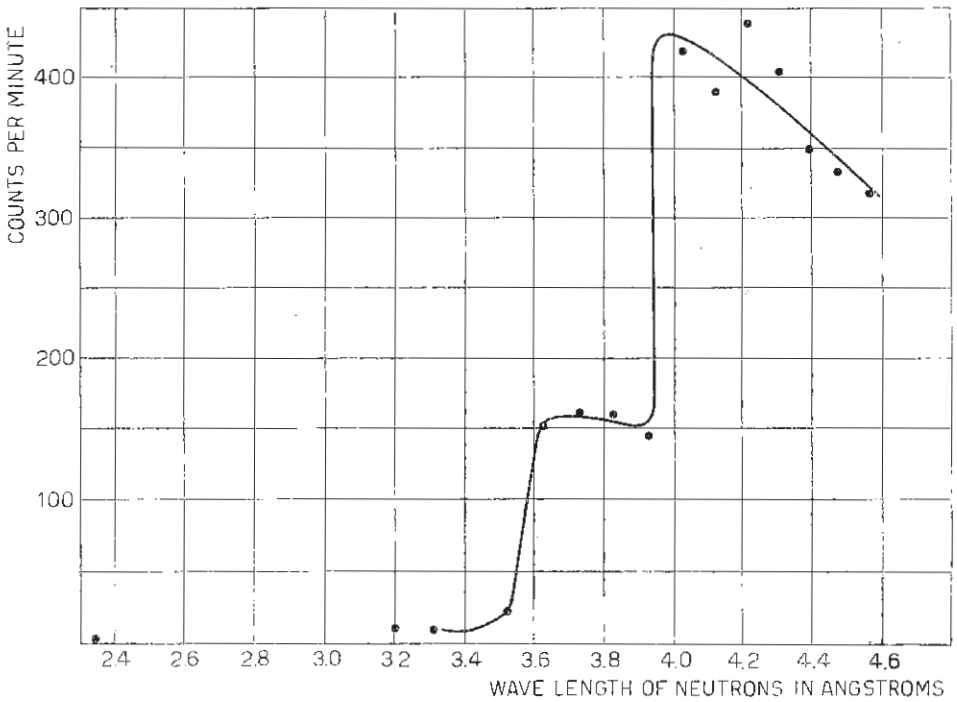

Fig. 1. – Spectrum of neutrons filtered through Be.

The scatterer was a thin circular foil of radius 2.7 cm (designated by S in fig. 2) containing 0.116 gms of indium alloyed with three times as much tin in order to give it sufficient stiffness. This scatterer was exposed to a collimated beam emerging from a hole in the shield of CP–3. The thermal neutrons were eliminated from this beam by a cadmium absorber. According to (3) a fraction ρ of the neutrons absorbed in this foil will be scattered. The scattered neutrons are detected by a foil D of pure In of weight 0.610 gms over an area of 24.9 cm^2. From the ratio of activities induced in the detector by the scattered neutrons and in the scatterer by the primary beam one can calculate ρ. Since the activity of the scatterer is relatively weak care must be taken to minimize backgrounds.

For this the detector was backed by a thick indium plate, and enclosed in a cadmium box to protect against stray thermal neutrons. Furthermore the experiment was made in a large evacuated container in order to eliminate the air scattering.

The scattering effect was measured as the difference in activity of the detector when the scatterer was put in and out of the beam. The saturated activities so obtained are summarized in Table II.

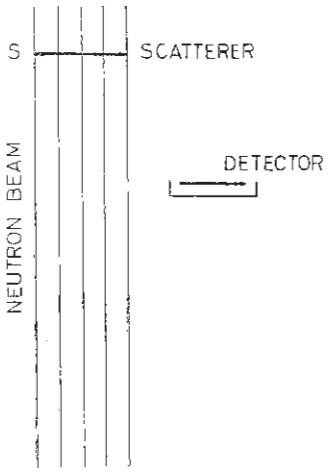

Fig. 2. – Resonant Scattering.

The net average activity of the detector must be increased by 3 % due to presence of a 1/32'' brass plate in front of the detector, giving 1140 counts/min. The activity of the scatterer is, of course, much greater and could not be compared directly on a counter with such a low activity. For this reason after irradiation of the detectors the scatterer was diluted by alloying it with much additional tin. From this alloy was made a foil equal in size and weight to the detector, and it was measured using the same geometry as was used for the detector. The final result of the measurement was a saturated activity for the scatterer of 7.90×10^6 counts/min. For the ratio of activities of detector to scatterer we therefore took $1140/7.90 \times 10^6 = = 1.45 \times 10^{-4}$.

TABLE II.

Saturated Activity of Scatterer in counts/min.

	With scatterer	No scatterer	Net
Front	4410	3041	1369
Back	3650	2801	849
		net average effect = 1109 counts/min.	

A similar measurement for the 22 sec activity of Ag was made. The scatterer and detector had the same areas as in the previous case, and were out from a sheet of Ag of 0.0276 gms/cm^2. The measurement was carried out essentially like that for indium the only difference being in the measurement of the high activity of the scatterer which was complicated due to the short life. The pile was run at a high and at a very low intensity and the two fluxes compared with an In monitor. At low power the activity of the scatterer was directly measurable ou a counter and the activity at high power

was obtained by multiplying by the ratio of the fluxes. The final results were

$$\frac{\text{Activity of detector}}{\text{Activity of scatterer}} = \frac{6100 \text{ counts/min.}}{2.91 \times 10^7 \text{ counts/min.}} = 2.10 \times 10^{-4}.$$

The ratio of activity of detector to scatterer can be expressed in terms of ω with the formula:

$$(6) \qquad \frac{\omega\rho}{4\pi} = \frac{\displaystyle\int_{-\infty}^{\infty} \frac{1+y'^2}{1+y'^2+\frac{1+y^2}{\cos\alpha}} \left\{1 - e^{-\frac{\sigma_R \delta}{(1+y'^2)\cos\alpha}}\right\} \left\{1 - e^{-\sigma_R s\left(\frac{1}{1+y^2}+\frac{1}{\cos\alpha\,(1+y'^2)}\right)}\right\} dy}{\displaystyle\int_{-\infty}^{\infty} \left(1 - e^{-\frac{\sigma_R s}{1+y^2}}\right) dy}$$

where δ and s are the atoms of In per cm² in detector and scatterer, ω is the solid angle under which the detector is seen from the scatterer, and the angle α is indicated in the figure. The integration variable y is $(E - R)/\Gamma$, and is related to y' by the relationship

$$(7) \qquad y' = y + \frac{2R}{\Gamma}\,\frac{(1+\cos\alpha)}{A}$$

where A is the atomic weight. The difference between y' and y arises from the fact that the neutrons lose energy when they are scattered. In deriving the formula the small contribution of the Doppler effect has been neglected, and Γ has been assumed small compared with R and Γ_n small compared with Γ.

The integrals in (6) have been calculated numerically with the following results. For indium

$$\frac{\text{Activity of detector}}{\text{Activity of scatterer}} = 0.00392\,\rho.$$

From the observed ratio of activities we deduce

$$\rho_{In} = \frac{1.45 \times 10^{-4}}{0.00392} = 0.037.$$

For Ag

$$\frac{\text{Activity of detector}}{\text{Activity of scatterer}} = 0.00202\,\rho$$

and

$$\rho_{Ag} = \frac{2.10 \times 10^{-4}}{0.00202} = 0.104.$$

The Breit-Wigner level of indium at 1.44 ev has been investigated relatively carefully by various investigators; (McDaniel, Rainwater and Havens with velocity selector; also self absorption and activation measurements by others). The current values for the Breit-Wigner constants are R = 1.44 ev, $\sigma(R)_{total} = 27{,}200 \times 10^{-24}$ cm², $\int \sigma(E)\,dE/E = 3{,}350 \times 10^{-24}$ cm² for the isotope In^{115}. The nuclear spin I of this isotope is 9/2. From these data one can calculate:

$$(8) \qquad \left(1 \pm \frac{1}{10}\right)\frac{\Gamma_n}{\Gamma} = 0.030.$$

The experiment gives:

$$\frac{\Gamma_n}{\Gamma_\gamma} = 0.037.$$

Therefore:

$$\frac{\Gamma_n}{\Gamma} = 0.036.$$

From (8) we find that $\Gamma_n/\Gamma = 0.027$ or 0.033 according to whether the spin of the compound nucleus is 3 or 4. The agreement, especially with the second value is excellent, but the overall experimental accuracy is not sufficient to allow one to decide between the possibilities.

In the case of Ag, no reliable measurements of σ (R) are to be found in the literature. For this reason we took a self-absorption curve of the *22* sec activity of Ag, using extremely thin detectors of 5 mg/cm². The neutron beam was that used in the previous experiment. The intensities in arbitrary units found for various Ag absorbers are reported in Table III below.

TABLE III.

Absorber mg Ag/cm²	Activity of Ag detector (5 mg/cm²) corrected for 2.3 min life
0	56.7 ± 0.4
5	49.6 ± 0.8
10	44.5 ± 0.7
15	39.3 ± 0.5
30	30.3 ± 0.3
60	21.7 ± 0.3
120	16.4 ± 0.4

Since there is a current belief that this absorption curve is strongly influenced by Doppler effect, we attempted to detect the influence of temperature on this absorption curve but we did not find any clear indication of it within our experimental accuracy of about 1–2 percent. From the data of Table III a background of 2.85 due presumably to weaker absorption levels of Ag has been subtracted. By comparison with the theoretical absorption curve, a value of $\sigma(R)_{total}$ of $11{,}300 \times 10^{-24}$ cm² for the natural isotopic mixture, corresponding to $23{,}800 \times 10^{-24}$ cm² for the isotope Ag^{109} has been calculated. The current values for the Breit-Wigner constants are $R = 5.2$ ev and $\int \sigma(E)\, dE/E = 1660$ cm² for Ag^{109}. The nuclear spin I of this isotope is $1/2$. From these data one calculates:

$$\left(I \pm \frac{1}{2}\right)\frac{\Gamma_n}{\Gamma} = 0.095. \tag{9}$$

The experiment of anomalous scattering gives:

$$\frac{\Gamma_n}{\Gamma_\gamma} = 0.104.$$

From these it follows that

$$\frac{\Gamma_n}{\Gamma} = 0.094.$$

From (9) result the two possible values $\Gamma_n/\Gamma = 0.190$ or $\Gamma_n/\Gamma = 0.063$ according to whether the spin of the compound nucleus is 0 or 1. The second value agrees somewhat better with the experimental figure. One may conclude that the spin of the compound nucleus is probably 1.

On the basis of this evidence we believe that the most probable Breit-Wigner constants are as follows:

For In:
$R = 1.44$ ev
$\Gamma_n = 0.0015$ ev
$\Gamma_\gamma = 0.042$ ev
Spin of compound nucleus $= 4$?

For Ag:
$R = 5.2$ ev
$\Gamma_n = 0.0065$ ev
$\Gamma_\gamma = 0.062$ ev
Spin of compound nucleus $= 1$.

It should be noted that our knowledge of these values is still quite incomplete, and quite large errors in the given values are possible.

4. Cross section of H_2 and D_2 molecules.

The cross section of these 2 molecules was measured at liquid nitrogen temperature (77,5° K) in order to obtain the spin dependence of the scattering length for deuterium. The measurement of H_2 was taken as a control of the method since the results for this case are already known. In the case of D_2 it was found that the scattering length for the 2 states with neutron spin parallel and anti-parallel to the spin of the D nucleus are not sufficiently different to give an appreciable reduction in the interference phenomenon. One can conclude that both scattering lengths for the 2 different orientations have the same sign and that their ratio is not more than a factor of 2.

5. Average Wave Length of BeO Filtered neutrons.

BeO filtered neutrons are often used as a source of neutrons of long wave length. In interpreting the results obtained with this source one must know the effective wave length of these neutrons. The effective wave length was obtained by measuring the absorption of the filtered spectrum for enriched boron. The effective wave length was found to be 5.5 Å.

6. Polarization of neutrons.

An attempt was made to detect a polarization of neutrons after Bragg reflection in the 2nd order of the 111 planes of magnetite. No effect was detected.

N° 232 and 233.

Fermi's interest in the peculiarly small interaction of the μ mesons with nuclear matter was excited by the work of M. Conversi, E. Pancini and O. Piccioni. In a colloquium at which Fermi was absent, I happened to hear about this work. A few days later I told Fermi about the puzzling fact found by the Italian group that decay of negative μ mesons seems more probable than reaction with the nuclear matter in the carbon nucleus. It was at once obvious that this points toward a very weak interaction of μ mesons and nucleons. Weisskopf had arrived at a similar conclusion and through correspondence we arranged a short joint note.

At the same time Fermi felt that alternative explanations should be investigated as vigorously as possible. He wondered whether the process of capturing the μ meson into its lowest orbit around the carbon nucleus may perhaps take a considerable length of time. If so, the relatively great number of μ meson decays might take place during the time of capture. As a result we looked into the capture process in very great detail. Actually in our conversations I was most of the time the listener. Due to the fact that the statistical (Fermi-Thomas) picture of the atom proved adequate, the answer could be obtained in a straightforward and convincing way. There was only one somewhat difficult question: Whether a relatively high number of μ mesons could he trapped in high angular momentum states around the nucleus. (Energy loss from these states is more difficult). In the end an orderly survey of the energy loss mechanisms in varying substances proved feasible.

At the time when this article was written Fermi and I shared a secretary (Nancy McMillan) who had a degree in chemistry. The paper was actually written by giving dictation to Mrs. McMillan. Since Fermi and I frequently interrupted each other in the actual formulation the first draft became a little confused. That a draft was produced at all was due to the excellent work of our secretary. It was then my job to transform the first draft into a manuscript, *The Capture of Negative Mesotrons in Matter*. This I did (I am afraid) with limited success.

E. TELLER.

232.

THE DECAY OF NEGATIVE MESOTRONS IN MATTER

E. FERMI, E. TELLER, *University of Chicago, Chicago, Illinois*
and V. WEISSKOPF, *Massachusetts Institute of Technology, Cambridge, Massachusetts*

(Received February 7, 1947)
« Phys. Rev. », *71*, 314–315, (1947).

In a recent experiment Conversi, Pancini, and Piccioni [1] observed separately the behavior of positive and negative mesotrons coming to rest in iron or in graphite. They find that in iron the disintegration electrons are observed only for positive mesotrons. This was indeed to be expected [2]

(1) M. CONVERSI, E. PANCINI, and O. PICCIONI, « Phys. Rev. », *71*, 209 (1947).
(2) S. TOMONAGA and G. ARAKI, « Phys. Rev. », *58*, 90 (1940).

because negative mesotrons after being slowed down can approach the nuclei and disappear by nuclear interactions. If, on the other hand, graphite is used for stopping the mesotrons, delayed disintegration electrons are observed to be about equally abundant for positive and negative mesotrons. This is in sharp disagreement with current expectations and seems to indicate that the interaction of mesotrons with nucleons according to the conventional schemes is many orders of magnitude weaker than usually assumed. The disappearance of a negative mesotron can be analyzed into a process of approach of the mesotron to the nucleus and the process of capture by short range interaction of the mesotron and the nucleons.

The slowing down of mesotrons to an energy of about 2000 ev takes place according to the conventional theory. In estimating the energy loss for lower energies we have considered energy exchange with electrons and radiation. We consider the electrons as a degenerate gas with a maximum velocity v_0 and assume that the velocity V of the mesotron is small compared to v_0. Then the energy loss to the electrons per unit time is of the order of magnitude $e^4 m^2 \mathrm{T}/(\hbar^3 \mu)$. Here m and μ are the masses of the electrons and the mesotrons, respectively, and T is the kinetic energy of the mesotron. This formula allows losses of energy even when the total energy is negative (mesotron bound to an atom), and is valid as long as the mesotron moves outside the K orbit. At closer distances the formula will be somewhat modified and, at the lowest energies, loss by radiation will predominate. The mesotron reaches its lowest orbit around the nucleus in most solids in not more than 10^{-12} second. This orbit is 200 times smaller than the radius for the K shell, which is for carbon about 10 times the nuclear radius and for iron about twice the nuclear radius. After reaching this orbit the mesotron can be found within the nucleus with a probability of 1/1000 in the case of carbon and a probability 1/10 in the case of iron.

According to the conventional mesotron theories, one will have to assume that the capture now proceeds according to one of the following schemes:

$$\mathrm{P} + \mu^- = \mathrm{N} + h\nu \tag{1}$$

$$\mathrm{X} + \mu^- = \mathrm{N} + \mathrm{Y}. \tag{2}$$

Here P and N stand for proton and neutron, μ signifies the mass of the mesotron, $h\nu$ is a light quantum, and X and Y stand for initial and residual nuclei in the capture process. The first calculation of these processes for a special form of mesotron interaction is due to Kobayasi and Okayama, and Sakata and Tanikawa [3]. The results depend to some extent upon the spin of the mesotron and the form of the interaction assumed. For example, in the case of pseudoscalar mesotrons with an interaction energy given by $\Sigma_i \frac{\hbar}{\mu c} (4\pi)^{1/2} g \tau_i \int (\psi^* \sigma \psi) \operatorname{grad} \Phi_i \, dv$ (ψ is the wave function of the nucleons, Φ_i of the mesotrons, μ is the mesotron mass, the index i refers to the charge,

(3) KOBAYASI and OKAYAMA, « Proc. Phys.-Math. Soc. Japan », *21*, 1 (1939); SAKATA and TANIKAWA, « Proc. Phys.-Math. Soc. Japan », *21*, 58 (1939).

and τ is the isotopic spin operator), one obtains for the time of capture by process (1) for a mesotron already captured in its lowest orbit 10^{-18} and 10^{-20} second in carbon and iron, respectively. Process (2) is likely to lead to 10 times shorter lives. This is negligible compared to the life of a negative mesotron of 2×10^{-6} second.

The experimental result [1] leads to the conclusion that the time of capture from the lowest orbit of carbon is not less than the time of natural decay, that is, about 10^{-6} second. This is in disagreement with the previous estimate by a factor of about 10^{12}. Changes in the spin of the mesotron or the interaction form may reduce this disagreement to 10^{10}.

If the experimental results are correct, they would necessitate a very drastic change in the forms of mesotron interactions. The result is significant also for the production of single mesotrons by artificial sources. Indeed the creation of a mesotron by x–rays or fast protons is the reverse of processes (1) and (2). If the interaction according to these two processes is much weaker than expected, one would conclude the same for the reverse processes. Thus one might be in doubt as to whether one can produce abundant numbers of artificial mesotrons with bombardment-energies only a little above the threshold for single-mesotron production. Predictions concerning the creation of mesotron pairs by electromagnetic radiation are, of course, not affected by these arguments.

N° 233.

For the introduction to this paper see paper N° 232.

233.

THE CAPTURE OF NEGATIVE MESOTRONS IN MATTER

E. FERMI and E. TELLER
Institute for Nuclear Studies, University of Chicago
(Received May 28, 1947)
« Phys. Rev. », *72*, 399-408 (1947).

A detailed discussion of the energy loss of negative mesotrons in matter is presented. The energy range considered is from + 2000 ev to the lowest quantized orbit of the mesotron. The most important mechanism for energy loss is that of electron collisions except very near the nucleus, where radiation losses are important.

The time for the over-all process is of the order of 10^{-13} sec in condensed matter and 10^{-9} sec in normal air. In chemical compounds the probability of capture near the various atoms is roughly proportional to their atomic numbers.

1. INTRODUCTION.

Recently the significance of experimental results [1] on the capture of negative mesotrons in matter has been discussed from the point of view of the information that it gives concerning the interaction between mesotrons and nucleons. The interaction of slow negative mesotrons with matter has been described as consisting of two steps: [2] first, one in which the mesotron is captured in the Bohr orbit with a radius of the order of 10^{-12} cm near the nucleus; second, a step in which more typically nuclear interactions play a role during which the mesotron is destroyed by its collisions with the nearby nucleons. The present paper will be primarily concerned with the detailed description of the first step.

The chief purpose of a detailed description of the capture process is to make sure that the time required for it is short compared with the natural decay time of the mesotron ($\sim 2 \times 10^{-6}$ sec). We propose to discuss in particular how the physical and chemical state of matter influences the capture process. In this connection we shall investigate also the relative probabilities of the capture of mesotrons near various types of nuclei in case the slowing down material is not a pure element.

(1) M. CONVERSI, E. PANCINI, and O. PICCIONI, « Phys. Rev. », *71*, 209 (1947).

(2) E. FERMI, E. TELLER, and V. WEISSKOPF, « Phys. Rev. », *71*, 314 (1947). [See paper N° 232. (Editors' note)].

Throughout the greater part of the capture process the wave-length of the mesotron is short as compared to the geometric dimensions of the field in which this particle is moving. It is therefore permissible in most of our arguments to consider the motion of the mesotron as purely classical.

2. Energy Loss of Electrons Over 2000 ev.

As long as the energy of the mesotron is more than 2000 ev, the velocity of the mesotron is greater than the velocity of the valence electrons. The slowing down of the mesotrons can then be treated according to the conventional methods applicable to fast heavy particles. In the slowing down of the mesotron the longest time is spent in the state when the mesotron moves with relativistic velocities. The consequences of the decay of the mesotron during this phase of cosmic radiation are well known and will not be discussed here. The time needed to slow a mesotron from the relativistic 10^8 volts to 2000 ev is about 10^{-9} to 10^{-10} second in condensed matter, or 1000 times as long in air. This part of the slowing process is again not our primary concern. It will be found that the time involved is considerably longer than the time needed for the later parts of the capture process. The probability of spontaneous decay during this phase, which corresponds to a range in condensed matter of a few centimeters, is only of the order of 10^{-4}. Consequently a negligible fraction of the decays observed with the ordinary experimental arrangements can be attributed to it [3]. Most of this time of 10^{-10} second is spent in the phases when the mesotrons still have velocities close to the light velocity. Actually the formula for energy loss per unit time is

$$-\frac{dW}{dt} = \frac{4\pi e^4 NZ}{mV} \log\left(\frac{b_{max}}{b_{min}}\right). \tag{1}$$

Here W is the energy of the mesotron, V its velocity, m the electron mass, N is the number of atoms with atomic number Z per cubic centimeter; b_{max} and b_{min} are the extreme values of the collision parameters. The logarithmic factor decreases during this interval of time from a value of the order 10 to zero. The latter value is reached when the mesotron velocity becomes equal to the velocity of an electron. Thus the contributions of successive electrons vanish. Finally, the velocity of the mesotron drops below that of the valence electrons. From then on we shall discuss the process of further energy loss in detail.

3. Loss of Energy to a Degenerate Electron Gas.

When the energy of the mesotron has dropped below 2000 ev, and its velocity is therefore less than the velocity of the valence electrons, formula (1) no longer represents a useful approximation, and the loss of energy to electrons can better be approximated in the following way.

(3) Decays during this phase are completely eliminated if the observations are carried out by delayed coincidence.

We consider the mesotron moving inside a degenerate electron gas with a velocity V much smaller than the maximum velocity v_0 of the electrons. In this case we can estimate the energy loss as follows: in an individual collision between an electron and the mesotron, the change in speed of the electron will be of the order of magnitude V. Indeed for a head-on collision it would be 2 V. Since the electrons belong to a degenerate gas, it is clear that all the collisions for which the final velocity of the electron lies inside the occupied zone of the velocity space will be forbidden on account of the Pauli principle. Only electrons with speeds close to v_0 by amounts of the order of V will, therefore, be capable of colliding. Their number per unit volume is of the order of magnitude

$$n \approx \frac{m^3 v_0^2 \mathrm{V}}{\hbar^3} . \tag{2}$$

The collision cross section σ for collisions in which the deflection is appreciable is, on the other hand, of the order of magnitude:

$$\sigma \approx \left(\frac{e^2}{m v_0^2}\right)^2 . \tag{3}$$

The energy transferred in collisions of this type not forbidden by the Pauli principle will always be positive and of the order of magnitude

$$\mathrm{W} \approx m v_0 \mathrm{V}. \tag{4}$$

From (2, 3 and 4) we can calculate the order of magnitude of the energy loss per unit time:

$$-\left(\frac{d\mathrm{W}}{dt}\right) \approx \mathrm{W}\sigma n v_0 \approx \frac{m^2 e^4 \mathrm{V}^2}{\hbar^3} \approx \frac{m^2 e^4 \mathrm{T}}{(\mu\hbar^3)} \approx \frac{\mathrm{T}}{t_0} , \tag{5}$$

where T is the kinetic energy of the mesotron, $t_0 = \frac{\mu\hbar^3}{m^2 e^4} = 4.84 \times 10^{-15}$ sec, and μ is the mass of the mesotron. We have set $\mu = 200\, m$.

The difference in the velocity dependence of the energy loss according to (1) and (5) which hold, respectively, for high and low velocities of the mesotron should be noticed. For high velocities the energy loss per unit time is inversely proportional to the velocity of the mesotron; for low velocities it is directly proportional to the square of the velocity. There is, therefore, a maximum in the energy loss which is found near the boundary of validity of the two formulae; namely, for mesotron velocities of the order of the electron velocity v_0. One might wonder why the energy loss (5) is independent of the density of the degenerate electron gas through which the mesotron moves. Actually the collisions occur between the mesotrons and the fastest electrons, and the collision cross section decreases as $1/v_0^4$. This strong dependence on v_0 just suffices to cancel the effect of great electron density, great energy loss per collision, and great relative velocity of the colliding particles. Naturally, if (5) were taken strictly, one would obtain the absurd result that the energy loss remains unchanged even when the density of the electrons becomes extremely small.

Actually there are two reasons that limit the validity of (5) for low electron density. One is expressed by the condition

$$V \ll v_0 \tag{6}$$

that the mesotron should move slowly with respect to the electrons. The second is due to the fact that when a negative mesotron moves through an electron gas, the density of electrons near it is reduced by the electrostatic repulsion. This rarefaction of the electrons near the mesotron effectively neutralizes its charge at distances of the order:

$$\left(\frac{a\hbar}{mv_0}\right)^{1/2}, \tag{7}$$

where a is the Bohr radius

$$\frac{\hbar^2}{me^2}. \tag{8}$$

The quantitative treatment of the electron-mesotron collision can be carried out according to the Born approximation method. This is justified if the formula

$$\frac{e^2}{\hbar v_0} < 1 \tag{9}$$

holds. Now if the Born approximation is applicable, the region in which the relevant collisions take place has dimensions equal to the de Broglie wave-length of the scattered particle. In order that expression (5) be applicable we must demand that this wave-length be less than the length given in (7). It follows that

$$\frac{\hbar}{mv_0} < \left(\frac{a\hbar}{mv_0}\right)^{1/2} \quad \text{or} \quad \frac{mv_0}{\hbar} > \frac{1}{a}. \tag{10}$$

The left-hand side of the last inequality is approximately equal to the cube root of the density of the electron gas. Condition (10) means, therefore, that the density of the electron gas must be such that, on the average, more than one electron is found in a cube having a side equal to the Bohr radius. Inequalities (9) and (10) are identical in content. It is easy to show that if they are not fulfilled (5) does not apply, and the mesotron loses energy at a much slower rate than the one given by (5). Conditions (6) and (10) are independent, and the more restrictive of the two will apply. Condition (10) is usually fulfilled approximately in condensed matter of not too small density. In the case of gases, however, it will be satisfied only within the atoms, and therefore the energy loss will be confined to these regions.

Quantitatively, the energy loss of a slow mesotron in an ideal degenerate electron gas is expressed by the following integral:

$$\frac{me^4 V^2}{8\pi\hbar^3} \int_0^{\pi}\int_0^{\pi}\int_0^{2\pi} \frac{(\cos\theta - \cos\theta')\sin\theta\, d\theta \sin\theta'\, d\theta'\, d\varphi}{\sin^4\left(\frac{1}{2}\psi\right)}. \tag{11}$$

The meaning of the integration variables is the following: θ and θ' are the angles between the directions of initial and final electron velocity and

the direction of the mesotron velocity; ψ is the angle of deflection for the electron; and φ is given by

$$\cos\psi = \cos\theta\cos\theta' + \sin\theta\sin\theta'\cos\varphi. \tag{12}$$

The integral diverges logarithmically near $\psi = 0$. The divergence can be removed by taking into account the fact that collisions involving a small value of ψ occur at large distances where the mesotron charge is screened.

Collisions at a distance greater than (7) will not contribute, and one needs to consider only momentum changes greater than

$$\left(\frac{\hbar m v_0}{a}\right)^{1/2}, \tag{13}$$

which is $\hbar$ divided by the length (7). From this one finds that the integration need be carried down only to a value

$$\psi_{\min} = \left(\frac{\hbar m v_0}{a}\right)^{1/2}(m v_0)^{-1} = \left(\frac{e^2}{\hbar v_0}\right)^{1/2} = \left(\frac{c}{137\, v_0}\right)^{1/2}. \tag{14}$$

One should notice that if (10) is fulfilled, $\psi_{\min}$ is small compared with unity, as it should be. Eliminating the divergence with this prescription, one can evaluate (11) and find finally the following estimate for the rate of energy loss:

$$-\frac{dW}{dt} = \frac{4}{3\pi}\frac{m^2 e^4 V^2}{\hbar^3}\log\frac{1}{\psi_{\min}} = \frac{2}{3\pi}\frac{m^2 e^4 V^2}{\hbar^3}\log\frac{137\, v_0}{c}, \tag{15}$$

or finally,

$$-\frac{dW}{dt} = \frac{4}{3\pi}\frac{m^2 e^4 T}{\mu\hbar^3}\log\frac{137\, v_0}{c}. \tag{16}$$

The logarithm will be of a small numerical order of magnitude and will have somewhat larger values in the deep portions of the atom. For estimates of the order of magnitude it will be permissible to use formula (5).

The previous theory will be applicable to those cases in which the electrons in the vicinity of the mesotron can properly be described as a degenerate gas. In particular, the theory will break down within the K shells of the atoms, since the electron density there is less than the value corresponding to the degenerate gas. We shall return to this question in the next section. We shall have to give special consideration to the case of insulators and gases where electrons may be excited only by discontinuous amounts. The case that most nearly approaches the ideal conditions is that of the metals, which we shall now discuss.

4. Metals.

In order to calculate the energy loss as a function of the mesotron energy, we have to calculate the average value of the kinetic energy $\overline{T}$ which is to be substituted in formula (5). In calculating average values of T, one makes use of the fact that the probability of finding the mesotron in a given volume element is weighted by the square root of the kinetic energy that the mesotron has at this position. The reason for this weighting is that the vol-

ume in the momentum space available to the mesotron is proportional to

$$T^{1/2}\,dT = T^{1/2}\,dW. \tag{17}$$

The average kinetic energy is therefore:

$$\bar{T} = \frac{\int (W-U)^{3/2}\,d\tau}{\int (W-U)^{1/2}\,d\tau}\,. \tag{18}$$

where U is the potential energy and $d\tau$ is the volume element.

For high mesotron energy U will be negligible compared with W, and $\bar{T}$ will be equal to W. As the energy approaches zero, namely, that value for which the mesotron can no longer freely pass from one atom to another, the average kinetic energy becomes appreciably larger than W because U is negative. For W negative, the mesotron is bound to a definite atom. For negative values of energy the kinetic energy is of the order of magnitude of the absolute value of W, as will be discussed later.

For positive W values one obtains a low limit for $\bar{T}$ and the energy loss replacing $(W-U)^{3/2}$ by the smaller expression $W^{3/2}+(-U)^{3/2}$ in the numerator of the integral, and replacing $(W-U)^{1/2}$ by the larger expression $W^{1/2}+(-U)^{1/2}$ in the denominator. The error caused by these substitutions is a maximum when W is equal to the absolute value of U, and is then a factor 2. We write thus

$$\bar{T} \approx \frac{\int W^{3/2}\,d\tau + \int (-U)^{3/2}\,d\tau}{\int W^{1/2}\,d\tau + \int (-U)^{1/2}\,d\tau}\,. \tag{18 a}$$

We shall use the potential obtained from the statistical model

$$U = -\frac{Z^{4/3}e^2}{b}\,\frac{\varphi(x)}{x}\,, \tag{19}$$

where we have set for the distance from the nucleus $r = xb\,Z^{-1/3}$ and the length b is

$$b = \left(\frac{9\pi^2}{128}\right)^{1/3} \times \text{Bohr radius} = 0.47 \times 10^{-8}\ \text{cm}. \tag{20}$$

The function φ has been tabulated [4]. In some of the following calculations we use the crude approximation [5]

$$\varphi = \frac{0.4}{x}\,. \tag{21}$$

Approximating a lattice cell by a sphere one obtains $\bar{T}$ by integrating (18 a) over the cell. The second integral in the numerator can be performed

(4) E. FERMI, «Zeits. f. Physik», *48*, 73 (1928). [See paper N° 49. (Editors' note)].

(5) From $x = 0.5$ up to almost $x = 8$ the quantity $x\varphi$ remains between the limits 0.3 and 0.5.

by partial integration using the differential equation [4] for φ. One finds

$$\bar{T} = \frac{N^{-1} W^{3/2} + 4\pi e^3 b^{3/2} Z [1 - \varphi(x_0) + x_0 \varphi'(x_0)]}{N^{-1} W^{1/2} + 4\pi e b^{5/2} Z^{-1/3} \int_0^{x_0} \varphi^{1/2} x^{3/2} dx} \tag{22}$$

Here N is the number of atoms per cubic centimeter, and x_0 is the value of x at the edge of the cell. Using (21) we get

$$\bar{T} = \frac{N^{-1} W^{3/2} + 4\pi Z e^3 b^{3/2} [1 - (0.8/x_0)]}{N^{-1} W^{1/2} + 3.96\, e b^{5/2} Z^{-1/3} x_0^2}, \tag{23}$$

where x_0 is given by the relation:

$$1/N = 4\pi b^3 x_0^3/3Z. \tag{24}$$

Values of $\bar{T}$ as obtained from (23) are given in Table I for graphite and iron. One finds that $\bar{T}$ has a flat minimum at 7 ev and 20 ev, respectively. This will be, therefore, the value of the energy at which energy is lost at the slowest rate. At higher energies Table I shows that $\bar{T}$ becomes less than W. This is because of the approximation which we made in substituting (18) by (18a). Actually $\bar{T} > W$ always holds, and we underestimate $\bar{T}$ if we use $\bar{T} = W$ for high values of W. From Table I and formula (5), one can calculate, for the two cases in question, the time needed for the mesotron to lose energy from 2000 ev to zero. One finds 2.6×10^{-14} sec in graphite and 2.2×10^{-14} sec in iron. Somewhat longer times would be found in condensed matter of lower density. As a practical average time for crossing the interval from 2000 ev to zero we take for all types of condensed matter about 3×10^{-14} sec.

We proceed now to the question of energy loss when W is negative, when the mesotron can be considered bound to a special atom. If the energy is negative and its absolute value is sufficiently large, it is a sufficient approximation to set the kinetic energy

$$\bar{T} = \alpha |W|, \tag{25}$$

where α is a number of the order of unity. (Actually $\alpha = 1$ for a Coulomb field and $\alpha > 1$ for the statistical potential). Expression (25) will lead to a very small loss of energy for small absolute values of W. Actually at $W = 0$ the kinetic energy does not vanish, and may be obtained from (23):

$$\bar{T}(0) = \frac{3.2\, e^2 Z^{4/3}}{b x_0^2} \left(1 - \frac{0.8}{x_0}\right). \tag{26}$$

Since at $W = 0$, $\bar{T}$ increases with decreasing W we may use (26) as a lower limit of $\bar{T}$ at negative energies. We shall use for the energy-loss expression (5), and substitute for $\bar{T}$ expression (25) or (26), whichever is the greater. Expression (26) will be relevant from $W = 0$ to $-W \approx 50$ ev. The time required to cross this energy region is of the order of $t_0 = 4.84 \times 10^{-15}$ sec.

In the range where $\overline{T}$ is estimated by (25), W as a function of time is given by

$$-W \approx \overline{T}(0)\, e^{\alpha t/t_0}. \tag{27}$$

This formula is valid as long as the statistical model is permissible, i.e., as long as the mesotron moves outside of the radius of the K–shell. At distances smaller than this radius the actual electron density is less than the density obtained from the statistical model. Nevertheless the energy loss of the mesotron continues to proceed according to the formulas (16), (5), and (27) even when the mesotron is somewhat closer to the nucleus than the radius of the K–shell. The reason for this is that the energy loss of the mesotron does not depend on the electron density, and thus the failure of the statistical model to predict the correct density within the K–shell has no direct effect on the behavior of the mesotron.

TABLE I.

Average kinetic energy as a function of the total energy.

W (ev)	$\overline{T}$ (ev)	
	Graphite	Iron
0	36	86
5	23	62
10	24	56
20	27	55
30	32	57
50	45	65
100	83	95

When the mesotron moves inside the K–shell it is not permissible, however, to apply the method of deriving formulas (16) and (5) which we have given above. In a collision the energy $mv_0 V$ is exchanged, and a time not shorter than $\hbar/mv_0 V$ is needed to describe such a collision. During this time the mesotron moves through a distance $\hbar/mv_0$. Our discussion so far has assumed that during a collision the mesotron moves in a straight line. When the mesotron moves along the K–orbit of the atom its path has a radius of curvature equal to $\hbar/mv_0$. For orbits on or within the K–shell it will be a better approximation to consider the time-dependent dipole consisting of the mesotron and a unit positive charge located on the nucleus. One may then calculate, by applying perturbation theory to the statistical model, the energy exchange between the mesotron and the electrons.

If one assumes that the mesotron moves on a circular orbit one may evaluate the rate of energy loss dW/dt. The result of the calculation is identical with (16) provided that the minimum momentum change of the electrons $(\hbar m v_0/a)^{1/2}$ obtained from (7) is greater than the minimum momentum change $\hbar\omega/v_0$ compatible with the requirement that a mesotron with angular velocity ω exchanges energy with the electrons in quanta $\hbar\omega$. At radii somewhat smaller than the radius of the K–shell the inequality $(\hbar\omega/v_0) > (\hbar m v_0/a)^{1/2}$ holds for not too light atoms. Then (16) must be replaced by

$$-\frac{dW}{dt} = \frac{8\,e^4 m^2 T}{3\pi\mu\hbar^3}\log\left(\frac{m v_0^2}{\hbar\omega}\right). \tag{28}$$

Expression (5) remains a satisfactory approximation as long as the logarithmic factor does not become small compared to unity, i.e., as long as the energy $\hbar\omega$ transferred to the electrons is smaller than the maximum kinetic energy $m v_0^2/2$ of the electrons. For $m v_0^2 \ll \hbar\omega$ the perturbation calculation gives

$$-\frac{dW}{dt} = \frac{2^{5/2}\pi m^{1/2} n_0 e^4 r^2}{3\hbar^{3/2}}\left(\frac{Ze^2}{\mu r^3}\right)^{1/4}, \tag{29}$$

where n_0 is the electron density near the nucleus and r is the radius of the circular orbit of the mesotron. Expression (29) agrees with the results of calculations on internal conversion, for the non-relativistic case, provided that the energy of the ejected electron is great compared with the energy of the K–electrons[6]. It is of interest to note that (28) holds if the radius r of the mesotron orbit is greater than

$$r_1 = \left(\frac{m}{\mu}\right)^{1/3} r_K = 0.171\, r_K\,. \tag{30}$$

Here r_K is the radius of the K–shell. For $r < r_1$ expression (29) is valid.

For very small values of r, energy loss by radiation is faster than energy loss due to interaction with electrons. For circular mesotron orbits one finds by comparing (29) with the radiated energy that radiation becomes predominant for $r < r_2$, where

$$r_2 = 4^{-1/7}\left(\frac{m}{\mu}\right)^{1/3}\left(\frac{\hbar c}{e^2}\right)^{3/7} Z^{-5/21} r_c = \left(\frac{4.5}{Z^{5/21}}\right)\times 10^{-11}\ \text{cm}, \tag{31}$$

where $r_c = \hbar/mc$ is the Compton wave-length divided by 2π.

From (29) one can calculate the time needed to drop from r_1 to r_2

$$t_{r_1\to r_2} = \frac{1}{6\sqrt{2}}\left(\frac{m}{\mu}\right)^{3/4}\left[\left(\frac{r_K}{r_2}\right)^{9/4} - \left(\frac{r_K}{r_1}\right)^{9/4}\right] t_0 = \left[\frac{103}{Z^{12/7}} - 0.117\right] t_0. \tag{32}$$

While the classical expression for the radiation by an accelerated charge gives the time spent between r_2 and the lowest quantum orbit $r_0 = \frac{\hbar^2}{Z\mu e^2}$,

$$t_{r_2\to r_0} = \frac{\mu^2 c^3}{4e^4 Z}(r_2^3 - r_0^3) = \frac{\mu}{4mZ}\left[\left(\frac{r_2}{r_c}\right)^3 - \left(\frac{r_0}{r_c}\right)^3\right] t_0 = \left[\frac{78}{Z^{12/7}} - \frac{16}{Z^4}\right] t_0\,. \tag{33}$$

(6) See, e.g., RASETTI, *Elements of Nuclear Physics* (Prentice-Hall, New York 1936), pp. 134–139.

For heavy nuclei r_1 becomes smaller than r_2, and there is no region in which (29) determines the energy loss. Further consequences of high Z–values are that r_0 becomes less than the nuclear radius and that pair production begins to play a role in the last steps of the slowing-down process. All these effects shorten the time the mesotron needs to get close to the nucleus.

TABLE II.

Summary of slowing-down times in graphite and iron.

Energy range (ev)	Time	
	Graphite	Iron
$2000 \to 0$	$5.4\, t_0$	$4.5\, t_0$
$0 \to -Ze^2/r_1$	$5.3\, t_0$	$7.4\, t_0$
$-Ze^2/r_1 \to -Ze^2/r_2$	$4.6\, t_0$	$0.3\, t_0$
$-Ze^2/r_2 \to -Ze^2/r_0$	$3.6\, t_0$	$0.3\, t_0$
$2000 \to -Ze^2/r_0$	$18.9\, t_0$	$12.5\, t_0$
(total " slow " range)	9.2×10^{-14} sec	6.1×10^{-14} sec

For carbon and iron, Table II summarizes the times (measured in units $t_0 = 4.84 \times 10^{-15}$ sec) the mesotron needs to cross the energy regions indicated in the first column of the table.

One sees that the slowing down time is less than 10^{-13} sec. This is very short compared with the lifetime of the mesotron, 2×10^{-6} sec.

5. INSULATORS.

The case of insulators differs from that of metals because the amount of energy that may be delivered to electrons in a metal can be arbitrarily small, whereas in an insulator it must be at least as large as the gap between two Brillouin zones. This usually amounts to several volts. The loss of energy to electrons will be thereby reduced in those cases in which energy is transferred in small individual amounts.

In a collision the amount of energy transferred to the electron is of the order of magnitude $mv_0 V$, and we can expect that Eq. (5) will hold only if

$$mv_0 V > G, \tag{34}$$

where G is the " Brillouin gap," i.e., the minimum energy that the electrons can accept. In case (34) is not fulfilled, the rate of energy loss will be smaller. This limitation will necessitate a change in formula (18) where the integral in the numerator will no longer be extended to all portions of space accessible to the mesotron but only to those for which in addition (34)

is fulfilled. For positive W, the effect on dW/dt is most important at and near $W = 0$. For $Z \geq 6$ actual calculation based on the statistical atom model shows that the rate of energy loss is not changed in this critical region by more than a factor $1/2$. The corresponding increase in the slowing-down time is less than 10^{-14} sec.

For positive energies, regions close to nuclei where (34) is fulfilled will occasionally be visited by the mesotron. For negative energies regions close to the nucleus may be avoided if the mesotron is captured into an almost circular orbit. Therefore the possibility arises of the mesotron spending a long time in such a circular orbit. We shall show that actually the mesotron will spend in a circular orbit a time which is not long compared to the other times we have obtained in the slowing-down process.

Circular orbits of negative energy exist only at a considerable depth within the atom. This can be proved using the statistical potential (19). Circular orbits of negative energy exist only where $x\varphi(x)$ is an increasing function of x [7]. The value of $x\varphi(x)$ is zero at $x = 0$, increases to a maximum reached at $x = 2.25$, and decreases beyond this point. Consequently, circular orbits of negative energy are to be found only within a distance from the nucleus corresponding to $x = 2.25$; namely,

$$r = \frac{2.25\, b}{Z^{1/3}}. \tag{35}$$

For a circular orbit at exactly this radius the energy is equal to zero, and the kinetic energy of the mesotron is equal to

$$\frac{0.09\, e^2 Z^{4/3}}{b} = 2.7\, Z^{4/3}\ \text{ev}. \tag{36}$$

If a mesotron is captured into an orbit which is not circular, its closest approach to the nucleus will be even smaller than the distance given by formula (35), and the maximum kinetic energy will be larger than that given by (36). Applying condition (34), we find that energy loss to the electrons will be possible from at least one part of the orbit if the condition

$$\frac{0.09\, e^2 Z^{4/3}}{b\ \text{ev}} > \frac{1}{2}\left(\frac{\mu}{m}\right)^{1/2} G \tag{37}$$

is fulfilled. If we set for G the fairly large value of 7 volts, we see that relation (37) is fulfilled if Z is 9 or greater. Actually relations (34) and (37) are not to be taken in a quite strict sense because head-on collisions between electrons and mesotrons will give an energy exchange twice as large as assumed in (34). If this is taken into account an additional factor of $1/2$ appears in the right-hand side of (34). If we again assume 7 volts for G the limiting value of Z drops from 9 to 6.

Stable circular orbits of positive energy exist for x values greater than 2.25. The condition of stability for a circular orbit is:

$$\varphi - x\varphi' - x^2\varphi'' > 0. \tag{38}$$

(7) This statement does not refer to circular orbits outside the core of an atom. In condensed matter there is usually no room available for orbits of such very large radius.

This condition is fulfilled up to $x = 3.3$, or

$$r = 3.3\, b\, Z^{-1/3}. \tag{39}$$

A mesotron moving on a circular orbit of this radius has a smaller velocity than one moving on the radius given by (35), and one may expect increased difficulties in the energy exchange between mesotron and electron. Actually, in light atoms the greatest stable circular radius (39) differs from (35) by less than the uncertainty due to the spread of the wave function of the mesotron. At the same time the difference in angular momenta between the greatest circular orbit and (35) is small. For $Z = 6$ this difference is less than $\hbar$. Thus a mesotron moving in a stable orbit of positive energy will not lose energy at a much smaller rate than will a mesotron whose wave function has its maximum at the radius given by (35).

We can conclude that the circular orbits will hardly ever be too stable. Even in case they should be formed around an element like lithium or beryllium the total time of energy loss will probably be less than the lifetime of a mesotron.

Furthermore, the actual size of the Brillouin gap is affected by the localization of the mesotron on one lattice atom. Since, at least in the critical cases, the mesotron is captured fairly far inside the atom, the atom is effectively turned into an element with atomic number $(Z - 1)$. If we were dealing with an isolated atom, this would lower the ionization energy of the atom and turn it into the much smaller value which usually is called the electron affinity of the atom of charge $(Z - 1)$. Actually this electron affinity may even be zero. In the special case of mesotron capture by the hydrogen atom, it is found that when the mesotron approaches the nucleus to a distance of 0.639 Bohr radii, the binding energy of the electron becomes zero. In the closed shell structures usually found in insulators, an electron affinity of two or three volts is likely to remain. As a consequence of this the mesotron, after it is captured, may lose as a first step an energy smaller than the Brillouin gap. After this loss the atom in which the mesotron is now localized does not have a closed shell, and further excitation may still require less energy than the width of the Brillouin gap. Of course, further ionizations would tend to raise the ionization potential, but the local electron deficiency will be promptly filled by capturing electrons from neighbors.

A special situation arises when the mesotron is captured on a hydrogen atom, as may happen for instance in paraffin. In that case the hydrogen and the mesotron circulating around it form a small neutral system which will move along and will readily permeate to any part of the lattice. As a result one will expect that the mesotron will eventually be caught in the field of a more highly charged nucleus.

After the mesotron has attained negative energies of an absolute value greater than 100 ev, the further energy loss proceeds in insulators as it does in metals.

In conclusion we see that the total time needed for energy loss in insulators is apt to be a little longer than in metals, because of the diffi-

culty in bridging the Brillouin gap. There will be, however, no change in the order of magnitude of the total time which the mesotron needs to reach its lowest orbit.

6. Gases.

In gases, as in insulators, electrons cannot accept from the mesotron arbitrarily small amounts of energy. The lowest electronic excitation energy, I, of a gas molecule plays the same role as the Brillouin gap does in insulators.

For positive values of W the energy loss proceeds according to (5) and (18). The upper limit of the integrand in the numerator is determined by the condition

$$mv_0 V = I. \tag{40}$$

The integral in the denominator is extended over the whole space. As a result the average value of the energy loss $-dW/dt$ is reduced by the ratio of gas density to insulator density. Under conditions of normal temperature and density the energy loss in a gas is about a thousand times smaller than in a solid insulator. The time needed to slow down the mesotrons from $W = 2000$ ev to $W = 0$ is approximately 3×10^{-11} seconds.

For negative values of W the mesotron is localized on a specific molecule. As the energy transfer to electrons proceeds, it is likely that enough energy will be given to nuclear motion to cause dissociation of the molecule on which the mesotron is found. Thus we may confine our attention to the atom which carries the mesotron along. The energy loss of the mesotron causes progressive ionization of this atom, and, as a result, the minimum excitation energy I is increased. This may lead to an effective stoppage of the energy loss if the mesotron happens to be moving on a nearly circular orbit. The energy loss may stop when the relation

$$\hbar\omega \approx I \tag{41}$$

is fulfilled. Here ω is the frequency of the mesotron in a circular orbit.

Further energy loss of the mesotron may thus be delayed until the ion carrying the mesotron makes a collision with another molecule. Then a substantial part of the ionic charge will be neutralized, and the energy transfer from the mesotron to the electron cloud will be resumed. We assume that the excitation energy I of the atom which carries the mesotron may be written in the form

$$I = Ki^2, \tag{42}$$

where i is the degree of ionization and K is a constant. The total energy E needed to raise the ionization from zero to i is

$$E = \frac{1}{3} Ki^3. \tag{43}$$

We assume that between two collisions of the mesotron-carrying atom the energy of the mesotron W will change by E/2. We have then

$$-\frac{dW}{dt}=\frac{1}{2}NE=\frac{1}{6}NKi^3, \tag{44}$$

where N is the number of collisions per unit time $\sim 10^{10}\,\mathrm{sec}^{-1}$.

The energy loss of the mesotron will be smallest if the mesotron continues to move on circular orbits. For the radius r of this orbit we write as previously

$$r=xb\,Z^{-1/3}. \tag{45}$$

Using (19), (21), and (41) we get

$$I=\frac{\hbar e\,Z}{\mu^{1/2}\,b^{3/2}\,x^{1/2}}\left[-\frac{d}{dx}\left(\frac{\varphi}{x}\right)\right]^{1/2}=2.06\,Zx^{-2}\ \mathrm{ev}. \tag{46}$$

From (42), (43), and (44) we now obtain

$$-\frac{dW}{dt}=0.493\,NK^{-1/2}(eV)^{3/2}Z^{3/2}x^{-3}. \tag{47}$$

If W is calculated for a circular orbit from the statistical model one obtains

$$W=-\frac{Z^{4/3}e^2}{2bx}\,d(x\varphi)/dx. \tag{48}$$

Here the approximation (21) is not sufficient. In the region where circular orbits of negative energy are possible we may use for the expression $x\varphi$

$$x\varphi=0.489-0.025\,(x-2.25)^2+0.015\,(x-2.25)^3. \tag{49}$$

For $x<0.5$, expression (49) is not a good approximation. This region, however, contributes little to the slowing-down time and (49) suffices, therefore, for our purpose.

We calculate the total time by integrating

$$t=\int_{2.25}^{0}\frac{dt}{dx}\,dx=\int_{0}^{2.25}\left[\frac{dW}{dx}\Big/\left(-\frac{dW}{dt}\right)\right]dx \tag{50}$$

$$=\frac{1}{N}\int_{0}^{2.25}\frac{Z^{4/3}e^2(2b)^{-1}[(0.34/x^2)-0.045]}{0.493\,Z^{3/2}(eV)^{3/2}K^{-1/2}x^{-3}}\,dx=15.5\left(\frac{K}{eV}\right)^{1/2}\frac{Z^{-1/6}}{N}.$$

A reasonable value of K is 5 ev. This gives

$$t=35\,\frac{Z^{-1/6}}{N}. \tag{51}$$

The total time needed for the energy-loss process at negative energies will therefore be of the order of 10^{-9} second even if the mesotron continues to move on circular orbits.

7. Chemical compounds.

It is of interest in experiments on the disappearance of negative mesotrons in chemical compounds to find out with what relative probability the mesotron is captured by the different kinds of atoms. We are led by

crude estimates to the conclusion that the capture probability is proportional to the nuclear charge Z. This may be seen as follows.

It is simplest to set the capture probability proportional to the energy loss of the mesotrons near the various atomic species. At low positive mesotron energy, which is the relevant region for our argument, the energy loss is given by an expression whose numerator contains the numerator of (23). For $W = 0$ this is proportional to Z. The denominator is a constant integral for all atomic species and does not enter in the evaluation of the ratio of energy losses.

The capture probability will actually be proportional to the rate of energy loss only if the ratio of these rates does not change too rapidly near $W = 0$. In particular it is necessary to demand that this ratio should not be strongly altered by the energy change due to a single passage of the mesotron through an atom. For this energy loss δW we may write

$$\delta W = \int \left[\frac{1}{2}(W - U)\right]^{1/2} \frac{ds}{t_0} . \tag{52}$$

Near $W = 0$ we get

$$\delta W = 2.3\, eVZ^{1/3} \log\left(\frac{x_0}{x_{\min}}\right) \tag{53}$$

where $x_{\min}$ corresponds to the distance of minimum approach. The energy given in (53) is small enough so that it does not yet affect significantly the numerator in (23). Thus the ratios of energy losses are hardly affected by δW, and we may conclude that the ratios of capture probabilities are proportional to Z.

8. Conclusions.

The over-all conclusions can be summarized as fcllows. In condensed substances, both conductors and insulators, a negative mesotron is captured in its orbit nearest to the nucleus in about 10^{-13} sec. In a gas the corresponding time is a little longer than is indicated by the ratio of densities. In particular, in normal air it is of the order of 10^{-9} sec. In both cases this time is very short compared with the mesotron natural lifetime of 2×10^{-6} sec so that the mode of ultimate disappearance of the negative mesotron is governed by the balance between natural decay and typically nuclear phenomena leading to mesotron disappearance.

N° 234.

When the neutron experiments were at the end of their obvious and interesting extension, Leona Marshall and Fermi sat down and discussed the various possible neutron interactions. Mrs. Marshall recalls that her suggestion and urging led to the experiment on neutron-electron interaction (in xenon gas), described in this paper. They hoped that such an experiment might reveal an interaction due to meson effects. The result was negative, but with a limit of error smaller than the magnitude of the effect which they estimated from meson theory. They were not aware of the interaction between the Pauli moment and the electric field of the electron, discovered only later by Foldy (L. L. Foldy, « Phys. Rev. », *87*, 688 and 683 (1952)).

At the same time when Fermi and Marshall were doing their experiment, Havens, Rabi and Rainwater at Columbia looked for the same effect by a somewhat different technique and obtained a positive result (Havens, Rabi, and Rainwater, « Phys. Rev. », *72*, 634 (1947)). Later experiments (Havens, Rabi, and Rainwater, « Phys. Rev. », *82*, 345 (1951)); Hammermesh, Ringo, and Wattenberg, « Phys. Rev. », *85*, 483 (1952); Goldberg, Harvey, Hughes, and Stafne, « Phys. Rev. », *90*, 497 (1953) established the existence of the small effect accounted for by the Foldy term. (See also B. D. Fried, « Phys. Rev. », *88*, 1142 (1952)).

See also the introduction to papers 226 and 227.

Paper N° 234 was circulated also as document MDDC–1183, by the Atomic Energy Commission, Technical Information Division, Oak Ridge, Tennessee, (August 7, 1947).

H. L. ANDERSON.

234.

ON THE INTERACTION BETWEEN NEUTRONS AND ELECTRONS (*)

E. FERMI and L. MARSHALL
Argonne National Laboratory and Institute for Nuclear Studies, University of Chicago, Chicago, Illinois

(Received September 2, 1947)
« Phys. Rev. », *72*, 1139–1146 (1947).

The possible existence of a potential interaction between neutron and electron has been investigated by examining the asymmetry of thermal neutron scattering from xenon. It has been found that the scattering in the center-of-gravity system shows exceedingly little asymmetry. By assuming an interaction of a range equal to the classical electron radius, the depth of the potential well has been found to be 300 ± 5000 ev. This result is compared with estimates based on the mesotron theory according to which the depth should be 12000 ev. It is concluded that the interaction is not larger than that expected from the mesotron theory; that, however, no definite contradiction of the mesotron theory can be

(*) Footnote added in proof: HAVENS, RABI and RAINWATER, « Phys. Rev. », *72*, 634 (1947) have published results similar to the present ones obtained by a somewhat different method. Their results are in essential agreement with those of the present work.

drawn at present, partly because of the possibility that the experimental error may have been underestimated, and partly because of the indefiniteness of the theories which makes the theoretical estimate uncertain.

INTRODUCTION.

The purpose of this paper is to investigate an interaction between neutrons and electrons due to the possible existence of a short range potential between the two particles. If such a short range force should exist, one would expect some evidence of it in the scattering of neutrons by atoms. The scattering of neutrons by an atom is mostly due to an interaction of the neutrons with the nucleus. In addition, there is a somewhat smaller interaction of neutrons and the electron system which has been observed by Bloch and his co-workers in their work on polarization of neutrons. This interaction is due to the magnetic field produced by the electronic currents within the atom acting on the magnetic moment of the neutron and will be referred to as magnetic interaction. Except for negligible higher order perturbations that will be discussed later, the magnetic interaction should not exist for atoms in which the electrons are bound in closed shells. In the present work, noble gases have been used in order to eliminate perturbations due to this magnetic interaction.

Besides the magnetic interaction, one might expect also the existence of a spin independent potential energy between neutron and electron. Such an interaction could be expected, for example, according to the current mesotron theories of nuclear forces. According to these theories, proton and neutron are basically two states of the same particle, the nucleon. A neutron can transform into a proton according to the reaction:

$$N = P + \bar{\mu} \tag{1}$$

(N = neutron, P = proton, $\bar{\mu}$ = negative mesotron).

Actually, a neutron will spend a fraction of its time as neutron proper (left-hand side of Eq. (1)) and a fraction of its time in a state that can be described as a proton with a negative mesotron nearby, (right-hand side of Eq. (1)). The system oscillates with extremely high frequency between these two forms and the fraction of the time spent in either of them is different depending on the specific form of mesotron theory.

According to the estimate given in Section 4, the neutron may spend 20 percent of the time as proton and negative mesotron and 80 percent of the time as neutron proper.

If these views are correct, in the immediate vicinity of a neutron one would expect an electric field of a strength equal to that produced by a charge 0.2 e, e being the proton charge. Of course, this field would extend only to a very small distance, because it would be screened by the negative charge of the mesotron, which is present whenever the nucleon is in the proton form. Indeed, the range of this electric force would be of the order of magnitude of the distances of the negative mesotron from the nucleon, that is

about 10^{-13} cm. This force should be attractive and could be represented as a potential hole of extremely small diameter. In the present paper, an attempt to detect an interaction of this type between neutrons and electrons is described.

If the scattering of neutrons were due only to nuclear interaction, one would expect the scattering to be spherically symmetrical in the center-of-gravity system whenever the wave-length of the neutron is large compared with nuclear dimensions. This last condition is very amply fulfilled for thermal neutrons which have a wave-length of the order of 2×10^{-8} cm, about 20,000 times larger than the nuclear dimensions. One would expect, therefore, that thermal neutrons should be scattered by nuclei in spherically symmetrical waves in the center-of-gravity system.

Deviations from the spherical symmetry can be due to several causes. The scattering atoms may be paramagnetic, in which case there is the magnetic interaction already discussed. A second reason for possible asymmetries in the scattering is interference of the waves scattered by different atoms. Such interference will be expected, both in solid and liquid elements and in gases with more than one atom in the molecule. Finally, asymmetric scattering could be due to a short range potential interaction whose investigation is the main object of this paper.

In order to eliminate the first two types of asymmetry, the experiments to be described were performed on xenon at pressures of the order of one atmosphere. An attempt was made to detect deviations from the spherical symmetry in the scattering of slow neutrons by this element.

If a short range potential interaction between neutron and electron should actually exist, one would expect the scattered waves to result from the interference of a spherically symmetrical wave scattered by the nucleus and a non-symmetrical wave scattered by the electrons. This last wave is expected to be non-symmetrical because the electrons are spread through a region of dimensions of the order of 10^{-8} cm, comparable to the wave-length of the neutrons. The interference of these two waves should make the intensity of the scattered beam a function of the scattering angle, as will be discussed in detail in Section 3.

Section 1.—Experimental procedure.

The apparatus used for the experiment is shown in fig. 1. It consists of a tank of the dimensions and shape indicated in the figure, lined with cadmium as indicated, except for the four windows A, B, W_1, W_2. A beam of thermal neutrons from the thermal column of the heavy water pile at the Argonne National Laboratory was allowed to pass along the axis of this tank. The beam was collimated by the cadmium diaphragms D, D'', D' 1 1/2 inches in diameter. The tank was filled with xenon at the pressure of about one atmosphere and the neutrons scattered by the gas were recorded by the 2 BF_3-counters C_1 and C_2. The counter C_1 records the neutrons scattered at an angle of about 45° with the direction of the primary beam and

the counter C_2 records neutrons scattered at an angle of 135°. In order to correct unavoidable differences in sensitivity and geometry between the two counters, all the apparatus can be turned around, so that the neutrons enter through window B instead of entering through window A. Cadmium screens could be inserted in front of the windows W_1 and W_2. In all measurements Cd differences were taken.

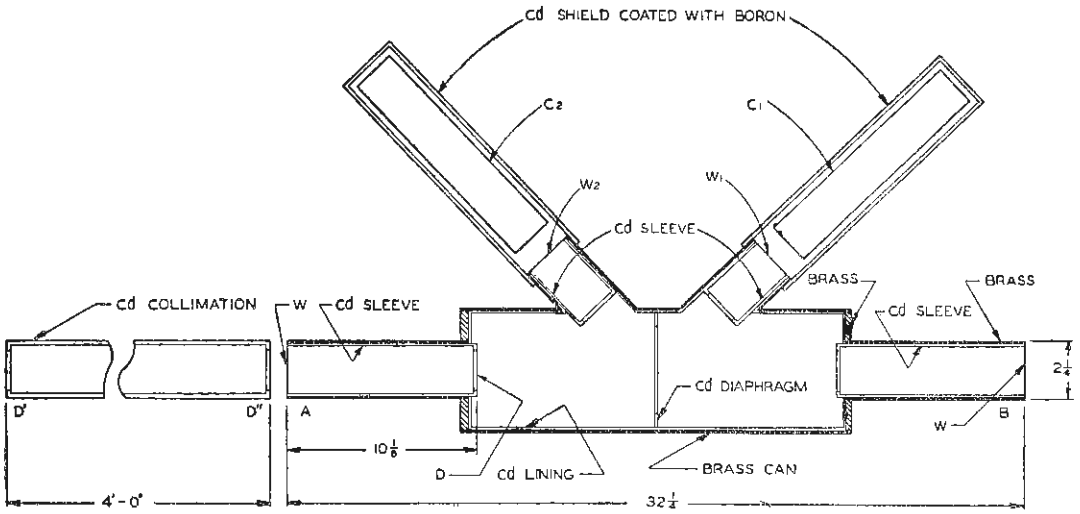

Fig. 1. – Diagram of apparatus.

Each run of the experiment consisted of four measurements, each of which was a cadmium difference. Two of them were taken with the apparatus in the position indicated in the figure (position A) and two with the apparatus turned around (position B). With the apparatus in position A, one takes first the number of counts in C_1 and C_2 with xenon inside the tank. The counts so observed must be corrected for a background. This is obtained by taking a second series of counts while the xenon is frozen out of the tank into a liquid air trap, not shown in the figure. Let n_{1a} and n_{2a} be the net number of counts per minute in the two counters. The same two measurements are performed successively with the whole tank in position B. Let n_{1b} and n_{2b} be the net number of counts observed in the counters C_1 and C_2 on this second measurement. The expression

$$\rho = \left[\left(\frac{n_{1a}}{n_{2a}}\right)\left(\frac{n_{2b}}{n_{1b}}\right)\right]^{1/2} \tag{2}$$

gives the ratio of the scattering in the two directions at 45° and 135° corrected for the possible differences in sensitivity of the two counters.

The numbers from a typical run are given in Table I.

Two series of measurements were made, with two different pairs of counters. In each series, ten complete measurements like the one given above were taken. The consistency of the two series may be seen in Table II.

The result is

$$\rho = 1.0235 \pm 0.0085. \tag{3}$$

TABLE I.

Data of a typical run.

Position	Counter	Cd	Xe	c/min	c/min cadmium difference	Net
A	C_1	no	yes	720	434	$448 = n_{1a}$
		yes	yes	286		
		no	no	276	— 14	
		yes	no	290		
A	C_2	no	yes	690	429	$421 = n_{2a}$
		yes	yes	261		
		no	no	262	8	
		yes	no	254		
B	C_1	no	yes	726	414	$406 = n_{1b}$
		yes	yes	312		
		no	no	311	8	
		yes	no	303		
B	C_2	no	yes	635	400	$392 = n_{2b}$
		yes	yes	235		
		no	no	227	8	
		yes	no	219		

The errors indicated are mean square errors obtained by a statistical study of the consistency of the various runs. They are only slightly larger than the statistical errors calculated from the actual number of counts.

SECTION 2.—CORRECTIONS.

Some corrections must be applied to the results (3) in order to arrive at the true ratio of the intensities scattered in the center-of-gravity system for scattering angles 45° and 135°.

Although xenon is rather heavy, one cannot altogether neglect the fact that the center of gravity of the neutron-atom system does not coincide with the center of the atom. In computing the correction due to this effect one must also take into account the fact that the scattering atoms are in thermal

agitation at room temperature. There is, in addition, a geometrical correction. Although the beam going through the tank is rather well collimated, it still diverges a little while going through the tank. This introduces an asymmetry which is not eliminated by switching the tank from position A to position B and must be, therefore, corrected by calculation. Here is a brief outline of the methods used for calculating these corrections.

TABLE II.

Comparison of data from two pairs of counters.

	$\frac{n_{1a}}{n_{2a}}$	$\frac{n_{2b}}{n_{1b}}$
First pair of counters	1.064	0.916
	1.064	0.975
	0.986	1.030
	1.017	0.920
	1.035	0.996
	1.104	1.019
	1.110	0.919
	1.155	1.019
	1.127	0.964
	—	0.955
Average	1.074 ± 0.018	0.968 ± 0.014
	$\rho = \left(\frac{n_{1a}\, n_{2b}}{n_{2a}\, n_{1b}}\right)^{1/2} = 1.020 \pm 0.012$	
Second pair of counters	0.943	1.031
	1.000	1.091
	0.892	1.047
	1.059	1.074
	0.884	1.116
	1.035	1.109
	1.020	1.028
	0.932	1.044
	0.971	1.100
	1.005	1.183
	—	1.093
Average	0.974 ± 0.019	1.083 ± 0.014
	$\rho = \left(\frac{n_{1a}\, n_{2b}}{n_{2a}\, n_{1b}}\right)^{1/2} = 1.027 \pm 0.012$	

Combined result: $\rho = 1.0235 \pm 0.0085$.

a) *Doppler Effect Correction.*

We consider an infinitely collimated beam of monochromatic neutrons being scattered by a gas, whose atoms move with a Maxwell distribution of velocity. The scattered neutrons are observed in a direction forming an

angle θ with the direction of the primary beam and are observed with a counter covering a small solid angle $\Delta\omega$. Two alternative assumptions are made as to the sensitivity of this counter: (1) the counter is a " thin " detector, in which case the sensitivity follows the $1/v$–law; (2) the counter is a " thick " detector, in which case the sensitivity is independent of the velocity of the neutron. If one assumes that the scattering of the neutrons is spherically symmetrical in the center-of-gravity system, one can calculate in a straightforward way the dependence upon θ of the number of counts recorded. One finds that the angular dependence is represented by the following factors: For assumption 1,

$$1 + \frac{\cos\theta}{A}\left(1 + \frac{kT}{MV^2}\right), \tag{4}$$

and for assumption 2,

$$1 + \frac{1}{A}\left(2\cos\theta - 1 + \frac{kT}{MV^2}\right). \tag{5}$$

A is the atomic weight of the scattering atoms, M and V are mass and velocity of the neutrons. In both formulae, terms of the order of $1/A^2$ have been neglected.

In the actual case, the neutrons used were not monochromatic, but had approximately a Maxwellian distribution corresponding to room temperature. The correction factors (4) and (5) must, therefore, be averaged for such a distribution. The correction factors so averaged are for assumption 1,

$$1 + \frac{2\cos\theta}{A}, \tag{6}$$

and for assumption 2,

$$1 + \frac{2\cos\theta - \frac{1}{2}}{A}. \tag{7}$$

In the actual cases, θ has the two values 45° and 135°, and we are interested in the ratio of the correction factors for these two values. Within our approximation, this ratio is the same for assumptions (1) and (2) and equal in both cases to:

$$1 + \frac{2\sqrt{2}}{A} = 1.022 \quad \text{for Xe } (A = 130). \tag{8}$$

b) *Other Geometrical Corrections.*

The experimental results must also be corrected for another reason. The beam entering the tank is collimated by an opening of 1.5 in. diameter at D and an opening of equal diameter at D', the distance between the two being 178 cm. The beam that passes through these two diaphragms is slightly spread and is, therefore, surrounded by a penumbra which increases with the distance from D. Consequently the two counters C_1 and C_2 see a beam of slightly different shape. As already pointed out, this difference between the two counters is not corrected by inversion of the tank.

In order to correct for this effect, the following procedure was adopted. An auxiliary experiment was carried out in order to determine the sensitivity of the counters to thermal neutrons originating at different places. A counter was surrounded with cadmium, shaped as in fig. 2, and was mounted on the tool holder of a lathe so that it was possible to move it parallel to itself into any desired position. A small source of thermal neutrons was obtained by exposing a small copper plate weighing about one gram to a beam of thermal neutrons. The neutrons scattered by this copper plate were re-

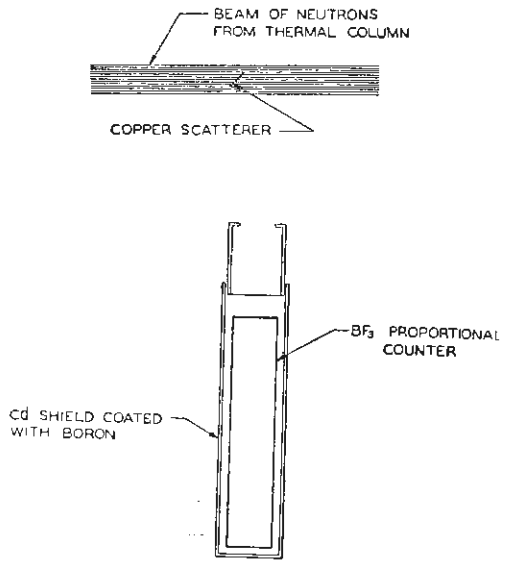

Fig. 2. – Arrangement used to make geometrical corrections.

corded for a number of positions of the counter. In all cases the average of the readings obtained with the counter at two positions symmetrical with respect to a plane perpendicular to the neutron beam and passing through the copper scatter was taken. This procedure corrects for the asymmetries of the source. In this way, the sensitivity of the counter surrounded by its cadmium shield was mapped as a function of the relative position of the source of scattered neutrons with respect to the counter.

The geometric corrections were calculated by dividing the volume of the beam seen by either of the counters C_1 or C_2 in about 200 parts. For each such section, the intensity of the radiation scattered into each counter was computed using the previously described calibration of the counter sensitivity and all the results were added. In this calculation, the Doppler correction and the correction due to the absorption of the beam were included. This rather lengthy calculation gave the following result.

If the scattering were symmetrical in the center-of-gravity system, the front counter C_1 would record a slightly larger number of counts than the back counter C_2. The ratio of the number of counts would be $\rho = 1.024$ in the case of Xe. It should be noticed that this number is quite close to the corresponding number (8) obtained by applying only the Doppler correction

and assuming that otherwise the geometry is ideally well collimated. This indicates that the error due to lack of collimation is a minor one. The calculated values of ρ should be compared with the observed value (3). The difference can be attributed to a deviation of the scattering from the spherical symmetry in the center-of-gravity system.

The observed relative difference between forward and backward scattering, with all corrections, is therefore

$$-0.0005 \pm 0.0085. \tag{9}$$

Section 3.—Calculation of an Upper Limit for the Electron-Neutron Interaction.

Both the sign and magnitude of the interaction between neutrons and electrons can be calculated from the ratio of the scattering intensities for the scattering angles 45° and 135°.

A short-range interaction between the neutron and other particles such as the nucleus or the electrons can always be represented in the Hamiltonian by terms proportional to the δ-function of the vector leading from the other particle to the neutron. Accordingly, the interaction of the neutron with the nucleus shall be represented by:

$$a\delta(\boldsymbol{r}), \tag{10}$$

and the interaction with each electron by terms of the form,

$$b\delta(\boldsymbol{r} - \boldsymbol{r}_e), \tag{11}$$

where $\boldsymbol{r}$ is the radius vector from the nucleus to the neutron, and $\boldsymbol{r}_e$ is the radius vector from the nucleus to one of the electrons. The constants a and b give a measure of the interactions of the neutron with the nucleus and with one electron. They have the dimensions of energy times volume. Indeed, when the interaction is weak, as is the case for the neutron-electron interaction, the coefficient b is simply equal to the volume integral of the potential energy between the two particles. If the potential energy between electron and neutron is a function $U(r)$ of the distance r between the two particles, then

$$b = 4\pi \int_0^\infty U(r)\, r^2\, dr\,. \tag{12}$$

We can now apply the Born approximation in order to find out the scattering in the various directions due to the interactions (10) and (11). A straightforward calculation, based on the Born approximation gives the following differential cross section for scattering within the element of solid angle $d\omega$:

$$d\sigma = \frac{M^2\, d\omega}{4\pi^2 \hbar^4} (a + bZ\mathfrak{F}(\theta))^2. \tag{13}$$

$\mathfrak{F}(\theta)$ represents the form factor of the electron distribution. A simple

expression for the form factor has been given by Bethe. [1] By means of his results, the form factors at 45° and 135° can be calculated for Xe (Z = 54). One finds

$$\mathfrak{F}(45^\circ) = 0.776,$$

$$\mathfrak{F}(135^\circ) = 0.515.$$

The difference of the form factor for the two scattering angles is responsible for the asymmetry in the scattering.

In the parenthesis of formula (13), the second term is very small compared with the first and one can neglect terms containing b^2. It follows that the ratio of the intensity scattered in two directions at 45° and 135° is given by:

$$1 + 2Z[\mathfrak{F}(45^\circ) - \mathfrak{F}(135^\circ)]\frac{b}{a} = 1 + 28.2\frac{b}{a}. \tag{14}$$

Comparison of these values with the experimental result (9) allows one to determine the ratio b/a between the interaction constants for neutron-electron and neutron-xenon nucleus. One finds

$$\frac{b}{a} = -0.00002 \pm 0.00030. \tag{15}$$

In order to obtain b, we calculate the nuclear interaction constant a from the scattering cross section.

The scattering cross section of xenon was determined by comparison of the scattered intensity (average of the net counts in the two counters C_1 and C_2) when the tank was filled with xenon or nitrogen. The scattering cross section of the molecule N_2 was assumed to be 20×10^{-24}. It was found in this way that the scattering cross section of xenon is 4.4×10^{-24}. Disregarding the very small correction due to the electron interaction term b, it follows from (13) that the scattering cross section is given by

$$\frac{M^2 a^2}{\pi\hbar^4}. \tag{16}$$

From this formula one finds

$$a = 2.46 \times 10^{-24} \text{ ergs} \times \text{cm}^3 \quad \text{for Xe}. \tag{17}$$

The sign of a is almost certainly positive. This choice is justified by the fact that nuclear interaction constants have been found to he positive for almost all nuclei. [2]

From (15) and (17) the value of b can be calculated. One finds

$$b = (-5 \pm 74) \times 10^{-47} \text{ ergs} \times \text{cm}^3. \tag{18}$$

As previously stated, the experimental error is a mean square error computed from the coherence of the various sets of measurements and it is only slightly in excess of the statistical error. In spite of that, one cannot guarantee that the actual value of b will lie within the limits as indicated in formula (18).

(1) H. A. BETHE, « Ann. d. Physik », *5*, 385 (1930).

(2) E. FERMI and L. MARSHALL, « Phys. Rev. », *71*, 666 (1947). [See paper N° 228 (Editors' note)]

and assuming that otherwise the geometry is ideally well collimated. This indicates that the error due to lack of collimation is a minor one. The calculated values of ρ should be compared with the observed value (3). The difference can be attributed to a deviation of the scattering from the spherical symmetry in the center-of-gravity system.

The observed relative difference between forward and backward scattering, with all corrections, is therefore

$$-0.0005 \pm 0.0085. \tag{9}$$

Section 3.—Calculation of an Upper Limit for the Electron-Neutron Interaction.

Both the sign and magnitude of the interaction between neutrons and electrons can be calculated from the ratio of the scattering intensities for the scattering angles 45° and 135°.

A short-range interaction between the neutron and other particles such as the nucleus or the electrons can always be represented in the Hamiltonian by terms proportional to the δ-function of the vector leading from the other particle to the neutron. Accordingly, the interaction of the neutron with the nucleus shall be represented by:

$$a\delta(\boldsymbol{r}), \tag{10}$$

and the interaction with each electron by terms of the form,

$$b\delta(\boldsymbol{r} - \boldsymbol{r}_e), \tag{11}$$

where $\boldsymbol{r}$ is the radius vector from the nucleus to the neutron, and $\boldsymbol{r}_e$ is the radius vector from the nucleus to one of the electrons. The constants a and b give a measure of the interactions of the neutron with the nucleus and with one electron. They have the dimensions of energy times volume. Indeed, when the interaction is weak, as is the case for the neutron-electron interaction, the coefficient b is simply equal to the volume integral of the potential energy between the two particles. If the potential energy between electron and neutron is a function $U(r)$ of the distance r between the two particles, then

$$b = 4\pi \int_0^\infty U(r)\, r^2\, dr\,. \tag{12}$$

We can now apply the Born approximation in order to find out the scattering in the various directions due to the interactions (10) and (11). A straightforward calculation, based on the Born approximation gives the following differential cross section for scattering within the element of solid angle $d\omega$:

$$d\sigma = \frac{M^2\, d\omega}{4\pi^2 \hbar^4} (a + bZ\mathfrak{F}(\theta))^2. \tag{13}$$

$\mathfrak{F}(\theta)$ represents the form factor of the electron distribution. A simple

It should be noted that the interaction constant b is found to be of the order of 10,000 times smaller than the constant of the interaction between a neutron and a proton or even smaller.

If the constant b should ultimately turn out to be negative it would mean that the potential between neutron and electron is negative (attractive force).

According to (12), b is the volume integral of the potential hole. Experiments of the type here discussed do not allow an independent determination of the depth and volume of the potential hole. If one assume arbitrarily, that the potential hole has a volume equal to the classical volume of the electron,

$$V_{el} = \left(\frac{4\pi}{3}\right)\left(\frac{e^2}{mc^2}\right)^3 = 0.94 \times 10^{-37}\ \text{cm}^3, \tag{19}$$

one finds from (18) the depth of the attractive potential to be

$$\overline{U(r)} = b/V_{el} = (-6 \pm 79) \times 10^{-10}\ \text{ergs} = -300 \pm 5000\ \text{ev}. \tag{20}$$

Before concluding this section, the effect of two possible perturbations should be discussed. It has been stated in the introduction that for atoms in which the electrons are bound in closed shells, no magnetic interaction between the neutron-electron system is to be expected. While this is certainly true in first approximation, one might, in reality, expect a small perturbation of this type to appear in second approximation, through the interaction of the magnetic moment of the neutron with currents in virtual excited states of the noble gas electron system. A closer discussion shows, however, that the contribution of the second order effect is quite negligible. By applying the conventional methods of quantum mechanics, one can readily estimate the interaction constant corresponding to this perturbation. This constant is found to be of the order of magnitude

$$(e\hbar/2Mc)^2\,(e^2\lambda\!\!\!^{-2}/mc^2\,R^3) \approx 10^{-48}\ \text{ergs} \times \text{cm}^3. \tag{21}$$

In this formula $e\hbar/(2Mc)$ is the nuclear magneton, $\lambda\!\!\!^{-}$ is its wave length divided by 2π, R is the average radius of the electronic orbit.

It is seen that the correction (21) is entirely negligible compared with the value (18) of b.

There is a second possible interaction between neutron and atom that could lead to an asymmetric scattering. When the neutron passes by the atom and penetrates the electronic system, it is exposed to an electric field due to the unscreened part of the nuclear charge. Since the neutron is moving, this electric field in the frame of reference of the neutron gives rise to an apparent magnetic field. This last interacts with the magnetic moment of the neutron, giving rise to a mutual energy, which might be capable of contributing a scattering asymmetry. A closer discussion shows that the error introduced by neglecting this effect is negligible. The main reason is that scattering due to the interaction just mentioned is always connected with a change in the spin direction of the neutron. There can be, therefore, no strengthening of this effect by interference with the large nuclear scattering, since in the latter case, change of the spin direction of the neutron on scattering in always coupled with a change in the spin state of the nucleus.

SECTION 4.—COMPARISON WITH THE MESOTRON THEORY.

The results (18) or (20) should be compared with the expectations of the mesotron theory.

From the qualitative discussion already given in the introduction it is clear that, according to the mesotron theory, a short-range attractive potential between neutron and electron should be expected. On the other hand, because of the indefiniteness of the mesotron theories, it is not feasible to predict in a precise way the strength of the interaction to be expected. Indeed, most mesotron theories require elimination of divergences by cutting off the field at a distance from the nucleon of the order of 10^{-13} cm, which is just the expected range of the electric field surrounding the neutron.

A second point that should be mentioned in this connection is the influence on the neutron-electron interaction of the size of the electron. If we take the classical picture of the electron as a small sphere throughout whose volume negative electricity is spread, and we assume also, in a purely classical way, that the neutron is surrounded by a short range electric field, one would expect that the range of the interaction is of the order of magnitude of the largest of the two lengths, radius of the electron and range of the electric field surrounding the neutron. If the radius of the electron is larger than the range of the electric field, the interaction will extend, therefore, to a distance of the order of the electron radius. In this sense, the size of the electron influences the expected potential hole in that if the radius of the electron is taken larger, the potential hole becomes shallower and wider. Actually, one can determine on this classical model that the interaction constant, namely, the volume integral over the potential hole, is not influenced by the size of the electron. We can, therefore, in these estimates, regard the electron as a point-charge.

One possible approach to a semi-quantitative estimate of the interaction to be expected, according to the mesotron theory, is the following.

According to the most simple forms of mesotron theory, the wave function describing the mesotrons in the vicinity of the nucleus is of the form

$$\frac{\exp[-\mu cr/\hbar]}{r}, \tag{22}$$

where μ is the mesotron mass. To this wave function there corresponds a density distribution of the mesotrons proportional to the square of (22); namely, to

$$\frac{\exp[-2\mu cr/\hbar]}{r^2}. \tag{23}$$

One can then calculate in an elementary way the electric field E at a distance r from the center of the neutron,

$$\mathrm{E} = \frac{ze}{r^2}\exp[-2\mu cr/\hbar], \tag{24}$$

where z is the fraction of the time that the neutron spends in the state represented by the right-hand side of Eq. (1) (proton and negative mesotron).

From (24) one can immediately calculate the potential energy for an electron in the electric field surrounding the neutron. One finds

$$U = -e\int_r^\infty E\,dr = -ze^2\int_r^\infty \left(\frac{dr}{r^2}\right)\exp[-2\,\mu cr/\hbar]. \tag{25}$$

From (25) and (12) we obtain finally the interaction constant

$$b = -\left(\frac{\pi}{3}\right)\left(\frac{ze^2\hbar}{\mu^2 c^2}\right)^2. \tag{26}$$

A simple procedure for estimating the value of z is given here. One of the objectives of the mesotron theory is to explain the neutron magnetic moment as the magnetic moment of the virtual mesotron field surrounding the neutron. If such an interpretation is correct and if we assume further that each mesotron bears a magnetic moment equal to $e\hbar/2\,\mu c$, we are led to the estimate that the average number of mesotrons near a neutron is 0.2. Therefore, in calculating the numerical value of (26), we shall use $z = 0.2$. Assuming a mesotron mass 200 times larger than the electron mass, we find from (26)

$$b = -1.8 \times 10^{-45}. \tag{27}$$

If we spread the interaction over the potential hole having the volume (19) we find that the depth of the potential hole is 12,000 ev.

Section 5.—Conclusions.

The comparison of the last result with the experimentally found depth of -300 ± 5000 ev indicates an experimental value appreciably less than the theoretical estimate. This does not necessarily mean that this experiment decisively contradicts the mesotron theory. On one hand, the experimental error may be somewhat larger than has been indicated. On the other hand, the theory outlined is obviously exceedingly crude. It may very well be that some mesotron theory eventually will lead to a lower estimate of the depth of the well. It would seem that the experimental result is sufficiently conclusive to exclude the so-called strong coupling theories according to which $z = 0.5$ and the depth is therefore about 30,000 ev which appears to be well outside of our experimental error.

A final conclusion one might draw from these experiments is that no interaction of an order of magnitude larger than that predicted by the mesotron theory exists between neutron and electron.

Our thanks are due to Dr. A. Wattenberg for help in this experiment.

N° 235.

For the introduction to this paper see paper N° 227.

235.

SPIN DEPENDENCE OF SLOW NEUTRON SCATTERING BY DEUTERONS (*)

E. FERMI and L. MARSHALL
Argonne National Laboratory and Institute for Nuclear Studies, University of Chicago, Chicago, Illinois

(Received November 8, 1948)
« Phys. Rev. », 75, 578–580 (1949).

The cross section of deuterium gas at liquid air temperature for neutrons of average wave-length 5.43 A is found to be 21.3×10^{-24} cm² per molecule. The cross section of deuterium atoms for neutrons of a few volts is found to be 3.44×10^{-24} cm² per atom. These two values are used to obtain information on the spin dependence of the neutron scattering by the deuteron. It is found that the two scattering lengths a_4 and a_2, corresponding to neutron spin parallel or antiparallel to the deuteron spin, have the same sign but may differ in magnitude by as much as a factor 2.

I. INTRODUCTION.

The purpose of the present experiment is to obtain information on the spin dependence of the slow neutron scattering by deuterium. The scattering properties of slow neutrons are determined by the scattering lengths (1) for the various spin orientations. The spins of the neutron and the deuteron can take two relative orientations with resultant spins 1/2 and 3/2. To these correspond two scattering lengths, a_2 for the doublet state, $S = 1/2$,

(*) This paper was circulated also as document AECD–2343 by the Atomic Energy Commission, Technical Information Division, Oak Ridge, Tennessee (October 20, 1948) (Editors' note)

(1) E. FERMI and L. MARSHALL, « Phys. Rev. », 71, 666 (1947). [See paper N° 228. (Editors' note)].

and a_4 for the quartet state, S = 3/2. If these two quantities and their signs were known, the scattering properties of the deuterium nucleus would be completely characterized.

The corresponding two quantities for hydrogen have been obtained by determining separately the cross sections of the ortho– and parahydrogen. The most recent of these measurements is due to Sutton *et al.* [2]

Since no liquid hydrogen was available for the present work and the ortho– and paradeuterium could not be separated, a somewhat different method was used. The cross section of the deuterium molecule at liquid air temperature was measured, using neutrons of very long wave-length in order to emphasize the interference phenomena. The ratio of this cross section to that of deuterium for epithermal neutrons was compared with a value of the same ratio calculated as a function of a_4/a_2. From the comparison one can assign limits to the possible values of a_4/a_2.

Unfortunately, a_4/a_2 turns out to be not very different from one—a value for which the sensitivity of the method is extremely poor. Consequently, a_4/a_2 could be determined only within rather wide limits.

II. Determination of the Cross Section of D_2 for Filtered Neutrons.

The deuterium gas was contained in a heavy-walled steel tube, the inside dimensions of which were 74.93 cm in length and 2.72 cm in diameter. In order to prevent condensation of water on the ends of the tube, when it was cooled to liquid air temperature, the ends of the tube were extended by false ends and the space in between was evacuated. The tube, together with the adjoining parts of the false ends, was immersed in liquid nitrogen. The temperature of the tube was measured by a thermocouple and was found to be quite constant at 77.5° K.

A beam of thermal neutrons from the thermal column of the Argonne heavy water pile was filtered through 40 cm of sintered BeO. This filter removes neutrons whose wave-length is less than 4.5 A from the thermal beam.[1] The average wave-length of the neutron beam so obtained was determined in a separate experiment, which will be described below, and found to be 5.43 A.

The neutron intensity transmitted by the deuterium was measured with a long BF_3 counter. The intensity was measured both with the tube empty and with the tube containing deuterium at a pressure of 406.9 cm Hg. Without deuterium the beam intensity was measured as 1672.1 ± 5 counts per minute with a background of 86 ± 2 c/min, corresponding to a net count of 1586 ± 6 c/min. With the deuterium in the tube the count was 781.9 ± 4 c/min with a background of 74.8 ± 2 c/min, corresponding to a net count of 707 ± 5 c/min.

(2) Sutton, Hall, Anderson, Bridge, De Wire, Lavatelli, Long, Snyder, and Williams, « Phys. Rev. », *72*, 1147 (1947).

From these data the cross section of the deuterium molecule at 77.5° K for BeO filtered neutrons is found to be $(21.3 \pm 0.2) \times 10^{-24}$ cm².

The average wave-length of the BeO filtered neutrons used in this experiment was measured by a subsidiary experiment. The cross section of B^{10} in the form of BF_3 was measured for monochromatic neutrons of known wave-length obtained by reflection from a (1 , 1 , 1) face of a LiF crystal, and for the filtered neutrons. Assuming a $1/v$ law for the boron absorption, the average wave-length of filtered neutrons is then calculated. The particular face (111) of LiF was chosen, because for it the correction caused by high orders in the range of wave-lengths used is negligible.

In order to measure transmissions of the order of 0.5 for a large range of wave-lengths, two interconnected transmission tubes filled with $B^{10}F_3$ were used. One was 3.569 cm long and the other was 17.556 cm. The short transmission tube was used to measure the cross section of the filtered neutrons, and the long tube was used to measure the cross sections of the monochromatic neutrons whose wave-length ranged from 0.8 A to 1.3 A. The average wave-length, after correcting for air absorption and for scattering, was found to be 5.43 A.

III. Determination of the Cross Section of D_2 for Epithermal Neutrons.

The cross section of deuterium for epithermal neutrons was measured for resonance neutrons of indium and silver. A beam of neutrons coming from the surface of the pile and which contained therefore a large amount of epithermal neutrons was used. A cadmium foil was inserted into the beam to absorb the thermal neutrons.

When a resonance detector like silver or indium is used, the activity induced is due to some extent to very high energy neutrons. One expects that the cross section of deuterium is smaller for such neutrons than for neutrons of a few volts. In order to minimize the contribution of the high energy neutrons, each measurement of induced activity is taken with and without a thin absorber made of the same element as the detector, and the difference is used. In this way, only neutrons belonging to the low resonance bands are counted.

The deuterium was in the form of 99.74 percent pure D_2O, the contaminant being H_2O. If the cross section of oxygen were well known, itc ould be directly substracted, since for epithermal neutrons interference phenomena are negligible. In order to minimize the error introduced by inaccuracies in the oxygen cross section, the following method to cancel it was used. In one measurement, the absorber in the neutron beam was n moles of D_2O and n moles of Be. The intensity transmitted through this absorber was compared with the intensity transmitted in a second measurement in which the absorber was n moles of BeO. The difference in these two transmitted intensities is due to the deuterium only.

Actually, the absorbers used in the two measurements contained the following quantities:

Absorber 1	moles/cm²	Absorber 2	moles/cm²
D_2O	0.2999	BeO	0.3016
H_2O	0.0008	O_2	0.00004
Be	0.3051	N_2	0.00018

If R is the ratio of the intensity transmitted by absorber 2 to that transmitted by absorber 1, one finds

$$\log R = 0.6023\,[0.5998\,\sigma_D + 0.0035\,\sigma_{Be} - 0.0010\,\sigma_O + 0.0016\,\sigma_H - 0.00036\,\sigma_N].$$

The σ's represent the cross sections of the respective elements in units of 10^{-24} cm². All cross sections except σ_D appear with very small coefficients so that an error in their values is unimportant. The values which were used were $\sigma_{Be} = 6.1$, $\sigma_O = 4.1$, $\sigma_H = 21$, $\sigma_N = 10$.

The measurement with silver gave

$$\log R = 1.293 \pm 0.023.$$

That with indium gave

$$\log R = 1.247 \pm 0.021.$$

The average of these two, 1.27 ± 0.02, was then used to calculate σ_D. One finds $\sigma_D = 3.44 \pm 0.06$.

IV. Theory.

The above esperiments have determined the cross section of the deuterium molecule for neutrons of average wave-length 5.43 A at 77.5° K ($\sigma(D_2) = 21.3 \times 10^{-24}$ cm²) and of the deuterium atom for neutrons of a few volts ($\sigma(D) = 3.44 \times 10^{-24}$ cm²).

These two cross sections can be expressed in terms of the scattering lengths a_2 and a_4 corresponding to antiparallel and parallel orientation of spins of the neutron and the deuteron, respectively.

$\sigma(D)$ is simply expressed by the formula

$$\sigma(D) = 4\pi\left(\frac{2}{3}a_4^2 + \frac{1}{3}a_2^2\right).$$

In this formula the factors 2/3 and 1/3 correspond to the probabilities of parallel and of antiparallel orientation. The calculation of the scattering cross section of the deuteron is more complicated and is similar to that made by Schwinger and Teller [3] for the scattering cross section of the hydrogen mol-

(3) J. Schwinger and E. Teller, «Phys. Rev.», 52, 286 (1937).

ecule. In the experiments the ortho-para ratio was unchanged from that at room temperature. On the other hand, the distribution of the rotational states was that for a temperature of 77.5° K. $\sigma(D_2)$ is an average of the values for the individual states corresponding to this distribution. The results of the calculation of the ratio $\sigma(D_2)/\sigma(D)$, not including the correction of the Doppler effect, are given below:

g	$\sigma(D_2)/\sigma(D)$
0.0	$5.76 - 1.92\,\delta + (0.0035/g) + (0.035\,\delta/g)$
0.2	$5.65 - 1.67\,\delta$
0.4	$5.23 - 1.58\,\delta$
0.6	$4.58 - 1.36\,\delta$
0.8	$3.85 - 0.98\,\delta$
1.0	$3.13 - 0.55\,\delta$
1.1	$2.81 - 0.36\,\delta$

In this table g is the relative velocity measured in units of $5\hbar/(2\,\mathrm{M}r)$ where M is the proton mass and r is the interatomic distance in the deuterium molecule, 0.747×10^{-8} cm. δ is the following function of a_2 and a_4:

$$\delta = \frac{(a_4 - a_2)^2}{(2\,a_4^2 + a_2^2)}\,.$$

The cross section becomes infinite at zero velocity. However, the coefficient of the infinite terms is very small.

The Doppler correction was calculated using the formula

$$\sigma_{\mathrm{eff}} = \frac{2\exp(-q^2/q_0^2)}{(\pi)^{1/2}\,q_0\,q^2}\int_0^\infty g^2\,\sigma(g)\sinh(2qg/q_0^2)\exp(-g^2/q_0^2)\,dg\,,$$

where q is the velocity of the neutrons in units $5\hbar/(2\,\mathrm{M}r)$ and q_0 is the characteristic velocity of the Maxwell distribution written in the form $\exp(-q^2/q_0^2)$. For deuterium at 77.5° K, q_0 is 0.269. The integral is obtained by a numerical integration.

The following values were found for the ratio $\sigma(D_2)/\sigma(D)$ corrected for the Doppler effect:

q	$\sigma(D)_2/\sigma(D)$
0.3	$6.851 - 2.022\,\delta$
0.368	$6.047 - 1.768\,\delta$
0.4	$5.782 - 1.680\,\delta$

The effective wave-length of the neutrons used in the determination of $\sigma(D_2)$ was 5.43 A, for which q is 0.346. By interpolation one finds, for $q = 0.346$,

$$\frac{\sigma(D_2)}{\sigma(D)} = 6.271 - 1.865\,\delta .$$

The measured value of this ratio is 21.3/3.44 or 6.19. Consequently, δ is very small

$$\delta = 0.04 \pm 0.10.$$

Since δ is essentially positive, this results enables one to assign to δ only an upper limit, namely, 0.14. If δ were zero, a_4 would be equal to a_2. To each value of δ there correspond two values of the ratio a_4/a_2, one greater and one less than one. For the upper limit, $\delta = 0.14$, the two corresponding values of a_4/a_2 are 0.53 and 2.25. Since δ is between zero and 0.14, the ratio a_4/a_2 must lie between 0.5 and 2.3.

Therefore, it can be concluded that a_4 and a_2 have certainly the same sign. Their magnitudes, however, may differ by somewhat more than a factor 2. The sensitivity of this method is low when the value of a_4 is rather close to that of a_2. Consequently, only the above wide limits can be given for their ratio.

It is notable that deuterium does not share the peculiarities of hydrogen for which the two scattering lengths are of opposite sign and of such magnitudes that the neutron interference effects almost cancel as a result of the almost complete cancellation of the contributions of the two spin orientations.

N° 236.

In the spring of 1948, a group of people at the Argonne National Laboratory, including Fermi, Maria Mayer, James Alexander, Elmer Eisner, and myself, were studying the applicability of Monte Carlo to reactor calculations. A practical difficulty not present in the earlier Monte Carlo work was caused by the enormous spread of neutron velocities in a moderated chain-reacting system. As a remedy, it was proposed to base census-taking on distance travelled rather than elapsed time so that comparable numbers of collisions would be followed for fast and slow neutrons. Although it seemed intuitively evident (at least to Fermi) that this would give correct results for a critical system, if the calculated neutron spectrum were suitably reinterpreted, it was felt that a more formal justification was desired, and the following paper written by Fermi and myself in the summer at Los Alamos, was the result.

This paper was circulated also as document AECD–3164 (July 11, 1941) and as document LADC–946.

R. D. RICHTMYER.

236.

NOTE ON CENSUS-TAKING IN MONTE-CARLO CALCULATIONS

E. FERMI and R. D. RICHTMYER
Document LAMS–805 (July 11, 1948).

ABSTRACT

An analysis is given of the proposal, made by investigators at the Argonne Laboratory, that in some Monte Carlo problems census taking should be made on the basis of distance travelled rather than time elapsed. The analysis given is restricted to critical systems, and it is shown how to interpret the resulting neutron distribution in this case.

We consider a "Monte Carlo" type treatment of a neutron chain reaction according to which the detailed history of a typical reaction in the given system is produced, whereby the position $\boldsymbol{x}$, velocity $\boldsymbol{v}$ and genealogy of every neutron is known at every time t. Let $n(\boldsymbol{x}, \boldsymbol{v}, t)$ be the density in phase-space $\boldsymbol{x}, \boldsymbol{v}$ of these neutrons at time t. For a stationary population n is independent of t except for statistical fluctuations. In practice n is found by determining the position and velocity of every neutron present at some time t^*, called a census time, and observing the distribution of the position and velocity values thus found. This procedure is called taking a census.

This report discusses alternative methods of census taking. They yield distributions simply related to $n(\boldsymbol{x}, \boldsymbol{v}, t)$ in the case of a stationary population.

While the procedure described above is suited to discussion of fast multiplying systems in which the neutrons essentially involved do not differ greatly in velocity, it is impractical for systems where neutrons of vastly

different velocities are of importance. This is the case, for example, in a reactor near critical condition when both fast and thermal neutrons contribute appreciably to the reactivity. A ratio of about 10,000 in the speeds of the two kinds of neutrons would force one in this case to follow up the life history of a fast neutron for an enormous number of generations before any of the slow neutrons has moved a single free path.

In such cases one must change the census procedure. One might, for example, divide the study of a neutron into intervals traversed by the neutron or by its ancestors. This " census distance " procedure is applicable, of course, only to critical systems or to systems that are conventionally made critical by adding a " time absorption. " As will be shown, a distribution of neutrons at a given value of the census distance corresponds to the flux distribution instead of the density distribution that one would obtain from the " census time " prescription.

Given that a neutron is present at point $\boldsymbol{x}$, $\boldsymbol{v}$ of phase space at time $t > 0$, we can trace a unique trajectory backward to time zero by following backward the path of this neutron and of each of its direct ancestors in turn until we reach $t = 0$. In particular, the speed v is a unique function of t on this trajectory.

Let $g(v)$ be a given function of v and define

$$\tau = \int_0^t g(v(t'))\, dt' \tag{1}$$

where $v(t)$ is the speed as function of time on the trajectory defined above. Each neutron has associated with it at each instant a certain value of τ. τ is called a census parameter. If $g(v) = 1$, it is the elapsed time; if $g(v) = v$, it is the distance traversed.

Now consider all points, in a space $(\boldsymbol{x}, \boldsymbol{v}, t)$, corresponding to a particular value of τ. These points have various different times t as well as different positions in phase space $(\boldsymbol{x}, \boldsymbol{v})$, but we focus our attention on their distribution in phase space, ignoring the time differences; and we call $N(\boldsymbol{x}, \boldsymbol{v}, t)$ the density of these points in phase space.

To establish the connection between the distributions n and N for a stationary population, we investigate the change in N caused by a small change in τ, by methods similar to those used in deriving the Boltzmann equation, and in this way obtain an equation for $\partial N/\partial\tau$, which will eventually be equated to zero

In the neighborhood of a given point of phase space the neutrons move along trajectories $\boldsymbol{x} = \boldsymbol{v}t + \text{const}$, $\boldsymbol{v} = \text{const}$, between collisions, and there is a change δN in the density, in time δt, due just to the motions, apart from collisions, amounting to:

$$\delta N = -[(\boldsymbol{v}\cdot\boldsymbol{\nabla})\, N]\, \delta t; \tag{2}$$

but, according to (1), $\delta t = \delta\tau/g(v)$ where $\delta\tau$ is the increment of τ under consideration. Therefore the motions contribute to $\partial N/\partial\tau$ an amount $-(\boldsymbol{v}\cdot\boldsymbol{\nabla})\frac{N}{g}$.

Other contributions to $\partial N/\partial\tau$ can be similarly obtained. In particular, if σ is a cross section for any process, the number of such processes per unit volume of phase space and having values of τ lying in the interval $\delta\tau$ is:

$$v\sigma\, N\, \delta t = v\sigma\, N \frac{\delta\tau}{g(v)} . \tag{3}$$

For a system in which fission, elastic scattering, inelastic scattering and absorption take place, the complete equation is, in customary notation:

$$\left.\begin{aligned} \frac{\partial N}{\partial\tau} = &- (\boldsymbol{v}\cdot\nabla)\frac{N}{g} - v\sigma_t \frac{N}{g} + \frac{\nu\varphi(v)}{4\pi}\int_{\text{all velocity space}} v'\,\sigma_f(v')\frac{N(\boldsymbol{x},\boldsymbol{v}',\tau)}{g(v')}\,d\boldsymbol{v}' \\ &+ \frac{1}{4\pi}\int_{\text{all velocity space}} v'\,\sigma_i(v',v)\frac{N(\boldsymbol{x},\boldsymbol{v}',\tau)}{g(v')}\,d\boldsymbol{v}' \\ &+ \int_{\substack{\text{all directions of } \boldsymbol{v}',\\ \text{with } v'=v}} v\sigma_e(v,\alpha)\frac{N(\boldsymbol{x},\boldsymbol{v}',\tau)}{g(v)}\,d\omega(\boldsymbol{v}') \end{aligned}\right\} \tag{4}$$

where α is the angle between $\boldsymbol{v}'$ and $\boldsymbol{v}$.

We now suppose that after the calculation has proceeded sufficiently, the distribution represented by N becomes independent of τ, except for statistical fluctuations. We therefore replace the left member of (4) by zero, and if we furthermore replace $\frac{N(\boldsymbol{x},\boldsymbol{v})}{g(v)}$ by $n(\boldsymbol{x},\boldsymbol{v})$, equation (4) reduces exactly to the Boltzmann equation for a neutron population n independent of the time t, and we are therefore justified in identifying n with N/g, because, for systems of the sort considered, there is only one stationary solution of the Boltzmann equation in the absence of sources and sinks. If $g(v)$ is equal to v, so that τ is the census distance, the distribution N represents the distribution of neutron flux, nv, in the system.

The application to Monte Carlo calculations is this: one maintains a current record of τ rather than t, for each neutron, and discriminates, at each collision, to see whether τ has exceeded a preassigned value τ^*, and if so, one calculates where the neutron was when $\tau = \tau^*$ and prints a census card.

As an application we consider the proposal, made sometime ago in the Theoretical Physics Division of the Argonne Laboratory, that for chain reacting systems in which both fast and slow neutrons are important (e.g. both 1 Mev and 1 ev neutrons) one should use a census distance $\tau = \int v\,dt$ rather than a census time. The advantage of this can be seen as follows. The mean free path is of the same order of magnitude for both fast and slow neutrons, so that if one used a census time long enough to allow a 1 ev neutron to make several collisions, a fast one would make several thousand in each census interval, and the calculation would be prohibitively long. This difficulty is largely avoided by use of a census distance. An even stronger dependence of $g(v)$ on v (e.g. perhaps $g = v^{3/2}$) may be indicated in some cases, such as that of a system containing large volumes of graphite or other moderator, in which a neutron may make many collisions (of the order of 100) before emerging as a slow neutron.

N° 237 and 238

With paper N° 235 Fermi's experimental work at Argonne came to a close. He gave up his regular excursions to the Argonne for two main reasons. The first was the very stimulating atmosphere which had developed at the University. Many interesting questions came up, and Fermi wanted more and more time to look into them. More and more frequently could he be found at his blackboard examining his equations. The second reason had to do with Mrs. Marshall, who felt compelled to do some of her own work independently of Fermi. These reasons, together with the absence yet of good experimental facilities at the new Institute for Nuclear Studies, combined to convert Fermi once more to theoretical physics.

Paper N° 237 was a direct outcome of heated disputes with Edward Teller on the origin of the cosmic rays. It was written to counter the view that the cosmic rays were principally of solar origin and that they could not extend through all galactic space because of the very large amount of energy which would then be required. Taking up the study of the intergalactic magnetic fields, Fermi was able to find not only a way to account for the presence of the cosmic rays, but also a mechanism for accelerating them to the very high energies observed.

He presented these same views on the origin of cosmic rays, though less extensively, in a talk at the Como International Congress on the Physics of Cosmic Rays (paper N° 238).

H. L. ANDERSON.

N° 237, 238, and 264

Fermi mentioned to me his interest in the origin of cosmic rays as early as 1946. Several years before that time he mentioned the subject in some lectures in Chicago. He had the suspicion that magnetic fields could accelerate the cosmic particles.

In 1948 Alfvén visited Chicago. He had been interested in electromagnetic phenomena on the cosmic scale for quite some time. At that time I was playing with the idea that cosmic rays might be accelerated in the neighborhood of the sun. I had discussed this question with Alfvén, and he visited us in Chicago in order to carry forward the discussion.

During this visit Fermi learned from Alfvén about the probable existence of greatly extended magnetic fields in our galactic system. Since this field would necessarily be dragged along by the moving and ionized interstellar material, Fermi realized that here was an excellent way to obtain the acceleration mechanism for which he was looking.

As a result he outlined a method of accelerating cosmic ray particles which serves today as a basis for most discussions on the subject. In his papers published in 1949 (N° 237 and 238) he explained most of the observed properties of cosmic rays with one important exception: it follows from his originally proposed mechanism that heavier nuclei will not attain as high velocities as protons do. This is in contradiction with experimental evidence. Fermi returned to this problem in his paper *Galactic Magnetic Fields and the Origin of Cosmic Radiation* (N° 264).

Some details concerning the origin of cosmic rays have not been settled conclusively by Fermi's papers. Another competing theory has been proposed by Sterling Colgate and Montgomery Johnson according to which cosmic rays are produced by shock mechanism in exploding supernovae. The actual origin of cosmic rays continues to remain in doubt.

E. TELLER.

237.

ON THE ORIGIN OF THE COSMIC RADIATION

« Phys. Rev. », 75, 1169–1174, (1949).

A theory of the origin of cosmic radiation is proposed according to which cosmic rays are originated and accelerated primarily in the interstellar space of the galaxy by collisions against moving magnetic fields. One of the features of the theory is that it yields naturally an inverse power law for the spectral distribution of the cosmic rays. The chief difficulty is that it fails to explain in a straightforward way the heavy nuclei observed in the radiation.

I. Introduction.

In recent discussions on the origin of the cosmic radiation E. Teller [1] has advocated the view that cosmic rays are of solar origin and are kept relatively near the sun by the action of magnetic fields. These views are amplified by Alfvén, Richtmyer, and Teller.[2] The argument against the conventional view that cosmic radiation may extend at least to all the galactic space is the very large amount of energy that should be present in form of cosmic radiations if it were to extend to such a huge space. Indeed, if this were the case, the mechanism of acceleration of the cosmic radiation should be extremely efficient.

I propose in the present note to discuss a hypothesis on the origin of cosmic rays which attempts to meet in part this objection, and according to which cosmic rays originate and are accelerated primarily in the interstellar space, although they are assumed to be prevented by magnetic fields from leaving the boundaries of the galaxy. The main process of acceleration is due to the interaction of cosmic particles with wandering magnetic fields which, according to Alfvén, occupy the interstellar spaces.

Such fields have a remarkably great stability because of their large dimensions (of the order of magnitude of light years), and of the relatively high electrical conductivity of the interstellar space. Indeed, the conductivity is so high that one might describe the magnetic lines of force as attached to the matter and partaking in its streaming motions. On the other band, the magnetic field itself reacts on the hydrodynamics [3] of the interstellar matter giving it properties which, according to Alfvén, can pictorially be described by saying that to each line of force one should attach a material density due to the mass of the matter to which the line of force is linked. Developing

(1) Nuclear Physics Conference, Birmingham 1948.
(2) Alfvén, Richtmyer, and Teller, « Phys. Rev. », to be published.
(3) H. Alfvén, « Arkiv Mat. f. Astr., o. Fys. », *29 B*, 2 (1943).

this point of view, Alfvén is able to calculate a simple formula for the velocity V of propagation of magneto-elastic waves:

$$V = \frac{H}{(4\pi\rho)^{1/2}}, \tag{1}$$

where H is the intensity of the magnetic field and ρ is the density of the interstellar matter.

One finds according to the present theory that a particle that is projected into the interstellar medium with energy above a certain injection threshold gains energy by collisions against the moving irregularities of the interstellar magnetic field. The rate of gain is very slow but appears capable of building up the energy to the maximum values observed. Indeed one finds quite naturally an inverse power law for the energy spectrum of the protons. The experimentally observed exponent of this law appears to be well within the range of the possibilities.

The present theory is incomplete because no satisfactory injection mechanism is proposed except for protons which apparently can be regenerated at least in part in the collision processes of the cosmic radiation itself with the diffuse interstellar matter. The most serious difficulty is in the injection process for the heavy nuclear component of the radiation. For these particles the injection energy is very high and the injection mechanism must be correspondingly efficient.

II. The Motions of the Interstellar Medium.

It is currently assumed that the interstellar space of the galaxy is occupied by matter at extremely low density, corresponding to about one atom of hydrogen per cc, or to a density of about 10^{-24} g/cc. The evidence indicates, however, that this matter is not uniformly spread, but that there are condensations where the density may be as much as ten or a hundred times as large and which extend to average dimensions of the order of 10 parsec. (1 parsec $= 3.1 \times 10^{18}$ cm $= 3.3$ light years). From the measurements of Adams [4] on the Doppler effect of the interstellar absorption lines one knows the radial velocity with respect to the sun of a sample of such clouds located at not too great distance from us. The root mean square of the radial velocity, corrected for the proper motion of the sun with respect to the neighboring stars, is about 15 km/sec. We may assume that the root-mean-square velocity is obtained by multiplying this figure by the square root of 3, and is therefore about 26 km/sec. Such relatively dense clouds occupy approximately 5 percent of the interstellar space. [5]

Much less is known of the much more dilute matter between such clouds. For the sake of definiteness in what follows, the assumption will be made that this matter has a density of the order of 10^{-25}, or about 0.1 hydrogen atoms

(4) W. S. Adams, «A. p. J.», *97*, 105 (1943).
(5) B. Stromgren, «A. p. J.», *108*, 242 (1948).

per cc. Even fairly extensive variations on this figure would not very drastically alter the qualitative conclusions. If the assumption is made that most of this material consists of hydrogen atoms, it is to be expected that most of the hydrogen will be ionized by the photoelectric effect of the stellar light. Indeed, one can estimate that some kind of dissociation equilibrium is established under average interstellar conditions, outside the relatively dense clouds, for which

$$\frac{n_+^2}{n_0} \approx (T_1)^{1/2}, \tag{2}$$

where n_+ and n_0 are the concentrations of ions and neutral atoms per cc, and T_1 is the absolute kinetic temperature in degrees K. Putting in this formula $n_+ = 0.1$, one finds that the fraction of undissociated atoms is of the order of 1 percent, even assuming a rather low kinetic temperature of the order of 100° K.

It is reasonable to assume that this very low density medium will have considerable streaming motions, since it will be kept stirred by the moving heavier clouds passing through it. In what follows, a root-mean-square velocity of the order of 30 km/sec will be assumed. According to Alfvén's picture, we must assume that the kinetic energy of these streams will be partially converted into magnetic energy, that indeed, the magnetic field will build up to such a strength that the velocity of propagation of the magneto-elastic waves becomes of the same order of magnitude as the velocity of the streaming motions. From (1) it follows then that the magnetic field in the dilute matter is of the order of magnitude of 5×10^{-6} gauss, while its intensity is probably greater in the heavier clouds. The lines of force of this field will form a very crooked pattern, since they will be dragged in all directions by the streaming motions of the matter to which they are attached. They will, on the other hand, tend to oppose motions where two portions of the interstellar matter try to flow into each other, because this would lead to a strengthening of the magnetic field and a considerable increase of magnetic energy. Indeed, this magnetic effect will have the result to minimize what otherwise would be extremely large friction losses which would damp the streaming motions and reduce them to disordered thermal motions in a relatively short time.

III. Acceleration of the Cosmic Rays.

We now consider a fast particle moving among such wandering magnetic fields. If the particle is a proton having a few Bev energy, it will spiral around the lines of force with a radius of the order of 10^{12} cm until it "collides" against an irregularity in the cosmic field and so is reflected, undergoing some kind of irregular motion. On a collision both a gain or a loss of energy may take place. Gain of energy, however, will be more probable than loss. This can be understood most easily by observing that ultimately statistical equilibrium should be established between the degrees of freedom of the wandering fields and the degrees of freedom of the particle. Equipartition evidently

corresponds to an unbelievably high energy. The essential limitation, therefore, is not the ceiling of energy that can be attained, but rather the rate at which energy is acquired. A detailed discussion of this process of acceleration will be given in Section VI. An elementary estimate can be obtained by picturing the " collisions " of the particles against the magnetic irregularities as if they were collisions against reflecting obstacles of very large mass, moving with disordered velocities averaging to $V = 30$ km/sec. Assuming this picture, one finds easily that the average gain in energy per collision is given as order of magnitude by

$$\delta w = B^2 w, \tag{3}$$

where w represents the energy of the particle inclusive of rest energy, and $B = \frac{V}{c} \approx 10^{-4}$. This corresponds, therefore, for a proton to an average gain of 10 volts per collision in the non-relativistic region, and higher as the energy increases. It follows that except for losses the energy will increase by a factor e every 10^8 collisions. In particular, a particle starting with non-relativistic energy will attain, after N collisions, an energy

$$w = Mc^2 \exp (B^2 N). \tag{4}$$

Naturally, the energy can increase only if the losses are less than the gain in energy. An estimate to be given later (see Section VII) indicates that the ionization loss becomes smaller than the energy gain for protons having energy of about 200 Mev. For higher energy the ionization loss practically becomes negligible. We shall discuss later the injection mechanism.

IV. Spectrum of the Cosmic Radiation.

During the process of acceleration a proton may lose most of its energy by a nuclear collision. This process is observed as absorption of primary cosmic radiation in the high atmosphere and occurs with a mean free path of the order of magnitude of 70 g/cm^2, corresponding to a cross section of about

$$\sigma_{abs} \approx 2.5 \times 10^{-26} \text{ cm}^2 \tag{5}$$

per nucleon.

In a collision of this type most of the kinetic energy of the colliding nucleons is probably converted into energy of a spray of several mesons.

It is reasonable to assume that the cosmic rays will occupy with approximately equal density all the interstellar space of the galaxy. They will be exposed, therefore, to the collisions with matter of an average density of 10^{-24}, leading to an absorption mean free path

$$\Lambda = 7 \times 10^{25} \text{ cm}. \tag{6}$$

A particle traveling with the velocity of light will traverse this distance in a time

$$T = \frac{\Lambda}{c} = 2 \times 10^{15} \text{ sec} \tag{7}$$

or about 60 million years.

The cosmic-ray particles now present will therefore, in the average, have this age. Some of them will have accidentally escaped destruction and be considerably older. Indeed, the absorption process can be considered to proceed according to an exponential law. If we assume that original particles at all times have been supplied at the same rate, we expect the age distribution now to be

$$\exp(-t/\mathrm{T})\, dt/\mathrm{T}. \tag{8}$$

During its age t, the particle has been gaining energy. If we call τ the time between scattering collisions, the energy acquired by a particle of age t will be

$$w(t) = \mathrm{M}c^2 \exp(\mathrm{B}^2 t/\tau). \tag{9}$$

Combining this relationship between age and energy with the probability distribution of age given previously, one finds the probability distribution of the energy. An elementary calculation shows that the probability for a particle to have energy between w and $w + dw$ is given by

$$\pi(w)\, dw = \frac{\tau}{\mathrm{B}^2\,\mathrm{T}} (\mathrm{M}c^2)^{\tau/\mathrm{B}^2\mathrm{T}} \frac{dw}{w^{1+(\tau/\mathrm{B}^2\mathrm{T})}}. \tag{10}$$

It is gratifying to find that the theory leads naturally to the conclusion that the spectrum of the cosmic radiation obeys an inverse power law. By comparison of the exponent of this law with the one known from cosmic-ray observations, that is, about 2.9, one finds a relationship which permits one to determine the interval of time τ between collisions. Precisely, one finds: $2.9 = 1 + (\tau/\mathrm{B}^2\,\mathrm{T})$, from which follows

$$\tau = 1.9\, \mathrm{B}^2\,\mathrm{T}. \tag{11}$$

Using the previous values of B and T, one finds $\tau = 4 \times 10^7 \approx 1.3$ years. Since the particles travel with approximately the velocity of light, this corresponds to a mean distance between collisions of the order of a light year, or about 10^{18} cm. Such a collision mean free path seems to be quite reasonable.

The theory explains quite naturally why no electrons are found in the primary cosmic radiation. This is due to the fact that at all energies the rate of loss of energy by an electron exceeds the gain. At low energies, up to about 300 Mev, the loss is mainly due to ionization. Above this energy radiative losses due to the acceleration of the electrons in the interstellar magnetic field play the dominant role. This last energy loss is instead quite negligible for protons. Also, the inverse Compton effect discussed by Feenberg and Primakoff [6] will contribute to eliminate high energy electrons.

V. The Injection mechanism. Difficulties with the Injection of Heavy nuclei.

In order to complete the present theory, the injection mechanism should be discussed.

In order to keep the cosmic radiation at the present level it is necessary to inject a number of protons of at least 200 Mev, to compensate for those

(6) E. Feenberg and H. Primakoff, « Phys. Rev. », *73*, 449 (1948).

that are lost by the absorption process. According to recent evidence, [7] the primary cosmic radiation contains not only protons but also some relatively heavy nuclei. Their injection energy is much higher than that of protons, primarily on account of their large ionization loss. (See further Section VII). Such high energy protons and heavier nuclei conceivably could be produced in the vicinity of some magnetically very active star. [8] To state this, however, merely means to shift the difficulty from the problem of accelerating the particles to that of injecting them unless a more precise estimate can be given for the efficiency of this or of some equivalent mechanism. With respect to the injection of heavy nuclei I do not know a plausible answer to this point.

For the production of protons, however, one might consider also a simple mechanism which, if the present theory is at all correct in its general features, should be responsible for at least a large fraction of the total number of protons injected. According to this mechanism the cosmic radiation regenerates itself as follows. When a fast cosmic-ray proton collides in the interstellar space against a proton nearly at rest, a good share of the energy will be lost in the form of a spray of mesons, and two nucleons will be left over with energy much less than that of the original cosmic ray. Estimates indicate that in some cases both particles may have an energy left over above the injection threshold of 200 Mev, in some cases one and in some cases none. We can introduce a reproduction factor k, defined as the average number of new protons above the injection energy arising in a collision of an original cosmic-ray particle. As in a chain reaction, if k is greater than one the overall number of cosmic rays will increase; if k is less than one it will decrease; if k is equal to one it will stay level.

Apparently the reproduction factor under interstellar conditions is rather close to one. This is perhaps not a chance, but may be due in part to the following self-stabilizing mechanism. The motions of the interstellar matter are not quite conservative, in spite of the reduced friction, caused by the magnetic fields. One should assume, therefore, that some source is present which steadily delivers kinetic energy into the streaming motions of the interstellar matter. Probably such a source of energy ultimately involves conversion of energy from the large supplies in the interior of the stars. The motions of the interstellar medium are in a dynamic equilibrium between the energy delivered by this source and the energy losses caused by friction and other causes. In this balance the amount of energy transferred by the interstellar medium to cosmic radiation is by no means irrelevant, since the total cosmic ray energy is comparable to the kinetic energy of the streaming, irregular motions of the galaxy. One should expect, therefore, that if the general level of the cosmic radiation should increase, the kinetic energy of the interstellar motion would decrease, and vice versa. The reproduction factor depends upon the density. As the density increases, the ionization

(7) FREIER, LOFGREN, NEY, and OPPENHEIMER, « Phys. Rev. », *74*, 1828 (1948); H. L. BRADT and B. PETERS, « Phys. Rev. », *74*, 1828 (1948).

(8) See for example W. F. G. SWANN, « Phys. Rev. », *43*, 217 (1933) and HORACE W. W. BABCOCK, « Phys. Rev. », *74*, 489 (1948).

losses will increase proportionally to it. This tends to increase the injection energy and consequently to decrease the reproduction factor. On the other hand, also, the rate of energy gained will change by an amount which is hard to define unambiguously. One might perhaps assume, however, that the velocity of the wandering magnetic fields increases with the $1/3$ power of the density, as would correspond to the virial theorem, and that the collision mean free path is inversely proportional to the $1/3$ power of the density, as one might get from geometrical similitude. One would find that the rate of energy increase is proportional only to the $2/3$ power of the density. The net effect is an increase of the injection energy and a decrease of the reproduction factor with increasing density. If the reproduction factor had been initially somewhat larger than one, the general level of the cosmic radiation would increase, draining energy out of the kinetic energy of the galaxy. This would determine a gravitational contraction which would increase the density and decrease k until the stable value of one is reached. The opposite would take place if k initially had been considerably less than one.

But even if this stabilizing mechanism is not adequate to keep the reproduction factor at the value one, and therefore an appreciable change in the general level of the cosmic radiation occurs over periods of hundreds of millions of years, the general conclusions reached in Section IV would not be qualitatively changed. Indeed, if k were somewhat different from one, the general level of the cosmic radiation would increase or decrease esponentially, depending on whether k is larger than or less than one. Consequently the number of cosmic particles injected according to the mechanism that has been discussed will not be constant in time but will vary exponentially. Combining this exponential variation with the exponential absorption (8), one still finds an exponential law for the age distribution of the cosmic particles at the present time, the only difference being that the period of this exponential will be changed by a small numerical factor.

The injection mechanism here proposed appears to be quite straightforward for protons, but utterly inadequate to explain the abundance of the heavy nuclei in the primary cosmic radiation. The injection energy of these particles is of several Bev, and it is difficult to imagine a secondary effect of the cosmic radiation on the diffuse interstellar matter which might produce this type of secondary with any appreciable probability. One might perhaps assume that the heavy particles originate at the fringes of the galaxy where the density is probably lower and the injection energy is therefore probably smaller. This, however, would require extreme conditions of density which are not easily justifiable. It seems more probable that heavy particles are injected by a totally different mechanism, perhaps as a consequence of the stellar magnetism. [8]

If such a mechanism exists one would naturally expect that it would inject protons together with heavier nuclei. The protons and perhaps to a somewhat lesser extent the α–particles would be further increased in numbers by the "chain reaction" which in this case should have $k < 1$. Indeed their number would be equal to the number injected during the lifetime T increased by the factor $1/(1 - k)$. Heavy particles instead would slowly

gain or slowly loose energy according to whether their initial energy is above or below the injection threshold. They would, however, have a shorter lifetime than protons because of the presumably larger destruction cross section. Their number should be approximately equal to the number injected during their lifetime.

One should remark in this connection that a consequence of the present theory is that the energy spectrum of the heavy nuclei of the cosmic radiation should be quite different from the spectrum of the protons, since the absorption cross section for a heavy particle is presumably several times larger than that of a proton. One would expect, therefore, that the average age of a heavy particle is shorter than the age of a proton, which leads to an energy spectrum decreasing much more rapidly with energy for a heavy particle than it does for protons. An experimental check on this point should be possible.

VI. Further Discussion of the Magnetic Acceleration.

In this section the process of acceleration of the cosmic-ray protons by collision against irregularities of the magnetic field will be discussed in somewhat more detail than has been done in Section III.

The path of a fast proton in an irregular magnetic field of the type that we have assumed will be represented very closely by a spiraling motion around a line of force. Since the radius of this spiral may be of the order of 10^{12} cm, and the irregularities in the field have dimensions of the order of 10^{18} cm, the cosmic ray will perform many turns on its spiraling path before encountering an appreciably different field intensity. One finds by an elementary discussion that as the particle approaches a region where the field intensity increases, the pitch of the spiral will decrease. One finds precisely that

$$\frac{\sin^2 \vartheta}{H} \approx \text{const}, \tag{12}$$

where ϑ is the angle between the direction of the line of force and the direction of the velocity of the particle, and H is the local field intensity. As the particle approaches a region where the field intensity is larger, one will expect, therefore, that the angle ϑ increases until $\sin \vartheta$ attains the maximum possible value of one. At this point the particle is reflected back along the same line of force and spirals backwards until the next region of high field intensity is encountered. This process will be called a "Type A" reflection. If the magnetic field were static, such a reflection would not produce any change in the kinetic energy of the particle. This is not so, however, if the magnetic field is slowly variable. It may happen that a region of high field intensity moves toward the cosmic-ray particle which collides against it. In this case, the particle will gain energy in the collision. Conversely, it may happen that the region of high field intensity moves away from the particle. Since the particle is much faster, it will overtake the irregularity of the field and be reflected backwards, in this case with loss of energy. The net result will be an average gain, primarily for the reason that head-on col-

lisions are more frequent than overtaking collisions because the relative velocity is larger in the former case.

Somewhat similar processes take place when the cosmic-ray particle spirals around a curve of the line of force as outlined in fig. 1 ("Type B" reflection). Here again, the energy of the particle would not change if the magnetic field were static. On the other hand, the lines of force partake of the streaming motions of the matter, and it may happen that the line of force at the bottom of the curve moves in the direction indicated by the arrow *a*, or that it moves in the direction indicated by the arrow *b*. In the former case there will be an energy gain (head-on collision) while in case *b* (overtaking collision) there will be an energy loss. Gain and loss, however, do not average out completely, because also in this case a head-on collision is slightly more probable than an overtaking collision due to the greater relative velocity.

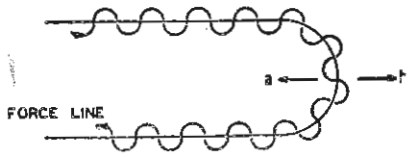

Fig. 1. – Type B reflection of a cosmic-ray particle.

The amount of energy gained or lost in a collision of the two types described can be estimated with a simple argument of special relativity, without any reference to the detailed mechanism of the collision. In the frame of reference in which the perturbation of the field against which the collision takes place is at rest, there is no change of energy of the particle. The change of energy in the rest frame of reference is obtained, therefore, by first transforming initial energy and momentum from the rest frame to the frame of the moving perturbation. In this frame an elastic collision takes place whereby the momentum changes direction and the energy remains unchanged. Transforming back to the frame of reference at rest, one obtains the final values of energy and momentum. This procedure applied to a head-on collision, gives the following result,

$$\frac{w'}{w} = \frac{1 + 2\,B\beta\cos\vartheta + B^2}{1 - B^2}, \tag{13}$$

where βc is the velocity of the particle, ϑ is the angle of inclination of the spiral, and Bc is the velocity of the perturbation. It is assumed that the collision is such as to produce a complete reversal of the spiraling direction by either of the two mechanisms outlined previously. For an overtaking collision, one finds a similar formula except that the sign of B must be changed. We now average the results of head-on and overtaking collisions, taking into account that the probabilities of these two types of events are proportional to the relative velocities and are given therefore by $(\beta\cos\vartheta + B)/2\,\beta\cos\vartheta$ for a head-on collision and $(\beta\cos\vartheta - B)/2\,\beta\cos\vartheta$ for an overtaking collision. The result for the average of $\log(w'/w)$ up to terms of the order of B^2 is:

$$\langle\log(w'/w)\rangle_{Av} = 4\,B^2 - 2\,B^2\,\beta^2\cos^2\vartheta \tag{14}$$

which confirms the order of magnitude for the average gain of energy adopted in Section III.

As a result of the extreme complication of the magnetic field and of its motion, it does not appear practical to attempt an estimate by more than the order of magnitude.

One might expect that after a relatively short time the angle ϑ will be reduced to a fairly low value so that Type A reflections will become infrequent. This is due to the fact that when ϑ is large, fairly large increases in energy and decreases of ϑ may occur, if the particle should be caught between two regions of high field moving against each other along a force line. One can prove that Type B reflections change gradually and rather slowly the average pitch of the spiral. It appears, therefore, that except for the beginning of the acceleration processes the Type A will not give as large a contribution as one otherwise might expect.

VII. Estimate of the Injection Energy.

Acceleration of a cosmic-ray particle will not be possible unless the energy gain is greater than the ionization loss. Since this last is very large for protons of low velocity, only protons above a certain energy threshold will be accelerated. In Section III a value of 200 Mev for this "injection energy" has been given; a justification for this assumed value will be given now. In estimating the injection energy we will assume that the particle, during its acceleration, finds itself both inside relatively dense clouds and in the more dilute material outside of the clouds for lengths of time proportional to the volumes of these two regions. The ionization loss will be due, therefore, to a material of an average density equal to the average density of the interstellar matter, which has been assumed to be 10^{-24} g/cm^2, consisting mostly of hydrogen. In Table I the energy loss per g/cm^2 of material traversed is given as a function of the energy of the proton. In the third column of the table the corresponding energy gain is given. It is seen that the loss exceeds the gain for particles of energy less than about 200 Mev, as has been stated.

Table I.

Energy loss per g/cm^2 *of material traversed.*

Energy	Loss/gr cm^{-2}	Gain/gr cm^{-2}
10^7 ev	94×10^6 ev	7.8×10^6 ev
10^8	15×10^6	8.6×10^6
10^9	4.6×10^6	16.1×10^6
10^{10}	4.6×10^6	91×10^6

A similar estimate yields for the acceleration of α–particles an injection energy of about 1 Bev, for the acceleration of oxygen nuclei the initial energy required is about 20 Bev, and for an iron nucleus it would amount to about 300 Bev. As already stated, it does not appear probable that the heavy nuclei found in the cosmic radiation are accelerated by the process here described, unless they should originate at some place in the galaxy where the interstellar material is extremely dilute.

I would like to acknowledge the help that I had from several discussions with E. Teller on the relative merits of the two opposing views that we are presenting. I learned many facts on cosmic magnetism from a discussion with H. Alfvén, on the occasion of his recent visit to Chicago. The views that he expressed then were quite material in influencing my own ideas on the subject.

N° 238.

For the introduction to this paper see paper N° 237.

238.

AN HYPOTHESIS ON THE ORIGIN OF THE COSMIC RADIATION

« Nuovo Cimento », Suppl. 317–323 (1949).

Cosmic rays are more and more being recognised as a phenomenon of cosmic importance. As an introduction I would like to give a few figures that stress this importance. We know the intensity of the cosmic radiation that comes from the outside into the atmosphere. The number of particles with an energy of the order of or greater than four billions of electron volt is about 0.1 particles per square centimetre per steradian per second. From this figure we can estimate the energy present per cm^3 in the form of cosmic rays of over 4 Gev. One finds $6 \cdot 10^{-13}$ erg/cm^3.

Very probably, particles of lower energy are also present and may be cut of by magnetic field action, perhaps by the magnetic field of the sun. By a rather uncertain estimate one may be led to increase the previous figure by a factor 3. The cosmic rays represent therefore an energy density of $22 \cdot 10^{-12}$ erg/cm^3. This energy should be compared with other astronomical or cosmic energies.

If one assumes that radiation with this average density occupies all the interstellar space of the galaxy, one obtains the result that the overall energy of the cosmic radiation is of the same order of magnitude as the kinetic energy of the disordered motions of the stars. The amount of energy is so large that one might legitimately doubt whether or not it is possible to find a mechanism capable of producing cosmic radiation in such a staggering amount. For this reason Teller has recently proposed a "Non-Cosmic Theory" of the cosmic radiation by assuming that the cosmic radiation instead of extending to the insterstellar space is confined to the immediate vicinity of the sun. This hypothesis was later developed by Teller, Richtmyer and Alfvén.

I will not discuss it now because I believe that Prof. Alfvén will do so next, and I will not even discuss the hypothesis considered in Bagge's report concerning a possible stellar origin of the cosmic radiation. I would like

instead to discuss a different possibility according to which cosmic rays acquire most of their energy while travelling through space.

I want to assume: first, that the cosmic radiation is a galactic phenomenon, whereby I mean that the cosmic radiation fills with more or less uniform energy distribution all the space of our galaxy. This assumption requires a mechanism capable of holding the cosmic ray particles within the galaxy. It has been often assumed that this may be due to a galactic magnetic field with closed in lines of force. Before making further assumptions, I would like to investigate what one can deduce from this hypothesis.

Our galaxy comprises stars and matter. The diffuse matter has an average density of about 10^{-24} g/cm^3, a figure easy to remember because it corresponds approximately to one hydrogen atom per cm^3. A simple calculation shows that the probability of collision of a cosmic ray against a star is extremely small. However, the probability that the cosmic ray particle may have a nuclear collision is not at all negligible. Indeed, we can make a crude estimate of this probability as follows: We know directly from cosmic ray experiments that when cosmic ray particles enter from the outside into the earth's atmosphere they soon collide with air nuclei. The mean free path for this collision is of the order of magnitude of one hundred grams per cm^2. Since the density is 10^{-24}, the corresponding mean free path for a cosmic ray particle travelling through the galaxy will be about 10^{26} cm. Since the particle travels with almost the velocity of light, the time taken for traversing this distance will be $10^{26}/3 \cdot 10^{10} = 3 \cdot 10^{15}$ sec $= 10^8$ years. In the following calculations I have used slightly different figures yielding:

$$T = 7 \cdot 10^7 \text{ years}, \tag{1}$$

for the average time that a cosmic ray particle travels before a nuclear collision happens that effectively destroys it.

This time is rather short compared to the age of the universe estimated to be two or three billion years. We are therefore led to the conclusion that only very few of the cosmic ray particles that we now observe can be as old as the galaxy. It seems necessary, therefore, to assume the existence of a mechanism that continuously produces new cosmic ray particles.

Without discussing yet what this mechanism may be, we want to introduce as a second assumption that the production is uniform in time. Since a particle has a mean life of 70 million years, its probability of survival after a time, t, will be

$$\exp\left(\frac{-t}{T}\right). \tag{2}$$

This expression gives the age distribution law of the particles that are now in existence.

One can now make two alternate assumptions: one is that the cosmic radiation particles are originally produced with a energy equal to or higher than their present energy. The other one is that the cosmic ray particles are originally produced at a relatively low energy and are gradually accelerated. In what follows we shall take this second point of view which has the advan-

tage to require an injection mechanism less powerful than the one that would be required for the first assumption.

We assume, therefore, the existence of an accelerating process whereby the energy of a particle gradually increases as its age increases and is a function of the age. The dependence of the energy upon the age may then be determined from the knowledge of the energy distribution of the cosmic radiation. The experimentally known energy distribution of cosmic ray particles is rather complicated at low energies but takes the form of a simple power law for energies above a few Gev. We will assume this simplified law:

$$I(E)\,dE = kE^{-2.9}\,dE. \tag{3}$$

the exponent 2.9 is chosen to fit the observations.

We have assumed that the energy of a particle is a function of its age, t

$$E = f(t) \tag{4}$$

From the knowledge of the age distribution (2), and the energy distribution (3), one can determine $f(t)$. Indeed, the number of particles with age between t and $t + dt$ is proportional to $\exp\left[\frac{-t}{T}\right] dt$, and the number of particles with energy between E and E + dE is proportional to

$$\frac{dE}{E^{2.9}} = \frac{df}{f^{2.9}}$$

we find, therefore,

$$\frac{df}{f^{2.9}} = a \exp\left[\frac{-t}{T}\right], \tag{5}$$

where a is a proportional constant. Integration yields

$$\frac{1}{1.9 f^{1.9}} = \frac{a}{T} \exp\left[\frac{-t}{T}\right], \tag{6}$$

where the integration constant has been set to equal zero because for large t, f becomes infinite. This equation can be rewritten in the form:

$$f(t) = E_0 \exp\left[\frac{t}{(1.9\,T)}\right], \tag{7}$$

where E_0 is a new constant that represents the initial energy of the particle. From our assumptions follows a very specific law (7) whereby the energy of the cosmic ray particles must increase with time. According to (7), the energy must increase every year by a fraction of about 10^{-8} of its value, so for a proton with energy equal to its rest energy, the energy will increase at the rate of about only 10 ev per year and will increase correspondingly faster for protons of higher energy. It is clear, however, that in any case the rate of increase of the energy will be quite slow since it takes about 100 million years to double the initial value of the energy.

A very simple process that leads to the acceleration law (7), is due to the collision against large moving objects. Without specifying yet what particular objects will be considered as likely obstacles against which the collisions take place, we want to assume that a cosmic ray frequently collides against large moving obstacles. That the energy of the cosmic ray will

on the average increase in such collisions is clear from the fact that ultimately statistical equilibrium would be established with equipartition of energy between the obstacles and the cosmic ray particles. This corresponds, of course, to an extremely high energy very many orders of magnitude beyond the maximum energy observed in cosmic rays. What limits the efficiency of this process in increasing the energy of the cosmic ray particles is, therefore, not the maximum energy attainable which is effectively infinite, but rather the rate at which the energy is transmitted.

Not all collisions will accelerate the particle. Actually, head-on collisions will produce an acceleration and over-taking collisions will produce a deceleration. On the average, there is acceleration primarily because head-on collisions are somewhat more probable than over-taking collisions since the relative velocity is larger in the former case. One can compute in an elementary way the order of magnitude of the average increase, δE, per collision of a particle of energy E (including rest energy) colliding against objects moving with velocity, V. The result is:

$$\delta E \sim \frac{E V^2}{c^2} . \tag{8}$$

If we assume that the collision cross-section is independent of the energy, the number of collisions per unit time will also be approximately independent of the energy since the velocity of the cosmic ray particles is practically constant and equal to c. It follows from (8) that the gain in energy per unit time is proportional to the energy. The energy therefore increases according to an exponential law.

We shall take V of the order of 30 km/sec. This gives (8) $\delta E \sim 10^{-8} E$. That is again an average gain of energy per collision of one part in 10^8.

After N collisions the energy will be:

$$E = E_0 \exp [N B^2] , \tag{9}$$

where

$$B^2 = \frac{V^2}{c^2} = 10^{-8} .$$

In order to estimate the number of collisions, we introduce a scattering mean free path λ. The number of collisions after a time, t, since the initiation of the process will be $N = \frac{ct}{\lambda}$, since the particle travels practically at the velocity of light. Consequently we get:

$$E = E_0 \exp \left[\frac{ct B^2}{\lambda} \right] . \tag{10}$$

Comparing (10) with (7) one obtains

$$\lambda = 1.9 B^2 cT \sim 10^{18} \text{ cm} = 1 \text{ light year.} \tag{11}$$

We will now further specialize our assumptions and introduce the hypothesis that the collisions responsible for the increase in energy are against moving irregularities in a cosmic magnetic field.

The idea of the existence of such a moving magnetic field is due to Dr. Alfvén who has made a thorough magneto hydro-dynamic study of the influence that the extremely tenuous interstellar matter has on the propagation of a magnetic field that penetrates it.

Unfortunately, I do not have the time to explain in detail his very stimulating ideas on this subject. I shall only mention that due to the relatively high electrical conductivity of the interstellar medium, the lines of force are practically attached to the matter so that they are dragged by the turbulent motion of the interstellar matter. A cosmic ray particle will be deflected by the action of the magnetic field and will gain energy in the process as previously discussed. In order to obtain agreement with the experimentally observed spectrum, we must assume that the size of the minimum vortices which drag the lines of force is of the order of one light year, a value which does not appear implausible.

Nothing has been said so far of the injection mechanism of the particles of relatively low energy which will be further accelerated by the proposed method. In order that a particle so injected may eventually become an energetic cosmic ray, it is necessary that its initial energy be above a certain limit which will be called the injection threshold. Indeed, the accelerating mechanism will function only when the energy gained by the accelerating mechanism is greater that the energy lost by ionization. An estimate of the injection threshold yields for various particles the following values:

Protons	–	100 Mev
α Particles	–	1 Gev
Oxygen nuclei	–	1 Gev per nucleon
Iron nuclei	–	5 Gev per nucleon

It is seen that the injection threshold is quite large for heavy nuclei and this represents the most serious difficulty for the proposed theory. Even without special assumption as to the origin of the initial protons and α particles the injection of these light components of the cosmic radiation may be understood perhaps as due to the collisions of the cosmic radiation itself with the nuclei of the interstellar matter. From this point of view, cosmic radiation would be a self regenerating process.

No such simple explanation, however, seems adequate for the injection of heavier nuclei like, for instance, oxygen or iron, since no known mechanism could yield an iron nucleus with 5 Gev per nucleon without destroying the nucleus itself. One must assume, therefore, a special injection mechanism for these particles, perhaps like the one suggested recently by Spitzer [1].

In conclusion, the proposed theory seems to be quite adequate for understanding the main features of the proton components of the cosmic radiation and perhaps also of the α particle component. It does not seem adequate to understand the presence in the cosmic radiation of a significant fraction of heavier nuclei. If the general features of the present theory should prove correct, there should be an independent and very powerful injection mechanism, of the heavy component of the cosmic radiation.

BIBLIOGRAPHY.

1] LYMAN SPITZER, Jr., « Phys. Rev. », *76*, 583 (1949).

DISCUSSIONE E OSSERVAZIONI.

E. BAGGE, *Hamburg*:

Bei dem von Fermi diskutierten Mechanismus für die Beschleunigung und Aufsammlung der Höhenstrahlungsteilchen innerhalb der Milchstrasse scheint es wichtig zu sein, die Frage zu diskutieren, welcher Teil kosmischer Strahlung an der Oberfläche des galaktischen Systems in den Weltraum hinauswandert. Da das von Fermi postulierte galaktische Magnetfeld grosse räumliche Schwankungen besitzen muss, wenn der Beschleunigungsprozess überhaupt wirksam werden soll, wird es unter anderem auch nahezu feldfreie Bereiche geben und dies kann besonders an den Randbereichen der Milchstrasse das Entweichen der Höhenstrahlungsteilchen ermöglichen.

E. FERMI, *Chicago*:

In order to avoid a large loss of particles out of the boundaries of the galaxy it is sufficient to assume that the lines of force are closed or at least that very few of them escape to the outer space.

L. JANOSSY, *Dublin*:

The injection process of protons is helped by the circumstance that a nucleon colliding with a nucleus is likely to retain an appreciable fraction of its energy and thus remain very much above the injection energy. The question is raised whether heavy fragments arising out of nuclear collisions can serve to inject heavier nuclei.

E. FERMI, *Chicago*:

Naturally I hope that you are right. On the other hand it seems to me very difficult to understand the fact from the theoretical point of view. But, of course, if the fact should prove to be true it will have some theoretical explanation.

N° 239.

At the end of the Second World War Fermi joined the University of Chicago, in the physics department and in the newly established Institute for Nuclear Studies (which now bears his name). That was the time when academic research work and graduate teaching were being resumed in the universities, and students, delayed by the war, thronged back to the campus. The University of Chicago had a particularly large enrollment of graduate students of physics. How many of them were attracted to Chicago by the name of Fermi we probably shall never know. In the case of myself, who was one of them, it had been my determination, in coming to the U. S. from China in November 1945, to study with Fermi or with Wigner. But I knew that war work had taken them from their universities. I remember that one day, soon after my arrival in New York, I trudged uptown and went up to the eighth floor of Pupin to inquire whether Professor Fermi would be giving courses soon. The secretaries met me with totally blank faces. I then went to Princeton, and found to my deep despair that Wigner would be mostly unavailable to students for the next year. But in Princeton I learned through W. Y. Chang that there were rumors of a new Institute to be established at Chicago and that Fermi would join the Institute. I went to Chicago, registered at the University, but did not feel completely secure until I saw Fermi with my own eyes, when he began his lectures in January 1946.

As is well known, Fermi gave extremely lucid lectures. In a fashion that is characteristic of him, for each topic he always started from the beginning, treated simple examples and avoided as much as possible " formalisms ". (He used to joke that complicated formalism was for the " high priests "). The very simplicity of his reasoning conveyed the impression of effortlessness. But this impression is false: The simplicity was the result of careful preparation and of deliberate weighing of different alternatives of presentation. In the spring of 1949 when Fermi was giving a course on Nuclear Physics (which was later written up by Orear, Rosenfeld and Schluter and published as a book), he had to be away from Chicago for a few days. He asked me to take over for one lecture and gave me a small notebook in which he had carefully prepared each lecture in great detail. He went over the lecture with me before going away, explaining the reasons behind each particular line of presentation.

It was Fermi's habit to give, once or twice a week, informal unprepared lectures to a small group of graduate students. The group gathered in his office and someone, either Fermi himself or one of the students, would propose a specific topic for discussion. Fermi would search through his carefully indexed notebooks to find his notes on the topic and would then present it to us. I still have the notes I took of his evening lectures during October 1946—July 1947. It covered the following topics in the original order: theory of the internal constitution and the evolution of stars, structure of the white dwarfs, Gamow-Schönberg's idea about supernovae (neutrino cooling due to electron capture by nuclei), Riemannian geometry, general relativity and cosmology, Thomas-Fermi model, the state of matter at very high temperatures and densities, Thomas factor of 2, scattering of neutrons by para and ortho hydrogen, synchrotron radiation, Zeeman effect, " Johnson effect " of noise in circuits, Bose-Einstein condensation, multiple periodic system and Bohr's quantum condition, Born-Infeld theory of elementary particles, brief description of the foundation of statistical mechanics, slowing down of mesons in matter, slowing down of neutrons in matter. The discussions were kept at an elementary level. The emphasis was always on the essential and the practical part of the topic; the approach was almost always intuitive and geometrical, rather than analytic.

The fact that Fermi had kept over the years detailed notes on diverse subjects in physics, ranging from the purely theoretical to the purely experimental, from such simple problems

as the best coordinates to use for the three-body problem to such deep subjects as general relativity, was an important lesson to all of us. We learned that *that* was physics. We learned that physics should not be a specialist's subject, physics is to be built from the ground up, brick, by brick, layer by layer. We learned that abstractions come *after* detailed foundation work, not before. We also learned in these lectures of Fermi's delight in, rather than aversion to, simple numerical computations with a desk computer.

Besides the formal and informal classes Fermi also devoted almost all of his lunch hours to the graduate students (at least that was the state of affairs before 1950). The conversations in these lunch hours naturally covered a wide range of subjects. We observed Fermi as a somewhat conservative man with a very independent mind. We observed his dislike of pretension of whatever kind. Sometimes he would give general advice to us about our research work. I remember his emphasizing that as a young man one should devote most of one's time attacking simple practical problems rather than deep fundamental ones.

Paper N° 239 was written by Fermi and me in the summer of 1949. As explicitly stated in the paper, we did not really have any illusions that what we suggested may actually correspond to reality. In fact, I was inclined to bury the work in notebooks and not publish it at all. Fermi said, however, that as a student one solves problems, but as a research worker one raises questions; and he considered the question we raised as worthy of publication. I may add here that the question remains unsolved today (1963).

As remarked by Segrè in his introduction to this collected works of Fermi, a very important question which Fermi had helped to raise was the spin orbit interaction in the shell model of nuclei; [See M. G. Mayer, « Phys. Rev. » *75*, 1969 (1949), acknowledgement at end of paper]. Another question that Fermi was the first to raise was the concept of the conservation of nucleons. [See C. N. Yang and J. Tiomno, « Phys. Rev. », *79*, 495 (1950), footnote 12]. I may also mention that Fermi was always very much interested in the question of parity conservation. [See the *Proceedings of the International Conference on Nuclear Physics and the Physics of Elementary Particles*, edited by J. Orear, A. H. Rosenfeld and R.A. Schluter, The Institute for Nuclear Studies, The University of Chicago, 1951, p. 2 and p. 109]. (See paper N° 245).

Fermi fell critically ill in the fall of 1954. Murray Gell-Mann, who was then at Columbia University, and I went to Chicago to see him in Billings Hospital. As we entered his room he was reading a book which was a collection of stories about men who by their will power succeeded in overcoming fantastic natural obstacles and misfortune. He was very thin, but only a little sad. He told us very calmly about his conditions. The doctors had said that in a few days he may go home, but he would not have more than months to live. He then showed us the notebook by his bedside, and said that it was his own notes on nuclear physics. He planned, when he left the hospital, in the two months' time left, to revise it for publication. Gell-Mann and I were so overwhelmed by his simple determination and his devotion to physics that we were afraid for a few moments to look into his face. (Fermi died within three weeks of our visit).

It has been said that the length of a man's life should not be measured in years, but in the different careers that he successfully goes through. Enrico Fermi, in one of his many careers, as a teacher in Chicago, had directly and indirectly influenced so many physicists of my generation that the record speaks for itself. The following is a list of the names of some of the physicists who received their graduate education in Chicago in the years 1946–1949. (I left Chicago in 1949 and am not familiar with Fermi's later students): H. M. Agnew, H. V. Argo, O. Chamberlain, G. F. Chew, G. W. Farwell, R. L. Garwin, M. L. Goldberger, D. Lazarus, T. D. Lee, A. Morrish, J. R. Reitz, M. N. Rosenbluth, W. Selove, J. Steinberger, R. M. Sternheimer, S. Warshaw, A. Wattenberg, L. Wolfenstein, H. A. Wilcox, C. N. Yang.

C. N. YANG.

239.

ARE MESONS ELEMENTARY PARTICLES?

E. FERMI and C. N. YANG (*)
Institute for Nuclear Studies, Univeristy of Chicago, Chicago, Illinois
(Received August 24, 1949)
« Phys. Rev. », *76*, 1739 (1949).

The hypothesis that π–mesons may be composite particles formed by the association of a nucleon with an anti-nucleon is discussed. From an extremely crude discussion of the model it appears that such a meson would have in most respects properties similar to those of the meson of the Yukawa theory.

I. INTRODUCTION.

In recent years several new particles have been discovered which are currently assumed to be "elementary," that is, essentially, structureless. The probability that all such particles should be really elementary becomes less and less as their number increases.

It is by no means certain that nucleons, mesons, electrons, neutrinos are all elementary particles and it could be that at least some of the failures of the present theories may be due to disregarding the possibility that some of them may have a complex structure. Unfortunately, we have no clue to decide whether this is true, much less to find out what particles are simple and what particles are complex. In what follows we will try to work out in some detail a special example more as an illustration of a possible program of the theory of particles, than in the hope that what we suggest may actually correspond to reality.

We propose to discuss the hypothesis that the π–meson may not be elementary, but may be a composite particle formed by the association of a nucleon and an anti-nucleon. The first assumption will be, therefore, that both an anti-proton and an anti-neutron exist, having the same relationship to the proton and the neutron, as the electron to the positron. Although this is an assumption that goes beyond what is known experimentally, we do not view it as a very revolutionary one. We must assume, further, that between a nucleon and an anti-nucleon strong attractive forces exist, capable of binding the two particles together. We assume that the π–meson is a pair of nucleon and anti-nucleon bound in this way. Since the mass of the π–meson is much smaller than twice the mass of a nucleon, it is necessary to assume that the binding energy is so great that its mass equivalent is equal

(*) Now at the Institute for Advanced Study. Princeton, New Jersey.

to the difference between twice the mass of the nucleon and the mass of the meson.

According to this view the positive meson would be the association of a proton and an anti-neutron and the negative meson would be the association of an anti-proton and a neutron. As a model of a neutral meson one could take either a pair of a neutron and an anti-neutron, or of a proton and an anti-proton.

It would be difficult to set up a not too complicated scheme of forces between a nucleon and an anti-nucleon, without about equally strong forces between two ordinary nucleons. These last forces, however, would be quite different from the ordinary nuclear forces, because they would have much greater energy and much shorter range. The reason why no experimental indication of them has been observed for ordinary nucleons may be explained by the assumption that the forces could be attractive between a nucleon and an anti-nucleon and repulsive between two ordinary nucleons. If this is the case, no bound system of two ordinary nucleons would result out of this particular type of interaction. Because of the short range very little would be noticed of such forces even in scattering phenomena.

Ordinary nuclear forces from the point of view of this theory will be discussed below.

Unfortunately we have not succeeded in working out a satisfactory relativistically invariant theory of nucleons among which such attractive forces act. For this reason all the conclusion that will be presented will be extremely tentative. It would be undesirable to assume that the attraction is due to a special field of force since in this case the quanta of this new field would be themselves new elementary particles which is just what we hope to be able to avoid. Therefore, only forces of zero range appear compatible with relativistic invariance. In Section II the attempt will be discussed to represent the interaction by a term of the fourth degree in the amplitudes of the nucleon fields. We do not know whether this attempt can be made mathematically self-consistent and we have not succeeded in finding a way to treat it, except by the most crude approximation. The main difficulty is that no stationary state exists with one pair of nucleons only, but only mixed states with one pair, two pairs and many pairs. In our simplified discussion we have neglected this important factor, and treated the problem of a nucleon and an anti-nucleon alone. Assuming hopefully that these mathematical difficulties can be overcome, we have investigated the symmetry properties of the quantum states of the system of a nucleon and an anti-nucleon, in particular for the states of total angular momentum zero, ${}^1S_0$ and ${}^3P_0$. The former of these two states corresponds to a pseudoscalar meson and the latter to a scalar meson. If the ground state of the two-nucleon system had a resultant angular momentum 1, one could get in a similar way a model of the vector meson.

A peculiarity of the wave functions of the meson is that they decrease extremely rapidly with the distance between the two nucleons, so that the dimensions of the meson appear to be of the order of magnitude of the Compton wave-length of the nucleon, which is roughly 1/10 of the classical electron

radius. This feature may make the experimental detection of the complex nature of the meson extremely difficult.

In the Yukawa theory of nuclear forces it is postulated that virtual mesons are continuously created and re-absorbed in the vicinity of a nucleon. When two nucleons are close to each other, the process of absorption by one nucleon of the virtual meson originated by the other is responsible for the nuclear forces. According to the present view, the main features of this theory can be kept even when the assumption that the meson is an elementary particle is dropped.

One finds that in the vicinity of an isolated nucleon there is a tendency to pair formation of nucleons and anti-nucleons, which will be predominantly formed in the bound state, that is as π–mesons, because such bound states are energetically much lower. From this point on, the Yukawa theory can be taken over almost unchanged as a description of the mechanism of nuclear forces (see Section III).

If the program that has been outlined could be carried out in a mathematically satisfactory way, one might hope to be able eventually to establish a relationship between the strength of the ordinary nuclear forces and the meson mass. Indeed, the difference between the mass of two nucleons and the mass of the meson is the binding energy of the nucleon and the anti-nucleon system. In a consistent theory, therefore, the strength of the coupling term between a nucleon and an anti-nucleon should be adjusted to give the correct value for this binding energy. On the other hand, it is this same coupling which is responsible for the creation of virtual mesons near a nucleon and determines, therefore, the strength of the ordinary nuclear forces. In Section III an estimate of the nuclear forces, calculated as far as is possible according to this program, is given. Considering the extremely primitive mathematical means used; the agreement is not worse than what might be expected.

II. Mesons as Bound States of a Nucleon and an Anti-Nucleon.

We proceed now to discuss the mathematical formalism needed in order to carry out the outlined program.

For this it is necessary to introduce attractive forces between a nucleon and an anti-nucleon capable of binding the two particles together into what we assume to be a meson.

As long as no requirements of relativistic invariance are introduced, this could be done merely by postulating an interaction potential of suitable depth and range. It is useful for what follows to formulate this in the language of the field theory as follows: Two types of particles, for example, protons and anti-neutrons, are described neglecting spin and relativity by two fields, P and A. It is convenient to use here these letters rather than the more usual ψ_P and ψ_A. The following Hamiltonian can be assumed in order to include the attractive potential:

$$(1)\quad \frac{\hbar^2}{2M}\int \nabla P^* \nabla P d^3\boldsymbol{r} + \frac{\hbar^2}{2M}\int \nabla A^* \nabla A d^3\boldsymbol{r} - \iint P^{*\prime} P' A^{*\prime\prime} A'' V(|\boldsymbol{r}' - \boldsymbol{r}''|) d^3\boldsymbol{r}' d^3\boldsymbol{r}''.$$

The first two terms are the kinetic energy of protons and anti-neutrons and the last term introduces the interaction. In this non-relativistic case, states with one proton and one anti-neutron do not mix with any other states. One can therefore confine one's attention to such states only and it is well known that the Hamiltonian (1) is then completely equivalent to that of a two-particle problem with an interaction $V(|\boldsymbol{r}' - \boldsymbol{r}''|)$.

Unfortunately no such simple situation obtains for relativistic particles in the hole theory. There are two reasons for this. One is that two-particle states mix with states in which additional pairs of particles form. The second is that only zero range forces can be used relativistically without adding an essentially new force field. For zero range forces no bound two-particle solution exists.

Since neutrons and anti-neutrons are symmetrical particles, it is immaterial whether we call the anti-neutrons "holes" in a negative neutron sea or vice versa. Since we are interested primarily in an interaction between protons and anti-neutrons, the second alternative is preferable.

The simplest relativistically invariant interactions between these two fields are the usual [1] five types: [2]

$$(2)\qquad \begin{cases} \int A^* \beta A P^* \beta P \, d^3\boldsymbol{r} & \text{(Scalar)} \\ \int \{A^* A P^* P - A^* \alpha A \cdot P^* \alpha P\} \, d^3\boldsymbol{r} & \text{(Vector)} \\ \int \{A^* \beta\sigma A \cdot P^* \beta\sigma P + A^* \beta\alpha A \cdot P^* \beta\alpha P\} \, d^3\boldsymbol{r} & \text{(Tensor)} \\ \int \{A^* \sigma A \cdot P^* \sigma P - A^* \gamma_5 A P^* \gamma_5 P\} \, d^3\boldsymbol{r} & \text{(Pseudovector)} \\ \int A^* \beta\gamma_5 A P^* \beta\gamma_5 P \, d^3\boldsymbol{r} & \text{(Pseudoscalar).} \end{cases}$$

The vector interaction in (2), like the Coulomb forces, has opposite signs for the interaction between a proton and a neutron and between a proton and an anti-neutron. It turns out that the tensor interaction also has this property while the scalar, pseudovector and pseudoscalar interactions have the same sign for a proton-neutron pair and a proton-anti-neutron pair.

As explained in the introduction, one needs an interaction that is attractive for a proton-anti-neutron pair and repulsive for a proton-neutron pair.

(1) These are very similar to the interactions used in β–decay theory. See, e.g., H. A. BETHE, « Rev. Mod. Phys. », *8*, 82 (1936). We use the same notation as Bethe's for α–, β–, and γ–matrices.

(2) In the hole theory to make the vacuum expectation value of these interactions zero one needs actually to subtract from (2) certain terms. For example the correct scalar interaction to take is:

$$\int [N^* \beta N - \langle N^* \beta N \rangle_{\text{vac}}] \, [P^* \beta P - \langle P^* \beta P \rangle_{\text{vac}}] \, d^3\boldsymbol{r},$$

where $\langle \ \rangle_{\text{vac}}$ means vacuum expectation value.

Thus the vector and tensor interactions in (2) are the possible choices. For definiteness we shall take in what follows the vector interaction and write:

$$H^{int} = G\int \{A^* A P^* P - A^* \alpha A P^* \alpha P\}\, d^3r. \tag{3}$$

This Hamiltonian represents a δ–function interaction between a proton and an anti-neutron. Indeed, (3) may be written:

$$H^{int} = G\iint A^{*\prime} P^{*\prime\prime} \times [\delta(r' - r'')(1 - \alpha_A \alpha_P)]\, A' P''\, d^3r'\, d^3r''. \tag{4}$$

It has proved impossible to solve exactly the interaction problem of a proton and an anti-neutron to yield the "meson" bound state. We had to limit ourselves to the extremely crude description in terms of two-particle states only, disregarding thereby the complications due to multiple pair creation.

The following qualitative argument leads us to believe that this approximate description may be fairly good when the two particles are relatively far from each other and may break down when they are close. For a proton-anti-neutron state the unperturbed energy is larger than the actual energy by a little bit less than $2Mc^2$. For a state with an additional pair (two-pairs state), the energy difference [3] is $4Mc^2$, for an N–pairs state, $2NMc^2$. One might expect that an N–pair state will last a time of the order of $\hbar/2NMc^2$ during which the particles can move away about $\hbar/2NMc$. We expect, therefore, nucleons to be found away from the center up to about this distance. As N increases such configurations will become smaller and smaller. As a confirmation of this qualitative argument we find that actually for the two-nucleon state the wave function depends on the distance approximately as $\exp(-Mcr/\hbar)$.

We have attempted therefore to regard the effect of multiple pairs as perturbing the near parts of the single pair wave function as if the δ–function interaction were smeared over a region of dimensions about $\hbar/Mc$. This procedure is not relativistically invariant and should be substituted by a correct multiple-pairs theory. In lack of this we propose to follow up the two-particle theory assuming instead of the contact interaction one of range $\hbar/Mc$. The interaction will be modified accordingly by introducing instead of $G\delta(r' - r'')$ a finite range attractive potential $-V(|r' - r''|)$. With this the interaction term becomes

$$H^{int} = -\iint A^{*\prime} P^{*\prime\prime} V(r)(1 - \alpha_A \cdot \alpha_P) A' P''\, d^3r'\, d^3r''. \tag{5}$$

For simplicity we will take for V a step function

$$\begin{cases} V(r) = 0 & \text{for } r > \hbar/Mc \\ V(r) = V_0 = \text{constant} & \text{for } r < \hbar/Mc, \end{cases} \tag{6}$$

where

$$r = |r' - r''| \quad , \quad r = r'' - r'.$$

(3) See, however, Section III, especially footnote 5.

We now adopt the two-particle approximation whereby the Schrödinger function will be a function of the spin and positional coordinates of the proton and the anti-neutron. The two spin indices running from 1 to 4 each yield a 16–component wave function. For states of zero total momentum each of the 16 components will depend only on the relative position $\boldsymbol{r}$.

The Schrödinger equation is:

$$\{-chi\,(\alpha_P-\alpha_A)\cdot\Delta+Mc^2\beta_A+Mc^2\beta_P-V(r)(1-\alpha_A\cdot\alpha_P)\}\,\psi=E\psi.$$

It is convenient to arrange the 16 compoents of ψ into a 4×4 matrix with the proton spin index vertical and the anti-neutron index horizontal.

For a $^1S_0$ state the rotational invariance specifies the dependence of the 16 components on the angular variables as follows:

$$(7)\qquad \psi(^1S_0)=\begin{vmatrix} 0 & -if_1 & \frac{f_2}{r}(-x+iy) & \frac{f_2}{r}z \\ if_1 & 0 & \frac{f_2}{r}z & \frac{f_2}{r}(x+iy) \\ \frac{f_3}{r}(-x+iy) & \frac{f_3}{r}z & 0 & -if_4 \\ \frac{f_3}{r}z & \frac{f_3}{r}(x+iy) & if_4 & 0 \end{vmatrix},$$

where f_1, f_2, f_3 and f_4 are functions of the distance r only. The other state of total angular momentum zero, namely, $^3P_0$, has a wave function similar *in form* to (7) in which, however, the first and second rows are interchanged with the third and fourth rows. The $^1S_0$ state yields a particle that behaves as a pseudoscalar meson, whereas the $^3P_0$ state behaves as a scalar meson. This fact surprised us because we had thought that the opposite would be the case. The reason is connected with the different transformation properties under space reflection of the large and small components of the wave functions of a Dirac particle. No such unexpected behavior would have been found if the neutron had been treated in the sense of the hole theory as the particle and the anti-neutron as the anti-particle.

Substituting in (6) one finds for f_1, f_2, f_3, f_4 the equations:

$$(8)\qquad \begin{cases} 2\left[r\frac{d}{dr}\left(\frac{f_2}{r}\right)+3\frac{f_2}{r}\right]=\frac{-2Mc^2+E+V}{c\hbar}f_1+\frac{3V}{c\hbar}f_4 \\ \qquad\qquad =\frac{2Mc^2+E+V}{c\hbar}f_4+\frac{3V}{c\hbar}f_1, \\ \frac{d}{dr}(f_1+f_4)=-\frac{E}{c\hbar}f_2, \\ f_2=f_3. \end{cases}$$

The lowest eigenvalue must be $E=\mu c^2$, the rest energy of the meson. This condition determines [4] the depth V_0 of the potential (6). Assuming

(4) There are some undesirable solutions of (8) with energy values E that go to zero when $V_0\to0$. These solutions are discarded because they do not adiabatically approach the state of two free particles when $V_0\to0$. Also they would not appear at all if we had taken the neutron and the proton to be of different masses.

the ratio 6.45 between the proton and meson masses one finds:

$$V_0 = 26.4\,Mc^2 = 24.6\ \text{Bev}. \tag{9}$$

The corresponding normalized solution in a large volume Ω is:

$$r > r_0 = \frac{\hbar}{Mc} \begin{cases} f_1 = -\dfrac{0.236}{(r_0^3\Omega)^{1/2}}\,\dfrac{1}{u}\,e^{-u} \\ f_2 = f_3 = -\dfrac{0.218}{(r_0^3\Omega)^{1/2}}\,e^{-u}\left[\dfrac{1}{u} + \dfrac{1}{u^2}\right] \\ f_4 = \dfrac{0.202}{(r_0^3\Omega)^{1/2}}\,\dfrac{1}{u}\,e^{-u}, \end{cases} \tag{10}$$

$$r < r_0 \begin{cases} f_1 = -\dfrac{0.0136}{(r_0^3\Omega)^{1/2}}\,\dfrac{\sin v}{v} \\ f_2 = f_3 = \dfrac{0.370}{(r_0^3\Omega)^{1/2}}\left[\dfrac{\cos v}{v} - \dfrac{\sin v}{v^2}\right] \\ f_4 = -\dfrac{0.0147}{(r_0^3\Omega)^{1/2}}\,\dfrac{\sin v}{v}, \end{cases} \tag{11}$$

where

$$u = \frac{rc}{\hbar\,(M^2 - \mu^2/4)^{1/2}} \quad , \quad v = 2.03\,(r/r_0).$$

Notice that the wave function at large distances decreases like $\exp\left[-\dfrac{rc}{\hbar\,(M^2-\mu^2/4)^{1/2}}\right]$; thus the geometrical size of the meson is of the order of $\hbar/Mc$ which is the Compton wave-length of the nucleon.

The inconsistencies of this representation should be emphasized. In particular we have given arguments to prove that the two-particle description breaks down at distances $\hbar/Mc$ and this very distance turns out to be the size of the meson. One could, therefore, state that the wave function becomes reliable only where it vanishes. Our only excuse in adopting it is that we have been unable to do better.

III. Relationships with the Yukawa Theory.

In spite of the differences between the Yukawa elementary particle model of the meson and the present model, most features of the Yukawa theory can be taken over even when the meson is pictured as a proton-anti-neutron bound pair denoted briefly as (P + A).

The fundamental process of Yukawa's theory

$$P \to N + \pi^+ \tag{12}$$

now becomes

$$P \to N + (P + A). \tag{13}$$

This last process essentially is the addition to a proton P of a neutron-anti-neutron pair: N , A. Such pair formation will be induced by the postulated interaction (5). Since the energy of the bound (P + A)-system is much

lower than that of the free particles the state (13) will be formed rather than a three free-particles state. [5] The matrix element is obtained from (5) by substituting for P the wave function of the proton that disappears, for A the wave function of the anti-neutron that disappears (neutron that appears), for A'* P''* the complex conjugate of the wave function (7) of the bound proton-anti-neutron that appears. In order to express the wave function of the disappearing anti-neutron in terms of that of the neutron that is created, one uses the charge conjugation transformation

$$A = \gamma_2 \tilde{N}^*,$$

where $\sim$ means transposed and * transposed and complex conjugate.

We calculate the matrix element for a transition from a slow proton to a slow neutron and a meson at rest. The calculation is straightforward and gives the following result:

$$\int\int V(r)\, N^{*\prime}\, Q(r)\, P''\, d^3r'\, d^3r'', \tag{14}$$

where Q is the matrix

$$Q = 2i(f_1 + f_4)\,\gamma_1\gamma_2\gamma_3 + i(f_1 - f_2)\,\gamma_1\gamma_2\gamma_3\gamma_4. \tag{15}$$

If the wave-length of the proton is long compared to $\hbar/Mc$, (14) can be approximated by

$$\int N^* RP\, d^3r, \tag{16}$$

where

$$R = \int V(r)\, Q(r)\, d^3r. \tag{17}$$

Using (10), (11), and (15), and carrying out the integration one finds:

$$R = i\left(\frac{2\pi\hbar^3 c^3}{\Omega\mu c^2}\right)^{1/2}(5.3\,\gamma_1\gamma_2\gamma_3 + 0.11\,\gamma_1\gamma_2\gamma_3\gamma_4). \tag{18}$$

This expression can be compared with the conventional interaction of a pseudoscalar meson with nucleons in the Yukawa theory. [6] There are two essentially independent coupling constants: f, the so-called pseudoscalar interaction, and g, the pseudovector interaction. The nucleon-meson interaction Hamiltonian is:

$$i\int N^*\left\{f\gamma_1\gamma_2\gamma_3\varphi + \sum_\nu \frac{\hbar}{\mu c} g\gamma_1\gamma_2\gamma_3\gamma_\nu \frac{\partial\varphi}{\partial x_\nu}\right\} P d^3r \tag{19}$$

where φ is the pseudoscalar meson field.

(5) The contribution to the forces of the virtual creation of free particle pairs has been discussed in Section II. It was interpreted there as modifying the interaction only a extremely short distances (Order $\hbar/Mc$). Creation of bound pairs yields inter-nucleon forces of range $\hbar/\mu c$.

(6) See for example: G. WENTZEL, « Rev. Mod. Phys. », *19*, 1 (1947).

The corresponding matrix element for the production of a meson at rest is

$$i\frac{\hbar c}{(2\Omega\mu c^2)^{1/2}}\int N^*(f\gamma_1\gamma_2\gamma_3+g\gamma_1\gamma_2\gamma_3\gamma_4)\,P d^3\boldsymbol{r}.$$

Comparison with (18) gives

$$f=(4\pi\hbar c)^{1/2}\times 5.3 \quad , \quad g=(4\pi\hbar c)^{1/2}\times 0.11. \tag{20}$$

It has been proved by Case [7] that the terms f and g produce up to the second approximation nuclear forces of the same type. Indeed, their joint contribution is the same as would be obtained by putting $f=0$ and substituting g by

$$g'=g+f\left(\frac{\mu}{2M}\right). \tag{21}$$

We find, therefore,

$$g'=(4\pi\hbar c)^{1/2}\times 0.52$$

yielding for $g'^2/4\pi\hbar c$, that is for the analog of the fine structure constant, the value 0.27, which appears quite reasonable.

Naturally the similarity between the present point of view and the Yukawa theory can be carried on only up to a limited extent. The similarity breaks down on the one hand because of the finite size of the meson which introduces naturally a cut-off at short distances. On the other hand it breaks down for phenomena in which sufficiently high energies are involved to break up the meson.

(7) K. M. CASE, « Phys. Rev. », 76, 14 (1949).

240.

CONFERENZE DI FISICA ATOMICA

(*Fondazione Donegani*)

Accademia Nazionale dei Lincei (1950).

Nell'ottobre 1949 Enrico Fermi, accogliendo un invito rivoltogli dalla « Fondazione Donegani », tenne sei conferenze a Roma e tre a Milano sopra vari argomenti di fisica atomica, conferenze seguite con vivo interesse da un pubblico numeroso che affollava l'aula dell'Istituto fisico di Roma e la grande sala della Società Montecatini a Milano. Queste conferenze, registrate e stenografate, furono poi redatte da alcuni professori ed assistenti di Fisica delle Università di Roma e Milano; ogni conferenza reca il nome del redattore.

Nel presentare oggi al pubblico il volume contenente le dette conferenze, l'Accademia Nazionale dei Lincei, alla quale è annessa la « Fondazione Donegani », desidera rinnovare l'espressione della sua gratitudine al conferenziere illustre che, dopo undici anni di assenza, ha fatto risuonare la sua voce tra noi ed ha dimostrato il suo interesse alla giovane scuola di fisica italiana, a cui egli aveva dato il primo impulso; ringrazia la Società Montecatini che col suo munifico contributo ha permesso di attuare subito i nobili propositi a favore della scienza espressi da Guido Donegani nel suo testamento; ringrazia infine i professori e gli assistenti che con cura ed amore si sono accinti al compito non lieve di adattare alla stampa conferenze inizialmente preparate per la esposizione orale.

La nostra Accademia confida che il presente volume possa contribuire al progresso della fisica moderna nel nostro paese ed all'estero.

G. CASTELNUOVO.

PRIMA CONFERENZA (*)

LE PARTICELLE ELEMENTARI (PRIMA PARTE)

(redatta dal dott. S. SCIUTI)

Conformemente al programma che è stato concertato con la Fondazione Donegani, delle sei lezioni che terrò qui a Roma, la prima sarà di carattere piuttosto generale, mentre le altre cinque saranno di carattere alquanto specifico, dedicate particolarmente ai fisici.

(*) Tenuta il 3 ottobre 1949 nell'aula dell'Istituto Fisico dell'Università di Roma.

L'argomento che tratterò oggi riguarda « le particelle elementari ». Ma se voi mi domandaste che cosa si intenda per particella elementare, resterei imbarazzato in quanto il termine « elementare » va inteso in senso piuttosto relativo alle nostre conoscenze.

Se si fosse chiesto ai chimici o ai fisici di una cinquantina d'anni fa se l'atomo poteva considerarsi come una particella elementare, probabilmente molti di essi avrebbero risposto affermativamente, perchè allo stato delle conoscenze di allora non si conosceva la struttura dell'atomo, anzi non si sospettava nemmeno che ne potesse avere una. Poi, quando esso si rivelò come un organismo complesso e quando questa natura complessa fu più profondamente esplorata, la nozione di elementarità si trasferì ad oggetti più piccoli, e cioè al nucleo; ma oggi anche questo ha rivelato molto della sua natura complessa. In generale si potrebbe dire quindi che ad ogni stadio della scienza si chiamano elementari le particelle di cui non si conosce la struttura, e che pertanto si possono considerare come punti.

Nell'ambito di queste considerazioni di carattere assai generale, se ne può fare anche un'altra, che riguarda il numero delle particelle. Se un fisico o un chimico che non sapesse nulla di struttura atomica, cominciasse ad esplorare la natura degli oggetti chimici e scoprisse un primo atomo, ad esempio un atomo di ferro, potrebbe supporre trattarsi di una particella elementare. Ma poi se, dopo questo atomo di ferro, il chimico scoprisse un atomo di altra natura, per esempio di zolfo, e poi un atomo di ossigeno e così via (naturalmente l'ordine che vi dò è assolutamente arbitrario), logicamente la confidenza di questo ricercatore nella elementarità dell'atomo andrebbe gradualmente diminuendo perchè un numero così elevato di particelle sarebbe in contraddizione col concetto stesso di elementarità. Anche per le particelle elementari che oggi si conoscono, si sta verificando una situazione non interamente dissimile da quella or ora accennata.

La prima particella elementare è, come sapete, l'elettrone, scoperto circa cinquanta anni fa ed oggi così familiare, che il suo nome si ritrova correntemente nella stampa quotidiana. In seguito si scoprì il protone, e così le particelle elementari furono per qualche tempo due; poi ancora si scoprì il neutrone, arrivando così a tre particelle elementari.

Le particelle elementari che possiamo, al momento presente, considerare come bene accertate sono in definitiva le seguenti:

1° l'elettrone (normalmente negativo, con la sua varietà di elettrone positivo);

2° il protone;

3° il neutrone;

4° il mesone π (diviso in due varietà, una con elettricità positiva ed una con elettricità negativa);

5° il mesone μ (anche questo nella varietà positiva e negativa);

6° il fotone.

Queste, con tutte le loro varietà, sono nove particelle e costituiscono un numero abbastanza grande per far sorgere il dubbio sulla elementarità di alcune di esse.

Al momento presente però non si hanno molte indicazioni, nè sperimentali nè teoriche, per scartare decisamente questa ipotesi e quindi dobbiamo accontentarci, almeno provvisoriamente, dello schema suddetto.

Per completare infine l'elenco delle particelle elementari, se ne dovrebbero ricordare un'altra mezza dozzina che presento però con una certa riserva perchè non si possono considerare bene accertate. Ciascuna di esse ha soltanto il 50 % di probabilità e quindi soltanto tre potranno forse sopravvivere alle ricerche future.

Tra queste particelle vi è il *neutrino*, che finora è sempre sfuggito ad ogni indagine sperimentale e la cui esistenza è stata stabilita in via teorica per giustificare la sparizione di una certa quantità di energia in alcuni processi. Questo ammanco di energia avrebbe infirmato la validità del principio di conservazione dell'energia e dell'impulso (contro la tradizionale convinzione che la loro validità è indiscutibile) qualora non si fosse appunto postulato che la quantità di energia in esame non scompariva ma veniva bensì trasferita ad una particella elettricamente neutra, probabilmente senza massa ed estremamente difficile ad osservarsi sperimentalmente. Oggi però si parla di esperienze che forse condurranno alla sua scoperta, ammesso che essa esista effettivamente.

Vi è poi una particella molto di secondo ordine, chiamata *gravitone*, che sarebbe il « quanto » del campo gravitazionale. Questa è una particella che molto probabilmente esiste, ammesso che le nostre idee teoriche sul come questi fenomeni vanno interpretati siano giuste. Ad ogni modo sarà molto difficile osservarla direttamente, perchè è quasi altrettanto inosservabile quanto il neutrino.

Non nominerò in dettaglio le altre quattro particelle; ricorderò soltanto che la loro esistenza è suggerita o da ragioni teoriche non assolutamente definitive, oppure da esperienze tutt'altro che complete ed attendibili al momento presente.

In definitiva possiamo dire che, considerando tre dei nominativi della seconda lista come particelle abbastanza probabile, si hanno complessivamente circa una dozzina di particelle elementari. È questo un numero troppo grande per considerare l'attuale uno stadio definitivo.

A questo punto si presenta la necessità di fare una sistematica, per cui si riesca a capire per quale ragione alcune di queste particelle si osservano in natura, ed altre no. Questo è, allo stadio presente, un desiderio molto logico ma interamente non soddisfatto, poichè nessuno finora è riuscito nell'intento con successo. Comunque, non vorrei discutere in questo momento i problemi teorici connessi a queste particelle, ma piuttosto parlare di alcuni dei metodi sperimentali e delle circostanze in cui le particelle si osservano e si producono.

I metodi di osservazione sono in gran parte noti da molto tempo; non starò quindi a descriverli in particolare: tutti hanno sentito parlare del contatore di Geiger e Müller come di un metodo per rivelare le particelle ionizzanti; della camera di Wilson, come di un metodo in cui queste particelle lasciano lungo il loro percorso una traccia che può venire fotografata.

In anni più recenti sono stati sviluppati nuovi metodi: uno di essi è il metodo fotografico che si basa su di un principio estremamente semplice, ma che ha richiesto, per arrivare allo sviluppo di oggi, un raffinamento di tecnica assai elevato. Una particella ionizzante passando nella gelatina di una lastra fotografica, produce per ionizzazione una piccola traccia di annerimento; questa, per essere osservata, richiede un ingrandimento di 1000 ÷ 2000 diametri. Dall'esame di queste tracce, e cioè dal loro comportamento geometrico e dalla loro densità, si possono trarre delle conclusioni circa la natura delle particelle.

Un altro metodo, che si è andato affermando negli ultimi anni, è quello che, in linea di principio, veniva già usato agli inizi degli studi di radioattività, particolarmente da Lord Rutherford e dai Curie: è il metodo delle così dette scintillazioni, basato sul fatto che una particella, incidendo sopra uno speciale schermo, produce una scintillazione visibile al microscopio. Un tempo gli studiosi passavano ore ed ore al microscopio, nel faticoso intento di osservare e contare queste scintillazioni; oggi, invece, si sostituisce all'occhio un contatore fotoelettrico a moltiplicazione elettronica, cosicchè la parte incerta e penosa di ieri è fatta ora automaticamente, con grande vantaggio di tempo e di precisione.

A titolo di introduzione vorrei mostrare ora alcune diapositive per far vedere come si presentano queste particelle elementari all'osservatore.

La figura 1 rappresenta una fotografia in camera di Wilson di un elettrone veloce: la traccia prodotta da questa particella è costituita da una serie di goccioline le quali danno una chiara indicazione del passaggio di un elettrone di elevata energia che attraversa, senza subire alcuna deviazione, il campo della camera. Si notano inoltre alcune tracce molto marcate dovute ad elettroni lenti; questi urtano le molecole del gas attraverso cui si propagano e subiscono una serie di deviazioni, che conferiscono alla traccia un aspetto contorto. Si può anche notare in questa fotografia, che la traccia degli elettroni veloci è molto più sottile e che quindi contiene un numero di goccioline minore di quello relativo alla traccia degli elettroni lenti; questo è dovuto semplicemente al fatto che questi ultimi producono una più intensa ionizzazione degli altri.

Nella figura 2 si vede la traccia di una particella (non è un elettrone ma una particella che parimenti si osserva nei raggi cosmici) che urta quasi centralmente un elettrone il quale è balzato in avanti percorrendo una traiettoria quasi circolare. Ciò avviene perchè in questa come nella maggior parte delle esperienze del genere, la camera di Wilson è immersa in un forte campo magnetico allo scopo appunto di produrre delle deviazioni. Da uno studio quantitativo di esse si può, in molti casi, calcolare la velocità delle particelle in esame.

Nella figura 3 si vede un elettrone positivo che arriva nella camera e traversa una lastra di materiale perdendo energia, come si vede dal fatto che la sua traiettoria, poco incurvata nella prima parte, lo è apprezzabilmente di più dopo aver superato l'assorbitore: questo vuol dire che la particella ha perduto velocità, perchè nell'attraversare lo schermo ha perduto energia.

Nella figura 4 si presenta per ben tre volte il fenomeno della formazione di coppie (elettroni positivi e negativi) da parte di raggi gamma. Dei raggi γ, non visibili in questo tipo di osservazione, arrivano su una lastra di materiale e creano una coppia di elettroni la cui traiettoria è ben visibile. Si nota in particolare, che le traiettorie di ogni coppia sono incurvate in direzione opposta, e ciò corrisponde appunto al fatto che i due elettroni di ogni coppia hanno cariche opposte. In questa figura si nota inoltre una traccia che si avvolge in molti cerchi. Essa è dovuta ad un elettrone positivo così lento da essere incurvato dal campo magnetico applicato, secondo un cerchio di raggio abbastanza piccolo.

La figura 5 mostra dei fenomeni più complicati, che non sto a descrivere in particolare e che si osservano nello studio della radiazione cosmica: sono i così detti sciami. È un fenomeno molto complesso, che oggi non è nemmeno interamente capito, e che consiste in parte in una formazione di elettroni positivi e negativi.

È interessante notare dal punto di vista tecnico che questa figura è costituita da due fotografie essenzialmente simili: esse sono state prese con due macchine fotografiche poste ad angolo retto tra loro e si possono, con opportuni metodi, trattare come fotografie stereoscopiche, per ricostruire la effettiva natura del fenomeno che si presenta, non solo nel piano di proiezione ma anche nello spazio.

Nella figura 6 si vede un altro sciame (da notare che questa fotografia è stata fatta senza campo magnetico quindi le tracce appaiono rettilinee) che sottopongo alla vostra attenzione semplicemente per dimostrare come questi fenomeni, quando siano rivelati con mezzi opportuni, siano veramente spettacolosi.

Mostrerò ora due altre fotografie in cui si presenta un fenomeno assai notevole e cioè il fenomeno del trasformarsi di una delle particelle elementari in un'altra: la conversione in un elettrone del cosiddetto mesone μ. Esso ad un certo punto si ferma nel gas della camera, ma non vi si trattiene per molto tempo; infatti dopo uno o due milionesimi di secondo si trasformerà spontaneamente in un'altra particella e cioè in un elettrone.

Vedete infatti nelle figure 7 e 8 la traccia di un mesone μ, che si riconosce da varie caratteristiche, particolarmente dall'alta densità di ionizzazione ed anche da una certa incertezza della traccia (la qual cosa indica che la particella subisce urti abbastanza frequenti con le molecole del gas); ad un certo punto, la particella si ferma e dopo pochi milionesimi di secondo muore trasformandosi in un elettrone il quale dà una traccia più sottile.

Dove si producono queste particelle elementari?

Naturalmente non vorrei parlare degli elettroni, che sono ben noti ai più tanto che hanno perduto ogni carattere di novità. Vorrei piuttosto parlare di particelle più nuove e particolarmente dei mesoni.

L'officina più comune nella quale queste particelle vengono fabbricate è costituita dai raggi cosmici; quando questi arrivano nell'alta atmosfera producono, urtando i nuclei dell'aria od i nuclei dei vari materiali con cui si fanno le osservazioni, delle disintegrazioni in cui appunto vengono prodotte particelle come i mesoni.

Per rendere la cosa più evidente vorrei mostrare ancora alcune fotografie (figg. 9 e 10) di fenomeni di questo tipo. Esse sono state ottenute mediante un forte ingrandimento dell'ordine di dieci-centomila volte e riproducono dei fenomeni avvenuti nell'interno della gelatina di una lastra fotografica appositamente preparata.

Queste disintegrazioni hanno l'aspetto di stelle con un gran numero di raggi, ciascuno dei quali rappresenta la traccia di uno dei prodotti di disintegrazione di un nucleo.

Nella figura 9 il proiettile entrante, che proviened a una direzione verticale, ha urtato ad un certo punto un nucleo d'argento producendo una esplosione di grossa dimensione nella quale sono proiettati frammenti di nucleo in tutte le direzioni. Fra questi raggi alcuni hanno le caratteristiche di particelle pesanti (tracce molto marcate) altri corrispondono a particelle di alta velocità e piccola carica; probabilmente fra questi ultimi vi sono parecchi mesoni.

Nella figura 10 si vede una stella prodotta da una particella veloce, che spezza un nucleo; si nota in particolare un raggio il quale ha un tracciato talmente lungo che, per farlo rientrare nelle dimensioni della fotografia, è stato necessario dividerlo in due parti, di cui la seconda viene riprodotta isolatamente sotto la prima. Esso è prodotto da un nucleo di berillio, che salta fuori da un nucleo più pesante.

Ho voluto mostrare alcune fotografie (naturalmente se ne potrebbero mostrare a centinaia, raccolte nei vari laboratori di raggi cosmici ed in particolare nel laboratorio della Testa Grigia) perchè forse alcuni di voi avrebbe potuto pensare che tutto ciò di cui si è parlato risultasse soltanto dalla teoria. Invece, come si è visto, si tratta di fatti sperimentalmente provati mediante materiali e mezzi ordinari, come per esempio la lastra fotografica.

Vorrei ora illustrare un po' in particolare le ricerche che portarono alla scoperta del mesone. Incidentalmente detto, questa particella si chiama mesone perchè con ciò si vuole indicare che la sua massa sta tra quella dell'elettrone, più leggero e quella del protone, più pesante. La massa del mesone corrisponde a circa trecento volte quella dell'elettrone.

L'idea del mesone fu introdotta nel 1935 per la prima volta in base ad una considerazione teorica da un fisico giapponese, Yukawa, il quale « inventò » questa particella, o meglio propose una teoria in cui ipoteticamente ammise la sua esistenza per spiegare la natura delle forze nucleari. Il tempo a disposizione non mi consente di descrivere in dettaglio la teoria; ma vorrei piuttosto esporre alcuni punti di vista che sono interessanti. In particolare vorrei giustificare il motivo per cui una particella, con una massa abbastanza considerevole come il mesone, si adatta a spiegare forze di piccolo raggio di azione come le forze nucleari.

Riferiamoci innanzi tutto, come base, al campo elettromagnetico. Precisamente, se consideriamo due particelle A e B, ad una certa distanza tra loro, le forze elettriche a cui esse sono sottoposte vengono trasmesse da un campo e si può dire che la particella A produce attorno a sè un campo elettrico entro cui verrà a trovarsi la particella B che in tal modo risulta assoggettata alla sua azione (e viceversa). Il campo è quindi l'intermediario che trasmette la forza tra le due particelle.

Ora le forze elettriche hanno una peculiarità, sono cioè forze di lunga portata, che arrivano a grande distanza; decrescono bensì con la distanza, ma soltanto col quadrato di essa, cioè con una legge abbastanza lenta, cosicchè anche particelle lontane interagiscono tra loro. Ma non così le forze nucleari, le quali sono di tal natura che possono agire solo se le due particelle sono vicinissime (e, quando dico vicinissime, intendo ad una distanza dell'ordine di grandezza di 10^{-13} cm., cioè a una distanza centomila volte più piccola del raggio dell'atomo che è dell'ordine di 10^{-8} cm); in una parola, le forze nucleari sono forze di corta portata. Il meccanismo, tuttavia, si può considerare analogo a quello svolto per il campo elettromagnetico, cioè si può immaginare che anche forze di così corta portata siano trasmesse da un campo, che non sarà naturalmente un campo elettrico, ma un tipo di campo differente e la cui natura si tratta ora di chiarire. Come il campo elettrico ha i suoi fotoni, che sono per così dire dei quanti di energia elettromagnetica e che si comportano in tutto e per tutto come particelle, così essendo questa una proprietà generale di tutti i campi, il campo delle forze nucleari avrà il suo analogo dei fotoni che chiameremo mesoni.

Quali saranno le caratteristiche di questi quanti per far sì che le forze vengono ad avere un piccolo raggio di azione? La risposta di Yukawa è che essi debbono avere una massa relativamente grande; la ragione di ciò si può capire quasi senza formule, almeno per coloro che hanno una certa familiarità coi metodi della meccanica quantistica. Si considerino due particelle, un protone ed un neutrone, a una certa distanza tra loro; ognuna di esse si circonderà del proprio campo, il quale dovrà agire sull'altra. Circondarsi del proprio campo vuol dire emettere dei quanti di questo campo e quindi le particelle emetteranno dei mesoni; ma emettere un mesone costa energia e se esso ha una massa M, l'energia richiesta per la sua sola creazione sarà data da:

$$E = Mc^2 \qquad (1)$$

[c velocità della luce].

Nella meccanica quantistica si può prendere, in un certo senso, dell'energia a prestito, a patto però che la scadenza sia molto breve. Praticamente, se si vuol prendere a credito una certa quantità di energia, diciamo per esempio Mc^2, secondo la relazione di Einstein, questo si può fare ma solo per un tempo dell'ordine di grandezza dato da:

$$t = \frac{h}{Mc^2} \qquad (2)$$

[h costante di Planck].

Dalla (2) si vede che se si vuol prendere a credito una grossa energia il termine del credito deve essere corto perchè l'energia che si prende a credito sta al denominatore; la (2) rappresenta quindi il tempo in cui il mesone può stare fuori dal nucleo nello spazio libero. Se allora si suppone che la velocità di questo mesone libero sia la massima velocità a cui una particella possa muoversi, cioè la velocità della luce, si vede che la massima distanza a cui esso può arrivare prima di essere richiamato per saldare il debito è data, come ordine di grandezza, dal prodotto del tempo per la velocità massima con cui la particella può muoversi:

$$d = \frac{h}{Mc}. \qquad (3)$$

La (3) esprime quindi, a meno di alcuni coefficienti numerici, il raggio di azione delle forze nucleari. Se si vogliono allora rappresentare le forze nucleari, si deve ammettere che la distanza (3) debba essere appunto dell'ordine di grandezza di 10^{-13} (che è il valore sperimentale del raggio di azione di queste forze) e siccome sia la costante di Planck che la velocità della luce sono note, si può ricavare la massa del mesone o almeno il suo ordine di grandezza.

Yukawa, che ideò questa teoria e la sviluppò matematicamente in modo assai elaborato e completo, arrivò alla conclusione che, se c'era qualcosa di vero, almeno dal punto di vista qualitativo (non ne era sicuro perchè sia in quell'epoca come oggi non si può dare una chiara interpretazione a questi fenomeni) dovevano esistere certe particelle, la cui massa, calcolata essenzialmente in base al ragionamento or ora fatto, doveva essere dell'ordine di grandezza di 200 o 300 volte la massa dell'elettrone.

Poco dopo due gruppi di fisici che studiavano i raggi cosmici (precisamente il gruppo di Anderson in California ed il gruppo di Stevenson nel Massachusetts), trovarono nelle loro lastre delle particelle che avevano una massa circa 200 volte la massa dell'elettrone. Essi conclusero che si trattava delle particelle di Yukawa; però in seguito si potè precisare che ciò non era perchè si accertò che le nuove particelle scoperte, non avevano nulla a che fare con esse. La prima chiara indicazione che le nuove particelle non erano i mesoni di Yukawa, venne da una esperienza che fu condotta qui a Roma da Conversi, Pancini e Piccioni (i lavori furono fatti, almeno in buona parte, in una cantina durante il periodo della resistenza, mentre questi ragazzi erano nascosti per ragioni politiche). Il risultato di questa esperienza si può riassumere all'incirca nel modo seguente: un mesone positivo o negativo si arresta in un blocco di materia. Se positivo, non potrà entrare nei nuclei specialmente da fermo perchè la repulsione elettrica lo tiene all'infuori di essi, lasciandolo praticamente nello spazio libero. Qui, dopo un tempo dell'ordine del milionesimo di secondo, disintegra emettendo un elettrone come nelle figure 7 e 8. Se il mesone è negativo, esso verrà attratto dai nuclei degli atomi in mezzo ai quali si ferma, ed in tal caso cadrà molto rapidamente in uno di essi. Se questo mesone ha le stesse caratteristiche della particella di Yukawa e cioè se è proprio il quanto che determina le forze nucleari, l'interazione con i nuclei sarà così violenta che esso sarà da questi assorbito in un tempo dell'ordine di 10^{-22} sec.

Orbene le esperienze di Conversi, Pancini e Piccioni dimostrarono che il mesone in particolari circostanze sparisce effettivamente, ma ciò dopo un tempo relativamente grande, rivelando in tal modo una interazione con i nuclei piuttosto piccola: questa infatti è circa un milione di milioni di volte più piccola di quella che ci si attende dal mesone di Yukawa. Si tratta quindi di una differenza tra le previsioni teoriche e il risultato sperimentale, che non può dipendere evidentemente da errori di dettaglio.

Tutta la teoria di Yukawa fu allora messa in dubbio non solo in questioni di dettaglio ma anche nella sua base generale, e questo stato di cose permase fin quando la soluzione dell'enigma venne dai lavori di Powell e Occhialini (Bristol) nei quali si mise in evidenza il fatto che esistono due

specie di mesone, una con le caratteristiche del mesone di Yukawa, ed una altra che si osserva più comunemente nella radiazione cosmica: dico più comunemente, perchè ormai si osservano entrambi i tipi. Questi autori mostrano inoltre che il primo tipo cioè il mesone π si converte spontaneamente nell'altro mesone (mesone μ), come mostrerò con due fotografie.

La figura 11 rappresenta una stella che, a prima vista, appare molto simile alle precedenti; in realtà essa offre un interessante particolare, e cioè una traccia (contrassegnata dalla lettera π) che dall'esame di tutte le caratteristiche sembra appartenere ad un mesone. Nel punto in cui questa particella si è fermata, si produce una disintegrazione nucleare, che rivela una forte interazione del mesone con i nuclei: si tratta quindi di una particella corrispondente alla teoria di Yukawa.

Nella figura 12 si vede la traccia di un altro mesone π che avendo una carica positiva, non può interagire coi nuclei, a causa della repulsione coulombiana. Ad un certo punto esso si ferma e disintegra dando luogo ad un mesone dell'altro tipo, cioè ad un mesone μ, che, dopo aver percorso un certo tratto nella gelatina (traccia piuttosto lunga) si ferma e disintegra a sua volta in un elettrone.

Da quel che ho detto, risulta che ogni speranza di capire con un certo dettaglio quelle che sono le proprietà del nucleo atomico (che attualmente conosciamo in via puramente empirica ma che non siamo in grado di calcolare o di capire in dettaglio) è nettamente legata allo studio delle proprietà del mesone π. Probabilmente le sue proprietà saranno piuttosto simili a quelle indicate nella teoria di Yukawa, o più propriamente nelle « teorie di Yukawa » potendosene fare parecchie (al momento presente non si ha nessun modo per decidere quale di esse sia la buona, ammesso che una lo sia, perchè non sappiamo ancora abbastanza della natura di questi fenomeni).

Vorrei aggiungere ancora due parole sulla questione delle particelle elementari che, come ho detto, sono particelle senza struttura o per lo meno con una struttura che noi non conosciamo. Ma in realtà molte di esse rivelano una certa struttura, cosicchè ogni diritto di considerarle elementari viene a svanire. Per esempio nello schema precedentemente descritto, in cui un protone si circonda del suo campo ed emette mesoni, non va in realtà considerata la particella protone, ma piuttosto un punto con due particelle che ogni tanto arrivano a distanza molto piccola tra loro ma non infinitesima. Lo stesso dirò anche per particelle più comuni e familiari, come l'elettrone. Quest'ultimo è circondato da un campo elettromagnetico che rappresenta essenzialmente una struttura e che, più o meno modificato, lo accompagna in tutti i suoi movimenti. Questo stato di cose, cioè l'elettrone fisico, si potrebbe descrivere come un miscuglio di un certo elettrone idealizzato, puntiforme, e di una nuvola di fotoni che lo circonda e che rappresentano il campo elettromagnetico. Quindi queste che noi seguitiamo a chiamare ancora particelle elementari, sono in realtà oggetti complicati. Nel cercare di analizzare questa complicazione si riscontrano notevoli difficoltà per la teoria; si trova per esempio che la massa elettromagnetica, che è la massa dovuta al campo circondante l'elettrone, risulta infinita.

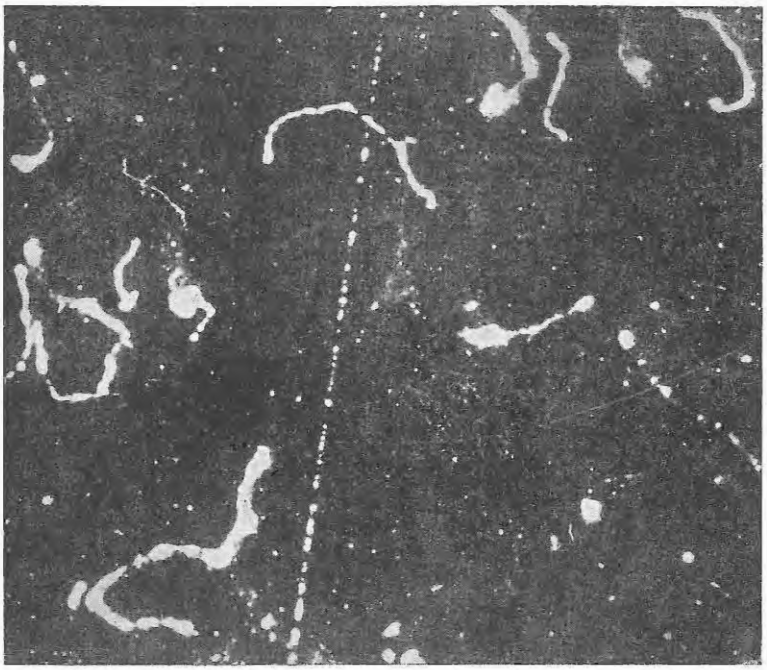

Fig. 1.

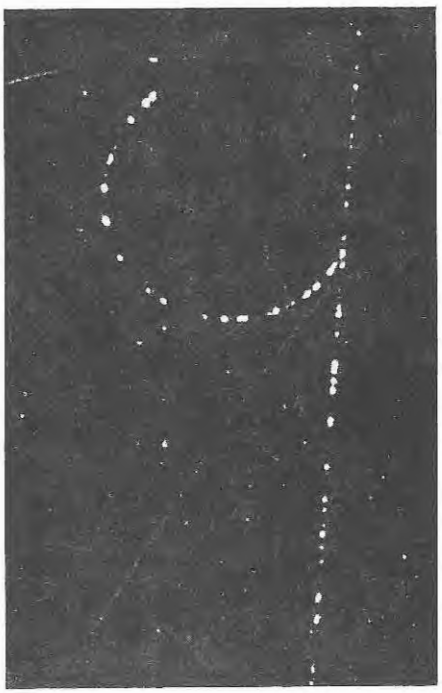

Fig. 2.

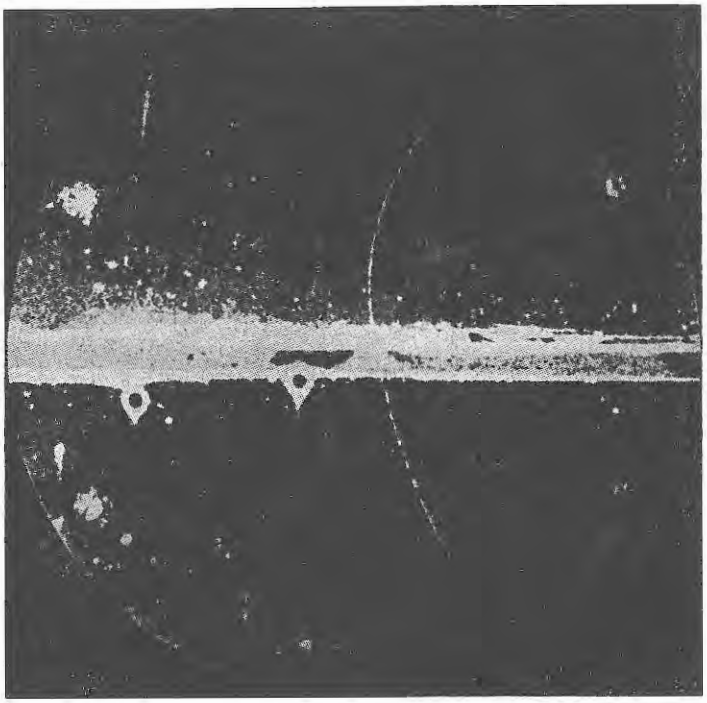

Fig. 3.

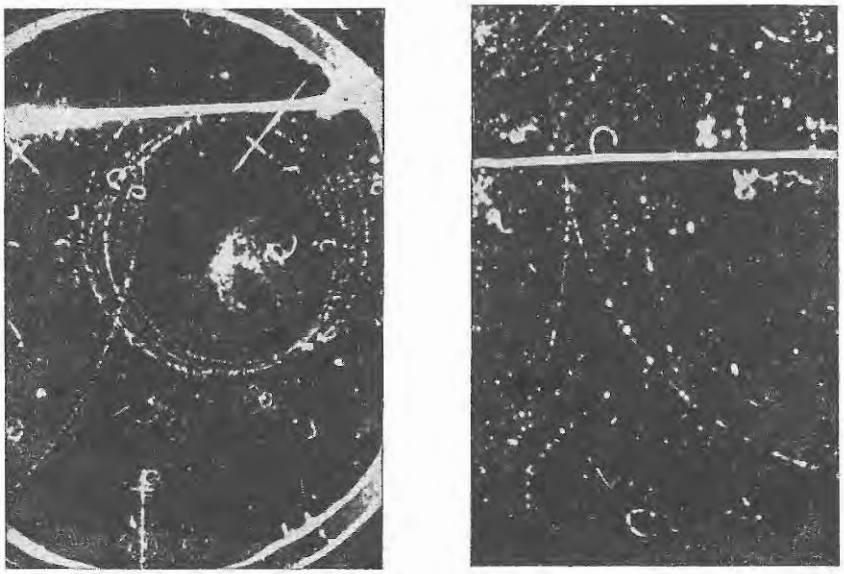

Fig. 4.

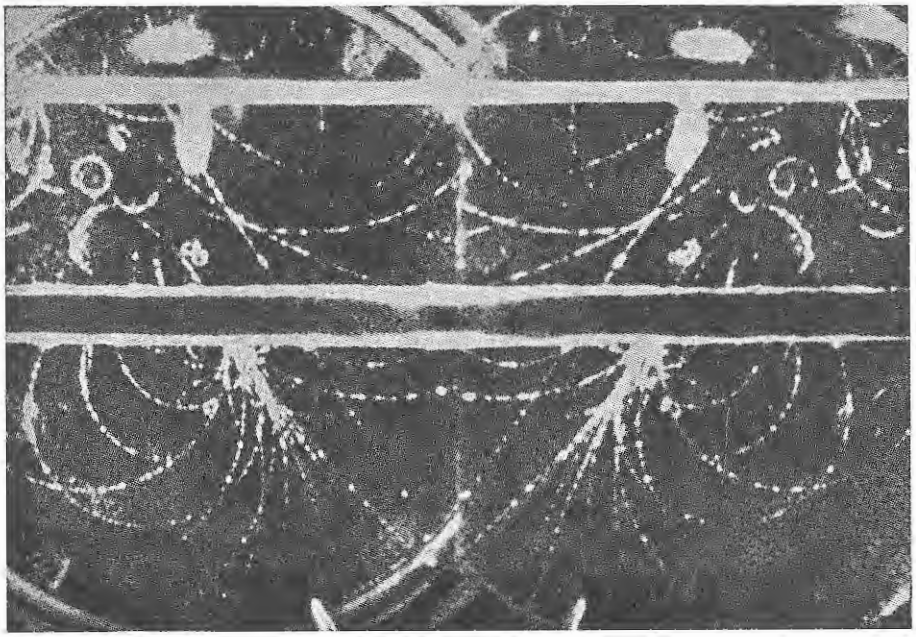

Fig. 5.

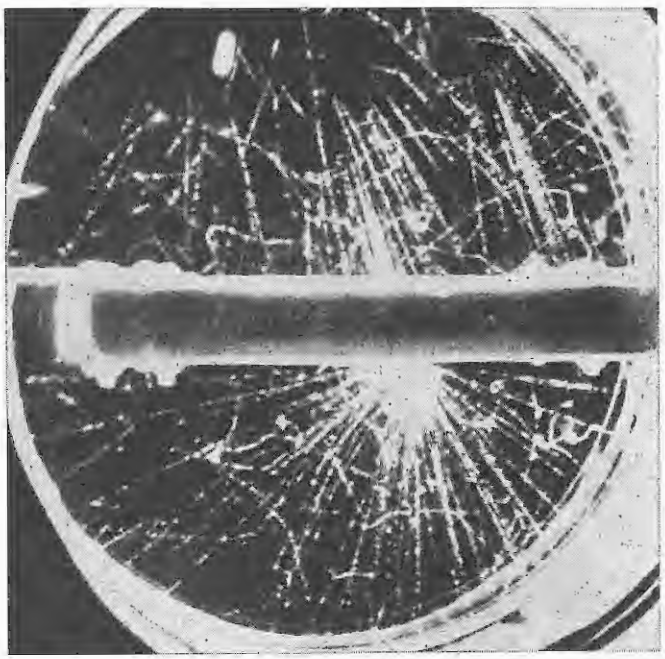

Fig. 6.

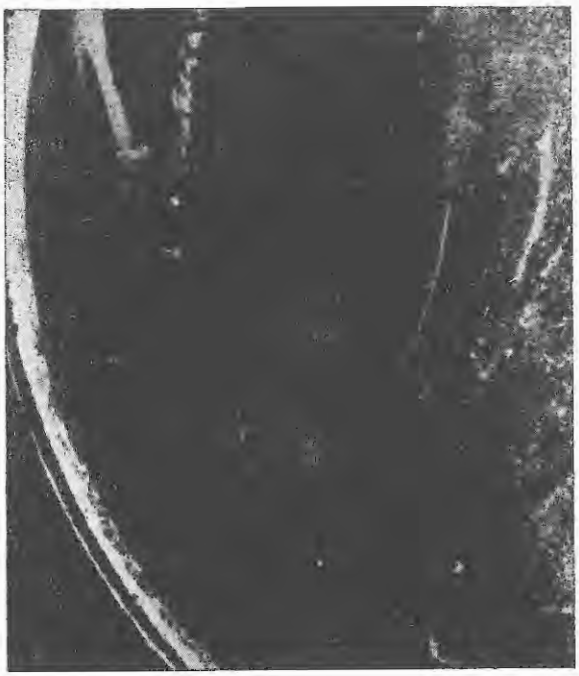

Fig. 7.

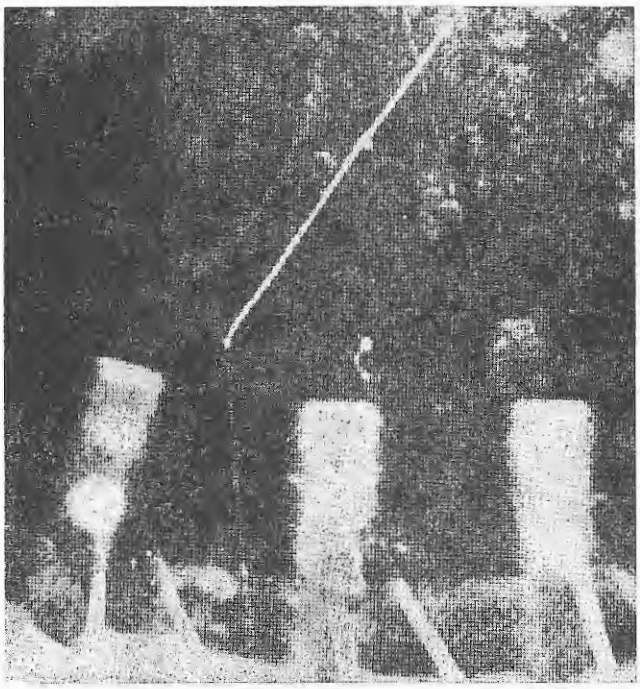

Fig. 8.

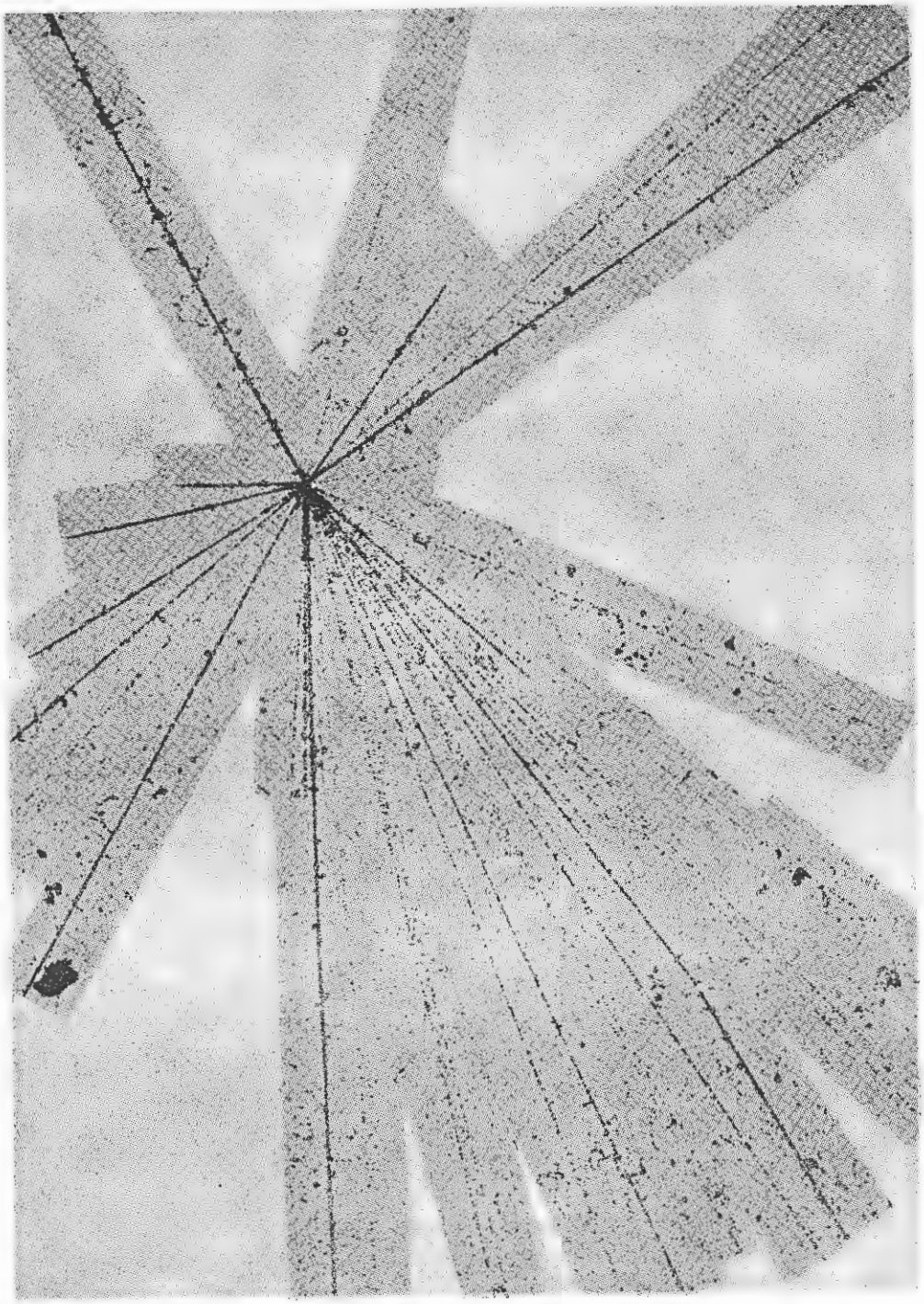

Fig. 9.

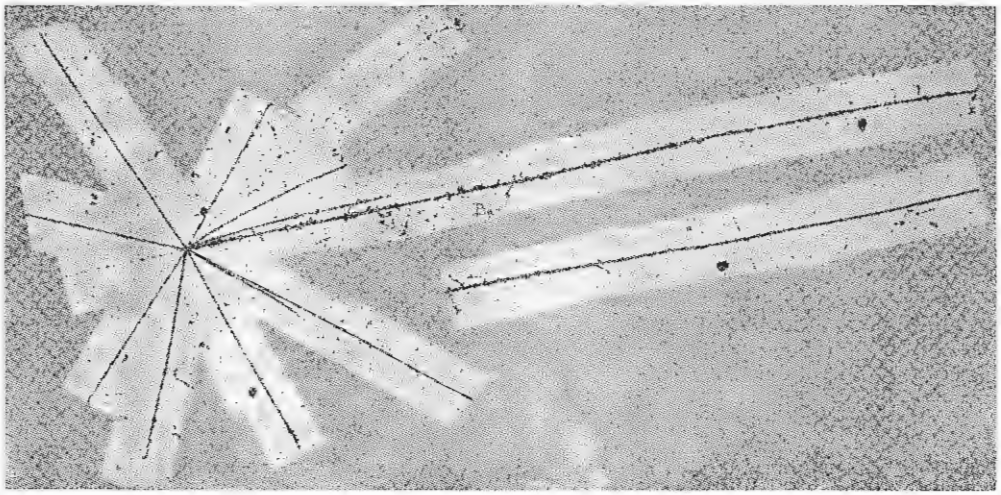

Fig. 10.

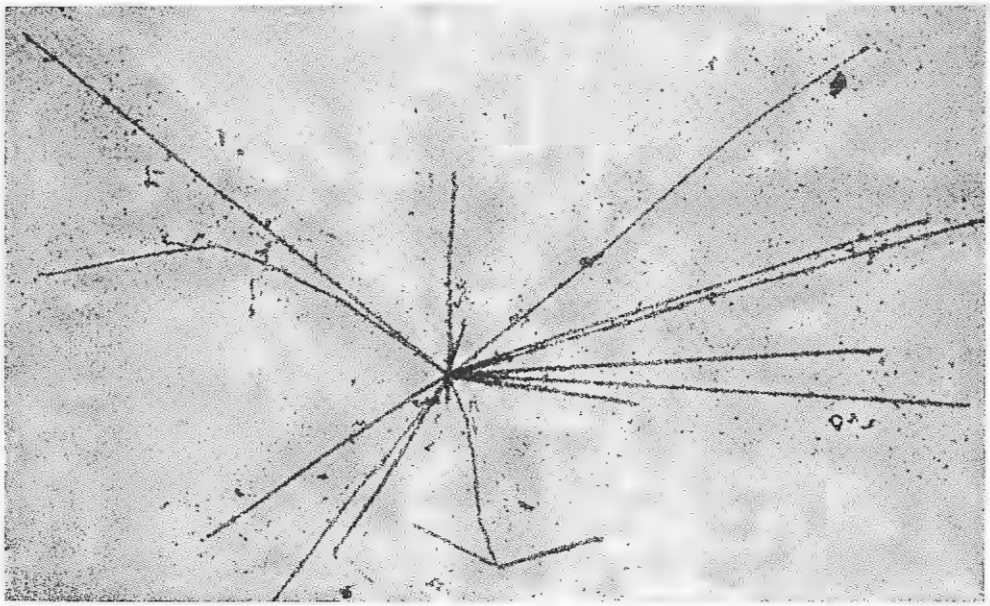

Fig. 11.

Fig. 12.

E così si arriva penosamente a quella che è oggi la frontiera delle nostre conoscenze nel campo delle particelle elementari. È una frontiera naturalmente in movimento, una frontiera fluida, una frontiera che si consoliderà probabilmente via via che nuovi dati sperimentali verranno ottenuti nei laboratori, dati che serviranno a indirizzare il pensiero dei fisici teorici verso un campo più circoscritto.

E quando ciò avverrà, si potrà realizzare un grande progresso nella fisica, perchè è presumibile che la risoluzione di questo problema si accompagnerà alla risoluzione del problema delle forze nucleari e permetterà pertanto di fare una vera teoria del nucleo e non un empirismo, come abbiamo oggi, in cui ci si sa servire del nucleo ma non si sa come è fatto.

Ma naturalmente al di là di questa frontiera ce ne saranno altre ed altre ancora, perchè sembra sia il destino della scienza che ogni gruppo di scoperte, ampliando l'area del sapere, debba ampliare anche quella delle cose sconosciute!

SECONDA CONFERENZA (*)

LE PARTICELLE ELEMENTARI (SECONDA PARTE)

(redatta dal dott. L. MEZZETTI)

Nella lezione precedente abbiamo elencato un certo numero di particelle elementari; parleremo oggi un po' più in dettaglio delle loro proprietà, o per lo meno di alcune delle loro proprietà.

Queste sono molte. In parte sono note, in parte sono ignote; forse, anzi certamente, la più gran parte sono ignote; ma ci sono certi fatti che o si conoscono, o si sospettano, e che permettono, attraverso una analisi matematica, di iniziare la costruzione di una teoria di esse. Dico incominciare, e voglio sottolineare questa espressione, perchè siamo estremamente lontani dal finirla.

La particolarità forse più notevole che risulta dallo studio sperimentale di queste particelle sta nel fatto che esse, in vari casi, si trasformano le une nelle altre; oppure, in altri casi, appaiono improvvisamente particelle che prima non erano osservabili. Questo non è un fatto interamente nuovo nella fisica dei fenomeni quantistici; e forse il primo caso in cui si è presentato in modo chiaro è quello della emissione della luce. Questo fenomeno veniva interpretato, nella fisica classica, come una graduale emissione di onde dovute, diciamo così, allo scuotere del campo elettromagnetico da parte degli elettroni dell'atomo. Ma, dal punto di vista quantistico, l'emissione della luce avviene invece per « quanti »; ad un certo momento un atomo emette un quanto; ma non si può dire in alcun modo (e l'analisi che si fa matematica-

(*) Tenuta il 5 ottobre 1949 nell'aula dell'Istituto Fisico dell'Università di Roma.

mente di questo fenomeno non indica in alcun modo) che il quanto fosse preesistente nell'atomo e ad un certo punto ne esca fuori: bisogna invece pensare che il quanto si formi nello stesso momento in cui avviene la transizione quantistica fra i due livelli energetici dell'atomo e la luce viene emessa.

Questo fenomeno di emissione della luce si può perciò indicare schematicamente con una equazione, che è il modello di altre equazioni dello stesso tipo, che verranno scritte tra un momento:

$$e \rightarrow e' + \gamma$$

dove abbiamo indicato con la lettera e l'esistenza di un elettrone in una certa orbita (livello energetico) che ad un certo momento si trasforma in un elettrone e' situato in una orbita diversa e in un quanto di luce, che abbiamo indicato con la lettera γ. Dove prima esisteva una sola particella elementare (un elettrone), ne è comparsa un'altra: un quanto di luce.

Via via che si sono andate scoprendo nuove particelle elementari e via via che la nostra conoscenza di esse, seppure incompleta, si è andata gradualmente approfondendo, nuove reazioni, analoghe a quella ora scritta, si sono andate aggiungendo, così che ora ne conosciamo in tutto una decina, o poco meno. In alcuni casi, queste reazioni sono note incompletamente, perchè si vedono uscire alcune particelle, ma si sospetta che ne escano anche delle altre che non si osservano. In generale la particella che si sospetta esca, anche se non si osserva, è il neutrino.

Nel seguito di questa discussione assumeremo senz'altro che il neutrino esista, facendo una ipotesi che in realtà non è particolarmente giustificata fino ad ora dai fatti sperimentali, ma che probabilmente si può usare, almeno come una ipotesi di lavoro.

Come esempio di reazione incompletamente nota prendiamo la reazione che avviene nella emissione dei raggi beta. La emissione dei raggi beta consiste essenzialmente nella trasformazione di un neutrone N del nucleo in un protone P, con emissione di un elettrone e^- e di un neutrino ν, secondo lo schema seguente:

$$\text{(1)} \qquad N \rightarrow P + e^- (+ \nu).$$

La carica negativa dell'elettrone emesso neutralizza la carica positiva del protone, in modo che la carica totale dei prodotti della reazione è nulla come la carica del neutrone originario. Il neutrino è necessario per completare il bilancio dell'energia e della quantità di moto; la parentesi indica che si tratta di una particella la cui presenza non è osservata sperimentalmente, ma solo supposta; ma d'ora in poi ci risparmieremo questa cautela.

Incidentalmente osserviamo che tutte queste reazioni andrebbero sempre indicate col doppio segno, perchè avviene sempre, o vi è sempre in linea di principio la possibilità, che ad una di queste reazioni possa contrapporsi la reazione opposta. L'equazione (1), per esempio, scritta nella forma più generale

$$e \rightleftarrows e' + \gamma$$

indica l'emissione di un quanto di luce, se letta nel verso da sinistra a destra,

secondo la freccia superiore, e l'assorbimento di un fotone se letta da destra a sinistra, secondo la freccia inferiore.

Ma ve ne sono altre. Abbiamo parlato nella lezione scorsa del mesone cosiddetto μ. Il mesone μ è, come abbiamo visto, quello, dei due mesoni, che non interagisce fortemente con la materia nucleare. Le osservazioni sperimentali, fatte con diverse tecniche (camera di Wilson, lastre fotografiche, contatori) mostrano che quando un mesone μ si ferma lontano dai nuclei della materia, cioè nel vuoto (il che avviene segnatamente per i mesoni μ positivi che sono tenuti lontani dai nuclei dalla repulsione coulombiana), ben presto emette spontaneamente un elettrone, positivo o negativo a seconda del segno della carica del mesone stesso, e dotato di grande energia cinetica.

Ma, naturalmente, ciò non basta; e ciò non basta per la semplice ragione che se la reazione consistesse unicamente nella emissione, da parte di un mesone fermo, di un elettrone veloce violerebbe il principio della conservazione della quantità di moto. La quantità di moto iniziale è infatti nulla (mesone fermo), mentre l'elettrone emesso possiede una notevole quantità di moto.

Per rimettere le cose a posto occorre ammettere che esista una compensazione per la quantità di moto portata via dall'elettrone; e questo si potrebbe fare ammettendo che nella direzione opposta venga emesso con la stessa quantità di moto dell'elettrone un neutrino. Ma una analisi più dettagliata del problema indica che ciò verosimilmente non basta: se il fenomeno consistesse nell'emissione di un elettrone e di un solo neutrino, ci si dovrebbe infatti attendere che l'energia cinetica dell'elettrone emesso fosse sempre la stessa, perchè la energia di massa mc^2 del mesone originario (che, incidentalmente, vale circa 100 milioni di ev) dovrebbe ripartirsi in quantità quasi esattamente uguali tra il neutrino e l'elettrone; quest'ultimo quindi porterebbe via $50 \cdot 10^6$ ev e l'invisibile neutrino ne porterebbe via altrettanti. Invece i risultati sperimentali sono diversi. Le esperienze indicano decisamente che gli elettroni emessi, benchè abbiano una energia massima non lontana dai 50 milioni di volt, hanno talvolta energia minore: alcune volte 30, alcune volte 20, altre volte 40 Mev, assumendo, con probabilità diverse, tutti i valori compresi fra zero e 50 milioni di ev. Ciò indica che non è una sola particella quella che noi non vediamo e che serve a ristabilire il bilancio della quantità di moto, ma che vengono emesse almeno due particelle.

In realtà, nelle speculazioni che si fanno sul meccanismo di questo processo (e si tratta di speculazioni che hanno, almeno per il momento, un carattere assai ipotetico), si usa ammettere che due particelle invisibili vengano emesse; e, per fare economia di particelle, assumeremo che siano tutte e due neutrini.

Concludendo, potremo dunque indicare la reazione in esame con lo schema:

$$\mu^{\pm} \rightarrow e^{\pm} + 2\,\nu\,. \tag{2}$$

Ce ne sono delle altre. Anche l'altro mesone, il mesone π, può disintegrarsi, come si vede chiaramente nelle lastre fotografiche. Ne abbiamo viste alcune nella lezione scorsa; vi si vede la traccia di un mesone π, che, arri-

vato alla fine del suo percorso, si disintegra, emettendo, in una direzione qualsiasi, un secondo mesone avente una notevole energia cinetica, e riconoscibile, dalle caratteristiche della traccia che esso lascia nella gelatina, per un mesone del tipo μ.

Anche qui, naturalmente, occorre salvaguardare il bilancio della quantità di moto; ed anche qui, per fare economia di ipotesi e non introdurre più particelle di quello che è strettamente necessario, possiamo ammettere che la particella emessa in direzione opposta, a compensazione della quantità di moto, sia di nuovo un neutrino. E in questo caso la situazione è diversa dalla precedente, perchè sperimentalmente si osserva che il mesone μ viene emesso sempre con la stessa energia: ciò indica che in questo caso viene presumibilmente emesso un solo neutrino.

Possiamo dunque, se le nostre speculazioni sono corrette, scrivere la seguente reazione:

$$\pi \to \mu + \nu . \tag{3}$$

Di altre reazioni dello stesso tipo parleremo più tardi, quando se ne presenterà l'occasione; tratteremo ora del punto di vista che si segue oggi nei tentativi di costruire una teoria dei fenomeni del tipo che ho descritto. Si tratta, a dire il vero, di semplici tentativi e di essi non direi in alcun modo che sono soddisfacenti, come altri rami della fisica teorica: ma sono per ora il meglio che si riesca a fare e, in attesa di qualche migliore idea, costituiscono il metodo che si segue nella discussione di quei fenomeni.

Prendiamo uno qualsiasi degli esempi citati, per esempio la disintegrazione del mesone π, secondo la reazione

$$\pi \leftrightarrows \mu + \nu$$

che scriviamo con la doppia freccia, per indicare la possibilità della reazione inversa. L'equazione rappresenta la possibilità di una transizione del sistema da uno stato iniziale, in cui è presente un mesone π, che in generale sarà dotato di una certa velocità, e potrà quindi descriversi mediante il suo vettore quantità di moto, ed uno stato finale, in cui sono presenti due particelle, entrambe diverse da quella originaria, e dotate di certe quantità di moto, in direzione generalmente diverse da quella del mesone primario. Se rappresentiamo gli stati mediante i corrispondenti vettori quantità di moto (fig. 1) avremo dunque una transizione fra lo stato A e lo stato B.

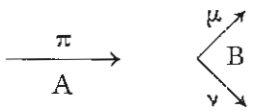

Fig. 1.

Questa descrizione della trasformazione in termini dello stato iniziale e dello stato finale del sistema è in realtà assai incompleta; e lo è per due ragioni: una di carattere secondario che, con un po' più di analisi, si potrebbe eliminare facilmente, è dovuta al fatto che sono state trascurate le quantità

di moto intrinseche delle particelle. In altre parole, le abbiamo considerate tutte come particelle senza spin. Ma questo è un vizio di forma che si può correggere senza effettiva difficoltà. Una più grave omissione consiste nell'aver trascurato tutto quello che avviene durante la trasformazione. In altre parole, se abbiamo un mesone π, che viaggia tranquillamente nello spazio, senza interagire con alcunchè, possiamo presumibilmente attribuirgli una quantità di moto determinata; ma quando le particelle presenti sono più di una (e durante la trasformazione, per un certo periodo di tempo, le dobbiamo pensare presenti tutte e tre) e vicine l'una all'altra, ci sono naturalmente delle interazioni; le particelle si disturbano mutuamente e, per parlare classicamente, le loro orbite saranno incurvate e la quantità di moto di ciascuna di esse non sarà costante.

Occorrerebbe dunque cercare di descrivere anche la fase in cui la transizione sta avvenendo, in cui perciò lo stato è una mescolanza dello stato iniziale e dello stato finale. Una indicazione del tipo della figura 1 rappresenta quindi correttamente soltanto quello che avviene molto prima che la trasformazione incominci, e molto dopo che la reazione è avvenuta; ma la fase veramente interessante, che è quella durante la quale la trasformazione, per così dire, è in atto, viene descritta in modo assai incompleto.

Nel descrivere fenomeni di questo tipo la meccanica quantistica usa di solito la teoria delle perturbazioni; ed usa la teoria delle perturbazioni semplicemente come un ripiego, perchè una teoria esatta dei fenomeni quantistici non è possibile con la nostra matematica, salvo poche eccezioni. La teoria delle perturbazioni dà un metodo approssimato che, almeno talvolta, serve a dare un'idea abbastanza accurata di quello che avviene; in altri casi, l'approssimazione che si riesce a raggiungere è piuttosto insoddisfacente.

Ad ogni modo, con il metodo delle perturbazioni si ottiene una formula che permette di calcolare la probabilità di transizione da un determinato stato iniziale di un sistema ad un determinato stato finale; essa risulta espressa come probabilità che il processo in esame avvenga per unità di tempo (o, se si vuole, come numero di processi che avvengono nell'unità di tempo in un insieme di un grande numero di sistemi che si trovano tutti nello stesso stato iniziale), ed ha perciò le dimensioni dell'inverso di un tempo. Scrivendola sotto la forma $1/\tau$, dove τ è un tempo che, come è noto, ha il significato di « vita media » del sistema per la transizione in esame, si ha dunque

$$\frac{1}{\tau} = \frac{2\pi}{\hbar} |H|^2 n \tag{4}$$

dove $\hbar$ rappresenta, come d'uso, la costante di Planck h divisa per 2π, H è l'elemento di matrice corrispondente al passaggio dallo stato iniziale allo stato finale, di cui fra poco discuteremo l'espressione esplicita; ed infine n rappresenta la « densità degli stati finali ». In generale, per densità degli stati finali si intende il numero di stati finali contenuti in un intervallo di energia unitario, o, se si vuole, il numero ΔN degli stati finali che cadono in un intervallo di energia ΔE diviso per l'ampiezza ΔE dell'intervallo stesso

$$n = \frac{\Delta N}{\Delta E}. \tag{5}$$

Si obietterà subito, a questo punto, che nel caso che stiamo esaminando la densità n degli stati finali risulta infinita; infatti, siccome le quantità di moto delle due particelle che costituiscono lo stato finale del nostro sistema sono limitate dalla sola condizione che la loro somma vettoriale deve essere uguale alla quantità di moto della particella iniziale, ma per il resto sono completamente arbitrarie, gli stati finali costituiscono un continuo, ed in ogni intervallo di energia ne cadono infiniti. Ma in compenso, come si vede dal calcolo, il fattore $|H|^2$ risulta in tal caso, e per la stessa ragione, infinitesimo; e il prodotto dei due fattori converge ad un limite finito. Più precisamente, l'artificio che si usa di solito per eseguire il calcolo di questo limite è il seguente: invece di considerare le particelle in esame come libere di muoversi in uno spazio infinito, le si pensano chiuse in una scatola di dimensioni finite e di volume Ω (che si fa poi tendere all'infinito in tutte le direzioni); eseguendo il calcolo per questo caso fittizio si trova che per ogni valore finito di Ω, gli stati finali non costituiscono un continuo, ma una successione discreta, per la quale è possibile definire una densità n finita; corrispondentemente anche il fattore $|H|^2$ è finito. Quando poi si fa tendere Ω all'infinito, $n \to \infty$ mentre $|H^2| \to 0$ e il prodotto $n|H|^2$, e quindi la probabilità $1/\tau$, tende ad un limite finito.

Il punto seguente è il calcolo degli elementi di matrice. Sia dunque in generale

$$A + B \to C + D$$

una transizione fra le particelle iniziali A e B e le particelle finali C e D (per semplicità consideriamo il caso in cui le particelle sono due e due, ma il ragionamento per il caso generale di un numero qualsivoglia di particelle non sarebbe sostanzialmente diverso). Secondo il metodo delle perturbazioni, l'elemento di matrice della transizione si rappresenta con un integrale

$$(6) \qquad H = \iiiint \psi_C^*(C)\,\psi_D^*(D)\,V(A, B, C, D)\,\psi_A(A)\,\psi_B(B)\,d\tau_A\,d\tau_B\,d\tau_C\,d\tau_D$$

dove $\psi_A(A)$ rappresenta la funzione d'onda della particella A calcolata nel punto occupato dalla particella stessa e che per economia di simboli indichiamo con la stessa lettera usata per indicare la particella; e analogamente $\psi_B(B), \cdots$; l'asterisco indica l'operazione di « complesso coniugato »; V è un fattore della natura di una energia di interazione delle varie particelle presenti, che, almeno in un certo ordine di approssimazione, si potrà descrivere come una energia potenziale mutua, funzione delle coordinate delle quattro particelle, $V(A, B, C, D)$; e l'integrale va esteso a tutte le posizioni che le particelle possono assumere, indipendentemente l'una dall'altra: si tratta dunque di un quadruplice integrale di volume.

In realtà la presenza del fattore $V(A, B, C, D)$, che rappresenta l'energia mutua di posizione fra le quattro particelle e che presumibilmente tenderà a zero quando le particelle si allontanano indefinitamente le une dalle altre, implica essenzialmente l'esistenza di una azione a distanza fra le varie particelle, che interagirebbero anche quando non sono in contatto (a meno di introdurre un campo, che sia il portatore di queste interazioni

il che implicherebbe l'esistenza di nuove particelle, quelle derivanti dalla quantizzazione del campo stesso; in altre parole, l'interazione fra le particelle in esame perderebbe il carattere di interazione fondamentale). Ora ci sono delle serie difficoltà teoriche – e le cito semplicemente senza entrare molto in dettagli – ad ammettere l'esistenza di azioni a distanza. La difficoltà consiste essenzialmente nella contraddizione con la teoria della relatività, perchè se due particelle A e B interagiscono a distanza e la particella A ad un certo istante si muove, la perturbazione dovuta a questo movimento dovrebbe giungere istantaneamente nel punto occupato dalla particella B, situata ad una distanza finita, invece di propagarsi con una velocità che, secondo la teoria della relatività, deve essere in ogni caso minore della velocità della luce.

Per ovviare a questo inconveniente, la funzione V che compare nella espressione dell'elemento di matrice deve scegliersi in modo alquanto singolare: si ammette cioè che essa sia diversa da zero (in realtà infinita) solo quando le quattro particelle sono in contatto, cioè, dato che le consideriamo come puntiformi, quando i quattro punti A , B , C , D coincidono. Questo permette evidentemente una sostanziale semplificazione dell'integrale della formula (6): le quattro funzioni $\psi_A, \psi_B, \psi_C, \psi_D$ andranno calcolate tutte nello stesso punto P e l'integrale quadruplo si riduce ad un solo integrale di volume, esteso a tutte le posizioni del punto P. Sviluppando il calcolo si trova

$$H = f \int \psi_C^*(P)\, \psi_D^*(P)\, \psi_A(P)\, \psi_B(P)\, d\tau \tag{7}$$

dove f è un coefficiente opportuno che rappresenta l'intensità dell'interazione fra le quattro particelle.

Accenniamo solamente, a questo punto, al fatto che l'espressione che stiamo deducendo in questo modo per l'elemento di matrice della transizione dipende in maniera essenziale dal modo che si sceglie di descrivere mediante funzioni d'onda le particelle e le loro interazioni: e di questi modi se ne possono scegliere molti e molto diversi fra loro. Prima di tutto, l'espressione scritta per H contiene soltanto le funzioni d'onda stesse e non le loro derivate: il che, in molti casi, non sarebbe contrario alla condizione di invarianza relativistica. In altri casi, e precisamente per tutte le particelle che hanno un momento angolare intrinseco, o, come si usa dire, uno « spin », la descrizione mediante una sola funzione d'onda è assolutamente inadeguata, ed al posto di quelle che io ho indicato come semplici funzioni scalari, andrebbero in realtà grandezze a più componenti. L'esempio più noto è quello del campo elettromagnetico, che si può descrivere per mezzo di un potenziale scalare e un potenziale vettore: così che l'onda elettromagnetica è caratterizzata in genere da quattro grandezze, le tre componenti del potenziale vettore e il potenziale scalare. Analogamente le particelle dotate di spin 1/2, come per esempio l'elettrone, sono rappresentate, nella teoria di Dirac, per mezzo di funzioni a quattro componenti. E così, in un gran numero di casi, nell'espressione (7), al posto di un prodotto di quattro funzioni scalari, comparirebbe una combinazione quadrilineare di tutte le componenti relative a tutte le particelle, combinazione che conterrebbe molti coeffi-

cienti, invece di uno solo come nel caso semplice da noi esaminato. I coefficienti non sarebbero completamente arbitrari, perchè limitati dalle condizioni di invarianza relativistica; rimarrebbe però, in ogni caso, una arbitrarietà sufficiente perchè non si possa affermare che il valore dell'elemento di matrice sia sostanzialmente dipendente da una sola costante.

Tuttavia, in molti calcoli in cui interessa soltanto l'ordine di grandezza, e talvolta anche perchè non si saprebbe fare di meglio, si usano espressioni semplificate del tipo (7), contenenti una sola costante, in attesa di conoscere il fenomeno più profondamente e di diventare, un po' alla volta, in grado di adoperare il formalismo più idoneo alla trattazione del problema.

Nell'espressione da noi scritta per l'elemento di matrice è inclusa già la necessità della conservazione della quantità di moto. Si vede infatti facilmente che questo integrale si annulla, se la conservazione della quantità di moto non è soddisfatta. Se, per esempio, lo stato della particella A è uno stato in cui la particella ha momento p_A, la funzione d'onda corrispondente contiene un fattore, dipendente dalle coordinate di spazio, che è un esponenziale immaginario del tipo

$$e^{i\frac{p_A \cdot r_A}{\hbar}}$$

dove il segno $\times$ rappresenta l'operazione di prodotto scalare ed r_A è il raggio vettore che individua la posizione della particella A.

La parte dipendente dallo spazio dell'integrando della (7) contiene perciò quattro fattori di quel tipo, i quali si possono riunire in un solo esponenziale:

$$e^{\frac{i}{\hbar} r \cdot (p_A + p_B - p_C - p_D)} \tag{8}$$

le quantità di moto delle particelle C e D compaiono all'esponente con il segno meno perchè nell'integrando della (7) comparivano le quantità complesse coniugate delle corrispondenti funzioni d'onda.

Se la quantità di moto si conserva,

$$p_A + p_B = p_C + p_D :$$

l'esponente della (8) si annulla e l'espressione stessa diviene costante ed uguale ad 1; viceversa, se la quantità di moto non si conserva, l'esponenziale (8) viene ad essere un fattore oscillante il cui integrale esteso a tutto lo spazio è sempre nullo: risulta allora nullo anche l'elemento di matrice. Ciò significa che non possono mai avvenire delle transizioni fra due stati tali che la quantità di moto totale finale è diversa da quella iniziale. Questa proprietà è comune anche a tutti gli altri integrali dello stesso tipo che si incontrano sviluppando la teoria in modo più completo: essi si annullano se non è soddisfatta la conservazione della quantità di moto.

Se lo stato iniziale e lo stato finale sono tali da soddisfare la conservazione della quantità di moto, l'esponenziale, come abbiamo visto, si riduce ad 1 e l'integrando diventa indipendente dalla posizione. L'integrazione dà quindi semplicemente il volume di integrazione, cioè il volume Ω della scatola a cui abbiamo accennato in principio; in più ci sarà un fattore dipen-

dente dai coefficienti di normalizzazione delle funzioni d'onda delle singole particelle: e questo è un punto su cui dobbiamo soffermarci un momento, perchè il comportamento di questi coefficienti risulta essere differente, a seconda che si tratti di particelle che obbediscono al principio di esclusione di Pauli, oppure di particelle che obbediscono alla statistica di Bose–Einstein.

Nel primo caso, il calcolo del coefficiente di normalizzazione è molto semplice. La presenza, nella nostra scatola di volume Ω, di una particella per esempio del tipo A, sarà rappresentata da una funzione d'onda del tipo accennato dianzi:

$$\psi_A = b e^{\frac{i}{\hbar} \boldsymbol{p} \cdot \boldsymbol{r}} \tag{9}$$

dove $\hbar$ è il coefficiente che vogliamo determinare. La condizione di normalizzazione richiede che l'integrale del quadrato del modulo della funzione d'onda, esteso a tutto il volume della scatola, sia uguale ad 1. Ma il quadrato del modulo dell'esponenziale è uguale ad 1, e l'integrazione sulle coordinate spaziali dà semplicemente il volume della scatola Ω. Si ha dunque

$$\int_{\Omega} |\psi_A|^2 d\tau = b^2 \Omega = 1 .$$

È quindi semplicemente

$$b = \frac{1}{\sqrt{\Omega}} .$$

Nel caso che la particella obbedisca alla statistica di Bose–Einstein, il calcolo non è più così semplice. Riferiamoci, per maggiore chiarezza, ad un caso concreto e familiare, che è quello del fotone e del campo elettromagnetico ad esso associato. Supponiamo dunque che nella scatola di volume Ω ci sia un fotone; per brevità faremo un calcolo puramente sugli ordini di grandezza, senza interessarci dei fattori numerici prossimi all'unità, per i quali metteremo i valori giusti nelle formule finali. La scatola sarà dunque sede di un sistema di onde elettromagnetiche, in cui il campo elettrico avrà un certo valore E, uguale, se si usa il sistema di unità di Gauss, al valore del campo magnetico H. La densità di energia w è data, come è noto, da

$$w = \frac{1}{8\pi} (E^2 + H^2) .$$

Ricordando che $E = H$ e disinteressandoci del fattore $\frac{1}{4\pi}$ possiamo dire che la densità di energia è dell'ordine di grandezza di E^2, e l'energia totale racchiusa nella scatola è dell'ordine di grandezza di $E^2 \Omega$. Questa deve essere uguale all'energia W del fotone; il che ci dà per l'intensità del campo elettrico, sempre come ordine di grandezza:

$$E = H \sim \sqrt{\frac{W}{\Omega}} . \tag{10}$$

Ma ciò che, nel caso di un'onda elettromagnetica, corrisponde all'ampiezza della funzione d'onda del fotone non è il campo elettrico, ma il potenziale vettore A, legato al campo elettrico della relazione

$$\mathbf{E} = -\frac{1}{c} \frac{\partial \mathbf{A}}{\partial t} .$$

Ora, la derivata temporale di una grandezza variabile periodicamente è dell'ordine di grandezza dell'ampiezza moltiplicata per la frequenza ν. Possiamo quindi scrivere, moltiplicando numeratore e denominatore per la costante di Planck h

$$\text{(11)} \qquad E \sim \frac{h\nu}{hc} A = \frac{WA}{hc}.$$

Confrontandola (10) con la (11) si ricava che A, analogo della funzione d'onda per il fotone, è data, come ordine di grandezza, dalla relazione

$$A \sim \frac{hc}{W} \sqrt{\frac{W}{\Omega}}.$$

Ritornando al caso generale, ed introducendo i fattori numerici corretti, si trova analogamente che il modulo della ampiezza della funzione di onda per una particella di energia totale W che obbedisca alla statistica di Bose–Einstein è

$$\text{(12)} \qquad |\psi| = \frac{\hbar c}{\sqrt{2\,\Omega W}}$$

e questa espressione viene spesso usata per il calcolo dell'elemento di matrice relativo ad una transizione in cui sia implicata una particella di quel tipo.

In realtà le cose sono spesso ancora meno semplici, e bisogna procedere con grande cautela; infatti, non è sempre vero che il potenziale di un'onda sia quello che si deve usare come analogo della funzione d'onda nel calcolo dell'elemento di matrice. Se si considera una particella, come per esempio il protone o meglio ancora il neutrone, dotata di un momento magnetico, si ha una interazione diretta del campo magnetico con il momento magnetico della particella; e per descriverla bisognerebbe moltiplicare la densità di probabilità che il neutrone sia in una certa posizione per il suo momento magnetico e per il campo magnetico dell'onda, il quale, come si vede dalla (10), è proporzionale a $W^{1/2}$, invece che a $W^{-1/2}$ come la funzione d'onda della formula (12). Questa è una fonte di considerevole indefinizione della teoria; se si sapesse come va fatta la teoria « vera », si saprebbe naturalmente in quali casi va usata una formula del tipo (12) ed in quali casi va usata una formula dell'altro tipo; ma la teoria « vera » non esiste, per il momento. Quel che si può dire è che in questa circostanza sta la giustificazione di certi peculiari fenomeni, che sono stati scoperti dai fisici teorici: per esempio del fatto che le interazioni elettromagnetiche di un mesone sono, alle alte energie, molto più forti, e crescono molto più rapidamente con l'energia se il mesone ha uno spin elevato, che non se il mesone ha uno spin nullo od uguale a $1/2$.

Per il resto, al momento presente, noi sappiamo così poco, che la scelta fra una formula del tipo (12) od una formula dell'altro tipo deve purtroppo farsi semplicemente a caso. E nell'esempio che ora descriveremo faremo uso, per semplicità, direttamente della formula (12).

Scegliamo, come esempio di applicazione dei metodi generali che abbiamo descritto, la più semplice delle reazioni a cui abbiamo accennato in principio: la conversione di un mesone π in un mesone μ e un neutrino

$$\text{(13)} \qquad \pi \to \mu + \nu.$$

Delle tre particelle coinvolte nella reazione si ritiene (ed anche questa affermazione va fatta con una certa cautela) che il mesone π obbedisca alla statistica di Bose–Einstein, mentre il mesone μ e il neutrino obbedirebbero al principio di Pauli. La formula (4) e le seguenti ci permettono allora di esprimere direttamente la probabilità di transizione, mediante una formula (che risulta esser valida sia per mesoni liberi, sia per mesoni comunque vincolati), che contiene una sola costante empirica f, quella che compare nell'espressione dell'elemento di matrice H. È opportuno soffermarci un momento a mostrare l'analogia di questo coefficiente con la carica elettrica. In un fenomeno di carattere elettromagnetico, l'interazione si può rappresentare sostanzialmente (e semplificando un po' le cose) mediante il prodotto della densità di carica ρ per il potenziale V, integrato su tutto lo spazio:

$$\int \rho V \, d\tau \,. \tag{14}$$

Trattandosi di un'onda elettromagnetica, avremmo dovuto far uso del potenziale vettore, ciò che non abbiamo fatto, come al solito, per ragioni di semplicità. D'altra parte la densità di carica si può scrivere come il prodotto della carica dell'elettrone per il quadrato del modulo della funzione d'onda dell'elettrone stesso

$$\rho = e\,|\psi|^2 \,. \tag{15}$$

Introducendo la (15) nella (14) si ottiene, per l'energia di interazione

$$e \int |\psi|^2 V d\tau \,;$$

questa rappresenta, come è noto, la perturbazione dell'energia di uno stato stazionario dell'elettrone dovuta all'interazione dell'elettrone stesso con il potenziale V. Nel caso che si voglia trattare, invece, un problema di transizione da uno stato all'altro, le regole della meccanica quantistica insegnano che al modulo quadrato della funzione d'onda corrispondente allo stato stazionario va sostituito il prodotto della funzione d'onda dello stato finale $\psi_{e'}$ per il complesso coniugato della funzione d'onda ψ_e, dello stato iniziale; mentre al potenziale d'interazione V si può sostituire la funzione d'onda ψ_γ del fotone che viene emesso nella transizione; l'elemento di matrice della transizione risulta dunque rappresentato dall'espressione.

$$e \int \psi_e^* \psi_{e'} \psi_\gamma \, d\tau$$

analoga alla (7), salvo che al posto del coefficiente f compare la carica dell'elettrone.

Questa si presenta dunque come il coefficiente che determina, per così dire, l'intensità dell'interazione tra l'elettrone e il campo elettromagnetico. Se invece di un elettrone avessimo considerato un protone, avremmo ottenuto un risultato analogo, ed il coefficiente sarebbe stato lo stesso, giacchè, per quanto ne sappiamo (benchè non ne sappiamo dare la spiegazione) la carica elettrica del protone è la stessa di quella dell'elettrone.

Nel caso della reazione $\pi \to \mu + \nu$ l'elemento di matrice si scrive

$$H = f \int_{\Omega} \psi_{\pi}^{*} \psi_{\mu} \psi_{\nu} \, d\tau; \tag{16}$$

il coefficiente f ha dunque per il fenomeno in esame un significato analogo a quello posseduto dalla carica elettrica per i fenomeni elettromagnetici ed anzi ha addirittura le stesse dimensioni della carica; per quel che riguarda il suo valore numerico, esso non può essere stabilito teoricamente a priori, ma deve essere determinato sperimentalmente.

L'integrale (16) si può calcolare agevolmente in base alle considerazioni che abbiamo svolto precedentemente: siccome la quantità di moto deve essere conservata, l'integrazione dei fattori dipendenti dalle coordinate spaziali dà semplicemente il volume Ω della scatola; e per i valori assoluti delle funzioni d'onda possiamo usare le espressioni (12) e (9), tenendo conto del fatto che il mesone π va considerato come un « Bosone », cioè come una particella che obbedisce alla statistica di Bose–Einstein, mentre mesone μ e neutrino obbediscono al principio di esclusione di Pauli. In formule

$$H = f \int_{\Omega} \psi_{\pi}^{*} \psi_{\mu} \psi_{\nu} \, d\tau = f \, |\psi_{\pi}| \, |\psi_{\mu}| \, |\psi_{\nu}| \int_{\Omega} d\tau \tag{17}$$

$$= f\Omega \frac{\hbar c}{\sqrt{2\,\Omega m_{\pi} c^{2}}} \cdot \frac{1}{\sqrt{\Omega}} \cdot \frac{1}{\sqrt{\Omega}} = \frac{f\hbar}{\sqrt{2\,\Omega m_{\pi}}}$$

dove per l'energia W_{π} del mesone π abbiamo posto l'energia di quiete $m_{\pi} c^{2}$ supponendo che, nello stato iniziale, il mesone π sia fermo.

Per calcolare la probabilità di transizione occorre ancora trovare l'espressione della densità n degli stati finali. Come al solito, semplificheremo il calcolo ammettendo che, siccome il neutrino ha una massa molto minore delle altre due particelle, ed in particolare del mesone μ, si possa trascurare, nello stato finale, la quantità di moto di quest'ultimo rispetto alla quantità di moto del neutrino; successivamente introdurremo senz'altro nella formula finale quelle modificazioni, facilmente comprensibili, che risultano da un calcolo più rigoroso. Detta dunque p_{ν} la quantità di moto del neutrino, il numero dN degli stati finali si ottiene, come è noto, dividendo per il cubo della costante di Planck h il volume dello spazio delle fasi corrispondenti ad una quantità di moto compresa fra p_{ν} e $p_{\nu} + dp_{\nu}$ e ad una posizione della particella interna alla scatola Ω; cioè, usando $\hbar$ invece che h

$$dN = \frac{4\pi p_{\nu}^{2} \, dp_{\nu} \, \Omega}{8\pi^{3} \hbar^{3}}$$

e la densità n degli stati si ottiene dividendo dN per l'intervallo di energia $dE = c \, dp_{\nu}$.

$$n = \frac{dN}{dE} = \frac{p_{\nu}^{2} \Omega}{2\pi^{2} \hbar^{3} c}. \tag{18}$$

Siamo ora in grado di calcolare il valore della probabilità di transizione $1/\tau$ introducendo nella formula (4) la espressione della densità degli stati finali data dalla (18) e il quadrato dell'elemento di matrice dato dalla (7); il volume

Ω della scatola, che ci eravamo trascinato dietro fino ad ora, si elide, ciò che è confortante; e si ottiene:

$$\frac{1}{\tau} = \frac{f^2}{2\pi\hbar^2 c m_\pi} p_\nu^2 .$$

Tenendo conto anche della quantità di moto del mesone che avevamo trascurato, il risultato viene leggermente modificato per l'aggiunta di un fattore numerico, prossimo ad 1:

$$\frac{1}{\tau} = \frac{f^2}{2\pi\hbar^2 c m_\pi} \frac{p_\nu^2}{1+\frac{v_\mu}{c}}$$

dove v_μ è la velocità con cui viene emesso il mesone μ, che è abbastanza piccola rispetto alla velocità c della luce.

Nel secondo membro della espressione ora scritta tutto è noto, tranne la costante f. Misurando sperimentalmente la vita media τ del mesone π per il processo in esame si può quindi determinare il valore di f, che, come abbiamo accennato, ha le dimensioni di una carica elettrica; il valore di f che così si ottiene risulta molto più piccolo della carica dell'elettrone, e conviene quindi esprimerlo come una frazione di questa carica; precisamente si ottiene

$$f \sim \frac{e}{4 \cdot 10^5} = 2{,}5 \; 10^{-6} e .$$

L'intensità della interazione che determina questa transizione è dunque circa due volte e mezzo un milionesimo dell'intensità dell'interazione fra elettrone e campo elettromagnetico.

Per concludere, voglio citare una circostanza notevolissima, che si presenta nello studio di questi fenomeni. Un calcolo analogo al precedente può essere sviluppato per molte altre reazioni; e in tutte le reazioni in cui è essenzialmente la carica elettrica che determina la interazione compare lo stesso coefficiente e, perchè tutte le particelle elementari conosciute, pur essendo essenzialmente diverse per tutte le loro altre caratteristiche, quando sono cariche (come il protone, il mesone, l'elettrone) hanno sempre la stessa carica, positiva o negativa, ma invariabile in valore assoluto: fatto del quale, come abbiamo già accennato, non si sa dare alcuna spiegazione soddisfacente (benchè siano state avanzate alcune ipotesi), ma che è sperimentalmente bene accertato. Ora, esistono tre reazioni di carattere non elettromagnetico, di due delle quali abbiamo già parlato in principio, nelle quali la costante di interazione ha le stesse dimensioni (che però non coincidono con quelle di una carica elettrica, essendo il prodotto di un volume per un lavoro). Le tre reazioni sono schematicamente le seguenti

$$(19) \qquad \begin{cases} \mathrm{N} \to \mathrm{P} + e + \nu \\ \mu^\pm \to e^\pm + 2\,\nu \\ \mathrm{P} + \mu^- \to \mathrm{N} + \nu . \end{cases}$$

La prima è la transizione β dei nuclei; la seconda è la disintegrazione del mesone μ, con vita media $\tau = 2.1 \; 10^{-6}$ secondi. La terza, di cui non abbiamo ancora parlato ed a cui accenneremo senza dare molti dettagli, è stata messa

in evidenza dalla esperienza di Conversi, Pancini, Piccioni sulla cattura, nella materia, dei mesoni μ: un mesone μ negativo verrebbe assorbito da un protone, che si trasformerebbe in un neutrone, con emissione di un neutrino. Naturalmente anche in questo caso la presenza del neutrino è puramente ipotetica; comunque, dallo studio dei risultati delle esperienze citate si traggono dei dati che permettono di calcolare anche in questo caso la costante di interazione.

Abbiamo dunque tre costanti di interazione f_1, f_2, f_3 aventi le stesse dimensioni e relative a tre reazioni che a priori, per quanto ne sappiamo al momento attuale, sono completamente diverse l'una dall'altra: anche assumendo senz'altro la validità degli schemi indicati (che invece, come abbiamo già visto, vanno presi con una certa cautela), si può osservare, per esempio, che nella seconda reazione vengono emessi due neutrini, mentre nella prima e nella terza ne viene emesso uno solo. Il fatto notevolissimo, e molto suggestivo, al quale ho accennato, e per il quale non esiste alcuna spiegazione, è che i valori numerici di queste costanti, calcolati con i metodi precedentemente indicati, risultano molto vicini tra loro. Non si può dire che siano esattamente uguali, ma sono compresi in un intervallo di circa 10 unità: tra 10^{-48} e 10^{-49}. Non sarebbe facile dire di più, perchè, come abbiamo più volte accennato, il nostro modo di vedere teorico su questi fenomeni è ancora estremamente rudimentale e possiamo considerarci fortunati se le formule rappresentano correttamente gli ordini di grandezza. Ma, come ordine di grandezza, queste quantità sono certo molto vicine, specialmente se si osserva che, dopo tutto, trattandosi di numeri tanto inusuali, si potrebbe considerare l'ordine di grandezza dei loro logaritmi, che sono rispettivamente —48, —49.

Questo fatto è stato notato indipendentemente da vari ricercatori: fra gli altri Wheeler e Puppi hanno segnalato la strana concordanza numerica di alcune di queste costanti ed osservato che questo suggerirebbe (se si vuole ardire una interpretazione di questo genere), l'esistenza di una proprietà analoga alla carica elettrica, che si presenta nello stesso modo in tutte le particelle elementari. Abbiamo già più volte osservato che anche nel caso elettromagnetico non conosciamo la ragione, che certamente è estremamente significativa, per la quale particelle tanto diverse come l'elettrone, il protone, il mesone, possiedono tutte la stessa carica elettrica. In quel caso la nostra conoscenza dei fenomeni elettromagnetici è tale da permetterci di asserire che la carica elettrica ha sempre, con grandissima approssimazione, lo stesso valore, e non semplicemente lo stesso ordine di grandezza. Nel caso delle reazioni del tipo (19) le nostre conoscenze sono molto più limitate, e non possiamo dire più di quanto abbiamo visto; può darsi, naturalmente, che ad una analisi più completa, quando sarà possibile farla, quei fenomeni appaiano fra loro simili ma i valori delle costanti non risultino esattamente uguali; nel qual caso quella concordanza sarebbe solamente un caso, forse un po' strano, ma non impossibile. Ma se, il giorno in cui si potrà fare una teoria rigorosa e non solamente grossolanamente approssimativa, si trovasse che la grandezza f analoga della carica elettrica è effettivamente, per quei tre fenomeni così diversi tra loro, la stessa, questa sarebbe certamente una indicazione di significato teorico grandissimo e probabilmente denso di conseguenze – benchè al momento presente queste conseguenze non si possano prevedere.

TERZA CONFERENZA (*)

TEORIE SULLE ORIGINI DEGLI ELEMENTI

(redatta dal Prof. E. PANCINI)

Tutta la materia conosciuta è costituita da vari elementi chimici presenti ciascuno con diversa abbondanza, onde sorge il problema, sperimentale dapprima, teorico poi, di comprendere per quale ragione alcuni elementi siano abbondanti, altri rari.

Il problema è innanzi tutto un problema sperimentale, e senza voler discutere qui la questione in dettaglio, bastano per comprenderlo alcune osservazioni di carattere generale. Quel che si cerca di stabilire è la quantità dei vari elementi chimici che si trovano, diciamo così, in tutto l'Universo, o almeno in una larga porzione di esso, e, naturalmente, il risultato che ci si può attendere di ottenere dipende in larga misura dai campioni di materia scelti per l'analisi. Per esempio, se si possono determinare le quantità relative di ossigeno, ferro, idrogeno e altri elementi che si trovano nella parte della crosta terrestre che è accessibile alle nostre osservazioni dirette si ricaverà, per ognuno di essi una certa abbondanza relativa; ma se si determina nvece, per esempio, la percentuale degli stessi elementi analizzando i meteoriti si riscontrerà una distribuzione di elementi diversa da quella che si trova nelle rocce superficiali della Terra.

Il problema, pertanto, più che un problema di analisi chimica è essenzialmente un problema di scelta degli esemplari da analizzare.

La questione naturalmente non è nuova; i dati che saranno qui presentati sono ottenuti da ricerche piuttosto recenti di Harrison S. Brown (1), dell'Università di Chicago, che ha esteso, ampliato e perfezionato i risultati di Goldschmidt (2). I dati sono stati ottenuti analizzando una grande quantità di esemplari e questo è garanzia della loro attendibilità perché dati ottenuti da un esemplare particolare rivelano piuttosto le caratteristiche speciali di esso che non quella che può essere considerata la distribuzione cosmica degli elementi.

È notevole il fatto che, a dispetto di questa osservazione, la conclusione di queste analisi è che, quando opportuna attenzione sia fatta alla scelta dei campioni da analizzare, i risultati sono estremamente uniformi anche se tratti da materiali di diversissima origine. Si riesce per esempio, in alcuni casi favorevoli, ad assegnare il rapporto dell'abbondanza cosmica di due elementi con una precisione dell'ordine dell'1 o 2 %.

Si noti che le misure dell'abbondanza degli elementi fatte sulla crosta terrestre, se pure hanno una grandissima importanza pratica, hanno una importanza teorica abbastanza più limitata perché la crosta terrestre, anzi

(*) Tenuta il 7 ottobre 1949 nell'aula dell'Istituto Fisico dell'Università di Roma.

(1) « Rev. Mod. Phys. », *21*, 625 (1949).

(2) V. M. GOLDSCHMIDT, « Geochemische Verteilungsgesetze der Elemente und der Atomarten », IX, Oslo 1938.

tutto il materiale di cui è costituita la Terra, è stato, durante le ere geologiche, assoggettato ad una profonda separazione chimica cosicché risultati significativi si potrebbero solo ottenere da una analisi fatta studiando campioni prelevati in zone che vanno dalla superficie della Terra fino al suo centro il che, naturalmente, è impossibile.

Fortunatamente questa impossibilità di prelevare i campioni nella parte interna della Terra può essere girata prendendo in esame la costituzione dei meteoriti che, a quanto dicono gli esperti, sono come esemplari prelevati in varie zone di pianeti scomparsi. Così se la Terra, per una catastrofe cosmica, andasse in pezzi, i meteoriti provenienti dalla sua crosta sarebbero meteoriti costituiti essenzialmente da pietra, mentre quelli provenienti dalla sua parte centrale sarebbero essenzialmente costituiti da ferro, o più precisamente da una lega costituita, in gran parte, da ferro e poi da nichel e poi in quantità sempre minori da altri elementi.

Effettivamente una analisi statistica dei meteoriti che arrivano sulla Terra (e i meteoriti che arrivano sulla Terra sono proprio di questi due tipi) indica che il rapporto fra le quantità di materia in forma di meteoriti di pietra e le quantità di materia in forma di meteoriti di ferro non è molto dissimile dal rapporto fra la parte pietrosa e la parte ferrosa della Terra quale risulta dalle investigazioni fatte in profondità per mezzo delle onde sismiche.

Le ricerche delle quali parliamo sono state fatte in gran parte raccogliendo pazientemente una grande quantità di meteoriti e facendo su di essi delle analisi quantitative estremamente accurate. Conviene rilevare che il problema di eseguire queste analisi è molto meno semplice di quel che possa sembrare perché molti degli elementi, anzi, come vedremo, la maggioranza degli elementi, sono tanto rari da essere presenti in quantità dell'ordine di alcune parti per milione ed anche meno. Una delle difficoltà più grandi del problema è quindi quella di trovare il modo di eseguire delle analisi chimiche quantitative di una delicatezza estrema. Per superare questa difficoltà si è dovuto perfino fare uso (almeno negli studi recenti che sono stati compiuti nell'Università di Chicago) delle pile atomiche che sono state usate per irradiare il materiale in esame onde poterne poi osservare le attività caratteristiche degli elementi ai quali si è interessati. Il riconoscimento degli elementi è fatto, dunque, per questa via essenzialmente con metodi radioattivi anziché chimici. Con questi mezzi si è riusciti ad analizzare il materiale che arriva sulla Terra sotto forma di meteoriti ferrosi e pietrosi e, prendendo sui dati ottenuti delle medie con opportuni criteri, è stata costruita una tabella che, per la maggioranza degli elementi, coincide assai bene con altri dati di origine assolutamente diversa come, per esempio, quelli ottenuti dalla osservazione spettroscopica della atmosfera stellare. Si ha così una indicazione che la materia della quale sono costituiti i meteoriti, non è sostanzialmente diversa da quella che costituisce le atmosfere stellari. Vi sono in realtà alcune eccezioni assai notevoli, ma facili da spiegare: ci sono per esempio alcuni elementi che praticamente mancano, o sono presenti in quantità assai minori del dovuto, nei meteoriti. Questo è il caso dei gas nobili che sono, sia nella Terra che nei meteoriti, presenti in quantità assai minore di quella competente alla loro abbondanza cosmica in quanto, nel processo di formazione dei pia-

neti, non sono stati in essi trattenuti. Un'altra eccezione ancora più notevole è quella dell'idrogeno, ma anche questa eccezione si spiega con ragionamenti analoghi a quelli fatti per i gas rari.

Fatti di questo genere rendono evidente come i risultati ottenuti dalla analisi dei meteoriti (dalla quale si trae il maggior numero dei dati quantitativi sull'abbondanza cosmica degli elementi) debbano essere rielaborati attraverso una accurata discussione chimica la quale, per altro, è purtroppo quasi del tutto arbitraria poiché coinvolge ipotesi sulle modalità di formazione dei meteoriti stessi e sulle caratteristiche chimico–fisiche dell'ambiente nel quale hanno passata la loro storia. Insomma l'analisi dei meteoriti, elemento per elemento, deve essere integrata attraverso considerazioni chimico–teoriche che consentano di giudicare se è da ritenersi o meno, che l'elemento in questione abbia conservate le proprie proporzioni cosmiche nei meteoriti.

Oltre che i meteoriti sono stati oggetto di studio le atmosfere stellari (attraverso l'analisi spettroscopica) e, in parte, le nuvole di materia dello spazio interstellare attraverso l'analisi del loro spettro di assorbimento. Questi ultimi dati sono peraltro estremamente scarsi e da usarsi unicamente come sussidiari. Ciò che è comunque assai notevole è il fatto che tutti questi dati (ove si tenga debito conto delle eccezioni citate, le quali si possono, peraltro, giustificare con argomenti molto persuasivi) tratti dall'analisi di oggetti celesti tanto diversi come l'atmosfera stellare, la materia interstellare o i meteoriti, coincidono assai bene. Variano invece notevolmente, come si è già detto, i dati che si possono ricavare dall'analisi della crosta terrestre poiché, ripetiamo la crosta terrestre non è un campione fedele di quello che può ritenersi essere il materiale di cui la Terra è costituita.

Ciò detto è interessante esaminare la tabella qui riportata nella quale sono dati dei numeri che rappresentano l'abbondanza relativa di vari elementi.

ABBONDANZA RELATIVA DEGLI ELEMENTI

	A	Z	Atomi per 10^4 atomi di silicio
H	1,01	1	$3{,}5 \times 10^8$
He	4	2	$3{,}5 \times 10^7$
Be	9,02	4	2×10^{-1}
C	12,01	6	8×10^4
O	16,00	8	1×10^5
Si	28,06	14	10^4
Cl	35,46	17	$2{,}5 \times 10^2$
Mn	54,93	25	1×10^2
Fe	55,85	26	$2{,}6 \times 10^4$
Co	58,94	27	$1{,}6 \times 10^2$
Ni	58,69	28	$2{,}0 \times 10^3$
Cu	63,57	29	7
Ga	69,72	31	5×10^{-3}
Sr	87,63	38	10^{-1}
Cd	112,41	48	2×10^{-2}
Cs	132,91	55	10^{-2}
Pt	195,23	78	10^{-1}
Pb	207,21	82	4×10^{-3}
Th	231,12	90	10^{-2}
U	238,07	92	3×10^{-3}

Questi dati sono tratti dai lavori di Harrison S. Brown che possono ritenersi i più aggiornati; i numeri elencati nella tabella si riferiscono ad alcuni degli elementi più significativi e sono sufficienti a mettere in luce alcune caratteristiche assai strane dell'andamento, in funzione del numero atomico, dell'abbondanza relativa dei vari elementi. Essi rappresentano il numero degli atomi di ciascun elemento presenti, in media, nella materia cosmica per ogni 10^4 atomi di silicio 14.

Nell'analizzare questa tabella conviene cominciare con l'idrogeno che è, non solo il più semplice fra gli elementi, ma anche quello più abbondante: il numero dei suoi atomi presenti nella materia cosmica per ogni 10^4 atomi di silicio è tre o quattro cento milioni. Dopo l'idrogeno sia nel sistema periodico degli elementi che nella scala delle abbondanze viene l'elio, l'abbondanza relativa del quale è, nella nostra scala, di 35 milioni. Per gli elementi che seguono l'elio l'abbondanza cala rapidissimamente a valori estremamente bassi: il litio, il berillio e il boro sono estremamente rari: l'abbondanza relativa del berillio, per esempio, è di 2 decimi (cioè per ogni atomo di berillio ce ne sono in media 50.000 di silicio). Come si vede fra elio e berillio c'è un salto di un fattore dell'ordine dei 100 milioni.

Gli altri elementi leggeri che seguono nel sistema periodico i tre ora citati hanno abbondanze poco diverse da quella del silicio: al carbonio, per esempio, va attribuita l'abbondanza 2×10^4. Subito dopo l'ossigeno segna una punta verso l'alto: 10^5. Esso è, dopo l'idrogeno e l'elio, l'elemento più abbondante in numero di atomi (ma non in peso).

Procedendo su questa scala si trovano abbondanze dell'ordine di qualche unità finché si giunge al ferro cui compete un'abbondanza notevolmente alta: $2{,}6 \cdot 10^4$. Poi il cobalto: $2{,}6 \cdot 10^2$, il nichel: $2 \cdot 10^3$, e, proseguendo nell'ordine del sistema periodico, a questo punto l'abbondanza comincia a calare rapidamente e non risale più. Dal gallio in poi fino all'uranio si trovano abbondanze che oscillano più o meno irregolarmente fra un decimo e un centesimo. Lieve eccezione è il piombo che ha un'abbondanza un po' superiore, ma si può pensare che la quantità di piombo sia aumentata per effetto del decadimento delle sostanze radioattive che si trovano immediatamente al di sopra di esso. Altra eccezione, in senso opposto, è l'uranio ma si può pensare che esso si sia impoverito a causa del suo decadimento radioattivo.

Tutti questi discorsi assumeranno probabilmente maggior evidenza se si rappresenta in un diagramma (fig. 1) l'abbondanza relativa degli elementi in funzione del numero atomico. Da questo diagramma si può vedere come subito dopo la punta estrema rappresentata dall'idrogeno e dall'elio vi sia tendenza a mostrare, benché con una grandissima irregolarità, un andamento decrescente dell'abbondanza relativa degli elementi. Cosicché uno che ardisse tracciare una curva attraverso questi punti, e non tenesse troppo conto delle irregolarità, potrebbe disegnare la curva riportata in figura 1. E, chi volesse ritenere che, giustificate le eccezioni, questa curva rappresenti con buona approssimazione l'abbondanza relativa degli elementi nella materia cosmica, dovrebbe concludere che l'abbondanza relativa di ciascun elemento è per esso una caratteristica essenziale come lo è, per esempio, il numero atomico, o la sua energia di formazione o la sua massa. Si ha dunque l'impres-

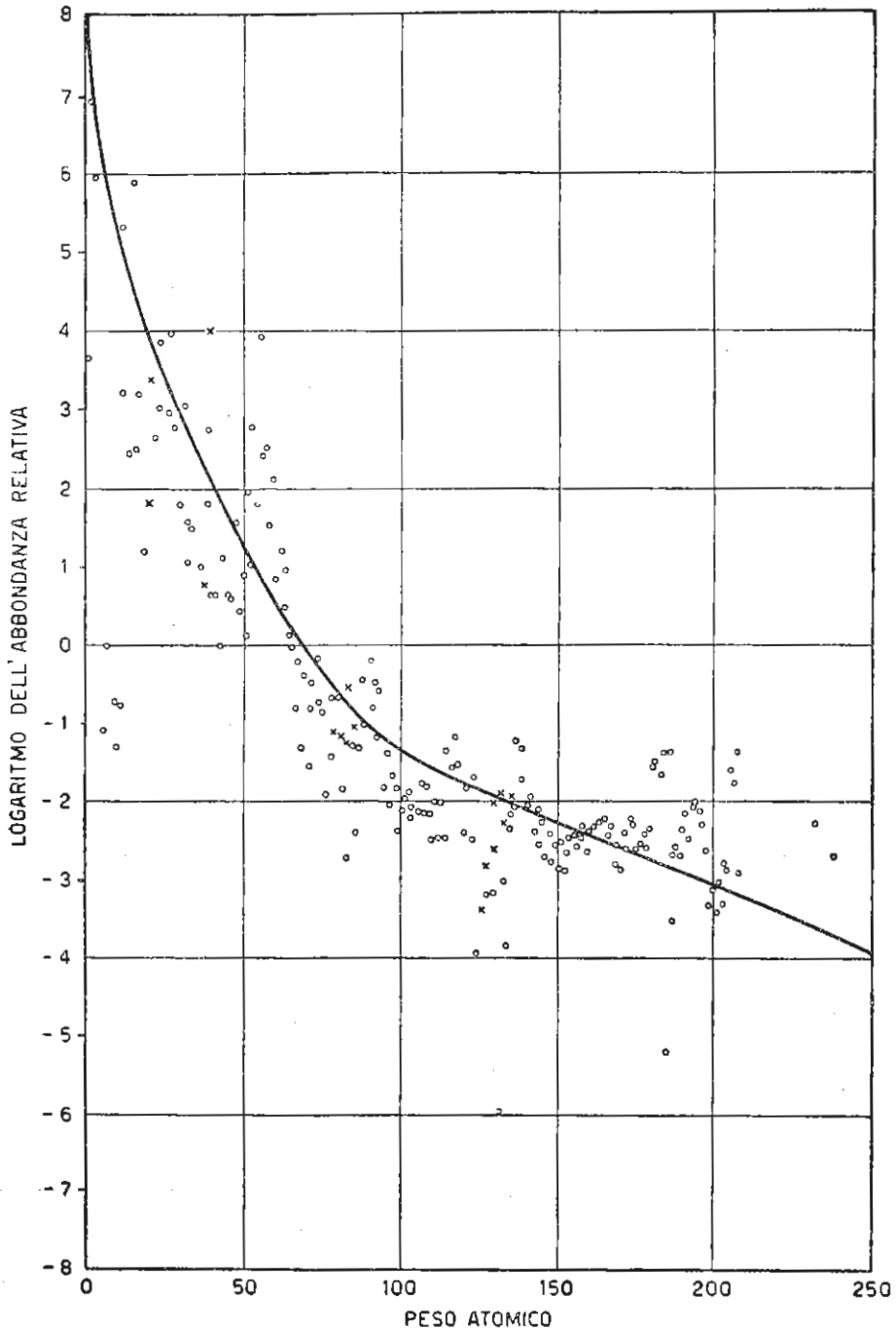

Fig. 1.

sione che l'abbondanza relativa di ciascun elemento sia realmente una sua proprietà, connessa, come è ovvio, sia con le altre proprietà dell'elemento sia col meccanismo, per altro ignoto, col quale l'elemento si è formato.

Naturalmente, in una discussione di questo genere si dovrà anche tenere conto dell'abbondanza dei singoli isotopi di ciascun elemento, ma questa

non è una complicazione del problema in quanto le abbondanze relative degli isotopi di ogni singolo elemento sono note e normalmente assai costanti: quindi nota l'abbondanza di ciascun elemento è semplice aritmetica calcolare l'abbondanza degli isotopi.

Anche studiando le abbondanze relative degli isotopi verrà fatto di notare delle regolarità sulle quali vale la pena di richiamare l'attenzione poiché su di esse ci sarà occasione di tornare in seguito.

In figura 2 è dato un diagramma degli isotopi portando in ascisse il numero dei protoni ed in ordinata il numero dei neutroni che costituiscono ciascun nucleo: come si vede i vari elementi sono distribuiti in una zona che ha inizialmente la direzione della bisettrice degli assi e poi piega in su (il che vuol dire che nei nuclei di piccolo numero atomico il numero dei protoni è uguale a quello dei neutroni mentre per i numeri atomici elevati la percentuale dei neutroni è, sempre più, superiore al 50 %). Ora si trova che quasi invariabilmente, nella parte bassa del sistema periodico – cioè per i nuclei leggeri – gli isotopi più abbondanti sono quelli più ricchi in protoni o, quel che è lo stesso, più poveri in neutroni; poi viene una zona di transizione e infine nella parte alta si osserva una tendenza del tutto opposta: gli isotopi più abbondanti tendono ad avere più neutroni che protoni.

Naturalmente l'idea di giustificare tutti questi fatti, giustificare cioè l'abbondanza dei singoli elementi e, per ciascun elemento, l'abbondanza dei suoi isotopi, è, certamente, un programma estremamente ambizioso e costituisce un problema dalla cui soluzione siamo, senza dubbio, molto lontani. Tuttavia vi sono stati recentemente dei tentativi in questo senso i quali, però, conducono a risultati che sono tutt'altro che soddisfacenti. Questo fatto non toglie che essi siano estremamente interessanti in quanto rappresentano un tentativo di ricerca in una direzione che sarà molto probabilmente una delle più importanti nell'avvenire. D'altra parte è ovvio che se le soluzioni oggi raggiunte non sono soddisfacenti non è da escludersi che, in seguito, si possano fare su questa strada passi conclusivi.

Una delle ipotesi più naturali che sia stata avanzata, e lo è stata infatti da vario tempo e da varie persone, è che gli elementi che noi troviamo in natura siano il risultato di un processo che si basa su una specie di equilibrio chimico o, come si dice, di equilibrio superchimico. In altre parole ci si può chiedere se sia lecito immaginare che ponendo in un calderone gli elementi costitutivi degli elementi, cioè protoni e neutroni, e poi scaldando il tutto a una opportuna temperatura e quindi, quando questa materia è, per così dire, cotta al punto giusto, freddando improvvisamente si possa ottenere un miscuglio di elementi che assomigli a quello che a noi sembra costituire l'Universo.

Molti tentativi in questo senso sono stati fatti ma i risultati ottenuti non sono, in verità, molto convincenti. Naturalmente le temperature e le pressioni che hanno sede in questa specie di calderone devono essere immaginate avere valori piuttosto sorprendenti se si vogliono ottenere risultati che non siano assolutamente discordanti da quelli sperimentali: la temperatura, per esempio, dovrebbe essere intorno ai 10 miliardi di gradi e la pressione intorno al milione di grammi per cm^2. La necessità di tali temperature

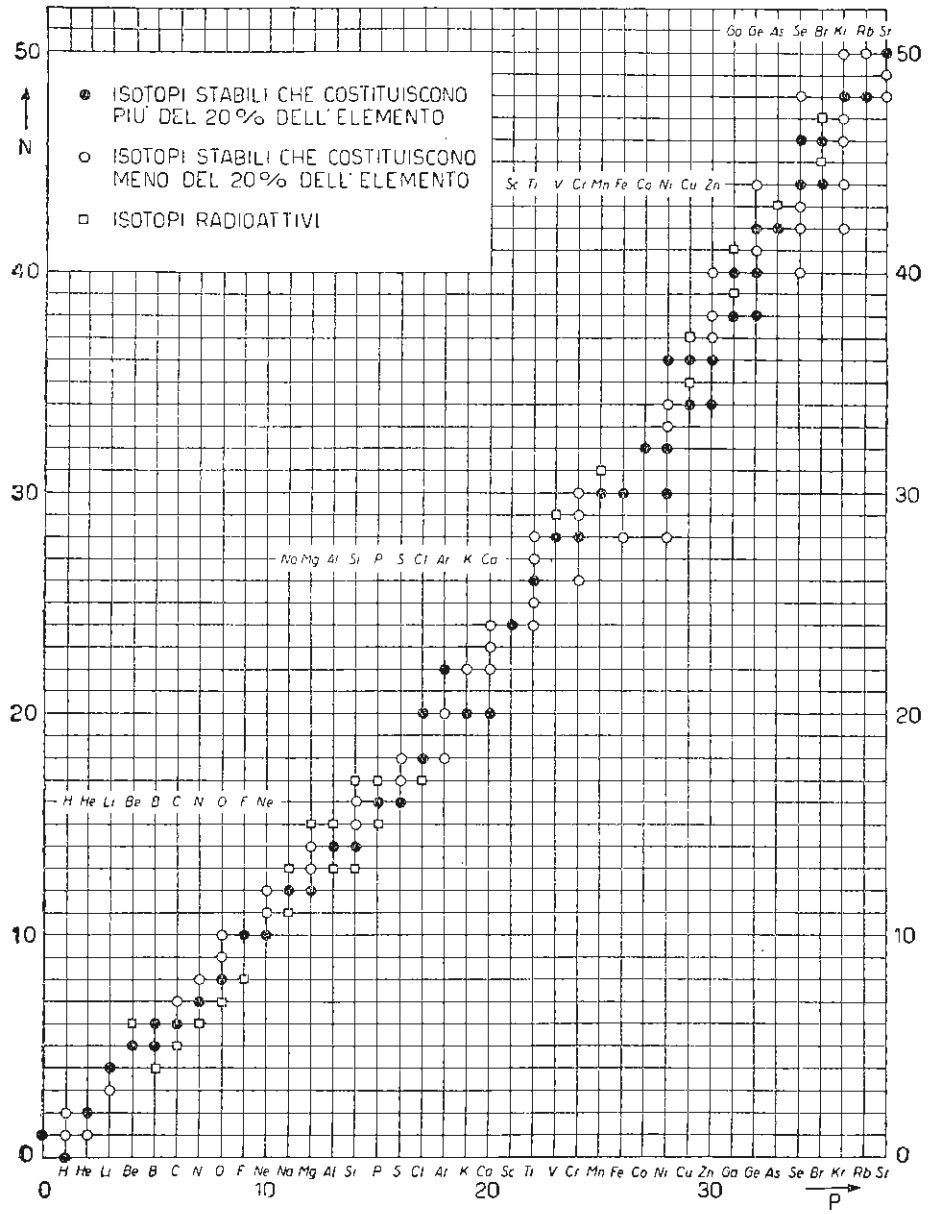

Fig. 2.

e di tali pressioni può essere compresa senza difficoltà appena si pensi che la temperatura deve essere molto grande per dare luogo, in maniera cospicua, a reazioni nucleari e che la pressione deve essere altissima perché ci sia la possibilità di formare nuclei molto pesanti. Infatti, se, a temperature così elevate, la pressione non fosse proporzionalmente alta, tutti i nuclei costituiti di molte particelle si disintegrerebbero e non ci sarebbe, quindi, possibilità di esistenza per i nuclei pesanti che invece si trovano in natura.

Sta di fatto, peraltro, che partendo da ipotesi siffatte non si riesce ad ottenere una distribuzione degli elementi che assomigli gran che a quella

reale: tanto per dire, le abbondanze relative dei vari isotopi, risultano distribuite completamente a caso e senza la minima somiglianza con quelle che si osservano sperimentalmente.

Le teorie più moderne si basano, invece, su di uno schema alquanto diverso: ci si limiterà qui a parlare di una sola di esse, quella che, a mio parere, è la più interessante benché non possa essere considerata, in alcun modo, capace di dare una spiegazione soddisfacente dei fatti. Essa è dovuta principalmente a Gamow il quale, essendo come tutti sanno un burlone, si è associato con altri due fisici, Alpher e Bethe, allo scopo, forse, di giocare sul fatto che, i tre nomi, Alpher, Bethe e Gamow, letti all'americana storpiando un po' le parole, possono sembrare i nomi delle prime tre lettere dell'alfabeto greco. In realtà, però, il contributo sostanziale dato alla teoria della quale trattiamo, è, sostanzialmente, quello di Gamow e, in parte, quello di Alpher: Bethe, invece, sembra essere stato associato soltanto per completare il gioco di parole.

Comunque sia, la teoria può dividersi, essenzialmente, in due parti. La prima ha per fondamento l'osservazione, in realtà non nuova, della possibilità di formare elementi, anche quando la temperatura e la pressione non assumano valori così sbalorditivi come quelli citati poco fa, purché si supponga di formare gli elementi attraverso successive aggiunte di neutroni. Senza soffermarci, per ora, a spiegare l'origine di questi neutroni cerchiamo di dare una idea del modo nel quale questa formazione può aver luogo.

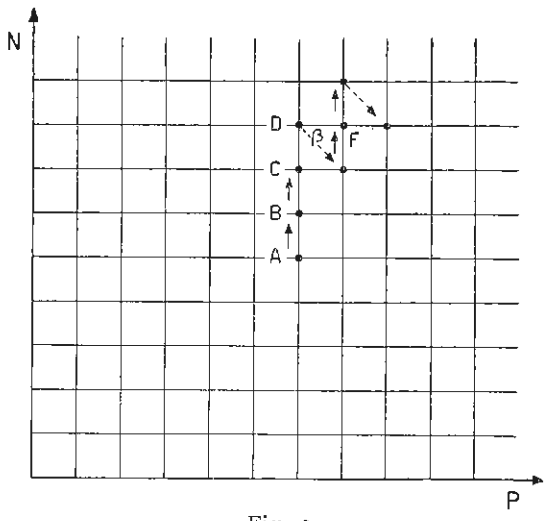

Fig. 3.

Riferiamoci ancora ad un diagramma P, N (fig. 2) nel quale ogni elemento è presentato da un punto la cui ascissa è uguale al numero di protoni e la cui ordinata è uguale al numero di neutroni in esso contenuti. Come si è già detto gli elementi stabili si trovano tutti in una zona molto ben definita.

Se supponiamo, ora, di esporre un certo elemento ad un « bagno » di neutroni potrà accadere che i suoi nuclei catturino uno di questi neutroni. Così, se la composizione di questo nucleo è rappresentata dal punto A di figura 3, dopo la cattura il nuovo nucleo formatosi avrà una composizione rappresentata dal punto B che si ottiene facendo da A un passo verso l'alto (infatti N è aumentato di uno e Z è rimasto costante).

Il nuovo nucleo potrà, a sua volta, assorbire un altro neutrone dando luogo ad un elemento rappresentato dal punto C e così via, fino a che si finirà per uscire dalla zona degli elementi stabili. L'elemento instabile formatosi sarà evidentemente radioattivo beta e quindi si disintegrerà con un processo beta che è un cambiamento di un neutrone in un protone: il nuovo punto

rappresentativo si otterrà, pertanto, facendo un passo verso il basso (diminuzione di un neutrone) ed un passo verso destra (aumento di un protone).

Se, ora, ci sono ancora neutroni presenti il nucleo così formatosi potrà assorbire un altro neutrone, poi ancora un altro neutrone quindi emetterà un raggio beta; e così poco alla volta si arrampicherà su per la china degli elementi stabili. Vengono così poco alla volta formandosi elemcnti molto pesanti attraverso un meccanismo di aggiunte successive di neutroni a nuclei leggeri che si suppongono essere preesistenti.

A questo punto, a volere essere ambiziosi (e come vedremo Gamow ha pretese ancora più ambiziose di queste), si può addirittura proporsi di spiegare la formazione di tutti gli elementi partendo da soli neutroni.

Supponiamo, infatti, che in una regione dello spazio, in un certo istante, siano contenuti dei neutroni. Ora, il neutrone, come si sa, non è una particella stabile, anzi la sua vita media è piuttosto corta (non è stata ancora misurata molto bene ma non può essere molto diversa da 15') e, pertanto, dopo circa dieci minuti, la metà dei neutroni sarà decaduta dando luogo ad altrettanti protoni. Ma neutroni e protoni hanno una certa affinità ed i neutroni tendono ad attaccarsi ai protoni, formando così dei nuclei di deuterio. Per questa via, partendo inizialmente da soli neutroni, per decadimento di essi ed associazione coi protoni generatisi, si potranno formare i primi nuclei leggeri, e poi da questi, con un processo del tipo di quello descritto poco fa, si potrà giungere presumibilmente alla formazione degli elementi pesanti.

Gamow ha fatto il tentativo di investigare questo modello (o meglio un modello simile a questo) dal punto di vista quantitativo. Naturalmente per una investigazione quantitativa è necessario introdurre dei dati sulla probabilità di cattura dei neutroni da parte di un certo elemento, perché è quella che essenzialmente determina la rapidità del processo di questo fenomeno. Ora, esistono molti dati sulla cattura dei neutroni lenti, ma presumibilmente fenomeni di questo tipo sono avvenuti ad una temperatura abbastanza elevata perché sia più conveniente prendere – e Gamow ha preso – dati corrispondenti alla cattura di neutroni abbastanza veloci. In figura 4 sono riportate le sezioni d'urto per la cattura di neutroni veloci in funzione del peso atomico.

Gamow semplificando, e forse semplificando anche troppo, quello che veramente i risultati sperimentali dànno, suppone che queste sezioni d'urto per la cattura di neutroni crescano linearmente per valori del peso atomico tra 0 e 100 e poi rimangano costanti così come è indicato dalla spezzata disegnata in figura 4. Ora, se si osserva la figura e si tiene conto che la scala delle ordinate è logaritmica, si può giudicare quanto sia energica la schematizzazione di Gamow: comunque prima di criticarla conviene seguire fino in fondo il ragionamento di Gamow.

Supposto dunque, per il momento, che le sezioni d'urto siano veramente quelle richieste da Gamow si possono scrivere molto semplicemente le equazioni differenziali che descrivono come avvenga il successivo formarsi di elementi sempre più pesanti. Chiamiamo N_a il numero di atomi di peso atomico a; la derivata di questo numero rispetto al tempo dipenderà da due

termini: uno che rappresenta la crescita del numero degli atomi di peso a dovuta all'aggregarsi di neutroni ad atomi di peso $a-1$ (e questo sarà un termine positivo proporzionale a N_{a-1}, alla sezione d'urto σ_{a-1} dell'elemento $a-1$ e proporzionale al flusso, $\Phi(t)$, dei neutroni). Poi ci sarà un termine negativo che similmente rappresenta la diminuzione di N_a per effetto dell'assorbimento dei neutroni che trasforma gli atomi a in atomi $a+1$. In formula

$$\frac{dN_a}{dt} = \Phi(t)\,(\sigma_{a-1} N_{a-1} - \sigma_a N_a) \qquad (a = 1 \cdot 2 \cdots 238).$$

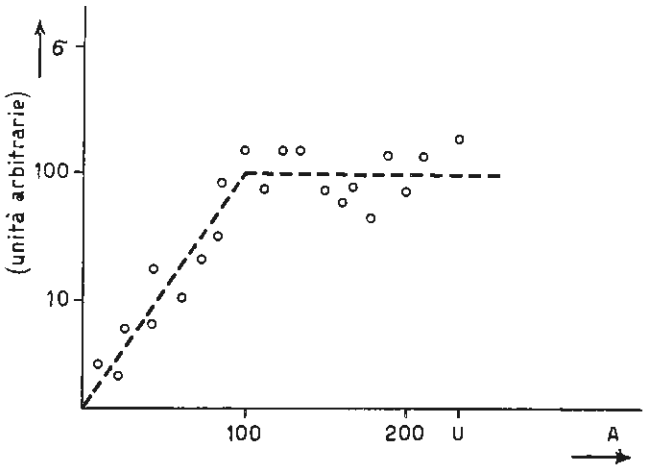

Fig. 4.

Equazioni come questa si dovranno scrivere per ogni valore di a e si otterrà un sistema che si potrà risolvere, una volta fissato il flusso dei neutroni, ricavando il modo nel quale si evolvono nel tempo le abbondanze dei singoli elementi.

Ora, il risultato più significativo (e che sarebbe ancor più significativo di quel che forse non sia se la curva delle sezioni di cattura scelta da Gamow fosse una rappresentazione più fedele dei fatti sperimentali) è che, per via della singolarità di questa curva – del fatto cioè che per un certo peso atomico la tendenza a crescere delle sezioni d'urto si arresta bruscamente – avviene che, scegliendo adatto il tempo e il flusso dei neutroni, si trova una distribuzione delle abbondanze degli elementi del tipo di quella rappresentata in figura 5 e che non è molto dissimile da quella sperimentale (fig. 1).

Naturalmente il risultato che si ottiene dipende dal tempo scelto nel senso che, se fissiamo un certo flusso di neutroni, il materiale deve essere esposto alla sua azione per un tempo adatto: infatti, se il tempo è troppo lungo, finiscono per formarsi troppi elementi pesanti, se è troppo breve per formarsene troppo pochi. Ma, « cuocendo » per così dire il materiale al punto giusto si riesce ad ottenere qualche cosa che ha una certa somiglianza coi dati sperimentali. Questa somiglianza giunge fino al punto da dare, per gli elementi a numero atomico elevato, una distribuzione degli isotopi simile a quella reale. Nella zona degli elementi leggeri il risultato è, invece, con-

trario a quello sperimentale ma si può pensare che un trattamento termico successivo, a temperature anche non eccessivamente elevate, possa aver modificata la situazione.

Gamow, come si è detto, non si è accontentato di questi risultati ed ha cercato di fare un passo più oltre, un passo molto arrischiato e quasi certamente errato. Quasi certamente errato come quello che si fa quando si pongono, per spiegare i fatti, delle ipotesi molto precise, perché, come è ovvio, tanto più precise sono le ipotesi tanto più facile è dimostrarne l'errore. Gamow, comunque, si è proposto di determinare il tempo nel quale la formazione degli elementi sopra descritta è avvenuta ricorrendo alla teoria della espansione dell'Universo. Questa teoria è collegata con quella della relatività generale e cercheremo di darne qui un cenno.

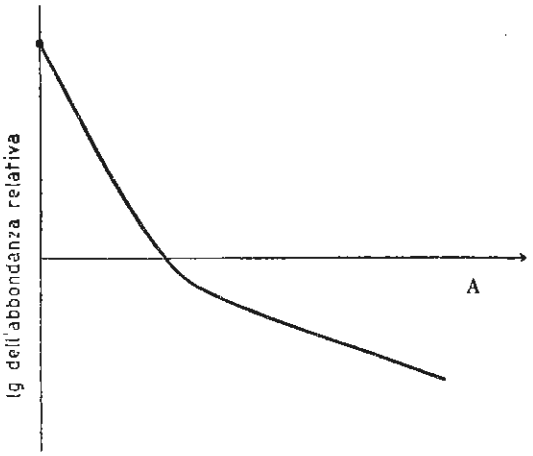

Fig. 5.

Disgraziatamente anche per la relatività generale, come per altre teorie fisiche, non esiste una sola teoria, e ciò implica sempre una certa libertà di scelta, scelta che al momento presente, non può essere fatta sulla base sicura delle indicazioni sperimentali. Ma se ci si basa sulla più semplice fra le teorie della relatività, quella nella quale non si tien conto dei cosidetti termini cosmologici, si può costruire, ed è stata costruita, una teoria della espansione dell'Universo secondo le seguenti linee generali.

Si parte dall'ipotesi – che se non altro ha il pregio di essere molto semplice – che la densità di energia (materia e radiazione) sia uniforme in tutto l'Universo, almeno quando si prendano medie su regioni molto estese di esso.

Si ammette inoltre che lo spazio abbia una curvatura costante il che è come dire che si richiede che l'Universo sia omogeneo non solo per quanto riguarda la densità di energia ma anche per le sue proprietà geometriche. Da questa ipotesi discende che la forma che ha l'Universo a un certo tempo determinato deve essere quella di una sfera oppure quella di una pseudo–sfera; per ragioni speciali, connesse con l'attuale densità della materia si deve scegliere la pseudo–sfera, che è una sfera a raggio immaginario non rappresentabile, in alcun modo, in una figura. Ma se per il momento prescindiamo dal fatto che l'oggetto di cui vogliamo parlare è una pseudo–sfera e non una sfera e per di più ci limitiamo a rappresentarne solo tre delle sue quattro dimensioni (il tempo e due coordinate spaziali) si potrà dare (fig. 6) l'idea di come l'Universo si evolva espandendosi. In figura 6 l'Universo è, rappresentato da cerchi il cui raggio va aumentando col passare del tempo.

Se ora, con le formule della relatività generale, si fanno i calcoli, si può trovare una relazione, che lega la velocità con cui si espande il raggio, $r = iu$, della pseudo–sfera con la densità dell'energia w:

$$\left(\frac{du}{dt}\right)^2 = c^2 + \frac{Kc^2}{3} u^2 w. \tag{2}$$

Questa formula dice che il quadrato della derivata rispetto al tempo del modulo del raggio u della pseudo sfera è uguale al quadrato della velocità della luce più un termine che contiene il raggio stesso, la densità di energia w e una costante K che è legata alla costante di gravitazione universale G nel modo seguente:

$$K = 8\pi \frac{G}{c^4}$$

ed ha un valore di circa $2 \times 10^{-48}\, dy\, n^{-2}$. Ora, se si vuole usare questa formula per descrivere l'espansione dell'Universo quando il suo raggio è molto piccolo, si può vedere che il primo termine del secondo membro diventa trascurabile in quanto la densità di energia cresce molto più rapidamente di quanto non diminuisca il quadrato del raggio. La formula (2) si semplifica allora nel modo seguente:

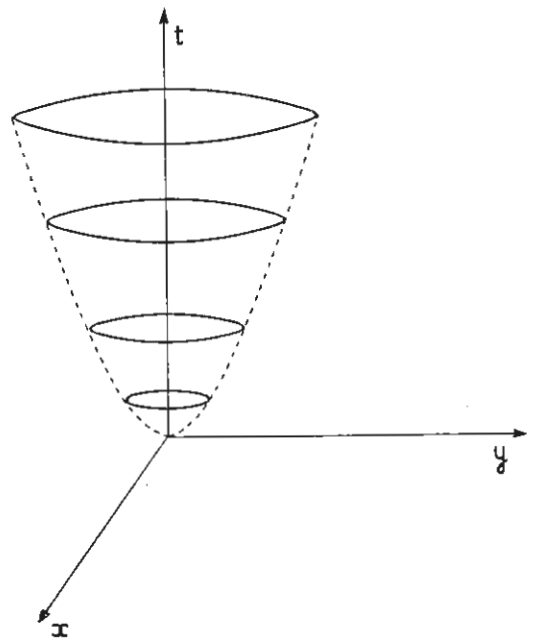

Fig. 6.

$$\left(\frac{du}{dt}\right)^2 = \frac{Kc^2}{3} u^2 w. \tag{3}$$

A questo punto Gamow ha fatto una osservazione molto interessante: se si ammette che, nei casi in cui sia usabile la formula 3, l'energia sia essenzialmente energia di radiazione, si può, usando la formula stessa, ricavare una relazione tra la temperatura e il tempo che non contiene altre co tanti che non siano costanti universali. Si viene, in questo modo, ad eliminare l'arbitrarietà sul valore della temperatura alla quale avrebbero avuto luogo le reazioni nucleari che hanno dato origine agli elementi, arbitrarietà, giocando sulla quale, si sarebbe potuto ottenere, entro certi limiti, qualsiasi risultato si fosse voluto. Diamo qui, senza dimostrazione, la formula che lega la temperatura al tempo trascorso dallo istante nel quale l'Universo aveva dimensioni infinitesime.

$$T = \left(\frac{3}{4Kc^2\sigma}\right)^{1/4} \frac{1}{\sqrt{t}} \text{gradi}. \tag{4}$$

In essa σ rappresenta la costante della legge di Stefan, T la temperatura assoluta e t il tempo. Come si è già avvertito essa è una formula appros-

simata e vale per valori di t non troppo grandi, per esempio, per valori non superiori ad alcuni milioni di anni.

Se, alle costanti che figurano nella formula (4), si sostituiscono i loro valori si ottiene

$$T = \frac{1{,}52 \cdot 10^{10}}{\sqrt{t}} \text{ gradi} \tag{5}$$

dalla quale si vede che quando t è, per esempio, eguale ad un secondo la temperatura è, come si poteva immaginare, spaventosamente alta: dell'ordine di 10^{10} gradi; ma decresce rapidissimamente cosicché, dopo mille secondi, è già ridotta ad avere l'ordine di grandezza di cento milioni di gradi valore questo già sufficientemente basso perché intensi fenomeni nucleari comincino a cessare di aver luogo.

La temperatura, dunque, varia nel tempo con una legge ben determinata e con una legge altrettanto determinata varia il pseudo raggio dell'Universo (esso è proporzionale al quadrato del tempo) e, pertanto, un solo parametro rimane indeterminato: la densità dei neutroni; Gamow si propone giocando su questo solo parametro arbitrario di riuscire a prevedere la distribuzione delle abbondanze degli elementi ed infatti in un certo senso vi riesce. Vi riesce, veramente, fintanto che ci si limiti a una analisi molto grossolana dei suoi risultati, ma, appena si cerchi di entrare nei dettagli, si incontrano subito delle difficoltà e probabilmente se ne incontrerebbero molte altre se si riuscisse a portare avanti questa analisi che è estremamente complicata da fare.

Le prime difficoltà si incontrano già nella parte bassa del sistema periodico appena che ci si domandi un po' in dettaglio come si vadano via via formando gli elementi. Come si è già detto il primo nucleo a formarsi sarà quello di idrogeno, poi per aggregazione di un protone con un neutrone si formerà il deuterio, quindi con l'aggiunta di un altro neutrone l'idrogeno tre, il quale decadrà attraverso un processo beta in elio tre. Per aggiunta di un nuovo neutrone l'elio tre si trasformerà in elio quattro. Già qui si presenta una piccola difficoltà perché l'elio tre catturando neutroni tende piuttosto a spezzarsi che a formare elio quattro, tuttavia si può sempre pensare che almeno una piccola frazione di elio tre si trasformi per cattura di un neutrone in elio quattro. Ma a questo punto la difficoltà che si presenta è molto più grande perché il nucleo di massa cinque non esiste: se si cercasse di formarlo per aggiunta di un neutrone all'elio quattro esso andrebbe immediatamente in pezzi creando una barriera insormontabile che impedisce la successiva formazione di elementi per aggiunta di neutroni.

In realtà si può trovare qualche modo per saltare, anzi meglio per girare questa barriera, ed è il seguente: in accordo con le formule che abbiamo scritto precedentemente, nel periodo di tempo in cui questi fenomeni dovrebbero aver luogo, la temperatura, benché sia già molto decresciuta, è sempre dell'ordine di 10^8 — 10^9 gradi e a temperature così alte possono ancora avere luogo, in maniera cospicua, delle reazioni termonucleari, reazioni, cioè, prodotte dagli urti fra i nuclei che si muovono sotto l'effetto della agitazione termica. Così non è impossibile pensare che possa formarsi un nucleo di massa

sei, senza che sia già esistente un nucleo di massa cinque, facendo reagire direttamente un nucleo di deuterio con un nucleo di elio quattro. In realtà questa reazione è estremamente improbabile, ma non impossibile, per modo che non è escluso che una piccola quantità di litio sei venga formandosi consentendo, per successive aggiunte di neutroni, la formazione di nuclei più pesanti. E difficoltà di questo tipo se ne incontrano molte altre, per esempio, anche il nucleo otto non esiste in nessuna forma stabile e questo gradino mancante dovrà essere superato con un artificio del tipo di quello già descritto.

Ma le difficoltà non finiscono qui, un'altra che non può essere taciuta è quella che, se si postula una densità di neutroni iniziale abbastanza grande perché essi possano formare elementi pesanti in quantità non infinitesime, si trova che la proporzione fra elio e idrogeno non ha nulla a che vedere con quella reale: si avrebbe cioè più elio che idrogeno contro l'evidenza sperimentale.

Non resta, dunque, che tristemente concludere che questa teoria è incapace di spiegare il modo come gli elementi sono venuti formandosi, il che era in fondo da aspettarsi.

È doveroso, però, rendere atto a Gamow del coraggio con cui si è accinto a costruire un tentativo di teoria basato su ipotesi estremamente determinate: la teoria è fallita il che vuol dire che qualcuna delle ipotesi è sbagliata, ma il risultato raggiunto in questo modo (di essere almeno certi di aver commesso un errore) è certamente più notevole di quello che si sarebbe potuto ottenere attraverso una teoria tanto vaga da essere capace di spiegare un notevole numero di fatti sperimentali, proprio attraverso il gran numero di arbitrarietà in essa contenute, ma da non mettere in evidenza quali sono i suoi punti certamente sbagliati consentendo di correggerli e di procedere alla costruzione di teorie nuove e più soddisfacenti.

QUARTA CONFERENZA (*)

LA RICERCA DI UN'ATTRAZIONE TRA ELETTRONE E NEUTRONE

(redatta dal Prof. N. B. CACCIAPUOTI)

Un problema che si presenta tutte le volte che si hanno due particelle è quello di conoscere quali forze agiscano tra di esse. Ora le particelle elementari la cui esistenza è accertata sono – come abbiamo detto – nove; ciò significa che il numero di problemi di questo tipo è

$$\frac{9\times 8}{2} \text{ cioè } 36.$$

Tuttavia è da tener presente, che questi trentasei problemi non si possono risolvere sempre; la soluzione del problema è infatti possibile solo in

(*) Tenuta il 10 ottobre 1949 nell'aula dell'Istituto Fisico dell'Università di Roma.

un numero limitato di casi ed il metodo classico per trovare quali siano le forze che agiscono tra due particelle – od almeno il metodo più classico – è quello di studiare l'urto tra le particelle stesse.

In realtà, già nelle famose ricerche di Rutherford sull'azione esercitata dai nuclei atomici sulle particelle alfa, l'applicazione di questo metodo aveva permesso di stabilire che le dimensioni del nucleo atomico sono piccole in confronto alle dimensioni dell'atomo. E tale metodo si sta seguendo tuttora con considerevole successo, benché non dia altro che risultati parziali, per determinare le forze tra neutrone e protone o tra protone e protone, dal punto di vista empirico.

Ma il problema che mi propongo di discutere oggi è un problema di importanza molto minore. È anche questo un problema che riguarda le forze agenti tra due particelle elementari, però le due particelle elementari considerate sono tali che tra di esse ben poche, e poco importanti forze, si esercitano.

Le due particelle in parola sono il *neutrone* e l'*elettrone*. Quindi il problema che ci proponiamo di discutere è: « le forze tra neutrone ed elettrone ».

Naturalmente, non esiste in questo caso la forza coulombiana, perché una delle due particelle è neutra. Vi è tuttavia una forza di origine elettrica o elettromagnetica, la cui esistenza è nota ed è stata osservata da circa una decina d'anni, che è dovuta alla seguente circostanza: il neutrone è provvisto di un piccolo momento magnetico; conseguentemente, quando attraversa un campo magnetico, è soggetto a delle forze perché c'è una energia mutua tra questo momento magnetico e il campo magnetico. Siccome l'elettrone, coi suoi movimenti, può produrre un campo magnetico, ne consegue una azione di carattere magnetico tra neutrone ed elettrone.

Questo fatto è stato per la prima volta suggerito teoricamente e quindi osservato sperimentalmente da Bloch, il quale ne ha dedotto alcune conseguenze assai importanti ed in particolare un metodo per polarizzare i neutroni, cioè per ottenere un fascio di neutroni aventi tutti il loro spin orientato in una certa direzione.

D'altra parte, per ciò che intendo discutere oggi, non è questo il tipo di azione del quale ci occuperemo; anzi le circostanze in cui si svolgono le esperienze che considereremo verranno sempre scelte in modo che tale azione sia eliminata; ciò si può fare scegliendo per queste esperienze sempre dei materiali non magnetici – atomi che non siano paramagnetici e tanto meno ferromagnetici, e non ci sia nulla con cui il momento magnetico del neutrone possa interagire. La scelta di queste particolari condizioni sperimentali è fatta deliberatamente, perché lo scopo che ci proponiamo è di ricercare se esistono delle forze di carattere attrattivo tra neutrone ed elettrone.

Consideriamo un neutrone N ed un elettrone e.

Per queste due particelle, delle quali non si conosce gran che, può darsi che esistano delle forze che agiscono tra l'una e l'altra. Cosicché, a parte ogni presupposto teorico che si possa immaginare, rimane aperto il seguente problema: esistono o non esistono, forze di carattere attrattivo, o repulsivo, forze aventi essenzialmente il carattere di forze centrali, fra queste due particelle?

Esiste però, in questo caso, un argomento più specifico per sospettare l'esistenza di forze di questo tipo; ed è il seguente: il neutrone, in realtà – secondo la teoria di Yukawa – non è proprio ed a stretto rigore una particella neutra; perché – secondo questa teoria – avviene un continuo scambio, con una continua reazione in sensi opposti, che abbiamo scritto già nella maniera seguente:

$$(1) \qquad N \rightleftarrows P + \pi^- \qquad$$

il neutrone può trasformarsi in ambedue le direzioni nel modo seguente: in un protone, più un mesone negativo che, in questo caso, sarebbe un mesone π^-.

E l'idea di Yukawa è che tra queste due forme del neutrone (sono tutte e due forme neutre, naturalmente) avvenga un continuo scambio, cosicché la particella passi una certa frazione del tempo in una forma, e la frazione complementare nell'altra forma.

Ora vi sono alcune ragioni indicative per ritenere che la particella sia per l'80 % nella forma N e per circa il 20 % del tempo nell'altra forma cioè $P + \pi^-$ [1]. Queste cifre sono puramente indicative e saranno usate unicamente per una valutazione degli ordini di grandezza.

Se, dunque, vogliamo rappresentare il neutrone con un modello molto rudimentale, possiamo dire: talvolta il neutrone si presenta come una particella priva di carica; talvolta il neutrone si trasforma in un protone avente in sua vicinanza un mesone negativo, conformemente alla formula (1). Naturalmente questo mesone negativo potrà trovarsi da qualsiasi parte, rispetto al protone; si troverà in media con una distribuzione avente simmetria sferica attorno al protone cosicché possiamo descrivere il neutrone da un punto di vista statistico come una particella definita dal valor medio degli eventi che si presentano; possiamo cioè distinguerla al modo seguente: al centro abbiamo, in media, una carica positiva, perché durante il 20 % del tempo totale abbiamo nel centro un protone: quindi si ha nel centro una carica, se mi è lecito così dire, di 0,2 volte la carica elementare. Attorno a questa carica centrale positiva a distanze variabili, ed in una posizione qualsiasi, si trova invece un mesone negativo, che dà una specie di distribuzione di elettricità negativa, la quale ha, in totale, lo stesso valore, ma questa volta col segno meno: $-0{,}2$ volte la carica elementare e.

E questo può essere un grossolano modello elettrico di come deve intendersi questo neutrone. Quindi il neutrone è neutro nel senso che la carica totale è nulla, però il campo elettrico non è nullo dappertutto, perché la carica positiva è localizzata nel centro, mentre la carica negativa è diffusa

(1) Si può avere una grossolana indicazione di questo fatto in base a considerazioni sui momenti magnetici: il momento magnetico del neutrone è dato approssimativamente da $-2\,M_0$, essendo M_0 il magnetone nucleare. Il momento magnetico del mesone è invece dell'ordine di $-10\,M_0$ (la massa del mesone è infatti dell'ordine di 1/10 della massa nucleonica). Secondo il modello da noi contemplato bisogna quindi ammettere che il mesone esista solo per il 20 % del tempo, in modo da dare luogo ad un momento magnetico medio uguale a $-2\,M_0$.

sfericamente, attorno a questo centro (fig. 1). Quindi se esploriamo il campo elettrico di questa distribuzione di elettricità, quando siamo lontani dalla particella il campo elettrico evidentemente si annulla e il potenziale è nullo; ma, quando ci avviciniamo ad un punto che penetri nell'interno di questa nuvola di carica negativa, allora in questo punto si risente l'azione della carica centrale positiva di valore 0,2 e, non completamente schermata dalla distribuzione negativa di carica, per modo che in tale punto si ha un campo elettrico; e questo campo elettrico diventa tanto più forte, quanto più ci si avvicina al centro, anzi, in vicinanza del centro, dove l'azione di schermo praticamente viene a cessare, la forza elettrica sarà quella dovuta ad una carica di 0,2 e.

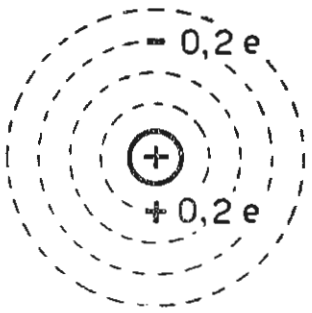

Fig. 1.

Se ora il neutrone viene investito da un elettrone, secondo questo modello possiamo aspettarci che, allorquando le due particelle vengano in estrema vicinanza l'una dall'altra, si esercitano delle forze tra queste. In realtà, se questo modello è corretto, la forza deve essere attrattiva e di assai corta portata, perché naturalmente la nuvola mesonica attorno al centro è di raggio molto piccolo; in una lezione precedente ho già segnalato che le distanze a cui il mesone si trova dal centro, sono dell'ordine di grandezza della cosiddetta lunghezza d'onda di Compton calcolata per la massa mesonica (e non per la massa elettronica). Quindi il raggio di distribuzione è dell'ordine di grandezza di

$$\frac{\hbar}{\mu c} = \frac{h}{2\pi\mu c}$$

dove h è la costante di Planck e μ rappresenta la massa del mesone; il raggio è quindi dell'ordine di grandezza di 10^{-13} cm.

Quindi, ne risulta che se questo meccanismo ha un effettivo significato fisico, si tratta di forze che arrivano fino ad una distanza di solo 10^{-13} cm. Anzi, si può a questo punto speculare sulla questione seguente:

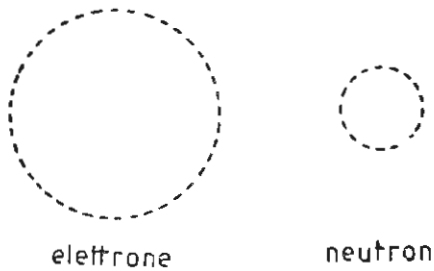

Fig. 2.

l'elettrone, probabilmente, non può considerarsi esso stesso come un punto; anche se accettiamo l'idea classica della massa elettromagnetica, dobbiamo attribuire all'elettrone delle dimensioni lineari che sono dell'ordine di 10^{-13} cm, anzi forse due o tre volte più grandi. Possiamo perciò rappresentare schematicamente l'elettrone e il neutrone con due sfere i cui raggi hanno delle dimensioni che stanno fra di loro nel rapporto 2: 1 oppure 3 : 1 circa, come è indicato nella fig. 2, sebbene una tale rappresentazione non significhi gran ché.

Quindi se prendiamo questa rappresentazione un po' alla lettera probabilmente più di quanto non sia lecito, dobbiamo dire che già quando certe

parti dell'elettrone cominciano a penetrare entro la nuvola mesonica che circonda la carica positiva del neutrone, le forze cominciano ad agire.

Ora, il problema principale, che è l'oggetto della ricerca che esporrò, è quello di cercare due cose: prima di tutto, se per caso non ci siano delle forze molto più grandi di quella da noi considerata, che agiscono tra elettrone e neutrone; poi, se questo non è il caso, vedere se si riesce ad osservare l'esistenza della forza di cui abbiamo ora descritto l'origine.

È chiaro che per orientarci circa il tipo di esperienza che si può fare, conviene conoscere l'ordine di grandezza dei valori a cui presumibilmente si deve arrivare e questo è abbastanza facile.

Debbo fare una osservazione a questo riguardo: per accertare o meno, l'esistenza di una forza del tipo considerato per mezzo di esperienze d'urto, è necessario sapere dalla teoria quale è l'effetto di un potenziale del tipo di quello che interviene nel modello ora descritto, che genere di fenomeni d'urto esso provoca e che genere di sezione d'urto esso determina. Ora, questo è un problema di meccanica quantistica molto classico che, nel caso di forze abbastanza deboli e di piccola portata, come si ha nel nostro modello, dà il risultato seguente: la sezione d'urto dipende non dai dettagli di questo potenziale che indicheremo con $u(r)$ ma semplicemente dall'integrale di $u(r)$ esteso a tutto il volume V. Si trova precisamente che la sezione d'urto σ è data dalla formula seguente:

$$\sigma = \frac{m^2 b^2}{\pi \hbar^4} \quad \text{essendo} \quad b = \int_V u(r)\, dV. \tag{2}$$

In questa formula m è la massa ridotta del sistema e vedremo che questa ha una certa importanza.

Quindi per risolvere il problema che consiste nel determinare quale sarebbe la sezione d'urto nella collisione tra un elettrone e un neutrone, secondo il modello da noi descritto bisogna calcolare o stimare l'ordine di grandezza dell'entità che abbiamo indicato con b. Una tale valutazione non è difficile (ora faccio un calcolo puramente di stima, dimenticandomi tutti i fattori numerici, che poi metteremo alla fine come si può), perché l'ordine di grandezza del potenziale è dato dal prodotto della carica centrale che è 0,2 e per la carica e dell'elettrone, diviso per la distanza fra queste due cariche. Per ottenere b bisogna integrare questo potenziale a tutto il volume; l'ordine di grandezza di questo integrale è dato essenzialmente dal potenziale moltiplicato per il volume. A parte un fattore numerico il volume è dato dal cubo del raggio della distribuzione di carica. Sempre per una valutazione di ordini di grandezza possiamo dare tanto al raggio della distribuzione che alla distanza fra le due cariche considerate, il valore $\hbar/\mu c$ che rappresenta, come abbiamo visto, il raggio delle forze. In conclusione troviamo

$$b \approx -\frac{0{,}2 \cdot e \cdot e}{\hbar/\mu c}\left(\frac{\hbar}{\mu c}\right)^3 \quad \text{ossia} \quad b \approx -0{,}2 \cdot e^2 \left(\frac{\hbar}{\mu c}\right)^2. \tag{3}$$

Ci si può domandare: si può far di meglio che non questa stima? Vedremo che al momento presente le esperienze sono ancora estremamente incerte, cosicché allo stato attuale non si può che fare un confronto di ordini

di grandezza; ma probabilmente le esperienze si affineranno, cosicché sorgerà il problema di confrontare il risultato ottenuto dalle esperienze, con quello ottenuto dalla teoria, in modo più accurato di quanto è richiesto da un grossolano confronto di ordini di grandezza.

Al momento presente, come ho detto, non si può fare di meglio che contentarci di questo confronto tra ordini di grandezza. E la ragione per cui non si può fare di meglio è, al solito, come ho già indicato in altre occasioni, che la teoria di Yukawa è una teoria che ha due difetti: prima di tutto non è una teoria sola, ma è una mezza dozzina di teorie; e dobbiamo dire più di mezza dozzina, perché la settima non la conosciamo ed è probabilmente quella buona. Secondariamente, anche se sapessimo che una di queste sei teorie che noi cono ciamo è quella buona, anche allora i nostri metodi matematici per trattare la teoria dei campi (sempre a parte la indefinitezza della teoria) sono estremamente rudimentali e dànno luogo a delle infinità che talvolta si accettano, talvolta si eliminano in modo piuttosto artificioso. Cosicchè in molti casi le sei teorie (non che siano proprio sei) dànno risultati indefiniti; inoltre probabilmente la teoria buona non è una di queste sei.

Quindi al momento presente non si può dare gran chè di più che una grossolana valutazione di ordini di grandezza di questo genere, la quale valutazione, sostituendo nella (3) i valori numerici, dà per risultato:

$$b \approx -9 \cdot 10^{-46} \text{ erg. cm}^3. \tag{4}$$

Si può vedere in modo un pochino più significativo che cosa vuol dire questo numero alla maniera seguente: secondo la nota convenzione abbiamo nel neutrone una certa buca di potenziale e ciò che conta è l'integrale di volume di questa buca. Fissiamo un certo volume standard al quale ci riferiremo sempre e diamo al potenziale un valore medio tale che il prodotto del potenziale per il volume standard sia uguale al valore di b dato dalla (4); quello che di solito si prende come volume standard è il volume classico dell'elettrone (fig. 3). Se così si fa, si trova che il valore medio che si deve assumere corrisponde ad un potenziale di circa 6.000 volt–elettroni.

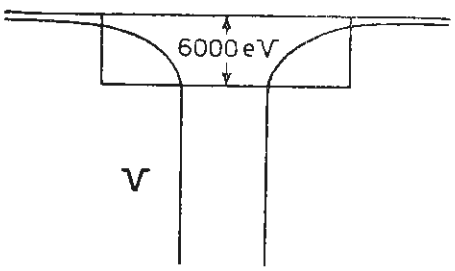

Fig. 3.

Da questo calcolo abbiamo una idea di quanto piccola sia questa interazione; noi la possiamo confrontare con le forze tra nucleoni, per esempio tra protoni e neutroni, che standardizzati allo stesso modo, cioè interpretati convenzionalmente come una buca di potenziale di raggio uguale al raggio classico dell'elettrone, corrispondono a dei potenziali che si aggirano in media attorno a 15 milioni di volt cioè a valori circa 2.000 volte più grandi.

Quindi, se esistono delle forze di questo tipo fra elettrone e neutrone esse corrispondono come importanza a circa 1/2000 delle forze tra nuclei.

Ma, per un momento, può sembrare che la situazione sia anche peggiore di quella che corrisponde a questo fattore 2.000. Se ci si propone, per esempio

(ammettendo che una forza di quest'ordine di grandezza veramente esista) di trovare la sezione d'urto tra elettrone e neutrone ci si deve servire della formula (2), che trascriviamo nuovamente:

$$\sigma = \frac{m^2 b^2}{\pi \hbar^4} \tag{2}$$

come valore della massa bisogna mettere la massa ridotta del sistema elettrone–neutrone e, siccome il neutrone ha massa molto più grande dell'elettrone, la massa ridotta è praticamente la massa dell'elettrone, che è piuttosto piccola e compare al quadrato nella (2).

Quindi il risultato è piccolo: precisamente il valore numerico è dato press'a poco da 2×10^{-37} cm^2 che è una sezione d'urto estremamente piccola se confrontata con la sezione d'urto dei neutroni coi nuclei, la quale è generalmente dell'ordine di 10^{-24}. Vi è cioè un fattore 10^{13} di differenza.

C'è da chiederci, allora, in qual modo si possa sperare di osservare una interazione corrispondente ad una sezione d'urto che è 10^{13} volte più piccola della sezione d'urto dei nuclei.

A questo punto possiamo cominciare a cercare di guadagnare qualche fattore in modo da presentare la situazione da un punto di vista più plausibile. C'è intanto un fattore un milione, che si può mettere direttamente senza difficoltà, per questa ragione: nella (2) compare m che è la massa ridotta. Ma dobbiamo proprio prendere la massa ridotta del sistema elettrone– neutrone? Questo sarebbe certo il caso se l'elettrone e il neutrone fossero particelle libere, cioè se avessimo soltanto un elettrone ed un neutrone che si urtano nel vuoto. Ma l'elettrone, in realtà, fa parte di un atomo al quale è attaccato in modo praticamente rigido, rispetto all'urto che riceve quando viene deflesso un neutrone lento. Conseguentemente (e questo si può giustificare con un calcolo accurato, ma il risultato si capisce abbastanza bene) un elettrone che fa parte di un atomo non è un elettrone libero ed agli effetti di fenomeni di questo genere si comporta anzi come un elettrone fisso.

Il sistema è dunque ora ridotto all'urto di un elettrone, che però è inchiodato in una posizione fissa, contro un neutrone: quindi per la massa ridotta che compare nella formula (2) noi dobbiamo prendere la massa del neutrone che è circa 2000 volte più grande di quella dell'elettrone ed essa compare al quadrato in tale formula.

Questo dà a nostro vantaggio un fattore $4 \cdot 10^6$ che non basta, naturalmente, per compensare un fattore di 10^{13}, ma aiuta. Inoltre possiamo, senza difficoltà, guadagnare un altro fattore, forse 50, se prendiamo un atomo abbastanza pesante, avente per esempio 50 elettroni (varie esperienze sono state fatte con xeno). Questi 2 fattori dànno insieme un fattore $50 \times 4 \times 10^6 = 2 \times 10^8$ che comincia ad avvicinarsi a 10^{13}. Rimane tuttavia sempre un fattore 100.000 di differenza ed è chiaro che non si possono fare le esperienze con la precisione di una parte su 100.000. Esperienze del tipo che stiamo considerando sono piuttosto difficili ed è già molto se si potrà arrivare ad una parte su 1000.

Ma c'è un altro fattore che ha importanza e questo è il fattore della interferenza. Dobbiamo infatti ricordarci che i fenomeni di questo tipo vanno

trattati con la meccanica ondulatoria. Ora per quanto si è detto prima il nostro problema consiste in sostanza nello studiare l'urto di un neutrone con un atomo il quale possiede un nucleo e degli elettroni. L'onda che rappresenta il neutrone viene dispersa sia dal nucleo, dando luogo ad una certa onda, sia dai vari elettroni, e per il momento ne consideriamo uno, dando luogo ad un'altra onda. Queste due onde interferiscono e siccome l'azione tra neutrone e nucleo è grande mentre l'azione tra neutrone ed elettrone è piccola, ne consegue che l'ampiezza dell'onda risultante sarà costituita di una parte grande A che è l'ampiezza dell'onda originata dal nucleo, più una parte piccola a che sarà l'ampiezza dell'onda originata dagli elettroni. L'intensità è proporzionale dal quadrato dell'ampiezza dell'onda: se ci fosse il solo nucleo l'intensità sarebbe quindi proporzionale ad A^2, mentre tenuto conto degli elettroni essa sarà $(A + a)^2 = A^2 + 2Aa$ (trascurando un termine a^2 che è molto piccolo).

D'altra parte le intensità sono proporzionali alle sezioni d'urto; indicando allora con $\sigma_{nucl.}$ la sezione d'urto del solo nucleo e con $\sigma_{el.}$ la sezione d'urto degli elettroni, avremo allora:

$$\frac{\sigma}{\sigma_{nucl.}} = \frac{A^2 + 2Aa}{A^2} = 1 + 2\frac{a}{A} = 1 + 2\frac{\sqrt{\sigma_{el.}}}{\sqrt{\sigma_{nucl.}}}$$

da cui:

$$\sigma = \sigma_{nucl.}\left(1 + 2\frac{\sqrt{\sigma_{el.}}}{\sqrt{\sigma_{nucl.}}}\right). \tag{5}$$

Ora noi abbiamo visto che il rapporto delle sezioni d'urto $\sigma_{el.}/\sigma_{nucl.}$ è circa $10^8/10^{13} = 10^{-5}$; tuttavia nella (5) compare fortunatamente la radice quadrata di questo rapporto moltiplicata per 2, il che dà per risultato circa 1/100.

Noi vediamo dunque che per effetto dell'interferenza, in cui interviene la dispersione da parte del nucleo, gli effetti che si possono prevedere, vengono ad essere dell'ordine di 1 %, mentre siamo partiti da 10^{-13}, che sarebbe stato addirittura fuori discussione.

Ora, due esperienze sono state fatte, per tentare di mettere in luce questo fenomeno ed hanno dato fin'ora soltanto dei risultati molto parziali, puramente di ordini di grandezza; ma probabilmente esse verranno affinate ed alla fine, io spero, si potrà raggiungere un risultato attendibile.

Un primo tipo di esperienza è stato effettuato dal gruppo della Columbia University capitanato da Rabi; altre esperienze sono state fatte da L. Marshall e da me a Chicago. Entrambe queste esperienze sono basate essenzialmente sull'idea di osservare l'interferenza di cui abbiamo parlato, ma il dispositivo è diverso nei due casi e per brevità, dato che mi è più familiare la esperienza fatta da me, descriverò questa in maggior dettaglio.

L'idea dell'esperienza è la seguente: consideriamo la dispersione dei neutroni da parte di un gas nobile. Nelle esperienze effettuate si usava come gas nobile lo xeno.

Consideriamo un atomo costituito dal suo nucleo e dai suoi elettroni periferici (fig. 4) e cerchiamo di osservare la dispersione di un fascio di neutroni lenti da parte di questo atomo. I neutroni lenti hanno una lunghezza d'onda di de Broglie, che è dell'ordine di 2×10^{-8} cioè dell'ordine di gran-

dezza delle dimensioni lineari dell'atomo di xeno che sono $2 \cdot 10^{-8}$, mentre è di parecchi ordini di grandezza più grande delle dimensioni del nucleo, che è praticamente puntiforme: le dimensioni lineari del nucleo sono circa 20.000 volte più piccole di quelle dell'atomo e quindi della lunghezza d'onda dei neutroni lenti.

Quindi, se non ci fosse l'azione degli elettroni (che per il momento eliminiamo) e si considerasse semplicemente la diffusione dell'onda da parte di un nucleo relativamente puntiforme, ci si aspetterebbe una distribuzione avente esattamente simmetria sferica, appunto perché la lunghezza d'onda è molto più grande dell'ostacolo costituito dal nucleo. Ma a questa azione del nucleo, che è l'azione principale, deve sovrapporsi l'effetto della nuvola di elettroni, i quali elettroni sono distribuiti, come ho detto prima, sopra una regione dell'ordine di grandezza della lunghezza d'onda.

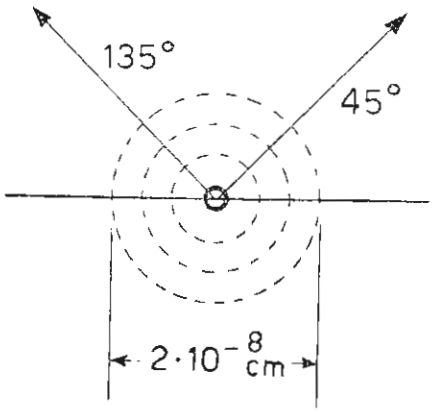

Fig. 4.

Quindi, se osserviamo la radiazione dei neutroni che vanno in una certa direzione, troveremo dei fenomeni di diffrazione, perché gli elettroni sono distribuiti su una regione dell'ordine di grandezza della lunghezza d'onda. Ci si può dunque aspettare che, per esempio, osservando l'intensità dei neutroni diffusi in una direzione a 45° con la direzione dei neutroni incidenti, oppure 135° con la direzione dei neutroni incidenti, ci siano delle differenze; dall'osservazione di queste differenze si può risalire a quale è l'effetto degli elettroni.

Ripeto: se non ci fosse alcuna azione con gli elettroni, le intensità in queste due direzioni dovrebbero essere uguali: gli elettroni produrranno, per via dell'interferenza, una piccola differenza.

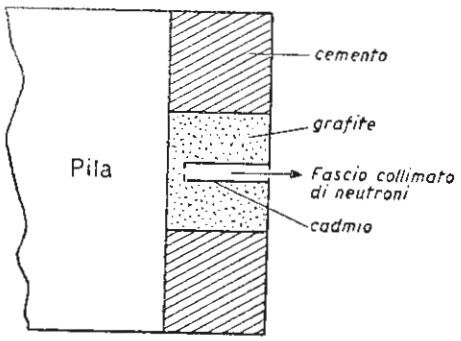

Fig. 5.

L'esperienza è stata condotta nel modo seguente: è una di quelle esperienze in cui è assai utile avere a disposizione le enormi intensità di neutroni che si possono ottenere da una pila ad uranio. La pila è circondata da un grosso schermo di cemento; in questo schermo di cemento vi è una grossa cavità, del diametro di un metro e mezzo, che penetra nell'interno della pila; tale cavità però non è vuota, ma è piena di grafite (fig. 5). Questa grafite costituisce la cosidetta « colonna termica »: in realtà si tratta di una colonna sdraiata. In alcune macchine, fatte in principio, questa colonna era effettivamente verticale: perciò è stata chiamata « colonna » e si è mantenuto questo nome.

Lo scopo di questa grafite è di purificare i neutroni lenti dalla massa dei neutroni di tutte le energie che si producono nella pila; i neutroni entrano nella grafite dove cominciano a subire un gran numero di collisioni contro gli atomi del carbonio della grafite ed in questi vari urti perdono energia; cosicché, dopo essersi diffusi attraverso uno strato relativamente piccolo di questa grafite, tutti i neutroni veloci sono praticamente eliminati e alla uscita della colonna termica si hanno solamente neutroni dotati di velocità di agitazione termica, che sono quelli con cui si può fare l'esperienza. Inoltre è necessario che il fascio di neutroni termici sia abbastanza ben collimato e per questo si procede nella maniera seguente: nel centro della colonna termica si pratica un foro cilindrico, lungo l'asse, nel quale si infila un tubo di cadmio. Il cadmio è una sostanza che gode della proprietà di assorbire fortemente i neutroni termici: li assorbe praticamente al 100 %. Se comple-

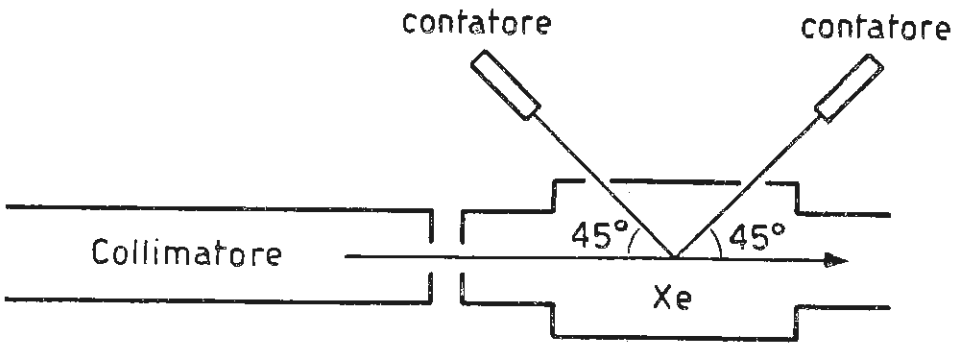

Fig. 6.

tiamo l'estremità esterna del tubo di cadmio con uno schermo di cadmio provvisto di un foro centrale, si ottiene un collimatore tale che solo i neutroni che lo attraversano possono uscire dal foro.

A questa maniera veniamo ad avere un fascio collimato di neutroni di considerevole intensità.

Nella fig. 6 è disegnato nuovamente il collimatore di neutroni, unitamente all'apparecchio che serve per le misure. Si fa entrare il fascio di neutroni nell'apparecchio propriamente detto, che è una specie di scatola che si può o evacuare o riempire di xeno a seconda dei casi. Nel disegno della fig. 6 è disegnata solamente la parte fatta in cadmio che è la parte interessante per i neutroni. Il tutto è, naturalmente, racchiuso in una scatola di ottone per poter contenere il gas.

Nella parte superiore dell'armatura in cadmio vi sono due finestre al di là delle quali sono collocati due contatori che permettono di rivelare i neutroni diffusi a 45° ed a 135° rispetto alla direzione di incidenza. Allora i neutroni passando attraverso il gas che si trova in questo recipiente subiscono degli urti di modo che alcuni di essi vanno a finire nell'uno, e alcuni di essi nell'altro contatore: ed essenzialmente misurando il rapporto del numero di neutroni che arrivano nell'uno e nell'altro contatore si trova il rapporto tra la intensità della diffusione nelle due direzioni.

Vi è un numero considerevole di correzioni da apportare, che non starò a descrivere; comunque se si fa l'esperienza completa, il risultato che si trova è il seguente: il rapporto tra la intensità diffusa a 45° con la direzione del neutrone primario, e l'intensità diffusa a 135°, viene ad essere leggermente diverso da uno e precisamente si trova il valore:

$$\frac{I_{45°}}{I_{135°}} = 1{,}0235 \pm 0{,}0085. \tag{6}$$

Tuttavia questa differenza è dovuta in gran parte (forse per la totalità, ma certamente per la maggior parte) ad un fenomeno spurio. Precisamente si presenta il fatto seguente: lo xeno ha un peso atomico di circa 130, quindi è molto più pesante del neutrone, che ha peso atomico 1; ciò nonostante il rapporto delle masse non è infinito. Se questo rapporto delle due masse fosse infinito si potrebbe considerare l'urto come un processo in cui l'atomo di xeno è fermo e il neutrone rimbalza su di esso.

In realtà, in questo urto il centro di gravità del sistema si muove un pochino. Bisogna allora, con un calcolo molto elementare, ridursi al caso di un urto riferito al sistema del centro di gravità delle due particelle. E se si fa questo si trova che il rapporto dovrebbe essere 1.022, che è molto vicino al rapporto osservato.

Dunque se dal valore sperimentale della misura si toglie 1.022 e se quello che resta è dovuto all'effetto che stiamo cercando e non ad altre piccole correzioni, si tratta certamente di un effetto molto piccolo, in cui la probabilità di aver dimenticato qualche cosa non è trascurabile; ad ogni modo prendendo per buono questo risultato si può ricavare, diciamo così, il valore della buca di potenziale che corrisponde ad una profondità di praticamente: 0 ± 5.000 volt-elettroni.

Quindi, una esperienza di questo tipo, per ora, dà un risultato piuttosto negativo, perché il valore che ci aspettavamo era di 6.000 volt-elettroni, sia pure con una notevole incertezza. Tuttavia occorre tenere presente prima di tutto che la stima teorica può facilmente essere in errore; inoltre gli errori sperimentali si stimano in base ad elementi che non sono sempre sicuri, quindi se diciamo che l'errore è 5.000 in realtà esso può anche essere 10.000, se c'è stata una serie di infortuni, tutti producenti dei piccoli errori nella stessa direzione. Appare perciò evidente che non vi è certo contraddizione tra il risultato teorico e quello sperimentale.

Come programma futuro penso che questa esperienza si possa certo raffinare molto. In particolare, io sono convinto che l'errore sperimentale può ridursi in modo tale che si riesca ad uscire da questa situazione sgradevole, e trovare se c'è un principio di accordo tra la teoria e l'esperienza, oppure no. Al momento quel che si può dire in base a questa esperienza è che non vi è certamente niente altro di molto importante e l'effetto da noi cercato può esserci, o può non esserci. Le esperienze future permetteranno di giudicare.

Il metodo di Rabi è basato essenzialmente sullo stesso tipo di idea teorica, ma il dispositivo è del tutto diverso. Nell'esperienza di Rabi si usano dei fasci di neutroni monocromatici. Nella monocromatizzazione del neu-

trone c'è una certa perdita di intensità di modo che l'intensità non è sufficiente per fare una esperienza accurata di diffusione; perciò ci si limita semplicemente ad una misura della sezione d'urto totale.

Per di più, sempre per ragioni di intensità, non si può usare un gas e si ricorre quindi ai liquidi (le esperienze sono state fatte con bismuto e piombo liquido). L'esperienza consiste nel misurare molto accuratamente come varia la sezione d'urto in funzione dell'energia dei neutroni.

Ora se si misurasse l'effetto dovuto ad un solo nucleo senza elettroni e senza altri nuclei, ci si dovrebbe aspettare, nella regione di energia di circa un centinaio di elettroni–volt, di trovare che la sezione rimane costante al variare dell'energia. Se esiste un piccolo effetto dovuto agli elettroni, si deve tenere conto del seguente fatto: la lunghezza d'onda degli elettroni è inversamente proporzionale alla loro velocità, quindi è inversamente proporzionale alla radice quadrata dell'energia. Quando si va ad energie abbastanza alte (quindi a lunghezze d'onda abbastanza piccole), l'effetto degli elettroni viene distrutto interferenzialmente, perché le fasi delle onde associate ai vari elettroni che circondano il nucleo vengono in media ad opporsi l'una all'altra. Viceversa quando si va verso le energie più basse, quindi a lunghezze d'onda via via più grandi, questa distribuzione interferenziale dell'effetto degli elettroni va gradualmente diminuendo: e questo fenomeno dà luogo ad un effetto che si può calcolare. Dunque si può dire che qualora non ci fosse l'effetto degli elettroni si otterrebbe, nella nostra approssimazione, che la sezione d'urto è costante al variare dell'energia; nel caso invece che esista questo effetto si dovrebbe osservare una piccola deviazione della sezione d'urto da questo valore costante.

C'è un punto sgradevole, in questa esperienza: in realtà, anche i soli nuclei non darebbero una sezione d'urto costante e questo a causa dei fenomeni interferenziali tra i nuclei medesimi. Si tratta qui di un fenomeno assai simile a quello che succede quando si fanno passare dei raggi X attraverso un liquido. Un liquido ha delle proprietà di correlazione tra le posizioni dei suoi vari centri che ricordano un po' quelle di un cristallo; questo dà luogo a fenomeni interferenziali. Per questo motivo anche i soli nuclei devono dare, e in realtà dànno, un andamento della sezione d'urto in funzione dell'energia che è pressoché costante per basse energie ma variabile per energie maggiori.

È chiaro quindi che l'esperienza per vedere l'eventuale effetto degli elettroni dovrà essere fatta in quella zona di energia in cui la perturbazione dovuta all'effetto interferenziale dei nuclei è molto piccola. Tuttavia un residuo di questa perturbazione costituisce sempre un elemento di incertezza nell'esperienza descritta, anche se una valutazione assai grossolana mostra che tale perturbazione è in realtà abbastanza piccola.

Comunque sia, l'impressione è che dai dati di Rabi risulti un valore del potenziale che è probabilmente negativo e dello stesso ordine di grandezza di quello teorico. Più precisamente sembra che il valore sperimentale possa essere eventualmente di un ordine di grandezza inferiore, ma non certo superiore a quello del valore teorico.

Questa, è dunque, la conclusione a cui portano le esperienze di questo genere. Sono esperienze in cui sono possibili, come ho detto, dei miglioramenti assai notevoli; quindi è abbastanza probabile che in un anno o due la situazione sia abbastanza chiarita. Se questo sarà il caso, si potrà avere una maggiore confidenza, di quella che si ha oggi, col meccanismo da noi descritto, secondo il quale i mesoni ogni tanto escono, per così dire, dal nucleo di modo che un neutrone ha in realtà una carica positiva per una piccola frazione di tempo, mentre il mesone si trova nelle sue vicinanze.

Dal punto di vista qualitativo questo risultato potrebbe permettere di decidere, almeno in parte, quale sia la vera teoria mesonica, o per lo meno di escludere quelle teorie che si trovano in contraddizione coi fatti sperimentali.

A meno che non si trovino metodi diversi e più precisi per fare questi esperimenti non credo personalmente che si possa, con un semplice raffinamento delle tecniche attuali, ottenere gran chè di più che forse il valore (-4.000 ± 1.000) ev.

Questo sarebbe già un risultato probabilmente vicino ai limiti di quello che le esperienze presenti possono consentire; ma sarebbe pur tuttavia un risultato di un certo valore: e si lavorerà in questa direzione per vedere sino a dove si possa arrivare.

QUINTA CONFERENZA(*)

ORBITE NUCLEARI

(redatta dal Prof. M. AGENO)

Uno dei problemi più importanti della fisica nucleare è il seguente: noto il numero di protoni e di neutroni costituenti un nucleo determinato, calcolare l'energia di legame di quest'ultimo, nel suo stato fondamentale. È naturalmente possibile allargare il programma contenuto in questo enunciato e proporsi di determinare, oltre all'energia di legame, anche tutte le altre grandezze relative al nucleo in questione, quali ad esempio la quantità di moto angolare intrinseca, il momento magnetico e così via.

Un problema interamente analogo si è già incontrato, ed è stato sostanzialmente risolto, nella fisica dell'atomo. In questo caso, dato un atomo di cui si conosca il numero atomico, si sa ch'esso è costituito da un nucleo centrale di data carica elettrica e da un corrispondente numero di elettroni: anche qui, uno dei problemi più importanti consiste nel determinare l'energia di legame di questo sistema in quello che si chiama di solito il suo stato fondamentale.

(*) Tenuta il 12 ottobre 1949 nell'aula dell'Istituto Fisico dell'Università di Roma.

La soluzione che è stata data a questo problema nel caso dell'atomo è una soluzione parziale, non tanto perché non si conoscano i principi in base ai quali calcolare una soluzione esatta, quanto perché il calcolo matematico relativo è troppo complicato per potersi effettivamente eseguire. Questa soluzione parziale si basa, com'è ben noto, sull'idea seguente. L'atomo è costituito dal nucleo centrale di carica positiva Ze e da Z elettroni. Fissiamo la nostra attenzione su un ben determinato elettrone: i restanti $(Z - 1)$ elettroni costituiscono una specie di nuvola di elettricità negativa che circonda il nucleo. L'elettrone considerato si muove dunque nel campo creato dalla carica $+ Ze$ del nucleo, e dalla carica negativa $-(Z - 1)\, e$ dei rimanenti elettroni. L'approssimazione che si fa di solito e che conduce a una certa comprensione qualitativa e spesso anche quantitativa delle proprietà dell'atomo, consiste nel considerare il campo dovuto agli elettroni, che sono molti ed in rapido movimento, come un campo centrale statico.

In tal modo, il problema viene ridotto per ciascun elettrone a quello di una sola particella che si muove in un campo di potenziale assegnato: questo è un problema relativamente facile da risolvere. Una tale approssimazione è naturalmente piuttosto grossolana; vi sono però due ragioni che la rendono assai migliore di quanto non potrebbe sembrare a prima vista. Anzitutto, il contributo del nucleo, che rappresenta un po' più del 50 % della carica generante il campo, è in questa approssimazione descritto in modo corretto. Ciò che non è descritto in modo corretto è naturalmente il contributo degli elettroni, dato che si trascura il fatto ch'essi sono essenzialmente delle cariche puntiformi in movimento. Tuttavia, le forze che questi elettroni esercitano sull'elettrone particolare su cui abbiamo fissato la nostra attenzione, sono forze coulombiane il cui potenziale è e^2/r: si tratta dunque di forze che decrescono abbastanza lentamente al crescere della distanza e quindi ancora sensibilmente efficaci ad una distanza relativamente grande dalla particella da cui esse provengono. Si può quindi affermare che su di un elettrone particolare agisce abbastanza intensamente un numero elevato di elettroni (almeno nel caso in cui Z è un numero abbastanza grande), per modo che una considerazione statistica del tipo sopra indicato, consistente nel sostituire all'azione complessiva degli elettroni individuali quella di una specie di nuvola di elettricità statica, porta in realtà ad un'approssimazione non troppo cattiva.

Si potrebbe ora pensare di svolgere una teoria approssimata del nucleo, che in particolare rispondesse alla domanda che ci siamo posti all'inizio, partendo da un'idea essenzialmente simile a questa. Consideriamo un nucleo costituito da Z protoni ed N neutroni ed ammettiamo che entrambi questi numeri siano abbastanza grandi. Le forze che si esercitano su di una particolare particella, per esempio su di un protone particolare, provengono da tutte le particelle rimanenti, cioè da $Z - 1$ protoni ed N neutroni. Ci si può chiedere se la forza risultante si possa anche qui, come nel caso di un elettrone atomico, rappresentare con una specie di campo di media indipendente dal tempo.

Fino a tempi molto recenti si è sempre data a questa domanda una risposta negativa. Un tale procedimento, si diceva, sarebbe nel caso del nucleo assai più grossolano che nel caso dell'atomo, per il fatto che i due

argomenti citati a suo favore nel caso precedente non sono più applicabili al nucleo. Da un lato, non si ha più in questo caso una carica centrale che determini da sola la maggior parte dell'energia potenziale; d'altro lato, le forze esercitantisi tra nucleoni sono tipiche forze a breve raggio d'azione. Se fosse quindi lecito farci del nucleo un modello assai grossolano, costituito da un certo numero di particelle più o meno addensate in una certa configurazione, ne deriverebbe che le particelle agenti su uno particolare dei nucleoni costituenti sono poche: quelle che sono con esso a contatto, se un qualche senso si può dare a questa espressione. Il fenomeno ha quindi un carattere statistico assai meno marcato che non nel caso dell'atomo.

Questo è quanto si diceva fino ad un paio d'anni fa circa. Si sono tuttavia andate via via accumulando informazioni a carattere sperimentale che sembrano indicare, a dispetto degli argomenti negativi ora esposti, che anche con una schematizzazione di questo tipo si possa ottenere un certo numero di resultati. Naturalmente, non si sa ancora oggi fino a che punto si possa giungere con idee di questo tipo.

Prima di addentrarmi nell'argomento, desidero dire due parole su un modello nucleare che è stato usato ed è ancora usato in molti casi e che permette di giuugere ad una grande quantità di risultati approssimati. Si tratta del modello a goccia, che parte dall'analogia tra un nucleo ed una goccia di liquido, le molecole della goccia corrispondendo ai nucleoni.

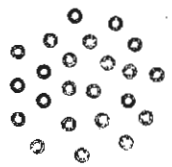

Fig. 1.

Questo modello a goccia corrisponde un po' ad una schematizzazione quale quella della figura 1. Sulla base di essa si potrà dire che una particella che si trovi nell'interno del nucleo è circondata da ogni parte da nucleoni: l'energia di legame conterrà quindi un termine proporzionale al volume del nucleo, cioè al numero di particelle che lo costituiscono. Le particelle invece che si trovano alla superficie del nucleo sono soggette ad un sistema di forze diverso dalle altre, poiché risultano in contatto con una frazione soltanto dei nucleoni che di solito circondano una di queste particelle.

Sviluppando questi concetti con argomenti molto semplici e di carattere semiempirico, è possibile scrivere una formula assai grossolana che risolve abbastanza bene il problema che ci siamo posto all'inizio, di determinare cioè l'energia di legame di un nucleo. Invece dell'energia di legame, si può rappresentare direttamente per mezzo di questa formula la massa di un nucleo, di numero di massa A e numero atomico Z. La formula che si ottiene è allora la seguente:

$$(1) \qquad M(A,Z) = \underbrace{0{,}99391\,A}_{1} - \underbrace{0{,}00085\,Z}_{2} + \underbrace{0{,}014\,A^{2/3}}_{3} +$$

$$+ \underbrace{0{,}083\,\frac{(A/2-Z)^2}{A}}_{4} + \underbrace{0{,}00063\,\frac{Z^2}{A^{1/3}}}_{5} + \underbrace{\delta}_{6}.$$

Il termine 1 di questa formula, essenzialmente proporzionale al numero dei nucleoni presenti non rappresenta la massa totale di questi ultimi. La massa di un nucleone è infatti pari a circa 1,008 unità di massa; il coefficiente di questo termine è invece minore, a causa della perdita di massa corrispondente all'energia di legame. Il termine 3 può spiegarsi come una energia dovuta alla tensione superficiale. Esso è infatti proporzionale alla superficie del nucleo: siccome il raggio del nucleo è proporzionale al numero totale di nucleoni elevato ad $1/3$, così la sua superficie è proporzionale ad $A^{2/3}$. Il coefficiente 0,014 è determinato empiricamente.

Non starò a spiegare in dettaglio l'origine del successivo termine 4. Esso assume evidentemente un valore minimo quando $A = 2Z$, quando cioè il nucleo contiene tanti neutroni quanti protoni; ha quindi essenzialmente la funzione di tener conto del noto fatto sperimentale che le forme nucleari più stabili tendono ad essere quelle contenenti numeri uguali di questi due tipi di particelle.

Il termine 5 ha un significato assai semplice: esso non è altro che l'energia coulombiana. Esso è infatti proporzionale al quadrato della carica ed inversamente proporzionale al raggio del nucleo ($r \sim A^{1/3}$).

Infine, c'è il termine che abbiamo indicato con δ e che è una funzione erratica di A e di Z. Più precisamente, esso tiene conto del fatto noto empiricamente che le varie forme nucleari sono più o meno stabili a seconda della parità o disparità del numero dei protoni e del numero dei neutroni. Questi numeri possono essere entrambi pari o entrambi dispari, oppure uno pari ed uno dispari, com'è indicato nella tabella seguente. La stabilità, a parità di altre condizioni, cresce marcatamente in direzione della freccia.

Z	N	
p	*p*	$\delta = -\frac{0{,}036}{A^{3/4}}$
p	*d*	$\delta = 0$
d	*p*	$\delta = 0$
d	*d*	$\delta = +\frac{0{,}036}{A^{3/4}}$

I valori di δ che si scelgono per rappresentare correttamente i fatti sperimentali sono indicati nella terza colonna.

La formula (1), che è come si è detto una formula semi-empirica suggerita nella sua struttura dal modello a goccia, è in realtà assai semplice, data la natura del problema che risolve; e è anche una formula assai potente, poiché rappresenta con accuratezza sorprendente le masse nucleari attraverso tutto il sistema periodico.

Ci si può però naturalmente proporre di studiare la questione più in dettaglio e domandare fino a che punto questa formula vada bene e che genere di errori si commettano affidandosi ad essa. Si trova che in genere

la formula dà resultati concordanti con l'esperienza: restano tuttavia delle irregolarità di dettaglio, che non possono rappresentarsi per mezzo di essa. Se ad esempio prendiamo in considerazione tutti i nuclei corrispondenti ad un certo valore del rapporto Z/A e rappresentiamo i difetti di massa dati per essi dalla formula (1) in un grafico, ponendo in ascisse il numero di massa A, otteniamo (a parte il termine 6) del quale per il momento non vogliamo occuparci, un andamento continuo del genere di quello rappresentato nella figura 2. Ora, si trova che l'andamento effettivo segue abbastanza bene nelle sue linee generali quello calcolato, pur essendovi delle deviazioni locali del genere di quelle rappresentate mediante la curva tratteggiata della figura 2. I punti singolari corrispondono a ben determinati valori del numero di protoni o del numero di neutroni nel nucleo. Questi valori, che vengono ormai comunemente chiamati numeri magici, sono i seguenti:

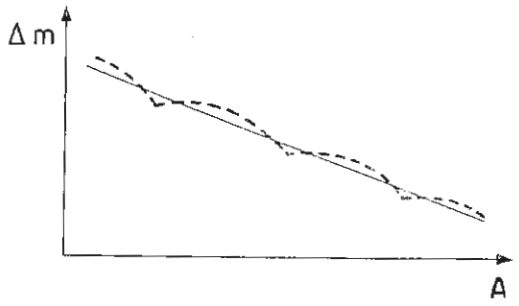

Fig. 2.

$$2\ ,\ 8\ ,\ 20\ ,\ 50\ ,\ 82\ ,\ 126.$$

Non mi soffermerò troppo a discutere le varie proprietà di questi numeri magici. Mi limiterò a porre in rilievo, sulla base della figura 2, ch'essi corrispondono a forme nucleari particolarmente stabili. La curva sperimentale della figura 2 un tratto della quale è rappresentato ingrandito nella figura 3, non è in realtà una curva continua: l'ascissa rappresenta un numero di particelle: quindi la curva è in realtà costituita da una successione di punti distanti di una unità sulle ascisse. Partiamo da un punto come il punto A, che si trovi poco prima di una cuspide. Il difetto di massa per l'aggiunta di una particella nel nucleo aumenta fortemente prima della cuspide: fino a questo punto, le singole particelle nel nucleo sono cioè assai fortemente legate, Tale aumento è invece assai minore subito dopo la cuspide: dopo questo punto cioè le particelle sono dapprima assai meno legate, poi al crescere di A divengono via via più legate fino a che si raggiunge nuovamente una situazione simile a quella del punto A subito prima di un nuovo punto di discontinuità.

Fig. 3.

Si ha in altre parole una situazione simile a quella che si ha nel caso degli atomi. Gli elettroni K sono qui i più legati, vengono poi gli elettroni L, che completano la seconda orbita, legati sempre con una certa energia. L'elettrone seguente è poco legato, ma l'energia di legame cresce via via che

si aggiungono nuovi elettroni sinché non si arriva a completare un'altra orbita, e così di seguito.

Le informazioni sperimentali su cui è basato il riconoscimento delle orbite nel caso dei nuclei, sono in buona parte del genere di quelle sopra esposte. Rappresentiamo i nuclei stabili nel solito diagramma, ponendo in ascisse il numero di protoni e in ordinate il numero di neutroni, e fissiamo la nostra attenzione sul numero di isotopi corrispondenti a valori fissi di N o di Z. Si trova che quando per esempio il numero di protoni corrisponde ad uno dei numeri magici il numero di isotopi esistente è assai più numeroso del solito. Infatti a causa della forte stabilità di questi nuclei, i nuclei adiacenti si trasformano in essi mediante transizioni beta. Lo stesso avviene quando il numero di neutroni corrisponde ad uno dei numeri magici.

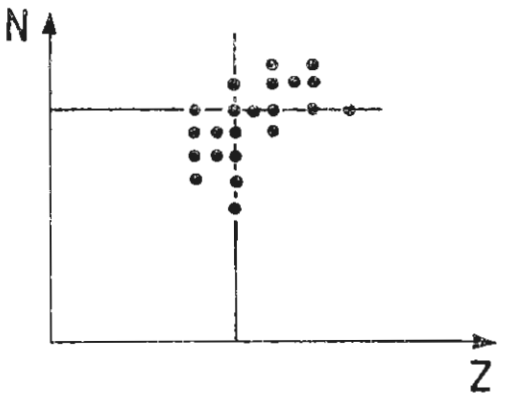

Fig. 4.

Si hanno poi anche dati di altra natura. Se per esempio si esaminano i dati relativi all'abbondanza cosmica degli elementi, si riconosce che i nuclei in cui Z od N è un numero magico sono particolarmente abbondanti. E si potrebbe, volendo, citare un'altra mezza dozzina di fatti di questa natura. Io mi limiterò a citarne uno solo, che si riferisce al comportamento dei nuclei molto pesanti e quindi ai numeri magici 82 e 126. Seaborg, bombardando con particelle di energie assai elevate prodotte col ciclotrone gigante di Berkeley, ha recentemente assai estesa la tavola delle radioattività alfa. Nell'estrema parte del sistema periodico, contenente gli elementi radioattivi, egli è riuscito a produrre e a identificare un numero enorme di nuclei che emettono particelle alfa e a determinare l'energia di queste particelle. E ciò non solo per nuclei vicini alla curva di stabilità, ma anche allontanandosi ampiamente da essa sia da una parte sia dall'altra. Usando i dati di Seaborg, riportando sul piano (N , Z) in una terza dimensione i difetti di massa, è possibile fare, introducendo pochissime ipotesi, un grafico tridimensionale (una specie di carta geografica) dell'andamento dei difetti di massa in questa zona, attraversata dalle linee magiche corrispondenti a 82 protoni, a 82 neutroni e 126 neutroni. Ciò che si

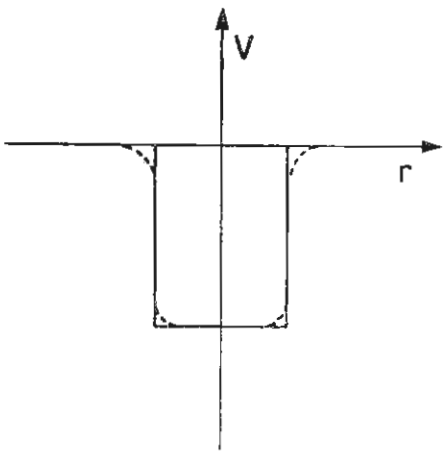

Fig. 5.

trova è l'analogo in tre dimensioni dell'andamento rappresentato nel caso bidimensionale nella figura 2.

Se è dunque vero che anche nel caso della struttura dei nuclei si trova una situazione simile a quella del sistema periodico degli elementi, ciò suggerisce che a dispetto degli argomenti in contrario esposti all'inizio, anche in un nucleo si possa parlare di orbite. Il primo tentativo che viene in mente di fare in proposito è il seguente. Il campo agente su di un nucleone all'interno di un nucleo può rappresentarsi per mezzo di quella che si chiama di solito una buca di potenziale: il potenziale è zero al di fuori di una zona che rappresenta grosso modo l'estensione del nucleo, mentre scende rapidamente a valori molto bassi all'interno. Lungo una sezione diametrale del nucleo, il potenziale sarà quindi rappresentato da una curva dall'andamento simile a quello della figura 5. Viene allora fatto di chiedersi quale sarà la sequenza delle orbite, per un nucleone sottoposto ad un campo del genere. Naturalmente per mettersi in condizioni più definite converrà assumere la buca di potenziale ad angoli vivi.

Questo problema si risolve abbastanza facilmente e porta ai resultati seguenti. Uso qui per indicare la quantità di moto areale delle orbite la notazione spettroscopica. Con l indico la quantità di moto areale misurata in unità $h/2\pi$; allora le lettere s, p, d, f, g, h, i significano rispettivamente $l = 0, 1, 2, 3, 4, 5, 6$. La successione delle orbite risulta essere la seguente:

orbita	numero di particelle
1 s	2
1 p	6
1 d	10
2 s	2
1 f	14
2 p	6
1 g	18
2 d	20
3 s	2
1 h	22
2 f	14
3 p	6
1 i	26
2 g	18
3 d	10
4 s	2

Se si fa il calcolo assumendo una buca di potenziale ad angoli vivi, le varie orbite, in questa successione, risultano spaziate da intervalli quasi

uguali. Se invece si arrotondano un po' gli angoli della buca gli intervalli diventano diseguali e si formano degli aggruppamenti di orbite, nel modo indicato dalle parentesi della tabella precedente. La seconda colonna della tabella indica il numero massimo di particelle che si possono mettere in ciascuna orbita, in base al « principio di Pauli ». Questo numero si calcola come nella fisica dell'atomo ed è dato da $4\,l+2$, essendo l il numero quantico azimutale. Ad esempio, nelle orbite s si possono mettere due nucleoni dello stesso tipo, neutroni o protoni, in un'orbita p se ne possono mettere 6, e così via.

Se la situazione dei nuclei fosse esattamente quella rappresentata nella tabella precedente, si potrebbero fare in base ad essa le previsioni seguenti. La prima orbita si riempie con due nucleoni, due protoni o due neutroni, con che è completo il primo gruppo. Dunque 2 è uno dei numeri magici. Il secondo gruppo coincide con la seconda orbita e si riempie con sei particelle, che aggiunte alle 2 precedenti dà 8, come secondo numero magico. Il terzo gruppo di orbite comprende due orbite con un totale di 12 particelle: il terzo numero magico risulta quindi essere 20. Sin qui come si vede le cose van bene e le previsioni coincidono coi dati sperimentali. Nel seguito però il modello cessa di funzionare, perché i numeri magici previsti risultano essere 40, 70 e 112 anziché 50, 82 e 126.

A dispetto di questo, E. Feenberg e L. Nordheim in due recenti pubblicazioni hanno cercato di far tornare le cose, ammettendo (in realtà in modo del tutto arbitrario) che le orbite della tabella precedente possano subire degli opportuni spostamenti. Date le nostre conoscenze abbastanza scarse sulle forze nucleari, c'è evidentemente in materia una certa libertà d'azione, ma alcune delle invenzioni ch'essi sono costretti a fare sembrano del tutto inattendibili. Non mi occuperò di conseguenza ulteriormente di questi tentativi, e passerò senz'altro a parlare di un altro, proposto indipendentemente da Maria Mayer a Chicago e da Suess. Costoro partono dall'idea che esista per le orbite di un nucleone nel nucleo, così come per le orbite di un elettrone atomico, un accoppiamento tra momento intrinseco e momento orbitale. Lo spin della particella può orientarsi parallelamente o antiparallelamente al momento orbitale, cosicché ad ogni valore di l vengono in realtà a corrispondere due orbite, una con momento risultante $l+1/2$ e l'altra con momento risultante $l-1/2$.

Si può ora ammettere che tra questi due livelli energetici esista una separazione abbastanza grande. Più precisamente, bisogna ammettere, per trovarsi in accordo coi resultati sperimentali, che tale separazione sia una funzione abbastanza rapidamente crescente di l, di guisa che per valori di l piccoli essa non alteri molto lo schema precedentemente descritto. Le differenze s'incominciano a produrre per i valori più elevati di l e si presentano nel modo seguente.

I primi tre gruppi rimangono inalterati. Al quarto gruppo viene ad aggiungersi una delle due orbite in cui viene a scindersi l'orbita $1\,g$ del quinto gruppo, precisamente quella che ha momento resultante $4+1/2=9/2$. Analogamente, una delle due orbite in cui si scinde l'orbita $1\,h$ del sesto gruppo viene ad aggiungersi alle orbite del quinto gruppo, ecc. In conclusione,

i gruppi risultano modificati come indicato nella prima colonna della tabella seguente.

gruppo	orbite	numero di particelle
I	$1s$	2
II	$1p$	6
III	$1d$ $2s$	12
IV	$1f$ $2p$ $1g_{9/2}$	30
V	$1g_{7/2}$ $2d$ $3s$ $1h_{11/2}$	32
VI	$1h_{9/2}$ $2f$ $3p$ $1i_{13/2}$	44

Calcolando come prima il numero di particelle in ciascun gruppo, si ottengono ora i numeri dell'ultima colonna. I numeri magici risultano quindi ora:

$$2 \ , \ 8 \ , \ 20 \ , \ 50 \ , \ 82 \ , \ 126.$$

come risulta dall'esperienza.

Con questa ipotesi abbastanza semplice si riesce quindi a prevedere esattamente il valore dei sei numeri magici. Potrebbe naturalmente ancora trattarsi di un caso e si può cercare di procurarsi delle indicazioni più precise che quella descritta sia effettivamente la situazione.

Si hanno effettivamente a questo proposito un certo numero di fatti abbastanza indicativi. Mi limiterò a citare il seguente. È un fatto sperimentale che tutti i nuclei che contengono un numero pari sia di protoni sia di neutroni hanno quantità di moto intrinseca zero. Ciò significa che se, per esempio, ad un nucleo che abbia un numero dispari di neutroni si aggiunge un neutrone la nuova particella si appaia col neutrone dispari preesistente nel nucleo in modo che la resultante delle loro quantità di moto intrinseche sia uguale a zero. Consideriamo allora un nucleo per il quale sia dispari il numero dei protoni oppure il numero dei neutroni: per esempio un nucleo con Z dispari ed N pari. Possiamo dire ch'esso è costituito da un numero pari di protoni e da un numero pari di neutroni, con l'aggiunta di un protone dispari. È ragionevole supporre che tutte le particelle, ad eccezione di quest'ultima, si associno tra loro in coppie, così da dare un momento angolare risultante uguale a zero. La quantità di moto angolare ed il momento magnetico del nucleo saranno allora dovuti sostanzialmente all'azione del protone dispari. Altrettanto si dirà se la particella dispari è invece un neutrone.

Consideriamo allora per esempio i nuclei della specie citata che si ottengono riempiendo successivamente le orbite del quarto gruppo, che hanno quindi un numero di protoni (o neutroni) uguale a qualunque numero dispari compreso tra 21 e 50 ed un numero pari di neutroni (o protoni). Se è vero che la quantità di moto angolare di questi nuclei è dovuta soltanto al nucleone dispari, si possono avere per essi soltanto certi valori dello spin nucleare e precisamente quelli che corrispondono ai valori del momento angolare risultante delle varie orbite. Saranno dunque

possibili per lo spin i valori: 9/2, corrispondente all'orbita 1 $g_{9/2}$, 3/2 e 1/2, corrispondenti alle orbite *p*, 7/2 e 5/2 corrispondenti alle orbite *f*. Questi sono dunque i soli valori dello spin possibili per i nuclei considerati. Le possibilità sono effettivamente parecchie, ma la condizione si può rendere assai più restrittiva considerando anche i valori del momento magnetico.

Uno stesso valore dello spin nucleare può ad esempio ottenersi talvolta sommando al momento orbitale il momento intrinseco della particella dispari $(l + 1/2)$, oppure sottraendo tale momento intrinseco dal momento orbitale $(l - 1/2)$. Il valore del momento magnetico indica, almeno in molti casi, se si tratta della prima o della seconda circostanza, poiché tale momento risulta diverso nei due casi. Se si tratta di un protone, al quanto azimutale l è associato un momento magnetico di l unità nucleari; se si tratta di un neutrone invece, il momento magnetico associato è nullo, perché il neutrone non ha carica e il suo moto orbitale non dà luogo ad un momento magnetico. A ciò si aggiunge poi nel caso di un protone un momento magnetico intrinseco pari a circa + 2,7 unità nucleari e nel caso del neutrone un momento magnetico pari a — 1,9 unità nucleari. Combinando i vettori con la regola di Landè si può quindi calcolare quale dovrebbe essere nei vari casi il momento magnetico del nucleo.

Non si può dire veramente che i valori sperimentali si accordino troppo bene coi valori teorici. Se per esempio si riportano in ascisse i valori di I e in ordinate i valori del momento magnetico, si ottengono, secondo questa semplice teoria, due curve corrispondenti ai due casi diversi sopra considerati. I valori sperimentali invece non cadono in genere sulle due curve, ma si distribuiscono nel piano press'a poco com'è indicato nella figura 6. In molti casi è tuttavia chiaro a quale delle due categorie appartiene il nucleo in questione, sicchè si può anche decidere, in molti casi senza ambiguità, quali siano i valori di l accettabili.

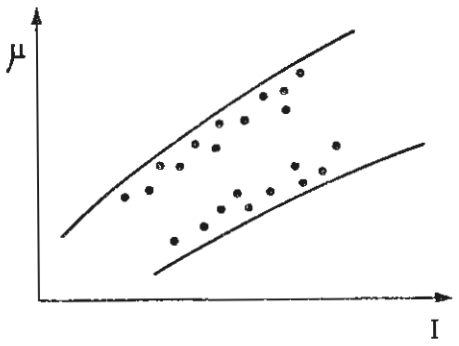

Fig. 6.

Applicando questo procedimento a tutta la successione dei nuclei, si trova circa una cinquantina di casi in cui questi dati possono effettivamente ottenersi e in tutti questi casi, con solo un paio di eccezioni, sembra che questa descrizione porti ad una descrizione corretta delle proprietà di momento angolare e di momento magnetico del nucleo atomico.

Sembra dunque che nel nostro modello ci sia effettivamente qualcosa di vero, anche se il modello stesso è certamente ben lontano dall'essere perfetto: v'è un'indicazione empirica molto decisa, che si può parlare, nel senso che ho indicato, di orbite nucleari.

Sorgono, di conseguenza, diverse questioni teoriche e prima di tutto viene fatto di chiedersi, dato che si può parlare, sia pure in via approssimata di orbite nucleari, come mai gli argomenti negativi citati all'inizio non abbiano in realtà quella validità che si era portati ad attribuir loro. Inoltre,

i fatti sperimentali indicano l'esistenza di un forte accoppiamento tra spin e orbita responsabile di quella scissione dei livelli che è necessaria per far andare a posto i numeri magici: ci si può chiedere qual'è l'origine fisica di questa energia mutua.

Posso qui soltanto accennare ad alcune idee ancora piuttosto vaghe che possono forse contenere alcuni degli elementi della risposta a queste due domande. Il fatto che nel nucleo sembrino esistere orbite individuali per i nucleoni potrebbe forse giustificarsi nel modo seguente. Consideriamo (fig. 7) una zona della materia nucleare ed un nucleone particolare che sta percorrendo una certa traiettoria. Evidentemente sarà lecito o illecito parlare di questa come di un'orbita nucleare, a seconda che si verifica l'uno o l'altro dei due fatti seguenti. Se il cammino libero medio per una forte collisione che alteri bruscamente la traiettoria del nucleone è corto, evidentemente l'orbita risulterà completamente distrutta. Se questo cammino libero medio è invece lungo almeno quanto il perimetro dell'orbita, in modo tale che il nucleone possa percorrere questa interamente almeno una volta, allora si potrà parlare dell'orbita stessa con un certo fondamento.

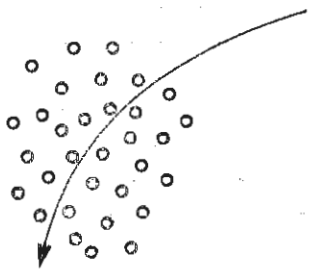

Fig. 7.

Se si computa il cammino libero medio sulla base delle sezioni d'urto tra nucleoni, si trova ch'esso risulta effettivamente assai corto, il che è stato molte volte portato come argomento per affermare che orbite non possono esistere. V'è però un punto che non sembra sia stato considerato in questa valutazione, ed è l'effetto del principio di Pauli. Di questo effetto ci si può render conto nel modo seguente. Il nucleone su cui abbiamo fissato la nostra attenzione passa attraverso una nuvola di altri nucleoni, nuvola che almeno in una certa approssimazione può considerarsi come costituita da un gas degenere di neutroni e da un gas degenere di protoni. Se avviene un urto, esso sarà accompagnato da uno scambio di energia in cui o l'energia del nucleone o l'energia della particella urtata diminuirà. Ma tutto ciò è proibito dal principio di Pauli, perché o l'una o l'altra di queste particelle andrebbe a cadere in una zona di piccola energia i cui livelli sono tutti occupati. Sembra quindi che si debba concludere che il cammino libero medio va sì calcolato in base alle sezioni d'urto, ma scartando tutte quelle possibilità d'urto che sono in contraddizione col principio di Pauli. Con ciò il numero di urti risulta grandemente diminuito e corrispondentemente allungato il cammino libero medio.

Questa potrebbe dunque essere, lo dico con molte riserve, la spiegazione del perché di orbite nucleari si può, nonostante tutto, parlare. V'è poi la questione del forte accoppiamento tra spin del nucleone ed orbita. Questa naturalmente è una questione di forze nucleari, che possiamo tentare di trattare almeno qualitativamente sulla base di una teoria mesonica. Una di queste teorie descrive il campo mesonico in una forma che è del tutto simile a quella del campo elettromagnetico: è la teoria del mesone vetto-

riale. Se questa fosse la teoria corretta, si potrebbe pensare ad un meccanismo d'interazione sostanzialmente simile a quello dell'accoppiamento tra quantità di moto intrinseca e momento orbitale nel caso di un elettrone. Quest'ultimo si produce così: l'elettrone si muove nel campo elettrico del nucleo, le cui linee di forza sono dirette come indicato nella figura 8. Nel sistema di riferimento dell'elettrone, tutto avviene dunque, per il noto effetto relativistico, come se vi fosse un campo magnetico pari al campo elettrico moltiplicato per il rapporto tra la velocità del nucleone e la velocità della luce. Siccome l'elettrone ha un suo momento magnetico intrinseco, questo si orienta e l'energia mutua risulta diversa a seconda che il momento intrinseco è parallelo o antiparallelo a questo campo virtuale. Una descrizione di questo tipo può tradursi nel linguaggio della teoria del mesone vettoriale, semplicemente sostituendo le grandezze elettromagnetiche con le corrispondenti quantità mesoniche.

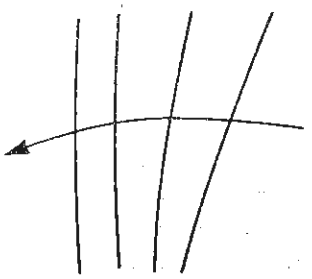

Fig. 8.

Disgraziatamente, un tentativo di fare una trattazione quantitativa dell'argomento, in questa teoria del mesone vettoriale, non può portare a nulla di più che ad un ordine di grandezza. E, naturalmente, non vi sono neppure molti argomenti per ritenere ch'essa sia proprio la teoria mesonica corretta. Ho voluto tuttavia accennare a questo argomento, per far vedere che vi è effettivamente la possibilità di arrivare, domani, per la via indicata ad una teoria consistente di tutti questi fenomeni.

A parte queste ultime considerazioni teoriche, le ricerche di cui ci siamo occupati aprono un campo abbastanza vasto, di carattere semiempirico: esse permettono in molti casi di raccogliere un buon numero di dati, per esempio sulla proprietà di spin non solo dello stato fondamentale di un nucleo, ma anche dei suoi stati poco eccitati. Se per esempio lo spin di un nucleo è $9/2$ e l'orbita è presumibilmente la $1g\,9/2$, gli stati poco eccitati del nucleo sono quelli in cui il nucleone dispari occupa una delle altre orbite dello stesso gruppo: le possibilità da prendere in considerazione sono quindi in numero piuttosto ristretto. Si può anzi notare che nuclei di questo tipo dànno spesso luogo ad isomeri. Questi si hanno quando l'orbita fondamentale è per esempio $9/2$ e quelle poco eccitate sono $1/2$ o $3/2$. Dato il forte cambiamento di momento angolare, tutte le transizioni sono allora proibite di un ordine assai elevato, così che gli stati poco eccitati hanno vita estremamente lunga e dànno quindi luogo ad isomeri.

In conclusione si può dire che queste ricerche aprono uno spiraglio di luce, per cominciare a costruire una sistematica dei nuclei. Naturalmente, prima che questa teoria possa venir considerata in alcun modo come definitiva, le domande fondamentali che ho posto, e cioè perché le orbite nucleari costituiscano un modello di discreta validità e perché ci sia un forte accoppiamento tra spin e orbita, dovranno essere completamente chiarite. Anche il materiale sperimentale andrà esaminato con molta maggior cura, per poter decidere se quelle regolarità che sono suggerite dal modello in questione effettivamente, entro certi limiti, si osservano.

SESTA CONFERENZA (*)

NUOVI SVILUPPI DELL'ELETTRODINAMICA QUANTISTICA

(redatta dal Dott. G. MORPURGO)

Subito dopo la scoperta della meccanica quantistica sorse il problema di estenderla al caso del campo elettromagnetico. È un caso in cui la estensione non è ovvia, perché il campo elettromagnetico, essenzialmente, è un sistema con infiniti gradi di libertà.

Il primo successo in questo tentativo è dovuto a Dirac, il quale stabilì per la prima volta una teoria della radiazione, che rendeva conto dei fatti fondamentali, già postulati nella vecchia teoria di Bohr: e cioè della relazione fra frequenza e livelli energetici, dell'intensità delle righe spettrali ecc.

La teoria di Dirac è essenzialmente una generalizzazione diretta dei metodi della meccanica quantistica fatta come è ben noto secondo lo schema seguente: se consideriamo il campo elettromagnetico in una cavità, in una scatola, per intenderci, di dimensioni finite (indichiamone con Ω il volume), da considerazioni di statistica e di elettromagnetismo, risulta che questo campo elettromagnetico è per molti riguardi equivalente ad un mezzo elastico che riempia la cavità e, come tale, ha certe frequenze caratteristiche; queste frequenze caratteristiche hanno uno spettro discreto, fino a che il volume della cavità è finito, mentre quando tale volume tende all'infinito, questo spettro discreto tende ad uno spettro continuo. Ed anzi, detto per inciso, la ragione per cui ci si immagina il nostro campo racchiuso in una cavità è associata al fatto che è più facile dal punto di vista analitico di procedere con uno spettro di frequenza discreto che con uno spettro continuo.

In particolare, un risultato delle considerazioni più sopra accennate è la formula che dà quale è il numero $d\mathrm{N}$ di frequenze caratteristiche comprese tra ν e $\nu + d\nu$:

$$d\mathrm{N} = \frac{8\pi}{c^3}\nu^2 d\nu \cdot \Omega \tag{1}$$

dove c è la velocità della luce.

Ciò premesso, la teoria di Dirac si fonda sull'idea di considerare ciascuna di queste frequenze come la frequenza di un oscillatore di proprietà simili a quelle di un oscillatore armonico meccanico; la meccanica quantistica di questo sistema viene quindi ridotta alla meccanica quantistica di un numero infinitamente grande di oscillatori armonici, con la distribuzione di frequenza data dalla (1).

Sarà bene rilevare fin d'ora una difficoltà che non è particolarmente grave, ma che è forse un primo indizio di difficoltà più gravi che s'incontrano in seguito. È noto che secondo la meccanica quantistica un oscillatore

(*) Tenuta il 14 ottobre 1949 nell'aula dell'Istituto Fisico dell'Università di Roma.

armonico, avente una certa frequenza caratteristica ν, ha una successione di livelli energetici E_N, che sono dati dalla formula

$$E_N = h\nu\left(N + \frac{1}{2}\right) \tag{2}$$

in cui $N = 0, 1, 2, 3 \cdots$ e $h =$ Cost. di Planck.

La (2) mostra l'esistenza di quella che di solito si chiama l'energia di zero, ossia mostra che anche nello stato di minima energia, l'oscillatore ha una energia finita e precisamente data da $h\nu/2$.

Se allora abbiamo non già *un* oscillatore ma *vari* oscillatori la energia di zero complessiva sarà la somma delle energie di zero; e precisamente se questi oscillatori sono in un numero di $8\pi\nu^2\Omega/c^3$ per unità di intervallo di frequenza caratteristica, l'energia di zero complessiva sarà data da:

$$\frac{4\pi^2}{c^3} h\Omega \int_0^\infty \nu^3 d\nu . \tag{3}$$

L'integrale in (3) diverge, onde l'energia di zero di questo sistema è un'energia infinita. Quella ora detta non è la peggiore delle infinità che si incontreranno nel seguito, per la semplice ragione seguente: è ben noto che nel caratterizzare l'energia di un sistema si può sempre lasciare libera una costante additiva indeterminata: quindi nel nostro caso, per evitare l'energia infinita, sarà sufficiente ridefinire in un modo leggermente diverso la scala delle energie, il modo cioè, che l'energia di uno di questi oscillatori, invece di contarla da quello che è lo zero convenzionale la contiamo a partire da $E_{N=0}$; l'energia di zero verrà così a sparire.

La (3) è però indicativa di un tipo di matematica che dà luogo alla maggior parte di quelle infinità che, come voi certamente sapete, sono una delle afflizioni della elettrodinamica e delle teorie dei campi; ed il meccanismo di tali divergenze è sempre grosso modo lo stesso: si tratta di effettuare quasi sempre somme estese a questo infinito numero di oscillatori; e talvolta queste somme (o integrali) danno risultati finiti; mentre talvolta, ed anche spesso, danno risultati infiniti.

Avremo occasione nel seguito di tornare su questo punto; e per proseguire ora nell'esposizione di quello che è stato lo sviluppo dell'elettrodinamica quantistica dirò che, dopo questo primo tentativo di Dirac di trattare il campo elettromagnetico, essa fu messa su una base formale abbastanza completa introducendo non solo il campo di radiazione che corrisponde a questi oscillatori, ma anche essenzialmente la parte non radiativa del campo elettromagnetico, in uno schema unico, del resto non molto differente da quello ora detto.

A questo riguardo vorrei fare una osservazione. Consideriamo un campo elettromagnetico non già isolato, ma con qualche carica presente; e il caso più semplice sarà quello in cui è presente soltanto un elettrone. L'Hamiltoniana di un tale sistema si può scrivere come la somma di tre termini: l'Hamiltoniana H_e dell'elettrone come se il campo elettromagnetico non ci fosse, più la Hamiltoniana $H_{em.}$ del campo elettromagnetico come se l'elettrone non ci fosse, più un termine di interazione $H_{int.}$ che naturalmente sarà pro-

porzionale alla carica dell'elettrone, e la cui forma risulta dalla formula seguente, dove $\boldsymbol{v}$ è la velocità dell'elettrone, $\mathbf{A}$ e φ i potenziali vettore e scalare nella posizione occupata dall'elettrone stesso

$$(4) \qquad H = H_e + H_{em.} + H_{int.} = H_e + H_{em.} - e\left(\frac{\boldsymbol{v}}{c}\cdot\mathbf{A} - \varphi\right);$$

$H_{int.}$ è effettivamente un termine di interazione in quanto in esso intervengono contemporaneamente elementi che dipendono dal campo elettromagnetico ed elementi che dipendono dal moto dell'elettrone; si noti che il termine di interazione porta a coefficiente la carica dell'elettrone e.

Ora, nella maggior parte delle trattazioni, il problema fondamentale della dinamica del nostro sistema « campo elettromagnetico + elettrone » che è quello di risolvere l'equazione di Schrödinger il cui Hamiltoniano è dato dalla (4), viene trattato matematicamente con un processo di approssimazione; e l'approssimazione consiste nel considerare $H_{em.} + H_e$ come la parte imperturbata del problema e $H_{int.}$ come la perturbazione. Si ottiene così il vantaggio ovvio di avere un problema imperturbato molto semplice; perché il campo elettromagnetico non è influenzato dall'elettrone e viceversa.

Secondo le normali prescrizioni della teoria delle perturbazioni tutti i risultati vengono poi ottenuti attraverso un processo di sviluppo in serie; ed il parametro rispetto al quale si sviluppa in serie di potenze in questo caso è la famosa espressione $e/\sqrt{\hbar c}$.

Tutto andrebbe benissimo, o abbastanza bene, se e fosse infinitesimo; ma e non è evidentemente infinitesimo dato che rappresenta la carica dell'elettrone; quindi sostituendo i valori numerici si ha

$$\frac{e}{\sqrt{\hbar c}} = \sqrt{\frac{e^2}{\hbar c}} = \frac{1}{\sqrt{137}}$$

e questa espressione è poco meno di un decimo (che è abbastanza piccolo, o abbastanza grande, secondo i gusti!).

Vorrei aggiungere a questo proposito quanto segue: naturalmente la teoria quantistica del campo elettromagnetico fu la prima a svilupparsi perché il campo elettromagnetico è certamente il campo con cui siamo più familiari; ma negli anni tra il 1930 e il 1940 ci fu una fioritura di teorie un po' simili a questa, in cui si trattava di altri campi. Una di queste teorie è la teoria dei raggi beta la quale differisce da questa in quanto in quel caso la costante di accoppiamento è effettivamente estremamente piccola (dell'ordine di 10^{-10} o 10^{-12}). In tale caso gli sviluppi in serie possono avere una certa vaga attendibilità. Ed un'altra è la teoria di Yukawa, la teoria delle forze nucleari trasmesse dal campo mesonico, in cui disgraziatamente il parametro di sviluppo è grande, ed in realtà circa eguale ad uno, o forse uguale ad un mezzo o forse uguale ad un terzo.

Nella discussione di oggi, però, mi limiterò al caso del campo elettromagnetico che ha il grande vantaggio, su tutti gli altri, di non contenere nessun elemento indefinito in quella che è l'approssimazione classica; poiché l'elettrologia è piuttosto bene stabilita e certamente è conosciuta infinitamente meglio di quel che non sia la teoria del campo mesonico.

Riallacciandomi a ciò che ho detto più sopra vorrei ora venire a parlare di alcune divergenze, che sono, come ho già accennato, il punto cruciale di tutte queste teorie. Il problema è questo: consideriamo nello schema più sopra detto un elettrone, e siano forze dovute al campo di radiazione le uniche forze che agiscono sull'elettrone; (non vi siano, in altre parole, campi esterni presenti). È ben noto allora che sia nella elettrodinamica quantistica, come nella elettrodinamica classica, l'accoppiamento fra il campo elettromagnetico e la carica in movimento si presenta come l'equivalente di una massa elettromagnetica, ed è anzi risaputo che tanto nell'una quanto nell'altra teoria questa massa elettromagnetica risulta essenzialmente infinita. Il tipo dell'infinità però risulta molto diverso nei due casi: essenzialmente nella teoria classica, la massa elettromagnetica di un elettrone in quiete che non sia proprio puntiforme ma abbia un raggio R, è data, come ordine di grandezza, dall'energia elettrostatica e risulta perciò dalla ben nota relazione:

$$mc^2 \cong \frac{e^2}{R} \quad \text{ossia} \quad m = \frac{e^2}{c^2 R} ;$$

onde questa massa elettromagnetica diventa infinita come $1/R$ se parliamo di elettrone puntiforme.

Nella teoria quantistica si ha pure una massa elettromagnetica, la cui divergenza è però di natura diversa da quella classica; la ragione di questa diversità è legata alla teoria di Dirac dell'elettrone (esistenza di stati di energia positiva e di energia negativa) e al fatto che si presenta una certa cancellazione di termini che rende la divergenza, come vedremo, assai debole. Precisamente, si trova che, se consideriamo un elettrone il quale abbia una massa m di origine *non elettromagnetica*, possiamo dire una massa *meccanica*, esso acquista, per effetto dell'accoppiamento col campo, una massa addizionale, che chiameremo $m_{el.}$ per indicare che si tratta di una massa elettromagnetica; la massa che misuriamo, la massa dell'elettrone fisico, m_f, risulta la somma di questa massa elettromagnetica più la massa meccanica; e la espressione della massa elettromagnetica è la seguente

$$m_{el.} \cong m \frac{e^2}{\hbar c} \log \frac{E_{max}}{mc^2} . \tag{5}$$

Vogliamo discutere brevemente la (5): $e^2/\hbar c$ è al solito il famoso $1/137$, poi c'è a fattore la massa meccanica ed infine il $\log \frac{E_{max}}{mc^2}$. A proposito di questo termine logaritmico possiamo dire quanto segue: esso risulta da una di quelle solite somme estese ad un numero infinito di oscillatori; ed in realtà, se la somma fosse estesa a tutti gli oscillatori, il termine stesso divergerebbe; se vogliamo che esso non diverga dobbiamo compiere un « taglio » cioè estendere la somma non a *tutti* gli oscillatori ma soltanto a quelli la cui energia è inferiore ad una certa E_{max}. Naturalmente un tale procedimento non è in alcun modo giustificato nell'ambito di una teoria coerente; il fatto però che l'infinità sia soltanto logaritmica e che l'energia E_{max} del taglio possa essere scelta estremamente grande rispetto alle usuali energie [1] autorizza a sperare

(1) L'ordine di grandezza di E_{max} può determinarsi nel modo seguente: E_{max} potrà essere scelto in modo tale che $m_{el.}$ sia dell'ordine di m. Se si vanno a fare i conti si vede che

che in una futura teoria (la quale si riduca eventualmente alla presente per le basse energie) $m_{el.}$ anziché divergere, converga.

In ogni caso nell'attuale teoria $m_{el.}$ diverge; e questa difficoltà non è che un caso particolare delle infinità che, negli studi di elettrodinamica quantistica che si svolsero sino ad un paio di anni fa, apparivano più o meno dappertutto tutte le volte che si è voluto essere troppo ambiziosi.

La situazione in cui si trovava l'elettrodinamica un paio di anni fa può riassumersi essenzialmente nel modo seguente: tutte le volte che si prosegue nello sviluppo in serie cui abbiamo accennato prima (corrispondente al metodo delle perturbazioni) per calcolare un certo fenomeno la procedura pratica era di arrestarsi appena si trovava un risultato diverso da zero perché, se si osava andare avanti la approssimazione seguente, in genere, era divergente; è questo un modo, evidentemente, non molto dignitoso di condurre un calcolo, ma era questa la regola pratica che si consigliava agli studenti.

Studi di questo genere sono stati ravvivati recentemente principalmente in seguito ad una esperienza di Lamb alla Columbia University, il quale ha ripreso colle tecniche recenti delle indagini spettroscopiche a mezzo delle microonde il problema della struttura fina dell'idrogeno.

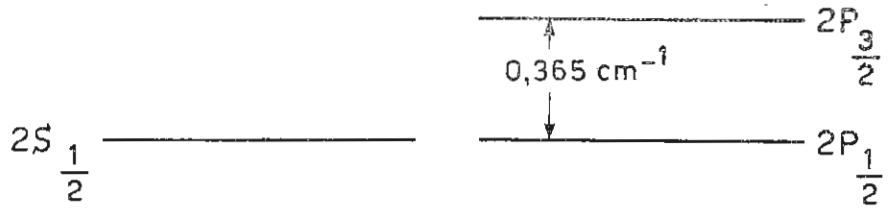

Fig. 1.

È ben noto che se si considera per esempio il termine $n = 2$ dello spettro dell'idrogeno, secondo la teoria che si legge nei libri, ad esempio nel libro di Sommerfeld, esso è costituito da un termine $2\,S_{1/2}$ con quantità di moto angolare totale $1/2$; e di un doppietto $2\,P_{1/2}$ e $2\,P_{3/2}$.

La posizione di questi termini secondo quanto si legge nel Sommerfeld è quella indicata nella figura 1 qui disegnata. Abbiamo i due termini $2\,P_{1/2}$ e $2\,P_{3/2}$ separati dalla differenza di frequenza di 0,365 cm^{-1}. Poi abbiamo un termine $2\,S_{1/2}$ coincidente esattamente con il $2\,P_{1/2}$. Bisogna dire ad onor del vero che gli spettroscopisti che avevano studiato questi fenomeni avevano timidamente espresso l'opinione che in realtà le cose non stessero così; ma siccome le esperienze non erano molto precise, e comunque la gente aveva probabilmente più fiducia nella teoria di quel che non dovesse esser lecito, la cosa non aveva colpito l'attenzione. Solo quando Lamb riattaccò il problema coi metodi più potenti che si hanno oggi per misurare le piccole differenze di frequenza a mezzo delle microonde, invece che con i sistemi della spettroscopia convenzionale, tutti si persuasero che in realtà lo schema non è quello

risulta $E_{max} \cong 10^{53}$ erg che è 100.000 volte la massa della terra tradotta in energia con la relazione di Einstein.

disegnato ora, e che, mentre la distanza tra i due livelli $2\,P_{1/2}$ e $2\,P_{3/2}$ è con grande approssimazione quella prevista dalla teoria, il livello $2\,S_{1/2}$ è spostato rispetto al $2\,P_{1/2}$ di qualcosa come 0,033 cm^{-1}, che è circa il dieci per cento della distanza totale fra i $2\,P_{1/2}$ e $2\,P_{3/2}$ (vedi fig. 2).

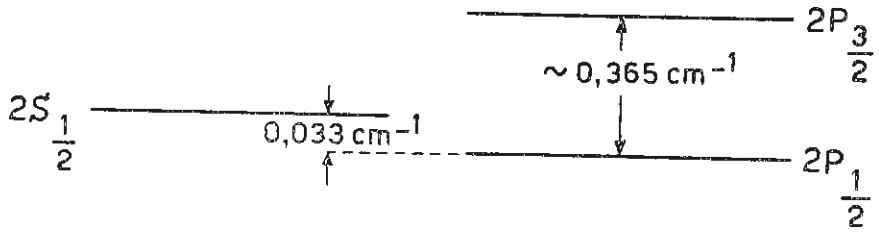

Fig. 2.

Sono, stati precisamente il tentativo ed i lavori che furono fatti per spiegare questa differenza tra teoria ed esperienza che condussero al progresso veramente notevole che c'è stato nella elettrodinamica quantistica negli ultimi due o tre anni. È difficile dare un nome a chi si deve questo progresso perché l'origine del lavoro avvenne in una conferenza alla quale partecipavano una trentina di fisici teorici e nella quale il problema fu discusso; e molte delle idee generali che sono state poi sviluppate furono, per lo meno qualitativamente espresse, senza arrivare a sviluppare in dettaglio i calcoli. Comunque il primo lavoro pubblicato, in cui questa situazione venne spiegata almeno al 99 %, è di Bethe, il quale calcolò l'effetto della perturbazione del termine $2\,S_{1/2}$ dovuto all'accoppiamento con tutti gli oscillatori di radiazione e con un artificio di sottrazione arrivò a giustificare che l'effetto doveva essere molto vicino, in realtà quasi esattamente, l'effetto sperimentale.

Per mostrare il ragionamento di Bethe dovrei riportarmi un momento alla (4) e mettere qualche cosa di più al posto delle espressioni H_e, $H_{em.}$ che erano state costà semplicemente indicate. H_e è l'energia dell'elettrone, la quale è la somma della sua energia cinetica che, non relativisticamente, si scrive $p^2/2m$, p essendo l'impulso, e della energia potenziale U dovuta all'interazione col nucleo; $H_{em.}$ lo possiamo lasciare semplicemente indicato e $H_{int.}$, nel caso di radiazione pura, si riduce a $(e/c)\,\boldsymbol{v}\cdot\mathbf{A}$; onde la (4) può essere riscritta:

$$H = \frac{p^2}{2m} + U + H_{em.} - e\frac{\boldsymbol{v}}{c}\cdot\mathbf{A}. \tag{6}$$

Se allora, applicando i metodi soliti della teoria delle perturbazioni, si studia lo spostamento dei termini dello spettro dell'atomo di idrogeno dovuto alla perturbazione $(e/c)\,\boldsymbol{v}\cdot\mathbf{A}$, il risultato è il seguente: la prima approssimazione dà zero e la seconda approssimazione diverge; cioè dei due primi termini dello sviluppo, il termine proporzionale a e (di prima approssimazione), ha per coefficiente zero; il termine proporzionale ad e^2 (di seconda approssimazione), ha per coefficiente uno dei soliti infiniti.

Di solito a questo punto ci si era scoraggiati e si era detto: evidentemente, la teoria non è abbastanza buona, per trattare di questi fenomeni.

L'osservazione molto semplice che venne fuori dalla conferenza a cui ho accennato è la seguente: consideriamo l'espressione $p^2/2m$; che cosa intendiamo con la m che vi compare? Siccome la spartizione della Hamiltoniana in tre termini è fondata sull'idea di separare quantità relative al solo elettrone, quantità relative al solo campo e interazione, la quantità $p^2/2m$ deve riferirsi al solo elettrone; ossia se si potesse, con un artificio inimmaginabile, escludere il campo elettromagnetico la massa m da mettere a denominatore della $p^2/2m$ sarebbe la massa meccanica. Nel fare i calcoli, noi mettiamo però al posto di m la massa fisica dell'elettrone che è $m_f = m_{\text{em.}} + m$ e chissà quanta di questa è massa meccanica e quanta massa elettromagnetica. Ciò non è evidentemente corretto. Poiché la massa fisica, quella che noi misuriamo, è la somma della massa meccanica e di quella elettromagnetica, se vogliamo riscrivere correttamente l'espressione (6) facendo uso di quello che conosciamo, e cioè della massa fisica, dobbiamo scriverla diversamente e precisamente:

$$\frac{p^2}{2(m_f - m_{\text{em.}})} + \mathrm{H}_{\text{em.}} - e\frac{\boldsymbol{v}}{c}\cdot\mathbf{A}. \tag{7}$$

Dobbiamo ora ricordarci che la massa elettromagnetica, come dicevo prima, è un effetto del secondo ordine e cioè proporzionale ad e^2; quindi, se vogliamo formalmente fare uno sviluppo consistente in potenze di e dobbiamo sviluppare il termine $\frac{p^2}{2(m_f - m_{\text{em.}})}$ ed associare la parte di esso che contiene la massa elettromagnetica a termini di ordine e^2; dobbiamo dunque riscrivere la (7) al modo seguente:

$$\frac{p^2}{2m_f} + \mathrm{H}_{\text{em.}} + \mathrm{U} + \frac{p^2}{2m^2}\left(\frac{m_{\text{em.}}}{e^2}\right)e^2 - e\frac{\boldsymbol{v}}{c}\cdot\mathbf{A}$$

in cui ho diviso e moltiplicato $\frac{p^2}{2m_f^2}m_{\text{em.}}$ per e^2 per ricordarmi che si tratta di un termine di ordine e^2. Cosicché veniamo ad avere, in un certo senso, due perturbazioni: una è quella che abbiamo considerato prima $(e/c)\,\boldsymbol{v}\cdot\mathbf{A}$, la quale dà risultato zero in prima approssimazione ed un risultato proporzionale a e^2 con coefficiente infinito in seconda approssimazione; ma abbiamo anche un altro termine di seconda approssimazione che viene direttamente da:

$$\frac{p^2}{2m_f^2}\left(\frac{m_{\text{em.}}}{e^2}\right)e^2 .$$

Nel calcolare il coefficiente del termine in e^2 intervengono tutt'e due queste perturbazioni ed entrambe danno luogo ad un coefficiente infinito. (Ricordo, come ho detto, che la massa elettromagnetica contiene quella certa infinità) [2]. Il punto essenziale è allora che le due parti infinite si cancellano; e quel che resta è un risultato finito che è estremamente vicino a quello che si osserva sperimentalmente. Dicendo questo non dico completamente la verità in quanto il lavoro di Bethe è un calcolo non relativistico. Esso è quindi un calcolo che evidentemente viene a cadere quando si arriva ad includere energie dell'ordine di $m_f c^2$; il risultato ora detto è vero se ai lavori di Bethe

(2) Il « tipo » dell'infinità dipende dal tipo di equazione d'onda cui obbedisce l'elettrone.

si aggiungono quelli di vari altri autori che hanno permesso di studiare il comportamento relativistico; ma di questo dirò qualche cosa in seguito.

Forse più a titolo di curiosità che altro, vorrei mostrare con un argomento molto semplice dovuto a Welton quale è, o quale si può considerare, il meccanismo del fatto che la interazione col campo elettromagnetico determina uno spostamento dei livelli S; disgraziatamente, non ho il tempo di svolgere l'argomento in dettaglio benché si tratti di un calcoletto facile; non so se crederei all'argomento, se non desse il risultato giusto ma in effetti esso lo dà.

Si tratta di questo: consideriamo un elettrone; se anche non ci sono fotoni presenti, vi sono sempre le fluttuazioni del campo elettromagnetico, le quali producono il ben noto fatto che se misuriamo per esempio il campo elettromagnetico in una certa posizione, in realtà, anche se non vi sono fotoni troviamo un valore diverso da zero, dovuto a queste fluttuazioni. Ora il campo di fluttuazione scuote l'elettrone forzandolo, se l'elettrone volesse stare in riposo, a muoversi con delle specie di oscillazioni forzate; cosicché l'elettrone viene a spandersi su una zona di estensione finita; ciò altera l'interazione tra l'elettrone e la carica, che possiamo considerare puntiforme, del nucleo, nel senso che quando l'elettrone si avvicina molto al nucleo, bisogna tener conto di questa estensione; e, se si fa il calcolo su questa base si trova precisamente lo stesso risultato ottenuto da Bethe. Si può quindi dire che l'effetto è dovuto alle fluttuazioni del campo elettromagnetico, che è anche il punto di vista cui si arriva del resto con la teoria più completa.

Diciamo qualche cosa di questa teoria più completa.

Essa è stata attaccata da vari ricercatori e forse le persone che più hanno contribuito a queste ricerche sono: Schwinger, Tomonaga, Feynman e Dyson. Non starò a dire quel che ciascuna di queste persone ha fatto; essi hanno contribuito in varie direzioni ed in vario limite.

Il problema risolto da Bethe è un problema non relativistico; e in realtà la soluzione è veramente alquanto incompleta, come ho già accennato, perché, per portarla a convergere, bisogna troncare il processo a energie dell'ordine $m_f c^2$, in cui l'elettrone comincia a comportarsi non relativisticamente, il che è in certo senso giustificato. D'altra parte senza una analisi approfondita non si potrebbe sapere che cosa succede a quel punto.

Sorge perciò il problema di stabilire una metodologia per fare calcoli di questo genere, relativisticamente corretti; e ciò richiede in particolare di scrivere le equazioni, diciamo così, del movimento del nostro sistema, in una forma che sia chiaramente invariante relativisticamente.

In tutte le rappresentazioni comuni della meccanica quantistica dei campi questa invarianza relativistica che pur sussiste, come si può vedere attraverso calcoli complicati, non è di solito molto evidente, per la semplice ragione che la equazione di Schrödinger, per esempio, rappresenta una legge di variazione dello stato al variare del tempo e conseguentemente nell'usare l'equazione di Schrödinger, si trattano variazioni rispetto a sezioni dello spazio–tempo a tempo costante; e questo procedimento non è certamente il migliore per mostrare la covarianza relativistica di una teoria.

L'idea di Tomonaga fu di sviluppare un metodo per trattare le teorie dei campi in cui il considerare lo stato ad un certo tempo viene a sparire. Si

potrebbe pensare naturalmente di procedere nel modo seguente: consideriamo accanto alle superficie $t = \text{cost.}$ « parallele » allo spazio del nostro laboratorio, le famiglie di superficie $t' = \text{cost}$ « parallele » allo spazio di un generico laboratorio e vediamo se ci è possibile cercare di stabilire, dato lo stato su una di queste sezioni, delle equazioni che permettano di lavorare sulle altre sezioni. Quello ora detto sarebbe un procedimento relativisticamente invariante; ma a quanto pare finora esso sarebbe matematicamente un po' più complicato del seguente procedimento più generale dovuto a Tomonaga: invece di considerare sezioni piane dello spazio-tempo consideriamo delle sezioni qualsiasi; consideriamo in altre parole una superficie arbitraria, con la sola restrizione che sia una superficie spaziale, cioè che, dati due punti qualsiasi di questa superficie, la loro distanza in tempo, moltiplicata per c, sia minore della distanza in spazio, la quale proprietà è notoriamente una proprietà relativisticamente invariante. Data una superficie spaziale σ qualsiasi si può ricercare una equazione che permetta, dato lo stato in tutti i punti di σ, di determinare lo stato stesso su una $\sigma' \neq \sigma$.

E precisamente la questione va posta nei termini seguenti: fissiamo anzi tutto l'attenzione sulla equazione di Schrödinger la quale, come è ben noto, ci dice come varia lo stato nel passaggio dall'una all'altra delle superficie $t = \text{cost}$ « parallele » allo spazio del nostro laboratorio. L'equazione di Schrödinger si scrive notoriamente:

$$\mathrm{H}\psi = i\hbar \frac{\partial \psi}{\partial t} \tag{8}$$

ψ essendo la funzione di stato del nostro sistema ed H essendone l'Hamiltoniana, che, nella teoria dei campi, si presenta sempre come integrale di volume di una certa densità di Hamiltoniana; indicherò quest'ultima con $\mathcal{H}$ onde $\mathrm{H} = \int \mathcal{H} d\mathrm{V}$.

Si tratta allora, nell'ordine di idee sopra discusso, di trovare una equazione di carattere funzionale che permetta di associare una funzione di stato non ad un tempo, come la (8), ma ad una superficie di carattere spaziale σ, e che goda delle proprietà seguenti: anzitutto tale equazione funzionale deve ridursi all'equazione di Schrödinger se la successione di superficie che si considera è una successione di superficie $t = \text{cost}$. In secondo luogo se si va da una superficie σ iniziale ad una superficie finale σ' in vari modi, passando attraverso superficie intermedie di varia forma, il risultato deve dipendere soltanto dalla specificazione della superficie iniziale e della superficie finale.

Ciò porta alla soluzione di questo problema, alla equazione di Tomonaga, che si scrive di solito nella notazione seguente che spiegherò subito [3]:

$$i\hbar c \frac{\delta \psi(\sigma)}{\delta \sigma(x')} = \mathcal{H}(x')\, \psi(\sigma). \tag{9}$$

In luogo del parametro tempo compare nella (9) come argomento di ψ la superficie σ che è il nostro parametro; il punto x' è un punto quadri-

(3) In effetti la grandezza $\mathcal{H}$ che compare nella (9) [e nella seguente (10)] non è proprio la densità di Hamiltoniana precedentemente definita ma la cosidetta densità di Hamiltoniana di interazione.

mensionale su questa superficie ed il simbolo $\delta/\delta\sigma(x')$ (derivata funzionale rispetto a σ del punto x') sta a ricordarci che $\psi(\sigma)$ è un funzionale del parametro superficie. La derivata funzionale va intesa come segue: supponiamo di modificare leggermente la superficie σ nelle vicinanze del punto x'; ciò porterà ad una variazione infinitesima di ψ; diciamo $\psi(\sigma)$ il valore di ψ relativo alla superficie σ; $\psi(\sigma + \delta\sigma)$ il valore di ψ relativo alla superficie $\sigma + \delta\sigma(x')$: allora la derivata funzionale è definita come la variazione di ψ divisa per il volume quadridimensionale che è stato aggiunto, quando quest'ultimo tende a zero seguitando a contenere il punto x'

$$\frac{\delta\psi(\sigma)}{\delta\sigma(x')} = \lim_{\delta\sigma(x')\to 0} \frac{\psi(\sigma+\delta\sigma)-\psi(\sigma)}{\int \delta\sigma(x')\,dV}.$$

Si può dimostrare molto facilmente che questa equazione di Tomonaga ha precisamente le proprietà richieste, purché sussista una relazione che è sempre verificata nei casi che si presentano, e cioè che le densità di Hamiltoniana prese a due punti quadridimensionali che siano però connessi da un vettore spaziale, commutino:

$$[\mathcal{H}(x), \mathcal{H}(x')] = 0. \tag{10}$$

L'equazione di Tomonaga ha il grande vantaggio di essere relativisticamente invariante a prima vista e pertanto è molto superiore per il calcolo pratico all'equazione di Schrödinger, tutte le volte che si debba stare attenti alla invarianza relativistica, in quanto questa invarianza si vede direttamente senza doverla dimostrare.

Messo il formalismo su una base relativisticamente invariante, non è certamente un'impresa facile dire come si procede nel metodo di Schwinger nel breve tempo che mi rimane! Accennerò ai punti essenziali: nel metodo di Schwinger si parte ancora da una espressione del tipo (4) e si compie uno sviluppo in serie in potenze di e. Il problema viene qui trattato direttamente con una equazione o con equazioni che sono del tipo di Tomonaga e si trovano naturalmente delle divergenze, ossia dei termini rappresentati da integrali, che sono divergenti.

Si cerca allora di raggruppare questi termini in modo conveniente. Si vede precisamente che:

1° taluni di essi hanno il carattere di massa; essenzialmente sono termini che rappresentano la massa elettromagnetica; e vengono associati alla massa meccanica nel dare la massa totale senza preoccuparsi del fatto che siano infiniti. Si dice: l'unica grandezza che abbia carattere di massa che noi possiamo conoscere è la massa totale, la massa fisica; e il distinguere tale massa in una massa meccanica e una massa elettromagnetica, probabilmente non ha senso; o comunque non sapremmo come fare se volessimo;

2° altri termini hanno la natura di una carica elettrica e vengono associati ad essa dando una « rinormalizzazione » della carica.

Non posso insistere molto su questo punto. Dirò semplicemente che come abbiamo introdotto una massa elettromagnetica, viene nella teoria di Dirac dell'elettrone a introdursi anche una specie, diciamo così, di carica elettromagnetica, che è connessa al così detto fenomeno della polarizzazione

del vuoto: il vuoto ha nella teoria di Dirac un carattere fisico, ed è polarizzabile, per modo che una carica, per la stessa natura del suo campo modifica il vuoto e cambia se stessa.

Si procede allora qui in modo completamente analogo a quello che si è fatto nel caso della massa dicendo: il distinguere una carica elettrica in carica elettrica, possiamo dire, originale e carica elettrica di polarizzazione non ha alcun senso; l'unica quantità che abbia carattere di carica che possiamo conoscere è la carica fisica, la carica totale: $e = 4{,}8 \cdot 10^{-10}$ u. e. s. E questa quantità è quella che dovremmo sostituire al posto di tutto quell'insieme di termini aventi il carattere di carica senza preoccuparci se tali termini sono infiniti;

3° restano infine altri termini di natura diversa, anch'essi divergenti, ma divergenti in modo, per così dire, indeterminato; nel senso che hanno parti positive e negative, cosicché sono divergenti o convergenti in dipendenza dell'ordine che si sceglie; qui si compie un atto di imperio ponendo tutti questi termini eguali a zero e giustificando la cosa nel modo seguente: lo schema deve naturalmente soddisfare alle condizioni generali dell'invarianza: invarianza relativistica da una parte e gauge–invarianza dall'altra; i termini suddetti hanno sempre la tendenza ad andar contro all'una o all'altra di queste, essendo coefficienti di espressioni non invarianti: poiché c'è la possibilità di farli eguali a zero, la filosofia della teoria è di dire: evidentemente in una teoria completa dovranno risultare zero per le necessità di invarianza. Quindi anticipiamo questa teoria definitiva ponendoli zero d'ufficio.

Quella che ho esposto è molto brevemente l'idea di Schwinger.

Le idee di Feynman e di Dyson sono un po' diverse, ma non essenzialmente distinte, almeno sino alla seconda approssimazione. In un certo senso sono più adatte a trattare problemi d'urto ed hanno il vantaggio che se ne può dimostrare la univocità in tutte le approssimazioni cosicché forse costituiscono effettivamente la risposta al problema della elettrodinamica quantistica.

Debbo dire che questa risposta, a quanto pare, è al momento presente limitata allo studio di elettroni che obbediscono all'equazione di Dirac: nel caso di particelle diverse le divergenze non si potrebbero eliminare col semplice artificio che ho indicato ma resterebbero in forma essenziale nella teoria.

Per finire voglio aggiungere per quanto riguarda i risultati sperimentali, che, oltre all'accennato risultato di Lamb, vi è un altro dato sperimentale che è stato interpretato in questo stesso schema teorico, ed è una lieve differenza tra il momento magnetico sperimentale dell'elettrone ed il magnetone di Bohr. È una differenza piccola, di circa una parte su mille in quanto il momento magnetico sperimentale dell'elettrone si vede essere uguale alla quantità seguente:

$$\text{Momento magnetico sperimentale} = \left(1 + \frac{1}{2\pi}\,\frac{1}{137}\right) \text{magnetoni di Bohr}$$

ma, naturalmente in una quantità così fondamentale come il momento magnetico dell'elettrone, non è una differenza trascurabile; ed anche questa è essenzialmente dovuta all'accoppiamento col campo elettromagnetico.

Cosicché possiamo concludere questa discussione al modo seguente: nella elettrodinamica propriamente detta c'è stato certamente un grande progresso. Non è ancora probabilmente la teoria definitiva, ma ci ha avvicinato sempre di più alla comprensione dei fenomeni. C'è una certa speranza che idee di questo genere si possano applicare anche, per esempio, alle teorie mesoniche, che sono ben più sconosciute che non il campo elettromagnetico e conseguentemente suscitano, al momento, molta più curiosità. Ci sono difficoltà serie e non è affatto sicuro e forse nemmeno particolarmente probabile che questi tentativi avranno molto successo. Evidentemente però, sono un campo di ricerche future di molto interesse. Può darsi invero, che la fisica del fenomeno sia ancora così imperfettamente compresa che il tentativo di farne una matematica troppo dettagliata sia necessariamente destinato all'insuccesso; oppure può darsi che la matematica permetta di arrivare a capire quale sia la vera fisica del fenomeno. Questo non si può dire al momento presente.

Ciò che posso dire è che c'è in questo momento un grande movimento: quasi tutti i giovani fisici teorici sono ansiosi di occuparsi di teorie dei campi e nient'altro che di teorie dei campi, forse anche in modo un pochino troppo unilaterale: ma questo solo l'avvenire potrà dire.

Voglio concludere ringraziando ancora l'uditorio che ha avuto la pazienza di seguirmi attraverso considerazioni talvolta astruse e talvolta noiose; e voglio ringraziare ancora la Fondazione Donegani e l'Accademia dei Lincei per avermi dato modo di passare queste due settimane all'Università di Roma.

SETTIMA CONFERENZA (*)

IL NEUTRONE

(redatta dal Prof. CARLO SALVETTI)

Voglio ringraziare il prof. Castelnuovo per le sue simpatiche parole nei miei riguardi e la mia gratitudine va all'Accademia dei Lincei e alla Fondazione Donegani che mi permettono di essere qui tra voi a parlarvi degli studi a cui mi sono dedicato per molti anni. Mi è particolarmente gradito che questa esposizione abbia luogo nella sala di una delle grandi industrie italiane. Si cita spesso, e con ragione, il fatto che la scienza contribuisce all'industria: in un certo senso tutti i grandi sviluppi industriali hanno la loro radice in una o più scoperte scientifiche. Si cita forse meno un altro fatto che è altrettanto vero e che è l'opposto di quello che ho detto e precisamente

(*) Tenuta il 18 ottobre 1949 nel salone delle assemblee della Società Montecatini di Milano.

quanto la scienza si avvantaggi del progresso industriale: sarebbe impossibile ogni scienza moderna senza il sussidio e l'apporto di quei mezzi tecnici che solo un grande sviluppo industriale rende possibile.

Io ho in programma di tenere qui a Milano tre lezioni, di cui questa è la prima. Questa e la seguente saranno dedicate a problemi della fisica dei neutroni e questa prima sarà di carattere piuttosto generale e introduttivo; la seguente sarà più specializzata; anche specializzata sarà la terza lezione sul monopolo magnetico di Dirac (una particella che probabilmente non esiste... ma che se esistesse sarebbe bella!).

Il neutrone è stato scoperto negli anni 1932 e 1933 per opera di una collaborazione che incomincia col tedesco Bothe, prosegue coi francesi Joliot–Curie, finisce con l'inglese Chadwick. È una particella relativamente pesante: ha la massa di una unità di peso atomico, come sapete, ed ha carica zero, il che le dà il nome. La sua grande importanza nella struttura della materia fu riconosciuta quasi immediatamente dopo la scoperta, per opera principalmente di Heisenberg, il quale riconobbe che il neutrone è una delle due particelle che formano il nucleo atomico; tuttavia i nuclei atomici, come certamente avete sentito dire molte volte, sono costituiti da un numero variabile di neutroni e di protoni che ne determinano la carica e la massa. Nell'illustrare brevemente la storia del neutrone, vi chiedo scusa se la considererò da un mio punto di vista personale e ciò perché ormai ho lavorato già per tanti anni coi neutroni che li considero un po' miei parenti.

Nel 1934 i Joliot–Curie, i due coniugi le cui ricerche ho citato un momento fa, fecero un'altra scoperta assai importante: bombardando un certo numero di sostanze con particelle alfa, scoprirono la radioattività artificiale ossia le sostanze bombardate si convertivano in sostanze radioattive. La scoperta era estremamente importante essendo il primo caso in cui la radioattività si sottraeva a quelle certe leggi di ineluttabilità per cui si riteneva fino allora che i fenomeni radioattivi non si potessero in alcun modo produrre; dopo le scoperte dei coniugi Joliot–Curie, si imparava per la prima volta a fabbricare le sostanze radioattive.

Ora i miei primi contatti personali col neutrone furono originati da questa scoperta dei coniugi Joliot–Curie. Un'idea piuttosto ovvia era che non solo le particelle alfa potessero produrre questa radioattività artificiale, ma probabilmente anche i neutroni; anzi, si sarebbe potuto presumere, ciò che l'esperienza confermò in seguito, che i neutroni dovessero presentare certi vantaggi sulle particelle alfa perché, essendo essi elettricamente neutri, avrebbero potuto avvicinarsi al nucleo positivo senza esserne respinti. Ma i neutroni sono un po' più difficili da produrre che non le particelle alfa perché non esistono sorgenti dirette di neutroni, ma sono essi stessi il prodotto di disintegrazione nucleare: quindi bisognava procurarsi una sorgente di neutroni.

A quel tempo, all'Istituto di Fisica di Roma dove io lavoravo in quegli anni, c'era una fortunata circostanza nel fatto che nell'Istituto stesso lavorava il prof. Trabacchi, direttore dell'Istituto di Fisica della Sanità Pubblica, il quale aveva a sua disposizione un apparecchio per estrarre l'emanazione

di radio: e fu principalmente con l'aiuto di Trabacchi e per l'aiuto di Trabacchi che mi fu possibile di procurarmi delle sorgenti di neutroni, estremamente esigue rispetto alla scala delle sorgenti di neutroni che si possono avere oggi, ma del tutto sufficienti per un numero considerevole di ricerche.

Vi posso descrivere brevemente come erano fatte queste semplicissime sorgenti. Una di queste aveva le dimensioni di circa 1,5 cm. Era un tubetto di vetro della forma rappresentata in figura 1 in cui si ponevano dei granuli di berillio; prima di saldare il tubo di vetro vi si introduceva una certa quantità di emanazione di radio proveniente dall'apparecchio di Trabacchi, per esempio, mezzo Curie. Le particelle alfa emesse dal radon vanno ad urtare in gran numero contro il berillio e vi producono dei neutroni; cosicché da questa piccola sorgente si sprigiona un gran numero di neutroni; una sorgente come quella che ho descritto ne produce alcuni milioni al secondo. Questa, naturalmente, non è l'unica nè la più perfezionata sorgente di neutroni; è forse la più piccola ed è certamente delle più comode perché è una sorgente che non richiede manutenzione. Una volta introdotta l'emanazione nel tubetto, essa seguita ad emettere particelle alfa per conto suo senza bisogno di nessun intervento o aiuto da parte dell'operatore. È anche una di quelle sorgenti che non si guastano mai; il che è anche un vantaggio.

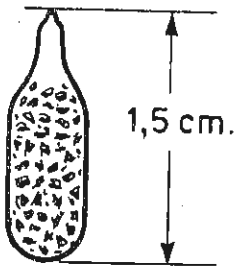

Fig. 1.

Ma poi naturalmente vi sono molte altre e molto più potenti sorgenti di neutroni, i ciclotroni e tutte le varie macchine che producono accelerazione di ioni ad energie dell'ordine di milioni di volt; queste macchine possono usarsi come sorgenti di neutroni, facendo cadere le particelle accelerate sopra un bersaglio per esempio di berillio; essenzialmente è lo stesso principio, soltanto invece di usare le particelle alfa naturali si usano particelle accelerate artificialmente. Si tratta di sorgenti che dànno in genere intensità molto più grandi ma che sono estremamente complicate date le dimensioni e il costo delle macchine acceleratrici.

Oggi, come dirò tra un momento, una delle sorgenti di neutroni più comode, ma anche questa piuttosto grande e macchinosa, è la pila in cui si producono le reazioni a catena dell'uranio e nella quale si arriva ad intensità di un ordine di grandezza parecchie volte maggiore di quello che si può ottenere con un ciclotrone.

Queste sono, in brevi parole, alcune delle principali sorgenti di neutroni.

Ora per produrre la radioattività artificiale per mezzo di neutroni si procede sperimentalmente in un modo assai semplice se si abbia a disposizione una di queste piccole sorgenti. Precisamente l'esperienza è fatta nel modo seguente: attorno alla sorgente di neutroni nelle sue immediate vicinanze si pone, per esempio, una lastrina di alluminio, una lastrina di ferro o una lastrina dell'elemento che si vuole studiare e la si lascia per un certo tempo che può essere di minuti, di ore, giorni, a seconda dei casi. I neutroni che escono dalla sorgente colpiscono alcuni dei nuclei di questa sostanza; avviene allora una varietà di reazioni che possono essere di tipo molto diverso e che possono grosso modo descriversi così. Quando il neutrone

si avvicina a un nucleo dell'elemento bombardato esso non è respinto perché neutro. La probabilità di giungere fino al nucleo è quindi piuttosto elevata. Naturalmente il nucleo è piccolo e quindi è difficile da colpire; ma il nucleo non si difende, per così dire. Quando il neutrone colpisce il nucleo possono avvenire diversi fenomeni. Può avvenire che il neutrone sia semplicemente inghiottito dal nucleo, il quale viene così eccitato. Esso può emettere delle radiazioni elettromagnetiche sotto forma di raggi gamma e trasformarsi in un nucleo il cui peso è cresciuto di una unità. Questa reazione si indica per solito col simbolo $(n\ ,\ \gamma)$. Le altre reazioni più comuni sono: la reazione che si indica con $(n\ ,\ p)$ che vuole dire che il neutrone entra e scaccia un protone; la reazione $(n\ ,\ \alpha)$ in cui un neutrone entra, ed esce una particella alfa. E ve ne sono altre, ma per il momento non le starò a citare.

In ognuna di queste reazioni si forma un nucleo diverso da quello colpito perché in un caso un neutrone si è aggiunto e negli altri casi esaminati un neutrone si è scambiato con un protone o con una particella alfa. Si parte in genere da un nucleo stabile e si va a finire il più delle volte in un nucleo non stabile, cioè in un nucleo radioattivo. Ora la radioattività si può misurare con metodi sperimentali di così raffinata sensibilità, i contatori di Geiger e Müller in particolare, che anche quando si disintegrino pochi atomi radioattivi ogni secondo od ogni minuto, il contatore riesce a scoprirli; ragione per cui il fenomeno, benché quantitativamente assai esiguo, è in realtà molto facilmente osservabile. Debbo confessare che, fino da quel tempo, e in buona parte anche dopo, sono stato prevalentemente un fisico teorico e se talvolta mi è riuscito di condurre a termine esperienze estremamente semplici, debbo dire che appena le esperienze diventano un po' complicate esse sono al di là della mia abilità sperimentale. Per fortuna in quel periodo all'Università di Roma lavoravo in collaborazione con un gruppo di studenti, prima, professori poi, e ora infine colleghi: c'era Amaldi, che è ora il direttore dell'Istituto Fisico di Roma, c'era D'Agostino, che era il chimico del gruppo (in ricerche di questo genere esiste la necessità di molto lavoro chimico, come dirò tra un momento); c'erano Pontecorvo, Rasetti e Segré. Tutti si lavorava in quel tempo sotto la paterna direzione del prof. Corbino, che era allora direttore dell'Istituto Fisico di Roma. Dunque quello che non sapevo fare io in questa tecnica sperimentale lo sapevano fare questi miei amici. Ho detto della chimica e vorrei indicare fin d'ora quale particolare chimica occorresse. Prendiamo, per esempio, il caso della reazione: Fe $(n\ ,p)$ Mn. Se il nucleo di ferro che contiene 26 protoni (perché ha carica 26) ne perde uno scambiandolo con un neutrone che è neutro perde una delle sue cariche e gliene rimangono 25: questo è il numero atomico non del ferro ma del manganese. Se si parte dal ferro di peso atomico 56 si forma il manganese di peso 56 che è un manganese radioattivo di vita media di due ore e mezzo. Ora se non si sa in precedenza quale reazione debba avvenire, solo la chimica può aiutare a capire cosa è successo. Nel ferro bombardato da neutroni si forma qua e là un certo numero, forse dell'ordine di qualche milione, di atomi di manganese radioattivo. E come facciamo a sapere che è proprio manganese?

A questo punto l'amico D'Agostino tirava fuori le sue provette e i suoi apparecchi di chimica ed operava, essenzialmente, una separazione del manga-

nese dal ferro. Per tale operazione si aggiunge in genere una piccola traccia di manganese perché i pochi atomi di manganese che si sono formati per bombardamento si sentono « confortati » e « guidati », per così dire, dalla presenza di un numero pure piccolo, ma sempre maggiore, di atomi di manganese vero, manganese comune. Comunque, dopo l'aggiunta del manganese si discioglie il tutto, si separa, e da una parte va la frazione manganese, dall'altra va la frazione ferro; portando ora semplicemente l'una o l'altra di queste frazioni vicino al contatore e osservando d'onde proviene l'attività si può decidere se l'attività è nel ferro, nel manganese oppure in qualche altra cosa. Questo è il tipo di lavoro chimico che si faceva a Roma, in quegli anni; lavoro condotto in serie, fino a fare separazioni chimiche di questo genere anche in un tempo inferiore al minuto quando si trattava di sostanze radioattive con vita media molto breve in cui non c'era tempo di dilungarsi in elaborate separazioni chimiche. Ora, come dicevo, i neutroni sono un mezzo molto potente per produrre la radioattività artificiale, tanto che nel periodo di circa un anno una cinquantina circa di nuovi elementi radioattivi furono identificati, nell'Istituto Fisico di Roma, con questo metodo. E in quel tempo eravamo tutti soddisfatti del lavoro compiuto e si riteneva che i neutroni avessero dato più o meno tutto quello che potevano dare. Ma poco dopo il nostro gruppo ebbe la fortuna di compiere una di quelle che si chiamano scoperte casuali. Fu una esperienza che francamente non mi sarei mai aspettato, benché essendo un fisico teorico dovrei essere capace di prevedere che cosa sta per succedere; ma invece questa scoperta accidentale capitò così per caso senza andarla a cercare e vi racconterò come si arrivò a scoprire i cosiddetti neutroni lenti.

Dunque in quel tempo c'era una certa confusione nel laboratorio; si lavorava necessariamente in condizioni non perfettamente riproducibili perché c'erano molti elementi da investigare e talvolta si dovevano investigare gli uni e talvolta gli altri in modo non sempre identico nell'uno e nell'altro caso. Ora, in questo modo un po' irregolare di procedere si cominciarono a notare delle differenze che parevano inspiegabili e cioè talvolta l'attività indotta in certe condizioni risultava piccola, talvolta risultava più grande. Capitò perfino che mettendo la lastra da irraggiare abbastanza lontano dalla sorgente, dove l'attività avrebbe dovuto essere quasi non misurabile, si misurasse invece una certa attività. Poiché il fenomeno, benché strano, si poteva riprodurre, si cominciò a fare una serie di osservazioni un po' a caso, mettendo gli oggetti da attivare ora qua ora là nella speranza di cogliere qualche circostanza che desse una chiave per risolvere il problema; e la chiave venne per caso quando accadde di interporre un piccolo pezzetto di paraffina tra la sorgente e l'oggetto da bombardare: questo pezzetto di paraffina fece crescere immediatamente, sia pur di poco, l'intensità ed allora ci si chiese: se poca paraffina fa questo, cosa farà molta ? Se ne mise molta e molta paraffina produsse in realtà un effetto molto grande: l'intensità risultò moltiplicata per un fattore dell'ordine di 20 o 30 o 50, così da indicare che si trattava effettivamente di un fenomeno strano: poi si capì che questo fenomeno strano era quello che si sarebbe dovuto probabilmente aspettare un fisico teorico: era cioè il fenomeno del rallentamento dei neutroni. Esso avviene nella paraffina, per il fatto che questa contiene una grande frazione di idrogeno. Il fenomeno, che

in modo del tutto simile è prodotto anche dall'acqua, consiste in questo: la sorgente di neutroni che ho indicato – come del resto quasi tutte le sorgenti di neutroni – emette neutroni con energia piuttosto grande, dell'ordine in genere di un milione di volt. Ma se questi neutroni vengono emessi entro un blocco di paraffina o entro una vasca d'acqua, essi urtano contro un atomo di idrogeno, e siccome il neutrone e l'atomo di idrogeno hanno, con grande approssimazione, la stessa massa, siamo all'incirca nel caso di una palla di biliardo che ne urta un'altra: l'energia cinetica della prima si suddivide in parti, in media, eguali tra la palla urtante e la palla urtata, così che la palla urtante va via con circa metà dell'energia in gioco; se poi essa subisce un secondo urto, e poi un terzo, e poi un quarto, dimezzando la propria energia in ognuno di questi processi, si ha che, dimezza e dimezza, l'energia si riduce a poca cosa; nel caso del neutrone l'energia andrebbe addirittura a zero se a un certo punto non intervenisse l'agitazione termica: ossia gli atomi di idrogeno dell'acqua o della paraffina sono in agitazione termica, cosìcché il fenomeno del rallentamento non va avanti illimitatamente, ma si ferma quando il neutrone ha perso tanta energia da essere in equilibrio termico con l'ambiente; sicché si forma da ultimo una specie di soluzione di neutroni nell'acqua. Naturalmente si tratta di una soluzione molto diluita e anche di una soluzione molto particolare, perché mentre le soluzioni normali si possono mantenere entro un recipiente, non esistono invece disgraziatamente recipienti per mantenere i neutroni. Quando il neutrone arriva alle pareti della vasca contenente l'acqua, prosegue e se ne va; quindi è una soluzione in stato di continua diffusione verso l'esterno e anche una soluzione in cui la sostanza disciolta sparisce continuamente perché i neutroni combinandosi con l'idrogeno vengono, sia pure in parte, catturati. Un neutrone in acqua, vive circa 200 microsecondi; questo tempo è abbastanza lungo per accumulare una soluzione che ha delle proprietà attivanti assai grandi; la proprietà di attivazione è assai grande perché in numerosissime reazioni nucleari la sezione d'urto dei neutroni lenti è molto maggiore di quella dei neutroni veloci, vale a dire i neutroni lenti hanno una probabilità molto maggiore dei veloci di essere catturati.

Così si fabbricano in modo molto semplice questi neutroni lenti; naturalmente sorge poi il problema di studiarne le proprietà: tali proprietà sono state studiate, dal tempo della loro scoperta fino ad oggi, con mezzi di potenza sempre crescente. Le prime esperienze furono fatte col metodo di assorbimento, selezionando questi neutroni lenti. Quando si parla di neutroni lenti non si deve intendere che abbiano tutti la stessa velocità; hanno tutti una velocità piccola, ma non la stessa; quindi si possono classificare in bande, diciamo così, alcune un po' più veloci, altre meno veloci a seconda della velocità ed a seconda dell'energia. Ora le prime indicazioni di proprietà peculiari di questi neutroni lenti riguardo all'assorbimento, furono ottenute da esperienze di assorbimento, di cui però ora non intendo parlare: oggi infatti questi tipi di esperimenti si conducono con metodi assai più potenti. Si sono trovati oggi metodi per produrre neutroni lenti, ma tutti della stessa velocità, ossia neutroni « monocromatici », vale a dire della stessa energia. Ora esistono due metodi per produrre neutroni monocromatici. Il primo di questi

metodi è basato sull'uso di una sorgente artificiale, per esempio, il ciclotrone. Il metodo consiste in questo: nel ciclotrone si produce una corrente di ioni che colpisce il bersaglio di berillio da cui al momento dell'urto nascono i neutroni. Ma in un ciclotrone è possibile modulare la sorgente in modo che questo bombardamento non abbia luogo in modo continuo, ma avvenga soltanto a certi intervalli di tempo determinati. Si tratta di aprire la sorgente solo per brevi istanti a intervalli di tempo regolari, ciò che si può ottenere con un metodo di modulazione elettrica. Si producono allora nel ciclotrone dei fasci di ioni intermittenti che, colpendo la targhetta di berillio, dànno origine a fiotti istantanei di neutroni con una modulazione regolabile a volontà. Ora se questi neutroni vengono rallentati, per esempio mediante paraffina, e poi inviati su un rivelatore posto ad una certa distanza, è chiaro che dei neutroni, tutti lenti, che escono dalla paraffina quelli meno lenti arriveranno sul rivelatore per primi, quelli più lenti per ultimi. Ora, se si selezionano con metodi elettrici quelli che arrivano in un certo intervallo di tempo, si selezionano neutroni appartenenti a una certa banda di velocità. Tale banda può scegliersi a volontà semplicemente spostando l'intervallo di tempo tra il momento dell'emissione ed il momento dell'arrivo. Questo è uno dei metodi. L'altro metodo verrà descritto in seguito: esso si basa sull'uso delle pile atomiche. Queste permettono di raggiungere grandi intensità di neutroni, per modo che questi ultimi possono essere riflessi su un cristallo: si producono così neutroni monocromatici con lo stesso metodo con cui si producono raggi X monocromatici per mezzo della diffrazione cristallina.

Con l'uno o con l'altro di questi due metodi si può esplorare la legge dell'assorbimento dei neutroni, legge che è talvolta assai semplice: in alcuni casi infatti la sezione d'urto, σ, è una funzione semplice della velocità dei neutroni e precisamente è inversamente proporzionale alla loro velocità. Ossia la sezione d'urto è data da $\sigma(v) = a/v$ (legge dell'$1/v$) (fig. 2). Questa non solo è la legge più semplice di assorbimento ma indica anche la ragione per cui i neutroni lenti, di piccola velocità, sono più attivi che non i neutroni veloci. Altre volte, in realtà assai spesso, la legge è più complicata: si trovano, per esempio, casi di elementi che assorbono i neutroni con una legge rappresentabile graficamente come in figura 3. In generale per piccole velocità vale la legge dell'$1/v$, ma a velocità maggiori la sezione d'urto presenta dei massimi (*risonanze*) talvolta molto pronunciati e stretti, che si susseguono in modo piuttosto complicato: è questo il fenomeno della risonanza nucleare, fenomeno su cui disgraziatamente non ho il tempo di dare molte notizie, ma che serve assai ad indicare certe peculiarità dei nuclei che sarebbero difficilmente osservabili in altro modo.

Nell'Istituto Fisico di Roma non avevamo grandi mezzi, naturalmente non avevamo pile e non avevamo un ciclotrone: solo più tardi, dopo che io avevo lasciato l'Istituto, fu costruita una macchina acceleratrice all'Istituto di Sanità Pubblica. Ma in quei tempi tali macchine non c'erano, quindi studi di questo genere non potevano farsi che coi metodi molto rudimentali di assorbimento: tali metodi sono basati sulla proprietà di assorbimento selettivo in corrispondenza delle righe di risonanza. Ora all'inizio dello studio di questi fenomeni, per alcuni anni, si cercò di capire almeno alcune delle peculiarità

di questi fenomeni che furono poi in seguito chiariti in modo assai più completo con esperienze di altro tipo. Dopo queste esperienze io pensai che i neutroni avessero più o meno dato tutto quello che potevano dare e che avrei potuto ritornare pacificamente ai miei studi di fisica teorica, ma un altro contrattempo venne con la scoperta della scissione.

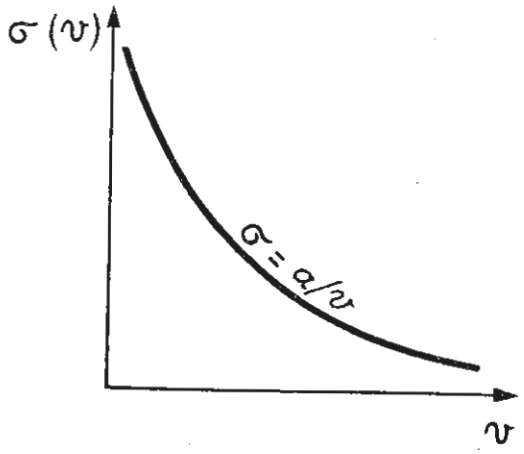

Fig. 2.

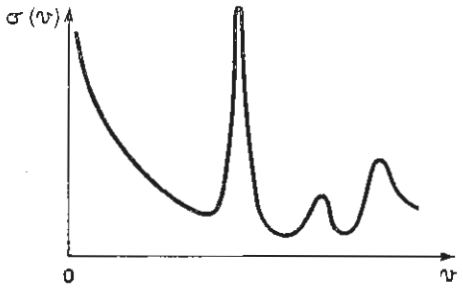

Fig. 3.

Già fin dai tempi di Roma, tra gli altri elementi bombardati con neutroni, vi era stato l'uranio: si era notato che l'uranio si comportava in un modo strano, ma non ci si era accorti di quanto singolare fosse veramente il suo comportamento. Bombardando l'uranio infatti si producevano numerose attività; si cercò, con la nostra chimica piuttosto primitiva, di individuare quali elementi fossero responsabili di queste attività ma non si riuscì. Si trovò che tale attività era sempre in elementi diversi da quelli che venivano esaminati. Si esaminò l'uranio, il protoattinio, il torio e giù giù per il sistema periodico fino, credo, all'emanazione, senza mai trovare l'attività cercata. Allora si pensò che si formassero elementi transuranici. In realtà elementi transuranici si formano, come senza dubbio sapete, ma in modo molto diverso ed in condizioni assai differenti da quelle che allora si pensava. La soluzione di questo strano comportamento dell'uranio fu trovata da Hahn e Strassmann, due fisico–chimici tedeschi, i quali, dopo molti errori, perché anche essi per un gran pezzo credettero di ripetere esperienze del tipo di quelle fatte a Roma, si accorsero che l'errore delle nostre esperienze consisteva nell'aver trascurato di proseguire l'indagine degli elementi verso la zona dei pesi atomici medi. Detti Autori trovarono precisamente che elementi situati verso la metà del sistema periodico si formano per il noto fenomeno della scissione dell'uranio, press'a poco nel seguente modo: un nucleo di uranio, concepito di forma sferica, colpito da un neutrone entra in vibrazione; siccome esso è già di per se poco stabile avviene che talvolta esce dalla posizione di equilibrio, allungandosi fino al punto in cui le forze di richiamo non sono più capaci di ricostituirne la forma sferica; ne consegue che esso passa attraverso tutta una serie di configurazioni (rappresentate in fig. 4) finché si scinde in due parti.

I due frammenti formati in questa maniera sono press'a poco eguali: generalmente uno è un po' più pesante dell'altro, pur essendo entrambi dello stesso ordine di grandezza. I due frammenti radioattivi che si formano scappano via in direzioni opposte. Sono infatti entrambi positivi e non appena il collo che li unisce si rompe, la repulsione elettrostatica fa sì che essi si allontanino l'uno dall'altro con energia enorme; è questa la ragione essenziale della grande quantità di energia che viene liberata nella scissione.

Il fenomeno della scissione venne a mia conoscenza nel gennaio del 1939. Ero appena arrivato a Nuova York e stavo un po' guardandomi attorno per cercare un campo in cui lavorare quando giunse dalla Germania la notizia di questa scoperta. Naturalmente vi fu un periodo di eccitazione nella fisica: in una dozzina di laboratori, contemporaneamente, gli sperimentatori si affrettarono a investigare le proprietà peculiari di questo nuovo tipo di disintegrazione nucleare. Fu allora che mi accorsi per la prima volta che un fenomeno di questo genere avrebbe potuto un giorno far uscire la fisica nucleare dal campo ristretto della ricerca pura, trasportandola in quello delle « cose grosse ». Ebbi allora l'idea, confermata poi dalle esperienze successive, che all'atto della scissione del nucleo in due frammenti potessero venire emessi anche dei neutroni, così come quando si spezza una goccia si vedono talvolta sprizzare via anche delle minute goccioline. Come conseguenza poteva avvenire, per esempio, che il primo neutrone che ha prodotto la scissione ne producesse in media, supponiamo, due: se così fosse, naturalmente, si avrebbe la possibilità di una reazione a catena in cui, da un neutrone originale, per raddoppiamenti successivi se ne potrebbe produrre un numero arbitrariamente grande finché rimanesse dell'uranio da scindere.

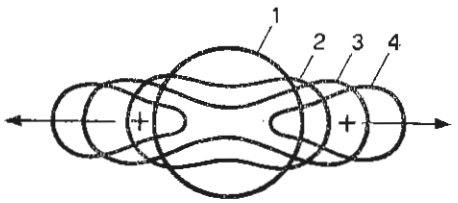

Fig. 4.

Queste idee vennero molto discusse in una riunione scientifica che fu tenuta a Washington nel gennaio del 1939. Cominciò allora un'altra fase delle mie relazioni coi neutroni in cui ricercavo una conferma di questa ipotesi. La dimostrazione sperimentale fu portata da Joliot con alcuni dei suoi collaboratori; da un gruppo che lavorava con me alla Columbia University e, più o meno indipendentemente, da Szilard e collaboratori. Da allora, per vari anni, dedicai tutta la mia attività ad esperienze di questo tipo per vedere fino a che punto si potesse arrivare. Tutto ciò succedeva in un momento politico estremamente teso; la guerra non era ancora scoppiata, ma si sentiva già molto nell'aria ed era facile presagire che sarebbe stata una guerra spietata, in cui la civiltà stessa sarebbe stata in giuoco. Queste ricerche, contrariamente alla tradizione scientifica, furono condotte in parte in segreto, e ciò avvenne, prima ancora che il Governo, le autorità militari od altri si interessassero del problema. Un gruppo di fisici parte americani, parte europei che vivevano in America in quel tempo si misero privatamente d'accordo per condurre queste ricerche con una certa riservatezza. Così s'andò avanti per un certo numero di anni prima senza, poi con limitati aiuti da parte del

governo americano e, in ultimo, con aiuti che alla fine avevano raggiunto cifre spettacolose. Del resto voi conoscete le tappe attraverso le quali si è passati. In particolare voglio ricordare qui che, già in una fase relativamente iniziale di questa ricerca, si arrivò a produrre una reazione a catena in una macchina in cui i neutroni sono rallentati dalla grafite. Questa macchina, la pila atomica, consistente in una grande massa di grafite, in cui vengono disposti con una geometria opportuna dei pezzi di uranio, quando abbia raggiunto dimensioni abbastanza grandi, comincia a funzionare spontaneamente; la reazione è perfettamente regolabile perché, se l'intensità cresce, basta introdurvi dei corpi che assorbano neutroni. Se si vuole invece crescere il livello di attività, si eliminano questi assorbitori così che si ha un dispositivo estremamente tranquillo, regolabile e non esplosivo.

Ma io non voglio parlarvi della pila né come strumento di carattere veramente industriale, né come prototipo di quelle reazioni che portarono poi alla bomba atomica; vorrei piuttosto parlarvi della pila come mezzo di ricerca, mezzo effettivamente potente, che avrà credo, a lungo andare, una influenza assai importante sopra lo sviluppo della scienza. Per prime vorrei ricordare le applicazioni scientifiche della pila quale sorgente di neutroni per esperienze di fisica. Come sorgente di neutroni essa presenta gran numero di vantaggi, accompagnati da un certo numero di inconvenienti. Il vantaggio principale è di fornire intensità enormi, assai maggiori di quelle ottenibili con ogni altro mezzo, e nello stesso tempo di essere assai costante e perfettamente regolabile.

L'inconveniente principale è che ben pochi laboratori ne possono disporre. Fortunatamente a Chicago ne avevamo due, cosicché si organizzò un certo numero di ricerche molte delle quali si riferiscono alle cosidette proprietà ottiche dei neutroni. Questi, come tutti i corpuscoli, obbediscono alla meccanica quantistica e perciò hanno il comportamento duale di particelle e di onde e, quando se ne sperimenti l'aspetto ondulatorio, si rifrangono, si riflettono e mostrano proprietà simili a quelle dei raggi X.

Altro tipo di applicazione è questo: una pila atomica è una sorgente di sostanze radioattive di grande varietà e di grande intensità. Queste sostanze radioattive si producono in due modi diversi. Prima di tutto il fenomeno stesso della scissione, su cui si basa il funzionamento della pila, porta alla produzione di sostanze radioattive (prodotti di scissione); si può quindi, con opportuni e talvolta complicati metodi chimici, estrarre, isolare, purificare e usare questi prodotti per gli scopi che vedremo.

L'altro modo per produrre sostanze radioattive è quello di introdurre nella pila una sostanza che assorba neutroni, per esempio secondo la reazione (n, γ), trasformandosi in sostanza radioattiva; data la grande varietà degli elementi che si possono introdurre, si comprende come si possa produrre un gran numero di isotopi radioattivi. Negli Stati Uniti la produzione e la distribuzione degli isotopi radioattivi si fa attualmente, in modo assai sistematico, con una organizzazione industriale che utilizza la pila di Oak Ridge. La Commissione dell'Energia Atomica americana li mette poi in commercio ad un prezzo nominale, che corrisponde, credo, grosso modo, ad un ventesimo del prezzo di costo, a disposizione di laboratori che ne abbiano una giustifi-

cata necessità. Gli isotopi servono ad una grande varietà di ricerche, nel campo della chimica, della biologia (come indicatori), e della medicina, anche come sostituti del radio. Naturalmente sia la fabbricazione che la distribuzione di questi isotopi presentano dei problemi non semplici. Per esempio la spedizione di quantità ingenti di sostanze radioattive non si può fare, ovviamente, avvolgendole soltanto in un pacchettino e mettendole in una buca delle lettere, ma richiede certe precauzioni a causa dell'attività che può essere pericolosa. Cosi per esempio, una quantità dell'ordine di un milligrammo di sostanza radioattiva viene spedita in un bussolotto di piombo di dimensioni considerevoli per protezione contro le radiazioni, il che ne aumenta peso e costo. Le richieste di sostanze radioattive ad Oak Ridge, provengono generalmente da Istituti americani ed anche europei; qualche invio è stato fatto anche all'Italia, per l'Istituto di Sanità Pubblica di Roma. L'invio è spesso abbastanza complicato, e richiede naturalmente un certo tempo, cosi che sostanze di vita breve non possono essere spedite; se una sostanza ha una vita media inferiore a qualche settimana può decadere prima di giungere a destinazione.

Per concludere voglio accennare a un'applicazione delle sostanze radioattive prodotte dai neutroni, che in questo caso non sono generati nè dalla pila né da alcuna delle sorgenti che ho detto, ma dal cosmo; cioè alla misura dell'età delle mummie, dei relitti storici o preistorici che contengano in qualunque maniera dei residui organici. Nel caso delle mummie le sostanze organiche sono contenute nei panni in cui venivano avvolte; negli altri casi possono essere usati travi di vecchie abitazioni, residui fossili, comunque conservati ecc., purché contenenti qualche traccia di carbonio. Il metodo, veramente molto ingegnoso, escogitato dal prof. Libby dell'Università di Chicago, consiste in questo: i raggi cosmici, disintegrando alcuni dei nuclei dell'atmosfera, producono neutroni in numero molto piccolo, dell'ordine di uno al secondo per una colonna d'aria di un centimetro quadrato di base. Data però l'estensione della Terra, il numero complessivo dei neutroni prodotti nell'atmosfera è considerevole. Essi vengono assorbiti dall'azoto, l'unico tra i costituenti dell'aria che ha un assorbimento notevole per neutroni secondo la reazione: $(N^{14} + n^1 = C^{14} + H^1)$ per la quale si ottiene un protone e un atomo di carbonio 14. Poiché questa reazione avviene continuamente nell'atmosfera, su ogni colonna di un centimetro quadrato di atmosfera si forma ogni secondo circa un atomo di carbonio 14, che è radioattivo con un periodo di dimezzamento di circa 5.000 anni; il C^{14} è il solo isotopo radioattivo del carbonio; gli altri due, il C^{12} (il comune carbonio) e il C^{13}, sono stabili. L'atomo di carbonio 14 così prodotto si ossida rapidamente, dando origine a anidride carbonica $C^{14}O_2$, che attraverso la funzione clorofilliana, rapidamente viene a far parte delle foglie, della materia vegetale; questa viene assimilata dagli animali, dagli uomini, alla morte dei quali il carbonio 14 ritorna nell'atmosfera. Esiste cioè una continua circolazione del carbonio 14 tra l'atmosfera e tutta la materia organica vivente, per cui esso viene a diluirsi con il carbonio di tutta la biosfera, così che ogni esemplare di carbonio, ottenuto da sostanza vivente, conterrà una percentuale, naturalmente molto piccola, di carbonio 14. Non vi starò a descrivere tutte le esperienze effettuate e le difficoltà a cui il Libby andò incontro per mettere in chiaro questo fenomeno.

Tra l'altro egli esaminò del metano di due origini: l'uno, molto antico, proveniente da pozzi di petrolio, contenente carbonio che in origine faceva parte di materia vivente milioni di anni fa, ma che attraverso i millenni in cui è rimasto nei giacimenti, ha finito col perdere ogni traccia di attività del carbonio 14 inizialmente contenuto; l'altro, estratto dalle fognature di Baltimora quindi di recente formazione organica, proviene dal ciclo descritto. Dopo un certo numero di ricerche e di perfezionamenti della tecnica il Libby arrivò a trovare che effettivamente il metano di Baltimora era più attivo del metano dei pozzi di gas naturali e indicava la presenza nel carbonio di una quantità minutissima, ma misurabile, di carbonio 14.

Ed ecco come si può applicare questa tecnica per trovare l'età di una mummia. Al momento della morte il corpo, che è stato poi mummificato, conteneva una certa percentuale di carbonio radioattivo e quindi possedeva una certa attività, ma nei tre–quattromila anni che sono trascorsi da allora, il carbonio presente nella mummia è decaduto con un periodo di dimezzamento di circa 5.000 anni; quindi, se la mummia fosse, mettiamo, vecchia di 5.000 anni, ne conterrebbe oggi la metà; se fosse vecchia di 10.000 anni, ne conterrebbe un quarto, così e di seguito. Misurando con precisione l'attività specifica del carbonio della mummia se ne può così stabilire l'età, con una approssimazione di circa 200 anni, la quale, almeno in alcuni casi, non è però grande rispetto alla approssimazione degli storici. Nel caso della storia egiziana, molto nota in genere, gli storici stabiliscono le date con più esattezza dei fisici, ma in parecchi casi di storia e in alcuni di preistoria e di recenti epoche geologiche questo metodo di dedurre le date dal carbonio radioattivo è di valore assai grande, e costituisce un prezioso aiuto in alcuni rami del sapere che, si penserebbe, poco avrebbero da aspettarsi dalla fisica e in particolare dalla fisica dei neutroni.

Ho scelto questo esempio, e avrei potuto sceglierne naturalmente molti altri, per indicare come lo studio delle sostanze radioattive, sostenuto anche da una certa dose di immaginazione, possa trovare applicazione nei campi più disparati di ricerca, oltre che in quelli più naturali della chimica, della biologia e della medicina.

Così io vorrei concludere, esprimendo la speranza che queste ricerche sui neutroni, alle quali ho dedicato tanti anni, producano infine non solo armi, ma soprattutto uno sviluppo scientifico che possa arricchire l'umanità ed estendere le frontiere della conoscenza umana.

OTTAVA CONFERENZA (*)

ANALOGIE OTTICHE NELLE PROPRIETÀ DEI NEUTRONI

(redatta dal Prof. C. SALVETTI)

Vorrei discutere questa sera alcuni aspetti della fisica dei neutroni, in cui si mette in evidenza il carattere ondulatorio di queste particelle. Secondo i risultati della meccanica quantistica o meccanica ondulatoria, tutte le par-

(*) Tenuta il 20 ottobre 1949 nel salone delle assemblee della Società Montecatini di Milano.

ticelle danno luogo a fenomeni di interferenza, simili a quelli di una radiazione luminosa, in cui la lunghezza d'onda è data dalla relazione di de Broglie ($\lambda = h/mv$): ossia dal rapporto tra la costante di Planck e la quantità di moto mv della particella. Perché si osservino fenomeni di questo tipo, è necessario che la lunghezza d'onda sia dell'ordine di grandezza di altre dimensioni geometriche contenute nel problema; conviene quindi indicarne senz'altro il valore. Per i neutroni cosiddetti termici, cioè neutroni che sono rallentati fino alle velocità di agitazione termica corrispondenti, alla temperatura ambiente, all'energia di circa 1/40 di elettrone Volt, si trova dalla relazione di de Broglie che la lunghezza d'onda è di circa $1.8 \cdot 10^{-8}$ cm. Poiché tale lunghezza è molto prossima alle distanze interatomiche, ci si aspetta di osservare per i neutroni fenomeni di diffrazione nei reticoli cristallini simili ai fenomeni che si osservano con i raggi X, i quali pure hanno lunghezza d'onda di questo ordine di grandezza.

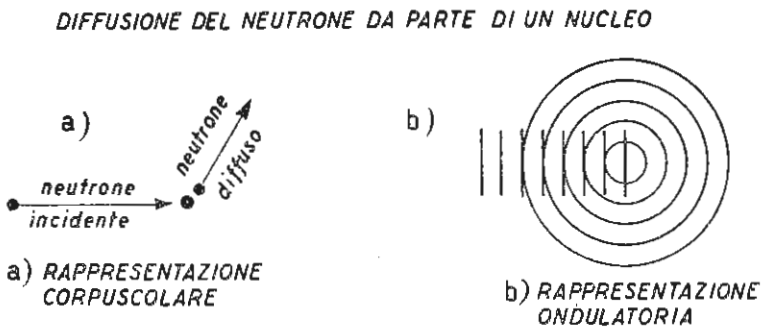

Fig. 1.

Ora, prima di entrare nella discussione dei vari esperimenti che sono stati fatti per osservare effettivamente proprietà di questo tipo, vorrei stabilire alcuni semplici fatti generali e alcune formule generali di cui ci serviremo in seguito. Supponiamo che su un atomo, meglio sul nucleo di un atomo (perché praticamente è sempre il nucleo che produce il fenomeno di diffusione dei neutroni) arrivi un neutrone che lo urti: il neutrone verrà diffuso secondo un certo angolo (fig. 1 *a*). Questo è lo schema nella rappresentazione corpuscolare; nella rappresentazione ondulatoria, si ha un gruppo di onde incidenti, le quali vengono diffuse come lo sarebbe la luce, cioè in un gruppo di onde sferiche irraggianti dal centro di diffusione (fig. 1 *b*). L'onda incidente piana propagantesi lungo la direzione positiva dell'asse delle x sia rappresentata con l'esponenziale

$$e^{ikx} \tag{1}$$

L'onda diffusa sarà un'onda sferica, che può scriversi

$$-a\frac{e^{ikr}}{r}. \tag{2}$$

Il fattore ikr rappresenta la fase (variabile) dell'onda sferica diffusa, il fattore $1/r$ indica che l'ampiezza dell'onda diffusa decresce con la distanza dal

centro diffondente con legge di proporzionalità inversa. Il che deve essere in conformità alle leggi di conservazione dell'energia, perché l'intensità dell'onda diffusa, che è proporzionale al quadrato dell'ampiezza, decresce come $1/r^2$.

Studiando l'onda diffusa e seguendola in una data direzione, ci si può domandare se vi è stata oppure no una differenza di fase all'atto della diffusione. La questione si può esaminare, almeno in parte, in base ad alcuni principi generali, sui quali tuttavia non mi soffermerò per ragioni di tempo. Vorrei piuttosto esporvi il risultato: fra l'onda incidente e l'onda diffusa vi sono in genere piccole differenze di fase, le quali però si concentrano molto vicino ai valori 0° e 180°. In questa diffusione quindi o non vi è quasi alcun mutamento di fase o vi è un mutamento di fase corrispondente a circa una inversione della fase di 180°. Come ripeto, non vorrei discutere in dettaglio perché soltanto questi due valori siano accettabili, tuttavia si può affermare che ogni cambiamento di fase che fosse molto diverso dall'uno o dall'altro di questi due valori corrisponderebbe ad un assorbimento assai forte. La differenza di fase è determinata dalla costante a che interviene nella (2) e precisamente: se la costante a è reale e negativa, la differenza di fase è 0°; se a è reale e positiva la differenza di fase è 180°; infine valori complessi di a corrispondono a valori intermedi della differenza di fase.

Mi limito a scrivere la relazione, che si potrebbe dimostrare assai speditamente, che lega la costante a con la sezione d'urto per diffusione:

$$\sigma = 4\pi a^2. \tag{3}$$

Vi è un altro punto che vorrei fissare prima di parlare dettagliatamente del lavoro sperimentale, e cioè, il significato di questa costante a nella meccanica quantistica, significato che può essere illustrato nel modo seguente. Osserviamo anzitutto, che la lunghezza d'onda è dell'ordine di 10^{-8} cm, mentre le dimensioni nucleari sono dell'ordine di 10^{-12} cm, e quindi la lunghezza d'onda è circa 10 mila volte le dimensioni dell'oggetto che produce la diffusione. Nel grafico di fig. 2 è riportata in ascisse la distanza r dal centro del nucleo, il nucleo stesso potendosi rappresentare schematicamente mediante una buca di potenziale d'un raggio dell'ordine di 10^{-12} cm, mentre in ordinate è riportato il prodotto di r per la funzione d'onda (nel caso di energia $E = 0$). Partendo da $r = 0$ la curva ha andamento sinusoidale fino al limite della buca di potenziale rappresentante il nucleo, per poi acquistare un andamento rettilineo. La teoria dell'urto consente di attribuire alla costante a il seguente significato geometrico: essa è uguale alla distanza dall'origine dell'intersezione con l'asse r del prolungamento della parte rettilinea del diagramma. La figura 2 si riferisce al caso $a > 0$; per $a < 0$ la intersezione cade dalla parte negativa dell'asse r (fig. 3).

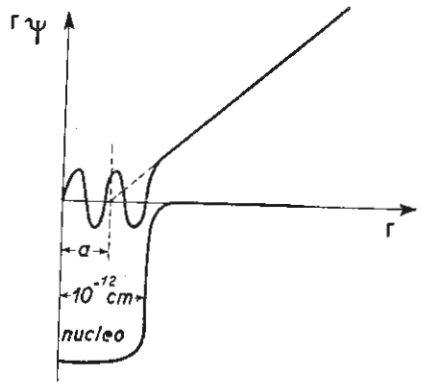

Fig. 2.

Dopo queste premesse, vorrei passare alla descrizione della semplice esperienza con cui si può verificare che effettivamente i neutroni si comportano rispetto ai fenomeni di diffrazione nei cristalli essenzialmente come i raggi X. Se sulla faccia di un cristallo tagliato, per esempio, parallelamente a una serie di piani reticolari si fanno cadere dei raggi X monocromatici (fig. 4) si trova che si ha riflessione solo per certe speciali direzioni. Queste sono individuate dalla ben nota relazione di Bragg:

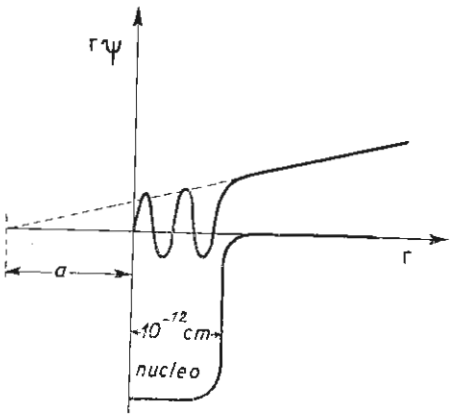

Fig. 3.

$$n\lambda = 2\,d \operatorname{sen} \vartheta \tag{4}$$

nella quale, n è un numero intero detto ordine della riflessione, λ è la lunghezza d'onda dei raggi X, d la distanza tra i successivi piani cristallini della serie considerata e ϑ il complemento dell'angolo di incidenza sul cristallo. Ora, se è vero il risultato generale della meccanica quantistica, che i neutroni si comportano sia come particelle, sia come radiazione di lunghezza d'onda $\lambda = h/mv$, ci potremo aspettare che un fenomeno simile abbia luogo anche per i neutroni; era proprio questo lo scopo della semplice esperienza che fu eseguita per la prima volta da Zinn. Per porsi in condizioni favorevoli occorre anzitutto disporre di una sorgente di neutroni molto intensa: flussi di neutroni molto intensi si hanno nelle pile atomiche e pertanto il dispositivo utilizzato da Zinn è quello rappresentato in figura 5. La pila è circondata da un grosso schermo di cemento per protezione contro le radiazioni; in cui, come in molte pile costruite per ricerche nel campo della fisica, è inserita la cosidetta « colonna termica » cioè una colonna di grafite, la cui estremità affonda nella pila, e che ha lo scopo di rallentare i neutroni veloci provenienti dalla pila stessa. Essi urtando contro i nuclei di carbonio della colonna termica perdono poco alla volta la loro energia iniziale fino a portarsi in equilibrio termico con i nuclei di carbonio nel blocco di grafite verso l'esterno. All'estremità della colonna di grafite è praticata, come mostra la figura, una cavità in guisa che i neutroni termici provenienti dal fondo vengono « grosso modo » incanalati verso l'esterno; così che all'uscita si ottiene un fascio (invero non troppo collimato) di neutroni, con distribuzione di energia corrispondente alla temperatura della colonna termica. Ma poiché per esperienze di questo tipo, occorre una collimazione ben maggiore, occorre cioè produrre un fascetto di neutroni abbastanza sottile, di direzione abbastanza ben definita, si introducono alcune limitazioni allo scopo

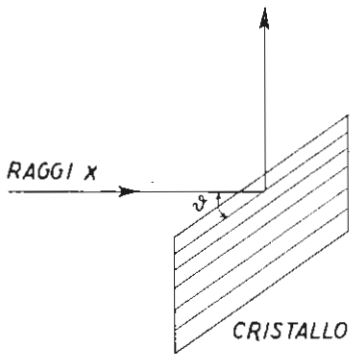

Fig. 4.

di selezionare soltanto i neutroni aventi una certa direzione. Per questo si fa uso di solito della proprietà del cadmio di essere un assorbitore fortissimo per i neutroni termici, tanto che uno strato di cadmio dello spessore di circa mezzo millimetro o di un millimetro, in pratica li assorbe completa-

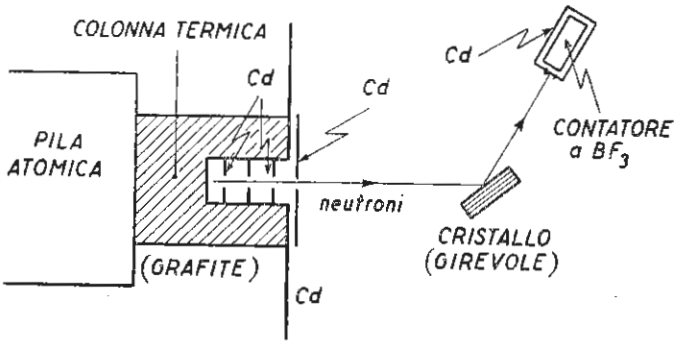

Fig. 5.

mente. Interponendo allora nella cavità praticata nella colonna termica dei diaframmi di cadmio si otterrà un fascio di neutroni termici abbastanza ben collimato. Poi l'esperienza si conduce in modo molto simile a quello descritto per i raggi X e cioè si fa incidere il fascio neutronico sopra un cristallo montato su una piattaforma girevole. A questo punto occorre però tener presente che i neutroni uscenti dalla colonna termica non sono monocromatici; lo spettro di velocità corrisponde più o meno a una distribuzione maxwelliana (fig. 6). Poichè la velocità è inversamente proporzionale alla lunghezza d'onda, l'asse delle ascisse di figura 6 è anche essenzialmente una scala di lunghezza d'onda decrescenti, o per meglio dire, è una scala degli inversi delle lunghezze d'onda. Quindi, ovviamente, ad ogni intervallo di velocità, corrisponde un intervallo di lunghezza d'onda. Diamo ora al cristallo una certa orientazione specifica rispetto al fascio incidente; la condizione di Bragg sarà verificata soltanto per un certo numero di lunghezze d'onda, non necessariamente per una sola, perché si hanno riflessioni dei vari ordini determinati dai differenti valori del numero n, che compare al 1° membro della (4). Fissando per il momento la nostra attenzione sul valore $n = 1$, di tutti i neutroni incidenti di varia velocità vengono riflessi soltanto quelli di una banda piuttosto stretta, quelli cioè che hanno velocità e quindi lunghezza d'onda tale da soddisfare alla relazione di Bragg:

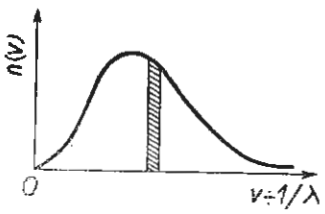

Fig. 6.

$$2\,d \sin \vartheta_1 = \lambda\,.$$

Gli altri neutroni del fascio in gran parte traversano il cristallo; perciò, nella direzione individuata da ϑ_1, uscirà solo un debole pennello di neutroni, rappresentante una piccola frazione di quelli incidenti; in altre parole sono stati selezionati quei neutroni che hanno una lunghezza d'onda determinata.

Per osservare i neutroni riflessi occorre predisporre un rivelatore di neutroni, per lo più un contatore a trifluoruro di boro; per rivelare i neutroni riflessi secondo un angolo ben definito conviene schermare il contatore con del cadmio, munito di una sottile apertura. Si possono allora eseguire esperienze come si farebbero con un tubo a raggi X, che emetta uno spettro continuo. Per esempio, se mantenendo fermo tutto il resto, si ruota la piattaforma su cui è posto il cristallo, si trovano in genere intensità piccolissime; quando però si raggiunge la condizione di angolo di incidenza eguale all'angolo di riflessione l'intensità sale all'improvviso assai rapidamente a valori notevoli; aumentando ancora l'angolo di rotazione l'intensità di nuovo cala bruscamente, cosicché se si rappresenta l'intensità in funzione dell'angolo di cui è ruotato il cristallo, si trova un diagramma come quello di figura 7 che presenta un massimo molto stretto e pronunciato.

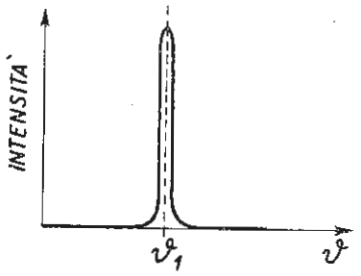

Fig. 7.

Tenendo fermo il cristallo in posizione corrispondente all'angolo ϑ_1 si possono così selezionare dallo spettro continuo i neutroni di una piccola banda monocromatica, corrispondenti alle condizioni di Bragg. Sin dalle prime esperienze, in cui questi fenomeni furono messi in luce, si cercò una conferma che la lunghezza d'onda così ottenuta fosse effettivamente correlata ai dati cristallografici e ai dati geometrici in modo da soddisfare alla relazione di Bragg; e poiché $\lambda = h/mv$ si cercò di controllare la relazione esistente fra la velocità dei neutroni e l'angolo ϑ. La più semplice esperienza diretta a questo scopo è di questo tipo: dopo di aver effettuato una misura, con il cristallo orientato secondo un angolo ϑ, ruotiamo di un certo angolo il contatore. Per far sì che i neutroni possano entrare nel contatore così ruotato, occorre ruotare anche il cristallo, sino ad una nuova posizione corrispondente ad un nuovo angolo ϑ_1; in questo modo possiamo selezionare una lunghezza d'onda λ_1 diversa da λ, selezionata in corrispondenza dell'angolo ϑ. Se per esempio $\vartheta_1 < \vartheta$ la lunghezza d'onda λ_1 è più piccola di λ. Di conseguenza si ottiene una banda di neutroni di diversa velocità. Come si può arrivare a conoscere il valore della velocità neutronica, in questi casi? In altre parole: come si possono verificare le relazioni precedenti? Il modo più semplice è quello di servirsi di un fenomeno di assorbimento; esistono infatti molte sostanze – una di queste è il boro – che assorbono i neutroni con una sezione d'urto inversamente proporzionale alla velocità. Se si interpone, lungo il cammino dei neutroni, dopo che essi sono stati riflessi, un assorbitore contenente boro e si misura così il coefficiente di assorbimento, si trova che esso è direttamente proporzionale al seno dell'angolo ϑ come deve essere appunto se valgono le relazioni di Bragg e di de Broglie; in tal caso infatti il coefficiente di assorbimento, dovendo essere inversamente proporzionale alla velocità v dei neutroni, sarà direttamente proporzionale alla loro lunghezza d'onda λ e quindi anche a sin ϑ. Si può così verificare che effettivamente valgono per i neutroni le relazioni di Bragg e di de Broglie.

In esperienze di questo tipo uno degli inconvenienti consiste nell'usare neutroni non monocromatici; sarebbe invece opportuno compiere esperienze più delicate usando neutroni tutti della stessa energia prodotti con opportuni dispositivi.

Si conduce l'esperienza presso a poco nel modo seguente (v. fig. 8): su un piccolo cristallo si fa incidere il fascio di neutroni non monocromatici la cui velocità è data dalla distribuzione di Maxwell. Nella esperienza che feci alcuni anni fa con Leona Marshall, il cristallo usato era, per ragioni di intensità, un cristallo di fluorite, ma qualsiasi altro cristallo va più o meno bene. Generalmente si lascia fisso il cristallo in una certa posizione, benché anche esso sia montato su una piattaforma girevole, in maniera che esso selezioni dal fascio di neutroni primari, dotati di una distribuzione continua di velocità, una banda monocromatica. Poiché nel processo di riflessione e di monocromatizzazione l'intensità del fascio neutronico diminuisce considerevolmente, occorre disporre di una sorgente di grande intensità, per avere alla fine neutroni monocromatici in numero sufficiente per l'esperienza. Lungo il cammino del fascio ormai monocromatizzato si pone poi un secondo cristallo, quello da studiare; si possono così esaminare le peculiarità della riflessione dei neutroni monocromatici da parte di vari cristalli.

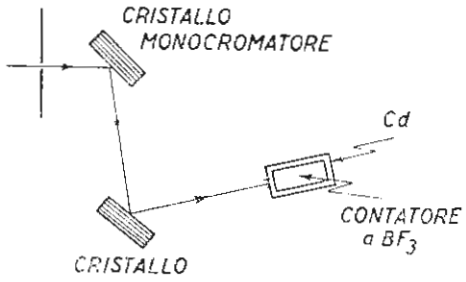

Fig. 8.

Il fascio riflesso sul secondo cristallo viene rivelato da un contatore a trifluoruro di boro munito di un rivestimento di cadmio nel quale è praticata una fenditura. Con esperienze di questo tipo è stata condotta una ricerca sistematica su una trentina di cristalli diversi; scopo principale di queste ricerche era di chiarire la questione riguardante la fase, cioè se a fosse negativo o positivo, se il cambiamento di fase fosse di circa 0° o di circa 180°. Citerò in seguito altri metodi per arrivare alla stessa conclusione; questo che ho descritto è basato sulla seguente argomentazione: supponiamo dunque di prendere un cristallo, per esempio il cloruro di sodio, la cui struttura ben nota, può rappresentarsi come in figura 9; in un piano si trovano atomi di sodio e di cloro alternati, nel piano contiguo gli stessi atomi sono ancora alternati ma il posto di ogni atomo di sodio è preso da un atomo di cloro e viceversa, e così di seguito. Se si considerano le cosiddette facce (100), che sono in definitiva le facce del cubo del cristallo, si vede che i vari piani riflettenti sono essenzialmente identici poiché contengono tutti per il 50 per cento atomi di cloro e per il 50 per cento atomi di sodio. Se invece si esaminano le facce diagonali del

Fig. 9.

cristallo, le cosiddette facce (III), si trova che i piani riflettenti sono diversi: infatti i piani che sono tutti costituiti da atomi di cloro, sono alternati con piani che sono tutti costituiti da atomi di sodio.

Supponiamo dapprima di considerare la riflessione alla Bragg dei neutroni su una faccia (III) del cristallo cioè su una famiglia di piani costituiti alternativamente da sodio e da cloro (fig. 10). Si ha riflessione del primo ordine quando la radiazione riflessa sul primo piano di sodio differisce in fase di 360° dalla radiazione riflessa sul secondo piano di sodio, di 720° dalla radiazione riflessa sul successivo piano di sodio, ecc. Naturalmente una differenza di fase di 360° vuol dire che i due raggi sono in fase. Si ha però anche una riflessione sopra il piano intermedio di cloro con una differenza di fase diversa dalle precedenti per ragioni geometriche; infatti la differenza di cammino ottico è tale da corrispondere ad una differenza di fase di 180°, ossia ad una inversione di fase: si ha perciò opposizione di fase tra i raggi provenienti

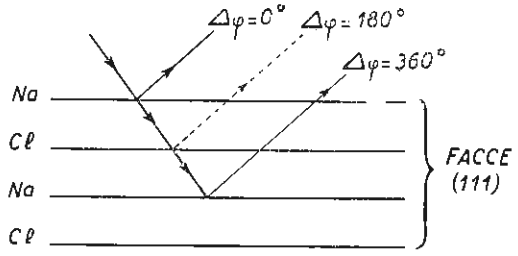

Fig. 10.

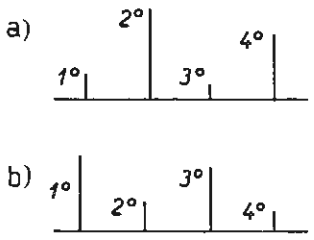

Fig. 11.

dal sodio e quelli provenienti dal cloro. Il cambiamento geometrico di fase farà dunque « lavorare » il sodio contro il cloro; quindi se sodio e cloro diffondono i neutroni con la stessa fase, il primo ordine sarà debole; se invece sodio e cloro diffondono con fase opposta il primo ordine sarà forte. Com'è la situazione nel secondo ordine? Nel secondo ordine le differenze di fase provenienti dai diversi cammini ottici sono tutte raddoppiate cioè sono 0°, 360°, 720°. In questo caso non esistono dunque differenze di fase provenienti da ragioni geometriche; 360° vuol dire infatti differenza di fase nulla, quindi si verifica il caso opposto, vale a dire: se sodio e cloro diffondono i neutroni nello stesso modo, le loro azioni si addizionano, se sodio e cloro diffondono i neutroni in modo opposto, le loro azioni si sottraggono. Se si osservano le intensità dei successivi ordini, nel caso che sodio e cloro diffondano con ugual fase i neutroni, si troverà il primo ordine debole, il secondo ordine forte, il terzo ordine debole, il quarto ordine forte e così via: in genere gli ordini dispari deboli, gli ordini pari forti (fig. 11 *a*). Nel caso invece di fasi differenziate si troverà la situazione opposta, e cioè primo ordine forte, secondo ordine debole, terzo ordine forte e così di seguito (fig. 11 *b*). In realtà la situazione è un pochino più complicata e chi abbia familiarità con esperienze analoghe eseguite con raggi X sa che, passando di ordine in ordine, c'è un decremento generale di intensità dovuto ad un numero di cause che non starò ad illustrare in questo momento, cosicché ad un andamento del genere de-

scritto, si trova sovrapposto un generico decremento di intensità dagli ordini bassi verso gli ordini elevati.

Se si fanno esperienze sopra facce (100), le quali, come ho detto prima, sono costituite da piani tutti eguali, ciascuno contenente il 50 per cento di atomi di una specie e 50 per cento di atomi di un'altra specie, si trova solamente il generale decremento di intensità. Voglio riportare alcuni valori numerici ricavati da misure effettuate con un cristallo di solfuro di piombo che ha la stessa struttura cristallina del cloruro di sodio; indicherò prima come si è condotto l'esperimento. Si accoppia meccanicamente il braccio che regge il rivelatore a BF_3, con la piattaforma che porta il cristallo in modo che a una rotazione di un certo angolo del cristallo corrisponda una rotazione di un angolo doppio del rivelatore; si è così certi che è sempre osservata, per qualunque angolo, la legge della riflessione (angolo di incidenza eguale ad angolo di riflessione). Partendo da angoli piccoli ed aumentando la rotazione verso angoli grandi si ottiene dapprima intensità nulla; poi l'intensità sale rapidamente tendendo a un massimo che viene raggiunto quando è soddisfatta la relazione di Bragg per la riflessione del primo ordine; continuando ancora la rotazione verso i valori crescenti degli angoli l'intensità diminuisce fino a che non si raggiunge un secondo massimo in corrispondenza della riflessione del secondo ordine, e così via di seguito per gli ordini successivi. Ecco i valori delle intensità (misurate in numeri di impulsi al minuto) osservate nella riflessione su una faccia (100) di un cristallo di solfuro di piombo: su tale faccia ci si deve attendere, come ho detto, solo il decremento generale di intensità senza complicazione di altra natura.

Faccia (100):	1° ordine	19600	impulsi al	minuto
	2° »	11400	»	»
	3° »	2250	»	»

tali valori mostrano un decremento abbastanza in accordo con la legge del decremento generale di intensità. Per la riflessione su una faccia (111) si trovano invece i seguenti valori.

Faccia (111):	1° ordine	7300	impulsi al	minuto
	2° »	10700	»	»
	3° »	808	»	»
	4° »	750	»	»

Da questi valori si vede ben chiaramente che, sovrapposto ad un decremento generale, si ha il primo ordine debole, il secondo molto intenso (perché l'aumento di intensità del secondo ordine è talmente grande da controbilanciare il generale decremento), il terzo ordine molto debole e così di seguito. La tabella indica chiaramente come gli ordini dispari siano deboli, gli ordini pari forti; se ne conclude, che piombo e zolfo diffondono i neutroni con la stessa fase.

Se si fa la stessa esperienza con un cristallo di fluoruro di litio anch'esso avente la stessa struttura del cloruro di sodio, (mi riferisco alla struttura

del NaCl semplicemente perché è molto nota, ma, naturalmente, si può, con opportuni calcoli, estendere queste considerazioni anche a cristalli con struttura più complicata) la riflessione sulle facce (111) fornisce le seguenti intensità:

1°	ordine	10080	impulsi	al minuto
2°	»	~ 0	»	»
3°	»	300	»	»

Questo è un caso assai significativo in cui la situazione è rovesciata completamente in quanto contro degli ordini dispari assai intensi si hanno degli ordini pari tanto deboli da sparire del tutto. Si conclude che litio e fluoro diffondono i neutroni con fasi opposte.

Dallo studio sistematico di un gran numero di cristalli si è trovato che la diffusione dei neutroni avviene quasi sempre con la stessa fase e precisamente quasi sempre con fase positiva, cioè la grandezza a è positiva; il che di per sè può fare molta meraviglia, quando si tenga presente il significato geometrico, precedentemente illustrato, della grandezza a. Infatti nelle figure 2, 3 il tratto rettilineo della funzione $r\psi$ parte parecchio distante dall'origine ed è perciò abbastanza improbabile che sia così poco inclinato da intersecare l'asse delle ascisse dalla parte negativa. Naturalmente la cosa non è impossibile: il verificarsi dell'una o dell'altra circostanza dipende dal particolare andamento della funzione $r\psi$; ma si comprende agevolmente come le intersezioni positive siano di gran lunga le più probabili. In realtà si trova una statistica di questo genere: su oltre una trentina di elementi studiati, solo tre dànno fase opposta e cioè: il litio, il manganese e l'idrogeno. Questo ultimo però rappresenta un caso molto complicato, che richiede una attenzione particolare. Come è ben noto, i raggi X si usano nella indagine sui cristalli per osservare la struttura e per determinare la posizione dei vari atomi nella cella elementare del cristallo. Coi raggi X non si riesce però a fissare la posizione dell'atomo di idrogeno perché questo, specie se jonizzato, non produce la rifrazione dei raggi X. Lo studio cristallografico coi raggi X dell'idrogeno è dunque impossibile. Una simile difficoltà non si incontra naturalmente coi neutroni perché essi sono diffusi non dagli elettroni, ma dal nucleo, e l'idrogeno può perdere i suoi elettroni, ma...se perdesse il nucleo, perderebbe anche se stesso.

Quindi sin dall'inizio di questi studi, si fece subito strada la convinzione che un campo di applicazione notevole avrebbe potuto essere quello della cristallografia dell'idrogeno. Disgraziatamente la cristallografia dell'idrogeno con questo metodo, pur non essendo impossibile è tuttavia tutt'altro che facile. In realtà gli inizi sono stati incoraggianti, ma non si è andati molto avanti, almeno quanto si sarebbe potuto sperare allora. La ragione è la seguente: il nucleo d'idrogeno, il protone, come molti altri nuclei e come del resto lo stesso neutrone è dotato di spin. Conseguentemente (e qui mi riferisco all'idrogeno, ma ciò che dico vale naturalmente per la diffusione di neutroni da parte di un qualsiasi nucleo dotato di spin) può avvenire che il neutrone dopo la diffusione abbia lo spin orientato nel senso primitivo o nel

senso opposto. Il cambiamento della quantità di moto angolare del neutrone è accompagnato, e compensato, da un cambiamento della quantità di moto angolare del nucleo. Se non si ha rovesciamento dello spin si ha diffusione coerente; se si ha rovesciamento dello spin si ha invece diffusione incoerente, ossia diffusione incapace di dare luogo a fenomeni di interferenza. Per renderci conto di questo fatto nel modo più semplice, supponiamo che su un cristallo, i cui nuclei abbiano lo spin orientato in determinate maniere, incida un neutrone, il quale venga diffuso in una certa direzione. Perché vi siano fenomeni di interferenza bisogna per così dire, che tutti questi nuclei collaborino al fenomeno. Ora se vi è un « ribaltamento » della direzione dello spin del neutrone diffuso, si avrà corrispondentemente ribaltamento dello spin di uno dei nuclei diffusori. Allora questo fatto stesso viene ad indicare quale è il « colpevole » dell'atto di diffusione: è stato quel nucleo che ha ribaltato il proprio spin: il fenomeno riguarda lui solo e non vi è nessuna possibilità di interferenza. Se invece non vi è ribaltamento dello spin del neutrone diffuso, non si può sapere quale dei nuclei sia responsabile dell'atto di diffusione: la responsabilità è divisa fra tutti e l'interferenza ha luogo. L'idrogeno ha una grossa sezione d'urto, il che sarebbe di per sè favorevole perché renderebbe l'idrogeno comodo da osservare, ma sfortunatamente questa grande sezione d'urto corrisponde (per il 95 %) a fenomeni in cui gli spin ribaltano, cioè a fenomeni di diffusione incoerente. Solamente il 5 % circa della sezione d'urto si riferisce a fenomeni di diffusione coerente, ed è utilizzabile per osservare il fenomeno di interferenza. La situazione per l'idrogeno si presenta sfavorevole in due sensi: da un lato perché l'intensità del contributo dell'idrogeno è piccola e quindi di per sè è difficile da osservare, dall'altro perché la diffusione coerente (fenomeni interferenziali) è piccola su un largo fondo dovuto alla diffusione incoerente che la rende ancora più difficile da osservare. Questa è la ragione per cui gli studi di identificazione della posizione dell'idrogeno nei cristalli mediante la diffrazione dei neutroni non hanno fatto ancora molto progresso benché, come dicevo, vi siano stati inizi incoraggianti; forse, poco alla volta, la tecnica si raffinerà fino a poterli usare in modo conveniente.

Ci sarebbero varie altre proprietà semiottiche dei neutroni che potrei citare, ma siccome non c'è molto tempo preferisco parlare di una in particolare e precisamente del fenomeno della riflessione dei neutroni, riflessione intesa non alla Bragg, ma per così dire, nel senso normale. Essa si osserva anche per i raggi X, però solo sotto incidenza estremamente radente quando cioè la radiazione arriva quasi parallela allo specchio. Lo stesso avviene nel caso dei neutroni, per la ragione che ora dirò. Prima di indicare come viene fatta l'esperienza voglio precisare che la riflessione dei neutroni si osserva solo quando il fascio incidente forma con lo specchio un'angolo dell'ordine di alcuni primi. Quindi per ottenere riflessione su uno specchio di un raggio con incidenza tanto radente occorre predisporre una fortissima collimazione: nelle prime esperienze la prima fenditura era, mettiamo, di 1 mm di larghezza e la seconda, della stessa larghezza, era posta a 5 metri di distanza in modo che il pennello presentava una delimitazione estremamente severa. Questa condizione naturalmente obbliga ad usare una sorgente di grande intensità,

altrimenti prima di trovare il neutrone che infili i due mirini bisognerà aspettare un gran pezzo. Al di là della seconda fenditura (fig. 12) è posto lo specchio, formato da una lastra lucida di materiale vario, di dimensioni di circa 10 cm per 20, inclinata sulla direzione del fascio incidente di un angolo accuratamente controllato di pochi minuti. Per osservare il fascetto riflesso a 5 m di distanza si poneva un contatore a trifluoruro di boro davanti al quale vi era un'altra fenditura praticata nello schermo di cadmio, anche questa di circa 1 mm di larghezza; si ruotava infine il contatore finché non si sorprendesse il raggio riflesso.

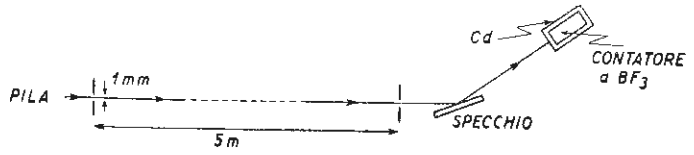

Fig. 12.

In realtà in una esperienza di questo genere per l'intensità del fascio riflesso si trovano due massimi in due diverse direzioni (fig. 13); il primo corrisponde a quei pochi neutroni diretti che passano attraverso lo specchio, il secondo, assai spesso più intenso, corrisponde ai neutroni riflessi. Se si ruota poi il cristallo, si trova che questi due massimi si spostano d'accordo con le leggi della riflessione.

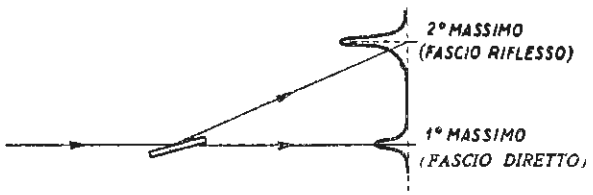

Fig. 13.

Anche il fenomeno della riflessione è desiderabile sia studiato con neutroni monocromatici; il che si può ottenere disponendo di intensità sufficienti e introducendo un monocromatore prima delle fenditure collimatrici. Con neutroni monocromatici, si può osservare l'intensità della riflessione al variare dell'angolo ϑ di cui ruota il cristallo. Riportando in un diagramma in ascisse l'angolo ϑ e in ordinate l'intensità del fascio riflesso, si trova che l'intensità si mantiene presso a poco costante fino ad un certo valore dell'angolo a partire dal quale cade bruscamente verso zero (fig. 14). Questo fatto indica che si tratta essenzialmente di un fenomeno non di riflessione ordinaria, ma di riflessione totale; infatti caratteristica della riflessione totale è che fintanto che si resta al di sotto dell'angolo limite la riflessione è forte, appena si raggiunge il valore dell'angolo limite o lo si oltrepassa di poco l'intensità scende a zero molto rapidamente. La riflessione totale dei neutroni è resa possibile dal fatto che l'indice di rifrazione per i neutroni è in

quasi tutte le sostanze, e precisamente nelle sostanze normali che dànno cambiamento di fase di 180°, un poco minore dell'unità, differendone di una quantità dell'ordine di alcuni milionesimi. Di conseguenza gli angoli limite sono estremamente piccoli, il che porta a condizioni geometriche di osservazione estremamente spinte.

A che è dovuto questo indice di rifrazione dei neutroni? Perché i neutroni si rifrangono? Essenzialmente per la stessa ragione per cui si diffondono; in realtà diffusione e rifrazione della luce, dei raggi X, dei neutroni o di qualsiasi altra radiazione, sono due fenomeni sempre assai intimamente legati. Consideriamo un'onda e poi interponiamo sul suo cammino una piccola lastra di un qualsiasi materiale; l'indice di rifrazione si presenta come una perdita di fase, o meglio come un cambiamento di fase. Se l'indice di rifrazione è, per esempio, maggiore dell'unità, nell'interno la lunghezza d'onda è un po' più breve, cosicché all'uscita l'onda si troverà con la fase spostata. Il legame tra il fenomeno della diffusione e quello della rifrazione, si può mettere anche in forma quantitativa mediante la relazione seguente:

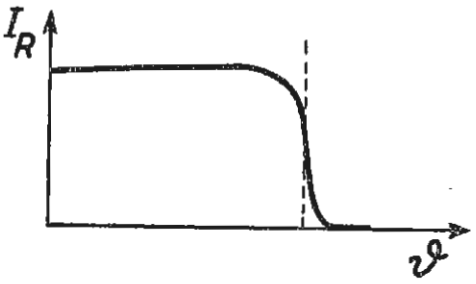

Fig. 14.

$$n = 1 - \frac{Na}{2\pi}\lambda^2 \tag{5}$$

dove N è il numero di atomi per cm³; a è la solita costante già introdotta caratteristica della diffusione e λ è la lunghezza d'onda di de Broglie; il termine $\frac{Na}{2\pi}\lambda^2$ è dell'ordine di qualche milionesimo. Dalla formula precedente si vede che se a è positivo l'indice di rifrazione è minore dell'unità; se a è negativo esso è maggiore dell'unità. Ma poiché per le ragioni già viste e come del resto risulta dalle esperienze, in quasi tutte le sostanze, (precisamente nel 90 % circa delle sostanze) a è positivo, ci si deve attendere nel maggior numero dei casi un indice di rifrazione minore dell'unità. Si può usare l'espressione precedente dell'indice di rifrazione per trovare il valore limite ϑ_0 dell'angolo radente ϑ (complementare dell'angolo di incidenza); in prima approssimazione si trova per l'angolo limite ϑ_0 l'espressione:

$$\vartheta_0 = \sqrt{2(1-n)} = \lambda\sqrt{\frac{Na}{\pi}} \tag{6}$$

o anche, ricordando che $a = \sqrt{\frac{\sigma}{4\pi}}$:

$$\vartheta_0 = \lambda\sqrt{\frac{N}{\pi}\sqrt{\frac{\sigma}{4\pi}}}\,. \tag{7}$$

Questa formula è suscettibile di verifica sperimentale, in quanto la lunghezza d'onda è nota, poiché si può lavorare con neutroni monocromatici, e i valori di N e σ sono pure noti.

Concluderò riproducendo una tabellina in cui compaiono i valori di ϑ_0 calcolati come sopra e i valori di ϑ_0 misurati sperimentalmente su specchi di varia natura. Per esempio è stato usato uno specchio di berillio che è un bel metallo, di facile pulitura, per il quale i valori di ϑ_0 risultano abbastanza prossimi. Poi l'esperienza è stata fatta con uno specchio di grafite, che non piglia bene la pulitura, ma richiede grande lavoro senza risultare mai molto bello; onde l'esperienza non risulta molto precisa, il che comporta differenza abbastanza grande fra i valori teorici e sperimentali di ϑ_0. In seguito sono stati provati altri specchi come ferro, nichel, zinco e rame i cui dati sono raccolti nella tabella seguente:

Specchio	ϑ_0 misurato	ϑ_0 calcolato
Be	12,0′	11,1′
C	(10,5′)	8,4′
Fe	10,7′	10,0′
Ni	11,5′	11,8′
Zn	7,1′	6,9′
Cu	9,5′	9,5′

Da qui si vede che in generale l'accordo è abbastanza buono: questo fatto sta a indicare che c'è una correlazione molto buona fra teoria ed esperienza.

Ci sarebbero in quest'ordine di considerazioni molti altri fenomeni da illustrare ma disgraziatamente non ne ho il tempo; vorrei invece fare alcune considerazioni sui risultati di questo lavoro, il cui scopo è forse in gran parte più didattico che scientifico. La meccanica quantistica è infatti di per sè ormai ben stabilita. Nessuno in realtà oggi potrebbe dubitare della relazione di de Broglie che fornisce la lunghezza d'onda associata ai corpuscoli. È interessante tuttavia farne una verifica in grande stile perché, dopo tutto, si tratta di una teoria che è basilare per le nostre cognizioni di fisica. Esperienze didattiche di questo tipo richiedono una pila (e di pile ce ne sono poche!) quindi sarebbe difficile portarle di fronte ad un uditorio come questo; quando però lo si può fare effettivamente, il vedere esperienze come queste che si possono montare con grande facilità, è veramente molto istruttivo.

Per quanto concerne il valore scientifico di queste ricerche, si può osservare che probabilmente il campo in cui potranno avere un certo seguito è un po' in concorrenza coi raggi X, per il problema della struttura dei cristalli. Da questo punto di vista, in genere, il vantaggio è tutto dalla parte dei raggi X, per due ragioni: 1° i raggi X si possono ottenere con intensità molto più forte dei neutroni; 2° un apparecchio a raggi X è un apparecchio molto corrente, mentre una pila è un apparecchio molto costoso di cui esistono pochi esemplari in tutto il mondo. Ci sono alcuni casi, invero non molti, in cui il vantaggio è dalla parte dei neutroni; uno di questi è il caso che ho citato prima e, cioè il caso dell'idrogeno, sul quale, mentre i raggi X non possono fare assolutamente nulla, i neutroni possono invece lavorare sia pure, almeno per ora, con difficoltà; certamente, però, poco alla volta, le difficoltà

verranno superate. Si tratta di aumentare l'intensità e il potere risolutivo: tutti problemi, questi, che si possono risolvere. Vi sono anche altri casi in cui i raggi X sono piuttosto in svantaggio. Supponiamo per esempio che si abbia una lega di Cu e di Zn; questi metalli nel sistema periodico sono contigui, quindi hanno all'incirca lo stesso numero di elettroni; perciò i raggi X, che sono diffusi degli elettroni non « distinguono », per così dire, il rame dallo zinco, ciò che possono fare invece i neutroni i quali « sentono » le proprietà nucleari dei nuclei di Cu e Zn tra cui non c'è nessuna similarità. In un problema, per esempio, di ordine e disordine in una lega di Cu e Zn, i raggi X non si accorgono se i due elementi sono stati scambiati, mentre i neutroni accusano immediatamente la differenza. Vi è dunque un certo numero di applicazioni, non spettacolose direi, ma pure di un certo interesse, a cui questo metodo si presta e sempre più si presterà in futuro.

NONA CONFERENZA (*)

IL MONOPOLO DI DIRAC

(redatta dal Prof. P. CALDIROLA)

Circa una ventina d'anni fa, il fisico teorico inglese Dirac (1) pubblicò alcune speculazioni sulla possibilità che esista una particella dotata, anziché di carica elettrica, di carica magnetica: in altre parole un polo magnetico isolato, un monopolo. Si tratta di una particella che nessun fisico ha finora « veduto » ma la cui esistenza è, almeno in linea teorica, possibile. Ora il mio interesse per questa particella è stato ravvivato, circa un paio d'anni or sono, dall'arrivo delle prime notizie (incomplete, frammentarie e in buona parte erronee) sulla scoperta di particelle pesanti nella radiazione cosmica. Precisamente si venne a sapere che, su lastre fotografiche inviate a grande altezza, erano state osservate delle particelle il cui potere jonizzante appariva assai più intenso di quello delle particelle leggere o delle solite particelle pesanti come i protoni e le particelle α; e in un primo momento, in alcune discussioni con il mio collega Edward Teller, si esaminò la possibilità che queste particelle anziché nuclei pesanti fossero invece monopoli di Dirac.

Quando poi furono pubblicati i resoconti delle esperienze eseguite, si potè riconoscere subito che l'interpretazione data originariamente era corretta e che cioè si trattava effettivamente di nuclei pesanti o perlomeno non leggeri, i quali, a quanto pare, fanno parte della componente primaria della radiazione cosmica.

(*) Tenuta il 21 ottobre 1949 nel salone delle assemblee della Società Montecatini di Milano.

(1) La teoria del monopolo magnetico è stata formulata da P. A. M. DIRAC in « Proc. Roy. Soc. » A, *133*, 60 (1931), ed è stata ripresa dallo stesso Autore in una recente Nota pubblicata sul « Phys. Rev. », *74*, 817 (1948).

Ma a quel tempo, per qualche giorno almeno fino a che la cosa non fu del tutto chiarita, ci si interessò al monopolo cercando di capirne il comportamento.

In questa lezione vorrei intrattenervi un poco sulla natura e sulle proprietà di questa ipotetica particella. La cosa, forse, non è del tutto oziosa perché, se la particella in questione dovesse effettivamente esistere, potrebbe un giorno capitare a qualcuno di osservarla: e ciò potrebbe avvenire in un Paese come l'Italia, in cui gli studi sui raggi cosmici sono tanto rigogliosi. Vale quindi la pena di cercare di rendersi conto, da un punto di vista generale, delle caratteristiche e degli effetti che una siffatta particella dovrebbe presentare.

Comincerò con una considerazione preliminare, che è la seguente: è noto come campo elettrico e campo magnetico siano due enti aventi proprietà assai simili; in altre parole, le equazioni cui obbedisce il campo elettrico nel vuoto sono quasi identiche a quelle corrispondenti cui obbedisce il campo magnetico. Nelle considerazioni che si fanno poi sulle proprietà di simmetria di questi due campi si usa dire che il campo elettrico è rappresentato da un vettore polare e il campo magnetico da un vettore assiale. Il che si cerca di illustrare nel modo seguente: in una riflessione dello spazio rispetto a un punto (operazione che dal punto di vista fisico non si può naturalmente eseguire) un vettore polare è un vettore che – come ad esempio il vettore spostamento da un punto A a un punto B – cambia di verso, mentre un vettore assiale è un vettore che conserva, in tale operazione, inalterato il suo segno. In realtà, siccome l'operazione di riflessione spaziale non è eseguibile, la natura polare e rispettivamente assiale del campo elettrico e del campo magnetico si stabilisce con considerazioni di vario genere; se per esempio supponiamo di avere (fig. 1) in O un protone e in A un elettrone, il campo elettrico è diretto dal protone all'elettrone, e, se si riflette lo spazio, l'elettrone viene a trovarsi in A' e il campo elettrico cambia perciò di verso. Se ammettiamo l'esistenza di un monopolo magnetico isolato, potremo concludere, con un argomento del genere di quello ora riportato, che anche il campo magnetico è rappresentabile con un vettore polare; la differenza di simmetria tra campo elettrico e campo magnetico verrebbe così turbata, a meno che naturalmente, accanto al nostro polo, non si ammettesse sempre l'esistenza di un altro polo di uguale massa e di segno opposto.

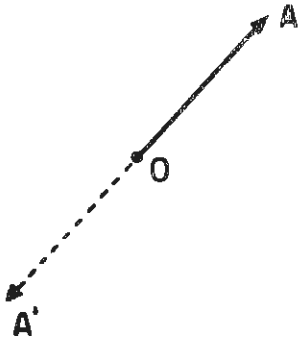

Fig. 1.

Dirac per la prima volta si pose il problema della possibilità di esistenza, dal punto di vista della meccanica quantistica, di un polo magnetico isolato arrivando a un risultato che non è del tutto evidente a priori: *la massa magnetica del supposto monopolo non può avere un valore arbitrario ma deve essere un multiplo intero di un certo quanto di magnetismo.*

Vorrei presentarvi ora, in un modo un po' semplificato, l'argomentazione di Dirac. Supponiamo di avere in un certo punto P dello spazio un

monopolo di massa magnetica m; esso darebbe luogo a un campo magnetico analogo al campo elettrico generato da una carica elettrica. In altre parole, a una distanza r dal monopolo avremo un campo magnetico $\mathbf{H}$ dato da:

$$\mathbf{H} = \left(\frac{m}{r^2}\right).$$

Tale campo evidentemente non avrebbe divergenza nulla, data l'esistenza di una sorgente in P. Descrivendo, come al solito, il campo magnetico $\mathbf{H}$ tramite il potenziale vettore $\mathbf{A}$, avremo [2]:

$$\mathbf{H} = \text{rot } \mathbf{A},$$

essendo $\mathbf{A}$ un vettore a divergenza nulla:

$$\text{div } \mathbf{A} = 0.$$

Il potenziale vettore $\mathbf{A}$ è completamente determinato da queste due equazioni, che la matematica insegna a risolvere. Per evitare però il calcolo esplicito conseguiremo lo stesso scopo facendo uso di una analogia elettrica. Supponiamo di avere un sistema di correnti di densità $\boldsymbol{j}'$, il quale dia luogo a un campo magnetico $\mathbf{H}'$ tale che

$$\begin{cases} \text{div } \mathbf{H}' = 0 \\ \text{rot } \mathbf{H}' = 4\pi \boldsymbol{j}'. \end{cases}$$

Confrontando queste equazioni con quelle precedenti cui soddisfa il vettore $\mathbf{A}$ si vede che il problema di determinare il potenziale vettore dato il campo magnetico $\mathbf{H}$ è matematicamente equivalente al problema di determinare il campo magnetico $\mathbf{H}'$ prodotto da un sistema di correnti di densità $\boldsymbol{j}'$. La corrispondenza fra questi due problemi può essere compendiata nella seguente tabella

problema originale		problema equivalente	
dato:	$\mathbf{H}$	dato:	$4\pi \boldsymbol{j}'$
cercato:	$\mathbf{A}$	cercato:	$\mathbf{H}'$

Siccome è ben noto e familiare come si calcoli il campo magnetico di una corrente per mezzo delle varie leggi di Laplace, Ampère, ecc., così anche il problema originale viene ad essere sostanzialmente risolto.

Nella nostra analogia dovremo avere un sistema di correnti uscenti da un punto in modo che ad una certa distanza r dalla sorgente in P si abbia

$$4\pi \boldsymbol{j}' = \left(\frac{m}{r^2}\right)\frac{\boldsymbol{r}}{r}.$$

(2) La relazione $\mathbf{H} = \text{rot } \mathbf{A}$ si deve naturalmente ritenere valida in tutti i punti dello spazio, ad eccezione del punto P ove è situata la massa magnetica m « sorgente » del campo. In tale punto è evidentemente $\text{div } \mathbf{H} \neq 0$.

Pertanto il punto P, ove trovasi il monopolo sorgente di un flusso costante di campo magnetico, viene ad essere, nell'analogia, sorgente di un *flusso costante* di corrente di densità $\boldsymbol{j}'$. È quindi necessario far affluire continuamente nel punto P della carica elettrica; ciò può pensarsi realizzato per mezzo di un filo conduttore di forma arbitraria il quale convogli in P una corrente concentrata di intensità I eguale a quella che da questo punto esce irradiandosi simmetricamente in tutte le direzioni [3]. Dovrà quindi essere:

$$I = \Phi(\boldsymbol{j}) = \boldsymbol{j}' \cdot 4\pi r^2 = \frac{m}{4\pi r^2} \cdot 4\pi r^2 = m,$$

dove $\Phi(\boldsymbol{j}')$ denota il flusso del vettore $\boldsymbol{j}'$ uscente da una superficie che racchiude il punto P. Essendo però arbitraria la scelta del conduttore che porta in P la corrente I, potendosi ciò fare in infiniti modi, ne risulta corrispondentemente anche un infinità di soluzioni del problema originale. Ora (fig. 2), se chiamiamo $\mathbf{A}_1$ e $\mathbf{A}_2$ due di queste soluzioni che corrispondono rispettivamente alla introduzione nel problema equivalente del filo (1) o del filo (2), la differenza $\mathbf{A}_1 - \mathbf{A}_2$ sarà numericamente eguale al campo magnetico $\mathbf{H}'$ che sarebbe prodotto da quella distribuzione di corrente che risulta facendo la differenza fra le correnti complessivamente passanti per P quando si supponga l'esistenza del filo (1) e quelle che vi passano quando si supponga l'esistenza del filo (2). Tali sistemi di correnti differiscono evidentemente solo per la corrente che nel primo caso affluisce in P lungo (1) e nel secondo lungo (2). Pertanto, detto $\mathbf{H}'$ (1) il campo generato dalla corrente che arriva in P lungo (1) e $\mathbf{H}'$ (2) quello generato dalla corrente che vi arriva lungo (2), avremo:

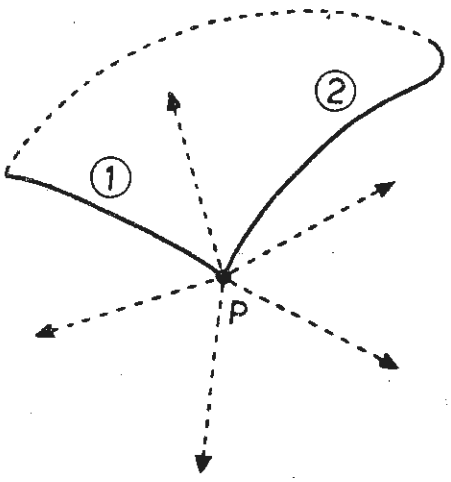

Fig. 2.

$$\mathbf{A}_1 - \mathbf{A}_2 = \mathbf{H}'(1) - \mathbf{H}'(2);$$

in altri termini la differenza tra i potenziali vettori $\mathbf{A}_1 - \mathbf{A}_2$ risulta eguale al campo magnetico generato da una corrente che, provenendo dall'infinito lungo (1), giunge in P e poi ne esce tornando all'infinito lungo (2). Ora si sa dall'elettrologia che un campo magnetico siffatto può rappresentarsi per mezzo di un potenziale che non è una funzione univoca, ma a più valori, e precisamente una funzione f il cui valore in un punto dello spazio cambia di 4π volte il valore della intensità di corrente ogni volta che si gira attorno al filo entro cui passa la corrente. Potremo così dire che:

$$\mathbf{A}_1 - \mathbf{A}_2 = \text{grad } f,$$

(3) L'introduzione di questi fili ideali adduttori di corrente nel punto P è richiesta dal fatto che ivi, come abbiamo precedentemente osservato, si ha $\text{div}\,\mathbf{H} \neq 0$ e quindi nel problema equivalente $\text{div}\,\boldsymbol{j}' \neq 0$.

ove dunque f è un potenziale a infiniti valori, il quale ogni volta che si passa attorno alla linea (1–2) cambia di $4\pi m$ (ricordiamo infatti che $I = m$). È appunto da questa proprietà di f che risulta la relazione di Dirac, denunciata all'inizio della lezione la quale dà come possibili solo certi valori molto particolari del polo magnetico m. È noto infatti che nella meccanica quantistica, la funzione d'onda ψ, che caratterizza una particella di carica e, cambia di fase allorquando si altera la definizione del potenziale vettore del campo che agisce su di essa per un gradiente; dunque se

$$\mathbf{A} \to \mathbf{A} + \operatorname{grad} f,$$

la ψ si trasforma nel modo seguente

$$\psi \to \psi \exp\left(\frac{ie}{\hbar c} f\right);$$

ossia, girando intorno alla linea (1–2), la ψ viene moltiplicata per un fattore

$$\exp\left(\frac{ie}{\hbar c} 4\pi m\right).$$

Ma questa espressione non può avere un valore diverso da 1, altrimenti le basi della stessa meccanica ondulatoria ne sarebbero scosse (è noto infatti che si richiede che la ψ deve sempre essere una funzione univoca). Quindi dovrà essere:

$$\exp\left(\frac{ie}{\hbar c} 4\pi m\right) = 1.$$

Il numero complesso più generale che è uguale a 1 è $\exp(2\pi i n)$, ove n è un arbitrario numero intero; quindi

$$\frac{ie}{\hbar c} 4\pi m = 2\pi i n$$

ossia

$$m = n\frac{\hbar c}{2e} = n\frac{\hbar c}{2e^2}\cdot e,$$

ove $\hbar c/e^2$ è il noto numero « 137 » (inverso della costante di struttura fine). Si ha quindi

$$m = n\frac{\text{« 137 »}}{2} e = n\, 68{,}5\, e,$$

ossia il monopolo può avere solo una massa magnetica che sia un multiplo intero della carica elettrica elementare moltiplicata per $137/2 = 68{,}5$.

A questa conclusione si può arrivare anche in un altro modo, che ora vorrei brevemente esporre pur senza entrare nei particolari. Uno dei fatti essenziali della meccanica quantistica è che la quantità di moto areale è quantizzata, e precisamente essa può prendere solo valori multipli di $\hbar/2$. Consideriamo (fig. 3) un monopolo m e una carica elettrica e, come in figura; nel punto P sarà:

$$\begin{cases} \mathbf{H} = \left(\dfrac{m}{r_2^2}\right)\dfrac{\boldsymbol{r}}{r} \\ \mathbf{E} = \left(\dfrac{e}{r_1^2}\right)\dfrac{\boldsymbol{r}}{r}. \end{cases}$$

Ora, il prodotto vettoriale di **E** per **H** (che viene ad essere un vettore perpendicolare al piano della figura) rappresenta, diviso per $4\pi c$, la densità di quantità di moto elettromagnetica. Ragionando in via approssimata sugli ordini di grandezza, se a è la distanza tra il monopolo e la carica sarà:

$$E \simeq \frac{e}{a^2} \quad , \quad H \simeq \frac{m}{a^2} \quad , \quad \left| \frac{\mathbf{E} \times \mathbf{H}}{4\pi c} \right| \simeq \frac{em}{a^4 c} .$$

Il « braccio » d sarà pure dell'ordine di a e il volume « efficace » d'integrazione sarà dell'ordine di a^3; perciò l'integrale che dà il momento totale della quantità di moto ha l'ordine di grandezza

$$\frac{em}{a^4 c} \cdot a \cdot a^3 = \frac{em}{c} ;$$

si ottiene cioè un risultato che non dipende dalla distanza tra polo e carica.

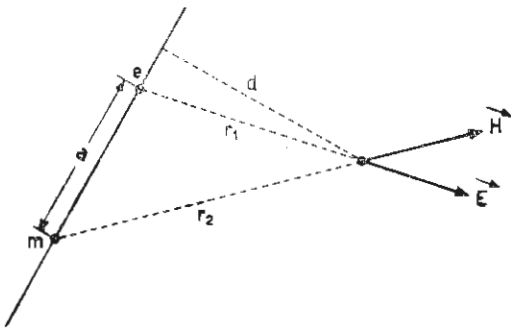

Fig. 3.

La condizione di quantizzazione dà poi:

$$\frac{em}{c} = \frac{\hbar}{2} n ;$$

che è la relazione ricavata più sopra.

Ora Dirac ha fatto un osservazione abbastanza curiosa ed è questa. Un fatto ben noto (e per il momento certo non spiegato) sta nella circostanza che esiste un quanto di carica elettrica, cioè la carica di tutte le particelle che noi conosciamo è sempre un multiplo intero di un valore elementare che è la carica dell'elettrone. Se noi ammettiamo che nell'universo esista almeno un monopolo si dovrà avere:

$$e = \frac{\hbar c}{2m} n ,$$

ossia la carica elettrica risulterà quantizzata; per di più alla massa magnetica del monopolo si dovrà attribuire un valore tale che la carica elettrica assuma conseguentemente i valori che si constatano sperimentalmente. In altre parole il valore della carica elettrica elementare, che noi conosciamo da infinite esperienze, « forza » il monopolo, se esiste, ad avere una massa magnetica quantizzata e viceversa.

Nell'elettrodinamica tutte le proprietà radiative dell'elettrone sono determinate essenzialmente dalla costante di struttura fina

$$\frac{e^2}{\hbar c} = \frac{1}{\text{« 137 »}}.$$

Ora, come abbiamo detto nella prima parte di questo corso [4], la circostanza che questa costante di struttura fina sia assai piccola è quella che permette di separare in prima approssimazione il campo radiativo dalla carica elettrica; in altri termini l'essere il suddetto parametro molto piccolo rispetto all'unità rende possibile l'adottare un procedimento di calcolo per approssimazioni successive in cui, in prima approssimazione, si considera separatamente l'elettrone e il campo elettromagnetico come non interagenti fra di loro. I fenomeni radiativi, in cui i due campi (quello dell'elettrone e quello del campo esterno) vengono a « mescolarsi », si presentano in una approssimazione superiore. Per i fenomeni corrispondenti legati all'esistenza del monopolo, la costante analoga di quella di struttura fina sarebbe

$$\frac{m^2}{\hbar c} \sim \text{« 34 »},$$

cioè un numero piuttosto grande rispetto all'unità, il che sta a significare che il separare il campo elettromagnetico dal monopolo stesso non è affatto un'approssimazione corretta; ne consegue che se il monopolo esiste esso si dovrà comportare in un modo abbastanza diverso da quello che ci si dovrebbe attendere per un ente magnetico puramente analogo ad una carica elettrica.

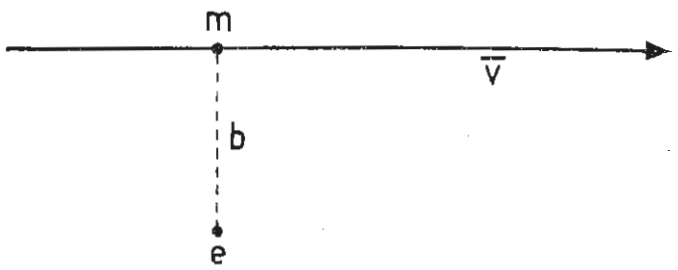

Fig. 4.

Comunque, senza curarci di queste difficoltà, passiamo a discutere come si presenterebbe un monopolo supposto ad esempio che un giorno dovesse capitare a qualcuno di osservarlo nella radiazione cosmica o come prodotto di reazioni ottenute mediante l'impiego di qualche ciclotrone gigante. Anzitutto esso ionizzerebbe (benché la sua sia una carica magnetica) in modo non troppo diverso da una carica elettrica, ma con alcune peculiarità cui ora desidero accennare.

Supponiamo che il monopolo viaggi secondo la linea disegnata in figura 4: sia b la minima distanza a cui esso passa da un elettrone e. L'elettrone verrà a trovarsi in un campo magnetico $H \simeq m/b^2$; ma, come è noto, un campo

(4) Vedasi la 6ª lezione.

magnetico generato da una particella in moto si presenta a un osservatore « fermo » come un campo elettrico di intensità

$$E \simeq \frac{m}{b^2}\frac{v}{c}.$$

Si noti che se passasse con velocità v una carica e, il campo elettrico da essa generato sarebbe semplicemente

$$E \simeq \frac{e}{b^2},$$

e siccome l'effetto di ionizzazione è essenzialmente determinato dal quadrato del campo E, si ha:

$$\frac{\text{effetto del monopolo}}{\text{effetto dell'elettrone}} \simeq \left(\frac{m}{e}\right)^2 \left(\frac{v}{c}\right)^2,$$

e per $v \simeq c$ il rapporto vale $\sim (m/e)^2 \simeq (68{,}5)^2 = 4692$, ossia il monopolo ionizza quanto un nucleo di numero atomico $Z \simeq 68$. Ed è questa la ragione per cui, quando vennero scoperti i nuclei pesanti nella radiazione cosmica, si pensò che potevasi trattare di monopoli.

Osserviamo ancora che a grandi velocità la ionizzazione di una carica elettrica è costante, mentre a bassa velocità è all'incirca proporzionale a $1/v^2$; nel caso invece del monopolo il fattore v^2 a numeratore elimina la dipendenza della velocità e ne risulta una ionizzazione praticamente costante al variare della velocità.

In una lastra fotografica la traccia di un monopolo e la traccia di un nucleo pesante di $Z = 68$ dovrebbero aver « grosso modo » l'aspetto disegnato in fig. 5. Verso la fine, la traccia del nucleo diviene sottile, perché il nucleo comincia a catturare elettroni, provocando così una diminuzione di carica e quindi di jonizzazione. La traccia del monopolo invece si manterrebbe sensibilmente uniforme, a parte il tratto estremo finale di cui è assai difficile prevedere l'aspetto. Un eventuale monopolo contenuto nella radiazione cosmica sarebbe poi influenzato dal campo magnetico terrestre, naturalmente in maniera diversa da come sono influenzati i nuclei. Infatti la Terra ha un campo magnetico le cui linee di forza sono disposte pressapoco come in figura 6. Se assimiliamo il campo magnetico terrestre a quello generato da un dipolo di momento μ, l'energia potenziale magnetica del monopolo sarebbe, se ϑ è la colatitudine:

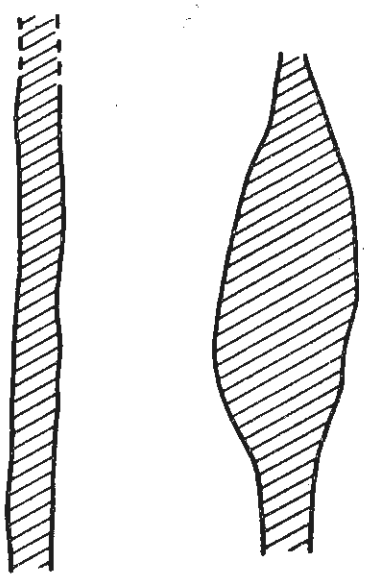

Fig. 5.

$$W_0 = 68 \cdot e \cdot \frac{\mu}{r^2} \cos\vartheta;$$

in particolare al polo

$$W_0 = \frac{\mu}{r^2} 68\, e \simeq 5 \cdot 10^{12}\, eV.$$

Ammettiamo ora che un monopolo entrato nell'atmosfera terrestre abbia perso la sua energia per ionizzazione. Il campo magnetico terrestre tenderebbe però sempre a farlo scorrere nell'aria e, a seconda che esso perda energia più o meno rapidamente di quanto la guadagni, verrebbe accelerato oppure si muoverebbe di moto viscoso. Orbene si trova facilmente che, per aria alla densità naturale, il valore critico del campo è di circa 10 gauss, e cioè un campo più intenso di 10 gauss è sufficiente per far vincere al monopolo la resistenza dell'aria e imprimergli un moto accelerato, un campo più debole gli imprimerebbe invece un moto uniforme.

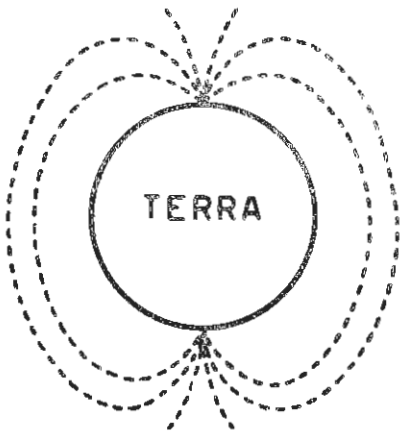

Fig. 6

Essendo il campo magnetico terrestre di circa 1/2 gauss, esso risulta quindi una ventina di volte troppo debole per accelerare il monopolo. Parrebbe quindi che gli ipotetici monopoli dovrebbero giungere alla Terra muovendosi di moto viscoso. I positivi cadrebbero nell'emisfero sud e i negativi nell'emisfero nord: essi tenderebbero così, se arrivassero in numero elevato, a neutralizzare il campo magnetico terrestre.

Si deve quindi concludere, dall'assenza di un simile effetto, che se anche i monopoli esistono in natura essi sono in numero assai limitato. D'altra parte però la conseguenza più importante della loro eventuale esistenza consiste nel fatto che basta l'esistenza anche di uno solo di essi per imporre la quantizzazione della carica elettrica.

Al termine di queste lezioni, desidero ringraziare tutti i miei ascoltatori ed esprimere la mia riconoscenza alla Fondazione Donegani dell'Accademia dei Lincei e alla Società Montecatini che, con il loro generoso contributo, hanno reso possibile questa mia piacevolissima permanenza in Italia.

N° 241 and 242.

During 1949–50 Fermi began to prepare for the developments in high energy physics which were starting to come out of Berkeley, and would soon be coming from many other laboratories as well. In particular, he began to prepare himself and his colleagues and students at Chicago for the experiments which they would soon be able to do with the pi-mesons from the new cyclotron nearing completion in the Institute for Nuclear Studies. Chicago is in a central position in the United States, an easy stopping place for those making the journey to either coast. Many physicists with a new result or a new idea were glad for the chance of a discussion with Fermi. To make these discussions useful Fermi needed a framework in which to set the information which came to him in this way.

For this he developed simplified methods for calculating the orders of magnitude of the pertinent quantities, the cross-sections of the processes of interest. His position was that the meson theories were not correct anyway, so why take the trouble to calculate anything with them exactly. Fermi's methods were a boon to the experimentalists, who had difficulty in following the sophisticated way in which the theorists liked to put forth their theories. Fermi explained his methods in lectures on elementary particles he gave at Chicago; some of the ideas appeared in the *Lezioni Donegani* (see paper N° 240), but they emerged most completely in his Silliman Lectures, later published in book form under the title *Elementary Particles* by Yale University Press.

One of the examples of this work was paper N° 241 which he submitted to the Japanese Journal of Theoretical Physics as his contribution to the " Commemoration of the 18th Anniversary of the Discovery of the Meson Theory by H. Yukawa ". The idea was to try to guess what would happen at extremely high energies in nucleon-nucleon collisions. These were observed to take place occasionally in the cosmic rays and might be expected in the laboratory, once the machines were made big enough. Fermi's model was an extremely simplified one which reduced the problem to a calculation of the available phase space. But one could get orders of magnitudes from such a calculation and this was certainly a good way to begin to understand what was going to happen. Rabi's comment after hearing Fermi present this paper at an American Physical Society meeting in Chicago is worth recording here. " If Fermi is right in saying that he can calculate what will happen at very high energies by purely statistical methods, then we will have nothing new to learn in this field. "

Rabi should have had nothing to fear. Fermi's theory was greatly oversimplified as he intended it to be, and while it did not give well the detailed results which were later found, it did serve as a standard against which one could make a first comparison of the experimental results of multiple production to reveal when something non-statistical was going on. In the later literature this made it appear that this theory was always wrong; a point that Fermi didn't enjoy at all.

He had always stressed the purpose and limitations of his calculations and referred ironically to his own authority and to those who took his results beyond what he intended them to be.

One particular high energy event which claimed a good deal of attention was the cosmic ray star found by Schein (Lord, Fainberg and Schein, « Phys. Rev. », *89*, 970 (1950)) in which a great multiplicity of high energy particles was observed. It was their peculiar angular distribution that Fermi tried to explain in paper N° 242.

Fermi has a very deep feeling for statistical methods and it is interesting to compare his treatment of the atom (papers N° 43 and following) with the present attempt in high energy physics.

H. L. ANDERSON.

241.

HIGH ENERGY NUCLEAR EVENTS

« Progr. Theor. Theoret. Phys. », 5, 570–583 (1950).

ABSTRACT

A statistical method for computing high energy collisions of protons with multiple production of particles is discussed. The method consists in assuming that as a result of fairly strong interactions between nucleons and mesons the probabilities of formation of the various possibile numbers of particles are determined essentially by the statistical weights of the various possibilities.

1. Introduction.

The meson theory has been a dominant factor in the development of physics since it was announced fifteen years ago by Yukawa. One of its outstanding achievements has been the prediction that mesons should be produced in high energy nuclear collisions. At relatively low energies only one meson can be emitted. At higher energies multiple emission becomes possible.

In this paper an attempt will be made to develop a crude theoretical approach for calculating the outcome of nuclear collisions with very great energy. In particular, phenomena in which two colliding nucleons may give rise to several π-mesons, briefly called hereafter pions, and perhaps also to some anti-nucleons, will be discussed.

In treating this type of processes the conventional perturbation theory solution of the production and destruction of pions breaks down entirely. Indeed, the large value of the interaction constant leads quite commonly to situations in which higher approximations yield larger results than do lower approximations. For this reason it is proposed to explore the possibilities of a method that makes use of this fact. The general idea is the following :

When two nucleons collide with very great energy in their center of mass system this energy will be suddenly released in a small volume surrounding the two nucleons. We may think pictorially of the event as of a collision in which the nucleons with their surrounding retinue of pions hit against each other so that all the portion of space occupied by the nucleons and by their surrounding pion field will be suddenly loaded with a very great amount of energy. Since the interactions of the pion field are strong we may expect that rapidly this energy will be distributed among the various degrees of freedom present in this volume according to statistical laws. One can then compute statistically the probability that in this tiny volume a certain number of pions will be created with a given energy distribution. It is then assumed that the

N° 241 and 242.

During 1949–50 Fermi began to prepare for the developments in high energy physics which were starting to come out of Berkeley, and would soon be coming from many other laboratories as well. In particular, he began to prepare himself and his collcagues and students at Chicago for the experiments which they would soon be able to do with the pi-mesons from the new cyclotron nearing completion in the Institute for Nuclear Studies. Chicago is in a central position in the United States, an easy stopping place for those making the journey to either coast. Many physicists with a new result or a new idea were glad for the chance of a discussion with Fermi. To make these discussions useful Fermi needed a framework in which to set the information which came to him in this way.

For this he developed simplified methods for calculating the orders of magnitude of the pertinent quantities, the cross-sections of the processes of interest. His position was that the meson theories were not correct anyway, so why take the trouble to calculate anything with them exactly. Fermi's methods were a boon to the experimentalists, who had difficulty in following the sophisticated way in which the theorists liked to put forth their theories. Fermi explained his methods in lectures on elementary particles he gave at Chicago; some of the ideas appeared in the *Lezioni Donegani* (see paper N° 240), but they emerged most completely in his Silliman Lectures, later published in book form under the title *Elementary Particles* by Yale University Press.

One of the examples of this work was paper N° 241 which he submitted to the Japanese Journal of Theoretical Physics as his contribution to the " Commemoration of the 18th Anniversary of the Discovery of the Meson Theory by H. Yukawa ". The idea was to try to guess what would happen at extremely high energies in nucleon-nucleon collisions. These were observed to take place occasionally in the cosmic rays and might be expected in the laboratory, once the machines were made big enough. Fermi's model was an extremely simplified one which reduced the problem to a calculation of the available phase space. But one could get orders of magnitudes from such a calculation and this was certainly a good way to begin to understand what was going to happen. Rabi's comment after hearing Fermi present this paper at an American Physical Society meeting in Chicago is worth recording here. " If Fermi is right in saying that he can calculate what will happen at very high energies by purely statistical methods, then we will have nothing new to learn in this field. "

Rabi should have had nothing to fear. Fermi's theory was greatly oversimplified as he intended it to be, and while it did not give well the detailed results which were later found, it did serve as a standard against which one could make a first comparison of the experimental results of multiple production to reveal when something non-statistical was going on. In the later literature this made it appear that this theory was always wrong; a point that Fermi didn't enjoy at all.

He had always stressed the purpose and limitations of his calculations and referred ironically to his own authority and to those who took his results beyond what he intended them to be.

One particular high energy event which claimed a good deal of attention was the cosmic ray star found by Schein (Lord, Fainberg and Schein, « Phys. Rev. », *80*, 970 (1950)) in which a great multiplicity of high energy particles was observed. It was their peculiar angular distribution that Fermi tried to explain in paper N° 242.

Fermi has a very deep feeling for statistical methods and it is interesting to compare his treatment of the atom (papers N° 43 and following) with the present attempt in high energy physics.

H. L. ANDERSON.

concentration of energy will rapidly dissolve and that the particles into which the energy has been converted will fly out in all directions.

It is realized that this description of the phenomenon is probably as extreme, although in the opposite direction, as is the perturbation theory approach. On the other hand, it might be helpful to explore a theory that deviates from the unknown truth in the opposite direction from that of the conventional theory. It may then be possible to bracket the correct state of fact in between the two theories. One might also make a case that a theory of the kind here proposed may perhaps be a fairly good approximation to actual events at very high energy, since then the number of possible states of the given energy is large and the probability of establishing a state to its average statistical strength will be increased by the very many ways to arrive at the state in question.

The statement that we expect some sort of statistical equilibrium should be qualified as follows. First of all there are conservation laws of charge and of momentum that evidently must be fulfilled. One might expect further that only those states that are easily reachable from the initial state may actually attain statistical equilibrium. So, for example, radiative phenomena in which photons could be created will certainly not have time to develop. The only type of transitions that are believed to be fast enough are the transitions of the Yukawa theory. A succession of such transitions starting with two colliding nucleons may lead only to the formations of a number of charged or neutral pions and also presumably of nucleon-anti-nucleon pairs. The discussion shall be limited, therefore, to these particles only. Notice the additional conservation law for the difference of the numbers of the nucleons and the anti-nucleons.

The proposed theory has some resemblance to a point of view that has been adopted by Heisenberg [1] who describes a very high energy collision of two nucleons by assuming that the pion "fluid" surrounding the nucleons is set in some sort of turbulent motion by the impact energy. He uses qualitative ideas of turbulence in order to estimate the distribution of energy of this turbulent motion among eddies of different sizes. Turbulence represents the beginning of an approach to thermal equilibrium of a fluid. It describes the spreading of the energy of motion to the many states of larger and larger wave number. One might say, therefore, in a qualitative way that the present proposal consists in pushing the Heisenberg point of view to its extreme consequences of actually reaching statistical equilibrium.

The multiple meson production has also been investigated in an interesting paper by Lewis, Oppenheimer and Wouthuysen [2]. These authors stress the importance of the strong coupling expected in the pseudoscalar meson theory for the production of processes of high multiplicity.

In the theory here proposed there is only one adjustable parameter, the volume Ω, into which the energy of the two colliding nucleons is dumped. Since the pion field surrounding the nucleons extends to a distance of the order $\hbar/\mu c$ where μ is the pion mass, Ω is expected to have linear dimensions of this order of magnitude. As long as the Lorentz contraction is neglected one could take for example a sphere of radius $\hbar/\mu c$. However, when the two nucleons

approach each other with very high energy in the center of gravity system, their surrounding pion clouds will be Lorentz contracted and the volume will be correspondingly reduced.

For this reason the volume Ω will be taken energy dependent according to the relationship:

$$\Omega = \Omega_0 \frac{2Mc^2}{W}, \tag{1}$$

where Ω_0 is the volume without Lorentz contraction. W is the total energy of the two colliding nucleons in the center of gravity system and M is the nucleon mass. The factor $2Mc^2/W$ is the Lorentz contraction. The uncontracted volume Ω_0 may be taken as a sphere of radius R:

$$\Omega_0 = 4\pi R^3/3. \tag{2}$$

It is found in the applications that one seems to get an acceptable agreement with known facts by assuming:

$$R = \hbar/\mu c = 1.4 \times 10^{-13} \text{ cm}. \tag{3}$$

This choice of the volume, although plausible as order of magnitude, is clearly arbitrary and could be changed in order to improve the agreement with experiment. One finds that an increase of Ω_0 would tend to favor processes in which a large number of particles is created.

According to this point of view the total collision cross-section of the two nucleons will be always of the order of magnitude of the geometrical cross-section of the pion cloud. In the numerical calculations, actually, the total cross-section has been taken equal to the area of a circle of radius R, namely,

$$\sigma_{tot} = \pi R^2. \tag{4}$$

Assuming (3) one finds $\sigma_{tot} = 6 \times 10^{-26}$ cm^2. In order to compute the partial cross-section for a phenomenon in which for example three pions are produced in the collision, one will multiply the total cross-section (4) by the relative probability that three pions instead of any other possible number and kind of particles are produced.

The probability of transition into a state of a given type is proportional to the square of the corresponding effective matrix element and to the density of states per unit energy interval. Our assumption of a statistical equilibrium consists in postulating that the square of the effective matrix element is merely proportional to the probability that, for the state in question, all particles are contained at the same time inside Ω. For example in the case of a state that describes n completely independent particles with momenta $p_1, p_2, \cdots, p_n$ this probability is $(\Omega/V)^n$ where V is the large normalization volume. The number of states per unit energy interval is

$$\left(\frac{V}{8\pi^3\hbar^3}\right)^n \frac{d}{dW} Q(W),$$

where Q (W) is the volume of momentum space corresponding to the total energy W. The probability for the formation of the state in question is therefore assumed to be proportional to the product:

$$S(n) = \left(\frac{\Omega}{8\pi^3\hbar^3}\right)^n \frac{dQ(W)}{dW}. \tag{5}$$

There are some complications arising from the fact that the particles are not independent.

(a) In the center of mass system the positions and momenta of only $n - 1$ of the n particles are independent variables. For this reason the exponent of Ω will be $n - 1$ instead of n. Also the momentum space Q (W) will be $3(n - 1)$–dimensional instead of $3n$–dimensional.

(b) Some of the particles may be identical and this fact should be taken into account in computing Q (W).

(c) Some of the particles may carry a spin and one should then allow for the corresponding multiplicity of the states.

(d) The conservation of angular momentum restricts the statistical equilibrium to states with angular momentum equal to that of the two colliding nucleons. In all cases considered $\lambda\!\!\!^{-}$ for the nucleons is smaller than the radius $\hbar/\mu c$ of the sphere of action. It is then meaningful to discuss separately collisions with various values of the impact parameter b (b is the distance of the two straight lines along which the nucleons move before the collision). In units of $\hbar$ the angular momentum is $l = b/\lambda\!\!\!^{-}$. The cross-section for collisions with impact parameter between b and $b + db$ is $2\pi b\,db = 2\pi\lambda\!\!\!^{-2}\,l dl$. One should treat separately collisions with different values of the impact parameter and compute for each of them the probability of the various possible events. The cross-section for a special event is then obtained by adding the contribution of the various l–values.

It is found in most cases that the results so obtained differ only by small numerical factors from those obtained by neglecting the conservation of angular momentum.

This has been done as a rule in order to simplify the mathematics. The corrections arising from the conservation of angular momentum have been, however, indicated in typical cases.

2. Example. Pion Production in Low Energy Nucleon Collisions.

As a first example the production of pions in a collision of two nucleons with relative energy barely above the threshold needed for emission of a pion will be discussed. This example is chosen because it is the simplest possible. It is, however, a case in which the statistical approach may be misleading, since only few states of rather low energy are involved. We will first simplify this example by disregarding the spin of the nucleons as well as the possible existence of a spin of the pions and by disregarding also the various possible electric charges of the particles in question. In the center of gravity system we will have therefore two nucleons colliding against each other. $T/2$ is the kinetic energy of each of the two nucleons. A pion can be emitted when $T > \mu c^2$. We shall assume that this inequality is fulfilled; that the kinetic energy, however, exceeds the threshold by only a small amount, so that both the two nucleons and the pion that may be formed will have non-relativistic energies.

Conservation of energy in this case allows only two types of states; Type (a) in which the two nucleons are scattered elastically without formation of pions; and type (b) in which a pion is formed and three particles, two nucleons and a pion, emerge after the collision.

The statistical weight of the state of type (a) is obtained as follows. Since the momenta of the two nucleons are equal and opposite the momentum space will be three-dimensional. We can compute the statistical weight with (5). s will be taken $= 1$ because the momentum of one particle determines that of the other. The reduced mass is $M/2$, the momentum $p = \sqrt{MT}$ and the phase space volume $Q(T) = 4\pi p^3/3$. According to (5) the statistical weight of this state has therefore the familiar expression:

$$S_2 = \frac{\Omega M^{3/2}}{4\pi^2 \hbar^3} \sqrt{T}. \tag{6}$$

S_2 should be compared with the statistical weight S_3 for case (b) in which three particles, two nucleons and one pion, emerge. Since the total momentum is zero, only the momenta of two of the three particles are independent and therefore in (5) $s = 2$. The calculation of the momentum volume involves some slight complication on account of the conservation of momentum. Let p be the momentum of the pion and let the momenta of the two nucleons be $-\frac{1}{2}p \pm q$. The kinetic energy will then be:

$$T_1 = \left(\frac{1}{2\mu} + \frac{1}{4M}\right) p^2 + \frac{1}{M} q^2 \tag{7}$$

where $T_1 = T - \mu c^2$ is the kinetic energy left over after a pion has been formed. Formula (7) represents an ellipsoid in the six dimensional momentum space of the two vectors p and q. Its volume is:

$$Q_3 = \frac{\pi^3}{3!} \left(\frac{4 M^2 \mu}{2M + \mu}\right)^{3/2} T_1^3. \tag{8}$$

The factor $\pi^3/3!$ is, for a six-dimensional sphere, the analog of the factor $4\pi/3$ in the volume of an ordinary sphere. Substituting in (5) one finds:

$$S_3 = \frac{\Omega^2}{16\pi^3 \hbar^6} \left(\frac{M^2 \mu}{2M + \mu}\right)^{3/2} T_1^2 \approx \frac{\Omega^2 M^{3/2} \mu^{3/2} T_1^2}{32\sqrt{2}\,\pi^3 \hbar^6}. \tag{9}$$

The last expression is simplified by assuming $\mu \ll M$. The probabilities of the two events (a) and (b) are proportional to S_2 and S_3. Since S_3 is very small, we may take the ratio S_3/S_2 to be the probability that the collision leads to pion formation. This is given by:

$$\frac{S_3}{S_2} = \frac{\Omega \mu^{3/2}}{8\sqrt{2}\,\pi \hbar^3} \frac{(T - \mu c^2)^2}{\sqrt{T}} \approx \frac{\Omega \mu (T - \mu c^2)^2}{8\sqrt{2}\,\pi \hbar^3 c}. \tag{10}$$

Since T is barely larger than the threshold energy μc^2, this value has been substituted for T in the denominator. In this case also the Lorentz contraction of the two colliding nucleons is negligible and we can therefore substitute for

Ω the value Ω_0 given by (2) and (3). One finds:

$$\frac{S_3}{S_2} = \frac{1}{6\sqrt{2}}\left(\frac{T}{\mu c^2} - 1\right)^2. \tag{11}$$

The cross-section for pion formation is given by the product of the total cross-section (4) and the probability (11). For example, in a bombardment of nucleons at rest with 345 Mev nucleons, (the proton energy available at Berkeley) one finds that the energy available in the center of gravity system is $T = 165$ Mev. On the other hand $\mu c^2 = 140$ Mev and the previous formula gives therefore $S_3/S_2 = 0.0038$. This means that at this bombarding energy a pion will be formed in about 0.4 percent of the nucleon collisions.

If one examines the process more in detail one will recognize that in a collision of two protons the probability of emission of a positive pion is twice (11) namely, 0.0076. Because if a positive pion is formed a proton and a neutron, instead of two protons, will also emerge. Their statistical weight is twice that for two protons because they are not identical particles. Similarly in the collision of a proton and a neutron the probability of emission of a positive pion is onehalf of (10) namely, 0.0019. The probability of emission of a negative pion is the same.

For example, when a carbon target is bombarded by 345 Mev protons the probabilities that the collision takes place between the proton and another proton or a neutron are the same. Hence, the probability of emission of a positive pion will be $0.0076/2 + 0.0019/2$; that is, 0.0048; and the probability of emission of a negative pion will be $0.0019/2 = 0.001$. Since the nuclear cross-section of carbon is about 3×10^{-25} cm^2, one will obtain the expected values of the cross-sections for emission of a positive and a negative pion by multiplying the nuclear cross-section by the above probabilities. The results are 1.4×10^{-27} cm^2 for the positive and 3×10^{-28} cm^2 for the negative pions. Considering the extremely crude calculation these values are in surprisingly good agreement with the experimental results.

In the above discussion the conservation of angular momentum has been disregarded. When a pion is produced the kinetic energy of the three emerging particles is small and they will therefore escape in an *s*–state. Consequently, only the initial states of zero angular momentum can contribute to this type of final state. Their maximum cross-section has the well known expression $\pi\lambda^2$ which is appreciably smaller than (4). However, also the competition of elastic scattering versus pion production is less since only the scattering states of zero angular momentum will contribute.

By carrying out the calculation one finds that the two effects almost cancel each other and that the conservation of angular momentum changes the previous results for the cross-section for pion production by only a factor 2/3. As long as the conservation of angular momentum is neglected one expects the scattering of the two nucleons to be spherically symmetrical in the center of mass system. This is no longer the case when the angular momentum is conserved. One finds then that the elastic scattering cross-section per steradian in the center of mass system instead of being constant is

approximately proportional to $1/\sin\theta$, where θ is the scattering angle in the same system.

3. Formulas for the Statistical Weights.

Some standard formulas expressing the statistical weights, S, for a number of simple cases will be collected here.

First, the case will be considered that after a collision n particles emerge with masses $m_1, m_2, \cdots, m_n$. Neglecting spin properties and assuming that the particles are statistically independent, and disregarding also the momentum conservation, one finds for S the following two formulas corresponding to the classical and to the extreme relativistic case:

$$S_n = \frac{(m_1 m_2 \cdots m_n)^{3/2}\,\Omega^n}{2^{3n/2}\,\pi^{3n/2}\,\hbar^{3n}}\,\frac{T^{3n/2-1}}{(3n/2-1)!}, \qquad \text{(classical case)} \tag{12}$$

$$S_n = \frac{\Omega^n}{\pi^{2n}\,\hbar^{3n}\,c^{3n}}\,\frac{W^{3n-1}}{(3n-1)!}. \qquad \text{(extr. relativistic case)} \tag{13}$$

In (12) T is the total classical kinetic energy of the n particles and in (13) W is the total energy including rest energy of the n particles. One can also compute a formula for the case that s of the particles, usually the nucleons, are classical and n, usually the pions, are extreme relativistic. Neglecting again spin statistics and momentum conservation and assuming further that all the classical particles have the nucleon mass, M, one finds:

$$S(s, n) = \frac{M^{3s/2}\,\Omega^{n+s}}{2^{3s/2}\,\pi^{2n+3s/2}\,\hbar^{3s+3n}\,c^{3n}}\,\frac{(W - sMc^2)^{3n+3s/2-1}}{(3n+3s/2-1)!}. \tag{14}$$

It is sometimes convenient to re-write (14) in the following form:

$$S(s, n) = \frac{M^{3s/2}\,\Omega^{s/2+1/3}}{2^{3s/2}\,\pi^{s/2+2/3}\,\hbar^{3s/2+1}\,c^{-3s/2+1}}\,\frac{\left(\dfrac{\Omega^{1/3}(W - sMc^2)}{\pi^{2/3}\hbar c}\right)^{3n+3s/2-1}}{(3n+3s/2-1)!}, \tag{15}$$

since it is thus easy to obtain an approximate expression for the sum of the statistical weights $S(s, n)$ over all values of n. The approximation applies to the cases when the average value of n is $\gg 1$. One finds then:

$$\sum_{n=0}^{\infty} S(s, n) \approx \frac{M^{3s/2}\,\Omega^{s/2+1/3}}{3\times 2^{3s/2}\,\pi^{s/2+2/3}\,\hbar^{3s/2+1}\,c^{-3s/2+1}} \exp\left(\frac{\Omega^{1/3}(W - sMc^2)}{\pi^{2/3}\hbar c}\right). \tag{16}$$

The numerical values of (15) and (16) adopting for Ω (1), (2) and (3) are:

$$Mc^2\,S(s, n) = \frac{6.31}{w^{1/3}}\left(\frac{98.8}{w}\right)^{s/2}\frac{\left(6.31\,\dfrac{w-s}{w^{1/3}}\right)^{3n+3s/2-1}}{(3n+3s/2-1)!} \tag{17}$$

and:

$$Mc^2 \sum_{n=0}^{\infty} S(s, n) \approx \frac{2.10}{w^{1/3}}\left(\frac{98.8}{w}\right)^{s/2} \exp\left(6.31\,\frac{w-s}{w^{1/3}}\right) \tag{18}$$

where one has put

$$w = \frac{W}{Mc^2} \tag{19}$$

and it has further been assumes $\mu/M = 0.15$.

In the previous formulas the momentum conservation has been disregarded. The formulas, however, can be generalized without difficulty so as to introduce at least approximately the requirement that the total momentum be zero. The approximation consists in assuming that the mass of the pion is very small compared to the nucleon mass. The momentum of the nucleons will then be much greater than the momentum of the pions since the kinetic energy is approximately equipartitioned among the various particles. Therefore, one can approximately apply the condition that the sum of the momenta vanishes to the nucleons only. One recognizes then that formula (15) must be changed as follows. (a) Instead of s one will write $s - 1$ at all places except in the term $W - s Mc^2$ since we have now $s - 1$ independent momenta of the heavy particles. (b) The factor $M^{3s/2}$ must be changed because instead of the mass one should substitute an expression which is the analog of a reduced mass. It is found that the factor in question must be substituted by $M^{3(s-1)/2}/s^{3/2}$. When the conservation of momentum is approximately taken into account formulas (17) and (18) should then be changed as follows:

$$Mc^2 S(s, n) = \frac{6.31}{s^{3/2} w^{1/3}} \left(\frac{98.8}{w}\right)^{(s-1)/2} \frac{[6.31 (w - s)/w^{1/3}]^{3n + 3s/2 - 1}}{(3n + 3s/2 - 1)!}, \tag{20}$$

$$Mc^2 \sum_{n=0}^{\infty} S(s, n) \approx \frac{2.10}{s^{3/2} w^{1/3}} \left(\frac{98.8}{w}\right)^{(s-1)/2} \exp[6.31 (w - s)/w^{1/3}]. \tag{21}$$

In all the preceding formulas the particles have been assumed to be statistically independent. As long as few nucleons and pions are involved, the error is not great. Larger errors are expected for high multiplicity. The formulas, however, become quite involved since there are at least three kinds of pions and four kinds of nucleons and anti-nucleons. No attempt has been made to introduce these complications for phenomena of relatively low energy. They have been calculated as if there were only one type of pions, one of nucleons and one of anti-nucleons statistically independent. This procedure is certainly inadequate and will give a too high multiplicity at high energy. For phenomena of extremely high energy it becomes simple to introduce the statistical correlations by substituting the statistical by a thermo-dynamical model. This case will be treated in Section 6.

In the previous expressions also the conservation of angular momentum has been neglected. The error introduced with this omission will be discussed in Section 6, where an appropriate correction factor for it will be given.

4. Transition from Single to Multiple Production of Pions.

In Section 2 the emission of a single low energy pion has been discussed. Collisions of higher energy in which besides the two original nucleons also several pions may be produced will be considered now. A rough indication

of the features of this process may be obtained by computing the relative probabilities for the emission of $0, 1, 2, \cdots, n, \cdots$ pions with (20). In that formula one will put $s = 2$. Statistical correlations and conservation of angular momentum will be neglected. Omitting a common factor, the probabilities of the various values of n are proportional to:

$$(22) \qquad \frac{\left[\frac{251}{w}(w-2)^3\right]^n}{\frac{3}{2}\cdot\frac{5}{2}\cdots\frac{6n+1}{2}}.$$

Table I gives the probabilities of pion production of different multiplicities calculated according to this formula. The first column of the table gives the energy, w, of the two nucleons in the center of gravity system in units of Mc^2. The second column gives the energy, w', of the primary particle in the laboratory frame of reference. The next eight columns are labeled by the number n, of pions produced and give the probabilities of various events in percents. The last column gives the average number of pions produced.

TABLE I.

w	w'	$n=0$	1	2	3	4	5	6	7	$\bar{n}$
2.5	2.1	49	47	4	—	—	—	—	—	0.6
3	3.5	9	59	30	2	—	—	—	—	1.2
3.5	5.1	2	31	46	18	3	—	—	—	1.9
4	7.0	—	13	40	33	11	2	—	—	2.5
5	11.5	—	2	15	34	31	14	3	1	3.5

Notice that already for a bombarding energy of about 1 Bev corresponding to the first line of the table the probability of elastic collision of the two nucleons is 50 percent. This probability decreases rapidly and drops below one percent for bombarding energies of about 5 Bev. As the bombarding energy increases the probability of multiple phenomena increases as indicated in the table. The most probable value of n according to (22) should be given approximately by $2.1\,(w-2)/w^{1/3}$.

It will be seen in Section 6 that at high energy very appreciable errors are introduced by neglecting the angular momentum conservation and the statistical correlations. Table I gives only a qualitative indication of the transition from elastic scattering to single and then multiple pion production. The quantitative features of the multiple production, however, should be more reliably represented by formula (32).

5. Production of Anti-Nucleons.

When the two colliding pions have a total energy $> 4Mc^2$ in the center of gravity system, competition with processes in which a nucleon-anti-nucleon pair is formed becomes possible. When the energy is barely above the $4Mc^2$–threshold, no pions can be formed accompanying the pair. As the energy increases, however, the pair will be as a rule accompanied by a number of pions. For moderate energy $w < 10$ one will use formula (20). Substituting in it $s = 4$ we obtain the statistical weight for nucleon pair formation associated with the emission of n pions. Substituting $s = 2$ we obtain an expression proportional to the probability that no pair is formed and the two original nucleons plus n pions emerge.

Omitting the common factor Mc^2 one obtains from (20):

$$S(4, n) = \frac{775}{w^{11/6}} \frac{[6.31\,(w-4)/w^{1/3}]^{3n+7/2}}{(3n+7/2)!}. \tag{23}$$

In normalizing these probabilities to total probability $= 1$, one can make use of the fact that the probability of pair formation in the range of energies here discussed is always less than one percent. One can therefore disregard the pair formation in the normalization factor which reduces to $\sum_n S(2, n)$. In calculating this sum one can use (21). One obtains in the end the following expression for the probability of pair formation accompanied by n pions:

$$P(4, n) = \frac{105}{w}\left(6.31\,\frac{w-4}{w^{1/3}}\right)^{3n+7/2} \frac{\exp[-6.31\,(w-2)/w^{1/3}]}{(3n+7/2)!}.$$

Table II.

w	w'	$n=0$	$n=1$	$n=2$	$n=3$	$n=4$	Total
$4+\varepsilon$	7.0	$1000\,\varepsilon^{7/2}$	—	—	—	—	$0.1\,\varepsilon^{7/2}$
4.5	9.1	14	0.6	—	—	—	15×10^{-4}
5	11.5	27	8	0.7	—	—	36×10^{-4}
5.5	14.3	21	21	5	0.5	—	47×10^{-4}
6	16.9	12	25	14	3	0.3	54×10^{-4}
Columns 3 to 7 inclusive $\times\,10^{-4}$							

Table II is calculated with this formula. Again the first and second columns represent in units of Mc^2 the total energy in the center of gravity system and the total energy of the bombarding particle in the laboratory system. The next five columns give the probabilities of pair formation accompanied by

n pions. These probabilities have been multiplied by a factor 10^4. The eighth column is the total probability of pair formation.

Again, in computing this table the statistical correlations mentioned in Section 3 and the conservation of angular momentum have been disregarded. For this reason the data of the table are merely indicative of the results that would be given by a more correct computation.

At the highest energy here considered the probability of anti-nucleon formation is 0.005. Since in a collision of this energy probably two or three pions are formed in the average one concludes that at these energies the ratio of anti-nucleons to pions formed is about 0.002. Therefore, anti-nucleons will be hard to find even in fairly high energy collisions.

6. Collisions of Extremely High Energy.

In discussing the collision of two nucleons with extremely high energy one can simplify the calculations by assuming that all the various particles produced are extreme relativistic and that thermo-dynamics may be applied instead of a detailed statistical computation of the probabilities of the various events.

In this discussion the conservation of angular momentum will first be neglected. Its effect will be given at the end of this section.

The extremely high energy density that is suddenly formed in the volume Ω will give rise to multiple production of pions and of pairs of nucleons and anti-nucleons. Since both kinds of particles are extreme relativistic, the energy density will be proportional to the fourth power of the temperature, T, as in Stefan's law.

The pions, like the photons, obey the Bose-Einstein statistics. Since we further assume that the temperature is so high that the rest mass is negligible, their energy momentum relationship will be the same as for the photons. Consequently the Stefan's law for the pions will be quite similar to the ordinary Stefan's law of the black body radiation. The difference is only in a statistical weight factor. For the photons the statistical weight is the factor, 2, because of the two polarization directions. If we assume that the pions have spin zero and differ only by their charge $\pm e$ or 0, their statistical weight will be 3. Consequently, the energy density of the pions will be obtained by multiplying the energy density of the ordinary Stefan's law by the factor 3/2. This energy density is therefore:

$$\frac{3 \times 6.494\,(kT)^4}{2\,\pi^2\,\hbar^3\,c^3}\,. \tag{25}$$

The numerical factor $6.494 = \pi^4/15$ is six times the sum of the inverse fourth powers of the integral numbers.

The contribution of the nucleons and anti-nucleons to the energy density is given by a similar formula. The differences are that the statistical weight of the nucleons is eight since we have four different types of nucleons and anti-nucleons and for each, two spin orientations. A further difference is due

to the fact that these particles obey the Pauli principle. In the extreme relativistic case their energy density is:

$$\frac{4 \times 5.682\,(kT)^4}{\pi^2 \hbar^3 c^3}\,. \tag{26}$$

Here the numerical factor 5.682 is $6 \sum_{1}^{\infty} (-1)^{n+1}/n^4$.

The temperature is obtained by equating the total energy to the product of the volume Ω times the sum of the two energy densities (25) and (26). Making use of (1) one obtains the temperature from the following equation:

$$(kT)^4 = 0.152\,\frac{\hbar^3 c^3 W^2}{Mc^2\,\Omega_0}\,. \tag{27}$$

In order to compute the number of pions, nucleons and anti-nucleons produced we need formulas for the density of the various particles. These are computed according to standard procedures of statistical mechanics. In the extreme relativistic case the density of the particles turns out to be proportional to the third power of the temperature. The total densities of the pions and of the nucleons are given by the following two expressions:

$$n_\pi = 0.367\,\frac{(kT)^3}{\hbar^3 c^3} \quad ; \quad n_N = 0.855\,\frac{(kT)^3}{\hbar^3 c^3}\,. \tag{28}$$

The total numbers of pions and nucleons are obtained by multiplying the expressions (28) by the volume Ω and by substituting in them the temperature calculated from (27). The result must be finally corrected in order to take into account the conservation of angular momentum. Only the result of this correction will be given. It is found that conservation of angular momentum has the effect of reducing the numbers of pions and nucleons by a factor that has been calculated numerically to be about 0.51. The conservation of angular momentum has the further effect that the angular distribution of particles produced is no longer isotropical but tends to favor somewhat, particles moving parallel to the original direction of the two colliding nucleons. Introducing these corrections one finds that the number of pions is:

$$\text{No. of pions} = 0.091\left(\frac{\Omega_0 M W^2}{c\hbar^3}\right)^{1/4} = 0.54\sqrt[4]{W/Mc^2} \tag{29}$$

and the number of nucleons plus anti-nucleons is:

$$\text{No. of nucleons and anti-nucleons} = 0.21\left(\frac{\Omega_0 M W^2}{c\hbar^3}\right)^{1/4} = 1.3\sqrt[4]{W\,Mc^2}. \tag{30}$$

From this follows that the number of charged particles that emerge out of an extremely high energy collision is given by:

$$1.2\,(W'/Mc^2)^{1/4} \quad (W' = \text{energy in the laboratory system}). \tag{30 a}$$

In these formulas Ω_0 has been substituted by its value, (2), (3).

These formulas apply only to extreme high energies. Substituting the value, (2), (3), for Ω_0 one finds from (27) that the relationship between temperature and energy can be written in the form:

$$kT/Mc^2 = 0.105\sqrt[4]{W/Mc^2}. \tag{31}$$

Relativistic conditions for the nucleons will be achieved therefore only when $W > 100\,Mc^2$. This corresponds in the laboratory system to an energy of the bombarding particles of more than 5×10^{12} ev. At somewhat lower energies the number of anti-nucleon pairs formed will decrease very rapidly, especially since an energy $2\,Mc^2$ is needed in order to form a pair. In this energy range the formation of pairs is probably better represented by the computation of Section 5.

A comparison of (29) and (30) indicates that in such collisions of extremely high energy the number of nucleons and anti-nucleons produced exceeds that of the pions. Naturally, the anti-protons which are the particles in which we are most interested from the experimental point of view are only one-fourth of the particles (30). Therefore, a somewhat larger number of pions than of anti-protons is formed, even at these high energies. The reason why so many nucleons of all kinds are formed compared to the pions is their statistical weight (8 for the nucleons, 3 for the pions).

In an intermediate energy range where the multiple production of pions is the relevant phenomenon one can still apply the thermo-dynamic method restricting, however, the thermo-dynamic equilibrium to the pion gas only, and assuming that the activation energy of the pairs is too high for producing a sizeable number of these particles at the given temperature. The energy density in this case will be given by (25). The numerical coefficient in formula (27) will be reduced for this reason from 0.152 to 0.046. Also in the same formula one will substitute W^2 by $W(W - 2Mc^2)$ since the energy of the two nucleons does not contribute to the energy of the pion gas. Introducing also the factor 0.51 for the conservation of angular momentum one finds that the number of pions in this approximation is given by:

$$(32) \qquad \text{No. of pions} = 0.323\,\frac{M^{1/4}\,R^{3/4}\,(W - 2\,Mc^2)^{3/4}}{\hbar^{3/4}\,c^{1/4}\,W^{1/4}} = 1.34\,\frac{(w-2)^{3/4}}{w^{1/4}}\,, \text{ (*)}$$

where $w = W/Mc^2$.

In the intermediate energy range of bombarding particles from 10 to 100 Bev this formula probably gives a better estimate of the multiplicities than do the computations of Table I. In particular it would appear that especially the multiplicities given in the last two lines of Table I are too large. According to (32) one would expect for these two energies multiplicities of about 2 instead of the considerably higher values given in Table I. The difference is due to two effects which have been disregarded in computing Table I; namely, the statistical correlation between various types of pions and the angular momentum conservation. Both factors are approximately taken into account in formula (32).

Since no observation of multiple production of an isolated nucleon is available at present, the comparison of these findings with experimental results is only tentative. The present theory seems to give rather low multiplicities except at extremely high energies of the order of 10^{12} to 10^{13} ev.

(*) The original paper gives a wrong formula which has here been corrected following M. KRETZSCHMAR, « ZS. f. Phys », *150*, 255 (1956) (Editors' note).

As more experimental results become available it may be possible to improve the agreement of the theory with experiment by changing the choice (3) of R. If experimentally the multiplicities should turn out to be larger than according to the theory, one wouid increase R or decrease it in the opposite case.

In the present theory we have considered only one type of mesons, the pions. If mesons of larger mass strongly bound to nucleons should exist, as seems to be indicated by the recent experiments of Anderson [3], these particles also could reach statistical equilibrium. Since their rest energy is large, however, they would compete unfavorably with the production of pions except at very high energies. One would expect therefore in most collisions that the number of pions produced should be appreciably larger than that of the heavier mesons.

REFERENCES.

[1] W. HEISENBERG, « Nature », *164*, 65 (1949); « ZS. f. Phys. », *126*, 569 (1949).
[2] H. W. LEWIS, J. R. OPPENHEIMER, and S. A. WOUTHUYSEN, « Phys. Rev. », *73*, 127 (1948).
[3] A. J. SERIFF, R. B. LEIGHTON, C. HSIAO, E. W. COWAN, and C. D. ANDERSON, « Phys. Rev. », *78*, 290 (1950).

N° 242.

For the introduction to this paper see paper N° 241.

242.

ANGULAR DISTRIBUTION OF THE PIONS PRODUCED IN HIGH ENERGY NUCLEAR COLLISIONS

« Phys. Rev. », *81*, 683–687 (1951).

The angular distribution of pions produced in a high energy collision of two nucleons is discussed in terms of the statistical theory of multiple meson production. The results are compared with experimental findings.

I. INTRODUCTION.

In a recent paper [1] a procedure for the calculation of the production of pions (π–mesons) in high energy nuclear collisions has been discussed. The basic assumption is made that the interaction between pions and nucleons is so strong that a statistical equilibrium is attained among all states that are compatible with the conservation theorems of energy, charge, angular momentum, etc. More precisely, it is assumed that when two high energy nucleons collide, the energy available in their center-of-mass system is released in a small volume having dimensions of the order of magnitude of the pion cloud surrounding the nucleons. By a succession of Yukawa processes this energy can give rise to states representing a certain number of pions in addition to the original two nucleons. The states into which the original two-nucleon state can be so converted are restricted by several conservation theorems. The basic assumption is made that the probability that the collision may result in the formation of one of the possible final states is proportional to the probability that the state in question will have all of its particles contained at the same time inside the small volume into which the energy has been concentrated.

(1) E. FERMI, « Prog. Theor. Phys. », *5*, 570 (1950), quoted as (**A**).

At relatively low energies when the Lorentz contraction is negligible this volume, V_0, may be taken equal to that of a sphere of radius R, and volume

$$V_0 = \frac{4\pi R^3}{3}. \tag{1}$$

R will be of the order of magnitude of $\hbar/\mu c$. Actually, the choice

$$R = \frac{\hbar}{\mu c} = 1.4 \times 10^{-13} \text{ cm} \tag{2}$$

seems to give results in fair agreement with the experimental data and has been adopted in the numerical computations.

The effect of the Lorentz contraction should be taken into account in the discussion of collisions at a higher energy. This has been done in **A** by reducing the volume from the uncontracted value, V_0, to

$$V = \left(\frac{2Mc^2}{W}\right) V_0. \tag{3}$$

Where W is the total energy (including rest energy) of the two colliding nucleons in the center-of-mass system, so that $2Mc^2/W$ is the Lorentz contraction factor. This point may be justified as follows.

One should bear in mind that at all the energies under consideration the de Broglie wave-length of the nucleons is very small compared with R. One might therefore think of the two nucleons that approach each other as of two nonquantized objects. Their surrounding pion fields will be Lorentz contracted. When the collision takes place, therefore, all the energy will be first deposited inside the contracted volume (3). Soon afterward a number of reactions take place while the volume in which the energy is concentrated begins to expand and the density of energy decreases. The assumption (3) is justified if one takes the point of view that the relevant time for the reaction is the one when the energy concentration is highest and that the equilibrium reached at that stage is frozen before the expansion has progressed appreciably.

On this assumption the expression (3) of the volume was used in **A** in order to calculate the probable number of charged particles formed in a very high energy nuclear collision. Two different formulas were found for this number, namely:

$$1.2 \left(\frac{W'}{Mc^2}\right)^{1/4} \tag{4}$$

or

$$1.06 \left(\frac{W'}{Mc^2}\right)^{1/4}, \tag{5}$$

depending upon whether one assumes that nucleon-antinucleon pairs are or are not possible. W' is the energy of the impinging nucleon in the laboratory frame of reference.

There is not much experimental material available for testing the formulas. Most of the cosmic-ray stars produced by the collision of a high energy

proton involve the break-up of a large nucleus under conditions in which plural production phenomena are obviously very important. Cases in which one might assume that the collision has effectively taken place between the cosmic-ray proton and a single nucleon are very rare. Recently Schein [2] and his collaborators have obtained a very spectacular example of this kind in which the collision is apparently due to a proton of about 30,000 Bev energy. Fifteen minimum ionization tracks are observed, several of them emerging within a core of about 0.003 radian aperture. The presence of only two lower energy tracks indicates that this collision must have taken place at the fringe of a nucleus, so that only one nucleon appears to have been seriously involved. Another photograph with similar characteristics, although apparently corresponding to a collision with a proton of much lower energy, has been published by the Bristol group [3] and may have been produced by a proton of about 3000 Bev. Formulas (4) and (5) for $W' = 30{,}000$ Bev give the for expected number of charged particles, respectively, 16 and 14 (observed 15). For the second star, assuming $W' = 3000$ Bev, one finds from the two formulas, respectively, 9 or 8 particles (observed 7). This agreement seems to indicate that the assumption that the volume V should be Lorentz contracted is not greatly in error. One should keep in mind, however, that the number of particles emitted in a collision of this type depends only on the fourth root of the volume V. A change by a factor of 2 or 3, therefore, would produce only a relatively minor variation in the expected number of particles.

II. The Angular Distribution.

The main purpose of the present paper is to discuss the angular distribution expected according to the statistical model. The angular distribution of the particles formed in high energy nuclear collisions when observed in the laboratory frame of reference seems to show a striking tendency to divide into a very narrow distribution containing about 50 percent of the particles and a second distribution containing the remaining particles spread over a cone of considerably wider aperture. Schein and his collaborators [2] have stressed this point strongly and have concluded that when the angular distribution is transformed to the center-of-mass system, one obtains a distribution with two concentrations of particles in the two polar directions. Although this concentration is very striking, it does not correspond in the center-of-mass system to extremely small angles, since particles are found in appreciable numbers up to angles of 40 or 50 degrees from the polar axis. In the Schein star the total energy available in the center-of-mass system is about 250 Mc^2. Including unobservable neutral particles one can assume that perhaps a total of 25 particles has been produced, each carrying an average energy of about 10 Bev, an estimate, incidentally, which is quite compatible with the direct

(2) Lord, Fainberg, and Schein, « Phys. Rev. », *80*, 970 (1950). I am indebted to the authors for informing me of their results before publication.

(3) Camerini, Fowler, Lock, and Muirhead, « Phil. Mag. », *41*, 413 (1950).

measurement of the energies observed in the laboratory frame of reference. Particles of 10 Bev have a de Broglie wave-length $\lambda\!\!\!^{-} \approx 2 \times 10^{-15}$. Since the range of the nuclear interactions is about $R = 1.4 \times 10^{-13}$ cm, one might perhaps guess that the allowable angular deviations from the polar axis are of the order of magnitude $\lambda\!\!\!^{-}/R \approx 0.015 \approx 1°$. This assumption is evidently in gross disagreement with the observations which give a much wider angular distribution.

We procced now to discuss the angular distribution to be expected according to the statistical theory. At first sight one might expect that this theory should give an isotropic distribution in the center-of-mass system because one might argue that the evaporation of particles from the volume, V, will obey some analog of the Maxwell distribution law and therefore be spherically symmetric. On closer analysis, however, it is recognized that this conclusion is incorrect and that actually one might expect an angular distribution rather similar to that observed experimentally. Qualitatively, this is explained by the following reason.

It is very improbable that the collision of the two original nucleons should be exactly centered. Far more probable are collisions in which the two particles collide somewhat on one side of each other, so that the system is left with a considerable amount of angular momentum. This angular momentum could easily amount in the case of the Schein star to several hundred or a thousand $\hbar$ units. Since the angular momentum must be conserved between initial and final state, the outgoing particles will have to carry away the initial amount of angular momentum. As a consequence of this fact, the angular distribution of the outgoing particles is not spherically symmetric even if one takes literally the statistical and thermodynamic procedures of calculation adopted in (**A**). The statistical distribution law is usually written on the assumption that the energy is the only conserved quantity, and should be changed when the system is such that other quantities, like the angular momentum, for example, also are conserved. The changes are of a nature to destroy, in general, the isotropy of the velocity distribution of the particles.

Before we proceed to a quantitative discussion of the case, the role of the Lorentz contraction flattening of the volume V should be discussed qualitatively. In fig. 1, a and b are the trajectories of the two nucleons in the center-of-mass system, and the line c represents the section of the flattened volume V in which the energy initially is deposited. Figure 1 is drawn for the case in which the angular momentum is directed perpendicular to the drawing and upward.

We introduce a system of axes, x, y, z, centered on the center of the volume V. The y axis is drawn parallel to the trajectories a and b of the two nucleons. The z axis (not drawn in the fig. 1) is perpendicular to the plane of a and b and is therefore the direction of the angular-momentum vector. After the collision the newly formed particles will emerge out of the volume V. Since this volume is very much flattened and the y-dimension can be neglected, the z-component of the angular momentum of a particle emerging at the point of coordinates x and z (y very small) will be

$$Z = xp \cos \vartheta, \tag{6}$$

where p is the momentum of the particle and ϑ is the angle between p and the y axis. Since the escaping particles must carry away a large amount of angular momentum, it is clear that particles emitted at places with positive x should have the $\cos\vartheta$ positive and as large as possible. That is, for them the angle ϑ should be small. Particles emerging from places with x negative will carry away a large positive angular momentum when $\cos\vartheta$ is negative and as large as possible in absolute value; that is, when ϑ is close to 180°.

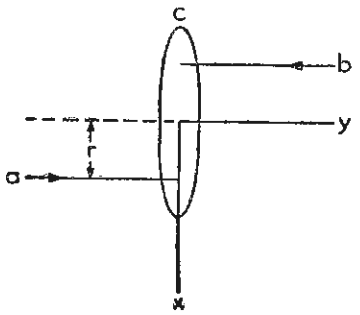

Fig. 1. – Trajectories of nucleons in the center-of-mass system.

In this way one understands qualitatively that the angular distribution of the particles will not be isotropic, but rather will favor the two polar directions $\vartheta = 0°$ and $\vartheta = 180°$. In order to estimate this effect quantitatively it would be necessary to know the actual shape of the volume V. The assumption that this is a very much flattened ellipsoid obtained by Lorentz contraction of the sphere (1) is evidently an oversimplification especially in the case represented in fig. 1, in which the two nucleons a and b collide with a relatively large value of the impact parameter. On the other hand, it would not be possible to specify the actual shape of the volume V without considerable arbitrariness. For this reason, in the calculations to follow, the assumption of a flattened ellipsoid of transverse axis R and very short symmetry axis has been adopted, with full realization of its crudeness.

The computation will be carried through in the thermodynamic approximation allowable when the energy involved is very large. If the energy W were the only quantity conserved during the collision process, one would expect that the average number of particles in a quantum state of energy w within the volume V should be

$$1/(e^{\beta w} - 1), \tag{7}$$

where $\beta = 1/kT$. The formula has been written for the case that the particles obey the Bose-Einstein statistics. Otherwise $+1$ should appear in its denominator instead of -1. It is found that the angular distribution in this approximation is independent of the type of statistics of the particles and therefore only the case of the Bose-Einstein statistics will be discussed in detail. Formula (7) is no longer applicable when the z–component of the angular momentum also is conserved. Instead of Eq. (7) one should use in this case

the following formula for the average number of particles in a given state:

$$1/(e^{\beta w-\lambda Z}-1). \tag{8}$$

The constants β and λ appearing in this formula should be adjusted in such a way that total energy and total z–component of the angular momentum have the correct values.[4]

We restrict the discussion to the case in which all particles in the center-of-mass system are extreme relativistic. We write, therefore, w and Z in the form

$$w = cp \quad , \quad Z = xp\eta, \tag{9}$$

where $\eta = \cos\vartheta$. Introducing further the notations

$$\gamma = c\beta \quad , \quad \rho = \frac{\lambda R}{c\beta}, \tag{10}$$

the distribution law (8) can be written

$$1/\{\exp[\gamma p\,(1-\rho\eta x/R)]-1\}. \tag{11}$$

The actual number of particles in a volume element of phase space is obtained by multiplying Eq. (11) by the volume element of phase space divided by $(2\pi\hbar)^3$. We consider an element of phase space corresponding to a volume element

$$\left(\frac{2Mc^2}{W}\right)\pi\,(R^2-x^2)\,dx \tag{12}$$

comprised between the abscissas x and $x+dx$, and a volume element in momentum space

$$2\pi p^2\,dp\,d\eta \tag{13}$$

corresponding to particles having momenta with magnitudes between p and $p+dp$, for which, in addition, $\cos\vartheta$ has value between η and $\eta+d\eta$. The number of particles in this volume element is

$$dn = \frac{Mc^2}{2\pi\hbar^3 W}\,\frac{(R^2-x^2)\,dx p^2\,dp\,d\eta}{\exp[\gamma p\,(1-\rho\eta x/R)]-1}. \tag{14}$$

Integration of this expression from zero to infinity for p, from $-T$ to $+R$ for x, and from -1 to $+1$ for η yields the total number N of particles of the given type. The result of the integration is

$$N = \frac{a}{2\pi}\,\frac{Mc^2 R^3}{W\hbar^3\gamma^3}\left(\frac{1+\rho^2}{\rho^3}\log\frac{1+\rho}{1-\rho}-\frac{2}{\rho^2}\right), \tag{15}$$

(4) Notice that not only the z–component of the angular momentun but also the x– and y–components are conserved. In spite of this, only the z–component appears in the formula, because the coefficients similar to λ for the other two components turn out to be zero when the components of the total angular momentum in these two directions vanish. For the same reason no terms corresponding to the momentum of the particles created appear in the exponent of Eq. (8), in spite of the fact that the momentum is also conserved. This arises from the fact that the total momentum vanishes in the center-of-mass system.

where

$$a = 2 \sum_{1}^{\infty} 1/n^3 = 2.413 \tag{16}$$

is the numerical constant that comes from the integration over p. Multiplication of Eq. (14) by the energy, cp, of a particle and performance of a similar integration yields the total energy W of the particles, which is given by the following formula:

$$W = \frac{b}{3\pi} \frac{Mc^3 R^3}{W\hbar^3 \gamma^4} \left(\frac{1}{\rho} \log \frac{1+\rho}{1-\rho} + \frac{2}{1-\rho^2} \right), \tag{17}$$

where

$$b = 6 \sum_{1}^{\infty} 1/n^4 = \pi^4/15 = 6.494. \tag{18}$$

One obtains finally the total z-component of the angular momentum of the particles by multiplication of Eq. (14) by the angular momentum $xp\eta$ of a particle and integration, with the result

$$M_z = \frac{b}{2\pi} \frac{Mc^2 R^4}{W\hbar^3 \gamma^4} \left(\frac{2}{\rho^3} + \frac{\left(\frac{4}{3\rho}\right)}{1-\rho^2} - \frac{1+\frac{1}{3}\rho^2}{\rho^4} \ln \frac{1+\rho}{1-\rho} \right). \tag{19}$$

Formulas (17) and (19) give the energy and angular momentum due to a single type of particle, for example, the neutral pions. When several types of particles are involved, such as neutral and charged pions or various types of nucleons and antinucleons, one obtains similar formulas, the only difference being in the value of the numerical constant, b. Formulas (17) and (19) can be used to determine the values of the parameters γ and ρ. In the collision represented in fig. 1 each of the two original nucleons a and b carry the energy W/2 and the momentum W/2 c. Consequently, the total angular momentum will be $M_z = Wr/c$, where r is the distance from the center of the volume V at which the nucleons collide. Using this expression of M_z and dividing Eq. (19) by Eq. (17) one finds

$$\frac{r}{R} = \frac{3 f_1(\rho)}{2 f_2(\rho)}, \tag{20}$$

where $f_1(\rho)$ is the function of ρ appearing in parenthesis in Eq. (19) and $f_2(\rho)$ is the function appearing in parenthesis in Eq. (17). The right-hand side of Eq. (20) is given in Table I, second column. The relationship (20) can be used for the computation of the parameter ρ appearing in the distribution law (11). This parameter vanishes for $r = 0$; that is, for a perfectly centered collision. In this case there is no angular dependence of the distribution law and η disappears from Eq. (11). For large values of r, ρ is close to unity and expression (11) becomes strongly dependent on the angle ϑ. In order to obtain the angular dependence explicitly we integrate Eq. (14) with respect to the variables p and x only. The result is the number of particles for which $\cos\vartheta$ lies between η and $\eta + d\eta$. One finds

$$\frac{dn}{d\eta} = \frac{a Mc^2 R^3 f_4(\rho\eta)}{2\pi W\hbar^3 \gamma^3}, \tag{21}$$

where f_4 is the following function:

$$f_4(\alpha) = \frac{2}{\alpha^2(1-\alpha^2)} - \frac{1}{\alpha^3}\log\frac{1+\alpha}{1-\alpha}. \tag{22}$$

Its numerical values are given in Table I.

TABLE I.

Numerical data for Eqs. (20) *and* (22).

ρ	$\frac{3f_1(\rho)}{2f_2(\rho)}$	$f_4(\rho)$
0	0.000	1.33
0.1	0.022	1.35
0.2	0.048	1.40
0.3	0.088	1.53
0.4	0.123	1.63
0.5	0.160	1.88
0.6	0.204	2.26
0.7	0.270	2.95
0.8	0.368	4.39
0.9	0.528	8.96
0.92	0.574	11.3
0.94	0.634	15.3
0.96	0.710	23.3
0.98	0.814	47.7
0.99	0.876	97.0
1.0	1.000	∞

III. Discussion.

Formula (21) gives the angular distribution. Since $d\eta = -\sin\vartheta d\vartheta$ is proportional to the element of solid angle, $dn/d\eta$ would be constant for an isotropic angular distribution. This would be the case, for example, when the collision impact parameter is zero because then ρ would also vanish. When r, and consequently ρ also, are different from zero, $f_4(\rho\eta)$ is not constant but has its maximum values for $\eta = \pm 1$. These maxima are most pronounced for values of ρ approaching unity.

It is to be expected that the impact parameter will be different from collision to collision and that r will range in value from zero to R. The median value of r will be $R/\sqrt{2}$. Collisions in which r is smaller or greater than this value will differ from the average because they give, respectively, a less or more strongly peaked angular distribution.

In fig. 2 the function $f_4(\rho\eta)$ is plotted *versus* η for a value of ρ of 0.959, corresponding to the median value of the impact parameter. This gives the plot of the angular distribution to be expected in an average collision. The plot is such that a straight line would correspond to an isotropic distribution. One can see that there is a very pronounced concentration at the two poles $\eta = \pm 1$. The concentration is still appreciable for the values

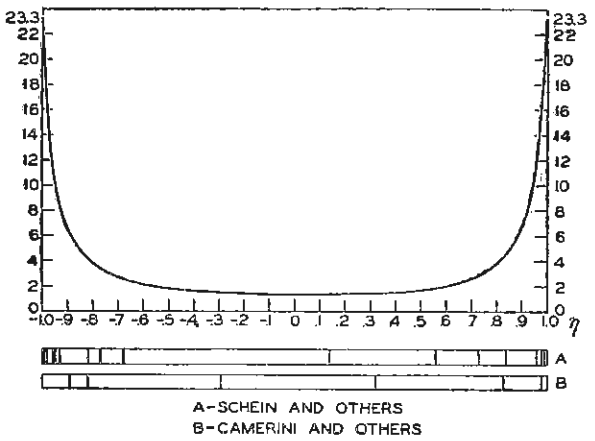

Fig. 2. – Functional dependence $f_4(0.959\,\eta)$ *vs* η.

$\pm$ 0.8 of η which correspond to ϑ values of 37° or 143°. For comparison an attempt has beem made to plot under the graph of fig. 2 a guess as to the angular distribution in the two stars already quoted.[2,3] This involves some arbitrariness in the conversion from the laboratory system to the center-of-mass system, so that the points indicated should not be taken to be more than a mere indication of the general type of experimental results. One can see, however, that the theoretical angular distribution is not at all incompatible with the results of the observation.

As pointed out, it is possible that in various collisions of the general type discussed here one might find a variety of different angular distributions. Centered collisions should give angular distributions more isotropic than fig. 2. Very eccentric collisions should give more peaked distributions.

The angular distribution calculated above is independent of the energy of the collision. The simple form of theory discussed here breaks down, however, at low energies for two reasons: The first is that the flattening of the volume V is no longer very pronounced, while the other is that it is no longer permissible to assume that all of the particles are extreme relativistic in the center-of-mass system.

N° 243, 244 and 245.

One of the several theoretical problems to which Fermi turned his attention at about this time was the instability of the surface dividing two fluids, when the heavier of them is accelerated by the lighter (Taylor Instability). This subject had been developed quite extensively at Los Alamos, principally by John von Neumann, because it is important for the implosion method of producing atomic bombs. Fermi felt that he ought to have a better understanding of the subject, and the three papers included here are some of the evidence of his efforts along these lines.

Paper N° 243 is an excerpt of a lecture that he gave at Los Alamos in September 1951. Paper N° 244 is Fermi's discussion of the Taylor instability at the surface of an incompressible liquid in a vacuum. It was written in September 1951, at Los Alamos. Almost two years later, in August 1953, he again took up the study of the Taylor instability at Los Alamos, with John von Neumann (Paper N° 245). Together they considered the more complex case of a surface dividing two incompressible liquids.

Paper N° 244 and 245 were first circulated as Parts 1 and 2 of the same document AECU–2979, under the title *Taylor Instability of Incompressible Liquids*, by Enrico Fermi and John von Neumann. This document was released in November 1955 by the Atomic Energy Commission, Technical Information Service, Oak Ridge, Tennessee.

H. L. ANDERSON.

243.

EXCERPT FROM A LECTURE ON TAYLOR INSTABILITY, GIVEN DURING THE FALL OF 1951 AT LOS ALAMOS SCIENTIFIC LABORATORY

Taylor instability is the instability of the surface between two fluids when the heavier material is being accelerated by the lighter material. It is traditionally illustrated by the instability of the surface between air and water when a beaker of water is turned upside down. The adequacy of this example can be seen by supposing the beaker to be in an elevator in a gravitationless region. If the elevator were accelerated in a direction corresponding to a vector drawn from the closed end to the open end of the beaker the surface would be stable. This acceleration corresponds to a gravitational field in the opposite direction (towards the closed end or bottom of the beaker). If the elevator were accelerated in a direction corresponding to a vector drawn from the surface of the liquid to the closed end of the beaker the surface would be unstable. This case corresponds to a gravitational field towards the open end of the beaker; i.e., when the beaker is turned upside down.

Now consider a stable liquid with a standing wave as shown in fig. 1. We will treat this in an approximate manner to illustrate the nature of the

equations. The amplitude is represented by a. Then the rate of change of amplitude is $\dot{a}$. To an order of magnitude $\dot{a}$ is the velocity of the material which flows from the through of the wave to the crest. In considering the motion of the fluid from the through to the adjoining crest as indicated in the figure, it is clear that we should not assume that the whole body of fluid moves, but we should consider a depth of fluid of the order of magnitude of one wavelength—certainly not more. The volume of fluid involved in the motion is thus of the order of magnitude of λ^2, and the order of magnitude of the kinetic energy is:

$$T \approx \rho\lambda^3 \dot{a}^2.$$

The potential energy can be represented as the weight of displaced fluid times the distance it is displaced. To a degree of approximation similar to

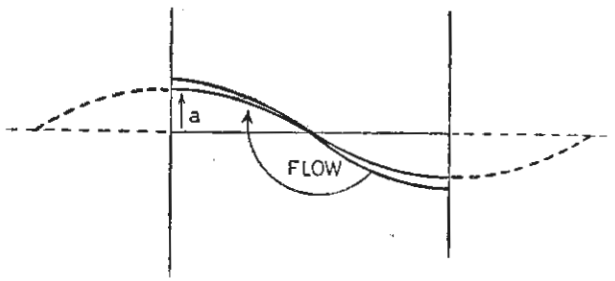

Fig. 1. – Profile of the liquid surface. The problem is treated in two dimensions. The fluid considered extends for a unit length in the direction perpendicular to the page.

that used above λa is the volume of fluid moved. Its center of gravity is displaced a distance about equal to a. Therefore the potential energy is: $U \approx \rho g \lambda a^2$, where ρ is the density and g is the acceleration due to gravity. Now we see that:

$$\text{mass} = \rho\lambda^2$$

$$\text{restoring force constant} = \rho g\lambda$$

and therefore the equation of motion of the liquid is:

$$\rho\lambda^2 \ddot{a} = -\rho g\lambda a$$

$$\ddot{a} = -\frac{ga}{\lambda}.$$

Now there have been many factors neglected in arriving at this equation. In this case, since it involves treatment of waves, the missing factors boil down, of course, to 2π, and the correct equation is:

(1) $$\ddot{a} = -\frac{2\pi}{\lambda} ga.$$

The solution for this is:

(2) $$a = a_0 \cos \sqrt{\frac{2\pi g}{\lambda}}\, t$$

which is a periodic oscillation the frequency of which is:

$$\omega = 2\pi\nu = \sqrt{\frac{2\pi g}{\lambda}}\, t. \tag{2'}$$

This is the case of gravity waves in liquids and corresponds to the stable surface, or to the beaker right side up.

The unstable case is the one in which the acceleration is in the opposite direction—when the beaker is turned upside down. In this case the acceleration of the whole body of material (or gravity in the example we have taken) no longer acts as a restoring force but acts to accentuate any existing displacements. The equation for a wave-like disturbance of the surface is then the same as before except that Equation 1 now becomes:

$$\ddot{a} = \frac{2\pi}{\lambda} g a \tag{3}$$

where the sign of the "restoring" force is reversed.

The solution for this is:

$$a = a_0 \cos \sqrt{-\frac{2\pi g}{\lambda}}\, t$$

or:

$$a_0 e^{\sqrt{\frac{2\pi g}{\lambda}}\, t}$$

The amplitude of the disturbance will thus increase exponentially with time, which constitutes the Taylor instability. It can also be seen that the exponential coefficient of the time is inversely proportional to $\lambda^{1/2}$; short wavelengths will increase in amplitude faster than long wavelengths.

N° 244.

For the introduction to this paper see paper N° 243.

244.

TAYLOR INSTABILITY OF AN INCOMPRESSIBLE LIQUID

Part I of Document AECU–2979 (September 4, 1951).

This is an attempt to discuss in a very simplified form the problem of the growth of an initial ripple on the surface of an incompressible liquid in presence of an acceleration, g, directed from the outside into the liquid.

The model is that of a heavy liquid occupying at $t = 0$ the half space above the plane $z = 0$. It is well known that this is a state of unstable equilibrium. Any tiny ripple on the surface at the initial time grows in amplitude, first exponentially and later, when its amplitude has became comparable to the wave length, by a more complicated law.

The case will be considered that there is initially a small-amplitude sinusoidal ripple of wave length λ. In a first phase this amplitude will increase exponentially like

$$\exp \sqrt{\frac{2\pi g}{\lambda}}\, t. \tag{1}$$

This exponential law, however, will break down when the amplitude has become comparable to $\lambda\!\!\!^{-} = \lambda/2\pi$. We propose to discuss what happens in the subsequent phase.

This will be done by grossly schematizing the shape of the wave as indicated in fig. 1.

Instead of a wave profile like the curve, a profile like ABCDEFGHIJ will be assumed.

It is clear from the symmetry of the problem that the points at the maximum and the minimum of the wave move in vertical directions. In fig. 2 a half wave, from a maximum to the successive minimum is represented with the notations adopted. OO′ is the initial level of the liquid. On account of the incompressibility the amount of liquid below the plane OO′, namely

CO′ DE, must be equal to the amount of liquid ABCO missing from above. This condition leads immediately to the relationship:

$$b = \frac{ax}{1-x} \cdot \tag{2}$$

Our schematic wave profile is then characterized by the two parameters a, x. The problem is to determine how they vary with time.

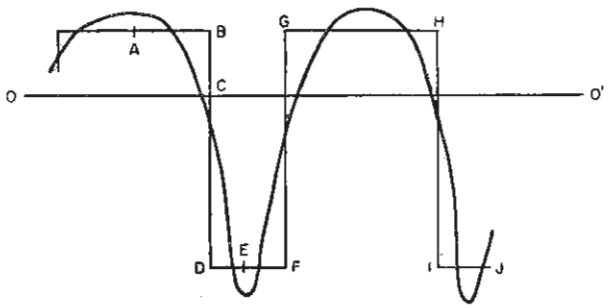

Fig. 1.

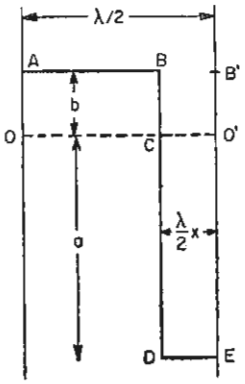

Fig. 2.

In principle the problem so simplified could be solved by expressing the kinetic energy T and the potential energy U of the liquid contained between the two boundaries OA, O′E as functions of $a, x, \dot{a}, \dot{x}$:

$$T = T(a, x, \dot{a}, \dot{x})$$

$$U = U(a, x).$$

One can then write the Lagrange equations:

$$\frac{d}{dt}\frac{\partial T}{\partial \dot{x}} - \frac{\partial T}{\partial x} = -\frac{\partial U}{\partial x} \quad ; \quad \frac{d}{dt}\frac{\partial T}{\partial \dot{a}} - \frac{\partial T}{\partial a} = -\frac{\partial U}{\partial a} \tag{3}$$

which describe the law of variation of the two wave parameters a, x.

The potential energy U can be written down immediately. It is due to having moved the liquid originally contained in ABOC (weight per unit length perpendicular to the plane of the drawing $= \rho g \frac{\lambda}{2} b (1-x)$, height of the center of gravity $= b/2$) to the lower position CDEO′ with the center of gravity at a height $-a/2$.

In what follows the following units will be used: Unit of length, $\lambda/2$; unit of acceleration, g; unit of density, ρ.

One finds, then, the potential energy:

$$U = -\frac{1}{2}\frac{a^2 x}{1-x} \cdot \tag{4}$$

The calculation of the kinetic energy is more difficult. In principle it could be carried out for a prescribed motion of the profile of the liquid by solving a Dirichlet problem. Instead of doing this, a much cruder method

was followed in keeping with the crude approximation chosen for the profile of the wave.

When the amplitude of the wave is very large it is evident that the kinetic energy is due primarily to the vertical component of the liquid velocity inside the domain BDEB'. The corresponding kinetic energy can be computed easily on the assumption that the vertical component of the velocity is constant on each horizontal section of BDEB'. One finds that this part of the kinetic energy is given by:

$$T_1 = \frac{a^3 \dot{x}^2}{6x(1-x)}. \tag{5}$$

For small and moderate amplitudes of the wave, additional terms in the kinetic energy become important. One of them is the kinetic energy due to the horizontal component of the motion of the liquid BDEB'. This term of the kinetic energy is given approximately by:

$$T_2 = \frac{ax\dot{x}^2}{6(1-x)}. \tag{6}$$

Finally, the kinetic energy due to the motion of the liquid above the line AB' should be estimated. An approximate expression for this term of the kinetic energy yields:

$$T_3 = \frac{\pi}{4}\frac{a^2\dot{x}^2}{(1-x)^2} + \frac{\pi}{2}\frac{ax\dot{a}\dot{x}}{1-x} + \frac{\pi}{4}x^2\dot{a}^2. \tag{7}$$

The kinetic energy is the sum of the three terms (5), (6), (7)

$$T = T_1 + T_2 + T_3 \tag{8}$$

As pointed out, the leading term at high amplitude is the first. For low amplitude all the three terms need to be considered.

Using the expressions (4) and (8) for potential and kinetic energy, one can write the Lagrange equations (3). That enables one to express the second time derivatives x and a in terms of $x, a, \dot{x}, \dot{a}$. One finds:

$$\ddot{x} = \frac{ED - FB}{AD - BC'} \quad , \quad \ddot{a} = \frac{AF - EC}{AD - BC} \tag{9}$$

where:

$$\begin{cases} A = \dfrac{a^2}{3y} + \dfrac{y}{3} + \dfrac{\pi}{2}a \quad , \quad D = a + \dfrac{\pi}{2}y \\ B = \dfrac{a}{2} + \dfrac{\pi}{2}y \quad , \quad C = \dfrac{a^2}{2y} + \dfrac{\pi}{2}a \end{cases} \tag{10}$$

$$E = \frac{a}{2} - \frac{\dot{a}^2}{2} - \frac{(4x-1)a^2\dot{x}^2}{6y^2} - \frac{a\dot{a}\dot{x}}{y} - \frac{\dot{x}^2}{6} - \frac{y\dot{x}\dot{a}}{3a} - \frac{\pi xy\dot{a}^2}{2a} - \frac{\pi ax\dot{x}^2}{2y} - \pi\dot{x}\dot{a} \tag{11}$$

$$F = a - \frac{\dot{a}^2}{2} + \frac{(1-2x)a^2\dot{x}^2}{2y^2} - \frac{a\dot{x}\dot{a}}{y} + \frac{\dot{x}^2}{6} - \pi\frac{y\dot{x}\dot{a}}{x}$$

and:

$$y = x(1-x). \tag{12}$$

These equations have been integrated numerically by Miriam Caldwell. Initial conditions corresponding to a wave of very low amplitude were chosen

as follows: $a = 0.01$, $\dot{a} = 0.0177$, $x = 0.5$, $\dot{x} = 0$. The results of the numerical integration are given in Table I.

TABLE I.

t	a	b	x
0.0	0.0100	0.0100	0.500
0.5	0.0243	0.0228	0.484
1.0	0.0628	0.0468	0.427
1.5	0.192	0.083	0.303
2.0	0.584	0.115	0.165
2.5	1.218	0.144	0.106
3.0	2.195	0.170	0.072

The four columns of the table give, respectively: the time in units $\sqrt{\frac{\lambda}{2g}}$; the two amplitudes of the wave, a and b, below and above the original surface of the liquid expressed in units $\lambda/2$; and the quantity x that measures the asymmetry of the wave ($x = 0.5$ corresponding to a symmetrical wave). $x < 0.5$ corresponds to a wave in which the half wave below the original liquid surface is narrower than the half wave above. From an inspection of the table one will recognize that up to about $t = 1$, the two amplitudes, a and b, have rather close values and they grow approximately exponentially with a period not far from the one computed from the correct hydrodynamical theory of small amplitude waves:

$$T = \sqrt{\frac{\lambda}{2\pi g}} = \frac{1}{\sqrt{\pi}} = 0.56 \text{ (in our units).} \tag{13}$$

Already, at $t = 1$, an appreciable asymmetry of the wave has developed. This becomes more and more noticeable for later times. At $t = 3$, for example, b is less than 1/10th of a.

The asymptotic behavior of a, b, and x for large values of the time is obtained from a discussion of the equations (9). One finds that a increases proportionally to the square of the time, b increases proportionally to the square root of the time, and x is inversely proportional to the 3/2 power of the time. More precisely, one finds the following limiting expressions:

$$a \to \frac{4}{7}(t - 1.04)^2 \tag{14}$$

$$b \to 0.12\,(t - 1.04)^{1/2} \tag{15}$$

$$x \to 0.21\,(t - 1.04)^{-3/2}. \tag{16}$$

In other words, the lower tip of the wave falls with uniformly accelerated motion and with acceleration equal to $8/7\,g$. The upper half wave grows much more slowly and its velocity decreases with time.

It is interesting to compare the results of this crude approximation with the experimental results obtained by D. J. Lewis,[1] as well as with the results of G. I. Taylor [2] and of Taylor and Davis.[3] The present theory seems to represent correctly one feature of experimental results, namely the fact that the half wave of the heavy liquid into the vacuum becomes rapidly narrower, whereas the half wave pushing into the heavy liquid becomes more and more blunt. On the other hand, the present theory fails to account for the experimental results according to which the front of the wave pushing into the heavy liquid moves with constant velocity. According to the present theory the displacement is expected instead to be proportional to the square root of the time.

(1) « Proc. Roy. Soc. (London) », *202 A*, 81 (1950).
(2) « Proc. Roy. Soc. (London) », *201 A*, 192 (1950).
(3) « Proc. Roy. Soc. (London) », *200 A*, 375 (1950).

N° 245.

For the introduction to this paper see paper N° 243.

245.

TAYLOR INSTABILITY AT THE BOUNDARY OF TWO INCOMPRESSIBLE LIQUIDS

E. FERMI and J. VON NEUMANN

Part 2 of Document AECU–2979 (August 19, 1953).

In a previous memorandum, *Taylor Instability of an Incompressible Liquid*, one of us has discussed the Taylor instability at the surface between an incompressible liquid and in a vacuum by using a very simplified model which consists in assuming that at all times the interface may be representedby a surface of a shape: (fig. 1).

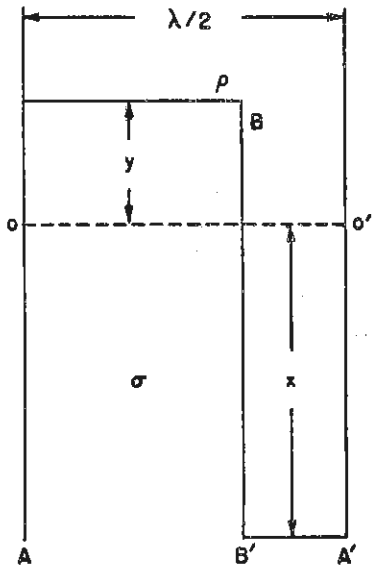

Fig. 1.

The vertical lines OA and O'A' are traces of planes of symmetry and their distance is half a wave length.

In the case previously discussed this model succeeded in representing correctly at least some features of Taylor instability. In particular, it was found that the heavy fluid penetrates into the vacuum with a spike which becomes thinner as the phenomenon progresses. Actually the front of this spike moves with uniformly accelerated motion with an acceleration that evidently should be equal to the gravitational acceleration g and which, due to the crudeness of the model, turns out to be $8g/7$. The upward motion of the vacuum bubble into the fluid is represented less correctly. According to the results of Taylor, this bubble should move upward with a constant limiting velocity. The model fails to reproduce correctly this feature and the displacement of the top of the bubble is asymptotically proportional to $\sqrt{t}$.

As a contribution to the discussion of the Taylor instability between two fluids of different densities, ρ and σ ($\rho > \sigma$), we have tried to explore a similar

model for this more complicated case. The notations are slightly different from those used in the previous memorandum and are clearly shown in fig. 1.

In order to write the Lagrangean equations for the system, it is necessary, to obtain an expression for the kinetic energy of the system as a function of the two parameters, x and y, that characterize its position and of their time derivatives, $\dot{x}$ and $\dot{y}$. This has been done using essentially the same procedure followed in the previous memorandum. In the present case we were interested particularly in a description of the late phases of the phenomenon and for this reason only one of the three terms of the kinetic energy previously used was maintained. This term represents the kinetic energy of the vertical motions in the two channels of length $x + y$ through which the heavy fluid of density ρ moves downwards and the light fluid of density σ moves upwards. The expression of this kinetic energy is given by two terms similar to expression (5) of the previous memorandum, rewritten with new notations. The expression of the kinetic energy is:

$$T = \frac{\lambda}{6}\left(\rho + \sigma\frac{y}{x}\right) y\dot{x}^2 + \frac{\lambda}{6}\left(\sigma + \rho\frac{x}{y}\right) x\dot{y}^2 + \frac{\lambda}{6}(\rho x + \sigma y)\,\dot{x}\dot{y} \tag{1}$$

The potential energy U is given by:

$$U = -\frac{\lambda(\rho - \sigma)}{2} g x y. \tag{2}$$

The Langrangean equations corresponding to (1) and (2) can be written immediately. One of them is:

$$\left(2\rho y + 2\sigma\frac{y^2}{x}\right)\ddot{x} + (\rho x + \sigma y)\,\ddot{y} - \sigma\frac{y^2}{x^2}\dot{x}^2 + \\ + \left(2\rho + 4\frac{\sigma y}{x}\right)\dot{y}\dot{x} - 2\rho\frac{x}{y}\dot{y}^2 - 3g(\rho - \sigma)\,y = 0. \tag{3}$$

The other Lagrangean equation is obtained by interchanging in (3) x and y and also ρ and σ in all terms except the last. Instead of using the two Lagrangean equations, we may, however, use equation (3) and the energy equation:

$$T + U = 0. \tag{4}$$

The total energy is taken to be zero because we assume that the system starts with zero velocity and with a flat horizontal interface. By a suitable change of the scales of x, y, and t, it is possible to write the equations (3) and (4) in a form in which ρ, σ and g do not appear. This is done by the following transformations:

$$\xi = \rho x \qquad \eta = \sigma y \qquad \tau = \sqrt{3g(\rho - \sigma)}\,t. \tag{5}$$

With these new coordinates, the equations (4) and (3) become:

$$\left(1 + \frac{\eta}{\xi}\right)\frac{\dot{\xi}^2}{\xi} + \left(1 + \frac{\xi}{\eta}\right)\frac{\dot{\eta}^2}{\eta} + \left(\frac{1}{\eta} + \frac{1}{\xi}\right)\dot{\xi}\dot{\eta} = 1 \tag{6}$$

$$\left(2 + 2\frac{\eta}{\xi}\right)\ddot{\xi} + \left(1 + \frac{\xi}{\eta}\right)\ddot{\eta} - \frac{\eta\dot{\xi}^2}{\xi^2} + \left(\frac{2}{\eta} + \frac{4}{\xi}\right)\dot{\xi}\dot{\eta} - 2\frac{\xi\dot{\eta}^2}{\eta^2} = 1. \tag{7}$$

The dots represent in these equations derivatives with respect to τ. By

making use of the similarity properties of these equations, they can be reduced to the first order. The appropriate transformations are the following:

$$(8)\qquad \begin{cases} \xi = e^{2s+2q} & \eta = e^{2s-2q} \\ 4p = \dfrac{\dot{\xi}}{\sqrt{\xi}} + \dfrac{\dot{\eta}}{\sqrt{\eta}} & r = \dfrac{dq}{ds} \end{cases}$$

By substitution one obtains the following equation of the first order:

$$(9)\qquad r\frac{dr}{dq} = (3 + r^2)\left(\operatorname{tgh} 2q - \frac{5}{3}r\right),$$

and also the additional equations:

$$(10)\qquad \begin{cases} \dot{s} = \dfrac{e^{-s}}{\sqrt{8(3+r^2)\cosh 2q}} \quad ; \quad \dfrac{\dot{\xi}}{\sqrt{\xi}} = \dfrac{e^{q}(1+r)}{\sqrt{2(3+r^2)\cosh 2q}} \\ \dfrac{\dot{\eta}}{\sqrt{\eta}} = \dfrac{e^{-q}(1-r)}{\sqrt{2(3+r^2)\cosh 2q}} \end{cases}$$

which can be used in passing from the solution of equation (9) to the solution of our physical problem.

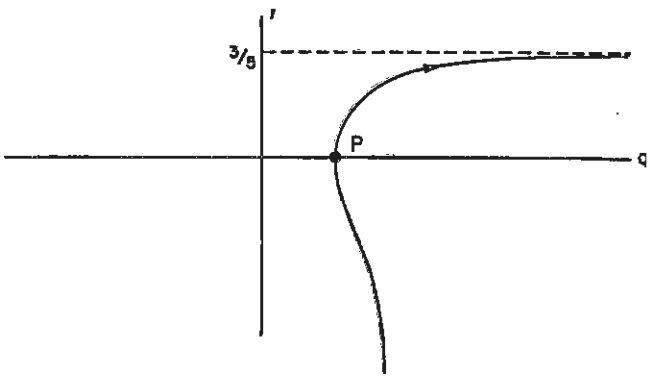

Fig. 2.

In selecting the solution of (9) corresponding to the actual case, one needs the initial values of q and r. These are obtained as follows. As long as the disturbance has very low amplitude, it is known that the wave is of sinusoidal shape and exponentially increasing amplitude. This phase of the phenomenon is not represented by our treatment which describes only the late phase of the motion. In fact, we may assume that the proper initial conditions for our problem correspond to the time when the exponential solution of the early phase breaks down. At this moment we have approximately $x = y$ and $dx/dt = dy/dt$. Making use of equation (5) and equation (8), this situation corresponds to:

$$(11)\qquad q = \frac{1}{4}\log\frac{\rho}{\sigma} \quad ; \quad r = 0.$$

In fig. 2 the shape of the solution of equation (9) corresponding to these initial conditions is outlined.

The initial point is P and the arrow indicates the direction of increasing time. As time increases q becomes positive infinite and r converges to the value $3/5$. One can now find without trouble the following asymptotic expressions

$$(12) \qquad \begin{cases} x \to \frac{1}{2}\,\frac{8}{7}\,g\,\frac{\rho-\sigma}{\rho}\,t^2 \\ y \sim t^{1/2}. \end{cases}$$

The first of these equations indicates that the heavy fluid moves into the light fluid with uniformly accelerated motion, as was found to be the case when $\sigma = 0$. The acceleration is $(8/7)\,[g\,(\rho - \sigma)]/\rho$. Presumably the factor $8/7$ in front of the expression should not be there in a more correct theory because the same factor was obtained also when $\sigma = 0$, in which case one would expect a free fall with acceleration g. We may, therefore, conclude tentatively that the heavy liquid should penetrate the light liquid with an acceleration:

$$(13) \qquad g\,\frac{\rho-\sigma}{\rho}\,.$$

Again we find that a bubble of the light liquid rises much more slowly into the heavy liquid. The fact that the height of this bubble is proportional to $\sqrt{t}$ and not to t is presumably due to the inaccuracy of the model.

Conclusions.

The present discussion makes it appear likely that the features of the Taylor instability at the interface between two liquids of different density are similar to those corresponding to the case of the boundary between a liquid and a vacuum. The main difference is that according to formula (13) the acceleration describing the fall of the heavy into the light liquid is reduced by the factor $(\rho - \sigma)/\rho$. There is, of course, another phenomenon that has been here entirely neglected and which may in some cases play a very important role. All along the line BB′ in fig. 1 one might expect Helmholtz instability to develop because the heavy liquid moves downwards on one side of the boundary and the light liquid moves upwards on the opposite side. This instability will presumably further contribute to the mixing and may, in particular, break up the spike of heavy liquid as soon as it becomes sufficiently thin.

N° 246.

In the spring of 1951 the big synchrocyclotron at Chicago started operating. It could accelerate protons to 450 MeV and a copious number of pions could be produced with these. The machine had been built with the idea that Fermi would be the principal user and when it was finally complete he spent a great deal of time familiarizing himself with its operation, laying out the pion beams and measuring their intensity and energy. He was very proud of at least one of his contributions to the construction. This was his trolley car, his device on wheels which carried the cyclotron target. It could be moved at will around the periphery of the magnet pole, controlled from outside by the action of the magnetic field on the currents which could be sent through the coils to which wheels were connected. He had constructed this himself in his own little shop and it worked well for years.

The new cyclotron was the occasion for calling an " International Conference on Nuclear Physics and the Fundamental Particles. " It was held from the 17th to the 22nd of September 1951, at the Institute for Nuclear Studies, as part of the joint program on nuclear physics of the Office of Naval Research and the Atomic Energy Commission. The proceedings of the conference were prepared by graduate students in physics at the University of Chicago.

Approximately 200 scientists attended the conference and forty of them came from foreign countries. The first experiments with the cyclotron on the scattering of pions through liquid hydrogen had been carried out during the summer, and it was possible to report some new and quite important results. Both theoretical and experimental questions were discussed, and the topics ranged from accelerator design to nuclear abundances in the cosmos and to photonuclear reactions.

Fermi took a lively interest in the conference, delivered the first paper, on fundamental particles (Paper N° 246), and participated in the discussions. The conference almost coincided with his fiftieth birthday, on September 29, and gave some of his old friends a chance to celebrate it informally, around the breakfast table.

H. L. ANDERSON.

246.

FUNDAMENTAL PARTICLES

Proceedings of the International Conference on Nuclear Physics and the Physics of Fundamental Particles. The University of Chicago (September 17 to 22, 1951). (Lecture)

E. Fermi presented the following list of 21 elementary particles.

e	electron	μ^+	positive muon
e^+	positron	G	graviton
P	proton	V^+	positive V–particle
$\bar{P}$	antiproton	V^-	negative V–particle
N	neutron	V°	neutral V–particle
$\bar{N}$	antineutron	τ^+	positive τ–meson
γ	photon	τ^-	negative τ–meson
π^+	positive pion	k^+	positive k–meson
π^-	negative pion	k^-	negative k–meson
π°	neutral pion	ν	neutrino
μ^-	negative muon		

Fermi expressed a belief in the existence of antinucleons. He defined the V, k, and τ particles during the discussion period.

Philosophically, at least some of these 21 particles must be far from elementary. The requirement for a particle to be elementary is that it be structureless. Probably some of these 21 particles are not structureless objects. They may even have some geometrical structure, if geometry has any meaning in such a small domain.

Fundamental particles are distinguished most easily by charge, mass, and spin. The spin of the positive pion has recently been determined by cyclotron results. This utilizes the principle of detailed balancing. Thus the result does not depend on any knowledge of the types of interactions involved. The reaction utilized is:

$$\pi^+ + D \rightleftarrows P + P \tag{1.1}$$

$$(2\,I_\pi + 1)(2\,I_P + 1)\,p_1^2\,\underset{\rightarrow}{\sigma} = (2\,I_P + 1)(2\,I_P + 1)\,p_2^2\,\underset{\leftarrow}{\sigma} \times \frac{1}{2} \tag{1.2}$$

$$3\,(2\,I_\pi + 1)\,p_1^2\,\underset{\rightarrow}{\sigma} = 2\,p_2^2\,\underset{\leftarrow}{\sigma}\,.$$

The factor 1/2 on the right hand side of eq. (1.2) is because the protons are identical particles (an interchange of the two protons does not give a new state). The experimental values give $2I + 1 \approx 1$ so $I = 0$. Since the π^+ and π^- are considered similar, both should have spin zero.

Recent results have shown that the pion is pseudoscalar. The parity of a particle is one of the most fundamental distinctions. Once we have decided the parity, we limit roughly by 1/2 the number of possible interactions. It should be noted that whether th pion is a true scalar or a pseudoscalar has no meaning for the pion by itself. It has meaning only in relation to interactions with other particles; for example, in $P \rightleftarrows N + \pi^+$. Once the parity of the nucleon is chosen, then experiments determine the pion parity. An analogous situation is the distinction of right and left. There is in natural laws no means of distinction between right and left. Thus if you were on a different planet and had forgotton which was your right hand, there would be no experiment which could tell you. Parity is really relative parity.

There is a recent paper of Yang and Tiomno, [1] « Phys. Rev. », *79*, 495 (1950), which puts spin 1/2 particles into four classes. Two of these classes can be illustrated by the following model in which the spin 1/2 particle is considered a two-particle system, composed of two sub-particles, one with intrinsic spin $I = 1/2$, one with $I = 0$, and a central force between them. Then states of the system can be described by S 1/2, P 1/2, P 3/2, D 3/2, D 5/2, etc. Notice that the first two states both have spin 1/2, but with different parities. In our present ignorance, we would call these two different elementary particles of spin 1/2. It would be a great help to have a simple model like this to explain more classes of "particles."

(1) This subject was discussed in a special session.

These 21 " fundamental particles " can change from one to another in various ways. A few of them are

$$e \rightleftarrows e + \gamma$$

$$P \rightleftarrows N + \pi^+$$

$$N \rightleftarrows P + e + \nu$$

$$N \rightleftarrows P + \mu + \nu$$

$$\mu \rightleftarrows e + 2\nu$$

$$\pi^0 \rightleftarrows 2\gamma$$

and so on.

Of course, the first two reactions happen only in the presence of other particles because of momentum and energy conservation. A free electron, photon, or nucleon can be in a well-defined specific state. This is not strictly true for a pion because it decays spontaneously by $\pi \to \mu + \nu$. Thus a pion state is not as well-defined as for an electron in the same situation.

Theoretical research may proceed on two tracks: 1. Collect experimental data, study it, hypothesize, make predictions, and then check. 2. Guess; if nature is kind and the guesser clever he may have success. The program I recommend lies nearer to the first track. It is desirable to arrange experimental data so as to exhibit most clearly the features which come from fundamental particle interactions taking place at " contact, " namely within about 10^{-13} cm. This may be done by assuming quantum mechanics holds in regions outside " contact " (there is little doubt in my mind that it does), and using it to remove from consideration phenomena which do not depend on what happens in the " contact " volume. The result is a compressed expression of experimental results, in which the nature of fundamental interactions between particles may be more easily discernible. This program won't work with the reaction $P \rightleftarrows N + \pi^+$, because there are too many other nucleons in contact. But nucleon-nucleon and pion-nucleon reactions can be treated. (In the session on Meson Theory, Fermi commented that reactions in which elementary particles are created were not the best subject for the program outlined above because particles with short wavelength must necessarily enter. He cited scattering of fairly low energy pions by nucleons as a good reaction for the purpose. He said, " Within a volume corresponding to 10^{-13} cm there are lions which will eat us if we get within. In a reaction like meson production we have at least one particle with wavelength shorter than 10^{-13}, so we cannot avoid the lions.")

Many of the reactions possible are not independent. One has a choice in deciding which of the reactions are primary. For example $\pi^+ \to \mu^+ + \nu$ may be considered primary, or it may be considered a second order consequence of the " primary " reactions

$$\pi^- \to N + \overline{P}$$

$$N' + \overline{P} \to \mu + \nu \qquad (\text{from } N \to P + \mu + \nu).$$

In fact with a little swindling on the infinities, the calculation based on these two independent interactions

$$\pi^- \to N + \bar{P} \to \mu + \nu$$

gives the correct answer. These types of arguments seem to work about 80 percent of the time. So there must be some element of truth in this approach. The above example isn't as good as it looks, since the path $\pi^- \to N + \bar{P} \to e + \nu$ predicts about the same decay constant for electron decay. But this has never been observed.

In meson production the number of basic linkages might be three. One of the possible paths for $P_1 + P_2 \to P_3 + N + \pi^+$ is

$$P_1 + P_2 \to P_1 + P_3 + \pi^0 \to P_4 + P_3 \to P_3 + N + \pi^+.$$

One hopes that the number of basic linkages is few, with most reactions coming as higher order.

The question of whether the proton is simple or complex can be raised because of the strong interaction $P \rightleftarrows N + \pi^+$. The physical proton should be in the $N + \pi^+$ state an appreciable part of the time. This is not the case for

$$P \to N + e + \nu$$

and

$$P \to N + \mu + \nu$$

because of the weak interactions in these cases. The proton would be in these states just 10^{-15} of the time.

N° 247.

The following article is based on the first of six invited papers presented during the symposium on contemporary physics which keynoted the Twentieth Anniversary Meeting of the Institute of Physics in Chicago last October. (*) An audience of three thousand assembled in the Chicago Civic Opera House to hear the addresses, four of which have appeared in recent issues of this journal.

From « Physics Today ».

247.

THE NUCLEUS

« Physics Today », 5, 6–9 (March 1952).

1.—In the twenty-year period since the founding of the American Institute of Physics, nuclear physics has been advancing perhaps as rapidly as any other branch of our science. Twenty years ago the neutron had not yet been discovered, and a favored hypothesis as to the structure of the atomic nucleus was that it consisted of protons and electrons. This very fact may give some idea of the exponential rate of our progress.

Perhaps, to think of another reference mark, consider that it was just about forty years ago when the discovery of the nucleus was announced by Rutherford.

In nuclear physics, as in many other branches of physics, the past four decades have seen advances in very many directions. These advances have occurred both in techniques and in fundamental knowledge. During the period with which we are concerned, voltages achieved in accelerating machines have been going up in steps roughly of 10—10^6, 10^7, 10^8, and very soon, we hope, 10^9 electron volts. The Cosmos is of course still far ahead, and provides a formidable challenge to the constructors of high energy accelerating machines.

Neutron sources have gone up in steps which are more nearly (in round numbers) of the order of one million each—from the small radium or radium-beryllium sources, to cyclotrons, to atomic reactors.

Of course quite sizeable steps have been taken in the amount of money used for research. Large steps have also been taken in the population growth of physicists, and in the audiences that come to listen to a symposium in physics—if I should judge from this audience.

Technical advances that have been less spectacular than those mentioned previously, but I believe no less significant, have taken place in the develop-

(*) October 1951 (Editors' note).

ment of detecting devices. Counters, ionization chambers, and the more recent and very important discovery of the scintillation counter should be mentioned. The latter does automatically what Rutherford and his pupils did so laboriusly in watching the minute scintillations that result when an alpha particle hits a crystal. The refined electronic techniques used in the scintillation counter have shortened the time of counting to the range of 10^{-9} seconds and less. One can thus measure directly the time taken by particles traveling close to the velocity of light to cross a distance of a few feet, and consequently obtain the velocity of the particle.

The Wilson cloud chamber has led to the development of the diffusion chamber, which promises to be one of the fundamental tools in investigating elementary particle reactions. Photographic plates have been developed to a very high degree of perfection as recorders of tracks of particles.

Now these technical developments have resulted in part in, and in good part have promoted, a very considerable advance in the knowledge of the nucleus and of its constituents. We have by now what seems to be the final understanding at least of the generalities of the nuclear structure—the nucleus built of neutrons and protons. We have some understanding of the features of the beta spectrum. We have discovered hundreds of nuclear reactions and hundreds of new radioactive isotopes, with the result that a new branch of the art of nuclear science has emerged which includes radiochemistry and all of the complex techniques in chemistry and biology for the use of tracers.

The discovery of fission has led to the realization of the possibility of chain reactions, soon followed by the actual construction of nuclear reactors. This has provided the starting point for the new science of nuclear engineering. The spectroscopy of the nucleus is approaching in complexity, although by no means in understanding, that of the atom. Charts of nuclear energy levels with corresponding gamma-ray and other transitions between them are beginning to acquire a complexity that may remind one of the early atlases of atomic levels that were in use in the early Twenties. Measurement of nuclear masses and moments, primarily with the technique of mass spectroscopy and radiofrequency resonances, has become an extremely precise art. We have learned a great deal about elementary particles and, with the help of the cosmic radiation, have discovered many new ones. Great progress has been made in the determination of beta spectra and recently even the beta disintegration of the neutron has been investigated quite thoroughly.

The mass of data resulting from these many discoveries presents a challenge for the understanding, and unfortunately the business of understanding is not as well in hand as one might wish. The present state might be illustrated by choosing, for purposes of discussion, two of the many topics in nuclear physics that are of current interest.

2.—In disentangling the problems of the atom, one of the major steps has been the recognition that it is useful to speak of individual orbits of the electrons in the atom. This, to be sure, is only an approximation, in fact a

crude approximation, but still it provides a quite invaluable starting point for the study of complex atoms containing large numbers of electrons.

When physicists became reasonably certain that the nucleus was constructed of protons and neutrons, questions were raised concerning the orbital behavior of these particles. Could nuclear structure be interpreted on the general pattern of atomic structure by attributing to the various neutrons and to the various protons within the nucleus something like individual orbits and individual states? If so, an understanding of the nuclear levels and the nuclear structure could possibly emerge from the much simpler pattern of the individual states.

No definite answer has ever been given to this question, although nuclear science has for a long time "officially" frowned on such attempts. Strong arguments were quoted for saying that the constituents of the nucleus are mixed so thoroughly and interact so rapidly that there is little basis for hoping that individual orbit considerations can lead to an understanding of nuclear structure.

Consider one nucleon in the nucleus travelling along its orbit among the other nucleons. If the collision mean free path is λ this nucleon would collide with the other neutrons and protons in the nucleus and its orbit would be lost after it had gone the distance of its free path. A criterion that one might adopt in deciding whether or not it is a sensible approach to talk of individual orbits is to compare the mean free path with the size of the expected orbit. If the mean free path is long, then we may take the orbital behavior seriously. But if the mean free path is much less than the size of the orbit, one expects the idea of orbit to become rather unusable. Now it is a very difficult problem to decide the length of the mean free path, but if one takes somewhat literally the strength of the interactions between the neutron and other components of the nucleus, one is led to a value that seems discouragingly short.

In spite of this argument, evidence has been accumulating for the last few years, both in this country and in Germany, to the effect that orbits do exist. The best-known feature of this evidence has been the discovery of the so-called "magic numbers." They are the numbers 2, 8, 20, 50, 82, 126. When a nucleus contains a number of either neutrons or protons equal to one of the magic numbers, it is particularly stable, as if a shell of either neutrons or protons had been closed.

This and other evidence to be discussed later indicate that the orbit approximation is much better than the discussion above may have suggested. It would appear that for some reason the mean free path must be longer than is given by a somewhat crude estimate of its length. One possible reason for this may be the Pauli principle, according to which collisions between two particles may be forbidden when, after the collision, one of the two particles would go to an occupied state.

Another possible explanation of the long mean free path may have to do with the saturation property of the nuclear forces. It has been suggested, for example, that the meson field responsible for these forces may have a non-linear character and reach a saturation level in nuclear matter due to

the high density of the nucleons present. In spite of the fact that neither of the two above possibilities has been worked out to the point that it can be considered a satisfactory theory, it is now rather generally believed that many features of the single particle model will ultimately prove correct.

Strong additional evidence for this model is the detailed explanation of the magic numbers in terms of the assumption of a very strong spin orbit coupling. Maria Mayer here in Chicago, and the investigators in Germany who developed independently similar ideas, have been able to point out very many features of the isomeric nuclear levels which lend strong support to these views.

There is at present no undestanding of the origin of the strong spin orbit coupling that is suggested by the empirical evidence. Such understanding perhaps will come only when a satisfactory theory of the nuclear forces will have been developed. At present we must take the existence of this coupling as an empirical fact.

In spite of our only partial understanding of the situation, the orbit theory of nuclear structure offers a hopeful model for at least a qualitative understanding of nuclear structure, and already it has been possible to fit into this picture a very great number of details.

3.—It is of course impossible to hope for any deep understanding of the structure of the nucleus without knowing a lot about the forces acting between the elementary constituents of the nucleus—between neutron and proton and between proton and proton and between neutron and neutron.

The classical experimental approach to investigations of nuclear forces has been the study of scattering. One hurls a neutron at a proton and sees how they are deflected. From the features of the deflection, the angular distribution, the energy dependence, and so on, one hopes to deduce the force responsible for the deflection. Early experiments by Tuve, Herb, and others, interpreted by Breit, gave the first knowledge of a short range interaction between nuclear nucleons that is responsible for the fact that particles stay together. Then came the Yukawa theory to give a great help to our understanding of the problem by offering for the first time a model for us to consider. The model is quite similar in many ways to that of the electromagnetic forces: one particle produces a field and the field acts on another particle. In this case, however, Yukawa was faced with the additional problem of designing a theory that would automatically account for the short-range character of the nuclear forces. Yukawa recognized that a field whose quanta have zero mass (like the photons) would have a long range, while a field whose quanta have a finite and relatively large mass would have a short range.

According to the Yukawa theory, a neutron will occasionally convert into a proton plus a pi-meson, which will then be reabsorbed and thrown out again and reabsorbed and so on. The nuclear field involved in this oscillation will extend as far from the original neutron as the continually emitted pimesons can reach. And how far can they reach? The argument runs as follows:

A meson has considerable mass, and to fabricate a meson with which to play this odd ball game requires an amount of energy equal to the mass of

the meson, μ, multiplied by the square of the velocity of light, c. Who pays for this amount of energy? Well, nobody; so if nobody pays one has to borrow. Now in the bank of energy there is a very special rule that should perhaps occasionally be adopted by commercial banks—namely, the larger the loan, the shorter the term. Quantitatively, this banking practice is represented by one of the forms of the Heisenberg uncertainty relation. One can borrow an amount of energy W for a time of the order of Planck's constant h divided by W; therefore the time t of the loan shall be $h/\mu c^2$. The meson will be capable of moving away from its source a distance equal at most to the time t multiplied by the velocity of light c; therefore the range of the nuclear forces according to this mechanism is essentially $h/\mu c$ and is inversely proportional to the mass. For short-range action, the quanta of the field that transmits the nuclear forces must be very massive; in fact, the early estimates of Yukawa indicated that the mass would have to be comparable to 300 times the electron mass.

Almost on the heels of the announcement of the Yukawa theory came the discovery of the meson in cosmic radiation, thus giving the theory a tremendous boost. The particle first found in the cosmic radiation, as is well known now but was not known at the time, is not the Yukawa meson, but is a son of the Yukawa meson. This was discovered recently when Powell found tracks in photographic plates that had been exposed at high altitudes, showing the existence of two different mesons. One of these, the so-called pi-meson, is the one responsible for nuclear forces; the other, the mu-meson, is a rather uninteresting offspring of the first—at least it seems uninteresting at present.

Then, of course, came another fundamental experimental result that was determined at least in part by the Yukawa theory: if two nucleons, each of which is surrounded by a meson field, collide with sufficient energy, some mesons are likely to be shaken loose. There was evidence from cosmic-ray studies of the actual existence of this process, but the most spectacular experimental result in this direction was obtained at Berkeley where Lattes and Gardner discovered that these mesons are actually produced in the high energy collisions in the synchrocyclotron. The discovery of an artificial means for the production of pi-mesons has put at the disposal of the physicists a source of this particle that is easily controllable and extremely more intensive than any cosmic-ray source. This is an ideal situation for investigating the properties of these new particles and research is going on actively in this direction in many laboratories. But again, what about the understanding?

4.—Perhaps, in outlining the Yukawa theory (which in my opinion certainly has a considerable amount of qualitative correctness), I should have included the warning that there is not just one theory, but that there are several theories, and that none of them seems to be really the correct one. It is sometimes difficult to say what is wrong with any particular theory because the mathematics involved is almost prohibitively complicated. But one can seldom manage to make a calculation that is really right because the theory is so complicated, and if one tries, more as a rule than as an exception,

one encounters divergent infinite terms which one usually attempts to eliminate by not perfectly orthodox procedures. Perhaps at the root of the trouble is the fact that the theory attempts to oversimplify a situation which may in fact be quite complicated. When the Yukawa theory first was proposed there was a legitimate hope that the particles involved, protons, neutrons and pi-mesons, could be legitimately considered as elementary particles. This hope loses more and more its foundation as new elementary particles are rapidly being discovered.

Perhaps the situation might be compared (although comparisons are always dangerous) to that of the early quantum theory, which provided a large amount of qualitative insight in the atomic structure, but nevertheless failed from the quantitative point of view. Perhaps the situation is similar; perhaps brilliant solutions of the same type will be forthcoming.

It is difficult to say what will be the future path. One can go back to the books on method (I doubt whether many physicists actually do this) where it will be learned that one must take experimental data, collect experimental data, organize experimental data, begin to make working hypotheses, try to correlate, and so on, until eventually a pattern springs to life and one has only to pick out the results. Perhaps the traditional scientific method of the textbooks may be the best guide, in the lack of anything better.

At present, rapid progress is being made in collecting data on nuclear forces, both by direct observation from scattering experiments and by indirect study of the mesons. Results are accumulating quite rapidly, and while they have not yet fallen into a satisfying pattern, perhaps they will before too long.

Some of the many Yukawa theories seem to be excluded by these experiments, and the favored one at present is the "pseudoscalar theory with pseudovector coupling," which in slightly plainer words means that the meson has spin zero and behaves like a pseudoscalar, a symmetry property that is certainly familiar to most physicists.

Of course, it may be that someone will come up soon with a solution to the problem of the meson, and that experimental results will confirm so many detailed features of the theory that it will be clear to everybody that it is the correct one. Such things have happened in the past. They may happen again. However, I do not believe that we can count on it, and I believe that we must be prepared for a long hard pull if we want to make sure that at the next anniversary celebration of the American Institute of Physics we shall have the solution to this problem.

N° 248, 249, and 250.

The principal work with the cyclotron was the study of the interaction of the pions with protons. The first experiments maesured the transmission of first negative and then positive pions through liquid hydrogen targets. Later the angular distribution of the pions scattered from hydrogen was studied in detail. It was a time consuming task and took a large part of Fermi's time for several years, although he was helped by a team whose steady members were D. E. Nagle and myself, and occasional members were E. A. Long, G. B. Yodh, and two younger students, R. Martin and M. Glicksman.

The difficulty was that the demands for the use of the cyclotron were so great that it was necessary to set up each experiment anew, rnn with it continnously for several days and nights, and then take away all the equipment again. For each experiment it was necessary to repeat the whole process of checking out the electronic equipment, lining up and calibrating the pion beams. The results were very rewarding.

The first paper on this work (N° 248) reported the measurements of the total cross sections for the negative pions in hydrogen and showed that this rose rapidly from the low value found at 85 Mev by Chedester, Isaacs, Sachs, and Steinberger, (« Phys. Rev. », *82*, 958 (1951)) until it reached the geometric value $(\hbar/\mu c)^2$ at 180 Mev. Since $\hbar/\mu c$ was just the range of interaction of a meson field, these results were indicative of the great strength of the pion-nucleon interaction. The rapid rise of the cross section with energy was characteristic of an interaction in which the orbital angular momentum is one unit. Many possible meson theories could be ruled out at once in the face of these simple characteristics.

With negative pions, there is the possibility, besides the ordinary elastic scattering, of scattering with exchange of charge. In this the negative pion is converted to the neutral, the proton to the neutron. Paper N° 249 reported the surprising results that this later process was about twice as frequent as the first.

Paper N° 250 reported on transmission measurements made with positive pions and held an even greater surprise. The cross section for positive pions mounted far above the maximum found for the negatives. This seemed particularly strange at first since with the positive pions only the elastic scattering is possible. An explanation by Brueckner anticipated this result by several days. In fact, Fermi could (and did) read the preprint of Brueckner's paper (F. A. Brneckner, « Phys. Rev. », *86*, 106 (1952)) the very day he found the high cross section. Brueckner had seized on the idea of the isotopic spin as being an essential element in the pion nucleon interaction. Arguing that the dominant state was one with total angular momentum 3/2 and isotopic spin 3/2 all the features of the experiments could be understood at once. It took hardly more than a glance at Brueckner's paper for Fermi to grasp the idea. Twenty minutes after he left the experimental room to work through the idea by himself in his office, he emerged with this happy conclusion. " The cross sections will be in the ratio 9 : 2 : 1 ", he announced. He was referring to the pi-plus elastic, the pi-minns charge exchange, and the pi-minus elastic processes in that order.

A few months later when he addressed the American Physical Society at it's New York meeting, he had a message to give. He had studied these pi-mesons and he could tell how they interacted with the nucleons. He had the facts about this, and also some explanation, and underlying, an important principle. In the strong interaction between the pion and the nucleon, the isotopic spin was conserved. Thus, an old idea, hitherto rather neglected, assumed a new importance.

H. L. ANDERSON.

248.

TOTAL CROSS SECTION OF NEGATIVE PIONS IN HYDROGEN (*)

H. L. ANDERSON, E. FERMI, E. A. LONG, (**) R. MARTIN, (***) and D. E. NAGLE
Institute for Nuclear Studies University of Chicag, Chicago, Illinois
(Received January 21, 1952)
« Phys. Rev. », *85*, 5, 934 (1952) (Letter).

The interaction of negative pions and protons has been investigated by Steinberger and co-workers (1) for pions of 85 Mev energy by transmission measurements and by Shutt and co-workers (2) for pions of 55 Mev by direct observation of pion tracks in a Wilson chamber. Both measurements indicate a surprisingly low value for the cross section in this range of energies. We have undertaken to extend the total cross section measurements to higher energies.

The negative pions are produced in the large Chicago cyclotron by protons of 450 Mev striking a target which in some of the experiments was copper and in others beryllium. The negative pions are bent in the fringing field of the cyclotron and enter channels in a 6–foot steel shield which separates the cyclotron from the experimental room where the measurements are taken. Further monochromatization and purification of the pion beams are carried out by a deflecting magnet located in the experimental room. In this manner one obtains a sharply collimated beam containing pions with energy defined within $\pm$ 3 percent. In addition to the pions this beam contains some muons and electrons of the same momentum. Their number has been determined from a range curve. The muons amount to between 5 percent and 10 percent. The electrons are present in negligible numbers for beams above 100 Mev. Below this energy the electron contamination increases rapidly. For this reason low energy measurements have been taken by reducing with a beryllium absorber the energy of the 122–Mev beam.

By using various channels we have taken measurements over the energy range from about 80 to 230 Mev.

The pion beam is monitored by two scintillation crystals of 1-inch-square cross section separated by a distance of about one meter. The coincidences of these two counters indicate the number of particles entering the equipment. Beyond the second crystal the pions enter the scattering chamber, which is a glass cylinder 3 inches in diameter and 7 1/2 inches long, closed by 0.005–inch copper windows. This chamber can be alternately filled with

(*) Research sponsored by the ONR and AEC.
(**) Institute for the Study of Metals, University of Chicago.
(***) AEC Predoctoral Fellow.
(1) CHEDESTER, ISAACS, SACHS, and STEINBERGER, « Phys. Rev. », *82*, 958 (1951).
(2) SHUTT, FOWLER, MILLER, THORNDIKE, and FOWLER, « Phys. Rev. », *84*, 1247 (1951).

and emptied of liquid hydrogen. The particles which are not scattered out of the beam are recorded by the coincidences which they give in a pair of liquid scintillation counters, of which one has a 3 inch diameter and the other a 4-inch diameter. The double coincidence rate of the first two scintillators is recorded and at the same time the quadruple coincidence rate of all four scintillators. The attenuation of the beam is obtained from a comparison of the ratio of the quadruple to double coincidence counts with and without the hydrogen and is computed as a cross section.

A number of corrections have been applied to the results on account of the following effects:

(1) Background due to accidentals (usually 1 percent or less).

(2) Angular spread of the beam due to geometry, diffraction scattering, and pi-mu decay. In some experiments the multiple scattering was compensated by means of an equivalent aluminum foil; in others it was computed. This correction is important only at low energies.

(3) Muon and electron component in the original beam. It is assumed that muons and electrons suffer only Coulomb scattering and have no specific nuclear interaction.

(4) Correction for scattered particles recorded by the end counters. This corrections was computed on the assumption of isotropic scattering in the center-of-mass system. It amounted to between 4 percent and 2 percent depending on whether the recoil protons are or are not recorded. The correction would be larger if the scattering were predominately forward but smaller if charge exchange scattering were important.[3] The results of the measurement are presented in Table I.

TABLE I.

Total cross sections negative pions on hydrogen.

Energy band Mev	Cross section 10^{-27} cm^2
89 ± 8	21 ± 8
112 ± 6	31 ± 9
135 ± 6	52 ± 6
176 ± 6	66 ± 6
217 ± 6	60 ± 6

The data show that the cross section rises rather rapidly above 80 Mev until it reaches the "geometrical" value $\pi(\hbar/\mu c)^2$ at 150 Mev, where the cross section seems to level off, or perhaps to go through a maximum, although our measurements do not permit a decision between these two possibilities.

(3) In view of the importance of the charge exchange process reported in the following Letter, it seems likely that the cross sections have been overcorrected by about 2 percent to 3 percent.

N° 249.

For the introduction to this paper see paper N° 248.

249.

ORDINARY AND EXCHANGE SCATTERING OF NEGATIVE PIONS BY HYDROGEN (*)

E. FERMI, H. L. ANDERSON, A. LUNDBY, D. E. NAGLE, and G. B. YODH
Institute for Nuclear Studies, University of Chicago, Chicago, Illinois
(Received January 21, 1952)
« Phys. Rev. », *85*, 935 (1952) (Letter).

In an accompanying letter some experiments on the total cross section of negative pions of various energies in liquid hydrogen have been described. Measurements of total cross sections, of course, do not give any indication as to the actual mechanism of the process. In particular, in the interaction of negative pions in hydrogen the following three processes are considered possible:

(1) $$p + \pi^- \to p + \pi^-$$

(2) $$p + \pi^- \to n + \pi^0 \to n + 2\gamma$$

(3) $$p + \pi^- \to n + \gamma.$$

The first two are scattering without or with exchange of charge. The last is the inverse process of the photoproduction of pions by the action of gamma-rays on neutrons. Estimates of the cross section of this last process, based on the principle of detailed balancing, indicate that its cross section must be of the order of magnitude of a few millibarns and is therefore rather small compared to the total cross section, which is of the order of 40 millibarns for pions of 120 Mev.

We have started a series of scattering experiments in order to distinguish between the process (1) and (2), as well as to give information as to the angular distribution of the scattered particles. We felt that the first results were of sufficient interest to be reported at this time.

(*) Research sponsored by the ONR and AEC.

The geometry used in this experiment is similar to the one adopted in the study of the total cross sections. The beam of pions enters the experimental space and is deflected by an analyzing magnet. After this, it is recorded by the coincidences of two 1–inch-square crystals and falls on the liquid hydrogen scattering chamber. The scattered products are observed by quadruple coincidences of these two counters with another pair of scintillators located directly under the scattering chamber in a direction at 90° to that of the incident pions. The latter two scintillators had diameters 4 inches and 3 inches and were placed, respectively, 8 inches and 11 inches below the center of the scattering chamber. The 118–Mev beam was chosen because of its high intensity. With 1–inch-square collimating crystals 10 inches apart, the coincidence counting rate was a about 150,000 per minute. The count of the scattered particles was instead, of the order of only a few per minute. In order to increase the sensitivity of the scattering detectors to gamma-rays, a lead radiator 1/4 inch thick was interposed in front of the third counter.

TABLE I.

Scattering of negative pions at 90°.

Liquid hydrogen	1/4–in. Pb radiator	Ratio quadruple to double coincidence
No	No	$(0.81 \pm 0.05) \times 10^{-4}$
Yes	No	$(1.21 \pm 0.08) \times 10^{-4}$
No	Yes	$(0.71 \pm 0.06) \times 10^{-4}$
Yes	Yes	$(1.73 \pm 0.09) \times 10^{-4}$

A standard measurement involved the observation of the ratio between scattered and incident particles with and without hydrogen in the scattering chamber, and with and without the lead converter of the gamma-radiation. Typical results are given in Table I. The difference with and without liquid hydrogen is due to the scattered particles. With no radiator this difference is $(0.4 \pm 0.15) \times 10^{-4}$; with the radiator it is $(1.02 \pm 0.11) \times 10^{-4}$. The sensitivity of the detector to gamma-rays without lead radiator is small but not negligible, because the radiation goes through the walls of the chamber and part of the third scintillator where it may produce pairs and be recorded. An attempt has been made to separate the number of scattering events recorded due to scattered π^- from those due to gamma-rays. We find the following:

Scattered π^- in the accepted solid angle: $(0.34 \pm 0.12) \times 10^{-4}$.

Photons in the accepted solid angle: $(1.41 \pm 0.32) \times 10^{-4}$.

The conversion of these numbers to a scattering cross section depends on the assumptions made as to the angular distribution. It also depends on the assumption that we have made in this paper that all neutral pions decay immediately into two photons. For example, if we assume that the angular distribution is fairly isotropic in the center-of-mass system and that the gamma-rays are produced in pairs by the decay of the neutral pions, the cross sections for the process (1) and (2) would be $(10 \pm 4) \times 10^{-27}$ and $(20 \pm 5) \times 10^{-27}$ cm^2. The cross section obtained for the charge exchange process is not very sensitive to the angular distribution adopted. It would be $(29 \pm 7) \times 10^{-27}$ cm^2 for a $\cos^2\theta$–distribution and $(18 \pm 4) \times 10^{-27}$ cm^2 for a $\sin^2\theta$–distribution.

N° 250.

For the introduction to paper see paper N° 248.

250.

TOTAL CROSS SECTIONS OF POSITIVE PIONS IN HYDROGEN (*)

H. L. ANDERSON, E. FERMI, E. A. LONG, (**) and D. E. NAGLE
Institute for Nuclear Studies, University of Chicago, Chicago, Illinois
(Received January 21, 1952)
« Phys. Rev. », *85*, 936 (1952) (Letter).

In a previous letter,(1) measurements of the total cross sections of negative pions in hydrogen were reported. In the present letter, we report on similar experiments with positive pions.

The experimental method and the equipment used in this measurement was essentially the same as that used in the case of negative pions. The main difference was in the intensity, which for the positives was much less than for the negatives, the more so the higher the energy. This is due to the fact that the positive pions which escape out of the fringing field of the cyclotron magnet are those which are emitted in the backward direction with respect to the proton beam, whereas the negative pions are those emitted in the forward direction. The difficulty of the low intensity was in part compensated by the fact that the cross section for positive pions turned out to be appreciably larger than for negative pions. The results obtained thus far are summarized in Table I.

TABLE I.

Total cross sections of positive pions in hydrogen.

Energy (Mev)	Cross section (10^{-27} cm^2)
56 ± 8	10 ± 10
82 ± 7	50 ± 13
118 ± 6	91 ± 6
136 ± 6	152 ± 14

(*) Research sponsored by the ONR and AEC.

(**) Institute for the Study of Metals, University of Chicago.

(1) ANDERSON, FERMI, LONG, MARTIN, and NAGLE, « Phys. Rev. », this issue. [See paper N° 248 (Editors' note)].

In fig. 1 the total cross sections of positive and negative pions are collected. It is quite apparent that the cross section of the positive particles is much larger than that of the negative particles, at least in the energy range from 80 to 150 Mev.

In this letter and in the two preceding ones,[1,2] the three processes: (1) scattering of positive pions, (2) scattering of negative pions with exchange of charge, and (3) scattering of negative pions without exchange of charge have been investigated. It appears that over a rather wide range of energies, from about 80 to 150 Mev, the cross section for process (1) is the largest, for process (2) is intermediate, and for process (3) is the smallest. Furthermore, the cross sections of both positive and negative pions increase rather rapidly with the energy. Whether the cross sections level off at a high value or go through a maximum, as might be expected if there should be a resonance, is impossible to determine from our present experimental evidence.

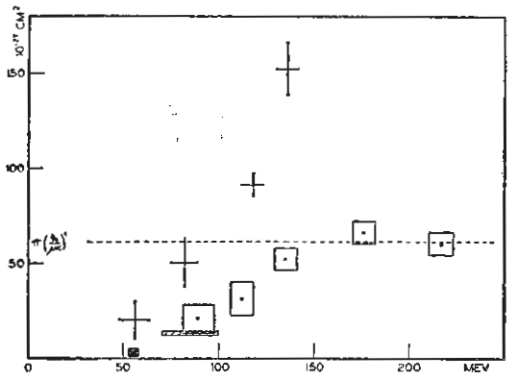

Fig. 1. – Total cross sections of negative pions in hydrogen (sides of the rectangle represent the error) and positive pions in hydrogen (arms of the cross represent the error). The cross-hatched rectangle is the Columbia result. The black square is the Brookhaven result and does not include the charge exchange contribution.

Brueckner [3] has recently pointed out that the existence of a broad resonance level with spin 3/2 and isotopic spin 3/2 would give an approximate understanding of the ratios of the cross sections for the three processes (1), (2), and (3). We might point out in this connection that the experimental results obtained to date are also compatible with the more general assumption that in the energy interval in question the dominant interaction responsible for the scattering is through one or more intermediate states of isotopic spin 3/2, regardless of the spin. On this assumption, one finds that the ratio of the cross sections for the three processes should be (9 : 2 : 1), a set of values which is compatible with the experimental observations. It is more dif-

(2) FERMI, ANDERSON, LUNDBY, NAGLE, and YODH, preceding Letter, this issue, « Phys. Rev. ». [See paper N° 249 (Editors' note)].

(3) K. A. BRUECKNER (private commmunication).

ficult, at present, to say anything specific as to the nature of the intermediate state or states. If there were one state of spin 3/2, the angular distribution for all three processes should be of the type $1 + 3\cos^2\theta$. If the dominant effect were due to a state of spin 1/2, the angular distribution should be isotropic. If states of higher spin or a mixture of several states were involved, more complicated angular distributions would be expected. We intend to explore further the angular distribution in an attempt to decide among the various possibilities.

Besides the angular distribution, another important factor is the energy dependence. Here the theoretical expectation is that, if there is only one dominant intermediate state of spin 3/2 and isotopic spin 3/2, the total cross section of negative pions should at all points be less than $(8/3)\pi\lambda^2$. Apparently, the experimental cross section above 150 Mev is larger than this limit, which indicates that other states contribute appreciably at these energies. Naturally, if a single state were dominant, one could expect that the cross sections would go through a maximum at an energy not far from the energy of the state involved. Unfortunately, we have not been able to push our measurements to sufficiently high energies to check on this point.

Also very interesting is the behavior of the cross sections at low energies. Here the energy dependence should be approximately proportional to the 4th power of the velocity if only states of spin 1/2 and 3/2 and even parity are involved and if the pion is pseudoscalar. The experimental observations in this and other laboratories seem to be compatible with this assumption, but the cross section at low energy is so small that a precise measurement becomes difficult.

N° 251 and 255.

The experiment on the scattering of pions by hydrogen were followed with great interest by the theoretical physicists at this time. These experiments seemed to hold the key to the understanding of the nuclear forces, and there had been a great many speculations about the nature of pion-proton interaction. The experiments would show which of the many possible theories came closest the truth.

This problem had captured the interest of the brilliant young American theorist, Richard Feynman, whom Fermi knew quite well from Los Alamos days. Feynmans's letter to Fermi about these experiments and how they might be analyzed is not reproduced here. It contains some predictions based on different meson theories, for nucleon pion cross sections. Fermi's reply shows how he was analyzing the observations. The use of the phase shift analysis was not new, but Fermi's adoption of the technique revived the interest in it, and it came into wide usage thereafter.

The phase shift analysis of the pion-proton scattering became a major occupation for Fermi. He spent the summer of 1952 at Los Alamos, putting the problem into the electronic computer there (see paper N° 257).

The experiment on the scattering of pions by protons commanded the center of the stage of nuclear physics. When the Rochester High Energy Nuclear Physics Conference was held, in December of that year, everyone was eager to hear Fermi's report. (He had attended regularly all meetings of the Rochester conferences since the first one in 1950). Some excerpts from the 1952 conference are reprinted here to give the flavor of that meeting and Fermi's part in it. (Paper N° 255).

H. L. ANDERSON.

251.

LETTER TO FEYNMAN

(1952)

Dr. R. P. Feynman
Miramar Palace Hotel
Copacabana
Rio de Janeiro, Brazil

Chicago, Illinois
January 18, 1952

Dear Dick:

I was very much interested in your letter of December 19, especially so because we have been thinking here along lines that are somewhat related to yours. We have some experimental results that seem to indicate the importance of the conservation of the resultant isotopic spin in the problem of scattering of pions by hydrogen. I am enclosing some letters to the « Physical Review » on this subject.

I have consulted my " experts " (*) on your assumption that the quantities X_1, X_2, etc. are real. As you may expect, they frown on such assumptions,

(*) In the special instance expert = Goldberger.

as experts would. I believe, however, that they are right and that the quantities are real only when they are small, but that phase differences develop when the cross section becomes comparable to $\lambda\!\!\!^{-2}$. For this reason I believe that your formulas need some changes at energies where this is the case. An approach to essentially the same discussion that seems to me above suspicion is the following.

Let's assume (a) that the resultant isotopic spin is a good quantum number; (b) that the scattering, at least in a certain energy interval, is due to p–waves only. In the scattering of pions of any charge by nucleons there are involved only states of isotopic spin $1/2$ and $3/2$. If we restrict ourselves to p–waves only, the true spin can have only the values $1/2$ and $3/2$. There are, therefore, only four combinations of isotopic and true spin that count, namely, $3/2$–$3/2$, $3/2$–$1/2$, $1/2$–$3/2$, and $1/2$–$1/2$. I shall abbreviate the notation by writing as indices the four combinations, 33, 31, 13, 11. From the assumptions made it follows that at a given energy all the scattering phenomena are characterized by four *real* quantities, namely the four phase shifts α_{33}, α_{31}, α_{13}, and α_{11} for these four states. These four real quantities are, of course, functions of the energy. In a scattering measurement, on the other hand, it is possible, in principle, to measure for each energy the three scattering cross sections of π^+ on protons and π^- on protons, without and with exchange of charge. Furthermore, each cross section can be measured at 0° and 90° in the center-of-mass system so that this gives for each energy six measurable quantities that can be expressed in terms of four phase shifts only, whereby two verifiable conditions are left over. The formulas are a little bit complicated and, if I have made no mistake, they are the following. σ_+, σ_-, σ_0 are the cross sections per steradian of the three processes. One finds:

$$\sigma_+(0^\circ) = \lambda\!\!\!^{-2}\{4\sin^2\alpha_{33} + \sin^2\alpha_{31} + 4\sin\alpha_{33}\sin\alpha_{31}\cos(\alpha_{33}-\alpha_{31})\}$$

$$\sigma_+(90^\circ) = \lambda\!\!\!^{-2}\{\sin^2(\alpha_{33}-\alpha_{31})\}$$

$$\begin{aligned}\sigma_-(0^\circ) = \frac{\lambda\!\!\!^{-2}}{9}\{&4\sin^2\alpha_{33} + \sin^2\alpha_{31} + 16\sin^2\alpha_{13} + 4\sin^2\alpha_{11}\\ &+ 4\sin\alpha_{33}\sin\alpha_{31}\cos(\alpha_{33}-\alpha_{31}) + 16\sin\alpha_{33}\sin\alpha_{13}\cos(\alpha_{33}-\alpha_{13})\\ &+ 8\sin\alpha_{33}\sin\alpha_{11}\cos(\alpha_{33}-\alpha_{11}) + 8\sin\alpha_{31}\sin\alpha_{13}\cos(\alpha_{31}-\alpha_{13})\\ &+ 4\sin\alpha_{31}\sin\alpha_{11}\cos(\alpha_{31}-\alpha_{11}) + 16\sin\alpha_{13}\sin\alpha_{11}\cos(\alpha_{13}-\alpha_{11})\}\end{aligned}$$

$$\begin{aligned}\sigma_-(90^\circ) = \frac{\lambda\!\!\!^{-2}}{9}\{&\sin^2(\alpha_{33}-\alpha_{31}) + 4\sin^2(\alpha_{13}-\alpha_{11})\\ &+ \sin(\alpha_{33}-\alpha_{31})\sin(\alpha_{13}-\alpha_{11})\cos(\alpha_{33}+\alpha_{31}-\alpha_{13}-\alpha_{11})\}\end{aligned}$$

$$\begin{aligned}\sigma_0(0^\circ) = \frac{2\lambda\!\!\!^{-2}}{9}\{&4\sin^2(\alpha_{33}-\alpha_{13}) + \sin^2(\alpha_{31}-\alpha_{11})\\ &+ 4\sin(\alpha_{33}-\alpha_{13})\sin(\alpha_{31}-\alpha_{11})\cos(\alpha_{33}+\alpha_{13}-\alpha_{31}-\alpha_{11})\}\end{aligned}$$

$$\begin{aligned}\sigma_0(90^\circ) = \frac{2\lambda\!\!\!^{-2}}{9}\{&\sin^2(\alpha_{33}-\alpha_{31}) + \sin^2(\alpha_{13}-\alpha_{11})\\ &- 2\sin(\alpha_{33}-\alpha_{31})\sin(\alpha_{13}-\alpha_{11})\cos(\alpha_{33}+\alpha_{31}-\alpha_{13}-\alpha_{11})\}\end{aligned}$$

Concerning the possibility of checking experimentally similar formulas, I am afraid that this may prove very difficult. At low energies, as far as we know, the cross sections of the pions on hydrogen become very small and in addition the influence of the *s*–scattering, which is small but not negligible, is probably important. One might think, of course, to add to the previously considered phase shifts of four *p*–waves also the two additional phase shifts of the *s*–waves. At the same time the experimentally observable quantities would increase from six to nine because when *s*–waves also are scattered, interference between *s*– and *p*–waves would make it meaningful to measure for each event the cross section forward, backward and at 90°. Apart from the difficulties of doing this with usable accuracy, there is one theoretical difficulty that arises from the fact that the isotopic spin at low energy is certinaly not too good a constant of motion because of the mass difference between the neutral and the charged pion, and also between the neutron and the proton. I have tried to see how this complication could be corrected for, and I think that it can be done, but I doubt that it is entirely unambiguous.

At higher energy, on the other hand, where the measurement would be more readily feasible, it is probable that higher angular momenta become important. Unfortunately, the energy range that is accessible to our experimentation is not adequate to decide whether and where the *d*–waves become important.

I wish I would also refresh my ideas by swimming off Copacabana.

Sincerely yours,
ENRICO FERMI

P. S.—I have had your letter duplicated and sent copies to the following: Weisskopf, Steinberger, Serber, Wheeler, Oppenheimer, Yang, Bethe, Marshak, Wick, Brueckner Chew, Christy, McMillan, Lepore.

P. P. S.—A few copies of your own letter as well as of this one will be sent to you by ordinary mail, along with the Letters to the « Physical Review ».

N° 252, 253, and 254.

Paper N° 252 reports the study of the pion scattering in deuterium instead of hydrogen, done to observe the behavior of the neutrons in the scattering process and to obtain some check on the isotopic spin ideas in a new situation.

To complete the study of the scattering of pions by protons, it was necessary to observe the angular distribution of the scattered particles. In this way the fate of the scattered particles was followed in detail, and a much more complete analysis of the process was possible (Paper N° 253). Fermi used the method of the phase shifts in analyzing these experiments, and was able thereby to select out in a quantitative way which states were important in the scattering. A more critical test of the principle of isotopic spin conservation was provided by these results.

With quantitative data available about the states involved in the scattering it became possible to connect the scattering with other experiments involving pions, in an ingenious application of the principle of detailed balance (paper N° 254). A connection was made between the scattering measurements and experiments in the photo-production of pions. The connecting link was the Panofsky ratio. The quantities involved were remeasured by different investigators many times and they finally came into agreement only after several improvements had been made quite a few years later (See: Cocconi, Fazzini, Fidecaro, Legros, Lipman, and Merrison, « Nuovo Cimento », *22*, 494 (1961)).

H. L. ANDERSON.

252.

DEUTERIUM TOTAL CROSS SECTIONS FOR POSITIVE AND NEGATIVE PIONS (*)

H. L. ANDERSON, E. FERMI, D. E. NAGLE, and G. B. YODH
Institute for Nuclear Studies, University of Chicago, Chicago, Illinois
(Received March 13, 1952)
« Phys. Rev. », *86*, 413 (1952) (Letter).

Recent communications from this laboratory report total cross sections of hydrogen for positive and negative pions. [1-3] [**] In these experiments scintillation counters were used to measure the transmission of hydrogen in the several pion beams of the large Chicago cyclotron. In the present experiment similar techniques were used to compare the transmission of H_2O and D_2O cells for charged pions. The immediate results, which we call $(\sigma_D - \sigma_H)'$, is the difference between the cross sections of deuterium and hydrogen for those events which produce no ionizing particles within the angular acceptance of the last counter.

(*) This work was supported the ONR and AEC.
(1) ANDERSON, FERMI, LONG, MARTIN, and NAGLE, « Phys. Rev. », *85*, 934 (1952).
(2) ANDERSON, FERMI, LONG, and NAGLE, « Phys. Rev. », *85*, 936 (1952).
(3) FERMI, ANDERSON, LUNDBY, NAGLE, and YODH, « Phys. Rev. », *85*, 935 (1952).
(**) [See papers N° 248–50 (Editors' note)].

One type of cell for either H_2O or D_2O was 2 inches long, and a second type was 4 inches long. For each pair of cells the numbers of atoms/cm² were very nearly the same, so that the energy loss, Coulomb scattering, and nuclear events due to oxygen were very nearly the same. The difference between the $\frac{1}{2}(H_2O)$ and $\frac{1}{2}(D_2O)$ cross sections observed is then $(\sigma_D - \sigma_H)'$.

TABLE I.

Cross sections of deuterium and hydrogen for π^+ and π^- at several energies.

Solid angle steradians	Energy band Mev	Observed $(\sigma_D - \sigma_H)'$ 10^{-27} cm² π^-	Corrected $(\sigma_D - \sigma_H)$ 10^{-27} cm² π^-	σ_H 10^{-27} cm² π^+	σ_D 10^{-27} cm² π^-
0.63	79 ± 10	31 ± 10	34 ± 10	48 ± 10	54 ± 13
0.63	109 ± 15	66 ± 4	72 ± 5	80 ± 10	103 ± 10
0.088	115 ± 9	87 ± 7	88 ± 7	95 ± 15	124 ± 11
0.63	115 ± 9	77 ± 18	84 ± 18		
0.43	127 ± 15	77 ± 7	84 ± 8	125 ± 15	129 ± 11
0.63	133 ± 9	66 ± 13	76 ± 15	135 ± 15	128 ± 16
0.088	164 ± 9	135 ± 13	139 ± 13		198 ± 12
0.63	164 ± 9	119 ± 11	128 ± 14		
0.088	179 ± 9	170 ± 10	172 ± 10		234 ± 12
0.63	179 ± 9	146 ± 9	163 ± 12		
0.43	209 ± 15	109 ± 24	131 ± 25		192 ± 26
		π^+	π^+	π^-	π^+
0.43	72 ± 17	24 ± 6	24 ± 6	15 ± 8	60 ± 9
0.63	79 ± 10	30 ± 13	31 ± 13	20 ± 8	79 ± 15
0.43	109 ± 15	28 ± 12	29 ± 12	31 ± 9	109 ± 16
0.43	127 ± 15	25 ± 15	26 ± 15	45 ± 10	151 ± 21

Table I presents the preliminary results. The solid angle in that of the last counter averaged over the absorber; hence it measures the "poorness" of the geometry. The energy band column lists the mean energy of the pions in the absorber, plus or minus half their energy spread. The energy spread is partly due to the spread in energy of the entering beam (± 3 Mev), but mostly due to the energy loss in the absorber. This information comes partly from magnetic analysis of the beam, partly from range curves, and from calculations of the energy loss in the sample. The $(\sigma_D - \sigma_H)'$ entries have been

corrected for the muon and electron contents of the beams, which in most channels is about 5 percent. The quoted error in $(\sigma_D - \sigma_H)'$ includes either the statistical or the consistency rms errors of the counts (whichever was greater), uncertainties in the corrections of the counting rates for chance coincidences (less the 1 percent), and uncertainties in the muon-electron correction (~ 2 percent).

It is desirable to correct the D — H difference for those specifically nuclear events which scatter particles into the last counter. For the purposes of this correction (which is of the order of 10 percent) we have taken $\sigma_D - \sigma_H$ for π^- equal to $\sigma_H(\pi^+)$. The correction was computed using the measured hydrogen cross sections [1,2] and assuming that the scattering is isotropic. Where $\sigma_H(\pi^+)$ was not available, we have taken $\sigma_H(\pi^+) = 3\,\sigma_H(\pi^-)$ (see reference 3). For π^+ the corresponding corrections are much smaller because of the importance of the charge exchange process.[4] The fourth column of Table I gives the corrected $\sigma_D - \sigma_H$. Values from different geometries are seen to agree within the experimental error. Justification of the assumption of the equivalence of $\sigma_D - \sigma_H$ for $\pi^\pm$ and σ_H for $\pi^\pm$ is seen from a comparison of columns 4 and 5 in Table I. There is some indication of deviations at the higher energies.

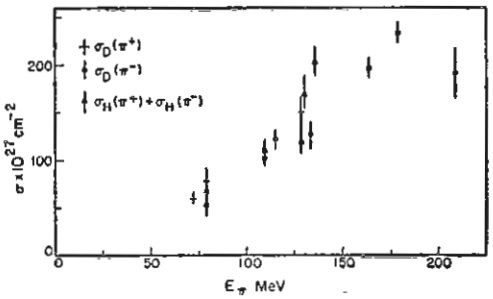

Fig. 1. – Total cross sections of deuterium for positive and negative pions.

Adding $\sigma_D - \sigma_H$, we obtain σ_D, as exhibited in column 6 of Table I and in fig. 1. Within the experimental errors σ_D is the same for pions of either sign. This has also been observed at 60 Mev by the Columbia workers. [4] This equality is predicted by the principle of charge symmetry, which requires for the free neutron and proton

$$\sigma_N(\pi^+) = \sigma_H(\pi^-) \quad , \quad \sigma_H(\pi^+) = \sigma_N(\pi^-).$$

For comparison, we have also plotted the sum $\sigma_H(\pi^+) + \sigma_H(\pi^-)$ in fig. 1. It will be seen that σ_D does not differ greatly from this sum, in accordance with the idea that the neutron and the proton in the deuteron scatter pions fairly independently.

At energies above 115 Mev there is some indication that σ_D is less than $\sigma_H(\pi^+) + \sigma_H(\pi^-)$. From such an effect it may be possible to obtain information about the relative phase of the scattering from neutrons and protons. We hope to extend our study of this effect in the near future.

(4) ISAACS, SACHS, and STEINBERGER, « Phys. Rev. », *85*, 802 (1952).

N° 253.

For the introduction to this paper see paper N° 252.

253.

ANGULAR DISTRIBUTION OF PIONS SCATTERED BY HYDROGEN (*)

H. L. ANDERSON, E. FERMI, D. E. NAGLE, and G. B. YODH
Insitute for Nuclear Studies, University of Chicago, Chicago, Illinois
(Received April 14, 1952)
« Phys. Rev. », *86*, 793 (1952) (Letter).

The angular distribution of the pions scattered by liquid hydrogen has been studied using the well collimated pion beams of the Chicago synchro-cyclotron. A pair of 2–inch diameter scintillation counters define the incident beam which passes through them into a liquid hydrogen cell (fig. 1). The

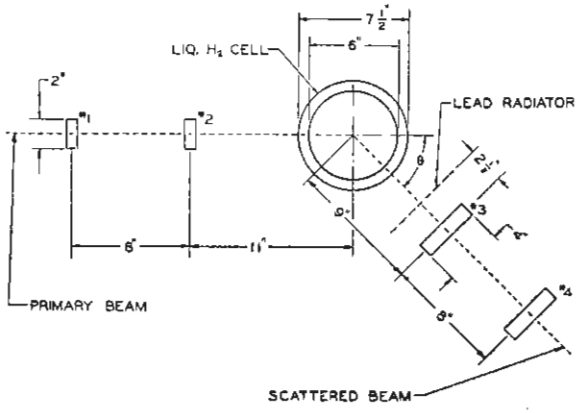

Fig. 1. – Experimental arrangement.

scattered particles are detected by two 4–inch diameter scintillation counters at suitable azimuth. A quadruple coincidence of all four counters requires a particle to pass through the first two counters and then to be scattered into the second pair. The quadruple coincidence rate, divided by the double coincidence rate of the first pair, which is recorded at the same time, gives the fraction of the beam which is scattered. The hydrogen cell was designed

(*) Research sponsored by the ONR and the AEC.

for rapid insertion and removal of the liquid hydrogen, to distinguish its effect from extraneous scattering. The charge exchange scattering was distinguished from the elastic scattering of negative pions by the insertion of a lead radiator in front of the second pair of counters, in order to enhance their sensitivity to gamma-rays.

The elastic scattering of positive pions at 110 Mev and 135 Mev, and both charge exchange and elastic scattering of negative pions at 135 Mev, were measured. The observations were taken at laboratory angles 45°, 90° and 135°.

The results, in the center-of-mass system, have been expressed in terms of the formula:

$$\frac{d\sigma}{d\omega} = a + b\cos\theta + c\cos^2\theta.$$

This angular distribution is expected when only s– and p–states contribute to the scattering. The values of the coefficients with their statistical errors are presented in Table I.

The integrated cross sections listed in Table I are in good agreement with those obtained previously [1] by transmission measurements. For negative pions the contributions of exchange and non-exchange scattering should be added, plus a small contribution of about 0.8×10^{-27} cm^2 due to the inverse photo effect ($\pi^- \to \gamma$).

TABLE I.

Coefficients for the differential cross sections.

Primary energy Mev	Process	a $10^{-27}\frac{\text{cm}^2}{\text{sterad}}$	b $10^{-27}\frac{\text{cm}^2}{\text{sterad}}$	c $10^{-27}\frac{\text{cm}^2}{\text{sterad}}$	$\int\left(\frac{d\sigma}{d\omega}\right)d\omega$ 10^{-27} cm^2
110	$\pi^+ \to \pi^+$	3.5 ± 0.6	-4.6 ± 0.8	7.2 ± 1.8	74.5 ± 5.4
135	$\pi^+ \to \pi^+$	3.8 ± 2.2	-6.8 ± 2.7	17.5 ± 6.6	121 ± 19
135	$\pi^- \to \pi$	1.2 ± 0.2	-0.1 ± 0.3	0.3 ± 0.7	16.2 ± 2.3
135	$\pi^- \to \pi^0$	1.1 ± 0.6	-2.5 ± 0.5	6.3 ± 1.9	40.6 ± 2.3

The elastic scattering of the positive pions is pronounced in the backward direction, an indication of interference of s– and p–waves. The same is true of the charge exchange scattering of the negative pions. The elastic scattering of the negative pions, on the other hand, is approximately isotropic.

A phase shift analysis has been made on the assumption that the scattering takes place in states characterized by isotopic spin 1/2 and 3/2 and

(1) H. L. ANDERSON, et al., « Phys. Rev. », *85*, 936 (1952). [See paper N° 250 (Editors' note)].

by angular momentum $S_{1/2}$, $P_{1/2}$ and $P_{3/2}$. The experimental data are well fitted by the following phase shift angles: At 135 Mev, $\mp 1°$, $\pm 19°$, and $\pm 1°$ for isotopic spin $1/2$; $\pm 25°$, $\mp 10°$, and $\mp 35°$ for isotopic spin $3/2$; at 110 Mev, $\pm 15°$, $0°$, and $\mp 25°$ for isotopic spin $3/2$. The angles are given in order for $S_{1/2}$, $P_{1/2}$ and $P_{3/2}$ and have an uncertainty of about $\pm 5°$.

The fact that at 135 Mev six phase shifts suffice to fit nine data demonstrates the fruitfulness of regarding the isotopic spin as a good quantum number. The pion-nucleon interaction is strongest in the $P_{3/2}$ state with isotopic spin $3/2$. However, the interaction in the $P_{1/2}$ state of isotopic spin $1/2$ is comparable. It appears to be responsible for the isotropy found in the π^- elastic scattering. The sizeable interaction found in the s–state of isotopic spin $3/2$ is believed to be responsible for the pronounced backward scattering observed in the other cases.

This research could not have been done without the active cooperation and advice of Professor Earl A. Long. We tank him and Dr. Lothar Meyer for generous supplies of liquid hydrogen. We are grateful to Messrs. Ronald Martin, Maurice Glicksman and Leo Slattery for contributing their time and skill to the preparation and conduct of these experiments.

N° 254.

For the introduction to this paper see paper N° 252.

254.

SCATTERING AND CAPTURE OF PIONS BY HYDROGEN (*)

H. L. ANDERSON and E. FERMI
Institute for Nuclear Studies, University of Chicago, Chicago, Illinois
(Received April 14, 1952)
« Phys. Rev. », *86*, 794 (1952) (Letter).

When a negative pion comes to rest in hydrogen, it is promptly captured in a Bohr-like orbit and almost immediately reacts with the proton. As shown by Panofsky and his co-workers, (1) the reaction produces either (a) a neutron and a photon, or (b) a neutron and a neutral pion, with about equal probability. Reaction (b) is closely related to the charge exchange scattering of the negative pion by the proton. The only difference is in the energy which is positive for the scattering, but slightly negative in the Panofsky case. It is the purpose of this note to show how these two phenomena may be correlated.

The experiments, in this laboratory, (2) on the scattering of pions by protons, have been interpreted in terms of the phase shifts of the s and p waves. At low energy, the p phase shifts, which vary as the cube of the momentum, become unimportant compared to the s phase shifts, which are proportional to the momentum. The scattering length a, which is the product of the s phase shift and the de Broglie wavelength, should be constant. From the experiments, $a_{3/2} = (3.8 \pm 0.7) \times 10^{-14}$ cm for the state of isotopic spin $3/2$ and $a_{1/2} = (0 \pm 1) \times 10^{-14}$ cm for the state of isotopic spin $1/2$.

The cross sections for exchange and nonexchange scattering at low energy can be expressed in terms of $a_{3/2}$ and $a_{1/2}$ by standard procedures of the collision theory. One should take into account the fact that states representing a proton and a negative pion, or a neutron and a neutral pion are linear

(*) Research sponsored by the ONR and AEC.

(1) PANOFSKY, AAMODT, and HADLEY, « Phys. Rev. », *81*, 565 (1951).

(2) ANDERSON, FERMI, NAGLE, and YODH, « Phys. Rev. », preceding Letter, this issue. [See paper N° 253 (Editors' note)].

combinations of pure states of isotopic spin 3/2 and 1/2. One finds the two cross sections

$$\sigma_- = \frac{4}{9}\pi (a_{3/2} + 2\, a_{1/2})^2 = 2 \times 10^{-27}$$

$$\sigma_0 = \frac{8}{9}\pi (a_{3/2} - a_{1/2})^2 \frac{v_0}{v} = (4 \times 10^{-27}) \frac{v_0}{v},$$

where v and v_0 are the relative velocities of the negative pion with respect to the proton and of the neutral pion with respect to the neutron, respectively.

From this value of σ_0 the rate of capture from the lowest Bohr orbit to give a neutral pion may he as obtained as

$$R_0 = \frac{\sigma_0 v}{\pi b^3} = 10^{15}\ \mathrm{sec}^{-1},$$

where we have taken for the radius of the mesonic Bohr orbit, $b = 2.2 \times 10^{-11}$ cm, and for the velocity of the emitted π^0, $v_0 = 8 \times 10^9$ cm/sec.

Unfortunately, a direct measurement of this rate is not available. However, we can use Panofsky's result that the rate of process (a) is equal to the rate of process (b). At low energy, therefore, the cross section σ_π for the process, $P + \pi^- \to N + \gamma$, must be equal to σ_0. By detailed balancing, the cross section σ_γ for the inverse reaction, which is the photomeson production process, is obtained. The result, near the threshold, is

$$\sigma_\gamma = \left(\frac{p_\pi^2}{2\, p_\gamma^2}\right)\sigma_\pi = \frac{1}{2} \times 4 \times 10^{-27} \frac{\mu_r^2 v_0 v}{p_\gamma^2}\ \mathrm{cm}^2,$$

where μ_r is the reduced mass of pion and proton and p_π and p_γ are the momenta of pion and photon in the center-of-mass system. Near the threshold $p_\gamma \approx \mu c$ and one finds the photo cross section

$$\sigma_\gamma = 4.0 \times 10^{-28} \frac{v}{c}\ \mathrm{cm}^2.$$

In comparing this formula with the measured values [3,4] of the photomeson production process, there is a certain arbitrariness in the extrapolation to the threshold. Moreover, some discrepancy can be expected because our formula refers to the photoeffect on neutrons, whereas the measurements have been on the photoeffect on protons. The agreement is within a factor of 4 in the worst case, Steinberger's [3] lowest point. It is quite close to the extrapolated curve given in Feld's [4] recent analysis of this and newer data.

It should be stressed that the coefficients in our formulas are affected by large experimental inaccuracies, owing to the combined errors in $a_{3/2}$ and $a_{1/2}$. The over-all uncertainty could well be as large as a factor 2.

(3) BISHOP, STEINBERGER, and COOK, « Phys. Rev. », *80*, 291 (1950).
(4) FELD, FRISCH, LEBOW, OSBORNE, and CLARK, « Phys. Rev. », *85*, 680 (1952).

N° 255.

For the introduction to this paper see paper N° 251.

255.

REPORT ON PION SCATTERING

Excerpts from the Proceedings of the Third Annual Rochester Conference (December 18–20, 1952).

1.—Fermi turned to a report on pion scattering from hydrogen by Anderson, Nagle and Fermi at Chicago. There are three types of pion scattering from hydrogen:

(1) $\pi^+ + P \rightarrow \pi^+ + P$, (2) $\pi^- + P \rightarrow N + \pi^\circ$, and (3) $\pi^- + P \rightarrow \pi^+ + P$,

where the second phenomenon is measured by observing one of the two π° decay photons. Process (1) has the largest cross section, then (2), and (3) has the smallest. From the experimental point of view this order has very umpleasant practical consequences for the measurement of reaction (3). The trouble arises since the photon background going in the direction of the counter is in many cases of the order of ten times the number of π^-. The observed cross sections for reaction (3) determined by previous measurements were somewhat in error.

The experimental setup consisted of π^- beam going into a liquid H target about 6″ in diameter; leaving the target were a mixture of photons and π^- having an intensity ratio of about 10 to 1 or 10 to 2 depending upon the angle of emission. The usual measurements consisted of the detection of the π^- meson with two scintillation counters without any material interposed. To detect the π° photons, a lead converter was placed in front of the first counter. Unfortunately, even without the lead interposed there is some photon conversion, mainly from the walls of the hydrogen Dewar. A new set of measurements are being made which are an improvement over the old ones, primarily because the Dewar walls have been made thinner. Expressed in radiation units the Dewar walls are not one half as thick. Fermi pointed out another disturbing fact about the old hydrogen Dewar that still cannot be explained. When calibrating the equipment by a Panofsky-type experiment where the π^- mesons are stopped in hydrogen, they found a pair conversion at birth coming from the region of the Dewar of about 4 percent of the photons after the calculated effect of the Dewar walls were subtracted off. This is a few times larger than both the theoretical value and also Stein-

berger's measurements using a thin-walled Dewar. With the new Dewar the same experiment gives an understandable yield much lower than the 4 percent. So the new data on the π^- interaction with hydrogen looks more convincing. The cross section for the π^0 exchange scattering has not changed, but there is a difference in the scattering results (see table below).

A characteristic feature to the π^+ scattering and the π^- exchange scattering is that they have a larger cross section in the backwards direction. However, the π^- elastic scattering cross section goes appreciably forward although not as much as the other reactions go backwards. This behavior can clearly be seen in the following table consisting of all the worthwhile measurements to date.

Chicago pion scattering data.

	$++$	ϑ	$--$	ϑ	$-\gamma$
78 Mev	$\eta = 0.973$				
54°	1.96 ± 0.33				
102°	2.26 ± 0.31				
143°	3.09 ± 0.34				
110 Mev	$\eta = 1.18$				
55°	3.3 ± 0.7				
103°	5.1 ± 0.7				
144°	12.3 ± 1.0				
120 Mev	$\eta = 1.24$				
		55°	1.02 ± 0.15	53°	3.0 ± 0.3
		104°	0.42 ± 0.15	100°	4.3 ± 0.3
		144°	0.88 ± 0.20	142°	8.0 ± 0.5
135 Mev	$\eta = 1.325$				
56°	5.7 ± 2.2				
104°	6.8 ± 2.2				
145°	21.6 ± 3.6				
144 Mev	$\eta = 1.375$				
		56°	1.63 ± 0.15	54°	5.0 ± 0.4
		105°	0.64 ± 0.15	102°	6.1 ± 0.4
		145°	1.10 ± 0.25	143°	10.5 ± 0.7

The data are expressed in millibarns per steradian in the C.M. system. The scattering angles are in the C.M. system. η is the meson momentum in units of μc. The heading $++$ stands for π^+ elastic scattering; notice the strong backward scattering. Also notice the similar behavior in the third column under the heading $-\gamma$ which stands for π^- charge exchange scattering. The new data is on the π^- elastic scattering and shows an increase in the forward direction.

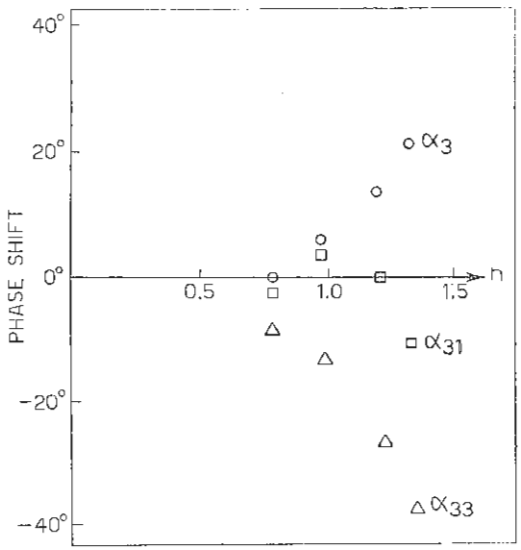

Fig. 1. – Phase shift angles for I = 3/2 in meson scattering from hydrogen.

These data can be correlated with the isotopic spin phase shifts. With the use of an electronic computer the phase shifts can be computed in five minutes, since there is one code for all calculations. With each calculation only taking about five minutes, one can learn something of the mathematics of the problem by varying the conditions a little. In particular, using the $++$ and $-\gamma$ measurements at three angles to compute the isotopic spin phase shifts, the phase shifts are then used to calculate the cross section. The results invariably want the cross section to look as they do experimentally. In this calculation only the S and P phase shifts are used. The following curves show how certain of the phase shifts depend upon energy. All the data are for the phase shifts calculated at Chicago as distinct from those of Yang.

The points labelled α_3 correspond to $I = 3/2$ and $S_{1/2}$. The ordinate scale is the meson momentum in the C.M. system and is expressed in units of μc. The points seem to fall on a curve. The meson energies are 135, 113, 78 and 55 Mev. The last point represents the Brookhaven data and has poor statistics. The curve through the points was theoretically suggested by Marshak. The points for $I = 3/2$ and $J = 3/2$ are denoted by α_{33}. They have a regular behavior and fit a curve varying with the cube of the momentum. This is the simplest law that one can expect for P level phase shifts. The points for $I = 3/2$ and $J = 1/2$ are denoted by α_{31} and do not show a

regular behavior. The data indicate that these points are small and slightly negative but the experimental errors are too large.

The next figure shows a schematic representation of the meson wave function for 135 Mev incident energy. S waves with and without a perturbation of the nucleus are rather similar except for the phase shift which is of the order of 20°. The nucleon radius is conventionally set at $\lambda/\mu c$ and the

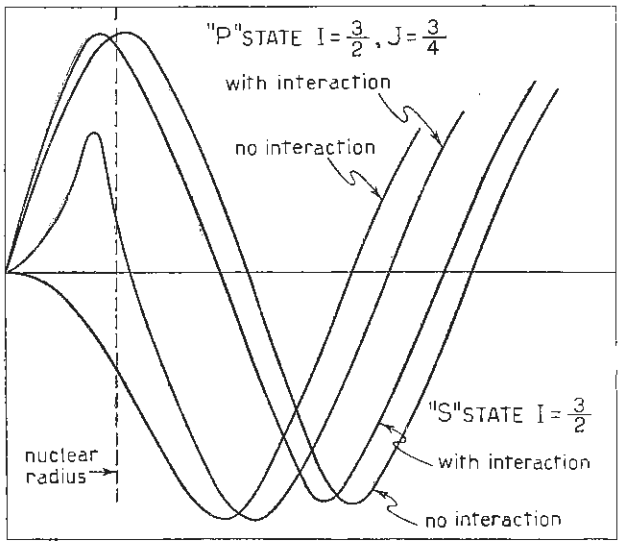

Fig. 2. – Meson wave functions (energy 135 Mev).

wave function goes to the origin by bending down sharper than a sine curve. The situation is different for the case of $I = 3/2$ and $J = 3/2$. The curves with and without nuclear interaction are two sine curves outside of the nucleon radius that have a separation of the measured phase shift. Inside the nucleon, however, the difference between the wave functions is very large even for a phase shift that is similar to that of the S wave.

Fermi pointed out that Yang's phase shifts agree with the data as well as the phase shifts computed at Chicago. These are compared in more detail in the Saturday morning session. There is hardly any difference for the S levels. The major difference is in the P states. There are probably no other solutions than these two. This limitation was suggested by the following calculation: 30 random samples of data were assumed and the phase shifts were computed, each set taking about 5 minutes with the electronic computer. The results fall into two minima corresponding to the phase shift analyses of Chicago and Yang. There was another minimum with a very large value, so that it is meaningless experimentally. The + or — signs of the phases have not been determined.

Brueckner asked whether the correct set of phases could be determined by a more accurate measurement. Fermi replied that this is probably so but if more accuracy is available then there is the added complication of the D and higher order phases. Anderson pointed out that the fact that

there are two sets of phase shifts is due to the $-\gamma$ process which can go either with or without spin flip for the proton. The uncertainty in the choice of phase shifts is due to the small contribution to the cross section from the spin flip part. Fermi pointed out that the two sets of phase shifts are distinctly different but in some respects quite close. For example, the S phases are roughly equal. Both sets of phase shifts appear to behave properly with energy. Probably a way to decide which set of phase shifts is correct is by interference methods.

2.—Fermi then presented the new data for which the conference had been waiting, first remarking that the courier when he got here handed him a small piece of paper on which there were written, in a cryptic fashion, as is proper for something that comes from Los Alamos, certain numbers which then had to be decoded. Fermi then presented to the conference certain essential results which he had converted from duo to decimal notation. He has since supplied us with the full and correct data, and these are given in the table below:

Mev	Type	Phase Angles (degrees)							
		η	α_3	α_1	α_{33}	α_{31}	α_{13}	α_{11}	
53	Conv.	0.78	0		— 9	— 2			Brookhaven
78	Conv.	0.97	6		— 13	3			
113	Conv.	1.20	13	— 7	— 27	— 1	12	14	Old Data
113	Yang	1.20	13	— 7	— 10	— 36	14	10	Old Data
135	Conv.	1.325	21	— 3	— 38	— 11	17	4	Old Data
135	Yang	1.325	20	— 2	— 21	— 49	15	9	Old Data
		New Data							Least Squares Sum
120	Conv.	1.24	17.8	— 10.2	— 31.6	— 4.1	0.3	3.1	1.44
120	Yang	1.24	30.1	4.6	— 13.1	— 29.5	6.3	10.5	6.05
135	Conv.	1.325	16.1	— 11.1	— 41.8	— 6.1	1.2	5.1	1.25
135	Yang	1.325	40.5	5.9	— 19.6	— 33.9	7.8	13.8	4.75

It will be noted that the calculated cross section represents the observed cross section very well. The phase shifts have no business to represent the observations so well. That is, for the nine measurements this set is inconsistent statistically with the errors given. The most striking difference from the previous results is in the α_{13} and α_{11} phase shifts. Fermi had noted more or

less empirically the extreme sensitivity of these angles to a change in cross section. They have never changed sign, but they have varied all over the map. He was sorry to report that Yang's solution is much worse with the new cross sections although this is really a trick of arithmetic and, cheer-up, maybe they are very good. The result can be expressed by giving the least square constant for the two solutions. For Fermi's solution the least square constant is approximately 1.44, which is a value that is very much too small. That is, the six variables are adjusted to minimize the least squares constant and if the errors were correctly given one would obtain the value 9; Yang's solution is much worse in the sense that it corresponds to a constant of 6.05 but this is still well within the experimental error. The change in Yang's solution due to the new data is much more striking than that in Fermi's, but it still has the feature of α_{31} being large and α_{33} being small, so that in this sense it is still recognizable. A second point about the new data is that the α_3 phase shift now is lower for the higher energy. This is probably a trick of the errors, and the cross section may easily still be rising with energy in this region, although the smoother dependence given originally no longer appears so convincing.

N° 256.

Fermi had a long standing interest in numerical analysis. Already in 1928, he had computed the solution of the differential equation of the Fermi-Thomas atom (N° 43) on a small calculator. In all his work he used to give prominence to numerical applications and examples. It is thus natural that the developments in computers which occurred in the forties should particularly interest him.

One day in the late summer of 1945, Fermi walked into the computer room at Los Alamos. We started to discuss some of the electro-mechanical accounting machines that were being used for scientific calculations, but before very long he casually reached into his shirt pocket for a piece of paper on which he "happened" to have written an equation and simply asked, "How would we do this on the machines?" It was a semi-empirical formula for atomic masses that he had derived. The question had immediate effects. The calculation was planned in terms of elementary steps, the so-called plug-boards were wired, a sample set of nuclei was punched on cards, the data was processed and the results printed that same afternoon. At each stage he would listen to a minimum of explanation and then proceed with the task at hand, doing every detail himself.

In the spring of 1952, Fermi and his collaborators at Chicago had measured the scattering of negative pions by hydrogen and had made a preliminary analysis of the data in terms of phase shifts using desk calculators. At about the same time, the computer at Los Alamos was completed. Fermi proposed that a more complete analysis using the new computer be made to include experimental results on positive pion scattering obtained by the Columbia and Carnegie groups. He spent the summer of 1952 in Los Alamos, and once again we were to witness that very straightforward and thorough approach.

The results of the specific calculations, together with a generalization of those techniques are contained in Paper N° 256. The following summer, the calculations were extended; the final results are in Paper N° 260.

Fermi had early recognized the potential capabilities of electronic computers; his sustained interest was a source of stimulation to those working in the field; but it was his direct approach and complete participation that had the greatest effect on the new discipline. His curiosity extended beyond the calculation problem at hand; he raised questions about the general logical structure of computers, and his remarks were always of a penetrating nature. He was equally interested in the various experimental techniques being developed. Whenever the computer would malfunction, as it often did in those early days, he always expressed surprise and admiration that it performed so well. Such a sympathetic reaction was atypical and refreshing.

Finally it may be mentioned that Fermi, in the summer of 1952, raised the question of the feasibility of automatically scanning and measuring, as well as analyzing, nuclear particle tracks in emulsions or photographs. Only a preliminary formulation of this problem was possible, but it was clear that Fermi had anticipated the intense efforts that would be made later.

N. METROPOLIS.

256.

NUMERICAL SOLUTION OF A MINIMUM PROBLEM

E. FERMI and N. METROPOLIS
Document LA–1492 (November 19, 1952).

ABSTRACT.

A particular non-linear function of six independent variables is minimized, using the Los Alamos electronic computer. The values of the variables at the minimum correspond to the phase shift angles in the scattering of pions by hydrogen.

The Los Alamos Maniac has been used in solving a numerical problem that is of importance in the interpretation of the scattering of pions by hydrogen. Mathematically, this problem consists of searching for the minimum of a rather complicated function of six angles. The procedure followed in solving this problem and the experience on the performance of the computer will be described. In the last section some general remarks on the use of similar methods in solving complicated systems of ordinary equations with many unknowns will be described.

THE PHYSICAL PROBLEM.

During the last year a series of experiments have been performed with the synchrocyclotron at the University of Chicago on the scattering of pions with energies of the order of 100 Mev by protons. The experimental results have been in part published.[1]

At each energy three different types of processes are investigated experimentally. They are the elastic scattering of positive and negative pions and the exchange scattering of the negative pions in which a negative pion incident on a proton loses its negative charge to the proton in the scattering process. The pion becomes thereby neutral and the proton is changed into a neutron. For each of these processes a complete angular distribution should be investigated. In the actual experiments data have been taken at three angles only, namely 45°, 90°, and 135° in the laboratory frame of reference. At each energy therefore nine cross sections are measured. Three of them,

(1) ANDERSON, FERMI, NAGLE, and YODH, « Phys. Rev. », *86*, 793 (1952). [See paper N° 253 (Editors' note)].

σ_-^1, σ_-^2, σ_-^3, are the elastic scattering cross sections of the negative pions for the three above angles converted to the center of mass reference. Similarly, the three cross sections, σ_+^1, σ_+^2, σ_+^3, for the elastic scattering of positive pions are measured. The exchange scattering cross sections cannot be measured directly because of the extremely short lifetime of the neutral pion. One can observe, however, the gamma rays that result from its disintegration. Three gamma ray cross sections, σ_γ^1, σ_γ^2, σ_γ^3, are measured in this case. In what follows, the nine cross sections will be referred to as $\sigma_1, \sigma_2, \cdots, \sigma_9$.

Attempts have been made to express all these cross sections in terms of phase shift angles. On the assumptions discussed in reference (1) all the cross sections at a given energy can be expressed in terms of six angles which will be here indicated by $\alpha_1, \alpha_2, \cdots, \alpha_6$. The first two angles are the phase shifts of the s–waves of isotopic spin $3/2$ and $1/2$, respectively, the angles α_3 and α_5 are the phase shifts of the p–waves of angular momentum $3/2$ and isotopic spins $3/2$ and $1/2$, and the angles α_4 and α_6 are the phase shifts of the p–waves of angular momentum $1/2$ and isotopic spins $3/2$ and $1/2$.

The Mathematical Problem.

The nine experimental cross sections $\sigma_1, \sigma_2, \cdots, \sigma_9$, are expressed in terms of the six angles α_1 to α_6 by formulas of the type

$$(1) \qquad \begin{cases} \sigma_1 = f_1(\alpha_1, \alpha_2, \cdots, \alpha_6) \\ \sigma_2 = f_2(\alpha_1, \alpha_2, \cdots, \alpha_6) \\ \cdots\cdots\cdots\cdots\cdots\cdots \\ \sigma_9 = f_9(\alpha_1, \alpha_2, \cdots, \alpha_6). \end{cases}$$

The actual form of the functions f_1 to f_9 will be given later. Because of the experimental error in the measured quantities σ_i the equations (1) will not be exactly verified and one tries to determine the best set of angles α by a least squares procedure. One searches for the set of angles that minimizes the following expression,

$$(2) \qquad M(\alpha_1, \alpha_2, \cdots, \alpha_6) = \sum_1^9 \left(\frac{\sigma_n - f_n(\alpha_1, \cdots, \alpha_6)}{\varepsilon_n} \right)^2 = \text{minimum}$$

in which ε_n is the experimental error of the quantity σ_n.

Because of the rather complicated structure of the functions f, a conventional numerical solution of the minimum problem (2) is very laborious and requires one or two weeks of fairly steady computation for solving one single problem. An approximate solution obtained by this method is quoted in Reference (1). Machine computation presents great advantages in handling this problem. One problem can be solved by the Maniac in approximately five minutes.

In order to define completely our problem, the form of the functions must be given. These functions are best expressed using complex notations.

For each of the six angles α_n one defines a corresponding quantity

$$e_n = \exp(2i\alpha_n) - 1 \tag{3}$$

from these quantities the following nine coefficients are computed

$$\left\{\begin{aligned} b_p &= \frac{e_1 + 2e_2}{3} \;;\; a_{\beta p} = \frac{\sqrt{2}}{9}(e_3 - e_4 + 2e_5 - 2e_6) \;;\; a_{\alpha p} = \frac{2e_3 + e_4 + 4e_5 + 2e_6}{9} \\ b_N &= \frac{\sqrt{2}}{3}(e_1 - e_2) \;;\; a_{\beta N} = \frac{2}{9}(e_3 - e_4 - e_5 + e_6) \;;\; a_{\alpha N} = \frac{\sqrt{2}}{9}(2e_3 + e_4 - 2e_5 - e_6) \\ b &= e_1 \;;\; a_\beta = \frac{\sqrt{2}}{3}(e_3 - e_4) \;;\; a_\alpha = \frac{2e_3 + e_4}{3}. \end{aligned}\right. \tag{4}$$

These nine coefficients represent physically the amplitudes of the scattered waves of different spin, angular momentum and electric charge for the three processes. These quantities are used for the computation of nine more quantities as follows:

$$\left\{\begin{aligned} A_- &= \frac{2|b_p|^2 + 9|a_{\beta p}|^2}{8} \;;\; B_- = \frac{3}{2} R(b_p a^*_{\alpha p}) \;;\; C_- = \frac{18|a_{\alpha p}|^2 - 9|a_{\beta p}|^2}{8} \\ A_o &= \frac{2|b_N|^2 + 9|a_{\beta N}|^2}{8} \;;\; B_o = \frac{3}{2} R(b_N a^*_{\alpha N}) \;;\; C_o = \frac{18|a_{\alpha N}|^2 - 9|a_{\beta N}|^2}{8} \\ A_+ &= \frac{2|b|^2 + 9|a_\beta|^2}{8} \;;\; B_+ = \frac{3}{2} R(b a^*_\alpha) \;;\; C_+ = \frac{18|a_\alpha|^2 - 9|a_\beta|^2}{8}. \end{aligned}\right. \tag{5}$$

The symbol R means "real part of". An asterisk means the complex conjugate. The cross sections are expressed in terms of these nine quantities by the following formulas:

$$\left\{\begin{aligned} \sigma_1 &= A_- + B_- \cos\chi_1 + C_- \cos^2\chi_1 \\ \sigma_2 &= A_- + B_- \cos\chi_2 + C_- \cos^2\chi_2 \\ \sigma_3 &= A_- + B_- \cos\chi_3 + C_- \cos^2\chi_3 \\ \sigma_4 &= A_+ + B_+ \cos\chi_1 + C_+ \cos^2\chi_1 \\ \sigma_5 &= A_+ + B_+ \cos\chi_2 + C_+ \cos^2\chi_2 \\ \sigma_6 &= A_+ + B_+ \cos\chi_3 + C_+ \cos^2\chi_3 \\ \sigma_7 &= 2A_o + \frac{2-q}{3} C_o + pB_o \cos\chi'_1 + qC_o \cos^2\chi'_1 \\ \sigma_8 &= 2A_o + \frac{2-q}{3} C_o + pB_o \cos\chi'_2 + qC_o \cos^2\chi'_2 \\ \sigma_9 &= 2A_o + \frac{2-q}{3} C_o + pB_o \cos\chi'_3 + qC_o \cos^2\chi'_3. \end{aligned}\right. \tag{6}$$

In these formulas the cross sections on the left hand side are expressed in units of $\lambda\!\!\!^{-2}$ where $\lambda\!\!\!^{-}$ is the de Broglie wave length in the center of mass system. They are, therefore, pure numbers. The quantities p and q are known

constants for each energy and are given by the following formulas:

$$p = \frac{2\gamma}{\eta} - \frac{1}{\eta^2}\log\frac{\gamma+\eta}{\gamma-\eta}$$

$$q = 2 + \frac{6}{\eta^2} - \frac{3\gamma}{\eta^2}\log\frac{\gamma+\eta}{\gamma-\eta}$$

in which γ and η are the total energy and the momentum of the pion in the center of mass system expressed in units μc^2 and μc, respectively, (μ = pion mass; c = velocity of light). The quantities χ_1, χ_2, and χ_3 are the angles at which the cross sections are measured (45°, 90°, 135°), converted to the center of mass system. χ_1', χ_2', χ_3' are the angles converted to the center of mass system for the case that the particle observed is a gamma ray. Both sets of angles are computed easily for each energy with the transformation formulas of relativity.

The Coding of the Problem.

In order to solve numerically the minimum problem (2) the Maniac must be instructed first to compute the quantity M for six given phase shift angles. These angles will then be changed by small steps according to a pattern to be described, searching for lower and lower values of M until a minimum is found. The coding consists therefore of a first part that contains the instructions for the computation of the function M and a second part with the instructions for the search of the minimum.

The first part is rather lengthy but logically quite straightforward. The machine computes in succession the real and imaginary parts of the quantities (4) and then combines them to compute the quantities (5) and the cross sections (6). Then it forms the sum of squares that appear in (2). For this computation the sines and cosines of the six angles are needed. For the initial values of the six angles the sines and cosines are given as part of the input of the problem. In the successive computation as the angles are changed, a simple routine is used that gives the new values of the trigonometric functions by using the old values and the addition theorem. The coding of this part of the problem requires approximately 150 memory positions. In spite of the complication of the function M, the machine computes its value in approximately 4/10 of a second, whereas a hand computation of the same function takes about 20 minutes.

The search for the minimum involves a sequence of successive computations of M for different values of the angles. Each time that new angles yield a value of M smaller than any of the preceding ones, this value is stored as a temporary minimum. The procedure stops when a set of angles, $\alpha_1, \alpha_2, \cdots, \alpha_6$, is found such that the values of M for this set are smaller than the 12 values of M obtained when one of the six angles is either increased or decreased by a specified small step. The smaller is the step, the higher is the accuracy of the minimum values found.

For a coarse search of the minimum, steps of $(1/2)°$ were chosen. After computing the value for M for the initial angles, the computer is instructed to seek a new value of M obtained by increasing α_1 by $(1/2)°$. If this value is smaller than the original, the computer keeps on calculating values of M, adding each time $(1/2)°$ to α_1 until the value of α_1 is reached such that adding $(1/2)°$ to it increases M instead of decreasing it. If the first addition of $(1/2)°$ to α_1 produces an increase in M, the computer is instructed to subtract from α_1 a half degree at a time until M stops decreasing. After this operation is completed, the computer repeats the same operation on α_2, and then on α_3, etc., up to α_6. This cycle is repeated until two successive cycles do not produce a further decrease of the value of M. After this coarse search for the minimum is completed the computer is instructed to go through a similar operation using this time a step of $(1/16)°$. After this second search is completed optimum angles and the values of the cross sections at the minimum are printed.

If the function M had one single minimum, one would expect that no matter what is the set of angles from which one starts, the procedure should always end very close to the same minimum position. Errors up to about $(1/2)°$ are possible because of the finite step of $(1/16)°$ used. For the practical problem errors of this magnitude are quite irrelevant. If the function M has several minima, one might expect that, depending on the set of angles from which one starts, the computer may end up at a different relative minimum.

In the present problem it was known that the function M had at least four minima, two of them corresponding to entirely different sets of angles, and two more obtained from them by changing the signs of all angles. In order to investigate whether there are any additional minima, it would be necessary to have a rather complete mapping of the function, a very staggering task for a function of six independet variables. This point was investigated partially as follows: A search of the minimum with the same experimental data was repeated some 30 times, starting each time with a different set of initial angles chosen at random. The minima obtained were recorded and classified. Three essentially different minima were found; for each of them sometimes one sign of the variables and sometimes the opposite is found. Two of the minima are in the vicinity of the positions that were already known, and the third is at quite different values of the angles. This last minimum, however, is irrelevant from the practical point of view, because it is only a relative minimum with a rather high value of M and would give therefore a very poor least square solution of the problem. While this procedure does not guarantee that no further minima exist, we feel that it is not very probable that any should have escaped this type of search.

RESULTS.

Tables I and II summarize the results obtained for 113 and 135 Mev pions. In each table, Column 1 indicates the quantity represented in the corresponding line. Column 2 gives the measured cross sections with experi-

mental error expressed in mb/sterad. The third and fourth columns, labeled "First Minimum" and "Second Minimum", give the results of the two solutions of the problem corresponding to the two lowest minima of M. In computing the fifth column the same code was used but the input was changed because the three errors of σ^1_-, σ^2_-, σ^3_- were increased by about a factor 1000. It is clear from (2) that if this is done the first three of the nine terms of M become negligibly small. The minimum value of M will then be very close to zero because, at least in general, it will be possible to find a set of six angles that represent exactly the remaining six cross sections. In the actual case the solution is not quite exact because of the finite step adopted in search for the minimum of M. One will notice that the cross sections for which the error has not been changed (lines 4–9 of the tables) are quite close to the measured values. The first three cross sections, for which the errors have been made practically infinite, are represented, instead, rather poorly.

TABLE I.

113 Mev.

	Measured	First Minimum	Second Minimum	ε_- increased	ε_+ increased	ε_γ increased
σ^1_-	0.55±0.23	0.707	0.702	1.362	0.603	0.672
σ^2_-	0.48±0.22	0.382	0.372	0.605	0.436	0.419
σ^3_-	0.73±0.19	0.698	0.705	0.931	0.740	0.711
σ^1_+	3.61±0.65	3.913	3.946	3.618	4.231	3.672
σ^2_+	5.29±0.62	5.034	5.041	5.258	4.383	5.207
σ^3_+	13.46±0.96	13.397	13.429	13.479	21.281	13.382
σ^1_γ	4.34±0.65	3.967	3.941	4.337	4.324	3.544
σ^2_γ	5.17±0.64	5.419	5.410	5.316	5.113	6.146
σ^3_γ	10.45±0.99	10.340	10.333	10.294	10.453	11.661
α_1		13.4°	13.3°	15.5°	16.8°	15.0°
α_2		— 6.8	— 6.9	— 2.1	— 1.9	— 13.2
α_3		— 27.1	— 10.3	— 26.4	— 27.6	— 26.5
α_4		— 1.1	— 35.8	— 0.8	— 18.0	— 0.8
α_5		11.8	13.7	12.1	5.0	11.7
α_6		14.0	10.4	20.3	15.6	12.0
M		1.584	1.786			

TABLE II.

135 Mev.

	Measured	First Minimum	Second Minimum	ε_- increased	ε_+ increased	ε_γ increased
σ_-^1	0.87±0.37	1.074	1.070	2.336	1.157	0.893
σ_-^2	0.65±0.35	0.400	0.370	0.732	0.481	0.618
σ_-^3	0.87±0.20	0.926	0.926	1.234	0.904	0.873
σ_+^1	5.66±2.18	6.399	6.688	5.818	9.423	5.723
σ_+^2	6.75±2.14	6.490	6.507	6.652	8.666	6.723
σ_+^3	21.64±3.55	22.100	22.344	21.610	26.834	21.497
σ_γ^1	6.50±1.00	5.581	5.606	6.486	5.881	4.137
σ_γ^2	6.70±0.90	6.676	6.462	6.687	6.826	5.310
σ_γ^3	12.80±0.90	12.683	12.762	12.806	12.766	10.461
α_1		21.2°	20.3°	24.2°	40.9°	25.2°
α_2		— 2.7	— 2.4	5.4	— 1.7	— 2.4
α_3		— 37.9	— 21.2	— 35.6	— 34.4	— 35.2
α_4		— 11.5	— 48.7	— 11.8	— 20.9	— 11.6
α_5		16.8	15.1	46.0	18.8	4.9
α_6		3.8	9.0	5.9	6.6	14.4
M		1.90	2.16			

A similar procedure was repeated by increasing once the errors of the three cross sections σ_+ (column 6) and once the errors of the cross sections σ_γ (column 7). In all of these three cases three of the cross sections were computed from the measured values of the remaining six, without any use of their experimental values being made in the computation. Inspection of the table shows that although the computed cross sections do not come very close to the measured values, they still have values somewhat similar to them.

SOLUTIONS OF MINIMUM PROBLEMS BY ELECTRONIC COMPUTERS.

The problem that has been here discussed is an example of a minimum problem for a function of many variables. In principle, problems of this type could be handled in two ways. One involves standard mathematical

procedure of equating to zero all the partial derivatives of the function and obtaining thereby a system of n equations with n unknowns (n number of variables). The second procedure is the one chosen in the present example: to search for the minimum value by computing the function at very many points until the minimum is attained.

There are, of course, no general criteria for preferring one method to the other and the choice may be different for different problems. The present procedure was chosen in our example because to solve the six equations with six unknowns obtained by equating to zero the partial derivatives would have been probably a more complicated task than to compute directly the values of the function.

The following experience was gathered: If one searches for a minimum without any previous knowledge of its location, one will start from an arbitrary set of initial angles. It usually takes a relatively long time before the first cycle of variation of the six variables has taken place. In the average, this may be approximately two minutes, corresponding to computing the function 400 times. The next cycle of variation of the six variables is usually much shorter, and may last on the average perhaps 30 seconds. In most cases the coarse minimum, corresponding to a step of $(1/2)^\circ$, is reached in about a dozen cycles, totaling three or four minutes.

The fine search of the minimum with steps of $(1/16)^\circ$ takes on the average between one and two minutes. Only exceptionally it has happened that the coarse minimum was actually rather far from the true minimum position and in this case the further approach to the minimum with the fine step is more lengthy.

A Method for Solving Systems of Equations with Many Variables.

The same general procedure followed in the present problem for obtaining a minimum may be applied to the problem of solving a complicated system of n equations with n unknowns. Let the equations be of the form:

$$\left\{\begin{array}{l} f_1(x_1 x_2 \cdots x_n) = a_1 \\ f_2(x_1 x_2 \cdots x_n) = a_2 \\ \cdots\cdots\cdots\cdots \\ f_n(x_1 x_2 \cdots x_n) = a_n . \end{array}\right. \tag{9}$$

Consider the expression:

$$M = \sum_1^n [f_i(x_1 \cdots x_n) - a_i]^2 \tag{10}$$

M vanishes for a solution of (9) and is greater than zero otherwise. A solution corresponds therefore to a minimum of M which can be found by a searching procedure of the same type used for our problem. Of course, only minima where $M = 0$ will correspond to actual solutions of the system (9) and there might be other relative minima that would have to be discarded.

An example of this procedure for solving a system of six equations with six unknown is given in the previous calculations in columns 5, 6 and 7 of the two tables. In fact the procedure followed would correspond exactly to the one described in this section if three of the errors had been made infinite instead of being only very large. The reason why the errors were made large but not infinite was merely a practical one, because by so doing one does not have to re-code the problem at all, but merely to change some of the input data.

Naturally, if one wanted to obtain more accurate solutions of the equation, one would have to use a smaller step. Probably it would save computing time to search for the solution to start with a coarse step and to reduce the step successively as closer and closer solutions are found.

It is questionable whether a procedure of this type would be practical in solving a system of linear equations. Probably in this case a method of successive elimination would be faster than the search for a minimum. On the other hand, it is likely that the search for a minimum may be a very practical approach for the case of complicated equations where the elimination procedure would not be easily feasible.

We wish to acknowledge the assistance of Mr. John B. Jackson during the course of computer operation.

N° 257 and 258.

It had been relatively easy and quite exciting to carry out the initial pion experiments. Something new and important came out each time. It was quite a different matter with the angular distribution measurements. These were necessary for a more detailed knowledge of the pion proton interaction. Fermi wanted to know the behavior of the phase shifts, at least the first six, as a function of energy. The first comprehensive report on this work did not appear until more than a year after he had undertaken it. Measurements were made at each of three energies with positive pions and at two energies with negative pions. In each case three angles were studied and for the negative pions the charge exchange scattering was sorted out from the elastic. It turned out to be quite an extensive task and it took a great deal of cyclotron time.

Fermi's group had to wait its turn for cyclotron time and for adequate supplies of liquid hydrogen, while maintaining the electronic equipment and scintillation counters in reliable working order was a continning chore. Only a small fraction of the time was spent taking actual measurements and it was difficult to get accurate data. Between runs the data were reduced and the phase shift analyses made. At first these were done by hand. Fermi was remarkably handy with a Marchant desk calculator. He could calculate the cross sections from a given set of phase shifts in 20 minutes and rarely made a mistake. But to find the best fit phase shifts this type of calculation had to be repeated many times.

In the summer of 1952 Fermi interrupted the experimental work and went to Los Alamos to analyze, with the electronic computer, the data so far collected (see previous paper, N° 256). He returned to Chicago the following fall, an expert in electronic computation and with a great deal of enthusiasm for the usefulness of such machines. He gave a very popular series of lectures on the use and programming of computers, and he also brought back the " best fit " phase shift solutions.

There was one trouble with these. It turned out that there were several possible sets of phase shifts which fit the data about equally well. For some years following the experts in pion physics talked about the different possible solutions. There was the Fermi solution and the Yang solution; then a new one called the Fermi-Metropolis solution, also the Steinberger solution, and finally the Bethe-de Hoffman solution. It wasn't until after Fermi's death that it was possible to demonstrate fairly convincingly that the Bethe-de Hoffman solution, which was really Fermi's original choice extended properly in the higher energy region, was most probably the correct one. Nevertheless, paper N° 257 is important. It demonstrated clearly how to proceed from scattering experiments to deduce information on the nature of the interaction between two elementary particles.

A word about the organization of this work might be in order here. There would be a session in Fermi's office which usually started rather informally out of a discussion between Fermi and myself, then broadened to include the others, always Nagle and usually some of the graduate students, Martin, Yodh, and later Glicksman. There wasn't much question about what experiment to do: this was always the same scattering experiment; but there was a constant development in the technique, improvements in counters, in electronics, ways to reduce the background, and of handling the liquid hydrogen better.

I handled the general organization of the work and saw to construction of necessary parts in the shop, arranging for the use of the cyclotron and auxiliaries, and for the availability of an adequate number of graduate students for the measurements at night. Nagle took care of everything having to do with the target and its liquid hydrogen, Martin with the help of our electronic technician, Leo Slattery, put the electronics in readiness. Fermi usually contrihuted in the preparatory stage by huilding some needed accessory in his own little shop. Frequently he took up the job of assembling some of the new scintillation counters and checking that they worked reliably. Sometimes he helped construct the cathode follower circuits which were used in conjunction with the photomultiplier tubes.

On the first day of the run all the equipment had to be set up and aligned. The electronic circuits had to be rolled into the experimental area and connected, the deflecting magnet had to be set correctly, hydrogen target set in place and aligned carefully, shielding arrangements made, and the counters set into place. Fermi worked hard at all of this, starting at 8 : 30 AM, his usual arrival time, continuing through until 6 or 6 : 30 PM, the time he liked to go home to dinner. He took off 1 hour for lunch and one hour or little over for each lecture he had to give.

Things were usually lined up to Fermi's satisfaction by noon and he would go off to his lunch at the Quadrangle Club. After lunch the cyclotron would be started up and Fermi would be in the counting room checking out the counters, measuring their plateaus, feed thru, accidental coincidences, efficiency. Liquid hydrogen would be brought in, the target cooled and the first few measurements taken before it was time for Fermi to leave for the day. Things being fairly well organized now, the evening and later the night crews would come in to continue the measurements until the next morning.

Fermi's first act the next morning was to take all the data up to his office to reduce it to cross sections and be sure that everything looked reasonable. Then he would be back down in the counting room to take over his share of the actual recording of the data, keeping a sharp eye out for any possible misbehaviors or oversights that might have gone by unnoticed by his less cautious collaborators. This routine continued for several days until the liquid hydrogen was gone. That was the end of the experiment.

With all aspects of the measurement under his control in the counting room, Fermi seemed happiest, most relaxed. He would watch to see that the lights of the scalers would behave properly. He would cut them off at the right moment and record the readings. Once the next measurement was started he would tap the Marchant calculator on the desk in front of him, and when the count had been reduced to a cross section and neatly listed with all the rest he might sit back and say, " You see, these pions like to scatter backwards. " When he wrote this fact in his paper it was not merely the result that finally appeared after reducing all the data, it was something he had been noticing all along.

With some knowledge of the phase shifts, Fermi tried to clarify their meaning. In particular the s–wave phase shifts could be thought of as arising from a potential well. He tried to draw what a phase shifted p–wave might look like. Some of these considerations appeared in his Varenna lectures (paper N° 270). He also uncovered the interesting fact that the recoil protons in the scattering would be polarized. A measurement of this polarization could, in fact, make a clear distinction between the various possible sets of phase shifts. This was the subject of paper N° 258.

H. L. ANDERSON.

257.

ANGULAR DISTRIBUTION OF PIONS SCATTERED BY HYDROGEN (*)

H. L. ANDERSON, E. FERMI, R. MARTIN, and D. E. NAGLE
Institute for Nuclear Studies, University of Chicago, Chicago, Illinois
(Received March 6, 1953)
« Phys. Rev. », *91*, 155-168 (1953).

The angular distribution of pions scattered by liquid hydrogen has been studied using the collimated pion beams from the Chicago synchrocyclotron. Differential cross sections have been measured for the laboratory angles 45°, 90°, and 135° for positive pions of energies

(*) Research supported by a joint program of the U. S. Office of Naval Research and the U. S. Atomic Energy Commission.

78 Mev, 110 Mev, and 135 Mev, and for negative pions of 120 Mev and 144 Mev. For negative pions, separate results were obtained for the elastic scattering and for the charge exchange scattering. The scattering of positive pions and charge exchange scattering of negative pions show a larger intensity in the backward direction. The elastic scattering of negative pions is mostly forward.

The results have been interpreted in terms of phase shift analysis on the assumption that the scattering is mainly due to states of isotopic spins 3/2 and 1/2 and angular momenta $s_{1/2}$, $p_{1/2}$ and $p_{3/2}$.

The experimental results are represented quite accurately by the following phase shifts expressed in degrees for the angular momentum states in the order indicated above: at 120 Mev, phase shifts ∓ 15, ± 4, ± 30 for isotopic spin 3/2 and ± 9, ∓ 3, ± 2 for isotopic spin 1/2; at 135 Mev, ∓ 14, ± 5, ± 38 for isotopic spin 3/2 and ± 10, ∓ 5, ± 2 for isotopic spin 1/2.

In earlier communications [1,2] measurements of the total cross sections of hydrogen for both negative and positive pions at various energies were reported. In order to study in greater detail the features of the interaction between pions and protons, it appeared important to investigate also the nature and the angular distribution of the scattered particles. [3] (*) The experiments are being carried out with the well-collimated pion beams of the Chicago Synchrocyclotron using scintillation counter techniques. This is a report on the progress of this investigation.

I. Experimental Arrangement.

The pions are produced by a 450-Mev proton beam striking a beryllium target inside the cyclotron. Negative pions emitted in the forward direction are bent outward by the cyclotron magnetic field and emerge through a thin aluminum window from the vacuum chamber of the machine. A certain amount of focusing takes place, so that a sizeable fraction of the pions of given energy leave the cyclotron in a fairly parallel beam. The 12–foot thick steel and concrete shield which separates the cyclotron from the experiment room has channels cut through it to accept a number of these beams with different energies.

On the experiment side of the shield a sector magnet deflects the pions through an angle of about 45°. The beam is purified thereby from most of the unwanted radiation (mostly neutrons) which comes through the channel.

Positive pions are obtained by reversing the direction of both the cyclotron and the deflecting magnetic fields. The proton beam in the cyclotron then circulates counterclockwise, and the positive pions which are emitted backward from this direction follow the same trajectories and have the same energy as their negative counterparts. The backward emission is

(1) Anderson, Fermi, Long, Martin, and Nagle, « Phys. Rev. », *85*, 934 (1952).
(2) Anderson, Fermi, Long, and Nagle, « Phys. Rev. », *85*, 936 (1952).
(3) Anderson, Fermi, Nagle, and Yodh, « Phys. Rev. », *86*, 793 (1952).
(*) [For references (1), (2), and (3) see papers N° 248, 250, and 253 (Editors' note)].

unfavorable and the intensity of the positive pions which is obtained in this way is much smaller than that of the negatives.

The general arrangement is shown in fig. 1. The pion beam is defined by passing through two 2-in. diameter liquid scintillation counters, No. 1 and No. 2, and thereafter enters the hydrogen cell. The scattered particles are detected by a pair of scintillation counters, No. 3 and No. 4, arranged on a table to pivot around the central axis of the hydrogen cell. In some experiments these two counters were 4 in. in diameter; in others they were rectangles of 4 in. $\times$ 6 in. A quadruple coincidence is recorded when a par-

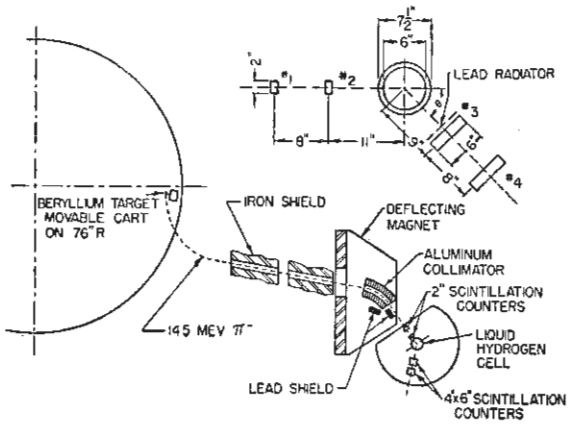

Fig. 1. – General experimental arrangement. In the inset the details of the scattering geometry are given.

ticle passes through the first two counters and is scattered so as to pass through the second pair. The double coincidences of the first pair are recorded at the same time. The fraction of the incident beam which is scattered is given by the ratio of the quadruple to double coincidences. The hydrogen cell was designed for rapid insertion and removal of the liquid hydrogen in order to distinguish the effect of the hydrogen from the scattering by surrounding materials. The resolving power of the coincidence equipment was fast enough (2×10^{-8} second), and the general background of stray radiation in the room was small enough, that chance coincidences were very few.

II. Scintillation Counters.

Liquid scintillation counters were found convenient in this work because they can be made with large areas of sensitivity over which their response is quite uniform. Their speed is quite high (6×10^{-9} second). The use of low density and low Z materials makes the absorption and scattering of pions in them tolerably small. The design of the 2–in. scintillation cell is shown in fig. 2. The cell is made of clear Lucite 3/4–in. thick over-all

with 1/16-in. thick Lucite windows. The liquid is phenylcyclohexane with 3 grams per liter of terphenyl and 10 mg per liter of diphenylhexatriene according to the prescription of Kallman.[4] The end of the Lucite cell is shaped to fit the photocathode of a 5819 tube and good optical contact is assured by a thin layer of clear silicone grease. The whole cell is wrapped in thin aluminum foil which enhances the light collecting efficiency. Phototube and scintillation cell are light-proofed with black Scotch electric tape. An iron shield is necessary to protect the photomultiplier from the stray magnetic field of the cyclotron.

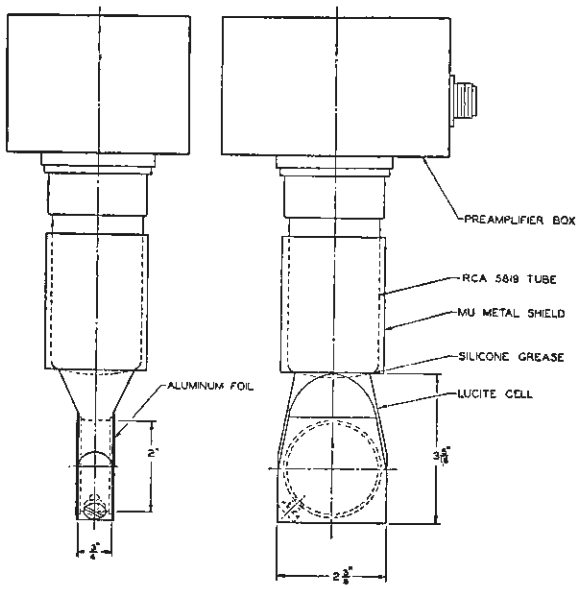

Fig. 2. – Two-inch diameter scintillation counters.

Two different types of counters No. 3 and No. 4 have been used at different times. In the earlier experiments 4-in. diameter scintillation counters were used; later the counters were changed to a newer type with a sensitive region of 4 in. × 6 in. The 4-in. diameter counters were 1 in. thick over all with 1/16-in. thick Lucite windows. The ends of the Lucite cell were shaped to fit the large cylindrical photocathode of an RCA C-7157 photomultiplier. The Lucite cell and the photomultiplier were enclosed in a steel box for magnetic shielding. The box was provided with 1/32-in. mu-metal windows in front and in back of the sensitive area of the cell.

The design of the 4 in. × 6 in. scintillation cells is shown in fig. 3. They are also made of clear Lucite with 1/16-in. thick Lucite windows. The over-all thickness is 1/2-in. The ends are shaped to fit the large cylindrical photocathode of the RCA C-7157 photomultiplier. The photomultiplier is protected from the stray magnetic field of the cyclotron by a cylindrical iron

(4) H. KALLMAN and M. FURST, « Phys. Rev. », *81*, 853 (1951).

enclosure not shown in the figure. The scintillation cell itself was wrapped in thin aluminum foil to improve the light collecting efficiency and to keep out stray light.

The response of both types of scintillators is uniform within 5 percent over their area. This was shown by making traverses with a narrow 1/4–in. beam of Co^{60} gamma-rays across the diameters parallel and perpendicular to the photocathode and reading the anode current of the photomultiplier directly on a microammeter.

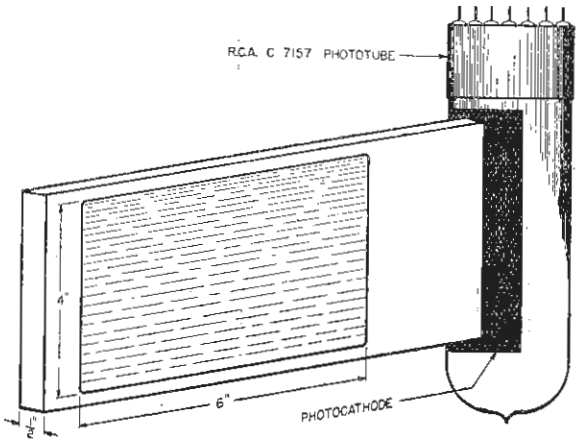

Fig. 3. – Rectangular 4–in.×6–in. scintillation counters.

For meson counting the photomultipliers were connected to a preamplifier which incorporated a 200–ohm line, 8 feet long, to clip the pulses into a fairly square shape of 2×10^{-6} second duration. The pulses were fed to the cyclotron control room through some 150 feet of 95–ohm RG7–U cable. The pulses were amplified tenfold by means of 100–ohm distributed amplifiers and fed to the coincidence circuits.

The coincidence circuits were designed using some of the ideas of Garwin. [5] The circuit used is given in fig. 4. It can be arranged to record either the single pulses from any given scintillator, or the double, triple, quadruple coincidences of any chosen combination, by the manipulation of suitable switches. The outputs of the first two scintillation counters were fed into the first coincidence circuit set to record doubles, and also into the second coincidence circuit set to record quadruples of all four scintillators. The coincidence circuits operate with negative pulses of 2 volts or more provided their duration is greater than 1×10^{-8} second. The photomultipliers were operated to deliver about 0.4 volt from meson pulses. With the amplification by 10, this was ample for reliable operation of the coincidence circuits. The meson pulses, as seen with the fast Tektronix Type 517 Oscilloscope, were quite uniform in amplitude.

(5) R. L. Garwin, « Rev. Sci. Instr. », *21*, 569 (1950).

The counting efficiency of these scintillators should be very close to 100 percent. An over-all check was obtained by comparing the quadruples to doubles rate with counters No. 3 and No. 4 between No. 1 and No. 2 in the line of the pion beam. The ratio obtained was usually quite close to unity.

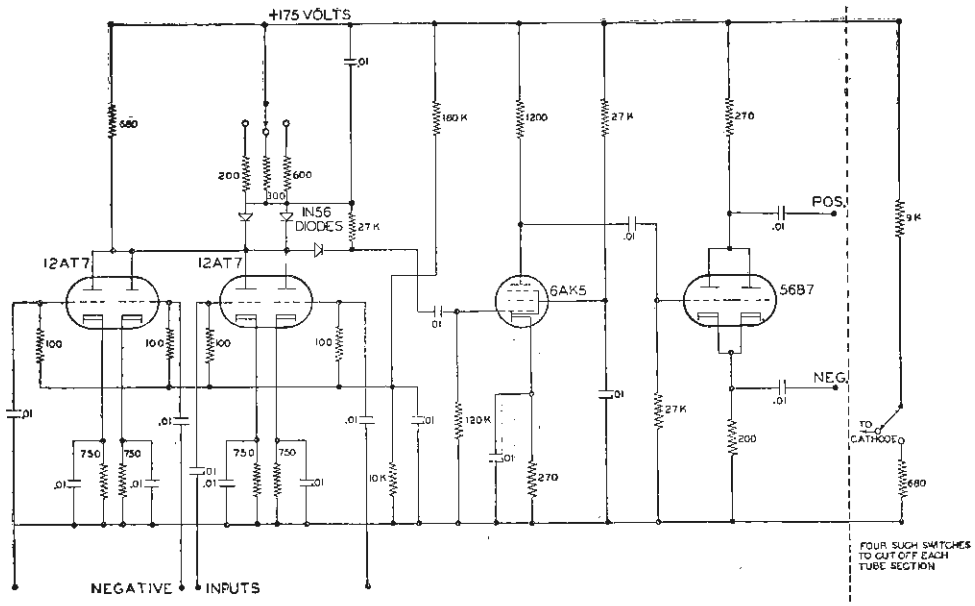

Fig. 4. – Diagram of the coincidence circuits.

III. Target.

The beryllium target in which the mesons are produced has a calibrated thermocouple arrangement which records on a Brown potentiometer the power in watts delivered to the target by the proton beam. Most of this energy is due to ionization loss, some is due to nuclear reactions, but in any case the energy delivered is closely proportional to the path length of protons in the target and hence to the number of mesons produced.

The readings obtained from the thermocouple target do not enter in any essential way in the present experiments. However, by reducing the counting rate to unit energy in watt minutes developed in the target, an over-all check on the operation of the equipment is provided which is useful not only during a given run, but also in judging the reproducibility of the arrangement from one day's run to the next.

In the present experiments the beryllium target was of dimensions 2-in. in the direction of the beam, 1/2-in. in height and 1/4-in. in thickness. In most of the runs the intensity ranged from 10 to 25 watts. At the level of operation of 12 watts the double coincidences of counters No. 1 and No. 2 which register the pions entering the equipment were as follows: For positive pions of 78 Mev, 36,000 per minute; for positive pions of 110 Mev, 6,000

per minute; for positive pions of 135 Mev, 900 per minute; for negative pions of 120 Mev, 230,000 per minute; and for negative pions of 114 Mev, 65,000 per minute.

IV. Hydrogen Container.

During the course of this investigation two different liquid hydrogen containers were used. They differed primarily in the materials and the thickness of the two walls of the liquid hydrogen Dewar. One was used in all measurements on positive pions and the other in the measurements of negative pions.

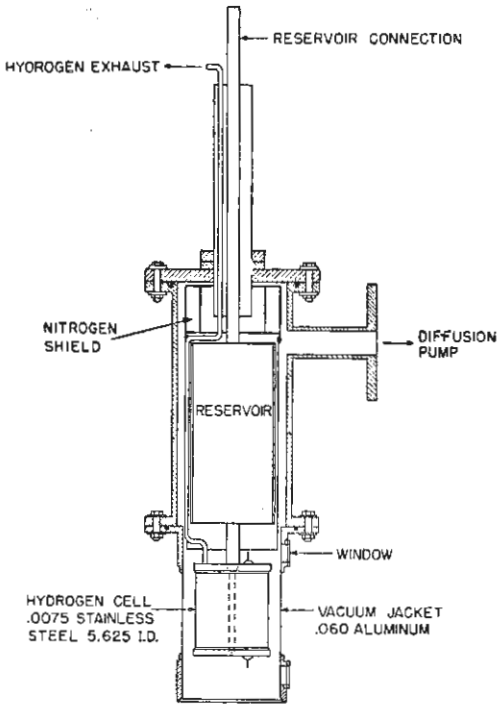

Fig. 5. – Liquid hydrogen container.

The apparatus for holding the liquid hydrogen is shown in fig. 5. The mesons passed horizontally through the lower section, where the walls were thinned. In the cell used for the positive pion measurements the outer wall was 0.032–in. stainless steel and the inner wall 0.020–in. brass, and the internal diameter 5.8–in. For the measurements on negative pions, the outer wall was 0.060–in. aluminum and the inner wall 0.0075–in. stainless steel, internal diameter 5 5/8–in. The space between the walls was evacuate to a pressure of about 10^{-6} mm of mercury. The inner cylindrical cell which held the liquid hydrogen had a volume of about 4 liters. A reservoir of 12 liters capacity was directly above the cell and connected to it by a 3/8–in. diameter tube extending nearly to the bottom of the cell. At the top of

the cell there was an exhaust tube which carried off the vapors when liquid filled the cell. Whenever it was required to remove the liquid from the cell, the exhaust tube was closed externally by a valve: whereupon the vapor pressure forced the liquid up into the reservoir. Opening the exhaust valve allowed the liquid to fall back into the cell under gravity. By this method successive measurements of the pion scattering could be taken with the cell full or empty of liquid.

Two parallel plate condensers, one above and one below the cell, were used to indicate when the cell was full or empty of liquid, use being made of the sizeable increase in capacity which results when liquid hydrogen fills the space between the condenser plates.

The reservoir was shielded from radiation by a liquid nitrogen jacket so that the evaporation rate was about 0.6 liter per hour. With a 50–liter supply of liquid hydrogen it was possible to continue an experiment for about 24 hours.

V. Energy of the Primary Pions.

The energy of the primary pions is known approximately from the channel through which they pass. These channels were laid out according to a rather detailed study of the trajectories of the pions of different energy. The channel energy is only nominal, however, because it depends on the target position and on the value of the cyclotron magnetic field, and these are not always precisely reproduced.

For this reason, it is more reliable to measure directly the energy of the pion beam used in each experiment. This has been done sometimes by taking a range curve of the pions and sometimes by observation of the Panofsky effect. A typical range curve is plotted logarithmically in fig. 6. This was obtained with the positive pion beam from the channel of nominal energy 122 Mev. The four counters were put in line with no hydrogen in the scattering cell, and copper absorbers were inserted between counters No. 2 and No. 3. The absorption curve shows two sharp drops corresponding to the end of the range of the pions and of the muons. The uncorrected mean ranges from the curve are 38.4 and 59.8 g/cm² copper.

In order to compute the energy of the pions in the center of the liquid hydrogen, one must correct these ranges, on account of the different amount of absorbers present in the absorption measurement and in the scattering experiment. The range is finally converted to energy using the range energy tables for protons given by Aron [6] and adopting as a mass ratio 6.65 for the proton to pion. The range curve of fig. 6 can also be used in order to estimate the contamination of the beam by muons and by electrons. For example, it was estimated that the muon contamination in this case was 7 percent.

(6) W. A. Aron, Berkeley Report UCRL 1325, 1951 (unpublished).

In some of the experiments the beam energy was determined by means of the Panofsky effect. One of the geometries used for this type of measurement is shown in fig. 7. A 1/4-in. lead sheet was placed in front of counter

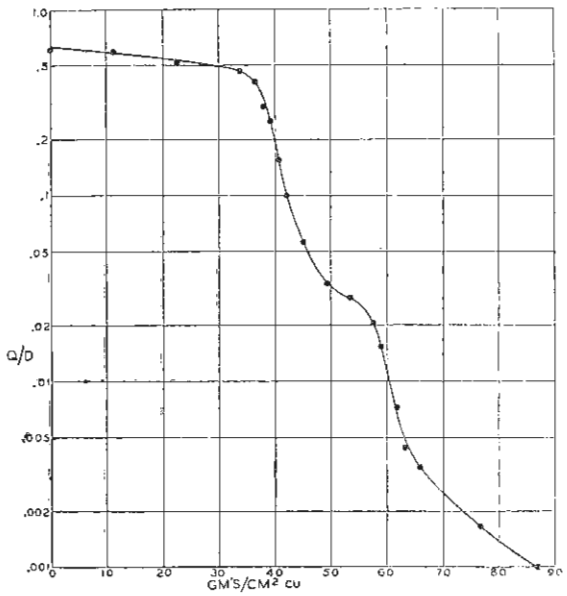

Fig. 6. – Range curve of $\pi+$ in copper.

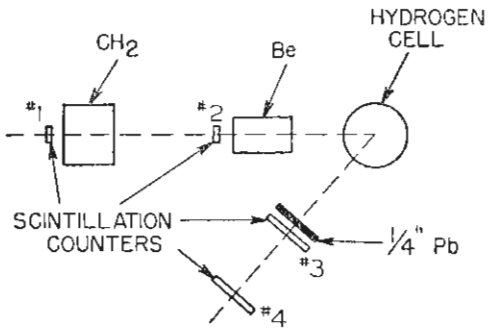

Fig. 7. – Arrangement for Panofsky effect.

No. 3 to increase its sensitivity to gamma-radiation. Light atomic weight absorbers, beryllium and polyethylene, were interposed in the beam in front of the liquid hydrogen cell. In fig. 8 the ratio of quadruple to double coincidences is plotted *versus* the thickness of absorber. The curve shows a sharp maximum at 23.8 g/cm² beryllium. To this one should add the absorber (11.24 g/cm² polyethylene) between counters No. 1 and No. 2. The beryllium equivalent of this is 14.6 g/cm². In conclusion the amount of beryllium necessary to reduce the energy of the pions to the point that they stop in the hydrogen is 38.4 g/cm², corresponding to an energy of 110 Mev.

In the upper part of fig. 8 there is plotted the absorption curve obtained in the same geometry of the Panofsky effect, and its derivative. One can see the maximum in the derivative curve matching the Panofsky maximum. A discussion of the quantitative comparison between the two curves will be found in Sec. VIII.

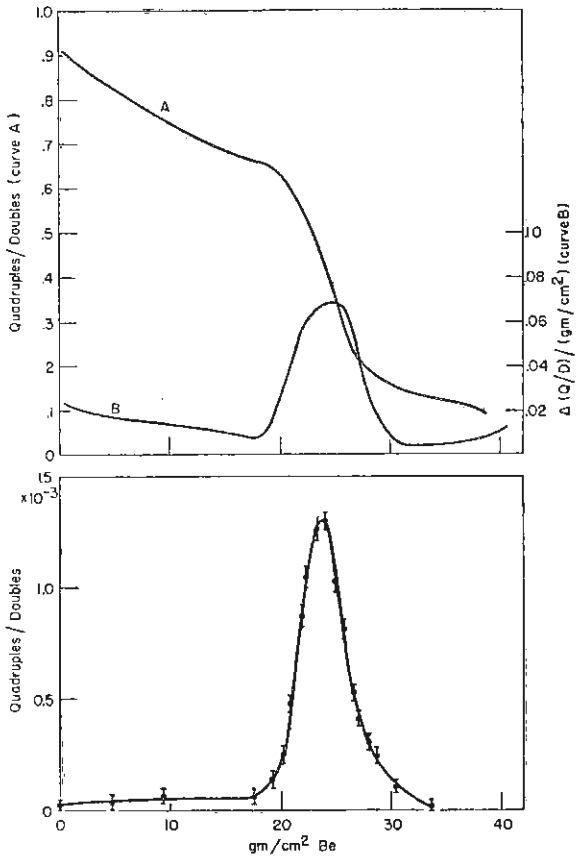

Fig. 8. – Abscissas, amount of Be absorber; lower curve, intensity of the Panofsky gamma-radiation; upper curves, absorption curve and its derivative. The additional absorber of 11.24 g/cm² polyethylene between counters No. 1 and No. 2 is not indicated.

VI. Scattering of Positive Pions.

For positive pions only the elastic scattering, represented by

(1) $$\pi^+ + p \to \pi^+ + p$$

was considered possible. After the scattering, a pion and a proton are produced which share the kinetic energy of the primary pion. In our experiment the conditions were always such that the protons could not be detected because they did not have sufficient range to penetrate the detecting counters No. 3 and No. 4. For this reason all observed scattering was attributed to

the scattered positive pions. Scattering measurements of positive pions have been performed at three energies of primary pions, 78 Mev, 110 Mev, and 135 Mev (mean energy at center of hydrogen). Measurements were taken for three scattering angles, 45°, 90°, and 135°. At each of these positions, counts were taken both with and without hydrogen in the scattering cell, and the difference of the two results attributed to the hydrogen scattering.

In the measurements at 110 Mev and 135 Mev the 4–in. diameter detecting counters were used in positions 3 and 4. In the 135–Mev measurement the distances of No. 3 and No. 4 from the center of the scattering cell were the "standard" distances 9 in. and 17 in. In some of the measurements at 110 Mev distances of 8.7 in. and 16.7 in. were used, in others the distances were 10.8 in. and 18.8 in. The data for this case are corrected to the "standard" geometry. One measures in both cases the ratio Q/D of quadruple to double coincidences. The results are given in Table I.

TABLE I.

Observed value of 10^6 Q/D *for* 110 Mev *and* 135 Mev *positive pions.*

(4–in. diameter counters, corrected to standard geometry).

Angle	With hydrogen	Without hydrogen	Net
	110 Mev		
45°	262.6 ± 15.0	162.3 ± 18.4	100.4 ± 19.8
90°	124.0 ± 10.5	21.0 ± 6.7	103.0 ± 12.5
135°	243.5 ± 12.7	50.5 ± 8.1	193.0 ± 15.1
	135 Mev		
45°	454 ± 47	280 ± 47	174 ± 67
90°	199 ± 32	63 ± 28	136 ± 43
135°	403 ± 45	74 ± 30	329 ± 54

In order to compute from these data the corresponding scattering cross section for each angle, the effective solid angle subtended by counters No. 3 and No. 4 is needed. For the scattering angles 45° and 135°, this was 0.0435 steradian. For the 90° geometry, the effective solid angle was 0.0410 steradian, slightly less because some of the particles scattered at the entrance or at the exit of the scattering cell could enter counter No. 4, but not counter No. 3, and would be missed. In computing the cross sections, the fact that only 93 percent of the primary beam were pions was taken into account. The muons, and possibly some few electrons in the beam were assumed not to be scattered appreciably.

The mean path length of pions traversing the hydrogen in these experiments was 14.4 cm. When the cell was filled with liquid hydrogen, the

number of atoms/cm³ was 4.2×10^{22}. When the cell was empty, it still contained gaseous hydrogen at liquid hydrogen temperature amounting to 0.07×10^{22} atoms/cm³. The difference, 4.13×10^{22}, multiplied by the effective length of the scattering cell, gives 5.95×10^{23} H atoms/cm².

The efficiency of counters No. 3 and No. 4 for counting a scattered pion that geometrically should be accepted by both counters was not 100 percent because the counter efficiency was not perfect (98 percent), and nuclear absorption in the first counter and in the hydrogen cell further reduced the efficiency to about 93 percent. The cross sections per steradian are given in Table II in the laboratory and in the center-of-mass systems.

The probable errors given in Table II are those due to statistics alone. Uncertainties in the beam energy and its pion content as well as in the estimates of the efficiency of detection all contribute to the inaccuracy of the experiment. These additional errors have not been added in this case because the statistical error was believed to be dominant.

TABLE II.

Differential cross sections for positive pions.

Energy Mev	Laboratory system		Center-of-mass system	
	Scattering angle (degrees)	Differential cross section 10^{-27} cm²/sterad	Scattering angle (degrees)	Differential cross section 10^{-27} cm²/sterad
78	45°	1.96 ± 0.33	53.8°	1.50 ± 0.25
	90°	2.26 ± 0.31	102.0°	2.34 ± 0.32
	135°	3.09 ± 0.34	143.2°	4.29 ± 0.47
110	45°	4.48 ± 0.88	54.9°	3.33 ± 0.65
	90°	4.88 ± 0.59	103.2°	5.09 ± 0.62
	135°	8.62 ± 0.67	143.9°	12.34 ± 0.96
135	45°	7.77 ± 3.00	55.7°	5.66 ± 2.18
	90°	6.42 ± 2.03	104.2°	6.75 ± 2.14
	135°	14.70 ± 2.41	144.5°	21.64 ± 3.55

The measurement with 78-Mev positive pions was performed at a later date using as detecting counters No. 3 and No. 4 the rectangular 4 in. × 6 in. counters. In this case the distances of the two counters No. 3 and No. 4 from the center of the scattering cell were respectively 9 in. and 17 in. The beam intensity at the average operation level of 23 watts yielded approximately 70,000 doubles per minute. The results of the measurement are collected in Table III. The conversion of these data to cross sections is similar to the previous cases. We assumed in this case that 92 percent of the doubles were due to pions. The solid angle was approximately 0.083 with

very minor geometrical and scattering corrections. The cross sections in the laboratory and in the center-of-mass system are given in Table II. It will be noticed that in all these cases $(d\sigma/d\omega)$ is appreciably larger in the backward than in the forward direction. This fact seems to indicate a negative interference between the scattering due to the s and the p waves, as will be discussed later.

TABLE III.

Observed values of 10° Q/D, 78–Mev *positive pions.*
(4–in. × 6–in. counters, standard geometry).

Angle	With hydrogen	Without hydrogen	Net
45°	510.9 ± 10.4	425.7 ± 9.8	85.2 ± 14.3
90°	217.5 ± 10.4	121.5 ± 7.8	96.0 ± 13.0
135°	390.9 ± 11.4	256.6 ± 9.3	134.4 ± 14.8

The differential cross sections in the laboratory system can be integrated over the solid angle in order to obtain the total cross sections. The results are given in column 2 of Table IV. In column 3 of the same table are reported the cross sections at the same energy obtained by interpolation from the data of the transmission measurements.[2] The agreement is within the experimental error.

TABLE IV.

Total cross sections of positive pions.

Mev Energy	Total cross section 10^{-27} cm²	
	From integration	From transmission
78	31 ± 3	45 ± 13
110	77 ± 6	82 ± 8
135	126 ± 20	149 ± 14

VII. SCATTERING OF NEGATIVE PIONS.

The measurement of the scattering of negative pions was carried out for two energies of the primary beam, 120 and 144 Mev (mean energy at the center of the hydrogen). Three processes are believed to be possible:

(2) $$\pi^- + p \rightarrow \pi^- + p,$$

(3) $$\pi^- + p \rightarrow \pi^0 + n \rightarrow 2\gamma + n,$$

(4) $$\pi^- + p \rightarrow \gamma + n.$$

Equation (2) represents the elastic scattering of negative pions and protons. Equation (3) represents scattering with charge exchange, in which the proton is converted to a neutron and the negative pion is converted to a neutral pion which almost immediately disintegrates into two photons. Equation (4) is the inverse reaction of the photoeffect in which a photon produces a negative pion by striking a neutron. The cross section of process (4) is estimated by detailed balancing from the inverse process [7] to be only about 0.8×10^{-27} cm^2. The present measurements confirmed the fact, previously reported, [8] that process (3) is appreciably more intensive than process (2).

The sensitivity of the pair of counters No. 3 and No. 4 to photons produced in the scattering process is normally rather low. However, it can be increased very appreciably by interposing in front of counter No. 3 a lead sheet to convert the gamma-rays into electron-positron pairs which are detected by the counters. For this reason, with π^-, four measurements were taken at each angle, namely, measurements of the ratio Q/D with and without liquid hydrogen in the scattering chamber and with and without a 1/4–in. thick lead radiator in front of counter No. 3. The net effect due to the hydrogen is computed as the difference with and without hydrogen.

In order to obtain separately the numbers of scattered pions and photons entering the detecting counters No. 3 and No. 4 it is necessary to know the efficiencies for the two types of particles. The counters used in the experiments on negative pions were thinner than those used in the positive pion experiments. There was a smaller loss due to absorption. The over-all efficiency without lead radiator was estimated to be 97 percent. With the lead radiator the efficiency is reduced both by nuclear absorption and by scattering. The latter effect depends on the energy of the pions and therefore also on the scattering angle. Moreover, the geometry at 90° is somewhat different than at 45° and 135°. An estimate of these effects gives the efficiencies listed in Table V.

In the same table the efficiencies for photon detection with and without lead are listed. The procedure for calculating these efficiencies is described in Sec. VIII.

The energies of the primary negative pions used in these two measurements were determined from the amount of absorber needed to produce a maximum in the Panofsky radiation. In one set of measurements the absorber was 44.3 g/cm^2 of aluminum corresponding to a pion energy of 120 Mev. In the other measurements it was 57.3 g/cm^2 of aluminum corresponding to 144 Mev. In both cases the detecting counters No. 3 and No. 4 had a sensitive area of 4×6 sq in., and were placed respectively, at 9 in. and 17 in. from the center of the scattering cell.

(7) BISHOP, STEINBERGER, and COOK, « Phys. Rev. », *80*, 291 (1950); FELD, FRISCH, LEBOW, OSBORNE, and CLARK, « Phys. Rev. », *85*, 680 (1952).

(8) FERMI, ANDERSON, LUNDBY, NAGLE, and YODH, « Phys. Rev. », *85*, 935 (1952). [See paper N° 249 (Editors' note)].

TABLE V.

Efficiencies of the detecting counters.

Mev Energy	Angle	Lead	Efficiency for pions (percent)	Efficiency for photons (percent)
120	45°	out	97	4
120	45°	in	91	67
120	90°	out	97	4
120	90°	in	88	61
120	135°	out	97	4
120	135°	in	88	59
135	45°	out	97	4
135	45°	in	92	70
135	90°	out	97	4
135	90°	in	89	63
135	135°	out	97	4
135	135°	in	88	60

Each individual measurement consists of a determination of the ratio Q/D of the quadruple coincidences to the double coincidences. The results of the measurements with their statistical errors are collected in Table VI.

For each primary energy and for each scattering angle, one needs the numbers Π and Γ of pions and photons per million primaries whose line of propagation enters the solid angle subtended by counter No. 4. These two numbers are obtained by solving two linear equations. For example, for 120-Mev pions and 90° scattering angle, we have from Table VI counts per million with and without lead 103.4 ± 4.0 and 25.6 ± 3.2. Using the efficiencies listed in Table V, one obtains the two equations

$$0.61\,\Gamma + 0.88\,\Pi = 103.4 \pm 4.0,$$
$$0.04\,\Gamma + 0.97\,\Pi = 25.6 \pm 3.2.$$

These equations have the solution

$$\Gamma = 139.8 \pm 8.7 \quad , \quad \Pi = 20.6 \pm 3.6.$$

In order to convert these numbers to differential cross sections they must be divided by the following factors: 930,000 (this is the number of pions per million primaries, the remainder of 7 percent being due to muons and electrons which are assumed to have no appreciable nuclear scattering),

0.083 (this is the solid angle subtended by counter No. 4), 5.9×10^{23} (this is the average number of hydrogen atoms per cm² traversed by the primary beam). Dividing the values of Π and Γ by the product of these factors, one obtains the following cross sections per steradian at 90°, for 120-Mev negative pions:

$$d\sigma_{-}/d\omega = (0.45 \pm 0.08)\times10^{-27} \text{ cm}^2/\text{sterad},$$

and

$$d\sigma_{\gamma}/d\omega = (3.08 \pm 0.20)\times10^{-27} \text{ cm}^2/\text{sterad}.$$

TABLE VI.

Observed values of $(Q/D)\times10^6$ *for negative pions.*

Angle	Lead	With hydrogen	Without hydrogen	Net
		120 Mev		
45°	out	235.6 ± 3.3	167.2 ± 2.8	68.4 ± 4.5
90°	out	82.0 ± 2.3	56.4 ± 2.1	25.6 ± 3.2
135°	out	112.7 ± 2.8	75.1 ± 3.1	37.6 ± 4.2
45°	in	290.6 ± 4.3	150.4 ± 3.4	140.2 ± 5.6
90°	in	161.4 ± 3.2	58.0 ± 2.4	103.4 ± 4.0
135°	in	223.9 ± 3.9	75.8 ± 3.1	148.1 ± 5.0
		144 Mev		
45°	out	237.6 ± 4.9	126.0 ± 4.0	111.6 ± 6.4
90°	out	93.3 ± 3.4	55.0 ± 3.0	38.3 ± 4.6
135°	out	135.3 ± 3.9	88.5 ± 4.2	46.8 ± 5.8
45°	in	355.9 ± 6.0	115.1 ± 1.8	240.8 ± 7.1
90°	in	202.2 ± 5.0	52.3 ± 3.0	149.9 ± 5.9
135°	in	264.1 ± 5.2	75.3 ± 4.3	188.8 ± 6.8

The errors indicated in these two cross sections comprise only the statistical error. Other sources of error are, in order of importance, the uncertainty in the efficiencies listed in Table V in the actual pion content and energy of the beam, and geometrical errors. We have estimated that the over-all effect of these errors may amount to 10 percent, and this error has been combined with the statistical error in the final results.

In Table VII are collected the values of the differential cross sections in the laboratory and in the center-of-mass frames of reference.

TABLE VII.

Differential cross sections for negative pions.

Energy Mev	Process	Laboratory system		Center-of-mass system	
		Scattering angle (degrees)	Diff. cross section (10^{-27} cm^2/sterad)	Scattering angle (degrees)	Diff. cross section (10^{-27} cm^2/sterad)
120	$\pi^- \to \pi^-$	45	1.44 ± 0.18	55.2	1.06 ± 0.14
		90	0.45 ± 0.09	103.6	0.47 ± 0.10
		135	0.67 ± 0.12	144.3	0.97 ± 0.18
120	$\pi^- \to \gamma$	45	2.64 ± 0.36	53.0	2.07 ± 0.30
		90	3.08 ± 0.37	100.5	3.19 ± 0.39
		135	4.53 ± 0.51	142.0	5.98 ± 0.69
144	$\pi^- \to \pi^-$	45	2.35 ± 0.29	56.0	1.70 ± 0.21
		90	0.69 ± 0.14	104.6	0.73 ± 0.15
		135	0.83 ± 0.17	144.6	1.23 ± 0.25
144	$\pi^- \to \gamma$	45	4.48 ± 0.55	54.0	3.43 ± 0.42
		90	4.25 ± 0.51	101.6	4.43 ± 0.53
		135	5.71 ± 0.66	142.6	7.78 ± 0.90

As an over-all check the total cross sections obtained by integration from the data of Table VII may be compared w th the results of total cross-section measurements by transmission.[1] The results of the integration are collected in Table VIII, column 2 and 3. The contribution of the $\pi^- \to \gamma$ process to the total cross section is about one-half the cross section listed in column three because each neutral pion produced in the exchange scattering process yields two photons. A very small correction has been included on account of the contribution of the inverse photoeffect. The total cross section obtained from the contributions of columns 2 and 3 is given in column 4. The total cross section given in column 5 is obtained instead by interpolation of the results of the transmission measurements. The two sets of results agree within the experimental errors.

VIII. SENSITIVITY OF THE DETECTING COUNTERS FOR PHOTONS.

The sensitivity of the detecting counters No. 3 and No. 4 for the photons produced in the decay of neutral pions is very small without lead radiator and is of the order of magnitude of 50 percent with the lead radiator in place.

TABLE VIII.

Integrated cross sections of negative pions (10^{-27} cm^2).

Energy Mev	$\pi^- \to \pi^-$	$\pi^- \to \gamma$	Total	Total from transmission
120	11.3 ± 1.6	43.4 ± 5.4	33.4 ± 3.2	38 ± 9
144	17.0 ± 2.4	61.2 ± 7.5	48.1 ± 4.5	55 ± 6

Without the lead radiator a photon may be detected when it materializes while traversing the hydrogen, the wall of the hydrogen cell, or counter No. 3, provided in this latter case that the materialization does not take place too close to the exit of the photon out of the sensitive region of the counter because the pulse will then be too small to be recorded. Finally, according to Dalitz, [9] a photon has a probability of 0.63 percent of being converted into a pair by internal conversion at the moment of its formation. In order to compute these various effects, the cross section for pair formation was obtained by interpolation between the data of Lawson [10] at 88 Mev and the data of De Wire, Ashkin, and Beach [11] at 280 Mev. Some small contribution to the detection of gamma-rays comes from Compton electrons. A Compton electron, however, has a high probability to give a coincidence of counters No. 3 and No. 4 only when its energy is an appreciable fraction of the energy of the photon. For this reason only one-half of the Compton cross section was added to the pair formation cross section, in order to obtain an effective cross section for materialization. The cross sections finally adopted are given in Table IX.

The probability of observing a photon without the lead radiator computed for the average energy photon emerging in the various directions and for the actual thickness of material traversed was in all cases about 4 percent, and this value has been adopted in Table V. With the lead radiator in place (7.36 g/cm^2), the probability of pair formation is greatly increased. For example, for 90–Mev photons, it is 51 percent.

The probability of pair formation, however, gives only a rough indication of the efficiency. There are primarily two reasons for this, namely, absorption of the electrons and effect of the multiple scattering. The first effect leads to a reduction, the second to an increase in efficiency. In order to understand the reason for the increase, we observe that if a single particle and not a pair were produced in the materialization, the effect of the multiple scattering would be cancelled in first approximation because some particles would be scattered in and some would be scattered out. In the case of a

(9) R. H. DALITZ, « Proc. Roy. Soc. (London) », *A 64*, 667 (1951).
(10) J. L. LAWSON, « Phys. Rev. », *75*, 433 (1949).
(11) DE WIRE, ASHKIN, and BEACH, « Phys. Rev. », *83*, 505 (1951).

pair, however, it is sufficient that one electron only of the pair be detected; therefore a photon is lost if both electrons are scattered out but is detected if both electrons or even only one of them is scattered in. An attempt was made to calculate these effects by assuming that all the pairs originate in the middle of the lead radiator. It was assumed further that the energy of the photon is divided evenly between the electron and the positron. The calculation was carried out for photons of 90 and 135 Mev. From the results of Wilson [12] it was estimated that the probability of a pair electron traversing the lead with sufficient energy to be recorded is 0.76 for photons of 90 Mev and 0.85 for photons of 135 Mev.

TABLE IX.

Cross sections for materialization σ *pair* $+\frac{1}{2}\sigma$ *Compton* (cm^2/g).

Element	90 Mev	135 Mev
H	0.0097	0.0097
C	0.0135	0.0143
Al	0.0240	0.0256
Fe	0.0422	0.0543
Cu	0.0454	0.0487
Pb	0.0909	0.0983

Consider now a photon whose line of propagation crosses the plane of counter No. 4 at a certain position. If a pair is formed, the probability q of observing the positron of the pair will be obtained by multiplying the probability that the positron of the pair escapes the lead with sufficient energy to be counted times the probability that after multiple scattering the positron falls inside counter No. 4. There is, similarly, an equal probability q of observing the electron of the pair. The probability of observing the photon that has materialized is the probability of observing either the electron or the positron or both. This probability is given by $q(2-q)$. Multiplying this probability by the probability of materialization of the photon, one obtains the probability of observing the photon. Integrating this probability over the area, one obtains an effective area of counter No. 4. We define the efficiency as the ratio of the effective to the true area of the counter. The geometry is slightly different at 90° and at 45° and 135°. The computed efficiencies are given in Table X. It is seen that the efficiency has an appreciable energy dependence. The mean energy of the photons produced by neutral pion decay in the scattering experiment depends on the energy of

(12) R. R. WILSON, « Phys. Rev. », *84*, 100 (1951).

the primaries and the scattering angle as is given in Table XI. The efficiencies were then computed by linear interpolation from the data of Table X and are given in Table V.

TABLE X.

Efficiency for photons.

Angle of scattering	90 Mev	135 Mev
45° or 135°	0.567	0.691
90°	0.558	0.681

TABLE XI.

Mean energy of the photons (Mev).

Primary pions \ Angle	45°	90°	135°
120 Mev	126	109	97
144 Mev	137	117	102

An attempt was made to obtain an experimental confirmation of the results of the efficiency calculation described in this section. This is done by an absolute measurement of the sensitivity of the detecting counters No. 3 and No. 4 to the gamma-rays emitted in the Panofsky effect. In fig. 8 the ratio of quadruple to double coincidences is plotted *versus* the thicknesses of absorber for the geometry represented in fig. 7. By integration of the curve of fig. 8 one finds that the total area of the Panofsky bulge after subtracting background is

$$P = 6430 \text{ counts per million} \times \text{g/cm}^2 \text{ Be.}$$

In the same figure is plotted also the derivative of the absorption curve. The derivative curve shows a bulge matching in position the Panofsky bulge. Its integrated area after subtracting background is found to be

$$A = 4.41 \times 10^5 \text{ counts per million.}$$

The thickness of hydrogen traversed by the pions is in the average 0.987 g/cm². Using for short range pions the equivalence factor in stopping power of hydrogen to beryllium of 2.58 one finds that this amount of hydrogen is equiv-

alent to 2.546 g/cm² Be. Denoting this factor by H, we obtain now the effective solid angle ω of the detecting counters from the following relationship:

$$P = \frac{fAH\omega}{4\pi},$$

where f is the average number of photons emitted when a negative pions comes to rest within the liquid hydrogen. According to Panofsky [13] one has $f = 1.485 \pm 0.054$. We obtain in this way $\omega = 0.0485 \pm 0.005$. The error includes an estimate of the uncertainties in the various quanties that enter in the determination of ω. The efficiency is the ratio of the effective solid angle ω to the geometrical solid angle which is 0.083. We obtain, therefore, an efficiency of 0.58 ± 0.06. The average energy of the pions to which this result refers is about 90 Mev. In Table X the efficiency was found, in excellent agreement, to be 0.57.

IX. Analysis of the Scattering Data.

The data of Secs. 6 and 7 may be analyzed by assuming that the scattering is due mainly to the contributions of s and p waves. The angular distribution of the scattered particles in the center-of-mass system will then have the form

$$\frac{d\sigma}{d\omega} = a + b\cos\chi + c\cos^2\chi, \tag{5}$$

where χ is the scattering angle in the center-of-mass system. The coefficients a, b, and c for the elastic scattering of 78, 110, and 135 Mev π^+ and for the elastic scattering of 120 and 144 Mev π^- are readily computed from the data of Tables II and VII.

The calculation of these coefficients for the charge exchange scattering is complicated by the fact that the direct measurement gives the cross section for the production of gamma-rays, and the angular distribution of these differs somewhat from that of the neutral pions which decay into them.

The problem can be solved by imagining the angular distribution of the neutral pions in the center-of-mass system to be analyzed into spherical harmonics. Each spherical harmonic component in the original distribution of the neutral pions gives rise, in the gamma-ray distribution, to a component proportional to the same spherical harmonic multiplied by a constant coefficient. The value of this coefficient depends upon the order of the spherical harmonic in question. It is equal to 2 for spherical harmonics of the order zero; to

$$k_1 = \frac{2\gamma}{\eta} - \frac{1}{\eta^2}\log\frac{\gamma+\eta}{\gamma-\eta} \tag{6}$$

for spherical harmonics of order one; and to

$$k_2 = 2 + \frac{6}{\eta^2} - \frac{3\gamma}{\eta^3}\log\frac{\gamma+\eta}{\gamma-\eta} \tag{7}$$

(13) Panofsky, Aamodt, and Hadley, « Phys. Rev. », *81*, 565 (1951).

for spherical harmonics of order two. In the above equations η and γ are the momentum and the total energy of the neutral pion in the center-of-mass system, in units of $\mu_0 c$ and $\mu_0 c^2$, respectively.

Writing (5) for neutral pions as the sum of spherical harmonics

$$a + \frac{1}{3} c + b \cos\chi + c\left(\cos^2\chi - \frac{1}{3}\right), \tag{8}$$

and applying the above coefficients, the angular distribution for the π^0 gamma-rays in the center-of-mass system is found to be

$$\frac{d\sigma_\gamma}{d\omega} = 2a + \frac{1}{3}(2 - k_2)\, c + k_1\, b \cos\chi + k_2\, c \cos^2\chi. \tag{9}$$

It is seen that the gamma–rays originating from the π^0 decay also have an angular distribution of the type (5) and one can readily compute the coefficients for the angular distribution of the neutral pions from the measured coefficients for the angular distribution of the photons.

TABLE XII.

Coefficients of $d\sigma/d\omega = a + b \cos\chi + c \cos\chi^2$ *for various processes* (10^{-27} cm^2/sterad).

Energy Mev	$\lambda\!\!\!^{-}$ (10^{-13}cm)	Process	a	b	c
53	1.777	$+ \to +$	0.46 ± 0.39	-0.08 ± 0.84	3.60 ± 1.46
78	1.439	$+ \to +$	1.9 ± 0.3	-1.7 ± 0.4	1.6 ± 0.9
110	1.186	$+ \to +$	3.6 ± 0.7	-4.8 ± 0.8	7.5 ± 1.9
135	1.057	$+ \to +$	3.9 ± 2.3	-7.1 ± 2.8	18.0 ± 6.8
120	1.129	$- \to -$	0.49 ± 0.11	0.34 ± 0.16	1.16 ± 0.34
144	1.018	$- \to -$	0.82 ± 0.16	0.73 ± 0.24	1.52 ± 0.50
120	1.129	$- \to \gamma$	2.68 ± 0.40	-2.39 ± 0.46	2.29 ± 1.20
114	1.018	$- \to \gamma$	3.80 ± 0.55	-2.49 ± 0.62	3.17 ± 1.62
120	1.129	$- \to 0$	0.6 ± 0.4	-1.9 ± 0.5	3.2 ± 1.7
144	1.018	$- \to 0$	1.05 ± 0.5	-1.9 ± 0.5	3.9 ± 2.0

Table XII summarizes the values of the coefficients a, b, and c for all the reactions studied. The first column gives the energy of the primary beam in Mev, the second column gives the de Broglie wavelength divided by 2π, in the center-of-mass system. The third column indicates the type of reaction; 0, +, and – are used to indicated neutral, positive, and negative pions, γ for the photons. The next three columns are the coefficients a, b, and c

for the reaction in question. The data at 53 Mev are computed from cross-sections measured at Brookhaven with a diffusion cloud chamber. [14]

Striking features of the table are the rather large values of the coefficients b and c which indicate strong deviations from spherical symmetry. The negative values of b for $\pi^+ \to \pi^+$ and $\pi^- \to \pi^0$ corresponds to the predominance of the backward scattering of these processes. The coefficient b has a positive value for $\pi^- \to \pi^-$ because, in this case, by contrast, the scattering is more pronounced in the forward direction.

X. Phase Shift Analysis.

The data may be analyzed on the assumption that in the scattering of pions by nucleons the isotopic spin is conserved, or more precisely, that the isotopic spin behaves as a quantized angular momentum vector in isotopic spin space. [15] In the scattering of positive pions by protons only the isotopic spin 3/2 will be involved because both the proton and the pion have their isotopic spin vectors "up." In the scattering of negative pions by protons, on the other hand, the orientation of the vectors is mixed and both isotopic spins, 3/2 and 1/2, will be involved.

From this basic assumption, it follows that the scattering features at any given energy will be determined by the phase shifts of the different states of given isotopic spin, orbital and total angular momentum. If it is assumed, as was done in the previous section, that only s– and p–states are important, there will be six phase shifts at each energy. They correspond to the possible values 3/2 and 1/2 of the isotopic spin, and, for each isotopic spin value, to the s–wave shifts and to the phase shifts of the two p–waves of angular momenta 3/2 and 1/2.

A complete set of measurements at any given energy consists of nine data: the values of the differential cross sections for each of the three processes $\pi^+ \to \pi^+$, $\pi^- \to \pi^0$, and $\pi^- \to \pi^-$, at each of three angles. Alternately the experiments supply nine constants, a, b, and c for each of the three reactions observed. If the assumptions are correct, these nine data will be expressible in terms of the six phase shifts, a situation which permits a check of the soundness of the procedure.

To obtain a complete set of data at each of two energies we have interpolated the π^+ data obtained at 110 Mev and 135 Mev to give values at 120 Mev to go with the π^- data at this energy. We interpolated the π^- data between 120 Mev and 144 Mev to give values at 135 Mev to go with the π^+ data at this energy. The measurements at 78 Mev, on the other hand, are incomplete because only the π^+ reaction was investigated. However, in this case, only the three phase shifts for isotopic spin 3/2 are involved. The data allow

(14) Fowler, Fowler, Shutt, Thorndyke, and Whittemore, « Phys. Rev. », *86*, 1053 (1952).

(15) N. Kemmer, « Proc. Cambridge Phil. Soc. », *34*, 354 (1938); W. Heitler, « Proc. Roy. Irish Acad. », *51*, 33 (1946).

these phase shifts to be calculated but nothing remains for an internal check.

The phase shifts of the s waves of isotopic spin $3/2$ and $1/2$ will be indicated by α_3 and α_1. The phase shifts of the p waves will be indicated by α_{33}, α_{31}, α_{13}, α_{11}, where the first index is twice the isotopic spin of the state in question and the second index is twice the angular momentum. The quantities a, b, and c for the reaction $\pi^+ \to \pi^+$ will be indicated by a_+, b_+, c_+. Similarly they will be indicated by a_+, b_+, c_+, for the reaction of elastic scattering of the negative pions, and by a_0, b_0, c_0 for the exchange scattering of the negative pions. In order to express the nine quantities a, b, c in terms of the six angles α, it is convenient to introduce the following notation:

$$e_3 = e^{2i\alpha_3} - 1, \cdots, e_{11} = e^{2i\alpha_{11}} - 1. \tag{10}$$

By applying the standard procedures of the phase shift analysis of the collision theory, the amplitudes of the scattered waves may be expressed in terms of these quantities. There are nine such amplitudes in all. Three corresponding to the scattering of positive pions; amplitude of the scattered s wave and amplitudes of the scattered p waves with and without spin flip. These are indicated by B, A_β, and A_α. The scattering of the negative pions contributes six amplitudes because in each case scattering without and with exchange of charge must be considered. The corresponding amplitudes are indicated by B_p, $A_{p\beta}$, and $A_{p\alpha}$ for the non-exchange process, and B_n, $A_{n\beta}$, and $A_{n\alpha}$ for the exchange process. These nine scattering amplitudes are given in terms of the quantities e of (10) by the relations

$$\left.\begin{aligned}
&B = e_3 \quad ; \quad A_\beta = \tfrac{1}{3}\sqrt{2}\,(e_{33} - e_{31}) \quad ; \quad A_\alpha = \tfrac{1}{3}(2e_{33} + e_{31}) \; ; \\
&B_p = \tfrac{1}{3}(e_3 + 2e_1) \quad ; \quad A_{p\beta} = (\sqrt{2}/9)(e_{33} - e_{31} + 2e_{13} - 2e_{11}) ; \\
&\qquad\qquad A_{p\alpha} = (1/9)(2e_{33} + e_{31} + 4e_{13} + 2e_{11}) ; \\
&B_n = \tfrac{1}{3}\sqrt{2}\,(e_3 - e_1) \quad ; \quad A_{n\beta} = (2/9)(e_{33} - e_{31} - e_{13} + e_{11}) \; ; \\
&\qquad\qquad A_{n\alpha} = (\sqrt{2}/9)(2e_{33} + e_{31} - 2e_{13} - e_{11}).
\end{aligned}\right\} \tag{11}$$

The coefficients a_+, b_+, c_+ for the scattering of positive pions are given by

$$\frac{a_+}{\lambda^2} = \frac{1}{4}|B|^2 + \frac{9}{8}|A_\beta|^2 \quad ; \quad \frac{b_+}{\lambda^2} = \frac{3}{4}(BA_\alpha^* + B^* A_\alpha) \; ; \tag{12}$$

$$\frac{c_+}{\lambda^2} = \frac{9}{4}|A_\alpha|^2 - \frac{9}{8}|A_\beta|^2.$$

In these formulas a star means complex conjugation. The quantities a_-, b_-, c_- and a_0, b_0, c_0 are given by similar formulas in which B, A_β, and A_α are replaced, respectively, by B_p, $A_{p\beta}$, $A_{p\alpha}$ and B_n, $A_{n\beta}$, $A_{n\alpha}$. It is possible, of course, to eliminate the intermediary quantities e, B, A from (10), (11), and (12), and to express directly the nine quantities a, b, c in terms of the six angles α. The formulas, however, are more complicated and not as well suited to numerical calculations.

If the accuracy of our measurement of the nine cross sections at a given energy were high enough, it would be possible to use six of them for determin-

ing the six angles α. Then, if the basic assumptions were right, the remaining three cross sections would be given correctly in terms of the same angles. Since, however, the experimental errors are rather large, this procedure is not very effective and it is more fruitful to try to use all the available experimental information in determining for each energy the best set of angles α by a least squares method. Some attempts to obtain by this method a set of "best" phase shifts were made by numerical computation on a preliminary set of cross-section values already published.[3]

The problem of determining the best set of phase shifts at each energy is managed much more efficiently with a modern electronic computer.[16] We are indebted to Dr. N. Metropolis for carrying out these computations for us using the Los Alamos Maniac computer. Given a set of nine measured cross sections, with the experimental errors, the machine finds the best set of six phase shifts according to the least squares criterion. Such a solution minimizes a least square sum $M = \sum_1^9 (\Delta_i/\varepsilon_i)^2$, where ε_i is the experimental error in the ith cross section, and Δ_i is the deviation of the calculated from the observed cross section.

This procedure does not permit a determination of the sign of the phase shifts. One recognizes easily that if the sign of all the phase shifts is changed the cross sections are not affected. It would be possible in principle to determine the signs by a study of the interference of the nuclear scattering with the Coulomb scattering. Thus far, however, measurements of the scattering at angles sufficiently close to the forward direction to observe this interference have not been carried out. Aside from this indeterminacy of the sign, one might raise the question whether the determination of phase shifts is unique. It appears that there are two fairly equivalent sets of angles that yield a rather low value of the least square sum. One of them corresponds to angles fairly close to those already published [3] and will be called "first solution." Yang has pointed out [17] that there is a second solution, that, although not equivalent to the first, is in many cases almost equally good. An extensive numerical analysis of the problem [16] has indicated that the first solution and the Yang solution are very probably the only two for which the least square sum is small. There is apparently another set of angles that yields a relative minimum of M. This, however, is so high as to make it of no practical value.

In Tables XIII and XIV are collected the cross sections for 120 Mev and for 135 Mev, together with the cross sections computed from the best sets of phase shifts. Results corresponding to the first solution and to the Yang solution are given. The agreement with the experimental results is extremely close for both solutions. Only a very considerable improvement in the experimental accuracy would permit to distinguish between the two.

(16) E. FERMI and N. METROPOLIS, Los Alamos unclassified report LA-1492, 1952 (unpublished). [See paper N° 256 (Editors' note)].

(17) C. N. YANG, private communication.

TABLE XIII.

Cross sections computed from phase shifts at 120 Mev (10^{-27} cm²/sterad).

Process	Measured cross sections	Computed	
		Firts solution	Yang solution
$-\to-$	1.06 ± 0.14	1.06	1.06
	0.47 ± 0.10	0.48	0.47
	0.97 ± 0.18	1.02	1.02
$+\to+$	4.26 ± 1.16	4.15	4.12
	5.75 ± 1.16	5.13	5.14
	16.00 ± 1.82	15.15	15.09
$-\to\gamma$	2.07 ± 0.30	2.06	2.07
	3.19 ± 0.39	3.38	3.40
	5.98 ± 0.69	6.01	6.00

PHASE SHIFTS

First solution:

$\alpha_3 = -15.2^\circ$; $\alpha_1 = 9.0^\circ$; $\alpha_{33} = 29.6^\circ$; $\alpha_{31} = 3.9^\circ$; $\alpha_{13} = 1.8^\circ$; $\alpha_{11} = -2.8^\circ$.

Yang solution:

$\alpha_3 = -15.4^\circ$; $\alpha_1 = 9.1^\circ$; $\alpha_{33} = 12.9^\circ$; $\alpha_{31} = 38.6^\circ$; $\alpha_{13} = -1.4^\circ$; $\alpha_{11} = 3.8^\circ$.

TABLE XIV.

Cross sections computed from phase shifts at 135 Mev (10^{-27} cm²/sterad).

Process	Measured cross sections	Computed	
		First solution	Yang solution
$-\to-$	1.46 ± 0.19	1.45	1.45
	0.63 ± 0.13	0.63	0.63
	1.13 ± 0.23	1.20	1.21
$+\to+$	5.66 ± 2.18	6.35	6.20
	6.75 ± 2.14	5.95	5.90
	21.64 ± 3.55	18.13	17.95
$-\to\gamma$	2.92 ± 0.38	2.85	2.85
	3.96 ± 0.47	4.07	4.11
	7.10 ± 0.82	7.40	7.36

PHASE SHIFTS

First solution:

$\alpha_3 = -14.0^\circ$; $\alpha_1 = 10.3^\circ$; $\alpha_{33} = 37.9^\circ$; $\alpha_{31} = 5.4^\circ$; $\alpha_{13} = 2.0^\circ$; $\alpha_{11} = -4.6^\circ$.

Yang solution:

$\alpha_3 = -14.2^\circ$; $\alpha_1 = 10.4^\circ$; $\alpha_{33} = 17.2^\circ$; $\alpha_{31} = 49.3^\circ$; $\alpha_{13} = -2.9^\circ$; $\alpha_{11} = 5.6^\circ$.

In figs. 9 and 10 are plotted the cross sections in the center-of-mass system *versus* the scattering angle χ. The curves are computed from the scattering angles of the first solution. Also the experimental points are put on the same graph for reference.

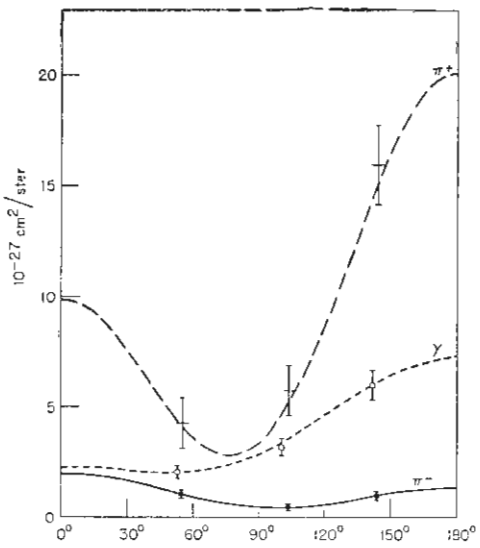

Fig. 9. – Computed and observed cross sections at 120 Mev.

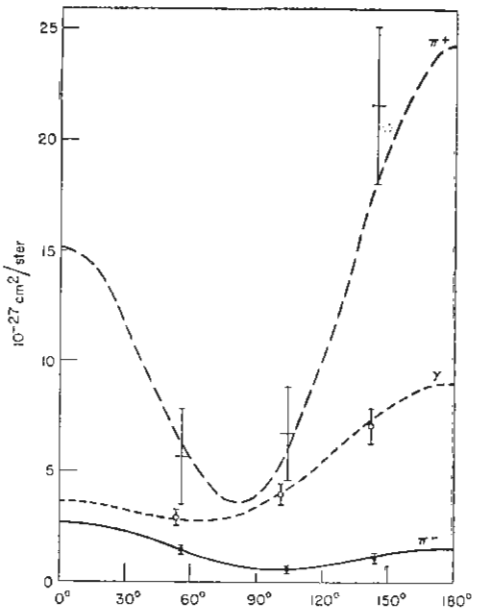

Fig. 10. – Computed and observed cross sections at 135 Mev.

As pointed out above, the sign of all the phase shifts could be changed without affecting the cross sections. The sign chosen corresponds to the assumption that the interaction of the state with both isotopic spin and angular momentum equal to $3/2$ is attractive. Some arguments in favor of this assumption have been advanced by Peaslee [18] on the basis of an analysis of the scattering of negative pions by carbon.

At 78 Mev only the scattering of positive pions has been measured and consequently only three of the phase shifts could be determined. They are $\alpha_3 = -6°$, $\alpha_{33} = 13°$, $\alpha_{31} = -3°$. Also a similar analysis can be made on the data for scattering of 53–Mev positive pions by hydrogen published by the Brookhaven group.[14] The result is $\alpha_3 = 0°$, $\alpha_{33} = 9°$, $\alpha_{31} = 2°$. In Table XV are collected the various values of the phase shifts (first solution only). The second column gives the pion momentum in the center-of-mass system in units of μc. Due to experimental errors the phase shifts given above have an uncertainty of perhaps 5°. Experience gathered in successive calculations of the phase shifts has indicated, however, that some of them appear to be not very sensitive to changes in the cross sections, whereas others

(18) Quoted by H. Bethe at the Rochester Conference, December, 1952. See also G. F. CHEW, « Phys. Rev. », *89*, 591 (1953).

have a higher sensitivity and are for this reason less reliable. This appears to be particularly true of the phase shifts α_{13} and α_{11}.

TABLE XV.

Phase shift angles.

Mev	η	Phase shifts in degrees					
		3	1	33	31	13	11
53	0.78	0		9	2		
78	0.97	— 6		13	— 3		
120	1.24	— 15	9	30	— 12	2	— 3
135	1.32	— 14	10	38	5	2	— 5

XI. CONCLUSIONS.

(1) The fact that 9 cross sections measured at each energy can be represented in terms of 6 phase shifts is a demonstration of the fruitfulness of regarding the isotopic spin as a good quantum number. Such a demonstration would be even more meaningful if the experimental errors were smaller.

(2) According to quantum mechanics one might expect that the phase shifts at sufficiently low energy should be proportional to the relative momentum η of the 2 colliding particles for s–terms and to η^3 for p–terms. In fig. 11 some of the data of Table XV are plotted. The values of η are on the abscissas and the phase shifts of isotopic spin 3/2 are plotted on the ordinates. One might expect that the phase shift α_3 should lie on a straight line through the origin. Actually the points do not at all show this property and this may or may not be due to the rather large experimental error. If one attempts to draw the " best " straight line through these points the coefficient of η would be approximately —10°. On the other hand, the points suggest an appreciably stronger dependence of α_3 on the energy. This in fact would be quite compatible with the possibility that α_3 may actually change sign at about 60 Mev, a possibility whose implications have been discussed by Marshak.[19] The ratio α_3/η at low energy gives the scattering length in units $\hbar/\mu c$. A coefficient of — 10° would correspond to a scattering length $a_3 = -0.24 \times 10^{-13}$. However, this value for the reasons explained is quite tentative and even its sign could be wrong. Similarly from the data of Table XV we may make an equally tentative guess that the scattering length of the s–state of isotopic spin 1/2 may be 0.18×10^{-13} cm.

The phase shifts α_{33} fit fairly well a proportionality to η^3 with a coefficient of about 16°. Very little can be said of the energy dependence of the other

(19) R. E. MARSHAK, « Phys. Rev. », *88*, 1208 (1952).

phase shifts α_{31}, α_{13}, and α_{11} which are so small that even their sign relative to that of the other phase shifts is uncertain with our present experimental accuracy.

(3) We have already commented on the difficulties of deciding experimentally with our present accuracy between the phase shifts corresponding to the first solution and to the Yang solution of the problem. The previous conclusions are obtained on the assumption that the first solution is correct and would have to be modified appreciably if the Yang solution ultimately would turn out to be the right one. Similarly the over-all sign of the phase shifts is uncertain, and the opposite sign to the one chosen here may well be correct.

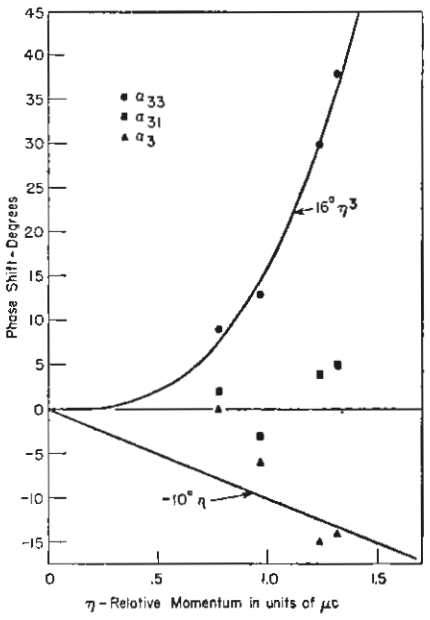

Fig. 11. – Phase shifts plotted *versus* relative momentum.

(4) One might attempt to interpret phenomenologically the scattering as if it were due to a force acting between the nucleon and pion. Inspection of the variety of phase shifts obtained indicates immediately that this force should be quite different for different states. Assuming again the first solution to be correct, one would further conclude that the force is very large for the state of isotopic spin 3/2 and angular momentum 3/2. One can recognize that the same potential produces a much larger phase shift in the s terms than it does in the p–terms. For example, phase shifts of the order of magnitude observed could be attributed to a potential of radius $\hbar/\mu c$ and of a magnitude of about 40 Mev for the s terms, while the depth of this potential hole should be of the order of several hundred Mev in order to produce a phase shift α_{33} of the observed magnitude. It is very questionable whether it is rewarding to adopt this potential model without a thorough study of its relativistic behavior.

(5) From partial evidence on the scattering of pions by hydrogen previously reported,[8] a tentative conclusion had been reached that the states of isotopic spin 3/2 are dominant. If this were exactly correct one would expect the cross sections for scattering of positive pions and for scattering of negative pions with and without charge exchange to be in the ratio 9 : 2 : 1 in all directions. That this is not so, is evident from a direct inspection of the cross sections which shows that the angular distribution for the scattering of positive pions and that of negative pions with charge exchange is mostly backward, whereas the elastic scattering of negative pions is mostly forward. Apparently this difference in angular distribution is due primarily to the phase shift α_1 of isotopic spin 1/2 which is the largest phase shift with isotopic spin different from 3/2.

On the assumption that the first solution is correct, the largest phase shift is α_{33} corresponding to a state for which the existence of a resonance has been suspected.[20] Our data do not extend far enough in energy to support the resonance hypothesis. If the hypothesis were correct, one would expect that at some higher energy the phase shift α_{33} should rise appreciably more rapidly than with the η_i^3 law and rather rapidly cross over from values less to values larger than 90°. It is possible, however, that α_{33} may go through a maximum and start decreasing before reaching 90°.

(6) The present experimental data are utterly inadequate to allow any conclusions to be drawn about the *d* terms, which have been neglected in our analysis. If the interaction of the *d* levels were of the order of magnitude μc^2, the phase shifts would be a fraction of a degree. This makes our neglect of the *d*–terms justifiable but not necessarily correct.

This work could not have been carried out without the active cooperation and advice of Professor Earl A. Long. We thank him and Dr. Lothar Meyer for generous supplies of liquid hydrogen. Mr. Gaurang B. Yodh and Mr. Maurice Glicksman took an active part in the work of preparing the experimental equipment and carrying out the measurements; we are indebted to them for their time and skill. Mr. Leo Slattery contributed to the development of the electronic equipment. We are particularly grateful to Mr. Lester Kornblith for the efficient operation of the cyclotron.

(20) K. A. BRUECKNER, « Phys. Rev. », *86*, 106 (1952).

N° 258.

For the introduction to this paper see paper N° 257.

258.

NUCLEON POLARIZATION IN PION PROTON SCATTERING (*)

« Phys. Rev. », *91*, 947–948 (1953).

The polarization of the recoiling nucleons after the scattering of a pion by a nucleon is calculated. It is found that the recoiling nucleons are polarized in a direction perpendicular to the scattering plane and that the intensity ratio for spin parallel or antiparallel to this direction in several cases is quite large. Simple formulas are given for computing the polarization as a function of the scattering angle in terms of the phase shifts.

When a pion is scattered by hydrogen, the recoiling proton will be polarized with the spin oriented preferentially in a direction perpendicular to the plane in which the scattering takes place. The purpose of this paper is to calculate the amount of polarization to be expected.

In this discussion, we will take as a basis the analysis of the scattering process in terms of phase shifts, (1) and in particular, we will assume that only the phase shifts of the s and p waves will be important. We consider first the scattering of positive pions. The primary pion wave $\exp(ikz)$ may be scattered by a proton with spin up or with spin down. Let α and β be the proton spin wave functions corresponding to the two cases. If initially the proton has spin up (α state), the scattered wave contains a superposition of states with spin up and with spin down. We can write, therefore, this scattered wave as follows:

$$S_{\alpha\alpha}\,\alpha + S_{\alpha\beta}\,\beta, \tag{1}$$

where $S_{\alpha\alpha}$ is the scattering amplitude for the wave with spin up and $S_{\alpha\beta}$ for the wave with spin down. Similarly, if the spin was initially down (β state), the scattered wave will be

$$S_{\beta\alpha}\,\alpha + S_{\beta\beta}\,\beta. \tag{2}$$

(*) Research supported by a joint program of the U. S. Office of Naval Research and the U. S. Atomic Energy Commission.

(1) ANDERSON, FERMI, NAGLE, and YODH, « Phys. Rev. », *86*, 793 (1952); ANDERSON, FERMI, MARTIN, and NAGLE, « Phys. Rev. », *91*, 155 (1953), quoted as A. [See papers N° 253 and 257 (Editors' note)].

By straightforward application of the scattering theory,[2] one can express the scattering amplitudes S as follows:

$$S_{\alpha\alpha} = S_{\beta\beta} = f(r)\{e_3 + (2e_{33} + e_{31})\cos\theta\}, \tag{3}$$

$$S_{\alpha\beta} = f(r)(e_{31} - e_{33})\sin\theta\, e^{i\varphi}, \tag{4}$$

$$S_{\beta\alpha} = -f(r)(e_{31} - e_{33})\sin\theta\, e^{-i\varphi}. \tag{5}$$

The notation is the same as in A. The quantities e_3, e_{33}, e_{31} are expressed in terms of phase shifts by

$$e_3 = e^{2i\alpha_3} - 1 \quad , \quad e_{33} = e^{2i\alpha_{33}} - 1 \quad , \quad e_{31} = e^{2i\alpha_{31}} - 1. \tag{6}$$

α_3 is the phase shift of the s wave; α_{33} and α_{31} are the phase shifts of the p waves of the angular momentum $3/2$ and $1/2$, respectively. All these phase shifts belong to the isotopic spin $3/2$ because in the scattering of positive pions by protons this is the only isotopic spin state. The function $f(r)$ is

$$f(r) = \exp(ikr)/(2ikr). \tag{7}$$

θ and φ are the polar angles defining the direction of the scattered pion in the center-of-mass system. We shall consider a scattering process in which the pion is scattered in the x, z plane corresponding to $\varphi = 0$. In this case, from (4) and (5) one has $S_{\alpha\beta} = -S_{\beta\alpha}$. If the spin of the proton before collision is down, the scattering wave given by (2) becomes then

$$-S_{\alpha\beta}\,\alpha + S_{\alpha\alpha}\,\beta. \tag{8}$$

If the protons against which the collision takes place are nonpolarized, there will be 50 percent probability that the initial spin is α and 50 percent probability that it is β. In the two cases the scattered waves shall be (1) and (8). It is clear from these formulas that the probability that the spin after the scattering is α is 50 percent; that is, the scattering will produce no polarization in the z direction as is otherwise evident for reasons of symmetry. Similarly, one would find that there is no polarization of the scattered proton in any direction parallel to the x, z plane.

One finds, however, a polarization in the direction y perpendicular to the scattering plane. The amount of polarization can be obtained immediately by analyzing the scattered waves (1) and (8) in terms of the spin eigenfunctions,

$$\gamma = (\alpha + i\beta)/\sqrt{2} \quad \text{and} \quad \delta = (\alpha - i\beta)/\sqrt{2}, \tag{9}$$

corresponding to spin parallel or antiparallel to the y direction. If the initial spin was α, the scattered wave (1) can be written

$$\frac{1}{\sqrt{2}}(S_{\alpha\alpha} - iS_{\alpha\beta})\gamma + \frac{1}{\sqrt{2}}(S_{\alpha\alpha} + iS_{\alpha\beta})\delta. \tag{10}$$

(2) See, for example, C. L. CRITCHFIELD and D. C. DODDER, « Phys. Rev. », *76*, 602 (1949).

In this case the probabilities that the spin is parallel or antiparallel with respect to y after the scattering are, therefore, proportional to

$$(11) \qquad |S_{\alpha\alpha} - iS_{\alpha\beta}|^2 \quad \text{and} \quad |S_{\alpha\alpha} + iS_{\alpha\beta}|^2.$$

Similarly, if the initial spin was β, the scattered wave (8) can be analyzed in terms of γ and δ and one finds that also for this case the probabilities for the resultant spin to be parallel or antiparallel to the y direction are proportional to the expressions (11). Observe that these two probabilities in general will be different because $S_{\alpha\alpha}$ and $S_{\alpha\beta}$ are complex quantities.

Substituting in (11) the expressions (3) and (4) with $\varphi = 0$, one finds that the probabilities that the scattered proton has spin parallel or antiparallel to y are proportional to

$$(12) \qquad I_{\pm} \sim |e_3 + (2e_{33} + e_{31})\cos\theta \mp i(e_{31} - e_{33})\sin\theta|^2,$$

where the upper sign corresponds to spin parallel and the lower sign corresponds to spin antiparallel to y. The degree of polarization will, therefore, depend on the scattering angle.

For ample, the scattering of 120–Mev pions on protons has been interpreted in A in terms of a set of phase shifts,

$$(13) \qquad \begin{cases} \alpha_3 = -15.2^\circ \;, & \alpha_1 = 9.0^\circ \;, & \alpha_{33} = 29.6^\circ, \\ \alpha_{31} = 3.9^\circ \;, & \alpha_{13} = 1.8^\circ \;, & \alpha_{11} = -2.8^\circ. \end{cases}$$

Substituting these phase angles in (12), one obtains

$$(14) \qquad I_{\pm} \sim 1 - 1.56\cos\theta + 3.56\cos^2\theta \mp (0.66 - 0.34\cos\theta)\sin\theta.$$

For example, for $\theta = 90^\circ$, this formula gives $I_+ = 1.66$ and $I_- = 0.34$. The ratio of the intensities polarized in opposite directions is therefore almost 5.

The phase shifts (13) are not the only set that is compatible with the experiments. A second set can be obtained by changing the signs of all the phase shifts. Such a change does not affect the cross sections except at very small scattering angles where the interference with the Coulomb scattering becomes appreciable. On the other hand, changing the sign of the phase shifts has the effect of inverting the polarization direction, as one can see immediately from (12) and (6). Therefore, if it were possible to observe the polarization of the recoil protons, one could immediately decide which is the appropriate sign of the phase shifts.

In addition to the indeterminacy of the signs, there is another set of angles that was given in A which represents the experimental data with about the same accuracy as the angles (13). This is the set of the Yang phase angles which are

$$(15) \qquad \begin{cases} \alpha_3 = -15.4^\circ \;, & \alpha_1 = 9.1^\circ \;, & \alpha_{33} = 12.9^\circ, \\ \alpha_{31} = 38.6^\circ \;, & \alpha_{13} = -1.4^\circ \;, & \alpha_{11} = 3.8^\circ. \end{cases}$$

Also for this case one can compute the intensities I_+ and I_- of the scattered protons polarized parallel and antiparallel to the y direction, and one finds

that they are

$$(16) \qquad I_{\pm} = 1 - 1.56 \cos\theta + 3.49 \cos^2\theta \mp (0.82 - 1.40 \cos\theta) \sin\theta.$$

The polarization for the Yang solution differs appreciably from the one corresponding to the phase angles (13), so that again observation of the polarization might permit a discrimination between these two sets of phase shifts.

We give now similar numerical results for the polarization produced in the scattering of negative pions by protons. In this case we must distinguish between the elastic scattering in which the recoiling nucleon is a proton and the charge exchange scattering in which the recoiling nucleon is a neutron. In the former case one obtains the polarization from a formula like (12) in which, however, e_3, e_{33}, and e_{31} are replaced by

$$(e_3 + 2e_1)/3 \quad , \quad (e_{33} + 2e_{13})/3, \quad \text{and} \quad (e_{31} + 2e_{11})/3.$$

For the case of the exchange scattering again the polarization of the recoiling neutron is obtained from a formula similar to (12) with the substitution of

$$\sqrt{2}\,(e_3 - e_1)/3 \quad , \quad \sqrt{2}\,(e_{33} - e_{13})/3, \quad \text{and} \quad \sqrt{2}\,(e_{31} - e_{11})/3,$$

in place of e_3, e_{33}, and e_{31}. Assuming the phase shift angles (13), one finds at 120 Mev the following polarization formulas: For elastic scattering,

$$I_{\pm} = 1 + 0.65 \cos\theta + 2.42 \cos^2\theta \pm (0.28 + 0.21 \cos\theta) \sin\theta.$$

For the recoil neutron in the exchange scattering the corresponding formulas are

$$I_{\pm} = 1 - 2.30 \cos\theta + 3.06 \cos^2\theta \pm (0.72 - 0.54 \cos\theta) \sin\theta.$$

If one assumes the phase angles (15) instead of (13), the polarization for elastic scattering is

$$I_{\pm} = 1 + 0.67 \cos\theta + 2.47 \cos^2\theta \mp (0.20 - 0.62 \cos\theta) \sin\theta.$$

For the exchange scattering, one finds

$$I_{\pm} = 1 - 2.22 \cos\theta + 2.87 \cos^2\theta \mp (0.92 - 1.37 \cos\theta) \sin\theta.$$

In many cases the polarization effect according to these formulas are very large and their observation, if possible, would offer an interesting method for improving our knowledge of the scattering of pions by nucleons.

N° 259.

Fermi did one final experiment on the pion scattering. He needed more data for the next summer's phase shift analysis he wanted to do at Los Alamos. I was recuperating from a long and difficult illness and did not participate in this work.

H. L. ANDERSON.

259.

SCATTERING OF NEGATIVE PIONS BY HYDROGEN (*)

E. FERMI, M. GLICKSMAN, R. MARTIN, and D. NAGLE (**)
Institute for Nuclear Studies, University of Chicago, Chicago, Illinois
(Received June 24, 1953)
« Phys. Rev. », *92*, 161–163 (1953).

The scattering of negative pions by liquid hydrogen has been studied with the 450-Mev synchrocyclotron, using the pion beams of energy 169 Mev, 194 Mev, and 210 Mev. Angular distributions for ordinary scattering and for photon production are presented for each of the three primary energies. The differential cross sections for ordinary scattering and for charge-exchange scattering are computed for the center-of-mass system. The charge-exchange cross sections when plotted as a function of the energy appear to go through a maximum at about 180 Mev. On the other hand, the ordinary scattering cross sections appear to increase steadily with the energy. The charge exchange cross sections, which at lower energies are predominantly backward, become rapidly forward as the energy increases, and are strongly forward at the highest energy.

The scattering of negative pions by hydrogen has been investigated in this laboratory using the pion beams of the 450-Mev synchrocyclotron. In the present paper, the results of previous measurements [1] are extended to a higher energy range. With our present technique this is possible only for negative pions because the intensity of the external positive pion beams from the cyclotron becomes extremely small at high energy. In the work here reported, the elastic and the charge-exchange scattering of negative pions on hydrogen have been investigated for primary pion beams of 169 Mev, 194 Mev, and 210 Mev. The equipment and the experimental technique used in this measurement are essentially the same as those already described in A.

(*) Research supported by a joint program of the U. S. Office of Naval Research and the U. S. Atomic Energy Commission.

(**) Aided by a grant from the Guggenheim Foundation.

(1) ANDERSON, FERMI, MARTIN, and NAGLE, « Phys. Rev. », *91*, 155 (1953), quoted here as A. [See paper N° 257 (Editors' note)].

A beam of pions of the desired energy passes through two scintillation counters No. 1 and No. 2 and after that traverses a thin-walled liquid hydrogen Dewar. The scattered particles are detected by two other counters No. 3 and No. 4. The double coincidences of No. 1 and No. 2, indicated by D, give a measure of the number of primary particles. The quadruple coincidences of the four counters, indicated by Q, give a measure of the number of scattered particles that are detected by the detecting counters No. 3 and No. 4. For an average rate of cyclotron operation corresponding to 20 watts on the target, the double coincidences per minute were approximately 190,000 at 169 Mev, 53,000 at 194 Mev, and 35,000 at 210 Mev.

For the details and geometry of this arrangement, we refer to Sec. I of A. One difference in the present experiments was in the construction of counters No. 1 and No. 2, which had the same diameter of 2 in. as in A, but were much thinner. Counter No. 1 in these experiments was a liquid scintillator with an over-all thickness of 1/4 in., and counter No. 2 was a plastic scintillator 1/8 in. thick. The background due to star production from the collisions with counter No. 2 is thereby reduced very considerably. In the previous experiments the thickness of the detecting counters was sufficient to prevent the detection of the recoil protons even for the measurements at 45° scattering angle. In the present measurements at higher energies, it was necessary in some cases to insert some additional absorber in front of counter No. 4 in order to make sure that no recoil protons could be detected. Such additional absorbers were used only in the measurements at 194 Mev and 210 Mev and only for scattering angle of 45°. In the measurements at 194 Mev an extra absorber of 5/8–in. aluminum was inserted in the runs without lead radiator. In the measurements at 210 Mev, an extra absorber of 1/8–in. aluminum was used when the lead radiator was in place; without lead radiator, the extra absorber was 7/8–in. aluminum. Otherwise the procedure followed in the calculation and reduction of the data is identical to the one described in Sec. VII of A.

Scattering measurements are taken for the laboratory scattering angles 45°, 90°, and 135° and at each position four measurements of the ratio Q/D between quadruple and double coincidences are taken with and without liquid hydrogen in the Dewar and with and without a lead plate of 7.36 g/cm² placed in front of counter No. 3. The difference of the measurements with and without liquid hydrogen is taken as the effect due to the presence of the liquid hydrogen. The lead plate increases the sensivity of the detecting counters to the photons produced in the decay of the neutral pions in the charge exchange process. Table I summarizes the observed values of the ratio Q/D obtained in the present measurements. This table is the analog of Table VI of A.

In order to compute from the data of this table the numbers of scattered pions and photons entering the detecting counters No. 3 and No. 4, one needs the efficiencies with and without lead radiator for the two types of particles. The procedure for calculating these efficiencies is described in Sec. VIII of A. The only difference is the extra absorption due to the aluminum absorbers which were put in some of the measurements in front of counter No. 4 in order

to stop all the recoil protons. The efficiencies adopted in the calculation are summarized in Table II.

TABLE I.

Observed values of $(Q/D)\times 10^6$ *for negative pions.*

Angle	Lead	169 Mev (94 % pions)		Net
		With hydrogen	Without hydrogen	
45°	out	269.4 ± 7.9	141.7 ± 5.1	127.7 ± 9.4
90°	out	100.8 ± 4.3	60.5 ± 3.6	40.3 ± 5.7
135°	out	160.9 ± 5.4	83.2 ± 4.1	77.7 ± 6.8
45°	in	488.8 ± 11.1	121.5 ± 5.1	367.3 ± 12.1
90°	in	243.4 ± 6.7	58.8 ± 3.5	184.6 ± 7.6
135°	in	303.8 ± 7.4	77.4 ± 4.0	226.4 ± 8.4
		194 Mev (96 % pions)		
45°	out	295 ± 11	137 ± 8	158 ± 14
90°	out	112 ± 6	53 ± 4	59 ± 7
135°	out	176 ± 8	91 ± 5	85 ± 9
45°	in	638 ± 15	169 ± 9	469 ± 18
90°	in	278 ± 10	63 ± 6	215 ± 12
135°	in	344 ± 6	92 ± 6	252 ± 8
		210 Mev (98 % pions)		
45°	out	288 ± 14	121 ± 8	167 ± 16
90°	out	146 ± 9	72 ± 6	74 ± 11
135°	out	171 ± 11	89 ± 7	82 ± 13
45°	in	633 ± 20	155 ± 9	478 ± 22
90°	in	222 ± 12	63 ± 6	159 ± 14
135°	in	263 ± 13	93 ± 7	170 ± 15

For each primary energy and each scattering angle, one computes with these efficiencies, from the data of Table I, the numbers Π and Γ of pions and photons entering the solid angle subtended by counter No. 4. This is done by solving two equations with two unknowns as described in A.

The numbers Π and Γ can immediately be converted to cross sections per steradian for the two processes. In order to do this, they must be divided by the product of the following factors: (a) the number of pions per million

doubles. This number was obtained as in A, from a study of the absorption curve. The percentage of pions in the beam of the various energies is given in Table I. (b) The solid angle subtended by counter No. 4. This was as in A, 0.083 steradians. (c) The number of hydrogen atoms per cm^2 traversed by the beam. As in A, this number was 5.9×10^{23}. (d) A correction factor due to the attenuation of the primary beam while traversing the hydrogen cell. For the three energies these correction factors were estimated to be 0.988, 0.986, and 0.990.

TABLE II.

Efficiencies of the detecting counters.

Energy (Mev)	Angle	Lead	Efficiency for pions (percent)	Efficiency for photons (percent)
169	45°	out	97	4
	45°	in	92	71
	90°	out	97	4
	90°	in	90	64
	135°	out	97	4
	135°	in	89	61
194	45°	out	92	4
	45°	in	92	72
	90°	out	97	4
	90°	in	91	66
	135°	out	97	4
	135°	in	90	62
210	45°	out	90	4
	45°	in	91	73
	90°	out	97	4
	90°	in	91	67
	135°	out	97	4
	135°	in	91	63

The differential cross sections so obtained and their conversions to the center-of-mass system are collected in Table III. The errors listed in this table are compounded out of the statistical error plus a 10 percent error that

we estimate may be due to our imperfect knowledge of the sensitivity of the detecting equipment.

TABLE III.

Differential cross sections for negative pions.

Energy (Mev)	Process	Laboratory system		Center-of-mass system	
		Scattering angle (degrees)	Diff. cross section (10^{-27} cm^2/sterad)	Scattering angle (degrees)	Diff. cross section (10^{-27} cm^2/sterad)
169	$\pi^- \to \pi^-$	45	2.56 ± 0.35	56.6	1.82 ± 0.25
		90	0.69 ± 0.16	105.4	0.73 ± 0.17
		135	1.51 ± 0.22	145.2	2.31 ± 0.34
169	$\pi^- \to \gamma$	45	8.05 ± 0.94	54.9	6.05 ± 0.71
		90	5.37 ± 0.63	102.8	5.65 ± 0.66
		135	5.95 ± 0.72	143.4	8.37 ± 1.01
194	$\pi^- \to \pi^-$	45	3.28 ± 0.50	57.3	2.30 ± 0.35
		90	1.08 ± 0.20	106.0	1.16 ± 0.21
		135	1.62 ± 0.27	145.6	2.54 ± 0.42
194	$\pi^- \to \gamma$	45	9.87 ± 1.23	55.6	7.24 ± 0.90
		90	5.53 ± 0.74	103.7	5.87 ± 0.79
		135	6.41 ± 0.77	143.9	9.29 ± 1.12
210	$\pi^- \to \pi^-$	45	3.49 ± 0.53	57.9	2.43 ± 0.37
		90	1.47 ± 0.29	106.7	1.59 ± 0.31
		135	1.64 ± 0.36	146.0	2.61 ± 0.57
210	$\pi^- \to \gamma$	45	9.43 ± 1.27	56.1	6.83 ± 0.92
		90	2.99 ± 0.66	104.4	3.19 ± 0.70
		135	3.31 ± 0.77	144.4	4.88 ± 1.14

From the differential cross sections in the laboratory system one obtains immediately by integration the total cross sections listed in Table IV. In columns 2 and 3 are given the total cross sections for elastic scattering and for the photon producing process. The contribution of this last process to the total cross section is only half the cross section listed in column 3, because each disintegrating neutral pion yields two photons. For this reason, the total cross sections given in column 4 are obtained by adding half the cross section for photon production to the elastic scattering cross section. A small

amount of approximately 0.5 mb has been added in order to take into account the contribution of the inverse photoeffect. In the last column the values of the total cross section from transmission experiments are listed for comparison. They are obtained by interpolation from data already published.[2]

TABLE IV.

Integrated cross sections of negative pions (10^{-27} cm^2).

Energy (Mev)	$\pi^- \to \pi^-$	$\pi^- \to \gamma$	Total	Total from transmission
169	21.2 ± 2.0	82.8 ± 5.9	63 ± 4	64 ± 6
194	26.4 ± 2.7	93.9 ± 7.2	74 ± 5	66 ± 6
210	28.7 ± 3.1	69.1 ± 7.2	64 ± 5	61 ± 6

On the assumption that only s and p levels contribute to the interaction, one expects that all the cross sections in the center-of-mass system should be of the form

$$a + b \cos \vartheta + c \cos^2 \vartheta. \tag{1}$$

The assumption that the contribution of d scattering is negligible becomes, of course, less and less plausible as the energy increases and it is very questionable whether it is correct for pions of approximately 200 Mev. A check on this assumption and formula (1) that derives from it would require a more thorough study of the angular dependence of the scattering than has been possible until now. Assuming formula (1) to be correct, one can compute from the data of Table III the values of the coefficients a, b, and c that represent the experimental data. These values are collected in Table V.

CONCLUSIONS.

In fig. 1 we have plotted the observed differential cross sections in the laboratory system listed in Table III *versus* the energy of the primary pions. For comparison also the cross sections obtained in A at the energies of 120 and 144 Mev have been included. Examination of this figure shows a rather striking difference in behavior of the cross sections for the elastic scattering and for the photon producing process. The former cross sections increase steadily with energy without any apparent sharp feature. On the other hand, the cross sections for photon production appear to go through a maximum at approximately 180 Mev. A second feature of these cross sections is the

(2) ANDERSON, FERMI, LONG, MARTIN, and NAGLE, « Phys. Rev. », *85*, 934 (1952). [See paper N° 248 (Editors' note)].

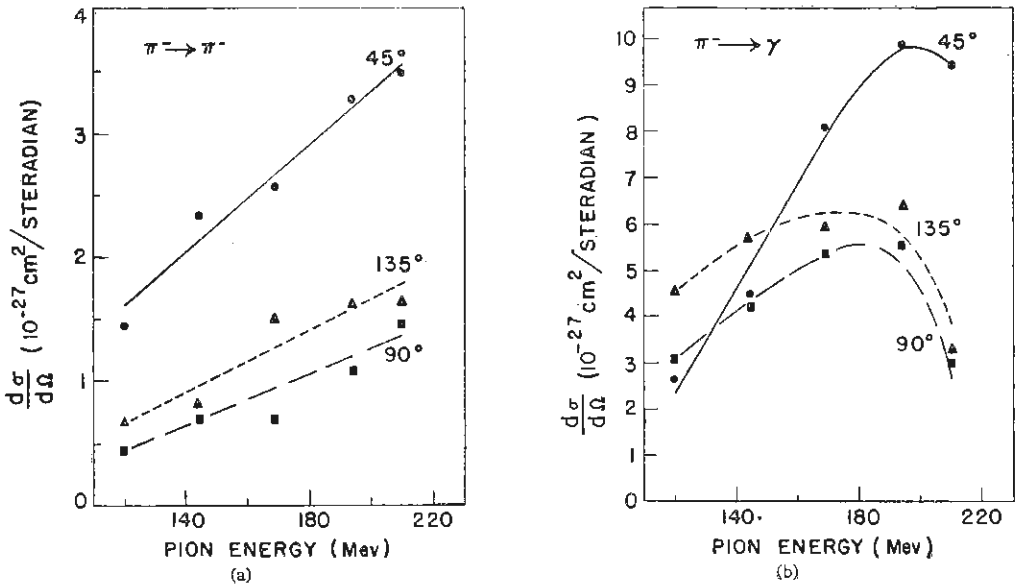

Fig. 1. Differential cross sections in the laboratory system for negative pions on hydrogen as functions of the primary pion energy.

(a) Elastic Scattering. The threes curves correspond to laboratory scattering angle 45°, 90°, and 135°. The curves are graphical interpolations of the data. (b) Cross sections for photon production at the same angles.

very rapid increase of the forward cross section with respect to the others. Due to this increase, the scattering which is mostly backward at the low energies becomes mostly forward at the high energies. This feature is recognizable also from the data of Table V which show a change in sign from negative to positive in the coefficient b for the exchange scattering.

TABLE V.

Coefficients of $\frac{d\sigma}{d\omega} = a + b\cos\vartheta + c\cos^2\vartheta$ *for various processes* (10^{-27}cm^2/sterad).

Energy (Mev)	$\lambda\!\!\!^{-}$ (10^{-13}cm)	Process	a	b	c
169	0.928	$-\rightarrow-$	0.64 ± 0.19	0.47 ± 0.29	3.04 ± 0.62
		$-\rightarrow\gamma$	5.28 ± 0.69	-0.84 ± 0.86	3.76 ± 2.00
		$-\rightarrow 0$	1.85 ± 0.72	-0.61 ± 0.62	4.25 ± 2.27
194	0.856	$-\rightarrow-$	1.12 ± 0.24	0.65 ± 0.40	2.87 ± 0.80
		$-\rightarrow\gamma$	5.53 ± 0.83	-0.13 ± 1.06	5.59 ± 2.48
		$-\rightarrow 0$	1.73 ± 0.80	-0.09 ± 0.74	5.89 ± 2.61
210	0.817	$-\rightarrow-$	1.56 ± 0.34	0.50 ± 0.47	2.14 ± 1.09
		$-\rightarrow\gamma$	3.55 ± 0.75	2.82 ± 1.06	5.48 ± 2.28
		$-\rightarrow 0$	0.84 ± 0.70	1.94 ± 0.73	5.56 ± 2.31

N° 260.

In the summer of 1953 Fermi returned to Los Alamos to feed his data to the electronic computer. The publication of the phase shift analysis which he did then with N. Metropolis and E. Alei was delayed somewhat: after he left Los Alamos at the end of the summer, the work was expanded and extended by de Hoffmann, Metropolis, Alei and Bethe (« Phys. Rev. », *95*, 1586 (1954)) using new data that began to emerge from other laboratories, and the two papers were published together. The solution obtained by Fermi gave the phase shift α_{33} non-resonant, which turned out to be not correct.

H. L. ANDERSON.

260.

PHASE SHIFT ANALYSIS OF THE SCATTERING OF NEGATIVE PIONS BY HYDROGEN (*)

E. FERMI, *Institute of Nuclear Studies, University of Chicago, Chicago, Illinois*
and
N. METROPOLIS and E. F. ALEI, *Los Alamos Scientific Laboratory, Los Alamos, New Mexico.*

(Received May 6, 1954)
« Phys. Rev. », *95*, 1581–1585, (1954).

A phase shift analysis of the scattering of negative pions by hydrogen in the range 115 to 215 Mev is presented. In the present paper two solutions are given that represent the data within the experimental error by two rather different sets of phase shifts. One of these solutions is excluded on the basis of some information on the scattering of positive pions. The other solution is compatible with all the experimental data known at present. It is pointed out, however, that this is not the only solution that has such properties. In addition, calculations carried out on scattering of positive and negative pions at 61.5 Mev are presented.

I. INTRODUCTION.

This paper describes some systematic attempts to analyze in terms of phase shifts the experimental data on pion-hydrogen scattering.[1,2] Two essentially independent calculations are described. Part I is concerned with the analysis of the experimental results of B on the scattering of negative

(*) Research supported by a joint program of the U. S. Office of Naval Research and the U. S. Atomic Energy Commission.

(1) ANDERSON, FERMI, MARTIN, and NAGLE, « Phys. Rev. », *91*, 155 (1953), quoted as A; FERMI, GLICKSMAN, MARTIN, and NAGLE, « Phys. Rev. », *92*, 161 (1953), quoted as B. [See papers N° 257 and 259 (Editors' note)].

(2) BODANSKY, SACHS, and STEINBERGER, « Phys. Rev. », *90*, 997 (1953); *93*, 918, 1367 (1954).

pions in the energy range 115 to 215 Mev. These calculations that are now being published have been completed during the spring and summer of 1953 and have been circulated privately. In the intervening period there have been a number of other attempts at interpreting essentially the same data.[3]

We refer to fig. 1 of B where the experimental results are summarized. From this figure one can see that the charge exchange apparently goes through a maximum somewhat below 200 Mev, and also that at about the same energy the angular distribution of this process changes from being mostly backward to being mostly forward. It has been suggested [4] that some features of the pion-nucleon scattering and of the pion photoeffect may indicate the existence of a resonance level in a state of isotopic spin 3/2 and ordinary spin 3/2 at approximately this energy. The features of the negative pion scattering in the vicinity of 200 Mev might be due to the effect of this hypothetical resonance level. For this reason it appeared worthwhile to see whether a phase shift analysis of the data would support the hypothesis of the existence of such a level. The solutions obtained in the present paper do not show this resonance level; however, solutions that are compatible with the existence of such a resonance are quoted in reference 3.

In Sec. IV we describe the phase shift calculations carried out on the experimental data of Bodansky, Sachs, and Steinberger [2] at 61.5 Mev. These authors suggested that we analyze their data to confirm their earlier calculations and to search for other solutions, as well as to determine the sensitivity of the analysis to small deviations in the phase shifts. We are indebted to them for the preparation of the data and for several useful discussions. For these relatively low pion energies, it is necessary to include a term corresponding to the Coulomb scattering.

After this work was completed, a preprint of a paper by Homa, Goldhaber, and Lederman [5] was received. In this work some results on the scattering of positive pions by hydrogen at 151 and 188 Mev are given. Other results on total cross sections of positive pions have been reported by Ashkin, Blaser, Stern, Gorman, and Feiner.[6] The relationship of these results with the results of the present calculation will be discussed at the end of this paper.

There are two reasons why a phase shift analysis of the experimental data presented in B is not very reliable. One is that only experimental results on the scattering of negative pions were available when this calculation was undertaken. Therefore there is no check of a set of phase shifts on the joint behavior of positive and negative pions. The second is that with our present experimental information it is impossible to include in the phase shift analysis

(3) M. GLICKSMAN, « Phys. Rev. », *94*, 1335 (1954); R. MARTIN, this issue [« Phys. Rev. », *95*, 1583 (1954)]; and in particular DE HOFFMANN, METROPOLIS, ALEI, and BETHE, following paper [« Phys. Rev. », *95*, 1586 (1954)], where the calculations presented in this paper are extended and attempts are made to choose one out of several possible solutions.

(4) K. A. BRUECKNER, « Phys. Rev. », *86*, 106 (1952).

(5) HOMA, GOLDHABER, and LEDERMAN, « Phys. Rev. », *93*, 554 (1954).

(6) ASHKIN, BLASER, STERN, GORMAN, and FEINER, quoted by Ashkin at the Fourth Annual Rochester Conference on High Energy Nuclear Physics, January 1954 (University of Rochester Press, Rochester, to be published).

any contribution of the d levels. Neglecting the d–level phase shifts is probably allowable at low energies, but becomes less plausible at higher energies where the relative de Broglie wavelength of the pion-nucleon system becomes appreciably smaller than the Yukawa radius.

For these reasons, the phase shift analysis of the Chicago data here presented may be seriously in error. It should be noted that the ambiguity is somewhat reduced by the fact that some results on the positive pion cross section have now become available, but even when these data are included some considerable ambiguity remains in the interpretation. These ambiguities are discussed in the following paper [3] where an attempt is made to arrive at the choice between the various possibilities on the basis of certain theoretical hypotheses.

II. The Mathematical Problem.

The general procedure followed in the computation of the phase shifts for the s– and p–waves has already been described in A.[1] We elaborate on that discussion and remark on two variants in the method; the simplification for the analysis of the Columbia data [2] at lower energy is also discussed. At a given energy the differential cross sections for all the scattering processes,

$$\pi^+ \to \pi^+, \quad \pi^- \to \pi^-, \quad \text{and} \quad \pi^- \to \pi^0 \to 2\gamma, \tag{1}$$

are expressed in terms of the six phase shift angles of the s– and p–waves of isotopic spins $3/2$ and $1/2$. For these six angles, we use the same notation of A and we indicate them by α_3, α_1, α_{33}, α_{31}, α_{13}, α_{11}. In the phase shift calculations described in A, differential cross sections were available for the three processes (1), each measured at three different angles.

At a point in the six-dimensional space of the phase shifts, one can compute the above-mentioned nine cross sections using the formulas given in A (Sec. X). Then one can evaluate the function

$$M(\alpha_3, \alpha_1, \alpha_{33}, \alpha_{31}, \alpha_{13}, \alpha_{11}) = \sum_{i=1}^{9} \left(\frac{\Delta i}{\varepsilon_i}\right)^2, \tag{2}$$

where Δ_i is the difference between the experimentally measured and the computed cross section, and ε_i is the corresponding experimental error. The value of M is a measure of the approximation to the nine experimental data. The mathematical problem then is to explore the six-dimensional space for the minimum (or minima) of the function M.

With the use of the Los Alamos electronic computer, the MANIAC, two methods were used. In the first, one starts at some point and proceeds along the first coordinate axis, α_3, in steps of, say, $1/2°$ until a minimum is reached. Then one moves along the second axis, and so on, until no further improvement is found. The completed procedure is refined by using a smaller step of $1/16°$. In the second method, one first computes the gradient and then proceeds along that direction until a minimum is found. There the

gradient is again computed and the process repeated until a (relative) minimum is found. In general, the second method is faster, although in certain instances this was not so, simply because the computation of the gradient is relatively time-consuming.

Under the assumptions stated in A, the differential cross sections may be written

$$\frac{d\sigma_n}{d\omega} = a_n + b_n \cos\chi + c_n \cos^2\chi , \tag{3}$$

where n corresponds to the three processes (1), and χ is the scattering angle in the center-of-mass system. The coefficients a_n, b_n, c_n are the quantities that are first evaluated for a set of phase shifts. By means of Eq. (3) one finds then the cross section for the various values of χ. An alternate procedure, therefore, is to find a least-squares solution of the coefficients instead of the cross sections. The former may be regarded as the more fundamental quantities, but the experimental errors on them are larger.

For energies up to 135 Mev, experimental results were used for all three processes (1). However, for higher energies, only measurements for the scattering of negative pions were available. The differential cross sections for each of the two processes are measured at three angles. In this case, therefore, the six phase shift angles α_i are determined from six cross sections only, with no internal checking of the procedure being possible. However, for each solution, one can compute the total cross section for the scattering of positive pions and compare with the corresponding experimental value.

At each energy where a computation is made, it is found that, in general, more than one solution exists; i.e., several relative minima of Eq. (2) are reached. In order to correlate a solution at one energy with that at another, use may be made of a continuity principle. One may make a graphical interpolation of the experimental cross sections (or coefficients) and then find a set of solutions to the minimum problem at rather close intervals of energy. The starting point for the search of a minimum at each energy step may conveniently be taken as the solution in the preceding energy step. In this way one chooses a solution that is near the one obtained immediately before. This " tracking " procedure may enable one to select a set of solutions that represents the data within the experimental errors and is consistent with the total positive pion cross sections. It has the advantage to average out in part the very sizable experimental errors.

III. Calculational results for the energy range 115 to 215 Mev.

Results on the phase shifts for the energies of 120 and 135 Mev were given in A. Both positive- and negative-pion measurements were used there. It was found that two sets of almost equivalent solutions, the " first solution " and the " Yang solution " existed.(7) A third minimum was found with

(7) E. Fermi and N. Metropolis, Los Alamos unclassified report LA–1492, 1952 (unpublished). [Paper N° 256 (Editors' note)].

a very large value of M, hence a very poor least-squares solution of the problem.

For the higher energies, where only negative-pion cross sections were used, two rather different solutions have been found that correspond to two somewhat different interpolations of the experimental results.

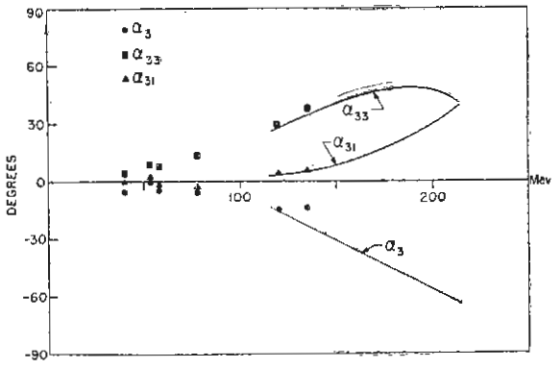

Fig. 1. – Phase shifts of the states of isotopic spin 3/2 plotted *versus* the energy of the primary pion for solution 1. For comparison, values of the same phase shifts at lower energies are also plotted.

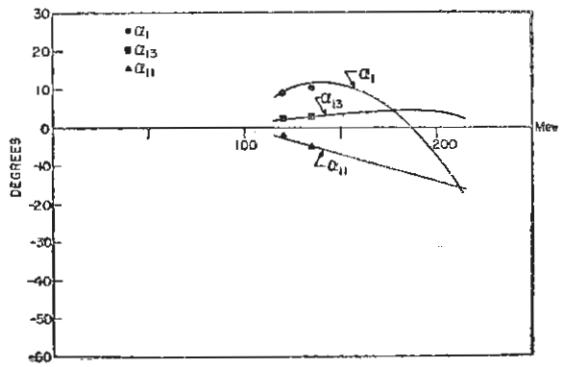

Fig. 2. – Phase shifts of the states of isotopic spin 1/2 plotted *versus* the energy of the primary pion for solution 1. Values previously obtained at 120 and 135 Mev are also plotted.

In both calculations we have chosen for the lowest energy a solution close to the "first solution" obtained in A. No attempt has been made in the work described in this paper to investigate the high-energy behavior of the Yang solution. This point is discussed, among others, in the next paper.[3]

The two sets of solutions obtained are presented in Tables I and II, and the first set is shown graphically in figs. 1 and 2. The first of these solutions actually was obtained by following a somewhat mixed procedure.

TABLE I.

First solution.

Energy (Mev)	Phase shifts (degrees)						Computed cross sections in the c. m. system corresponding to the laboratory scattering angles 45°, 90°, 135° (10^{-27} cm²/sterad)									Total cross section of π^+ (10^{-27} cm²)
	α_3	α_1	α_{33}	α_{31}	α_{13}	α_{11}	—	→	—	—	→	γ	+	→	+	
115	— 13.4	8.2	26.0	2.7	1.6	— 2.1	0.90	0.41	0.85	1.69	2.86	5.01	3.34	4.42	12.69	75
125	— 18.4	10.3	30.6	3.7	2.0	— 3.5	1.13	0.53	0.98	2.20	3.74	6.59	4.29	5.70	15.89	95
135	— 23.5	11.3	34.9	5.0	2.4	— 4.9	1.35	0.65	1.15	2.79	4.50	7.88	5.57	6.84	18.59	115
145	— 28.5	11.3	38.9	6.7	2.8	— 6.3	1.52	0.76	1.32	3.44	5.03	8.70	7.10	7.67	20.46	133
155	— 33.6	10.3	42.6	9.2	3.2	— 7.7	1.66	0.85	1.53	4.17	5.35	9.13	8.84	8.16	21.73	149
165	— 38.6	8.2	45.8	12.3	3.6	— 9.1	1.78	0.92	1.76	4.96	5.48	9.16	10.72	8.36	22.38	163
175	— 43.7	5.1	48.3	16.6	4.0	— 10.5	1.86	1.00	2.01	5.70	5.36	8.73	12.45	8.16	22.23	173
185	— 48.7	0.9	49.8	20.8	4.2	— 12.0	1.94	1.09	2.30	6.47	5.12	8.16	14.10	7.72	21.92	181
195	— 53.8	— 4.2	49.4	26.5	4.2	— 13.4	2.05	1.22	4.68	7.02	4.68	7.37	15.19	7.01	21.16	184
205	— 58.8	— 10.5	46.9	32.6	3.6	— 14.8	2.23	1.43	2.74	7.31	4.11	6.45	15.65	6.25	19.81	181
215	— 63.9	— 17.7	41.0	39.8	2.0	— 16.2	2.53	1.70	2.66	7.20	3.46	5.44	15.21	5.68	17.60	170

TABLE II.

Second solution.

Energy (Mev)	Phase shifts (degrees)						Computed cross sections in the c. m. system corresponding to the laboratory scattering angles 45°, 90°, 135° (10^{-27} cm²/sterad)									Total cross section of $\pi+$ (10^{-27} cm²)
	α_3	α_1	α_{33}	α_{31}	α_{13}	α_{11}	—	→	—	—	→	γ	+	→	+	
115	— 10.9	8.5	23.2	9.8	3.0	— 8.2	0.99	0.50	0.73	1.39	2.49	5.03	2.69	2.82	12.26	64
125	— 14.0	9.7	33.1	5.1	1.3	— 2.8	1.21	0.47	1.04	2.47	3.76	6.76	5.19	5.36	16.62	102
135	— 16.5	10.5	39.7	3.8	1.0	— 0.4	1.42	0.50	1.32	3.38	4.66	7.86	7.08	6.88	19.29	126
143	— 18.5	10.8	44.3	2.8	1.1	1.1	1.56	0.55	1.52	3.99	5.14	8.33	8.40	7.80	20.53	141
155	— 17.9	10.7	51.8	1.9	1.5	1.4	1.74	0.66	1.78	4.77	5.47	8.70	10.32	8.53	21.61	159
167	— 8.9	10.0	61.6	0.3	1.6	1.4	1.91	0.81	2.01	5.46	5.47	8.50	12.26	8.78	22.00	173
173	— 3.3	9.4	66.6	—0.2	1.8	1.1	1.98	0.89	2.11	5.73	5.34	8.27	13.09	8.76	21.81	177
184	6.9	7.3	74.8	3.2	3.3	— 3.4	2.11	1.06	2.29	6.22	5.01	7.74	14.60	8.42	21.25	184
188	9.4	6.6	69.6	10.6	4.0	— 14.9	2.16	1.13	2.36	6.38	4.86	7.50	13.48	6.87	19.93	174
192	11.0	6.4	61.7	15.1	3.1	— 25.5	2.21	1.20	2.43	6.57	4.80	7.27	13.47	5.03	17.66	156
196	12.7	5.9	51.3	22.2	1.3	— 35.9	2.24	1.26	2.47	6.67	4.48	6.94	11.87	2.56	14.60	128
200	14.4	5.3	46.9	25.6	0.0	— 40.5	2.28	1.34	2.53	6.81	4.26	6.62	11.37	1.62	12.87	117
208	18.1	3.7	40.3	31.5	— 3.1	— 46.7	2.35	1.48	2.63	7.05	3.78	5.93	10.89	0.57	10.03	103
216	20.7	0.3	35.4	38.6	— 5.5	— 49.7	2.42	1.63	2.73	7.27	3.26	5.17	10.74	0.28	8.49	97

First, two sets were computed starting from two different graphic interpolations of the experimental data. The corresponding phase shifts were rather similar. They were combined and smoothed out in order to obtain the phase shifts and it was verified that they represent the experimental cross sections within the experimental error.

The second set was obtained from a different interpolation of the experimental data. In this case an analytical interpolation formula was used. This calculation was carried out twice with different analytic interpolation and gave in both cases rather similar results. Only one of them is reported here in detail.

IV. Analysis of Columbia experiment at 61.5 Mev.

Bodansky, Sachs, and Steinberger [2] provided us with the experimental measurements given in Table III. The data represent extrapolations of their measured values to 61.5 Mev from 58 Mev for the positive pions and from 65 Mev for the negative pions. This extrapolation was done in order to have a complete set for both positive and negative pions at a single energy. Thus a least-squares procedure was used for fourteen cross sections. At this relatively low energy it is possible to use somewhat simpler expressions for the cross sections obtained by expanding the exponentials of A, formula (10), and keeping first-order terms. This expansion is permissible because all phase shifts should be small at this energy. It is necessary, however, to include a term for the Coulomb scattering, that is important at low energy.

Two computations were made starting at two points corresponding to approximate solutions of the problem previously obtained by Bodansky, Sachs, and Steinberger. In addition to these, twenty-two computations were made starting at randomly selected points. Seven different solutions were found. These are given in Table IV. The first two are similar to those found by Bodansky, Sachs, and Steinberger.

It is known from purely algebraic considerations that the multiplicity of solutions may be large. With our assumption of small phase shifts, whenever the p–phase shifts for one of the two isotopic spin states, say $T = 1/2$, are approximately equal, there exists a twofold multiplicity of p–phase shifts for $T = 3/2$.[8] These latter are related as follows:

$$(4) \qquad \begin{cases} 2\,\alpha_{33} + \alpha_{31} = 2\,\alpha'_{33} + \alpha'_{31} \\ \alpha_{33} - \alpha_{31} = \alpha'_{31} - \alpha'_{33}\,, \end{cases}$$

corresponding to the two multiple sets. These conditions hold approximately for minima 1,2; and 6,7 of Table IV for $T = 3/2$; and for 3,4 for $T = 1/2$. Minimum 5 shows no multiplicity because for both isotopic spins, the p–wave shifts are neither small nor equal.

(8) This is exactly the multiplicity of p–phase shifts found in an analysis of p–He^4 elastic scattering angular distribution by C. L. Critchfield and D. C. Dodder, « Phys. Rev. », *76*, 602 (1949).

TABLE III.

Extrapolated data of Columbia experiments.

$\pi^+ \longrightarrow \pi^+$	
θ	$d\sigma/d\omega$
36°	0.27 ± 0.12
47	0.53 ± 0.09
64	0.74 ± 0.07
101	1.39 ± 0.08
129	2.36 ± 0.12
155	3.13 ± 0.17
$\pi^- \longrightarrow \pi^-$	
θ	$d\sigma/d\omega$
42°	0.83 ± 0.12
53	0.47 ± 0.07
70	0.28 ± 0.05
101	0.21 ± 0.05
151	-0.01 ± 0.10
$\pi^- \longrightarrow 2\gamma$	
θ	$d\sigma/d\omega$
50°	0.69 ± 0.05
97	1.76 ± 0.07
150	2.88 ± 0.16

TABLE IV.

Analysis of Columbia data.

	α_3	α_1	α_{33}	α_{31}	α_{13}	α_{11}	Relative minimum
1	— 5.4	9.4	8.3	— 1.8	— 2.0	0.1	86
2	— 5.4	9.4	1.6	11.6	— 0.7	— 2.7	86
3	13.0	— 3.6	— 2.7	— 1.1	6.3	— 1.2	143
4	13.0	— 3.6	— 1.6	— 3.1	1.3	9.0	143
5	— 11.2	0.9	4.0	0.4	— 8.3	0.5	250
6	8.5	— 2.5	— 0.7	— 10.3	5.9	5.2	324
7	8.5	— 2.5	— 6.9	2.7	5.4	5.8	324

TABLE V.

Change in phase angles separately to produce a given change in the minimum function M.

	$+\delta$	$-\delta$
α_3	1.1°	— 1.4°
α_1	0.9	— 1.0
α_{33}	0.6	— 0.8
α_{31}	0.9	— 1.1
α_{13}	0.9	— 0.8
α_{11}	1.7	— 1.7

Finally, we took minimum 1 of Table IV and varied separately each of the phase shifts in turn until the value of M of Eq. (2) increased from its minimum value of 86 to 128. The results are summarized in Table V. This gives a measure of the sensitivity of the solution to small changes in the phase shifts. Both positive and negative changes are shown.

V. CONCLUSIONS.

We first observed that solution 2 is almost certainly to be discarded. This was not evident when the solution was first obtained in the summer of 1953 but appears now well established because it seems to be incompatible with the data on positive-pion cross sections that have since become available.[5,6,9] This, of course, does not prove that solution 1 is correct, because there are other solutions that have been found subsequently [3] that are about equally compatible with the experimental data. About solution 1, one may remark that it does not show a resonance of the state of isotopic spin 3/2 and angular momentum 3/2. This can be seen because the corresponding phase shift α_{33} does not reach 90° but starts decreasing after going through a maximum of approximately 50°. It has already been pointed out that other solutions quoted in reference 3 show the resonance feature. Otherwise they are about equivalent to solution 1 in accuracy in which they represent the experimental data, so that a decision between them on this basis does not appear possible at the present time. A decision can be obtained only by introducing theoretical arguments as has been done, for example, in the following paper. At the present status of the theory, such arguments must of necessity be somewhat hypothetical.

(9) FOWLER, LEA, SHEPHARD, SHUTT, THORNDIKE, and WHITTEMORE, « Phys. Rev. », *92*, 832 (1953).

$\beta = \frac{V}{c}$ $\beta^2 \approx 10^{-8}$

$1+\beta^2$ $W = Mc^2 e^{\beta^2 N} = Mc^2 e^{\frac{\beta^2 t}{\tau}}$

$N = \frac{t}{\tau}$

τ = time bet. collisions

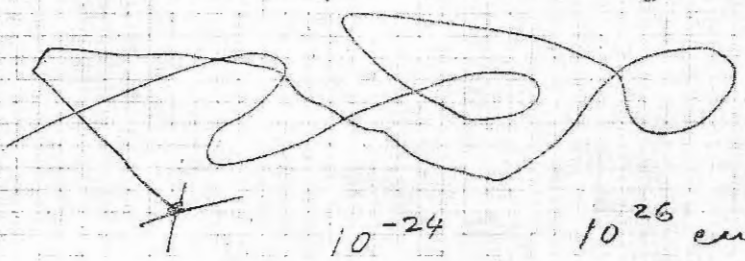

10^{-24} 10^{26} cm

$T = \frac{10^{26}}{3 \times 10^{10}} = 3 \times 10^{15}$ sec

$e^{-\frac{t}{T}} dt$ = age distr

$\frac{dw}{w^{(1+\frac{\tau}{\beta^2 T})}}$ = energy distr

$\frac{dw}{w^{(2.9)}}$

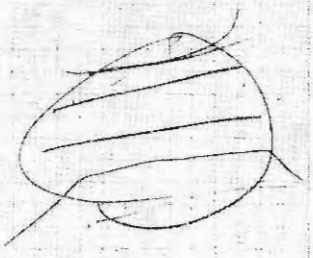

$\frac{\tau}{\beta^2 T} = 1.9$ $\tau = 1.9 \beta^2 T = 2 \times 10^{-8} \times 3 \times 10^{15}$

$= 6 \times 10^7 = 2$ years

$\beta^2 \approx 10^{-8}$ diam ≈ 2 l.y.

magn field

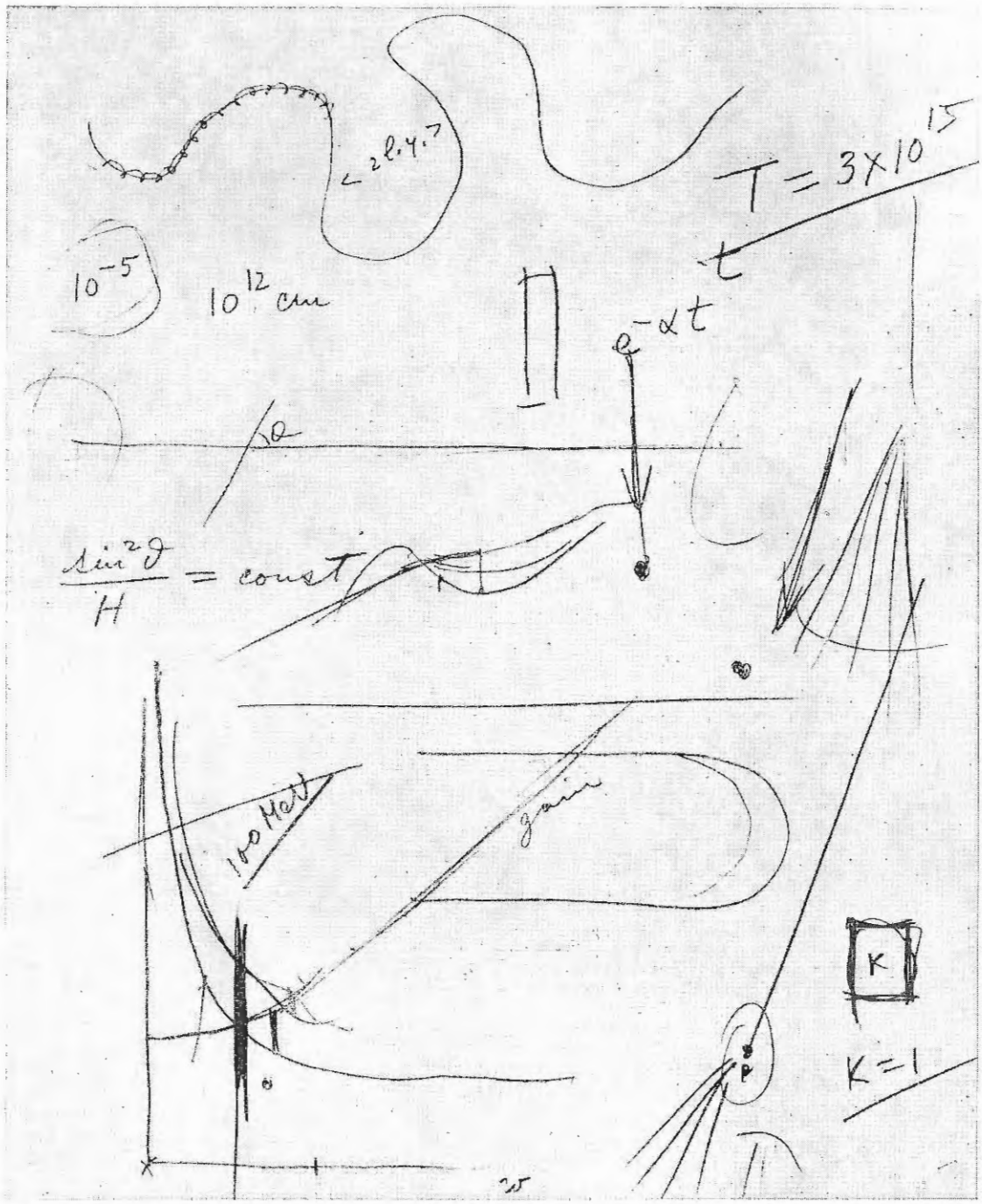
T = 3×10^15
t
10^-5
10^12 cm
e^-αt
sin²ϑ / H = const
150 Hett
gain
K
K=1
P
25

N° 261 and 262.

Paper N° 259 concludes Fermi's experimental work. He never wrote another experimental paper. Through my illness he lost a major supporter who was willing to help smooth the way and to cater to his way of doing things. His new students, Rosenfeld, Orear and Taft asked his guidance and advice but wanted their work to be their own. So Fermi changed his role; he spent more and more time helping others by discussion and frequently lending a hand in the experiment, but never again to the extent that would allow him to admit that the work was his own. Thus freed from the time consuming experimental work, he could consider the possibility of working together with Chandrasekhar on problems of astrophysical interest, somewhat related to his earlier concern with the origin of the cosmic rays. The collaboration with Chandrasekhar was in part brought about by the character of the Institute of Nuclear Studies which tried to range of a much broader field of science than high energy physics and elementary particles. Fermi tried very hard to encourage and support this tendency.

Paper N° 261 is an estimate of the magnetic field in the galactic spiral arms. Paper N° 262 is a more extensive study of the gravitational stability in the presence of a magnetic field, and demonstrates, perhaps, Fermi's willingness to solve any problem of physics.

H. L. ANDERSON.

N° 261, 262, and 265.

I.

During the fall of 1952 and the winter and the spring of 1953, I saw Fermi regularly: we met for two hours every Thursday morning and we discussed a variety of astrophysical problems bearing on hydromagnetics and the origin of cosmic radiation. The principal results which came out of these discussions are included in the two papers N° 261 and 262 which we wrote together. It is worth remarking that these discussions were begun at Fermi's instance: a testimony to his wide interests which went far beyond the fundamental questions of physics with which he was principally occupied.

During all my discussions with Fermi, I never failed to marvel at the ease and clarity with which he analyzed novel situations in fields in which, one might have supposed, he was not familiar and, indeed, was often not familiar prior to the discussion. In the manner in which he reacted to new problems, he always gave me the impression of a musician who, when presented with a new piece of music, at once plays it with a perception and a discernment which one would normally associate only with long practise and study. The fact, of course, was that Fermi was instantly able to bring to bear, on any physical problem with which he was confronted, his profound and deep feeling for physical laws: the result invariably was that the problem was illuminated and clarified. Thus, the motions of interstellar clouds with magnetic lines of force threading through them reminded him of the vibrations of a crystal lattice; and the gravitational instability of a spiral arm of a galaxy suggested to him the instability of a plasma and led him to consider its stabilization by an axial magnetic field.

II.

Fermi always had a lively interest in astrophysical problems. He was, for example, quite familiar with the applications of his statistics (with the required relativistic modifications) to the theory of the structure of the white dwarf stars: indeed, T. D. Lee, as a graduate

student of Fermi's, wrote his Ph. D. thesis on the *Hydrogen Content and Energy-Productive Mechanism of White Dwarf Stars* (« Ap. J. », *111*, 625 (1950)). And Fermi followed with considerable detail the developments relating to the origin of the elements and the source of energy of the stars. Thus, when Gamow put forward his ideas on the origin of the elements during the very early stages of an expanding universe by successive neutron captures in a non-equilibrium process, Fermi, together with Anthony Turkevich, examined very carefully the formation of the lightest nuclei during the " first 2000 seconds of the universe." Fermi and Turkevich considered all thermonuclear reactions (28 in all) which are less endothermic than the disintegration of the deuteron and which can go on between neutrons, protons, deuterons, tritons and the isotopes of helium of masses three and four; and they deduced the varying relative abundances of these nuclei during the early phase ($t < 2000\ s$). This detailed examination of the process of element formation in an expanding universe led them to the discovery of the deep " crevasse " which occurs at He^5; and of the unsurmountable difficulty which this presents to stepping over He^5 to the formation of the elements of higher atomic weight. These considerations of Fermi and Turkevich were never published; but an account of them will be found in the article *Theory of the Origin and Relative Abundance Distribution of the Elements* (« Rev. Mod. Phys. », *22*, 194–197 (1950)) by R. A. Alpher and R. C. Herman.

Fermi's interest in astrophysical problems became more than that of an onlooker (albeit a most critical onlooker) when the role of hydromagnetics in astrophysics came to be realized. In this field Fermi made some of the most original and fundamental contributions.

III.

The years after World War II were to witness a phenomenal growth of interest in hydromagnetics. The subject is a difficult one: part of the difficulty arises from one's inability to clearly visualize the often conflicting tendencies to which the motions of an electrically conducting fluid are subject in the presence of a magnetic field. With his interest in problems which challenge a physical understanding, it was natural that Fermi should have been fascinated by this subject; and he was the first to realize how important magnetic fields can be for the structure and the evolution of the galaxy.

IV.

In the fall of 1948, Edward Teller was advancing the view that cosmic rays are of solar origin. Fermi was wont to say—half-jokingly—that this inspired him to take an opposing view and advocate a galactic origin of the cosmic rays.

The argument (then current) against the view that cosmic rays pervaded all of galactic space is the very large amount of energy that should be present in the form of cosmic radiation if it were to occupy such a " huge " volume. Fermi met this objection by proposing a mechanism for the acccleration of the cosmic ray particles and suggesting that cosmic rays originate and are accelerated, primarily, in the interstellar space. (See also Teller's introduction to paper N° 237).

Fermi's acceleration mechanism (as it has come to be called) depends on the interaction of the cosmic ray particles with " wandering magnetic fields; " and Fermi supposed that such magnetic fields existed in interstellar space for the successful operation of his mechanism.

At the time Fermi proposed his acccleration mechanism, the assumption of interstellar magnetic fields was a " speculation. " But Fermi made its prevalence a matter of theoretical necessity by examining the physical conditions which had then been independently deduced for interstellar space. The discovery at about the same time of the phenomenon of interstellar polarization by Hiltner and Hall was soon to make the assumption of interstellar magnetic fields a matter of practical necessity.

Fermi developed his ideas on the origin of cosmic radiation in November 1948. How completely his ideas were crystallized, already at the outset, is evident from all the essential elements of theory clearly written on the two sheets of paper reproduced here as he explained his ideas within a day or two of his first thoughts on the subject.

The importance of magnetic fields and cosmic rays for the energy balance in the galaxy was realized by Fermi at once. In recognizing this, Fermi discovered a most significant fact for astronomy. His description of turbulent interstellar matter and prevailing magnetic fields as a moderator for maintaining a constant level of cosmic ray intensity is grand in its concept and inception.

When subsequent studies on interstellar polarization revealed that the galactic magnetic field is not irregular but exhibits a pattern and a uniformity, Fermi made the alternative suggestion that " spiral arms are magnetic tubes of force. " The changes which this new concept of the interstellar magnetic field (as well as the relatively large abundances of α–particles and other nuclear species in the primary cosmic rays which became well established by 1952) implied for his original theory were briefly examined by Fermi in his Henry Norris Russell Lecture [2] of the American Astronomical Society. (See paper N° 265). The concluding sentence of this Lecture was a prophetic utterance and is worth quoting:

" In conclusion, I should like to stress that, regardless of the details of the acceleration mechanism, cosmic radiation and magnetic fields in the galaxy must be counted as very important factors in the equilibrium of interstellar gas. "

V.

As I have already stated, Fermi and I discussed astrophysical problems regularly during 1952–53. The paper *Problems of Gravitational Stability in the Presence of a Magnetic Field* (N° 262) was an outcome of these discussions. Referring to this largely mathematical paper, several persons have remarked that it is " out of character " with Fermi. For this reason I may state that the problems which are considered in this paper were largely at Fermi's suggestion. The generalization of the virial theorem; the existence of an upper limit to the magnetic energy of a configuration in equilibrium under its own gravitation; the distortion of the spherical shape of a body in gravitational equilibrium by internal magnetic fields; the stabilization of the spiral arms of a galaxy by axial magnetic fields; all these were Fermi's ideas, novel at the time. But they had to be proved; for, as Fermi said:

" It is so very easy to make mistakes in magneto-hydrodynamics that one should not believe in a result obtained after a long and complicated mathematical derivation if one cannot understand its physical origin; in the same way, one cannot also believe in a long and complicated piece of physical reasoning if one cannot demonstrate it mathematically. "

If only this dictum were followed by all!

VI.

Fermi's interest in hydromagnetic turbulence led him to inquire into the physics of ordinary hydrodynamic turbulence. Confessing ignorance of this subject, Fermi asked me (early in 1950) to come to his office and tell him about the ideas of Kolmogoroff and Heisenberg which were then very much in the vogue. However, when I went to tell him, I found that it was not necessary for me to say beyond a few words: such as isotropy, the cascade of energy from large to small eddies etc. With only such words as clues, Fermi promptly went to the blackboard (" to see if I understand these words ") and proceeded to derive the Kolmogoroff spectrum for isotropic turbulence (in the inertial range) and the basis of Heisenberg's elementary theory. Fermi's manner of arguing is worth recording for its transparent simplicity.

Divide the scale of $\log k$ (where k denotes the wave number) into equal divisions, say $(\cdots, n, n+1, \cdots)$. In a stationary state the rate of flow of energy across " n " must be equal to the rate of flow across " $n+1$ ". Therefore:

$$(1) \qquad E_{n,n+1} = \rho \frac{v_n}{k_n} (v_n k_n)^2 - \rho \frac{v_{n+1}}{k_{n+1}} (v_{n+1} k_{n+1})^2,$$

(2) It may be noticed in passing that so far Fermi has been the sole exception to the rule that only professional astronomers are invited to give the Russell Lecture.

if one remembers that the characteristic time associated with " eddies " with wave numbers in the interval $(n, n+1)$ is $(v_{n+1} k_{n+1})^{-1}$. From this relation it follows that:

$$v_n = \text{Constant} \times k_n^{-1/3}, \tag{2}$$

and this is equivalent to Kolmogoroff's law. For decaying turbulence, equation (1) should be replaced by:

$$\frac{d}{dt}(\rho v_n^2) = E_{n,n+1} \tag{3}$$

and this equation expresses the content of Heisenberg's theory.

An amusing incident took place during this meeting with Fermi and it is worth narrating for it reveals some of his characteristic attitudes:

In the beginning of our discussion I had mentioned that in isotropic turbulence the longitudinal and the transverse velocity correlations are related by the equation of continuity. (3) Fermi did not seem interested in this; he wanted me to go on into the more physical aspects of isotropic turbulence. It happened that some time during this discussion I was temporarily called away. And when I returned after some twenty minutes, I found that Fermi had spent the time (while I was gone) deriving for himself the relation between the two correlations. There it was derived on the blackboard from first principles; and Fermi was " dutifully " transcribing the essential parts of the derivation into his " notebook. " I conld not resist telling him: " I have caught you red-handed; " and he did look embarrassed!

VII.

Fermi's aversion to mathematical technicalities is well known. Even when a mathematical argument had played a role in his initial thinking of a problem, he was careful to erase all its traces from his final account.

I was once to talk to a seminar and when I expressed my doubts as to what I should talk about, he advised: " If I were you, I would not be technical. " And I asked: " Do you mean, if I were you or you were me? " This baffled him: it was the only occasion I got the better of him.

VIII.

Others with greater competence have written about Fermi's fundamental contributions to physics. But his own account of the critical moment when the effect of the slowing down of neutrons on their ability to induce nuclear transformations was discovered is perhaps worth recording.

I described to Fermi Hadamard's thesis regarding the psychology of invention in mathematics, namely, how one must distinguish four different stages: a period of conscious effort, a period of " incubation " when various combinations are made in the subconscious mind, the moment of " revelation " when the " right combination " (made in the subconscious) emerges into the conscious, and finally the stage of further conscious effort. I then asked Fermi if the process of discovery in physics had any similarity. Fermi volunteered and said: (4)

" I will tell you how I came to make the discovery which I suppose is the most important one I have made. " And he continued: " We were working very hard on the neutron induced radioactivity and the results we were obtaining made no sense. One day, as I came

(3) The relation in question is the following: $g = f + \frac{1}{2} r \, \partial f / \partial r$ where $\langle u_1^2 \rangle f(r, t) = \langle u_{\parallel}(0) \, u_{\parallel}(r) \rangle$ and $\langle u_1^2 \rangle g(r, t) = \langle u_{\perp}(0) \, u_{\perp}(r) \rangle$ in an obvious notation.

(4) His account made so great an impression on me that though this is written from memory, I believe that it is very nearly a truly verbatim account.

to the laboratory, it occurred to me that I should examine the effect of placing a piece of lead before the incident neutrons. And instead of my usual custom, I took great pains to have the piece of lead precisely machined. I was clearly dissatisfied with something: I tried every "excuse" to postpone putting the piece of lead in its place. When finally, with some reluctance, I was going to put it in its place, I said to myself, 'No! I do not want this piece of lead here; what I want is a piece of paraffin.' It was just like that: with no advanced warning, no conscious, prior, reasoning. I immediately took some odd piece of paraffin I could put my hands on and placed it where the piece of lead was to have been."

S. CHANDRASEKHAR.

261.

MAGNETIC FIELDS IN SPIRAL ARMS

S. CHANDRASEKHAR and E. FERMI, *University of Chicago*
(Received March 23, 1953)
« Astrophys J. », *118*, 113-115 (1953).

ABSTRACT.

In this paper two independent methods are described for estimating the magnetic field in the spiral arm in which we are located. The first method is based on an interpretation of the dispersion (of the order of 10°) in the observed planes of polarization of the light of the distant stars; it leads to an estimate of $H = 7.2 \times 10^{-6}$ gauss. The second method is based on the requirement of equilibrium of the spiral arm with respect to lateral expansion and contraction: it leads to an estimate of $H = 6 \times 10^{-6}$ gauss.

The hypothesis of the existence of a magnetic field in galactic space [1] has received some confirmation by Hiltner's [2] observation of the polarization of the light of the distant stars. It seems plausible that this polarization is due to a magnetic orientation of the interstellar dust particles [3]; for such an orientation would lead to different amounts of absorption of light polarized parallel and perpendicular to the magnetic field and, therefore, to a polarization of the light reaching us. On this interpretation of the interstellar polarization we should expect to observe no polarization in the general direction of the magnetic lines of force and a maximum polarization in a direction normal to the lines of force. And if we interpret from this point of view the maps [4] of the polarization effect as a function of the direction of observation, it appears that the direction of the galactic magnetic field is roughly parallel to the direction of the spiral arm in which we are located.

(1) E. FERMI, « Phys. Rev. », *75*, 1169 (1949). [See paper N° 237 (Editors' note)].

(2) W. A. HILTNER, « Ap. J. », *109*, 471 (1949).

(3) Of the two theories which have been proposed (L. SPITZER and J. W. TUKEY, « Ap. J. », *114*, 187 (1951), and L. DAVIS and J. L. GREENSTEIN, « Ap. J. », *114*, 206 (1951)), that by Davis and Greenstein appears to be in better accord with the facts.

(4) W. A. HILTNER, « Ap. J. », *114*, 241 (1951).

In this paper we shall discuss some further consequences of this interpretation of interstellar polarization, in an attempt to arrive at an estimate of the strength of the interstellar magnetic field.

As we observe distant stars in a direction approximately perpendicular to the spiral arm, it appears that the direction of polarization is only approximately parallel to the arm. There are indeed quite appreciable and apparently irregular fluctuations in the direction of polarization of the distant stars.[4] This would indicate that the magnetic lines of force are not strictly straight and that they may be better described as "wavy" lines. The mean angular deviation of the plane of polarization from the direction of the spiral arm appears to be about $\alpha = 0.2$ radians.[4] There must clearly be a relation between this angle, α, and the strength of the magnetic field, H. For, if the magnetic field were sufficiently strong, the lines of force would be quite straight and α would be very small; on the other hand, if the magnetic field were sufficiently weak, the lines of force would be dragged around in various directions by the turbulent motions of the gas masses in the spiral arm and α would be large. To obtain the general relation between α and H, we proceed as follows:

The velocity of the transverse magneto-hydrodynamic wave is given by

$$V = \frac{H}{\sqrt{(4\pi\rho)}}, \tag{1}$$

where ρ is the density of the diffused matter. In computing the velocity, V, we should not include in ρ the average density due to the stars, since the stars may be presumed to move across the lines of force without appreciable interaction with them, whereas the diffused matter in the form of both gas and dust has a sufficiently high electrical conductivity to be effectively attached to the magnetic lines of force in such a way that only longitudinal relative displacements are possible.

According to equation (1), the transverse oscillations of a particular line of force can be described by an equation of the form

$$y = a \cos k (x - Vt), \tag{2}$$

where x is a longitudinal co-ordinate and y represents the lateral displacement. We take the derivatives of y with respect to x and t and obtain

$$y' = -ak \sin k (x - Vt) \tag{3}$$

and

$$\dot{y} = -akV \sin k (x - Vt). \tag{3'}$$

From these equations it follows that

$$V^2 \overline{y'^2} = \overline{\dot{y}^2}. \tag{4}$$

The lateral velocity of the lines of force must be equal to the lateral velocity of the turbulent gas. If v denotes the root-mean-square velocity of the turbulent motion, we should have

$$\overline{\dot{y}^2} = \frac{1}{3} v^2. \tag{5}$$

to the laboratory, it occurred to me that I should examine the effect of placing a piece of lead before the incident neutrons. And instead of my usual custom, I took great pains to have the piece of lead precisely machined. I was clearly dissatisfied with something: I tried every " excuse " to postpone putting the piece of lead in its place. When finally, with some reluctance, I was going to put it in its place, I said to myself, ' No! I do not want this piece of lead here; what I want is a piece of paraffin. ' It was just like that: with no advanced warning, no conscious, prior, reasoning. I immediately took some odd piece of paraffin I could put my hands on and placed it where tbe piece of lead was to have been. "

S. CHANDRASEKHAR.

261.

MAGNETIC FIELDS IN SPIRAL ARMS

S. CHANDRASEKHAR and E. FERMI, *University of Chicago*
(Received March 23, 1953)
« Astrophys J. », *118*, 113–115 (1953).

ABSTRACT.

In this paper two independent methods are described for estimating the magnetic field in the spiral arm in which we are located. The first method is based on an interpretation of the dispersion (of the order of 10°) in the observed planes of polarization of the light of the distant stars; it leads to an estimate of $H = 7.2 \times 10^{-6}$ gauss. The second method is based on the requirement of equilibrium of the spiral arm with respect to lateral expansion and contraction: it leads to an estimate of $H = 6 \times 10^{-6}$ gauss.

The hypothesis of the existence of a magnetic field in galactic space [1] has received some confirmation by Hiltner's [2] observation of the polarization of the light of the distant stars. It seems plausible that this polarization is due to a magnetic orientation of the interstellar dust particles [3]; for such an orientation would lead to different amounts of absorption of light polarized parallel and perpendicular to the magnetic field and, therefore, to a polarization of the light reaching us. On this interpretation of the interstellar polarization we should expect to observe no polarization in the general direction of the magnetic lines of force and a maximum polarization in a direction normal to the lines of force. And if we interpret from this point of view the maps [4] of the polarization effect as a function of the direction of observation, it appears that the direction of the galactic magnetic field is roughly parallel to the direction of the spiral arm in which we are located.

(1) E. FERMI, « Phys. Rev. », *75*, 1169 (1949). [See paper N° 237 (Editors' note)].

(2) W. A. HILTNER, « Ap. J. », *109*, 471 (1949).

(3) Of the two theories which have been proposed (L. SPITZER and J. W. TUKEY, « Ap. J. », *114*, 187 (1951), and L. DAVIS and J. L. GREENSTEIN, « Ap. J. », *114*, 206 (1951)), that by Davis and Greenstein appears to be in better accord with the facts.

(4) W. A. HILTNER, « Ap. J. », *114*, 241 (1951).

The factor 1/3 arises from the fact that only one component of the velocity is effective in shifting the lines of force in the y-direction. The quantity y', on the other hand, represents the deviation of the line of force from a straight line projected on the plane of view. Hence,

$$\overline{y'^2} = \alpha^2. \tag{6}$$

Now, combining equations (1), (4), (5), and (6), we obtain

$$H = \left(\frac{4}{3}\pi\rho\right)^{1/2} \frac{v}{\alpha}. \tag{7}$$

In equation (7) we shall substitute the following numerical values, which appear to describe approximately the conditions prevailing in the spiral arm in which we are located: [5]

$$\rho = 2\times 10^{-24}\ \mathrm{gm/cm^3}\ , \quad v = 5\times 10^5\ \mathrm{cm/sec}, \quad \text{and} \quad \alpha = 0.2\ \text{radians}. \tag{8}$$

With these values equation (7) gives

$$H = 7.2\times 10^{-6}\ \text{gauss}. \tag{9}$$

An alternative procedure for estimating the intensity of the magnetic field is based on the requirement of equilibrium of the spiral arm with respect to lateral expansion and contraction. As an order of magnitude, we may expect to obtain the condition for this equilibrium by equating the gravitational pressure in the spiral arm to the sum of the material pressure and the pressure due to the magnetic field. In computing the gravitational pressure, we should allow for the gravitational force due to all the mass present, i.e., of the stars as well as of the diffused matter. We are interested, however, in computing the gravitational pressure exerted on the diffused matter only. Assuming for simplicity that the spiral arm is a cylinder of radius R with uniform density, one finds for the gravitational pressure:

$$p_{\mathrm{grav}} = \pi G \rho\ \rho_t\, R^2, \tag{10}$$

where G denotes the constant of gravitation, ρ is the density of the diffused matter only, and ρ_t is the total mean density, including the contribution of the stars. The kinetic pressure of the turbulent gas is given by

$$p_{\mathrm{kin}} = \frac{1}{3}\rho v^2 \tag{11}$$

while the magnetic pressure is given by

$$p_{\mathrm{mag}} = \frac{H^2}{8\pi}. \tag{12}$$

And for the equilibrium we must have

$$p_{\mathrm{grav}} = p_{\mathrm{kin}} + p_{\mathrm{mag}}. \tag{13}$$

(5) For ρ, the estimate of J. H. OORT (cf. « Ap. J. », *116*, 233 (1952)) from observations of the 21-cm line is used; while the value of v adopted is that of A. BLAAUW, « B.A.N. », *11* 405 (1952).

In computing p_{grav} we shall assume a radius of the spiral arm of 250 parsecs or $R = 7.7 \times 10^{20}$ cm. As before, we shall take $\rho = 2 \times 10^{-24}$ gm/cm^3; and for ρ_z we shall assume [6] 6×10^{-24} gm/cm^3. For these values of R, ρ, and ρ_z equation (9) gives $p_{grav} = 1.5 \times 10^{-12}$ dynes, while p_{kin} computed with the values already given is 0.2×10^{-12} dynes. We attribute the difference to the magnetic pressure. Hence

$$\frac{H^2}{8\pi} = 1.3 \times 10^{-12}, \tag{14}$$

or

$$H = 6 \times 10^{-6} \text{ gauss}. \tag{15}$$

The two independent methods of estimating H therefore agree in giving essentially the same value for the field strength. A field of about 7×10^{-6} gauss indicated by these estimates is ten times smaller than that which Davis and Greenstein [3] have estimated as necessary for producing an adequate orientation of the dust particles to account for the interstellar polarization. If the present estimate of 7×10^{-6} gauss is correct, one should conclude that the mechanism of orientation is somewhat more effective than has been assumed by Davis and Greenstein.

Since this paper was written, our attention has been drawn to the fact that the idea underlying the first of the two methods by which we estimate the magnetic field in the spiral arm is contained in an earlier paper by Leverett Davis Jr. (« Phys. Rev. », *81*, 890 (1951)). We are sorry that we were not aware of this paper when we wrote ours. However, since with the better estimates of the astronomical parameters now available the value of H derived is a great deal different from Davis' value and since further the value we have derived is in accord with our second independent estimate, we have allowed the paper to stand in its original form.

(6) Cf. J. H. OORT, « Ap. J. », *116*, 233 (1952).

N° 262.

For the introduction to this paper see paper N° 261.

262.

PROBLEMS OF GRAVITATIONAL STABILITY IN THE PRESENCE OF A MAGNETIC FIELD

S. CHANDRASEKHAR and E. FERMI, *University of Chicago*
(Received March 23, 1953)
«Astrophys. J.», *118*, 116–141 (1953).

ABSTRACT.

In this paper a number of problems are considered which are related to the gravitational stability of cosmical masses of infinite electrical conductivity in which there is a prevalent magnetic field. In Section I the virial theorem is extended to include the magnetic terms in the equations of motion, and it is shown that when the magnetic energy exceeds the numerical value of the gravitational potential energy, the configuration becomes dynamically unstable. It is suggested that the relatively long periods of the magnetic variables may be due to the magnetic energy of these stars approaching the limit set by the virial theorem. In Section II the adiabatic radial pulsations of an infinite cylinder along the axis of which a magnetic field is acting is considered. An explicit expression for the period is obtained. Section III is devoted to an investigation of the stability for transverse oscillations of an infinite cylinder of incompressible fluid when there is a uniform magnetic field acting in the direction of the axis. It is shown that the cylinder is unstable for all periodic deformations of the boundary with wave lengths exceeding a certain critical value, depending on the strength of the field. The wave length of maximum instability is also determined. It is found that the magnetic field has a stabilizing effect both in increasing the wave length of maximum instability and in prolonging the time needed for the instability to manifest itself. For a cylinder of radius $R = 250$ parsecs and $\rho = 2 \times 10^{-24}$ gm/cm^3 a magnetic field in excess of 7×10^{-6} gauss effectively removes the instability. In Section IV it is shown that a fluid sphere with a uniform magnetic field inside and a dipole field outside is not a configuration of equilibrium and that it will tend to become oblate by contracting in the direction of the field. Finally, in Section V the gravitational instability of an infinite homogeneous medium in the presence of a magnetic field is considered, and it is shown that Jeans's condition is unaffected by the presence of the field.

1. *Introduction.*—In this paper we shall consider a number of problems relating to the dynamical and gravitational stability of cosmical masses in which there is a prevalent magnetic field. In the discussion of these problems, the assumption will be made that the medium is effectively of infinite

electrical conductivity. This latter assumption implies only that the conductivity is large enough for the magnetic lines of force to be considered as practically attached to the matter during the length of time under consideration; it has been known for some time that this is the case in most astronomical connections.[1]

The abstract gives an adequate summary of the paper.

I. The Virial Theorem and the Condition for Dynamical Stability.

2. *The virial theorem.*—In a subject such as this it is perhaps best that we start by establishing theorems of the widest possible generality. The extension of the virial theorem to include the forces derived from the prevailing magnetic field provides such a starting point. We shall see that under conditions of equilibrium this extension of the virial theorem leads to the relation

$$2\,\mathrm{T} + 3\,(\gamma - 1)\,\mathfrak{U} + \mathfrak{M} + \Omega = 0 \tag{1}$$

between the kinetic energy (T) of mass motion, the heat energy ($\mathfrak{U}$) of molecular motion, the magnetic energy ($\mathfrak{M}$) of the prevailing field, and the gravitational potential energy (Ω), where γ denotes the ratio of the specific heats. That a relation of the form (1) should exist is readily understood: For the balance between the pressures p_{kin}, p_{gas}, and p_{mag} due to the visible motions, the molecular motions, and the magnetic field, on the one hand, and the gravitational pressure, p_{grav}, on the other, requires

$$p_{\mathrm{kin}} + p_{\mathrm{gas}} + p_{\mathrm{mag}} = p_{\mathrm{grav}}, \tag{2}$$

while the order of magnitudes of these pressures are given by

$$p_{\mathrm{kin}} = c_1 \frac{\mathrm{T}}{\mathrm{V}} \quad , \quad p_{\mathrm{gas}} = c_2 \frac{\mathfrak{U}}{\mathrm{V}} \quad , \quad p_{\mathrm{mag}} = \frac{\mathrm{H}^2}{8\pi} = c_3 \frac{\mathfrak{M}}{\mathrm{V}}, \tag{3}$$

and

$$p_{\mathrm{grav}} = \text{Density} \times \text{gravity} \times \text{linear dimension} = -c_4 \frac{\Omega}{\mathrm{V}}, \tag{3 a}$$

where V denotes the volume of the configuration and c_1, c_2, c_3, and c_4 are numerical constants. A relation of the form (1) is therefore clearly implied. We now proceed to establisb the exact relation (1).

With tbe usual assumptions of hydromagnetics, the equations of motion governing an inviscid fluid can be written in the form

$$\rho \frac{du_i}{dt} = -\frac{\partial}{\partial x_i}\left(p + \frac{|\mathbf{H}|^2}{8\pi}\right) + \rho \frac{\partial \mathrm{V}}{\partial x_i} + \frac{1}{4\pi} \frac{\partial}{\partial x_j} \mathrm{H}_i \mathrm{H}_j, \tag{4}$$

where ρ denotes the density, p the pressure, V the gravitational potential, and **H** the intensity of the magnetic field. (In eq. (1) and in the sequel, summation over repeated indices is to be understood).

(1) Cf. L. Biermann, «Annual Review of Nuclear Science», 2 (Stanford: Annual Reviews, Inc., 1953) 349.

Multiply equation (4) by x_i and integrate over the volume of the configuration. Reducing the left-hand side of the equation in the usual manner, we find

$$(5) \qquad \iiint \rho x_i \frac{du_i}{dt}\, dx_1\, dx_2\, dx_3 = \int_0^M x_i \frac{d^2 x_i}{dt^2}\, dm = \frac{1}{2}\frac{d^2}{dt^2}\int_0^M r^2\, dm - \int_0^M |\, \boldsymbol{u}\,|^2\, dm\,,$$

where $dm = \rho\, dx_1\, dx_2\, dx_3$ and the integration is effected over the entire mass, M, of the configuration. Letting

$$(6) \qquad I = \int_0^M r^2\, dm \quad \text{and} \quad T = \frac{1}{2}\int |\, \boldsymbol{u}\,|^2\, dm$$

denote the moment of inertia and the kinetic energy of mass motion, respectively, we have

$$(7) \qquad \frac{1}{2}\frac{d^2 I}{dt^2} - 2T = -\iiint x_i \frac{\partial}{\partial x_i}\left(p + \frac{|\,\mathbf{H}\,|^2}{8\pi}\right) dx_1\, dx_2\, dx_3$$

$$+ \frac{1}{4\pi}\iiint x_i \frac{\partial}{\partial x_j} H_i\, H_j\, dx_1\, dx_2\, dx_3 + \int_0^M x_i \frac{\partial V}{\partial x_i}\, dm\,.$$

The last of the three integrals on the right-hand side of this equation represents the gravitational potential energy, Ω, of the configuration. The remaining two volume integrals can be reduced by integration by parts. Thus the first of the two integrals gives

$$(8) \qquad -\iiint x_i \frac{\partial}{\partial x_i}\left(p + \frac{|\,\mathbf{H}\,|^2}{8\pi}\right) dx_1\, dx_2\, dx_3$$

$$= -\int \left(p + \frac{|\,\mathbf{H}\,|^2}{8\pi}\right) \boldsymbol{r}\cdot d\mathbf{S} + 3\iiint \left(p + \frac{|\,\mathbf{H}\,|^2}{8\pi}\right) dx_1\, dx_2\, dx_3.$$

The surface integral (over $d\mathbf{S}$) vanishes, since the pressure (including the magnetic pressure $|\,\mathbf{H}\,|^2/8\pi$) must vanish on the boundary of the configuration. The assumption that $\mathbf{H}$ vanishes on $\mathbf{S}$ may require the placing of $\mathbf{S}$ at infinity; and the volume integral over p and $|\,\mathbf{H}\,|^2/8\pi$ is readily expressible in terms of the internal energy ($\mathfrak{U}$) and the magnetic energy ($\mathfrak{M}$) of the configuration. Thus we have

$$(9) \qquad -\iiint x_i \frac{\partial}{\partial x_i}\left(p + \frac{|\,\mathbf{H}\,|^2}{8\pi}\right) dx_1\, dx_2\, dx_3 = 3(\gamma - 1)\,\mathfrak{A} + 3\,\mathfrak{M}\,,$$

where γ denotes the ratio of the specific heats. In the same way the second volume integral in equation (7) gives

$$(10) \qquad \frac{1}{4\pi}\iiint x_i \frac{\partial}{\partial x_j} H_i\, H_j\, dx_1\, dx_2\, dx_3 = -2\,\mathfrak{M}\,.$$

Now, combining equations (7), (9), and (10), we have

$$(11) \qquad \frac{1}{2}\frac{d^2 I}{dt^2} = 2T + 3(\gamma - 1)\,\mathfrak{U} + \mathfrak{M} + \Omega\,.$$

This is the required generalization of the virial theorem; it differs from the usual one only in the appearance of $\mathfrak{M} + \Omega$ in place of Ω.

3. *The condition for dynamical stability.*—If the configuration is one of equilibrium, then it follows from the virial theorem that

$$3(\gamma - 1)\,\mathfrak{U} + \mathfrak{M} + \Omega = 0. \tag{12}$$

On the other hand, the total energy, $\mathfrak{E}$, of the configuration is given by

$$\mathfrak{E} = \mathfrak{U} + \mathfrak{M} + \Omega. \tag{13}$$

Eliminating $\mathfrak{U}$ between equations (12) and (13), we obtain

$$\mathfrak{E} = -\frac{3\gamma - 4}{3(\gamma - 1)}(|\,\Omega\,| - \mathfrak{M}). \tag{14}$$

From this equation for the total energy it follows that *a necessary condition for the dynamical stability of an equilibrium configuration is*

$$(3\gamma - 4)(|\,\Omega\,| - \mathfrak{M}) > 0. \tag{15}$$

Thus, even when $\gamma > 4/3$ (the condition for dynamical stability in the absence of a magnetic field) a sufficiently strong internal magnetic field can induce dynamical instability in the configuration. In fact, according to formula (15), the condition for dynamical stability, when $\gamma > 4/3$, is

$$\mathfrak{M} = \frac{1}{8\pi}\iiint |\,\mathbf{H}\,|^2\,dx_1\,dx_2\,dx_3 = \frac{1}{6}R^3\,(H^2)_{av} < |\,\Omega\,|, \tag{16}$$

where $(H^2)_{av}$ denotes the mean square magnetic field.

For a spherical configuration of uniform density,

$$\Omega = -\frac{3}{5}\frac{GM^2}{R}, \tag{17}$$

where M is its mass, R is its radius, and G is the constant of gravitation. We can use this expression for Ω to estimate the limit imposed by the virial theorem on the magnetic fields which can prevail. On expressing M and R in units of the solar mass and the solar radius, we find from equations (16) and (17) that

$$\sqrt{(H^2)_{av}} < 2.0 \times 10^8 \frac{M}{R^2}\,\text{gauss}. \tag{18}$$

For the peculiar A stars for which Babcock has found magnetic fields of the order of 10^4 gauss, we may estimate that

$$M \simeq 4\odot \quad \text{and} \quad R \simeq 5\,R_\odot \quad (\text{A star});$$

and expression (18) gives

$$\sqrt{(H^2)_{av}} < 3 \times 10^7\,\text{gauss} \quad (\text{A stars}). \tag{19a}$$

Of greater interest is the limit set by expression (18) for an S-type star for which Babcock has found a variable magnetic field of the order of 1000 gauss. For an S-type star we can estimate that

$$M \simeq 15\odot \quad \text{and} \quad R \simeq 300\,R_\odot \quad (\text{S star}); \tag{20}$$

and (18) now gives

$$\sqrt{(H^2)_{av}} < 3 \times 10^4\,\text{gauss} \quad (\text{S star}). \tag{20a}$$

Thus the limit set by (18) is seen to be two to three orders of magnitude larger than the surface fields observed by Babcock. However, the fields in the interior may be much stronger than the surface fields; and it is even possible that the actual root-mean-square fields in these stars are near their maximum values. Indeed, from the fact that the periods of the magnetic variables are long compared with the adiabatic pulsation periods they would have if they were nonmagnetic, we may surmise that $\sqrt{(H^2)_{av}}$ is near the limit set by (18); for, as is well known, we may lengthen the period of the lowest mode of oscillation of a system by approaching the limit of dynamical stability; and we can accomplish this by letting $\mathfrak{M} \to |\Omega|$.

Note added June 17.—Since we wrote this paper, Dr. Babcock has informed us that he has measured a variable magnetic field (+ 2000 to — 1200 gauss) for the star VV Cephei. It has been estimated that for this star $M = 100\odot$ and $R = 2600\, R_\odot$. With these values, inequality (18) gives $\sqrt{(H^2)_{av}} < 3000$ gauss. We may conclude that this star must be on the verge of dynamical stability and, anticipating the result established in Section IV, probably highly oblate.

4. *The virial theorem for an infinite cylindrical distribution of matter.*— Some care is needed in applying the results of §§ 2 and 3 to a distribution of matter which can be idealized as an infinite cylinder (such as, for example, a spiral arm); for the potential energy per unit length of an infinite cylinder is infinite. For this reason it is perhaps best that we consider the problem *de novo*.

We shall consider, then, an infinite cylinder in which the prevailing magnetic field is in the direction of the axis of the cylinder; and we shall suppose that all the variables are functions only of the distance r from the axis of the cylinder. Under these conditions the equations of motion reduce to the single one

$$\rho \frac{du_r}{dt} = -\frac{\partial}{\partial r}\left(p + \frac{H^2}{8\pi}\right) - \frac{2Gm(r)}{r}\rho, \tag{21}$$

where $m(r)$ is the mass per unit length interior to r.

Multiplying equation (21) by $2\pi r^2 dr$ and integrating over the entire range of r, we find in the usual manner that

$$\frac{1}{2}\frac{d^2}{dt^2}\int_0^M r^2\, dm - \int_0^M \left(\frac{dr}{dt}\right)^2 dm = 2(\gamma - 1)\mathfrak{A} + 2\mathfrak{M} - GM^2, \tag{22}$$

where M denotes the mass per unit length of the cylinder and $\mathfrak{A}$ and $\mathfrak{M}$ are the kinetic and the magnetic energies per unit length of the cylinder, respectively.

From equation (22) it follows that, under equilibrium conditions, we should have

$$2(\gamma - 1)\mathfrak{A} + 2\mathfrak{M} - GM^2 = 0. \tag{23}$$

A necessary condition for equilibrium to obtain is, therefore,

$$\mathfrak{M} < \frac{1}{2}GM^2. \tag{24}$$

We can rewrite the condition (24) alternatively in the form

$$\mathfrak{M} = \frac{1}{4}\int_0^R H^2\, r dr = \frac{1}{8}(H^2)_{av} R^2 < \frac{1}{2}\pi^2 R^4 \bar{\rho}^2 G, \tag{25}$$

or

$$\sqrt{(H^2)_{av}} < 2\pi R\bar{\rho} G. \tag{25 a}$$

This last condition on the root-mean-square field is essentially equivalent to one of the formulae used in the preceding paper [2] (eq. (13)) for estimating the magnetic field in the spiral arm; the difference between the two formulae arises from the fact that in that paper the gravitational attraction was not limited to the interstellar gas only; allowance was also made for the stars contributing to the gravitational force acting on the gas.

II. The Radial Pulsations of an Infinite Cylinder.

5. *The pulsation equation.*—In view of the inconclusive nature of the current treatments [3] of the adiabatic pulsations of magnetic stars, it is perhaps of interest to see how the corresponding problem in infinite cylinders can be fully solved. We consider, then, the radial pulsation of an infinite cylinder, along the axis of which there is a prevailing magnetic field.

Choosing the time t and the mass per unit length, $m(r)$, interior to r, as the independent variables, we can write the equations of continuity and motion in the forms

$$\frac{\partial}{\partial m}(\pi r^2) = \frac{1}{\rho} \tag{26}$$

and

$$\frac{\partial^2 r}{\partial t^2} = -2\pi r \frac{\partial P}{\partial m} - \frac{2Gm(r)}{r}\ , \tag{27}$$

where

$$P = p + \frac{H^2}{8\pi} \tag{28}$$

denotes the total pressure. Distinguishing the values of the various parameters for the equilibrium configuration by a subscript zero and writing

$$r = r_0 + \delta r\ ,\quad P = P_0 + \delta P\ ,\quad \rho = \rho_0 + \delta\rho, \text{ etc.} \tag{29}$$

we find that the equations governing radial oscillations of small amplitudes are

$$\frac{\partial}{\partial m}(2\pi r_0 \delta r) = -\frac{\delta\rho}{\rho_0^2} \tag{30}$$

(2) «Ap. J.», *118*, 113 (1953). [See paper N° 261 (Editors' note)].

(3) M. Schwarzschild, «Ann. d'ap.», *12*, 148 (1949); G. Gjellestad, *Rep. No. 1, Inst. Ther. Ap.* (Oslo 1950), and «Ann. d'ap.», *15*, 276 (1952); V. C. A. Ferraro and D. J. Memory, «M. N.», *112*, 361 (1952); T. G. Cowling, «M. N.», *112*, 527 (1952).

and

$$\frac{\partial^2}{\partial t^2}\delta r = -2\pi\delta r\frac{\partial P_0}{\partial m} - 2\pi r_0\frac{\partial}{\partial m}\delta P + \frac{2Gm}{r_0^2}\delta r. \tag{31}$$

Using the equation

$$2\pi r_0\frac{\partial P_0}{\partial m} = -\frac{2Gm}{r_0}, \tag{32}$$

which must obtain in equilibrium, we can rewrite equation (31) in the form

$$\frac{\partial^2}{\partial t^2}\delta r = -2\pi r_0\frac{\partial}{\partial m}\delta P + \frac{4Gm}{r_0^2}\delta r. \tag{33}$$

We shall now evaluate δP. For an adiabatic pulsation,

$$\delta P = \delta p + \frac{\mathbf{H}_0\cdot\delta\mathbf{H}}{4\pi} = \gamma\frac{p_0}{\rho_0}\delta\rho + \frac{\mathbf{H}_0\cdot\delta\mathbf{H}}{4\pi}. \tag{34}$$

Now when the medium is of infinite electrical conductivity, the change, $\Delta\mathbf{H}$, *at a given point* in a prevailing magnetic field, $\mathbf{H}_0$, caused by a displacement $\delta\boldsymbol{r}$, is given quite generally by

$$\Delta\mathbf{H} = \operatorname{curl}(\delta\boldsymbol{r}\times\mathbf{H}_0). \tag{35}$$

This relation is derived in § 14 below (see eq. (130)); but we may note here that it merely expresses the fact that the changes in the magnetic field are simply a consequence of the lines of force being pushed aside. According to equation (35), the change in the magnetic field, $\delta\mathbf{H}$, *as we follow the motion*, is given by

$$\delta\mathbf{H} = \operatorname{curl}(\delta\boldsymbol{r}\times\mathbf{H}_0) + (\delta\boldsymbol{r}\cdot\operatorname{grad})\,\mathbf{H}_0. \tag{36}$$

When $\mathbf{H}_0$ is the z–direction and $\delta\boldsymbol{r}$ is radial, the only nonvanishing component of $\delta\mathbf{H}$ is

$$\delta H_z = -\frac{1}{r}\frac{\partial}{\partial r}(H_0 r\delta r) + \delta r\frac{\partial H_0}{\partial r} = -\frac{H_0}{r}\frac{\partial}{\partial r}(r\delta r), \tag{37}$$

in the z–direction. Hence in the case under consideration

$$\frac{\mathbf{H}_0\cdot\delta\mathbf{H}}{4\pi} = -\frac{H_0^2\rho_0}{4\pi}\frac{\partial}{\partial m}(2\pi r_0\delta r), \tag{38}$$

and the expression for δP becomes

$$\delta P = -\left(\gamma p_0 + \frac{H_0^2}{4\pi}\right)\rho_0\frac{\partial}{\partial m}(2\pi r_0\delta r), \tag{39}$$

where we have substituted for $\delta\rho$ in equation (34) in accordance with equation (30).

With δP given by equation (38), equation (33) takes the form

$$\frac{\partial^2}{\partial t^2}\delta r = 4\pi^2 r\frac{\partial}{\partial m}\left\{\left(\gamma p + \frac{H^2}{4\pi}\right)\rho\frac{\partial}{\partial m}(r\delta r)\right\} + \frac{4Gm}{r^2}\delta r. \tag{40}$$

In writing equation (40), we have suppressed the subscripts zero distinguishing the equilibrium configuration, since there is no longer any cause for ambiguity.

When all the physical variables vary with time like $e^{i\sigma t}$, equation (40) reduces to

$$(41) \qquad \left(\sigma^2 + \frac{4Gm}{r^2}\right)\delta r = -4\pi^2 r \frac{d}{dm}\left\{\left(\gamma p + \frac{H^2}{4\pi}\right)\rho \frac{d}{dm}(r\delta r)\right\}$$

where δr has now the meaning of an amplitude.

The boundary conditions,

$$(42) \qquad \delta r = 0 \quad \text{at} \quad m = 0 \quad \text{and} \quad \delta P = 0 \quad \text{at} \quad m = M,$$

in conjunction with the pulsation equation (41) will determine for σ^2 a sequence of possible characteristic values, σ_k^2. And it can be readily shown that the solutions, δr_k, belonging to the different characteristic values, are orthogonal:

$$(43) \qquad \int_0^M \delta r_k \, \delta r_l \, dm = 0 \qquad (k \neq l).$$

In view of this orthogonality of the functions δr_k, we should expect that the characteristic values themselves could be determined by a variational method. The basis for this method is developed in the following section.

6. *An integral formula for σ^2 and a variational method for determining it.*—Multiply equation (41) by δr and integrate over the range of m, i.e., from zero to M. We obtain

$$(44) \quad \sigma^2 \int_0^M (\delta r)^2 \, dm + 4G \int_0^M \left(\frac{\partial r}{r}\right)^2 dm = -4\pi^2 \int_0^M r\delta r \frac{d}{dm}\left\{\left(\gamma p + \frac{H^2}{4\pi}\right)\rho \frac{d}{dm}(r\delta r)\right\} dm .$$

By integrating by parts the integral on the right-hand side, we obtain

$$(45) \quad \sigma^2 \int_0^M (\delta r)^2 \, dm + 4G \int_0^M \left(\frac{\delta r}{r}\right)^2 dm = 4\pi^2 \int_0^M \left(\gamma p + \frac{H^2}{4\pi}\right)\rho \left[\frac{d}{dm}(r\delta r)\right]^2 dm .$$

Writing $p = (P - H^2/8\pi)$ in equation (45), we obtain, after some elementary reductions,

$$(46) \qquad \sigma^2 \int_0^M (\delta r)^2 \, dm = \gamma \int_0^M \frac{P}{\rho}\left[\frac{1}{r}\frac{d}{dr}(r\delta r)\right]^2 dm - 4G \int_0^M \left(\frac{\delta r}{r}\right)^2 m \, dm$$

$$+ \frac{1}{8\pi}(2 - \gamma) \int_0^M \frac{H^2}{\rho}\left[\frac{1}{r}\frac{d}{dr}(r\delta r)\right]^2 dm .$$

It can be shown that the foregoing equations give a minimum value for σ^2 when the true solution δr belonging to the lowest characteristic value of the pulsation equation is substituted; and any other function δr (satisfying the boundary conditions) will give a larger value for σ^2. These facts can clearly be made the basis of a variational procedure for determining σ^2.

In the theory of the adiabatic pulsations of ordinary stars, it is known [4] that we get a very good estimate of σ^2 (for the fundamental mode) by setting

$$\delta r = \text{Constant } r, \tag{47}$$

in an integral formula for σ^2 similar to equation (46). We shall assume that this will continue to be the case in our present problem. Therefore, making the substitution (47) in equation (46), we obtain

$$\sigma^2 \int_0^M r^2 dm = 4\gamma \int_0^M \frac{P}{\rho} dm - 2GM^2 + (2-\gamma) \int_0^R H^2 r dr. \tag{48}$$

On the other hand,

$$\int_0^M \frac{P}{\rho} dm = 2\pi \int_0^R Pr\, dr = -\pi \int_0^R r^2 \frac{dP}{dr} dr = G \int_0^M m dm = \frac{1}{2} GM^2. \tag{49}$$

Hence

$$\sigma^2 \int_0^M r^2 dm = 2(\gamma - 1) GM^2 + (2-\gamma) \int_0^R H^2 r dr. \tag{50}$$

An alternative form of this equation is (cf. eq. (23))

$$\sigma^2 \int_0^M r^2 dm = 4(\gamma - 1)\left[\frac{1}{2} GM^2 - \mathfrak{M}\right] + 4\mathfrak{M} = 4[(\gamma-1)^2 \mathfrak{U} + \mathfrak{M}]. \tag{51}$$

III. The Gravitational Instability of an Infinitely Long Cylinder when a Constant Magnetic Field is Acting in the Direction of the Axis.

7. *The formulation of the problem.*—In Section II we have seen that an infinitely long cylinder in which there is a prevalent magnetic field in the direction of the axis is stable for radial oscillations. But the question was left open as to whether the cylinder may not be unstable for transverse or for longitudinal oscillations. In Section III we shall take up the discussion of the transverse oscillations; however, in order not to complicate an already difficult problem, we shall restrict ourselves to the case when the medium is incompressible in addition to being an infinitely good electrical conductor.

We picture to ourselves, then, an infinite cylinder of uniform circular cross-section of radius R_0, along the axis of which a constant magnetic field of intensity H_0 is acting. Since any transverse perturbation can be expressed as a superposition of waves of different wave lengths, the question of stability can be investigated by considering, individually, perturbations of different wave lengths. We suppose, then, that the cylinder is subject to a perturbation, the result of which is to deform the boundary into

$$r = R + a \cos kz. \tag{52}$$

(4) P. Ledoux and C. L. Pekeris, «Ap. J.», *94*, 124 (1941).

Since the fluid is assumed to be incompressible, the mass per unit length must be the same before and after the deformation; this, clearly, requires that

$$R_0^2 = R^2 + \frac{1}{2}a^2. \tag{53}$$

We shall see that, as a result of the deformation, the mean field in the z–direction is also changed by an amount of order a^2 (see eq. (87) below).

The investigation of the stability of the cylinder consists of two parts. First, we must calculate the change in the potential energy, $\Delta\Omega$, and the magnetic energy, $\Delta\mathfrak{M}$, per unit length resulting from the perturbation. Then, depending on whether $\Delta\Omega + \Delta\mathfrak{M}$ is positive or negative, we shall have stability or instability. We shall see presently that $\Delta\Omega + \Delta\mathfrak{M} < 0$ for all k less than a certain determinate value depending on H_0. In other words, the cylinder is unstable for all wave lengths exceeding a certain critical value λ_*. The determination of λ_* is the first problem in the investigation of stability. The second problem concerns the specification of the wave number k_m (say) for which the instability will develop at the maximum rate. We can determine this mode of maximum instability by considering the amplitude of the deformation (cf. eq. (52)) as a function of time, constructing a Lagrangian for the cylinder and determining the manner of increase of the amplitudes of the unstable modes. We shall find that whenever $\lambda > \lambda_*$ (or $k < k_*$), the amplitude increases like e^{qt}, where q is a function of k (and H_0). The mode of maximum instability is clearly the one which makes q (for a given H) a maximum.

Before proceeding to the details of the calculations, we may state that the method we have described derives from an early investigation of Rayleigh's [5] on the stability of liquid jets.

8. *The change in the potential energy per unit length caused by the deformation.*—Following the outline given in § 7, we shall first calculate the change in the potential energy, $\Delta\Omega$, per unit length caused by the deformation which makes the cross-section change from one of a constant radius R_0 to one whose boundary is given by equation (52). Since the potential energy per unit length of an infinite cylinder is infinite, the evaluation of $\Delta\Omega$ requires some care. We proceed as follows:

Let U and V denote the external and the internal gravitational potentials of the deformed cylinder. They satisfy the equations

$$\nabla^2 U = 0 \quad \text{and} \quad \nabla^2 V = -4\pi G\rho. \tag{54}$$

We shall first solve these equations to the first order in the amplitude a appropriately for the problem on hand. The solutions must clearly be of the forms

$$U = -2\pi G\rho\, R^2 \log r + aAK_0(kr)\cos kz + c_0 \tag{55}$$

(5) Lord RAYLEIGH, «Scientific Papers» (Cambridge: At the University Press, 1900), 2, 361; also *Theory of Sound* («Dover Reprints» [New York 1945]), 2, 350–362.

and

$$V = -\pi G\rho r^2 + aBI_0(kr)\cos kz, \tag{55 a}$$

where c_0 is an additive constant (with which we need not further concern ourselves), A and B are constants to be determined, and I_n and K_n are the Bessel functions of order n for a purely imaginary argument, which have no singularity at the origin and at infinity, respectively.

The constants A and B in solutions (55) are to be determined by the condition that U and V and $\partial U/\partial r$ and $\partial V/\partial r$ must be continuous on the boundary (52). Carrying out the calculations consistently to the first order in a, we find that the continuity conditions require

$$AK_0(kR) = BI_0(kR) \tag{56}$$

and

$$AK_1(kR) + BI_1(kR) = \frac{4\pi G\rho}{k}. \tag{56 a}$$

Solving these equations, we find

$$A = 4\pi G\rho\, RI_0(kR) \quad \text{and} \quad B = 4\pi G\rho\, RK_0(kR). \tag{57}$$

The required solution for V is, therefore,

$$V = -\pi G\rho r^2 + 4\pi G\rho R\, aK_0(kR)\, I_0(kr)\cos kz + O(a^2). \tag{58}$$

Now suppose that the amplitude of the deformation is increased by an *infinitesimal* amount from a to $a + \delta a$. The change in the potential energy, $\delta\Delta\Omega$, consequent to this infinitesimal increase in the amplitude, can be determined by evaluating the work done in the redistribution of the matter required to increase the amplitude. For evaluating this latter work, it is necessary to specify in a quantitative manner the redistribution which takes place; and we shall now do this.

An arbitrary deformation of an incompressible fluid can be thought of as resulting from a displacement ξ applied to each point of the fluid. The assumed incompressibility of the medium requires that $\operatorname{div}\xi = 0$; and, since no loss of generality is implied by supposing that the displacement is irrotational, we shall write

$$\xi = \operatorname{grad}\psi, \tag{59}$$

and require that

$$\nabla^2\psi = 0. \tag{60}$$

A solution of equation (60) which is suitable for considering the deformation of a uniform cylinder into one whose boundary is given by (52) is

$$\psi = A\, I_0(kr)\cos kz, \tag{61}$$

where A is a constant. The corresponding radial and z–components of ξ are

$$\xi_r = Ak I_1(kr)\cos kz \quad \text{and} \quad \xi_z = -Ak I_0(kr)\sin kz. \tag{62}$$

Since at $r = R$, ξ_r must reduce to $a \cos kz$ (cf. eq. (52)), we must have

$$A = \frac{a}{kI_1(kR)}. \tag{63}$$

The displacements,

$$\xi_r = a \frac{I_1(kr)}{I_1(kR)} \cos kz \quad \text{and} \quad \xi_z = -a \frac{I_0(kr)}{I_1(kR)} \sin kz, \tag{64}$$

applied to each point of the cylinder will deform it into the required shape. The displacement $\delta\xi$, which must be applied to increase the amplitude from a to $a + \delta a$, is therefore,

$$\delta\xi_r = \delta a \frac{I_1(kr)}{I_1(kR)} \cos kz \quad \text{and} \quad \delta\xi_z = -\delta a \frac{I_0(kr)}{I_1(kR)} \sin kz. \tag{65}$$

The change in the potential energy, $\delta\Delta\Omega$, per unit length involved in the infinitesimal deformation (65) can be obtained by integrating over the whole cylinder the work done by the displacement $\delta\xi$ in the force field specified by the gravitational potential (58). It is therefore given by

$$\delta\Delta\Omega = -2\pi\rho \left\{ \int_0^{R+a\cos kz} \delta\xi \cdot \text{grad } V r \, dr \right\}_{av}, \tag{66}$$

where the averaging is to be done with respect to z. Substituting for V and $\delta\xi$ from equations (58) and (65), we obtain

$$\begin{aligned} \delta\Delta\Omega = -2\pi\rho\, \delta a \Bigg\{ & \int_0^{R+a\cos kz} \cos kz \frac{I_1(kr)}{I_1(kR)} \left[-2\pi G\rho r + 4\pi\rho GR\, ak\, K_0(kR)\, I_1(kr) \cos kz \right] r dr \\ & + \int_0^{R+a\cos kz} \sin kz \frac{I_0(kr)}{I_1(kR)} \left[4\pi\rho\, GR\, ak\, K_0(kR)\, I_0(kr) \sin kz \right] r dr \Bigg\}_{av}. \end{aligned} \tag{67}$$

Evaluating the foregoing expression consistently to the first order in a, we find

$$\delta\Delta\Omega = 2\pi^2\rho^2 GR^2 a\delta a - 4\pi^2\rho^2 GR\, a\delta a \frac{kK_0(kR)}{I_1(kR)} \int_0^R \left[I_1^2(kr) + I_0^2(kr) \right] r dr, \tag{68}$$

or, using the readily verifiable result,

$$\int_0^R \left[I_1^2(kr) + I_0^2(kr) \right] r dr = \frac{R}{k} I_0(kR)\, I_1(kR), \tag{69}$$

we have

$$\delta\Delta\Omega = 4\pi^2\rho^2 GR^2 \left[\frac{1}{2} - I_0(x)\, K_0(x) \right] a\delta a, \tag{70}$$

where for the sake of brevity we have written

$$x = kR. \tag{71}$$

Finally, integrating equation (70) over a from 0 to a, we obtain

$$\Delta\Omega = 2\pi^2\rho^2 GR^2 \left[\frac{1}{2} - I_0(x)\, K_0(x) \right] a^2. \tag{72}$$

This is the required expression for the change in the potential energy per unit length caused by the deformation.

9. *The change in the magnetic energy per unit length caused by the deformation.*—The changes in the magnetic field inside the cylinder can best be determined from the condition that the magnetic induction across any section normal to the axis of the cylinder must remain unaffected by the deformation. This condition follows from the assumed infinite electrical conductivity of the medium. Thus, if

$$\mathrm{H}\,\mathbf{1}_z + \boldsymbol{h} \tag{73}$$

represents the magnetic field inside the cylinder (where 1_z is a unit vector in the z–direction, $\boldsymbol{h}$ is a field, of order a, varying periodically with z, and H is the mean field), we must require that

$$\mathrm{N} = \int_0^{\mathrm{R}} \mathrm{H}_0\, rdr = \int_0^{\mathrm{R}+a\cos kz} (\mathrm{H} + h_z)\, rdr = \text{Constant}. \tag{74}$$

Turning to the determination of H and $\boldsymbol{h}$, we may first observe that $\boldsymbol{h}$ can be derived from a magnetostatic potential φ satisfying the equation $\nabla^2 \varphi = 0$. For the problem on hand we can represent φ as a series in powers of a of the form

$$\varphi = \sum_{n=1}^{\infty} \frac{a^n \mathrm{A}_n}{nk} \mathrm{I}_0(nkr) \sin nkz\,, \tag{75}$$

where the A_n's are constants to be determined. Retaining terms up to the second order in a, we have

$$h_r = a\mathrm{A}_1 \mathrm{I}_1(kr) \sin kz + a^2 \mathrm{A}_2 \mathrm{I}_1(2\,kr) \sin 2\,kz \tag{76}$$

and

$$h_z = a\mathrm{A}_1 \mathrm{I}_0(kr) \cos kz + a^2 \mathrm{A}_2 \mathrm{I}_0(2\,kr) \cos 2\,kz, \tag{77}$$

for the components of $\boldsymbol{h}$.

With h_z given by equation (77), the magnetic induction across a normal section of the cylinder is given by

$$\mathrm{N} = \int_0^{\mathrm{R}+a\cos kz} \{\mathrm{H} + a\mathrm{A}_1 \mathrm{I}_0(kr) \cos kz + a^2 \mathrm{A}_2 \mathrm{I}_0(2\,kr) \cos 2\,kz\}\, rdr\,. \tag{78}$$

Evaluating N correct to the second order in a, we obtain

$$\mathrm{N} = \tfrac{1}{2}\mathrm{H}\left(\mathrm{R}^2 + \tfrac{1}{2}a^2\right) + \tfrac{1}{2}\, a^2 \mathrm{A}_1 \mathrm{RI}_0(k\mathrm{R}) + a\left[\mathrm{HR} + \frac{\mathrm{A}_1}{k}\, \mathrm{I}_1(k\mathrm{R})\,\mathrm{R}\right] \cos kz$$
$$+ a^2\left[\tfrac{1}{4}\,\mathrm{H} + \tfrac{1}{2}\,\mathrm{A}_1 \mathrm{RI}_0(k\mathrm{R}) + \frac{\mathrm{A}_2}{2k}\, \mathrm{RI}_1(2\,k\mathrm{R})\right] \cos 2\,kz\,; \tag{79}$$

and according to equation (74) this must be identically equal to (cf. eq. (53))

$$\tfrac{1}{2}\,\mathrm{H}_0\,\mathrm{R}_0^2 = \tfrac{1}{2}\,\mathrm{H}_0\left(\mathrm{R}^2 + \tfrac{1}{2}\,a^2\right). \tag{80}$$

Hence we must require that

$$\frac{1}{2}\,H\left(R^2+\frac{1}{2}\,a^2\right)+\frac{1}{2}\,a^2\,A_1\,RI_0(kR)=\frac{1}{2}\,H_0\left(R^2+\frac{1}{2}\,a^2\right), \tag{81}$$

$$HR+\frac{A_1}{k}\,I_1(kR)\,R=0, \tag{82}$$

and

$$\frac{1}{4}\,H+\frac{1}{2}\,A_1\,RI_0(kR)+\frac{A_2}{2k}\,RI_1(2kR)=0. \tag{83}$$

From equations (82) and (83) we find:

$$A_1=-\frac{H}{R}\,\frac{x}{I_1(x)} \tag{84}$$

and

$$A_2=\frac{H}{R^2}\,\frac{x}{I_1(2x)}\left\{\frac{xI_0(x)}{I_1(x)}-\frac{1}{2}\right\}, \tag{85}$$

where $x=kR$ (cf. eq. (71)).

With A_1 given by equation (84), equation (81) gives (correct to order a^2)

$$H_0=H\left\{1-\frac{a^2}{R^2}\,\frac{xI_0(x)}{I_1(x)}\right\}, \tag{86}$$

or, equivalently,

$$H=H_0\left\{1+\frac{a^2}{R^2}\,\frac{xI_0(x)}{I_1(x)}\right\}. \tag{87}$$

This equation shows that the mean field inside the deformed cylinder is larger than that in the undeformed cylinder; the difference is of order a^2 and depends on the wave number of the deformation.

Equations (76), (77), (84), (85), and (87) determine the field inside the cylinder correct to the second order in a. It may be noted here that the same solution can also be derived from the alternative (but equivalent) condition that the magnetic lines of force follow the boundary of the cylinder (52).

With the field inside the cylinder determined, we can now evaluate the magnetic energy, $\mathfrak{M}$, per unit length. We have

$$\mathfrak{M}=\frac{1}{4}\left\{\int_0^{R+a\cos kz}|\mathbf{H}|^2\,rdr\right\}_{av}=\frac{1}{4}\left\{\int_0^{R+a\cos kz}(H^2+2Hh_z+h_z^2+h_r^2)\,rdr\right\}_{av}, \tag{88}$$

where the averaging is to be done with respect to z. Substituting for h_r and h_z from equations (76) and (77) and evaluating $\mathfrak{M}$ correct to the second order in a, we obtain (cf. eq. (69))

$$\begin{aligned}\mathfrak{M}&=\frac{1}{8}\,H^2\left(R^2+\frac{1}{2}\,a^2\right)+\frac{1}{2}\,aH\left\{\cos kz\int_0^{R+a\cos kz}A_1\,I_0(kr)\,rdr\right\}_{av}\\&+\frac{1}{2}\,a^2HA_2\left\{\cos 2kz\int_0^{R+a\cos kz}I_0(2kr)\,rdr\right\}_{av}+\frac{1}{8}\,a^2A_1^2\int_0^{R}[I_0^2(kr)+I_1^2(kr)]\,rdr\\&=\frac{1}{8}\,H^2\left(R^2+\frac{1}{2}\,a^2\right)+\frac{1}{4}\,a^2HA_1\,RI_0(kR)+\frac{1}{8}\,a^2A_1^2\,\frac{R}{k}\,I_0(kR)\,I_1(kR).\end{aligned} \tag{89}$$

On making further use of equations (53), (84), and (87), we can reduce this last expression for $\mathfrak{M}$ to the form

$$\mathfrak{M} = \tfrac{1}{8} H_o^2 R_o^2 + \tfrac{1}{8} a^2 H^2 \frac{x I_o(x)}{I_1(x)} . \tag{90}$$

But the magnetic energy per unit length of the undeformed cylinder is $\frac{1}{8} H_o^2 R_o^2$. Hence

$$\Delta\mathfrak{M} = \tfrac{1}{8} a^2 H^2 \frac{x I_o(x)}{I_1(x)} . \tag{91}$$

10. *The modes of deformation which are unstable.*—Combining the results of §§ 8 and 9, we have

$$\Delta\Omega + \Delta\mathfrak{M} = \left\{ 2\pi^2 \rho^2 G R^2 \left[\tfrac{1}{2} - I_o(x) K_o(x) \right] + \tfrac{1}{8} H^2 \frac{x I_o(x)}{I_1(x)} \right\} a^2 . \tag{92}$$

Letting

$$H_s^2 = 16\pi^2 \rho^2 R^2 G \quad \text{or} \quad H_s = 4\pi \rho R \sqrt{G}, \tag{93}$$

we can rewrite equation (92) more conveniently in the form

$$\Delta\Omega + \Delta\mathfrak{M} = 2\pi^2 \rho^2 R^2 G \left\{ \left[\tfrac{1}{2} - I_o(x) K_o(x) \right] + \frac{x I_o(x)}{I_1(x)} \left(\frac{H}{H_s} \right)^2 \right\} a^2 . \tag{94}$$

Whether the mode of deformation considered is stable or unstable will depend upon the sign of the quantity in braces in the foregoing expression.

Now the asymptotic behaviors of the Bessel functions which appear in equation (94) are:

$$I_o(x) \to 1 \quad , \quad I_1(x) \to \tfrac{1}{2} x , \quad \text{and} \quad K_o(x) \to -\left(\gamma + \log \tfrac{1}{2} x \right) \quad (x \to 0) , \tag{95}$$

where γ (not to be confused with the ratio of the specific heats) is Euler's constant $0.5772\cdots$, and

$$I_o(x) \to \frac{e^x}{(2\pi x)^{1/2}} \quad , \quad I_1(x) \to \frac{e^x}{(2\pi x)^{1/2}} , \quad \text{and} \quad K_o(x) \to \left(\frac{\pi}{2x} \right)^{1/2} e^{-x} \quad (x \to \infty) . \tag{96}$$

Hence $\Delta\Omega$ (cf. eq. (72)) tends to minus infinity logarithmically as $x \to 0$ and tends monotonically to the positive limit $\pi^2 \rho^2 R^2 G$ as $x \to \infty$, while $\Delta\mathfrak{M}$ (cf. eq. (91)) tends to the positive limit $\frac{1}{4} a^2 H^2$ as $x \to 0$ and increases monotonically to infinity (linearly) as $x \to \infty$. These behaviors of $\Delta\Omega$ and $\Delta\mathfrak{M}$ are illustrated in fig. 1, in which the functions $\left[\tfrac{1}{2} - I_o(x) K_o(x) \right]$ and $\frac{x I_o(x)}{I_1(x)}$ are plotted.

From the asymptotic behaviors of $\Delta\Omega$ and $\Delta\mathfrak{M}$ it follows that the equation

$$\tfrac{1}{2} - I_o(x) K_o(x) + \frac{x I_o(x)}{I_1(x)} \left(\frac{H}{H_s} \right)^2 = 0 \tag{97}$$

allows a single positive root. Let $x = x_*$ denote this root. Then

$$\Delta\Omega + \Delta\mathfrak{M} > 0 \quad \text{for} \quad x > x_* , \tag{98}$$

and

$$\Delta\Omega + \Delta\mathfrak{M} < 0 \quad \text{for} \quad x < x_* . \tag{98 a}$$

Hence *all modes of deformation with* $x < x_*$ *are unstable.* Since $x = kR$, x_* specifies the minimum wave number (in units of $1/R$) for a stable deformation; alternatively, we could also say that *all modes of deformation with wave lengths exceeding*

$$\lambda_* = \frac{2\pi R}{x_*} \tag{99}$$

are unstable.

In Table I we have listed x_* for a few values of H/H_s. This table exhibits the strong stabilizing effect of the magnetic field: this is shown in the pres-

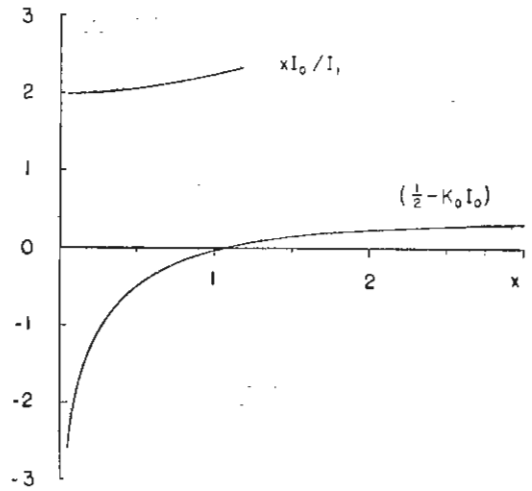

Fig. 1. – The dependence of the changes in the potential energy, $\Delta\Omega$, and magnetic energy, $\Delta\mathfrak{M}$, per unit length of an infinitely long cylinder on the wave number of the deformation; $\Delta\Omega$ is proportional to $[1/2 - I_0(x)\,K_0(x)]$, while $\Delta\mathfrak{M}$ is proportional to $xI_0(x)/I_1(x)$, where x is the wave number measured in the unit $1/R$.

ent connection by the very rapid increase, with increasing H, of the wave length at which instability sets in. In fact, for $H > H_s$ this increase becomes exponential; this can be shown in the following way:

Since $x_* = 0.092$ already for $H = H_s$, for $H > H_s$ we may replace the Bessel functions which occur in equation (97) by their dominant terms for $x \to 0$; thus,

$$\tfrac{1}{2} + \gamma + \log \tfrac{1}{2} x_* + 2\left(\frac{H}{H_s}\right)^2 = 0 \qquad (H > H_s) . \tag{100}$$

Hence

$$x_* = 2 \exp\left\{-\left[\gamma + \tfrac{1}{2} + 2\left(\frac{H}{H_s}\right)^2\right]\right\} \qquad (H > H_s), \tag{101}$$

or, numerically,

$$x_* = 0.6811\, e^{-2(H/H_s)^2} \qquad (H > H_s). \tag{102}$$

TABLE I.

Dependence of Wave Numbers x_* and x_m at which Instability First Sets in and at which it is Maximum, on Prevailing Magnetic Field.

H/H_s	x_*	x_m	$q_m/(4\pi G\rho)^{1/2}$
0	1.067	0.58	0.246
0.25	0.832	0.47	0.208
0.50	0.480	0.28	0.133
0.75	0.232	0.14	0.0685
1.00	0.092	0.057	0.0281
1.25	0.0299	0.0182	0.0091
1.50	0.00757	0.00459	0.00229
2.00	0.000228	0.000139	0.0000693

11. *The mode of maximum instability.*—In the preceding section we have seen that an infinite cylinder is gravitationally unstable for all modes of deformation with wave lengths exceeding a certain critical value. We shall now show that there exists a wave length for which the instability is a maximum. For this purpose we shall suppose that the amplitude, a, of the deformation is a function of time and seek an equation of motion for it.

We have already seen that the potential energy (gravitational plus magnetic) per unit length of the cylinder measured from the equilibrium state is

$$\mathfrak{B} = \Delta\mathfrak{M} + \Delta\Omega = -2\pi^2\rho^2 R^2 GF(x)\, a^2, \tag{103}$$

where

$$F(x) = I_0(x)\, K_0(x) - \frac{1}{2} - \left(\frac{H}{H_s}\right)^2 \frac{xI_0(x)}{I_1(x)}. \tag{104}$$

Defined in this manner, $F(x) > 0$ for $x < x_*$, i.e., it is positive for all unstable modes and negative for all stable modes.

To obtain the Lagrangian function for the cylinder, we must find the kinetic energy of the motion resulting from the varying amplitude. Since we have assumed that the fluid is incompressible, a velocity potential, ψ, exists which satisfies Laplace's equation. And the solution for the velocity potential appropriate to the problem on hand is

$$\psi = BI_0(kr)\cos kz, \tag{105}$$

where B is a constant to be determined. The components of the velocity derived from the foregoing potential are

$$u_r = \frac{\partial\psi}{\partial r} = +Bk\, I_1(kr)\cos kz \tag{106}$$

and

$$u_z = \frac{\partial \psi}{\partial z} = - \mathrm{B}k\, \mathrm{I}_0(kr) \sin kz. \tag{106 a}$$

The constant of proportionality, B, in the foregoing equations must be determined from the condition that the radial velocity, u_r, at $r = \mathrm{R}$ must agree with that implied by equation (52); i.e., we should have

$$\mathrm{B}k\, \mathrm{I}_1(k\mathrm{R}) \cos kz = \frac{da}{dt} \cos kz. \tag{107}$$

Hence

$$\mathrm{B} = \frac{1}{k\mathrm{I}_1(x)} \frac{da}{dt}. \tag{108}$$

From equations (106) we obtain, for the kinctic energy per unit length, the expression (cf. eq. (69))

$$\left\{ \begin{aligned} \mathfrak{T} &= \tfrac{1}{2} \pi\rho\, \mathrm{B}^2 k^2 \int_0^{\mathrm{R}} [\mathrm{I}_0^2(kr) + \mathrm{I}_1^2(kr)]\, r dr \\ &= \tfrac{1}{2} \pi\rho\, \mathrm{B}^2 k^2 \frac{\mathrm{R}}{k} \mathrm{I}_0(x)\, \mathrm{I}_1(x), \end{aligned} \right. \tag{109}$$

or, substituting for B from equation (108), we have

$$\mathfrak{T} = \tfrac{1}{2} \pi\rho\, \mathrm{R}^2 \frac{\mathrm{I}_0(x)}{x\mathrm{I}_1(x)} \left(\frac{da}{dt}\right)^2. \tag{110}$$

The Lagrangian function (per unit length) for the infinite cylinder is therefore given by

$$\mathfrak{L} = \mathfrak{T} - \mathfrak{B} = \tfrac{1}{2} \pi\rho\, \mathrm{R}^2 \frac{\mathrm{I}_0(x)}{x\mathrm{I}_1(x)} \left(\frac{da}{dt}\right)^2 + 2\pi^2 \rho^2\, \mathrm{R}^2\, \mathrm{GF}(x)\, a^2. \tag{111}$$

The equation of motion for a derived from the Lagrangian (111) is

$$\pi\rho\, \mathrm{R}^2 \frac{\mathrm{I}_0(x)}{x\mathrm{I}_1(x)} \frac{d^2 a}{dt^2} = 4\pi^2 \rho^2 \mathrm{R}^2 \mathrm{GF}(x)\, a, \tag{112}$$

or, alternatively,

$$\frac{d^2 a}{dt^2} = 4\pi\, \mathrm{G}\rho \left\{ \frac{x\mathrm{I}_1(x)}{\mathrm{I}_0(x)} \left[\mathrm{I}_0(x)\, \mathrm{K}_0(x) - \frac{1}{2} \right] - \left(\frac{\mathrm{H}}{\mathrm{H}_s}\right)^2 x^2 \right\} a, \tag{113}$$

where we have suhstituted for $\mathrm{F}(x)$ in accordance with equation (104). The solution for a is therefore of the form

$$a = \text{Constant}\ e^{\pm qt}, \tag{114}$$

where

$$q^2 = 4\pi\, \mathrm{G}\rho \left\{ \frac{x\mathrm{I}_1(x)}{\mathrm{I}_0(x)} \left[\mathrm{I}_0(x)\, \mathrm{K}_0(x) - \frac{1}{2} \right] - \left(\frac{\mathrm{H}}{\mathrm{H}_s}\right)^2 x^2 \right\}. \tag{115}$$

Accordingly, q is purely imaginary for $x > x_*$ and is real for $x < x_*$; this is in agreement with the fact that all modes with $x > x_*$ are stable, while all modes with $x < x_*$ are unstable.

As defined by equation (115), $q = 0$ both for $x = 0$ and for $x = x_*$. There is, therefore, a determinate intermediate value of x—say, x_m—for which

q attains a maximum—say, q_m. *The wave number x_m clearly represents the mode of maximum instability*; for it is the mode for which the amplitude of the deformation increases most rapidly. The wave length

$$\lambda_m = \frac{2\pi R}{x_m}, \tag{116}$$

corresponding to the wave number x_m, gives approximately the length of the "pieces" into which the cylinder will ultimately break up: for the component with the wave length λ_m, in the Fourier analysis of an arbitrary perturbation, is the one whose amplitude will increase most rapidly with time and, therefore, represents the mode in which the instability will first assert itself. Finally, it is clear that $1/q_m$ gives a measure of the time needed for the instability to make itself manifest.

In Table I the values of x_m and $q_m/(4\pi G\rho)^{1/2}$ area also listed. As in the case of x_* (§ 10), we can give explicit formulae for x_m and q_m for $H > H_s$. Since for $H > H_s$ we are concerned only with values of $x \ll 1$, we may replace the Bessel functions which occur in the expression for q^2 by their dominant terms for $x \to 0$. Thus

$$q^2 = 4\pi G\rho\left\{-\tfrac{1}{2}x^2\left(\gamma + \tfrac{1}{2} + \log\tfrac{1}{2}x\right) - x^2\left(\frac{H}{H_s}\right)^2\right\} \qquad (H > H_s). \tag{117}$$

The expression on the right-hand side attains its maximum when

$$\left(\gamma + \tfrac{1}{2} + \log\tfrac{1}{2}x\right) + \tfrac{1}{2} + 2\left(\frac{H}{H_s}\right)^2 = 0. \tag{118}$$

Hence

$$x_m = 2\exp\left\{-(\gamma+1) - 2\left(\frac{H}{H_s}\right)^2\right\} = 0.4131\, e^{-2(H/H_s)^2} \qquad (H > H_s). \tag{119}$$

The corresponding expression for q_m is

$$q_m = \tfrac{1}{2}x_m(4\pi G\rho)^{1/2} \qquad (H > H_s). \tag{120}$$

These formulae emphasize the fact, apparent from an examination of Table I that, as the strength of the magnetic field increases, not only does the wave length of the mode of maximum instability increase exponentially, but the time needed for the instability to manifest itself also increases exponentially.

12. *Numerical illustrations.*—To illustrate the theory developed in the preceding sections we shall take, as typical of a spiral arm of a galaxy,

$$R = 250 \text{ parsecs} \quad \text{and} \quad \rho = 2\times 10^{-24}\ \text{gm/cm}^3. \tag{121}$$

The corresponding value of H_s is (cf. eq. (93))

$$H_s = 5.0\times 10^{-6}\ \text{gauss}. \tag{122}$$

For these values of the physical parameters, the nondimensional results given in Table I can be converted into astronomical measures; they are given in Table II. From the values given in this table it follows that between $H = H_s$ and $H = 2H_s$ the characteristic time of the instability becomes so long that, for all practical purposes, the instability is effectively removed by the presence of the magnetic field.

TABLE II.

Wave Lengths λ_* *and* λ_m *at which Instability Sets in and at which it is Maximum and Characteristic Time,* q_m^{-1}, *Needed for Instability to Manifest Itself for Case* R = 250 Parsecs *and* $\rho = 2\times 10^{-24}$ gm/cm^3.

H (Gauss)	λ_* (Parsecs)	λ_m (Parsecs)	q_m^{-1} (Years)
0	1.5×10^3	2.7×10^3	1.0×10^8
1.25×10^{-6}	1.9×10^3	3.3×10^3	1.2×10^8
2.5×10^{-6}	3.3×10^3	5.6×10^3	1.8×10^8
3.75×10^{-6}	6.8×10^3	1.1×10^4	3.6×10^8
5.0×10^{-6}	1.7×10^4	2.8×10^4	8.7×10^8
6.25×10^{-6}	5.2×10^4	8.6×10^4	2.7×10^9
7.5×10^{-6}	2.1×10^5	3.4×10^5	1.1×10^{10}
10.0×10^{-6}	6.9×10^6	1.1×10^7	3.5×10^{11}

IV. THE FLATTENING OF A GRAVITATING FLUID SPHERE UNDER THE INFLUENCE OF A MAGNETIC FIELD.

13. *The formulation of the problem.*—In this section we shall consider the gravitational equilibrium of an incompressible fluid sphere with a uniform magnetic field inside and a dipole field outside. We shall show that under these circumstances the sphere is not a configuration of equilibrium and that it will become oblate by contracting along the axis of symmetry.

We suppose, then, that initially the magnetic field in the interior of the sphere is uniform and of intensity H in the z–direction. In spherical polar co-ordinates (r, θ, φ) the components of **H** in the radial (r) and the transverse (θ) directions are

$$H_r^{(i)} = H\mu \quad \text{and} \quad H_\theta^{(i)} = -H(1-\mu^2)^{1/2} \qquad (r < R), \tag{123}$$

where $\mu = \cos\theta$ and the superscript i indicates that these are the components of the field *inside* the sphere.

When the field inside the sphere is uniform, that outside the sphere must be a dipole field given by

$$H_r^{(e)} = H\left(\frac{R}{r}\right)^3 \mu \quad \text{and} \quad H_\theta^{(e)} = \frac{1}{2} H\left(\frac{R}{r}\right)^3 (1-\mu^2)^{1/2}, \tag{124}$$

where R denotes the radius of the sphere.

The energy, $\mathfrak{M}$, of the magnetic field specified by equations (123) and (124) is given by

$$(125)\qquad \left\{\begin{aligned} \mathfrak{M} &= \frac{H^2}{8\pi}\left(\frac{4}{3}\pi R^3\right) + \frac{1}{4}H^2\int_R^\infty\int_{-1}^{+1}\left(\frac{R}{r}\right)^6\left\{\mu^2 + \frac{1}{4}(1-\mu^2)\right\}r^2\,dr\,d\mu \\ &= \frac{1}{4}H^2R^3. \end{aligned}\right.$$

Let the sphere be now deformed in such a way that the equation of the bounding surface is

$$(126)\qquad r(\mu) = R + \varepsilon P_l(\mu),$$

where $\varepsilon \ll R$, $\mu = \cos\theta$ (θ being the polar angle), and $P_l(\mu)$ denotes, as usual, the Legendre polynomial of order l. We shall call such a deformation of the sphere a "P_l–deformation." We shall investigate the stability of the sphere by examining whether or not it is stable to a P_l–deformation.

14. *The change in the magnetic energy of the sphere due to a* P_l*–deformation.*—As we have already pointed out in § 8, an arbitrary deformation of an incompressible body can be thought of as the result of applying to each point of the body a displacement $\boldsymbol{\xi}$. And if, as in § 8 (eqs. (59) and (60)), we express $\boldsymbol{\xi}$ as the gradient of a scalar function ψ, the solution of Laplace's equation satisfied by ψ appropriate to a P_l–deformation of a sphere is

$$(127)\qquad \psi = Ar^l P_l(\mu),$$

where A is a constant. The corresponding expressions for the components of $\boldsymbol{\xi}$ are

$$(128)\qquad \xi_r = \frac{\partial\psi}{\partial r} = Alr^{l-1}P_l(\mu)$$

and

$$(128\,a)\qquad \xi_\theta = \frac{1}{r}\frac{\partial\psi}{\partial\theta} = -Ar^{l-1}(1-\mu^2)^{1/2}P_l'(\mu),$$

where a prime is used to denote differentiation with respect to μ. According to equation (126), at $r = R$, $\xi_r = \varepsilon P_l(\mu)$; this determines A, and we have

$$(129)\qquad \xi_r = \varepsilon\left(\frac{r}{R}\right)^{l-1}P_l(\mu) \quad\text{and}\quad \xi_\theta = -\frac{\varepsilon}{l}\left(\frac{r}{R}\right)^{l-1}(1-\mu^2)^{1/2}P_l'(\mu).$$

Now the deformation of a body will alter the prevailing magnetic field; and, since in a medium of infinite electrical conductivity a change in the existing magnetic field can be effected only by bodily pushing aside the lines of force, it follows that

$$(130)\qquad \delta\mathbf{H} = \operatorname{curl}(\boldsymbol{\xi}\times\mathbf{H}).$$

The truth of this last relation can be established in the following way: Suppose that the displacement $\boldsymbol{\xi}$ takes place as a slow continuous movement so that if $\boldsymbol{u}$ denotes the velocity, $\boldsymbol{u} = \partial\boldsymbol{\xi}/\partial t$ (i.e., if quantities of the second order of smallness are neglected). On the other hand, when the electrical conductivity is infinite,

$$\delta\mathbf{E} = -\boldsymbol{u}\times\mathbf{H},$$

where $\delta\mathbf{E}$ is the electrical field resulting from the changing magnetic field $\delta\mathbf{H}$ in accordance with Maxwell's equation,

$$\operatorname{curl}\delta\mathbf{E} = -\frac{\partial}{\partial t}\delta\mathbf{H}.$$

Combining the last two equations, we have

$$\operatorname{curl}\left(\frac{\partial\boldsymbol{\xi}}{\partial t}\times\mathbf{H}\right) = \frac{\partial}{\partial t}(\delta\mathbf{H}).$$

The relation (130) is simply the integrated form of this equation].

When the fluid is incompressible (i.e., when $\operatorname{div}\boldsymbol{\xi} = 0$ in addition to $\operatorname{div}\mathbf{H} = 0$), equation (130) can be written alternatively in the form

$$\delta\mathbf{H} = (\mathbf{H}\cdot\operatorname{grad})\,\boldsymbol{\xi} - (\boldsymbol{\xi}\cdot\operatorname{grad})\,\mathbf{H}. \tag{131}$$

And when the initial field is homogeneous, equation (131) simplifies still further to

$$\delta\mathbf{H} = (\mathbf{H}\cdot\operatorname{grad})\,\boldsymbol{\xi}. \tag{132}$$

In spherical polar co-ordinates the foregoing equation is equivalent to

$$\delta H_r = \left(H_r\frac{\partial}{\partial r} + \frac{H_\theta}{r}\frac{\partial}{\partial\theta}\right)\xi_r - \frac{H_\theta\,\xi_\theta}{r} \tag{133}$$

and

$$\delta H_\theta = \left(H_r\frac{\partial}{\partial r} + \frac{H_\theta}{r}\frac{\partial}{\partial\theta}\right)\xi_\theta + \frac{H_\theta\,\xi_r}{r}. \tag{133 a}$$

These equations in conjunction with equations (123) and (129) give

$$\delta H_r^{(i)} = \varepsilon H\,(l-1)\,\frac{r^{l-2}}{R^{l-1}}\,P_{l-1}(\mu) \tag{134}$$

and

$$\delta H_\theta^{(i)} = -\varepsilon H\,\frac{r^{l-2}}{R^{l-1}}\,(1-\mu^2)^{1/2}\,P'_{l-1}(\mu). \tag{134 a}$$

The corresponding change in the internal magnetic energy density is given by

$$\delta\left(\frac{|\mathbf{H}|^2}{8\pi}\right) = \frac{1}{4\pi}\mathbf{H}^{(i)}\cdot\delta\mathbf{H}^{(i)} = \varepsilon\,\frac{H^2}{4\pi}\,\frac{r^{l-2}}{R^{l-1}}\left\{(l-1)\,\mu P_{l-1}(\mu) + (1-\mu^2)\,P'_{l-1}(\mu)\right\}. \tag{135}$$

On further simplification this reduces to

$$\delta\left(\frac{|\mathbf{H}|^2}{8\pi}\right) = \varepsilon\,(l-1)\,\frac{H^2}{4\pi}\,\frac{r^{l-2}}{R^{l-1}}\,P_{l-2}(\mu). \tag{136}$$

Hence, when averaged over all directions, this is zero except when $l = 2$, in which case

$$\delta\left(\frac{|\mathbf{H}|^2}{8\pi}\right) = \frac{\varepsilon}{4\pi}\,\frac{H^2}{R} \qquad (l=2); \tag{137}$$

the corresponding change in the internal magnetic energy, $\Delta\mathfrak{M}^{(i)}$, is given by

$$\Delta\mathfrak{M}^{(i)} = \frac{1}{3}\varepsilon H^2 R^2. \tag{138}$$

15. *The change in the external magnetic energy of the sphere due to a* P_l*–deformation.*—Writing the magnetic field outside the deformed sphere in the form

$$H_r^{(e)} = H\left(\frac{R}{r}\right)^3 \mu + \delta H_r^{(e)} \tag{139}$$

and

$$H_\theta^{(e)} = \tfrac{1}{2} H\left(\frac{R}{r}\right)^3 (1-\mu^2)^{1/2} + \delta H_\theta^{(e)}, \tag{139 a}$$

we shall suppose that $\delta H_r^{(e)}$ and $\delta H_\theta^{(e)}$ are derivable from a magnetic potential $\delta\varphi^{(e)}$. Since the magnetic potential satisfies Laplace's equation, the solution for $\delta\varphi^{(e)}$ must be expressible as a linear combination of the fundamental solutions $P_j(\mu)/r^{j+1}$, which vanish at infinity.

We shall find it convenient to write the solution for $\delta\varphi^{(e)}$ in the form

$$\delta\varphi^{(e)} = -\varepsilon H\left\{\frac{l-1}{l}\left(\frac{R}{r}\right)^l P_{l-1}(\mu) + \Sigma A_j\left(\frac{R}{r}\right)^{j+1} P_j(\mu)\right\}, \tag{140}$$

where the A_j's are coefficients to be determined. The expressions for $\delta H_r^{(e)}$ and $\delta H_\theta^{(e)}$ derived from this potential are

$$\delta H_r^{(e)} = \varepsilon H\left\{(l-1)\frac{R^l}{r^{l+1}} P_{l-1}(\mu) + \Sigma A_j (j+1)\frac{R^{j+1}}{r^{j+2}} P_j(\mu)\right\} \tag{141}$$

and

$$\delta H_\theta^{(e)} = \varepsilon H\left\{\frac{l-1}{l}\frac{R^l}{r^{l+1}} P_{l-1}^1(\mu) + \Sigma A_j \frac{R^{j+1}}{r^{j+2}} P_j^1(\mu)\right\}. \tag{141 a}$$

The coefficients A_j in equations (141) and (141a) can be determined from the condition that the component of the magnetic field normal to a bounding surface must be continuous. To the first order in ε this condition requires that

$$\{H_r^{(e)}\}_{R+\varepsilon P_l} + \{H_\theta^{(e)}\}_R \frac{\varepsilon}{R}(1-\mu^2)^{1/2}\frac{\partial P_l}{\partial\mu} = \{H_r^{(i)}\}_{R+\varepsilon P_l} + \{H_\theta^{(i)}\}_R \frac{\varepsilon}{R}(1-\mu^2)^{1/2}\frac{\partial P_l}{\partial\mu}, \tag{142}$$

where $-(\varepsilon/R)(1-\mu^2)^{1/2}\partial P_l/\partial\mu$ is the angle (to the first order in ε) which the deformed boundary makes with the θ–direction; the terms in H_θ in the foregoing equation arise from this latter circumstance. Now, according to equations (124), (139), and (140),

$$\{H_r^{(e)}\}_{R+\varepsilon P_l} + \{H_\theta^{(e)}\}_R \frac{\varepsilon}{R}(1-\mu^2)^{1/2}\frac{\partial P_l}{\partial\mu} = H\mu\left(1 - 3\frac{\varepsilon}{R}P_l\right) + \tfrac{1}{2} H\frac{\varepsilon}{R}(1-\mu^2)\frac{\partial P_l}{\partial\mu} + \frac{\varepsilon}{R} H\{(l-1)P_{l-1} + \Sigma A_j (j+1) P_j\}, \tag{143}$$

while, according to equations (123) and (134),

$$\{H_r^{(i)}\}_{R+\varepsilon P_l} + \{H_\theta^{(i)}\}_R \frac{\varepsilon}{R}(1-\mu^2)^{1/2}\frac{\partial P_l}{\partial\mu} = H\mu + \frac{\varepsilon}{R} H(l-1)P_{l-1} - \frac{\varepsilon}{R} H(1-\mu^2)\frac{\partial P_l}{\partial\mu}; \tag{143 a}$$

and the equality of the expressions on the right-hand sides of equations (143) and (143 a) requires

$$(144)\qquad \Sigma A_j (j+1)\, P_j = 3\mu\, P_l - \frac{3}{2}(1-\mu^2)\frac{\partial P_l}{\partial \mu} = \frac{3}{2(2l+1)}\{(l+1)(l+2)\, P_{l+1} - l(l-1)\, P_{l-1}\}.$$

Hence

$$(145)\qquad A_{l-1} = -\frac{3(l-1)}{2(2l+1)}\quad,\quad A_{l+1} = \frac{3(l+1)}{2(2l+1)}\,,$$

and

$$(145\,a)\qquad A_j = 0 \quad \text{for} \quad j \neq l-1 \quad \text{or} \quad l+1.$$

Inserting these values of A in equations (141) and (141 a), we obtain

$$(146)\quad \delta H_r^{(e)} = \varepsilon H\left\{\frac{(l-1)(l+2)}{2(2l+1)}\,\frac{R^l}{r^{l+1}}\,P_{l-1}(\mu) + \frac{3(l+1)(l+2)}{2(2l+1)}\,\frac{R^{l+2}}{r^{l+3}}\,P_{l+1}(\mu)\right\}$$

and

$$(146\,a)\qquad \delta H_\theta^{(e)} = \varepsilon H\left\{\frac{(l-1)(l+2)}{2l(2l+1)}\,\frac{R^l}{r^{l+1}}\,P_{l-1}^1(\mu) + \frac{3(l+1)}{2(2l+1)}\,\frac{R^{l+2}}{r^{l+3}}\,P_{l+1}^1(\mu)\right\}.$$

Returning to equations (139) and (139 a), we can write the change in the external magnetic energy, $\Delta\mathfrak{M}^{(e)}$, to the first order in ε, in the form

$$(147)\quad \Delta\mathfrak{M}^{(e)} = \frac{H^2}{8\pi}\iiint_{R+\varepsilon P_l \geq r \geq R}\left(\frac{R}{r}\right)^6\left\{\mu^2 + \frac{1}{4}(1-\mu^2)\right\} r^2\, dr\, d\mu\, d\varphi + \frac{H^2}{8\pi}\iiint_{r>R}\left(\frac{R}{r}\right)^3\{2\,P_1(\mu)\,\delta H_r^{(e)} + P_1^1(\mu)\,\delta H_\theta^{(e)}\}\, r^2\, dr\, d\mu\, d\varphi.$$

After some minor reductions we find

$$(148)\quad \Delta\mathfrak{M}^{(e)} = -\frac{1}{4}\varepsilon H^2 R^2\int_{-1}^{+1}\left\{\frac{1}{2}P_2(\mu) + \frac{1}{2}\right\}P_l(\mu)\,d\mu + \frac{1}{2}\varepsilon H^2\int_R^\infty dr r^2\int_{-1}^{+1} d\mu\left(\frac{R}{r}\right)^3 P_1(\mu)\cdot\left\{\frac{(l-1)(l+2)}{2(2l+1)}\,\frac{R^l}{r^{l+1}}\,P_{l-1}(\mu) + \frac{3(l+1)(l+2)}{2(2l+1)}\,\frac{R^{l+2}}{r^{l+3}}\,P_{l+1}(\mu)\right\} + \frac{1}{4}\varepsilon H^2\int_R^\infty dr r^2\int_{-1}^{+1} d\mu\left(\frac{R}{r}\right)^3 P_1^1(\mu)\cdot\left\{\frac{(l-1)(l+2)}{2l(2l+1)}\,\frac{R^l}{r^{l+1}}\,P_{l-1}^1(\mu) + \frac{3(l+1)}{2(2l+1)}\,\frac{R^{l+2}}{r^{l+3}}\,P_{l+1}^1(\mu)\right\}.$$

From this equation it is evident that $\Delta\mathfrak{M}^{(e)}$ vanishes (to the first order in ε) for all deformations except a P_2–deformation. And for a P_2–deformation we have

$$(149)\quad \Delta\mathfrak{M}^{(e)} = -\frac{1}{8}\varepsilon H^2 R^2\int_{-1}^{+1}[P_2(\mu)]^2\,d\mu + \frac{1}{5}\varepsilon H^2 R^5\int_R^\infty\int_{-1}^{+1}\frac{dr}{r^4}\left\{\frac{1}{2}P_2(\mu) + \frac{1}{2}\right\}d\mu$$

or

$$(150)\qquad \Delta\mathfrak{M}^{(e)} = \frac{1}{60}\varepsilon H^2 R^2 \qquad (l=2).$$

Finally, combining equations (138) and (150), we obtain

$$\Delta\mathfrak{M} = \Delta\mathfrak{M}^{(i)} + \Delta\mathfrak{M}^{(e)} = \frac{7}{20}\varepsilon H^2 R^2, \tag{151}$$

for the total change in the magnetic energy due to a P_2–deformation; it vanishes to this order for all higher deformations.

We have, therefore, shown that *the change in the magnetic energy is of the second order in* ε *for all deformations of the sphere except a* P_2*–deformation; and for a* P_2*–deformation it is of the first order in* ε *and is given by* (151). Moreover, for a P_2–deformation $\Delta\mathfrak{M} > 0$ when the deformation is in the sense of making the sphere into a prolate spheroid; and $\Delta\mathfrak{M} < 0$ when the deformation is in the sense of making the sphere into an oblate spheroid.

16. *The change in the gravitational potential energy and the instability of the sphere to a* P_2*–deformation.*—The change in the potential energy, $\Delta\Omega$, due to a P_l–deformation can also be computed. The result is well known for a P_2–deformation. For a general P_l–deformation we can evaluate $\Delta\Omega$ by following the procedure used in § 8. We shall not give here the details of the calculations, which lead to the result

$$\Delta\Omega = \frac{3(l-1)}{(2l+1)^2}\left(\frac{\varepsilon}{R}\right)^2 \frac{GM^2}{R}. \tag{152}$$

The change in the potential energy is therefore always positive and is of the second order in ε. This is in contrast to $\Delta\mathfrak{M}$, which as we have seen, is of the first order in ε for a P_2–deformation and is negative for a deformation which tends to make it oblate. We can therefore conclude that the sphere is unstable and that it will tend to collapse toward an oblate spheroidal shape. To estimate the extent to which this collapse may proceed, let us consider $\Delta\Omega + \Delta\mathfrak{M}$ for a P_2–deformation. We have (cf. eqs. (151) and (152))

$$\Delta\Omega + \Delta\mathfrak{M} = \frac{3}{25}\frac{GM^2}{R^3}\varepsilon^2 + \frac{7}{20}H^2R^2\varepsilon \qquad (l=2). \tag{153}$$

As a function of ε, $\Delta\Omega + \Delta\mathfrak{M}$ has a minimum which it takes when

$$\frac{6}{25}\frac{GM^2}{R^3}\varepsilon + \frac{7}{20}H^2R^2 = 0, \tag{154}$$

or

$$\frac{\varepsilon}{R} = -\frac{35}{24}\frac{H^2R^4}{GM^2}. \tag{155}$$

If H_* denotes the value of the constant magnetic field inside the sphere for which $\mathfrak{M}$ (given by eq. (125)) is equal to the numerical value of the gravitational potential energy $\Omega\,(= -3\,GM^2/5\,R)$, then

$$\frac{1}{4}H_*^2R^3 = \frac{3}{5}\frac{GM^2}{R}. \tag{156}$$

In terms of H_* defined in this manner, we can rewrite equation (155) in the form

$$\frac{\varepsilon}{R} = -3.5\left(\frac{H}{H_*}\right)^2. \tag{157}$$

We may interpret this relation by saying that when a star has a magnetic field approaching the limit set by the virial theorem (cf. Sec. I), then it tends to become highly oblate; in this respect the magnetic field has the same effect as a rotation.

V. The gravitational instability of an infinite homogeneous medium in the presence of a magnetic field.

17. *The statement of the problem.*—It is well known that, by considering the propagation of a wave in an infinite homogeneous medium and allowing for the gravitational effects of the density fluctuations, Jeans [6] showed that the velocity of wave propagation is given by

$$V_J = \sqrt{c^2 - (4\pi G\rho/k^2)}, \tag{158}$$

where $c = \sqrt{(\gamma p/\rho)}$ denotes the convectional velocity of sound and k is the wave number. Accordingly, when

$$k < (4\pi\rho G)^{-1/2}/c, \tag{159}$$

the velocity of wave propagation becomes imaginary; and under these circumstances the amplitude of the wave will increase exponentially with time.

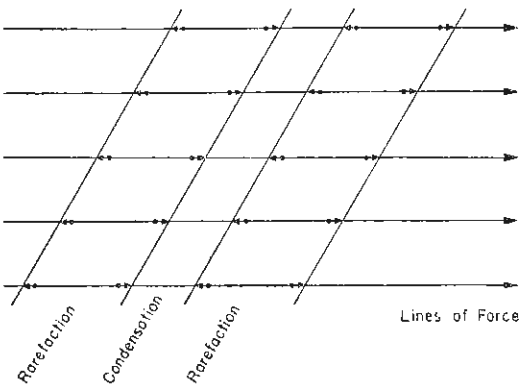

Fig. 2. – Illustrating why the presence of a magnetic field does not affect Jeans's condition for the gravitational instability of an infinite homogeneous medium.

The inequality (159) is therefore the condition for gravitational instability; this is Jeans's result. In this Section we shall show that Jeans's condition (159) is unaffected by the presence of a magnetic field. The physical reason for this is evident for a deformation in which the density waves are perpendicular to the lines of force because the motion of the particles in this case will be parallel to the lines of force and therefore will not be impeded by the magnetic field. But also a density wave forming an angle with the lines of force may be obtained by particle motions parallel to the lines of force, as shown in fig. 2.

(6) *Astronomy and Cosmogony* (Cambridge: At the University Press, 1929), pp. 345–347.

18. *The three modes of wave propagation in the presence of a magnetic field and the condition for gravitational instability.*—Consider an extended homogeneous gaseous medium of infinite electrical conductivity, and suppose that there is present a uniform magnetic field of intensity **H**. Then the fluctuations in density ($\delta\rho$), pressure (δp), magnetic field ($\boldsymbol{h}$), and gravitational potential (δV) are governed by the equations

$$(160)\qquad \begin{cases} \rho \dfrac{\partial \boldsymbol{u}}{\partial t} = \dfrac{1}{4\pi}(\operatorname{curl} \boldsymbol{h} \times \mathbf{H}) - \operatorname{grad} \delta p + \rho \operatorname{grad} \delta V, \\ \dfrac{\partial \boldsymbol{h}}{\partial t} = \operatorname{curl}(\boldsymbol{u} \times \mathbf{H}), \\ \dfrac{\partial}{\partial t}\delta\rho = -\rho \operatorname{div} \boldsymbol{u}, \end{cases}$$

and

$$\nabla^2 \delta V = -4\pi G \delta\rho.$$

If the changes in pressure and density are assumed to take place adiabatically, then

$$(161)\qquad \delta p = c^2 \delta\rho.$$

We shall seek the solutions of equations (160) and (161) which correspond to the propagation of waves in the z–direction. Then $\partial/\partial z$ is the only non-vanishing component of the gradient. And if we further suppose that the orientation of the co-ordinate axes is so chosen that

$$(162)\qquad \mathbf{H} = (0, H_y, H_z),$$

it readily follows that $h_z = 0$; and we find that equations (160) and (161) break up into the two noncombining systems:

$$(163)\qquad \rho \frac{\partial u_x}{\partial t} = \frac{H_z}{4\pi}\frac{\partial h_x}{\partial z}, \qquad \frac{\partial h_x}{\partial t} = H_z \frac{\partial u_x}{\partial z};$$

and

$$(164)\qquad \begin{cases} \rho \dfrac{\partial u_y}{\partial t} - \dfrac{H_z}{4\pi}\dfrac{\partial h_y}{\partial z} = 0, \\ \rho \dfrac{\partial u_z}{\partial t} + \dfrac{H_y}{4\pi}\dfrac{\partial h_y}{\partial z} + c^2 \dfrac{\partial}{\partial z}\delta\rho - \rho \dfrac{\partial}{\partial z}\delta V = 0, \\ \dfrac{\partial h_y}{\partial t} + H_y \dfrac{\partial u_z}{\partial z} - H_z \dfrac{\partial u_y}{\partial z} = 0, \\ \dfrac{\partial}{\partial t}\delta\rho + \rho \dfrac{\partial u_z}{\partial z} = 0, \\ \dfrac{\partial^2}{\partial z^2}\delta V + 4\pi G \delta\rho = 0. \end{cases}$$

Equations (163) can be combined to give

$$(165)\qquad \frac{\partial^2 h_x}{\partial t^2} = \frac{H_z^2}{4\pi\rho}\frac{\partial^2 h_x}{\partial z^2} \quad \text{and} \quad \frac{\partial^2 u_x}{\partial t^2} = \frac{H_z^2}{4\pi\rho}\frac{\partial^2 u_x}{\partial z^2}.$$

These equations are the same as those leading to the ordinary hydromagnetic waves of Alfvén propagated with the velocity

$$V_A = \frac{H_z}{\sqrt{(4\pi\rho)}}. \tag{166}$$

This mode of wave propagation is therefore unaffected by gravitation and compressibility.

Turning next to solutions of equations (164), which also represent the propagation of waves in the z–direction, we can write

$$\frac{\partial}{\partial t} = i\omega \quad \text{and} \quad \frac{\partial}{\partial z} = -ik, \tag{167}$$

where ω denotes the frequency and k the wave number. Making the substitutions (167) in equations (164), we obtain a system of linear homogeneous equations which can be written in matrix notation in the following form:

$$\left|\begin{array}{ccccc|c} \rho\omega & k\frac{H_z}{4\pi} & 0 & 0 & 0 & u_y \\ 0 & -k\frac{H_y}{4\pi} & \rho\omega & -kc^2 & k\rho & h_y \\ kH_z & \omega & -kH_y & 0 & 0 & u_z \\ 0 & 0 & -k\rho & \omega & 0 & \delta\rho \\ 0 & 0 & 0 & 4\pi G & -k^2 & \delta V \end{array}\right| = 0. \tag{168}$$

The condition that equation (168) has a nontrivial solution is that the determinant of the matrix on the left–hand side should vanish. Expanding the determinant, we find that it can be reduced to the form

$$\left(\frac{\omega}{k}\right)^4 - \left\{\frac{H^2}{4\pi\rho} + \left(c^2 - \frac{4\pi G\rho}{k^2}\right)\right\}\left(\frac{\omega}{k}\right)^2 + \frac{H_z^2}{4\pi\rho}\left(c^2 - \frac{4\pi G\rho}{k^2}\right) = 0. \tag{169}$$

In terms of the velocity of wave propagation, $V = \omega/k$, we can rewrite equation (169) in the form

$$V^4 - (V_A^2 \sec^2\vartheta + V_J^2)V^2 + V_A^2 V_J^2 = 0, \tag{170}$$

where ϑ denotes the angle between the directions of **H** and of wave propagation and V_J and V_A have the same meanings as in equations (158) and (166).

It is seen that equation (170) allows two modes of wave propagation. If V_1 and V_2 denote the velocities of propagation of these two modes, we conclude from equation (170) that

$$V_1 V_2 = V_A V_J$$

and

$$V_1^2 + V_2^2 = V_A^2 \sec^2\vartheta + V_J^2. \tag{171}$$

Accordingly, *if* V_J *is imaginary, then either* V_1 *or* V_2 *must be imaginary.* In other words, one of the two modes of wave propagation will be unstable if Jeans's condition (159) is satisfied. The condition for gravitational instability is therefore unaffected by the presence of the magnetic field. How-

ever, as to which of the two modes will become unstable will depend on the strength of the magnetic field. Thus for $H \to 0$, the two modes given by equation (170) approach, respectively, Jeans's mode and Alfvén's mode. And if we suppose that

$$V_1 \to V_J \quad \text{and} \quad V_2 \to V_A \quad \text{as} \quad H \to 0, \tag{172}$$

then it follows from equation (170) that so long as $V_J^2 > 0$,

$$V_1 \to V_A \sec \vartheta \quad \text{and} \quad V_2 \to V_J \cos \vartheta \quad \text{as} \quad H \to \infty. \tag{173}$$

Hence, for $H \to \infty$, the mode, which will become unstable when Jeans's condition is satisfied, will be the mode which for $H \to 0$ is Alfvén's mode; and the mode, which for $H \to 0$ is Jeans's mode, becomes a hydromagnetic wave for $H \to \infty$ and is unaffected by gravitation. This " crossing-over " of the two modes with increasing strength of the magnetic field is in agreement with what is known [7] from the theory of wave propagation in a compressible medium in the absence of gravitation.

(7) Cf. H. VAN DE HULST, *Symposium: Problems of Cosmical Aerodynamics* (Dayton Ohio: Central Air Documents Office, 1951), chap. vi; also N. HERLOFSON, « Nature », *165*, 1020 (1950).

N° 263 and 264.

In paper N° 263 Fermi applied his earlier statistical theory (paper N° 241) to the case of multiple production due to pions at cosmotron energies (up to 2.5 Bev). He showed how to take into account the consequences of charge independence. The paper was intended to serve to show how purely statistical effects enter in the analysis of experiments of this type which were being carried out with the cosmotron at Brookhaven. Originally intended as a personal communication, it was printed in Brazil.

Paper N° 264 is similar but applies to pions produced in nucleon-nucleon collisions.

H. L. ANDERSON.

263.

MULTIPLE PRODUCTION OF PIONS IN PION-NUCLEON COLLISIONS

« Academia Brasileira de Ciências », *26*, 61–63 (1954).

ABSTRACT.

The multiple production of pions in collisions of a nucleon against a pion with a laboratory energy of the order of 1 Bev is discussed with the statistical theory.

The statistical theory [1] of multiple production of pions has been recently applied to a discussion of multiple production for nucleon-nucleon collisions at the energies obtained with the Brookhaven cosmotron. In the present paper, this discussion is extended to the calculation of the result of collisions of pions against nucleons in the same range of energies. It is assumed that the result of the collision will be a nucleon and n pions. The mathematical problem is simplified by assuming that the pions are extremely relativistic in the center of mass system, and that the mass of the nucleon is very large compared to the pion mass. As a consequence of this latter assumption the nucleon carries the major fraction of the momentum of the system and therefore is considered to be at rest after the collision in the center of mass system. The conservation of angular momentum is disregarded. With these assumptions one can apply the formula (13) of A,

$$S_n = \frac{\Omega^n}{\pi^{2n}\hbar^{3n}c^{3n}} \frac{W^{3n-1}}{(3n-1)!}. \tag{1}$$

(1) E. FERMI, « Prog. Theor. Phys. », *5*, 570 (1950), quoted as A; « Phys. Rev. », *81*, 683 (1951). [See papers N° 241 and 242 (Editors' note)].

TABLE I.

$\Pi^+ + P$ *Collisions.*
Statistical Weights of the Various Charge States.

Charge State	Weight
$p+$	1
$p+o$	0.6
$p++$	0.4
$p++-$	0.333
$p+oo$	0.233
$n+o$	0.267

TABLE II.

$\Pi^- + P$ *Collisions.*
Statistical Weights for Various Charge States for $T = 1/2$ *and* $T = 3/2$.

Charge State	$T = 1/2$	$T = 3/2$
$p-$	2/3	1/3
no	1/3	2/3
$po-$	1/3	7/15
$n+-$	1/2	6/15
noo	1/6	2/15
$p+--$	0.2	0.2
$p-oo$	0.133	0.167
$n+o-$	0.3	0.4
$nooo$	0.033	0.067

TABLE III.

$\Pi^+ + P$ *Collisions.*

Outcome	Probabilities in percent for primaries of				
	0.5 Bev	1.0 Bev	1.5 Bev	2.0 Bev	2.5 Bev
$p+$	75.3	43.1	23.6	13.4	7.8
$p+o$	14.2	29.1	32.2	31.3	27.0
$n++$	9.4	19.4	22.2	20.8	18.0
$p++-$	0.4	3.2	7.7	12.0	15.4
$p+oo$	0.3	2.3	5.4	8.4	10.8
$n++o$	0.3	2.6	6.2	9.6	12.3
$p++o-$	0.0	0.2	0.8	1.9	3.7
$p+ooo$	0.0	0.0	0.2	0.6	1.1
$n+++-$	0.0	0.0	0.2	0.6	1.1
$n++oo$	0.0	0.1	0.4	1.0	1.9

S_n is proportional to the probability of obtaining a final state of definite charge structure containing n pions. In this formula W is the energy available for pion production in the center of mass system. Ω is the reaction volume. In the numerical computations this has been taken as a sphere of radius $\hbar/\mu c$ (μ is the pion mass) with a relativistic contraction factor determined by the velocity of the nucleon in the center of mass system.

In computing the various charge states, isotopic spin conservation has been assumed. The two cases of physical interest are collisions of either a positive or a negative pion against a proton. In the former case, only states of isotopic spin 3/2 are involved. In Table I the statistical weights of the various charge possibilities for this case are listed.(*)

For the collisions $\Pi^- + P$ two isotopic spin states, $T = 1/2$ and $T = 3/2$ are involved. They are present in the initial state in the amounts of 2/3 and 1/3, respectively. In Table II are listed the statistical weights corresponding to this type of collision for the two possible values of the isotopic spin.

TABLE IV.

$\Pi^- + P$ *Collisions.*

Outcome	Probabilities in percent for primaries of				
	0.5 Bev	1.0 Bev	1.5 Bev	2.0 Bev	2.5 Bev
$p-$	41.4	24.2	13.5	7.8	4.6
$n0$	33.1	19.3	10.7	6.1	3.6
$p0-$	8.8	18.5	21.4	20.5	17.9
$n+-$	12.1	22.9	26.5	25.4	22.3
$n00$	3.7	7.6	8.8	8.5	7.4
$p++-$	0.3	2.0	4.8	7.5	9.8
$p-00$	0.2	1.4	3.5	5.5	7.0
$n+0-$	0.4	3.3	7.9	12.5	16.2
$n000$	0.1	0.4	1.0	1.6	2.1
$p+0--$	0.0	0.1	0.5	1.3	2.4
$p000-$	0.0	0.0	0.2	0.4	0.8
$n++--$	0.0	0.0	0.2	0.6	1.2
$n+00-$	0.0	0.1	0.5	1.3	2.4
$n0000$	0.0	0.0	0.0	0.1	0.2

(*) For the notation see paper N° 264 (Editors' note).

The probabilities of a given outcome of a collision are proportional to the product of S_n given by (1) times the statistical weight given in Tables I and II. For the $P + \Pi^-$ case, one should take the average of the results obtained from columns 2 and 3 of Table II, weighted respectively by 2/3 and 1/3. The probabilities in percents computed on this basis are given in Tables III and IV for various energies of the primary pion in the laboratory system. In computing these tables, the statistical weights for the cases in which four pions are emitted have only been estimated.

It is remarkable that the multiplicity of pions obtained in collisions of this kind should be, according to this theory, appreciably greater than for nucleon bombardment at the same energies. This is due in part to the fact that at the same bombardment energies, more energy is available in the center of mass system because of the lighter mass of the pion. Also the reacting volume is not very much contracted relativistically and events of higher multiplicity are thereby favored.

N° 264.

For the introduction to this paper see paper N° 263.

264.

MULTIPLE PRODUCTION OF PIONS IN NUCLEON-NUCLEON COLLISIONS AT COSMOTRON ENERGIES (*)

« Phys. Rev. », *92*, 452–453 (1953).

The statistical theory of multiple pion production is applied in some detail to the discussion of nucleon-nucleon collisions for primary energies of 1.75 Bev and 2.2 Bev. Probabilities are given for single and multiple productions of pions and nucleons with different charges.

The availability of high-energy nucleons from the Brookhaven cosmotron makes it now possible to compare the results of the statistical theory [1] of multiple pion production with experiment. [2] In Table I of A, a tentative estimate of the relative probabilities that in a nucleon-nucleon collision various numbers n of pions are emitted together with two nucleons was given. According to formula (22) of A, these probabilities for bombarding energies of a few Bev should be proportional to

$$f_n(w) = \frac{\left[\frac{251}{w}(w-2)^3\right]^n}{\frac{3}{2}\times\frac{5}{2}\times\cdots\times\frac{6n+1}{2}}. \tag{1}$$

In this formula w is the total energy of the two colliding nucleons in the center-of-mass system including their rest energy. The nucleon rest energy is taken as unit of energy. A number of crude simplifying approximations have been introduced in A in deriving the preceding formula. One of them was to neglect the effects of the different possible charges of the nucleons and of the pions. We propose to improve the earlier results by a consideration of this factor. This will be done for low multiplicity production up to a maximum number of pions $n = 3$. In doing this we shall make use of the conservation of isotopic spin as a limitation to the possible types of transitions.

(*) Research supported by a joint program of the U. S. Office of Naval Research and the U. S. Atomic Energy Commission.

(1) E. FERMI, « Progr. Theoret Phys. (Japan) », *5*, 570 (1950), quoted as A; « Phys. Rev. », *81*, 683 (1951). [See paper N° 241 and 242 (Editors' note)].

(2) FOWLER, SHUTT, THORNDIKE, and WHITTEMORE, « Phys. Rev. » (to be published).

TABLE I.

Number of states of isotopic spin 1 *and* 0 *for a system of two nucleons and n pions.*

n	0	1	2	3
p_n	1	2	4	9
q_n	1	1	2	4

The fundamental hypothesis of the statistical calculation of high-energy nuclear events is that in a collision process, all possible final states are formed with a probability proportional to the statistical weight of the final state. In listing all the possible final states, however, one should exclude all those that cannot be reached from the ground state because of conservation theorems. In addition to the classical conservation theorems of energy, momentum, and angular momentum, one should include in the present discussion also the conservation of isotopic spin and, of course, of charge. To be sure, the conservation of isotopic spin is not exact. It is believed, however, that only weak transitions are possible between states of different isotopic spin. Therefore, the statistical equilibrium postulated in A will normally not have time to be established except for states of equal isotopic spin.

In a collision of two nucleons, the initial state may have either isotopic spin $T = 1$ or $T = 0$. In computing the final states, only those with isotopic spin 1 or 0 shall have to be counted. For each final state characterized, for example, by the momenta of its particles, there are a number of different charge possibilities. Let p_n be the number of such possibilities for states of isotopic spin 1 with the given total charge, and q_n the similar number for isotopic spin 0. In Table I, we list the numbers p_n and q_n for states of two nucleons and n pions.

For example, in the collision of two high-energy protons, the isotopic spin of the initial state is $T = 1$. A final state will be formed abundantly only when its isotopic spin is also 1 and we may assume that the probability of its formation will be proportional to $f_n(w)$ given by Eq. (1). In computing the relative probabilities for the formation of n pions, we shall take into account, however, that there are p_n states of isotopic spin 1. Therefore, the probabilities to form n pions will be proportional to $p_n f_n$ and be given by

$$P_n = \frac{p_n f_n}{\Sigma p_n f_n} . \tag{2}$$

If the two colliding nucleons are a neutron and a proton, the initial state is a mixture of 50 percent isotopic spin 1 and 50 percent isotopic spin 0. If the initial state has $T = 1$, the probability to form n pions will again be given by Eq. (2). For $T = 0$, the probability will be given by a similar expression with p_n replaced by q_n:

$$Q_n = \frac{q_n f_n}{\Sigma q_n f_n} . \tag{3}$$

The resultant probability will be, therefore, the arithmetic average of Eqs. (2) and (3).

In discussing the comparison of these figures with experiment, it is important to give not only the number of pions that accompany the two nucleons in the final state, but also their charges. In order to do this, we must subdivide the numbers p_n and q_n of states with n pions into numbers of states corresponding to the different possible charges of the particles emitted. For example, according to Table I there are two states of isotopic spin 1 containing two nucleons and one pion. If we are discussing the collision of two protons (total charge = 2) the two states can be written as follows:

$$(-1/\sqrt{2})(pp\,0) + (1/2)(pn\,+) + (1/2)(np\,+) \tag{4}$$

and

$$(1/\sqrt{2})(pn\,+) - (1/\sqrt{2})(np\,+), \tag{5}$$

where, for example, $(pn\,+)$ means a state in which the first nucleon is a proton, the second a neutron, and the pion is a positive pion. If the final state were Eq. (4), the probability would be 1/2 that in the final state there is a proton, a neutron, and a positive pion and 1/2 that there are two protons and a neutral pion. If the final state were Eq. (5), the only possible final state would be a neutron, a proton, and a positive pion. In this case, therefore, the number $P_2 = 2$ is divided in a part 3/2 for the formation of a neutron, a proton and positive pion, and a part 1/2 corresponding to the formation of two protons and a neutral pion. The weights computed in this manner for the various cases are listed in Tables II and III.

Table II illustrates the case of a collision between two protons. The first column gives the different types of particles that may appear in the final state compatible with charge conservation. The second column gives the weight of the state, the third is the number n of pions emitted and the fourth column is the number of charged particles emitted. The fifth and sixth columns will be discussed later.

Table III gives similar data for a neutron-proton collision. In this case two isotopic spins, T = 1 and T = 0, are possible, and therefore, two weights are given for each case in columns 2 and 3. Columns 4 and 5 give respectively the number of pions and the number of charged particles emitted. Again, the last two columns will be discussed later.

In order to show the use of the tables, we consider first the collisions of 1.75–Bev and 2.2–Bev protons against a proton at rest. One finds in this case $w = 2.781$ for 1.75 Bev and $w = 2.948$ for 2.2 Bev. The corresponding values of f_n are

$$f_0 = 1\ ;\ f_1 = 3.28\ ;\ f_2 = 0.88\ ;\ f_3 = 0.062\ ;\ \text{for 1.75 Bev.}$$

$$f_0 = 1\ ;\ f_1 = 5.53\ ;\ f_2 = 2.49\ ;\ f_3 = 0.30\ ;\ \text{for 2.2 Bev.}$$

The probability that the collision gives rise to an event of the type listed in the first column of Table II is given by the product of the weight listed in

column 2 of the same table times the appropriate f_n. The probabilities calculated in this manner and normalized to 1 are listed in columns 5 and 6.

TABLE II.

Weights for different final states in a collision of two protons.

State	Weight (*)	Number of pions	Number of prongs	Probabilities for primaries of energy	
				1.75 Bev	2.2 Bev
pp	1	0	2	8.6	4.0
pp o	1/2	1	2	14.1	11.3
pn +.	3/2	1	2	42.3	32.7
pp + —	1.2	2	4	9.1	12.2
pp oo	0.4	2	2	3.0	4.0
pn + o	1.8	2	2	13.6	18.2
nn + + ...	0.6	2	2	4.6	6.0
pp + — o	154/60	3	4	1.4	3.2
pp ooo	18/60	3	2	0.2	0.4
pn + + —	175/60	3	4	1.5	3.7
pn + oo	121/60	3	2	1.0	2.5
nn + + o	72/60	3	2	0.6	1.5

(*) See " Correction " below. (Editors' Note).

A similar calculation can be carried out for a collision of 1.75–Bev and 2.2–Bev neutrons with a proton. In this case, one should compute in a similar manner the probabilities corresponding to isotopic spin 1 and 0, and then take the average of the results. These averages are given in columns 6 and 7 of Table III. For example, one can see from Table III that the probabilities of having a star with 1, 3, or 5 prongs in a neutron-proton collision of 1.75 Bev are 61.3, 37.8, 0.6 percent, and for a 2.2–Bev neutron are 52.6, 46.2, 1.5 percent. In particular, notice the very low probability of 5–pronged stars at these energies.

In statistics of 3–pronged, stars, one will expect the probabilities of events in which a single negative pion, or at least a negative and a neutral pion, or a positive and a negative pion are produced should be 42, 15, 43 percent at 1.75 Bev and 28, 18, 54 percent at 2.2 Bev.

TABLE III.

Weights for different final states in a collision of a proton and a neutron for the cases T = 1 *and* T = 0.

Final state	T = 1 (*)	T = 0 (*)	Number of pions	Number of prongs	Probabilities primaries of energy	
					1.75 Bev	2.2 Bev
pn	1	1	0	1	12.3	6.0
pp —	1/2	1/3	1	3	15.7	12.9
pn o	1	1/3	1	1	22.8	18.5
nn + ...	1/2	1/3	1	1	15.7	12.9
pp — o	0.8	1/3	2	3	5.3	7.3
pn oo	0.6	1/3	2	1	4.6	6.3
pn + —	1.8	1	2	3	13.8	18.9
nn + o	0.8	1/3	2	1	5.3	7.3
pp — oo	0.9	0.4	3	3	0.4	1.0
pp — — + ...	1.2	0.6	3	5	0.6	1.5
pn ooo	0.6	0.2	3	1	0.2	0.6
pn + —o	4.2	1.8	3	3	2.0	4.6
nn + oo	0.9	0.4	3	1	0.4	1.0
nn + + —	1.2	0.6	3	3	0.6	1.5

(*) See " Correction " below. (Editors' Note).

It should be stressed that all these figures are at best indicative of orders of magnitude. Obviously, a statistical theory of the type under discussion can, at best, yield qualitative results. In addition, in deriving formula (1) in A, many features like statistical correlation of the various particles and conservation of angular momentum have been neglected and it is to be expected that some sizeable error may be introduced thereby in the results.

Correction:

«Phys. Rev.», *93*, 1434 (1954).

In computing the statistical weights of the various states discussed in this paper, a factor $1/n!$ (n = number of pions) was omitted. For this reason, the statistical weights given in column 2 of Table II and in columns 2 and 3 of Table III should be divided by the factorials of the number of pions given in column 3 of Table II and column 4 of Table III. Corresponding changes should be made in the computed probabilities for the two cases. This correction has the effect of reducing the probability of events with high multiplicity. For example, for a neutron-proton collision, the probabilities of stars with 1, 3, or 5 prongs for 1.75–Bev bombarding energy become 68, 32, and 0.13 percent; for bombarding energy of 2.2–Bev, the probabilities are 62, 38, and 0.3 percent. For 3–pronged stars the probabilities of a star containing a single negative pion, or at least a negative and a neutral pion, or at least a positive and a negative pion, for bombarding energy of 1.75–Bev energy are 61, 11, and 28 percent; and for 2.2–Bev bombarding energy 47, 14, and 39 percent.

In this computation the possibility of deuteron formation by proton-neutron binding, as well as the elastic shadow scattering have been neglected.

N° 265.

Fermi's interest in astrophysics was welcomed by the astrophysicists. They asked him to give the Sixth Henry Norris Russel Lecture of the American Astronomical Society. Fermi was quite pleased by this show of regard outside his own field and took the occasion to re-examine his earlier ideas about the origin of the cosmic rays in view of later developments in the knowledge of the strength and behavior of the magnetic fields. (See also the introduction to paper N° 237).

H. L. ANDERSON.

265.

GALACTIC MAGNETIC FIELDS AND THE ORIGIN OF COSMIC RADIATION

« Astrophys. J. », *119*, 1–6 (1954).

I became interested in the possible existence of magnetic fields extending through the volume of the galaxy in connection with a discussion on the origin of the cosmic radiation a few years ago.[1] The hypothesis was discussed then that the acceleration of cosmic-ray particles to extremely high energies was due to their interaction with a galactic magnetic field that was postulated to pervade the galactic space. According to Alfvén's ideas on magneto-hydrodynamics, this field would be strongly influenced by the turbulent motions of the diffuse matter within the galaxy. Indeed, the electric conductivity of this matter is so large that any lateral shift of the magnetic lines of force with respect to the matter is effectively prevented. A strong magnetic field quenches the transverse components of the displacement due to the turbulent motion. A weak field yield to the material motions, so that its lines of force are soon bent into a very crooked pattern.

The observation by Hiltner and Hall of an appreciable polarization of the light coming to us from distant stars has been interpreted [2] as due to the orientation of nonspherical dust grains by a magnetic field. If this general

(*) Sixth Henry Norris Russell Lecture of the American Astronomical Society delivered at Boulder, Colorado, on August 28, 1953.

(1) E. FERMI, « Phys. Rev. », *75*, 1169 (1949); cited hereafter as " R ". [See paper N° 237 (Editors' note)].

(2) DAVIS and GREENSTEIN, « Ap. J. », *114*, 206 (1951); SPITZER and TUKEY, « Ap. J. », *114*, 187 (1951).

type of interpretation is correct, the polarization gives us some information of the strength and the direction of the magnetic field. Hiltner's measurements [3] indicate that in the vicinity of the earth the magnetic field is approximately parallel to the direction of the spiral arm. This fact suggests that we may perhaps think that the spiral arms are magnetic tubes of force. In the following discussion we will assume that this is the case.

The direction of polarization of the stellar light indicates further that in our vicinity the magnetic lines of force show irregular deviations from parallelism of the order of 10°. This fact excludes the hypothesis that the lines of force yield completely to the turbulent motions of interstellar matter, because then they would be rapidly bent into shapes much more irregular than those observed. One is rather led to the conclusion that the field is sufficiently strong to yield only a little to the transverse component of the turbulent motion. Indeed, as was pointed out by Davis, the small deviations from parallelism of the field enable one to estimate that the intensity of the magnetic field must be of the order of 10^{-5} gauss. Recently Chandrasekhar and I [4] have re-examined this problem, considering, in particular, the balance between magnetic and gravitational effects in the spiral arm. Our conclusion is that the field intensity is about 6×10^{-6} gauss. Owing to the turbulence, the lines of force are irregularly pushed sidewise until the magnetic stress increases to the point of forcing a reversal of the material motion and of pushing back the diffuse matter, impressing on it some kind of very irregular oscillatory motion. One expects, therefore, that the lines of force sway back and forth and also that the field intensity will fluctuate along the same line of force.

A cosmic-ray particle spiraling around these moving lines of force is gradually accelerated. The acceleration mechanism was discussed in R, although the shape of the lines of force assumed then was quite different from what we now believe it to be. A cosmic-ray proton of 10 Bev energy is bent in a magnetic field of 6×10^{-6} gauss in a spiral having a radius of the order of one-third the radius of the earth's orbit. This is very small on the galactic scale. The motion of a proton with this energy and also of one with much greater energy is, therefore, properly described as a very small radius spiral around a line of force. Apart from the very rapid changes due to the spiraling, the general direction of motion may change for two reasons. One is that the line of force around which the particle spirals may be curved. In R a change of direction of this kind was called a "collision of type *b*." A second type of event, called a "collision of type *a*," takes place when the particle in its spiraling encounters a region of high field strength.

Let ϑ be the angle between the direction of the line of force and the direction of motion of the spiraling particle. The angle ϑ will be called the "angle of pitch." One can prove that, in a static magnetic field, the quantity

$$q = \frac{\sin^2\vartheta}{H} \tag{1}$$

(3) «Ap. J.», *114*, 241 (1951).
(4) «Ap. J.», *118*, 113 (1953). [See paper N° 261 (Editors' note)].

is approximately constant with time. For this reason, in a static field, the particle cannot enter a region where

$$H > \frac{1}{q} . \tag{2}$$

When the particle approaches such a region, its pitch decreases until $\vartheta = 90°$, at which moment the particle is reflected and spirals backward in the direction whence it came.

In a variable magnetic field both *a*– and *b*–type collisions may cause changes in energy. As a rule, the energy will increase or decrease according to whether the irregularity of the field that causes the collision moves toward the particle (head-on collision) or away from it (overtaking collision). It was shown in R that, on the average, the energy tends to increase primarily because the head-on collisions are more probable than the overtaking collisions. In the present discussion the same general acceleration mechanism will be assumed. The details, however, will be quite different from those previously assumed.

It was shown in R that through this mechanism the energy of the particle increases at a rate that, for extreme relativistic particles, is proportional to their energy. The energy E, therefore, increases exponentially with time:

$$E(t) = E_0 \, e^{t/A} . \tag{3}$$

According to this law, the oldest particles should have the highest energy.

The time A needed for a energy increase by a factor e was estimated in R to be about 100 million years. If this estimate was correct, A would be comparable to the time B for nuclear collisions of the particle. Assuming that a nuclear collision effectively destroys the particle, the probability that a particle has the age t should be

$$e^{-t/B} \frac{dt}{B} . \tag{4}$$

Combining conditions (3) and (4), one readily finds that the probability that a particle observed now has energy E should be proportional to

$$\frac{dE}{E^n} , \tag{5}$$

with

$$n = 1 + \frac{A}{B} . \tag{6}$$

An exponent law like (5), with n of the order of 2 or 3, seems to fit fairly well the observed energy spectrum of the cosmic radiation.

Two main objections can be raised against the theory proposed in R. One is that, according to present evidence, the structure of the galactic magnetic field is much more regular than was assumed in R. We shall try to make plausible the conclusion that, in spite of this fact, the acceleration may still take place at an adequate rate. Indeed, as will be discussed below, it will be necessary to provide an acceleration process five to ten times more efficient than was previously supposed. The second difficulty arises from the

fact that the protonic and the nuclear components of the cosmic radiation have very much the same energy spectrum. Heavy nuclei have a larger nuclear collision cross-section than protons. Their mean life B, therefore, should be shorter, and the exponent n given by equation (6) should be larger.

This difficulty would be removed if the process that eliminates the particles were equally effective against protons and against larger nuclei, because B would then be the same for both kinds of particle. For example, collisions against stars or planets do not differentiate between protons and nuclei. On the other hand, a simple estimate shows that the probability of collisions against such massive objects is quite negligible, even in a time equal to the age of the universe. Another means of removing cosmic-ray particles that is equally effective for protons and nuclei is diffusion outside the galaxy. Assume, for example, that the lines of force follow the spiral arms. The stretched-out length of the galactic spiral is about a million light-years, and the particles travel with a velocity very close to that of light. They could, therefore, escape in a time of the order of a million years. The escape time, of course, would be longer if the particle occasionally reversed its direction, owing, for example, to collisions of type *a*.

In a theory that yields essentially the same energy spectrum for cosmic-radiation protons and nuclei it will be necessary to assume that the escape time for diffusion outside the galaxy is appreciably shorter than the nuclear collision time. Then escape will be dominant with respect to nuclear collisions. We will assume that this is the case, and we will take, somewhat arbitrarily, in the numerical examples the escape time,

$$\mathrm{B} = 10 \text{ million years.} \tag{7}$$

The escape time is then about ten times shorter than the nuclear collision time.

Assuming 2.5 as an average value of the exponent n in quantity (5), we have, from equation (6),

$$\mathrm{A} = 1.5\,\mathrm{B} = 15 \text{ million years,} \tag{8}$$

in which A is the time through which the energy of the particle increases, on the average, by the factor e. This time, 15 million years, is appreciably shorter than was estimated in R.

It therefore appears necessary to modify the acceleration mechanism of R in two ways. The mean free path must be much longer, in order to allow the escape of the particles from the galaxy in a relatively short time. And the process of acceleration must be much faster. At first sight, these two requirements seem to be contradictory, and perhaps they are. On the other hand, there is an acceleration mechanism that is potentially much more efficient than the others. This process was discussed in R and was then dismissed as of little importance for certain reasons to be mentioned shortly. I propose to criticize those reasons and to make a case in favor of this acceleration mechanism.

First of all, we observe that the knowledge that we now have of the general shape of the magnetic field makes the collisions of type *b* rather unim-

portant. We shall therefore concentrate our attention on type–*a* collisions. They take place, as will be remembered, when the particle encounters a region of large field strength, where condition (2) is fulfilled. A particle that finds itself between two such regions will be trapped on the stretch of line of force comprised between them. When this happens, the energy of the particle will change with time at a rate much faster than usual. It will decrease or increase according to whether the jaws of the trap move away from or toward each other.

Let H be the average value of the magnetic field and H_{max} the maximum field along the line of force that may be likely to cause a type–*a* reflection. If ϑ is the angle of pitch of the spiral where the field is average, reflections will occur only for particles having

$$\vartheta > \chi, \tag{9}$$

where

$$\sin \chi = \sqrt{\frac{H}{H_{max}}}. \tag{10}$$

A simple calculation shows that when a particle with $\vartheta > \chi$ is caught in a trap, both its energy and its angle of pitch will change with time, but the product,

$$E \sin \vartheta, \tag{11}$$

remains approximately constant. The particle can escape the trap only when ϑ has decreased to the point that condition (9) is no longer fulfilled. In this process the energy must increase by a factor

$$\frac{\sin \vartheta}{\sin \chi}. \tag{12}$$

This process may lead to a sizable energy gain in a relatively short time. For example, if the jaws of the trap are 10 light-years apart and move toward each other at 10 km/sec, the time needed for a 10 percent energy increase is only a few tens of thousands of years.

To be sure, the jaws will occasionally move away from each other, causing a loss instead of a gain of energy. But in this case ϑ will increase, making the particle more easily caught in similar traps. The process ends only when the energy has increased to the point that ϑ has become less than χ, because only then will the particle be capable of passing without reflection through occasional maxima of the field intensity that it may encounter along its path.

When this condition is reached, the process of acceleration becomes exceedingly slow. Indeed, if q in equation (1) were exactly a constant of motion, the particle would always keep on spiraling in the same direction and would eventually escape from the galaxy. It is for this reason that the process of acceleration in a trap was not considered of major importance in R. The process may become important only if there is machinery whereby the angle of pitch, after having been reduced to a small value in the process of acceleration in a trap, can be increased. If this is the case, the trap mechanism again becomes operative, and the energy may be increased by a further factor.

Now one finds that q is almost exactly a constant as long as the particle is not caught in a trap and there are no sharp variations in the magnetic field either in time or in space. When I first discussed the acceleration of cosmic rays by magnetic fields, I was not aware of the possibility of sharp discontinuities of the field and for this reason did not think that the traps could be the dominant factor. I propose now to show that discontinuities in the direction of the magnetic field should not be too exceptional in the galaxy.

Recently de Hoffmann and Teller [5] have discussed the features of magnetohydrodynamic shocks. They show, in particular, that at a shock front sudden variations in direction and intensity of the field are likely to occur. One is tempted to identify the boundaries of many clouds of the galactic diffuse matter with shock fronts. If this is correct, we have a source of magnetic discontinuities. Probably many of these discontinuities will be rather small. However, either their cumulative effect or the effect of some occasional major discontinuity will tend to convert the angle of pitch that a previous trap acceleration has reduced to a small value back to a statistical distribution corresponding to isotropy of direction. At this moment the particle is ready for a new trap acceleration.

Probably our knowledge of the galactic magnetic field is still inadequate for a realistic discussion of the process here proposed. I would like, nevertheless, to list here in a purely hypothetical way a set of parameters that may be compatible with our present knowledge. We assume that a particle for part of the time has $\vartheta < \chi$ and that it spirals in the same direction along the line of force without being caught in traps. Let λ be the average distance of travel while the particle is in this state, measured along the line of force. After the mean path λ, the particle will change ϑ back to a high value and for a period of time will be frequently caught in traps, until its energy increases by a factor f and ϑ decreases again to $\vartheta < \chi$. After this the process repeats itself. Let T be the average duration of one such cycle. The time A for acceleration by a factor e, then, is

$$A = \frac{T}{\log f}. \tag{13}$$

The escape time B can be estimated as follows. Let L be the stretched-out length of the galaxy. The motion of the particle along L can be described as a random walk, with steps of duration T. The mean displacement in a step is given in first approximation by λ, because the particle, during the acceleration phase, changes its direction very frequently and does not move far. Estimating B with the diffusion theory, one finds

$$B = \frac{T\,(L/\lambda)^2}{\pi^2}. \tag{14}$$

A set of parameters that yields A = 15 million years and B = 10 million years is the following.

$$L = 1.3 \times 10^{24} \text{ cm}, \qquad \lambda = 2 \times 10^{23} \text{ cm};$$

$$T = 2.3 \times 10^{6} \text{ years}, \qquad f = 1.17.$$

(5) « Phys. Rev. », *80*, 692 (1950).

Naturally, these values are given here merely as an indication of possible orders of magnitude. Only a much more thorough discussion of the actual conditions in the galaxy may enable one to find reliable values of these quantities.

Two important questions should be discussed further. One is the injection mechanism that should feed into interstellar space an adequate number of particles of energy large enough for the present acceleration mechanism to take over. This problem was discussed in R, but no definite conclusion was reached there. The fact that the acceleration by the galactic magnetic field discussed here is appreciably faster than in R makes the requirements of the injection somewhat less stringent. Nevertheless, one still needs a very powerful injection mechanism. Recent evidence that cosmic-ray-like particles are emitted by the sun indicates the stars, or perhaps stars of special types, as the most likely injectors.

A second question has to do with the energy balance of the turbulence of the interstellar gas. If it is true that the cosmic radiation leaks out of the galaxy in a time of the order of 10 million years, it is necessary that its energy be replenished a few hundred times during a time equal to the age of the universe. A simple estimate shows that the energy present in the galaxy in the form of cosmic rays is comparable to the kinetic energy due to the turbulence of the intergalactic gas. According to the present theory, the cosmic rays are accelerated at the expense of the turbulent energy. This last, therefore, must be continuously renewed by some very abundant source, perhaps like a small fraction of the radiation energy of the stars.

In conclusion, I should like to stress the fact that, regardless of the details of the acceleration mechanism, cosmic radiation and magnetic fields in the galaxy must be counted as very important factors in the equilibrium of interstellar gas.

N° 266.

After the war, during one of his frequent summer visits to Los Alamos, Fermi became interested in the development and potentialities of the electronic computing machines. He held many discussions with me on the kind of future problems which could be studied through the use of such machines. We decided to try a selection of problems for heuristic work where in absence of closed analytic solutions experimental work on a computing machine would perhaps contribute to the understanding of properties of solutions. This could be particularly fruitful for problems involving the asymptotic—long time or " in the large " behavior of non-linear physical systems. In addition, such experiments on computing machines would have at least the virtue of having the postulates clearly stated. This is not always the case in an actual physical object or model where all the assumptions are not perhaps explicitly recognized.

Fermi expressed often a belief that future fundamental theories in physics may involve non-linear operators and equations, and that it would be useful to attempt practice in the mathematics needed for the understanding of non-linear systems. The plan was then to start with the possibly simplest such physical model and to study the results of the calculation of its long-time behavior. Then one would gradually increase the generality and the complexity of the problem calculated on the machine. The Los Alamos report LA–1940 (paper N° 266) presents the results of the very first such attempt. We had planned the work in the summer of 1952 and performed the calculations the following summer. In the discussions preceding the setting up and running of the problem on the machine we had envisaged as the next problem a two-dimensional version of the first one. Then perhaps problems of pure kinematics e.g., the motion of a chain of points subject only to constraints but no external forces, moving on a smooth plane convoluting and knotting itself indefinitely. These were to be studied preliminary to setting up ultimate models for motions of system where " mixing " and " turbulence " would be observed. The motivation then was to observe the *rates* of mixing and " thermalization " with the hope that the calculational results would provide hints for a future theory. One could venture a guess that one motive in the selection of problems could be traced to Fermi's early interest in the ergodic theory. In fact, his early paper (N° 11 *a*) presents an important contribution to this theory.

It should be stated here that during one summer Fermi learned very rapidly how to *program* problems for the electronic computers and he not only could plan the general outline and construct the so-called flow diagram but would work out himself the actual *coding* of the whole problem in detail.

The results of the calculations (performed on the old MANIAC machine) were interesting and quite surprising to Fermi. He expressed to me the opinion that they really constituted a little discovery in providing intimations that the prevalent beliefs in the universality of " mixing and thermalization " in non-linear systems may not be always justified.

A few words about the subsequent history of this non-linear problem. A number of other examples of such physical systems were examined by calculations on the electronic computing machines in 1956 and 1957. I presented the results of the original paper on several occasions at scientific meetings; they seemed to have aroused considerable interest among mathematicians and physicists and there is by now a small literature dealing with this problem. The most recent results are due to N. J. Zabusky. [1] His analytical work shows, by the way, a good agreement of the numerical computations with the continuous solution up to a point where a discontinuity developed in the derivatives and the analytical work had to be modified. One obtains from it another indication that the phenomenon discovered

(1) Exact Solutions for the Vibrations of a non-linear continuous string. A. E. C. Research and Development Report. MATT–102, Plasma Physics Laboratory, Princeton University, October 1961.

is not due to numerical accidents of the algorithm of the computing machine, but seems to constitute a real property of the dynamical system.

In 1961, on more modern and faster machines, the original problem was considered for still longer periods of time. It was found by J. Tuck and M. Menzel that after one continues the calculations from the first " return " of the system to its original condition the return is not complete. The total energy is concentrated again essentially in the first Fourier mode, but the remaining one or two percent of the total energy is in higher modes. If one continues the calculation, at the end of the next great cycle the error (deviation from the original initial condition) is greater and amounts to perhaps three percent. Continuing again one finds the deviation increasing—after eight great cycles the deviation amounts to some eight percent; but from that time on an opposite development takes place! After eight more i.e., sixteen great cycles altogether, the system gets very close—better than within one percent to the original state! This supercycle constitutes another surprising property of our non-linear system.

Paper N° 266 is not the only work that Fermi and I did together. In the summer of 1950 we made a study of the behavior of the thermonuclear reaction in a mass of deuterium and wrote a report, LA–1158, which is still classified. The problem is of enormous mathematical complexity, involving the hydrodynamics of the motion of the material, the hydrodynamics of radiation energy, all interwoven with the processes of the various reactions between the nuclei whose probabilities and properties depend i.a., on temperature, density, and the changing geometry of the materials. The aim of this work was to obtain, by a schematized but still elaborate picture of the evolution of all these physical processes, an idea of the propagation of such a reaction. This was to complement a previous work by Everett and myself, dealing with the problem of ignition of a mass deuterium. Assuming an ignition somehow started in a large volume, one wanted to evaluate the prospects of propagation of the reactions already started. Many ingenious schematizations and simplifications had to be introduced in order to describe the process, without the possibility of calculating in exact detail the innumerable geometrical and thermodynamical factors. The results of our computations on the chances of propagation were negative and the report played an important role in channeling imagination and energies towards a search for a different scheme for a successful hydrogen reaction. This was indeed found later on on a different basis. All the calculations on which the work of the report is based were performed on desk computers and slide rules. The subsequent massive and lengthy work on the electronic computer machines (organized and performed by von Neumann, F. and C. Evans and others) confirmed in large lines, qualitatively and to a good degree quantitatively the behavior of the system as estimated and predicted in our report—with its combination of intuitive evaluations, schematized equations and hand calculations.

S. M. ULAM.

266.

STUDIES OF NON LINEAR PROBLEMS

E. FERMI, J. PASTA, and S. ULAM
Document LA–1940 (May 1955).

ABSTRACT.

A one-dimensional dynamical system of 64 particles with forces between neighbors containing nonlinear terms has been studied on the Los Alamos computer MANIAC I. The nonlinear terms considered are quadratic, cubic, and broken linear types. The results are analyzed into Fourier components and plotted as a function of time.

The results show very little, if any, tendency toward equipartition of energy among the degrees of freedom.

The last few examples were calculated in 1955. After the untimely death of Professor E. Fermi in November, 1954, the calculations were continued in Los Alamos.

This report is intended to be the first one of a series dealing with the behavior of certain nonlinear physical systems where the non-linearity is introduced as a perturbation to a primarily linear problem. The behavior of the systems is to be studied for times which are long compared to the characteristic periods of the corresponding linear problems.

The problems in question do not seem to admit of analytic solutions in closed form, and heuristic work was performed numerically on a fast electronic computing machine (MANIAC I at Los Alamos).[1] The ergodic behavior of such systems was studied with the primary aim of establishing, experimentally, the rate of approach to the equipartition of energy among the various degrees of freedom of the system. Several problems will be considered in order of increasing complexity. This paper is devoted to the first one only.

We imagine a one-dimensional continuum with the ends kept fixed and with forces acting on the elements of this string. In addition to the usual linear term expressing the dependence of the force on the displacement of the element, this force contains higher order terms. For the purposes of numerical work this continuum is replaced by a finite number of points (at most 64 in our actual computation) so that the partial differential equation defining the motion of this string is replaced by a finite number of total differential equations. We have, therefore, a dynamical system of 64 particles with forces acting between neighbors with fixed end points. If x_i denotes the displacement of the i–th point from its original position, and α denotes the coefficient of the quadratic term in the force between the neighboring mass points and β that of the cubic term, the equations were either

$$(1) \qquad \ddot{x}_i = (x_{i+1} + x_{i-1} - 2x_i) + \alpha\,[(x_{i+1} - x_i)^2 - (x_i - x_{i-1})^2] \qquad (i = 1, 2, \cdots, 64),$$

or

$$(2) \qquad \ddot{x}_i = (x_{i+1} + x_{i-1} - 2x_i) + \beta\,[(x_{i+1} - x_i)^3 - (x_i - x_{i-1})^3] \qquad (i = 1, 2, \cdots, 64).$$

α and β were chosen so that at the maximum displacement the nonlinear term was small, e.g., of the order of one-tenth of the linear term. The corresponding partial differential equation obtained by letting the number of particles become infinite is the usual wave equation plus non-linear terms of a complicated nature.

Another case studied recently was

$$(3) \qquad \ddot{x}_i = \delta_1 (x_{i+1} - x_i) - \delta_2 (x_i - x_{i-1}) + c$$

(1) We thank Miss Mary Tsingou for efficient coding of the problems and for running the computations on the Los Alamos MANIAC machine.

where the parameters δ_1, δ_2, c were not constant but assumed different values depending on whether or not the quantities in parentheses were less than or greater than a certain value fixed in advance. This prescription amounts to assuming the force as a broken linear function of the displacement. This broken linear function imitates to some extent a cubic dependence. We show the graphs representing the force as a function of displacement in three cases.

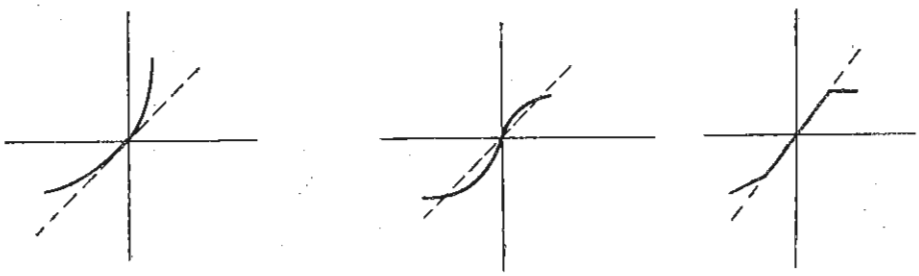

Quadratic Cubic Broken Linear

The solution to the corresponding linear problem is a periodic vibration of the string. If the initial position of the string is, say, a single sine wave, the string will oscillate in this mode indefinitely. Starting with the string in a simple configuration, for example in the first mode (or in other problems, starting with a combination of a few low modes), the purpose of our computations was to see how, due to nonlinear forces perturbing the periodic linear solution, the string would assume more and more complicated shapes, and, for t tending to infinity, would get into states where all the Fourier modes acquire increasing importance. In order to see this, the shape of the string, that is to say, x as a function of i and the kinetic energy as a function i were analyzed periodically in Fourier series. Since the problem can be considered one of dynamics, this analysis amounts to a Lagrangian change of variables: instead of the original $\dot{x}_i$ and x_i, $i = 1, 2, \cdots, 64$, we may introduce a and $\dot{a}_k$, $k = 1, 2, \cdots, 64$, where

$$a_k = \Sigma x_i \sin \frac{ik\pi}{64} . \tag{4}$$

The sum of kinetic and potential energies in the problem with a quadratic force is

$$\mathrm{E}^{\mathrm{kin}}_{x_i} + \mathrm{E}^{\mathrm{pot}}_{x_i} = \frac{1}{2}\dot{x}_i^2 + \frac{(x_{i+1} - x_i)^2 + (x_i - x_{i-1})^2}{2} \tag{5 a}$$

$$\mathrm{E}^{\mathrm{kin}}_{a_k} + \mathrm{E}^{\mathrm{pot}}_{a_k} = \frac{1}{2}\dot{a}_k^2 + 2\,a_k^2 \sin^2 \frac{\pi k}{128} \tag{5 a}$$

if we neglect the contributions to potential energy from the quadratic or higher terms in the force. This amounts in our case to at most a few percent.

The calculation of the motion was performed in the x variables, and every few hundred cycles the quantities referring to the a variables were computed by the above formulas. It should be noted here that the calculation of the motion could be performed directly in a_k and $\dot{a}_k$. The formulas, however become unwieldy and the computation, even on an electronic computer, would take a long time. The computation in the a_k variables could have been more instructive for the purpose of observing directly the interaction between the a_k's. It is proposed to do a few such calculations in the near future to observe more directly the properties of the equations for $\ddot{a}_k$.

Let us say here that the results of our computations show features which were, from the beginning, surprising to us. Instead of a gradual, continuous flow of energy from the first mode to the higher modes, all of the problems show an entirely different behavior. Starting in one problem with a quadratic force and a pure sine wave as the initial position of the string, we indeed observe initially a gradual increase of energy in the higher modes as predicted (e.g., by Rayleigh in an infinitesimal analysis). Mode 2 starts increasing first, followed by mode 3, and so on. Later on, however, this gradual sharing of energy among successive modes ceases. Instead, it is one or the other mode that predominates. For example, mode 2 decides, as it were, to increase rather rapidly at the cost of all other modes and becomes predominant. At one time, it has more energy than all the others put together! Then mode 3 undertakes this role. It is only the first few modes which exchange energy among themselves and they do this in a rather regular fashion. Finally, at a later time mode 1 comes back to within one percent of its initial value so that the system seems to be almost periodic. All our problems have at least this one feature in common. Instead of gradual increase of all the higher modes, the energy is exchanged, essentially, among only a certain few. It is, therefore, very hard to observe the rate of " thermalization " or mixing in our problem, and this was the initial purpose of the calculation.

If one should look at the problem from the point of view of statistical mechanics, the situation could be described as follows: the phase space of a point representing our entire system has a great number of dimensions. Only a very small part of its volume is represented by the regions where only one or a few out of all possible Fourier modes have divided among themselves almost all the available energy. If our system with nonlinear forces acting between the neighboring points should serve as a good example of a transformation of the phase space which is ergodic or metrically transitive, then the trajectory of almost every point should be everywhere dense in the whole phase space. With overwhelming probability this should also be true of the point which at time $t = 0$ represents our initial configuration, and this point should spend most of its time in regions corresponding to the equipartition of energy among various degrees of freedom. As will be seen from the results this seems hardly the case. We have plotted (figs. 1 to 7) the ergodic sojourn times in certain subsets of our phase space. These may show a tendency to approach limits as guaranteed by the ergodic theorem. These limits, however, do not seem to correspond to equipartition even in the time average. Certainly, there seems to be very little, if any, tendency towards equipartition

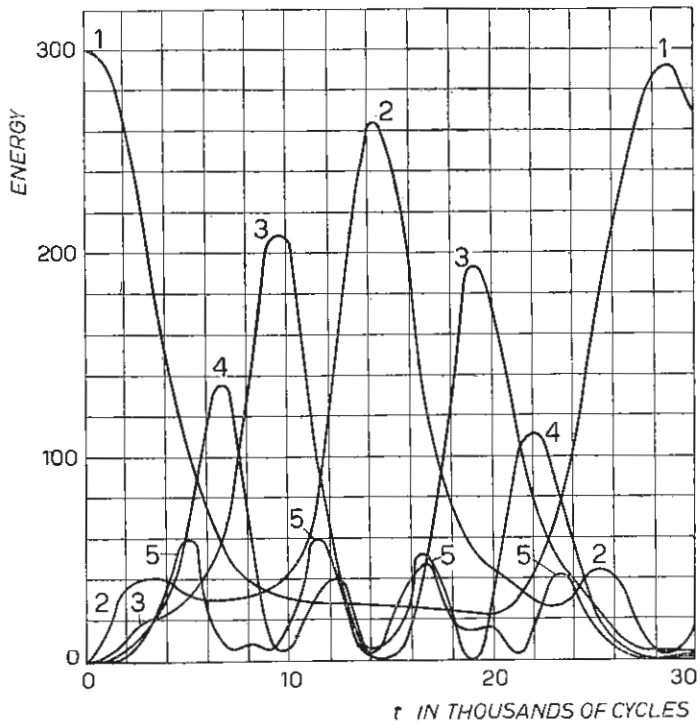

Fig. 1. – The quantity plotted is the energy (kinetic plus potential in each of the first five modes). The units for energy are arbitrary. $N = 32$; $\alpha = 1/4$; $\delta t^2 = 1/8$. The initial form of the string was a single sine wave. The higher modes never exceeded in energy 20 of our units. About 30,000 computation cycles were calculated.

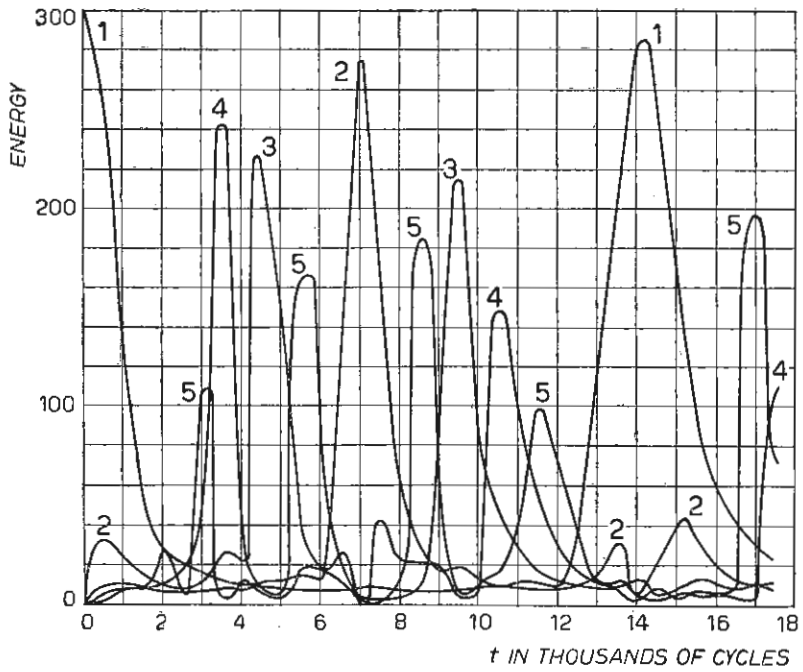

Fig. 2. – Same conditions ad fig. 1 but the quadratic term in the force was stronger. $\alpha = 1$. About 14,000 cycles were computed.

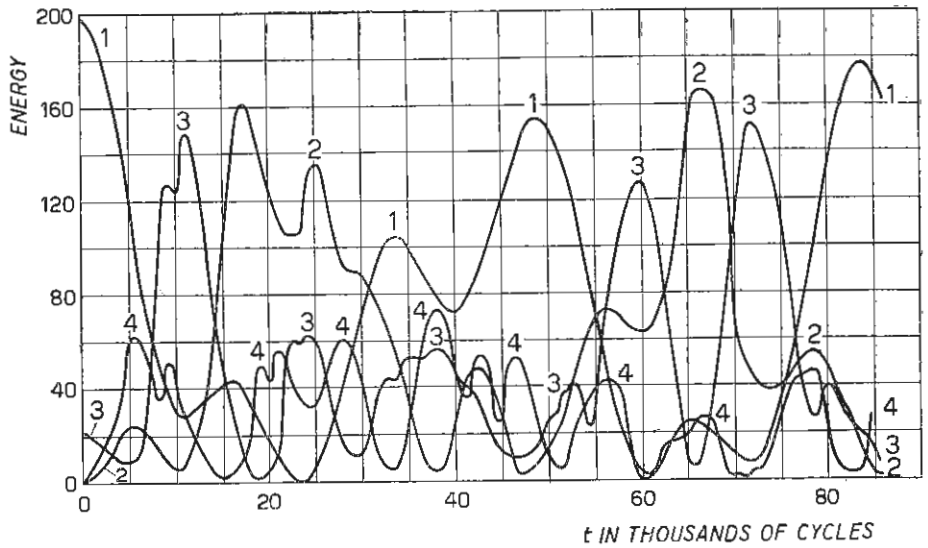

Fig. 3. – Same conditions as in fig. 1, but the initial configuration of the string was a " saw-tooth " triangular-shaped wave. Already at $t = 0$, therefore, energy was present in some modes other than 1. However, modes 5 and higher never exceeded 40 of our units.

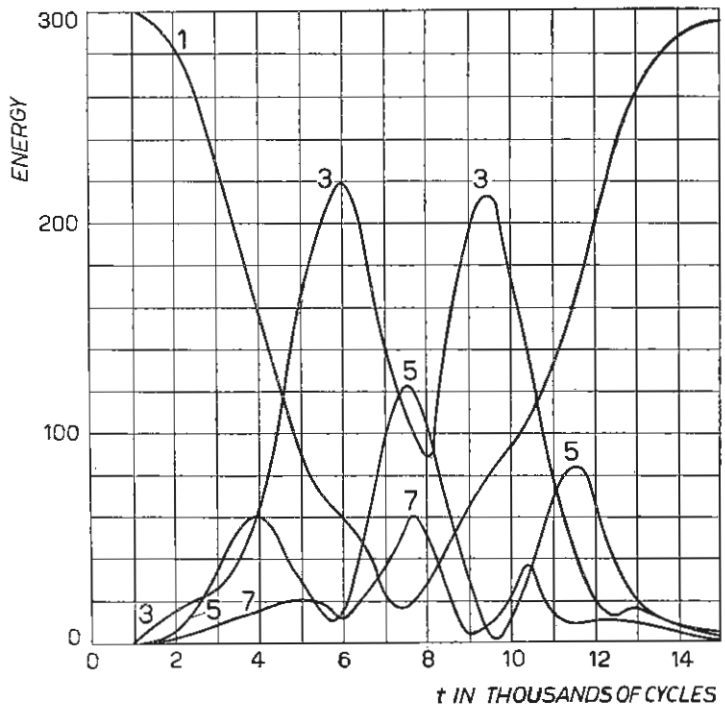

Fig. 4. – The initial configuration assumed was a single sine wave; the force had a cubic term with $\beta = 8$ and $\delta t^2 = 1/8$. Since a cubic force acts symmetrically (in contrast to a quadratic force), the string will forever keep its symmetry and the effective number of particles for the computation is $N = 16$. The even modes will have energy 0.

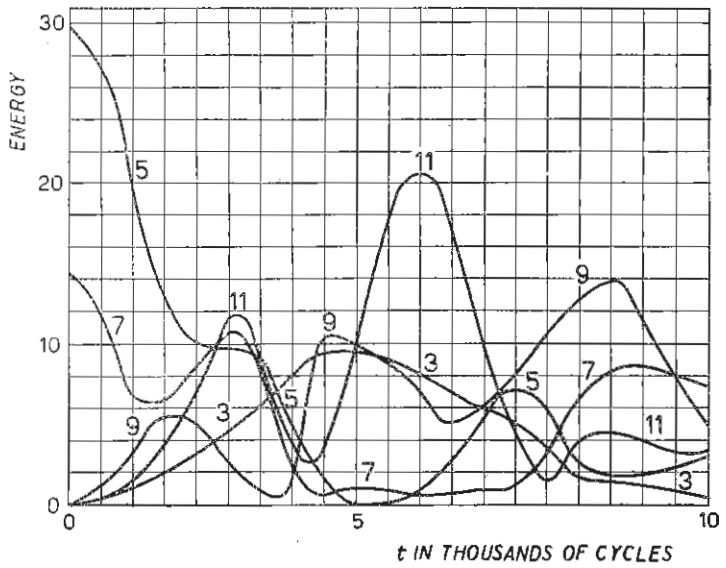

Fig. 5. – N = 32; $\delta t^2 = 1/64$; $\beta = 1/16$. The initial configuration was a combination of 2 modes. The initial energy was chosen to be 2/3 in mode 5 and 1/3 in mode 7.

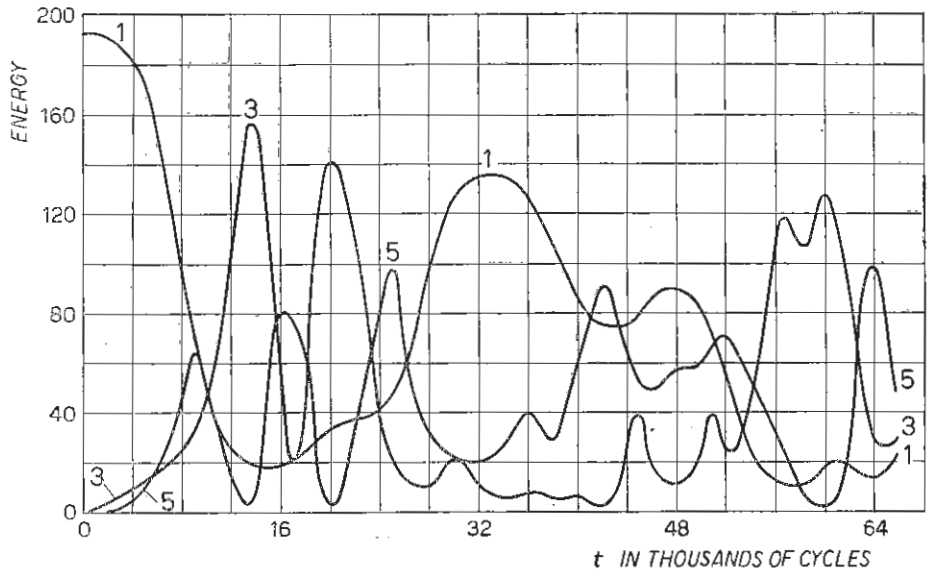

Fig. 6. – $\delta t^2 = 2^{-6}$. The force was taken as a broken linear function of displacement. The amplitude at which the slope changes was taken as $2^{-5} + 2^{-7}$ of the maximum amplitude. After this cut-off value, the force was assumed still linear but the slope increased by 25 percent. The effective N = 16.

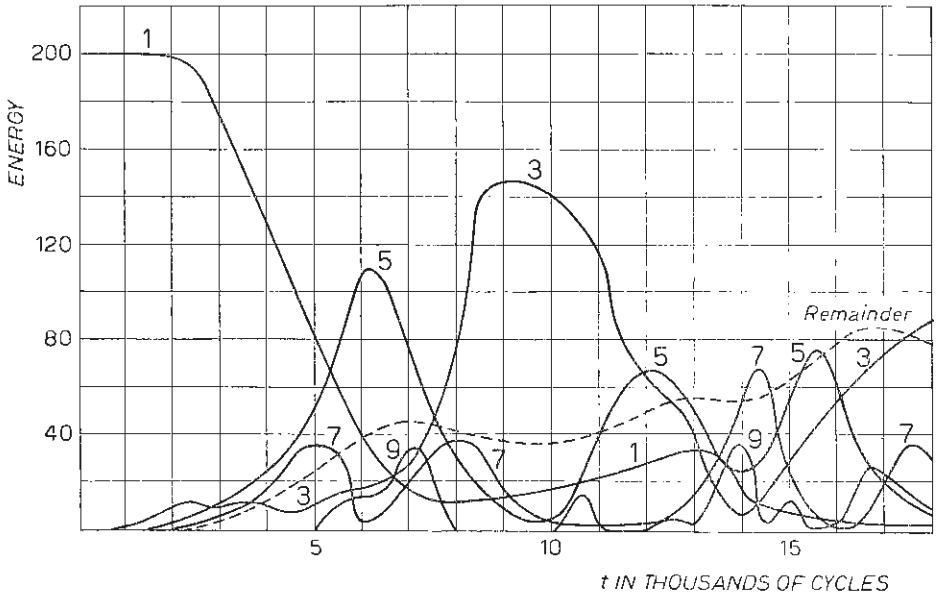

Fig. 7. – $\delta t^2 = 2^{-6}$. Force is again broken linear function with the same cut-off, but the slopes after that increased by 50 percent instead of the 25 percent charge as in problem 6. The effective N = 16.

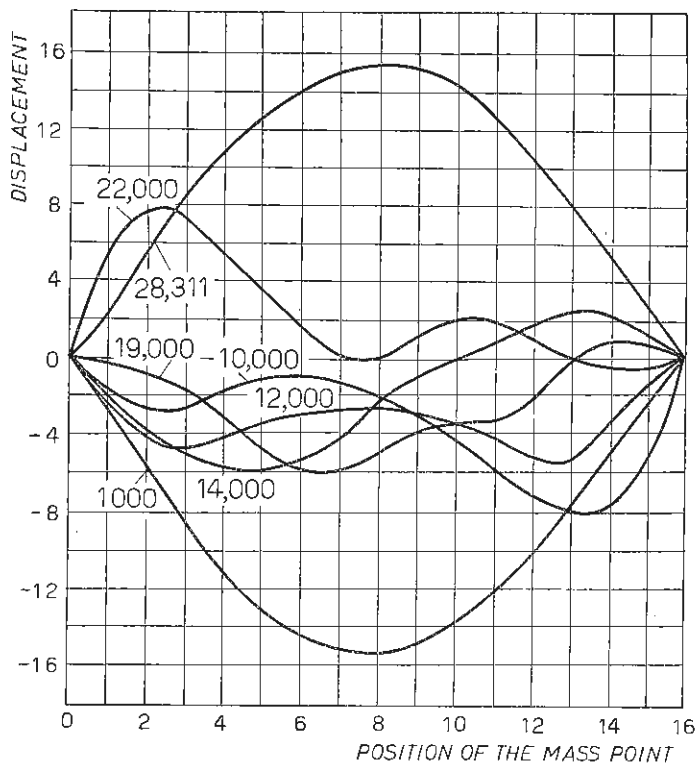

Fig. 8. – This drawing shows not the energy but the actual *shapes*, i.e., the displacement of the string at various times (in cycles) indicated on each curve. The problem is that of fig. 1.

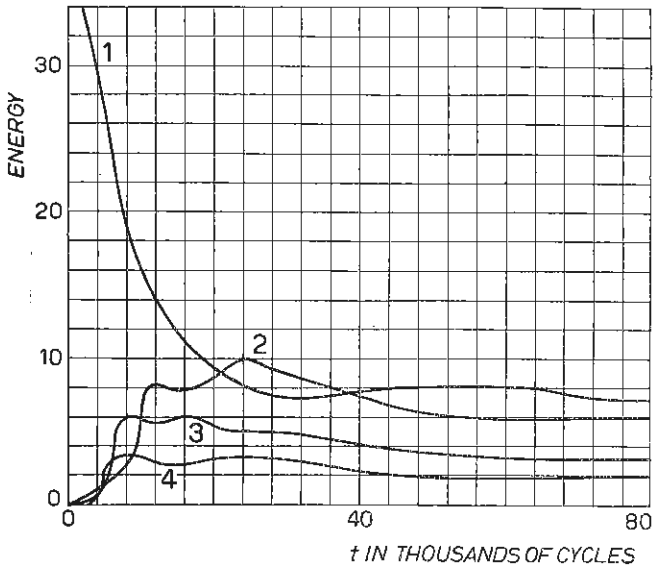

Fig. 9. This graph refers to the problem of fig. 6. The curves, numbered 1, 2, 3, 4, show the time averages of the kinetic energy contained in the first 4 modes as a function of time. In other words, the quantity is $\frac{1}{\nu}\sum_{i=1}^{\nu} T^i_{a_k}$. ν is the cycle no., $k = 1, 3, 5, 7$.

of energy among all degrees of freedom at a given time. In other words, the systems certainly do not show mixing. (2)

The general features of our computation are these: in each problem, the system was started from rest at time $t = 0$. The derivatives in time, of course, were replaced for the purpose of numerical work by difference expressions. The length of time cycle used varied somewhat from problem to problem. What corresponded in the linear problem to a full period of the motion was divided into a large number of time cycles (up to 500) in the computation. Each problem ran through many "would-be periods" of the linear problem, so the number of time cycles in each computation ran to many thousands. That is to say, the number of swings of the string was of the order of several hundred, if by a swing we understand the period of the initial configuration in the corresponding linear problem. The distribution of energy in the Fourier modes was noted every few hundred of the computation cycles. The accuracy of the numerical work was checked by the constancy of the quantity representing the total energy. In some cases, for checking purposes, the corresponding linear problems were run and these behaved correctly within one percent or so, even after 10,000 or more cycles.

It is not easy to summarize the results of the various special cases. One feature which they have in common is familiar from certain problems in me-

(2) One should distinguish between metric transitivity or ergodic behavior and the stronger property of mixing.

chanics of systems with a few degrees of freedom. In the compound pendulum problem one has a transformation of energy from one degree of freedom to another and back again, and not a continually increasing sharing of energy between the two. What is perhaps surprising in our problem is that this kind of behavior still appears in systems with, say, 16 or more degrees of freedom.

What is suggested by these special results is that in certain problems which are approximately linear, the existence of quasi-states may be conjectured.

In a linear problem the tendency of the system to approach a fixed "state" amounts, mathematically, to convergence of iterates of a transformation in accordance with an algebraic theorem due to Frobenius and Perron. This theorem may be stated roughly in the following way. Let A be a matrix with positive elements. Consider the linear transformation of the n–dimensional space defined by this matrix. One can assert that if $\bar{x}$ is any vector with all of its components positive, and if A is applied repeatedly to this vector, the directions of the vectors $\bar{x}$, $A(\bar{x}), \cdots, A^i(\bar{x}), \cdots$, will approach that of a fixed vector $\bar{x}_0$ in such a way that $A(\bar{x}_0) = \lambda(\bar{x}_0)$. This eigenvector is unique among all vectors with all their components non-negative. If we consider a linear problem and apply this theorem, we shall expect the system to approach a steady state described by the invariant vector. Such behavior is in a sense diametrically opposite to an ergodic motion and is due to a very special character, linearity of the transformations of the phase space. The results of our calculation on the nonlinear vibrating string suggest that in the case of transformations which are approximately linear, differing from linear ones by terms which are very simple in the algebraic sense (quadratic or cubic in our case), something analogous to the convergence to eigenstates may obtain.

One could perhaps conjecture a corresponding theorem. Let Q be a transformation of a n–dimensional space which is nonlinear but is still rather simple algebraically (let us say, quadratic in all the coordinates). Consider any vector $\bar{x}$ and the iterates of the transformation Q acting on the vector $\bar{x}$. In general, there will be no question of convergence of these vectors $Q^n(\bar{x})$ to a fixed direction.

But a weaker statement is perhaps true. The directions of the vectors $Q^n(\bar{x})$ sweep out certain cones C_α or solid angles in space in such a fashion that the time averages, i.e., the time spent by $Q^n(\bar{x})$ in C_α, exist for $n \to \infty$. These time averages may depend on the initial $\bar{x}$ but are able to assume only a finite number of different values, given C_α. In other words, the space of all direction divides into a finite number of regions R_i, $i = 1, \cdots, k$, such that for vectors $\bar{x}$ taken from any one of these regions the percentage of time spent by images of $\bar{x}$ under the Q^n are the same in any C_α.

The graphs fig. 1–9 show the behavior of the energy residing in various modes as a function of time; for example, in fig. 1 the energy content of each of the first 5 modes is plotted. The abscissa is time measured in computational cycles, δt, although figure captions give δt^2 since this is the term involved directly in the computation of the acceleration of each point.

In all problems the mass of each point is assumed to be unity; the amplitude of the displacement of each point is normalized to a maximum of 1. N denotes the number of points and therefore the number of modes present in the calculation. α denotes the coefficient of the quadratic term and β that of the cubic term in the force between neighboring mass points.

We repeat that in all our problems we started the calculation from the string at rest at $t = 0$. The ends of the string are kept fixed.

N° 267 and 268.

On February 11th, 1954 I went to visit Fermi in Chicago for a few days and related to him the recent results of some experiments on polarization of scattered protons which my group and I had performed at Berkeley. Similar experiments had been attempted previously at the University of Chicago with negative results, and Fermi and I had discussed the problem already in November of 1953. When I reported definite results with quantitative measurements, Fermi was very interested and wanted to check whether the spin orbit coupling, which plays such an important role in the shell model, could account also for the polarization in high energy scattering. The calculation reported in paper N° 267 was performed on the blackboard in Fermi's office from ten in the morning to about noon. He made first a false start in using the Born approximation, which gives a null result, but corrected it very soon and proceeded rapidly while I took notes for myself and for the paper, which was completed within very few days. Fermi liked the simplicity of the method and of the results, and lectured on it later at Varenna (see paper N° 270). This was the last time in which I saw him solving a problem in the old style so familiar to me from the Roman period. It is probably his last published original work, preceding his final illness only by a few months.

After completing paper N° 267 Fermi undertook an exact calculation to prove the validity of the Born approximation. He presented the results of this calculation in a private communication, which was not published then (paper N° 268).

E. SEGRÈ.

267.

POLARIZATION OF HIGH ENERGY PROTONS SCATTERED BY NUCLEI

« Nuovo Cimento », *11*, 407-411 (1954)

SUMMARY.—The attempt is made to explain the polarization recently observed in protons of several hundred Mev scattered by nuclei in terms of the same spin orbit coupling that is assumed in the nuclear shell model. It is found that the extrapolation to high energy of the spin orbit coupling observed at low energy is adequate to yield the correct order of magnitude of the polarization.

It has recently been observed [1] that protons of a few hundred Mev become strongly polarized when scattered by nuclei. A somewhat weaker polarization has also been observed in proton scattering. The polarization is observed by a double scattering experiment. The beam is polarized by a

(1) C. L. C. OXLEY, W. F. CARTWRIGHT, J. ROUVINA, E. BASKIR, D. KLEIN, J. RING, and W. SKILLMAN, « Phys. Rev. », *91*, 419 (1953); O. CHAMBERLAIN, E. SEGRÈ, R. TRIPP, C. WIEGAND, and T. YPSILANTIS, « Phys. Rev. », in press.; J. MARSHALL, L. MARSHALL, and H. G. DE CARVALHO, « Phys. Rev. », in press.

first scattering on a target usually located inside the cyclotron tank. The scattered and polarized beam is scattered a second time on a target of various materials and the polarization is shown by a difference in intensity of the scattering by the second target at equal angles to the right and to the left of the beam. According to Marshall, Marshall, and De Carvalho [1] the elastically scattered protons are even more strongly polarized than those that are scattered inelastically.

In the present paper an attempt will be made to explain the polarization of the elastically scattered beam with the effect of the spin orbit coupling that is postulated in the nuclear shell model of Mayer and Jensen. The evidence of nuclear structure indicates the existence of a spin orbit interaction which tends to depress the energy of the nucleonic orbits with spin parallel to the orbital angular momentum. This coupling is presumably present in the nucleon nucleon forces but not enough is known about them at present to substantiate this conjecture. One might expect, of course, that also in a nucleus there should be a spin orbit coupling corresponding to the so-called Thomas correction.[2] This coupling, however is much weaker than the coupling that is observed empirically in nuclear levels. For example it has been estimated by Heisenberg that the shell model of nuclear structure requires a coupling about 15 times stronger.

We will assume, therefore, that in the potential that the nucleus exerts on a nucleon there is a term 15 times larger than the Thomas correction, namely:

$$H_s = -15 \frac{\hbar}{2 M^2 c^2} \frac{V_1'(r)}{r} \boldsymbol{\sigma} \cdot \boldsymbol{r} \times \boldsymbol{p}. \tag{1}$$

$V_1(r)$ is the real part of the potential to be discussed later. It is clearly a risky extrapolation to extend the spin orbit coupling (1) known to be present in bound nucleon orbits to protons of 200 or 300 Mev. It appears worthwhile, however, to discuss the consequences of this extrapolation for the polarization phenomena.

In addition to the spin orbit coupling (1) we shall assume that the nucleus exerts a central potential $V(r)$ on the nucleon. This potential will consist of a real and an imaginary part:

$$V = V_1 + iV_2. \tag{2}$$

The imaginary part of the potential represents in the usual way the absorption properties of the nuclear matter.[3] For simplicity we will assume that both the real and the imaginary part of V have the shape of a potential well

$$V_1 + iV_2 = \begin{cases} -B - iB_a & \text{for } r < r_0 \\ 0 & \text{for } r > r_0 \end{cases} \tag{3}$$

where r_0 is the nuclear radius. We will discuss the scattering by the po-

(2) L. H. THOMAS, « Nature », *117*, 514 (1926).

(3) See for example, S. FERNBACH, R. SERBER, and T. B. TAYLOR, « Phys. Rev. », *75*, 1352 (1949).

tentials (1) and (3) in Born approximation. This method is probably adequate to give correctly qualitative results and we hope to be able to improve on it at a later date.

In order to compute the scattering cross-section we need the matrix elements of (1) and (3) between the final state 2 and the initial state 1. We take as initial state a plane wave of momentum p parallel to the x axis, with spin up. We are interested in the scattering in the xy plane, perpendicular to the spin direction. Our final state, therefore, will be a plane wave with momentum equal in magnitude to p, parallel to the xy plane, and forming an angle ϑ with the x axis. Observe that with this notation ϑ positive corresponds to scattering to the left and ϑ negative to scattering to the right.

In computing the matrix element of (1), V_1' will he given by:

$$V_1' = B\delta(r - r_0) \tag{4}$$

in accordance with (3). The calculation of the matrix element is straightforward. One finds:

$$\langle 2 \mid H_s \mid 1 \rangle = -30\,\pi i\,(p/Mc)^2 r_0^3\,B \sin\vartheta \left\{ \frac{\sin q}{q^3} - \frac{\cos q}{q^2} \right\}, \tag{5}$$

where

$$q = \frac{2pr_0}{\hbar} \sin\frac{\vartheta}{2}. \tag{6}$$

The matrix element of the potential (3) is given by:

$$\langle 2 \mid V \mid 1 \rangle = -4\,\pi r_0^3\,(B + iB_\alpha) \left\{ \frac{\sin q}{q^3} - \frac{\cos q}{q^2} \right\}. \tag{7}$$

Both matrix elements (5) and (7) cause no change of the spin direction. The differential scattering cross-section $d\sigma/d\omega$ is proportional to the square modulus of the sum of the matrix elements (5) and (7). The proportionality coefficient is $M^2/(4\,\pi^2\,\hbar^4)$. One finds:

$$\frac{d\sigma}{d\omega} = \frac{4\,M^2}{\hbar^4} r_0^6\,B^2 \left\{ \frac{\sin q}{q^3} - \frac{\cos q}{q^2} \right\}^2 \left[1 + \left\{ \frac{B_\alpha}{B} + \frac{15}{2} \left(\frac{p}{Mc} \right)^2 \sin\vartheta \right\}^2 \right]. \tag{8}$$

The scattering depends on the sign of ϑ and scattering by the same angle to the right and to the left will be different.

The intensity of the polarization effects is usually described by an expression

$$e(\vartheta) = \frac{I\,(\text{right}) - I\,(\text{left})}{I\,(\text{right}) + I\,(\text{left})} \tag{9}$$

where I (right) and I (left) are the intensities of the scattering to the right and to the left of the beam. Formula (8) gives:

$$e(\vartheta) = \frac{15 \left(\frac{p}{Mc} \right)^2 \frac{B_\alpha}{B} \sin\vartheta}{1 + \left(\frac{B_\alpha}{B} \right)^2 + \frac{225}{4} \left(\frac{p}{Mc} \right)^4 \sin^2\vartheta}. \tag{10}$$

Notice that according to this formula the polarization effects are proportional

to the imaginary component of the potential. In Born approximation the matrix element (5) of the spin orbit coupling interferes only with the imaginary part of the matrix element (7) of the potential V. It may be that this feature will be in part reduced by an exact calculation. Notice also that the right eft asymmetry vanishes for an infinitely strong absorptive potential.

In the numerical estimates of the right left asymmetry for 340 Mev polarized protons we have computed the absorptive potential B_a of nuclear matter assuming a proton-neutron cross-section of $32 \cdot 10^{-27}$ cm^2 and a proton-proton cross-section of $24 \cdot 10^{-27}$ cm^2. With a nuclear radius $r_0 = 1.4 \cdot 10^{-13} A^{1/3}$ one finds the absorption mean free path in nuclear matter $\lambda = 4.1 \cdot 10^{-13}$ cm. This corresponds to an imaginary component of the potential

$$B_a = \frac{\hbar v}{2\lambda} = 16 \text{ Mev}.$$

v is the velocity of the protons, equal to 0.68 c. The real part of the potential has been assumed B = 27 Mev. In Table I the calculated values of the asymmetry are listed. The first column is the scattering angle in degrees, the second column is the asymmetry parameter $e(\vartheta)$, the third column is the differential cross-section computed from (8) for carbon, taking the average between the values to the right and to the left.

TABLE I.

Asymmetry in the Scattering of a 340 Mev Polarized Proton Beam.

Scattering angle (degrees)	Asymmetry $e(\vartheta)$	$\frac{d\sigma}{d\omega} \cdot 10^{24}$ (for carbon)
0	0	2.7
5	0.40	2.2
10	0.51	1.2
15	0.49	0.3
20	0.42	0.02
30	0.33	0.01
40	0.27	0.03
50	0.23	0.01

These values of the asymmetry are in reasonably good agrement with the experimental observations. It should be noticed that at large scattering angles the elastic scattering (see column 3) becomes practically negligible compared to the inelastic scattering which is not included in the present theory,

because it is due to those protons that have been eliminated by the imaginary component of the potential.

This theory leads to a definite prediction as to the sign of the polarization effect. A proton with spin up should according to it be scattered with smaller intensity to the right than to the left. No experimental information is available at present on this point.

If further research should indicate that the results of this theory are in good agreement with experiment, an interesting consequence would be that the spin orbit coupling (1) of the shell model persists with about the same intensity up to very high nucleon energies.

RIASSUNTO. — Si fa l'ipotesi che la polarizzazione recentemente osservata nello scattering di protoni di alcune centinaia di Mev sia dovuta all'accoppiamento tra spin e orbita che viene postulato nel modello nucleare a shells di Mayer e Jensen. L'esistenza di questo accoppiamento noto da fenomeni nucleari di bassa energia permette di spiegare l'ordine di grandezza dei fenomeni di polarizzazione osservati ad alte energie. L'effetto di polarizzazione è dovuto all'interferenza dell'accoppiamento tra spin e orbita con la componente immaginaria del potenziale nucleare.

N° 268.

For the introduction to this paper see paper N° 267.

268.

POLARIZATION IN THE ELASTIC SCATTERING OF HIGH ENERGY PROTONS BY NUCLEI

University of Chicago
Private communication (March 24, 1954).

The polarization effects in the scattering of high energy protons by nuclei have been recently interpreted as due to the action of the spin orbit coupling that manifests itself at much lower energies in the nuclear shell structure.[1]

The present calculation has been undertaken in order to establish the validity of the Born approximation used in I. For this reason an exact calculation has been carried out for the scattering of 340 Mev nucleons on carbon, using potentials identical to those used in the Born approximation. Namely, a square potential well with a real part 27 Mev deep and an imaginary part 16 Mev deep, and a spin orbit coupling 15 times larger than the Thomas correction. The radius of the carbon nucleus was assumed 3.2×10^{-13} cm. The calculation is rather tedious because spherical harmonics up to about the order of 20 are involved.

The results are presented in fig. 1. The two curves give the computed values of the differential elastic cross sections at the various scattering angles to the left and to the right with respect to the direction of polarization. As one can see, the "left" curve is, at most angles, higher than the "right" curve, indicating that the beam is normally scattered preferentially to the left as is predicted by the Born approximation. There are, however, limited angular regions where this model predicts inversion of the normal polarization effect in the vicinity of 16° and of 28°. These anomalies are clearly connected with the fact that the interference minima for the scattering to the left appear

(1) E. FERMI, *Polarization of High Energy Protons Scattered by Nuclei*, « Il Nuovo Cimento », April 1954; quoted hereafter as I. [See paper N° 267 (Editors' note)]. After completion of this paper I have been informed that at least two other groups are working independently on the same general type of explanation of the polarization. They are W. HECKROTTE and J. V. LEPORE of Berkeley (paper submitted to the « Physical Review »), and BERTRAND J. MALENKA of Harvard (abstract submitted to the 1954 Washington meeting.)

to be at somewhat smaller angles than the interference minima in the scattering to the right. The model chosen overemphasizes the interference effects because of the sharp edges of the potential well. It is likely, therefore, that in reality qualitative features as indicated in the figure will be less sharp,

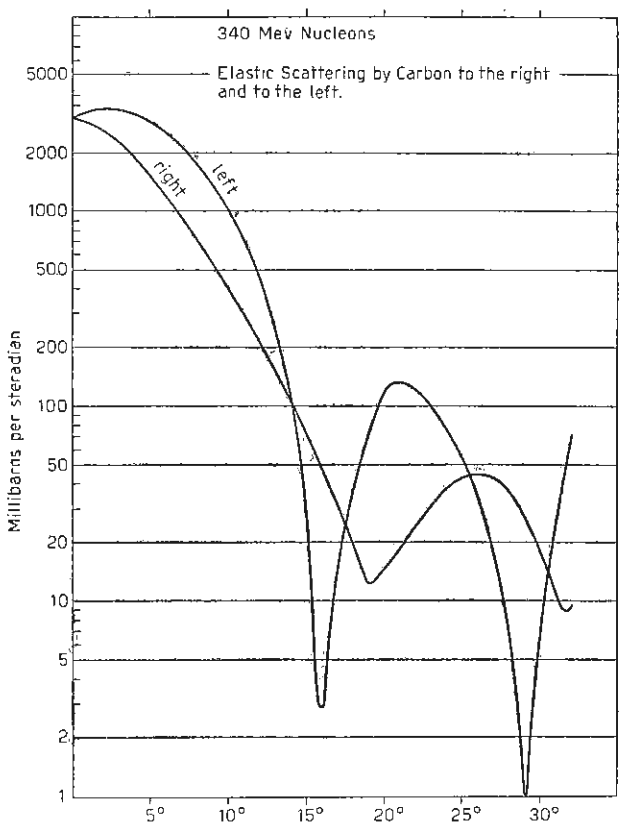

Fig. 1. – 340 Mev Nucleons Elastic Scattering by Carbon to the right and to the left.

and they may not be large enough to cause an actual inversion of the polarization where it should be according to fig. 1. Except for these features the results of the exact calculation are in this case in fair quantitative agreement with the results of the Born approximation. One might expect, however, that the agreement would be worse for a larger nucleus.

Thanks are due to Miss Caroline Littlejohn for help in the computations.

N° 269.

The following is a verbatim transcript of Enrico Fermi's last address before the American Physical Society, delivered, informally and without notes at Columbia University's McMillin Theater on Saturday morning, January 30, 1954. His retiring presidential address was delivered one day earlier. The present speech, transcribed from a tape recording, is left deliberately in an unpolished and unedited form. Such informality would no doubt have been frowned upon by Fermi, who was very particular about his published writings. For those who knew Fermi or heard him speak, however, the verbatim transcript may serve (as no formal document could ever serve) to bring back for a moment the very sound of his voice. The paper was presented as part of the session "Physics at Columbia University" during the Society's 1954 annual meeting.

From « Physics Today », November 1955.

A tape recording and records of this speech are in possession of the American Institute of Physics.

269.

PHYSICS AT COLUMBIA UNIVERSITY

The Genesis of the Nuclear Energy Project

« Physics Today », *8*, 12-16 (November 1955).

Mr. Chairman, Dean Pegram, fellow Members, Ladies and Gentlemen:

It seems fitting to remember, on this 200th anniversary of Columbia University, the key role that the University played in the early experimentation and the organization of the early work that led to the development of atomic energy.

I had the good fortune to be associated with the Pupin Laboratories through the period of time when at least the first phase of this development took place. I had had some difficulties in Italy and I will always be very grateful to Columbia University for having offered me a position in the Department of Physics at the most opportune moment. And in addition this offer gave me, as I said, the rare opportunity of witnessing the series of events to which I have referred.

In fact I remember very vividly the first month, January, 1939, that I started working at the Pupin Laboratories because things began happening very fast. In that period, Niels Bohr was on a lecture engagement in Princeton and I remember one afternoon Willis Lamb came back very excited and said that Bohr had leaked out great news. The great news that had leaked

out was the discovery of fission and at least an outline of its interpretation; the discovery as you well remember goes back to the work of Hahn and Strassmann and at least the first idea for the interpretation came through the work of Lise Meitner and Frisch who were at that time in Sweden.

Then, somewhat later that same month, there was a meeting in Washington organized by the Carnegie Institution in conjunction with George Washington University where I took part with a number of people from Columbia University and where the possible importance of the new-discovered phenomenon of fission was first discussed in semi-jocular earnest as a possible source of nuclear power. Because it was conjectured, if there is fission with a very serious upset of the nuclear structure, it is not improbable that some neutrons will be evaporated. And if some neutrons are evaporated, then they might be more than one; let's say, for the sake of argument, two. And if they are more than one, it may be that the two of them, for example, may each one cause a fission and from that one sees of course a beginning of the chain reaction machinery.

So that was one of the things that was discussed at that conference and started a small ripple of excitement about the possibility of releasing nuclear energy. At the same time experimentation was started feverishly in many laboratories, including Pupin, and I remember before leaving Washington I had a telegram from Dunning announcing the success of an experiment directed to the discovery of the fission fragments. The same experiment apparently was at the same time carried out in half a dozen places in this country and in three or four, in fact I think slightly before, in three or four places in Europe.

Now a rather long and laborious work was started at Columbia University in order to firm up these vague suggestions that had been made as to the possibilities that neutrons were emitted and try to see whether neutrons were in fact emitted when fission took place and if so how many they would be, because clearly a matter of numbers is in this case extremely important because a little bit greater or a little bit lesser probability might have made all the difference between possibility and impossibility of a chain reaction.

Now this work was carried on at Columbia simultaneously by Zinn and Szilard on one hand and by Anderson and myself on the other hand. We worked independently and with different methods, but of course we kept close contact and we kept each other informed of the results. At the same time the same work was being carried out in France by a group headed by Joliot and von Halban. And all the three groups arrived at the same conclusion—I believe Joliot may be a few weeks earlier than we did at Columbia—namely that neutrons are emitted and they were rather abundant, although the quantitative measurement was still very uncertain and not too reliable.

A curious circumstance related to this phase of the work was that here for the first time secrecy that has been plaguing us for a number of years started and, contrary to perhaps what is the most common belief about secrecy, secrecy was not started by generals, was not started by security officers, but was started by physicists. And the man who is mostly responsible for this certainly extremely novel idea for physicists was Szilard.

I don't know how many of you know Szilard; no doubt very many of you do. He is certainly a very peculiar man, extremely intelligent (*laughter*). I see that is an understatement. (*laughter*). He is extremely brilliant and he seems somewhat to enjoy, at least that is the impression that he gives to me, he seems to enjoy startling people.

So he proceeded to startle physicists by proposing to them that given the circumstances of the period—you see it was early 1939 and war was very much in the air—given the circumstances of that period, given the danger that atomic energy and possibly atomic weapons could become the chief tool for the Nazis to enslave the world, it was the duty of the physicists to depart from what had been the tradition of publishing significant results as soon as the « Physical Review » or other scientific journals might turn them out, and that instead one had to go easy, keep back some results until it was clear whether these results were potentially dangerous or potentially helpful to our side.

So Szilard talked to a number of people and convinced them that they had to join some sort of—I don't know whether it would be called a secret society, or what it would be called. Anyway to get together and circulate this information privately among a rather restricted group and not to publish it immediately. He sent in this vein a number of cables to Joliot in France, but he did not get a favorable response from him and Joliot published his results more or less like results in physics had been published until that day. So that the fact that neutrons are emitted in fission in some abundance—the order of magnitude of one or two or three—became a matter of general knowledge. And, of course, that made the possibility of a chain reaction appear to most physicists as a vastly more real possibility than it had until that time.

Another important phase of the work that took place at Columbia University is connected with the suggestion on purely theoretical arguments, by Bohr and Wheeler, that of the two isotopes of uranium it was not the most abundant uranium 238 but it was the least abundant uranium 235, present as you know in the natural uranium mixture to the tune of 0.7 of a percent, that was responsible at least for most of the thermal fission. The argument had to do with an even number of neutrons in uranium 238 and an odd number of neutrons in uranium 235 which, according to a discussion of the binding energies that was carried out by Bohr and Wheeler, made plausible that uranium 235 should be more fissionable.

Now it clearly was very important to know the facts also experimentally and work was started in conjunction by Dunning and Booth at Columbia University and by Nier. Nier took the mass spectrographic part of this work, attempting to separate a minute but as large as possible amount of uranium 235, and Dunning and Booth at Columbia took over the part of using this minute amount in order to test whether or not it would undergo fission with a much greater cross section than ordinary uranium.

Well, you know of course by now that this experiment confirmed the theoretical suggestion of Bohr and Wheeler, indicating that the key isotope of uranium, from the point of view of any attempt of—for example—constructing a machine that would develop nuclear energy, was in fact uranium 235.

Now you see the matter is important primarily for the following reasons that at the time were appreciated perhaps less definitely than at the present moment.

The fundamental point in fabricating a chain reacting machine is of course to see to it that each fission produces a certain number of neutrons and some of these neutrons will again produce fission. If an original fission causes more than one subsequent fission then of course the reaction goes. If an original fission causes less than one subsequent fission then the reaction does not go.

Now, if you take the isolated pure isotope U^{235}, you may expect that the unavoidable losses of neutrons will be minor, and therefore if in the fission somewhat more than one neutron is emitted then it will be merely a matter of piling up enough uranium 235 to obtain a chain reacting structure. But if to each gram of uranium 235 you add some 140 grams of uranium 238 that come naturally with it, then the competition will be greater, because there will be all this ballast ready to snatch away the not too abundant neutrons that come out in the fission and therefore it was clear at the time that one of the ways to make possible the production of a chain reaction was to isolate the isotope U^{235} from the much more abundant isotope U^{238}.

Now, at present we have in our laboratories a row of bottles labeled, more or less, isotope—what shall I say—iron 56, for example, or uranium 235 or uranium 238 and these bottles are not quite as common as would be a row of bottles of chemical elements, but they are perfectly easily obtainable by putting due pressure on the Oak Ridge Laboratory (*laughter*). But at that time isotopes were considered almost magically inseparable. There was to be sure one exception, namely deuterium, which was already at that time available in bottles. But of course deuterium is an isotope in which the two isotopes hydrogen one and hydrogen two have a ratio of mass one to two, which is a very great ratio. But in the case of uranium the ratio of mass is merely 235 to 238, so the difference is barely over one percent. And that, of course, makes the differences of these two objects so tiny that it was not very clear that the job of separating large amounts of uranium 235 was one that could be taken seriously.

Well, therefore, in those early years near the end of 1939 two lines of attack to the problem of atomic energy started to emerge. One was as follows. The first step should be to separate in large amounts, amounts of kilograms or maybe amounts of tens of kilograms or maybe of hundreds of kilograms, nobody really knew how much would be needed, but something perhaps in that order of magnitude, separate such at that time fantastically large-looking amounts of uranium 235 and then operate with them without the ballast of the associated much larger amounts of uranium 238. The other school of thought was predicated on the hope that perhaps the neutrons would be a little bit more and that perhaps using some little amount of ingenuity one might use them efficiently and one might perhaps be able to achieve a chain reaction without having to separate the isotopes, a task as I say that at that time looked almost beyond human possibilities.

Now I personally had worked many years with neutrons, and especially slow neutrons, so I associated myself with the second team that wanted to

use nonseparated uranium and try to do the best with it. Early attempts and studies, discussions, on how to separate the isotopes of uranium were started by Dunning and Booth in close consultation with Professor Urey. On the other hand, Szilard, Zinn, Anderson, and myself started experimentation on the other line whose first step involved lots of measurements.

Now, I have never yet quite understood why our measurements in those days were so poor. I'm noticing now that the measurements that we are doing on pion physics are very poor, presumably just because we have not learned the tricks. And, of course, the facilities that we had at that time were not as powerful as they are now. It's much easier to carry out experimentation with neutrons using a pile as a source of neutrons than it was in those days using radium-beryllium sources when geometry was the essential item to control or using the cyclotron when intensity was the desired feature rather than good geometry.

Well, we soon reached the conclusion that in order to have any chance of success with natural uranium we had to use slow neutrons. So there had to be a moderator. And this moderator could have been water or other substances. Water was soon discarded; it's very effective in slowing down neutrons, but still absorbs a little bit too many of them and we could not afford that. Then it was thought that graphite might be perhaps the better bet. It's not as efficient as water in slowing down neutrons; on the other hand little enough was known of its absorption properties that the hope that the absorption might be very low was quite tenable.

This brings us to the fall of 1939 when Einstein wrote his now famous letter to President Roosevelt advising him of what was the situation in physics—what was brewing and that he thought that the government had the duty to take an interest and to help along this development. And in fact help came along to the tune of $ 6000 a few months after and the $ 6000 were used in order to buy huge amounts—or what seemed at that time when the eye of physicists had not yet been distorted—(*laughter*) what seemed at that time a huge amount of graphite.

So physicists on the seventh floor of Pupin Laboratories started looking like coal miners (*laughter*) and the wives to whom these physicists came back tired at night were wondering what was happening. We know that there is smoke in the air, but after all... (*laughter*).

Well, what was happening was that in those days we were trying to learn something about the absorption properties of graphite, because perhaps graphite was no good. So, we built columns of graphite, maybe four feet on the side or something like that, maybe ten feet high. It was the first time when apparatus in physics, and these graphite columns were apparatus, was so big that you could climb on top of it—and you had to climb on top of it. Well, cyclotrons were the same way too, but anyway that was the first time when I started climbing on top of my equipment because it was just too tall—I'm not a tall man (*laughter*).

And the sources of neutrons were inserted at the bottom and we were studying how these neutrons were first slowed down and then diffused up the column and of course if there had been a strong absorption they would

not have diffused very high. But because it turned out that the absorption was in fact small, they could diffuse quite readily up this column and by making a little bit of mathematical analysis of the situation it became possible to make the first guesses as to what was the absorption cross section of graphite, a key element in deciding the possibility or not of fabricating a chain reacting unit with graphite and natural uranium.

Well, I will not go into detail of this experimentation. That lasted really quite a number of years and required really quite many hours and many days and many weeks of extremely hard work. I may mention that very early our efforts were brought in connection with similar efforts that were taking place at Princeton University where a group with Wigner, Creutz and Bob Wilson set to work making some measurements that we had no possibility of carrying out at Columbia University.

Well, as time went on, we began to identify what had to be measured and how accurately these things that I shall call "eta," f, and p—I don't think I have time to define them for you—these three quantities "eta," f, and p had to be measured to establish what could be done and what could not be done. And, in fact, if I may say so, the product of "eta", f, and p had to be greater than one. It turns out, we now know, that if one does just about the best this product can be 1.1.

So, if we had been able to measure these three quantities to the accuracy of one percent we might have found that the product was for example 1.08 plus or minus 0.03 and if that had been the case we would have said let's go ahead, or if the product had turned out to be 0.95 plus or minus 0.03 perhaps we would have said just that this line of approach is not very promising, and we had better look for something else. However I've already commented on the extremely low quality of the measurements in neutron physics that could be done at the time—where the accuracy of measuring separately either "eta," or f, or p was perhaps with a plus or minus of 20 percent (*laughter*). If you compound, by the well-known rules of statistics, three errors of 20 percent you will find something around 35 percent. So if you should find, for example, 0.9 plus or minus 0.3—what do you know? Hardly anything at all (*laughter*). If you find 1.1 plus or minus 0.3—again, you don't know anything much. So that was the trouble and in fact if you look in our early work—what were the detailed values given by this or that experimenter to, for example, "eta" you find that it was off 20 percent and sometimes greater amounts. In fact I think it was strongly influenced by the temperament of the physicist. Shall we say optimistic physicists felt it unavoidable to push these quantities high and pessimistic physicists like myself tried to keep them somewhat on the low side (*laughter*).

Anyway, nobody really knew and we decided therefore that one had to do something else. One had to devise some kind of experiment that would give a complete over-all measurement directly of the product "eta," f, p without having to measure separately the three, because then perhaps the error would sort of drop down and permit us to reach conclusions.

Well, we went to Dean Pegram, who was then the man who could carry out magic around the University, and we explained to him that we needed a

big room. And when we say big we meant a really big room, perhaps he made a crack about a church not being the most suited place for a physics laboratory in his talk, but I think a church would have been just precisely what we wanted (*laughter*). Well, he scouted around the campus and we went with him to dark corridors and under various heating pipes and so on to visit possible sites for this experiment and eventually a big room, not a church, but something that might have been compared in size with a church was discovered in Schermerhorn.

And there we started to construct this structure that at that time looked again in order of magnitude larger than anything that we had seen before. Actually if anybody would look at that structure now he would probably extract his magnifying glass (*laughter*) and go close to see it. But for the ideas of the time it looked really big. It was a structure of graphite bricks and spread through these graphite bricks in some sort of pattern were big cans, cubic cans, containing uranium oxide.

Now, graphite is a black substance, as you probably know. So is uranium oxide. And to handle many tons of both makes people very black. In fact it requires even strong people. And so, well we were reasonably strong, but I mean we were, after all, thinkers (*laughter*). So Dean Pegram again looked around and said that seems to be a job a little bit beyond your feeble strength, but there is a football squad at Columbia (*laughter*) that contains a dozen or so of very husky boys who take jobs by the hour just to carry them through College. Why don't you hire them?

And it was a marvelous idea; it was really a pleasure for once to direct the work of these husky boys, canning uranium—just shoving it in—handling packs of 50 or 100 pounds with the same ease as another person would have handled three or four pounds. In passing these cans fumes of all sorts of colors, mostly black, would go in the air (*laughter*).

Well, so grew what was called at the time the exponential pile. It was an exponential pile, because in the theory an exponential function enters—which is not surprising. And it was a structure that was designed to test in an integral way, without going down to fine details, whether the reactivity of the pile, the reproduction factor, would be greater or less than one. Well, it turned out to be 0.87. Now that is by 0.13 less than one and it was bad. However, at the moment we had a firm point to start from, and we had essentially to see whether we could squeeze the extra 0.13 or preferably a little bit more. Now there were many obvious things that could be done. First of all, I told you these big cans were canned in tin cans, so what has the iron to do? Iron can do only harm, can absorb neutrons, and we don't want that. So, out go the cans. Then, what about the purity of the materials? We took samples of uranium, and with our physicists' lack of skill in chemical analysis, we sort of tried to find out the impurities and certainly there were impurities. We would not know what they were, but they looked impressive, at least in bulk (*laughter*). So, now, what do these impurities do?—clearly they can do only harm. Maybe they make harm to the tune of 13 percent. Finally, the graphite was quite pure for the standards of that time, when graphite manufacturers were not concerned with avoiding those special im-

purities that absorb neutrons. But still there was some considerable gain to be made out there, and especially Szilard at that time took extremely decisive and strong steps to try to organize the early phases of production of pure materials. Now, he did a marvelous job which later on was taken over by a more powerful organization than was Szilard himself. Although to match Szilard it takes a few able-bodied customers (*laughter*).

Well, this brings us to Pearl Harbor. At that time, in fact I believe a few days before by accident, the interest in carrying through the uranium work was spreading; work somewhat similar to what was going on at Columbia had been initiated in a number of different Universities throughout the country. And the government started taking decisive action in order to organize the work, and, of course, Pearl Harbor gave the final and very decisive impetus to this organization. And it was decided in the high councils of the government that the work on the chain reaction produced by nonseparated isotopes of uranium should go to Chicago.

That is the time when I left Columbia University, and after a few months of commuting between Chicago and New York eventually moved to Chicago to keep up the work there, and from then on, with a few notable exceptions, the work at Columbia was concentrated on the isotope-separation phase of the atomic energy project.

As I've indicated this work was initiated by Booth, Dunning, and Urey about 1940, 1939, and 1940, and with this reorganization a large laboratory was started at Columbia under the direction of Professor Urey. The work there was extremely successful and rapidly expanded into the build-up of a huge research laboratory which cooperated with the Union Carbide Company in establishing some of the separation plants at Oak Ridge. This was one of the three horses on which the directors of the atomic energy project had placed their bets, and as you know the three horses arrived almost simultaneously to the goal in the summer of 1945. I thank you. (*Applause*).

N° 270.

Fermi's greatness as a teacher stemmed from the fact that he made little, if any, distinction between teaching and research. His famous power, of finding the simple and clear physical model for understanding a seemingly complicated idea, can be seen as well in his papers as in his lectures. His ability of recalling, for the solution of some new problem, an appropriate example from no matter which field in which the problem had already been solved, he applied in reverse in his courses; the examples employed in his course in Thermodynamics were frequently exciting excursions along the frontiers of nuclear physics.

I learned thermodynamics, and a great deal more, when, as a young graduate student at Columbia soon after Fermi's arrival, I had the good fortune to be assigned as reader for his elementary courses. That was the year that Fermi gave a course in Geophysics, in which he demonstrated so beautfully how to extract the physical essence from a field with a century old, beautifully intricate but overcomplicated superstructure of mathematical formalism. While waiting for the discovery of fission, Fermi had been amusing himself by looking into a number of different fields; but this period of waiting had not lasted long.

My final experience with Fermi the teacher was in Varenna on Lake Como in 1954, that last summer before his death, when he gave his great series of lectures on Meson Physics (paper N° 270). Later, I was to have the unhappy privilege of editing the lecture notes, but there was no foretaste of tragedy in the lectures themselves. Here was Fermi at the height of his powers, bringing order and simplicity out of confusion, finding connections between seemingly unrelated phenomena; wit and wisdom emerging from lips white, as usual, from contact with chalk, in that clear, resonant voice that had never lost the soft Italian vowel endings on a perfectly colloquial American delivery.

B. T. FELD.

270.

LECTURES ON PIONS AND NUCLEONS

« Nuovo Cimento », *2*, Suppl., 1793 (1955).

CONTENTS. – *Preface.*

PREFACE

It was with considerable misgiving that I agreed to edit this set of notes, based on the lectures of Enrico Fermi at Varenna. The notes were originally prepared by students at the school, making liberal use of tape recordings of the lectures. Many portions are, essentially word-for-word, in the original form.

This is certainly not the form in which Fermi would have written them for publication, for his methods of oral and of written presentation were very different. In their present form, however, they illustrate (subject to the limitations of those who transcribed and edited them) the unique qualities of Fermi as an expositor and teacher.

In the hope of preserving this quality, I have tried to minimize the changes from the original notes, confining my role of editor to the occasional correction of obvious errors on the part of the transcribers and to occasional interpolations, mostly to fill in omissions on the part of the transcribers.

In working on these notes, I have been rewarded by frequently encountering sections which are so unique in their language and approach as to evoke for me, again, the picture of Fermi as he lectured during those lovely mornings in the beautiful setting of the Villa Monastero on Lake Como. It is to be hoped that these notes have succeeded, in some small measure, in capturing the spirit of those unforgettable lectures.

12 Feb. 1955. B. T. FELD.

A) ISOTOPIC SPIN

1.—NUCLEONS.

The isotopic spin notation was invented by Heisenberg [1] in the early 30's almost immediately after the discovery of the neutron. The neutron appeared to be a particle with properties similar to those of the proton, and the idea was that they could both be described as different states of the same particle. Thus we can say that a particular nucleon, which I shall indicate by the symbol $\mathfrak{N}$ can have two forms p or n, proton or neutron. The idea at this stage is purely formal and it could be adapted, though probably not fruitfully, to distinguish any two objects. As time went on, the fruitfulness of the notation became apparent, because the properties of nucleons are such that they make the notation more valuable than a purely formal device. However, just for a short time, let me pursue the purely formal consequences of this notation. We are here presented with what is usually called a dichotomic variable, i.e., a variable that can take on essentially two values. If we represent, as is usual, a function of a dichotomic variable by a vertical slot containing the two values a and b, $f = \left| \begin{matrix} a \\ b \end{matrix} \right|$, then this is a function which for the first of the variables takes the value a and for the second takes the value b.

There is in physics a wide amount of experience as to the behaviour of these functions of dichotomic variables. They were encountered for the first time when Pauli [2] worked out the theory of the spin 1/2, which is also a dichotomic variable. The state may be specified by saying that the spin is "up" or "down". There are certain standard linear operators that operate on variables of this type, and they are essentially the Pauli operators.

(1) W. HEISENBERG, «Zeits. f. Phys.», *77*, 1 (1932).
(2) W. PAULI, «Zeits. f. Phys.», *43*, 601 (1947).

We may consider adding the unity operator $\begin{vmatrix} 1 & 0 \\ 0 & 1 \end{vmatrix}$ to the three Pauli operators:

$$\begin{vmatrix} 0 & 1 \\ 1 & 0 \end{vmatrix}, \quad \begin{vmatrix} 0 & -i \\ i & 0 \end{vmatrix}, \quad \begin{vmatrix} 1 & 0 \\ 0 & -1 \end{vmatrix}.$$

We then have a list of four operators which are linear and have the following property. They and their linear combinations are all the possible linear operators on any function of a dichotomic variable. Whether this is a spin, or a variable which tells us whether the particle is a proton or a neutron, makes no difference whatsoever. We shall define:

$$2\tau_1 \equiv \begin{vmatrix} 0 & 1 \\ 1 & 0 \end{vmatrix} \quad ; \quad 2\tau_2 \equiv \begin{vmatrix} 0 & -i \\ i & 0 \end{vmatrix} \quad ; \quad 2\tau_3 \equiv \begin{vmatrix} 1 & 0 \\ 0 & -1 \end{vmatrix}.$$

The factors 2 here introduced will prove convenient later.

What is, for instance, the significance of the operator $2\tau_1$, when applied to a proton p? The function which represents the proton state is, in this notation

$$p = \begin{vmatrix} 1 \\ 0 \end{vmatrix}.$$

Similarly we shall introduce another function $n = \begin{vmatrix} 0 \\ 1 \end{vmatrix}$, which defines the neutron. Now,

$$\begin{vmatrix} 0 & 1 \\ 1 & 0 \end{vmatrix} p = \begin{vmatrix} 0 & 1 \\ 1 & 0 \end{vmatrix} \begin{vmatrix} 1 \\ 0 \end{vmatrix} = \begin{vmatrix} 0 \\ 1 \end{vmatrix} = n.$$

means a linear operation with coefficients indicated by the square matrix $\begin{vmatrix} 0 & 1 \\ 1 & 0 \end{vmatrix}$ applied to the function $\begin{vmatrix} 1 \\ 0 \end{vmatrix}$ and this yields $\begin{vmatrix} 0 \\ 1 \end{vmatrix}$. So, we see that $2\tau_1$ changes p to n and, as can be shown, also changes n into p. $2\tau_1$ is thus the operator that interchanges a proton and a neutron. Similarly one can show the operational significance of the others.

Now let me consider just one application, which would make this notation worth considering even if all our problems were concerned with only a single nucleon. (To be sure, in this case, the notations would be somewhat superfluous). Suppose we consider the operators $\left(\frac{1}{2} + \tau_3\right)$ and $\left(\frac{1}{2} - \tau_3\right)$.

$$(1.1) \quad \begin{cases} \text{Now} \quad \left(\frac{1}{2} + \tau_3\right) = \begin{vmatrix} \frac{1}{2} & 0 \\ 0 & \frac{1}{2} \end{vmatrix} + \begin{vmatrix} \frac{1}{2} & 0 \\ 0 & -\frac{1}{2} \end{vmatrix} = \begin{vmatrix} 1 & 0 \\ 0 & 0 \end{vmatrix} \\ \quad \text{therefore} \quad \left(\frac{1}{2} + \tau_3\right) p = p \quad ; \quad \left(\frac{1}{2} + \tau_3\right) n = 0; \\ \text{similarly} \quad \left(\frac{1}{2} - \tau_3\right) = \begin{vmatrix} \frac{1}{2} & 0 \\ 0 & \frac{1}{2} \end{vmatrix} - \begin{vmatrix} \frac{1}{2} & 0 \\ 0 & -\frac{1}{2} \end{vmatrix} = \begin{vmatrix} 0 & 0 \\ 0 & 1 \end{vmatrix} \\ \quad \text{therefore} \quad \left(\frac{1}{2} - \tau_3\right) n = n \quad ; \quad \left(\frac{1}{2} - \tau_3\right) p = 0. \end{cases}$$

These are called projection operators.

Now consider a nucleon which may be a proton with a certain amplitude a and a neutron with a certain amplitude b, $\mathfrak{N} = \left|\begin{matrix} a \\ b \end{matrix}\right| = ap + bn$. If we apply our operator $\left(\frac{1}{2} + \tau_3\right)$ to the wave function $ap + bn$; the result is

$$\left(\frac{1}{2} + \tau_3\right)(ap + bn) = ap .$$

In other words this operator projects out of a mixture of states that part which is a proton. For this reason $\left(\frac{1}{2} + \tau_3\right)$ is called a projection operator. It is a projection operator for protons. Similarly $\left(\frac{1}{2} - \tau_3\right)$ is a projection operator for neutrons.

Suppose that we want to write the Hamiltonian for a nucleon without specifying whether this nucleon is a neutron or a proton. How can we do that? Let H_p and H_n be the Hamiltonians for a proton and a neutron, respectively. In a simple case, for example, they may have the form:

$$(1.2) \qquad H_p = \frac{p^2}{2M_p} + U_p(x) \quad , \quad H_n = \frac{p^2}{2M_n} + U_n(x).$$

In general these Hamiltonians are different because $U_n \neq U_p$ since the forces acting on a proton will be different from the forces acting on a neutron. This is seen to be true if we consider that there are, for example, electrical forces. Part of the potential may be the Coulomb potential, which leaves the neutron unaffected and acts on the proton only. The kinetic energy parts are different, too, because of the small but appreciable difference in mass of the proton and neutron.

Now our task is to write a Hamiltonian for the nucleon, valid whether the particle is a proton or a neutron, or also, in the case which at present may seem meaningless, that the particle is both a neutron and a proton. In terms of the projection operators, it is very easy to do this. Let me write as an expression for the Hamiltonian H without index for the nucleon,

$$(1.3) \qquad H = H_p\left(\frac{1}{2} + \tau_3\right) + H_n\left(\frac{1}{2} - \tau_3\right) = \frac{H_p + H_n}{2} + (H_p - H_n)\,\tau_3 .$$

Now I claim that this is the right Hamiltonian for the nucleon.

This can be shown as follows: The nucleon wave function is a function of the coordinates; we summarise by x not only the positional coordinates but also the spin coordinates. In addition there will be what, for the time being, I will call the charge coordinate, which specifies whether the particle is a proton or a neutron. The isotopic spin operators τ operate on functions of the charge coordinates. Such a wave function can always be written in the following manner:

$$(1.4) \qquad \psi(x, c) = \left|\begin{matrix} \psi_1(x) \\ \psi_2(x) \end{matrix}\right| = \psi_1(x)\left|\begin{matrix} 1 \\ 0 \end{matrix}\right| + \psi_2(x)\left|\begin{matrix} 0 \\ 1 \end{matrix}\right| = \psi_1(x)\,p + \psi_2(x)\,n,$$

$\psi_1(x)$ and $\psi_2(x)$ is a pair of functions of the variables x only.

After these preliminaries, let us try to decide what this Hamiltonian operator does when applied to a function of this type

$$H\{\psi_1(x)\,p + \psi_2(x)\,n\} = H_p\,\psi_1(x)\,p + H_n\,\psi_2(x)\,n.$$

Thus the effect of H on the wave function is to operate on the proton part with the Hamiltonian H_p and on the neutron part with H_n. If our wave function consists of a proton part only, then it treats it just as a proton. If the wave function consist of the neutron part only, it treats it as a neutron.

2.—The Two-Nucleons System.

Up to this point it may be only a matter of curiosity that one can write a Hamiltonian which is ready to treat any nucleon whether it is a proton or a neutron. This is purely formal, and there is no physics involved in it. Incidentally, up to this point we could have taken, for example, a proton and an electron, introduced a variable which would tell us whether the particle were a proton or an electron (two very different particles), used the same type of formalism, and written a Hamiltonian which would act correctly on a particle whether it is a proton or an electron. We may begin to see the fruitfulness of this notation if we go on to the case of two nucleons, and this is the next case we will want to investigate. Let us denote the variables related to one of the two nucleons with one prime (x', c') and to the other, with two primes (x'', c''). Similarly with the operators, τ' $(\tau_1', \tau_2', \tau_3')$ and τ'' $(\tau_1'', \tau_2'', \tau_3'')$. The wave function of our system will be $\psi(x', x'', c', c'')$. Let us concentrate especially on the meaning involved in the various possible values of the two charge coordinates, (c', c'') which tell us whether the two particles are protons or neutrons. An immediate generalisation of what we have done in the previous case leads us to recognise that the charge possibilities of two nucleons are 4 (nn, pp, np, pn) so we see that a wave function of this kind can be written as

$$(2.1)\quad \psi(x', x'', c', c'') = p(c')\,p(c'')\,\psi_1(x', x'') + n(c')\,n(c'')\,\psi_2(x', x'') + p(c')\,n(c'')\,\psi_3(x', x'') + n(c')\,p(c'')\,\psi_4(x', x'').$$

In this case, then, the general wave function consists of four parts, which contain four functions of the space and spin coordinates of the two nucleons.

The next point is to try to do for two nucleons what we have done for one, namely, to write down a Hamiltonian that operates correctly on all charge possibilities. In doing this I want to begin by making a simplification; I propose to ignore the difference of the masses of proton and neutron. We shall call the common value M. This simplification is not essential but makes certain details simpler. In the Hamiltonian there will enter terms containing the potential energy. We will call the potential energy between two protons U_{pp}, and the potential energy between two neutrons U_{nn}. U_{nn} will certainly be different from U_{pp}, since, for instance, in U_{pp} there is a Coulomb part

which is missing in U_{nn}. In the case that one particle is a proton and the other a neutron it is known that the simple idea of potential is not applicable because there are also exchange potentials. We know that in the nuclear force between a neutron and a proton there are essentially two terms: one that acts in a straightforward way as a potential energy term, and the other that acts as a potential energy term combined with an exchange of the two particles. In the discussion of nuclear forces one considers various types of exchange (e.g., Majorana: exchange of the positional coordinates leaving the spin coordinates unchanged; Heisenberg: exchange of both position and spin coordinates). For our discussion it does not really matter what kind of exchange we consider. However, since we do not distinguish in our notation between the position and spin coordinates, it will be more convenient to use the Heisenberg exchange. We shall call the exchange operators E_x; thus

$$E_x \psi(x', x'') = \psi(x'', x'). \tag{2.2}$$

If we have two particles, of which one is a proton and one a neutron, we may write the potential U in two parts,

$$U = V + WE_x, \tag{2.3}$$

thus

$$U\psi(x', x'') = V\psi(x', x'') + W\psi(x'', x'). \tag{2.4}$$

Suppose $\psi(x', x'')$ is symmetric, i.e. $\psi(x', x'') = \psi(x'', x')$; then $U\psi = (V+W)\psi$. Or assume $\psi(x', x'')$ is anti-symmetric; then $U\psi = (V - W)\psi$.

We now note that any function can be written as a sum of a symmetric and an anti-symmetric part, as can be seen from the identity

$$\psi(x', x'') = \underbrace{\frac{\psi(x', x'') + \psi(x'', x')}{2}}_{\text{Symmetric}} + \underbrace{\frac{\psi(x', x'') - \psi(x'', x')}{2}}_{\text{Anti-symmetric}}. \tag{2.5}$$

Thus if we divide our function into symmetric and anti-symmetric parts we can write the potential in a simple way, namely

$$U_s = V + W \quad , \quad U_a = V - W, \tag{2.6}$$

which are the potentials to be adopted if ψ is symmetric or anti-symmetric respectively.

This leads us naturally to the discussion of the symmetry properties of the nucleon wave functions. In arriving at the symmetry properties we shall apply the Pauli principle, which tells us that the over-all wave function is anti-symmetric, provided that all the coordinates of one nucleon are interchanged at the same time with all the coordinates of the other. We must include in this exchange also the charge coordinate c. The demand of the Pauli principle is that an acceptable wave function changes its sign under interchange of all of its coordinates; i.e.

$$\psi(x', x'', c', c'') = -\psi(x'', x', c'', c'). \tag{2.7}$$

Using the previous expression for ψ, we obtain for the anti-symmetry condition

$$(2.8)\quad p(c')\,p(c'')\,\psi_1(x',x'')+n(c')\,n(c'')\,\psi_2(x',x'')+p(c')\,n(c'')\,\psi_3(x',x'')+n(c')\,p(c'')\,\psi_4(x',x'')=-\{p(c')\,p(c'')\,\psi_1(x'',x')+n(c')\,n(c'')\,\psi_2(x'',x')+p(c'')\,n(c')\,\psi_3(x'',x')+n(c'')\,p(c')\,\psi_4(x'',x')\}.$$

This identity is required by the Pauli principle, which is one of the best established laws of quantum mechanics. The conditions under which this identity is satisfied are

$$(2.9)\quad \begin{cases} a)\quad \psi_1(x',x'')=-\psi_1(x'',x') & \text{for the coefficients of } p(c')\,p(c''),\\ b)\quad \psi_2(x',x'')=-\psi_2(x'',x') & \text{for the coefficients of } n(c')\,n(c''),\\ c)\quad \psi_3(x',x'')=-\psi_4(x'',x') & \text{for the coefficients of } p(c')\,n(c''),\\ d)\quad \psi_4(x',x'')=-\psi_3(x'',x') & \text{for the coefficients of } n(c')\,p(c''). \end{cases}$$

This set of equations represents the complete symmetry requirement. The first two correspond to both particles being either protons or neutrons, respectively. The last two correspond to the particles being a proton and a neutron, and vice versa. The last two conditions are not immediately useful. However adding and subtracting equations *c*) and *d*), we obtain something simpler.

If we define

$$(2.10)\qquad \psi_3=\frac{1}{\sqrt{2}}(\psi_3+\psi_4)\quad\text{and}\quad \psi_6=\frac{1}{\sqrt{2}}(\psi_3-\psi_4),$$

it follows from the above equations that

$$(2.11)\qquad \psi_5(x',x'')=-\psi_5(x'',x')\quad\text{(anti-symmetric)}$$

and

$$(2.12)\qquad \psi_6(x',x'')=\psi_6(x'',x')\quad\text{(symmetric)}.$$

Now we can simplify the expression for $\psi(x',x'',c',c'')$. By substituting $\psi_3=(1/\sqrt{2})(\psi_5+\psi_6)$ and $\psi_4=(1/\sqrt{2})(\psi_5-\psi_6)$, we obtain

$$(2.13)\qquad \psi(x',x'',c',c'')=pp\psi_1+nn\psi_2+\frac{pn+np}{\sqrt{2}}\psi_5+\frac{pn-np}{\sqrt{2}}\psi_6,$$

where ψ_1, ψ_2, ψ_5 are anti-symmetric, ψ_6 is symmetric. Note that the pp, nn, and $(pn+np)$ parts which are symmetric, are multiplied respectively by ψ_1, ψ_2 and ψ_5 which are anti-symmetric. In addition the $(pn-np)$ part which is anti-symmetric is multiplied by ψ_1 which is symmetric.

If the particles are two protons, then the Hamiltonian which would act on the part of the wave function containing the factor pp would be

$$(2.14)\qquad H_{pp}=\frac{p'^2+p''^2}{2M}+U_{pp}.$$

For the part with the factor nn the two neutron Hamiltonian,

$$(2.15)\qquad H_{nn}=\frac{p'^2+p''^2}{2M}+U_{nn},$$

applies. The Hamiltonian we want to act on ψ_5 is

$$H_a = \frac{p'^2 + p''^2}{2M} + U_a \tag{2.16}$$

and the Hamiltonian we want to act on ψ_6 is

$$H_s = \frac{p'^2 + p''^2}{2M} + U_s. \tag{2.17}$$

All that is needed is a device for writing the general form of the Hamiltonian that automatically does the appropriate switching, namely applies to each part of the wave function the kind of Hamiltonian which is applicable to it. This requires the use of projection operators that select out of these mixtures of charge states the various parts. It is very easy to see that the projection operator which selects pp is

$$O_{pp} = \left(\frac{1}{2} + \tau_3'\right)\left(\frac{1}{2} + \tau_3''\right). \tag{2.18}$$

Similarly

$$O_{nn} = \left(\frac{1}{2} - \tau_3'\right)\left(\frac{1}{2} - \tau_3''\right). \tag{2.19}$$

We note that $\left(\frac{1}{2} + \tau_3'\right)\left(\frac{1}{2} - \tau_3''\right)$ projects out pn. But we need an operator which projects out $(pn + np)/\sqrt{2}$ and one which projects out $(pn - np)/\sqrt{2}$.

I will just write down these operators and leave the proof as an exercise. The operator which projects out the part with anti-symmetric ψ_5 is

$$O_a = \frac{1}{4} + \tau_1' \tau_1'' + \tau_2' \tau_2'' - \tau_3' \tau_3''. \tag{2.20}$$

The operator which projects out the part with symmetric ψ_6 is

$$O_s = \frac{1}{4} - \tau_1' \tau_1'' - \tau_2' \tau_2'' - \tau_3' \tau_3''. \tag{2.21}$$

So the Hamiltonian of 2 nucleons is

$$H = H_{pp} O_{pp} + H_{nn} O_{nn} + H_a O_a + H_s O_s. \tag{2.22}$$

The only physical condition which has been introduced so far (aside from the Pauli principle) has been the near equality of the masses of neutron and proton. Now we shall introduce the physical principle of the charge independence of nuclear forces. We shall postulate that the forces between two protons or two neutrons or also between a proton and a neutron are the same, provided in the latter case that the wave function of the two nucleons is of the antisymmetric type $\psi_a(x', x'')$. This assumption is supported to some extent by experiment. The only major difference that is known to exist among these forces is the Coulomb force, which in many nuclear phenomena, especially in light nuclei, plays only a secondary role. Thus we have

$$H_{pp} = H_{nn} = H_a. \tag{2.23}$$

In the other Hamiltonian, H_s, the potential energy is unmistakably different. The potential that corresponds to an antisymmetric state observed,

for example, in the virtual state of the deuteron, is about 10 Mev; the potential that corresponds to the symmetric state, the state of the bound deuteron, is about 20 Mev. So the difference between the two potentials is about a factor of 2.

The Hamiltonian can then be written

$$H = H_a (O_{pp} + O_{nn} + O_a) + H_s O_s \tag{2.24}$$

and if we put in the projection operators this becomes

$$H = H_a\left(\frac{3}{4} + \boldsymbol{\tau}' \cdot \boldsymbol{\tau}''\right) + H_s\left(\frac{1}{4} - \boldsymbol{\tau}' \cdot \boldsymbol{\tau}''\right) = \frac{3H_a + H_s}{4} + (H_a - H_s)\boldsymbol{\tau}' \cdot \boldsymbol{\tau}'', \tag{2.25}$$

where we have put

$$\boldsymbol{\tau}' \cdot \boldsymbol{\tau}'' = \tau_1' \tau_1'' + \tau_2' \tau_2'' + \tau_3' \tau_3''. \tag{2.26}$$

The first part is independent of the charge operators; the second term involves the analogue of the scalar product $\boldsymbol{\tau}' \cdot \boldsymbol{\tau}''$ which is a scalar not in ordinary space but corresponds to a scalar with respect to an orthogonal transformation of the axes 1, 2, and 3 of the charge space. Many consequences derive from this invariant structure of the Hamiltonian with respect to rotations in charge space. Eq. (2.25) is an approximation because we have neglected the Coulomb forces.

$\boldsymbol{\tau}$ for a nucleon is compounded of τ_1, τ_2, τ_3 which are the Pauli operators apart from a factor 2. These operators were introduced to represent the spin angular momentum; as such, they obey the angular momentum commutation rules and have all the formal properties of the angular momentum. So we may say that, as regards their mathematical properties, $\tau_1' \cdots \tau_3''$ obey all the same rules as the angular momentum components. But the three directions labeled 1, 2 and 3 are now not three directions in ordinary space, but in a fictitious space which we can call charge space or isotopic spin space.

The properties of angular momentum in ordinary space can be adapted then to the properties in this I.S. space. For example $\boldsymbol{\tau}$ is a vector in charge space and in the same way one may define the scalar product of two vectors for 2 nucleons $\boldsymbol{\tau}' \cdot \boldsymbol{\tau}''$ and their sum $\mathbf{T} = \boldsymbol{\tau}' + \boldsymbol{\tau}''$, $\mathbf{T}$ being called the total isotopic spin of the system. With respect to changes of the coordinate system in I.S. space (e.g. rigid rotations) the Hamiltonian (2.25) is invariant, i.e. it is a scalar. Then the total isotopic spin and its components will be constants of motion, in the same sense as the angular momentum vector is a constant of motion when the Hamiltonian is invariant under rotation in ordinary space. Further τ_1, τ_2, τ_3, in the same manner as the Pauli spin operators, obey the following commutation rules:

$$\begin{cases} \boldsymbol{\tau}' \times \boldsymbol{\tau}' = i\boldsymbol{\tau}', \\ \boldsymbol{\tau}'' \times \boldsymbol{\tau}'' = i\boldsymbol{\tau}'', \\ \mathbf{T} \times \mathbf{T} = i\mathbf{T}. \end{cases} \tag{2.27}$$

Making use of (2.27) one finds that the following operators commute with

the Hamiltonian: T_1, T_2, T_3, T^2; thus

$$[HT_1] = 0 \quad , \quad [HT_2] = 0 \quad , \quad [HT_3] = 0 \quad , \quad [HT^2] = 0 \tag{2.28}$$

and so T_1, T_2, T_3, T^2 are constants of the motion.

Since the same formal considerations apply and since H is a scalar, the properties of ordinary angular momentum can be applied to the isotopic spin dependence of the two–nucleon wave function. One can choose a diagonal representation of T^2 and T_3, where

$$\begin{cases} T^2_{op} = T\,(T+1) \\ T_{3\,op} = T\,,\, T-1\,,\cdots -T \end{cases} \qquad (T = \text{integer or half-integer}). \tag{2.29}$$

As in the case of the angular momentum for a system of 2 electrons, T then takes the values 0, 1. Another property which also follows is that all states of constant T should have the same energy, and, in fact, are the same state viewed from different directions in I.S. space.

Before leaving the two–nucleon system, we discuss a correction to the scheme of charge independence which indicates where this scheme is defective. One can write down immediately one term, at least, which has been neglected and must be added to the Hamiltonian (2.25). This term describes the coulomb interaction and will, of course, be present only if both nucleons are protons. This additional term may be expressed as

$$+\frac{e^2}{r} O_{pp}\,,$$

where e^2/r is the Coulomb energy of the two charges and the projection operator O_{pp} is that defined in Eq. (2.18), which selects the case in which both nucleons are protons. Writing it out, we obtain the following additional term to the Hamiltonian (2.25)

$$\frac{e^2}{r} O_{pp} = \frac{e^2}{r}\left\{\frac{1}{4} + \frac{\tau'_3 + \tau''_3}{2} + \tau'_3\,\tau''_3\right\}. \tag{2.30}$$

The new Hamiltonian is no longer an isotopic scalar invariant. Considering the commutators of H with the components of the total isotopic spin vector it is clear that

$$[HT_1] \neq 0 \quad , \quad [HT_2] \neq 0,$$

but even in this case $[HT_3] = 0$ (charge conservation), since $T_3 = \tau'_3 + \tau''_3$ commutes with all the terms in the new Hamiltonian.

3.—The Many-Nucleon System.

The generalization to a system of many nucleons is a straightforward extension of the previous considerations. Consider a collection of A nucleons, all of which have their associated isotopic spin vectors $\boldsymbol{\tau}^{(1)}$, $\boldsymbol{\tau}^{(2)}$, $\cdots$, $\boldsymbol{\tau}^{(A)}$. As regards the Hamiltonian, we do not know very much even about 2 nucleons let alone about a many-nucleon system. For example, 3–body forces may

well play a large part. As in the case of 2 nucleons we will postulate that the Hamiltonian for A nucleons is also invariant under rotation in I.S. space, i.e. a scalar. Then the total isotopic spin vector,

$$\mathbf{T} = \boldsymbol{\tau}^{(1)} + \boldsymbol{\tau}^{(2)} \cdots + \boldsymbol{\tau}^{(A)}, \tag{2.1}$$

will have all the properties of an angular momentum vector and will be a constant of the motion.

The charge operator, which in the case of a single nucleon has the form $(1/2 + \tau_i)$ and the eigenvalues 1 (proton) and 0 (neutron), may be extended to the present system if one defines the charge operator of a nucleus as the sum of the charge operators of all the nucleons:

$$Q = \sum_{j=1}^{A} \left(\frac{1}{2} + \tau_3^{(j)} \right) = \frac{A}{2} + T_3. \tag{3.2}$$

Since the charge of the nucleus and the number of nucleons are both constant it follows that T_3 must remain constant. For this reason T_3 is a true constant of the motion. The other isotopic spin components are only approximately constants of the motion. In this respect T_3 has a special position that has no analogue for angular momentum vectors for which all components are essentially equivalent.

Next, one may classify states of the nucleus in isotopic spin multiplets. The possible values of T defined here by $T(T + 1) =$ eigenvalue of $\mathbf{T}^2$ are

$$T = \begin{cases} A/2 \\ \vdots \\ 0 \end{cases}, \text{ A even}, \qquad T = \begin{cases} A/2 \\ \vdots \\ \frac{1}{2} \end{cases}, \text{ A odd}. \tag{3.3}$$

Each state of the system of nucleons may be characterised by a particular value of T and for a chosen value of T the possible values of T_3 are then T, $T - 1, \cdots - T$. For example in the case of $T = 1$, T_3 may have the values $1, 0, -1$, forming an isotopic spin triplet composed of 3 neighbouring isobars with respective charges $(A/2) + 1$, $A/2$, and $(A/2) - 1$. For $T = 1/2$ there occurs an isotopic spin doublet.

One of the first doublets to be recognised was the $^7Li_3 - {}^7Be_4$ pair:

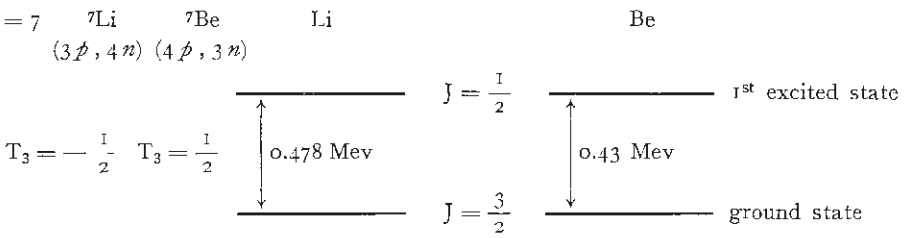

Fig. 1. – The energies and angular momenta of the ground and first excited states of the ^7Li–^7Be isotopic spin doublets.

The ground states of these nuclei are in fact closely similar (neglecting correction terms such as that due to the Coulomb potential) while the first excited states of these nuclei form another well known I.S. doublet.

Before leaving this question of I.S. as applied to a nucleus, it is interesting to remark that many reactions (e.g. α–particle emission) which, on grounds of energy, angular momentum, and parity, one would expect to occur strongly, often take place very slowly. This is frequently due to the fact that isotopic spin is not conserved in these reactions.

4.—Systems Containing Nucleons and π–Mesons.

The possible values for the isotopic spin of the pion can be obtained from the basic Yukawa reaction

$$\mathfrak{N} \rightleftarrows \mathfrak{N} + \pi. \tag{4.1}$$

We assume that isotopic spin is conserved in this reaction. From the fact that $\mathfrak{N}$ has isotopic spin $1/2$ it follows from the usual rules for the addition of angular momentum vectors that the pion can have only either $\tau = 1$ or $\tau = 0$. The fact that the pion is known to exist in three charge states, positive, neutral and negative, which behave like an isotopic triplet, suggests that the choice for the pion must be $\tau = 1$. Here also τ is defined by $\tau(\tau + 1)$ eigeuvalue of $\boldsymbol{\tau}^2$.

Observe that the relationship between the charge operator for a pion and a nucleon is different. For a pion T_3 gives directly the charge without the addition of the $1/2$ term:

$$\text{meson charge} = \tau_3 = \begin{cases} +1 \text{ for } \pi^+ \\ 0 \text{ for } \pi^0 \\ -1 \text{ for } \pi^- \end{cases} \tag{4.2}$$

Then for a system of A nucleons and B pions the total charge is

$$\sum_{\text{A nucleons}} \left(\frac{1}{2} + \tau_3\right) + \sum_{\text{B pions}} \tau_3 = \frac{A}{2} + T_3, \tag{4.3}$$

where T_3 is the 3–rd component of the total I.S. of the system and is again conserved since both the charge and the number of nucleons are constant.

We now introduce the postulate that even for a system of nucleons and pions the Hamiltonian is approximately a scalar invariant in charge space. As for the case of nucleons only, this hypothesis will apply only if the Coulomb forces are neglected and the mass differences between proton and neutron on the one hand and charged and neutral pions on the other are also neglected.

From this postulate it follows that the resultant isotopic spin (i.e. its three components and its magnitude) are time constants and have in addition all the formal properties of angular momentum vectors.

We consider a system composed of a nucleon and a pion: $(\mathfrak{N}, \pi)$. We have already seen that for a nucleon $\tau(\mathfrak{N}) = 1/2$ and for a pion $\tau(\pi) = 1$.

The total isotopic spin T can then take on the two values

$$T = \frac{2}{3} \quad , \quad T = \frac{1}{2}.$$

The following notation will be used for charge states:

$$n^+ \text{ means } n + \pi^+, \text{ etc.}$$

So we have six possible charge states:

$$p^+, p^0, p^-, n^+, n^0, n^-,$$

that we shall call "physical charge states," directly accessible to observation. [Remember, for analogy, that a given combination of an orbital and spin angular momentum forms a mixture of states of the different possible total angular momenta].

We use the function χ_3 as indicating a state with $T = 3/2$, and in order to fix the charge state we use the superscript $(2\,T_3)$ on it.

For $T = 3/2$.

$$(4.4) \qquad T_3 = \begin{cases} 3/2 \\ 1/2 \\ -1/2 \\ -3/2 \end{cases} \qquad \text{charge} = \frac{A}{2} + T_3 = \begin{cases} 2 \\ 1 \\ 0 \\ -1 \end{cases}$$

we obtain four functions

$$\chi_3^{(3)}, \chi_3^{(1)}, \chi_3^{(-1)}, \chi_3^{(-3)}.$$

$\chi_{2T}^{(2T_3)}$ in general is the wave function corresponding to isotopic spin T and charge state T_3.

The wave functions for the case of a nucleon and a pion are as follows:

$$T = \frac{3}{2} \qquad\qquad T = \frac{1}{2}$$

$$(4.5) \quad \begin{cases} (a) \quad \chi_3^{(3)} = p^+ \\ (b) \quad \chi_3^{(1)} = \sqrt{\frac{2}{3}}\, p^0 + \sqrt{\frac{1}{3}}\, n^+ \qquad (e) \quad \chi_1^{(1)} = \sqrt{\frac{1}{3}}\, p^0 - \sqrt{\frac{2}{3}}\, n^+ \\ (c) \quad \chi_3^{(-1)} = \sqrt{\frac{2}{3}}\, n^0 + \sqrt{\frac{1}{3}}\, p \qquad (f) \quad \chi_1^{(-1)} = -\sqrt{\frac{1}{3}}\, n^0 + \sqrt{\frac{2}{3}}\, p^- \\ (d) \quad \chi_3^{(-3)} = n^-. \end{cases}$$

The coefficients of combination here used are the Clebsch-Gordan coefficients. The χ's are all orthogonal.

We can experimentally realize a state of $T = 3/2$ by the bombardment of hydrogen by π^+, and, in principle, it is possible to obtain in a similar way the $T = 3/2$ state as an n^- state. The $T = 1/2$ state, however, cannot be obtained in a pure form in any single nucleon-meson combination.

B) EXPERIMENTS INVOLVING PIONS AND NUCLEONS

5.—Meson-Nucleon Scattering.

Let us now introduce the scattering amplitudes S_3 and S_1, corresponding to scattering in the different isotopic spin states, in the following way

$$(5.1) \qquad \begin{cases} e^{ikz}\,\chi_1 \to S_1\,\chi_1 \\ e^{ikz}\,\chi_3 \to S_3\,\chi_3\,, \end{cases}$$

where there first terms correspond to initial (plane wave incident pion) states, and the others to final (scattered pion) states.

In the scattering of positive pions on protons only the charge state p^+ is involved. Therefore the amplitude for this case is S_3.

For the case of π^- scattered by protons the initial state is a mixture of $\chi_3^{(-1)}$ and $\chi_1^{(-1)}$.

From (*c*) and (*f*) of (4.5) we have the following expressions

$$(5.2)\qquad \begin{cases} n^0 = \sqrt{\frac{2}{3}}\,\chi_3^{(-1)} - \sqrt{\frac{1}{3}}\,\chi_1^{(-1)}, \\ p^- = \sqrt{\frac{1}{3}}\,\chi_3^{(-1)} + \sqrt{\frac{2}{3}}\,\chi_3^{(-1)}. \end{cases}$$

So we can write (omitting the common upper index -1)

$$(5.3)\quad (p^-)\exp[ikz] = \sqrt{\tfrac{1}{3}}\chi_3 \exp[ikz] + \sqrt{\tfrac{2}{3}}\chi_1 \exp[ikz] \to \sqrt{\tfrac{1}{3}}\chi_3 S_3 + \sqrt{\tfrac{2}{3}}\chi_1 S_1$$
$$= \sqrt{\tfrac{1}{3}}\left(\sqrt{\tfrac{2}{3}}\,n^0 + \sqrt{\tfrac{1}{3}}\,p^-\right)S_3 + \sqrt{\tfrac{2}{3}}\left(-\sqrt{\tfrac{1}{3}}\,n^0 + \sqrt{\tfrac{2}{3}}\,p^-\right)S_1$$
$$= n^0\sqrt{2}\,(S_3 - S_1)/3 + p^-\,(S_3 + 2\,S_1)/3.$$

In this relation the first term describes the charge exchange scattering and the second one the elastic scattering.

At present it is experimentally possible to bombard protons with positive and negative pions. For instance, the cyclotron of Chicago accelerates protons to an energy of 460 Mev. These strike a Be target, producing positive and negative pions. (A Be target is particularly suitable for obtaining pions).

About 10 percent of the protons colliding with the target give rise to nuclear collisions, and only a few percent of these collisions give pions. The number of these is of the order of $10^{10} \div 10^{11}\ s^{-1}$.

In the collisions neutral pions are also produced, but these decay within $\sim 10^{-14}$ s, and their disintegration products can be eliminated before reaching the measuring devices.

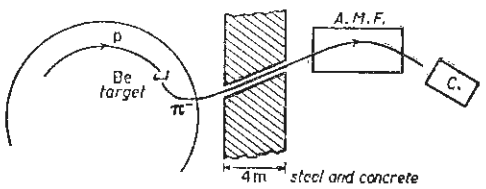

Fig. 2. – Schematic diagram of the method for producing negative pion beams at the University of Chicago synchrocyclotron.

Negative pions are deviated by the magnetic field of the cyclotron, pass through a hole in a shield of 4 m concrete and steel, then are purified, before reaching the measuring equipment, by an auxiliary magnetic field (A.M.F.), as shown in fig. 2.

Positive pions are obtained in a rather similar way by reversing the magnetic field of the cyclotron, but in this case it is not possible to reach the same intensity and energy as for negative pions since the pions observed are those emitted in the backward direction.

The techniques of observations use counters, diffusion cloud chambers and photographic plates.

A typical arrangement with scintillation counters is shown in fig. 3.

The beam of pions is not really pure, because there is always a rather large contamination of muons; but these are readily distinguished, as they have, for the same magnetic rigidity, a different range from the pions. This also applies to the electron component that is sometimes present.

If we plot in a diagram the intensity of the beam as a function of absorber thickness, R, we obtain a curve like the one shown in fig. 4, which enables us to determine the amount of contamination in the beam.

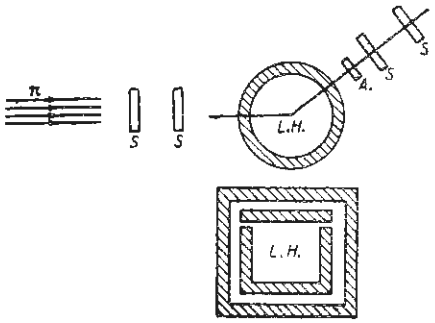

Fig. 3. – A typical arrangement for the observation of pion scattering from protons.

L. H., Liquid hydrogen; *S*, Scintillation counters; *A*, Anticoincidence, used when one wants to discriminate photons from charged pions. A convenient liquid hydrogen container can be made from styrofoam, having a specific gravity of only 0,03 g cm^{-3} and very easy to machine.

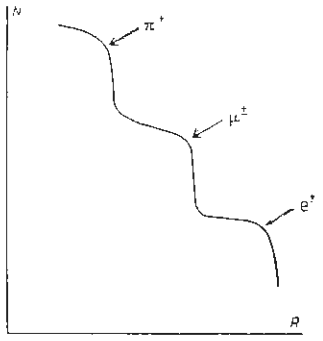

Fig. 4. – Counting rate vs. absorber thickness for a "pion" beam. The heights of the steps are proportional to the amounts of the various components in the beam.

Photographic plates are also a convenient means of detection: they have a concentration of hydrogen comparable to that in liquid hydrogen. The technique used is that of "area scanning" to find events like that shown in fig. 5.

At the place where one observes this event it is possible that one has a case of pion-proton scattering. One then tests the coplanarity and the relationship between the angles α, β.

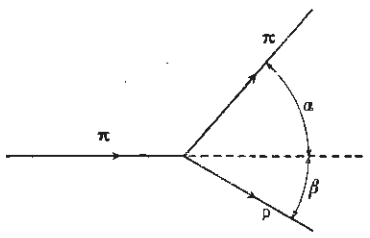

Fig. 5. – An event observed in a photographic emulsion which could correspond to a pion–proton scattering.

One may also use in these measurements a hydrogen filled diffusion cloud chamber, which has the advantage that it contains only hydrogen.

Bubble chambers are being developed now, and this technique too is very promising. Good tracks have been obtained by Hildebrand in Chicago, using pentane in the bubble chamber.

The three scattering processes shown in column 1 of Table I can be di rectly investigated experimentally. Now, we have seen that the scattering amplitudes of these three processes are expressible in terms of S_3 and S_1, the ampli-

tudes for scattering in the states with isotopic spin $T = 3/2$ and $1/2$, respectively, as shown in Table I.

The process $p^+ \to p^+$ is controlled directly by the amplitude S_3, because p^+ is a pure state of $T = 3/2$. Since p^- and n^0 are mixtures of the states $T = 3/2$ and $1/2$, the amplitude $((S_3/3) + (2\,S_1/3))$ describes the elastic scattering of negative pions by protons and the amplitude $(\sqrt{2}/3)\,(S_3 - S)_1$ describes the charge-exchange scattering. So in order to complete the scattering analysis and to find the cross-sections, it is necessary to obtain expressions for S_1 and S_3.

TABLE I.

Scattering amplitudes for the possible processes involving charged mesons on hydrogen.

Process	Amplitude
$p^+ \to p^+$	S_3
$p^- \to p^-$	$\frac{1}{3} S_3 + \frac{2}{3} S_1$
$p^- \to n^0$	$\frac{\sqrt{2}}{3} (S_3 - S_1)$

The expressions that we will arrive at for S_3 and S_1 are, however, obtained under the simplifying assumption that only s and p states are present. There is much discussion of the legitimacy of this assumption but it seems fairly clear that at sufficiently low energy this approximation should by justified.

In principle the waves of increasing angular momentum make contributions to the scattering which vary with increasing powers of the momentum; so, at sufficiently low energy one might say that the s–state should dominate and that only at somewhat higher energy the p–state will contribute significantly. At still higher energies one expects the d–wave and higher angular momentum states to become increasingly important.

We will see that there is good evidence that the interaction in the p–state is abnormally strong, so there is perhaps some point in including both s– and p–states in the analysis. One of course hopes that the d–state will not yet contribute appreciably at the energies of interest, not only because this is in accordance with the general sequence of importance of the various terms, but also because there is no reason to suspect that the interaction in the d–state is intrinsically as strong as that in the p–state.

Now if we make this assumption, the problem of expressing S_1 and S_3 becomes a rather conventional problem of collision theory in which all effects are interpreted in terms of phase shifts.

The only complication which remains to be taken into account is the spin of the nucleon; for example, S_3 should be labelled by another index

indicating the direction of the spin of the nucleon in the initial state. We shall consider the scattering of a pion wave which is incident along the z–direction. The target nucleon may have its spin parallel or anti-parallel to this direction. We shall distinguish these two possibilities by means of superscripts α, β, corresponding to spin up and spin down, respectively. So instead of only S_3, we now need the expressions for S_3^α and S_3^β.

Next let us introduce the phase shifts for the various angular momentum states. In the case of the s–state the resultant angular momentum is controlled by the spin of the nucleon only and thus there occurs only one angular momentum state, that with $J = 1/2$. For p–states, on the other hand, the spin of the nucleon may be parallel or anti-parallel to the orbital angular momentum $l = 1$ of the p–wave, giving two possibilities, namely $J = 1/2,\ 3/2$, as in ordinary doublet states. Therefore we have three different states, differing in orbital and total angular momentum, to each of which we must assign a phase shift. This number of states must be doubled when one considers that we are dealing with two possible values of the isotopic spin. Altogether, then, we have the six combinations of three possible angular momentum states and two possible charge states. The corresponding phase shifts are also six, and the notation usually adopted for them is shown in Table II.

TABLE II.

Notation adopted for the scattering phase shifts, assuming s– and p–wave scattering only.

	$s_{1/2}$	$p_{1/2}$	$p_{3/2}$
$T = 3/2$	α_3	α_{31}	α_{33}
$T = 1/2$	α_1	α_{11}	α_{13}

We expect that all scattering phenomena in a certain low energy range will be described by the set of these six α's. In particular S_3 will be described in terms of α_3, α_{31} and α_{33} and S_1 in terms of α_1, α_{13} and α_{11}. The expressions for S_3^α and S_3^β are the following:

$$\begin{pmatrix} S_3^\alpha \\ S_3^\beta \end{pmatrix} = \frac{\exp[ikr]}{kr}\left[\{e_3 + (2e_{33} + e_{31})\cos\theta\}\begin{pmatrix}\alpha\\ \beta\end{pmatrix} \pm (e_{31} - e_{33})\sin\theta\exp[\pm i\varphi]\begin{pmatrix}\beta\\ \alpha\end{pmatrix}\right], \tag{5.4}$$

where e^{ikr}/kr describes the outgoing spherical wave, while the e's are the following quantities:

$$\begin{cases} e_{31} = \exp[2i\alpha_{31}] - 1, \\ e_{33} = \exp[2i\alpha_{33}] - 1, \\ e_3 = \exp[2i\alpha_3] - 1. \end{cases} \tag{5.5}$$

The first term of (5.4) corresponds to no spin-flip, and the second to spin-flip. The expressions for S_1^α and S_1^β are the same, except that in place of e_{31} we must write e_{11}, and so forth.

We can obtain the intensity of the scattered wave by taking the square modulus of the coefficient in (5.4) of the term corresponding to one spin direction, and adding to it the square modulus of the coefficient for the other spin direction. So we have one term independent of the angle θ, another proportional to $\cos\theta$, another to $\cos^2\theta$. We are thus led to an angular distribution of the type

$$\frac{d\sigma}{d\Omega} = a + b\cos\theta + c\cos^2\theta . \tag{5.6}$$

If we had included, for example, *d*–states but no higher angular momentum states, then terms in $\cos^3\theta$ and $\cos^4\theta$ would have appeared in (5.6). In general each additional angular momentum state considered will result in the introduction of two further terms in this expansion in powers of $\cos\theta$.

There is a further complication which has been neglected in the above discussion of the scattering in *s*– and *p*–states. This is the perturbation due to the Coulomb scattering, resulting in an interference with the pure nuclear scattering. Let us consider the $p^+ \to p^+$ scattering as a simple example in which we are not troubled with the complication of charge exchange scattering. Suppose for a moment that we could switch on and off alternatively either the Coulomb force or the purely nuclear interaction. When we have only the Coulomb interaction, we get Rutherford scattering. This has an extremely large cross-section at small angles but decreases very rapidly, as the fourth power of the angle θ. Therefore $(d\sigma/d\Omega)_{\text{Coulomb}}$ is very important in the forward direction and becomes practically negligible at angles greater than say, 30° or 40°.

Now the question arises as to the effect of interference when both modes of scattering occur. The exact formula has been obtained by van Hove,[3] but the effect can be demonstrated in good approximation by the following considerations: we shall split $(d\sigma/d\Omega)$ into two nuclear parts, $(d\sigma/d\Omega)_1$ which is coherent with the Coulomb scattering and $(d\sigma/d\Omega)_2$ which is incoherent.

Then since the cross-section is proportional to the square of the amplitude, we have,

$$\frac{d\sigma}{d\Omega} = \left[\sqrt{\left(\frac{d\sigma}{d\Omega}\right)_1} + \sqrt{\left(\frac{d\sigma}{d\Omega}\right)_{\text{Coulomb}}}\right]^2 + \left[\sqrt{\left(\frac{d\sigma}{d\Omega}\right)_2}\right]^2 . \tag{5.7}$$

The coherent part of the amplitude $\sqrt{(d\sigma/d\Omega)_1}$ corresponds to "no spin-flip" of the nucleon, while the incoherent part $\sqrt{(d\sigma/d\Omega)_2}$ corresponds to "spin-flip," because in Coulomb scattering it is known that the major contribution arises from the "no spin-flip" process. The interference of nuclear and Coulomb scattering may be positive or negative depending on the sign of the amplitude of nuclear scattering and this enables one to determine this sign, as we shall see later.

(3) L. VAN HOVE, « Phys. Rev. », *88*, 1358 (1952).

Forgetting for the moment the effects of the Coulomb forces, which in most cases are a minor correction, we can make the comparison with experiment. Many experiments of the type in which we are interested, e.g.

$$p^+ \to p^+ \quad , \quad p^- \to p^- \quad \text{and} \quad p^- \to n^0.$$

have been carried out at a variety of energies.

The angular distributions in these reactions have been studied separately and each has been fitted by an expansion of the form $a + b\cos\theta + c\cos^2\theta$. The experimental results therefore yield, essentially, sets of quantities a^+, b^+, c^+ obtained from the angular distribution in the $p^+ \to p^+$ reaction; a^-, b^-, c^- from that of $p^- \to p^-$, and a^0, b^0, c^0 from the charge exchange scattering $p^- \to n^0$. These nine quantities constitute the maximum information that experiment can give provided of course that the assumed formula is correct. There have been many attempts to determine whether the contribution from higher angular momentum states appears in a significant way, especially at high energies. But so far, because of rather limited experimental accuracy, it has been impossible to draw any significant conclusion. Therefore we may say that even if higher angular momentum terms are present, they are too small to be observed at present.

For this reason I propose to ignore such terms, so that at each energy, the experimental distributions give us the value of the nine quantities a^+, b^+, c^+, etc. To determine the six phase shifts $\alpha_3, \alpha_1, \alpha_{33}, \cdots$, from the nine experimental coefficients is an overdetermined problem, which has a solution, provided that the theory is correct. Of course it could be solved within the experimental error, which is quite large, even if there were some appreciable deviation from isotopic spin conservation.

The method we could adopt is, for example, to consider first only the data on negative pion scattering. In other words, consider only the six coefficients $a^-, b^-, c^-, a^0, b^0, c^0$, and from them determine the six phase shifts. Then we can compute the coefficients a^+, b^+, and c^+ of the positive pion scattering and compare them with the direct measurements. This is, in a certain sense, an honest way of checking the theory, and it turns out to work fairly well. But there are unfortunately various ambiguities which are of the following kind. Suppose I follow this scheme, and try to solve the six equations for the six unknown quantities. Then I find a number of solutions, all of which give very similar values for the p^+ coefficients a^+, b^+, c^+, so that this procedure does not appear to yield a unique solution.

As long as the Coulomb scattering is neglected there is, in particular, the ambiguity that a change of sign of all phase shifts does not change the angular distribution. It is especially in this respect that the Coulomb forces are important. Because the Coulomb scattering is well knownand completly understood, one has the possibility of determining the sign of the nuclear phase shifts by observing the sign of the interference term. This has been done to some extent by many people. I cannot say that the results which have been obtained on this point are final. But they warrant the conclusion that the probability, that the signs that I am going to give are correct, is perhaps 90 percent. I am now going to present a set of phase

shifts that is compatible with the experimental data. It is not by any means the only solution but is the one which, for a variety of reasons, appears at present to be the most probable.

These solutions were first published by Glicksman [4] and are obtained by assuming that only α_3, α_1, and α_{33} are different from zero. This rather drastic assumption is perhaps not quite justified but yields a very simple fit of the experiments. With this simplification Glicksman found that α_{33} is approximately proportional to η^3.(*)

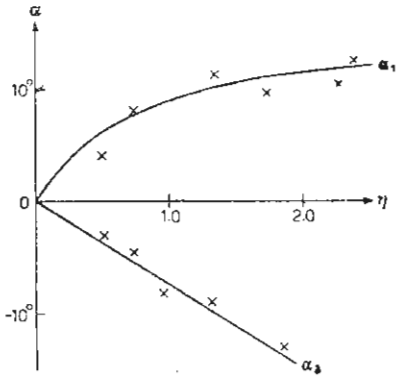

Fig. 6. – Experimental s–wave phase shifts as a function of $\eta = p/\mu c$ of the pion in the c.m.s.

The coefficient of η^3 is not quite constant but ranges from 0.26 radians at low energy to 0.31 at higher energy. This expression becomes equal to 90°, which is the conventional definition of a resonance, at about $\eta = 1.7$, corresponding to a laboratory energy a little below 200 Mev.

The experimental evidence concerning the phase shifts α_3 and α_1 is a bit confused. The experimental points are shown in fig. 6 with "reasonable" curves drawn through them.

Previous indications, reported at the Rochester conference in 1953,[5] appeared to indicate that α_3 could be positive at very low energy and become negative at somewhat higher energies. However, more recent data seem to favor the simpler solution shown in fig. 6.

Orear [6] has collected all pertinent data at low energy and proposes the following formulas for α_3 and α_1 at low energy:

$$(5.8) \qquad \begin{cases} \alpha_3 = -0.11\,\eta\,, \\ \alpha_1 = +0.16\,\eta\,; \end{cases}$$

$|\alpha_3|$ apparently increases linearly with η over a rather long interval, although it is difficult to predict what will happen at higher energies; α_1 instead reaches a plateau of about 10° and its behaviour becomes rather unclear at high energies (see fig. 6).

I should mention in this connection that in the Orear analysis somewhat more weight was given to the pion scattering experiments than to the photo-effect experiments. There exists a relation [7] between the photoeffect and the difference between α_1 and α_3 near $\eta = 0$. With the best data on the

(4) M. GLICKSMAN, « Phys. Rev. », *94*, 1335 (1954).

(*) η is the meson momentum, in the c.m.s., in units of μc (μ is the pion rest-mass).

(5) *Proceedings of the Fourth Annual Rochester Conference on High Energy Physics* (New York, 1954).

(6) J. OREAR, « Phys. Rev. », *96*, 176 (1954).

(7) H. L. ANDERSON and E. FERMI, « Phys. Rev. », *86*, 794 (1953). [See paper N° 254 (Editors' note)].

photoeffect $(\alpha_1 - \alpha_3)/\eta$ should be about 0.21 instead of 0.27 according to Orear. This corresponds to a discrepancy in the intensities by the factor $(0.27/0.21)^2 = 1.65$.

6.—Interpretation of the Phase Shifts.

We have described our experimental knowledge of the phase shifts in pion-nucleon interactions. The question now arises as to what quantitative conclusions we can draw from these phase shifts. Consider a system of two particles, say a pion and a nucleon. When they are far apart, our understanding of the system is as complete as that of any other two body problem; however, when the distance between them is small, say less than the interaction range, r_0, our understanding is very limited.

In order to obtain a simplified picture let us assume that a potential of short range, r_0, acts between the two particles. For a state of definite charge and angular momentum, we can write the equation for $r\psi = u(r)$. $u(r)$ obeys the radial Schrödinger equation,

$$u'' + \left[p^2 - \frac{l(l+1)}{r^2} - 2mU(r)\right] u = 0, \tag{6.1}$$

where we have used a system of units in which $\hbar = c = 1$, m is the reduced mass, and $p^2 = 2mE$. An exact solution of (6.1) may be obtained for values of $r > r_0$; for values $r < r_0$, this is not possible unless we know the potential. So, let us divide the equation into an inside part $(r < r_0)$ for which we can say very little and an outside one $(r > r_0)$.

For the outside (6.1) becomes

$$u'' + \left[p^2 - \frac{l(l+1)}{r^2}\right] u = 0. \tag{6.2}$$

The general solution of (6.2) is a linear combination of two fundamental solutions. Written in a normalized form they are:

$$\sqrt{\frac{\pi}{2}pr}\, J_{l+\frac{1}{2}}(pr) \equiv J(pr), \tag{6.3}$$

$$\sqrt{\frac{\pi}{2}pr}\, N_{l+\frac{1}{2}}(pr) \equiv N(pr), \tag{6.4}$$

where J and N are Bessel functions. J is regular at $r = 0$. On the other hand N is singular at $r = 0$.

The asymptotic expressions for these two solutions are, for large values of r,

$$J \to \sin\left(pr - \frac{\pi l}{2}\right) \quad \text{and} \quad N \to \cos\left(pr - \frac{\pi l}{2}\right), \tag{6.5}$$

for small values of r,

$$J \to \frac{(pr)^{l+1}}{(2l+1)!!} \quad \text{and} \quad N \to \frac{(2l-1)!!}{(pr)^l}. \tag{6.6}$$

The !! means that in the factorial multiplication, only odd numbers are included, i.e. $1 \cdot 3 \cdot 5 \cdot 7 \cdots (2l+1) \equiv (2l+1)!!$ If there were no interaction the solution should be regular at the origin and it would be J. When there is an interaction, however, we expect that for $r > r_0$, $u(r)$ will be a linear combination of the two asymptotic solutions, of the form $aJ + bN$.

This mixture can be determined if the phase shift is known. For a phase shift, α, we have the asymptotic solution $\sin(pr - (\pi l/2) + \alpha)$, instead of $\sin(pr - \pi l/2)$ which corresponds to zero phase shift.

The asymptotic form of the phase-shifted solution is then

$$\sin\left(pr - \frac{\pi l}{2}\right)\cos\alpha + \cos\left(pr - \frac{\pi l}{2}\right)\sin\alpha .$$

Its exact form in the region $r > r_0$ is then

$$u(r) = J\cos\alpha + N\sin\alpha \tag{6.7}$$

and since α is known experimentally, we can determine the coefficients. In the vicinity of r_0, for low meson momenta and thus small pr (we assume for simplicity $pr_0 \ll 1$) we may use (6.6). The solution is then:

$$u(r) \cong \cos\alpha \frac{(pr)^{l+1}}{(2l+1)!!} + \sin\alpha \frac{(2l-1)!!}{(pr)^l} . \tag{6.8}$$

For small α, with $\cos\alpha \cong 1$, $\sin\alpha \cong \alpha$, fig. 7 shows schematically the undisturbed solution J (in the absence of any phase shift), the phase shift correction αN, and the actual solution obtained by adding the two. For $r < r_0$ the above solution has no physical significance.

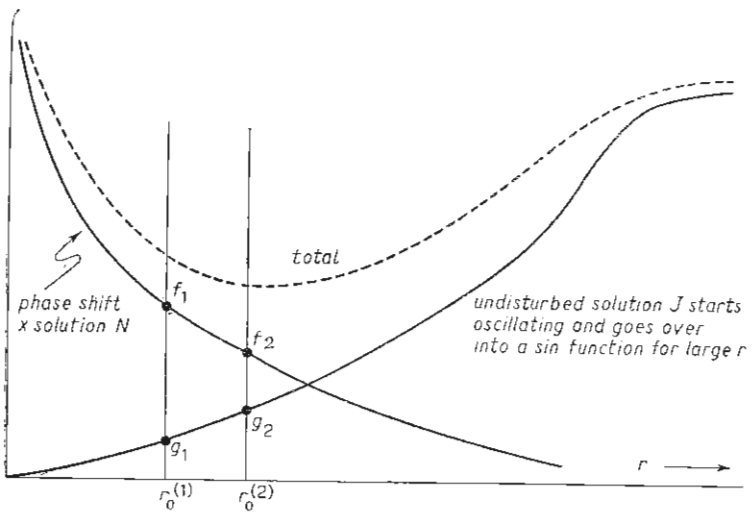

Fig. 7. – Schematic representation of the radial wave function $u(r)$ for an interaction of range r_0.

The question now arises: what is the magnitude of the perturbation arising from the phase shift? Clearly this is dependent on the magnitude of r_0. Thus (see fig. 7) if $r_0 = r_0^{(1)}$, the perturbation is measured by $(f_1/g_1)^2$ and if $r_0 = r_0^{(2)}$, it is $(f_2/g_2)^2$; these are very different.

We shall now demonstrate that, for an angular momentum l, the phase shift α, at low energy, is proportional to p^{2l+1}.

Consider a potential function U (r) of range r_0, the exact nature of which is unknown for $r < r_0$. In the vicinity of r_0 the solutions $u(r)$ of (6.2) computed for $r < r_0$ and $r > r_0$ must have equal values and derivatives

$$u(r_0 + \varepsilon) = u(r_0 - \varepsilon) \quad , \quad u'(r_0 + \varepsilon) = u'(r_0 - \varepsilon). \tag{6.9}$$

Because our equation (6.1) is linear, what is required is to match, on the two sides of r_0, the ratio $u(r)/u'(r)$. Put

$$\rho \equiv \frac{u_l(r_0)}{u_l'(r_0)} = \rho(E) \tag{6.10}$$

and assume that $\rho(E)$ is computed from the inside solution. Assuming for the outside solution the form (6.8) we obtain, by matching at r_0,

$$\rho(E) = \frac{\cos\alpha \dfrac{(pr_0)^{l+1}}{(2l+1)!!} + \sin\alpha \dfrac{(2l-1)!!}{(pr_0)^l}}{(l+1)\cos\alpha \dfrac{p^{l+1} r_0^l}{(2l+1)!!} - l\sin\alpha \dfrac{(2l-1)!!}{p^l r_0^{l+1}}}. \tag{6.11}$$

From this follows

$$\operatorname{tg}\alpha = \left[\frac{(l+1)\rho(E) - r_0}{l\rho(E) + r_0}\right] \frac{(pr_0)^{2l+1}}{(2l+1)!!\,(2l-1)!!}, \tag{6.12}$$

which expresses the phase shift α in terms of $\rho(E)$.

Near the threshold $\rho(E)$ can be substituted for by its values for zero energy $\rho(0)$. For small values of E this is an adequate approximation. Also for small values of p and consequently small α, $\operatorname{tg}\alpha \cong \alpha$. We then have $\alpha = \text{constant} \cdot p^{2l+1}$.

As the energy E is increased, the dependence of α on p will contain terms of higher power than $(2l+1)$. Thus, we may express the coefficient of (6.12) as an expansion in powers of E

$$\operatorname{tg}\alpha \cong [Y_0 + Y_1 E + \cdots] \frac{(pr_0)^{2l+1}}{(2l+1)!!\,(2l-1)!!}. \tag{6.13}$$

We note that the first correction to the phase shift gives a term proportional to p^{2l+3} (and not to p^{2l+2}).

It is clear that α cannot be computed as long as ρ is unknown. However, for most values of ρ the coefficient in (6.12) is of the order of one.(*)

(*) This is, of course, only true for $l \gtrsim 1$. For $l = 0$, (6.13) becomes

$$\operatorname{tg}\alpha = \left[\frac{\rho(E) - r_0}{r_0}\right] pr_0. \tag{6.14}$$

Only over a relatively small range of ρ values, in the region of $\rho \approx -r_0/l$, does the coefficient become very large. For this reason a value of

$$\alpha \gg \frac{(pr_0)^{2l+1}}{(2l+1)!!\,(2l-1)!!},$$

would indicate an exceptional condition well worth looking into.

The importance of the factorials in the denominator of (6.12) is shown in the following Table III.

TABLE III.

The factorials in the denominator of the dependence of phase shift on momentum, eq. (6.12).

l	$(2l+1)!!\,(2l-1)!!$
0	1
1	3
2	45
3	1575

The rapid increase in the denominator with increasing l is another reason why we expect the phase shifts near threshold to be negligible for $l \geq 2$.

The behavior of the coefficient in (6.12) and (6.14) is shown in fig. 8 for a number of l-values.

$$\operatorname{tg}\alpha = Y\,\frac{(pr_0)^{2l+1}}{(2l+1)!!\,(2l-1)!!}, \qquad Y \equiv \frac{(l+1)\,\rho\,(E) - r_0}{l\rho\,(E) + r_0}.$$

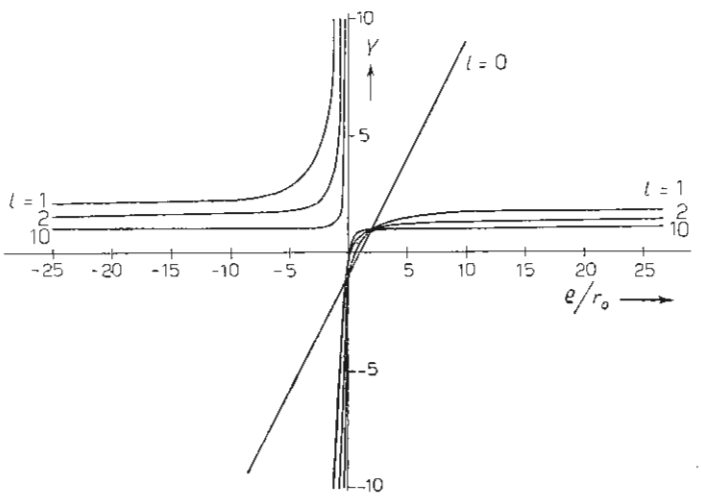

Fig. 8. – Dependence of the phase shift on the wave function at the interaction boundary.

We can now try to estimate from the phase shifts the actual magnitude of the perturbation introduced by the interaction. For this purpose let us evaluate the ratio of the total disturbed wave function (6.7) to the undisturbed wave function $J(pr)$. The square of this ratio may be referred to as the "enhancement factor." It represents the increase in probability, due to the interaction, for the two particles to be "in contact."

For small values of p

$$\cos\alpha \cong 1 \quad , \quad \sin\alpha \cong \alpha \cong a p^{2l+1},$$

$$\text{the undisturbed wave function} \cong \frac{(pr)^{l+1}}{(2l+1)!!},$$

$$\text{the perturbation term} \cong a p^{2l+1} \frac{(2l-1)!!}{(pr)^l}.$$

The phase-shifted wave function, which is the sum of the two expressions given above, is

$$\frac{(pr)^{l+1}}{(2l+1)!!} + a p^{2l+1} \frac{(2l-1)!!}{(pr)^l}.$$

The enhancement factor is, then

$$\text{E.F.} = \left\{ 1 + \frac{a(2l+1)!!\,(2l-1)!!}{r_0^{2l+1}} \right\}^2. \tag{6.15}$$

For the s–and p–waves we have previously obtained the phase shifts at low energies for $T = 3/2$ and $T = 1/2$ given in Table IV.

TABLE IV.

Experimental pion-nucleon scattering phase shifts at low energies.

Wave \ T	$\frac{3}{2}$	$\frac{1}{2}$
$s_{1/2}$	$\alpha_3 = -0.11\,\eta$	$\alpha_1 = 0.16\,\eta$
$p_{3/2}$	$\alpha_{33} = 0.26\,\eta^3$	—

Substituting these values we obtain for the enhancement factors:

$$\text{E.F.}(\alpha_3) \cong \left[1 - \frac{0.11}{r_0}\right]^2 \quad , \quad \text{E.F.}(\alpha_1) \cong \left[1 + \frac{0.16}{r_0}\right]^2, \tag{6.16}$$

$$\text{E.F.}(\alpha_{33}) \cong \left[1 + \frac{0.78}{r_0^3}\right]^2,$$

r_0 is measured in units of $\hbar/\mu c$.

For $r_0 \cong 1$, the enhancement factors are ~ 1 for α_3 and α_1 and ~ 3 for α_{33}. However, the "33" p–wave appears, from experimental observations, to be more important than is indicated by the enhancement factor 3. In fact, the experimental evidence from photomeson production suggest that the

factor is probably $\sim$ 10. This would be the case for $r_0 \approx 0.7$, which may be taken as an indication that the range of the interaction is somewhat $< \hbar/\mu c$.

TABLE V.

Enhancement factors for the wave function at $r = r_0$ corresponding to p–wave scattering in the (3.3) state.

η	α_{33}	E. F.			
		$r_0 = 0.5$	$r_0 = 0.6$	$r_0 = 0.7$	$r_0 = 1.0$
0	$(15^\circ\,\eta^3)$	53	22	10.8	3.2
0.5	1.88°	49	26	10.4	3.8
1	15°	62	36	12.5	4.6
1.5	58°	68	31	15.9	4.1
1.7 (*)	90°	57	19	11.0	1.6
2.0 (**)	145°	3.4	0.8	0.2	0.1

(*) This is the momentum corresponding to the "resonance" energy, at which $\alpha_{33} = 90^\circ$.

(**) The values of the E.F. for $\eta = 2$ are small and probably the exact values do not have any physical significance. For $r_0 = 1$, there is actually a node between $\eta = 1.7$ and $\eta = 2.0$. The general dependence of the E.F. on the value of α_{33} is indicated in fig. 9, from which we may see that the "resonance" behavior of the processes involving the (33) state is due to two factors. The rapid rise at low energies comes from the p^3 dependence of α_{33}; the rapid decrease above the resonance energy comes from the rapid falling off of the E.F.

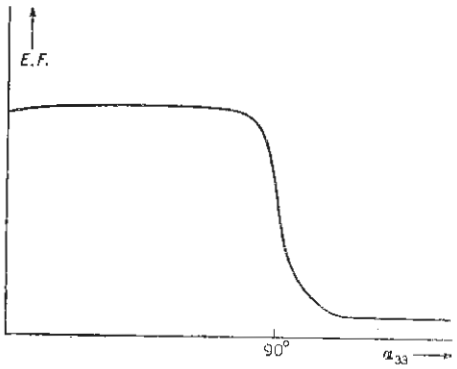

Fig. 9. – General behaviour of the enhancement factor in the (33) state as a function of the phase shift α_{33}.

Table V shows the enhancement factors for the (33) scattering as a function of relative meson momentum η, calculated for the measured α_{33} phase shifts and using the correct Bessel function solutions for the wave functions, for a number of assumed values of the interaction range, r_0.

7.—Photomeson Production.

We have heard from Bernardini's lectures (*) that at low energies, close to the threshold for the photoproduction of positive pions from hydrogen, the transition is to a state in which the pion is emitted in an s–state. This is indicated by the flatness of the angular distribution as well as by the excitation function, which seems to be proportional to the momentum of the pion. I would like now to discuss in a simplified form the mechanism of this photo-pions production and begin with an approach that does not lead to an adequate solution. We may argue as follows: According to Yukawa the nucleon alternates between a state of the bare nucleon, say a proton and a state which may be described as a neutron plus a positive pion which surrounds the neutron in some sort of a cloud

$$p \rightleftarrows n + \pi^+. \tag{7.1}$$

The incoming photon may catch the system in the latter state and produce a photo-disintegration by ejecting the pion. What estimate can we make of the intensity of this effect? We know that the initial state has $J = 1/2$ and even parity, being just a proton. (A nucleon is, by definition, treated as a particle with even parity).

In the final state, the pion, of intrinsic spin zero, is emitted in an s–state, i.e., with no orbital angular momentum. The spin of the system is thus essentially the spin of the remaining neutron, i.e. $1/2$. The pion is pseudoscalar and therefore the parity of the system in an orbital s–state will be odd. The transition is thus from a $J = 1/2\ (+)$ to $J = 1/2\ (-)$ state, a transition which is classified as an electric dipole (E 1) transition.

Now, what will happen to the direction of the nucleon spin in this transition? Let us take the z–axis in the direction of propagation of the photon and assume that the spin of the nucleon is up in the initial state; i.e. the initial spin state is α. After the transition the proton will change to a neutron and the pion can be considered as free. In this process the spin of the nucleon will be flipped so that the final spin state is β (spin down). The reason for this spin flip can be seen if we consider the angular momentum carried by the photon. The photon may be described by a scalar function, e^{ikz} which we may call the orbital part, and a polarization vector, which plays the role of an object with spin $s = 1$. The orbital part e^{ikz} can be expanded in spherical harmonic functions $Y_{l,m}$, which have the orbital angular momentum l. The z–component m of the orbital angular momentum is always zero, since e^{ikz} only depends on z.

The polarization state of the photon can be described in terms of two circularly polarized states of opposite directions, which in the case of a linearly polarized photon are mixed in equal proportions. The angular momentum of these two polarization states corresponds to a spin $s = 1$, with the z–component $s_z = \pm 1$. Since the z–component of the orbital angular momentum

(*) G. Bernardini, «Nuovo Cimento», *2*, Suppl. 104–139 (1955).

is $m = 0$, the total angular momentum has the z–component, $j_z = \pm 1$. The magnitude of the total angular momentum $\boldsymbol{j} = \boldsymbol{l} + \boldsymbol{s}$ can take all integral values, zero excluded. To each value of j there correspond three values of l, namely $l = j \pm 1$ and $l = j$ and two parities corresponding to an electric or a magnetic multipole interaction.

Since the nucleon spin in our initial state was stipulated as being up, i.e. $j_z = +1/2$, and the photon transfers an angular momentum component ± 1 in the z–direction, it follows that in the final state we must have for thewhole system $J_z = +3/2$ or $-1/2$. Since the final state is $S_{1/2}$, it follows that $j_z = -1/2$ is the only possibility for the nucleons. The spin of the nucleon is thus flipped in the transition and the final spin state must be a β–state.

We now try to account for the observed intensity of the photoeffect using the naive picture of a Yukawa nucleon, sometimes surrounded by a cloud of pions, which may then be ejected by the photon. For this we first have to write down the wave function of the initial state. We are interested only in that part of the initial state which has the form n^+ since in our simple picture the proton is photoelectrically active only in this form. In the expression for the wave function of the initial state

$$\psi_i = f\left(\sqrt{\frac{2}{3}}\, n^+ - \sqrt{\frac{1}{3}}\, p^0\right)\left(\sqrt{\frac{2}{3}}\,\beta Y_{1,1} - \sqrt{\frac{1}{3}}\,\alpha Y_{1,0}\right) g(r) \tag{7.2}$$

the factor f is the amplitude of this state. f is smaller than unity but probably not very much smaller. The next factor in (7.2) is the isotopic spin function $\chi_1^{(1)}$ (6.5), for the system $(\mathfrak{N} + \pi)$ in the $T = 1/2$, $T_3 = 1/2$ state. The next term specifies the spin and orbital angular momentum state of the system. In the decomposed form of the proton, this state must have angular momentum $1/2$ and even parity. To make the parity even the pion must be moving in a p–orbit around the neutron. The angular momentum $1/2$ of the system is obtained by combining the spin $s = 1/2$ of the neutron with the orbital angular momentum $l = 1$ of the pion. Stipulating the initial state of the system as an α–state with the total spin up, $J_z = +1/2$, we can have $m = 1$ and the neutron in a β–state, or $m = 0$ and the neutron in the α–state. The term in the wave function represents the proper mixture of these spin and angular momentum states according to Condon and Shortley.[8] We finally have the radial part $g(r)$ of the wave function on which we have very little information.

The final state also contains a pion and a nucleon. The pion is in a positive energy state, in the form of an outgoing wave. In the final state the isotopic state may be either $T = 1/2$ or $T = 3/2$, since the interaction with the photon may lead to $\Delta T = 0$ or $\Delta T = \pm 1$. We therefore have two wave-functions for the final state:

$$\begin{cases} \psi_3 = \left(\sqrt{\frac{1}{3}}\, n^+ + \sqrt{\frac{2}{3}}\, p^0\right)\beta\,\frac{u_3(r)}{r}, \\ \psi_1 = \left(\sqrt{\frac{2}{3}}\, n^+ - \sqrt{\frac{1}{3}}\, p^0\right)\beta\,\frac{u_1(r)}{r}. \end{cases} \tag{7.3}$$

(8) E. U. CONDON and G. H. SHORTLEY, *The Theory of Atomic Spectra* (Cambridge, 1935).

These contain the isotopic spin functions $\chi_3^{(1)}$ and $\chi_1^{(1)}$ from (4.5) corresponding to $T_3 = +1/2$ and $T = 3/2$ or $1/2$, respectively. The total spin of the final state is required to be down. Since the pion is in an s–state and has no intrinsic spin, the neutron spin must also be down, i.e. be in a β–state. Since the pion is in an s–state we have no angular part of the wave function. Finally we have the radial parts $u_3(r)/r$ and $u_1(r)/r$ of the wavefunction in the final state.

We must now compute the matrix element corresponding to the interaction of the photon with the system. The interaction of a particle with a photon is described by the term: $e\mathbf{A}\cdot\boldsymbol{v}$, where $\mathbf{A}$ is the vector potential of the electromagnetic field. We should thus calculate the matrix element of the velocity $\boldsymbol{v}$ or, in the non relativistic case, the momentum $\boldsymbol{p}$ of the pion.

In the special case of electrons in an atom it is proved that this amounts to taking the matrix element of the coordinates, but this is not permitted in the present case.

Before we write down the matrix element we note that in the initial and final states the terms containing p^0 do not contribute since the neutral pions give no current to interact with the photon.

Furthermore, since the interaction with the pion current does not change the spin of the nucleon, the part of the initial wavefunction containing the spin state α is irrelevant since the final spin state of the nucleon is a β–state.

We obtain e.g. for the x–component of the matrix element to the final state with $T = 3/2$

$$\langle \text{final} \mid p_x \mid \text{initial} \rangle = \text{const} \cdot f \int Y_{1,1}\, g(r) \frac{\partial}{\partial x} \frac{u_3(r)}{r}\, \mathrm{d}^3\boldsymbol{r}\,, \tag{7.4}$$

For the spherical harmonic function $Y_{1,1}$ we have

$$Y_{1,1}(\vartheta, \varphi) \sim \sin\vartheta \cdot e^{i\varphi} = \frac{x + iy}{r}\,. \tag{7.5}$$

In order to estimate the magnitude of the matrix element we must know something about $g(r)$ and $u(r)$. Of $g(r)$ we do not know anything at small distances, but for $r \gtrsim \hbar/\mu c$ it decreases rapidly with the distance from the nucleon, approximately as $\exp[-r\mu c/\hbar]$.

For the wavefunction $u(r)$ of the emitted pion we can use the previously given asymptotic expressions (6.5). For the case $l = 0$,

$$u_3(r) \sim \sin(\eta r + \alpha_3) \tag{7.6}$$

and

$$u_1(r) \sim \sin(\eta r + \alpha_1), \tag{7.7}$$

if we limit ourselves to low energies of the emitted pion.

We use the experimental values of Orear [6] for the phase shifts α_3 and α_1 which, for small values of η, are:

$$\alpha_3 = a_3\,\eta \quad \text{with} \quad a_3 = -0.11, \tag{7.8}$$

and

$$\alpha_1 = a_1\,\eta \quad \text{with} \quad a_1 = +0.16. \tag{7.9}$$

The asymptotic expressions for u_3 and u_1 are valid outside the range r_0 of the potential. Inside r_0 we do not know the shape of $u(r)$ except that it should go to zero for $r = 0$ (see fig. 10). However, the volume inside r_0 is small and does not contribute very much to the matrix element, the main part of the electromagnetic interaction being in the region of and outside r_0, so we can use the above expressions (7.6)–(7.9) for u_3 and u_1 in calculating the matrix elements. This conclusion will of course be valid only if the wavefunction $g(r)$ in the initial state has an appreciable tail, so that there is a fair probability for the pion to be found outside r_0. Using as an approximation, (7.6) with (7.8) the derivative of u_3 becomes (for $\eta r \ll 1$)

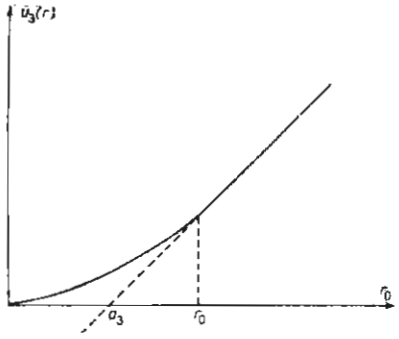

Fig. 10. – Shape of the radial function $u_3(r)$ for small values of r.

$$\frac{\partial}{\partial x}\frac{u_3(r)}{r} = \frac{\partial}{\partial x}\left(\eta + \eta\frac{a_3}{r}\right) = -\eta\frac{a_3}{r^3}x. \tag{7.10}$$

The matrix element (7.4) now becomes (after integrating over the angles)

$$\langle \text{final} \,|\, p_x \,|\, \text{initial}\rangle = \frac{\hbar}{i}\frac{2f}{9\sqrt{L}}\left\{\begin{matrix} a_3 \\ \sqrt{2}\,a_1 \end{matrix}\right\}\eta\int g(r)\,dr. \tag{7.11}$$

The factor $1/\sqrt{L}$ comes from the normalization of the wavefunctions (7.6), (7.7) of the final unbound state, the normalization volume being a sphere of radius L. (*) L, of course, disappears in the final result. The essential feature of (7.11) is that the matrix element is proportional to the phase shifts $a_3\,\eta$ and $a_1\,\eta$ respectively. To get numerical values we must make a guess at the function $g(r)$. It turns out that the result is not very different if we assume various reasonable forms. (E.g., one can take an exponential or a Bessel-function).

From these matrix elements one calculates the cross-section for the transition $p^\gamma \to n^+$. A numerical calculation gives:

$$\sigma(p^\gamma \to n^+) = 1.0\cdot 10^{-27}\cdot f^2\,\eta\left(\frac{a_3 + 2a_1}{3}\right)^2 \text{cm}^2. \tag{7.12}$$

For the probability f^2 that the proton is in a state consisting of a neutron and a pion, ready to be "photo-electric-effected," we can assume unity, an assumption which may be too large by perhaps a factor of 2.

The numerical part of (7.12), $1.0\cdot 10^{-27}$ cm^2 comes from the assumption that the wavefunction $g(r)$ has a range of the order of $\hbar/\mu c$, which gives a cross-section of nuclear dimensions. The remaining part of (7.12) consists of pure numbers since the momentum η is expressed in units of μc and the

(*) The appropriate normalization factor is, in this case, $(2\pi L)^{-1/2}$.

lengths a_3 and a_1 in units of $\hbar/\mu c$. If we introduce the experimental values (7.8), (7.9) for a_1 and a_3 we find

$$\sigma(p^{\nu} \to n^{+}) = 5 \cdot 10^{-30} \cdot \eta \text{ cm}^2. \tag{7.13}$$

This cross-section is much too small, the experimental value being about $150 \cdot 10^{-30}\,\eta$ cm^2, a factor of 30 larger.

Even though the above theoretical argument is very approximate, a drastic modification would be needed to account for a factor of 30. It should however be pointed out that the predicted energy dependence, proportional to the momentum η of the emitted particle, is correct. A more correct procedure would be to apply pseudoscalar meson theory to the problem as first suggested by Wentzel (unpublished). It does not make much difference if the pseudoscalar or pseudovector coupling is used for the calculation. We will for simplicity, assume PV–coupling following Chew.[9] However PS—PV theory is not renormalizable, as PS — PS theory is, and it is therefore frowned upon by the high priests of field theory.

There is a hope, somewhere between $\sim$ 5 and 95 percent, that PS — PS theory is the truth.

Chew takes a highly common sense approach to the problem, and is temporarily satisfied with a partial solution, which does not take into account, for example, relativistic effects. Within its limitations the theory appears to be fairly self-consistent and essentially convergent in the sense that the various terms in the approximation grow smaller as one proceeds with the evaluation.

Chew introduces the simplification that the mass M of the nucleon is very large compared to the pion mass so that the nucleon will remain at rest. This is really a weak point of the theory. The nucleon has then only its spin and its charge as dynamical variables. In addition Chew gives the nucleon a finite size in order to avoid convergence difficulties. The interaction between the nucleon and the surrounding pion field is taken as

$$H_{\text{int}} = \sqrt{4\pi}\,\frac{f}{\mu} \sum_{\lambda=1}^{3} \tau_\lambda \int \rho(\boldsymbol{r})\, \boldsymbol{\sigma} \cdot \nabla \varphi_\lambda \, \mathrm{d}^3 \boldsymbol{r}\,. \tag{7.14}$$

f is a coupling constant. The units are such that $\hbar = c = 1$. The interaction is written in an isotopic spin invariant form. In PV–coupling the interaction is between the spin $\boldsymbol{\sigma}$ of the nucleon and the gradient of the pion fields φ_λ. φ_3 is the neutral meson and φ_1 and φ_2 the charged meson field. The interaction has the form of a scalar product in charge space and is thus invariant.

Since Chew assumes the nucleon to have a finite size the interaction has to be averaged over the volume of the nucleon, using a weight function $\rho(\boldsymbol{r})$, normalized as follows

$$\int \rho(\boldsymbol{r})\, \mathrm{d}^3 \boldsymbol{r} = 1\,. \tag{7.15}$$

(9) G. F. CHEW, « Phys. Rev. », *95*, 1669 (1954).

Actually, for what we are discussing at present, photo-production near the threshold, we could omit the weighting function $\rho(\boldsymbol{r})$ and take a point interaction. For this particular problem, the result is essentially identical. However, we may as well leave it in the form (7.14).

The general idea of this type of explanation, as it was first proposed by Wentzel, is the following. Let us introduce in (7.14) the gauge-transformation, making this expression gauge-invariant when the e.m. field is introduced. This will add two terms, which are very suitable to describe directly the photo-effect. If the field φ had a definite charge, e, the gauge-transformation would consist in writing $(\boldsymbol{\nabla} - ie\mathbf{A})$ instead of $\boldsymbol{\nabla}$.

Now, there is a slight extra complication for the following reason. We have to deal with a field φ with its 3 real components φ_1, φ_2 and φ_3, which correspond to different charge states. In fact, the normal convention is to associate the field φ_3 to π^0. So, for example, in so far the φ_3 part of (7.14) is concerned, $e = 0$, and the transformation for the third component will be just no transformation at all $(\boldsymbol{\nabla} \to \boldsymbol{\nabla})$. There are however complications for φ_1 and φ_2 because φ_1 and φ_2 are not the amplitudes of the plus and minus pion fields, but are linear combinations of the two. In fact, the easy way to remember the rule is the following. Let us consider the spherical harmonics of order 1, since we are describing a system of isotopic spin 1 which behaves in charge space essentially as a spherical harmonic of order 1. They are, apart from a common normalisation factor,

$$(7.16)\qquad \begin{cases} Y_{11} \to \varphi^+ \alpha \dfrac{-\sin\vartheta \cdot \exp[i\varphi]}{\sqrt{2}} & \text{corresponding to } \pi^+, \\ Y_{10} \to \varphi_0 \alpha \cos\vartheta & \text{corresponding to } \pi^0, \\ Y_{1-1} \to \varphi^- \alpha \dfrac{\sin\vartheta \cdot \exp[-i\varphi]}{\sqrt{2}} & \text{corresponding to } \pi^-. \end{cases}$$

These spherical harmonics are respectively proportional to the expressions

$$(7.17)\qquad \frac{-x - iy}{\sqrt{2}} \quad , \quad z \quad , \quad \frac{x - iy}{\sqrt{2}}.$$

The three components φ_1, φ_2 and φ_3 form, essentially, a vector in charge space (not in the true space), like the Pauli operators σ_1, σ_2 and σ_3 of the spin of the nucleon, which also act as the components of a vector. Substituting in (7.17) φ_1, φ_2, φ_3 for x, y, z, we obtain the expressions

$$(7.18)\qquad \begin{cases} \varphi^+ = \dfrac{-\varphi_1 - i\varphi_2}{\sqrt{2}} & \text{corresponding to } \pi^+ \text{ amplitude}, \\ \varphi_0 = \varphi_3 & \text{corresponding to } \pi^0 \text{ amplitude}, \\ \varphi^- = \dfrac{\varphi_1 - i\varphi_2}{\sqrt{2}} & \text{corresponding to } \pi^- \text{ amplitude}. \end{cases}$$

The expressions $\boldsymbol{\nabla}\varphi^{\pm}$ is to be transformed into $(\boldsymbol{\nabla} \mp ie\mathbf{A})\,\varphi^{\pm}$. In (7.14) we have the gradients of φ_1, φ_2, φ_3. When we apply the gauge transformation, extra terms will be added. They are

$$(7.19)\qquad H' = \sqrt{4\pi}\frac{fe}{\mu}\int \boldsymbol{\sigma}\cdot\mathbf{A}\,(\tau_1\,\varphi_2 - \tau_2\,\varphi_1)\,\rho(\boldsymbol{r})\,\mathrm{d}^3\boldsymbol{x}.$$

These extra terms, added in order to satisfy the gauge condition, are precisely the terms which are responsible for the photo-production. Now, this should be fairly evident because, apart from nucleon spins and such things, (7.19) includes essentially the products of the vector **A** and one of the φ (φ_1 or φ_2) that correspond to the charged pion field. We know that in field theory the vector potential or its components are creation or destruction operators of photons. Similarly the operators φ_1, and φ_2 create or destroy a charged pion. In the reaction

$$\mathfrak{N} + \gamma \rightarrow \mathfrak{N} + \pi \tag{7.20}$$

we must destroy a photon (operator A) and create a pion (operator φ_1 or φ_2). Both operators are present in (7.19).

In order to arrive at a quantitative result, we need the matrix element of (7.19) corresponding to this transition. From it the cross-section can easily be computed. The easiest way is to go from the components φ_1 and φ_2, that are not definitely charge components, back to the φ^+ and φ^-, which are operators representing the creation of π^+ and π^-. Let me call, according to the usual notation,

$$\begin{cases} \varphi^+ = \varphi^* \\ \varphi^- = -\varphi . \end{cases} \tag{7.21}$$

Expression (7.19) becomes

$$H' = \sqrt{4\pi}\, i \sqrt{2}\, \frac{fe}{\mu} \int \boldsymbol{\sigma} \cdot \mathbf{A}\, (\tau^* \varphi + \tau \varphi^*)\, \rho\,(r)\, \mathrm{d}^3 \boldsymbol{x}, \tag{7.22}$$

where

$$\begin{cases} \dfrac{\tau_1 + i\tau_2}{2} = -\tau^* & \text{is the operator which transforms } n \text{ to } p, \\ \dfrac{\tau_1 - i\tau_2}{2} = \tau & \text{is the operator which transforms } p \text{ to } n, \\ \varphi^* & \text{is the operator which creates } \pi^+ \text{ and destroys } \pi^-, \\ \varphi & \text{is the operator which creates } \pi^- \text{ and destroys } \pi^+. \end{cases} \tag{7.23}$$

The matrix element for the reaction

$$\gamma + p \rightarrow n + \pi^+ \tag{7.24}$$

is, then, near the threshold

$$\mathrm{ME} = i \sqrt{8\pi}\, \frac{ef}{\mu}\, \sigma_\varepsilon \sqrt{\frac{2\pi}{\nu}}\, \frac{1}{\sqrt{2\omega}} \int \rho\,(r) \exp\,[i\nu x]\, \mathrm{d}^3 \boldsymbol{x}, \tag{7.25}$$

in which

σ_3 is the component of the σ vector in the polarization direction of **A** (ε is a unit vector in this direction);

$e^{i\nu x}$ is the propagation term introduced by the electro-magnetic field; the pion near the threshold (small pion momentum) does not contribute a corresponding propagation factor;

$\sqrt{2\pi}/\sqrt{\nu}$ is the normalization factor of **A**, corresponding to one photon per unit volume; likewise $1/\sqrt{2\omega}$ is a similar normalization factor for the pion; ν and ω are the energies, in appropriate units, of the photon and pion, respectively.

The form factor $\rho(r)$ has, in the most recent version of the Chew's theory, the radius: $\frac{1}{5}\cdot\frac{\hbar}{\mu c}$; on the other hand, $1/\nu$ is, at threshold, about $\hbar/\mu c$ and is therefore much longer than the range of ρ. The integral in (7.25) is therefore ≈ 1.

Equation (7.25) has been obtained on the assumption that the meson wavefunction can be expressed as a plane wave. Actually, the outgoing meson is in an s–state, with $r\psi(r) = u(r) = \sin(kr + \alpha) \cong kr + \alpha \approx kr$. (The term due to the phase shift, $\alpha = ka$, leads to a small correction, essentially that calculated in the preceding approximation, and is therefore neglected in the following). Using this wave function, appropriately normalized in a sphere of radius L, we obtain

$$\langle n^+ | H' | p^\gamma \rangle = \pm i \sqrt{\frac{4\pi}{L}} \frac{ef}{\mu} \frac{k}{\sqrt{\nu\omega}}, \tag{7.26}$$

where the $\pm$ sign corresponds to the nucleon spin antiparallel and parallel, respectively, to the photon polarization vector.

The passage from the matrix element to the cross-section is carried out by the usual formula

$$c\sigma = \frac{2\pi}{\hbar} |ME|^2 \rho_{\text{final}}, \tag{7.27}$$

where the density of final s–states is

$$\rho_{\text{final}} = \frac{L}{\pi\hbar v} = \frac{L}{\pi\beta}. \tag{7.28}$$

Near threshold, putting $\nu = \omega = \mu$, $k/\mu = v = \beta = \eta$, and converting from the $\hbar = c = 1$ to the ordinary CGS system, we obtain

$$\sigma = 8\pi\left(\frac{\hbar}{\mu c}\right)^2\left(\frac{e^2}{\hbar c}\right)\left(\frac{f^2}{\hbar c}\right)\eta \cong 0.15\cdot 10^{-27}\,\eta\ \text{cm}^2. \tag{7.29}$$ (*)

From (7.29) we derive the value of the renormalized coupling constant $f^2/\hbar c \cong 0.04$. This value can be improved upon by making use, instead of (7.29), of a similar expression in which certain nucleon recoil corrections are introduced. According to Bernardini and Goldwasser [10] this new analysis of the data yields

$$f^2/\hbar c = 0.058\ (**).$$

(*) The same cross section could have been obtained by using the plane wave approximation (7.25) for the matrix element, and using for the density of final states (for unit normalization volume)

$$\frac{dN}{dW} = \frac{p^2}{2\pi^2\hbar^3 v}. \tag{7.30}$$ [*Note by* B. T. Feld.]

(10) G. Bernardini and E. L. Goldwasser, « Phys. Rev. », *95*, 857 (1954).

(**) The authors give 0.066 ± 0.008 in ref. (10). [Note by B. J. Feld].

This value coincides with the one adopted by Chew [9] to account for the pion-nucleon scattering properties. It is certainly gratifying that the same value of the coupling constant is adequate to interpret both phenomena.

There is one point, however, on which I am not clear. The constant $f^2/\hbar c$, according to Chew [9], is a "renormalized" coupling constant. It is precisely because of this renormalization that Chew's scattering theory is fairly rapidly convergent. Now it would appear at first sight that a different renormalization should apply for the scattering than for the photo-effect. I do not know of any simple explanation why this, as indicated by the experimental evidence, does not appear to be the case.(*)

8.—Connections between Scattering and Photoproduction.

We want to establish certain formal relations which are useful for the phenomenological treatment of problems on which we have little theoretical information. The method itself has general applicability. We shall discuss the photo-effect as an example.

Thus the reaction we consider is

$$\gamma + \mathfrak{N} \rightarrow \mathfrak{N} + \pi. \tag{8.1}$$

We shall restrict ourselves to such low energies that s– and p–states give a sufficient description of the phenomena. In the following Table VI the possible states for this reaction are catalogued.

TABLE VI.

Possible states involved in photomeson production from nucleons.

a) Initial states				*b*) Final states		
nucleon	photon			nucleon + pion		
I parity		I	parity	state	I	parity
1/2 +	E 1	1	—	$s_{1/2}$	1/2	—
	M 1	1	+	$p_{1/2}$	1/2	+
	E 2	2	+	$p_{3/2}$	3/2	+

The possible transitions are shown in Table VII. We shall restrict ourselves to a set of states with definite values of I , I_z, and parity. Then, for the wave function of each physical state, only the radial part of the wave function will remain to be determined.

(*) It can be shown, however, that in the low energy limit the renormalized coupling constants are indeed the same, cf., G. F. Chew and F. Low, « Phys. Rev. », *101*, 1579 (1956) [*Note by* B. T. Feld].

TABLE VII.

Possible states in photomeson production leading to the emission of s– or p–wave mesons.

photon	state	meson
E 1	$1/2\ -$	$\rightarrow\ s_{1/2}\ -$
M 1	$1/2\ +$	$\rightarrow\ p_{1/2}\ +$
M 1	$3/2\ +$	$\rightarrow\ p_{3/2}\ +$
E 2	$3/2\ +$	$\rightarrow\ p_{3/2}\ +$

We will make use of the channel picture, as described in Blatt and Weisskopf.[11]

Consider a system of particles that may transform into each other on colliding. For example the transformations may be

$$p + \gamma \longleftrightarrow n + \pi^+ \longleftrightarrow p + \pi^0. \tag{8.2}$$

In general

$$A_1 + B_1 \longleftrightarrow A_2 + B_2 \longleftrightarrow A_3 + B_3 \longleftrightarrow \cdots. \tag{8.3}$$

Confining ourselves to states of definite angular momentum and parity we assign a "channel" to each set of two colliding particles. Channel 1 will describe the colliding particles $A_1 + B_1$ channel 2 the particles $A_2 + B_2$, and so forth. These channels may be pictured (see fig. 11) as converging into a "black box" in which we may consider that the reactions take place which change one type of particle into others. We may describe for example a collision between $A_1 + B_1$ as a wave packet heading along channel 1 for the black box. After the collision is completed there will be outgoing wave packets, not only in the original channel 1 but also in the others. (The collision may have changed the nature of the particles to $A_3 + B_3$, for example). What describes the essential properties of the reaction is the ensemble of all "reflection coefficients" including cross reflection from one channel into another.

These coefficients are n^2 in number for a black box with n channels, and may be ordered in the form of a matrix with n rows and n columns.

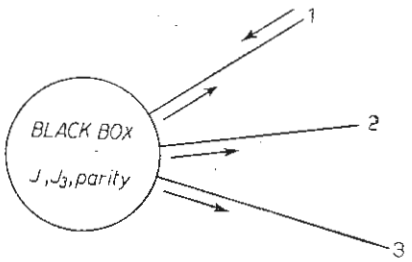

Fig. 11. – Schematic representation of the channels available for the reaction $A_i + B_i \rightleftarrows A_j + B_j$.

(11) J. M. BLATT and V. F. WEISSKOPF, *Theoretical Nuclear Physics* (New York 1952).

The S–matrix is essentially such a matrix. One must, however use a special type of normalization. Instead of normalizing the ingoing or outgoing waves to amplitude one, they are normalized to flux = 1.

For example an ingoing wave on channel λ will be

$$\frac{\exp[-ik_\lambda r_\lambda]}{\sqrt{v_\lambda}} \qquad \text{(units } \hbar = c = 1\text{)}, \tag{8.4}$$

where k_λ and v_λ are the momentum (in c.m.s.) and velocity of the incident particles A_λ at the given energy of the system. This ingoing wave may be reflected with the reflection coefficient $S_{\lambda\mu}$ into the channel μ (particles $A_\mu + B_\mu$). This reflected wave is

$$S_{\lambda\mu}\frac{\exp[ik_\mu r_\mu]}{\sqrt{v_\mu}} \equiv a_{\lambda\mu}\exp[ik_\mu r_\mu]. \tag{8.5}$$

The S–matrix is then

$$S = \begin{vmatrix} S_{11} & S_{12} & S_{13} & \dots \\ S_{21} & S_{22} & S_{23} & \dots \\ \dots & \dots & \dots & \dots \\ \dots & \dots & \dots & \dots \end{vmatrix} \tag{8.6}$$

If the incoming wave had an amplitude 1, the outgoing waves would have the coefficients $a_{\lambda\mu}$. However, for reasons of convenience we do not normalize the waves to amplitude 1, but to $1/\sqrt{v}$. This normalization corresponds to unit flux instead of unit particle density. Thus if we enter with one particle per second through a certain channel, through all channels there will emerge one particle per second.

We then call the S–matrix that matrix which consists of the coefficients $S_{\lambda\mu}$ of the waves, thus normalized. To describe the complete phenomenology of our three possible reactions (8.2) we need an S–matrix with 3 rows and 3 columns.

There are *two* formal properties of the S–matrix which will be quite useful.

(8.7) 1) The S–matrix is a *unitary* matrix. We denote by $\tilde{S}$ the Hermitian conjugate of S, $\tilde{S}_{ik} = S^*_{ki}$. Then this property means the matrix equation $S\tilde{S} = \tilde{S}S = 1$ (identity matrix).

(8.8) 2) Within certain limits, which are valid in a large number of cases, the S–matrix is *symmetric*; that is $S_{ki} = S_{ik}$.

The proof of these theorems can be found in Blatt and Weisskopf, and we will only look at the physical reasons for these properties.

1) We consider again the black box. We may enter this box with a very long but finite wave packet, which at the time $t = 0$ is heading for the box. A certain time after, it has entered the box and will be reflected into the various channels as outgoing packets moving out along the various channels. When the incoming flux is normalized to 1, the sum of the outgoing

fluxes must also be 1. An analysis of this " conservation of flux " property shows that it is expressed mathematically by the fact that the S–matrix is unitary.

2) The symmetry of S has its origin essentially in the property of time reversibility. This enters into the S–matrix in the following manner: we consider an incoming wave in channel 1, and an outgoing wave in channel 2, which have, respectively, the forms $\exp[-ik_1 r_1]/\sqrt{v_1}$ and $\exp[+ik_2 r_2]/\sqrt{v_2}$. Let us restrict ourselves to the case where the Hamiltonian describing the process is real. Then $H\psi = E\psi$, and also $H\psi^* = E\psi^*$. By going from ψ to ψ^* one interchanges ingoing and outgoing waves.

This establishes a relationship between the reflection coefficients $S_{12} = S_{21}$. A complete discussion shows that the relationship is $S_{12} = S_{21}$, which expresses the symmetry of the S–matrix.

Before we are ready to use these properties, I must still say what this matrix is like in the simple case where there is just one channel. What the black box does is to reflect the incoming wave to the outside with unchanged amplitude. So $|S_{11}| = 1$. We can write for the incoming wave $\exp[-ikr]/\sqrt{v}$ and for the outcoming wave $S_{11}\exp[ikr]/\sqrt{v}$.

It is clear that S_{11} has modulus 1 because all that goes in must come out, as there is only one channel. Thus, for S_{11} we can write $\exp[2i\alpha]$, α being a real number.

The overall wave function containing the incoming and outgoing part has the structure $\exp[2i\alpha]\cdot\exp[ikr] + \exp[-ikr]$ (the normalization factor $\sqrt{v}$ is left out for convenience). Dividing by $\exp[i\alpha]$ we obtain $\exp[i(kr+\alpha)] + \exp[-i(kr+\alpha)] = 2\cos(kr+\alpha)$. We call α the phase shift. If α is equal to zero it means that the box acts as an inert thing.

Suppose that we have not one but several channels, for instance three, but that there are no cross links. (The box is divided in black compartments). This is essentially the same thing as before, so we can write

$$S_0 = \begin{vmatrix} \exp[2i\alpha_1] & 0 & 0 \\ 0 & \exp[2i\alpha_2] & 0 \\ 0 & 0 & \exp[2i\alpha_3] \end{vmatrix}, \tag{8.9}$$

$\alpha_1, \alpha_2, \alpha_3$ being the phase shifts which determine the reflection coefficients of each compartment. The zero's indicate that there are no cross links.

Let us assume now that we have 3 channels and that in first approximation we have the same situation as before, i.e. no cross connections between the various channels (photon goes out as photon, π as π, etc.). But, as a second approximation, let us assume that there are weak interconnections between the channels i.e. that the cross reflectivity is there but it is small.

In this case, we may write for the overall matrix

$$S = S_0 + i\varepsilon, \tag{8.10}$$

where S_0 represents the unconnected matrix (8.9), with the phase shifts α_1, α_2, α_3, and where ε contains all the cross links. The elements of ε are small

and their squares shall be neglected. The factor i has been put in for convenience.

Now we shall apply to the overall S–matrix the 2 properties (8.7), (8.8). In doing this we shall neglect the quadratic terms in ε.

The hermitian conjugate of (8.10) is

$$\tilde{S} = \tilde{S}_0 - i\,\tilde{\varepsilon}. \tag{8.11}$$

Applying the unitary property, we obtain

$$1 = S\tilde{S} = S_0\tilde{S}_0 + i\,(\varepsilon\tilde{S}_0 - S_0\,\tilde{\varepsilon}). \tag{8.12}$$

Now, as $S_0\tilde{S}_0 = 1$ it follows

$$\varepsilon\,\tilde{S}_0 = S_0\,\tilde{\varepsilon}, \tag{8.13}$$

where the matrix $\tilde{S}_0$ is given by

$$\tilde{S}_0 = \begin{vmatrix} \exp[-2i\alpha_1] & 0 & 0 \\ 0 & \exp[-2i\alpha_2] & 0 \\ 0 & 0 & \exp[-2i\alpha_3] \end{vmatrix}. \tag{8.14}$$

Remember that the general form of an element (m, n) of the product of 2 matrices A and B is

$$(AB)_{mn} = \sum_l A_{ml}\,B_{ln}. \tag{8.15}$$

In the product $S_0 \cdot \tilde{\varepsilon}$ the first factor is diagonal, which means that we can write,

$$\sum_l A_{ml}\,B_{ln} = A_{mm}\,B_{mn}, \tag{8.16}$$

since only the elements with $l = m$ are different from zero.

So we can write

$$(S_0\,\tilde{\varepsilon})_{mn} = \exp[2i\alpha_m]\cdot\tilde{\varepsilon}_{mn} = \exp[2i\alpha_m]\cdot\varepsilon^*_{nm}, \tag{8.17}$$

$\varepsilon\tilde{S}_0$ has, similarly, the mn element $\varepsilon_{mn}\cdot\exp[-2i\alpha_n]$. We can rewrite the previous identity (8.13) $\exp[2i\alpha_n]\cdot\varepsilon^*_{mn} = \varepsilon_{mn}\cdot\exp[-2i\alpha_n]$. Now we will use the symmetry condition. As S_0 is symmetric, ε must also be symmetric and therefore $\varepsilon_{nm} = \varepsilon_{mn}$.

The above relation now becomes $\exp[2i\alpha_m]\cdot\varepsilon^*_{nm} = \varepsilon_{nm}\cdot\exp[-2i\alpha_n]$.

If we now multiply both sides by $\exp[i(\alpha_n - \alpha_m)]$ we obtain

$$\varepsilon_{mn}\cdot\exp[-i(\alpha_m + \alpha_n)] = (\varepsilon_{mn}\cdot\exp[-i(\alpha_m + \alpha_n)])^*. \tag{8.18}$$

Therefore $\varepsilon_{mn}\cdot\exp[-i(\alpha_m + \alpha_n)]$ is real and we can write

$$\varepsilon_{mn} = \rho_{mn}\exp[i(\alpha_m + \alpha_n)], \tag{8.19}$$

where ρ_{mn} is a real number. This applies generally to the case in which there are weak cross links between the channels (i.e., where most of the phenomenon is straight scattering in each of the channels, with the phase shifts α_1, α_2, α_3 in the various channels).

ε_{mn} represents one of the cross-links, which generally is a complex number. In order to determine it, experimentally or otherwise, we must usually determine two things: the real and the imaginary parts. Our procedure, however, saves us part of this labor: the phase parts being determined by the scattering, we have only to determine the real number ρ_{mn} (which can be positive or negative).

So now we can write schematically the matrix

$$(8.20)\quad S = \begin{vmatrix} \exp[2i\alpha_1] & i\rho_{12}\exp[i(\alpha_1+\alpha_2)] & i\rho_{13}\exp[i(\alpha_1+\alpha_3)] \\ i\rho_{12}\exp[i(\alpha_1+\alpha_2)] & \exp[2i\alpha_2] & i\rho_{23}\exp[i(\alpha_2+\alpha_3)] \\ i\rho_{13}\exp[i(\alpha_1+\alpha_3)] & i\rho_{23}\exp[i(\alpha_2+\alpha_3)] & \exp[2i\alpha_3] \end{vmatrix}$$

or the equivalent

$$S_{mn} = \delta_{mn}\exp[2i\alpha_m] + i\rho_{mn}\exp[i(\alpha_m+\alpha_n)],$$

with

$$(8.21)\qquad \rho_{mn} = \rho_{nm}.$$

Now let us see how this simplification works in the case of the photo-effect. First let us consider the following reactions in the case of very low energy (near the threshold):

$$(8.22)\qquad \begin{cases} p + \gamma \to n + \pi^+, \\ p + \gamma \to p + \pi^0. \end{cases}$$

The reaction $p + \gamma \to p + \pi^0$ is practically absent and only builds up very slowly with energy, which indicates that most of the π^0 effect is in p–wave pion production. We may ask why, in the presence of fairly strong exchange scattering, the internal exchange interaction of the π does not give rise to the second reaction, even if the first process occurs primarily.

First let us see whether any of these formal properties contradicts the experimental result. Let us consider specifically, the s–wave production caused by the electric dipole transition E1 having three channels, p^γ, n^+ and p^0 in a state of $J = 1/2$, $J_z = 1/2$ and odd parity.

We may expect, and this is supported by theory and experiment, that the electromagnetic interactions are weak (the electromagnetic coupling constant is small (1/137) so the cross-section for the photo-effect is of the order of 10^{-4} barns while the scattering cross-sections are of the order of several millibarns). Then we can, as a zero'th approximation, switch off the electromagnetic interaction. In this case, we have for the interaction matrix

$$(8.23)\qquad S_0 = \begin{array}{c} \begin{matrix} p^\gamma & n^+ & p^0 \end{matrix} \\ \begin{vmatrix} 1 & 0 & 0 \\ 0 & X & X \\ 0 & X & X \end{vmatrix} \end{array}.$$

The p^γ channel is not effective as we have switched off the electromagnetic interaction. But even if this is not assumed, the p^γ channel will hardly be important because, as we know, the electromagnetic field is hardly influenced

by the charge of the proton, and the photon scattering is very small. So we can put the phase shift α_γ equal to zero and can write:

$$\exp\,[2\,i\alpha_\gamma] = 1. \tag{8.24}$$

Now, a condition for applying the above formalism is that we have only diagonal elements in S_o. This is not the case for our choice of channels because the exchange scattering between n^+ and p° involves cross links.

In order to avoid this difficulty, we choose our channels not in terms of pure charge states but as linear combinations of them. We shall take as pure states the isotopic spin states corresponding to $3/2$ and $1/2$

$$\begin{cases} \chi_3 = \sqrt{\frac{1}{3}}\,n^+ + \sqrt{\frac{2}{3}}\,p^\circ \\ \chi_1 = -\sqrt{\frac{2}{3}}\,n^+ + \sqrt{\frac{1}{3}}\,p^\circ \end{cases} \tag{8.25}$$

since there are no cross links between these.

We can now write:

$$S_o = \begin{vmatrix} 1 & 0 & 0 \\ 0 & \exp\,[2\,i\alpha_3] & 0 \\ 0 & 0 & \exp\,[2\,i\alpha_1] \end{vmatrix} \tag{8.26}$$

and

$$S = \begin{vmatrix} 1 & i\rho_3 \exp\,[i\alpha_3] & i\rho_1 \exp\,[i\alpha_1] \\ i\rho_3 \exp\,[i\alpha_3] & \exp\,[2\,i\alpha_3] & X \\ i\rho_1 \exp\,[i\alpha_1] & X & \exp\,[2\,i\alpha_1] \end{vmatrix} \tag{8.27}$$

We are not interested in the off-diagonal scattering elements.

Now we can go back to the physical states. The charge state that is produced in the photo-effect is described by

$$i\rho_3 \exp\,[i\alpha_3]\left(\sqrt{\frac{1}{3}}\,n^+ + \sqrt{\frac{2}{3}}\,p^\circ\right) + i\rho_1 \exp\,[i\alpha_1]\left(-\sqrt{\frac{2}{3}}\,n^+ + \sqrt{\frac{1}{3}}\,p^\circ\right).$$

If we pick out the coefficients of the physical states, and get rid of the factor i, we obtain:

$$n^+\left(\sqrt{\frac{1}{3}}\,\rho_3 \exp\,[i\alpha_3] - \sqrt{\frac{2}{3}}\,\rho_1 \exp\,[i\alpha_1]\right) + p^\circ\left(\sqrt{\frac{2}{3}}\,\rho_3 \exp\,[i\alpha_3] + \sqrt{\frac{1}{3}}\,\rho_1 \exp\,[i\alpha_1]\right).$$

Now we are faced with the experimental fact that the coefficient of (n^+) is large and that of (p°) is small, or at least not measurable.

If we first put the phase shifts equal to zero, it follows that $\sqrt{\frac{1}{3}}\,\rho_3 - \sqrt{\frac{2}{3}}\,\rho_1$ is large and $\sqrt{\frac{2}{3}}\,\rho_3 + \sqrt{\frac{1}{3}}\,\rho_1$ is very small.

Our formalism therefore leads to no contradiction; it only tells us that ρ_3 and ρ_1 have opposite signs and that $\sqrt{2}\,\rho_3 \approx -\rho_1$. It would, however, be a real contradiction if the coefficient of (p^0) were exactly zero. In fact since the two complex vectors have different phase shifts, they will give us a residual vector different from 0, as shown in fig. 12.

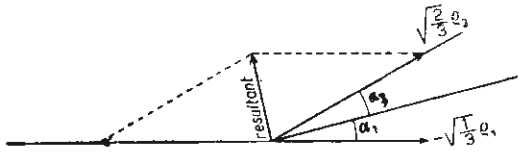

Fig. 12. – Diagram illustrating the effective cancellation of amplitudes giving rise to the small value of the p^0 electric dipole photoproduction.

If α_3 and α_1 are small, one obtains the following result for the ratio of the two cross-sections:

$$\frac{\sigma(\to p^0)}{\sigma(\to n^+)} \geqslant \frac{2}{9}(\alpha_1 - \alpha_3)^2 . \tag{8.28}$$

In others words, there is some justification for the assumption of an internal exchange scattering. So, if the two scattering cross-sections are known (we refer only to the s–wave part) and if $\alpha_1 \neq \alpha_3$ (as we know, they are unequal and of opposite sign) then there exists a minimum value of the cross-section for the p^0 process.

Near the threshold, $\alpha_3 - \alpha_1$ is approximately $10^\circ\,\eta$, which corresponds to $\sim 2 \cdot 10^{-1}\,\eta$ in radians. Thus the ratio of the cross-sections is

$$\frac{\sigma(\to p^0)}{\sigma(\to n^+)} \geq 10^{-2}\,\eta^2. \tag{8.29}$$

This value is too small and would not be observable at present.

There is another point. We know that near the threshold the phase shifts are proportional to the momentum and therefore $(\alpha_1 - \alpha_3)^2 \sim \eta^2$. But also the cross-section $\sigma(\to n^+) \sim \eta$, from which follows

$$\sigma(\to p^0) \geq c\eta^3. \tag{8.30}$$

This energy dependence is like the one for p–wave photomeson production and makes it extremely hard to distinguish experimentally a small s–wave contribution (*).

9.—Meson Production in Nucleon-Nucleon Collisions.

We consider the reaction

$$2\mathfrak{N} \rightleftarrows 2\mathfrak{N} + \pi . \tag{9.1}$$

Experimentally, it has been observed in considerable detail up to a bombarding energy of the incident nucleon of approx. 450 Mev. For this bombard-

(*) The presence of this small s–wave photoproduction has been detected by the observation of a small asymmetry ($\cos\theta$ term) in the angular distribution of the p^0 reaction, arising from interference between the s–wave and the dominant p–wave production [Y. Goldschmidt-Clermont, L. S. Osborne and M. Scott, « Phys. Rev. », 97, 188 (1955)] [*Note by* B. T. Feld].

ing energy, the pion energy is about 70 Mev in the centre of mass system. This energy is small compared to μc^2 and, consequently, we can apply some simplifications which are valid only near the threshold. The reaction takes a variety of forms:

(9.2) $$p + p \begin{cases} \nearrow p + p + \pi^0 \\ \searrow \underset{(d)}{p + n} + \pi^+ \end{cases}$$

(9.3) $$n + p \begin{cases} \nearrow p + p + \pi^- \\ \longrightarrow \underset{(d)}{p + n} + \pi^0 \\ \searrow n + n + \pi^+ \end{cases}$$

(9.4) $$n + n \begin{cases} \nearrow n + n + \pi^0 \\ \searrow \underset{(d)}{p + n} + \pi^-. \end{cases}$$

The symbol (d) indicates that the proton and the neutron, after the reaction, may be bound as a deuteron. Not all of these reactions have been observed. In particular, experiments on the processes (9.4) cannot be carried out directly, and have been performed using the loosely bound neutron of deuterium. However, the information obtained is not abundant and we may just as well disregard these processes. Actually reactions (9.2) and (9.4) are charge symmetric and we have good reason for expecting that these reactions will have essentially the same features.

In attempting to put some order into the rather abundant but still quite incomplete experimental material concerning the reactions (9.2) and (9.3), one may take isotopic spin conservation as the main guiding principle.

We observe that in the initial state we have 2 nucleons, which can form states with total I-spins T = 1 or 0. So we have, for the initial state, essentially 2 possibilities. In the case T = 1, depending on the orientation of the I.S. vector in charge space, the actual physical state may be pp, nn, or pn: the principle, however, is that the orientation of the I.S. vector in charge space is immaterial and the properties of the processes are controlled by the values of the vector and not by the values of its 3-rd component.

In the final state, the system consists of a pion, with T = 1, and 2 nucleons, of which the resultant total I.S., $T_{\pi 2\mathfrak{N}}$, may again be 1 or 0. The resultant I.S. of the 3 particle system, $\pi + 2\mathfrak{N}$, must be equal to the initial I.S. This suggests a classification of the possible processes by means of 2 indices, which represent the I.S. of the initial state (T = 0 or 1) and the I.S. of the 2 nucleons in the final state. So we would expect the possible combinations shown in Table VIII.

(For example, 01 indicates the reaction that occurs when 2 nucleons collide in the initial state in the combination T = 0 and in the final state the 2 nucleons form a system with T = 1, which is combined with the T = 1 of the π to give the resultant zero).

TABLE VIII.

Classification of the isotopic spin states of the two nucleons

$$\mathfrak{N} + \mathfrak{N} \to \mathfrak{N} + \mathfrak{N} + \pi.$$

Initial T	Final $T_{2\mathfrak{N}}$	Classification
1	1	11
1	0	10
0	1	01
(0)	(0)	(00)

The hypothesis of I.S. conservation evidently excludes the $T = 0$, $T_{2\mathfrak{N}} = 0$ combination. So the possibilities are reduced to 3. An important experimental question is to see whether, in fact, the variety of physical reactions can really be reduced to 3 by these considerations. This analysis has been performed by Rosenfeld.[12] In the following discussion I shall make use of these results. Let us introduce the following notation: we indicate with A_1, A_0, A_{-1} the charge states of the system of 2 nucleons having total I.S. = 1 and with B the only charge state corresponding to total I.S. = 0. We have

$$(9.5)\qquad \begin{cases} A_1 = pp \\ A_{-1} = nn \\ A_0 = \dfrac{pn + np}{\sqrt{2}} \quad \text{(symmetric combination)} \\ B = \dfrac{pn - np}{\sqrt{2}} \quad \text{(antisymmetric combination).} \end{cases}$$

Suppose e.g. that we start with a B state ($T = 0$). If we look at Table VIII, if $T = 0$ the final state must be $T_{2\mathfrak{N}} = 1$; so after the collision has taken place, the state will go into a state containing 2 nucleons in an A state and a pion, which has total I.S. = 1. We represent this final state with $(A\pi)_0$, where the subscript zero indicates that the total I.S. is zero.

So we write

$$(9.6)\qquad \begin{cases} B \to \Gamma_{01}\,(A\pi)_0 \\ A \to \Gamma_{10}\,(B\pi)_1 + \Gamma_{11}\,(A\pi)_1, \end{cases}$$

where Γ_{01}, Γ_{11}, Γ_{10} are the transition amplitudes which control the intensity of the processes. (In the second equation (9.6) we have 2 terms because the 2 nucleons in the final state may have I.S. = 0 or 1).

(12) A. H. ROSENFELD, «Phys. Rev.», *96*, 139 (1954).

In this manner the phenomenon is described in terms of the 3 transition amplitudes Γ_{01}, Γ_{11}, Γ_{10}. Using the standard rules for angular momentum vector combination, we have

$$(A\pi)_0 = \frac{1}{\sqrt{3}}(A_1\,\pi^- + A_{-1}\,\pi^+ - A_0\,\pi^0)$$

$$(9.7)\qquad (A\pi)_1 = \begin{cases} \frac{1}{\sqrt{2}}(A_1\,\pi^0 - A_0\,\pi^+) & T_3 = +1 \\ \frac{1}{\sqrt{2}}(A_1\,\pi^- - A_{-1}\,\pi^+) & T_3 = 0 \\ \frac{1}{\sqrt{2}}(A_0\,\pi^- - A_{-1}\,\pi^0) & T_3 = -1 \end{cases}$$

$$(B\pi)_1 = \begin{cases} B\pi^+ & T_3 = +1 \\ B\pi^0 & T_3 = 0 \\ B\pi^- & T_3 = -1 \end{cases}$$

where A_1, A_{-1}, A_0 may be expressed in terms of the physical states by use of (9.5). For example, let us consider an initial state with 2 protons ($T = 1$, $T_3 = 1$). According to (9.6) and (9.7) we have

$$(9.8)\qquad (pp) \to \Gamma_{10}(B\pi^+) + \Gamma_{11}\left(\frac{A_1\,\pi^0 - A_0\,\pi^+}{\sqrt{2}}\right).$$

The Γ coefficients are, in general, functions of the initial energy, the energy of the pion and its angle of emission. Eq. (9.8) may be written, by use of (9.5),

$$(9.9)\qquad (pp) \to \left(\frac{\Gamma_{10}}{\sqrt{2}} - \frac{\Gamma_{11}}{2}\right)(pn+) - \left(\frac{\Gamma_{10}}{\sqrt{2}} + \frac{\Gamma_{11}}{2}\right)(np+) + \frac{\Gamma_{11}}{\sqrt{2}}(pp\,0).$$

In both the cases $(pn+)$ and $(np+)$, there is a proton, a neutron and a π^+, but in the first case the proton comes first. There is actually a distinction between these 2 states, that depends on which we call the first and which the second nucleon. We shall call the first nucleon that one whose momentum in the c.m.s. (fig. 13) has the projection of largest magnitude on the direction of the pion momentum.

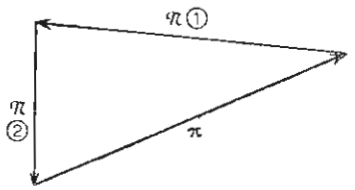

Fig. 13. – Diagram illustrating the method of classifying two identical nucleons in the reaction $\mathfrak{N} + \mathfrak{N} \to \mathfrak{N} + \mathfrak{N} + \pi$.

As long as we are interested in the cross-section integrated over all angles, the distinction between first and second nucleon has no meaning. Using the expression (9.9) we obtain, when we do not distinguish between $(pn+)$ and $(np+)$ states:

$$\sigma(pp) = \sigma(pp \to pp\,0) + \sigma(pp \to pn+)$$

with

$$(9.10)\qquad \begin{cases} \sigma(pp \to pp\,0) = \frac{1}{2}\int |\Gamma_{11}|^2\,dx \\ \sigma(pp \to pn+) = \int |\Gamma_{10}|^2\,dx + \frac{1}{2}\int |\Gamma_{11}|^2\,dx, \end{cases}$$

where the integration variable x summarizes all angular, energy, and other appropriate variables. We can, in a quite similar way, analyze all the other processes and express all the cross-sections in terms of the 3 following cross-sections:

$$(9.11)\qquad \begin{cases} \sigma_{11} = \frac{1}{2}\int |\,\Gamma_{11}\,|^2\,dx \\ \sigma_{10} = \int |\,\Gamma_{10}\,|^2\,dx \\ \sigma_{01} = \frac{1}{3}\int |\,\Gamma_{01}\,|^2\,dx\,. \end{cases}$$

One finds

$$(9.12)\qquad \begin{cases} \sigma\,(pp \to pp\,0) = \sigma_{11} \\ \sigma\,(pp \to pn\,+) = \sigma_{10} + \sigma_{11} \\ \sigma\,(np \to pp\,-) = \frac{1}{2}(\sigma_{01} + \sigma_{11}) \\ \sigma\,(np \to np\,0) = \frac{1}{2}(\sigma_{01} + \sigma_{10}) \\ \sigma\,(np \to nn\,+) = \frac{1}{2}(\sigma_{01} + \sigma_{11}) \end{cases}$$

where σ is, in general, a function of the energies

$$(9.13)\qquad \sigma = \sigma\,(E_{in}\,,\,E_{\pi}).$$

In the two reactions

$$pp \to pn\,+$$
$$np \to np\,0$$

there is a considerable probability (of the order of 50 percent) that the two nucleons come out bound as a deuteron. In these cases, the cross-sections are expressed by

$$(9.14)\qquad \begin{cases} \sigma\,(pp \to d\,+) = \sigma_{10}\,(d) \\ \sigma\,(np \to d\,0) = \frac{1}{2}\sigma_{10}(d) \end{cases}$$

(the simpler expressions are due to the fact that the deuteron has $T = 0$). $\sigma\,(d)$ is a function of the initial energy only, since we are dealing with a 2–body reaction.

We have a considerable amount of experimental information on various of these processes at various energies. Following Rosenfeld's work,[12] we will try to determine from the experimental data the values of σ_{11}, σ_{10} and σ_{01} as function of the parameters upon which they depend. If we measure the π^0–production in pp collisions we obtain directly σ_{11}; also $\sigma_{10}\,(d)$ appears isolated in reactions (9.14).

The experimental data on the reaction $pp \to d\pi^+$ are rather complete. Some of them are obtained from the direct, some from the inverse reaction.

The information on the other reactions is, on the other hand, rather meager.

Let us consider now in detail the angular momenta for the three processes 11 , 10 , 01. In Table IX are listed the possible angular momentum states compatible with the Pauli principle for two nucleons in a T = 0 or a T = 1 state.

TABLE IX.

Angular momentum states permitted by the Pauli principle for two nucleons in the two possible isotopic spin states.

T = 0	T = 1
$^3S_1$	$^1S_0$
$^1P_1$	$^3P_{0,1,2}$
$^3D_{1,2,3}$	$^1D_2$
$^1F_3$	$^3F_{2,3,4}$

The subscripts are the values of J. Let us consider first the process 10, on which the experimental information is most abundant; the possible final states of the two nucleons are shown in the left hand column of Table IX. For instance, we can have the 2 nucleons in the state $^3S_1$. In addition, we have a pion in the final state. For this we specify the angular momentum (s , p , d , $\cdots$) with respect to the c.m. system.

We indicate, for example, by the symbol ($^3S_1 p$) a final state in which the 2 nucleons are in a $^3S_1$ state and the pion in a p–orbit.

In Table X we have collected the most important initial and final states for the (1 , 0) process.

TABLE X.

Angular momentum states possible in the reaction $\mathfrak{N} + \mathfrak{N} \rightarrow \mathfrak{N} + \mathfrak{N} + \pi$, *in which the nucleons are initially in the* T = 1 *state and finally in the* T = 0 *state.*

Process	Initial state	Final state	I parity
(1 , 0)	$^3P_1$	($^3S_1$, s)	1 —
	$^1S_0$	($^3S_1$, p)	0 +
	$^1D_2$	($^3S_1$, p)	2 +

In constructing this Table we have listed only the final state of the types (Ss) and (Sp). Higher angular momenta of the pion are improbable at low energy. The nucleons, in addition, are very probably emitted in an S–state

because of the large enhancement of this state due to nucleon-nucleon forces. Observe that in Table X, the $({}^3S_1 p)$ final state with J = 1 is missing. The reason is that no initial state with T = 1 has the required angular momentum and parity.

TABLE XI.

Summary of the isotopic spin states involved in the various reactions leading to pion production by nucleon-nucleon collision.

Reaction	Coefficient of		
	σ_{01}	σ_{10}	σ_{11}
$pp \to pp\,0$	0	0	1
$\to np\,+$	0	1	1
$\to d\,+$	0	1	0
$np \to pp\,-$	1/2	0	1/2
$\to np\,0$	1/2	1/2	0
$\to d\,0$	0	1/2	0
$\to nn\,+$	1/2	0	1/2

We have previously found that the cross-sections, for the various processes of pion production considered, may be written as linear combinations of the quantities σ_{01}, σ_{10}, σ_{11}, which are functions of the initial energy of the two nucleons and of the energy of emission of the pion. The coefficients in the combination of these σ's for the various processes of interest are summarized in Table XI.

Consider, now, the experimental data on these various reactions. Except in the two cases in which a deuteron is produced in the final state, the pion emerges with a continuous spectrum of energies.

In fig. 14, taken from the quoted paper of Rosenfeld,[12] are presented curves consistent with the observed cross-sections for the various processes plotted against the maximum value of the pion momentum in the c.m.s. in μc units. (This momentum is denoted by η). These curves are based on the following considerations:

a) The experimental cross-sections for the reaction $pp \to d\,+$ agree quite well with an expression of the form $0.14\,\eta + 1.0\,\eta^3$. This formula has a semi-theoretical justification, which we shall consider later. From the table one can see that the cross-section involves only the term σ_{10}, and we indicate this by $\sigma_{10}\,(d)$ to remind us that it arises in the reaction in which a deuteron occurs in the final state.

b) Another experimental cross-section measured is that for $pp \to np\,+$, in which the neutron and proton emerge unbound. Experimentally it is

often easier to detect just the emergent pion, without knowing whether the nucleons remain bound or unbound. The curve of $\sigma_{\tau 0}$ in fig. 14 represents the sum of the two cross-sections $pp \to pn +$ and $pp \to d +$. The intensities of the two processes are roughly comparable.

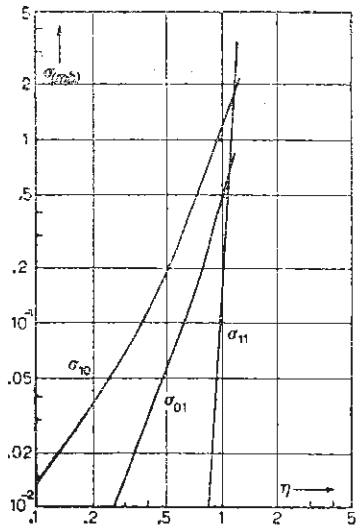

Fig. 14. – Cross-sections for the three fundamental reactions which govern pion production in nucleon-nucleon collisions, plotted against the maximum c.m.s. momentum of the pion.

c) At present there are only two experimental points known for σ_{11} (η), the cross-section for $pp \to pp\,0$. In the absence of further information, the best we can do to describe the excitation function is to join the two points (at 350 Mev and 450 Mev) by a straight line on our log — log graph. The equation for this line is $\sigma_{11} \cong 0.2\,\eta^8$.

d) We now discuss briefly the experimental techniques for studyingthe neutron-proton collision reactions, from which one obtains σ_{01}. A beam of neutrons may be obtained from the proton beam in an accelerator by charge exchange scattering in a suitable target, e.g. beryllium. The neutrons are not monochromatic and the spectrum of the emergent neutrons is about like the one plotted in fig. 15.

Essentially, two techniques have been used in the experiments we are considering. These are due to i) Yodh (unpublished), ii) Wright and Schluter.[13]

i) The Yodh technique has been used in studying the two np reactions in which positive and negative pions emerge. A liquid hydrogen target is

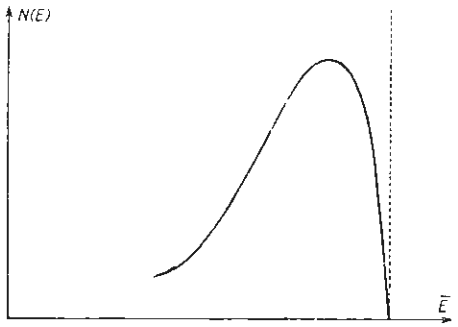

Fig. 15. – Neutron spectrum from the bombardment of a beryllium target by monoenergetic, high energy protons.

used and photographic plates are suitably positioned to record the pion tracks, as shown in fig. 16. In this manner the total cross-section and angular

(13) R. A. SCHLUTER, « Phys. Rev. », *95*, 639 (A) (1954).

distribution can be studied, for the reactions

$$np \nearrow pp -$$
$$\searrow nn +.$$

ii) Wright and Schluter have used, instead, a hydrogen filled diffusion cloud chamber operating at a pressure of 30 atmospheres in conjuction with a magnetic field. With the neutron beam, one can use a high flux of primary neutrons since they are not detected in the chamber unless they

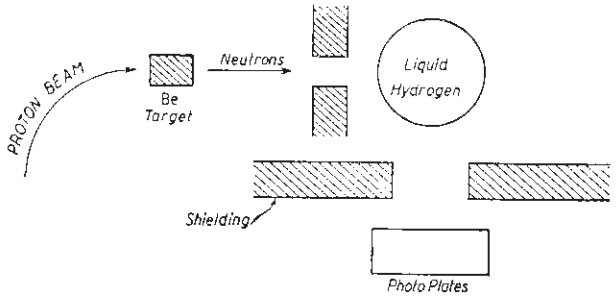

Fig. 16. – Method of Yodh for observing the pions produced in n–p collisions.

interact. Most of the events observed are neutron-proton scatterings and these are used to calibrate the primary neutrons both as to intensity and energy spectrum. The collimation in this experiment is extremely good, since the target and chamber can be separated by about ten metres, so that angular measurements can be carried out very accurately. By using a rather low pulse rate (~one every half-minute) to avoid local depletions of alcohol vapour, and strict temperature control, these workers have found it possible to distinguish between proton and deuteron tracks unambiguously on the basis of track density and curvature (see fig. 17). In this manner they separated the neutron-proton scattering events from some 100 cases corresponding to the reaction $n + p \to d + \pi^0$, and so derived the cross-section for this process.

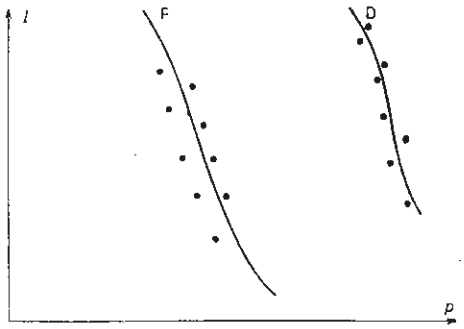

Fig. 17. – Plot of ionization vs. momentum for the tracks observed in a hydrogen-filled diffusion chamber bombardment by fast neutrons (in the experiment of Wright and Schluter).

This cross-section is given in Table XI as $\frac{1}{2}\sigma_{10}$. According to the theory therefore one should have

$$2\sigma(np \to d\,0) = \sigma(pp \to d\,+). \tag{9.15}$$

This was actually found to be the case.

In the same set of pictures, Wright and Schluter have many cases of the reactions $np \to pp -$ and $np \to nn +$. The first of these is very

easily recognized as a three prong event. A peculiarity of the reaction $np \to pp -$ is the angular asymmetry of the pion emission. In the c.m.s., the negative pions are emitted preferentially in the direction of the original neutron. The positive pions, instead, are more abundant in the opposite direction.

The cross-section σ_{01} has been measured at one energy only (average bombarding energy ~ 400 Mev). From Table XI, it follows that

$$\sigma(np \to nn +) + \sigma(np \to pp -) - \sigma(pp \to pp\,0) = \sigma_{01}. \tag{9.16}$$

It is expected that the excitation function for σ_{01} should be $\sim \eta^4$. On the basis of a single experimental point the coefficient of η^4 is about 0.5 mb.

We summarize the approximate values and energy dependences of the three basic processes:

$$\begin{cases} \sigma_{10} = \begin{cases} d \;\; ; \;\; 0.14\,\eta + 1.0\,\eta^3 \\ np \;\; ; \;\; 1.0\,\eta^4 \end{cases} \\ \sigma_{01} = 0.5\,\eta^4 \\ \sigma_{11} = 0.2\,\eta^8. \end{cases} \tag{9.17}$$

The dependences of the above cross-sections on η are in qualitative agreement, as far as the present experimental information goes, with the theoretical scheme of Brueckner, Serber and Watson [14] who stress the consequences of the hypothesis that pions are normally emitted into p-states. Consider the basic Yukawa reaction,

$$\mathfrak{N} \rightleftarrows \mathfrak{N} + \pi, \tag{9.18}$$

and assume that the nucleon, owing to its large mass, is effectively at rest. The angular momentum and parity of the state represented on the left hand side of (9.18) is $1/2\,+$). Because the pion is a pseudoscalar, the parity of the right hand state is $(-1)^{l+1}$. The pion, therefore, must be emitted into a state of odd l in order to conserve parity. The angular momentum $J = 1/2$ can then be obtained *only* with $l = 1$, which combines with the spin $1/2$ of the final nucleon to give a resultant spin of $1/2$.

The conclusion is, therefore, that a nucleon at rest emits pions in p-states only. The extension of this conclusion to pions emitted in the collision of two nucleons is not necessarily correct. The two nucleons in some of the intermediate states of the process may have large relative velocity, in which case the above argument breaks down. Moreover virtual formation of nucleon-antinucleon pairs may also play a role, and when this is the case pions may be emitted preferentially into s- rather than p-states.

It appears, however, that the preferential emission of pions into p-states is fairly well supported by experiment, at least at energies not too far from the threshold for pion production.

(14) K. BRUECKNER, R. SERBER, and K. WATSON, « Phys. Rev. », *84*, 258 (1951).

The energy dependence near the threshold of the excitation function for a reaction in which n particles are produced is controlled by the energy dependence of the transition matrix element and by the statistical weight of the final state. The statistical weight S near the threshold is

$$S = \text{const} \cdot p^{3n-5}, \tag{9.19}$$

where p is the maximum momentum of the emitted particles at the given energy. This result can be obtained by observing that S is dimesionally proportional to the ratio between the volume V_p in momentum space and the energy E. For n independent particles the momentum space has $3n$ dimensions. Because of the conservation of the center of mass, however, only the momenta of $n - 1$ particles can be assigned arbitrarily and the dimensions of V_p are therefore reduced to $3(n - 1)$.

Therefore

$$V_p \propto p^{3n-3}. \tag{9.20}$$

Also near the threshold where the emitted particles are non relativistic,

$$E \propto p^2. \tag{9.21}$$

Thus

$$S \propto V_p/E \propto p^{3n-5}. \tag{9.22}$$

If all particles were emitted into s–states, the matrix element near the threshold would be approximately energy independent and the reaction cross-section would be proportional to (9.19)

$$\sigma \propto p^{3n-5} \qquad (s\text{–states only}). \tag{9.23}$$

If particles are emitted preferentially into p–states, however, additional powers of p appear. The matrix element in this case is proportional to p^q where q is the number of particles emitted in p states.

In this case, then, (9.22) must be multiplied by the extra factor p^{2q}, since the cross-section is proportional to the square of the matrix element. We thus have

$$\sigma \propto \eta^{2q+3n-5} \qquad (q \text{ particles in } p\text{–states}). \tag{9.24}$$

We apply this formula to the reaction $\sigma_{10}(d)$ in which two particles, d and π, are produced. According to (9.24), the excitation function should be proportional to η or to η^3, depending on whether the pion is emitted into an s- or a p–state. Actually in (9.17) this reaction has been represented by two terms, of which the first corresponds to s–wave pion emission and the second (which is usually the largest) to p–wave pion emission.

The reaction $\sigma_{10}(np)$ and σ_{01} have a different energy dependence. For three particles, of which only one (the pion) is in a p–state, we would expect, according to (9.24) $\sigma \propto \eta^6$. But the two nucleons are not completely free, because they tend to have very low relative energy. This is due to the nucleon forces which tend to form a quasi bound, " virtual state " of two nucleons. If this were completely true and the two nucleons were in a bound state, we would expect a two particle reaction, with energy dependence η^3. In fact,

the situation is intermediate and an empirical interpolation between the two extremes, η^3 and η^6, yield approximately $\sigma \propto \eta^4$.

The steep excitation function of the σ_{11} process will be discussed later.

Let us consider the reaction

$$2p \to d + \pi^+ \tag{9.25}$$

in greater detail. Its cross-section is given by (9.17)

$$\sigma(pp \to d + \pi^+) = 0.14\,\eta + 1.0\,\eta^3 \text{ mb.}$$

which fits very smoothly the experimental data. The first term corresponds to the pion going into an s–state and the second, into a p–state. In the range of energy where there is experimental information, the main contribution is from the second term, the first one giving rise to a small deviation from the second. For this reason a fit to the experimental data does not give a reliable value of the coefficient of η. The adopted value 0.14 has been obtained by Rosenfeld [12] using a procedure introduced years ago by Brueckner, Serber and Watson,[15] in the interpretation of an experiment by Panofsky.[16]

In the Panofsky experiment a π^- stops in deuterium gas and attaches itself to a deuteron, forming a mesic atom; the meson has time enough to fall into the K orbit of the system. We have a system containing a d and a π^- at very low energy (slightly negative). According to Panofsky, two reactions occur

$$d + \pi^- \nearrow 2n \tag{9.26}$$

$$\searrow 2n + \gamma. \tag{9.27}$$

Panofsky's conclusion is that in 70 percent of the cases the first reaction takes place and in 30 percent of the cases, the second.

The inverse of the first reaction

$$2n \to d + \pi^- \tag{9.28}$$

is the charge symmetric twin of the reaction $2p \to d +$. We may expect, from general principles, that the intensities of these two reactions are comparable. From the rate of transition in the first branch (9.26) we could compute the cross-section for the inverse reaction by detailed balancing, and this would give the cross-section for the very similar reaction (9.25). In the Panofsky experiment, however, the two reactions (9.26) and (9.27) are too fast (of the order of 10^{-14} s) so that are we not able to determine their rates, but only the ratio of the two rates. We will try to estimate the rate of (9.27) and to deduce from it, and the known branching ratio between (9.26) and (9.27), a value for the rate of (9.26). We use the fact that the deuteron is a very loosely bound system of a proton and a neutron and instead of computing the rate of (9.27), we will compute the rate of

$$(p + n) + \pi^- \to 2n + \gamma, \tag{9.29}$$

(15) K. BRUECKNER, R. SERBER, and K. WATSON, « Phys. Rev. », *81*, 575 (1951).
(16) W. K. H. PANOFSKY, R. L. AAMODT, and J. HADLEY, « Phys. Rev. », *81*, 565 (1951).

which is closely related to

$$p + \pi^- \rightarrow n + \gamma. \tag{9.30}$$

(The extra neutron plays only a relatively minor role). An estimate of the ratio in the rates of (9.29) and (9.30) has been given by Brueckenr, Serber and Watson,[15] who find that it is $2/3$.

The reaction (9.30) is the inverse of the photo-effect $n + \gamma \rightarrow p + \pi^-$, which is related to $p + \gamma \rightarrow n + \pi^+$ by a factor of about 1.5; the last reaction was measured near the threshold by Bernardini and Goldwasser.[10] We have thus, all the information that is needed in order to compute the cross-section of (9.25) near the threshold. By carrying out the calculation one finds the term $0.14\,\eta$ millibarns of (9.17).

TABLE XII.

Angular distributions in the reaction $\mathfrak{D} + \mathfrak{D} \rightarrow d + \pi$ *on the assumption of s– and p–wave pion emission only.*

Initial		Final	Ang. distribution
$^3P_1$	$\rightarrow$	$(^3S_1, s)_{1-}$	isotropic
$^1S_0$	$\rightarrow$	$(^3S_1, p)_{0+}$	isotropic
$^1D_2$	$\rightarrow$	$(^3S_1, p)_{2+}$	$\frac{1}{3} + \cos^2\theta$

We consider, now, the angular distribution of the reaction (9.25). If we make the assumption that the π can be emitted in an s– or a p–state, we have only the three possibilities shown in Table XII.

The angular distributions given in the last column correspond to the case that only one value of the angular momentum contributes to the reaction. Otherwise, interference of different angular momentum states may take place.

The angular distribution in the first row of Table XII is isotropic because the π is emitted in an s–state. Also, in the second row we have an isotropic distribution because the state in question has $J = 0$.

In the third row of the table the angular distribution is $\frac{1}{3} + \cos^2\theta$, as may be seen by the following argument. The initial state $^1D_2$ is a state with $J = 2$ and no spin. The z–component of the angular momentum is equal to zero, as is found by expanding in spherical harmonics the plane wave e^{ikz}. Then, the final state must also have $J = 2$ and $m = 0$. The angular momentum of this state is the resultant of the deuteron spin $S = 1$ and the orbital angular momentum 1 of the pion emitted as a p–wave. From Condon and Shortley [8] one finds that the appropriate linear combination of spin function $S = 1$ and spherical harmonic $L = 1$ to give $J = 2$, $m = 0$, is

$$s_{+1} L_{-1} + s_{-1} L_{+1} + 2 s_0 L_0$$

where

$$(9.31)\quad L_{+1} = Y_{11} \propto -\frac{\sin\theta e^{i\varphi}}{\sqrt{2}}\ ,\ L_0 = Y_{10} \propto \cos\theta\ ,\ L_{-1} = Y_{1,-1} \propto \frac{\sin\theta e^{-i\varphi}}{\sqrt{2}}\ .$$

The angular distribution is given by the sum of the square moduli of the coefficients of the three spin functions and is therefore proportional to

$$2\cdot\frac{\sin^2\theta}{2} + 4\cos^2\theta = 1 + 3\cos^2\theta \propto \frac{1}{3} + \cos^2\theta\ .$$

If all the three states of Table XII contribute to the reaction, the angular distribution expected is not simply the sum of the three distributions, because of interference. We observe that the initial state $^3P_1$, does not interfere with the other two states in the table, which are singlet states ($^1S_0$ and $^1D_2$). These two are however capable of interfering. One finds that the interference of these two states results in the angular distribution of the pion of the form

$$(9.32)\quad \frac{d\sigma}{d\Omega} \propto A + \cos^2\theta\ ,$$

with

$$(9.33)\quad A = \frac{1 - 2\varepsilon_1 + \varepsilon_1^2 + \varepsilon_2^2}{3 + 6\varepsilon_1}\ ,$$

where $\varepsilon = \varepsilon_1 + i\varepsilon_2$ is the ratio of the (complex) transition amplitudes of the second and third processes of Table XII. To $A + \cos^2\theta$ we add the isotropic intensity B due to the first process of the table and we obtain the final angular distribution

$$(9.34)\quad \frac{d\sigma}{d\Omega} \propto C + \cos^2\theta \quad \text{where} \quad C = A + B\ .$$

One can measure C at various energies and plot C vs. the pion momentum η. One obtains a plot in which the points scatter widely because of the large experimental error. The points indicate, however, that at most energies C is not far from 1/3. This suggests that the third process of Table XII is strongly dominant. Following Rosenfeld,[12] one might attempt to separate the contributions to the total intensity of the three processes of Table XII. Due to the very low accuracy of the measurements of C this involves very great arbitrariness. However a set of relative intensities of the three processes that fits the data is the following

$$0.14\,\eta : 0.04\,\eta^3 : 0.96\,\eta^3$$

in the order in which the processes are listed in the Table.

The most striking feature is the relative importance of the third process in Table XII. One might conjecture that this feature is related to the strong enhancement factor of the p–state of the pion–nucleon system, with $J = 3/2$ $T = 3/2$ (the state (3, 3)). In order to test this conjecture, we postulate that, in the dominant process, the pion π and the nucleon $\mathfrak{N}_1$ that emits it are in the (3, 3) state. The other nucleon $\mathfrak{N}_2$ will be in an s–state with respect to $\mathfrak{N}_1$. The final state of (9.25) consists therefore of two parts:

$$\text{part 1}\quad (\mathfrak{N}_1 + \pi) \qquad \text{has}\quad T = \frac{3}{2}\quad J = \frac{3}{2}\quad \text{parity} +$$

part 2 the nucleon $\mathfrak{N}_2$ has $T = \frac{1}{2}$ $J = \frac{1}{2}$ parity $+$.

The possible values of the resultants for this kind of final state are, according to the quantum mechanical rules of vector addition:

$$T = 1 \text{ or } 2$$

$$J = 1 \text{ or } 2$$

$$\text{parity } +$$

These values of T, J and the parity of the final state must he the same as for the initial state consisting of two nucleons. The T–value for two nucleons is either 0 or 1; only T = 1 matches.

For T = 1, the possihle states of two nucleons are the following:

$$^1S_0 \ , \ ^3P_{0,1,2} \ , \ ^1D_2 \ , \ ^3F_{2,3,4} \ , \cdots .$$

Of these only

$$^1D_2$$

has the proper parity and J–value. Thus, we see that the hypothesis that the strong enhancement factor of the (3, 3) state determines the dominant process of reaction (9.25) leads naturally to the conclusion that the process of line 3 of Table XII should be dominant.

We now discuss the reaction

(9.35) $$p + p \to p + n + \pi^+ .$$

In this reaction, the pion has a continuous spectrum of energies, with a peak in the high energy region. What are the qualitative elements which enter into this energy distribution? The best way of discussing this is to compare the observed energy distribution with the one that would be expected near threshold (non-relativistic region) on the assumption that the shape of the spectrum is controlled only by the statistical weight of the final state. If this were the case the spectral distribution would be represented by the semicircular line in fig. 18.

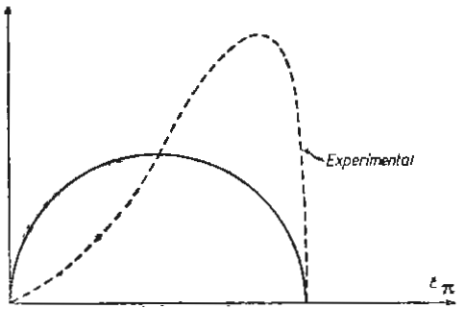

Fig. 18. – Experimental pion energy distribution in the reaction $p + p \to p + n + \pi^+$, compared to the theoretical distribution based on the assumption that the cross-section is determined only by the statistical weight of the final state.

Now, two factors tend to modify this shape: the first is an enhancement factor, coming from the forces between the two nucleons, which favors a small relative energy of the nucleons, that is a large energy of the pion. The second factor comes from the fact that the pion is emitted in a p–state. This means that the transition matrix element is proportional to the pion momentum, and the

intensity to its square. Both factors tend to modify the actual shape of the spectrum as shown in fig. 18.

By a more quantitative argument, Watson [17] found that this phenomenological description is in qualitative agreement with experiment. Quantitatively, however, the theory fails to predict correctly the ratio of the two branches of the reaction

$$p + p \begin{cases} \nearrow d + \pi^- \\ \searrow p + n + \pi^-. \end{cases} \tag{9.36}$$

The ratio of the second to the first branch is experimentally about twice the ratio predicted by the theory. This discrepancy could well be due to a perturbation of the enhancement factor of the two–nucleon wave function, due to the presence of the pion.

We have still to discuss the reactions 11 and 01. There is very little experimental information on them.

The first one apparently has a very steep excitation curve, which is approximately proportional to η^8; this is based mainly on data on the reaction

$$p + p \to p + p + \pi^0, \tag{9.37}$$

in which the process σ_{11} appears alone. There are only two experimental measurements: one made at a bombarding energy of ~ 345 Mev, at Berkeley, and the other at a hombarding energy of ~ 450 Mev, at Chicago. The two experimental points are fitted by the expression

$$\sigma_{11} \sim 0.2\, \eta^8, \tag{9.38}$$

but this formula may be modified by subsequent, more extensive and precise experiments.

Regarding the 01 process, even less is known. Information on this process is obtained from the two reactions

$$n + p \to p + p + \pi^-, \tag{9.39}$$

$$n + p \to n + n + \pi^+. \tag{9.40}$$

They have been observed at only one energy, at Chicago by Yodh. He bombarded hydrogen with neutrons having a continuous spectrum, centered at about 400 Mev. The cross-section thus obtained is due to the combined effect of the 01 and 11 processes, $\frac{1}{2}\sigma_{01} + \frac{1}{2}\sigma_{11}$. Cross-section σ_{01} can be obtained from the difference between this cross-section and the corresponding one on the σ_{11} curve. As there is only one experimental point, there is no question of drawing an excitation curve. But if one assumes that σ_{01} follows a η^4 law, as it should according to the following very rough arguments, then the coefficient should be about 0.5 millibarns,

$$\sigma_{01} \cong 0.5\, \eta^4. \tag{9.41}$$

This excitation function corresponds to the hypothesis that only two angular momentum states contribute to the 01 process, precisely the only two that are "favored" because, in the final state, the pion is in a p–state

(17) K.M. WATSON, «Phys. Rev.», *88*, 1163 (1952).

and the two nucleons in an S–state. The two possibilities are

$$(9.43) \qquad \begin{cases} {}^3S_1 \to ({}^1S_0\, p)_1\,, \\ {}^3D_1 \to ({}^1S_0\, p)_1\,. \end{cases}$$

The η^4 dependence then represents a compromise between the η^3 dependence for a bound ${}^1S_0$ state and the η^6 dependence for uninteracting nucleons (see eq. (9.24)).

The apparently much steeper excitation function for the II process, proportional to η^8, could be due to the fact that for this process there are no " favored " angular momenta. This process must then be due to the contributions of many unfavored processes. The excitation function suggests that most of them are of the (Pp)–type, which would lead to $\sigma \propto \eta^{4+9-5} = \eta^8$.

10.—Multiple Production of Pions.

Multiple production of pions has been observed at Brookhaven. Several experiments have been made with the Brookhaven beam, but much more work is needed to give a clear picture. The situation at high energies is more complicated than that at low energies because more particles are emitted.

As a basis for comparison we might use the statistical theory.[18] In many cases we will find very drastic deviations from this theory and then we must look for an explanation. Unfortunately, few data have been obtained directly from nucleon-nucleon collisions or pion-nucleon collisions. Most of the data have been obtained from nucleon– or pion-nucleus collisions. The interpretation of these data is obviously less simple.

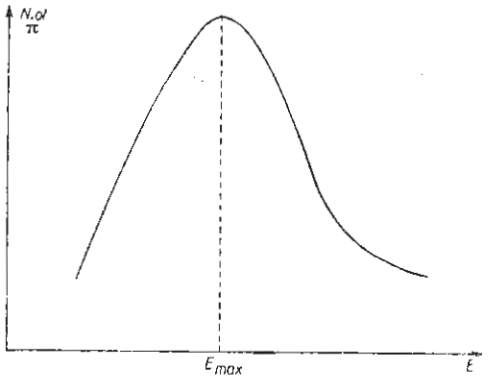

Fig. 19. – Pion energy distribution from bombardment of Be by protons from the Brookhaven Cosmotron, from the experiments of Yuan and Lindenbaum. The pion energies are in the c.m.s., computed on the assumption of production in a nucleon-nucleon collision.

In this category are the experiments of Yuan and Lindenbaum[19] relating to the emission of $\pi^{\pm}$ in the collision of protons, of 1.0 and 2.3 Gev, on beryllium. They observe the spectrum of emitted pions and the ratio of positive to negative pion production. The spectrum is of the shape indicated in fig. 19, in which the observed pion energies have been converted to their energies in the center of mass system, computed on the assumption of production in nucleon-nucleon collisions. The results of Yuan and Lindenbaum are summarized in Table XIII.

(18) E. Fermi, « Phys. Rev. », *92*, 452 (1953); *93*, 1434 (1954). [See paper N° 264 (Editors' note)].

(19) L. C. L. Yuan and S. J. Lindenbaum, « Phys. Rev. », *93*, 1431 (1954); S. J. Lindenbaum and L. C. L. Yuan, « Phys. Rev. », *95*, 638 (A) (1954).

The statistical predictions, according to calculations made by Yang (unpublished) are summarized in Table XIV.

The experimental figures are closer to the theoretical values of E_{max} for double pion production. This is in contradiction with the theoretical expectation of the statistical theory, that single production should still be dominant at these energies.

TABLE XIII.

Summary of the results of Yuan and Lindenbaum on meson production from the bombardment of Be *by protons from the Brookhaven Cosmotron.*

Primary Gev	π	E_{max} (Mev)	π^+/π^-
2.3	+	130	1.8
2.3	—	90	
1.0	+	90	4.5
1.0	—	80	

TABLE XIV.

Predictions of the statistical theory for the properties of meson production from proton bombardment of Be *at Cosmotron energies, according to Yang.*

Gev	Production	E_{max}	π^+/π^-
2	double	100	1.7
	single	450	
1	double	90	3.5
	single	172	

A set of data that can be compared more directly with theory was obtained in experiments carried out with a hydrogen filled diffusion cloud chamber by Shutt *et al.*,[20] who investigated the reactions of protons bombarded by the Cosmotron neutron beam (of about $1.7 \div 1.8$ Gev mean energy and 2.3 Gev maximum energy). For technical reasons, only the three-prong

(20) W. B. FOWLER, R. P. SHUTT, A. M. THORNDIKE, and W. L. WHITTEMORE, « Phys. Rev. », *95*, 1026 (1954).

events were recorded. There are many possible reactions, with end products such as those given in Table XV.

TABLE XV.

Some possible end products of the bombardment of hydrogen by fast neutrons.

End products	Observable prongs
$n\ p$	1
$p\ p-$	3
$n\ n+$	1
$p\ n\ 0$	1
$n\ p+-$	3
$p\ p-0$	3
$n\ n+0$	1
.....	....
$p\ p\ +--$	5

No five-prong events were observed out of some hundred events; so, the probability of such an event is of the order of a fraction of 1 percent. Three-prong events are rather abundant and attempts have been made to classify them in detail. This is not always feasible and the statistics given in Table XVI may still include some wrong assignments.

TABLE XVI.

Preliminary results of Shutt et al. on the events produced in a hydrogen filled diffusion chamber by Cosmotron neutron beam.

Event	Number observed
$p\ p-$	24
$p\ p-0$	30
$n\ p+-$	95

The ratio of the observed single pion production ($pp-$) to the observed double production ($np+-$) is, experimentally, $24/95 \cong 1/4$, whereas the expectation of the statistical theory is $4/1$. The discrepancy is about a factor 16 in favor of double pion production.

There are some elements of the angular distribution of the $(np + —)$ reaction that are worth noting. In the c.m.s. the neutron and the π^- are emitted preferentially in the original direction of the neutron; the proton and the π^+ tend to go off in the original direction of the proton.

One must look for the reason for such an angular distribution and, also, for the drastic deviation from the relative intensities expected from the predictions of the statistical model. It has been suggested by many people that they are related to the "resonant" state (33). For example Peaslee [21] and others consider as a first step of the reaction

$$n + p \rightarrow n^* + p^*, \tag{10.1}$$

where n^* and p^* are excited (resonant) states, $n^* = (n + \pi^-)$ and $p^* = (p + \pi^+)$, that almost istantaneously disintegrate into a nucleon and a pion.(*)

From measurements of the momenta of the charged particles one can compute the relative momentum of the proton and π^+ in their center of mass system and also, although with less certainty, of the neutron and π^-. One can then examine the energy of the $(p + \pi^+)$ or $(n + \pi^-)$. If the resonance were sharp, this energy should be well defined (of the order of 200 Mev). But, in fact the resonance is not at all sharp. Perhaps a better picture is given by the enhancement factor as a function of the energy of $(p + \pi^+)$ or $(n + \pi^-)$. This factor, as shown in Table V, is large up to the "resonance" energy and drops sharply beyond it. On this basis, one expects, then, that a plot of the observed values of the energies of $(p + \pi^+)$ and $(n + \pi^-)$ should yield most values in the energy range up to $\sim$ 200 Mev. There is some small experimental confirmation of this prediction.

The diffusion cloud chamber group has also studied the interactions of 1.37 Gev π^- with protons. (The interactions of the 1.37 Gev π^- beam in nuclear emulsions has also been investigated by Walker *et al.*[22]). On the basis of 94 events, Thorndike (unpublished) find the following tentative results:

$$\sigma_{\text{total}}\,(1.37\ \text{Gev}\ \pi^- + p) = 34\ \text{mb}, \tag{10.2}$$

for events of all types, including $p^- \rightarrow p^-$, n°, p^-°, $p^{-\infty}$, n^+-, etc. A special study has been made of the elastic scattering events (52 in number). Of these 43 are scattered through an angle $\theta < 20°$, while 9 are more or less uniformly scattered over the rest of the angular range. This indicates an appreciable "shadow" scattering with, roughly, $\sigma_{\text{shadow}} \approx 7.2$ mb, and $\sigma_{\text{real elastic}} \approx 1.5$ mb. Since $\sigma_{\text{shadow}} < \frac{1}{2}\sigma_{\text{total}}$, we conclude that the nucleon is partially transparent to 1.37 Mev pions. The above values indicate a nucleon transparency of $\sim$ 20 percent.

(21) D. C. PEASLEE, « Phys. Rev. », *94*, 1085 (1954).

(*) We have, of course, also the possibilities $n^* = (p + \pi^-)$ and $p^* = (n + \pi^+)$. However, since the states $(n + \pi^-)$ and $(p + \pi^+)$ are pure T = 3/2 states, the probability of their resonant formation is greater than for the mixed states $(p + \pi^-)$ and $(n + \pi^+)$. [*Note of* B. T. Feld].

(22) W. D. WALKER, J. CRUSSARD, and M. KOSHIBA, « Phys. Rev. », *95*, 852 (1954).

C) EXPERIMENTS WITH POLARIZED NUCLEONS

11.—Polarization in Nuclear Scattering.

The most detailed information which can be obtained at present on nuclear forces comes from scattering experiments. In the past, cross-sections and angular distributions for nucleon-nucleon scattering have been available up to energies of about 10 Mev; at these energies only *s*–states are involved. More recently, however, it has been possible to extend the range of observation up to about 400 Mev in the laboratory system. The most important information which has been obtained in this energy region is that concerning exchange forces, but in general, little progress has been made, and spin analyses of the various particles involved are still not normally possible.

In the last year or two, however, some progress has been made, particularly in the study of polarization phenomena in the scattering of protons in the high energy range. The attempts to discover such effects are, of course, not new and some early work was done at Berkeley [23] with neutrons. The polarization effects observed were only a few percent, and within the experimental uncertainties. The first really successful experiments on polarization in this energy range were performed by Oxley and co-workers [24] at Rochester, who worked with protons. Their experiment is typical of the methods used by later workers, aside from practical modifications rendered necessary by geometrical conditions in the different laboratories. The proton beam inside the synchro-cyclotron strikes a target (carbon, beryllium, and copper have been used; the material of the target is not critical for this experiment) and some of the protons are scattered. Several types of scattering occur, of which we shall consider three.

a) Coulomb scattering, which, at these energies, is limited to very small angles, and may be neglected.

b) Nucleon-nucleon scattering, in which the interaction may be regarded approximately as a nucleon-nucleon collision, and a recoil nucleon appears at roughly 90° to the direction of the scattered proton. Since the nucleons in the nucleus are not at rest and other nucleons are always involved in the collision, the angular distribution will not show a sharp maximum at 90°. Nevertheless, this type of collision will occur, and may be regarded as *pp* or *pn* scattering.

c) Shadow (elastic) scattering. This always occurs if absorption processes are present, because of wave conservation theorems. It is appreciable up to an angle $\theta \sim \lambda\!\!\!^{-}/R$, where R is the radius of the nucleus.

Other types of scattering will also occur, in which the incident nucleon collides several times within the nucleus, imparting considerable excitation energy, and giving rise to a diffuse beam of low energy particles.

(23) L. F. Wouters, « Phys. Rev. », *84*, 1069 (1951).

(24) C. L. Oxley, W. F. Cartwright, J. Rouvina, E. Baskir, D. Klein, J. Ring, and W. Skillman, « Phys. Rev. », *91*, 419 (1953).

We assume that the initial protons are unpolarized, so that half of them will have spin orientation "up" and half spin orientation "down". On striking the target, the protons will be scattered by each of these processes. If we consider scattering at an angle θ to the right or to the left of the incident direction, particles of one spin orientation will tend to be scattered preferentially to one side or the other; but it is not possible to predict from symmetry considerations alone the sign or amount of polarization in a given direction.

The degree of polarization can be measured by means of the azimuthal asymmetry in the scattering by a second scatterer.

The usual arrangement of first and second scatterers is shown in fig. 20. The fringing field of the cyclotron will deviate the scattered protons so that the direction of observation does not point directly at the target, and this will

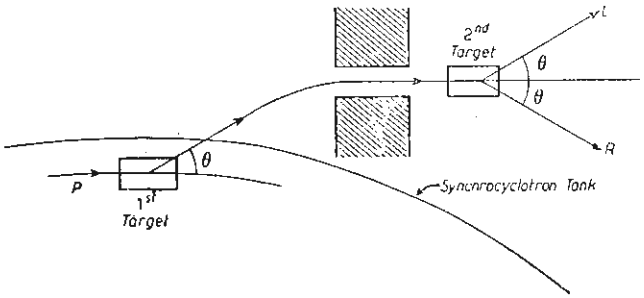

Fig. 20. – Typical arrangement used in the production and analysis of beams of polarized protons from a synchro-cyclotron.

reduce contamination by secondary neutrons. The magnetic field does not disturb the polarization of the scattered protons because the spin orientation is parallel or anti-parallel to magnetic field. If the primary beam is unpolarized, there will be no difference in the intensities of the left and right scattered beams, at a given angle, after the first scattering. These two beams will, however, be partially polarized.

The ratio of spin-up protons going into left and right beams will be

$$\frac{\text{Left}}{\text{Right}} = \frac{1+\varepsilon}{1-\varepsilon}, \tag{11.1}$$

and the ratio of spin-down protons in the two beams will be

$$\frac{\text{Left}}{\text{Right}} = \frac{1-\varepsilon}{1+\varepsilon}. \tag{11.2}$$

If we consider the beam scattered to the left the proportion between spin-up and spin-down is $(1+\varepsilon)$ to $(1-\varepsilon)$. We define the polarization as

$$P = \frac{\text{Number up} - \text{Number down}}{\text{Number up} + \text{Number down}} = \frac{(1+\varepsilon)-(1-\varepsilon)}{2} = \varepsilon, \tag{11.3}$$

Now if we carry out a second scattering as closely as possible identical with the first, the ratio of the left to right intensities will be:

$$\frac{\text{Left}}{\text{Right}} = \frac{(1+\varepsilon)(1+\varepsilon)+(1-\varepsilon)(1-\varepsilon)}{(1+\varepsilon)(1-\varepsilon)+(1-\varepsilon)(1+\varepsilon)} = \frac{1+\varepsilon^2}{1-\varepsilon^2}. \tag{11.4}$$

This allows the calculation of the polarization of the first scattered beam from

$$\frac{L-R}{L+R} = \varepsilon^2, \tag{11.5}$$

though the sign of ε cannot be determined in this way. The ratio observed experimentally for the intensities of the second scattering to the left and to the right is about 1.5–2, quite a large difference, and the corresponding ratio of spin-up to spin-down may be as high as 3.

A variant of this experiment had been attempted previously,[25] in which neutrons were observed from the first target, having undergone exchange scattering. In order to study the anisotropy of the neutron beam, protons were then observed from the second target. This method is experimentally simpler, since the path of the neutrons is unaffected by the field of the magnet; but the polarization observed is very much less than that for protons, the observed differences being in most cases comparable to the experimental error. We shall limit ourselves, therefore, to p–p scattering in both scatterers.

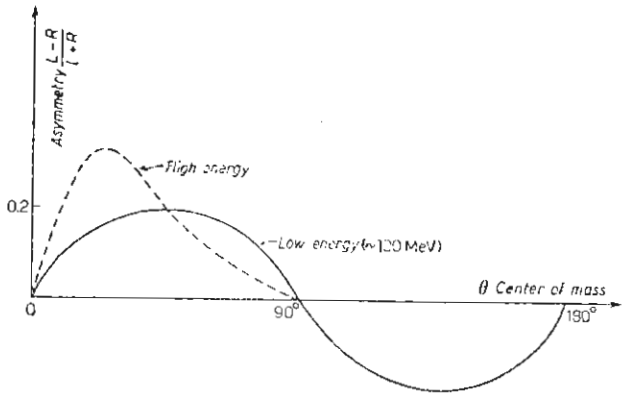

Fig. 21. – Summary of the experimental results on the left-right asymmetry in the scattering of polarized protons by hydrogen.

We start with a partially polarized beam of protons, whose degree of polarization is known approximately, and can use this to investigate proton-nuclear forces, correcting the results to correspond to 100 percent initial polarization. Any kind of target material can be used now as the second scatterer, and the angular distributions of the left-right asymmetry can be investigated.

Consider first scattering of polarized protons by liquid hydrogen. The experimental results [26,27] are shown in fig. 21. The maximum asymmetry

(25) H. BRADNER and R. E. DONALDSON, « Phys. Rev. », *95*, 663 (A) (1954).

(26) O. CHAMBERLAIN, E. SEGRÈ, R. TRIPP, C. WIEGAND, and T. YPSILANTIS, « Phys. Rev. », *93*, 1430 (1954).

(27) J. MARSHALL, L. MARSHALL, and H. G. DE CARVALHO, « Phys. Rev. », *93*, 1431 (1954); H. G. DE CARVALHO, E. HEIBERG, J. MARSHALL, and L. MARSHALL, « Phys. Rev. », *94*, 1796 (1954).

occurs, for low energies, at about 45° in the c.m.s. At higher energies the maximum is shifted to smaller angles. Most of the experimental points are for values of θ between 0 and 90°, and the results are corrected to 100 percent polarization. The experimental data are not yet very accurate, however.

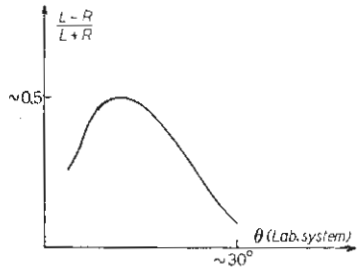

Fig. 22. – Left-right asymmetry observed in the scattering of polarized protons by complex nuclei.

Similar experiments may be carried out on the scattering of polarized protons by nuclei. A higher degree of asymmetry is observed here and $(L - R)/(L + R)$ may be about 0.5–0.6 (fig. 22). The results here are plotted in the laboratory system. The asymmetry becomes quite small at about 30°, and we have little information about the behavior at larger angles.

In considering the theoretical interpretation of the polarization effects in proton-proton scattering, we may adopt either of two methods. The first is to calculate the polarization expected on the basis of various proposed potentials, e.g. those of Jastrow, Levy, Chew and other workers. It is found that most of these models predict polarization effects smaller than those observed. This may be due to the fact that static potentials are used, in which velocity dependent forces are not included. It is not unlikely that velocity dependent forces are important, and this may vitiate any comparison, even with a valid form of the static potential.

The second method, which also has had little success so far, aims only at an empirical description of the facts. One may try to analyse the experimental data in terms of phase shifts. Due to the Pauli principle, the even l–states S , D , ··· have total spin zero (singlets) and odd l–states P , F , ··· have total spin 1 (triplets). This limits the number of possible states, but not sufficiently.

Attempts in this direction have shown that the data available at present are inadequate to determine a unique set of phase shifts. In part this is due to the fact that in the high energy collision of two nucleons very many angular momentum states are of importance. For this reason a much higher experimental accuracy than is available at present would be needed.

If we consider only the angular momentum states S and P, we require the 4 scattering phase shifts α_{lj} shown in Table XVII.

So far, attempts to describe the nucleon-nucleon scattering in this manner have been remarkably unsuccessful, and this is due to the great ambiguity in fitting the various parameters involved: one can find solutions, but not convincing ones, because they allow the phase shifts to be varied almost at will. There is some expectation that, by adding a new experimental fact to be explained, namely data on the polarization, the problem will become somewhat more confined.

The assumption that only the S and P–states contribute to the phenomena is, in this case, particularly unjustified since, for colliding nucleons of energies 200 ÷ 300 Mev, it is to be expected that quite appreciable angular

momenta will contribute. We make here this assumption only to get an idea of the form of the dependence of the scattering parameters on the phase shifts.

TABLE XVII.

States and phase shifts involved in p–p scattering at relatively low energies.

State	Phase shift
$^1S_0$	α_{00}
$^3P_0$	α_{10}
$^3P_1$	α_{11}
$^3P_2$	α_{12}

On this assumption, the angular distribution may be given by the formula (where $\lambda\!\!\!^{-}$ is taken in the c.m. system):

$$\frac{1}{\lambda\!\!\!^{-2}}\frac{d\sigma}{d\Omega} = A + B\cos^2\vartheta + C\sin\vartheta\cos\vartheta\cos\varphi\,, \tag{11.6}$$

when the nucleons are travelling along the z axis, with the spin direction parallel to the y–axis. The dependence on φ is what gives the right-left asymmetry in polarization phenomena; the coefficient C is the important one for the asymmetry. The coefficients A, B and C are expressible in terms of the phase shifts, in the following forms:

$$\left.\begin{aligned} A &= \sin^2\alpha_{00} + \sin^2\alpha_{10} + \frac{9}{4}\sin^2\alpha_{11} \\ &\quad + \frac{13}{4}\sin^2\alpha_{12} - 2\cos(\alpha_{10}-\alpha_{12})\sin\alpha_{10}\sin\alpha_{12} \\ &\quad - \frac{9}{2}\cos(\alpha_{11}-\alpha_{12})\sin\alpha_{11}\sin\alpha_{12}\,, \\ B &= \frac{9}{4}\sin^2\alpha_{11} + \frac{21}{4}\sin^2\alpha_{12} + 6\cos(\alpha_{10}-\alpha_{12})\sin\alpha_{10}\sin\alpha_{12} \\ &\quad + \frac{27}{2}\cos(\alpha_{11}-\alpha_{12})\sin\alpha_{11}\sin\alpha_{12}\,, \\ C &= 6\sin(\alpha_{10}-\alpha_{12})\sin\alpha_{10}\sin\alpha_{12} + 9\sin(\alpha_{11}-\alpha_{12})\sin\alpha_{11}\sin\alpha_{12}\,. \end{aligned}\right\} \tag{11.7}$$

Experimentally we know, in the case of p–p scattering, the total cross-section and the angular distribution averaged over right and left, so that the polarization terms disappear. What is remarkable about this distribution is that it is almost spherically symmetric, which would indicate that B is very small. Then one has the polarization factor or asymmetry that can be used to determine the magnitude of the coefficient C.

There is one point that indicates that the assumption made (only S and P–waves) is not very good, at least at the higher energies (about 250 Mev

or greater). The asymmetry predicted by (11.6) would have a shape like curve B of fig. 23, with a maximum at 45°; instead, at higher energies, the asymmetry seems to have a shape like curve A, with the maximum shifted towards smaller angles.

The coefficient C is controlled only by the P–phase shifts, since only the triplet part of the scattering is coupled with the spin. Also, if all the P–phase shifts were equal, C = 0.

The above theory could be expanded, as more precise data become available on p–p scattering and, with some principle of charge independence, extended to n–p scattering.

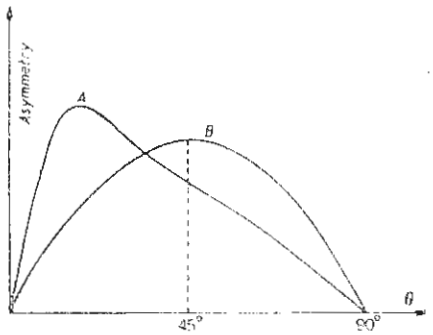

Fig. 23. – Comparison of shape of observed asymmetry, in the scattering of polarized protons by protons, with the prediction of the simple theory assuming S– and P–wave scattering only.

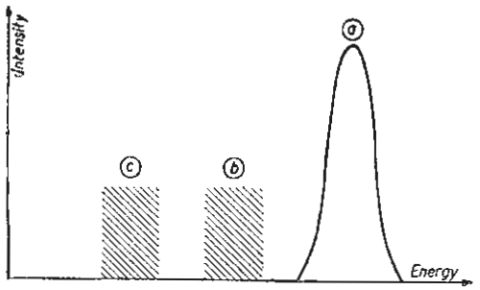

Fig. 24. – Spectrum of scattered nuc eons for an incident high energy nucleon on a complex nucleus.

When a polarized beam of nucleons hits a scatterer, three scattering processes can take place: elastic scattering (or shadow scattering); nucleon-nucleon scattering, and nucleon evaporation from excited nuclei. The resulting energy spectrum of the scattered nucleons is shown in fig. 24, where part *a*) represents the elastically scattered nucleons (with energy a little smaller than the primary energy, because of the small amount of energy that is taken up by the nucleus); part *b*) represents the nucleons from nucleon-nucleon collisions; and part *c*) represents the evaporation nucleons.

It is experimentally difficult to study the degree of polarization of the various components of this spectrum; in principle, it may be done by using a counter telescope with various absorbers, in order to isolate the various energy bands. Some experimental data (Marshall [27]) are summarized in fig. 25. We can conclude that the elastically scattered component is polarized, and that the polarization is higher for this component than for the other ones.

Of course, this pattern is some function of the angle θ, because the elastically scattered component has a sharp forward distribution; so, if we go to $\theta = 40° \div 45°$ (depending on the energy) the polarization effect becomes much harder to observe.

We will now give a rapid interpretation of the polarization of the elastically scattered component. The polarization of the elastically scat-

tered component is probably due to a spin-orbit coupling of the same nature as that present in the shell model of the nucleus (Mayer [28]). This model of the nucleus is essentially based on the observed shell structure, in which the assumption, that there is ast rong spin-orbit coupling, is very important. We describe the orbit as that of a particle in a potential well, characterized by the quantum numbers l and $j = l + s = l \pm 1/2$ (the plus or minus indicating spin parallel or antiparallel to the orbital angular momentum). To fit the experimental values, we have to assume that there is a considerable splitting between $l + 1/2$ and $l - 1/2$ levels, the coupling making the larger value of j more stable than the smaller value. This indicates that the energy corresponding to the "parallel" state is lower than that corresponding to the "antiparallel" state.

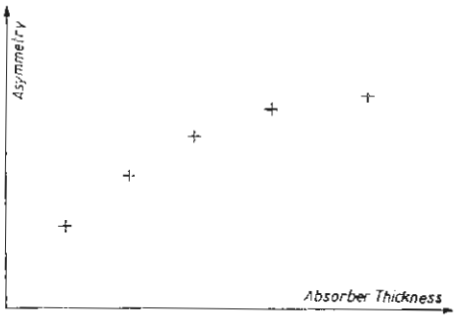

Fig. 25. – Asymmetry in the scattering of polarized protons from complex nuclei as a function of the thickness of absorber in the telescope used to detect the scattered protons.

One may say that the energy is proportional to $\boldsymbol{l}\cdot\boldsymbol{s}$, with a negative coefficient, i.e. $E = -c\boldsymbol{l}\cdot\boldsymbol{s}$. This is the type of spin-orbit coupling suggested by the nuclear structure.

What sort of interactions between spin and orbit are plausible in nuclear matter? Consider the extreme view of a nucleus where the density ρ as a function of the distance from the center is constant up to the edge of the nucleus, and then dropping to zero. The nuclear forces are of very short range (say a), as indicated in the fig. 26. Consider the large sphere of fig. 27 *a* to be the nucleus hit by the nucleon, travelling through nuclear matter of density ρ; the small circle inside represents the range of the nuclear forces. There will be essentially no forces on the average acting on the nucleon or its spin, at least as long as the nucleon travels in the uniform part of the nuclear matter. There will be, however, some attenuation of the beam in the direction of incidence, equivalent to an absorption due to collisions with other nucleons.

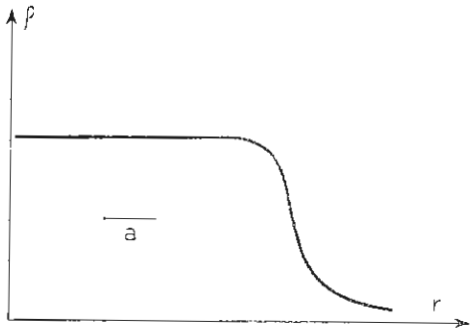

Fig. 26. – Schematic plot of the density of nuclear matter in a nucleus; the range of the nuclear forces is indicated by the distance a.

The situation differs as soon as the nucleon comes to the edge of the nucleus, where ρ decreases sharply, going to zero outside; the nucleon is then

(28) M. G. MAYER, « Phys. Rev. », *74*, 235 (1948); *75*, 1969 (1949); *78*, 16, 22 (1950).

in a sphere of action where on one side the density is ρ and on the other zero. (see fig. 27 *b*).

At this point, the spin-orbit coupling is controlled essentially by the following vector elements: the momentum $\boldsymbol{p}$ of the nucleon, the spin vector $\boldsymbol{\sigma}$ and finally a vector that is the gradient of the nuclear density; the spin-

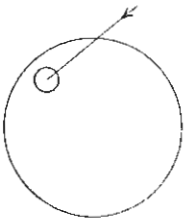

Fig. 27 *a*. – Nucleon passing through a nucleus in a region of essentially no net force.

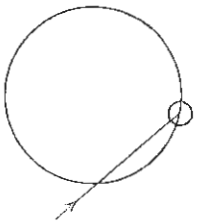

Fig. 27 *b*. – Nucleon passing through a nucleus in a region of strong forces.

orbit coupling energy is a scalar, and can be fabricated from the 3–vectors by the following combination: $\boldsymbol{\sigma}\cdot\boldsymbol{p}\times\boldsymbol{\nabla}\rho$. Other terms (functions of momentum, gradient of ρ, ρ) may be included, but will be neglected for the moment.

Taking into account the shape of the function ρ, we can transform the previous expression into:

$$(11.8) \qquad (\text{coeff.})\,\frac{\rho'}{r}\,\boldsymbol{\sigma}\cdot\boldsymbol{r}\times\boldsymbol{p},$$

where $\boldsymbol{r}\times\boldsymbol{p}=\boldsymbol{l}$ (in units of $\hbar$); the coefficient has a negative sign, which satisfies the conditions of the shell model.

Using (11.8) we can try to find out what polarization arises from the spin-orbit coupling. $\rho'=d\rho/dr$ is peaked around the edge of the nucleus, where ρ goes to zero; if we assume a sharp drop for ρ at the edge, then ρ' can be represented by a delta–function.

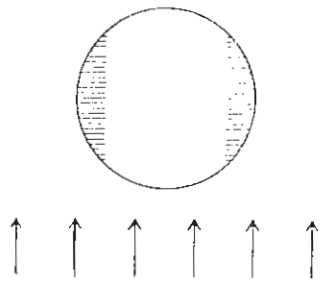

Fig. 28. – Beam of polarized protons (spin up) impinging on a spherical nucleus. The shaded areas represent the regions where the nuclear potential is distorted by the spin-orbit coupling.

Now, we may try to see, without formulae, the effects of such an interaction. Assume a nuclear potential (for instance with sharp corners) and a beam of particles completely polarized as in fig. 28; there will be a potential of the $\boldsymbol{\sigma}\cdot\boldsymbol{l}$ type; on the right hand side $\boldsymbol{\sigma}\cdot\boldsymbol{l}$ is positive, and, on the left side, negative. Then the potential well will be deformed as shown in fig. 29.

Another datum of importance in describing the potential is the main potential well depth (20 ÷ 30 Mev). In addition, there is absorption. If the observation is confined to the elastically scattered part of the beam, any particles that suffer non-elastic collisions will be considered as lost to the beam. This loss of particles (for example, by collisions against nucleons in the nucleus) manifests itself by an attenuation of the beam. The standard way to

describe these absorption properties is to add an imaginary component to the potential:

$$U = U_1 + iU_2 . \tag{11.9}$$

Then the Schrödinger equation takes the form

$$i\hbar \frac{\partial \psi}{\partial t} = (E_{kin} + U_1 + iU_2)\,\psi . \tag{11.10}$$

If we consider only the part depending on U_2, we get

$$\psi \propto \exp\,[(U_2/\hbar)\,t], \tag{11.11}$$

which, for $U_2 < 0$, represents an absorbed wave.

The magnitude of U_2 is controlled by the mean free path for collisions with nucleons in nuclear matter, which can be computed from the nuclear density and the nucleon-nucleon cross-sections at the given energy; for an energy of 200 ÷ 300 Mev, U_2 has a value of about — 7 Mev.

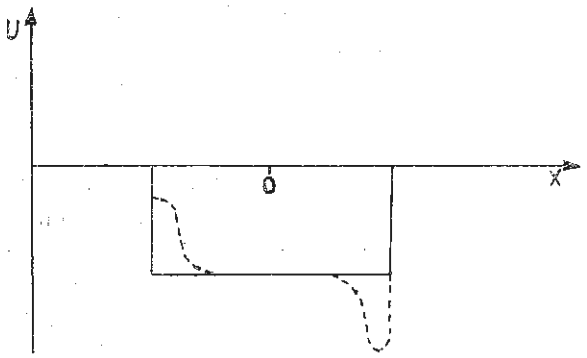

Fig. 29. – Deformation of the nuclear potential due to a spin-orbit coupling of the form of eq. (11.8).

What happens when a particle beam encounters a potential with a real and an imaginary part, and with a depression and a rise, is essentially a diffraction problem. The action of the central part of the potential is clearly symmetric; that of the depression and rise clearly asymmetric.

For a first description of the problem, consider a first approximation corresponding to the Born approximation: this corresponds essentially to considering each element of the potential as acting on the wave with an amplitude proportional to the local value of the potential. Consider scattering through a certain angle ϑ; the amplitude, after taking into account interference due to the path difference or phase difference resulting from scattering in different regions of the nucleus, is

$$\begin{aligned}(U_1 + iU_2)\exp\,[ikr] - D\exp\,[ik\,(r - R\vartheta)] + D\exp\,[ik\,(r + R\vartheta)] \\ = [(U_1 + iU_2) + 2iD\sin kR\vartheta]\exp\,[ikr]\,,\end{aligned} \tag{11.12}$$

where D is the ratio of the volume of the depression and rise near the nuclear edge to the total nuclear volume multiplied by the potential prevailing at

the nuclear edge. This potential may be considered real because for waves originating near the nuclear surface the absorption path is very small. R is the nuclear radius.

The amplitude of the scattered wave is therefore (removing the common factor exp [ikr])

$$U_1 + iU_2 + 2iD \sin kR\vartheta. \tag{11.13}$$

Now look for the terms that may make a right-left difference in the amplitudes for $+\vartheta$ and $-\vartheta$. It is evident that U_1 makes no difference in the intensity, which is the square of the modulus of the amplitude, i.e.

$$U_1^2 + (U_2 + 2D \sin kR\vartheta)^2 \tag{11.14}$$

$$= U_1^2 + U_2^2 + 4D^2 \sin^2 kR\vartheta + 4U_2 D \sin kR\vartheta.$$

This expression for the intensity is symmetric, except for the term containing $\sin kR\vartheta$; since U_2 is negative, this term means that the intensity to the left is greater than that to the right.

One may now argue as to the validity of this Born approximation procedure. It is medium good for light elements, and medium bad for heavy elements. The reason is the following: The condition for validity of the Born appr. is that the primary wave be not too strongly disturbed by the potential in question. Now, if one considers one factor only (and the others are of comparable importance), namely the effect of U_2, one sees that the wave is absorbed and its intensity reduced in traversing the nuclear matter. It turns out that for a rather large nucleus the intensity drops by about a factor 2, or that the wave loses about 30 percent of its amplitude. Now, 30 percent may be considered as small, or as large: we are in an intermediate situation, which may indicate that the Born approximation gives at least a qualitatively correct result for light nuclei, but probably we should make a more accurate calculation for the quantitative details.

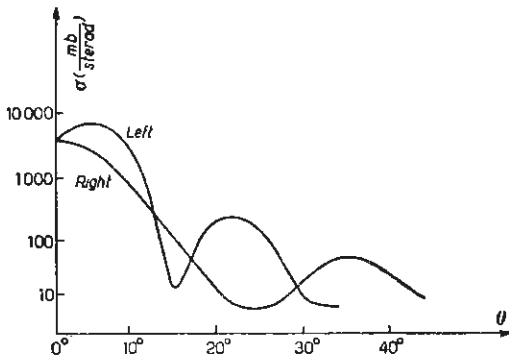

Fig. 30. – Differential elastic scattering cross-sections for 340 Mev polarized protons on carbon calculated for a square well complex potential with spin-orbit coupling.

More detailed calculations can be carried out on this wrong model (sharp potential well [29]): the results for 340 Mev protons on carbon are showed in fig. 30

(29) See, for example, G. A. SNOW, R. M. STERNHEIMER, and C. N. YANG, « Phys. Rev. », *94*, 1073 (1954); B. J. MALENKA, « Phys. Rev. », *95*, 522 (1954); W. HECKROTTE and J. V. LEPORE, « Phys. Rev. », *95*, 1109 (1954).

Interference maxima and minima occur at different angles for left and right scattering; in the region of small angles the left curve is higher than the right one, as was already foreseen in the previous more simple considerations. The right curve has maxima less sharp and shifted towards larger angles than the left one.

Experimentally, the situation is not yet quite clear. The values for the asymmetry, compared with those calculated from fig. 30, are shown in fig. 31. (Segrè at Berkeley, on C (1) and Al (2) [30]).

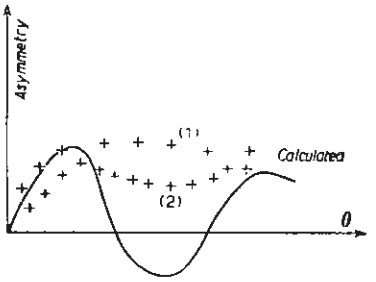

Fig. 31. – Comparison of observed asymmetries in the scattering of polarized protons from C (1) and Al (2) with the predictions from fig. 30.

We should remember that this theory applies only to the elastically scattered protons; as the angle ϑ increases the competition with the non elastically scattered protons becomes more and more important (the cross-section varies by a factor 100 from 0° to 30°), and it is difficult experimentally to separate the elastically scattered protons from the other components.

The aluminium curve shows a minimum, but no reversal of the polarization. An experimental situation of this kind is not unexpected, because of the extreme model used: in the sharp-edged nucleus model, with the δ–function in the l–s coupling, the interference terms are very strongly exaggerated. Presumably, if one eliminates the sharp boundary, one will wash out these interference patterns.

In a small nucleus the edges of the nucleus are something like in fig. 32; if one takes a nucleus with a larger radius (with the radius large compared to the diffuseness of the edges) then one can get a potential corresponding to something like fig. 33; here, interference effects presumably begin to appear. One can try to introduce a suitable degree of diffuseness to account for the experimental results.

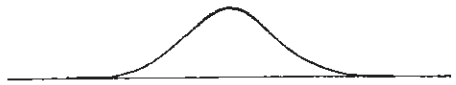

Fig. 32. – Density distribution in a light nucleus, showing the inadequacy of a model which assumes a sharp boundary.

Fig. 33. – Density distribution in a heavy nucleus.

Now two final remarks.

1) Sign of the polarization: a theory of this kind predicts that at small angles the particles with spin up go preferentially to the left; for this, there is no experimental confirmation. The sign of the polarization can be detected by two methods:

a) studying the interference with coulomb scattering;

b) slowing down a polarized beam, by ionization loss, to a few Mev, and detecting the sign of the polarization by means of processes of ordinary nuclear physics, which are sufficiently understood to give the sign of the

(30) O. CHAMBERLAIN, E. SEGRÈ, R. TRIPP, C. WIEGAND, and T. YPSILANTIS, « Phys. Rev. », *95*, 1105 (1954); *96*, 807 (1954).

polarization; there is sufficient reason to believe that during ionization loss there is very little probability of spin flip.(*)

2) In the Born approximation, the polarization phenomena appear as due only to the U_2 part of the potential; this is just a trick used in Born approximation, because the potential scatters with an amplitude given directly by the potential; if you go to higher approximations, things become more complicated.

What we have learned from the polarization effects is the following: there is good evidence that the l–s coupling of conventional nuclear physics persists with essentially the same strength at higher energies; this can presumably be tied to the primary origin of the l–s coupling, already present in a latent form in the nucleon-nucleon forces.

(*) This has recently been done at Chicago (L. MARSHALL and J. MARSHALL, « Nature », fasc. 1 (1955)), and the sign turns out to be as predicted by the theory of Fermi. [*Note by* B. T. Feld].

APPENDICE N. 1

LISTA DEGLI ONORI

Premio Matteucci, Medal of the "Società Italiana delle Scienze" detta dei XL, Roma, 1926.

Correspondent Member, "Accademia delle Scienze", Torino, August 8th–1928.

Correspondent Member, "Academy of Sciences", Leningrad, 1928.

Member, "Reale Accademia d'Italia", Roma, March 18th 1929.

Honorary Member, "Accademia Gioenia di Scienze Naturali", Catania, January 24th–1931.

Correspondent Member, "Accademia Nazionale dei Lincei", Roma, July 27th–1932 (National Member, May 6th–1935).

Member, "Società Italiana delle Scienze" detta dei XL, Roma, 1933.

Correspondent Member, "Academia Brasileira de Ciencias", Rio de Janeiro, August 26th–1934.

Member, "Kaiserlich Deutsche Akademie der Naturforscher", Halle–Saale, February 16th–1935.

Honorary Member, "Indian Academy of Sciences", Bangalore, 1935.

Honorary Degree, Doctor of Natural Sciences, "Ruprecht Karl Universität", Heidelberg, June 30th–1936.

Honorary Degree, Doctor of Science, "Rijksuniversiteit", Utrecht, July 20th–1936.

Foreign Correspondent Member, "Österreichische Akademie der Wissenschaften", Wien, 1937.

Nobel Prize in Physics, Stockolm, December 10th–1938.

Honorary Member, "Academia Română", Bucureşti, 1938.

Fellow, "American Philosophical Society", Philadelphia, Penna. April 31st–1939.

Hughes Medal of the "Royal Society", London, November 30th–1942.

Award, "United States Office of Scientific Research and Development", Washington D.C., March 1st–1945.

Member, "National Academy of Sciences", Washington (D.C.), April 24th–1945.

Award, United States War Department, Army Service Forces, Corps of Engineers, Manhattan District, Washington D.C., August 6th–1945.

Congressional Medal of Merit of the United States of America, Washington D.C., January 12th–1946.

Honorary Degree, Doctor of Science, "Washington University", St. Louis, Missouri, February 22nd–1946.

Honorary Member, "Franklin Institute", Philadelphia, Penna. April 16th–1946.

Lewis Prize of the "American Philosophical Society" Philadelphia, Penna. for 1945–46, April 12th 1946.

Honorary Member, "Sons of Italy in America", New–York, N.Y., March, 1946.

Honorary Degree, Doctor of Science, "Columbia University", New–York, N. Y., June 4th–1946.

Honorary Degree, Doctor of Science, "Yale University", New Haven, Conn., July 7th–1946.

Honorary President, "Fondazione Angelo della Riccia", Firenze, March 5th 1947.

Franklin Medal of the "Franklin Institute", Philadelphia, Penna, January 8th–1947.

Honorary Degree, Doctor of Law, "Rockford College", Rockford, Ill., February 23rd–1947

Trasenster Medal, "Association des Ingenieurs sortis de l'École de Liège", University of Liège, February 16th–1947.

Fellow, "American Academy of Arts and Sciences", Boston, Mass. March 13th–1947.

Honorary Degree, Doctor of Science "Harvard University" Cambridge, Mass. June 10th–1948.

Honorary Member, "Società Italiana di Fisica", Bologna, 1948.

Donegani Medal for Chemistry, "Accademia Nazionale dei Lincei", Roma, May 15th 1948.

Honorary Fellow, "Royal Society of Edinburgh", July 4th–1949.

Foreign Member, "The Royal Society", London, April 27th–1950.

Barnard Medal for Meritorious Service to Science, New–York, N.Y., June 8th–1950.

Honorary Member, "Italian Historical Society of America", New–York, N.Y., 1950.

Recognition Plaque, "Columbia University" for Participation in the Work of the Division of War Research, World War II, New–York, N.Y. [*no date*].

"Réaction en Chaine Medal" [*no date*].

Dr. Binala Churn Law Gold Medal of the "Indian Association for the Cultivation of Science", Calcutta, April 6th–1951.

Honorary Degree, Doctor of Science, "University of Rochester", Rochester, N. Y., January 4th–1952.

Popular Mechanics Hall of Fame, January, Chicago, Ill., 1952.

Rumford Medal of the "Academy of Arts and Sciences", Boston, March 27th–1953.

Planck Medal of Verband Deutscher Physikalischer Gesellschaften, Braunschweig, April 23rd–1954.

Medal of the "Italian–American Charitable Society", Boston, October 11th–1954.

Enrico Fermi Award, Atomic Energy Commission, United States of America, Washington, D.C., December 2nd 1954 (posthumous).

Honorary Member, "Swedish Engineers Society", Chicago, December 10th–1954 (posthumous).

APPENDICE N. 2

CRONOLOGIA

1901 – September 29th: Born in Rome, Via Gaeta 17 (now 19).

1911–1918: Attends Ginnasio and Liceo at school "Umberto I" in Rome.

1914 – Fall: Begins self training under Ingegner Adolfo Amidei.

1915 – Friendship with Persico begins.

1916 – January 12th: Brother Giulio dies in Rome.

1918 – Fall: Enters Reale Scuola Normale Superiore in Pisa; attends University of Pisa.

1922 – July 7th: Receives degree (Laurea) Doctor of Physics from University of Pisa.

1923 – From January to August is in Goettingen to study with Max Born (with a Fellowship of Ministero della Pubblica Istruzione).

1923–24: Teaches Mathematics for Chemists and Naturalists at the University of Rome. Meets George Uhlenbeck, from Leyden.

1924 – May 8: Mother dies in Viggiù.

1924 – From September to December is in Leyden to study with Ehrenfest.

1924 – (Fall) to 1926 (fall) Teaches Mathematical Physics and Theoretical Mechanics (Meccanica razionale) at the University of Florence (incarico).

1925 – March 2: Obtains "Libera Docenza" in Mathematical Physics.

1925 – December: Conceives idea of Statistics (published in 1926).

1926 – February: Is awarded second place in competition for chair of Mathematical Physics at Cagliari and does not get a position.

1926 – Summer: Writes "Introduzione alla fisica atomica".

1926 – Fall: Is Awarded first place in competition for the newly established chair of Theoretical Physics at the University of Rome, Becomes professor there.

1927 – May 7th: Father dies in Rome.

1927 – September: Attends Volta Congress in Como (Sommerfeld presents a paper Zur Elektronentheorie der Metalle und des Volta-Effektes nach der Fermischen Statistik. Fermi discusses Sommerfeld's paper).

1927 – October: Buys his first car (Bebé Peugeot).

1927 – Fall: The Rome physics group starts informally: Rasetti, Segrè, Majorana, Gentile, Amaldi.

1927–1929 (?) Secretary Comitato Nazionale per la fisica del C.N.R.

1928 – Spring: Declines invitation to succeed Schroedinger in Zürich.

1928 – July 19th: Marries Laura Capon in Rome.

1929 – March 18th: Is appointed a Member, Reale Accademia d'Italia, Rome.

1926–1929 (?) Redattore Enciclopedia Italiana.....

1929–1931 (?) Direttore di Sezione, Enciclopedia Italiana.

1930 – Spends the Summer at the University of Michigan, Ann Arbor, Mich. (First visit to the U.S.).

1931 – January 31st: Daughter Nella is born in Rome.

1931 – October 11–18: Attends International "Volta Conference" on Nuclear Physics of Reale Accademia d'Italia in Rome.

1932 – July 7th: Gives report on Nuclear physics at the "International Conference on Electricity" in Paris.

1933 – Vice President, Società Italiana per il Progresso delle Scienze.

1933 – Returns for the Summer to the University of Michigan, Ann Arbor, Mich.

1933 – October 22–29: Attends Solvay Conference on nuclear physics at Bruxelles, Belgium.

1933 – December: Theory of Beta Decay.

1934 – January: Theory of Beta Decay published in letter to « Ricerca Scientifica ».

1934 – March 21st: Obtains first radioactive isotopes by neutron bombardment.

1934 – Summer: Lectures in Argentina, Brazil, and Uruguay.

1934 – October 22: Rome, Explains effect of hydrogenated substances on radioactivity produced by neutron bombardment. (Slow neutrons).

1935–1938 March 28th, Member Consiglio di Amministrazione dell'E.I.A.R. (Ente Italiano Audizioni Radiofoniche).

1935 – July 16th – to 1938 Member Consiglio Superiore dell'Educazione Nazionale, Rome.

1935 – Spends the Summer at the University of Michigan, Ann Arbor, Mich.

1936 – February 16th: Son Giulio is born.

1936 – Spends the Summer at Columbia University, New York, N. Y. (Book: Thermodynamics).

1937 – Spends the summer at Stanford University, Palo Alto, Calif.

1937 – November 19th: Member Consiglio direttivo del Comitato Nazionale per la fisica e la matematica applicata del Consiglio Nazionale delle Ricerche, Rome.

1938 – September, Direttore Centrale dei Laboratori scientifici e di ricerche del Gruppo Industriale Magneti Marelli.

1938 – November 10th: Nobel Prize is announced.

1938 – Early December: Leaves Italy.

1938 – December 10th – Receives Nobel Prize in Stockholm.

1939 – January 2nd: Lands in the United States at New York.

1939 – January 26: At Fifth Conference on Theoretical Physics, sponsored jointly by George Washington University and Carnegie Institution, in Washington, D. C., discusses implications of fission with Bohr and advances hypothesis that neutrons might be emitted.

1939 – March 17th: Talks to Admiral S. C. Hooper about possibility of atomic energy for war purposes.

1939 – Spends the summer at the University of Michigan, Ann Arbor, Mich.

1939 – September: Settles in Leonia, N. J.

1939 – December 16th: Discusses Pu^{239} with Segrè.

1941 – December 8th: Becomes enemy alien as result of the U. S'. entry in the war.

1941 – End of December: Begins traveling to Chicago under war time regulations for enemy aliens.

1942 – Spring: Work on chain reaction is moved to Chicago. Fermi settles in Chicago.

1942 – December 2nd: Directs experiment in which the first self sustaining chain reaction is achieved.

1944 – September: Is present at the start up of the first Hanford pile at Hanford, Wash.; helps understand the pile poisoning.

1944 – Later in September: Joins project at Los Alamos, N. M.

1945 – July 16th: Participates in the test of first atomic bomb at Alamogordo, N. M.

1945 – December 31st: Leaves Los Alamos, N. M.

1946 – January 2nd: Returns to Chicago as member of the Institute for Nuclear Studies.

1946 – July 30 – September 3: is consultant at Los Alamos.

1946–50: Member, General Advisory Committee of the U. S. Atomic Energy Commission.

1947 – Part of June and July: lectures at the University of Washington, Seattle, Wash.

1947 – July 25 – September 21: is consultant at Los Alamos.

1948 – Second part of summer session: lectures at the University of California, Berkeley, Calif.

1948 – September 13–25: is consultant at Los Alamos.

1949 – September: Attends International meetings on the Physics of Cosmic Ray at Basel, Switzerland and Como Italy (Como meeting Sept. 11th–16th).

1949 – Fall: Delivers "Lezioni Donegani" in Rome and Milan, Italy.

1950 – April: Delivers Silliman Memorial Lectures at Yale University, New Haven, Conn. (Book: Elementary Particles).

1950 – July 3 – September 19: is consultant at Los Alamos.

1951 – June 15–17, July 25 – September 11: is consultant at Los Alamos.

1952 – Is elected Vice President of the American Physical Society.

1952 – July 24 – September 20: is consultant at Los Alamos.

1953 – July 25 – September 20: is consultant at Los Alamos.

1953 – Iselected President of the American Physical Society.

1954 – Summer: Is at Brookhaven National Laboratory, Upton, N. Y.; at the School af Theoretical Physics at Les Houches, France; at the International School of Physics at Varenna, Italy (later named "International School of physics Enrico Fermi") and at Heidelberg, Germany.

1954 – November 28: Dies in Chicago, and is buried there.

APPENDICE N. 3

DOCUMENTI E MANOSCRITTI DI E. FERMI

Due sono le principali raccolte di manoscritti e cimeli di Fermi. Una si trova nella « Domus Galilaeana » in Pisa, l'altra nella collezione di Libri Rari della Biblioteca dell'Università di Chicago.

Quando Fermi partì dall'Italia nel 1938 egli portò con sè la maggior parte delle carte che pensava gli sarebbero state utili nel suo lavoro futuro. Così, ciò che rimase in Italia si riferisce solo a lavori completamente conclusi prima del 1939 e non comprende quaderni cominciati o scritti in Italia ma che avrebbero potuto avere interesse in seguito.

La collezione di Pisa comprende 22 quaderni contenenti lavoro teorico datato dal 1926 al 1938. In essa si trovano i manoscritti di parecchi lavori importanti come i nn. 30, 50, 73, 76. Sono a Pisa tutti i quaderni che si riferiscono al lavoro sperimentale compiuto tra il 1935 e il 1938. Questi sono in numero di 8.

Nella « Domus Galilacana » si trova anche una raccolta degli strumenti originali usati dal gruppo di Roma per i lavori nucleari del 1934–1938: contatori Geiger–Müller, camere di ionizzazione, sorgenti di neutroni a radon e berillio, etc.

La collezione di Chicago comprende 49 scatole ed è divisa in tre sezioni principali: (1) Carte personali e miscellanea (scatola 1); (2) Carte professionali e oggetti (scatole 2–48); (3) Carte accademiche (scatola 49). La suddivisone (2) è ulteriormente suddivisa in: carte che si riferiscono alla sua attività (scatole 2–15), e carte contenenti informazioni (scatole 16–48).

Segue un inventario più particolareggiato di questa collezione.

Scat. 1: Carte personali e carte professionali varie. Queste carte si riferiscono a onorificenze e premi, documenti di famiglia, appunti di conferenze a cui aveva assistito, inviti non accettati.

Scat. 2–5: Certificati di premi, lauree *ad honorem*, cariche e onorificenze varie.

Scat. 6–7: Bibliografia e una collezione pressoché completa di estratti dei suoi lavori.

Scat. 8–9: Corrispondenza professionale, principalmente del periodo americano, ordinata alfabeticamente.

Scat. 10: Documenti riguardanti le sue funzioni di Presidente della American Physical Society.

Scat. 11: Corrispondenza relativa a contratti col Governo Federale, e altri rapporti col Governo Federale.

Scat. 12: Ulteriore corrispondenza col Governo Federale. Corrispondenza relativa al National Bureau of Standards (caso Astin), al caso Oppenheimer, e ad una controversia riguardante accuse fatte al Laboratorio di Los Alamos da Shepley–Blair.

Scat. 13: Corrispondenza e dati riguardanti ricerche.

Scat. 14: Manoscritti di libri.

Scat. 15: Richieste di brevetti.

Scat. 16: Diapositive per conferenze diverse.

Scat. 17–22: Appunti e lezioni ciclostilate e quaderni riguardanti ricerche. In questo gruppo di manoscritti si trovano i superstiti programmi dei corsi svolti alle università di Columbia e di Chicago. Molti di essi sono stati pubblicati in una forma o nell'altra. Vi sono programmi di corsi non pubblicati sulla Meccanica Statistica (Columbia, 1941), Equazioni differenziali della fisica classica (Chicago, 195?), particelle fondamentali (Chicago, 1953), e Stato solido (Chicago, 1951).

Scat. 23: Estratti.

Scat. 24–44: «Memoria artificiale». È questa una raccolta enciclopedica di appunti, estratti, calcoli, dati numerici etc., classificata in modo adatto per la consultazione. Il materiale è catalogato secondo una classificazione decimale inventata da Fermi, con indici e rinvii tali che Fermi poteva facilmente e rapidamente trovare tutto ciò che cercava. Uno schedario fornisce la chiave per la «Memoria artificiale». Questa contiene matematica, fisica, geofisica, astronomia, tecnica dei traccianti, organi di senso etc. La memoria artificiale non esisteva nel periodo romano, benché tra i manoscritti conservati alla «Domus Galilaeana» vi sia un quaderno intitolato «Thesaurus» contenente formule di uso comune. La memoria artificiale nella sua forma attuale deve essere stata accumulata principalmente a Chicago.

Quando era assai giovane Fermi compilò un quaderno (vedi Introduzione Biografica) nel quale cercò di concentrare tutta la fisica che conosceva. La «Memoria artificiale» fu la soluzione escogitata da Fermi per i problemi derivanti dall'immensa accumulazione di dati teorici e sperimentali in cui era interessato e che gli servivano per il suo lavoro, e dal relativo indebolimento della sua eccezionale memoria. Caratteristica dell'uomo è l'estrema cura nella scelta del materiale e nella sua classificazione.

Scat. 45: Appunti di conferenze tenute in Italia nel 1949 su argomenti di fisica.

Scat. 46–48: Miscellanea di alcuni libri della biblioteca personale di Fermi.

Scat. 49: Carte riguardanti gli inizi della sua carriera accademica in Italia e carte relative alla sua nomina a Chicago, contratti col governo, consulenze etc. In questa stessa scatola si trovano anche lettere e documenti relativi al suo insegnamento a Chicago.

Una descrizione più dettagliata della collezione di Chicago è stata preparata dal Dr. R. Rosenthal, curatore della Sala dei Libri Rari della Biblioteca dell'Università di Chicago. La presente descrizione abbreviata è basata su di essa.

ERRATA CORRIGE ALL'INDICE E ALLA BIBLIOGRAFIA DEL VOLUME I

Pag.	N°.	Errata.	Corrige.
VIII	23 *a*	(1925).	(1925); also « Rend. Linc. », *33*, 243–245 (1924).
VIII	27	*Resonanzstrahlung*.	*Resonanzstrahlung*. E. FERMI und F. RASETTI.
X	66	Sur la théorie de la radiation.	La théorie du rayonnement.
XI	72 *a*	La physique du noyau atomique.	État actuel de la physique du noyau atomique.
XI	74	(1933)	(1933); also « Nuovo Cimento», *10*, 333–338 (1933).
XIII	97	442–447.	442–451.
XIII	104	34–39.	34–39 (1934).
XIII	111	116–120.	116-120 (1935).
XIV	120	(1937).	(1937); also « L'Energia Elettrica », *14*, 85–86 (1937).